FEB - FRESENIUS ENVIRONMENTAL BULLETIN
Founded jointly by F. Korte and F. Coulston
Production by PSP - Vimy Str. 1e, 85354 Freising, Germany in
cooperation with PRT-Parlar Research & Technology
Vimy Str 1e, 85354 Freising
Copyright© by PSP and PRT, Vimy Str. 1e, 85354 Freising, Germany
All rights are reserved, especially the right to translate into foreign language or other processes - or convert to a machine language, especially for data processing equipment - without written permission of the publisher. The rights of reproduction by lecture, radio and television transmission, magnetic sound recording or similar means are also reserved.
Printed in Germany-ISSN 1018-4619

FEB-EDITORIAL BOARD

CHIEF EDITOR:
Prof. Dr. Dr. H. Parlar
Parlar Research & Technology-PRT
Vimy Str.1e
85354 Freising, Germany

MANAGING EDITOR:
Dr. P. Parlar
Parlar Research & Technology
PRT, Vimy Str.1e
85354 Freising, Germany

CO-EDITORS:

Environmental Spectroscopy
Prof. Dr. A. Piccolo
Universita di Napoli "Frederico II"
Dipto. Di Scienze Chemica Agrarie
Via Universita 100, 80055 Portici, Italy

Environmental Biology
Prof. Dr. G. Schuurmann
UFZ-Umweltzentrum
Sektion Chemische Ökotoxikologie
Leipzig-Halle GmbH,
Permoserstr.15, 04318
04318 Leipzig, Germany
Prof. Dr. I. Holoubek
Recetox-Tocoen
Kamenice126/3, 62500 Brno, Czech Republic
Prof. Dr. M. Hakki Alma
Kahramanmaras Sutcu Imam University
Avsar Kampusu, 46100 Kahramanmaras, Turkey

Environmental Analytical Chemistry
Prof. Dr. M. Bahadir
Lehrstuhl für Ökologische Chemie
und Umweltanalytik
TU Braunschweig
Lehrstuhl für Ökologische Chemie
Hagenring 30, 38106 Braunschweig, Germany
Dr. D. Kotzias
Via Germania29
21027 Barza(Va), Italy

Environmental Management
Dr. K. I. Nikolaou
Env.Protection of Thessaloniki
OMPEPT-54636 Thessaloniki
Greece

Environmental Toxicology
Prof. Dr. H. Greim
Senatkommision – DFG / TUM
85350 Freising, Germany

Environmental Proteomic
Dr. A. Fanous
Halal Control GmbH
Kobaltstr. 2-4
D-65428 Rüsselsheim, Germany

Environmental Education
Prof. Dr. C. Bayat
Esenyurt Üniversitesi
34510 Esenyurt, Istanbul, Turkey

Advisory Board
K. Bester, K. Fischer, R. Kallenborn
DCG. Muir, R. Niessner,W.Vetter,
A. Reichlmayr-Lais, D. Steinberg,
J. P. Lay, J. Burhenne, L. O. Ruzo

Marketing Manager
Cansu Ekici, B. of B.A.
PRT-Research and Technology
Vimy Str 1e
85354 Freising, Germany
E-Mail: parlar@wzw.tum.de
parlar@prt-parlar.de
Phone: +49/8161887988

Fresenius Environmental Bulletin is abstracted/indexed in:
Biology & Environmental Sciences, BIOSIS, CAB International, Cambridge Scientific abstracts, Chemical Abstracts, Current Awareness, Current Contents/Agriculture, CSA Civil Engineering Abstracts, CSA Mechanical & Transportation Engineering, IBIDS database, Information Ventures, NISC, Research Alert, Science Citation Index (SCI), Scisearch, Selected Water Resources Abstracts

CONTENTS

ORIGINAL PAPERS

PARTICULATE MATTER ASSESSMENT AT SELECTED POINTS IN AMBIENT AIR OF DISTRICT SIALKOT, PAKISTAN 5693
Muhammad Waseem Mumtaz, Muhammad Danish, Muhammad Asam Raza, Hamid Mukhtar, Muhammad Arshad, Saad Afzal, Muhammad Zubair, Syed Ali Raza

A NOVEL NaClO2-UV/O3 TREATING ACID TURQUOISE BLUE A IN AQUEOUS SOLUTION: DYNAMICS MODEL AND SYNERGISTIC EFFECT 5700
Yongjun Shen, Yuanyuan Hu, Qihui Xu, Peng Zhu, Kaixia Fan, Yao Sun

COMPARISON OF TWO STRATEGIES FOR THE START-UP OF A NEW BIOFILM REACTOR FOR THE TREATMENT OF SYNTHETIC AQUACULTURE WASTEWATER 5707
Xiaoma Xu, Siyao Wang, Jiejie Wu, Cheng Wei, Yuewu Pu

THE USAGE OF AUXINS WITH VARIOUS CULTURAL TECHNIQUES TO INCREASE FRUIT SIZE IN STAR RUBY GRAPEFRUIT 5717
Turgut Yesiloglu, Salih Koc, Berken Cimen

LOW COST MESO-POROUS CARBON DEVELOPED FROM JATROPHA HUSK, A BIO-DIESEL BYPRODUCT WASTE FOR ADSORPTION OF METHYLENE BLUE 5723
Alagarasan Jagadeesh Kumar, Rajendra Prasad Singh, Dafang Fu, Chinnaiya Namasivayam

EFFECTS OF ANTIBIOTICS AND METAL IONS EXPOSURE ON THE NATURAL TRANSFORMATION FREQUENCY OF AN ANTIBIOTIC RESISTANT PLASMID 5732
Yang Qingxiang, Wang Qiang, Zhuo Kaiyue

DISTRIBUTION AND CONTROLLING FACTORS OF PHYTOPLANKTON DURING A TIDE IN THE COASTAL AREA OF BOHAI BAY, CHINA 5737
Wenliang Zhang, Chao Wu, Haijiao Liu, Jun Sun, Gang Qian

RISK DECISION ANALYSIS OF FLOODWATER RESOURCE UTILIZATION BASED ON ADJUSTING FLOOD LIMITED WATER LEVEL OF RESERVOIR 5745
Guohua Fang, Yong Yang, Yu Yuan, Xianfeng Huang, Xin Wen

ASSOCIATIVE EFFECTS OF ENSILING SOYBEAN AND CORN PLANT AS MIXTURES ON THE NUTRITIVE VALUE, FERMENTATION AND METHANE EMISSION 5754
Mustafa Kizilsimsek, Cehre Ozturk, Kubra Yanar, Ibrahim Ertekin, Cagri Ozgur Ozkan, Adem Kamalak

THE DETERMINATION OF SOME GENOTYPIC AND PHENOTYPIC PARAMETERS FOR CHEMICAL COMPOSITION OF SOME BEAN GENOTYPES 5761
Omer Sozen, Ufuk Karadavut

HEAVY METAL BIOSORPTION OF COPPER IONS BY IMMOBILIZED BIOMASS OF Stichococcus subtilis (KÜTZING) KLERCKER 5769
Dilek Yalcin, Tulay Ozer, Ilkay Acikgoz Erkaya, Ahmet Furkan Kayis, Ozcan Yalcinkaya

EFFECT OF NUTRITIONAL NEEDS ON THE YIELD OF LIGNIN-DEGRADING ENZYME AND DYES DECOLOURIZATION USING HETEROBASIDION INSULARE 5775
Yue-Hua Zhang, Jing-Ni Yu, Jia-Lin Li, Zhi-Wen Luo

NOVEL APPROACH OF PREDICTING THE BIODEGRADABILITY OF CORROSION INHIBITORS BASED ON THEIR PHYSICOCHEMICAL PROPERTIES 5783
Amel Begbeg, Rabah Kerbachi, Mohamed Khodja, Malha Nazef-Allaoua

ADSORPTION BEHAVIOR OF 17A-ETHINYLESTRADIOL ONTO ACTIVATED SLUDGE DERIVED FROM MEMBRANE BIOREACTOR 5789
Hai-Liang Song, Xiao-Li Yang, Tong-Qing Chen

EFFECT OF SIMULATED CORROSION ENVIRONMENT ON MECHANICAL PERFORMANCES OF SAND FIXATION BY HYDROPHILIC POLYURETHANE 5797
Zhishui Liang, Zhiren Wu, Mohammad Noori, Lin Deng

NITROGEN MINERALIZATION VARIATION AMONG TREE SPECIES, INCUBATION METHOD AND INTRINSIC SOIL PROPERTIES 5806
Soner Oktay, Huseyin Baris Tecimen

PHYSIO-BIOCHEMICAL AND NUTRITIONAL RESPONSES OF ABELMOSCHUS ESCULENTUS (L.) MOENCH (OKRA) UNDER MERCURY CONTAMINATION 5814
Asiya Hameed, Tabasum Nazir Qadri, Mahmooduzzafar, Tariq Omer Siddiqi,Munir Ozturk, Volkan Altay, Parvaiz Ahmad

ENVIRONMENTAL AND ECONOMIC CONDITIONING OF THE BREEDING OF DAIRY CATTLE 5824
Andrzej Borusiewicz, Kamila Mazur

EXPERIMENTAL STUDY ON THE EFFECTS OF ULTRA-LOW SULFUR DIESEL FUEL TO THE EXHAUST EMISSIONS OF A FERRY 5833
Murat Durmaz, Saliha Saadet Kalender, Selma Ergin

NATURAL ANTIOXIDANTS OF HUMIC AND FULVIC ACIDS AGAINST OXIDATIVE STRESS INDUCED BY HYDROGEN PEROXIDE: IN-VIVO STUDIES 5841
Abd El-Moneim M R Afify, Osama K Konswa

OXIDATIVE STRESS RESPONSE AND CELL DEATH IN FISH INTESTINE DUE TO METRONIDAZOLE TOXICITY 5849
Beyhan Gurcu, Yucel Basimoglu Koca, Sevinc Inan, Mehmet Ibrahim Tuglu

A CASE STUDY: TREND ANALYSIS OF TOTAL ANNUAL RAINFALLS ON EASTERN ANATOLIA REGION IN TURKEY 5858
Serkan Senocak, Muhammed Fatih Emek

SCREENING OF HYDROLYTIC ENZYME PRODUCTION AND FAME (FATTY ACID METHYL ESTERS) ANALYSIS OF THERMOPHILIC BACTERIAFROM HOT SPRINGS 5865
Meral Yilmaz Cankilic, Emine Celikoglu, Umut Celikoglu

RAPID DETERMINATION OF NITROGEN IN OVERLYING RIVER WATER DURING INTERMITTENT AERATION USING INTERVAL PARTIAL LEAST SQUARES AND NEAR-INFRARED SPECTROSCOPY 5873
Jian Huang, Xiong Zhang, Hua Zhang, Qing-ye Sun, Xian-huai Huang, Xiao-kun Yu, Zhao-liang Wu

THE HIDDEN FRAGMENTATION AFTER LAND CONSOLIDATION IN TURKEY 5882
Muge Kirmikil, S Tulin Akkaya Aslan, Kemal S Gundogdu, Ismet Arici

ASSESSMENT OF SULPHUR EFFICIENCY OF DURUM AND BREAD WHEAT GENOTYPES 5891
Halil Erdem, Mustafa Bulent Torun

RAW KENAF BAST FIBER AS A GREEN BIOADSORBENT FOR CATIONIC AND ANIONIC DYES 5900
Ridwan Shamsudin, Azlan Kamari, Hanisom Abdullah

EFFECT OF THREE ENVIRONMENTAL FACTORS ON POTENTIAL NITRIFICATION RATES OF RIPARIAN SEDIMENT 5911
Xiaohong Zhou, Chunzi Wen, Yimin Li

HYDROLOGICAL RESPONSES TO ECOLOGICAL MANAGEMENT OF THE LOESS HILLY-GULLY AREA, CHINA 5917
Erjia Liu, Xiaoli Zhang, Xiaoping Zhang, Zhidong Luo, Aijuan Wang, Zhiguang Li

SOLAR ENERGY AS HEAT SOURCE FOR ENHANCING EXCESS SLUDGE REDUCTION 5929
Wei Zheng, Qi-Di Mao, Wei Zhang, Bing-Zheng Li, Xiao-Fang Guo

SEASONAL CHANGES IN ANTIOXIDANT DEFENCE SYSTEM ON BROWN TROUT (SALMO SP.) IN MUNZUR STREAM 5936
Erkan Can, Nuran Cikcikoglu Yildirim, Devrim Erdogan

OPTIMIZING FENTON PROCESS FOR OLIVE MILL WASTEWATER TREATMENT USING RESPONSE SURFACE METHODOLOGY 5942
Farzaneh Doosti, Reza Ghanbari, Hamzeh Ali Jamali, Hamid Karyab

EFFECTS OF SOIL ENVIRONMENTAL FACTORS ON VEGETATION COMMUNITIES IN THE DEGRADED TARIM RIVER WETLAND 5954
Peng Dong, Ming Li, Jiyuan Jiang, Jun Zhang, Qiling Chen, Yaojun Zhu

INDOOR AIR QUALITY: THE SAMPLES OF SAFRANBOLU BULAK MENCILIS CAVE 5965
Mehmet Cetin, Hakan Sevik, Ahmet Saat

OCCURRENCE OF PHARMACEUTICAL AND PERSONAL CARE PRODUCTS (PPCPS) IN THE AFRICAN AQUATIC ENVIRONMENT: A BRIEF REVIEW FOR THE FUTURE OF ENVIRONMENT 5971
Yongbum Kwon, Do Gyun Lee

THE STUDY OF THE UPSTREAM SLOPE OF A SIPHON SPILLWAY ON ITS DISCHARGE COEFFICIENT USING FLOW3D SOFTWARE 5980
Amir Abbas Kamanbedast, Ali Assareh

STUDY ON SYNTHESIS OF LUBRICATING OIL ADDITIVES OF SULFIDE ESTER 5987
Miao Changqing, Chen Yongkui, Ma Xin, Zhang Wei

EFFECT OF SUPER-ABSORBENT POLYMER (SAP) ON BASALT FIBER ENGINEERED CEMENTITIOUS COMPOSITE 5991
Qiang Du, Jing Wei, Jing Lv

CATALYTIC TREATMENT OF OILFIELD WASTEWATER BASED ON RESPONSE SURFACE METHOD 5999
Hai-xiang Zhang, Yang Li, Zhan-dong Li, Cang-ming Ma, Shu-xin Zhang, Hao Shi, Mi Tian, Haotian Dai, Wei Li

STUDY ON ANTIBIOTIC WASTEWATER TREATMENT BY NEODYMIUM COORDINATION POLYMER CATALYST 6004
Xu Jingyi, Zhou Zipeng

THE EFFECTS OF LAND USE CHANGE ON SOIL LOSS AND CARBON STOCK AMOUNTS 6007
Sezgin Hacisalihoglu, Mehmet Misir, Nuray Misir, Zafer Yucesan, Ercan Oktan, Selcuk Gumus, Ugur Kezik

EFFECT OF GLUCOSE AS CO-METABOLISM SUBSTRATE ON THE BIODEGRADATION OF DICHLOROPHENOLS 6017
Zhirong Sun, Jiangyang Li, Jinwei Zhang, Jianguang Wang, Xueyun Wang, Xiang Hu

STUDY ON COKING WASTEWATER TREATMENT BY CATALYTIC SUPERCRITICAL WATER OXIDATION 6028
Dong Xu, Peifeng Wang, Rui Yang

LEVELS OF CHLORINATED PESTICIDES IN HUMAN ADIPOSE TISSUE FROM BAGHDAD/ IRAQ 6035
Mahmoud A Alawi, Firas T Al-Tameemi, Sana'a Al-Aqqad

AN ESTIMATION OF SOME PLANT TRAITS WITH THE REMOTE SENSING METHOD IN THE NARBON BEAN (VICIA NARBONENSIS L.) 6043
Yasar Ozyigit

EFFECT OF FLOC RECYCLING ON GROWTH AND CHARACTERISTICS OF FLOCS FORMED BY POLYMERIC ALUMINIUM CHLORIDE 6049
Wei Wei, Jia Zhu, Chaosheng Zhang, Yongfeng Cao

RESPONSE OF SOIL ENZYMES TO VOLATILE ORGANIC COMPOUNDS EMITTED FROM CREOSOTE-TREATED WOOD 6058
Arkadiusz Telesinski, Krystyna Cybulska, Michal Strek, Maciej Platkowski, Martyna Snioszek, Robert Biczak

EVALUATION OF ECOLOGICAL TOLERANCE AND REQUIREMENTS OF EXOTIC CONIFERS IN THE URBAN LANDSCAPE OF BURSA 6064
Nilufer Seyidoglu Akdeniz, Elvan Ender, Murat Zencirkiran

INFLUENCE OF STORED PRODUCT INSECTS ON PLANTING CHICKPEA SEEDS 6071
Tawfiq M Al Antary, Talal A Thalji

SOIL CARBON MINERALIZATION IN ARBUTUS ANDRACHNE AND CUPRESSUS SEMPERVIRENS GROWING ON THE DIFFERENT ELEVATIONS 6078
Ilay Cevik, Husniye Aka Sagliker

EFFECTS OF ZINC AND UREA AS FOLIAR APPLICATION ON NUTRITIONAL PROPERTIES AND GRAIN YIELD IN BARLEY (HORDEUM VULGARE L. CONV. DISTICHON) UNDER SEMI ARID CONDITION 6085
Mehmet Yagmur, Digdem Arpali, Fusun Gulser

SEDIMENTS CHARACTERISTICS AND HEAVY METALS DISTRIBUTION OF A VERY SHALLOW PROTECTED COASTAL LAGOON, PROKOPOS LAGOON, MEDITERRANEAN SEA WESTERN GREECE 6093
Dimitrios Katsaros, Dionisios Panagiotaras, Nikolaos Kontopoulos, Pavlos Avramidis

A CONTRIBUTION TO CHEMICAL CONTAMINATION OF GROUNDWATER 6104
Sonja Ketin, Predrag Dasic, Vera Vukanic,Tatjana Jaksic, Predrag Vasic

A CALIBRATED HYDROLOGICAL MODEL FOR ALIBEYKÖY WATERSHED IN ISTANBUL, TURKEY INCORPORATING LID IMPLEMENTATION 6112
Sezar Gulbaz, Cevza Melek Kazezyilmaz-Alhan, Rouhollah Nasirzadeh Dizaji, Mehmet Dikici

THE EFFECT OF COAL ASH PRACTICES ON HEAVY METAL CONTENT IN THE SOIL 6121
Duygu Boyraz Erdem, Seyide Yilmaz

INCREASED 8-HYDROXYDEOXYGUANOSINE RESPONSES AS A MARKER OF DNA DAMAGE AFTER STRENUOUS ANAEROBIC EXERCISE IN SEDENTARY YOUNG CIGARETTE SMOKERS AND NONSMOKERS 6127
Hayriye Cakir-Atabek, Filiz Ozdemir

THE EFFECT OF BARLEY GRASS ON ANTIOXIDANT CAPACITY AND DNA DAMAGE IN RAT WITH RENAL FAILURE 6135
Bahat Comba, Leyla Mis, Sema Uslu, Arzu Comba

EFFECTS OF FENBUTATIN OXIDE ON ANTIOXIDANT SYSTEM OF DIFFERENT TISSUES IN Cyprinus carpio (L., 1758) 6141
Ferbal Ozkan-Yilmaz, Arzu Ozluer-Hunt, Suna Gul Gunduz, Mehmet Berkoz, Serap Yalin, Metin Yildirim

EVALUATION OF TURKISH MINE WASTE MANAGEMENT POLICY WITH RESPECT TO MARINE POLLUTION 6149
Esin Esen

PROTECTIVE EFFECT OF ASTAXANTHIN AGAINST ALUMINUM INDUCED LIVER OXIDATIVE DAMAGE 6159
H Turan Akkoyun, Aydin Sukru Bengu, Mahire Bayramoglu Akkoyun, Aykut Ulucan, Okan Arihan

DETERMINATION OF PROBABLE REPRODUCTION SEASON OF INDIVIDUALLY TAGGED SIBERIAN, ACIPENSER BAERII, AND DIAMOND, A. GUELDENSTAEDTII, STURGEON BROODSTOCK, WHICH ARE NEWLY RISED, VIA STEROID HORMONES, HAEMATOLOGICAL CHANGES AND ULTRASOUND IMAGERY 6166
Kubra Ak, Ilker Zeki Kurtoglu

COMPREHENSIVE BENEFIT EVALUATION OF VARIOUS TYPES OF MARINE DEVELOPMENT: A CASE STUDY OF JIANGSU 6175
Sheng Gao, Huihui Sun, Lin Zhao, Runjie Wang, Baiqiong Liu, Min Xu

ANALYSIS OF THE IMPORTANCE OF THE FACTORS THAT INFLUENCE UREA HYDROLYSIS THROUGH AN ARTIFICIAL NEURAL NETWORK 6184
Tao Lei, Xihuan Sun, Xianghong Guo, Juanjuan Ma

EVALUATION OF PREBIOTIC POTENTIAL OF SALEP OBTAINED FROM SOME ORCHIDACEAE SPECIES 6191
Buse Usta, Lutfiye Yilmaz-Ersan

EFFECTS OF DIFFERENT SOWING DATES ON FLOWERING PHENOLOGY OF PHACELIA (PHACELIA TANACETIFOLIA BENTHAM) 6199
Ayse Genc Lermi, Sahin Palta

COMPETITIVE ADSORPTION OF HEAVY METALS IN DIFFERENT SOILS 6205
Veli Uygur, Mehmet Ali Karaduman, Mehmet Kececi, Enise Sukusu, Metin Mujdeci

THE EFFECT OF TEBUCONAZOLE ON SERUM PARAOXONASE AND AMINOTRANSFERASE ACTIVITIES IN CYPRINUS CARPIO (L. 1758) 6212
Gokhan Nur, Muhitdin Yilmaz, Mahmut Karapehlivan, Inan Kaya, Ozlem Nur, Ayla Deveci

NATURA 2000: ITS STATUS QUO, OPPORTUNITIES AND CHALLENGES FOR FOREST BIODIVERSITY IN TURKEY 6217
Cumhur Gungoroglu

OPTIMIZATION OF MINERALIZED REFUSE ADSORBENT-FENTON-NACLO OXIDATION OF BIOLOGICALLY TREATED LANDFILL LEACHATE USING RESPONSE SURFACE METHODOLOGY 6225
Fa-hui Nie, Qing Yu, Wen-ting Li, Rong-rong Liu, Yong-xi Zhou

SPATIAL AND TEMPORAL DISTRIBUTION OF PHYTOPLANKTON IN KARKAMIS DAM LAKE (SANLIURFA/TURKEY) 6234
Feray Sonmez, Banu Kutlu, Ahmet Sesli

DETERMINATION OF THE ANTI-OXIDATIVE ACTIVITIES OF SIX MUSHROOMS 6246
Celal Bal, Hasan Akgul, Mustafa Sevindik, Ilgaz Akata, Onder Yumrutas

THE EFFECT OF PARTICLE SIZE ON PHOSPHORUS ADSORPTION KINETIC AND DESORPTION BY TURKISH NATURAL ZEOLITES 6253
Veli Uygur, Canan Sanli Celik, Enise Sukusu, Metin Mujdeci

SOME MATURITY PROPERTIES OF OKUZGOZU (VITIS VINIFERA L. CV.) GRAPE BERRIES 6261
Gultekin Ozdemir, Abdullah Sessiz, Resat Esgici

EFFECT OF TOPOGRAPHIC MAP SCALE ON QUALITY OF SOIL MAPS IN DETAILED SOIL SURVEYS OF UNDULATED LANDS 6266
Yakup Kenan Koca, Suat Senol, Mahmut Dingil, M Eren Oztekin

PREPARATION OF Γ-FE2O3/SIO2/TIO2 UNDER THE LOW-TEMPERATURE AND THE PHOTO-CATALYTIC DEGRADATION OF SULFAMETHAZINE IN WATER 6272
Qingzhu Jia, Xiaochen Jia, Hui Chen

THE SEMI-ANALYTICAL SOLUTION OF PARTICLE TRANSPORT IN POROUS MEDIA INDUCED BY SEEPAGE 6286
Bing Bai, Tao Xu, Huawei Li

© by PSP Volume 26 – No. 10/2017 pages 5693-5699 Fresenius Environmental Bulletin

PARTICULATE MATTER ASSESSMENT AT SELECTED POINTS IN AMBIENT AIR OF DISTRICT SIALKOT, PAKISTAN

Muhammad Waseem Mumtaz[1], Muhammad Danish[1,*], Muhammad Asam Raza[1], Hamid Mukhtar[2], Muhammad Arshad[3], Saad Afzal[1], Muhammad Zubair[4], Syed Ali Raza[3]

[1]Department of Chemistry, University of Gujrat, Gujrat, Pakistan
[2]Institute of Industrial Biotechnology, Government College University, Lahore-54000, Pakistan
[3]Department of Chemistry, Government College University, Lahore, Pakistan
[4] Institute of Geographical Information system, SCEE, NUST, Islamabad, Pakistan

ABSTRACT

Present study describes the state of particulate matter (PM) pollution in the ambient air of Sialkot city of Pakistan and associated common health issues. Monitoring of different size fractions of particulate matter was carried out at nine sampling sites using a light-scattering laser photometer. PM1.0, PM2.5 and PM4.0 levels were ranged from 282 – 528 µg/m^3, 360 – 677 µg/m^3, 382 – 724 µg/m^3, respectively whereas PM10 concentration ranged from 440 – 843 µg/m^3 at different sampling points on average basis. The PM levels were further interpolated for the whole city. China Chowk was found to be the most polluted area with highest levels of particulate matter. Particulate matter load in the ambient air of Sialkot city was depicted to be noncompliance with NEQS guideline values. Analysis of Variance (ANOVA) ascertained significant difference among PM concentrations at all sampling points on average basis with p-value < 0.05. Flu, cough, eye and skin problems were the most common health impacts being faced by the general public by 25.4, 37.3, 20.9 and 16.4%, respectively.

KEYWORDS:
Particulate matter; Health effects; Environmental effects; Air pollution; Sialkot

INTRODUCTION

Population explosion along with many other factors i.e. rapid urbanization, industrialization and heavy transportation resulted in unfavorable degradation of our ambient environment [1,2]. The air we breathe, should be in clean form; is now under severe stress because of the certain air pollutants i.e. smoke, soot, dust particles, odor, light, heat, electro-magnetic radiation, fumes, exhaust gases, noxious gases, hazardous and radioactive substances with concentration beyond the permissible limits thus posing threat to living organism [3]. The air quality usually depends on the levels of toxic pollutants and particulate matter in the ambient air [4]. Previous studies connecting air pollution with human health effects, concentrate on the particulate components due to their potential health hazards, persistence nature and scattering power [5-7]. Particulate matter (PM) usually consists of mixed components varying in number, size, surface area, chemical composition, concentration and source [6, 9].

Particulate matter influences the visibility, climate, individual health and thus the quality of life [10]. Most common health issues associated with the particulate matter pollution among roadside populations includes coughing, asthma, allergy, breathing difficulties, itching and headache etc. [11]. The exposure to particulates with the size of PM2.5 is associated with adverse health impacts like respiratory diseases, asthma attacks leading to decreased lung functioning, heart attacks and premature death [12]. The monitoring of outdoor particulate matter is gaining much attention by the governments, regulators, environmentalist and scientific global warming.

Pakistan is also facing intense problem regarding particulate matter pollution like many other developing countries. Previously, some researchers had reported the particulate matter load in ambient air of different cities of Pakistan and revealed that the values were higher than stipulated values as prescribed by National Environmental Quality Standards of Pakistan [4, 13, 14]. The city of Sialkot has emerged as industrial hub and numerous industries have been installed at micro and macro level with some demerits especially regarding the environmental degradation [15]. Current study was planned to monitor the particulate matter levels in ambient air at multiple sites of Sialkot city and to assess associated health implications as this core issue was never addressed before.

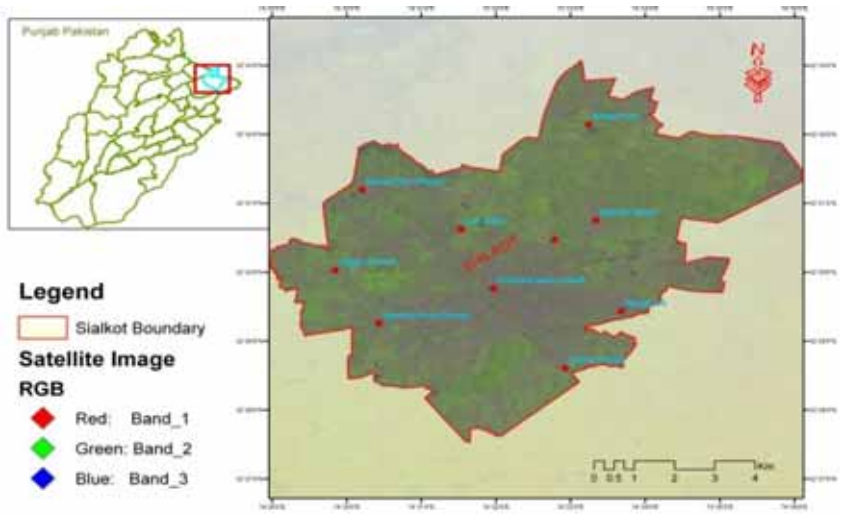

FIGURE 1
Sampling points selected for study

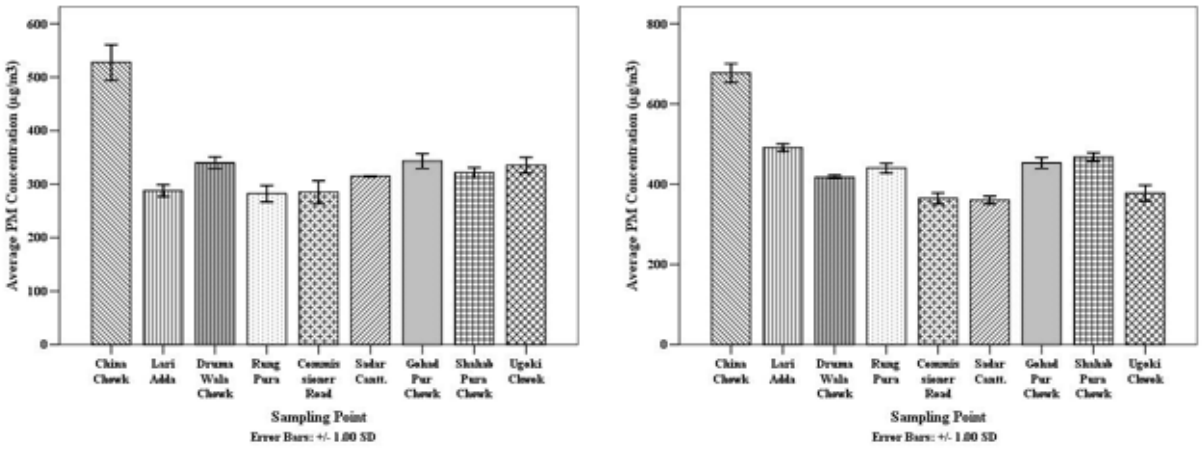

FIGURE 2
Average PM1.0 and PM2.5 concentration (µg/m^3) at different sampling points in ambient air of Sialkot Punjab, Pakistan

MATERIALS AND METHODS

Sampling Points. Taking into consideration heavy traffic and industrialization, extensive survey of Sialkot city, Punjab, Pakistan was carried out and nine sampling points were specified i.e. China Chowk, Lari Adda Chowk, Druma Wala Chowk, Rung Pura, Commissioner Road, Sadar Cantt., Gohad Pur Chowk, Shahab Pura Chowk and Ugoki Chowk, respectively for the monitoring of Particulate Matter (PM) Pollution (Figure 1).

Particulate matter monitoring. Monitoring of Particulate Matter concentrations regarding PM1.0, PM2.5, PM4.0, and PM10.0 size fractions was executed using the Dust Trak™ II Aerosol Monitor (model 8530), a light-scattering laser photometer. PM monitoring was carried out at all the specified sampling points of Sialkot city. All the estimations were carried out thrice.

Interpolation studies. The experimental results of sampling sites regarding PM concentration were used for interpolation using kriging techniques to estimate values for the remaining locations of the Sialkot city. Kriging is stochastic techniques to model and estimate unknown values using known data. Different kriging approaches (i.e. simple kriging, ordinary kriging etc.). Kriging interpolation model was developed in Geostatistical Analyst tool of ArcGIS.

Assessment of Associated Health Impacts. For the commonly observed health impacts assessment, in vicinity of the defined sampling points of Sialkot city, the population representatives having different exposure levels with ambient PM pollution were interviewed randomly during this study.

Statistical analysis. Experimental data were further compared and analyzed using different statistical methods like SPSS [16].

RESULTS AND DISCUSSIONS

Considering PM a potential ambient air pollutant, PM levels (PM1.0, PM2.5, PM4.0 & PM10) in Sialkot city were evaluated, their associated health impairments were assessed and results were further statistically analyzed.

Ambient PM1.0 concentration (µg/m^3) at defined sampling points of Sialkot i.e. China Chowk, Lari Adda Chowk, Druma Wala Chowk, Rung Pura, Commissioner Road, Sadar Cantt., Gohad Pur Chowk, Shahab Pura Chowk and Ugoki Chowk were found to be 527±33, 287±11, 340±10, 282±15, 285±21, 315±09, 343±14, 322±09, 335±15 µg/m^3, respectively on average basis. Highest PM1.0 concentration found at China Chowk could most probably be due to rubber industries and vehicular emissions, whereas lowest PM1.0 concentration was found in ambient air of Rung Pura Chowk. The order of PM1.0 concentration at different sampling points was depicted to be China Chowk > Gohad Pur Chowk > Druma Wal Chowk > Shahab Pura Chowk > Sadar Cantt > Lari Adda > Commissoiner Road > Rung Pura. Concentrations of PM2.5 levels at specified sampling points were found to be 677±23, 491±09, 417±05, 440±12, 364±14, 360±10, 453±13, 468±11 and 378±20 µg/m^3 in ambient air of China Chowk, Lari Adda Chowk, Druma Wala Chowk, Rung Pura, Commissioner Road, Sadar Cantt., Gohad Pur Chowk, Shahab Pura Chowk and Ugoki Chowk, respectively are given in Fig. 2. Thus PM2.5 concentration ranged from 360 – 677 µg/m^3 at different sampling stations, whereas the order was revealed to be China Chowk > Lari Adda Chowk > Shahab Pura Chowk > Gohad Pur Chowk > Rung Pura > Druma Wala Chowk > Ugoki Chowk > Commissioner Road >Sadar Cantt. The levels of PM2.5 at all the sampling points were found to be greater than the stipulated guideline value for PM2.5 i.e. 35 µg/m^3 as described in National Environmental Quality Standards (NEQS), Pakistan.

PM4.0 and PM10 were also monitored in the air of Sialkot city at defined sampling points. On the average basis, PM4.0 levels (µg/m^3) were found to be 724±24, 562±38, 681±26, 522±17, 450±37, 490±13, 542±25, 533±11 and 382±07 µg/m^3 whereas, PM10 levels (µg/m^3) were depicted to be 843±09, 647±27, 760±09, 600±8, 502±08, 577±20, 822±18, 608±07 and 440±28 µg/m^3 in ambient air of China Chowk, Lari Adda Chowk, Druma Wala Chowk, Rung Pura, Commissioner Road, Sadar Cantt., Gohad Pur Chowk, Shahab Pura Chowk and Ugoki Chowk, respectively.

PM4.0 concentration was found to be ranged from 382–724µg/m^3, whereas PM10 concentration ranged from 440–843 µg/m^3 at different sampling points on average basis. The levels of PM10 were also ascertained to be noncompliance with the NEQS guideline value i.e. 150 µg/m^3 for PM10 (Fig. 3). The order of PM4.0 concentration at different sampling points was depicted to be China Chowk > Druma Wala Chowk > Lari Adda Chowk > Gohad Pur Chowk > Shahab Pura Chowk > Rung Pura Chowk > Sadar Cantt. > Commissioner Road > Ugoki Chowk and for PM10, the order was found to be China Chowk > Gohad Pur Chowk > Druma Wala Chowk > Lari Adda Chowk > Shahab Pura Chowk > Rung Pura Chowk > Sadar Cantt. > Commissioner Road > Ugoki Chowk. China Chowk was ascertained to be most polluted area with respect to PM load in ambient air.

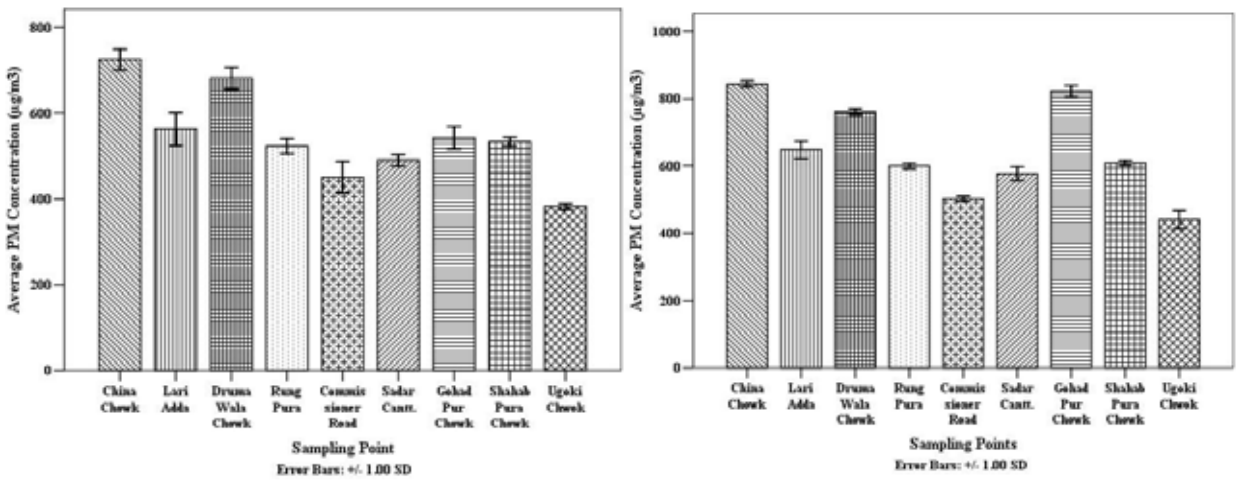

FIGURE 3
Average PM4.0 and PM10 concentration (µg/m^3) at different sampling points in ambient air of Sialkot Punjab, Pakistan

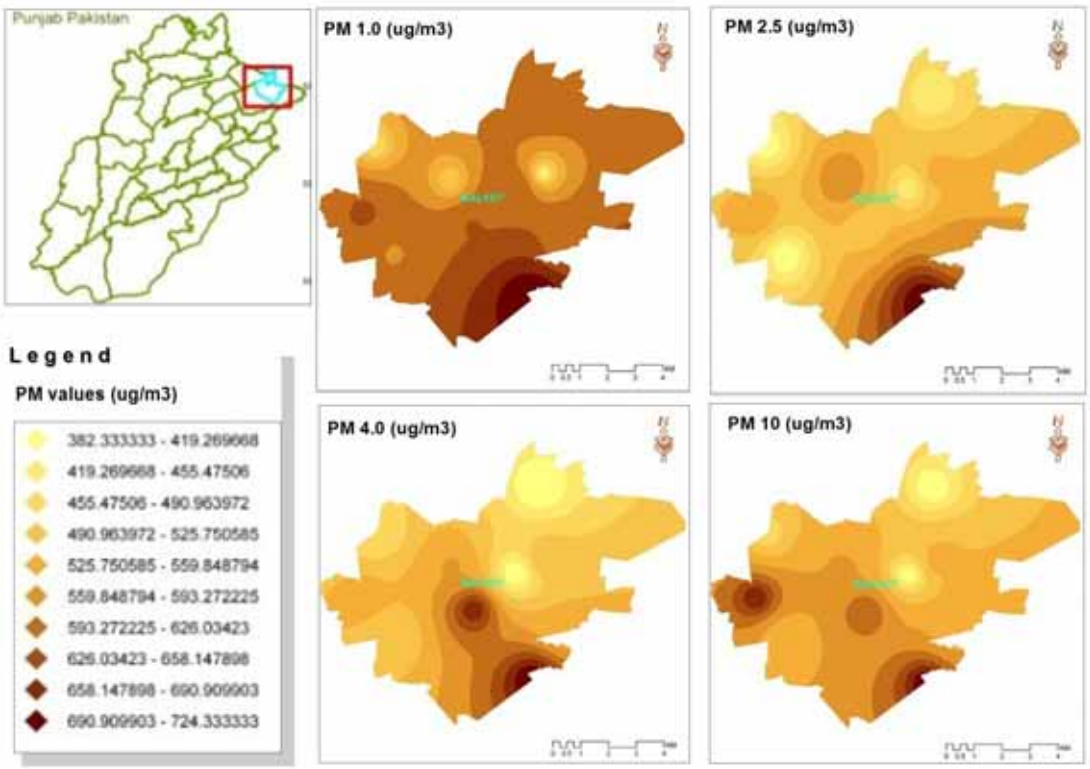

FIGURE 4
Interpolation maps for PM1.0, PM2.5, PM4.0 and PM10 concentration (µg/m^3) in ambient air of Sialkot Punjab, Pakistan

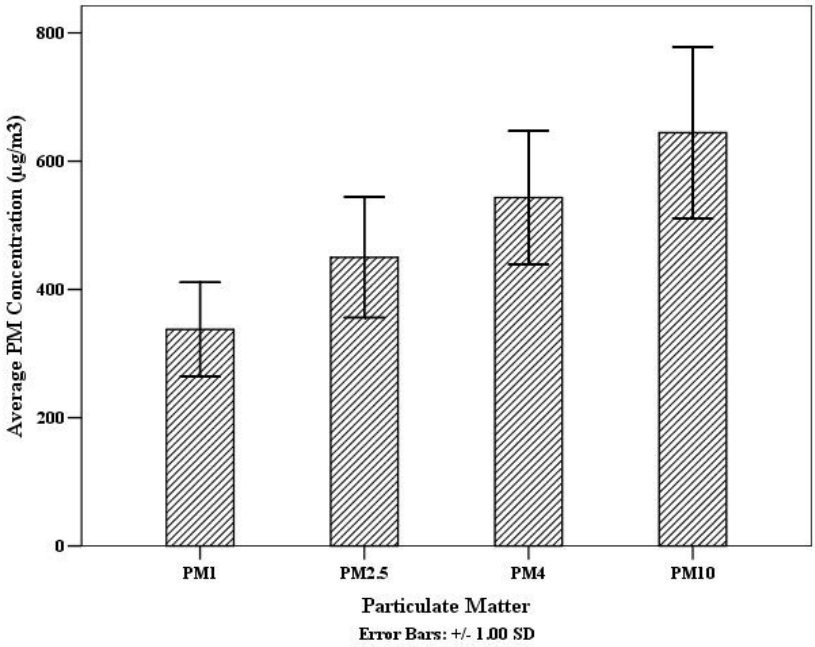

FIGURE 5
Average PM1.0, PM2.5, PM4.0 and PM10 concentration (µg/m^3) in ambient air of Sialkot Punjab, Pakistan

TABLE 1
Test Equality of Means of Readings with respect to Different PM Levels

Readings	Sum of Squares	df	Mean Square	F	Sig.
Between Groups	1388898.407	3	462966.136	43.072	.000
Within Groups	1117873.111	104	10748.780		
Total	2506771.519	107			

TABLE 2
Multiple comparison among PM1.0, PM2.5, PM4.0 and PM10 concentration at different sampling points of Sialkot

Readings LSD						
(I) PM	(J) PM	Mean Difference (I-J)	Std. Error	Sig.	95% Confidence Interval	
					Lower Bound	Upper Bound
PM 1	PM 2.5	-112.40741*	28.21712	.000	-168.3630	-56.4518
	PM 4	-205.59259*	28.21712	.000	-261.5482	-149.6370
	PM 10	-306.81481*	28.21712	.000	-362.7704	-250.8592
PM 2.5	PM 4	-93.18519*	28.21712	.001	-149.1408	-37.2296
	PM 10	-194.40741*	28.21712	.000	-250.3630	-138.4518
PM 4	PM 10	-101.22222*	28.21712	.001	-157.1778	-45.2666

* The mean difference is significant at the 0.05 level

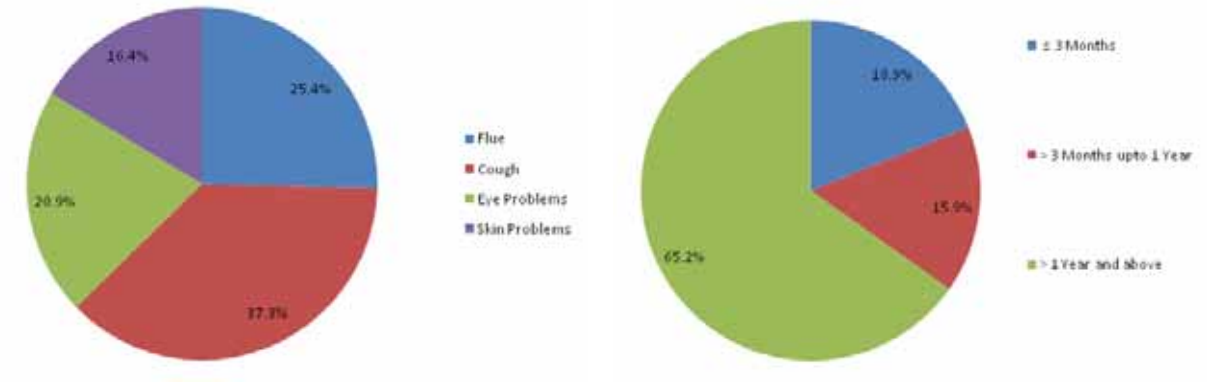

FIGURE 6
Health problems faced by the respondents due to direct exposure with the PM in ambient air of Sialkot

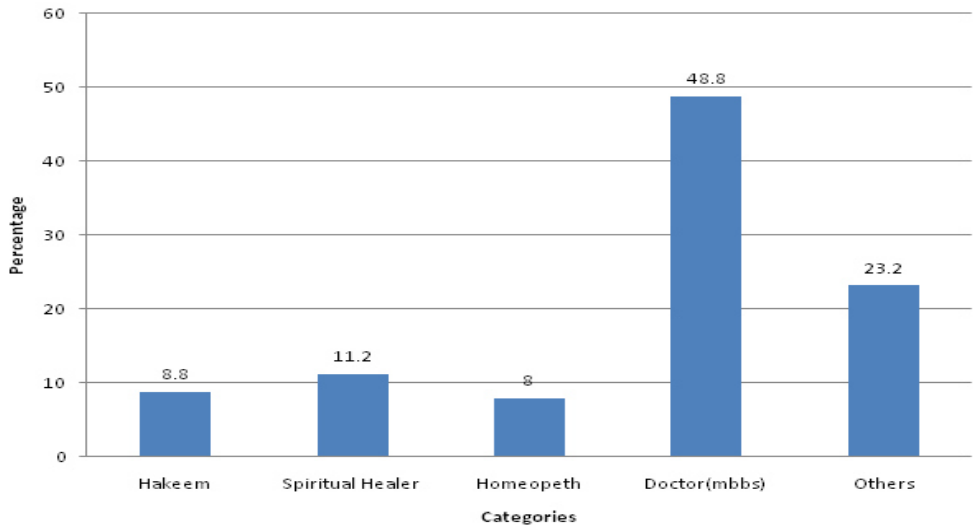

FIGURE 7
Medication used by the respondents for the treatment of health problems linked with PM pollution

The experimental data regarding PM1.0, PM2.5, PM4.0 and PM10 concentrations µg/m^{3}was further used for interpolation. The results of interpolation for the whole Sialkot city are presented in Fig. 4 (a-d).

On the average basis PM1.0, PM2.5, PM4.0 and PM10 concentrations µg/m^3 in the ambient air of Sialkot city were depicted to be 337±73, 450±94, 543±104 and 644±133, respectively (Fig. 5). It was found that the levels of the particulate matter in the ambient air of Sialkot city were comparatively higher than the NEQS guideline values. Shah et al. reported 119 µg/m^3 Total Suspended Particulate (TSP) in the urban areas of I-9, I-10 sectors of Islamabad Pakistan [14]. Our finding regarding the particulate matter concentration in ambient air of Sialkot were found to be higher than the findings of Shah et al. [14], lower than TSP concentration 2756 µg/m^3 in Gujranwala as reported by Awan et al. (2011) whereas comparable with the TSP levels i.e. 607 µg/m^3 in Lahore & 550 µg/m^3 in Faisalabad (4) as reported by Harrison et al. and Qadir and Zaidi, respectively [17, 18].

Analysis of Variance (ANOVA) was carried out based on the experimental results regarding average PM concentration with different size fractions at different sampling points in Sialkot (Table 1). *P*-value < 0.05 depicted significant difference among PM concentrations at all sampling points on average basis.

Furthermore, Post Hoc test was applied for multiple comparisons and it was ascertained that PM1.0 levels significantly differ relative to PM2.5, PM4 and PM10 levels with *P*- value < 0.05. Similarly when PM2.5 concentrations were compared with PM4.0 and PM10, significant difference was found between PM2.5 comparative to PM4.0 and PM10 concentrations on average basis. Furthermore, PM4.0 levels also differ significantly from PM10 levels with *P*- value < 0.05 (Table 2).

The results regarding the assessment of common health impacts linked with PM pollution revealed that the population having direct exposure with the ambient particulate matter is facing various acute and chronic diseases.

Of the respondents facing common health problems because of their exposure to particulate matters in the ambient air of Sialkot, the flue, cough, eye and skin problems were the most common by 25.4%, 37.3%, 20.9% and 16.4%, respectively. Furthermore, it was assessed that the respondents having health impairment issues experienced different levels of exposure with the ambient air particulate matter i.e. 18.9% with ≤ 03 months, 15.9% > 03 months up to 01 year and 65.2% > 01 year exposure levels (Fig. 6).

Majority of the patients (48.8%) were visiting physician for medication. About 8.8% were visiting Hakeem for their health care, 08% patients were found to have access to homoeopaths for medication. 11.2 % of the patients were going for spiritual treatment of diseases. The remaining 23.2% respondents were found to use conventional treatments and were depicted to have strong belief on the use of sweets, gur (Jaggery) and frequent use of tea to minimize health impairment issues (Fig. 7).

CONCLUSION

Particulate matter (PM) load in the ambient air of Sialkot city was depicted to be noncompliance with the NEQS guideline values, therefore causing severe health problems among the general public. The impact of particulate matter emitted during various anthropogenic activities is not ignorable and researchers should work to opt suitable preventive measures to stop further degradation of the natural environment due to the emission of PM and to work for the sustainable environment.

REFERENCES

[1] Wahid, A. (2006) Productivity losses in barley attributable to ambient atmospheric pollutants in Pakistan. Atmospheric Environment. 40, 5342-5354.

[2] Wahid, A. (2006) Influence of atmospheric pollutants on agriculture in developing countries: a case study with three new varieties in Pakistan. Science of the Total Environment, 371: 304- 313.

[3] Hamid, S.M. (1994) Fundamentals of Environmental Pollution. CBS publishers and Distributors, Delhi, India. p. 12.

[4] Awan, A.M., Ahmed, H.S., Aslam, R.M. and Qazi, A.I. (2011) Determination of Total Suspended Particulate Matter and Heavy Metals in Ambient Air of Four Cities of Pakistan. Iranica Journal of Energy &Environment, 2: 128-132.

[5] Brook, R.D., Brook, J.R., Urch, B., Vincent, R., Rajagopalan, S. and Silverman, F. (2002) Inhalation of fine particulate air pollution and ozone causes acute arterial vasoconstriction in healthy adults. Circulation, 105: 1534-1536.

[6] Brook, R.D., Franklin, B., Cascio, W., Hong, Y., Howard, G., Lipsett, M., Luepker, R., Mittleman, M., Samet, J. and Smith, S.C. (2004) Air pollution and cardiovascular disease: a statement for healthcare professionals from the Expert Panel on Population and Prevention Science of the American Heart Association. Circulation, 109: 2655-2671.

[7] Gold, D.R., Litonjua, A., Schwartz, J., Lovett, E., Larson, A., Nearing, B., Allen, G., Verrier, M., Cherry, R. and Verrier, R. (2000) Ambient pollution and heartrate variability. Circulation, 101: 1267-1273.

[8] Ibald-Mulli, A., Stieber, J., Wichmann, H.E., Koenig, W. and Peters, A., (2001) Effects of air pollution on blood pressure: a population-based approach. Am. J. Public Health, 91, 571-577.
[9] Wilson, W.E. and Suh, H.H. (1997) Fine and Coarse Particles: Concentrations Relations Relevant to Epidemiological Studies. J. Air Pollut. Control Assoc., 27: 46-51.
[10] Ruzer, L.S. and Harley, N.H. (2005) Aerosols Handbook: Measurement, Dosimetry, and Health Effects, CRC Press, Florida, USA.
[11] Bahauddin, M.K. and Salah Uddin, T. (2010) Status of Particulate Matter and Its Impact on Roadside Population of Dhaka City, Bangladesh: A Review Study. Proc. of International Conference on Environmental Aspects of Bangladesh (ICEAB10), Sept. 2010, Japan, 125-128.
[12] Kunzli, N., Jerrett, M., Mack, W.J., Beckerman, B., LaBree, L., Gilliland, F., Peters, D.T.J. and Hodis, H.N. (2004) Ambient air pollution and atherosclerosis in Los Angeles. Environmental Health Perspectives, 113: 201-206.
[13] Shah, M.H. and Shaheen, N. (2008) Annual and seasonal variations of trace metals in atmospheric suspended particulate matter in Islamabad. Pakistan. Water Air and Soil Pollution, 190: 13-25.
[14] Shah, H.M., Shaheen, N. and Nazir, R. (2012) Assessment of the trace elements level in urban atmospheric particulate matter and source apportionment in Islamabad, Pakistan. Atmospheric Pollution Research, 3: 39-45
[15] Rafique, U., Ashraf, A., Khan, A.K., Nasreen, S., Rashid, R. and Mahmood, Q. (2010). Toxic chromium from tanneries pollute water resources and soil of Sialkot (Pakistan). Journal of Chemical Society of Pakistan, 32: 644-649
[16] Steal, R.G.D., Torrie, J.H. and Dickey, D.A. (1997) Principles and procedures of statistics. New York: McGraw Hill.
[17] Harrison, R.M., Smith, D.J.T., Pio, C.A. and Castro, L.M. (1997) Comparative receptor modeling study of airborne particulate pollutants in Birmingham (United Kingdom), Coimbra (Portugal) and Lahore (Pakistan). Atmospheric Environment, 31: 3309-3321.
[18] Qadir, M.A. and Zaidi, J.H. (2006) Characteristics of the aerosol particulates in the atmosphere in an urban environment at Faisalabad, Pakistan. Journal of Radio analytical and Nuclear Chemistry, 267: 545-550.

Received: **23.09.2015**
Accepted: **19.03.2016**

CORRESPONDING AUTHOR

Muhammad Danish
Department of Chemistry,
University of Gujrat,
Gujrat, 50700 – PAKISTAN

Email: drdanish62@gmail.com

© by PSP Volume 26 – No. 10/2017 pages 5700-5706 Fresenius Environmental Bulletin

A NOVEL $NaClO_2$-UV/O_3 TREATING ACID TURQUOISE BLUE A IN AQUEOUS SOLUTION: DYNAMICS MODEL AND SYNERGISTIC EFFECT

Yongjun Shen*, Yuanyuan Hu, Qihui Xu, Peng Zhu, Kaixia Fan, Yao Sun

School of Chemistry and Chemical Engineering, Nantong University, Nantong 226019, China

ABSTRACT

The process sodium chlorite-ultraviolet/ozone ($NaClO_2$/UV-O_3) is utilized to deal with simulated wastewater of Acid Turquoise Blue A (ATBA). It is a brand-new mode which combined the advantages of both chlorine dioxide (ClO_2) and O_3. It achieves strong degradation effect in alkaline conditions. Commonly, it takes 15 minutes when the removal rate goes higher than 95%, but it only required about 3 minutes under the best operating conditions (pH=10, 150 mg/L dosing quantity of $NaClO_2$, 18 W UV intensity, 36 L/h O_3 flux, room temperature) when simulated wastewater of ATBA (25 mg/L, 1L) was treated. The degradation reaction was consistent with first-order kinetics model, and instant dynamics equation could be established to determine the values of its apparent rate constant k_{obs}. The pH had maximal influence on the kinetics model that had been discussed under two conditions of pH >5.8 and pH<5.8. When pH=10, the k_{obs} was maximum which was 1.6525. The synergistic cofactor E was obviously about 4.

KEYWORDS:
$NaClO_2$-UV/O_3, Acid Turquoise Blue A, dynamics, synergistic effect

INTRODUCTION

Since the printing and dyeing wastewater was in large amount, its composition was complex, plus its permeability was strong, the pollution was so serious that exceeded the environment self-purification ability [1]. So it required constant wastewater treatment process, in order to meet the environmentally friendly requirements.

The treatment technologies of wastewater in the printing and dyeing industry included adsorption coagulation, biological treatment, electrochemical oxidation, chemical oxidation and advanced oxidation processes (AOPs) [2]. In terms of modern processing technology, adsorption coagulation treatment could be generally used as the pretreatment of wastewater to treat macromolecular impurities. Biological treatment method worked well, but it needed a long time and would produce bad smell. Electrochemical oxidation treatment could not treat the waste water completely, and it consumed time and electric in the process of wastewater treatment in practical application [3]. The advanced oxidation process could produce the hydroxyl radicals during the treatment process. At present, the mainstream advanced oxidations about the wastewater treatment involve O_3 [4, 5] Fenton [6], O_3/Fenton [7], O_3/US [8], ClO_2 [9] and a series of combination processes.

ClO_2 was a kind of good disinfectant and strong oxidizer which had a better removal effect to many organic and inorganic pollutants in water. In addition, it hardly reacted with the organic matter to form halogenated organic matter in the water such as THMs. So the ClO_2 would not cause secondary pollution and would have broad application prospect in wastewater treatment. $NaClO_2$-UV technology had enormous potentiality to produce ClO_2 [10-12]. Ozone-based AOPs involved the generation of radical intermediates, especially the hydroxyl radicals (·OH) which were highly reactive with most organic compounds and could be widely used in dye industrial areas [13].

With the deterioration of environmental problems caused by dye wastewater pollution, the single process would not meet the requirements of environment. Therefore, in this paper, we creatively put forward the innovation where $NaClO_2$-UV was combined with O_3 to degrade wastewater. The newly combined process $NaClO_2$-UV/O_3 mainly depended on the strong oxidizing ability of ClO_2 and O_3, which could be widely used in future, and it was essential to establish the new kinetics model.

Therefore, the purpose of the present project was to study the feasibility of the combination of $NaClO_2$-UV/O_3 for the degradation of ATBA, the influence of operating reaction conditions, such as the solution pH, dye concentration, dosing quantity of $NaClO_2$, O_3 flux and temperature. The instant kinetics of combined process $NaClO_2$-UV/O_3 was studied in the treatment of dyeing wastewater.

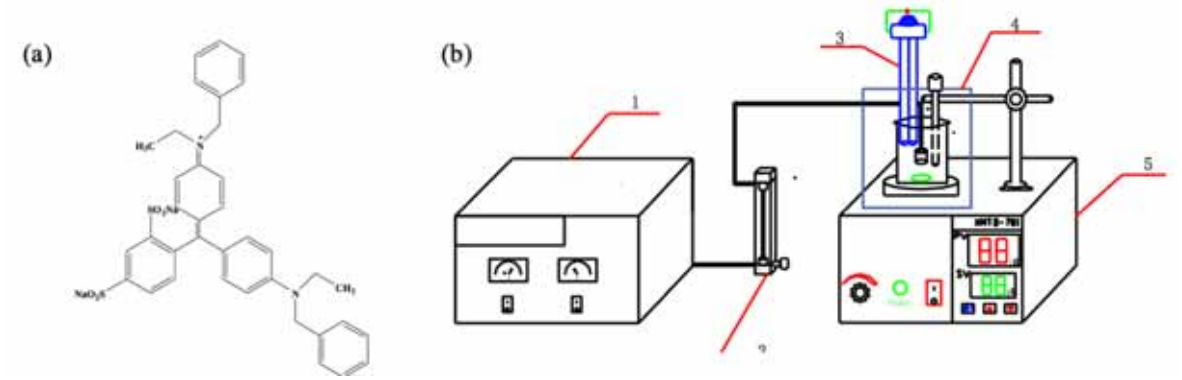

FIGURE 1
(a) the structural formula of ATBA), (b) $NaClO_2$ - UV and O_3 combined installation drawing

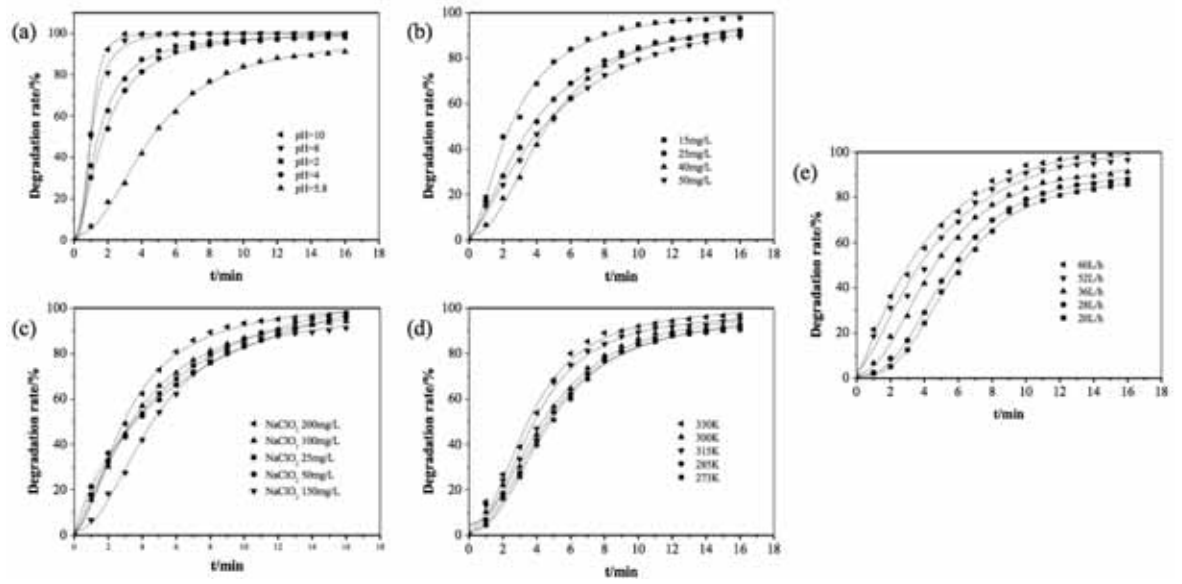

FIGURE 2
The effect of the influential factors under the $NaClO_2$-UV/O_3 joint action: (a) pH, (b) concentrations of ATBA, (c) dosages of sodium chlorite, (d) water bath temperatures, (e) fluxes of ozone

EXPERIMENT

The molecular formula of ATBA was $C_{37}H_{35}N_2NaO_6S_2$, which could be seen on Fig. 1a. Its molecular weight was 690.80 and the maximum absorption wavelength is 638 nm. $NaClO_2$-UV/O_3 process system was used in this experiment. The device could be seen on Fig. 1b (1.ozonator 2.rotameter 3. ultraviolet lamp 4. sealed box 5. temperature control magnetic stirrer). $NaClO_2$ was white granular crystal and had strong oxidizability, and its molecular weight was 90.44. The distilled water was used to clean a beaker, and to prepare mixed solution of ATBA and sodium chlorite according to the experiment (analytical pure, Shanghai Jiaying Co., Ltd.). NaOH or H_2SO_4 was used to adjust pH to a certain value. The absorbance of the reaction solution was determined by UV-Vis spectrophotometer (752N). We selected an 18-watt UV lamp in this experiment, and insert the tube to the solution in a closed environment, paid attention to the use of magnetic stirrer, and stir the mixed solution evenly. 1 L mixed solution of $NaClO_2$ and ATBA was degraded.

RESULTS AND DISCUSSION

Analysis of the influential factors. The initial pH. T= 285 K, $c_{0(ATBA)}$= 25 mg/L, $Q_{(O3)}$= 36 L/h, $P_{(NaClO2)}$= 150 mg/L. The impacts of the degradation of dye were studied, when the initial pH values were 2, 4, 5.8, 8 and 10, respectively. Fig. 2a showed that the effect on degradation was very obvious under strong alkaline and strong acidic conditions. In alkaline condition, the degradation

rate was more than 90% after 3 min. The dye was completely decoloured at 4th min. In strong acidic condition, the degradation rate was above 90% after 6 min. The dye was completely decoloured at 12th min. However, for the original solution whose pH had not been adjusted, it took 15 min until its degradation rate was above 90%. In addition, light blue solution would turn dark olive with pungent odor. The stronger the solution acidity was, the faster the degradation rate would be. The ClO_2 which was released in the degradation can partly degrade ATBA. It illustrated that chromophoric groups of ATBA had been partly destroyed under the partial acid. So the degradation reaction could work well under $NaClO_2$-UV/O_3. On the one hand, alkaline condition would propel the ozone to generate hydroxyl radicals with strong oxidability to degrade dye, and seriously inhibit the part reaction between ozone and sodium chlorite, avoiding worse degradation effect.

The initial concentration of dye. T= 285 K, pH= 5.8, $Q_{(O3)}$= 36 L/h, $P_{(NaClO2)}$= 150 mg/L. When the concentrations of ATBA were respectively 15, 20, 25, 30, 40 and 50 mg/L, the effects on the degradation of different dye concentrations were investigated. It could be seen from Fig. 2b that O_3 and ClO_2 produced by the combined process were certain during a certain period of time. When the concentration of ATBA increased, the concentration of reactants would also increase. In other words, increasing concentration of ATBA promoted the reaction. Actually, although the degradation rate of the high concentration dye was low, the amount of degradation was large. Relative to the low concentration dye, since the O_3 and ClO_2 were adequate, and reaction was more fully done, the degradation rate was relatively high.

The dosing quantities of $NaClO_2$. T= 285 K, pH= 5.8, $Q_{(O3)}$= 36 L/h, $c_{0(ATBA)}$= 25 mg/L. When the dosing quantities of sodium chlorite were respectively 25, 50, 100, 150, 200 and 500 mg/L, the impacts on the degradation of dye with different dosing quantities of sodium chlorite were studied. Fig. 2c showed that the degradation rate presented fluctuating upward with the increase of the amount of additive sodium chlorite. When dosing quantity of $NaClO_2$ was small, the degradation reaction gave priority to react with ozone oxidation, and oxidation of ClO_2 produced by $NaClO_2$ and UV would be complementary reaction. With the increase of dosing quantity of $NaClO_2$, O_3 oxidation weakened slowly, while ClO_2 oxidation was enhanced. However, effect of O_3 oxidation was little more obvious than that of ClO_2 oxidation in the same period of time. So there would be fluctuations about degradation rate. When dosing quantity of $NaClO_2$ continuously increased and was more than 200 mg/L, ClO_2 in heavy concentrations led to disproportionation reaction, and the effect of disproportionation abated the influence of ozonation, so the degradation effect was obvious under $NaClO_2$-UV/O_3 process.

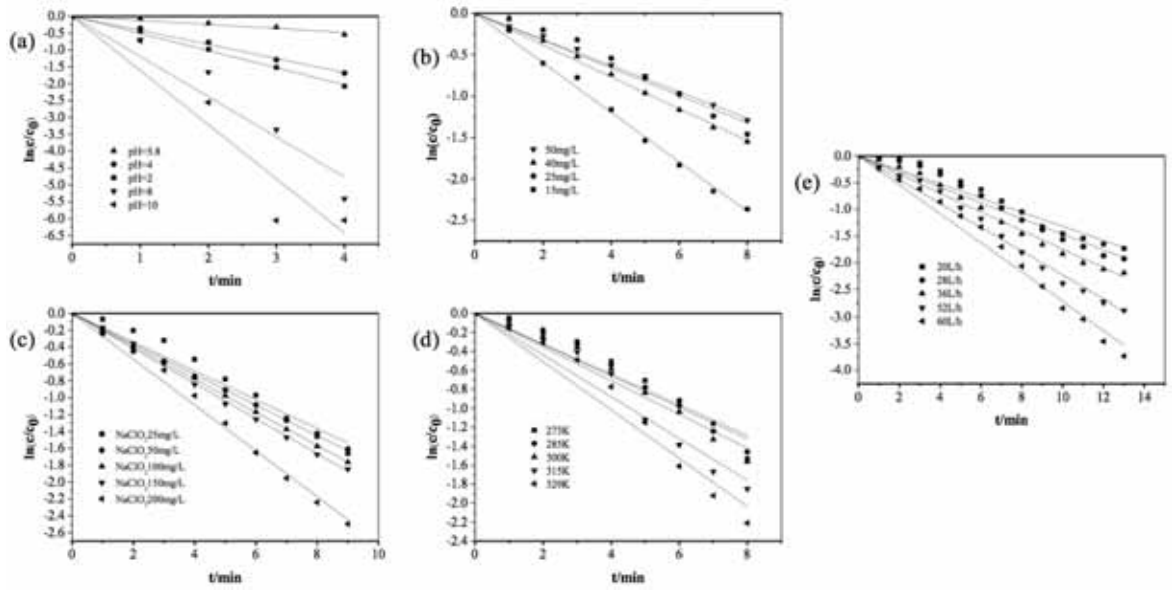

FIGURE 3
The ln (c/c_0) fitting figure of ATBA under the influential factors for the $NaClO_2$-UV/O_3 joint action: (a) pH, (b) concentrations of ATBA, (c) dosages of sodium chlorite, (d) water bath temperatures, (e) fluxes of ozone

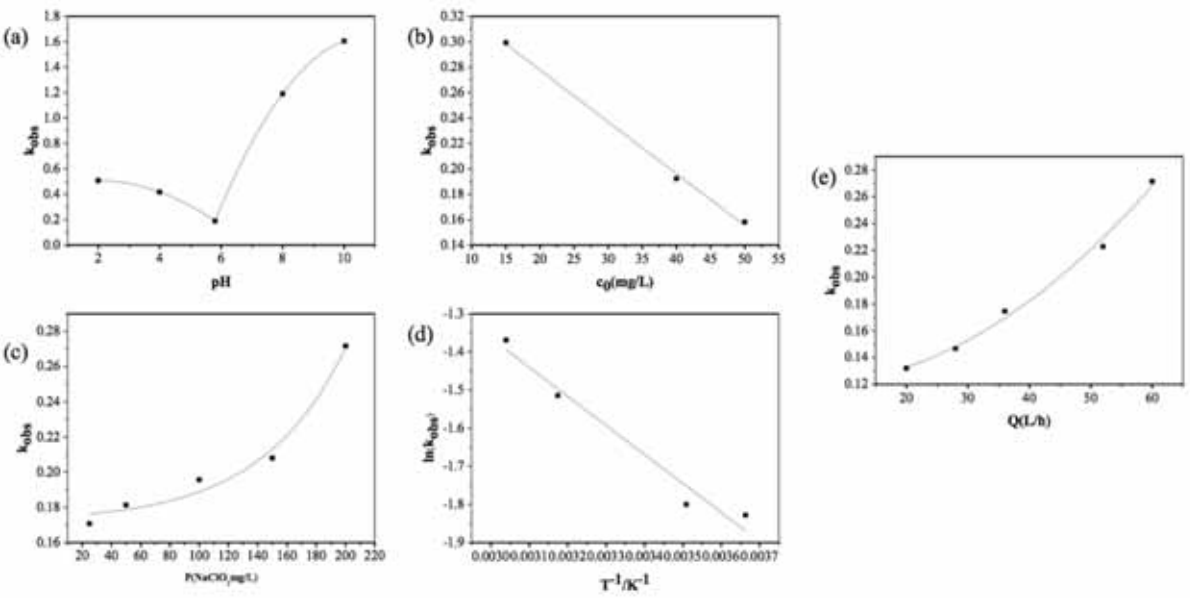

FIGURE 4
The fitting curves under $NaClO_2$-UV/O_3 (a) k_{obs}-pH (b) k_{obs}-c_0 (c) k_{obs}-P, (d) k_{obs}-T^{-1} (e) k_{obs}-Q

TABLE 1
The fitting sub-equations of k_{obs} vs. four factors by interpolation method

Factors	Classification	The fitted sub-equations	R^2	Figure
K-pH	pH<5.8	$K_{pH1} = -0.02104\,pH^2 + 0.08036\,pH + 0.43187$	-	Fig. 4a
	pH>5.8	$K_{pH2} = -0.059\,pH^2 + 1.26916\,pH - 5.18601$	-	
K-c_0	-	$K_{c_0} = -0.00408c_0 + 0.35931$	0.9945	Fig. 4b
K-P	-	$K_P = 0.00302 \times \exp(P/57.2778) + 0.17149$	0.96491	Fig. 4c
lnK-T^{-1}	-	$\ln(k_{obs}) = -954.71558/T + 1.51315$	0.93299	Fig. 4d
k_{obs}-T^{-1}	-	$K_T = k_{obs} = 4.541\exp(-954.71558/T)$		
K-Q	-	$K_Q = 4.5555\times10^{-5}\times Q^2 - 2.57443\times10^{-4}Q + 0.11963$	-	Fig. 4e

- no data

The water bath temperature. $P_{(NaClO2)}$= 150 mg/L, pH= 5.8, $Q_{(O3)}$= 36 L/h, $c_{0(ATBA)}$= 25 mg/L. When the temperatures were respectively 273, 285, 300, 285 and 329 K, the effects of different temperatures on the degradation were studied. Fig. 2d illustrated that the degradation rate also rose as temperatures rose. Most chemical reaction rate increased with the increase of temperature. The increase of temperature could accelerate the collision frequency between molecules. So the number of effective collision and activated molecule both increased. The degradation reaction was speeded up, and the degradation rate also increased.

The flux of ozone. $P_{(NaClO2)}$= 150 mg/L, pH= 5.8, T= 285 K, $c_{0(ATBA)}$= 25 mg/L. When the ozone fluxes were respectively 20, 28, 36, 44, 52 and 60 L/h, the impacts on the degradation of dye were studied under different dosing quantities of $NaClO_2$. Fig. 2e showed that the degradation rate increased with the increase of ozone flux. The increase of ozone flux meant that the amount of ozone participated in the degradation reaction in the solution would also increase. Although under the non-alkaline conditions, rejection action of $NaClO_2$ and O_3 would affect the degradation effect. However, with the great increase of ozone and the stable dosing quantity of sodium chlorite with 150 mg/L, the effect of O_3 oxidation tended to be more obvious, so degradation rate increased with equal increments.

The degradation dynamic of ATBA under $NaClO_2$-UV/O_3 process. The reaction was supposed to be zero-order, first-order or second-order reaction. Various reactions would be fitted respectively. It could be seen from the figure of the linear correlation that the results of experimental data analysis were consistent with the fitting of first-order reaction [14]. The first-order fitting diagrams of various affecting factors were shown as following.

Fig. 3 showed that there was a linear propor-

tion by inversion between the ln(c/c$_0$) of ATBA and time under the different factors. R^2 was more than 0.90 and the fitting degree was higher.

According to the Fig. 4, the fitted sub-equations of K versus four factors by interpolation method could be obtained. The results were showed in Table 1.

Establishment of dynamics model under $NaClO_2$-UV/O_3 process. From the discussion of the $NaClO_2$-UV/O_3 system, we can get the relation between a single controlled factor and $k_{obs1} = A_1 \cdot X_1$. So $NaClO_2$-UV/O_3 system containing more than one variable factor could get cumulative effects under the influence of single and multiple factors. It could be expressed by product, $k_{obs} = A \cdot X_1 \cdot X_2 \cdots\cdots X_n$, based on interpolation method. In practice, the MATLAB could be used to treat the following equations.

Through establishing the above sub-equations, the general equations of apparent rate constants were gotten:

①pH<5.8: $k_{obs} = \mathrm{A}K_{pH1}K_{c_0}K_P K_T K_Q$ (1)

②pH>5.8: $k_{obs} = \mathrm{A}K_{pH2}K_{c_0}K_P K_T K_Q$ (2)

Table 2 showed that A=3205.329, therefore:

①pH<5.8: $k_{obs} = 3205.329K_{pH1}K_{c_0}K_P K_T K_Q$ (3)

②pH>5.8: $k_{obs} = 3205.329K_{pH2}K_{c_0}K_P K_T K_Q$ (4)

Table 2 showed that the relative error was less than 5% under $NaClO_2$-UV/O_3. The model was better and could correctly reflect the need of the actual result.

The pseudo first-order reaction rate was acquired to use in the following equation.

$$Ln(S/S_0) = -k_{obs}t \quad (5)$$

Therefore, Equation 6 could be obtained:

$$S = S_0 \exp(-k_{obs}t) \quad (6)$$

$$S = S_0 \exp(-3205.329K_{pH}K_{c_0}K_P K_T K_Q t) \quad (7)$$

Then put k_{obs} into the above equation. k_{obs} was the pseudo-first-order rate constant and S was the concentration of organic compound at given reaction time, with S_0 being the initial concentration of organic compound in the bulk solution.

Comparison of degradation process. In order to facilitate comparison, several sets of controlled trials that the degradations under $NaClO_2$-UV, O_3 and UV were measured at pH=10

It could be seen from Fig. 5a that when the degradation time was 4 minutes, the dye degradation rate was 99.764% under $NaClO_2$-UV/O_3 system, the dye degradation rate was 65.826% under O_3, the dye degradation rate was 31.451% under $NaClO_2$/O_3, and the dye degradation rate was 0 under single UV. Make a comparison among the four kinds of processes' effects of degradation on ATBA, we can see that the degradation effect was best and most obvious under $NaClO_2$-UV/O_3, the degradation effect took second place under the condition of single ozone, the degradation effect took third place under the condition of sodium chlorite and ultraviolet, and it almost had no degradation effect in ATBA under the condition of UV alone. The gap between the four processes was obvious.

TABLE 2
k_{obs} under different experimental conditions and the stability analysis of dynamic model

pH	c_0/mg.L^{-1}	$NaClO_2$ dosing quantity P /mg.L^{-1}	T/k	Q(O_3)(L/h)	experimental-k_{obs}/min^{-1}	A	Calculative k_{obs}/min^{-1}	The relative error %
2	25	150	285	36	0.50845	3070.792	0.523289	1.4839
4	25	150	285	36	0.41675	3071.264	0.428846	1.2096
8	25	150	285	36	1.19125	3070.623	1.226083	3.4833
10	25	150	285	36	1.60557	3070.636	1.652511	4.6941
5.8	25	150	285	36	0.19334	3121.821	0.19573	0. 239
5.8	25	150	273	36	0.17016	3183.482	0.168927	0. 123
5.8	25	150	300	36	0.24112	3292.907	0.231418	0. 97
5.8	25	150	315	36	0.26453	3104.637	0.269282	0. 4752
5.8	25	150	329	36	0.29457	3038.899	0.306348	1.1778
5.8	15	150	285	36	0.22344	3114.069	0.226765	0. 3325
5.8	40	150	285	36	0.1642	3478.703	0.149176	1.502
5.8	50	150	285	36	0.1201	3212.828	0.118141	0. 196
5.8	25	25	285	36	0.1707	3331.421	0.161938	0. 876
5.8	25	50	285	36	0.1813	3487.669	0.164288	1.701
5.8	25	100	285	36	0.18754	3415.134	0.173552	1.399
5.8	25	200	285	36	0.27174	3451.528	0.24882	2.292
5.8	25	150	285	20	0.15674	3230.739	0.153328	0. 341
5.8	25	150	285	28	0.18342	3386.781	0.17116	1.226
5.8	25	150	285	52	0.25156	2999.208	0.265081	1.3521
5.8	25	150	285	60	0.29153	2973.43	0.309862	1.8332
						Average: 3205.329		

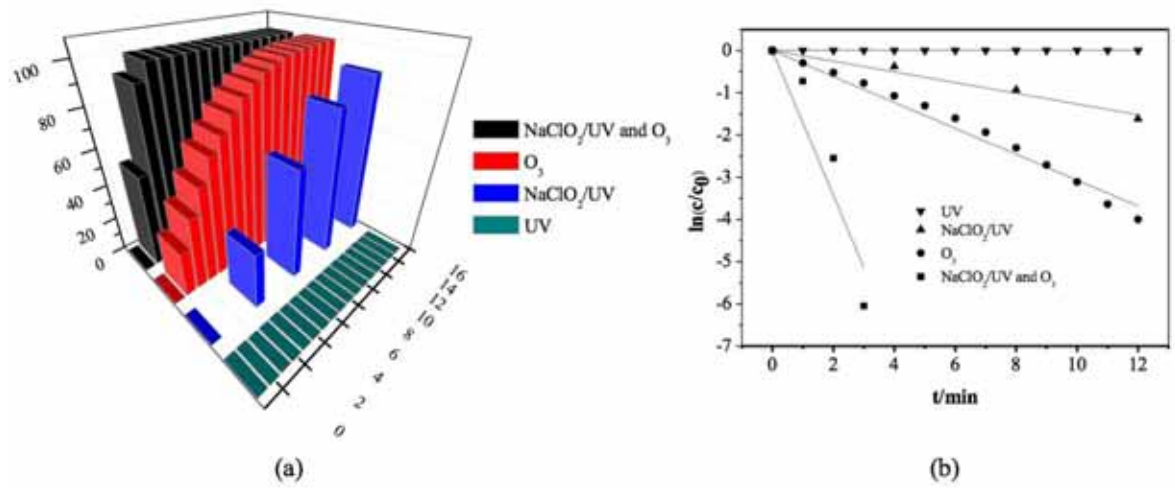

FIGURE 5
(a)the comparison chart of degradation rate under different process for pH=10, (b)process comparison

Synergistic effect of $NaClO_2$-UV/O_3. Fig. 5b showed that: when pH= 10, the apparent rate constant of single ultraviolet k_{UV}= 0, the apparent rate constant of ozone k_{O3}= 0.30701, the apparent rate constant of chlorine produced by sodium chlorite and ultraviolet $k_{NaClO2\text{-}UV}$= 0.12651, the apparent rate constant of combination of sodium chlorite and ultraviolet with ozone.

$k_{(NaClO2\text{-}UV)+O3}$ = 1.71235. So the synergistic cofactor E:

$$E = \frac{k_{(NaClO_2-UV)+O_3}}{k_{NaClO_2-UV} + k_{O_3} + k_{UV}} = \frac{1.71235}{0.12651 + 0.30701 + 0} = 3.9499 \quad (8)$$

The synergistic cofactor E was about 4, which illustrated that $NaClO_2$-UV/O_3 degradation process exerted a very significant synergistic effect only under the condition of alkaline. However, it had no joint effect under other conditions. Put the degradation effect as f.

In alkaline conditions:

$f_{(NaClO2\text{-}UV)+O3} >> f_{O3} > f_{O3/NaClO2} > f_{NaClO2\text{-}UV} > f_{UV}$ (f_{NaClO2})

In the other conditions:

$f_{O3} \approx f_{(NaClO2\text{-}UV)+O3} > f_{O3} > f_{O3/NaClO2} > f_{NaClO2\text{-}UV} > f_{UV}$ (f_{NaClO2})

CONCLUSION

Through the research of this paper, the dynamics research of $NaClO_2$-UV system got further improvement according to the degradation of ATBA. $NaClO_2$-UV/O_3 process system was further innovation on the basis of $NaClO_2$-UV system. Under alkaline conditions and room temperature, experiments obtained obvious degradation effect. The significant synergistic effect under the condition of alkaline indicated that the $NaClO_2$-UV/O_3 process had great application prospect.

ACKNOWLEDGEMENTS

The authors gratefully acknowledge the financial support from National Natural Science Foundation of China (No. 21246010) and Jiangsu Eastern Coast and Yangtse River Area Development Institute (Z201402).

Yongjun Shen and Qihui Xu contributed equally to this work and should be considered co-first authors

REFERENCES

[1] Panizza, M. and Cerisola, G. (2008) Removal of colour and COD from wastewater containing acid blue 22 by electrochemical oxidation. J. Hazard. Mater. 153, 83-88.

[2] Yu, H., Nie, E., Xu, J., Yan, S.W., Cooper, W.J. and Song, W.H. (2013) Degradation of Diclofenac by Advanced Oxidation and Reduction Processes: Kinetic Studies, Degradation Pathways and Toxicity Assessments. Water. Res. 47, 1909-1918.

[3] Chatzisymeon, E., Xekoukoulotakis, N.P., Coz, A., Kalogerakis, N. and Mantzavinos, D. (2006) Electrochemical treatment of textile dyes and dyehouse effluents, J. Hazard. Mater. 137, 998-1007.

[4] Turhan, K. and Turgut, Z. (2007) Reducing chemical oxygen demand and decolorization of direct dye from synthetic-textile wastewater by ozonization in a batch bubble column reactor. Fresen. Environ. Bull. 16, 821-825.

[5] Cakmakci, M., Yaman, F.B., Yetilmezsoy, K., Karadag, D., Ozkaya, B., Turkay, H. and Genc, T. (2016) Effect of pre-ozonation on anaerobic treatability of membrane concentrate. Fresen. Environ. Bull. 25, 1206-1220.

[6] Lee, H. and Shoda, M. (2008) Removal of COD and color from livestock wastewater by the Fenton method. J. Hazard. Mater. 153, 1314-1319.
[7] Shen, Y.J., Xu, Q.H., Liang, J. and Xu. W. (2016) Degradation of Reactive Yellow X-RG by O_3/Fenton system: response surface approach, reaction mechanism, and degradation pathway. Water Sci. Technol. 74, 2483-2496.
[8] Shen, Y.J., Xu, Q.H., Wei, R.R., Ma, J.L. and Wang. Y. (2017) Mechanism and dynamic study of reactive red X-3B dye degradation by ultrasonic-assisted ozone oxidation process. Ultrason. Sonochem. 38, 681-692.".
[9] Tian, F., Qiang, Z.M., Liu, C., Zhang, T. and Dong, B.Z. (2010) Kinetics and mechanism for methiocarb degradation by chlorine dioxide in aqueous solution. Chemosphere 79,646-651.
[10] Herd, C. and Ernst, W.R. (1994) Photodecomposition of Chlorine Dioxide and Sodium Chlorite in Aqueous Solution by Irradiation with Ultraviolet Light. Environ. Sci. Technol. 33, 1468-1475.
[11] Callerame, J. (1989) Process for the production of chlorine dioxide. US4874489.".
[12] Simpson, G.D. (2001) Chlorine dioxide generator.US6171558.
[13] Lopez-Lopez, A., Pic, J.S. and Debellefontaine, H. (2007) Ozonation of azo dye in a semi-batch reactor: a determination of the molecular and radical contributions. Chemosphere 66, 2120-2126.
[14] Shen, Y.J., Xu, Q.H., Pan, Y.W., Ding, J.D. and Wang, Y. (2016) Kinetics of the ozone oxidation of weak acid brilliant green in aqueous solution. Fresen. Environ. Bull. 25, 2554-2562.

Received: **11.05.2016**
Accepted: **10.07.2017**

CORRESPONDING AUTHOR

Yongjun Shen
School of Chemistry and Chemical Engineering,
Nantong University
No. 9, Seyuan Road,
Nantong, 226019 – CHINA

E-mail: zjuenv@163.com
shenyj@ntu.edu.cn

© by PSP Volume 26 – No. 10/2017 pages 5707-5716 Fresenius Environmental Bulletin

COMPARISON OF TWO STRATEGIES FOR THE START-UP OF A NEW BIOFILM REACTOR FOR THE TREATMENT OF SYNTHETIC AQUACULTURE WASTEWATER

Xiaoma Xu[1], Siyao Wang[1], Jiejie Wu[1], Cheng Wei[2], Yuewu Pu[1,*]

[1]School of Bioscience and Bioengineering, South China University of Technology, Guangzhou 510006, PR China
[2]Architecture & Civil Engineering, South China University of Technology, State Key Laboratory Building Science, Guangzhou, 510640, PR China

ABSTRACT

A newly foldaway DO (Dissolved Oxygen)-increased biofilm reactor (FDI-BfR) was designed for the treatment of synthetic aquaculture wastewater. Two strategies for the start-up of the biofilm reactor were designed in order to find the best operation conditions, with (phase B) and without (phase A) inoculum of activated sludge. The differences in the organic matter removal, ammonia nitrogen removal as well as the difference in physical properties of the biofilm were analyzed. The results showed that the start-up of the FDI-BfR is faster in phase A, from the start to the end, in both strategies. The average removal rate of COD and NH_4^+-N were above 90% and 70% respectively in 24 hours. More compact structure and stronger adhesion were observed by scanning electron microscope (SEM) in the biofilm started-up by adding activated sludge than that of natural-started biofilm. Moreover, the V3 regions in the 16S rRNA of the bacteria were sequenced to characterize the microbial community structures in both reactors. The diversity of the microbial community is higher after start-up when applied different strategies, though the difference of the removal efficiency for the two start-up strategies is insignificant.

KEYWORDS:
Biofilm reactor; Start-up; Removal efficiency; Microbial community

INTRODUCTION

Aquaculture has been developed steadily over last decade in response to the increasing world market demand for seafood. However, it also discharges an enormous amount of wastewater into environment which contains high concentration of nitrites, nitrates and phosphorus and eventually leads to eutrophication on receiving waters [1-2]. In recent years, researches have been focused on looking for advanced methods in treating aquaculture wastewater prior to recirculation or discharge into receiving waters.

The membrane biofilm reactor (MBfR), an emerging technology for water and wastewater treatment, is based on pressurized membranes that supply a gaseous substrate to the biofilm formed on the exterior of the membrane. MBfRs are uniquely suited for numerous applications of wastewater treatment such as the removal of carbon and nitrogen when oxygen is supplied, and the reduction of oxidized contaminants when hydrogen is supplied. According to recent researches, such an emerging technology has been successfully used for organic matter stabilization and nutrient control [3-4]. It has been employed in recent years for the treatment of various types of substrates especially aquaculture wastewater.

The performance of biofilm reactor includes sewage treatment capacity, biofilm attachment effects, mechanisms of fouling formation, etc. The performance may differ due to different aspects, such as biofilm carrier choice, reactor module design, operation and management methods, etc. [5-6]. Furthermore, many studies have indicated that the start-up strategy played an important role in biofilm reactor running. Recent studies focusing on bioreactor start-up period agreed that the "spontaneous" start-up of the membrane bioreactors is usually short and so easy to manage that an initial inoculum may not be required [2, 6–8]. Furthermore, the initial activated sludge inoculum has been considered only for its positive effect on the optimization of biological nutrient removal and Anammox process start-up. The start-up can constitute an aspect that critically influences MBR performance during its lifespan.

However, there were few works focused on the difference of bacterial community structure inside the biofilm applied different start-up strategies. Indeed, the biological technology for wastewater treatment is a complex biochemical process, in which several microorganisms are involved and they play a crucial role. It is affected by the survival conditions of the microorganisms and colonies, as well as the raw fermentation materials. The microbial community structure and activity level can greatly affect the rate of fermentation [7]. The techniques which have been developed in recent years [8], such as denaturing gradient gel electrophoresis/temperature gradient gel electrophoresis (DGGE/TGGE), 16S rRNA

clone library, deep sequencing, etc. together with corresponding analysis software [9] and databases, such as Genbank, EMBL (European Bioinformatics Institute), DDBJ (DNA Data Bank of Japan) and so on, have become powerful approaches in studying microbial community structure and diversity.

Based on the comprehensive analysis, we designed a simple, low cost foldaway DO (dissolved oxygen)-increased biofilm reactor (FDI-BfR) which uses two different strategies for the start-up. This study was to evaluate the influence on system performance and the rate of initial biofilm attachment of the two strategies. Moreover, the other primary objective of this study was to characterize and compare the microbial ecology of the biofilms in the FDI-BfR after adopted two different start-up strategies. Deep sequencing technique was used to scan and to compare the bacterial 16S rRNA genes and DGGE of archaeal 16S rRNA genes, to explore the microbial community diversity and start-up shift in this period.

MATERIALS AND METHODS

Experiment Design. The newly folding DO (Dissolved oxygen)-increased biofilm reactor (FDI-BfR) consists of a 150L lower water tank, the five layers of inclined plates, and a 20L higher water tank. The main part of the system is the five layers of inclined plates covered by ceramic tiles which are supported by the steel hobs. Fibers are used to adhere on the surface of ceramic tiles as a membrane. The inclined plates of 50 cm × 40 cm × 1 cm are placed on a steel hob of 60 cm × 40 cm × 160 cm with slope of 8° and a 10 cm drop between two inclined plates. Fiber packing was produced by biological company, model for CH430. An overflow outlet can be formed by placing the side opening of the places slightly lower. Sequencing batch and closed-circuit circulation method were adopted for this experiment, and artificial start-up with adding activated sludge and natural start-up without adding activated sludge were used as two different strategies respectively. Each cycle sustained 4 days with 100 L of aquaculture wastewater feeding to the high water tank of the FDI-BfR reactor by water pump from low water tank and flowing over membrane surface of the five places, finally the water flowed back into the lower water tank. The complete reactor layout is represented in Fig 1.

The entire experiment lasted 90 days and it was divided into two phase (45 days pre-phase). All of the cycles are continuous with no time interval between two adjacent cycles. During the first experiment phase (phase A), the system was started-up without any activated sludge addition, just under the condition of the natural environment and no sludge withdrawal was performed. Difficulty occurred during the second experimental phase (phase B). The system was started-up with activated sludge inoculum addition. Before inoculation, the sludge was domesticated for two days at room temperature under aeration cultivation control. The SV30 the concentration was 30% and 6000 mg/L, respectively. The cultivated sludge was mixed with wastewater by the ratio of 1:4 to 100L and was put into low water tank to start-up the system. After one cycle, the lower water tank was allowed to settle for 2 h to exchange the mixture with wastewater. The subsequent cycle was same as phase A. Overall experiments were operated in room temperature, and other operating conditions were kept constant in both start-up periods.

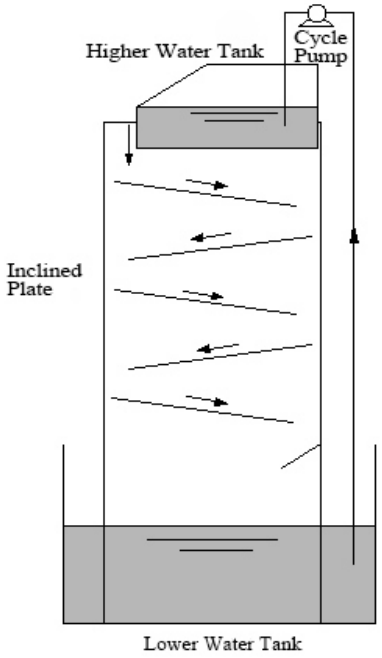

FIGRUE 1
The layout and schematic diagram of the newly folding DO (Dissolved oxygen)-increased biofilm reactor (FDI-BfR)

TABLE 1
Characterization of influent wastewater

	COD mg/L	BOD_5 mg/L	NH_4^+-N mg/L	N-NO_3 mg/L	N-NO_2 mg/L	TN mg/L	TP mg/L	pH
Phase A	83.767	37.712	8.579	<0.04	<0.04	12.308	12.56	7.03
Phase B	83.388	36.908	8.847	<0.04	<0.04	12.213	12.41	7.01

The activated sludge in this experiment was obtained from the secondary sedimentation of a municipal wastewater treatment factory in Guangzhou (China). The wastewater was collected from an aquaculture plant in Guangzhou (China). Before usage, it has been diluted with tap water in order to maintain an average constant influent COD concentration (500mg/L) to operate with a constant volumetric load rate. The wastewater characteristics are shown in Table 1.

Analytical Method. (1) Chemical index analysis. All the water samples in this experiment was collected every 12h in each cycle to measure the parameters of water quality, approximately 100 ml of well mixed reactor contents from lower water-tank were collected. And all of the analytical procedures were performed according to Standard Methods [10]. The solution chemical oxygen demand (sCOD) was analyzed according to the standard methods of Chinese State Environmental Protection Agency (CSEPA). Biochemical oxygen demand (BOD5) was measured by Biochemical oxygen demand BOD measurement instrument (BODTrakTM, Hach) using differential pressure measurement method. Ammonium, nitrate and nitrite nitrogen concentrations were measured through spectrophotometry using ultraviolet spectrophotometer for Laboratories (UV-2802SH, Yvonne ko (Shanghai) instrument Co.). The total phosphorus was determined by the method of Ammonium molybdate spectrophotometry. In addition, the pH, DO, temperature are measured by using digital pH meter (pHS-3C, China), Portable dissolved oxygen meter, and mercury thermometer, respectively.

The structure of biofilm was detected by scanning electron microscope (Car Zeiss EVO LS10, Zeiss British company), and the biofilm samples were pretreated by freeze-drying processing, and metal spraying before taking pictures.

(2) DNA extraction, amplification and DGGE analysis. An aliquot of biofilm sample suspension (250 mg) was centrifuged at 12,000 rpm for 10 min. The pellet was washed twice with distilled water (1 mL), repeating the centrifugation after each wash. A DNA extraction kit (Sangon Biotech, China) was used to extract the DNA from the washed biofilm pellet. Bacterial universal primers BAC-338F (50-ACTCCTACGGGAGGCAG-30) and BAC-518R (50-ATTACCGCGGCTGCTGG-30) were used to amplify the DNA. For DGGE analysis, a 40bp GC-clamp (50-CGCCCGCCGCGCGCGGCGGGCGGGGCGGGGGCACGGGGGG-30) was added to BAC-338F primer. The touchdown PCR program consisted of an initial denaturation step (5 min, 95°C), 20 cycles of denaturation (1 min, 95°C), annealing (0.75 min, 65°C) and extension (1 min, 72°C) steps with the annealing temperature decreased 0.5°C/cycle, followed by 10 cycles of denaturation (1 min, 95°C), annealing (0.75 min, 55°C) and extension (1 min, 72°C), and a final extension step (10 min 72°C).

The DGGE analysis was performed using a denaturant gradient ranging from 40% to 60%, where 100% was defined as 7 M urea containing for methane amide (40%, v/v), Electrophoresis was run at 60°C and 120 V for 6 h. The DGGE gel was stained using silver nitrate, as described by Sambrook et al.[11], and photographed. The densities and migration patterns of the bands were calculated by applying an image analysis system to the DGGE band profiles. Then, principle component analysis, based on the densities and migration of the bands, was performed using Quantity One software (version 4.4.0; Bio-Rad Laboratories, USA). The richness (R) values were calculated using the formula Ri =Li/LT, where Ri is the richness value of the bacterial community in lane i, Li is the number of bands in lane i, and LT is the total number of bands in the DGGE profile.

Individual bands were excised, immersed in doubled-distilled water and incubated overnight at 4℃. The dissolved DNA samples were further amplified with PCR using the corresponding primers without the GC-clamp. The amplified 16S ribosomal RNA (rRNA) gene fragments were purified by the DNA agarose gel purification kits(Invitrogen Biotech, China), and then cloned 16S rRNA gene fragment into TA cloning vector PCR 2.1. After amplification, it was transformed into competent cells; positive clones were selected for PCR verification by a blue-white screening. The positive clones were further amplified with PCR using the corresponding primers without the GC-clamp. Then the amplified 16S rRNA gene fragments were sequenced and the results were compared with the reference sequences in the GenBank database using BLAST program.

RESULTS AND DISCUSSION

Performance of System. Artificially added activated sludge to develop the biofilm and start-up spontaneously without any inoculums are the comparison of two conventional biofilm start-up strategies [12-13]. In this experiment, both of the two methods had been used. At the end of the both phases, a thick biofilm was developed successively. The biofilm on every inclined plate was about 2cm thick. There was a small, black, anaerobic area in the interior of the biofilm. Besides that, the removal efficiency of the organic matter was investigated as another important criterion.

Fig 2 shows the NH_4^+-N and COD concentration of inflow and effluent at 24 h during start-up without (phase A) and with (phase B) inoculums. The removal efficiency was presented, too. We found that the performance of removing organic matter has attained a good level, the NH_4^+-N removal

efficiency reached above 80%, and the COD removal rates even touched 91% at the end of start-up, no matter in phase A or B (Fig 3). It is an excellent comparison with conditional biochemical methods. It have been pointed out that the MBfR achieving high gas transfer rates makes it important for consideration in the literatures [14-15]. One of the original goals of the MBfR was to provide bubble-less aeration of wastewater for high rate treatment or high strength COD removal [16]. Previous studies showed the DO concentration in biofilm raw water pretreatment systems were various from 0.01 mg/L to saturation level according to different treatment objectives [17-18]. In this experiment, with the aid of a pump, sewage was pushed to flow from low to high water tanks, and then to flow through the five inclined plates of the system, through repeated cycles, required dissolved oxygen (DO) was supplied for microbial degradation. In the whole experiment, the measured concentration of DO is about 3.65mg/L on average. Former studies shown that the best value of dissolved oxygen is 3mg/L to 5mg/L. The MBfR have anaerobic, aerobic and facultative anaerobic biofilm environment simultaneously to supports luxuriant unique microbial community structures that allow for the simultaneous removal of COD and nitrogen from waste water [19].

(1) Start-up efficiency comparison. In addition, by comparing the left two graphs of Fig 2, it could be found that, for Ammonia nitrogen, under the condition of the inflow concentration was about 80-90 mg/L in phase A, the outflow concentration was 35mg/L initially and then reached a steady value which under 10mg/L until 22th day. During phase B, the ammonia nitrogen concentration of outflow was 34.1mg/L, which is similar with phase A. But decreased rapidly after the first cycle, and stabilized at about 10mg/L from the 10th day. Furthermore, the same phenomenon was also observed at the variation curve of COD concentration. The inflow COD concentration was from 70mg/L to 100mg/L both in phase A and phase B. For outflow COD concentration，when the biofilm was developed at the end of each phase, there was no much difference, both around 85mg/L. In terms of removal efficiency, we can find that it reached a stable value in phase B much faster than in phase A.

In order to investigate the effects of start-up strategies on speed of biofilm development, we have also counted the removal efficiency of COD and NH_4^+-N at 12 h, 24 h, which was showed in Fig 3 and Fig 4. It can be found that, in the phase A, named natural hanged biofilm start-up strategy, the removal rate of COD at the time of 24 h from the first day was 39%. It is a slow growth process, to fifth batch experiments, which is around at 25th day. Its removal rate reached more than 70%, and finally, the system got the steady rate at around 80%. Ammonia nitrogen treatment efficiency, 15.9% at the first day of the start, presented a slow growth process. Around 25th day, removal efficiency reached more than 70% but in the end, stabled at around 91%. Compared with phase A, the removal rate in phase B was much

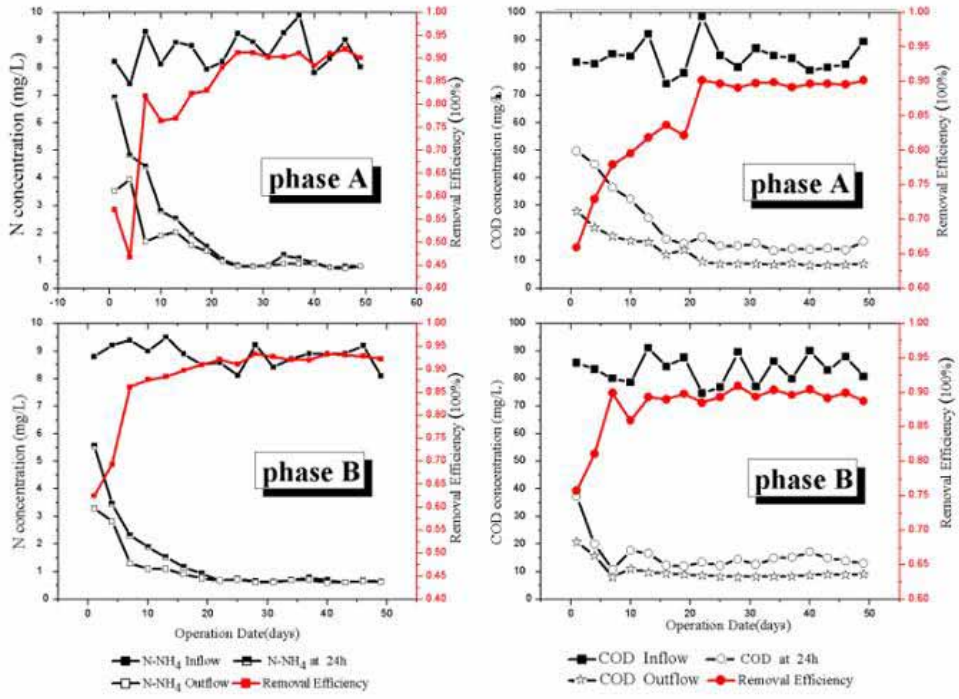

FIGURE 2
The NH_4^+-N, COD concentration in the inflow, outflow and at 24 h during start-up without (phase A) and with (phase B) inoculum. The removal efficiency was represented by the red curves

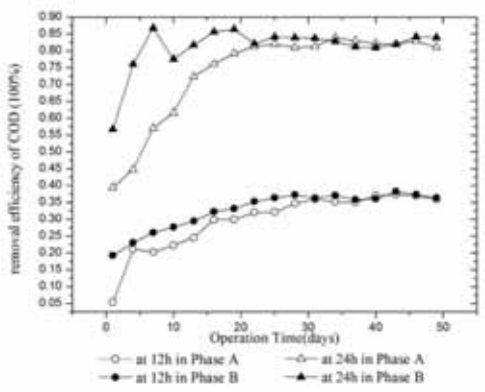

FIGURE 3
The removal efficiencies of COD at the 12th h, 24th h during phase A and phase B

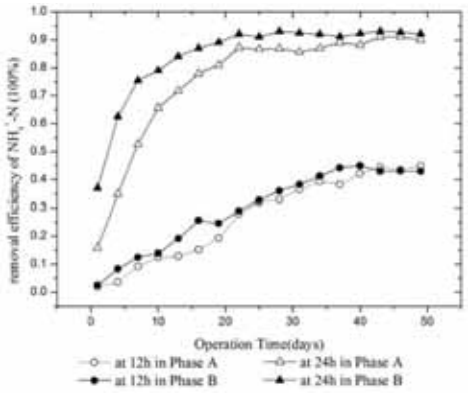

FIGURE 4
The removal efficiencies of NH_4^+-N at the 12th h, 24th h during phase A and phase B

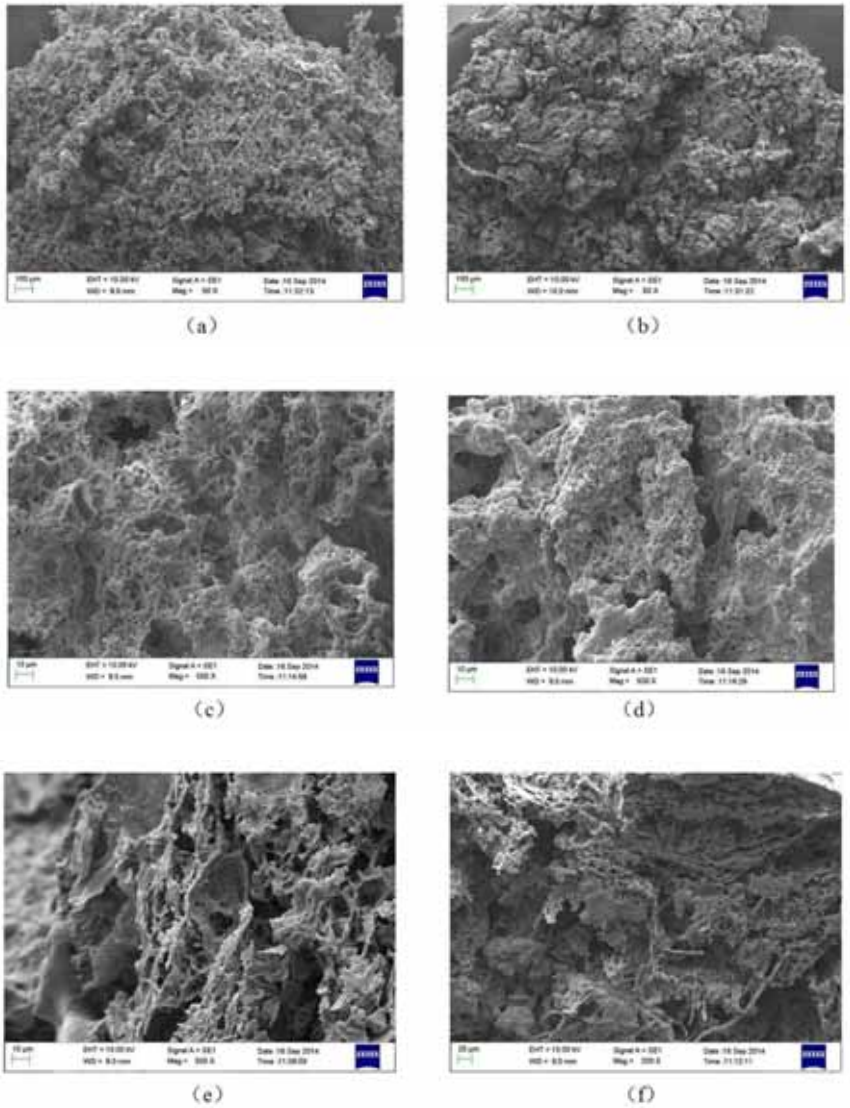

FIGURE 5
Scanning electron micrographs of the biofilm samples in different start-up methods
(a), (c): SEM micrographs of biofilm in natural start-up process (phase A)
(b), (d): SEM micrographs of biofilm in start-up process by adding activated sludge (phase B)
(e), (f): Longitudinal section micrographs of biofilm in phase A and B

TABLE 2
The Lane Similarity Matrix of 12 lanes

Lane	1	2	3	4	5	6	7	8	9	10	11	12
1	100.0	78.9	54.3	31.4	33.5	28.3	31.8	37.6	33.6	15.6	21.9	18.8
2	78.9	100.0	69.7	28.8	19.4	21.8	31.8	30.2	34.4	17.4	25.1	21.2
3	54.3	69.7	100.0	26.9	18.4	20.7	30.3	26.1	26.7	18.9	27.5	24.9
4	31.4	28.8	26.9	100.0	61.7	57.2	33.3	24.8	24.7	25.2	26.3	26.8
5	33.5	19.4	18.4	61.7	100.0	76.3	23.2	21.7	16.7	39.7	24.5	23.5
6	28.3	21.8	20.7	57.2	76.3	100.0	20.4	18.4	18.3	36.8	22.8	22.3
7	31.8	31.8	30.3	33.3	23.2	20.4	100.0	60.8	55.7	42.7	49.5	46.1
8	37.6	30.2	26.1	24.8	21.7	18.4	60.8	100.0	65.0	33.4	39.7	33.7
9	33.6	34.4	26.7	24.7	16.7	18.3	55.7	65.0	100.0	39.2	38.6	39.5
10	15.6	17.4	18.9	25.2	39.7	36.8	42.7	33.4	39.2	100.0	53.6	60.5
11	21.9	25.1	27.5	26.3	24.5	22.8	49.5	39.7	38.6	53.6	100.0	78.8
12	18.8	21.2	24.9	26.8	23.5	22.3	46.1	33.7	39.5	60.5	78.8	100.0

higher. At the beginning of the start-up, the removal rate of COD and ammonia nitrogen was 56.7% and 36.9%, respectively. It is important to notice that the removal rate of COD in 5 days reached to 76%, and after several wave appeared, the steady efficiency was attained at around 84%. At 10th day, ammonia nitrogen, removal performance was attained at more than 70% with a steady trend up to 90%.

Through the above analysis of removal performance during the start-up, it could be concluded that the start-up strategy with the addition of inoculum has a higher efficiency than the method without inoculum addition. The main difference of the two strategies is the addition of inoculum, which has a deep influence to the beginning biomass concentration. In conventional activated sludge systems (CASs), the start-up period represents a very important phase; most of the organic substrate in the influent wastewater cannot be biodegraded because the biomass concentration in biological reactors is very low at the beginning [20]. There were many studies try to shorten the start-up of CAS to a few days by inoculation with sludge from existing plants. On the other hand, for membrane biofilm reactors (MBR), it is able to completely retain all of TSS within the reactor from the first day, leading a quick increase of TSS concentration in the biological reactor. The sludge in this experiment was activated by the raw wastewater firstly, when inoculated to the reactor. The microorganisms were still alive, which contribute to the organic matter removal. At the beginning of phase A, the removal performance was much lower than that of in phase B. Moreover, the initial increased biomass had contributed to the subsequent microbial proliferation which further influenced the structure of microbial flora and the performance of system.

(2) The structural differences of biofilm. In order to compare the difference of surface structure of mature biofilm which started-up by two different methods, scanning electron microscopy (SEM) was used to characterize the structure. The result was showed in Fig 5, the skeletal structure of mature biofilm was obviously formed, and the mature biofilm pieced together with uniform gap in its surface.

Further the difference of surface structure of mature biofilm is compared (Fig 5a and Fig 5b, Fig 5c and Fig 5d). The result showed that the mature biofilm in phase B was more compact, and the gap structure was much more homogeneous and micromesh. While the biofilm during phase A was a little loose and the aperture in the biofilm had a bigger size. Research indicated that too compact biofilm structure is not only conducive to the exchange of matter and energy in biofilm, but also affect the supply of oxygen, thus affecting the efficiency of biofilm removal of organic contaminants; but if it is too loose, then poor adhesion of biofilms, extracellular polymeric substances (EPS) secreted less, the growth situation of microbial was not ideal, and affect removal efficiency of organic pollutants in the biofilm reactor [21].

To further investigate the difference between the inner structures of the biofilm, we cut biofilm with a razor blade to contrast the longitudinal section of biofilm in phase A and B, as shown in Fig 5e and Fig 5f. it is found that in the mature biofilms of phase B, the endothecium structure of biofilm was more compact, while the outer side was relatively loose, this level difference distribution strengthen the biofilm adhesion ability of biofilm, and ensured the biofilms have a certain mass transfer capability and the dissolved oxygen concentration [22]. But the mature biofilm structure in phase A do not have this level of difference in the overall structure of osteoporosis (Fig 5e), although beneficial biofilm internal mass transfer, and dissolved oxygen, but have poor adhesion.

DGGE Analysis of Microbial Community Diversity at The Period of Start-Up. (1) The analysis of lane similarity matrix. To study the diversity and the shift of the microbial community in the system, we had randomly selected a patch of biofilm on the first layer, third layer and fifth layer of inclined

plate at 4th and 45th day in both phases. The result of DGGE was showed in Fig 6, After the analysis by the Quantity One software, we had got the similar results. Matrix showed in Table 2 and the Phylogenetic Tree showed in Fig 5. From the results, we could find that, the first few days of each phase, the diversity between the biofilm at the same layer of two different start-up strategies was a little big. The similarity index of Lane 1 to 3 and Lane 7 to 9 was at average 28.85. The same phenomenon also appeared after the start-up. The index (similarity of Lane 4 to 6 and Lane 10 to 12) was a little lower down to 24.3. Those results indicated that, in terms of microbial community, the two start-up strategies have little or no similarity during the phase of start-up, even though their performance to degrade the organic matter after the start-up was similar. This may have the same contribution to the degradation because of the effect of different microorganisms.

However, in phase B, we could find that the microbial communities have a little shift during the whole period (the Similarity Index reached 41.15 on average). This is evident furtherly that the alive microorganism which in activated sludge have an obvious promotion to the development of biofilm. It was explained why the start-up strategy, with the addition of inoculum was just used for few days.

What is more, there is also a high similarity (the maxima reached 78.9) between the biofilm at different inclined plates, despite at which period or take which start-up strategy. This might take a Sequencing batch and closed-circuit circulation method because of the start-up experiment. In which, there is a little difference in terms of water quality parameters

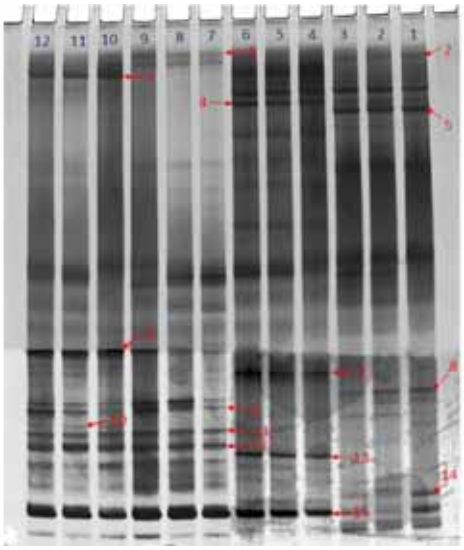

FIGURE 6
DGGE results in the analysis of the microbial communities. Lane 1-3 respectively represent the biofilm sample at the first, third and fifth layer at the forepart of phase A. Lane 4-6 and respectively represent the biofilm sample at the first, third and fifth layer at the rear-end of phase A. Accordingly Lane 7-9 and Lane 10-12 respectively represent the biofilm sample at the first, third and fifth layer at the forepart and the rear-end of phase B.

TABLE 3
Phylogenetic affiliation of the bands obtained by DGGE

Band(s)	Nearest sequence	Accession no.	% similarity
1,13	*Azoarcus sp.*	KP739958	98
		KP739970	100
2	*Lactococcus sp.*	KP739959	99
		KP739960	98
		KP739967	99
3,10,11,12,15	*Aeromonas caviae*	KP739968	98
		KP739969	100
		KP739972	99
4	*Bacteroidetes bacterium*	KP739961	99
5	*Bergeyella sp.*	KP739962	99
6	*Tolumonas osonensis*	KP739963	98
7, 9	*Flavobacterium sp.*	KP739964	100
		KP739966	96
8	*Trichococcus pasteurii*	KP739965	98
14	*Duganella sp.*	KP739971	95

and running environment (including dissolved oxygen). Indeed, many studies have indicated that the type of wastewater and the type of bioreactor determine the structure of the bacterial communities deeply [23-25].

(2) DGGE analysis of microbial community. DNA samples at the forepart and rear-end of the start-up were applied different strategies (with and without inoculum) and were analyzed by DGGE. The partial 16S rRNA gene fragments obtained from 15 bands (Fig 4) were sequenced and identified by comparison with the sequences in the GenBank database (Table 3).

From Table 3, we could find that the preponderant microorganisms of all the start-up period were mainly concentrated in the genera: *Lactobacillus, Aeromonas, Flavobacterium, Bacteroides, Tolumonas, Bergeyella, Trichococcus, Duganella* and *Azoarcus*. What is more, combined with Fig 4, we could also find that a lower number of visible bands were observed in phase A compared to phase B, when the start-up was finished. During the phase A, the main DGGE bands were the band 4,7,13 and 15. They were related to *Bacteroidetes bacterium, Flavobacterium sp, Azoarcus sp and Aeromonas caviae* respectively. All of them did not appear at the early stage of the start-up, the DGGE bands 4, 7, 13 were only appeared in phase A. It was reported that *Bacteroidetes bacterium* was strictly anaerobic and found to decolorize the dye and textile wastewater [26]. *Flavobacterium sp. w*as reported to degrade the organic matter and also had good decolorizing ability [27]. *Azoarcus sp* belongs to genus *Azoarucus.* Studies recognized that many strains of *Azoarcus* contributed significantly to the biodegradation of aromatic and other refractory compounds via a *meta*-cleavage pathway of the aromatic rings [28]. During phase B, eight bands (DGGE band 3, band 6, band 8-12 and band 15) were observed, and except band 3 and band 10, all of them were observed at the early stage of start-up, too. They are related to *Aeromonas caviae Tolumonas osonensi, Flavobacterium sp, Trichococcus pasteurii,* respectively. According to the previous work, *Aeromonas caviae* belongs to genus *Aeromonas*, Gram-negative, rod shaped, non-spore forming, oxidase-positive, and facultative anaerobe . Common in the biofilm it can ferment carbohydrates to acids [29-30]. *Tolumonas osonensis* is reported to be another kind of bacterium that can ferment carbohydrates to produce acids, and what's more, it is facultative anaerobic microorganism [31]. These results indicated that even there is big difference in the microbial community of the two start-up strategies, the main microbial flora have a good performance on the removal of organic matters. This study furtherly explains why the removal efficiency of two start-up strategies are not significantly different.

CONCLUSION

In this paper, a new foldaway DO (Dissolved oxygen)-increased biofilm reactor (FDI-BfR) was designed, focusing on the role of the initial inoculum of activated sludge. This experiment was aimed to study the difference of removal efficiency and microbial community between start-ups with and without the addition of activated sludge. Results showed that, both of the two strategies has a good performance on the removal of COD and NH_4^+-N, but the inoculum of activated sludge can help the biofilm mature much faster, comparing with the strategy without any inoculum. What is more, the addition of activated sludge can bring numerous activated bacteria to the system, and most of them have acclimatized to the new environment. They made a significant contribution to the removal of organics.

After the started-up, the structure of mature biofilm was contrasted by scanning electron microscopy, it is found that in phase A, the mature biofilm has a loose structure, and there have no significant differences between the inner and outer structure, although this structure is conducive to energy exchange between water and biofilm, but biofilm adhesion is poor. While in phase B, the mature biofilm structure was compact and existed significant differences between the inner and surface layers, in contrast with surface biofilm structure, the inner one is much tighter. This difference in the structure not only enhances the biofilm adhesion, makes it hard to be washed off, but also ensures the biofilm mass transfer capability and a certain concentration of dissolved oxygen.

It was also investigated that the bacterial community shifts during the start-up process and the variation of bacteria between the two start-up methods by PCR-DGGE. The results showed that, during the biofilm start-up process, the bacterial community changed obviously no matter in which start-up methods. The comparability index of bacterial community was only 32.7% and 42.5%, respectively. After the start-up, bacterial community between the two start-up strategies showed little similarity, and the maximum comparability index was only 25.2%. In addition, part of the biofilm microbial community of dominant bacteria was analyzed through the methods of cloning and sequencing. 15 bacterial 16S rDNA sequences were identified in both of two start-up methods, and with a homology over than 95% when compared with the bacteria of *Azoarcus sp., Bacteroidetes bacterium, Aeromonas caviae, Lactobacillus sp., Bergeyella sp., Tolumonas osonensis, Duganella sp.* and *Trichococcus pasteurii*., these strains played very important roles in the process of removing organic pollutants. The performance of each phase is not significantly different no matter at the early stage or when the biofilm had successfully developed, even there is a big difference between the two start-up strategies.

ACKNOWLEDGEMENTS

This work was supported by The National Key Technology R&D Program during the 12th Five-Year Plan period. (2014BAL06B02).

REFERENCES

[1] Mook, W.T., Chakrabarti, M.H., Aroua, M.K. Khan, G. M. A., Ali, B. S., and Islam, M. S. (2012) Removal of total ammonia nitrogen (TAN), nitrate and total organic carbon (TOC) from aquaculture wastewater using electrochemical technology: A review. Desalination, 285(3), 1-13

[2] Van Den Hende, S., Beelen, V., Bore, G., Boon, N., and Vervaeren, H. (2014) Up-scaling aquaculture wastewater treatment by microalgal bacterial flocs: from lab reactors to an outdoor raceway pond. Bioresource technology, 159, 342-354.

[3] Lee, K-C. and Rittmann, B.E. (2000) A novel hollow-fibre membrane biofilm reactor for autohydrogenotrophic denitrification of drinking water. Water Science and Technology, 41(4-5), 219-226

[4] Timur, H. (2001) Denitrification of wastewater in a fixed film reactor. Fresen. Environ. Bull., 10(4), 396-400.

[5] Guvensu, N. and Demir, S. (2012) Effects of magnesium and calcium cations on biofilm formation by sphingomonas paucimobilis from an industrial environment, Fresen. Environ. Bull., 21(12), 3685-3692.

[6] Mannina, G. and Di Bella, G. (2012) Comparing two start-up strategies for MBRs: Experimental study and mathematical modelling. Biochemical Engineering Journal, 68, 91-103.

[7] Hu, M., Wang, X., Wen, X., and Xia, Y. (2012) Microbial community structures in different wastewater treatment plants as revealed by 454-pyrosequencing analysis. Bioresource technology, 117, 72-79.

[8] Jung, J.Y., Lee, S.H., Kim, J.M., Park, M. S., Bae, J. W., and Hahn, Y. (2011) Metagenomic Analysis of Kimchi, a Traditional Korean Fermented Food. Applied and Environmental Microbiology, 77(7), 2264-2274.

[9] Reeder, J. and Knight, R. (2010) Rapidly denoising pyrosequencing amplicon reads by exploiting rank-abundance distributions. Nature Methods, 7(9), 668-669.

[10] American Water Works Association (1998) Water Pollution Control Federation. APHA (American Public Health Association). SM (2130).

[11] Deininger, P. (1990) Molecular cloning: A laboratory manual: 2nd ed. Edited by J. Full-size image. Cold Spring Harbor Laboratory Press, Cold Spring Harbor, NY, 1989 (in 3 volumes). Analytical Biochemistry, 186(1), 182-183.

[12] Ferraris, M., Innella, C. and Spagni, A. (2009) Start-up of a pilot-scale membrane bioreactor to treat municipal wastewater. Desalination, 237(1), 190-200.

[13] Pollice, A., Laera, G. and Blonda, M. (2004) Biomass growth and activity in a membrane bioreactor with complete sludge retention. Water Research, 38(7), 1799-1808.

[14] Martin, K.J. and Nerenberg, R. (2012) The membrane biofilm reactor (MBfR) for water and wastewater treatment: Principles, applications, and recent developments. Bioresource Technology, 122, 83-94.

[15] Qin, Y. Y., Zhang, X. W., Ren, H. Q., Li, D. T., and Yang, H. (2008) Population dynamics of ammonia-oxidizing bacteria in an aerated submerged biofilm reactor for micropolluted raw water pretreatment. Applied Microbiology and Biotechnology, 79(1), 135-145.

[16] Pankhania, M., Brindle, K. and Stephenson, T. (1999) Membrane aeration bioreactors for wastewater treatment: completely mixed and plug-¯ow operation. Chemical Engineering Journal, 73, 131-136.

[17] Vet, W. W. J. M. D., Dinkla, I. J. T., Muyzer, G., Rietveld, L. C., and Loosdrecht, M. C. M. V. (2009) Molecular characterization of microbial populations in groundwater sources and sand filters for drinking water production. Water Research, 43(1), 182-194.

[18] Han, M., Zhao, Z.-W., Gao, W., and Cui, F. Y. (2013) Study on the factors affecting simultaneous removal of ammonia and manganese by pilot-scale biological aerated filter (BAF) for drinking water pre-treatment. Bioresource Technology, 145(10), 17-24.

[19] Suzuki, Y., Hatano, N., Ito, S., and Ikeda, H. (2000) Performance of nitrogen removal and biofilm structure of porous gas permeable membrane reactor. Water Science and Technology, 41(4-5), 211-217.

[20] Bella, G. D., Durante, F., Torregrossa, M., and Viviani, G. (2010) Start-up with or without inoculum Analysis of an SMBR pilot plant. Desalination, 260(1-3), 79-90.

[21] Ahmadi, E., Gholami, M., Farzadkia, M., Nabizadeh, R., and Azari, A. (2015) Study of moving bed biofilm reactor in diethyl phthalate and diallyl phthalate removal from synthetic wastewater. Bioresource Technology, 183, 129-135.

[22] Ning, Y. F., Chen, Y. P., Shen, Y., Zeng, N., Liu, S. Y., and Guo, J. S. (2014) A new approach for estimating aerobic–anaerobic biofilm structure in wastewater treatment via dissolved oxygen microdistribution. Chemical Engineering Journal, 255(6), 171-177.

[23] Boon, N., Windt, W. D., Verstraete, W., and Top, E. M. (2002) Evaluation of nested PCR-DGGE (denaturing gradient gel electrophoresis)

with group-specific 16S rRNA primers for the analysis of bacterial communities from different wastewater treatment plants. FEMS Microbiol Ecol, 39(2), 101-112.

[24] Rowan, A. K., Snape, J. R., Fearnside, D., Barer, M. R., Curtis, T. P., and Head, I. M. (2003) Composition and diversity of ammonia-oxidising bacterial communities in wastewater treatment reactors of different design treating identical wastewater. FEMS Microbiology Ecology, 43(2), 195-206.

[25] Yang, Q., Wang, J., Han, X., Xu, Y., Liu, D., and Hao, H. (2014) Analysis of the bacterial community in a full-scale printing and dyeing wastewater treatment system based on T-RFLP and 454 pyrosequencing. Biotechnology and Bioprocess Engineering, 19(1), 191-200.

[26] Tamboli, D. P., Kagalkar, A. N., Jadhav, M. U., Jadhav, J. P., and Govindwar, S. P. (2010) Production of polyhydroxyhexadecanoic acid by using waste biomass of Sphingobacterium sp. ATM generated after degradation of textile dye Direct Red 5B. Bioresource Technology, 101(7), 2421-2427.

[27] Zhao, Y., Fang, Y., Jin, Y., Huang, J., Ma, X., and He, K. (2015) Microbial community and removal of nitrogen via the addition of a carrier in a pilot-scale duckweed-based wastewater treatment system. Bioresource Technology, 179, 549-558.

[28] Rabus R., Kube M., Heider J., Beck A., Heitmann K., Widdel F., and Reinhardt R. (2005) The genome sequence of an anaerobic aromatic-degrading denitrifying bacterium, strain EbN1. Archives of Microbiology, 183(1), 27-36.

[29] Percival, S.L. and Williams, D.W. (2014) Microbiology of Waterborne Diseases (Second Edition).

[30] Lee, C., Kim, J., Hwan, K. and Hwang, S. (2009) Fermentation and growth kinetic study of Aeromonas caviae under anaerobic conditions. Applied Microbiology and Biotechnology, 83(4), 767-773.

[31] Caldwell, M.E., Allen, T.D., Lawson, P.A. and Tanner, R.S. (2011) Tolumonas osonensis sp. nov., isolated from anoxic freshwater sediment, and emended description of the genus Tolumonas. International Journal of Systematic and Evolutionary Microbiology, 61(11), 2659-2663.

Received: **09.05.2016**
Accepted: **03.04.2017**

CORRESPONDING AUTHOR

Yuewu Pu
Guangzhou Higher Education Mega Centre
382 Zhonghuan Road East
Panyu District,
Guangzhou, 510006 – P.R. CHINA

E-mail: g96123@scut.edu.cn

© by PSP Volume 26 – No. 10/2017 pages 5717-5722 Fresenius Environmental Bulletin

THE USAGE OF AUXINS WITH VARIOUS CULTURAL TECHNIQUES TO INCREASE FRUIT SIZE IN STAR RUBY GRAPEFRUIT

Turgut Yesiloglu, Salih Koc, Berken Cimen*

Cukurova University, Faculty of Agriculture, Department of Horticulture, 01330, Adana, Turkey.

ABSTRACT

Fruit size is a key parameter for quality and increases the profitability for export markets in citrus production in Turkey. Fruit size can be enhanced by several techniques such as girdling and thinning. Various plant growth regulators are known to affect the growth and size of citrus fruit. Thus the effects of synthetic auxin applications (2,4-DP and 3,5,6-TPA) at different physiological periods, girdling practices, pruning practices, foliar application of potassium and various combinations of these practices on the fruit size and yield, fruit retention rate, and leaf chlorophyll concentration and fluorescence of Star Ruby grapefruit cultivar were investigated. As a result of pomological observations, treatments had different effects on fruit size and yield. The highest yield per tree were determined in Maxim (3,5,6-TPA) and Citrimax (2,4-DP) (605.33 and 601.83 kg/tree) treatments. The highest fruit diameter was determined from foliar spray of K (83.25 mm) on leafs whereas the lowest was obtained from control samples with 78.96 mm. The highest leaf chlorophyll concentration was determined in the leaf treated with foliar spray of K.

KEYWORDS:
Citrus, 3,5,6-TPA, 2,4-DP, yield, quality

INTRODUCTION

The cultivation of citrus fruits in Turkey is a traditional agricultural practice that has taken place for centuries, especially in the southern parts of the Taurus Mountains along the Mediterranean coast. In 2013, 3.681.158 million tons of citrus fruits were produced in Turkey. This amount consisted of 1.781.258 tons of oranges, 942.226 tons of mandarins, 726.283 tons of lemons and 228.799 tons of grapefruit [1]. The east Mediterranean Region produces 80% of Turkey's total citrus fruit and 99% of the grapefruit. The main grapefruit (*Citrus paradisi*) variety grown in Turkey is the 'Star Ruby' cultivar. In recent years, there has been a large increase in the exportation of citrus fruits, especially grapefruit. The planting of the 'Star Ruby' grapefruit has been extended in regions of Turkey that are already developed in terms of citriculture. The 'Star Ruby' grapefruit is desirable due to characteristics such as seedlessness, shape, smooth rind, color and taste. However, small fruit size is a common problem in 'Star Ruby' grapefruit, especially in the older trees of Star Ruby. Moreover, small fruit size is the main factors limiting the sales of Star Ruby grapefruit; thus, large fruit brings higher prices in the export market [2-3]. Consumers prefer large fruits; thus, there is a significant price difference between large and small fruits [4-6].

In terms of determining profitability, fruit size in citrus fruit has become as important as the yield. This phenomenon is readily apparent for small mandarin fruits, as well as lemons, sweet oranges and large grapefruit species [5]. Fruit size is affected by many factors including irrigation management, soil type, rootstock and ecological variables, which cannot be controlled by the producer. Moreover, fruit size is inversely proportional to yield and fruit number [7]. The availability of carbohydrates (increases fruit size), flower intensity (decreases fruit size), competition between flowers/fruitlets (decreases fruit size) and abiotic stresses (decrease fruit size) are the most important factors affecting the final fruit size of citrus fruits [8-10].

Synthetic auxins can be applied to increase fruit size [11-12]. Applying synthetic auxins during the cell division stage of fruit development significantly reduces the number of fruits and increases the final fruit size by reducing the competition for carbohydrates between fruitlets [8]. Synthetic auxins such as 2,4-dichlorophenoxy acetic acid (2,4-D), 2,4,5-trichlorophenoxy acetic acid (2,4,5-T), naphthalene acetic acid (NAA) and 2,4-dichlorophenoxypropionic acid (2,4-DP) have been shown to increase fruit size [3-4, 13-14]. In addition, cultural treatments such as pruning, irrigation and fertilization can be optimized in order to increase fruit size. For instance, techniques such as girdling [15] and thinning [5, 11, 16-17] are used in citrus production to increase fruit size.

Thus the effects of synthetic auxin applications (2,4-DP and 3,5,6-TPA) at different physiological periods, girdling practices, pruning practices, foliar

application of potassium and various combinations of these practices on the fruit size and yield, fruit retention rate, and leaf chlorophyll concentration and fluorescence of Star Ruby grapefruit cultivar were investigated in the present study.

MATERIALS AND METHODS

Trees and Treatments. The experiments were conducted on 20-year-old Star Ruby grapefruit trees planted on sour orange rootstock at 8 m x 8 m intervals at the Research Station of Cukurova University, Agricultural Faculty Citrus Experiment Station, Adana (Latitude, 35° 23′ N; Longitude, 36° 50′ E; altitude 27 m) during 2011. The trees were managed and selected for uniformity and crop load. In the experimental area, the soil was a clay loam (55% clay, 22% silt and 23% sand containing 11% $CaCO_3$), and the soil pH was between 7.29 and 7.37 at a depth of 0 cm – 90 cm. The trial was organized in a randomized complete block design with 10 replicates for each treatment.

T1: 2,4-DP (Citrimax, 50 g of dichlorophenoxypropionic acid per L) was applied to the entire tree at concentration of 150 ppm 3 weeks after full anthesis when the average fruit diameter was 13-15 mm. T2: 3,5,6-TPA (Maxim, 3,5,6-trichloro-2-piridil-oxi acetico, 10% (v/v), 1 tablet = 10 g) was applied to the entire tree at concentration of 20 ppm when the 85% of the average fruit diameter was higher than 22 mm. T3: First girdle was applied at the end of anthesis, and the second one was applied just after the June fruit drop. Thickness of the girdle was 4 mm in both applications. T4: Hand pruning was applied in the middle of February. T5: Mechanical pruning was applied in the middle of February in both side of the trees. T6: KNO_3 was applied at a concentration of 4% two times in the experiment by foliar spray to entire tree. First treatment was 6-8 weeks after full anthesis and the second one was applied in at the beginning of September. T7, T8 and T9 was performed by combining the selected treatments described above (see Table 1). T10: Control trees left without any of these treatments except fertigation and a recommended pest management program for grapefruits.

Fruit Yield, Size and Retention Rate. The fruit was harvested at the optimal harvest time (in October). The yield per tree (kg/tree) was obtained by weighing the harvested fruit. Tree height and canopy diameter in the two tree directions (to obtain the average diameter) were measured after harvesting. Canopy volume (CV) was calculated according to the equation reported by Turrell [18] as follow: CV = 0.5248 x canopy height x canopy diameter^2. In addition, scion trunk circumferences were measured 10 cm above the bud union. The scion trunk circumferences were converted into trunk cross-sectional area (TCSA). Yield efficiency was estimated as the ratio of fruit yield to canopy volume (kg/m^3) and trunk cross sectional unit area (kg/cm^2).

A random sample of 50 fruits from each tree was selected and marked on the branches in order to determine the average fruit size. The fruit was sized using a digital caliper (Mitutoyo CD-15CPX) at the equatorial diameter and graded according to the following commercial size classes: > 93 mm (class 1), 89 - 93 mm (class 2), 84 - 89 mm (class 3), 80 - 84 mm (class 4) and, < 80 mm (class 5) (MEA, 2009). In order to determine the fruit retention rate, the number of flowers, fruitlets and fruits were recorded during full blossom, fruitlet abscission (a couple of weeks after bloom), the June drop and pre-harvest drop. The observations were made on four randomly selected branches from the four quadrants (north, south, east, and west) of every tree.

Leaf Chlorophyll Concentration and Fluorescence. Leaf chlorophyll concentration was estimated by SPAD readings (SPAD-502 meter, Minolta Inc., Osaka, Japan) on five fully expanded young Star Ruby leaves (4th–5th leaf from the shoot apex) per each replicates. SPAD readings were used to estimate leaf Chl concentration because there is a strong relationship between SPAD readings and chlorophyll levels in citrus leaves [19]. Chlorophyll fluorescence parameter (*Fv'/Fm'*) = (Quantum yield in light adapted leaves) was measured with a portable fluorimeter (FluorPen FP100, Photon System Instruments Ltd, Drasov, Czech Republic) on five fully expanded young leaves (4th–5th leaf from the shoot apex) per each replicates.

Statistical Analysis. The experiment was arranged as 10 x 10, ten treatments, ten replicates, respectively, in a 'Complete Randomized Design'. Data were subjected to one-way analysis of variance (ANOVA) using SAS statistical software (SAS v9.0). The percentages recorded in fruit retention variable were analyzed after arc-sin transformation. To compare the means, a Tukey's multiple range test was performed to determine if the differences between treatments were significant at a confidence level of $P < 0.05$.

RESULTS AND DISCUSSION

Fruit Yield, Retention Rate and Size. The usage of auxins with various cultural techniques significantly affected fruit yield. As shown in Table 2, fruit yield of Star Ruby grapefruit had ranged between 393.75 kg/tree and 605.33 kg/tree regarding different treatments. The highest fruit yield per tree was obtained from T2, T1, T3, T4, T9, T6, T7, T8 treatments, respectively. These treatments were grouped in the same subset according to a Tukey's range (P<0.05). A foliar spraying treatment of 3,5.6-TPA

at the concentration of 20 ppm (T2) resulted the highest fruit yield per tree among these treatments. The lowest fruit yield was obtained from control trees. In addition, effects of treatments on yield efficiency (kg/cm^3 and kg/m^2) were found to be statistically significant considering canopy volume and trunk cross sectional unit area at a significance level of α=0.05 and α=0.01, respectively (Table 2). Regarding canopy volume, the highest fruit yield efficiency was determined in trees treated with T4 (11.528 kg/cm^3) whereas the lowest yield efficiencies were obtained from the trees treated with T3 (7.612 kg/cm^3) and C (7.500 kg/cm^3). As shown in Table 2, the lowest fruit yield, regarding trunk cross sectional unit area, also was determined in control trees (0.582 kg/cm^2) whereas the highest yield efficiencies were obtained from T1, T2, T3, T6 and T7. According to the results obtained in the present study, using synthetic auxins, double girdling and foliar spraying of K had increased the fruit yield significantly. Similar results were obtained by Chao et al. [20], who studied Fina Sodea Clementine mandarins, and found that a post-bloom application of 2,4-D (2,4-Dichlorophenoxyacetic acid) significantly increased the yield. Similarly, a significant increase in the fruit number per tree of Valencia and Shamouti oranges was obtained when 2,4-D (20 ppm) was applied 6-8 weeks after full bloom [21] and 2,4-DP application increased total yield of Valencia orange [3, 22].

TABLE 1
Treatments conducted at the experimental orchard

No	Treatment Code	Treatment
T1	2,4-DP	2,4-DP
T2	3,5,6-TPA	3,5,6-TPA
T3	DG	Double girdling
T4	HP	Hand pruning
T5	MP	Mechanical pruning
T6	K	Potassium treatment (KNO_3)
T7	K+DG	KNO_3 + Double girdling
T8	3,5,6-TPA+DG	3,5,6-TPA + Double girdling
T9	MP+DG	Mechanical pruning + Double girdling
T10	C	Control

TABLE 2
Effects of treatments on fruit yield (kg/tree), yield efficiency (yield/TCSA and CV) and fruit diameter (mm) of the Star Ruby grapefruit trees.

Treatment	Fruit yield (kg/tree)	Yield efficiency		Fruit diameter (mm)
		kg/cm^3	kg/cm^2	
2,4-DP	601.83 a[1]	10.423 ab	0.964 a	82.06 abc[y]
3,5,6-TPA	605.33 a	11.133 ab	0.935 a	82.77 ab
DG	589.00 a	7.612 c	0.956 a	81.23 a-d
HP	568.33 a	11.528 a	0.748 ab	83.23 a
MP	489.67 ab	9.604 abc	0.788 ab	80.22 bcd
K	561.00 a	9.383 abc	0.855 a	83.25 a
K+DG	564.14 a	9.090 bc	0.831 a	82.74 ab
3,5,6-TPA+DG	554.67 a	9.795 abc	0.813 ab	83.05 a
MP+DG	556.00 a	10.918 ab	0.814 ab	79.85 cd
C	393.75 b	7.500 c	0.582 b	78.96 d
Significance[2]	**	*	**	**
$D_{\%5}$	*131.980*	*2.104*	*0.179*	*2.557*

[1]Values within the columns followed by unlike letters are significantly different by Tukey's multiple range test at α=0.05.

[2]*: significant at 0.05 level; **: significant at 0.01 level.

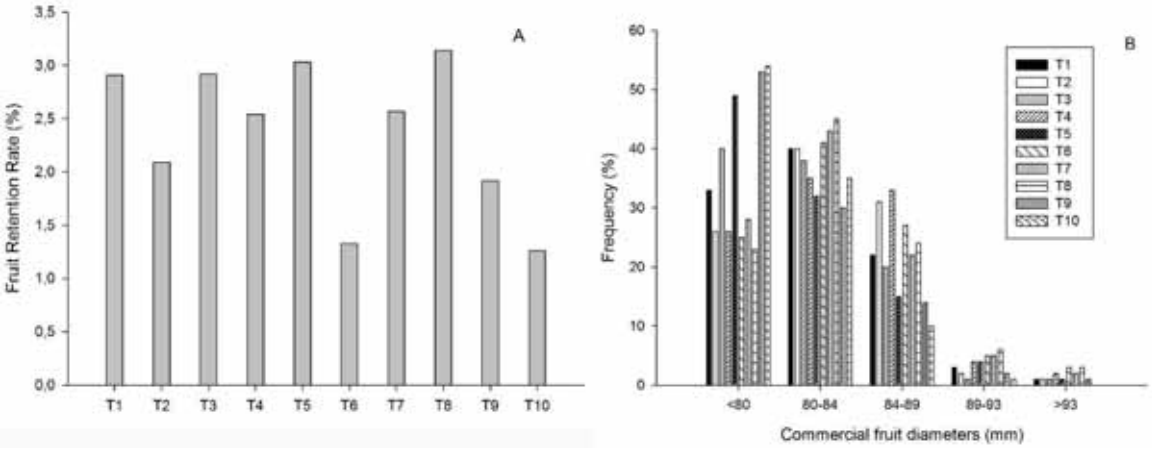

FIGURE 1
Effects of treatments on fruit retention rate (%) of the diameter of Star Ruby grapefruits at harvest (A). Frequency distribution of the diameter of Star Ruby grapefruits at harvest (B).

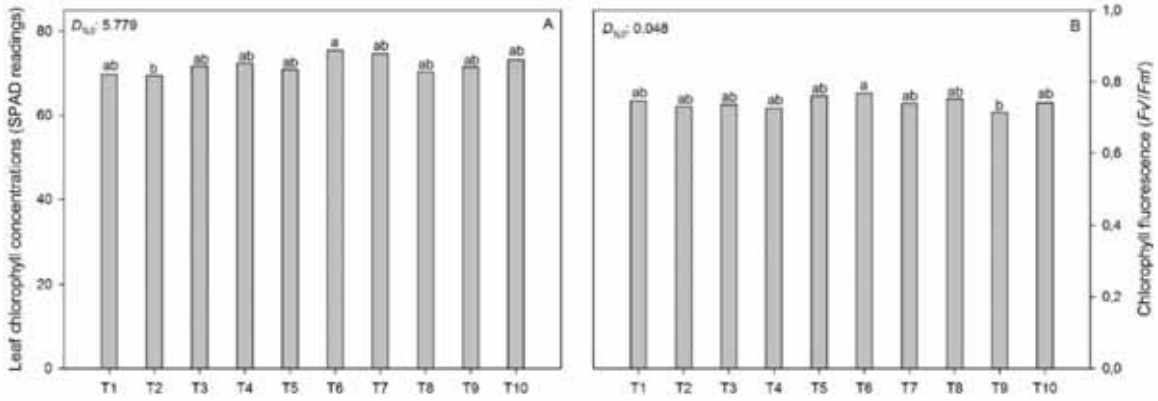

FIGURE 2
Effects of treatments on chlorophyll concentrations (SPAD readings) (A) and chlorophyll fluorescence (*Fv'/Fm'*, in light adapted stage) efficiency (B) of Star Ruby grapefruit.

Fig. 1A shows the effects of different treatments on the fruit retention rate of Star Ruby fruits. According to a one-way ANOVA conducted to the retention rate data after arc sin transformation, there were no significant differences on the fruit retention rate among the treatments (data not presented). However, when the fruit retention percentages were examined without arc sin transformation, it can be said that markable differences were observed among treatments. In the present study, the fruit retention rates ranged between 1.26% (control treatment) and 3.14% (3,5,6-TPA + DG treatment) as shown in Fig. 1A. All treatments conducted in this study had resulted higher fruit retention rate in comparison with the control trees. The application of mechanical pruning, double girdling and synthetic auxins led to an increase in the fruit retention rate. Specifically, the application of 20 ppm 3,5,6-TPA together with double girdling resulted in high fruit retention rates. In addition, this study showed that application of synthetic auxins did not have a thinning effect on the trees, and an increase in the fruit retention rate was observed in comparison with the control treatment. The results obtained in the present study are in concordance with those of Saraswathi et al. [23], who demonstrated that the highest fruit retention rate was obtained (28.32%) from trees treated with 20 ppm 2,4-D. In comparison, the fruit retention rate of the control trees in the aforementioned study was only 20.32%. In a previous study, the application of 2,4-D delayed the abscission of navel oranges [24]. Moreover, foliar applications of 2,4-DP significantly reduced abscission in mature Washington navel sweet oranges [25].

In terms of fruit diameter distribution at maturity, treatments had significant effects on fruit diameter at a significance level of α=0.05 (Table 1). All treatments had higher fruit diameter in comparison with fruits obtained from control trees as presented in Table 1. Star Ruby fruits obtained from hand pruned (83.23 mm), K sprayed (83.25 mm) and 3,5,6-TPA+DG (83,05 mm) trees had the highest

fruit diameter at maturity. In this study, the lowest fruit diameter was obtained from the fruits of control trees and recorded as 78.96 mm. The results indicated that all treatments inspected in this study had positive effects on fruit diameter and increased the fruit size. Fruit size is one of the most important factors affecting the marketing of fresh citrus fruits. Thus, synthetic auxins are commonly used to increase the size of fruit for fresh consumption together with fruit thinning and pruning. In previous studies, fruits harvested from trees treated with 2,4-DP were significantly larger than that of the control trees, indicating that the application of 2,4-DP and 2,4-D increased fruit size [6, 14, 20-22, 25-26]. Also, according to El-Otmani et al. [14], 2,4-DP improved fruit size by affecting juice sac development through an enhancement of cell enlargement rather than cell division. Similar results have also been reported for other auxins. For instance, applications of 10-20 ppm 3,5,6-trichloro-2-pyridiloxyacetic acid (3,5,6-TPA) increased the fruit size of Fino lemons [27], satsuma mandarins [4] and Clementine mandarins [8].

Fig. 1B shows the effects of treatments conducted in this study on the distribution of the crop within commercial fruit size classes. In this study a total of 3250 fruits were analyzed in terms of their diameter in order to obtain the frequency distribution. The results showed that 1157 fruits (35.60%) were smaller than 80 mm diameter, 1229 fruits (37.82%) were between 80-84 mm diameter, 708 fruits (21.79%) were between 8489 mm diameter, 110 fruits (3.38%) were between 89-93 mm diameter and 46 fruits (1.41%) were larger than 93 mm diameter.

Leaf chlorophyll concentration and fluorescence. The SPAD measurements were used as an estimate of leaf chlorophyll concentration, because there is a positive linear relationship between these two parameters ($r^2 > 0.8$, [19]). In the present study, there were significant effects ($p \leq 0.05$) on leaf Chl concentrations among treatments. The lowest Chl concentration was determined in the leaves treated with 3,5,6-TPA, whereas the leaves of shoots treated with a foliar spray of potassium at a concentration of 4% had the highest Chl concentration. Furthermore, all the other treatments were grouped the same subset according to a Tukey's multiple range test at $\alpha=0.05$ (Fig. 2A).

As shown in Fig. 2B, there were differences in Star Ruby leaves among treatments in terms of chlorophyll fluorescence. The highest *Fv'/Fm'* ratio was recorded in leaves treated with a foliar spray of potassium at a concentration of 4% (0.7682) whereas the lowest *Fv'/Fm'* ratio was determined in MP + DG treatment (0.7133). The rest of the treatments were grouped the same subset according to a Tukey's multiple range test at $\alpha=0.05$, resulting as the same effect on leaf PSII activity (Fig. 2B).

CONCLUSIONS

In this study, we tried to describe how fruit yield and size affected by the usage of auxins with various cultural techniques. As a conclusion regarding the parameters estimated in this study, treatments had positive effects on fruit yield and size in Star Ruby grapefruit. According to the results, foliar spraying of 3,5,6-TPA at a concentration of 20 ppm and 2,4-DP at a concentration of 150 ppm had increased the fruit yield up to fifty percent in comparison with the control trees. In addition foliar spraying of 4% potassium increased the leaf Chl concentration and fluorescence. Considering the fruit number in the frequency distrubition of commercial fruit diameter at class 84-89 mm, all treatments had better results than control trees in terms of diameter.

ACKNOWLEDGEMENTS

Special thanks are due to the Cukurova University, Scientific Research Projects Coordinating Office (project CU-BAP-ZF2011YL12) for supporting the present study.

REFERENCES

[1] FAO (2015) Food and agriculture organization. The database of annual production. FAOSTAT. Statistical database. http://faostat.fao.org.

[2] Yildirim, B., Yesiloglu, T., Incesu, M., Kamiloglu, M., Ozguven, F., Tuzcu, O. and Aka Kacar, Y. (2010) The effects of mechanical pruning on fruit yield and quality in 'Star Ruby' grapefruit. Journal of Food, Agriculture & Environment. 8(2): 834-838.

[3] Yildirim, B., Yesiloglu, T., Incesu, M., Kamiloglu, M., Cimen, B. and Tamer, S. (2012) Effects of 2,4-DP (2,4-dichlorophenoxypropionic acid) plant growth regulator on fruit size and yield of Valencia oranges (*Citrus sinensis* Osb.). New Zealand Journal of Crop and Horticultural Science, 40(1), 55-64.

[4] Agusti, M., Almela, V., Juan, M., Primo-Millo, E., Trenor, I. and Zaragoza, S. (1994) Effects of 3,5,6-trichloro-2-pyridyloxyacetic acid on fruit size and yield of clausellina mandarin (*Citrus unshiu* Marc.). Journal of Horticultural Science 69(2): 219-223.

[5] Guardiola, J.L., and Garcia-Luis, A. (2000) Increasing fruit size in Citrus. Thinning and stimulation of fruit growth. Plant Growth Regulation 31: 121-132.

[6] Erner, Y., Tagari, F., Hamou, M. and Katzir, I. (2004) Enhancing citrus fruit size: An overview of opportunities and achievements in Israel. Proc. Int. Soc. Citriculture 2: 495-501.

[7] Guardiola, J.L. (1997) Increasing citrus fruit size with synthetic auxins. In: Futch, S.H. and Kender, W.J. (eds.) Citrus Flowering and Fruiting Short Course. Univ. of Florida. 79-86.
[8] Agusti, M., El-Otmani, M., Aznar, M., Juan, M. and Almela, V. (1995) Effect of 3,5,6-trichloro-2-pyridyloxyacetic acid on Clementine early fruitlet development and on fruit size at maturity. Journal of Horticultural Science 70(6): 955-962.
[9] Goldschmidt, E.E., and Koch, K.E. (1996) Citrus. In: Zamski, E. and Schafer, A.A. (eds.), Photoassimilate distribution in plants and crops. Source-sink relationships. Marcel Dekker, Inc., New York, pp.797-823.
[10] El-Otmani, M., Coggins, C.W., Agusti, M. and Lovatt, C. (2000) Plant growth regulators in citriculture: World current uses. Critical Reviews in Plant sciences. 19: 395-447.
[11] Wheaton, T.A. (1981) Fruit thinning of Florida mandarins using plant growth regulators. Proc. Int. Soc. Citriculture 1: 263-268.
[12] Gallasch, P.T. (1988) Chemical thinning of heavy crops of mandarins to increase fruit size. Proc. 6th Int. Citrus Congress 1: 395-405.
[13] Guardiola, J.L., Agusti, M., Garcia-Mari, F. and Almela, V. (1982) The regulation of fruit size in citrus by tree factors. XXIst Int. Hortic. Congress. 1:1363 (Abst. No).
[14] El-Otmani, M., Agusti, M., Aznar, M. and Lmela, V. (1993) Improving the size of Fortune mandarin fruits by auxin 2,4-DP. Scientia Horticulturae 55(3-4): 283-290.
[15] Cohen, A. (1984) Citrus fruit enlargement by means of summer girdling. J. Hortic. Sci. 59:119-125.
[16] Hirose, K. (1981) Development of chemical thinners for commercial us efor satsuma mandarin in Japan. Proc. of Int. Soc. of Citriculture 1: 256-260.
[17] Zaragoza, S., Tenor, I., Alonso, E., Primo-Millo, E. and Agusti, M. (1992) Treatments to increase the final fruit size on Satsuma Clausellina. Proc. Int. Soc. Citriculture 2: 725-728.
[18] Turrel, F.M. (1946) Tables of surfaces and volumes of spheres and of prolate and oblate spheroids and spheroidal coefficients. University of California, Press. Berkeley.
[19] Jifon, J.L., Syvertsen, J.P. and Whaley, E. (2005) Growth environment and leaf anatomy affect nondestructive estimates of chlorophyll and nitrogen in Citrus sp. leaves. Journal of American Society Horticulture Science 130: 152–158.
[20] Chao, C.T., Lowatt, C. and Ferguson, L. (2004) Effcacy of plant growth regulators and fertilizers to increase fruit set and fruit size of Fina Sodea Clementine mandarins in California. Proc. Int. Soc. Citriculture 2: 547.
[21] Erner, Y., Kaplan, Y., Artzi, B. and Hamou, M. (1993) Increasing citrus fruit size using auxins and potassium. Acta Horticulturae 329: 112-119.
[22] Greenberg, J., Eshel, G. and Gotfreed, A. (1996) Effects NAA, 2,4-D and 2,4-DP on yield, fruit size and creasing of Valencia orange. Proc. Int. Soc. Citriculture 2: 934-937.
[23] Saraswathi, T., Rangasamy, P. and Azhakiamanavalan, R.S. (2003) Effect of preharvest spray of growth regulators on fruit retention and quality of mandarins. South Ind. Hort. 51(1/6): 110-112.
[24] Stewart, W.S. and Klotz, L.J. (1947) Some effects of 2,4- dichlorophenoxypropionic acid on fruit drop and morphology of oranges. Bot. Gaz. 109: 150-162.
[25] Agusti, M., Juan, M., Martinez-Fuentes, A., Mesejo, C. Reig, C. and Almela, V. (2006) Application of 2,4-dichlorophenoxypropionic acid 2-ethylhexyl ester reduces mature fruit abscission in *Citrus* navel cultivars. Journal of Horticultural Science & Biotechnology 81(3): 532-536.
[26] Fang, J.G., Wu, C.J., Zheng, Y.S. and Chao, C.T. (2008) Application of 2,4-D for fruit size and yield increase of W. Murcott mandarin and Minneola tangelo in California. 11th Int. Citrus Congress. 26-30 October 2008, China. Abs. No: 158. p 81-82.
[27] Garcia-Lidon, A., Porras-Castillo, I., Ortiz Marcide, J. and Molina, R. (1992) Early harvesting of Fino lemon using a new synthetic auxin. Proc. Int. Soc. Citriculture 1: 473-474.

Received: **20.07.2016**
Accepted: **31.07.2017**

CORRESPONDING AUTHOR

Berken Cimen
Cukurova University,
Faculty of Agriculture,
Department of Horticulture,
Adana 01330 – TURKEY

E-mail: bcimen@cu.edu.tr
berken@mailzf.cu.edu.tr

© by PSP Volume 26 – No. 10/2017 pages 5723-5731 Fresenius Environmental Bulletin

LOW COST MESO-POROUS CARBON DEVELOPED FROM JATROPHA HUSK, A BIO-DIESEL BYPRODUCT WASTE FOR ADSORPTION OF METHYLENE BLUE

Alagarasan Jagadeesh Kumar[1,2], Rajendra Prasad Singh[1,*], Dafang Fu[1] , Chinnaiya Namasivayam[2]

[1]Department of Municipal Engineering, Southeast University, Nanjing, Jiangsu 210096, China
[2]Department of Environmental Sciences, Bharathiar University, Coimbatore 641 046, India

ABSTRACT

The adsorption of Methylene Blue (MB) dye from aqueous solution using Jatropha husk mesoporous activated carbon was investigated. The structural, chemical and morphologies of the prepared Jatropha husk carbon (JHC) were characterized by different analytical techniques including Scanning Electron Microscopy (SEM), X-ray powder diffraction (XRD), Fourier Transform Infrared Spectroscopy (FTIR) and Batch adsorption experiments were carried out and the parameters investigated include effect of time, dose, pH and temperature. The JHC equilibrium adsorption data were analyzed using two widely applied kinetics and isotherms: first order and second order kinetics, Langmuir, Freundlich and Dubinin-Radushkevitch (D-R) isotherms. The results revealed that kinetics well fit with current findings. The JHC have the maximum adsorption capacity (Q_0) of about 66.66 mg g^{-1}, obeying Freundlich isotherm. Kinetics analysis was conducted using first and second-order kinetics models and intraparticle model. The adsorption kinetics better obeyed second-order model. The activation energy of system (E) was calculated as 10 $kJmol^{-1}$. Thermodynamic parameters e.g. standard enthalpy (ΔH^o), standard entropy (ΔS^o) and standard free energy (ΔG^o) with regard to temperature effect were also studied. The adsorption was found to be endothermic in nature. Alkaline pH was constructive for the adsorption of MB. The pH effect and desorption studies showed that ion-exchange mechanism seems to be the major mode of adsorption for MB.

KEYWORDS:
Activated Carbon, Adsorption Kinetics, Isotherms, Jatropha Husk, Methylene Blue, FTIR, XRD, SEM.

INTRODUCTION

Environmental pollution has been increased in recent years with increasing industrial and urban development. The textile industry plays vital role in the economy of developing countries across the world. Dyeing is an essential operation during textile fibre processing. This process cause the fabrication of more or less colored wastewaters, depending on the quantity of fixation of the dyestuffs on the substrates, which difference with the nature of the substances, the preferred strength of coloration, and the main application method [1]. Dye manufacturing process industries, pulp and paper mills, tanneries, distilleries, food processing industries and host of other manufacturing industries discharge the colored wastewater pollution [2]. Methylene blue (MB) is the widely used stuff for dying wood, silk and cotton. While MB is not strongly harmful, it can cause some damaging effects. Critical exposure to MB can cause increased heartbeat rate, vomiting (emesis), shock, jaundice, cyanosis, and tissue necrosis in humans [3]. Therefore, removal of such dyes from processed effluents becomes environmentally important. The discharge of dyes to the environment is a matter of concern for toxicological and esthetical reasons, causing severe water contamination problems to aquatic life due to reduced light penetration [4-5]. There are several processes accessible for the removal of dye by conventional treatment technologies including biological and chemical oxidation, foam flotation, biodegradation, advanced oxidation, photocatalysis [6]. Among these techniques adsorption method is considered as the better treatment of dyeing wastewater based on its higher efficiency, lower cost, simple operation, insensitive to toxic substance, etc. The traditional absorbent is commercial activated carbon. However, the higher cost and complicated production technology of activated carbon limited its wildly application [7]. A low-cost and more easily available adsorbent would formulate the removal of pollutants an economically viable alternative [8]. The cost effect involved look for alternative adsorbent that could provide an economical solution is very important for developing countries [9].

Many studies have been made on use of different adsorbents materials for ACs like, coir pith, banana pith, peanut hull, orange peel, peat, sawdust, bagasse pith, rice husk, fenugreek mucilage and various blends of these. However search for cost-effective, efficient adsorbent is continuing. Large quantities of Jatropha husk (JH) is generated as an agro-industrial solid waste in to the bio-diesel by product industries. JH constitutes nearly 80% of the dried

vegetable [10]. The JH Waste biomass have been utilized by many researchers for adsorption of MB using agriculture solid waste activated carbons prepared by different activators such as such as periwinkle shells by KOH [11], rice husk by H_2SO_4 [12], commercial activated carbon by NaOH [13], thermally activated coir pith carbon [14], harmal seeds residue by HNO_3 [15], rice husk by HCL [16], $ZnCl_2$ coir pith carbon [17], bone char [18], $ZnCl_2$ Activated buriti shells [19]. In the present study, a novel adsorbent Jatropha husk carbon was investigated for its efficiency in the removal of dye, namely MB, from aqueous solution.

MATERIALS AND METHODS

Jatropha husk was collected from Tamil Nadu Agricultural University, Coimbatore, India. The dry raw material (JH) was washed with tap water and then washed with double distilled water to remove earthy impurities. It was dried in a hot air oven at 105 ± 5 °C for 8 h.

Physical method. The washed, dried and crushed JH was filled in a stain less steel container by a tight lid. This container was located in another concentric stain less steel container with another lid. The linear space was filled with sand which was consolidated layer by layer up to the brim of the outer container. The arrangement achieved a close to whole absence of exposure of the carbonizing material to air, allowing only a limited presence of O_2 trapped in the voids of the material being carbonized. This prepare set up was kept in a muffle furnace for 1 h at 800 ± 5 °C. After cooling, the carbon was washed with distilled water to remove impurities similar to tars. This material was subsequently oven-dried at 105 ± 5 °C for 8 h and sieved to 250-500 µm size (60-35 mesh ASTM) and designated as Jatropha Husk carbon (JHC) and stored in air tight plastic container.

Preparation of Methylene Blue (MB) Solution. Molecular formula of MB $C_{16}H_{18}CIN_3S$ with molecular weight is 319.85. It is water – soluble, which is blue in color (ʎmax, 665 nm). Prepare stock solution was dissolving an appropriate amount of MB in distilled water. The functioning solutions were prepared in diluting the stock solution with distilled water for appropriate concentration of the working solutions.

Experimental procedures. Adsorption experiments were carried out by agitating 25 mg of JHC with 50mL of dye solution of desired concentration and pH at 200 rpm, 35 °C in a thermo stated rotary shaker (ORBITEK, Chennai, India). MB concentration was estimated spectrophotometrically by monitoring the absorbance at 665 nm using UV- Vis Spectrophotometer (Specord 200, Analytic Jena, Germany). pH was measured using pH meter (Elico, model LI-127, Hyderabad, India). The dye solution was separated from the adsorbent by centrifugation at 2500 rpm for 30 min and its absorbance was measured. Effect of adsorbent dosage was studied with different adsorbent doses (25–200 mg) along with 50 mL of dye solution and agitated for equilibrium time. Langmuir, Freundlich, and Dubinin–Radushkevich (DR) isotherms were employed to investigate the equilibrium adsorption. Effect of pH was investigated by adjusting the pH of dye solutions using dilute HCI and NaOH solutions and the solutions were agitated with 25 mg/50 mL adsorbent dose at 140 min for all concentrations. Desorption investigated for the adsorbent were used for the adsorption of 100 and 120 mg L^{-1} of dye solution which was separated from the supernatant by centrifugation. The MB-loaded adsorbent were filtered by Whatman filter paper and washed softly with water to remove any unabsorbed dye. Several such samples were prepared and the spent adsorbent was agitated for 120 min with 50 mL of distilled water and adjusted to different pH values. The desorbed MB was estimated as before. For temperature studies, adsorption of all conc. of MB by 25 mg/50 ml adsorbent was carried out at 35, 40, 50 and 60 °C in a thermo stated rotary shaker.

Characterization. Structural studies and surface morphologies of the loaded and unloaded JHC were characterized by different analytical methods. Infrared spectrums of the samples were obtained by Fourier transform infrared spectroscopy (FTIR) (Bruker, Germany). The morphology and elemental analysis of loaded and unloaded JHC was examined by scanning electron microscope (SEM-JSM, 840A, JEOL, Japan). The carbon samples were filtered using a suction pump on qualitative filter paper and kept in a vacuum desiccator, which was used for further instrumental analysis.

RESULTS AND DISCUSSION

X-ray powder diffraction (XRD) pattern was used to analyze the crystallinity and phases of the as-prepared JHC from Jatropha husk (JH) activated by physically and MB adsorbed JHC. Figure 1 shows that there are two peaks centred around 26°and 43°, which are assigned to the reflection from the (002) plane and the overlapped reflections from the (100) and (101) planes, respectively. The appearance of the peak at around 26° confirmed the regularity of crystalline structure, which resulted in a better layer alignment. The crystalline carbonaceous structure in a typically, perhaps graphite, the interlayer distance among two adjacent carbon sheets is 0.335 nm. The peak corresponds to an interlayer distance of 0.338 nm, which is quite similar to that of graphite. Peaks at 20

and 44° were due to the creation of pores through the corrosion of carbon along the direction of the graphic structures. This produced relatively well-organized aromatic carbon that was more stable than amorphous-like carbon [20].

The FTIR spectra of the JHC and MB adsorbed JHC are shown in Fig. 1. A large number of peaks are present on FTIR spectrum of JHC and dyes loaded samples. It may be due to the availability of the volatiles such as lignin, fibre and hemi-cellulose. Generally, the locations of the hydrogen-bonded OH groups are usually in the range of 3200–3650 cm^{-1} for alcohols and phenols. The band at about 3435-3419 cm^{-1} is attributed to *ν*(O–H) vibrations. The band located around 2924 cm^{-1} corresponds to *ν*(C–H) vibrations in the methylene groups. The band at 1323 cm^{-1} can be attributed to υ(C–O) vibrations in carboxylate groups [21]. The bands among the 1300 and 900 cm^{-1} could be assigned to C–O stretching vibrations [22].The band 3500 cm^{-1} can be assigned to the O–H stretching mode of hydroxyl functional groups [23]. For JHC-MB, the band around 3431 cm^{-1} was shifted to ca. 3695 cm^{-1} and showed an increase of intensity. This band can be attributed to the N–H stretching combined with the O–H vibration. The band at 1584 cm^{-1} was shifted to ca. 1434 cm^{-1} and can be attributed to N–H vibration coupled with C–N stretching mode, indicating the saturation of the material with MB dye. The decrease in the group at ca. 600 cm^{-1} may be due to the interaction of MB with aromatic rings of JHC.

Morphology of JHC and MB loaded JHC observed through SEM micrographs Fig. 2(a, b) shows tremendous, perfect and constructed pore structure on top of the surface JHC. The carbon is compressed and the lanky structure is due to the formation of more interspaces between mono layers of the carbon by activation of thermal JHC. The SEM picture of JHC clearly shows honeycomb void structure similar to that of char based carbon. Basically, the high surface area and pore structure are the basic parameters for an effective adsorbent. It showed that the dye was strongly adsorbed on the surface of the JHC as shown in Fig. 2(c, d).

Initial pH of the MB solutions with various concentrations (100 - 180 mg L^{-1}) was varied from 2.0 to 10, by adding either 0.1 N Sodium hydroxide (NaOH) or 0.1 N hydrochloric acid (HCl) solutions, to assess the effect of pH on the dye adsorption onto the JHC. Figure 3(c) shows the effect of initial pH on the adsorption of MB onto JHC. The percent adsorption of MB was at pH 2.0 and higher at pH 10. At pH 10, negatively charged surface sites on the adsorbent favor the adsorption of dye cations due to the electrostatic attraction and hence dye removal was high (more than 20%) for JHC adsorbents. Basically, cationic dyes are produce an intense molecular cation (C^+) and reduced ions (CH^+). At higher pH, the OH^- ions on the surface of adsorbent obey the removal of cationic dye molecules. Earlier studies have reported that the % adsorption of MB usually increases with increase in the pH [24-26].

Desorption studies as a function of pH were conducted to analyze the possibility of reuse of the adsorbent for further adsorption and to make the process more effective and economical. At lower pH the hydrogen ion (H^+) concentration increases in solution, which then displaces adsorbed dye cations into solution. The percent desorption decreased from 7.80 % at pH 2.0 to 4.26 % at pH 10 for the dye concentrations of 100 and 120 mg L^{-1}as shown in Fig. 3(d) [27]. The reversibility of adsorbed dyes is in agreement with the pH depenant results obtained. Desorption of dye at lower pH indicates that adsorption of MB onto JHC may be due to ion exchange mechanism [28].

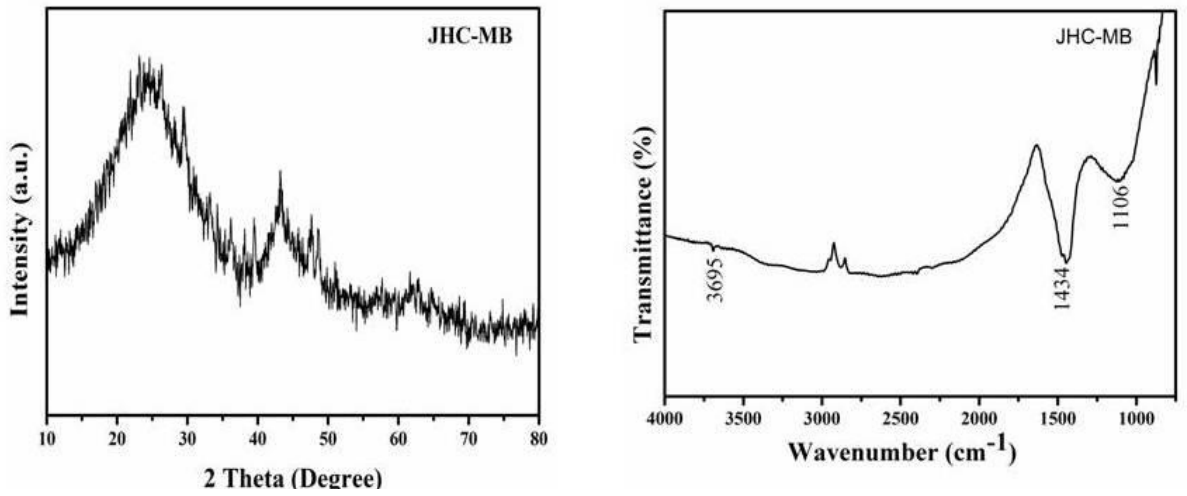

FIGURE 1
MB after adsorption of X-ray patterns and FTIR of JHC

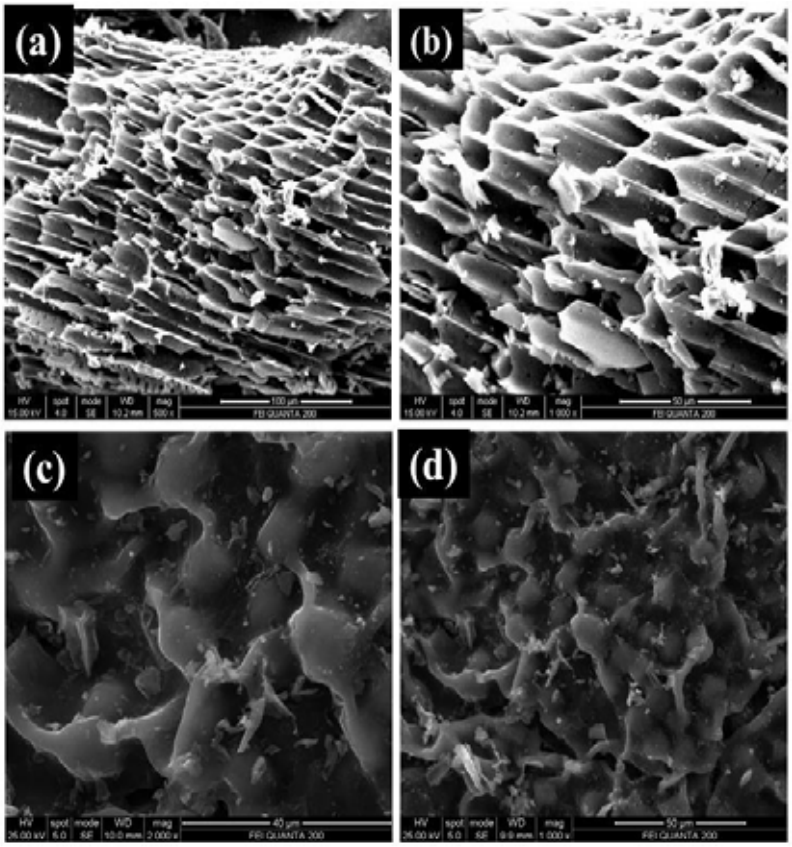

FIGURE 2
SEM with different magnification images of (a, b) Raw JHC; and (c, d) JHC with adsorbed MB

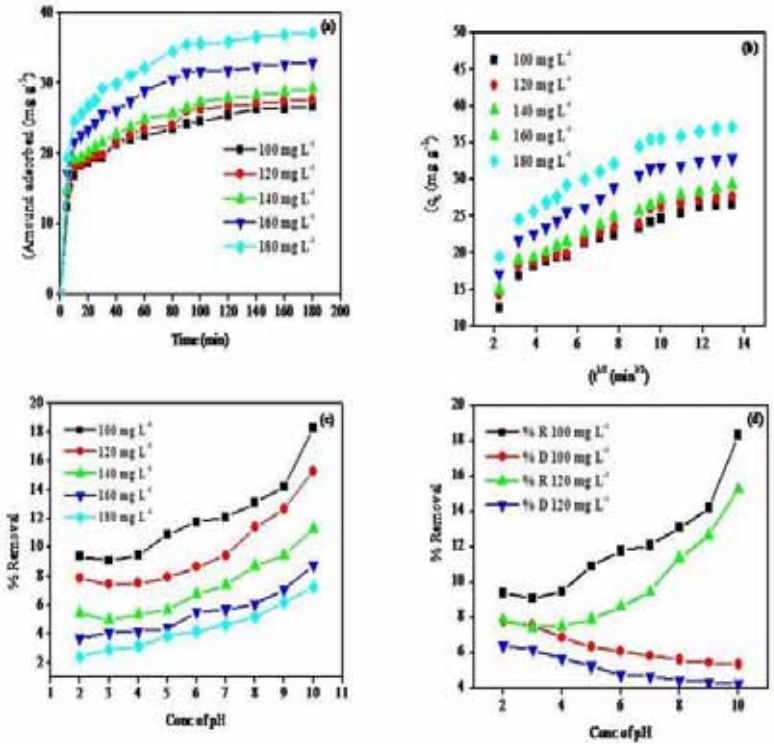

FIGURE 3
Effect of agitation time and initial MB concentration on (a) JHC; Intraparticle diffusion plots for adsorption of MB on to (b) JHC; Effect of pH on (c) JHC; and (d) desorption of MB

TABLE 1
Kinetic parameters for the removal of MB onto JHC

Adsorbate	Initial conc. (mg L^{-1})	q_e(exp) (mg g^{-1})	First order kinetics			Second order kinetics		
			k_1 (min^{-1})	q_e (cal) (mg g^{-1})	R^2	k_2 ($gmg^{-1}min^{-1}$)	q_e (cal) (mg g^{-1})	R^2
JHC MB	100	26.36	0.02	12.24	0.975	0.007	25.00	0.997
	120	27.17	0.03	14.89	0.946	0.007	25.64	0.996
	140	28.29	0.03	14.72	0.962	0.004	29.41	0.996
	160	32.38	0.03	16.94	0.975	0.003	34.48	0.996
	180	36.57	0.03	18.03	0.979	0.003	38.46	0.997
		Conc. (mg L^{-1})	q_e exp (mg g^{-1})	k_{id} (mg $g^{-1}h^{-1/2}$)		C	R^2	
Intraparticle diffusion		100	26.36	1.097		13.35	0.926	
		120	27.17	1.124		14.05	0.949	
		140	28.29	1.167		14.87	0.954	
		160	32.38	1.305		17.54	0.923	
		180	36.57	1.438		20.14	0.921	
		Initial Conc. (mg L^{-1})	Kb (ml (g L^{-1}))	α		R2		
Bangham's model		100	0.21	1.33		0.965		
		120	0.20	1.37		0.977		
		140	0.20	1.49		0.988		
		160	0.19	1.42		0.984		
		180	0.17	1.43		0.982		

A series of contact time experiments for adsorption of MB dye were carried out at different initial concentrations (100-180 mg L^{-1}) at 35ºC Fig. 3(a). Adsorption of MB reached equilibrium at 140 min for all concentrations. The percent removal decreased with increasing initial dye concentration, but the amount of dye adsorbed per unit mass of carbon increased with increase in MB concentration. It means that the adsorption is extremely dependent on initial concentration of MB. At lower concentration, ratio of the initial number of dye molecules is low available surface area. Consequently the incomplete adsorption becomes independent of initial concentration. However, at high concentration of MB the available sites of adsorption turn into less and therefore the percent removal of dye is dependent upon initial concentration.

Removal of MB by JHC was studied at different adsorbent doses from 25 - 200 mg/50ml and different initial concentrations of MB from 100 to 180 mg L^{-1}. It was found that increase in adsorbent dose increased the removal of MB and quantitative removal occurred at 25, 50, 75, 100, 150 and 200 mg/50ml for 100-180 mg L^{-1} of MB, respectively. Increase in adsorption by adsorbent dose is attributed to more surface area and the availability of more adsorption sites.

The results obtained from the first and second order kinetic equilibrium models along with the experimental *qe*. The calculated *qe* values of the Lagergren second order kinetics are generally closer to the experimental q_e values compared to the calculated q_e values from first order kinetics. Therefore, the adsorption process follows Lagergren second order kinetic model. The initial curved segment is attributed to the bulk diffusion effect, the linear portion to the intraparticle diffusion rate effect and the plateau to the kinetic equilibrium. The linear portions of the plots do not pass through the source representative that intraparticle diffusion is not the only rate controlling step for adsorption process shows in Fig. 3 (d). These linear portions are attributed to the instantaneous utilization of the majority readily available adsorbing sites on the adsorbent surface [29]. Bangham's kinetic equation was used to evaluate whether the adsorption was pore-diffusion controlled. Table 1 were found to be linear for different concentrations at 35ºC, which confirmed that the adsorption was pore-diffusion-controlled for MB.

Adsorption isotherms are mathematical models, which are used to describe the distribution of the adsorbate species among solid and liquid phases. The adsorption data were investigated by using three types of the most common isotherms: Langmuir, Freundlich and Dubinin-Radushkevich models [30]. Langmuir model suggests a monolayer adsorption with no lateral interaction among the adsorbed molecules. Plot of C_e/q_e vs C_e gives a straight line with slope $1/Q_0$ and intercept $1/Q_0b$. Langmuir constants Q_0 and b, were found to be 66.66 mg g^{-1} and 0.006 (L mg^{-1}), respectively. The necessary characteristics of the Langmuir isotherm can be expressed by a dimensionless constant called equilibrium parameter R_L. The calculated R_L values were found to be between 0 and 1 which specify favorable adsorption. The R_L values are shown in Table 2. Freundlich model assumes heterogeneous adsorption. The Freundlich constants, k_f and n were calculated from the linear plot of log q_e vs log C_e are presented in Table 2. The adsorption isotherms followed Freundlich Isotherm.

This adsorption potential is independent of temperature, but it adsorbent and adsorbate are varies the depending on the nature. The mean free energy of adsorption gives information about adsorption mechanism as ion-exchange. The mean energy of the MB adsorption was calculated as 10 kJ=mol^{-1}, which indicates that the adsorption of MB on the JHC occurred with ion-exchange mechanism. Figure 4 presents different adsorption isotherms along with the experimental data. In order to compare the validity of isotherms, a normalized deviation, Δq (%). where superscripts 'exp' and 'cal' are the experimental and calculated values, respectively, and 'n' is the number of measurements. From the results it was found that Freundlich isotherm shows lowest Δq and so it is most suitable than other isotherms shown in Table 3.

Increase in the temperature increased the percent removal. Temperature changes into standard free energy, enthalpy and entropy of adsorption. Positive values of ΔH° (268.4 J mol^{-1}K^{-1}) show the endothermic nature of adsorption. The negative values of ΔG° indicate the spontaneous nature of adsorption for MB. Positive values of ΔS° (-192.81 J mol^{-1}K^{-1}) which suggest an increased randomness at the solid/solution interface during the adsorption of dye on JHC shown in Table 4. Thermodynamic parameters such as changes in Gibbs free energy (ΔG^0), entropy (ΔS^0) and enthalpy (ΔH^0) were calculated by using following thermodynamic relations [31]. Current study revealed that adsorption of dyes on JHC was found to non- spontaneous. The raw material for the carbon, namely, JH is bio-diesel production industries waste. The AC developed from the agricultural waste material can be used for the effective and economic adsorption of toxic ions and dyes the organics from waters. Approximate calculations show that the cost of the JH carbon is \$0.50 kg^{-1}, while that of the commercial carbon for dye removal is \$3.00 kg^{-1} [32].

CONCLUSIONS

In the present study, we have successfully developed JHC from Jatropha husk activated by physical method. The structural characterization of pure JHC and MB adsorbed JHC were characterize with FTIR, XRD, and SEM. Jatropha husk, a biodiesel by- product solid waste, was used for the development of activated carbon by JHC shows the excellent surface area. The S_{BET} and micropore volume obtained were 421.1 m^2/g. The pore structure, morphology and elemental composition of the JHC was experiential through SEM micrographs. The prepared JHC shows an excellent dye adsorption from aqueous solution. Parameters such as pH level, initial dye concentration, adsorbent dosage, agitation time and temperature and their effects on removal of the MB by JHC were investigated in the current study. The percent adsorption of MB was at pH 2.0 and higher at pH 10. At pH 10, negatively charged surface sites on the adsorbent favor the adsorption of dye cations due to the electrostatic attraction and hence dye removal was high (>20%) for JHC adsorbents. The equilibrium adsorption closely followed second order kinetics. The equilibrium data yielded good fit with Freundlich isotherm. Adsorption was non spontaneous and endothermic in nature. Desorption studies showed that the ion-exchange mechanism seems to be the major mode of adsorption for MB onto JHC.

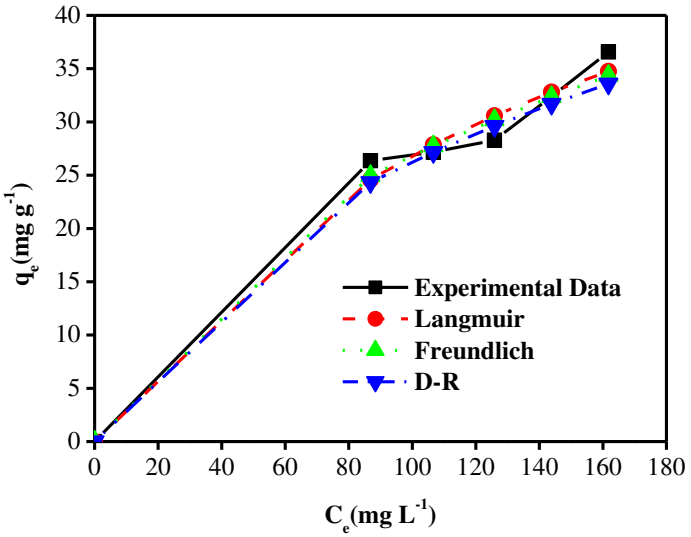

FIGURE 4
Comparison of Langmuir, Freundlich and D-R isotherms for adsorption of MB on to JHC

TABLE 2
Langmuir, Freundlich and Dubinin- Radushkevich isotherm constants for MB onto JHC

			Langmuir			
Adsorbate	Conc. mg L^{-1}	Q_0 (mg g^{-1})	b (L mg^{-1})	R^2	R_L	Δq (%)
MB	100 120 140 160 180	66.66	0.006	0.772	0.59 0.55 0.51 0.48 0.45	5.98
			Freundlich			
Adsorbate	Conc. mg L^{-1}	k_f $mg^{1-1/n}L^{1/n}g^{-1}$	n	R^2		Δq (%)
MB	100 120 140 160 180	2.53	1.94	0.84		5.36
			D-R			
Adsorbate	Conc. mg L^{-1}	q_m (mg g^{-1})	β ($mol^2J^2x10^{-9}$)	R^2		Δq (%)
MB	100 120 140 160 180	222.2	5	0.840		6.16

TABLE 3
Comparison of Langmuir, Freundlich and D-R constants for Adsorption of MB by various adsorbents reported in literature

Adsorbent	Langmuir isotherm		Freundlich isotherm		D-R isotherm		Ref
	Q_0 (mg g^{-1})	b (mg L^{-1})	k_f ($mg^{1-1/n}L^{1/n}g^{-1}$)	n	E (kJ mol^{-1})	B (L mg^{-1})	
JHC	66.66	0.006	2.53	1.94	10.0	5	This work
Coir pith carbon	5.87	0.93	1.19	0.70	*	*	[14]
Poly(Vinyl alcohol)	13.80	27.8	0.50	0.86	*	*	[33]
Raw clay	27.49	13.99	14.85	0.15	*	*	[34]
Calcined clay	56.31	8.88	9.01	0.061	*	*	[34]
Saw dust	32.26	0.38	14.58	0.26	*	*	[35]
Date stones char (DSAC)	*	*	42.65	2.46	*	*	[36]

TABLE 4
Thermodynamic parameters for the adsorption of MB onto JHC

T (K)	K_c	ΔG (kJ mol^{-1})	ΔH (kJ mol^{-1})	ΔS (J mol^{-1} K^{-1})
308	0.112	5.59	-	-
313	0.113	5.66		
323	0.114	5.83	268.44	-192.81
333	0.116	5.94		

ACKNOWLEDGEMENTS

This research was supported by the National Natural Science foundation of China NSFC Grants No. (51650410657) and Jiangsu Province Post Doctoral Research funds Grant No. (110500334).

REFERENCES

[1] Orfao, M.J.J., Silva, A.I.M., Pereira, J.C.V., Barata, S.A., Fonseca, I.M. and Faria, P.C.C. Pereira, M.F.R. (2006) Adsorption of a reactive dye on chemically modified activated carbons-Influence of pH. J. Colloid Interface Sci., 296, 1480-489.

[2] Sayed, G.O.E., Yehia, M.M. and Asaad, A.A. (2014) Assessment of activated carbon prepared from corncob by chemical activation with phosphoric acid. Water Resour. Ind., 8, 66-75.

[3] Theydan, S.K. and Ahmed, M.J. (2012) Adsorption of methylene blue onto biomass-based activated carbon by $FeCl_3$ activation: Equilibrium, kinetics, and thermodynamic studies. J. Anal. App. Pyro. 97, 116-122.

[4] Rafatullah, M., Sulaiman, O., Hashim, R. and Ahmad, A. (2010) Adsorption of methylene

blue on low-cost adsorbents: a review. J. Hazard. Mat. 177, 70-80.
[5] Robinson, T., McMullan, G., Marchant, R. and Nigam, P. (2001) Remediation of dyes in textiles effluent: a critical review on current treatment technologies with a proposed alternative. Bioresour. Technol.77, 247-255.
[6] Mazaheri, H., Ghaedi, M., Asfaram, A. and Hajati, S. (2016) Performance of CuS nanoparticle loaded on activated carbon in the adsorption of methylene blue and bromophenol blue dyes in binary aqueous solutions: using ultrasound power and optimization by central composite design. J. Mol. Liq. 219, 667-676.
[7] Fan, S., Tang, J., Wang, Y., Li, H., Zhang, J., Tang, Z., Wang, X. and Li. (2016) Biochar prepared from co-pyrolysis of municipal sewage sludge and tea waste for the adsorption of methylene blue from aqueous solutions: kinetics, isotherm, thermodynamic and mechanism. J. Mol. Liq. 220, 432-441.
[8] Namasivayam, C. and Kavitha, D. (2002) Removal of Congo red from water by adsorptiononto activated carbon prepared from coir pith, an agricultural solid waste. Dyes Pig. 54, 47-58.
[9] Ponnusami, V., Krithika, V.,Madhuram R. and Srivastava, S.N. (2007) Biosorption of reactive dye using acid-treated rice husk: Factorial design analysis. J. Hazard. Mat. 142, 397-403.
[10] Ramakrishnan, K. and Namasivayam, C. (2009) Development and Characteristics of activated carbons from jatropha husk, an agro industrial solid waste, by chemical activation methods. J. Environ. Eng. Manage. 193, 173-178.
[11] Olugbenga, S.B., Idowu, A.A., John, C.A. and Ezekiel, O.F. (2008) Adsorption of methylene blue onto activated carbon derived from periwinkle shells: kinetics and equilibrium studies. Chem. Ecol. 244, 285-295.
[12] Ming, C.S. (2012) Kinetics of the batch adsorption of methylene blue from aqueous solutions onto rice husk: effect of acid-modified process and dye concentration. Desalin. Water Treat. 37, 200-214.
[13] Christianah, O.I.,Ji, I.C., Da, H.H., Hye, Y.C.,Se, J.O. and Dong, S.K. (2010) Methylene Blue adsorption from aqueous solution by activated carbon: effect of acidic and alkaline solution treatments. J. Environ. Sci. Heal. A. 45, 958-967.
[14] Kavitha, D. and Namasivayam, C. (2007) Experimental and kinetic studies on methylene blue adsorption by coir pith carbon. Biores. Technol. 98, 14-21.
[15] Maryam, A.T. and Toraj, M. (2013) Methylene blue adsorption onto granular activated carbon prepared from Harmal seeds residue, Desalin. Water Treat. 1-11.
[16] Muhammad, N.A., Muhammad, N.U.H., Tahira, A., Ambreen, S., Ashfaq, M. and Muhammad, N. (2012) Methylene blue adsorption onto granular activated carbon prepared from Harmal seeds residue. Desalin. Water Treat. 49, 376-383.
[17] Kumar, A.J. and Namasivayam, C. (2014) Uptake of endocrine disruptor bisphenol-A onto sulphuric acid activated carbon developed from biomass: Equilibrium and kinetic studies, Sustain. Environ. Res. 24(1), 73-80.
[18] Avila, H.E.R., Castillo, D.I.M. and Petriciolet, A.B. (2016) Relevance of anionic dye properties on water decolorization performance using bone char: Adsorption kinetics, isotherms andbreakthrough curves. J. Mol. Liq. 219, 425-434.
[19] Pezoti, J.O., Cazetta, A.L., Souza, I.P.A.F., Bedin, K.C., Martins, A.C., Silva, T.L. and Almeida, V. (2014) Adsorption studies of methylene blue onto $ZnCl_2$-activated carbon produced from buriti shells *Mauritia flexuosa* L. J. Ind. Eng. Chem. 20(6), 4401-4407.
[20] Kennedy, L.J., Vijaya, J.J. and Sekaran, G. (2004) Effect of two-stage process on the preparation and characterization of porous carbon composite from rice husk by phosphoric acid Activation. Ind. Eng. Chem. Res. 43, 1832-1838.
[21] Baccar, R., Bouzid, J., Feki, M. and Montiel, A. (2009) Preparation of activated carbon from Tunisian olive-waste cakes and its application for adsorption of heavy metal ions. J. Hazard. Mat. 162, 1522-1529.
[22] Lua, A.C. and Yang, T. (2005) Characteristics of activated carbon prepared from pistachio-nut shell by zinc chloride activation under nitrogen and vacuum conditions. J. Colloid Interface Sci. 290, 505-513.
[23] Xiong, G., Pal, U., Serrano, J.G., Ucer, K.B. and Williams, R.T. (2006) Photoluminescence and FTIR study of ZnO nanoparticles: the impurity and defect perspective. Phys. Stat. Sol. 310, 3577-3581.
[24] Heibati, B., Couto, S.R., Ghouti, M.A.A, Asif, M., Tyagi, I., Agarwal, S. and Gupta, V.K. (2015) Kinetics and thermodynamics of enhanced adsorption of the dye AR 18 using activated carbons prepared from walnut and poplar woods. J. Mol. Liq. 208, 99-105.
[25] Singh, K.P., Mohan, D., Sinha, S., Tondon, G.S. and Gosh, D. (2003) Color removal from wastewater using low-cost activated carbon derived from agricultural waste material. Ind. Eng. Chem. Res. 42, 1965-1976.
[26] Janos, P. (2003) Sorption of basic dyes onto iron humate. Environ. Sci. Technol. 37, 5792-5798.
[27] Chen, M., Ding, W.,Wang, J. and Diao, G. (2013) Removal of azo dyes from water by combined techniques of adsorption, desorption, and electrolysis based on a supramolecular sorbent. Ind. Eng. Chem. Res. 52, 2403-2411.

[28] Ofomaja, E. and Ho, Y.S. (2008) Effect of temperatures and pH on methyl violet bio sorption by Mansonia wood sawdust. Biores. Technol. 99, 5411-5417.
[29] Blanchard, G., Maunaye, M. and Martin, G. (1984) Removal of heavy metals from water by means of natural zeolites. Water. Res. 18, 1501-1507.
[30] Serkan, K., Murside, K., Leman, S. and Hurriyet, P. (2012) Adsorption of methylene blue from aqueous solution on high lime fly ssh: kinetic, equilibrium, and thermodynamic studies. J. Disper. Sci. Technol. 33, 15-23.
[31] Jia, Z., Li, Z., Li, S., Li, Y. and Zhu, R. (2016) Adsorption performance and mechanism of methylene blue on chemically activated carbon spheres derived from hydrothermally-prepared poly(vinyl alcohol) microspheres. J. Mol. Liq. 220, 56–62.
[32] Karthick, K., Dinesh, C. and Namasivayam, C. (2014) Utilization of ZnCl2 activated Jatropha husk carbon for the removal of reactive and basic dyes: Adsorption equilibrium and kinetic studies, Sustain. Environ. Res. 242, 139-148.
[33] Ayse, Z.A., Gulen, J. and Evers, R.H. (2008) Adsorption of methylene blue from aqueous solution on pyrolyzed petrified sediment. Biores. Technol. 99, 1503-1508.
[34] Ghosh, D. and Bhattacharyya, K.G. (2002) Adsorption of methylene blue on kaolinite. Appl. Clay Sci. 20, 295-300.
[35] De, D.S. and Basu, J.K. (1998) Adsorption of Methylene blue on to a low cost adsorbent developed from saw dust. Ind J. Environ. Prot. 19, 416-421.
[36] Foo, K.Y. and Hameed, B.H. (2011) Preparation of activated carbon from date stones by microwave induced chemical activation: application for methylene blue adsorption. Chem. Eng. J. 170, 338-341.

Received: **09.09.2016**
Accepted: **14.07.2017**

CORRESPONDING AUTHORS

Rajendra Prasad Singh
Department of Municipal Engineering
Southeast University
Nanjing, Jiangsu 210096 – CHINA

E- mail: 101002314@seu.edu.cn
101100623@seu.edu.cn

© by PSP Volume 26 – No. 10/2017 pages 5732-5736 Fresenius Environmental Bulletin

EFFECTS OF ANTIBIOTICS AND METAL IONS EXPOSURE ON THE NATURAL TRANSFORMATION FREQUENCY OF AN ANTIBIOTIC RESISTANT PLASMID

Yang Qingxiang[1,2,*], Wang Qiang[1,2], Zhuo Kaiyue[1]

[1]College of Life Sciences, Henan Normal University, Xinxiang 453007, China
[2]Key Laboratory for Microorganisms and Functional Molecules (Henan Normal University), University of Henan Province, Xinxiang 453007, China

ABSTRACT

Although the relationship between the horizontal gene transfer of antibiotic resistant genes and metal or antibiotic pollution in environments are growing concern, the effects of metals or antibiotics on the natural transformation frequency are unavailable. In this study, the transformation frequencies of a multi-antibiotics resistance plasmid pYN1 that possesses high transfer ability were investigated among different recipient bacteria under exposure of various concentrations of antibiotics or metal ions. As the results, antibiotics and metal ions significantly altered natural transformation frequencies of this plasmid under exposure of the reported residual concentration ranges in various environments. But the alteration varied depending on the recipient bacterial species and the types of antibiotics or metals. In general, the transformation frequencies of *Bacillus subtilis* and *Proteus vulgaris* increased by 100 to 1000 times in the presence of Cephalexin, tetracycline, or kanamycin; while exposure of these three antibiotics decreased transformation frequencies when *Bacillus cereus* and *Bacillus thuringiensis* were used as recipients. Overall, the investigated metal ions, Cu^{2+}, Zn^{2+}, Mn^{2+} and Fe^{2+}, facilitated the transformation of plasmid pYN1 to recipient bacterial strains except to *Bacillus cereus* under low concentration levels, although these effects weakened with the increase of concentrations.

KEYWORDS:
antibiotic, metal ion, ARGs, natural transformation, horizontal gene transfer

INTRODUCTION

It is well known that antibiotic resistance genes (ARGs) as emerging environmental contaminants are becoming one of the most serious threats to global public health. Although antibiotic resistance bacteria (ARB) are easy to be killed, the ARGs released from ARB can steadily exist and disseminate in environments for a long time [1]. Horizontal gene transfer (HGT) is considered to be a main reason contributing to the emergence and dissemination of ARGs [2-4].

Horizontal gene transfer involves three independent mechanisms: conjugation, transduction, and transformation. Conjugative transfer which requires direct contact between the donor and the recipient cells is the main approach to spread genes. Transduction relies on the transducing phages that package and transfer infected host DNA to new hosts. Because the phages generally have narrow host ranges, so phage-mediated genes transfer is considered to be restricted [5]. Natural transformation is defined as the active uptake and heritable integration of extracellular DNA (plasmid and chromosomal) [6]. Unlike conjugation and transduction, transfer of DNA by natural transformation is initiated by the recipient cell and doesn't rely on extrachromosomal genetic elements [7]. As is well-known, the development of physiological state of competence is essential for a recipient cell to uptake extracellular DNA in natural transformation processes. More than 70 species of bacteria can develop competence under natural conditions. Prudhomme et al. found that some antibiotics can induce the competence development in *Streptococcus pneumoniae* [8]. Obviously, the constant exposure to antibiotics may induce the generation of ARGs and push them spreading. The ratio of resistant bacteria significantly elevated in the antibiotic-polluted environments, resulting from the selective pressure imposed by continual exposure to antibiotics. Importantly, lots of researches have shown that metal contamination plays an important role in the maintenance and dissemination of ARGs [9-11]. Compared with antibiotics, metals are more difficult to be degraded and subsequently produce a long-term selection pressure [11]. It has been known for several decades that metal- and antibiotic- resistance genes are linked, particularly on plasmids. This physical linkage results in the co-selection for resistant genes located on the same element [12].

Although large researches have shown that the prevalence of ARGs and resistant bacteria was elevated in metal- and/or antibiotic-polluted environments, the effects of metals or antibiotics exposure

on the natural transformation frequencies of antibiotic resistant plasmids are unavailable [11, 13]. In our previous study, an *Escherichia coli* Ls1 strain resistant to at least eight types of antibiotics was isolated from chicken manure, and the multi-resistance plasmid pYN1 was isolated from this bacterium strain which contained multiple ARGs, especially Glo_EDI_BRP_like superfamily which regulated multiple metal- and antibiotic- resistance (data unpublished). This plasmid was detected in several different species and genera of multi-resistance bacterial strains. In this study, the effects of metals or antibiotics exposure on the natural transformation frequencies of the plasmid pYN1 in different species of recipient bacteria were researched.

MATERIALS AND METHODS

Plasmid. To obtain a potential donor strain for natural transformation, several multidrug-resistance strains were isolated from the surrounding environment of livestock farms. After antibiotic resistance exploration, an *Escherichia coli* strain resistant to at least eight types of antibiotics was used as the donor strain. The strain was named as *E. coli* Ls1. From this strain, a plasmid named pYN1 was isolated and further sequenced. This plasmid was used here for natural transformation tests.

Recipient bacteria. The recipient strains were *Bacillus subtilis*, *Bacillus cereus*, *Bacillus thuringiensis*, and *Proteus vulgaris*, which preserved in Key Laboratory for Microorganisms and Functional Molecules (Henan Normal University), University of Henan Province. The antibiotic sensitivity for each recipient strain was tested to assure they were sensitive to cephalexin, tetracycline, and kanamycin. Plasmid extraction and agarose gel electrophoresis detection were performed to assure that no plasmid was contained in the bacterial strains.

Natural transformation. Plasmid pYN1 was extracted by alkaline lysis according to omega plasmid mini kit manual (Omega Bio-Tek, USA). The concentration and purity of plasmid were determined by colorimetric assay using ultraviolet spectrophotometer. 1.5 μg total plasmids isolated from *E. coli* Ls1 were co-cultured with 100 μL each of the four recipient bacteria in logarithmic phase, respectively. After 18 h static co-cultured, all four fractions were appropriately diluted and plated on Luria-Bertani solid selective (adding 50 μg ml^{-1} cephalexin, 20 μg ml^{-1} tetracycline, and 100 μg ml^{-1} kanamycin) and nonselective media to determine resistant CFU and total CFU, respectively. The transformants were verified by antibiotic sensitive tests on Luria-Bertani (LB) agar plates, isolation plasmid and agarose gel electrophoresis. The transformation frequency was defined as the number of resistant colonies per total colonies.

RESULTS

Effects of antibiotic exposure on transformation frequency. Cephalexin, tetracycline, and kanamycin were chosen to test their effects of different exposure concentrations on transformation frequency. As shown in Fig. 1, addition of antibiotics significantly altered the transformation frequencies in all the recipient bacteria, in which the transformation frequencies of *Bacillus subtilis* and *Proteus vulgaris* sharply increased by 100 to 1000 times in the presence of various antibiotics. But the dosage effects of antibiotics exposure were not significant in the range of tested concentrations. On the contrary, these three antibiotics contributed to the decrease of *Bacillus cereus* and *Bacillus thuringiensis* transformation frequencies. And the transformation frequency presented a slight decrease with the increase of antibiotic concentrations, however, without significant difference among the three antibiotics.

Effects of metal ions on transformation frequency. The effects of heavy metals, Cu^{2+}, Zn^{2+}, Mn^{2+} and Fe^{2+}, on transformation frequencies were depending on the types of ions and types of recipient bacterial strains as shown in Fig. 2. Overall, metal ions facilitated the transformation of plasmid pYN1 to recipient bacterial strains except to *Bacillus cereus* under low concentration levels, although these effects weakened with the increase of concentrations. For examples, copper ion obviously increased transformation frequency of *Bacillus subtilis*, *Bacillus thuringiensis*, and *Proteus vulgaris* by 100 to 1000 times, but obviously inhibited *Bacillus cereus*. The effects of manganese ion and zinc ion were also significant. Low-concentration manganese ion contributed to the increase of transformation frequencies by 10-100 times. The transformation frequencies of *Bacillus subtilis* and *Bacillus thuringiensis* evidently increased in the presence of zinc ion. In comparison, the influence of ferrous ion seemed mediocre. Therefore, the kinds of both metal ions and recipient bacterial strains affected the natural transformation frequencies.

DISCUSSION

It has been an indisputable fact that exposure of antibiotics and heavy metals promoted the prevalence of antibiotic resistant / multiple antibiotic resistant bacteria in various environments or even the horizontal gene transfer of ARGs [11, 13-15]. However, very limited reports were involved in how this process was developed and what extents of such effects made on the environments. According to traditional selective pressure theory, resistant strains are

easily survival and enriched under the condition of high dosage antibiotic exposure, because the remaining susceptible population are killed. However, recent studies have shown that extremely low antibiotic concentrations (in the ng per ml range) can also promote the dissemination of resistant genes [16]. That theory might not be appropriate in environmental conditions since most of the extremely low level of antibiotics cannot efficiently inhibit the antibiotic sensitive microorganisms. It is therefore possible that there is an alternate mechanism such as horizontal gene transfer (HGT) for the dissemination of antibiotic resistance traits in environments. For example, some antibiotics (such as fluoroquinolones, β-lactams and aminoglycosides) or metals can damage the genomic DNA and consequently induce the SOS response and the RpoS regulon [17, 18]. The consequences of induction can lead to genetic alterations that are associated with the movement of mobile elements (such as the induction of prophages, integrative conjugative elements (ICEs) and transposons), activation of recombinases [19] (such as integrases and transposases) and an increase in the rate of mutagenesis during chromosome replication (by the induction of error-prone DNA polymerases and the suppression of mismatch repair) [20, 21]. Natural transformation of plasmids in environments is an important way of horizontal gene transfer. From our results, the effects of antibiotics and heavy metal ions on the natural transformation were affirmative. However, such effects were highly depending on the types of antibiotics or metals, and also depending on the bacterial species. In this study, the abilities of receiving exogenous plasmids were contrary under exposure of various antibiotics or metals between *Bacillus subtilis* and *Bacillus cereus* although they belonged to the same genus. This phenomenon may exert a kind of selection to promote the evolution of microbial community, especially in antibiotic or metal polluted environments.

From the results, we can see that the dosage effect was not very clear in most tests, which might be due to the exposure concentrations used. The investigated concentration range of each antibiotic or metal was determined according to references about the residual concentrations in soil or other environments. According to available literature, the concentration of common antibiotics reached a fraction of milligram to a dozen of milligrams per kilogram in antibiotic-polluted environment such as manure or livestock farms in China [22, 23]. And the heavy metals concentration ranged from dozens of milligrams to hundreds of milligrams per kilograms in these environments [24, 25]. These residual concentrations of antibiotics or metals were possibly sub-inhibiting dosages for most bacterial species but might play important roles in gene transfer in environments. Therefore, the investigated exposure concentrations of antibiotics or metals represented real environmental significance although further study should be conducted under enlarged exposure dosage ranges and also under co-occurrence of antibiotics, metals or antibiotics plus metals. Certainly, the rate of natural transformation also depended on various environmental microorganism-associated factors such as recipient species. In this study, the influencing effects of antibiotic or metal exposure were case by case depending on recipient species without a clear rule intra- or inter- genus. More species and genera of recipient bacteria should be tested to explore the effects of different bacterial species in the further study.

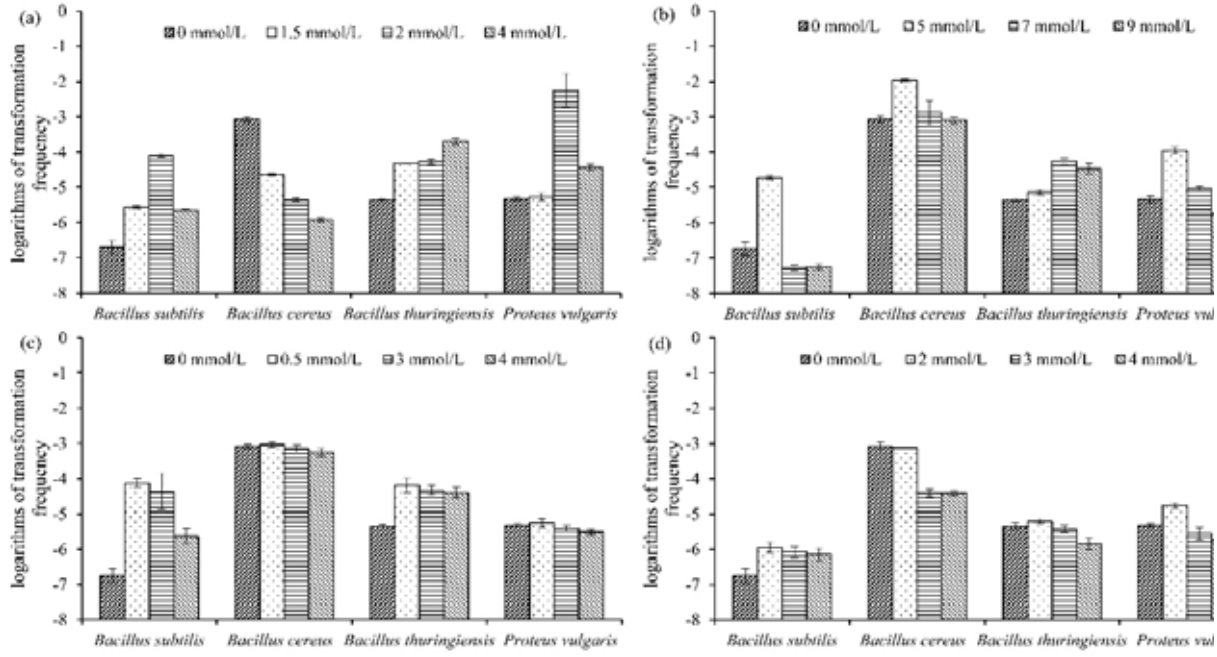

FIGURE 1
Effect of antibiotics on transformation frequency. (a) cephalexin; (b) tetracycline, (c) kanamycin

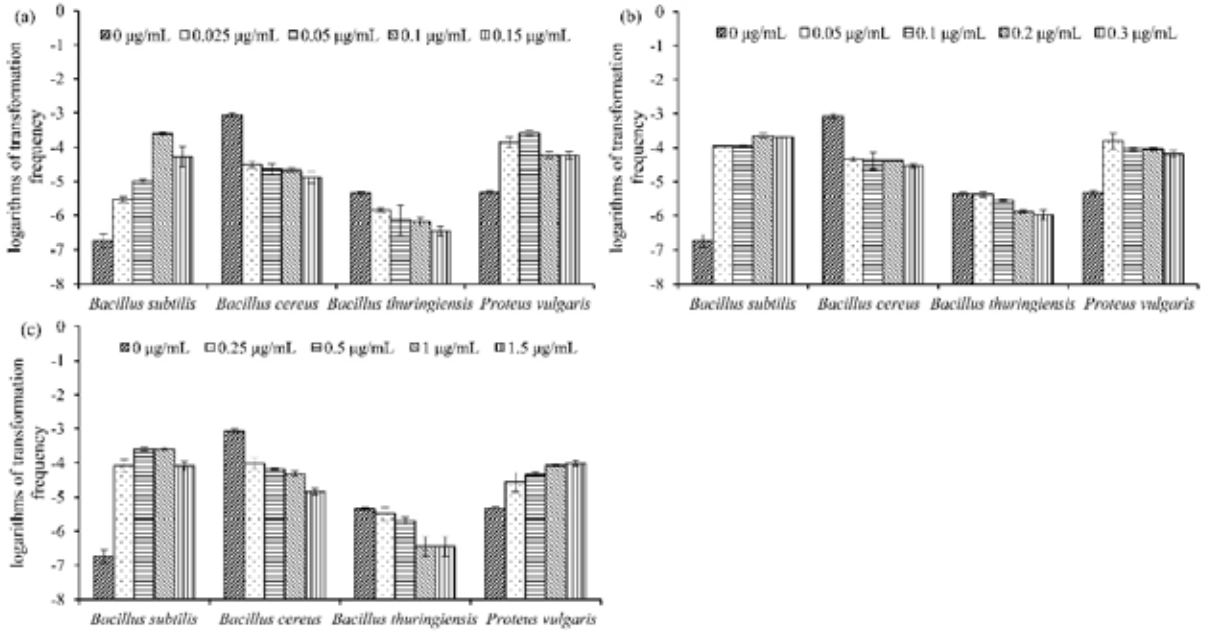

FIGURE 2
Effect of metal ions on transformation frequency. (a) copper ion, (b) manganese ion, (c) zinc ion, (d) ferrous ion

CONCLUSION

Although further studies should be conducted, the present study has revealed that antibiotic or metal exposure significantly influenced the transformation frequencies of a multi-antibiotics resistance plasmid pYN1. And these effects were unfavorable because the transformation frequencies increased in most cases. Therefore, the effects of metal- and antibiotic-pollution on ARGs natural transformation should be given more attentions.

ACKNOWLEDGEMENTS

The authors would like to acknowledge the financial support from the National Natural Science Foundation of China (NSFC 21277041 and NSFC 21477035), the Specialized Research Fund for the Doctoral Program of Higher Education (20134104110006), the Outstanding Talented Persons Foundation of Henan Province (144200510007), the Key Project of Natural Science of the Education Department of Henan Province, China (16A180029), and the Doctoral Scientific Research Foundation of Henan Normal University (qd15177).

REFERENCES

[1] Pruden, A., Pei, R., Storteboom, H. and Carlson, K.H. (2006) Antibiotic resistance genes as emerging contaminants: Studies in northern colorado. Environmental Science & Technology 40, 7445-7450.

[2] Chaturvedi, S., Chandra, R. and Rai, V. (2008) Multiple antibiotic resistance patterns of rhizospheric bacteria isolated from phragmites australis growing in constructed wetland for distillery effluent treatment. Journal Of Environmental Biology 29, 117-124.

[3] Dian, D., Straub, J., Scholz, C., Mylonas, I., Rack, B., Sommer, H. and Janni, W. (2006) Frequency of transferable multiple antibiotic resistance amongst coliform bacteria isolated from a treated sewage effluent in antofagasta, chile. Electronic Journal of Biotechnology 9, 533-540.

[4] Selvaratnam, S. and Kunberger, J. (2004) Increased frequency of drug-resistant bacteria and fecal coliforms in an indiana creek adjacent to farmland amended with treated sludge. Canadian Journal Of Microbiology 50, 653-656.

[5] Brabban, A.D., Hite, E. and Callaway, T.R. (2005) Evolution of foodborne pathogens via temperate bacteriophage-mediated gene transfer. Foodborne Pathogens & Disease 2, 287-303.

[6] Lorenz, M.G. and Wackernagel, W. (1994) Bacterial gene transfer by natural genetic transformation in the environment. Microbiological Reviews 58, 563-602.

[7] Johnsborg, O., Eldholm, V. and Havarstein, L.S. (2007) Natural genetic transformation: Prevalence, mechanisms and function. Research In Microbiology 158, 767-778.

[8] Prudhomme, M., Attaiech, L., Sanchez, G., Martin, B. and Claverys, J.P. (2006) Antibiotic

stress induces genetic transformability in the human pathogen *streptococcus pneumoniae*. Science 313, 89-92.
[9] Summers, A.O., Wireman, J., Vimy, M.J., Lorscheider, F.L., Marshall, B., Levy, S.B. and Bennett, S. (1993) Mercury released from dental "silver" fillings provokes an increase in mercury- and antibiotic-resistant bacteria in oral and intestinal floras of primates. Antimicrobial Agents & Chemotherapy 37, 825-834.
[10] Alonso, A., Sánchez, P. and Martínez, J.L. (2001) Environmental selection of antibiotic resistance genes. Environmental Microbiology 3, 1-9.
[11] Stepanauskas, R., Glenn, T.C., Jagoe, C.H., Tuckfield, R.C., Lindell, A.H. and Mcarthur, J.V. (2005) Elevated microbial tolerance to metals and antibiotics in metal-contaminated industrial environments. Environmental Science & Technology 39, 3671-3678.
[12] Foster, T.J. (1983) Plasmid-determined resistance to antimicrobial drugs and toxic metal ions in bacteria. Microbiological Reviews 47, 361-409.
[13] Knapp, C.W., Singh, B.K., Campbell, C.D., Hudson, G. and Graham, D.W. (2011) Antibiotic resistance gene abundances correlate with metal and geochemical conditions in archived scottish soils. Plos One 6, 1119-1119.
[14] Jiang, L., Hu, X., Xu, T., Zhang, H., Sheng, D. and Yin, D. (2013) Prevalence of antibiotic resistance genes and their relationship with antibiotics in the huangpu river and the drinking water sources, shanghai, china. Science Of The Total Environment 458-460, 267-272.
[15] Ramunas, S., Glenn, T.C., Jagoe, C.H., Cary, T.R., Lindell, A.H., King, C.J. and Mcarthur, J.V. (2006) Coselection for microbial resistance to metals and antibiotics in freshwater microcosms. Environmental Microbiology 8, 1510-1514.
[16] Kim, S., Yun, Z., Ha, U.H., Lee, S., Park, H., Kwon, E.E., Cho, Y., Choung, S., Oh, J. and Medriano, C.A. (2014) Transfer of antibiotic resistance plasmids in pure and activated sludge cultures in the presence of environmentally representative micro-contaminant concentrations. Science Of The Total Environment 468-469, 813-820.
[17] Lopez, E. and Blazquez, J. (2009) Effect of subinhibitory concentrations of antibiotics on intrachromosomal homologous recombination in *escherichia coli*. Antimicrobial Agents & Chemotherapy 53, 3411-3415.
[18] Baharoglu, Z., Krin, E. and Mazel, D. (2013) Rpos plays a central role in the sos induction by sub-lethal aminoglycoside concentrations in vibrio cholerae. Plos Genetics 9, e1003421-e1003421.
[19] Lopez, E., Elez, M., Matic, I. and Blázquez, J. (2007) Antibiotic-mediated recombination: Ciprofloxacin stimulates sos-independent recombination of divergent sequences in *escherichia coli*. Molecular Microbiology 64, 83–93.
[20] Dan, I.A. and Hughes, D. (2014) Microbiological effects of sublethal levels of antibiotics. Nature Reviews Microbiology 12, 465-478.
[21] Thi, T.D., López, E., Rodríguez-Rojas, A., Rodríguez-Beltrán, J., Couce, A., Guelfo, J.R., Castañeda-García, A. and Blázquez, J. (2011) Effect of reca inactivation on mutagenesis of *escherichia coli* exposed to sublethal concentrations of antimicrobials. Journal Of Antimicrobial Chemotherapy 66, 531-538.
[22] An, J., Chen, H., Wei, S. and Gu, J. (2015) Antibiotic contamination in animal manure, soil, and sewage sludge in shenyang, northeast china. Environmental Earth Sciences 74, 5077-5086.
[23] Du, L.S., Wang, Y., Wang, J.H., Liu, Q., Zhang, J.J., Sun, C.Y. and Liu, J.S. (2014) Effects of livestock farms on heavy metal pollution in farmland soils. Advanced Materials Research 955-959, 1210-1215.
[24] Chen, H., Teng, Y., Lu, S., Wang, Y. and Wang, J. (2015) Contamination features and health risk of soil heavy metals in china. Science Of The Total Environment 512–513, 143-153.
[25] Ji, X., Shen, Q., Liu, F., Ma, J., Xu, G., Wang, Y. and Wu, M. (2012) Antibiotic resistance gene abundances associated with antibiotics and heavy metals in animal manures and agricultural soils adjacent to feedlots in Shanghai; China. Journal of Hazardous Materials. 235-236, 178-185.

Received: **21.09.2016**
Accepted: **14.07.2017**

CORRESPONDING AUTHOR

Yang Qingxiang
College of Life Sciences
Henan Normal University
Xinxiang 453007 – CHINA

E-mail: yangqx@htu.edu.cn

© by PSP Volume 26 – No. 10/2017 pages 5737-5744 Fresenius Environmental Bulletin

DISTRIBUTION AND CONTROLLING FACTORS OF PHYTOPLANKTON DURING A TIDE IN THE COASTAL AREA OF BOHAI BAY, CHINA

Wenliang Zhang[1,2], Chao Wu[3], Haijiao Liu[3], Jun Sun[4,*], Gang Qian[4]

[1]School of Environmental Science and Engineering, Tianjin University, Tianjin, 300072, China
[2]Tianjin Bohai Marine Monitoring and Surveillance Management Center, Tianjin, 300480, China.
[3]Institute of Marine Science and Technology, Shandong University, Jinan 250110, China
[4]College of Marine and Environmental Sciences, Tianjin University of Science and Technology, Tianjin 300457, China

ABSTRACT

A comprehensive survey was conducted in the coastal area of Bohai Bay (117º50'E～118º9'E and 39º 4'N～39º 12'N) during May 7 to 11, 2009. Environmental factors were surveyed in a grid of 20 stations during a rising tide and a falling tide. Phytoplankton samples were collected from 16 stations and microscopically examined in the lab. A total of 33 species which belongs to 3 phyla were detected in the study area, including Bacillariophyta (31 species, accounting for 93.94%), Cryptophyta (1 species, accounting for 3.03%) and Chlorophyta (1 species, accounting for 3.03%). The main phytoplankton groups were eurythermal and neritic autochthonous species, the dominant species were *Skeletonema* sp., *Ditylum brightwellii*, *Nitzschia longissima*, *Coscinodiscus excentricus*, *Thalassiosira rotula*, *Rhizosolenia styliformis* and *Coscinodiscus jonesianus* in this season. Cell abundance ranged from 2.429×10^4 cells/L to 4.51×10^5 cells/L with an average of 1.386×10^5 cells/L. Dissolved inorganic nitrogen (DIN) and soluble reactive phosphorus (SRP) ratios were 39.4:1 in rising tide and 41.64:1 in falling tide. Combined with history literatures, the nutrient limiting factor for phytoplankton growth could shift to phosphorus limitation from nitrogen limitation due to anthropogenic emissions in the last decade. Correlation analysis proved that SRP and pH were the main factors that control the phytoplankton growth in rising tide, while these factors had no obvious effect in falling tide. The periodic change of the phytoplankton community structure was not only influenced by physical process, but also influenced by the sea surface temperature (SST), nutrient concentration and other environmental factors.

KEYWORDS:
phytoplankton, tidal, Bohai Bay, nutrient, correction

INTRODUCTION

Phytoplankton, a primary producer which can convert solar energy to organic compounds, contributes greatly to material circulation and energy flow in the marine ecosystems [1,2]. Its species composition and quantity can largely restrict the development of ocean primary productivity directly or indirectly, thus it is an important indicator to the development and utilization of marine biotic resources [3,4]. To a large extent, the state of phytoplankton communities determines the stability of local marine ecosystems, and the investigation of phytoplankton communities is a crucial method to estimate the health level of the seawaters [5].

Bohai Bay is a typical semi-enclosed basin situated in the western region of Bohai Sea in northeast China, with an area of 1.6×10^4 km^2 and an average water depth of 12.5m [6]. Of particular note is that red tide happened frequently in this bay, mainly caused by eutrophication in water bodies [7]. A survey from the literature available showed that about 1 billion tons of sewage was discharged annually into the offshore of Bohai Bay from the peripheral city [8]. Nutrients in untreated sewage were poured into seawater, and stimulated algae overgrowth to form red tide ultimately. Many reports have focused on eutrophication in the offshore of Bohai Bay. Peng [6] reported that DIN was the main pollutant in Bohai Bay, and responsible for the eutrophication risk here. Xu [9] demonstrated that nutrients have great effect on phytoplankton biomass in Bohai Bay by using structural equation model, and a strong relationship was observed in nutrients and physical environment. Similar literature can be found somewhere else, with an identical consequence that Bohai Bay are facing the plight of eutrophication, and nutrients may be the principal culprit to such dilemma [10].

Note that Bohai Bay is an irregular semidiurnal tide, with a diurnal tidal range 2-3 m [11]. Previous works on spatio-temporal distribution of phytoplankton were ample, but few documents have focused on recording variation of the phytoplankton biomass during a tide in Bohai Bay. Environmental forcing by tidal cycles is a significant driver of phytoplankton community in coastal waters [12]. Thus, research

on how tidal cycles act on phytoplankton is necessary. Here we conducted a survey during a tide in the coastal area of Bohai Bay in 2009, our aims were (1) to investigate the distribution of phytoplankton in coastal area of Bohai Bay, and identify the dominant species in this area; (2) to compare the difference of phytoplankton biomass, as well as the primary productivity, between rising tide and falling tide; (3) to recognize the crucial environmental factors that driving the change of phytoplankton biomass.

.

MATERIALS AND METHODS

Field sampling. Samples were collected at 20 stations (5 sampling sections) in waters around Hangu distinct (117º50'E～118º9'E and 39º 4'N～39º 12'N) during May 7 to 11, 2009 (Fig. 1). Hereafter we use S1～S20 to represent the collection stations, and T1～T5 to represent the 5 sampling sections. Directions of sampling cross-sections were substantially parallel to the direction of the main current. We collected water samples in all of the 20 stations, and among which 16 stations were used for biological analysis except for Stn. S9, S13, S17 and S20. Rising tide and falling tide water samples were included in the field experiment, the whole investigation lasted for five days. Water samples were collected at 0.5 m below the surface in all stations with 5L Niskon bottles. Then the water samples were transferred to acid-cleaned polyethylene bottles, and samples were kept from light until analyzed in the laboratory.

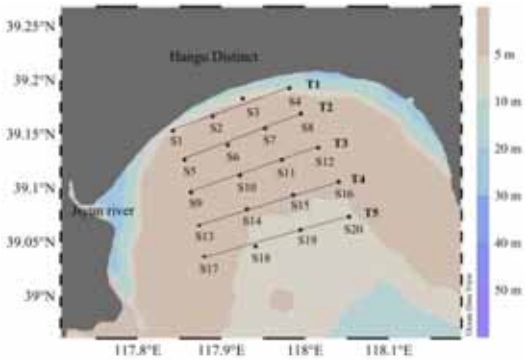

FIGURE 1
Study area and sampling stations in the coastal area of Bohai Bay

Water samples measurement. Depth were measured in situ by a onboard echo measure instrument. Temperature (T), pH and salinity (Sal) were recorded by corresponding equipments with detection limits of 0.1□, 0.01 and 2, respectively. Dissolved oxygen (DO) were measured in the laboratory by iodometry with a detection limits of 0.02mg/L.

Nutrient analysis were conducted in the lab, including ammonium (NH_4-N), nitrate(NO_3-N), nitrite (NO_2-N) and SRP. Concentrations of NH_4-N were determined by hypobromite oxidation method with a detection limit of 5.0 μg/L. Zinc cadmium reduction method and azo photometric method were used in our experiments to measure the concentrations of NO_3-N and NO_2-N, and the two methods had a common detection limit of 5.0μg/L. For convenience, we use dissolved inorganic nitrogen (DIN) to represent the assumption of NH_4-N, NO_3-N and NO_2-N. SRP concentrations were determined with the method of phosphorus molybdenum blue spectrophotometric method and had a detection limit of 1.4 μg/L.

Two liters of seawater were filtered through 25 mm Whatman GF/F filters and stored frozen until analysis. Pigments were extracted in cold acetone (90%) for 24h, and the concentrations of chlorophyll a (Chla) were analyzed by spectrophotometry. We translated 250 ml seawater to polyethylene (PE) bottles for phytoplankton analysis, and the samples were buffered with formaldehyde (final concentration of 1%) solution. PE bottles were stored in dark until further analyze in laboratory. Phytoplankton cells were observed and counted with an optical microscope.

Statistics analyses. In this paper, a method recommended by the United Nations Educational Scientific and Cultural Organization (UNESCO) was used to calculate the primary productivity (*PP*): $PP=(Chla \cdot Q \cdot D \cdot E)/2$, where Q represents different levels of assimilation arithmetic mean index (3.7); D is daytime (14 h); E is the depth of euphotic layer. Diversity of phytoplankton community were described by the Shannon-Wiener diversity index (*H'*), Pielou's evenness(*J'*) and Margalef's calculation. Detailed formulas and annotations were saved in some literature [2].

Pearson correlation analysis and Canonical correlation analysis (CCA) were used in our analysis to determine the key environmental factors. Pearson correlation analysis were conducted in SPSS 21.0 program (Statistical Product and Service Solutions, USA). Biplots of the two tides were made with the MVSP3.1 program package (Kovach Computing Services, UK).

RESULTS

Environmental conditions. Corresponding environment factors of rising tide and falling tide in the survey area were shown in Tab.1. This area is a typical inshore sea, with a mean depth of 5.51 m in rising tide and 4.36 m in falling tide. Obviously, the depth of the middle two sampling cross-

TABLE 1
Mean (±standard error) values of physico-chemical parameters of five sections in study area

	H (m)	WT (℃)	pH	Sal (psu)	DO (mg/L)	DIN (mg/L)	SRP (mg/L)	DIN/SRP	Chla (μg/L)	PP
Rising tide										
T1	3.5±1.36	20.78±0.95	8.11±0.04	31.19±0.44	9.36±0.41	0.87±0.09	0.025±0.019	47.66±23.1	4.68±1.81	197.8±123.6
T 2	4.25±1.17	19.58±1.43	8.18±0.07	31.06±0.43	9.25±0.52	1.01±0.16	0.033±0.032	62.43±46.5	4.59±2.4	178.5±123.1
T 3	5.9±1.02	18.5±1.29	8.15±0.03	30.92±0.27	9.90±1.23	0.78±0.17	0.035±0.016	23.75±5.1	3.99±0.80	142.6±65.9
T 4	6.68±1.66	18.03±0.79	8.11±0.02	31.16±0.27	9.47±0.72	0.87±0.17	0.040±0.025	27.25±12.62	1.49±0.70	57.7±36.1
T 5	7.23±1.05	17.4±0.16	8.13±0.01	31.22±0.26	10.11±0.83	0.65±0.15	0.030±0.03	39.07±25.03	3.30±0.86	156±54.8
Mean	5.51±1.84	18.86±1.53	8.14±0.05	31.11±0.33	9.61±0.78	0.84±0.18	0.032±0.02	39.4±27.1	3.61±1.78	146.50±90.5
Falling tide										
T 1	2.78±0.97	20.78±0.95	8.08±0.03	31.18±0.44	9.61±0.78	0.90±0.07	0.028±0.02	41.64±19.02	5.09±1.29	183.2±111.8
T 2	3.2±1.02	19.58±1.43	8.16±0.1	31.04±0.43	9.52±0.75	1.05±0.17	0.036±0.034	58.29±43.42	4.28±0.44	124.2±31.2
T 3	4.65±1.16	18.5±1.29	8.14±0.03	30.9±0.27	9.76±0.27	0.80±0.21	0.037±0.015	22.98±4.58	2.85±1.53	88.5±53
T 4	5.4±1.62	18.03±0.79	8.08±0.06	31.10±0.31	9.24±0.45	0.92±0.21	0.044±0.025	24.8±9.45	1.36±0.72	44.8±33.9
T 5	5.75±1.05	17.4±0.16	8.12±0.02	31.21±0.25	9.73±0.07	0.67±0.14	0.033±0.03	35.68±24.11	2.70±0.82	106.4±40
Mean	2.78±0.97	20.78±0.95	8.08±0.03	31.18±0.44	9.61±0.78	0.90±0.07	0.028±0.02	41.64±19.02	5.09±1.29	109.41±70.1

TABLE 2
Dominant species of phytoplankton in study area

Taxa	Phylum	Abundance ratio (%)	Frequency (f_i)	Dominance (Y)
Skeletonema sp.	Diatom	31.49	0.75	0.2362
Ditylum brightwellii	Diatom	16.80	0.88	0.1478
Nitzschia longissima	Diatom	11.64	0.94	0.1094
Coscinodiscus excentricus	Diatom	9.52	1	0.0952
Thalassiosira rotula	Diatom	10.23	0.56	0.0573
Rhizosolenia styliformis	Diatom	9.25	0.63	0.0583
Coscinodiscus jonesianus	Diatom	7.14	0.69	0.0493

sections are overtop than the others. Seawater temperature, showed no significant difference during rising tide and falling tide, varying between 17.2℃ and 22.1℃. A distinct decrease of seawater temperature, from coastal waters to open waters can be observed in study area. Salinity was always thought to be a critical index in the ocean, and in our experiment, mean salinity during the two tides were nearly constant. The distribution of salinity was relatively uniform except for the area close to the mouth of Jiyun river and the offshore of Hangu distinct. pH and dissolved oxygen (DO) demonstrated an identical distribution during the two tides, and the five sections showed little variation. The DIN concentration during rising tide (mean concentration is 0.84 mg/L) was slightly lower than the falling tide (mean concentration is 0.87 mg/L), and the coastal waters had higher DIN concentration than that of deeper waters. The soluble reactive phosphorus (SRP) value was always well similar during the study period and had no significant difference between the two tides. DIN/SRP values were higher than 16 during both tides, and the values during the rising tide were slightly higher than the falling tide. It can be concluded that this area was characterized with high nutrients ascribed to anthropogenic inputs.

Chlorophyll a concentrations and primary productivity. Chla concentration could reflect the change rule of phytoplankton and characterize the standing crop of the primary producers in waters, and was often used as a vital indicator for evaluating eutrophication status. The survey revealed that concentrations of Chla were belonging to intermediate or low level, varying between 0.46 mg/m^3 to 8.17 mg/m^3. Mean concentrations of Chla during rising tide and falling tide were 3.61 μg/L and 3.25 μg/L, respectively. Mean value of Chla during rising tide were greater than the value during falling tide somewhat. Maximum value of Chla appeared in Sta.S8 during rising tide, while the minimum value was in Sta.S15 during falling tide. Chla concentrations were gradually decreased from coastal waters to offshore waters during rising tide, and a local low value region emerged in the deepest of monitoring waters during falling tide.

According to the formula shown in Section 2.3, we calculated the primary productivity (PP) in this area (Tab.2). Consistent with the Chla values, mean PP value of rising tide exceeded the value of falling tide. Values of mean PP in rising tide and falling tide were 146.5 and 109.4, respectively. Minimum values of PP were appeared in Sta.S15 in both tides, while maximum values showed in Sta. S8 during rising tide and Sta. S2 during falling tide (Dates not shown here).

Species composition and dominant species composition. In total, 33 species were identified during our research, including Bacillariophyta (31 species, accounting for 93.94%), Cryptophyta (1 species, accounting for 3.03%) and Chlorophyta (1 species, accounting for 3.03%). *Coscinodiscus* was the most frequently observed genus in this area, followed by *Nitzschia* and *Rhizosolenia*, accounting for 51.52%、6.06% and 6.06%, respectively. Phytoplankton cell

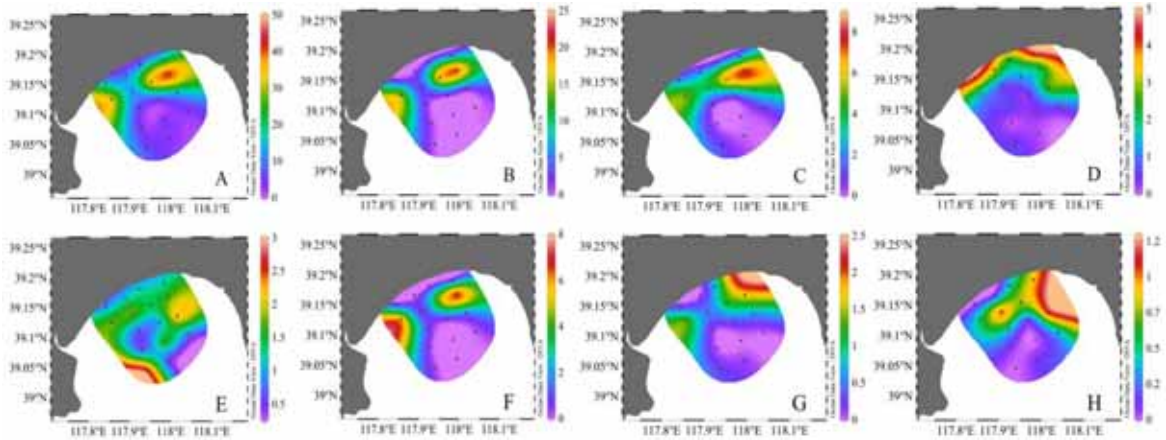

FIGURE 2

Horizontal distribution of dominant cells abundance in the surface water in the surveyed area (×10^4 cells/L). A:Phytoplankton; B: Skeletonema sp.; C: Ditylum brightwellii; D: Nitzschia longissima; E: Coscinodiscus excentricus; F: Thalassiosira rotula; G: Rhizosolenia styliformis; H: Coscinodiscus jonesianus.

TABLE 3

The Pearson correlation coefficients between biotic and abiotic variables in rising tide and falling tide

	H (m)	WT (℃)	pH	Sal (psu)	DO (mg/L)	DIN (mg/L)	SRP (mg/L)	DIN/SRP
Rising tide								
Chla	-0.408	0.135	0.623**	0.351	0.082	-0.041	-0.475*	0.556*
H′	-0.105	0.246	-0.612*	-0.146	-0.252	-0.165	0.378	-0.649**
J′	0.150	-0.078	-0.582*	0.082	-0.105	-0.360	0.290	-0.633**
Phytoplankton	-0.596*	0.306	0.724**	-0.056	-0.171	0.524*	-0.269	0.610*
Falling tide								
Chla	-0.569**	0.651**	0.227	0.043	0.217	0.288	-0.259	0.399
H′	0.065	0.246	-0.497	-0.154	-0.048	-0.152	0.388	-0.680**
J′	0.203	-0.078	-0.437	0.071	0.066	-0.359	0.301	-0.673**
Phytoplankton	-0.709**	0.306	0.608*	-0.030	0.111	0.474	-0.268	0.615*

abundances were shown in Fig. 2. Surface phytoplankton cell concentrations ranged from 2.429×10^4 cells/L to 4.51×10^5 cells/L, and the mean concentration was 1.386×10^5 cells/L. Compared with deeper waters, section T1 and section T2 were close to the offshore and more easily affected by anthropogenic nutrient inputs. Thus, an apparent difference in cell abundance could be observed between coastal waters and deeper waters. Phytoplankton cell abundance was highest in Stn. S8 and lowest in Stn. S14 (Dates not shown here).

The dominance species in the study area were all diatoms. In order, *Skeletonema* sp., *Ditylum brightwellii*, *Nitzschia longissima*, *Coscinodiscus excentricus*, *Thalassiosira rotula*, *Rhizosolenia styliformis* and *Coscinodiscus jonesianus* were the most common diatoms in this season (Fig.2). Among them, *Skeletonema* sp. were the first dominant species, its mean cell quantity reached 4.36×10^4 cells/L, accounting for 31.49%. Maximum values of *Skeletonemas* sp. appeared in Stn.S8. The second and third dominant species were *Ditylum brightwellii* and *Nitzschia longissima*, accounting for 16.80% and 11.64%, respectively. Appearance frequency (f_i) analyses were conducted to explore the highest occurrence frequency species. From the statistics, *Coscinodiscus excentricus* emerged in every sampling station, closely followed by *Nitzschia longissima* and *Ditylum brightwellii*. In general, a small quantity of phytoplankton was found in this study area.

Pearson correlation analysis and CCA between phytoplankton and environmental variables. Pearson correlation analysis between organism and environmental factors are shown in Tab.3, it's quite useful to determine the critical factors that influence the growth of phytoplankton. Chla concentration showed a positively relationship with pH ($p<0.01$) and DIN/SRP ($p<0.01$) during rising tide, while it was positively related with WT ($p<0.01$) and negatively correlated with H ($p<0.01$) during falling tide. This correlation results revealed different nutrient strategies during a tide. Phytoplankton cell concentrations had come out virtually unanimously outcomes during both correlation analysis. They were positively related with pH, DIN and DIN/SRP, and negatively correlated with H. Other factors haven't showed significant correlation with phytoplankton cell concentrations. Compared with phytoplankton cell concentrations, Shannon-Wiener diversity index (*H'*) and Pielou's evenness values (*J'*) displayed an

adverse correlation. This two indicators were all negatively correlated with DIN/SRP ($p<0.01$) in both tides. In addition, *H'* and *J'* showed negatively correlation with pH ($p<0.01$) during rising tide while similar results haven't found during falling tide.

CCA is a useful tool to explain the internal relations between species and environmental factors. Similar location of species in CCA bioplots have a consistent response with the ecological adaptability of the environment. To better reflect ecological requirements of dominance species in study area, we analyzed the congruent relationship between seven dominance species and environmental factors. The position of phytoplankton in the map can reflect dependence severity of dominance species on different environmental factors. Often, for various species, the more closer relationship in taxonomy, the more closer distribution in the biplot. In rising tide, the abundance of *Skeletonema* sp., *Nitzschia longissima* , and *Coscinodiscus excentricus* were positively related to temperature, DIN and SRP. While the abundance of *Ditylum brightwellii* and *Rhizosolenia styliformis* mostly related to salinity. And, in falling tide, the abundance of *Ditylum brightwellii* and *Rhizosolenia styliformis* showed positive correlation with temperature, salinity, DIN and SRP. Other dominance species didn't show correlation with environment factors.

DISCUSSION

Diversity of phytoplankton community. Biological community diversity, one of the most important properties for biogenesis, reflects a function relation between the types and individual numbers of biological communities. It can be evaluated by species diversity index and evenness. Shannon-Wiener diversity index (*H'*) and Pielou's evenness (*J'*) are two characterizations of community stability index [13]. Generally speaking, higher values of *H'* and *J'* indicate more stability and maturity of the ecosystem. Based on the formula given in Sun [14], we calculated the relevant indexes as shown in Tab.4. *H'* ranged from 2.03 to 3.31, with a mean value of 2.76. Mean section values of H', except for section T2,

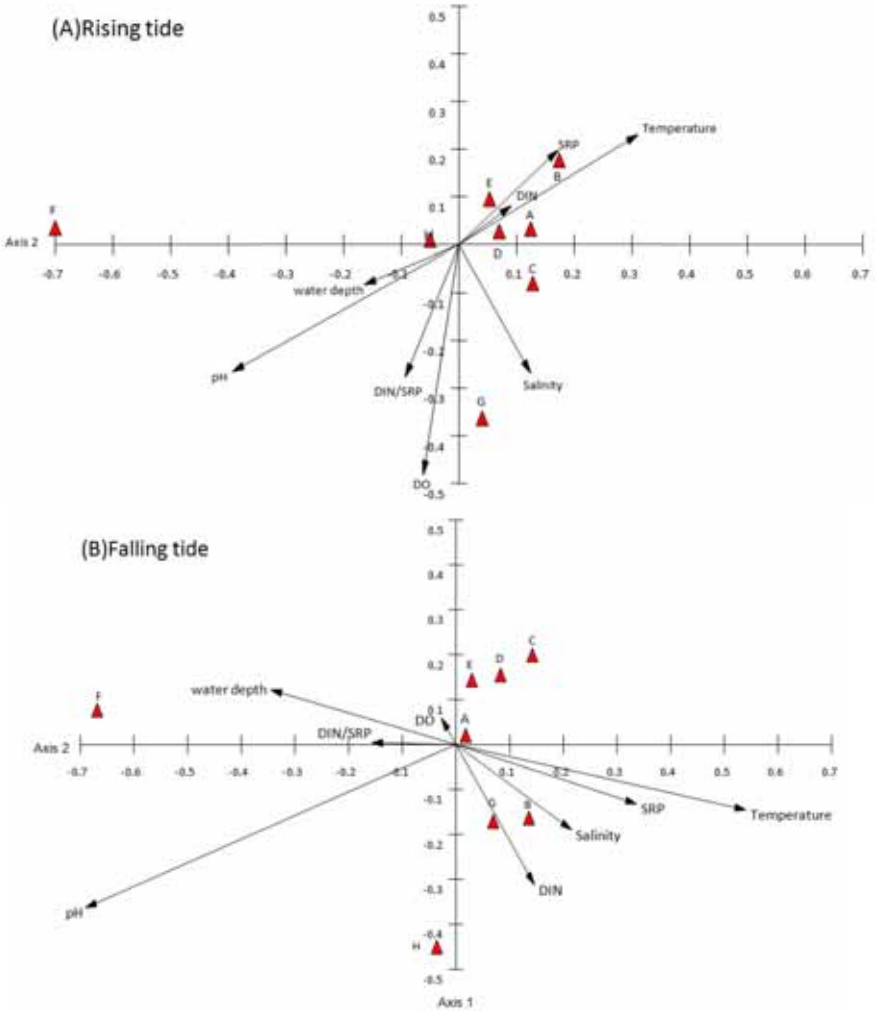

FIGURE 3

Biplots of dominant species and environment factors in study area in (A) rising tide and (B) falling tide. A: Chla; B: Skeletonema sp.; C: Ditylum brightwellii; D: Nitzschia longissima; E: Coscinodiscus excentricus; F: Thalassiosira rotula; G: Rhizosolenia styliformis; H: Coscinodiscus jonesianus.

TABLE 4
Phytoplankton diversity index, evenness and abundance in study region

Station	*H′*	*J′*	d	Eutrophication status	Station	*H′*	*J′*	d	Eutrophication status
S1	3.20	0.84	3.47	Slight	S11	3.31	0.87	9.20	Slight
S2	2.83	0.79	3.38	Moderate	S12	2.84	0.82	2.64	Moderate
S3	3.29	0.84	4.20	Slight	S14	3.05	0.82	9.37	Slight
S4	3.08	0.83	2.89	Slight	S15	2.67	0.80	3.86	Moderate
S5	2.26	0.65	1.94	Moderate	S16	2.73	0.91	4.42	Moderate
S6	2.85	0.82	2.99	Moderate	S18	2.49	0.75	3.31	Moderate
S7	2.10	0.63	1.71	Moderate	S19	2.08	0.66	4.44	Moderate
S8	2.03	0.72	1.09	Moderate	Range	2.03～3.31	0.63～0.91	1.09～9.37	/
S10	3.28	0.89	5.23	Slight	Mean	2.76	0.79	4.01	Moderate

TABLE 5
Comparison of dominant species with historical data in the same season

Location	Time	Dominant species	Reference
117º6'E～118º2'E 38º 6'N～39º 2'N	May,2013	*Noctilucas cintillans* *Coscinodiscus oculus-iridis* *Coscinodiscus asteromphalus* *Coscinodiscus* spp.	[21]
117º46'E～118º04'E 38º39'N～39º 05'N	May,2012	*Rhizosolenia delicatula* *Skeletonema costatum* *Chaetoceros curvisetus*	[22]
117º50'E～118º9'E 39º 4'N～39º 12'N	May 7 to 11,2009	Tab.2	This study
117º50'E～118º1'E 38º 5'N～39º 2'N	May,2005	*Paralia sulcate* *Skeletonema costatum* *Coscinodiscus* spp. *Chaetoceros* spp.	[23]
Coastal area of Bohai Bay	May,1998	*Coscinodiscus* spp. *Chaetoceros* spp. *Rhizosolenia* spp. *Ceratium* spp.	[16]
West of Bohai Bay(118º25'E)	1964～1981	*Skeletonema costatum* *Eucampoia zoodiacus* *Rhizosolenia stolterfothii* *Leptocylindrus danicus* *Thalassionema nitzschioides*	[24]

gradually decrease from section T1 to section T5. Reasons for this distribution trend were higher cell abundance in coastal waters than deeper waters, and the community composition structure became complicated and diversified. For section T2, despite its higher cell abundance, the total number of species were relatively low and the cell abundance ratio of minority dominant species were comparatively high. For instance, at Stn.S8 we only detected 8 species that all belong to diatoms, among them *Skeletonema* sp. and *Ditylum brightwellii* accounted for almost 70%, a similar situation discovered in other low diversity sites. Pielou's evenness values (*J′*) ranged from 0.63 to 0.91, and the mean value was 0.79. Similar to the Shannon-Wiener diversity index, Pielou's evenness value (*J′*) in section T2 was lower than other sections. Combined with the distribution of dominant cells abundance in this survey, lower values of *J′* also corresponded to areas with higher phytoplankton abundance, suggesting that the existence of dominant species would reduce the region phytoplankton diversity to some extent.

Eutrophication status in study area. Species diversity index is an important attribute of the biological community structure, and it can be used as the biological indexes for evaluate water quality and predict the occurrence of red tides. Shannon-Wiener diversity index (*H'*) can be used in any biological group theoretically. In terms of phytoplankton, its computational error is very small due to each species are small and homogeneous. Judgment criterion of diversity index is: *H'*=0 represents severe pollution; *H'*< 1 represents heavy pollution; *H'= 1* and *J'=0.1* represents occurrence threshold of phytoplankton red tides; *H'*= 1～3 represents middle level pollution; *H'> 3* represents slight pollution. According to this criteria, we could come to the conclusion that this area is moderately polluted.

The nutrients limitation in study area. The growth and propagation of phytoplankton are mainly influenced by nutrients levels and uptake processes among these species [13]. This progress is recognized as bottom-up effects or nutrients limiting [15]. According to Redfield ratio, the most suitable N and P ratio for phytoplankton growth is 16:1. In this survey, DIN concentration in rising tide was lower than that in falling tide, while SRP concentration showed a reverse trend. N and P ratio was much higher than Redfield ratio, with a mean ratio of 39.4:1 in rising tide and 41.64:1 in falling tide. The two mean ratios

were not vary too much, it implied that the nutrients structure didn't vary wildly during the two tides. According to the literature, nitrogen was the predominant limiting nutrient in the 1980s in Bohai, while this ratio approached 16:1 in the 1990s [1]. In our investigation, this ratio was much higher than the values previously reported. The main reason for this situation was caused by untreated sewage discharged into the offshore of Bohai bay from the peripheral city. These history ratio and their changes suggested that the nutrient limiting factor for phytoplankton growth could turn to phosphate limitation from nitrogen limitation in the last decade. This is in keeping with more recent studies conducted in this area [16].

Relationship between phytoplankton and environmental factors. Chla is an important indictor to characterize the phytoplankton standing stock, and it can reflect the change rule of phytoplankton. In simple numerical terms, mean concentration of Chla in rising tide was lower than that in falling tide. One reason for this was fresh water with low phytoplankton biomass entered into Bohai Bay diluted the original waters. Pearson correlation analysis and CCA showed different strategies during the two tides. In rising tide, SRP and pH were the main factors that control the phytoplankton growth, while these factors had no obvious effect in falling tide. This might caused the increase of SRP concentration in rising tide which could remit P limitation. The influence mechanism of tides on phytoplankton structure may attribute to horizontal migration, diffusion and aggregation processes. The periodic change of the phytoplankton community structure can be further influenced by the surface layer water temperature, nutrient concentration and other environmental factors.

Comparative analysis of dominant species with history. Compared with history date, dominant species in Bohai Bay were diatom before 2012. A investigation conducted in 2013, however, showed a distinct change that *Noctilucas cintillans* which belonged to dinoflagellate became the first dominant species [1]. It partly explained that some changes of phytoplankton community structure have taken place in coastal area of Bohai Bay for the past few years. Many researches have indicated that dominance species will change to dinoflagellate from diatom with the increase of N and P ratio [17]. Though such phenomenon haven't found in our survey, the raise of N/P would driven this change definitely. Notably, *Skeletonema*, *Coscinodiscus* proved to be the major dominant genuses in this bay though the cell abundance changed a lot. *Skeletonema,* a eurythermic and euryhaline genus which could result in red tides, was always extensively distributed in coastal waters [18]. It always reached the maximal biomass in April to May and August to September. Literature has recorded that this species incurred red tides in the Yellow Sea, the Bohai sea and the South China Sea [19]. *Coscinodiscus* is a neritic genus which always shown in Bohai Bay, preferred living in waters with high salinity [20]. These two species needs more nitrogen to support their growth, while the increase of DIN can just provide a good material basis.

CONCLUSION

In summary, our preliminary investigation of phytoplankton community structure showed that diatoms were the major groups in this area. Compared with history data, diatom was the major group before 2012 and then dinoflagellate hold the advantage. It means that the nutrients change have lead to the variation of phytoplankton structure. Tidal effects on phytoplankton community structure were reflected not only in physical effects, but also in physiological functions by environment factors. However, the real effect of tidal on phytoplankton is still mysterious for us. Further studies, such as the field time-series station work and long-term monitory program, should conducted in this area to better explain the phytoplankton change during the period of a tide.

ACKNOWLEDGEMENTS

This work was supported by the Natural Science Foundation of China (41676112), the Key Project of Natural Science Foundation for Tianjin (17JCZDJC40000), the strengthening the ocean by science and technology for Tianjin (KJXH2013-22), the University Innovation Team Training Program for Tianjin (TD12-5003), and the Program for Changjiang Scholars to Jun Sun.

REFERENCES

[1] Guo, S.J., Li, Y.Q., Zhang, C.X., Zhai, W.D., Huang, T., Wang, L.F., Ma, W., Jing, H. L., and Sun, J. (2014). Phytoplankton community in the Bohai Sea and its relationship with environmental factors. Marine Science Bulletin , 33(1), 95-105. [in Chinese]

[2] Yuan, M.L., Zhang, C.X., Jiang, Z.J., Guo, S.J., and Sun, J. (2014). Seasonal Variations in Phytoplankton Community Structure in the Sanggou, Ailian, and Lidao Bays. Journal of Ocean University of China, 13(6), 1012-1024.

[3] Sun, J. (2011). Marine phytoplankton and biological carbon sink, Acta Ecologica Sinica, 31(18), 5372-5378. [in Chinese]

[4] Ren, Y. C., Wang, F., Dong, S. L., and LIU F. (2010). Seasonal characteristics of primary pro-

duction of sea cucumber (Apostichopus japonicus) culture ponds in Jinghai Bay, Rongcheng. Periodical of Ocean University of China, 40(3), 24-28. [in Chinese]
[5] Zhang, C.X., Chen, T., Huang, X., Guo, S.J., Zhai, W.D., and Sun, J. (2014). Phytoplankton Communities in the Northern Yellow Sea in Summer. Transactions of Oceanology & Limnology, 1, 81-92. [in Chinese]
[6] Peng, S.T., Qin, X.B., Shi, H.H., Ran, Z., Dai, M.X., and Ding, D.W. (2012). Distribution and controlling factors of phytoplankton assemblages in a semi-enclosed bay during spring and summer. Marine Pollution Bulletin, 64(5), 941-948.
[7] Tang, D.L., Kawamura H., Im, S.O., and Joe, B. (2006). Satellite evidence of harmful algal blooms and related oceanographic features in the Bohai Sea during autumn 1998. Advances in Space Research, 37(4), 681-689.
[8] Duan, L.Q., Song, J.M., Li, X.G., Yuan, H.M., and Xu, S.S. (2010). Distribution of selenium and its relationship to the eco-environment in Bohai Bay seawater. Marine Chemistry, 121(1-4), 87-99.
[9] Xu, X.F., and Tao, J.H. (2011). Application of structural equation model for exploring the influence of environmental factors on phytoplankton in Bohai Bay. Advanced Materials Research, 347, 1832-1835.
[10] Peng, S.T., Dai, M.X., Hu, Y.D., Bai, Z.P., and Zhou, R. (2009). Long-term (1996–2006) variation of nitrogen and phosphorus and their spatial distributions in Tianjin Coastal Seawater. Bulletin of Environmental Contamination and Toxicology, 83(3), 416-421.
[11] Chen B.C., and Wen, H., (2013). Simulation of the Tide and Current in the Bohai Bay with FVCOM. Journal of Tianjing University of Science & Technology, 8(4), 40-43. [in Chinese]
[12] Arindam, C., Gadi, P., and Amit, K.G. (2015). Tidal variation of phytoplankton in the coastal waters of South Andaman, India. Journal of Environmental Biology, 36(1), 207-214.
[13] Liu, H.J., Hhuang, Y.J., Zhai, W.D., Guo, S.J., Jin, H.L., and Sun, J. (2015). Phytoplankton communities and its controlling factors in summer and autumn in the southern Yellow Sea, China. Acta Oceanologica Sinica, 34(2), 114-123.
[14] Sun, J., and Liu D.Y. (2004). The application of diversity indices in marine phytoplankton studies. Acta Oceanologica Sinica, 26(1), 62-75. [in Chinese]
[15] Sun, J., Feng, Y.Y., Wang, D., Song, S.Q., Jiang, Y., Ding, C.L., and Wu, Y. (2013). Bottom-up control of phytoplankton growth in spring blooms in Central Yellow Sea, China. Deep sea Research Part II, 97(12), 61-71.
[16] Wang, J. (2003) Species composition and quantity variation of phytoplankton in inshore waters of the Bohai Sea. Marine Fisheries Research, 24(4), 44-50. [in Chinese]
[17] Egge J K. (1998). Are diatoms poor competitors at low phosphate concentrations? Journal of Marine Systems, 16(3-4), 191-198.
[18] Wiebe, H.C.F.K., Diana, S., Sergio B., Gu, H.F., Robert, A.A., and Adriana, Z. (2008). Global Diversity and Biogeography of Skeletonema Species (Bacillariophyta). Protist, 159(2), 177-193.
[19] Dou, Y., Gao, J.W., Shi, X.T., Chen, R.N., and Zhou, W.L. (2015). Outbreak frequency and factors influencing red tides in nearshore waters of the South China Sea from 2000 to 2013. Journal of Hydroecology, 36(3), 31-37. [in Chinese]
[20] Francisco, V.C., Francisco, J.G.M., and Maria, E.M.D.C. (2010). Phytoplankton assemblages in two compartmentalized coastal tropical lagoons (Carretas-Pereyra and Chantuto-Panzacola, Mexico). Journal of Plankton Research, 32(9), 1283-1299.
[21] Wang, Y., Liu, L.S., Zhu, Y.Z., Lin, K.X., Zhou, J., and Xia, Y. (2016).The community structure of phytoplankton sampled by nets in the coastal seawaters of Bohai bay in spring and autumn. Marine Environmental Science, 35(4), 564-570. [in Chinese]
[22] Yin, C.L., Zhang, Q.F., Niu, F.X., Shi, H.M., Xu, Y.S., and Tu, J.B. (2015). Primary Productivity and net-phytoplankton composition in Tianjin nearshore waters of Bohai Bay from 2012 to 2013. Journal of Marine Sciences, , 33(2), 82-92. [in Chinese]
[23] Xu, Y.S, Liu, X.B., and Zhang, Q.F. (2009). Studies on Species Diversity of Phytoplankton in the Offshore Marine Areas of the Bohai Bay. Journal of Salt and Chemical Industry, 38(6), 11-14. [in Chinese]
[24] Kang Y.D. (1986). Ecological characteristics of phytoplankton in the Yellow Sea and its relationship with fishery. Marine Fisheries Research, 2, 51-53. [in Chinese]

Received: **26.09.2016**
Accepted: **26.03.2017**

CORRESPONDING AUTHOR

Jun Sun
College of Marine and Environmental Sciences, Tianjin University of Science and Technology, Tianjin 300457, China

e-mail: phytoplankton@163.com

© by PSP Volume 26 – No. 10/2017 pages 5745-5753 Fresenius Environmental Bulletin

RISK DECISION ANALYSIS OF FLOODWATER RESOURCE UTILIZATION BASED ON ADJUSTING FLOOD LIMITED WATER LEVEL OF RESERVOIR

Guohua Fang*, Yong Yang, Yu Yuan, Xianfeng Huang, Xin Wen

College of Water Conservancy and Hydropower Engineering, Hohai University, Nanjing, China

ABSTRACT

On the basis of analyzing the factors affecting the floodwater resource utilization by adjusting flood limited water level (FLWL), the floodwater resources utilization risk evaluation index system was constructed. And based on the risk analysis and multi-objective decision-making theory, risk decision-making model regarding the maximum comprehensive benefit as the target was established. The China's Shilianghe reservoir was selected as a case study. The results indicate that the risk evaluation index system and the risk decision-making model can be used to analyze and demonstrate the FLWL adjustment problem. As the FLWL gradually improving, water storage benefit gradually increases, showing linear relationship. The contribution rate of different water storage benefits indices to water storage benefit is different. Dam safety risk loss is the main aspect of adjusting FLWL risk loss, followed by downstream river channel security risk loss, environmental risk loss is a small part in total risk loss. As the FLWL gradually improving, total risk loss gradually increases. As the FLWL gradually improving in a certain range, comprehensive benefit gradually increases. When the level reaches a certain value, the comprehensive benefit is largest. After the threshold, comprehensive benefit gradually decreases.

KEYWORDS:
Floodwater resource utilization; Adjustment of FLWL; Risk evaluation index system; Decision-making model; Comprehensive benefit; Shilianghe reservoir

INTRODUCTION

Downstream areas are always economically developed and the core areas of the national economy industry in china, such as the lower areas of the Yangtze River, the Pear River and Huaihe River. With social progress and economic development, water demand in these areas is growing[1]. Water supply and demand contradictions have become increasingly prominent. In order to alleviate the situation, floodwater resource utilization is one of effective ways easing the shortage of water resources[2]. Adjustment of FLWL of reservoir is an important way of floodwater utilization[3]. Rising FLWL can improve the economic benefits of water supply, generating electricity and irrigation, etc. However, it may also correspondingly increase the risk of flood control, water quality security and ecological environment security, etc.[4]. Thus, in order to use floodwater resource safely and efficiently, determine the optimized scheme, risk analysis of floodwater resource utilization by adjusting FLWL must be carried out.

In the process of the study on the risk of floodwater resources utilization, Cao et al. expounded the implementation approach, main risks and risk management countermeasures of flood water resources utilization[5]. Wang et al. proposed that the risk management mode is a feasible mode of flood management in China and the core and main goal of flood risk management is making full use of floodwater resource[6]. Fang et al. assessed the risk items of flood resources utilization by considering risk level and risk degree[7]. Gu et al. studied the risk of floodwater resource configuration by considering the resource quantity, and established multivariate risk analysis model based on stochastic simulation technique to provide basis for configuration scheme[8]. Li et al. pointed out that random process theory was an effective tool for risk analysis of floodwater resource utilization under the unstable condition[9].

At present, the main research aspect of flood resources utilization is adjustment of FLWL. Wurbs et al. drew a relatively reasonable FLWL by considering flood losses from an economic view point and comparing the losses with the benefits obtained from adjusting FLWL[10]. Salmon et al. combined the probability of dam failure caused by adjusting FLWL with the losses caused by dam failure by using tolerance risk analysis method[11]. Fu et al. set up a risk analysis model of adjusting FLWL of large reservoir by using systematic analysis method, and the calculated results showed the relationship between different FLWL and the maximum flood hazard risk rate[12]. Yin et al. defined the concept of risk degree

and used risk degree to evaluate the risk of adjustment of FLWL scheme[13]. Wang et al. took Biliuhe reservoir for example to analyze the risk caused by adjusting FLWL, adopted the method of combination of FLWL and flood frequency to calculate dam safety risk ratio, and comprehensive considered flood calamity strength, the density and the vulnerability of disaster bearing body in calculating risk losses[14].

For now, research on the theoretical approaches and practical application of risk analysis of floodwater resource utilization based on adjusting FLWL is in continuous development and improvement. The current research results are focused on flood risk analysis method[15]. Such as probability and mathematical statistics method, limit analysis method and Monte Carlo stochastic simulation method, etc. The research on risk decision-making model is relatively less.

In this paper, risk evaluation index system and risk decision-making model of adjusting FLWL regarding the maximum comprehensive benefit as the target were constructed to provide theoretical basis for selection of reservoir flood resources utilization plan. The indices considered in the model were water storage benefits and risk losses. The main objective of this study was to develop the decision making model system for determining the FLWL of Shilianghe reservoir in China. And the study provides a useful framework for similar studies in other regions of the word.

MATERIALS AND METHODS

Risk decision-making model of adjusting FLWL.(1) Construction of risk evaluation index system of decision-making.FLWL is important for the flood control security and its economic benefits[16]. Many factors, such as dam protection, downstream protection and water storage benefits, are involved in the determination and adjustment of FLWL. On the one hand, the flood control capacity of reservoir, the highest flood level in front of the dam in theprocess of reservoir flood routing and risks of dam safety, downstream river channel security and environmental safety etc. are determined by FLWL. On the other hand, FLWL has direct influence on the water storage capacity of the reservoir during and after the flood season, which directly determines the water storage benefits. Thus, on the premise of ensuring flood risk, the FLWL should be raised in order to increase the water storage capacity and the economic benefits.

The key of floodwater resources utilization by adjusting FLWL is the objective quantitative evaluation of risk loss and benefit. Considering various factors synthetically, the floodwater resources utilization risk evaluation index system based on adjusting FLWL was constructed (Figure 1).

(2) Water storage benefit indices. The main aspects of water supply benefits are industry water supply, agriculture water supply, domestic water supply and the third industry water supply benefits. Industrial value added method and benefit allocation coefficient method were used to calculate these benefits.

The equation for industry water supply, agriculture water supply and the third industry water supply benefits is as follows[17]:

$$B_{123} = Vqk = (I / W) fqkB_4 \quad (1)$$

The equation for domestic water supply benefit is as follows:

$$B_4 = Vqk = (re / p) fqk \quad (2)$$

where B_i is water supply benefit, i=1,2,3,4; V is water price; q is increased water supply; k is water resource utilization; I is industrial added value; W is the total water consumption; f is benefit allocation coefficient; r is disposable income of Chinese households; e is Engel's coefficient; p is per capita yearly water consumption.

The calculated results mainly reflect the benefits of flood resources applied to industry growth. The higher industrial added value is, the more benefits of floodwater resources utilization is.

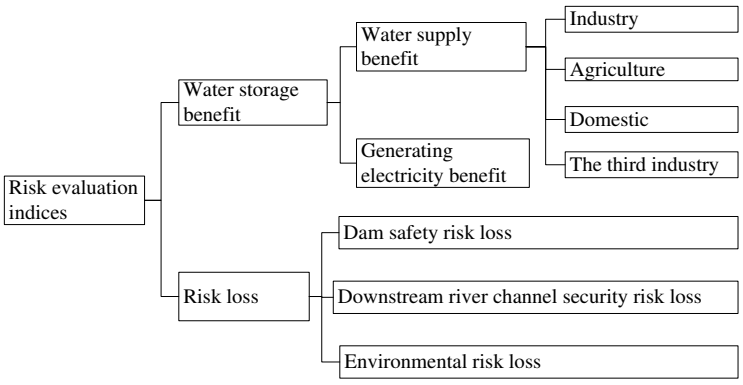

FIGURE 1
FLWL risk evaluation index system of decision-making.

After the FLWL was adjusted, certainly the water head for power generation would be changed correspondingly. And the annual average generating capacity of the hydropower station would also be changed. The annual average generating capacity was calculated according to the water loss rate of each unit of electrical energy. The equation for generating electricity benefit is as follows[18]:

$$B_5 = \frac{\Delta V}{\varphi} \times \delta \quad (3)$$

where B_5 is generating electricity benefit; ΔV is increased water storage can be used in electricity generation; $\varphi$is the water consumption of each unit of electrical energy; $\delta$is regional average on-grid electricity prices.

(3) Risk loss indices. The direct integral method, based on the theory of probability and mathematical statistics, has been used in dam water level analysis[19]. In the reservoir flood control dispatching, indeterminacy risk factors obey the typical probability distribution, such as Pearson Type III distribution and normal distribution etc. According to the characteristic distribution and parameters of these variables, using probability statistical analysis method can calculate the reservoir flood dispatching risk.

Improving reservoir water limit level in flood seasons can increase the reservoir storage and economic benefit, but decrease flood control capacity, increase the risk of surpassing design standard level (Z_d). The equation for the risk is as follows:

$$R = p\{Z_m(t) \geq Z_d\} \quad (4)$$

where Z_d is the value of design standard level, used to calculate the risk ratio, and the value range is between design flood level and check flood level; $Z_m(t)$ is the possible highest water level through the stochastic simulation of inflow flood and flood regulating calculation under a certain FLWL.

There are many uncertainty factors, such as hydrological process, hydraulic change and engineering structure, in the reservoir flood control. Because of this, the risk can be further stated as follows:

$$R = p\{Z_m(t) \geq Z_d\} = \int_{Z_d}^{\infty} f(z)dz \quad (5)$$

where *f(z)* is the probability density function of reservoir water level, when the statistical data is enough, *f(z)* can be replaced by inflow flood data.

The dam safety risk ratio, downstream river channel security risk ratio and environmental risk ratio, caused by adjusting FLWL, can be calculated based on the above theory.

The probability density function of dam safety risk is difficult to determine, so that it is unable to establish integral equation. This study used historical flood data to calculate dam safety risk ratio by flood routing of reservoir. The equation for the risk ratio is as follows:

$$f_1(H_i) = \frac{n}{N+1} \quad (6)$$

where $f_1(H_i)$ is the risk ratio of surpassing design standard level (Z_d) when the FLWL is H_i; N is the total number of flood in historical flood data; n is the number of occurring surpassing design standard level (Z_d) through flood routing when the FLWL is H_i.

The calculation of inundation loss is associated with inundated area, inundated time, inundated depth and flow velocity[20, 21]. In this study, inundated area was used to calculate inundation loss. The equation for the risk loss is as follows:

$$L_1(H_i) = f_1(H_i) \times L_1 \quad (7)$$

$$L_1 = (1+\alpha)\beta A + C_p \quad (8)$$

where $L_1(H_i)$ is the dam safety risk loss when the FLWL is H_i; L_1 is the dam safety risk loss of unitized risk ratio; $\alpha$is indirect loss coefficient; β is direct loss of unit area; A is inundated area; C_p is cost of flood-relief efforts.

The downstream river coast will face risk when the water release discharge is bigger than downstream safety discharge. And the bigger water release discharge the more losses. There is also threat when water release discharge is less than downstream safety discharge but close. The threat potential of water release discharge is measured by flow range, and membership grade function of flow range is used to calculate downstream river channel security risk. The equation for the risk ratio is as follows:

$$f_2(H_i) = \sum V_i \in A \mu_A(V_i) \times p(V_i) \quad (9)$$

where $f_2(H_i)$is downstream river channel security risk ratio when the FLWL is H_i;$f_2(H_i)$is the probability of water release discharge belonging to a certain flow range V_i;$\mu_A(V_i)$ is the membership grade of a certain flow range V_i.

In order to avoid overlap with dam safety risk loss, the dam was assumed safety when calculating downstream river channel security risk loss. In this study, inundated area, located on either side of levees, was used to calculate the loss. The equation for the risk loss is as follows:

$$L_2(H_i) = f_2(H_i) \times L_2 \quad (10)$$

$$L_2 = (1+\alpha)\beta A + C_p \quad (11)$$

where $L_2(H_i)$ is the downstream river channel security risk loss when the FLWL is H_i; L_2 is the downstream river channel security risk loss of unitized risk ratio.

Ecological environmental impacts are mainly demonstrated as river self-purification capability decreased and the deterioration of creature's living environment caused by water release discharge diminished. And the local environmental changes resulted from reservoir operates at a high water level. Ecological environmental impacts are hard to quantitative calculate, and is usually simulate by subjective estimate according to regional history data. The equation for the risk ratio is as follows:

$$f_3(H_i)=\sum_{j=1}^{n} f_3(H_i,T_j) \quad (12)$$

$$f_3(H_i,T_j)=k_{31}\times f_{31}(T_j)+k_{32}\times f_{32}(T_j)+k_{33}\times f_{33}(T_j) \quad (13)$$

where $f_3(H_i)$is the environmental risk ratio when the FLWL is H_i; $f_{31}(T_j)$ is the loose rate of upstream flood during the period of T_j; $f_{32}(T_j)$is the incremental rate storage capacity during the period of T_j; $f_{33}(T_j)$ is the probability of downstream river flow is less than the lowest environmental water demand during the period of T_j; k_{31}、 k_{32} and $k_{33}$are weight coefficients.

Change of flow rate has influence on the structure and function of river ecosystem[22]. Floodwater resource utilization will change the former river ecosystem and the ecosystem service value of the river. In this study, according to the research results of Costanza and Xie, ecosystem service value coefficient per area of China's terrestrial ecosystems was used to calculate environmental risk loss[23]. The equation for the risk loss is as follows:

$$L_3(H_i)=f_3(H_i)\times\sum_{i=1}^{n} A_i\times d_i \quad (14)$$

where $L_3(H_i)$ is the environmental risk loss when the FLWL is H_i; A_i is the area of different land ecosystem influenced by floodwater resource utilization; d_i is ecosystem service value coefficient per area of different land ecosystem.

(4) Construction of risk decision-making model. Risk decision is the ultimate purpose of risk analysis[24]. This study discussed risk benefits and risk losses, constructed risk decision model. The results provide a basis for selection of different flood utilization projects.

The objective of risk decision model is most optimal comprehensive benefit. The value of linear combination of the water storage benefits and risk losses was considered as the evaluation index in this paper. The relation between water storage benefits and risk losses is contradictory. Risk losses are calculated in term of economic losses. The maximum comprehensive benefits can be calculated in the dynamic changes of the risk benefits and risk losses according to the decision-making model. The equation for the model is as follows:

$$F(H_i)=\sum_{j=1}^{n} B_j(H_i)-\sum_{j=1}^{m} L_j(H_i) \quad (15)$$

where $B_j(H_i)$ is the risk benefits when the FLWL is H_i; $L_j(H_i)$is the risk losses when the FLWL is H_i; n is the number of risk benefit, n=5; m is the number of risk loss, m=3.

Study case. (1) Study area. Shilianghe reservoir, located in Lianyungang city between latitude of 34°44′~35°49′N and longitude of 118°44′~118°52′E, controls drainage area of 15673 km^2. The annual precipitation in the study area is 1785mm. Shilianghe reservoir, with a total capacity of 5.31×10^8m^3, is the largest reservoir in Jiangsu Province. The utilizable capacity is 2.34×10^8m^3. The current FLWL is 23.5 m, design flood level is 26.81m and checkflood level is 27.95m, peak discharge of design flood is 7367 m^3/s, peak discharge of check flood is 9640 m^3/s, maximum discharge is 10131 m^3/s. Shilianghe reservoir is a large-scale comprehensive hydro project privileged to irrigation and flood control, incorporating with urban water supply, electric power generation and aquiculture. The location map of Shilianghe reservoir studied in this paper can be seen in Figure 2.

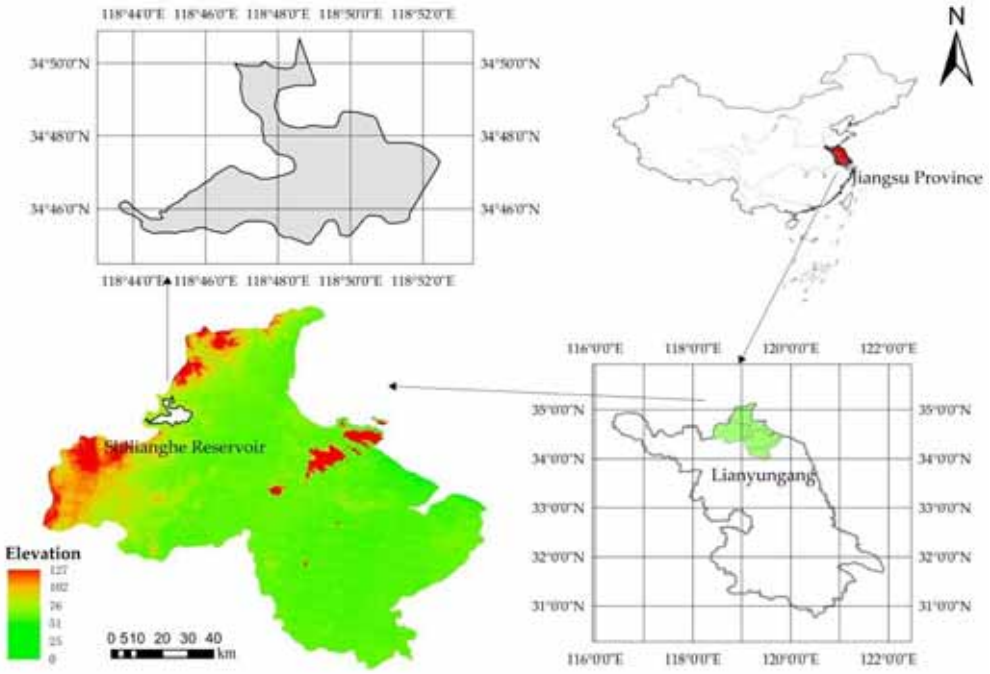

FIGURE 2
Location map of Shilianghe reservoir studied in this paper.

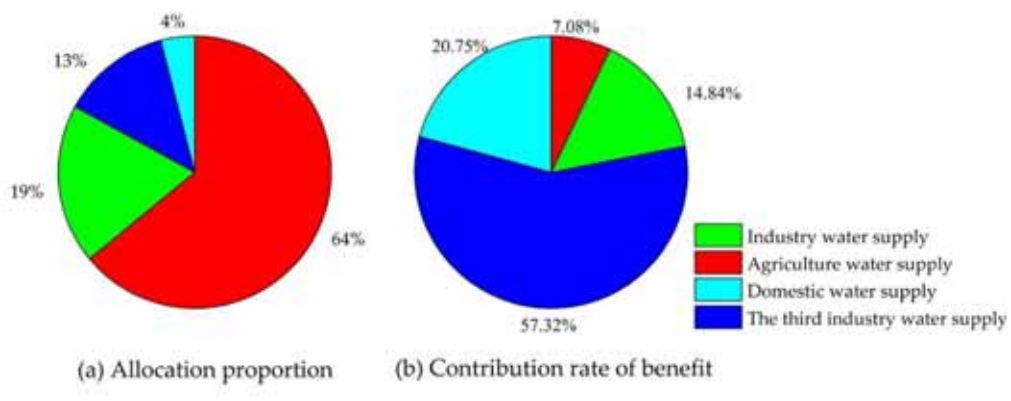

FIGURE 3
The water supply allocation proportion and contribution rate of benefit of industry water supply, agriculture water supply, domestic water supply and the third industry water supply: (a) allocation proportion, (b) contribution rate of benefit.

(2) Calculation of water storage benefit indices. The main functions of Shilianghe reservoir are water supply and flood control. Flood control is mainly discussed in risk losses. The reservoir has a small hydropower station and its installed capacity is small, therefore generating electricity benefit can be ignored. This paper mainly discusses the water supply benefit generated from adjusting FLWL of Shilianghe reservoir.

By coordinating and calculating the datum of Water Resource Communique and the Statistical Yearbook in 2014 of Lianyungang city. The parameter values used in calculating industry water supply benefit are as follows: $I$is 18.38×10^8Yuan, k is 0.9, f is 0.1. As for Agriculture water supply benefit, I is 1.95×10^8Yuan, k is 0.9, f is 0.45. As for domestic water supply benefit, k is 0.9, f is 0.3, R is 1.2×10^4Yuan, e is o.4, p is 588 m^3. As for the third industry water supply benefit, I is 14.7×10^8Yuan, k is 0.9, f is 0.3.

(3) Calculation of risk loss indices. According to statistical data of Shilianghe reservoir, the highest water level is 26.82m since its run-off, 0.1m more than design flood level. And based on the definition of design standard level in formula (4), the design flood level was taken as design standard level in this paper (Z_d=26.81m). According to the statistics results of reservoir's inflow, Pearson Type III hydrological frequency curve was plotted. And the possible flood and its frequency were obtained by flood control operation.

In consideration of the safety discharge of Xinshu River, located in the downstream of Shilianghe reservoir, and the effect of sedimentation, the value of safety discharge is $2000m^3/s$ in calculating downstream river channel security risk ratio. In the flood control operation of reservoir, the highest water level was kept below the design flood level, in order to ensure that the downstream river channel security risk ratio would not overlap with the dam safety ratio.

Time factor was considered in calculating environmental risk ratio. The dry season in Lianyungang city is from October to May and Shilianghe reservoir is the main source of water supply in the dry season. In the initial water supply the water level is normal water level (26.00m). And when the water supply period is over, the water level is down to FLWL.

The values of the parameters used in calculating dam safety risk loss are as follows: α is 0.25, β is 7.2×10^5Yuan/km^2, A is 200 km^2, the ratio of flood-relief efforts cost in direct loss is 15%. As for downstream river channel security risk loss, α is 0.25, β is 2.0×10^5Yuan/km^2, A is 55 km^2, the ratio of flood-relief efforts cost in direct loss is 15%.

In the calculation of environmental risk loss, the area of the land ecosystem influenced by flood-water resource utilization is the urban flood control dike on the right bank of Xinshu River. The comprehensive ecosystem service value coefficient (d_i) is 5.6×10^4Yuan/km^2.

RESULTS AND DISCUSSION

Water storage benefit analysis. Figure3 shows the water supply allocation proportion and contribution rate of benefit of industry water supply, agriculture water supply, domestic water supply and the third industry water supply. The water supply allocation proportions of industry, agriculture, domestic water supply and the third industry are 19%, 64%, 4% and 13% respectively according to the actual situation of water supply in Lianyungang city. The contribution rates of benefit are 14.84%, 7.08%, 20.75% and 57.32% respectively, according to the calculation result. Proportion of agricultural water supply is the biggest part, but the contribution rate of benefit is the lowest. Proportion of domestic water supply and the third industry water supply are smaller, but

the contribution rates of benefit are higher.

According to the above result, in the allocation of floodwater resource, increasing the proportions of urban water supply and the third industry water supply and decreasing the proportion of agricultural water supply are efficient way to increase the profits of floodwater resource utilization. This finding agree well with the literature which reports that with the development of economy, urban water supply and the third industry water supply have higher water supply economic benefit[25].

Risk loss analysis. Figure 4 shows the relation curve of dam safety risk ratio and FLWL. As the FLWL gradually increasing, the dam safety risk ratio gradually increases. When the dam safety risk ratio is less than 6%, the risk is low and controllable. When the risk ratio is between 6% and 10%, the risk is moderate. When the risk ratio is more than 10%, the risk is high and uncontrollable. According to the relation curve, when the FLWL increased from 23.5m to 24.75m, the increasing degree of dam safety risk ratio is relatively minor, from 1.53% to 5.98%, and less than 6%. When the FLWL increased from 24.95m to 25.3m, the risk ratio increased rapidly, from 7.55% to 15.01%.

Figure5 shows the percentage of various kinds of risk losses in total risk loss of different FLWL. As the FLWL gradually increasing, the percentage of dam safety risk loss gradually increases (from 68.58% to 87.93%), and the average is 78.92%. Next is downstream river channel security risk loss, and the average is 18.35%. Environmental risk loss is a small part in the total risk loss, and the average is 2.73%. The dam safety risk loss is the main aspect of risk losses caused by adjusting FLWL.

Determination of floodwater resource utilization scenario. Figure 6 shows the relation curve of water storage benefit, total risk loss and comprehensive benefit with FLWL. As the FLWL gradually increasing, the total water storage benefit gradually increases showing linear relationship, and the total risk loss gradually increases, after the FLWL is more than 24.80m, the total risk loss increases rapidly. The comprehensive benefit of floodwater resource utilization increases with the increase of FLWL and the comprehensive benefit reaches maximum when the FLWL is 24.9m. The comprehensive benefit shows a downtrend when the level continues to rise. Jiang et al. analyzed the comprehensive benefit in Fengtan reservoir, and the trend is similar with the result in this paper[26].

In this paper, three kinds of floodwater resource utilization scenarios were proposed. The FLWL of the scenarios are 24.5m, 24.9m and 25.3m respectively. Table 1 shows the specific situation of the three scenarios. According to the aforementioned analysis, dam safety risk loss is the highest in total risk losses, accounting for 78.9% of the total. Dam safety risk loss can be directly represented by dam safety risk ratio. Thus, dam safety risk ratio is a major consideration in scenario decisions.

When the dam safety risk ratio is less than 6%, the risk ratio grows slowly and the flood control capacity is enough. So that, when the FLWL ranges from 23.5m to 24.75m, the risk ratio is low and controllable. As for scenario 1 (FLWL is 24.5m), the increased water storage volume is $5.743\times10^7 m^3$, accounting for 24.5% of utilizable capacity. The dam safety risk ratio is 4.32%. The total risk loss is 1.077×10^7Yuan. The water storage benefit is 2.287×10^7Yuan. The comprehensive benefit is 1.210×10^7Yuan.

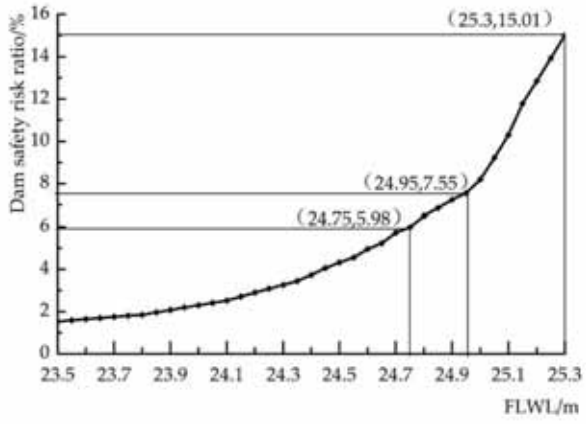

FIGURE 4
The relation curve of dam safety risk ratio and FLWL.

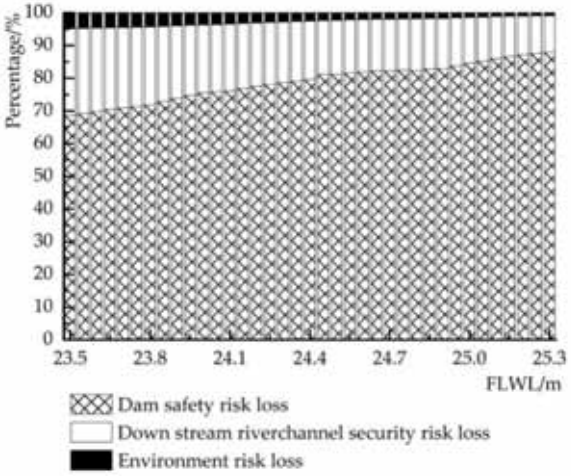

FIGURE 5
The percentages of various kinds of risk losses in total risk loss of different FLWL.

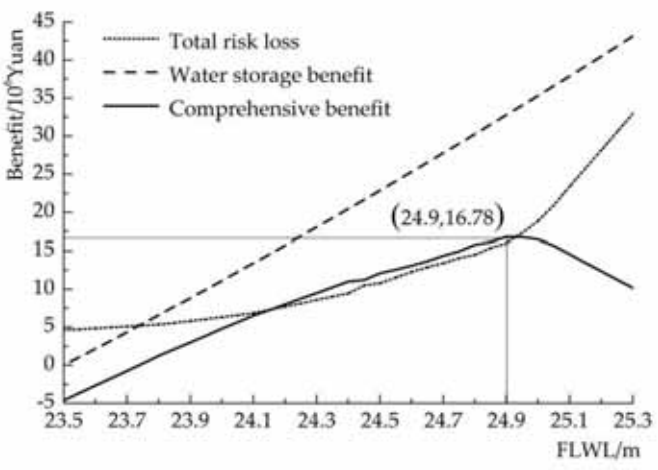

FIGURE 6
The relation curves of total risk loss, water storage benefit and comprehensive benefit with FLWL.

TABLE 1
The specific situation of the three scenarios.

Scenarios	FLWL/ m	Dam safety risk ratio/ %	Dam safety risk loss/10^6Yuan	Total risk loss/ 10^6 Yuan	Increased water storage volume/ 10^6m^3	Water storage benefit/ 10^6 Yuan	Comprehensive benefit/ 10^6 Yuan
Scenario 1	24.5	4.32	8.74	10.77	57.43	22.87	12.10
Scenario 2	24.9	7.25	13.26	16.00	82.33	32.78	16.78
Scenario 3	25.3	15.01	29.00	32.98	108.00	43.14	10.16

When the risk ratio is between 6% and 10% (the corresponding interval of FLWL is from 24.75~25.1m), the risk ratio is moderate. The upstream water is an important factor in calculating dam safety risk ratio. When the FLWL of Shilianghe reservoir is 25.1m and the upstream water is 10-year flood, the water level by flood routing surpasses the design standard level (Z_d), which constitutes threat to dam safety. But the safety can be insured by increasing water release discharge. As for scenario 2 (FLWL is 24.9m), the increased water storage volume is $8.233\times10^7m^3$, accounting for 35.2% of utilizable capacity. The dam safety risk ratio is 7.25%. The total risk loss is 1.600×10^7Yuan. The water storage benefit is 3.278×10^7Yuan. The comprehensive benefit is 1.678×10^7Yuan, which is the largest.

When the FLWL exceeds 25.1m, the dam safety risk ratio grows rapidly, and the risk is high and uncontrollable. As for scenario 3 (FLWL is 25.3m). The dam safety ratio is 15.01% which is much bigger than scenario 1 and 2. The comprehensive benefit is 1.016×10^7Yuan which is less than scenario 1 and 2.

In conclusion, when the FLWL of Shilianghe reservoir is raised to 24.9m (scenario 2), the comprehensive benefit (1.678×10^7Yuan) is the largest and the dam safety risk ratio (7.25%) is moderate. It is a comparatively ideal plan of floodwater resource utilization.

CONCLUSIONS

In this paper, on the basis of analyzing the factors affecting the floodwater resource utilization by adjusting FLWL, the risk evaluation index system and risk decision-making model of adjusting FLWL regarding the maximum comprehensive benefit as the target were established to provide theoretical basis for selection of reservoir flood resources utilization plan. The model was applied to Shilianghe reservoir in China. The following conclusions are drawn from the study.

1) The risk evaluation index system and risk decision-making model of adjusting FLWL have common significance, and can be used to analyze the problem of adjusting FLWL.

2) As the FLWL gradually improving, water storage benefit gradually increases, showing linear relationship. The contribution rate of different water storage benefits indices to water storage benefits is different. As for Shilianghe reservoir, the proportion of agricultural water supply is the biggest part, but the contribution rate of benefit is the lowest. Proportion of domestic water supply and the third industry water supply are smaller, but the contribution rates of benefit are higher. Urban water supply and the third industry water supply have higher water supply economic benefit.

3) Dam safety risk loss is the main aspect of adjusting FLWL risk losses. As the FLWL gradually

improving, total risk losses gradually increase. As for Shilianghe reservoir, dam safety risk loss is the main aspect of adjusting FLWL risk losses, followed by downstream river channel security risk loss, environmental risk loss is a small part in total risk loss. The total risk loss increases slower when the FLWL increases from 23.5m to 24.8m. And after the flood limited water level is more than 24.80m, the total risk loss increases rapidly.

4) As the FLWL gradually improving in a certain range, comprehensive benefit gradually increases. When the level reaches a certain value, the comprehensive benefit is largest. After the threshold, comprehensive benefit gradually decreases.

5) When the FLWL of Shilianghe reservoir is raised to 24.9m, dam safety risk ratio (7.25%) is moderate, and the comprehensive benefit (1.678×10^7Yuan) is the largest. It is a comparatively ideal plan of floodwater resource utilization.

The study approach will provide useful information and reference for similar studies to be conducted in other regions, and the results will have useful implications for adjusting FLWL and determining reservoir flood resources utilization plan in the region.

ACKNOWLEDGEMENTS

This work was financially supported by the Fundamental Research Funds for the Natural Science Foundation of Jiangsu Province (BK20130849), Water Conservancy Science and Technique of Jiangsu Province (2014064), the Fundamental Research Funds for the Central Universities (2014B25314), and Science and Technique Project of Lianyungang City (SH1429).

REFERENCES

[1] Wang, B., Zhou, H. and Zhang, G. (2007) Review on the dynamic control of reservoir normal level in flood season. South-to-North Water Transfers and Water Science and Technology, (03), 43-46.

[2] Yun, R. and Singh, V.P. (2008) Multiple duration limited water level and dynamic limited water level for flood control, with implications on water supply. Journal of Hydrology, 354(1-4), 160-170.

[3] Bender, M.J., Hranisavljevic, D., Bernardin, R. and Bianchi, R.(2002) Dynamic operating rules for water supply reservoirs in La Paz. Water science and technology, 46(6-7), 247-254.

[4] Qiu, R., Wang, B. and Zhou, H.(2004) New idea for controling the limited elevation of reservoirs in flood season. Advances in Water Science, (01), 68-72.

[5] Cao, Y. (2004) Study on Floodwater Utilization and Management. Resources and Industries, (02), 21-23.

[6] Wang, H. and Yin, J. (2004) Review of risk management on flood resource utilization. Water Resources Development Research, (05), 4-8.

[7] Fang, H., Wang, Y. and Hu, Q. (2009) Integrative risk evaluation of regional floodwater utilization. Advances in Water Science, (05), 726-731.

[8] Gu, W., Shao, D., Huang, X. and Dai, T.(2008) Multi-objective risk assessment on water resources optimal deployment. Shuili Xuebao, (03), 339-345.

[9] Li, Y. and Lence, B. (2005) On risk analysis of water resources systems under non-stationary conditions. in Impacts of Global Climate Change. ASCE.

[10] Wurbs, R.A. and Cabezas, L.M. (1987) Analysis of reservoir storage reallocations. Journal of Hydrology. 92(92), 77-95.

[11] Salmon, G.M. and Hartford, D. (1995) Risk analysis for dam safety. in International Journal of Rock Mechanics and Mining Sciences and Geomechanics Abstracts.

[12] Fu, X. and Ji, C. (1998) Study on the maximum flood hazard risk rate in reservoir flood-season operation. Water Resources and Power, (02), 13-16.

[13] Yin, J. (2002) Research and Application on Fuzzy Set and Risk Analysis for City Flood Control and Water Supply. Dalian University of Technology.

[14] Wang, B., Zheng, D., Zhou, H. and Ma, X.(2007) Study of index system and fuzzy optimum model on schemes of dynamic flood control limited water level of a reservoir. Journal of Dalian University of Technology, (01), 113-118.

[15] Liu, P., Li, L., Guo, S., Xiong, L., Zhang, W., Zhang, J. and Xu, C., (2015) Optimal design of seasonal flood limited water levels and its application for the Three Gorges Reservoir. Journal of Hydrology. 527, 1045-1053.

[16] Hu, S., Gao, B. andWang, Z.(2002) Safe utilization of flood in the Hai River basin. China Water Resources, (10), 105-108.

[17] Liu, D., Li, X., Guo, S., Dan, R. and Chen, H.(2015) Using a Bayesian Probabilistic Forecasting Model to Analyze the Uncertainty in Real-Time Dynamic Control of the Flood Limiting Water Level for Reservoir Operation. Journal of Hydrologic Engineering, 20(2).

[18] Feng, P., Han, S. and Li, J. (2006) Analysis on risk and benefit of adjusting limited reservoir water level for flood control. Shuili Xuebao, (04), 451-456.

[19] Li, X., Guo, S., Liu, P. and Chen, G., (2010) Dynamic control of flood limited water level for reservoir operation by considering inflow uncertainty. Journal of Hydrology, 391(1), 124-132.

[20] Shi, G. and Zhou, Z. (1990) Classification of

flood losses and calculation method. Haihe Water Resources, (03), 42-45.
[21] Li, L., Wang, R., Sheng, J., Wang, Z., Peng, X. and Zhang, S., (2006) Dam risk evaluation and risk management, Beijing: China Water and Power Press.
[22] Wang, Z., Zhang, B. and Zhang, S. (2004) Study on the effects of land use change on ecosystem service values of Jilin Province. Journal of Natural Resources, (01), 55-61.
[23] Xie, G., Lu, C., Leng, Y., Zheng, D. and Li, S.(2003) Ecological assets valuation of the Tibetan Plateau. Journal of Natural Resources, (02), 189-196.
[24] Chang, F.-J. and Y.-T. Chang, (2006) Adaptive neuro-fuzzy inference system for prediction of water level in reservoir. Advances in Water Resources, 29(1), 1-10.
[25] Norton-Brandao, D., Scherrenberg, S.M. and van Lier, J.B. (2013) Reclamation of used urban waters for irrigation purposes--a review of treatment technologies. Journal of Environmental Management, 122C(10), 85-98.
[26] Jiang, Z., Sun, P., Ji, C. and Zhou, J.(2015) Credibility theory based dynamic control bound optimization for reservoir flood limited water level. Journal of Hydrology. 529, 928-939.

Received: **28.11.2016**
Accepted: **07.08.2017**

CORRESPONDING AUTHOR

Guohua Fang
College of Water Conservancy and
Hydropower Engineering,
Hohai University.
1 Xikang Road,
Nanjing 210098 – CHINA

E-mail: yyhhu_151413@163.com

© by PSP Volume 26 – No. 10/2017 pages 5754-5760 Fresenius Environmental Bulletin

ASSOCIATIVE EFFECTS OF ENSILING SOYBEAN AND CORN PLANT AS MIXTURES ON THE NUTRITIVE VALUE, FERMENTATION AND METHANE EMISSION

Mustafa Kizilsimsek[1,*], Cehre Ozturk[2], Kubra Yanar[2], Ibrahim Ertekin[2], Cagri Ozgur Ozkan[3], Adem Kamalak[4]

[1]Kahramanmaras Sutcu Imam University, Faculty of Agriculture, Field Crops Department Kahramanmaras, Turkey
[2]Kahramanmaras Sutcu Imam University, Natural and Applied Science Institute, Kahramanmaras, Turkey
[3]Kahramanmaras Sutcu Imam University, Goksun Vocational School, Organic Farming Department Kahramanmaras, Turkey
[4]Kahramanmaras Sutcu Imam University, Faculty of Agriculture, Animal Science Department, Kahramanmaras, Turkey

ABSTRACT

The aim of the current experiment was to determine the fermentation characteristics and nutritive value of soybean and corn plants silage either as sole crops or as four different mixtures rates. Two forages were ensiled in plastic bags for 60 days at room temperature as mixtures containing 100:00, 80:20, 60:40; 40:60; 20:80; 0:100 of soybean:corn plant on a fresh weight basis. The resultant silages were evaluated using the chemical analysis and *in vitro* gas production technique. Ensiling of soybean with whole corn plant has a significant effect on the chemical composition, fermentation parameters, organic matter digestibility (OMD), metabolisable energy (ME) and aerobic stability of the resultant silages. As the proportion of corn plant increase in silage mixture, crude protein (CP), neutral detergent fiber (NDF), acid detergent fiber (ADF), crude ash (CA), pH, acetic acid, butyric acid contents and aerobic stability decreased while dry matter content (DM), Fleig score (FS), dry matter recovery (DMR), lactic acid, gas production, methane production, ME and OMD of the resultant silages were increased. This study clearly showed that good quality silages with high ME and OMD can be produced with soybean:corn plant ratios of 60:40, 40:60 and 20:80. Ensiling of soybean plant with corn plant improved more or less the quality and nutritive value of the resultant silages irrespective of mixing ratio. Ensiling the soybean plant with corn plant overcome some of drawbacks associated with low DM, pH and nutritive value of soybean silage. It can be recommended that soybean plant can be ensiled with corn plant at the ratio of 60:40, 40:60 and 20:80 as green herbage basis. This experiment clearly indicated that high quality silage could be obtained through mixing of soybean plant with corn plant. However, *in vivo* experiments with ruminants are required to determine the effect of associative effects on animal performance.

KEYWORDS:
Soybean, Corn, Silage, Nutritive Value, *In Vitro* Gas production, Aerobic stability

INTRODUCTION

Recently silage production from green cereal and legume plants such as corn, sorghum, alfalfa and soybean has been increased at the expense of hay or grazing in the most parts of world [1]. Corn silage is known as one of the most important livelihood [2] for many farms interesting in livestock production. When compared to cereal plants, legumes are difficult to ensile due to their lower water-soluble carbohydrate content and higher buffering capacity [3, 4]. Although silage is a very important component of ruminant animal diets, the quality of silages included in to ruminant diets vary depending on type of plant ensiled. Cereal plants silages have high quality whereas the CP content of cereal silage is lower than that of legume silages. The low level of CP content of cereal silages is one of the limiting factors for ruminant animal requirements [5]. Recently ensiling of two plants, that have a similar growth cycle, has become a practice to obtain high quality silage with a sufficient CP content to meet ruminant animal requirements [5, 6, 7, 8, 9, 10]. Ensiling of alfalfa plant with whole crop corn improved the pH, OMD and ME of the resultant silage [6]. Ensiling of whole crop corn with soybean increased not only CP content but also ME and taste of the resultant silage [11] without affecting other quality parameters [8]. So far limited studies have been carried out to provide detailed information on feasibility of ensiling of whole soybean plant with whole corn plant. However, the optimal combination and the associative effects of soybean and corn plants for ensilage have not been studied in detail. Therefore the aim of the current experiment was to determine the fermentation characteristics and nutritive value of silage mixtures with six different soybean and corn mixture rates.

TABLE 1
Silages combinations used in the current experiment

Silages	Soybean (%)	Corn (%)
SS	100	0
S80C20	80	20
S60C40	60	40
S40C60	40	60
S20C80	20	80
CS	0	100

TABLE 2
Classification of silage quality according to Fleig scores

Fleig Scores	85 and 100	60 and 80	55 and 60	25 and 40	<20
Silage Quality	Very good	Good	Moderate	Satisfying	Worthless

MATERIALS AND METHODS

A commercial soybean (Yesilsoy) was sown in June, 2015 at the seed rate of 7 kg da^{-1} with N (8 kg $/da^{-1}$) and P_2O_5 (8 kg/ha-1) fertilizer application. The soybean plant was harvested at the seeding stage. A commercial corn hybrid (Truva) was sown in June, 2015 at the seed rate of 3.5 kg da^{-1} with N (20 kg $/da^{-1}$) and P_2O_5 (8 kg/da^{-1}) fertilizer application and was harvested at 2/3 milk line maturity stage. Both plants were sown as second crop after wheat. Representative soybean and corn plant were chopped to 2-3 cm in theoretical length and ensiled in six different mixture rates in plastic bags for two months as indicated in Table 1.

DMR of the silages were determined as a rate of DM content of initial silage to that of resultant silages [12]. After two months fermentation period, plastic bags silos were opened and 20 gram fresh silage sample were blended with 180 ml distilled water for 5 min followed by filtration through two layers of cheesecloth to obtain the filtrate. The pH of silage was determined from the supernatant using pH meter (HANNA Inst., HI 2215 model). The lactic acid and volatile fatty acids were determined by HPLC following the method described by Muck and Dickerson [13] after a sample cleaning procedure. The HPLC was run at 41 °C, 0,6 ml/min flow rate and RID detector was used. The FS of the resultant silages were estimated by the method described by Fleig [14] as follows.

FS = 220 + (2xDM%-15) - (40xpH)

After 60 day storage period, the resultant silages were subjected to an aerobic stability test for 162 hours, in which temperature of the resultant silages were recorded to determine the aerobic deterioration [15]. Subsamples of 50 g per silage type were dried at 78ºC in a ventilated oven and ground to pass through a 1mm sieve using a mill. The DM, EE and CA contents of silages were determined according to AOAC [16] procedures. Nitrogen contents of silages were measured by the Kjeldahl method [16]. The CP contents of samples were calculated as N X 6.25. The NDF and ADF contents of silages were determined using the method described by van Soest et al. [17].

***In vitro* gas and methane production.** Silage samples (0.200 g) were incubated in calibrated glass syringes of 100 ml with 30 ml buffered rumen fluid in a water bath at 39°C for 24 hours according to Menke et al. [18] procedure. Rumen fluid was obtained from three fistulated sheep fed twice daily with a diet containing alfalfa hay (800 g) and barley (400 g). Net gas productions of silages were determined after correction for blank and hay standard (University of Hohenheim, Germany).

The ME and OMD of silages were estimated using equation suggested by Menke and Steingass [19].

ME (MJ7kg DM): 2.0 + 0.1298GP + 0.045CP + 0.303EE

OMD (%) = 15.38 + 0.8453GP + 0.595CP +0.675CA

GP: Gas production at 24 h incubation, CP: Crude protein (%), EE: Ether extract (%), CA: Crude ash (%).

Methane contents (%) of total gas produced at 24 h fermentation of silages were determined by an infrared methane analyzer (Sensor Europe GmbH, Erkrath, Germany) [20].

Methane production (mL) was calculated as follows and presented as ml or percentage.

Methane production (mL) = Total gas production (mL) X Percentage of Methane (%)

RESULTS AND DISCUSSION

There is considerable variation among silages in point of chemical composition (Table 3). The DM contents of silages ranged from 20.93 to 34.18%

with the highest being for CS and lowest for SS. The DM contents of the silage mixtures increased with increasing level of CS in the mixture. This increase in the DM contents of mixture silage was expected since the DM content of CS was higher than that of SS at the beginning of ensiling. The CP, NDF, ADF and CA contents of silages ranged from 7.46 to 14.77%, 35.65 to 49.33%, 24.11 to 46.63%, 5.78 to11.02% respectively, with the highest being for SS and lowest for CS. The CP, NDF, ADF and CA contents of mixture silages decreased with increasing level of CS in the mixture due to dilution effect of CS. As can be seen from Table 2, The CP, NDF, ADF and CA contents of CS was significantly lower than those of SS. In the current experiment the DM contents of the resultant silages increased with increasing level of corn in the mixtures since DM content of corn plant was higher than that of soybean plant at harvest. On the contrary, Demirel et al. [8] showed that the DM contents of the resultant silages decreased with increasing level of corn in the mixtures since DM content of soybean plant was higher than that of corn plant at harvest. Therefore the chemical compositions of the resultant silages depend on the plants, which are ensiled in combination. It is reasonable that if two plants with different chemical composition are ensiled in combination, the percentage of constituents of the resultant silages are decreased or increased at the expense of the other.

Although the CP contents of soybean-corn mixture silages fell into range of the minimum level of 7-8% of DM for optimum rumen function and feed intake in ruminant animals [21], soybean-corn mixture silages should be supplemented with concentrate with high CP content to obtain high performance from ruminant animals.

The DM, NDF and ADF contents of SS obtained in the current study were similar to those obtained by Magalhaes et al. [22]. On the other hand CP, CA and NDF of SS obtained in the current study were similar to those indicated by Lima et al. [7] even if there is a significant differences in DM contents of these two studies. The DM content of SS obtained in the current study was lower than that reported by Lima et al. [7]. The differences in DM content between two studies are possibly associated with maturity at harvest. It is well known that the DM content of plant increased with advancing maturity.

Although the DM, NDF and ADF contents of CS obtained in the current experiment were comparable with those of Basso et al. [23], the DM, NDF and ADF contents of CS obtained in the current experiment were different from those obtained by Ozturk et al. [6]. The differences in terms of chemical composition among these experiments are associated with harvesting maturity of corn plant. Bal et al. [24] clearly showed that cell wall contents (NDF and ADF) decreased at the expense of starch with advancing maturity of corn plants since the percentage of grain with high starch content increased in the whole plant as plant matured.

Data on the fermentation parameters of silages is given in Table 4. There is considerable variation among silages in terms of fermentation parameters. Lactic acid contents ranged from 2.18 to 13.12 % with the highest being for CS and lowest for SS. Lactic acid of the silage mixture increased with increasing level of CS in the mixtures. Acetic acid, propionic acid and butyric acids contents ranged from 1.89 to 12.55%, 1.75 to 5.09% and 0.00 to 9.58% respectively, with the highest being for SS and lowest for CS. Acetic acid, propionic acid and butyric acids contents decreased with increasing level of CS in the mixtures. As can be seen from Table 4, fermentation of SS-CS mixtures was dominated by production of lactic acid rather than acetic acid or butyric acid, irrespective of proportion.

The higher content of acetic and butyric acids in SS and S80C20 than other silages indicated that these combinations were not sufficiently fermented due possibly to low water soluble carbohydrate contents of these combination. The increase in lactic acid production rather than rather than acetic acid or butyric acid is associated possibly with high water soluble sugar of corn plant in silage mixture since water soluble sugars are quickly available to lactic acid producing bacteria in silage [25].

TABLE 3
The chemical composition (%) of soybean, corn and their mixture silage (on DM basis)

	Silages							
Constituents	SS	S80C20	S60C40	S40C60	S20C80	CS	SEM	Sig
DM	20.93^{d}	23.48^{cd}	25.55^{c}	29.66^{b}	31.69^{ab}	34.18^{a}	0.818	***
CA	11.02^{a}	9.49^{a}	8.50^{ab}	6.71^{bc}	6.61^{bc}	5.78^{c}	0.764	***
CP	14.77^{a}	12.72^{b}	10.87^{c}	8.85^{d}	8.48^{de}	7.46^{e}	0.340	***
NDF	49.33^{a}	45.06^{ab}	41.03^{bc}	38.73^{bc}	37.25^{c}	35.65^{c}	2.024	***
ADF	45.63^{a}	39.69^{b}	32.15^{c}	27.08^{d}	26.81^{d}	24.11^{d}	1.488	***
EE	2.69^{b}	3.95^{a}	3.72^{a}	4.08^{a}	3.41^{ab}	3.61^{a}	0.227	***

^{abc} Row means with common superscripts do not differ (P>0.05); SEM: Standard error mean; Sig. – significance level; DM: Dry matter (%), CA: Crude ash (%), CP: Crude protein (%), NDF: neutral detergent fiber (%), ADF: Acid detergent fiber (%), EE: Ether extract (%),***P<0.001

TABLE 4
The lactic acid, volatile fatty acids contents, pH, Fleig score and dry matter recovery of soybean, corn and their mixture silages

	Silages							
Parameters	SS	S80C20	S60C40	S40C60	S20C80	CS	SEM	Sig
Lactic	2.18^{c}	7.55^{b}	12.77^{a}	12.97^{a}	13.12^{a}	13.75^{a}	0.400	***
Acetic	12.55^{a}	8.72^{b}	6.89^{c}	4.98^{d}	4.10^{d}	1.89^{e}	0.399	***
Propionic	5.09^{a}	3.02^{b}	2.04^{bc}	1.90^{c}	1.91^{bc}	1.75^{c}	0.332	***
Butyric	9.58^{a}	6.81^{a}	0.71^{b}	0.41^{b}	0.00^{b}	0.00^{b}	0.831	***
pH	5.81^{a}	5.11^{b}	4.51^{c}	4.44^{c}	4.33^{c}	4.13^{c}	0.140	***
FS	14.20^{d}	47.43^{c}	75.43^{b}	86.43^{ab}	95.20^{ab}	108.03^{a}	6.983	***
DMR	0.85b	0.89^{ab}	0.92^{ab}	0.92^{ab}	0.93^{a}	0.95^{a}	0.023	***

^{abc} Row means with common superscripts do not differ (P>0.05); SEM: Standard error mean; Sig. – significance level; FS: Fleig score, DMR: Dry matter recovery, ***P<0.001

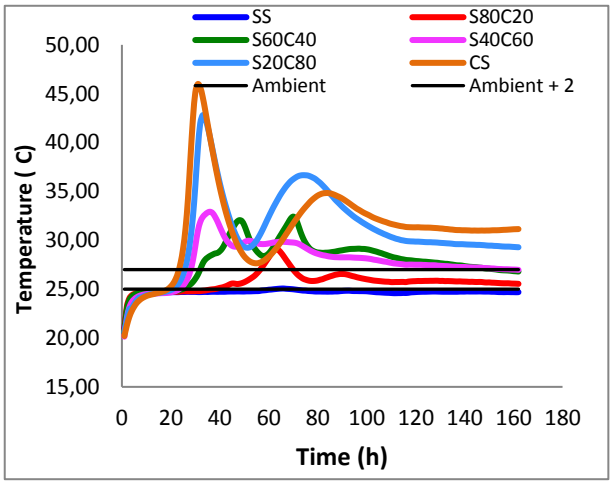

FIGURE 1
The aerobic stability of corn, soybean and their mixture silages

The similar trend was also observed by Lima et al. [7], who ensiled the soybean with sorghum plant. It has been previously reported that there is inverse relationship with between pH decline and lactic acid production in well managed and preserved silages [25]. In the current experiment the accumulation in lactic acid was accompanied with pH decline. Lactic acid is the more preferable acid over the other fermentation acids since it is major organic acid which is responsible for reducing the silage pH [26]. The pH of silages ranged from 4.13 to 5.81% with the highest being for SS and lowest for CS. The pH of mixture silages decreased with increasing level of corn in the mixtures. The FS ranged from 14.20 to 108.03 with the highest being for CS and lowest for SS. The FS or quality of mixture silages increased with increasing level of CS in the mixtures. It is reasonable to expect that the higher FS should be obtained with increasing corn plant in the mixture since silage pH decreased and DM content increased with increasing level of corn plant in the mixture. As can be seen from the equation, FS is positively correlated with DM and negatively correlated with silage pH.

The DMR of silages ranged from 0.85 to 0.95 with the highest being for CS and lowest for SS. The DMR of silage mixtures increased with increasing level of CS in the mixtures.

The aerobic stability of the resultant silages was given in Figure 1. As can be seen from Figure 1, all silages except for SS had the temperature rise of more than 2 °C above the ambient temperature (25°C) while SS silage remained stable during the full aerobic stability measurement period of 162 hours. The CS, S20C80, S40C60, S60C40 and C80C20 silages had the temperature rise of more than 2 °C above the ambient temperature (25°C) after 24, 26, 29, 32 and 58 hour aerobic exposure respectively. As can be seen from Figure 1, the aerobic stability decreased with increasing level of corn in the mixtures. It is well known that the aerobic deterioration begins when the silage is exposed to air, especially during the feed-out period since fermentation

end products and water soluble carbohydrate of the resultant silages are used by aerobic bacteria, yeast and molds and converted to H_2O, CO_2 and heat. The heat production results in increase in the temperature of the resultant silages [27, 28]. Aerobic deterioration result in not only loss of fermentation products and water soluble carbohydrate, which are potentially digestible but also production of undesirable microbial spores [27] and toxins [29, 30, 31]. It was reported that the increase in temperature is positively associated with DM content of the resultant silages since the heat requirement of wetter silages to raise the temperature is higher than that required for drier material [25, 32]. The similar trend was observed in the current experiment in which the temperature increase of the resultant silages with high DM contents such as CS and S20C80 was considerably higher than those of the silages with lower DM contents.

Ohyama et al. [33] showed that acetic acid and butyric acids contents of the resultant silage were positively correlated with the time for the temperature to rise during exposure to air. The similar relationship was observed in the current experiment in which the silages with higher acetic and butyric acids contents had a higher aerobic stability. As mentioned before, the silages with higher acetic and butyric acids contents were deteriorated within longer time or remained stable within air exposure time.

Data on the gas, methane, ME and OMD of silages is given in Table 4. There is considerable variation among silages in terms of gas, methane, ME and OMD. Gas, methane, ME and OMD of silages ranged from 25.82 to 49.34 ml, 4.73 to 8.39 ml, 6.83 to 8.83 MJ/kg DM, 53.43 to 65.43 % with the highest being for CS and lowest for SS. Gas, methane, ME and OMD of the silage mixtures increased with increasing level of CS in the mixture.

The gas production and ME of SS obtained in the current experiment was comparable with those reported by Magalhaes et al. [22] found that the gas production and ME of SS was 22.44 ml and 6.44 MJ/kg DM respectively. The gas production of CS obtained in the current experiment was comparable with those reported by Valentin et al. [34] found that the gas production of CS was 47.74 ml. On the other hand the gas production, ME and OMD of CS obtained in the current study were lower than those reported by Canbolat et al. [35] but higher than those obtained by Cetinkaya and Erdem [36]. The differences in the gas production, ME and OMD among the studies are possibly associated with differences in chemical composition of maize silages used.

The associative effect of combining soybean with corn plants is given in Table 6. The obtained gas production, methane production, ME and OMD were higher than those predicted in all silage mixtures. However, the extent of associative effect obtained in the current experiment was not constant with mixing groups. The extent of associative effect varied depending on the percentage of each plant included into mixtures. As can be seen from Table 6, the extent of associative effect decreased with increasing ratio of corn in the mixtures. The associative effect was considerably higher at low level inclusion of corn plant into silages.

TABLE 5
The gas production, methane production, metabolisable energy and organic matter digestibility of soybean, corn and their mixture silages

	Silages							
Constituents	SS	S80C20	S60C40	S40C60	S20C80	CS	SEM	Sig
Gas (ml)	25.82^{c}	40.01^{b}	44.51^{ab}	47.27^{a}	47.44^{a}	49.34^{a}	1.717	***
CH_4 (ml)	4.73^{c}	6.80^{b}	7.75^{b}	8.31^{a}	8.34^{a}	8.39^{a}	0.343	***
CH_4 (%)	18.30	17.01	17.40	17.77	17.52	16.89	0.436	**NS**
ME	6.83^{c}	8.96^{b}	9.39^{ab}	9.77^{a}	9.57^{ab}	9.83^{a}	0.228	***
OMD	53.43^{b}	63.18^{a}	65.20^{a}	65.06a	65.06^{a}	65.43^{a}	1.356	***

^{abc} Row means with common superscripts do not differ (P>0.05); SEM: Standard error mean; Sig. – significance level; ME: Metabolisable energy (MJ/kg DM), OMD: organic matter digestibility (%), ***P<0.001

TABLE 6
Relative differences (%) between observed and predicted parameters

	Silage mixture			
	S80C20	S60C40	S40C60	S20C80
Gas	23.70***	20.66***	15.22*	5.88**
CH_4	19.85***	14.35*	11.53*	8.26*
ME	17.07***	14.35***	11.53**	3.52*
OMD	11.62***	10.60*	6.70*	3.12*

ME: Metabolisable energy (MJ/kg DM), OMD: organic matter digestibility (%), *P<0.05, **p<0.01, ***P<0.001

Although the meaning of an associative effect is clear, the reasons for an associative effect are clear [37]. The associative effects obtained in the current experiment are possibly associated with completion of missing nutrients in the mixtures required by the rumen microorganisms when the two different plants are ensiled together. The synchronization of energy and protein might have also contributed the associative effects obtained in the current experiment. The synchronization of energy and protein might have stimulated the microbial activity when soybean plant is ensiled with corn plant.

CONCLUSION

Ensiling of soybean plant with corn plant improved more or less the quality and nutritive value of the resultant silages irrespective of mixing ratio. Ensiling the soybean plant with corn plant overcome some of drawbacks associated with low dry matter, pH and nutritive value of soybean silage. It can be recommended that soybean plant can be ensiled with corn plant at the ratio of 60:40, 40:60 and 20:80 as green herbage basis respectively. This experiment clearly indicated that high quality silage could be obtained through mixing of soybean plant with corn plant. However, in vivo experiments are required to determine the effect of associative effects on animal performance.

REFERENCES

[1] Danner, H., Holzer, M., Mayrhuber, E. and Braun, R. (2003) Acetic acid increases stability of silage under aerobic conditions. Appl. Environ Microbiol. 69, 562-567.

[2] Baran, M.F. and Gokdogan, O. (2016) Comparision of energy use efficiency of different tillage methods on secondary crop corn silage production. Fresen. Environ. Bull., 25(9), 3808-3814.

[3] Davies, D.R., Merry, R.J., Willams, A.P., Bakewell, E.L., Leemans, D.K and Tweed, J.K.S. (1998) Proteolysis during ensilage of forages varying in soluble sugar content. Journal of Dairy Science, 81, 444-453.

[4] Singh, K. Honig, H., Wermke, M. and Zimmer, E. (1996) Fermentation pattern and changes in cell wall constituents of straw-forage silages, straw and partners during storage. Animal Feed Science and Technology, 61, 137-153.

[5] Zhang, S.J., Chaudry, A.S., Oman, A., Shi, C.O., Edwards, G.R., Dewhurst, R.J. and Cheng, L. (2016) Associative effect of ensiling mixtures of sweet sorghum and alfalfa on nutritive value, fermentation and methane characteristics. Animal Feed Science and Technology. 206, 29-38.

[6] Ozturk, D., Kizilsimsek, M., Kamalak, A., Canbolat, O. and Ozkan, C.O. (2006) Effects of ensiling alfalfa with whole crop maize on the chemical composition and nutritive value of silage mixtures. Asian-Aust. J. Anim. Sci. 19(4), 526-532.

[7] Lima, R., Lourenco, M., Diaz, R.F., Castro, A. and Fievez, V. (2010) Effect of combined ensiling of sorghum and soybean with or without molasses and lactobacilli on silage quality and *in vitro* rumen fermentation. Animal Feed Science and Technology. 155, 122-131.

[8] Demirel, M., Celik, S., Temur, C., Guney, M. and Celik, S. (2009) Determination of fermentation properties and digestibility characteristics of combination of corn-soybean and corn silages. Journal of Animal and Veterinary Advances. 8(4), 711-714.

[9] Kaplan, M. (2011) Effect of ensiling alfalfa with sorghum on the chemical composition and nutritive value of silage mixtures. Journal of Animal and Veterinary Advances. 10(18), 2368-2371.

[10] Martinez-Garcia, C.G., Valencia-Nunez, K., Bastida-Lopez, J., Estrada-Flores, J.G., Mirande-de la Lama, G.C., Cruz-Monterrosa, R.G. and Rayas-Amor, A.A. (2015) Effect of different combinations of soybean-maize silage on its chemical composition, nutrient intake, degradability, and performance of Pelibuey lamb. Trop Anim Health Prod. 47, 1561-1566.

[11] Blaunt, A.R., Wright, D.L., Sprenkel, R.K., Hewitt, T.D. and Myer, R.O. (2006) Forage soybeans for grazing, hay and silage. University of Florida, Florida, FL. SS-AGR-180, 1-4.

[12] Lynch, J.P., O'Kiely, P. and Doyle, E.M. (2012) Yield, quality and ensilage characteristics of whole-crop maize and of the cob and stover components: harvest date and hybrid effects. Grass and Forage Science, 67, 472–487.

[13] Muck, R.E. and Dickerson, J.T. (1988) Storage temperature effects on proteolysis in alfalfa silage. Trans. ASAE 31:1005–1009

[14] Fleig, O. (1938) A key for the evaluation of silage samples. Futterbau und Giirfutterbereitung, 1, 112-128.

[15] Kung, L., Jr., Taylor, C.C., Lynch, M.P. and Neylon, J.M. (2003) The effect of treating alfalfa with Lactobacillus buchneri 40788 on silage fermentation, aerobic stability, and nutritive value for lactating dairy cows. J. Dairy Sci. 86, 336-343.

[16] AOAC (1990) Official Method of Analysis. Association of Official Analytical Chemists, 15th Edition, Washington, DC. USA

[17] Van Soest, P.J., Robertson, J.B. and Lewis, B.A. (1991) Methods for dietary fiber, neutral detergent fiber, and nonstarch polysaccharides in relation to animal nutrition. Journal of Dairy Science, 74(10), 3583-3597.

[18] Menke, K.H., Raab, L., Salewski, A., Steingass, H., Fritz, D. and Schneider, W. (1979) The estimation of digestibility and metabolizable energy content of ruminant feedstuffs from the gas production when they incubated with rumen liquor *in vitro*. Journal of Agricultural Science (Cambridge), 92, 217-222.
[19] Menke, K.H. and H. Steingass (1988) Estimation of the energetic feed value obtained from chemical analysis and *in vitro* gas production using rumen fluid. Anim. Res. Dev. 28, 7-55.
[20] Goel, G., Makkar, H.P.S. and Becker, K. (2008) Effect of *Sesbania sesban* and *Carduus pycnocephalus* leaves and Fenugreek (*Trigonella foenum-graecum* L) seeds and their extract on partitioning of nutrients from roughage-and concentrate-based feeds to methane. Animal Feed Science and Technology, 147(1-3), 72-89.
[21] Van Soest, P.J. (1994) Nutritional ecology of ruminants. 2nd ed. Cornell University Press Ithaca, New York USA.
[22] McDonald, P., Edwards, R.A., Greenhalgh, J.F.D. and Morgan, C.A. (2002) Animal Nutrition, 6th ed. John Willey & Sons, New York.
[23] Basso, F.C., Bernardes, T.F., Roth, A.P.T.P., Lodo, B.N., Berchielli, T.T. and Reis, R.A. (2012) Fermentation and aerobic stability of corn silage inoculated with *Lactobacillus buchneri*. R. Bras. Zootec, 41(7), 1789-1794
[24] Bal, M.A., Shaver, R.D., Shinners, K.J., Coors, J.G., Lauer, J.G., Straub, R.J. and Koegel, R.G. (2000) Stage of maturity, processing, and hybrid effects on ruminal in situ disappearance of whole-plant corn silage. Animal Feed Science and Technology, 86, 83-94.
[25] McDonald, P., Henderson, A.R. and Heron, S.J.E. (1991) The biochemistry of silage, 2nd ed. Marlow, UK: Chalcombe Publications.
[26] Umana, R., Staples, C.R., Bates, D.B., Wilcox, C.J. and Mahanna, W.C. (1991) Effects of a microbial inoculant and (or) sugarcane molasses on the fermentation, aerobic stability, and digestibility of bermudagrass ensiled at two moisture contents. J. Anim. Sci. 69, 4588–4601.
[27] Pahlow, G., Muck, R.E., Driehuis, F., Oude, Elferink, S.J.W.H. and Spoelstra, S.F. (2003) Microbiology of ensiling. In: Buxton, D.R., Muck, R.E. and Harrison, J.H. (eds.) Silage science and technology, pp. 31–93. Madison, WI, USA: Agronomy Publication No. 42, American Society of Agronomy.
[28] Ranjit, N.K. and Kung, L. Jr. (2000) The effect of *Lactobacillus buchneri*, *Lactobacillus plantarum* or chemical preservative on the fermentation and stability of corn silage. Journal of Dairy Science, 83, 526–535.
[29] Pitt, R.E. (1995) A model of aflatoxin formation in stored products. Transactions of the American Society of Agricultural Engineering, 38, 1445–1453.
[30] Wilkonson, J.M. (1999) Silage and animal health. Natural Toxins, 7, 212–230.
[31] Cavallarin, L., Tabacco, E., Antoniazzi, S. and Borreani, G. (2011) Aflatoxin accumulation in whole crop maize silage as result of aerobic exposure. Journal of the Science of Food and Agriculture, 91, 2419-2425.
[32] Crawshaw, R. and Woolford, M.K. (1979) Aerobic deterioration of silage in and out of the silo. ADAS Quarterly Review, 34, 151–178.
[33] Ohyama, Y., Hara, S. and Masaki, S. (1980) Analysis of the factors affecting aerobic deterioration of grass silages. In: Thomas, C. (ed.) Forage conservation in the 80s. BGS Occasional Symposium No.11, pp. 257–261. Reading, UK: British Grassland Society.
[34] Valentin, S.F., Williams, P.E.V., Forbes, J.M. and Sauvant, D. (1999) Comparison of *in vitro* gas production technique and the nylon bag degradability technique to measure short-and long term processes of degradation of maize silage in dairy cows. Animal Feed Science and Technology, 78, 81-99.
[35] Canbolat, O., Karaman, S. and Filya, I. (2010) The effect of different doses of oregano oil on corn silage digestive and rumen fermentation. Kafkas Univ Vet Fak Derg. 16(6), 933-939.
[36] Cetinkaya, N. and Erdem, F. (2015) Effects of different Juncus acutus: Maize silage ratios on digestibility and rumen cellulolytic bacteria. Kafkas Univ Vet Fak Derg. 21(4), 499-505.
[37] Robinson, P.H., Gatechew, G. and Cone, J.W. (2009) Evaluation of the extent of associative effects of two groups of four feeds using an *in vitro* gas production procedure. Animal Feed Science and Technology. 150, 9-17.

Received: **08.12.2016**
Accepted: **21.07.2017**

CORRESPONDING AUTHOR

Mustafa Kizilsimsek
University of Kahramanmaras Sutcu Imam
Faculty of Agriculture, Field Crops Department
46100 Kahramanmaras – TURKEY

E-mail: mkizil@ksu.edu.tr

© by PSP Volume 26 – No. 10/2017 pages 5761-5768 Fresenius Environmental Bulletin

THE DETERMINATION OF SOME GENOTYPIC AND PHENOTYPIC PARAMETERS FOR CHEMICAL COMPOSITION OF SOME BEAN GENOTYPES

Omer Sozen[1,*], Ufuk Karadavut[2]

[1]Ahi Evran University, Faculty of Agriculture, Department of Field Crops, Kirsehir, Turkey
[2]Ahi Evran University, Faculty of Agriculture, Department of Biometry and Genetics, Kirsehir, Turkey

ABSTRACT

This study was conducted in producer fields in Central Anatolia Region in 2009-2012. Ten different genotypes were used as planting material. Trials were conducted in the randomized blocks design with four replications. The objective of the study was to determine the genotypic and phenotypic parameters for chemical compositions of bean genotypes with respect to yield and several quality aspects. Quality data were analyzed for each genotype. Consequently, a substantial variation was observed for all analyzed characteristics. Phenotypic and genotypic variances were observed for higher water uptake and lower calcium content. Therefore, the environmental variation was the highest for water uptake ratio and the lowest for phosphorus and copper content. Average genetic gain was the highest for crude oil content with 51.18% where it was the lowest for copper content with 17.89%.

KEYWORDS:
Genetic progress, quality, chemical content, variance, yield, bean

INTRODUCTION

Seed yield in plants is placed among the most important agronomic characteristics. However, the variation in this characteristic is quite high because it is controlled by lots of genes. Beside of the genetic structure, environmental conditions are crucial to see the genetical capacity of plants. Both environment and genotype should be evaluated together when genotype is wanted to develop at a particular level in terms of yield and quality [1]. Genetic development is the difference between averages of breeding plants that are selected by phenotypic morphological, agronomic or yield traits among them [2]. Success in genetic variety evaluations at breeding programs is dependent upon the collecting data with precise measurements of quality parameters. Climatic variances (temperature, precipitation, scarcity or abundance of precipitation etc.) which occurred during genotypes' development change particularly year by year highly. Consequently, genotype x environment interaction is occurred. Genotype x environment interaction decreases the correlations between phenotypes and genotypes [3]. Success in predictions on genetic progress decreases significantly due to the descending correlation [4, 5]. Consequently, this leads significant issues for breeding studies. Researchers reduce this correlation via conducting their experiments at either the same or the different places to deal with this issue [6].

Altınbas and Sepetoglu [7] tried to estimate the genetic progress, and explored that winter chickpea's inheritance degree were between 0.15-0.86, and genetic capacity could be improved. Lalic et al. [8] explored that the inheritance degree of all parameters with seed yield was over 0.85 at their study about broad bean, but they did not find the same success in genetic improvement.

Some studies were conducted in determining maize growth parameters that they turned into quite complicated structure at different level of growth [9]. Blum et al. [10] explained that the same characteristics of plant, vegetation temperature, harvest index, biomass, yield and yield components were different according to genotypes and environmental factors.

The current results have showed that the drought stress after the brooding period increased with the increased number of spikes per square meter and that the translocation activities of the old varieties are better than the modern varieties due to their tallness. Yield was negatively affected by arid conditions so that the late flowering resulted in a decrease in productivity. Merah et al. [11] studied the drought indicator in the durum wheat genotype, leaf relative water content, osmotic potential, harvest index and yield. As a result, relative water content can be the selection criterion for drought tolerance of osmotic potential in the Mediterranean region.

Royo et al. [12] studied 25 varieties of durum wheat in Spain and two different Carbon isotope difference in area, vegetation temperature, thousand grain weight, total carbon content and grain yield with making regression analysis. The carbon isotope technique gives the best correlation with the genotypic variation, this is followed by the weight of a thousand-seed, and the planting temperature is weak relationship.

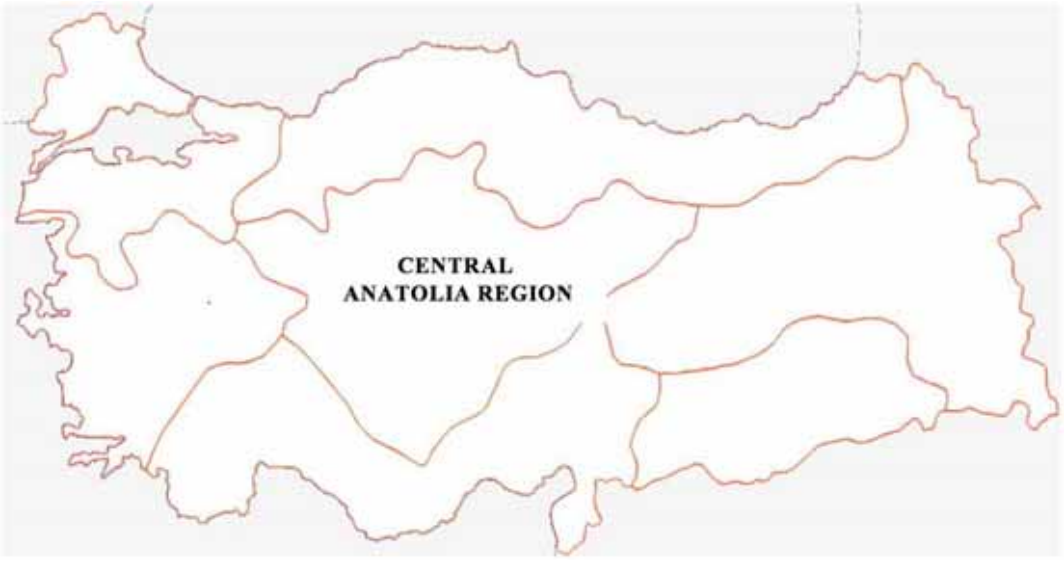

FIGURE 1
Central Anatolia Region map.

Genetic analyses of starch characteristics were studied in the study about rice, and it was determined that inheritance degree was above 0.60, and early generation increase selection success [13, 14]. Also, in different studies, genetic analyses were conducted to determine plants' growth at different stages [15-18].

Caylak et al. [19] found inheritance degree as 0.98, and 0.99 that are quite high values for tuber yield index. However, they reported these values changed in terms of years and locations in their study.

Alghamdi [20] determined Giza's development was quite well in terms of all characteristics, and found inheritance degree as 0.96 at flowering period, as 0.95 for seed number per plant, as 0.90 in ripening period.

Arshad et al. [5] stated that the production of per grain for legumes was controlled by many factors, because of that genetic progress was quite difficult. This study was aimed to find out some genotypic and phenotypic parameters particularly chemical composition for bean and seed yield.

MATERIALS AND METHODS

In this study, 6 standard cultivars (Eskisehir 855, Karacasehir 90, Sehirali 90, Yalova 5, Yalova 17, Yunus 90) and 4 local genotypes, totally 10 bean genotypes were used in private fields where were in Sarikaya province in Yozgat (Figure 1) which is located in Central Anatolia Province, during three years as between 2009 and 2012 years.

Information including beans characteristics belong to bean varieties are given at Table 1. When Table 1 investigated, it was seen that although varieties were breaded at different places, they had close to each other with respect to the observed characteristics. In this study, the local genotypes have been grown at this ecology for many years, without scientific knowledge on their genetic potentials.

A randomized block design was used with four replications for trials, and seeds of cultivars were sown by hand per parcel which was consisted of 4 rows in 5 m length and as 50 cm row spacing. After sowing, soil was pressed well to make seeds grow well. Soil structure of the experiment fields is given in Table 2.

When Table 2 was investigated, it was seen that the experimental field (soil) was quite poor in terms of organic substance (1.39%), phosphor, and rich in terms of potassium and non-saline, and its pH was 7.4. When experiments fields' rainfall was regarded, there were 128 mm rainfalls in the first year, 134 mm in the second year, 135 mm rainfall in the third year in terms of months which the experiment was conducted.

Average values of the moisture ratios were 62%, 67%, and 63% respectively. It was determined that there were not any fluctuations with respect to long years' averages, and there were similar climate data with long years' averages. Row irrigation was applied for four times during experiments.

The first irrigation was applied with sowing, the second irrigation was applied after 20 days of germination, the third irrigation was applied after flowering, and the last irrigation was applied at the pod maturation period. 20 kg pure nitrogen and 50 kg phosphor fertilizer were applied per hectare with the sowing. The potassium content of soil was detected as adequate, so potassium fertilizer was not given. Weed control was managed by hand twice during the study. Ten plants were selected randomly

for per variety, and each experimental parcel belong to local genotype, and their seed yield (kg da^{-1}), 100-seed weight (g), water intake rate (%), total nitrogen (%), chlorophyll content (ppm), prolin (ppm), canopy temperature (°C), stoma conductivity (mmol/m^2/sn), oil (%), protein rate in seed (%), carbohydrate (%), potassium (ppm), phosphor (ppm), calcium (ppm), magnesium (ppm), copper (ppm), and zinc (ppm) characteristics were determined. Phenotypic variance, genotypic variance, environmental variance, heritability, genetic progress expected, the average genetic gain, genotypic variation coefficient, phenotypic variation coefficient, phenotypic correlation coefficient, genotypic correlation coefficient, environment correlation coefficients were calculated in this study. Obtained data were analyzed by GLM procedure of SPSS statistical software (Windows version of SPSS, release 16.00) [21-27].

RESULTS AND DISCUSSION

When genotypes which were used in the experiment were investigated, significant differences were determined between genotypes. Descriptive statistics belong to observed characters, and sum of squares were given in Table 3. When Table 3 was observed it was seen that 100-seed weight was 17.44 g, and water intake ratio was 162.23%. Besides, it was found that protein ratio was high as 24.17%; crude oil was low as 1.24%.

Additionally, the average calcium content was found as 0.85 ppm, magnesium content as 1.22 ppm, and zinc content as 5.63 ppm. Genetic parameters belong to observed characteristics in this study are given in Table 4. When Table 4 was observed, it was determined that the highest phenotypic variance was observed in water intake ratio (396.13), and the lowest ratio was obtained from copper (0.01 ppm), and calcium (0.01 ppm).

The highest variance was observed in water intake ratio (28.4%) in plants that were affected by environmental conditions. This value is very important since it defines the environmental effects on water intake ratio directly. These conclusions are agreeing with Lalic et al. [8]'s findings. The obtained inheritance degree was between 0.29 and 0.99 for studied parameters.

TABLE 1
Some plant characteristics of varieties in the study

Varieties	Some Plant Characteristics
Eskisehir 855	It has dwarf and cock seed. Its pods are non-smooth and can be ready for harvest for 110-115 days. Its pods' length 12-13 cm and it has 4-5 numbers of pods per plant. Seed color is white, and 100 seed weight is 61.5g.
Karacasehir 90	It has 55-65 cm plant height, white, and plump seed, and it is a semi dwarf. Small plump's blending ability is so good, and its 100 seed weight is 18-19g. The numbers of pods per plant are 6-7.
Sehirali 90	It has dwarf and cock seed. Its pods are non-smooth, and can be ready for harvest for 105-110 days. Its pods' length 12-12.2 cm and it has 4-5 numbers of pods per plant. Seed color is white, and 100 seed weight is 45-47g
Yalova 5	It has a dwarf character; its pods are smooth and ready for the harvest for 55 days. Its pods' heights are 10-12 cm, their widths are 1.4-1.6 cm, oblate ellipse, and green. Its grains are white and kidney-shaped. Its white grains are coarse, and its 100 seed weight is 48-50g.
Yalova 17	It can give a crop for 40 days. It is smooth, a little bit dark green, flat Yalova type, dwarf variety. Average ripening period is 45-50 days.
Yunus 90	It has dwarf and plump seed. Its pods are non-smooth and can be ready for harvest for 115-120 days. Its pods' length 14.3-14.5 cm and it has 4-5 numbers of pods per plant. Seed color is white, and 100 seed weight is 41-43g.

TABLE 2
The soil structure of research area

Characters	Depth (0-40 cm)	Characters	Depth (0-40 cm)
pH (%)	7.40	Sand (%)	68.752
Salt (%)	0.027	Clay (%)	18.561
Usable P_2O_5	10.468	Mil (%)	12.056
Usable K_2O	97.112	Organic substances (%)	1.386
Usable N	105.86		

TABLE 3
The average values and the sum of squares of the characters

Character	Average	Standard Deviation	The Average Sum of Squares
Seed yield (kg da^{-1})	155.60	14.68	1807.28
100-seed weight (g)	17.44	7.52	68.712
Water intake rate (%)	162.23	39.14	1644.38
Total Nitrogen (%)	2.85	0.13	1.036
Protein (%)	24.17	6.21	49.24
Oil (%)	1.24	0.58	0.3574
Carbohydrate (%)	40.49	11.71	148.83
Chlorophyll content (ppm)	37.21	3.05	137.25
Proline (ppm)	2.38	0.48	1.662
Canopy temperature (°C)	24.56	6.34	56.28
Potassium (ppm)	0.98	0.97	0.1469
Stoma conductivity (mmol/m^2/sn)	64.71	9.37	184.236
Phosphor (ppm)	0.72	0.32	0.0763
Calcium (ppm)	0.85	0.22	0.0506
Magnesium (ppm)	1.22	0.36	0.1452
Copper (ppm)	0.99	0.21	0.0390
Zinc (ppm)	5.63	1.96	3.9861

The lowest inheritance degree was obtained from seed yield per plant as 0.29%; the highest inheritance degree was obtained from calcium content as 0.98%. When inheritance evaluated in general, seed yield per plant had quite higher value than inheritance degree that measured for all characters. It was determined that additive gene effect rose due to environmental effect, and genetic progress was over the average. While the lowest average genetic gain was determined for copper content as 17.89%, the highest genetic gain was determined for crude oil as 51.18%. In this respect, genetic gain studies help to reveal input which was obtained from breeding studies, allowing to make breeding strategies. It was determined that while seed yield's genetic gain was 29.52%; 100-seed weight's genetic gain was 40.38%. Besides, protein ratio's genetic gain was high as 28.04%. When traits were observed in terms of phenotypic variance, it was seen that all traits had nearly similar values to each other. Seed yield per plant was determined as 16.84%, 100-seed weight as 20.04%, protein ratio as 16.44% in terms of phenotypic variance coefficient respectively.

While phenotypic variance coefficient reached over 14% values for all quantitative characters such as seed yield per plant and 100-seed weight, these values were below 14% for the percentage of water intake rate (11.56%), and copper content (9.51%). When the inheritance degree of protein ratio was considered as 0.98, suggesting that it can be a protein selection criterion for variance studies [16]. When environmental variance was observed, it was seen that there was a wide variance in general. This is significant because it reveals that high inheritance degree leads high genetic varieties for plants. The estimated phenotypic coefficient of variation was greater than their corresponding genotypic coefficients of variation for most characters evaluated [28-30].

The determined plant water content can provide genetic gain compared to previous generations is quite a significant issue. Because in studies conducted for genetic gain not estimated genetic gain but materialized genetic gain was stated. Genetic variances changed too little by the experiment years. These results were contrary with Da Silva et al. [31]'s findings. The most significant estimated reason of it was that researchers used over geographical regions in their studies. The most significant parameter which is used to estimate expected selection gain is inheritance degree. Because of this reason, genetic variance can include dominant and epistatic effects [32]. Consequently, this will affect the success to increase plants which are selected positively.

Munjal and Rana [33] reported that it is important to keep the cover cool, to have a significant physiological development during the grain filling period in wheat. Venora and Calcagno [34] explained in the vicinity of the surfaces of the plants, evaporation from the leaf surfaces. When the temperature is dropped compared to the ambient temperature, plants will keep their stomata open under drought stress.

Vegetation temperature, hot and dry in wheat highly correlated with the conditions, high in heritability and early in the generations [35]. Photosynthesis in plants under heat stress decreases chloroplasts, by causing structural and functional damage to chloroplasts and chlorophyll [36]. Chlorophyll biosynthesis is affected negatively when plants are exposed to high temperatures [37]. The amount of proline has been reported to decrease, especially in water stressed leaves [38].

TABLE 4
Genetic parameters of the investigated characters

Character	Phenotypic variance	Genotypic variance	Environmental variance	Heritability (%)	Genetic progress expected	The average genetic gain (%)	Genotypic variation coefficient (%)	Phenotypic variation coefficient (%)	Phenotypic correlation coefficient	Genotypic correlation coefficient	Environment correlation coefficients
Seed yield (kg da^{-1})	20.14	12.51	5.84	0.29	5.84	29.52	20.58	16.84	-	-	-
100-seed weight (g)	19.26	18.15	1.26	0.94	7.38	40.38	20.19	20.04	0.152	0.214	0.251
Water intake rate (%)	396.13	412.57	28.34	0.95	40.07	21.19	10.26	11.56	-0.049	-0.106	0.003
Protein (%)	12.67	11.87	0.46	0.98	6.76	28.04	15.26	16.44	0.016	-0.211	0.054
Oil (%)	0.04	0.08	0.0002	0.98	0.59	51.18	20.84	21.18	-0.096	-0.094	0.017
Chlorophyll (ppm)	2.56	1.28	6.31	0.66	0.37	24.56	14.36	20.14	0.075	0.107	-0.112
Proline (ppm)	2.67	41.12	38.94	0.75	0.88	26.13	12.48	18.96	0.134	0.039	-0.131
Total nitrogen (%)	3.47	4.85	14.12	0.58	0.41	19.62	16.28	16.47	0.117	0.084	-0.074
Stoma cond. (mmol/m^2/sn)	4.66	7.12	24.19	0.33	0.27	30.25	15.07	13.89	0.098	0.057	-0.201
Carbohydrate (%)	36.28	39.17	1.64	0.97	11.44	27.55	14.88	15.06	0.022	-0.044	0.007
Canopy temperature (ºC)	2.12	3.34	3.29	0.61	0.18	21.78	14.68	12.38	0.018	0.088	0.046
Potassium (ppm)	0.02	0.03	0.0003	0.95	0.40	38.14	21.06	21.08	0.156	0.216	0.006
Phosphor (ppm)	0.02	0.02	0.0002	0.96	0.28	30.22	20.54	21.14	0.184	0.251	0.078
Calcium (ppm)	0.01	0.02	0.006	0.99	0.36	27.74	15.49	15.84	0.035	0.196	-0.054
Magnesium (ppm)	0.05	0.04	0.0004	0.94	0.19	30.88	14.93	14.69	0.126	0.116	0.071
Copper (ppm)	0.01	0.06	0.0002	0.96	1.24	17.89	6.58	9.51	0.106	0.184	0.114
Zinc (ppm)	1.12	1.10	0.0015	0.96	2.06	30.69	16.48	16.52	0.086	0.072	0.112

These results were in line with Sengul and Sagsoz [39] and Gastol and Swiatkiewicz's [40] findings. Actually, the genetic variance was not changed too much in their studies for desirable characteristic. When genetic variance is low, the selection will lead to decrease yield [41]. However, the studies carried out on genetic selection showed that the lack of phenotypic variance affected genetic selection naturally. In our study, it was found that phenotypic variance alteration according to characteristics was wider than genotypic variance since environmental conditions directly affected the observed data regarding current traits. Any time or place, any stress factors will affect agronomic traits, consequently allowing variations depending upon acclimatization ability of plant to different environmental conditions. Since the genotypic variations at different environments, and the greatness of inheritance degree are the main pillars to determine the effects of the environmental conditions on genetic gain [42].

Heterosis, i.e., new gene combinations will be possible as obtaining synthetic variation to select individuals whose general combination ability are higher in terms of the studied parameters or traits. When plants have better values than those of parents regarding studied parameters, the genetic improvement is maintained, thus, reflecting to yield. And this shows that the breeding studies are carried out successfully. The similar genetic and phenotypic correlation values will be normal. In this case, we saw that the phenotypic/genetic correlation ratio has to be less than the geometric mean of the heritability. When phenotypic correlation is lower than genetic correlation, the environmental conditions affects parameters negatively [43].

A phenotypic correlation is less than its genetic counterpart; it has a small positive environmental correlation. Environmental correlation has a small value its value will be large (positive or negative). Because of the environment affects an individual in all its parts. Genotypic coefficient of variation showed genetic variability in the genotypes for various traits. It doesn't get full scope to assess the variation for heritage [44]. The most important function of the heritability is the reliability of the phenotypic value for breeding value [45].

CONCLUSIONS

According to the obtained results, the genotypes which have been studied on may not give similar results at other regions due to the possible interactions seen in yields and environmental conditions. However, it is a true and substantial approach that they are evaluated at similar fields ecologically. It was well known that the genetic variance is quite narrow in small locations. Thus, the desirable variance will be composed more successfully since plants are cultivated at a suitable ecology for their physiologies, and consequently this may allow genetic gain.

In studying the inheritance of quantitative characters, the examined the proportional sizes of the additive and dominant genetic variance and environmental variance elements will not only be the ideal genotype to be improved (homozygous, heterozygous) but also provide useful information to the breeder if the optimal breeding method is specified. Successful genetic selection can be made in early generations, especially in those with a high degree of heredity in the narrow dimension. The number of leaves, the second important feature in terms of yield and quality. The variations in total sugar contents of beans may reduce the effectiveness of selection in early generations in terms of yield and quality, as it requires selection for recessive genes with lower frequencies. Therefore, it may be useful for the breeder to work with large populations, which will allow for the desired gene recombination, in order to increase the efficacy of selection on these traits.

REFERENCES

[1] Sreedhar, J., Reddy, T.D. and Ramesha, M.S. (2011) Genotype x Environment interaction and stability for yield and its components in hybrid rice cultivars (*Oryza sativa* L.). International Journal of Plant Breeding and Genetics, 1-15.

[2] Panwar, L.L., Joshi, V.N. and Ali, M. (2008) Genotype x Environment interaction in scented rice. Oryza, 45, 103-108.

[3] Comstock, R.E. and Moll, R.H. (1963) Genotype-Environment Interactions (statistical genetics and plant breeding. Edit. W.D. Hansen and H.F. Robinson) NAS-NRC Publ., Washington, 982, 164-196.

[4] Karadavut, U. and Palta, C. (2010) Chemical performance of multi-environment trials in lens (*Lens culinaris* M.). Journal of the Science of Food and Agriculture, 90(1), 117-120.

[5] Arshad, M., Bakhsh, A., Haqqani, M. and Bashir, M. (2003) Genotype–environment interaction for grain yield in chickpea (*Cicer arietinum* L.) Pak. J. Bot., 35, 181–186.

[6] Ozdemir, S. and Karadavut, U. (2003) Comparison of the Performance of autumn and Spring Sowing of Chickpeas in a Temperate Region. Turkish Journal of Agriculture and Forestry, 27, 345-352.

[7] Altinbas, M. and Sepetoglu, H. (2003) The Relationship of Performance with Adaptation for Yield and Some Agronomic Traits of Chickpea Lines Sown in winter. Ege Journal of Faculty of Agricultural, 40(1), 49-56.

[8] Lalic, A., Novoselovic, D., Kovacevic, J., Drezner, G., Darko, B., Abicic, I. and Dvojkovic, K. (2010) Genetic gain and selection criteria effects on yield and yield components in barley (*Hordeum vulgare* L.), Periodicum Biologorum, 112(3), 311-316.

[9] Bello, O.B., Ige, S.A., Azeez, M.A., Afolabi, M.S., Abdulmaliq, S.Y. and Mahamood, J. (2012) Heritability and Genetic Advance for Grain Yield and its Component Characters in Maize (*Zea Mays* L.). International Journal of Plant Research, 2(5), 138-145.

[10] Blum, A., Golan, G., Mayer, J., Sinmena, B., Shpiler, L. and Bura, J. (1999) The drought response of landraces of wheat from the northern Negev Desert in Israel. Euphytica, 43, 87-96.

[11] Merah, O., Deleens, E., Souyris, I. and Monaeveux, P. (2001) Ash content might predict carbon isotope discrimination and grain yield in durum wheat. JSTOR: New Phycologist, 149(2), 275-282.

[12] Royo, C., Villegas, D., Garcia del Moral, L.F., Elhani, S., Aparicio, N., Rharrabti, Y. and Araus, J.L. (2002) Comparative performance of carbon isotope discrimination and canopy temperature depression as predictors of genotype differences in durum wheat yield in Spain. Australian Journal of Agricultural Research, 53(5), 561-569.

[13] Bao, J.S. and Sun, M. (2002) Analysis of genetic behavior of some starch properties in indica rice (*Oryza sativa* L.): thermal properties, gel texture, swelling volume. Theoretical and Applied Genetics, 104, 408-413.

[14] Bao, J.S., Corke, H. and Sun, M. (2002) Microsatellites in starch-synthesizing genes in relation to starch physicochemical properties in waxy rice (*Oryza sativa* L.). Theoretical and Applied Genetics, 5, 898-905.

[15] Laghari, K.A., Sial, M.A., Afzal Arain, M.A., Mirbahar, A.A., Pirzada, A.J., Dahot, M.U. and Mangrio, S.M. (2010) Heritability studies of yield and yield associated traits in bread wheat. Pak. J. Bot., 42(1), 111-115.

[16] Ahmad, S.Q., Khan, S., Ghaffar, M. and Ahmad, F. (2011) Genetic diversity analysis for yield and other parameters in maize (*Zea mays* L.) genotypes. Asian J. Agric. Sci., 3(5), 385-388.

[17] Kashiani, P., Saleh, G., Abdullah, N.A.P. and Abdullah, S.N. (2010) Variation and genetic

studies on selected sweet corn inbred lines. Asian J. Crop Sci., 2(2), 78-84.

[18] Waqar-Ul-Haq, M., Malik, F., Rashid, M., Munir, M. and Akram, Z. (2008) Evaluation and estimation of heritability and genetic advancement for yield related attributes in wheat lines. Pak. J. Bot., 40(4), 1699-1702.

[19] Caylak, O., Caliskan, C. and Aygun, H. (2004) Genotype x Environment Interactions and Their Interpretations in Potato Breeding. Ege Journal of Faculty of Agricultural, 41(3), 123-131.

[20] Alghamdi, S.S. (2007) Genetic behavior of some selected Faba bean genotypes. African Crop Science Society, 8, 709-714.

[21] Bates, L.S., Waldren, R.P. and Tear, I.D. (1973) Rapid determination of free prolin for water-stress studies. Plant and Soil, 39, 205-207.

[22] Jackson, R.D., Idso, S.B., Reginato, R.J. and Pinter, P.J. (1981) Canopy Temperature as a Crop Water Stress Indicator. Water Resources Research, 17(4), 1133-1138.

[23] Adamsen, F.J., Pinter, P.J., Barnes, E.M., Lamorte, R.L., Wall, G.W., Leavitt, S.W. and Kimball, B.A. (1999) Measuring Wheat Senescence with a Digital Camera. Crop Ecology, Production and Management, Crop Sci., 39, 719-724.

[24] Novoselovic, D., Marijana, B., Drezner, G., Gunjaca, J. and Lalic, A. (2004) Quantitative inheritance of some wheat plant traits. Genetics and Molecular Biology, 27(1), 92-98.

[25] Killi, F., Efe, L. and Mustafayev, S.A. (2005) Genetic and environmental variability in yield, yield components and lint quality traits of cotton. International Journal of Agriculture and Biology, 7(6), 1007-1010.

[26] Johnson, H.W., Robinson, H.F. and Comstock, R.E. (1955) Estimates of genetic and environmental variability in soybean. Agron Journal, 47, 314-318.

[27] AOAC (2012) Official methods of analysis of the association of agricultural chemists. Official Methods of Analysis 19th Ed.

[28] Kadams, M.A. and Sajo, A.A. (1998) Variability and correlation studies in yield and yield components in bambara groundnut (*Vigna subterranean* L. Verdc). Journal of Applied Science and Management, (2), 66-70.

[29] Agbor, C.U. and Obi, I.U. (2005) Genetic variability of the yield and agronomic characters of breeding lines of rice (*Oryza sativa* L) in Nsukka genetic society of Nigeria, 30th Annual National Conference, Nsukka, 193-199.

[30] Jonah, P.M., Aliyu, B. and Jibung, Y.G.G. (2013) Phenotypic and Genotypic Variance and Heritability Estimates in Bambara Groundnut (*Vigna subterranea* L. Verdc) in Mubi, International Journal of IT, Engineering and Applied Sciences Research, 2(2), 66-71.

[31] Da Silva, F.F., Pereira, M.G., Ramos, H.C.C., Junior, P.C.D., Pereira, T.N.S., Gabriel, A.P.C., Pio Viana, A. and Ferreguetti, G.A. (2008) Selection and estimation of the genetic gain in segregating generations of papaya (*Carica papaya* L.). Crop Breeding and Applied Biotechnology, 8, 1-8.

[32] Serin, Y., Seker, H., Tan, M., Gokkus, A., Koc, A., Erkovan, H.I. and Bulut, S. (2001) Evaluation of biometrical properties with some components at Smooth bromegrass (*Bromus inermis leyss*). Field Crops Congress, Tekirdag, 193-198.

[33] Munjal, R. and Rana, R.K. (2003) Evaluation of Physiological Traits in Wheat (*Triticum aestivum* L.) for Terminal High Temperature Tolerance. Proceedings of the Tenth International Wheat Genetics Symposium, 2(3), 804-805.

[34] Venora, G. and Calcagno, F. (1991) Study of stomatal parameters for selection of drought resistance varieties in Triticum durum Desf. Euphytica, 57, 275-283.

[35] Yildirim, M., Akinci, C., Koc, M. and Barutcular, C. (2009) Applicability of Canopy Temperature Depression and Chlorophyl Content in Durum Wheat Breeding. Anadolu J. Agric. Sci., 24(3), 158-166.

[36] Xu, Q., Chitnis, V.P., Ke, A. and Chitnis P.R. (1995) Structural Organization of Photosystem I. In Mathis, P. (ed.), Photosynthesis: From Light to Biosphere. Kluwer Academic Publishers, Dordrecht, Netherlands, 87-90.

[37] Havaux, M. (1993) Rapid Photosynthetic Adaptation to Heat Stress Triggered in Potato Leaves by Moderately Elevated Temperatures, Plant Cell Environ., 16, 461-467.

[38] Stewart, C.R. and Hanson, A.D. (1980) Proline accumulation as a metabolic response to water stress. In: Turner NC, Kramer PJ, Adaptation of plants to water and high temperature stress. New York: Wiley Interscience, 173-189.

[39] Sengul, S. and Sagsoz, S. (2004) Evaluation of some biometric parameters of dry matter and seed yield components in alfalfa ecotypes (*Medicago sativa L)* as criterion for selection. Ataturk Journal of Faculty of Agricultural, 35 (1-2), 5-10.

[40] Gastol, M. and Swiatkiewicz, I.D. (2013) Genotype-Environment interactions in vitis vinifera-trace element contents in 13 grapevine cultivars. Fresen. Environ. Bull., 22(4), 1003-1007.

[41] Khayatnezhad, M., Gholamin, R., Somarin, S.J. and Mahmoodabad, R.Z. (2010) Investigation and Selection Drought Indexes Stress for Corn Genotypes. American-Eurasian J. Agric. & Environ. Sci., 9(1), 22-26.

[42] Talebi, R. (2009) Effective selection criteria for assessing drought stress tolerance in durum wheat (*Triticum durum* Desf.). General and Applied Plant Physiol., 35(1-2), 64-74.

[43] Searle, S.R. (1961) Phenotypic, Genetic and Environmental Correlations Author(s): Source: Biometrics, 17(3), 474-480.
[44] Singh, B.D. (2000) Plant breeding: principles and methods. Kalyani Publishers, New Delhi.
[45] Dabholkar, A.R. (1992) Elements of biometrical genetics. Concept Publishing Company, New Delhi, India.

Received: **14.12.2016**
Accepted: **23.07.2017**

CORRESPONDING AUTHOR

Omer Sozen
Ahi Evran University,
Faculty of Agriculture,
Department of Field Crops,
40100 Kirsehir - TURKEY

E-mail: eekim_55@hotmail.com
omer.sozen@ahievran.edu.tr

© by PSP Volume 26 – No. 10/2017 pages 5769-5774 Fresenius Environmental Bulletin

HEAVY METAL BIOSORPTION OF COPPER IONS BY IMMOBILIZED BIOMASS OF *STICHOCOCCUS SUBTILIS* (KÜTZING) KLERCKER

Dilek Yalcin[1,*], Tulay Ozer[2], Ilkay Acikgoz Erkaya[3], Ahmet Furkan Kayis[4],Ozcan Yalcinkaya[4]

[1]Department of Biology Education, Faculty of Education, Gazi University, Ankara, Turkey
[2]Department of Biology, Faculty of Arts and Science, Ahi Evran University, Kırşehir, Turkey
[3]Department of Environmental Engineering, Faculty of Architecture and Engineering, Ahi Evran University, Kırşehir, Turkey
[4]Department of Chemistry, Faculty of Science, Gazi University, Ankara, Turkey.

ABSTRACT

In this study, the ability of *Stichococcus subtilis* (Kützing) Klercker was used for heavy metal removal adsorbstion capacity. The sorption ability of *S. subtilis* was investigated using Cu metallic solutions. In the analysis, pH effect, equilibrium timing, initial metal ions concentration and temperature ranges were investigated. For single-metal systems, sorption isotherms were well-fitted to the Langmuir model. The results of the maximum Cu biosorption capacities were found as 2.70 and 10.4 mg/g for alginate and alginate–cells, with pH 5.5, corresponding to the initial Cu concentration of 50 mg/L. Cu biosorption on all the tested biosorbents agreed with Langmuir adsorption isotherm model.

KEYWORDS:
Copper, *Stichococcus subtilis*, alginate, immobilization, biosorption

INTRODUCTION

Being very hazardous and toxic materials for living organisms when in great amount, heavy metals become very serious environmental concerns [1]. To remove heavy metal ions from aqeous wastes, different methods are being used [2]. The use of biomass from live materials, eg, microalgae to adsorption multimetal ions in waste water has been gathering momentum. Therefore, a low cost biosorption process using microalgae as an adsorbent has recently been introduced as an option [3]. Biosorption, when compared with conventional treatment methods brings the following to the fore: cheap, high effiiciency, reduce of chemical and biological mud, renovation of biosorbent and a feasible metal recovery [4].

Microalgae have evolved natural method of responding to metals such as copper, lead, and cadmium via passive accumulation in cells and through surface binding to various functional groups [5]. The sorption characteristics of Chlorophyta have shown to be affected by different environmental parameters such as, pH, temperature, studied metal ion and other metal ions concentrations. Chlorophyta has been observed to be efficient in biosorption of copper, nickel, zinc and cadmium [6]. There are several studies focusing on demonstrating the toxic effects of heavy metals on different species of algae [7, 8, 9]. Heavy metal biosorption capacity of algae proved to be the highest because of the algal cell wall, which is composed of a fiberlike organization and an amorphous-embedding matrix of numerous polysaccharides [10]. The aim of this study was to evaluate the effect of copper metal on some physiological activities of *S. subtilis* with special references to metal bioaccumulation.

MATERIALS AND METHODS

Microalgae culture condition. *S. subtilis* species were collected from eutrophic freshwater lakes in Ankara and isolation with purification done through dilution and plating technique [11]. It was grown in 250 mL flasks with 100 mL BG11 medium [12], incubated at 22±1°C, and irradiance of 50 µmol photos m^{-2} s^{-1} provided by white fluorescent lamps set on 16D:8L h photo-period. Algal cells were incubated for enrichment in nutrients medium for 96 h [13]. After harvesting, the algal biomass was washed with ultrapure water and oven-dried at 100°C for 2 h before use.

Immobilization of *Stichococcus subtilis*. The immobilization of *S. subtilis* by entrapment was done as follows: Na-alginate (2.0 g; Sigma Chem. Co., USA) was dissolved in ultrapure water (50mL) and mixed with the algal suspension (50mL, containing 1.0g algal cells). The mixture was poured into a solution containing (0.1M $CaCl_2$) with a burette and stirred to avoid aggregation of the algal cell immobilized Ca-alginate beads. The beads, approx. 4 mm in diameter, were left in the solution for about 1 h, before washing 3x with 150 mL of sterile

ultrapure water. The hardened beads were then allowed in 5 mM $CaCl_2$ solution at 4°C until use. After drying the alginate beads for a night in an oven at 50°C, the dry weight of the biomass was assertained [14].

Reagent. As an instruction, every chemical used, was of analytical reagent grade. Ultrapure deionized H_2O was applied in the study. Cu stock solution (1000 mg/L) was prepared using $CuSO_4.5H_2O$ (Merck). The working solutions were prepared by diluting the stock solution to relevant volumes. NH_3 (27%), HCl (37%) and HNO_3 (30%) were got from Merck.

Apparatus. Flame atomic absorption spectrometer (FAAS), Varian AAS240FS model (Palo Alto, CA, USA) equipped with a Cu hallow-cathode lamp and a deuterium lamp for background correction, was used for copper determination following the manufacturer's instructions. Lamp current, wavelength, band width of the slit and acetylene flow rate were 10.0 mA, 324.8 nm, 0.5 nm and 1.4 L/min, respectively. WTW 720 model pH meter was used in all the measurements (Weilheim, Germany). To determine the adsorption capacity, a shaking thermostatic bath (Nüve ST 402, Turkey) at the temperatures (range of 298K-328K), at a fixed speed of 150 rpm was applied.

Batch Adsorption Procedure. Batch method was used in the determination of adsorption kinetics of Cu (II) ions on immobilized algae. Batch equilibrium tests were done using 50 mL of Cu (II) solutions in 100 mL Erlenmeyer flasks containing 0.01 g of adsorbent. The pH of the solutions were adjusted to 5.5 using 0.1 mol/L HCl and 0.1 mol/L of NH_3 solution and the flasks, placed into a mechanical shaker and stirred for 2 h at the desired temperature (range of 298K-328K) on a constant speed of 150 rpm. To find out the effect of mass transfer, the range of concentrations of prepared Cu (II) solution was varied from 1 to 50 mg/L. These suspensions were filtered after 2 h and the filtrates, analyzed for the determination of Cu (II) by FAAS with the required dilution. Equilibrium adsorption q_{eq} (mg/g) is calculated as follows:

$$q_{eq} = \frac{(C_0 - C_{eq})V}{X} \qquad (1)$$

with, C_0 and C_{eq} being the beginning and equilibrium concentrations (mg/L) of solutions, respectively, V the volume of solutions, (L) and X, the mass of the immobilized algae and alginat(g).

RESULTS AND DISCUSSIONS

Different parameters such as pH, equilibrium time and temperature were optimized to obtain the removal of copper ion on immobilized algal beads.

Effect of pH. Firstly, to be optimized in the sample solution was the pH, being important factor that influence, not only site dissocation, but also, the heavy metals solution chemistry. Hyrolysis, redox reaction and precipitation were strongly influenced by pH. To find the effect of pH on the solid phase extraction, pH of 50 mL model solution containing 500µg of Cu (II) was adjusted to 2.0-10.0 with 0.1 mol/L HCl and 0.1 mol/L. Amonia solutions flasks were placed in a mechanical shaker and mixed for 2 h at a constant rate of 150 rpm.The suspensions were filtered after 2 h and the filtrates analyzed for the detection of copper ions by FAAS with the required dilution. As can be seen on (Fig. 1), maximum removed copper was obtained at pH 5.5-6.0. According to this result, copper ions could be made and it is possible to separate from aqua solutions.

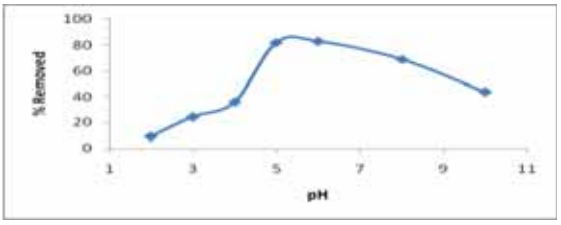

FIGURE 1
pH effect on the removed of copper by immobilized *Stichococcus subtilis*.

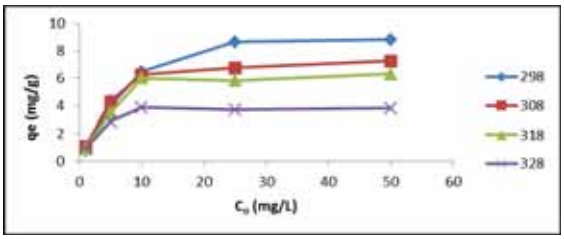

FIGURE 2
The effect of initial concentration of Cu (II) on adsorption at differnt temperatures (Sample volume; 50 mL, pH:5.5) for Stichococcus subtilis.

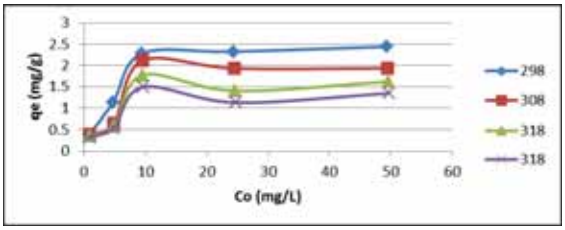

FIGURE 3
The effect of initial concentration of Cu (II) on adsorption at different temperatures (Sample volume; 50 mL, pH:5.5) for CA.

Adsorption Kinetics and Thermodynamic Parameters. Effect of initial Cu (II) concentration on adsorption capacity. In order to determine Cu (II) initial concentration effect on the adsorption capacity of both, *S. subtilis* and Ca-alginate (CA) beads, batch method was used at pH 5.5 with different initial Cu (II) concentrations under four different

temperatures and the results obtained are given on (Fig. 2 and 3). Generally, adsorption capacity of resin increases with initial metal concentration up to the equilibrium formed because, the initial metal concentration provides a driving force to overcome mass transfer resistance between the aqueous and solid phase. As seen on (Fig. 2 and 3), the adsorption equilibrium capacity was increased by increasing the initial concentration and decreased with increasing temperature up to 30 mg/L. So, equilibrium concentration was taken as 30 mg/L and used in determining the adsorption kinetics.

In order to explain the experimental results, the adsorption isotherms were formed showing the equilibrium relationship between adsorbent and adsorbate. For this purpose, Langmuir and Freundlich isotherm models were used in doing the analysis.

Langmuir Isotherm. Langmuir adsorption isotherm is ordinarily used in adsorption of solute from a solution. The basic assumption of this theory is that adsorbent until the saturated monolayer adsorption to be achieved. The saturated monolayer Langmuir isotherm equation is as follows:

$$\frac{C_{eq}}{q_{eq}} = \frac{1}{K_L q_m} + \frac{C_{eq}}{q_m} \quad (2)$$

such that, C_{eq} is the equilibrium concentration (mg/L), q_{eq} the amount of metal ion adsorbed (mg/g), q_m, the monolayer adsorption capacity of adsorbent (mg/g), and K_L the Langmuir adsorption constant (L/mg) related with the free energy of adsorption. The plot C_{eq}/q_{eq} versus C_{eq} indicates a straight line of slope $1/q_m$ and an intercept of $1/K_L q_m$ (Fig. 4).

Freundlich Isotherm. Freundlich isotherm model assumes heterogeneous adsorption active sites with different energy [15]. The linearized Freundlich model is as folllows:

$$\log q_{eq} = \log K_F + \frac{1}{n}\log C_{eq} \quad (3)$$

with, K_F as constant relating with the adsorption capacity and 1/n, an empirical parameter showing the adsorption intensity, and varies with the heterogeneity of the adsorbent. Langmuir and Freundlich isotherms were plotted using experimental data and the values obtained given on Table 1.

It is seen on Table 1 that Langmuir model is more acceptable than Freundlich model by comparing the results of correlation values at different temperatures. Besides, the experimental adsorption capacities are near the theoretical adsorption capacities of Langmuir model at high temperatures. In addition, the shape of the isotherm can be used to predict whether an adsorption system is favorable or unfavorable. For this purpose, Langmuir isotherm can be expressed in terms of equilibrium parameter R_L, defined in the following equation:

$$R_L = \frac{1}{1+K_L C_0} \quad (4)$$

Where, C_o is the initial concentration of copper (mg/L) and K_L, the Langmuir constant described above. There are four probabilities for the value R_L: (i) favorable adsorption $0<R_L<1$, (ii) unfavorable adsorption $R_L>1$, (iii) linear adsorption $R_L=1$, and (iv) irreversible adsorption $R_L=0$ [16]. In this study, all R_L values calculated for all initial concentrations (1-50 mg/L) and all temperatures are between 0 and 1. This shows that the adsorption of copper on *S. subtilis* at each defined temperature is favorable.

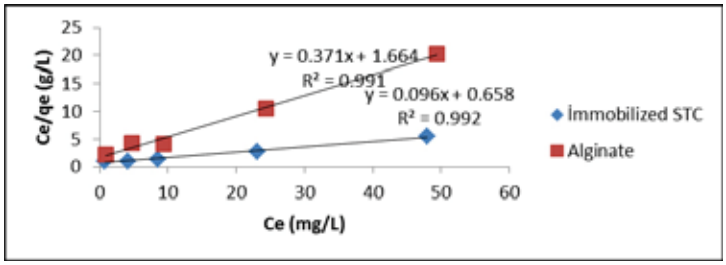

FIGURE 4
The linearized Langmuir isotherm at 298 K (pH: 5.5)

TABLE 1
The Isotherm parameters of Cu (II)

Temperature (K)	q_{exp} (mg/g)	Langmuir model			Freundlich model		
		q_m(mg/g)	K_L(L/mg)	R^2	K_F	n	R^2
298	8.8	8.6	0.081	0.9910	1.27	1.68	0.8812
308	7.3	7.2	0.073	0.9885	1.66	2.19	0.8381
318	6.3	6.3	0.061	0.9890	1.40	2.14	0.8290
328	3.8	3.7	0.058	0.9903	1.34	2.29	0.8010

TABLE 2
Kinetic parameters for the adsorption of Cu(II) at different temperatures

Temperature (K)	Pseudo-first order			Pseudo-second order			Second order		
	q_e mg/g	k_1 min^{-1}	R^2	q_e mg/g	k_2 g/min.mg	R^2	q_e mg/g	k_3 g/min.mg	R^2
298	6.486	0.0207	0.9700	20.06	$2.13x10^{-4}$	0.8661	16,6	0.0102	0,8276
308	6.261	0.0210	0.9810	18.48	$2.34x10^{-4}$	0.8773	24.3	0.0118	0,7985
318	6.008	0.0225	0.9881	16.30	$2.41x10^{-4}$	0.8581	41.5	0.0210	0,8118
328	3.815	0.0233	0.9792	15.64	$2.73x10^{-4}$	0.8779	36.25	0.0185	0,8665

Adsorption Kinetics. To determine the adsorption kinetics of copper ions on *S. subtilis*, 50 mL 10 mg/L Cu (II) solution (50 mL) containing adequate amount of adsorbent (0.01 g) was stirred at various time intervals (15-120 min) at the desired temperature at a fixed speed of 150 rpm. Lagergren's pseudo-second and pseudo-first order kinetic models [16], were applied to the experimentally obtained data. The linearized form of the pseudo-first order rate equation is given as:

$$\log(q_{eq} - q_t) = \log q_{eq} - \frac{k_1}{2.303} t \quad (5)$$

such that, q_{eq} and q_t (mg/g) are the metal ions adsorbed equilibrium with time *t* (min), respectively, and k_1 the rate constant of the process (min^{-1}). The adsorption rate constants were determined experimentally by plotting log (q_{eq}-q_t) versus *t* (Fig. 5) as given on Table 2.

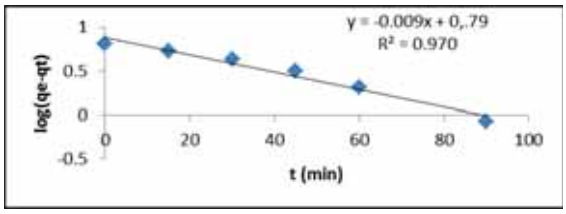

FIGURE 5
Pseude-first order kinetic model

Lagergren's pseudo-second order kinetic model was also applied to the experimental data which is given in the following form:

$$\frac{t}{q_t} = \frac{1}{k_{2.ad} q_{eq}^2} + \left(\frac{1}{q_{eq}}\right) t \quad (6)$$

Where, k_2 (g/mg.min) is the rate constant of the second order kinetic. The t/qt values were plotted againts t and the rate constant calculated were given in Table 2.

Second order kinetic model was also applied to the experimental data given in the following form:

$$\frac{1}{(q_{eq} - q_t)} = \frac{1}{q_{eq}} + kt \quad (7)$$

that, k (g/mg.min) is the rate constant of the second order kinetic. The $1/(q_{eq}-q_t)$ values were plotted versus t and the rate constant calculated were given in Table 2.

It is clear from these results that the adsorption of copper by *S. subtilis* fit the pseudo-first order kinetics, because its R^2 values (0.9700-0.9881) are very high against the R^2 values of the pseudo-second order kinetics (0.8581-0.8779) and the R^2 values of the second order kinetics (0.7985-0.8665).

Thermodynamic study. Adsorption capacity of *S. subtilis* for Cu (II) ions was decreased with increment in the temperature of solutions. This reveals that the adsorption of Cu (II) ion by *S. subtilis* surfaces is an exothermic process. The amounts of adsorption of Cu (II) ions by *S. subtilis* was measured in the temperature range of 298–328 K. Thermodynamic parameters, i.e. free energy (ΔG°), enthalpy (ΔH°), and entropy (ΔS°) changes, were determined using the following relations:

$$\Delta G^o = -RT \ln K_c^o \quad (8) \qquad \ln K_c^o = \frac{\Delta H^o}{RT} - \frac{\Delta S^o}{R} \quad (9)$$

where T (K) is the absolute temperature, *R* (kJ/mol K) is the ideal gas constant, and K_c° (L/mol) is the Langmuir equilibrium constant.

From eq. (9), it appears that both ΔH° and ΔS° of adsorption of Cu (II) by *S. subtilis* can be determined plotting K_c^o versus 1/T. The Gibbs free energy change (ΔG°) was calculated using eq. (8) at different temperatures. The thermodynamic parameters are shown on Table 3. The -ΔGs° demonstrated the feasibility of the process and the spontaneous nature of the adsorption with a high affinity of Cu (II) to *S. subtilis* at lower temperatures. The -ΔGs° change (-7.37 kJ/mol) showed the exothermic nature of the adsorption. The decrease in adsorption capacity with increase in temperature was seen to be due to the weakening adsorptive forces between the active sites on the *Stichococcus subtilis* and the metal ions species and also, between Cu (II) ions on the adsorbed phase as in other studies [17]. The low and negative value of ΔS° reflects the decreased randomness at the solid–solution interface during adsorption.

TABLE 3
Thermodynamic parameters for the adsorption of Cu(II)

Temperature (K)	ΔG^0 kJ/mol	ΔH^0 kJ/mol	ΔS^0 J/mol.K
298	-0.689		
308	-0.816	- 4.57	- 3.19
318	-0.973		
328	-2.082		

Most of the cell walls of green algae are made up of cellulose and a large percentage of proteins are bonded to polysaccharides in the form of glycoproteins. These compounds with functional

groups such as amino, carboxyl, sulphate and hydroxyl play an important role in the biosorption step [18]. The efficiency of algal (*Chlorella* sp., *Scenedesmus obliquus*, *Stichococcus* sp., *Phormidium sp*.) and bacterial species associations in the remediation of industrial wastewater of a pond in Russia, was investigated [19]. The results showed that *Stichococcus* and *Phormidium* cells had adsorped copper up to 62 %. The use of *Chlorella vulgaris* and *Scendesmus* sp. which is a Chloropyta genus, algal cells for copper biosorption was studied different researchers. In a Fraile's study over the heavy metal biosorption of microalgae, it is expressed that the adsorption of isotherm has best fitted to Langmiur Model [6]. As a result of our study, Langmiur model has proven to be the best adsorption isotherm model again. N. R. Bishnoi found that *Spirogyra* species carried out Cu (II) biosorption better at pH 6.0-7.0 and at contact time of 30 min [20].

Stichococcus species have been studied by researchers regarding heavy metal adsorption, but there are not much work on *S. subtilis for* copper adsorption. *S. subtilis* was applied as efficient adsorbent for the removal of Cu (II) ions from aqueous solutions. The effects of influential parameters such as pH, initial Cu (II) ion concentration and temperature were investigated under optimized conditions. A. Fraile have indicated that pH is an important factor in the sorption process due to competition between protons and metal cations for the active sites of the biomass [6]. Monolayer adsorption capacity of *S. subtilis* was found for Cu (II) ions as 8.8 mg/g at 298 K. The kinetic data revealed that the adsorption of Cu onto *S. subtilis* followed pseudo first-order kinetics. The -ΔGs support the spontaneous and favorable adsorption of Cu (II) ions while -ΔH causes exothermic nature of adsorption. The +ΔS indicates increased randomness at solid-liquid interface.

REFERENCES

[1] Leppard, G.G. (1981) Trace Element Speciation in Surface Waters. Plenum Press, New York.

[2] Matheickal, J.T., Yu, Q. (1999) Biosorption of lead (II) and copper (II) from aqueous solution by pretreated biomass of Australian marine algae. Bioresour Technol 69, 223-229.

[3] Smidsrød, O., Braek, G. (1990) Alginate as immobilization matrix for cells. Tibtech 8,71-78.

[4] Das, N., Vimala, D., Karthika, P. (2008) Biosorption of heavy metals. Indian Journal of Biotechnolog 7, 159-169.

[5] Gardea-Torresdeya, J.L., Arenasb, J.L., Franciscob, N.M.C., Tiemanna, K.J., Webbb, R. (1998) Abilty of immobilized Cyanobacteria to remove metal ions from solution and demonstration of the presence of metallothionein genes in various strains. J of Hazardous Substance R 1, 1-18.

[6] Fraile, A., Penche, S., González, F., Blázquez, M.L., Muñoz, J.A., Ballester, A. (2005) Biosorption of copper, zinc, cadmium and nickel by Chlorella vulgaris. Chemistry and Ecology 21, 61-75.

[7] El-Sheekh, M.M., El-Naggar, A.H., Osman, M.E.H., El-Mazaly, E. (2003) Effect of Cobalt on growth, pigments and the photosynthetic electron transport in Monoraphidium minutum and Nitzchia perminuta. Braz J Plant Physiol 15, 159-166.

[8] Anne, H.L.J., Marie, C., Veronique, D., Jean-Francois, B., Jean-Franc, L. (2006) Effect of copper sulphate treatment on natural phytoplanktonic communities. Aquat Tox 80, 267-280.

[9] Afkar, E., Ababna, H., Fathi, A.A. (2010) Toxicological Response of the Green Alga C.vulgaris, to Some Heavy Metals. American Journal of Environment Sciences 6 (3), 230-237.

[10] Khani, M.H. (2011) Statistical analysis and isotherm study of uranium biosorption by Padina sp. algae biomass. Environ Sci Pollut Res 18,790–799.

[11] CSIRO (Commonwealth Scientific and Industrial Research Organisation) (2016) Availale via DIALOG. http://www.csiro.au/ Accessed 15 February 2016.

[12] UTEX (Culture Collection of Algae at The University of Texas) (2016) Availale via DIALOG.https://utex.org/pages/algal-collections Accessed 15 February 2016.

[13] Duygu, D., Udoh, A.U., Ozer, B.T., Akbulut, A., Erkaya, A.I., Yıldız, K., Deniz, G. (2012) Fourier transform infrared (FTIR) spectroscopy for identification of Chlorella vulgaris Beijerinck 1890 and Scenedesmus obliquus (Turpin) Kützing 1833. African J of Biotech 11(16), 3817-3824.

[14] Katircioglu, H., Aslım, B., Tunçeli, A. (2012) Chromium (VI) Biosorption from aqueous solutions by free and immobilized biomass of Oscillatoria sp. H1 isolated from freshwater. ISIJ International 52(7), 1173–1178.

[15] Ozcan, A.S., Tunalı, S., Akar, T., Özcan, A. (2009) Biosorption of lead(II) ions onto waste biomass of Phaseolus vulgaris L.: estimation of equilibrium, kinetic and thermodynamic parameters. Desalination 244, 188-198.

[16] Ho, Y.S., McKay, G. (1999) Pseudo-second order model for sorption proceses. Process Biochem 34, 451-465.

[17] Tan, I.A.W., Ahmad, A.L., Hameed, B.H. (2008) Adsorption of basic dye on high-surface-area activated carbon prepared from coconut husk: Equilibrium, kinetic and thermodynamic studies. J Hazard Mater 154, 337-346.

[18] Romera, E., González, F., Ballester, A., Blázquez, M.L., Muñoz, J. (2007) Comparative

study of biosorption of heavy metals using different types of algae. Bioresour Technol 98, 3344-3353.
[19] Safonova, E., Kvitko, K., Iankevitch, M., Surgko, L., Afti, I. (2004) Biotreatment of industrial wastewater by selected algal-bacterial consortia. Eng Life Sci 4, 347–353.
[20] Bishnoi, N.R., Pant, A. (2004) Biosorption of copper from aqueous solution using algal biomass. Journal of scientific & Industrial Research 63, 813-816.

Received: **28.12.2016**
Accepted: **25.07.2017**

CORRESPONDING AUTHOR

Dilek Yalcin
Gazi University Faculty of Education, Department of Biology Education 06500 Ankara - Turkey

e-mail: dilekduygu06@hotmail.com

© by PSP Volume 26 – No. 10/2017 pages 5775-5782 Fresenius Environmental Bulletin

EFFECT OF NUTRITIONAL NEEDS ON THE YIELD OF LIGNIN-DEGRADING ENZYME AND DYES DECOLOURIZATION USING *HETEROBASIDION INSULARE*

Yue-Hua Zhang[1,*], Jing-Ni Yu[2], Jia-Lin Li[2], Zhi-Wen Luo[2]

[1]Institute of Agricultural-Environmental Biotechnology, Jiamusi University, Jiamusi, Heilongjiang Province, China, 154007
[2]College of Life Science, Jiamusi University Jiamusi, Heilongjiang Province, China, 154007

ABSTRACT

A research was made on glyoxal oxidase, manganese peroxidase and laccase produced under the impact of *Heterobasidion Insulare* (HIJ-2234) medium components. The change in the concentrations of copper could positively affect the secretion of lignin-degrading enzyme. *H. Insulare* extracellular fluid would enable the maximum production of lignin (161mU/ml glyoxal oxidase, 46.01 U/ml laccase and 241.6 mU/ml MnP), which demonstrates the maximum capabilities of decolorizing dyes Ponceau 2R, anthraquinone blue, malachite green and Ponceau 2R (a xylidine derivative) (at a velocity of 2.41, 1.53 and 3.0 mg ml^{-1} h^{-1}, separately). Simultaneously, the decolonization rate of the lignin and the activities of the enzyme were analyzed through multivariate regression. The experimental results meet the linear acceleration mode of interaction. Response surface was obtained through comparison, which manifests that manganese peroxidase activity plays a main role in malachite green decolorization even though laccase is of greater importance in dimethyl aniline degradation.

KEYWORDS:
laccase-producing; nutrient requirements; biochemical properties; *Heterobasidion Insulare*: decolorization;

INTRODUCTION

There are 10 million different kinds of dyes and dyestuffs widely and extensively applied in dyeing and printing industry all over the world each year. Synthetic dyes and commonly used industrial dyes with diverse chemical structures can be turned into insoluble azo dyes with triphenylmethane or heterocyclic polymer structure [1]. This product processing process tends to produce a large amount of waste water, which accounts for 10-15% of dye sewage. Some dyes are impacted by light irradiation and temperature. The performance of micro-organisms is fairly stable, and they could form a stable compound [2]. White-rot fungi belong to basidiomycetes, which secrete a group of lignin degradation enzymes. They have the potential for bioremediation [3]. This capability is degraded by the extracellular lignin as well as non-stereo-selective and nonspecific enzyme from the paint system formed by lignin peroxidase and manganese peroxidase (MNPs), hydrogen peroxide enzymes and secondary metabolites together. White-rot fungi need one enzyme or more to degrade lignin synthesis. Maybe this is the only reason for nonspecific mechanism, which can also degrade lignin degradation and a variety of contaminants, including chlorinated phenols, dyes and dioxin, polychlorinated biphenyls, as well as insecticide and explosives. The purified laccase, lignin peroxidase and MnPs with different chemical structures can undergo a dye-bleach process [4]. Previous studies are focused on lignin-degrading enzymes *Phanerochaete chrysosporium* and *Coriolus versicolor*. Recently, the interest in the study of white-rot fungi and ligninase has been increasing. The biological points of view have been compared, and a better system has been found for the biotechnological applications of lignin degradation [5]. Although the study of white-rot fungi rarely gets attention, it can increase the ability of laccase to degrade pollutants. For example, PCBs, PAHs degradation of dyes and polycyclic aromatic compounds have been demonstrated recently [6]. Economic cost is one of the main factors affecting the wide application of enzymes. The optimization of industrial fermentation medium may reduce operating costs. These statistical methods are more powerful than the practical method of controlling a single variable. The objective of the present study was to assess the effect of various nutrients on *H. Insularein* submerged fermentation and their relative importance for the production of lignin-degrading enzymes. Besides, we studied the culture medium of different synthetic textile dyes and bleaching effect of lignin-degrading enzymes. Lecter-Burman (PB) designed experiments [13] for enzyme production and the maximization of decolorization efficiency [7].

MATERIALS AND METHODS

Microorganism. *Heterobasidion Insulare* (HIJ-2234) was obtained from the Key Laboratory of Forest Protection, Northeast Forestry University, Heilongjiang Province, China. White-rot fungal strains were grown in modified PDA (potato-dextrose) at 28℃ for 7 days. Then, cell blocks of equal quantity and size were inoculated in modified PDB (potato-dextrose-) for liquid inoculation.

Culture media. Synthetic liquid medium was produced. (The compositions included: HK_2PO_4, 0.6g; $MgSO_4 \cdot 7H_2O$, 0.5g; KH_2PO_4,0.5g; zinc chloride, 3.5 mg; ferric chloride, 1.0 mg; thiamine hydrochloride, 0.1 mg; H_3BO_3, 0.07 mg; $Na_2MoO_4 \cdot 2H_2O$, 0.02mg; glucose concentration gradient (l), 10.0-20.0g; concentration gradient 2-Amino-3-carbamoylpropanoicacid, 0.50-4.0g; concentration gradient $CuSO_4 \cdot 5H_2O$, 1.50-700mg; concentration gradient $MnCl_2 \cdot 4H_2O$, 0.54-667mg; concentration gradient veratridine (3,4-dimethoxyphenyl) ethanol, 0.00-2.00mg; Tween-40 concentration gradient, 0.0-2.0 mg; double distilled water, 1 l) The starting pH of the medium was HCl 1.0N, which was adjusted by NaOH 1.0N. After autoclaving, the value was 4-6.5. The content of Bacto-agar was 2%.

Culture conditions. Cultures were incubated at 18-28℃ in 250ml erlenmeyer flask containing 25ml of medium under a stationary condition. The bacteria were grown in 2% agar for 5-day-old colonies. 2 agar blocks (per 0.25 cm^2) were inoculated. On the 23rd day, the fungal culture was screened out by using a Buchner funnel, and the culture supernatant was used as an enzyme source of filter paper.

Design of experiments and statistical analyses. Plackett Burman designed experiments to assess the *H. Insularein* submerged fermentation of various nutrients for the production of lignin-degrading enzymes and their relative importance. The planning assumption is that there is no interaction among the media with different components, taking the scope of the parameters into consideration. In a linear manner, it is considered as an adequate screening.

$$Y = \beta_0 + \Sigma\beta_i\chi_i (i = 1,2,3.....,k_i) \quad (1)$$

Wherein, variable "Y" is an estimate function of the object, and "β_i" is the regression analysis coefficient. The $\sum\beta$ is designed as the fraction of reason and analysis experimental schema. Significant impact (control coefficient, b) can be analogous to a simple calculation method, which is generally measured with a value coefficient and a high level of average (+1). The difference between the designs of the high assessment construction is at a low level (1). The determination of the effectiveness of the control coefficient permits every component. A massive control coefficient is a positive or negative factor that can indicate a significant impact on potency; nevertheless, the near-zero coefficient implies a factor that does not work or has little effect. The value of "*P*" is the probability of a comparison, because coefficient value suggests the variability of stochastic processes. Low-value "P" specifies "real" and means significant results. Discussion the variables are through the application of learning "t" test to detect [8]. Seven variables were used to represent 6 nutritional compositions and the original pH of the culture medium. Test results of variable parameters of high (+1) and low (-1) concentrations are shown in Table 1. Table 2 presents 2 distinct experimental representative lines, with each column representing the different variables. The experiment was run in three consecutive

TABLE 1
Plackett-Burman programming for optimized of medium, individual variable parameters the level used in the test

Parameter Design	Experimental variables						
	Asparagine (g/l)	Cu^{2+} (mM)	Glucose (g/l)	Mn^{2+} (mM)	pH	Tween 80 (mM)	VA (mM)
High factor	1.8	3.9	226	321	6.5	3	671
Low levels	0.1	0.6	10	4.9	3.9	1.7	0.39

TABLE 2-1
Plackett-Burman as media optimized and planning for the detect of response

Test parameters	groups											
	1	2	3	4	5	6	7	8	9	10	11	12
L-asparagine(g /l)	0.4	0.4	5	5	5	0.4	5	0.4	0.4	5	0.4	5
Cu^{2+} (mM)	667	667	667	1.6	1.6	1.6	667	1.6	667	1.6	1.6	667
Glucose (g/l)	10	10	20	10	20	10	20	20	20	10	20	10
Mn^{2+} (mM)	667	0.54	0.54	667	0.54	0.54	667	0.54	667	667	667	0.54
pH	4.0	6.0	6.5	6.5	4.0	4.0	4.0	6.0	6.5	6.0	4.0	4.0
Tween (mM)	0.0	1.6	0.0	0.0	0.0	0.0	1.6	1.6	0.0	1.6	1.6	1.6
VA (mM)	2.0	2.0	2.0	0.0	2.0	0.0	0.0	0.0	0.0	2.0	2.0	0.0

TABLE 2-2
Plackett-Burman Model Construction respond to media optimization and measured

groups		1	2	3	4	5	6	7	8	9	10	11	12
Equal enzyme activity	Laccase (U/ml)	17.20	2.20	45.90	1.10	2.21	0.10	18.40	0.30	1.41	0.79	0.65	2.51
	MnP (mU/ml)	48.00	10.49	215.5	3.9	59	2.0	104.5	3.0	4.0	10.0	3.0	19.95
	GLOX (mU/ml)	31.50	36.15	117.0	5.29	25.4	0.0	0.48	0.0	6.49	6.79	2.10	21.89
Decolorized arguments (DA/(min)	Ponceau2R	1.69	0.49	1.79	0.43	0.59	0.03	0.68	0.10	0.19	0.21	0.16	0.39
	Malachite-green	7.10	3.48	7.58	2.25	3.39	0.40	4.67	0.50	2.19	0.89	0.78	2.40
	Anthraquinone blue	530	450.1	677.5	94.53	508.6	9.00	544.7	13.50	38.26	24.76	29.26	182.32

replicates. Statistics analyses were conducted using software Minitab v13.1, and regression analysis was carried out with Primary V 2.2 through multiple regression and variance amount [9].

Enzymatic analysis. The activity of laccase was measured with 2, 2 O-azino bis (3-ethylbenzthiazoline-6-sulphonic acid) (ABTS) in 0.1 M acetate buffer (pH 4.0) at 28℃. ABTS oxidation reactions were detected and elevated in A_{410} (E_{410}= 40 mM/cm) [10]. The activity of MnPs in manganese peroxidase, was measured in 0.1M sodium dim ethyl succinate buffer (pH 4.0) at 28 ℃ (E_{600}=22.20 mM/cm) [11]. Phenolsulfonphthalein was used as a reference substrate GLOX assay used peroxidase conjugated with methylglyoxalsynthase, the GLOX as the reference substrate, and the phenolsulfonphthalein determination as reference peroxidase substrate (E_{600}= 22.20 mM/cm) [12]. The LIP was tested using the Resazurin with sodium salt-B determination method [13]. Activity represents the culture filtrate as per U/ml in international enzyme unit (U) (mmol product / min).

In vitro microbial cells decolorization. The reaction of decoloration mixture was observed in a monitor tube at 28℃. The reactant system contained sodium acetate buffer (10.0 mM; pH 4.0). The crude filtrate aliquots of enzyme were dispensed in a test tube with a total volume of 4.0 ml, to determine whether it is an azo dye Ponceau 2R (7.5mg/l), triphenylmethane dyestuff of malachite green (3.0 mg/l), anthraquinone or anthraquinone blue dyeware (50.0 mg /l). The dyes were adjusted to have an identical initial absorbance in 1.0 units. Their near-infrared wavelengths were in the visible ligut spectral range. Bleaching vitality reduced the visible wavelength of the specified dyes with a maximum absorbance (500, 616 and 625 nm, respectively). Nonetheless, the extracellular fluid with distilled water was in the control of duplicate samples. The results are displayed at DA / (min).

Chemicals reagents. All the standard dyes involved in the experiment were purchased from Sigma Co., Ltd, Shanghai, China.

RESULTS AND DISCUSSION

Results. Statistical methodology for optimizing the culture medium has been proven to be a perfect and biotechnologically useful tool. Accordingly, it attempts to compare the several factors between the two stages, and optimizes the formulations of the medium applications using Plackett-Burman trial design simultaneously. Factors detected comprised medium components of varying concentrations, including asparagine, cupric ions, glucose, bivalent manganese ion, and tween-80. Their reservation was properly done, and initial pH values were calculated. Besides, they were sterilized. These factors were the most promising in maintaining strains based on previous research on the optimization of strain fermentation [14]. Cultures were harvested on the 23rd day, which were previously detected in different media; *H. Insulare* culture began fermentation during the breeding period. Although it peaked before laccase and mycelium activity showed GLOX (i.e. they existed in principal growth stage), they began to take on the greatest activity in the secondary metabolic stage. From another aspect, manganese peroxidase activity was primarily detected during the breeding season. Dextrose in the culture medium was depleted with the decrease in the dry weight of mycelia [15]. Sampling time was set at 23 days to ensure that the significant levels of three enzymes could be tested.

Variable data experiments and their varying levels given are summarized in Table 1. The productions of lignin dye decolorization enzyme in different media were compared in Table 2-1 and Table 2-2. According to the experimental design, medium "3" had most significant laccase production. In media “7” and “1”, the increase in production were notable. Maximum conditions were suitable and supplementary to the culture medium generated regarding incorporation. GLOX potency increased 500 times in laccase. LiP was utilized to detect whether the experiment was successful or not. Negative LiP test results indicate various fungi growing conditions for this enzyme or no significant production needs. LiP concentration could be detected earlier, if the target strains were grown in the medium containing lignocellulose [16]. The finest enzymatic activity reached a peak value (44.89 U/ ml laccase, 220.40 mU/ml MnPs and

TABLE 3
Experimental design of based on various media components Plackett Burman experimental design degrading enzyme secretion of lignin *H. Insulare*

parameter		Aspara-gine	Glucose	Constant	Tween-60	Mn^{2+}	pH	VA	Cu^{2+}
Laccase activ-ity	*b*	7.89	7.31	7.21a	7.32	2.12	1.49	7.60	14.11c
	P-value	NS*I*s	*I*sb	0.110	*I*s	*I*s	*I*s	*I*s	0.082
MnP activity	*b*	56.97	50.11	36.89	29.97	24.43	0.98	35.11	52.97
	P-value	0.085	0.112	0.021	*I*s	*I*s	*I*s	*I*s	0.067
GLOX activity	*b*	24.13	15.12	25.11	13.04	18.14	9.41	24.13	34.86
	P-value	0.087	*I*s	0.012	*I*s	*I*s	*I*s	0.058	0.021
Ponceau 2R decoloration	*b*	0.26	0.08	0.58	0.46	0.02	0.08	0.56	0.68
	P-value	*I*s	*I*s	0.011	0.089	*I*s	*I*s	0.086	0.031
Malachite green decolorization	*b*	1.21	0.49	3.21	1.77	0.19	0.28	1.79	3.21
	P-value	*I*s	*I*s	<0.002	0.087	*I*s	*I*s	0.068	0.010

Note: The main influencing of factors (b) (laccase activity (U / ml), MnP vitality (MU / ml), GLOX vitality (mu / ml), malachite green and Ponceau 2R decolorizing (DA / (dl), and significance level (P-values) for experimental groups) the main effect (b) (paint activity). A Constant is expressed as presumption constant. The step b*I*s is: P <0.1. C expressed significant positive role.

121.05mU/ml GLOX). The culture medium contained 20.0g/l of glucose, 4.0g /l of asparagine, 766.0 mM of copper, 0.54 mM of Mn-ion and 2.0 mM of resveratrol. The initial pH value was 6.0. This kind of media formulation was also obtained to measure the maximum dye-decolorizing capacity.The crude enzyme solution was obtained in a medium. Such conditions also demonstrated the ability to measure the decolorization degree. The P value was a powerful tool to check each significant factor. Their analysis results show that only a significant positive impact on the factors tested may due to copper on laccase, manganese peroxidase and GLOW. MnP of the secretion also had higher influence on glucose and asparagine concentration. The GLOX production in the culture medium was increased by asparagine and resveratrol stimulus. Resveratrol, Cu^{2+} concentration of methyl aniline and malachite green decolorizing showed significant positive influence. Other factors were not proven to be statistically significant (P < 0.1).

Cu^{2+} consistently demonstrated in several species enjoyed a strong laccase inducer. It is known that the Cu^{2+} the intervention of laccase would induce transcription activities in DNA. Cu^{2+} concentration increased in proportion to the increase in activity. Under experimental conditions, *H. Insulare* manganese peroxidase and GLOX-inducing activity were previously observed [17]. Aromatic alcohols such as resveratrol (from white-rot fungi, it is well known for participating in the use of lignin and secondary metabolites LiP xenobiotic contaminants lignin degradation cofactors culture produced) have been reported to induce the production of laccase [18]. Within the range of measurement, the *H. Insulare* laccase and manganese peroxidase production had no significant effect either with or without VA, though it induced LOX production. On the contrary, VA was recognized to reduce the activity of extracellular GLOX [19, 22] in *P. chrysosporium*. Whether MnP induce or inhibit production in basic medium was affected by different fungi with different functions [20]. VA production increased the concentrations of enzyme production and level of toxicity [21].

LiP is usually utilized for the production under the best conditions of nitrogen starvation; when the concentration of N in the medium is large enough, many white-rot fungi generate a large number of laccase and manganese peroxidase [22]. Previous studies have demonstrated that *H. Insulare* produces the highest amount of laccase, a high concentration of nitrogen in the medium and the presence of carbon, manganese peroxidase and GLOX of expression in accordance with its constitutive lignin system expression [23].

The breakdown of lignin peroxidases in the participation extracellular H_2O_2 production was required. GLOX vitality for producing extracellular and secondary metabolism was illustrated, while lignin was also expressed in *P. chrysosporium*. It has been demonstrated to lead to the synthesis of hydrogen peroxide major enzyme [18]. GLOX depends on the high level expression of active *H. Insulare* (high up to 0.09 U/ml). Only a small portion of sample strains of were analyzed and measured . Degradative enzyme activity attained to 0.004 U/ ml. Kersten usually optimized a liquid medium to obtain 0.023 U/ml of GLOX activities in *P. chrysosporiumv* [24]. Previous profiles indicate that the oxidized process of white-rot fungi's synthetic xenobiotic compounds yielding peroxide cannot be improved without increasing the endogenously produced H_2O_2 [25]. Therefore, H_2O_2 produced had high lignin and vitality. Those crude culture filtrates produced by the *H. Insulare* (HIJ-2234) had different chemical structures capable of decoloration of dyes. Based on the order of magnitude of the resulting colorant, it can be used in the bioremediation of textile processing wastewater as a good candidate.

TABLE 4
Reveal of variance (ANOVA) for the Specified linear together interactive model for malachite Ponceau 2R (B) and green (A)decolonization by *H. Insulare*

Group A	Sum of squares	Degrees freedom	Mean squares	F-ratio	P-value	Group A	Sum of squares	Degrees freedom	Mean squares	F-ratio	P-value
Model	63.43	6	10.57	63.23	<0.001	Model	4.121	6	0.687	124.87	<0.001
Linear	49.40	3	9.67	58.23	<0.001	Linear	3.361	3	0.496	90.18	<0.001
Interaction	14.03	3	4.68	28.15	0.001	Interaction	0.760	3	0.253	46.04	<0.001
Residuals	0.83	5	0.17	–	–	Residuals	0.028	5	0.006	–	–
Total	64.26	11	–	–	–	Total	4.148	11	–	–	–

The relationship between lignin and decolorization enzyme activity was obtained in the experiments through multivariate linear regression analysis (Table 3). The decolorizations of Ponceau 2R and malachite green obtained obey the following equation:

$$Yi = \beta_0 + \sum \beta_i X_i + \sum \beta_{ij} X_i X_j \quad (2)$$

Wherein, *Yi* predicts the reactions. *Xi* and *Xj* are the variables in response to the impact of the input variable parameter *Y*. β_0 and β_i, represent the regression parameters. β_{ij} means model. Quadratic term was not statistically obvious. Accordingly, they are denied. (ANOVA) Variance corresponding analyses are summarized in Table 4. Determination (R2) of the coefficient values provides how the observed variability of response by experimental factors with the interaction between them to explain the measure. The model R2 (0.987 to Ponceau 2R bleaching, 0.978 and 0.976 malachite green and blue anthraquinone decomposition) is demonstrated in Table 4. Recommend fitting the linear model can explain and communicate, respectively accounting for 99.4%, 97.8% and 97.0% of the change. This means the expressed satisfaction by procedure model in the F-value (64.12, 125.12 and 24.98); P <0.001 Ponceau 2R, P<0.001 malachite green and similar anthraquinone blue discoloration respectively indicate optimism prediction of the model of the research conclusions. The P-value indicates the coefficients laccase and manganese peroxidase activity with nonlinear effects (MnP having a value of 0.049 and 0.019, respectively) of/between laccase (0.009) and the interaction). Manganese peroxidase / GLOX (0.041) and laccase/GLOX (0.076) activity suggest significant decolorization of malachite green. In other words, the active GLOX cannot significantly influence the decolorization of such dyes. Nevertheless, the activity does not linearly affect GLOX significantly in the decolorization of malachite green. In the detection scope, its impact cannot be entirely negative, because interaction affects laccase and manganese peroxidase activity. Despite the interaction between laccase and manganese peroxidase activity between the Ponceau 2R decolorized statistical significance (P=0.008), other factors indicate that the data are not statistically obvious (P <0.1).

Differences in the results gained in sample dyes indicate that this fungus strain achieves different react mechanisms to split the various chemical structure of the dye. Factors anthraquinone blue decolorized analysis demonstrates no statistical significance as P <0.01. Similar structure of anthraquinone blue could easily be decreased by *H. Insulare*. Participating in its degrading enzyme activity is probably not in a limited quantity. It means obvious difference based on the analysis of variance expression. From another aspect, an anthraquinone blue decolorized without considering the impact may be affected by other variables in this exercise. Malachite green decolorized by fitting regression model equation is given below:

$$Y = 0.905 + 1.448A - 0.20B - 0..12AB - 0.026AC + 0.01BC \quad (3)$$

Ponceau 2R decolorization enables optimum prediction based on the model:

$$Y = 0.085 - 0.002AB \quad (4)$$

Wherein, *Y* is the decolorization (DA/ (dl)). A denotes laccase, B signifies MVP and C represents GLOX activity. The 3D surface regression is the equation for Ponceau 2R (Fig. 1A), and malachite green decolonization has a graphical representation (Fig. 1B-D). The groups of pair-wise interactions describe the effect parameters.

After restricting the third parameter trends, the primary purpose is the efficient use of response surface grabs variables. Consequently, the best maximizes numerical values accordingly. Fig.1A illustrates the effect of the coordinating role on decolorization in laccase and manganese peroxides titers of Ponceau 2R. Fig.1B describes the degradation of malachite green and complementary role of two activities. Comparison of the obtained reaction surface demonstrates that laccase activity is of greater importance for dimethyl-aniline derivative decolorization, and MnP effect plays a primary role in the malachite green decolorization. Higher manganese peroxidase activity and GLOX were observed and increased in the dye decolorization (Fig. 1 C). This is consistent with the manganese peroxidases involved malachite green decolorization major enzyme, and the GLOX provides necessary H_2O_2 activity. That is to say, the high secretion of laccase by centrifugation liquid shrink their efficiency in splitting the molecular structure of malachite green, especially in the apparent expression of concentration GLOX existence

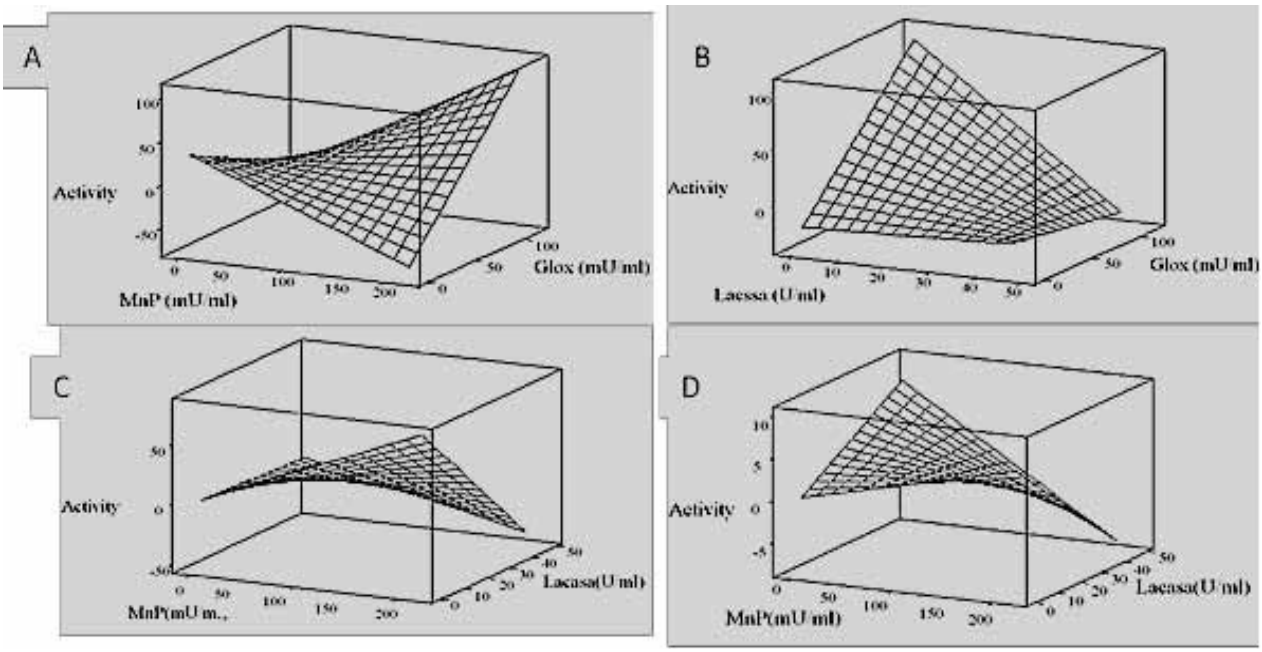

FIGURE 1

(A) Lecter-Burman's design for Ponceau 2R degradation by metabolite of *H. Insulare* production in laccase and MnP activities; (B) Lecter-Burman's design for malachite green degradation by metabolite of *H. Insulare* in laccase and MnP activities The vitality of GLOX was maintained at level 0 (47 mU/ml); (C) capability of MnP and GLOX function, with the activity of in laccase maintained at level 0 (22.075 U/ml); (D) capability of laccase and GLOX activities, with the activity of MnP maintained at level 0 (97.85 mU/ml)

Note: The capability of laccase is expressed in U/ml. MnP and GLOX capability are expressed in mU/ml. The decolorization values of dyes are demonstrated in DA/(min).

(denoted with B and D in Fig. 1). The possible reason lies in the competition between the two oxidizations: GLOX and paint enzymes present in the medium of active oxygen.

The outer *H. Insulare* at the highest production of lignin obtained *H. Insulare* cell laccase decolorization Ponceau 2R ideal efficiency. The sample of dyes in anthraquinone blue and malachite greenwere decolorized at rates of 1.53mg and 2.8mg dye/(ml.h), correspondingly. Different proportions represent different efficiency characteristics in *H. Insulare* crude product culture filtrates. The dyes with a different chemical structure were removed. There are documents that demonstrate anthraquinone dye is insoluble by the fungus whereas decolorization of azoic dyes is easier and faster [26]. The decolorization of insoluble azo dyes has a low efficiency, compared with other types of dyes, according to another report about *P. chrysosporium* and *I. lacteus* [27].

Natural microbial degradation of insoluble azo dye is formidable due to sulfo group, and an azo group is xenobiotics. Therefore, sulfonated azo dyes fight enzyme attacks. Insoluble azo biodegradation is dependent on the existence of extremely accurate changes in a functional group in the molecule structure. Dyes include those anthraquinone derivatives, Ponceau 2R, and some derived from RBBR and synthetic polymer, white-rot fungi act as the lignin-degrading enzyme in the enzymatic system of wood decay.

It is also used as lignin decolorization activity indicators for assessment. Anthraquinone, azo dyes and indigo dye *T.versicolor* laccase were discolorated [28]. However, laccase's catalytic decomposition of mechanism depends on the structure of the dye, which is different. The anthraquinone direct enzymatic oxidation paint, substrate interactions and small molecule metabolites insoluble azo dye and indigo paint are not mediated between the enzyme and dye. The decolorization rate of non-base dye is mediated by the compound rather than laccase concentration in solution [29]. Scholars have reported that the decolorization rate obtained with other white-rot fungi previously reported is comparable to the decolorization rate of azo dye Congo red, i.e. 2.9 and 3.9 mg/ml respectively [30]. *P. chrysosporium* and *P. ostreiformis* were cultivated in liquid media. Congo red, Ponceau 2R and methyl red including and regarding anthraquinone RBBR triphenylmethane bromophenol blue show a rate of 10, 20 and 35 mg/ml respectively in culture medium I. lacteus is described. *T. versicolor* decolorization of anthraquinone dye acid green 27 has a speed of 156 mg / (ml.h) [28].

The experimental results have revealed that *H. Insulare* strain may be utilized to remove color from

industrial wastewater in biological processes. Furthermore, this does not require rigorous secondary metabolites to create lignin-degrading enzyme. This enzyme needs non-stringent regulation than other extensively researched decolorization by white-rot fungi such as *P. chrysosporium*. Moreover, it has more other advantages. In the industrial decolonization of dye wastewater, nutrients and carbon source may remain present.

The degradation capability of white-rot fungi in allusion to a variety of environmental POPs manifests their potential uses in the treatment of pollution. Better exploration of the mechanism of these fungi secreting laccase system allows the development of technology and application of these microorganisms in cleaning both aquatic and land environments.

ACKNOWLEDGEMENTS

The work has been supported by the Natural Science Foundation of Heilongjiang Province, China. №: C201452.

REFERENCES

[1] Yagub, M.T., Sen, T.K., Afroze, S., & Ang, H.M. (2014). Dye and its removal from aqueous solution by adsorption: a review. Advances in colloid and interface science, 209, 172-184.

[2] Razzak, N.R.B. (2014). Effectiveness of fenton's reagent in the treatment of textile effluent.

[3] Elisashvili, V., Kachlishvili, E., Tsiklauri, N., Metreveli, E., Khardziani, T., & Agathos, S.N. (2009). Lignocellulose-degrading enzyme production by white-rot Basidiomycetes isolated from the forests of Georgia. World Journal of Microbiology and Biotechnology, 25(2), 331-339.

[4] Wesenberg, D., Kyriakides, I., & Agathos, S.N. (2003). White-rot fungi and their enzymes for the treatment of industrial dye effluents. Biotechnology advances, 22(1), 161-187.

[5] Cañas, A.I., & Camarero, S. (2010). Laccases and their natural mediators: biotechnological tools for sustainable eco-friendly processes. Biotechnology advances, 28(6), 694-705.

[6] Reddy, C.A., & Mathew, Z.A.C.H.A.R.I.A. (2001, November). Bioremediation potential of white rot fungi. In British Mycological Society Symposium Series, 23(1), 52-78.

[7] Levin, L., Herrmann, C., & Papinutti, V.L. (2008). Optimization of lignocellulolytic enzyme production by the white-rot fungus Trametes trogii in solid-state fermentation using response surface methodology. Biochemical Engineering Journal, 39(1), 207-214.

[8] Saeys, Y., Inza, I., & Larrañaga, P. (2007). A review of feature selection techniques in bioinformatics. bioinformatics, 23(19), 2507-2517.

[9] Rolston, A., Meade, C., Boyle, S., Kakouli-Duarte, T., & Downes, M. (2009). Intraspecific variation among isolates of the entomopathogenic nematode Steinernema feltiae from Bull Island, Ireland. Nematology, 11(3), 439-451.

[10] Erel, O. (2004). A novel automated direct measurement method for total antioxidant capacity using a new generation, more stable ABTS radical cation. Clinical biochemistry, 37(4), 277-285.

[11] Kamat, R.B. (2014). Phytoremediation for dye decolorization. Kansas State University.

[12] Vares, T., Kalsi, M., & Hatakka, A. (1995). Lignin Peroxidases, Manganese Peroxidases, and Other Ligninolytic Enzymes Produced by Phlebia radiata during Solid-State Fermentation of Wheat Straw. Applied and Environmental Microbiology, 61(10), 3515-3520.

[13] Khandare, R.V., Kabra, A.N., Kurade, M.B., & Govindwar, S.P. (2011). Phytoremediation potential of Portulaca grandiflora Hook.(Moss-Rose) in degrading a sulfonated diazo reactive dye Navy Blue HE2R (Reactive Blue 172). Bioresource technology, 102(12), 6774-6777.

[14] Alvira, P., Tomás-Pejó, E., Ballesteros, M.J., & Negro, M.J. (2010). Pretreatment technologies for an efficient bioethanol production process based on enzymatic hydrolysis: a review. Bioresource technology, 101(13), 4851-4861.

[15] Ahamed, A., & Vermette, P. (2008). Culture-based strategies to enhance cellulase enzyme production from Trichoderma reesei RUT-C30 in bioreactor culture conditions. Biochemical Engineering Journal, 40(3), 399-407.

[16] Huang, D. L., Zeng, G. M., Feng, C. L., Hu, S., Zhao, M. H., Lai, C., & Liu, H. L. (2010). Mycelial growth and solid-state fermentation of lignocellulosic waste by white-rot fungus Phanerochaete chrysosporium under lead stress. Chemosphere, 81(9), 1091-1097.

[17] Levin, L, Forchiassin F, Viale, A. (2005) Ligninolytic enzyme production and dye decolorization by Trametes trogii: application of the Plackett–Burman experimental design to evaluate nutritional requirements. Process Biochemistry, 40(3): 1381-1387.

[18] Saratale, R.G., Saratale, G.D., Chang, J.S., & Govindwar, S.P. (2011). Bacterial decolorization and degradation of azo dyes: a review. Journal of the Taiwan Institute of Chemical Engineers, 42(1), 138-157.

[19] Wymelenberg, A. V., Minges, P., Sabat, G., Martinez, D., Aerts, A., Salamov, A., & Dosoretz, C. (2006). Computational analysis of the Phanerochaete chrysosporium v2. 0 genome database and mass spectrometry identification of peptides in ligninolytic cultures reveal complex mixtures of secreted proteins. Fungal Genetics and Biology, 43(5), 343-356.

[20] Haritash, A. K., & Kaushik, C. P. (2009). Biodegradation aspects of polycyclic aromatic hydrocarbons (PAHs): a review. Journal of hazardous materials, 169(1), 1-15.
[21] Upadhaya, S.D, Park, M.A, Ha, J.K. (2010) Mycotoxins and their biotransformation in the rumen: a review. Asian-Australasian Journal of Animal Sciences, 23(9): 1250-1260.
[22] Baldwin, N.C., Bycroft, B.W., Dewick, P.M., & Gilbert, J. (1986). Metabolie Conversions of Trichothecene Mycotoxins: Biotransformation of 3-AcetyldeoxynivaIenoI into Fusarenon-X. Zeitschrift für Naturforschung C, 41(9-10), 845-850.
[23] Luo, F. (2011). The promotion of laccase expression induced by interspecies interaction and its application to biomass pretreatment (Doctoral dissertation).
[24] Zhao, J., & Janse, B.J. (1996). Comparison of H2O2-producing enzymes in selected white rot fungi. FEMS microbiology letters, 139(2-3), 215-221.
[25] Ten Have, R., & Teunissen, P.J. (2001). Oxidative mechanisms involved in lignin degradation by white-rot fungi. Chemical reviews, 101(11), 3397-3414.
[26] Dykstra, C.M. (2011). Decolorization of an azo and anthraquinone textile dye by a mixture of living and non-living Trametes versicolor fungus.
[27] Rauf, M.A., Meetani, M.A., & Hisaindee, S. (2011). An overview on the photocatalytic degradation of azo dyes in the presence of TiO_2 doped with selective transition metals. Desalination, 276(1), 13-27.
[28] Eichlerová, I., Homolka, L., & Nerud, F. (2006). Synthetic dye decolorization capacity of white rot fungus Dichomitus squalens. Bioresource Technology, 97(16), 2153-2159.
[29] Rodwell, T.C., Valafar, F., Douglas, J., Qian, L., Garfein, R.S., Chawla, A., & Catanzaro, D. (2014). Predicting extensively drug-resistant Mycobacterium tuberculosis phenotypes with genetic mutations. Journal of clinical microbiology, 52(3), 781-789.
[30] Younes, S.B., Bouallagui, Z., & Sayadi, S. (2012). Catalytic behavior and detoxifying ability of an atypical homotrimeric laccase from the thermophilic strain Scytalidium thermophilum on selected azo and triarylmethane dyes. Journal of Molecular Catalysis B: Enzymatic, 79, 41-48.

Received **07.11.2016**
Accepted: **04.05.2017**

CORRESPONDING AUTHOR

Yue-Hua Zhang
Institute of Agricultural-Environmental Biotechnology, Jiamusi University, Jiamusi, Heilongjiang Province, China, 154007

e-mail: _zhangyaohua_2008@163.com

© by PSP Volume 26 – No. 10/2017 pages 5783-5788 Fresenius Environmental Bulletin

NOVEL APPROACH OF PREDICTING THE BIODEGRADABILITY OF CORROSION INHIBITORS BASED ON THEIR PHYSICOCHEMICAL PROPERTIES

Amel Begbeg[1,2,*], Rabah Kerbachi[2], Mohamed Khodja[1], Malha Nazef-Allaoua[1]

[1] Sonatrach/R&D Center, 1th November Avenue, Boumedes, 35000, Algeria
[2] Environment Department, Ecole Nationale Polytechnique, Avenue Hassen Badi BP 182 El Harrach 16200 Algiers, Algeria

ABSTRACT

Corrosion inhibitors (CIs) are widely used in petroleum industry for protecting equipment from deterioration and hence reducing the enormous cost losses. In this context, extensive efforts have been made in R&D domain to look for green and cost effective CIs, because the common used CIs are toxic and not biodegradable. The main goal of this study is to develop a methodology for selecting friendly environmental CIs that can be used in oil and gas fields on the base of their physicochemical properties taken from the Material Security Data sheets (MSDS) and their chemical composition. More than twenty CIs are selected wherein the biodegradability, is determined experimentally under international standard ISO9408 (equivalent to OECD 301F). Several correlations are developed, the generated data indicates that some developed correlations can be used efficiently to predict the biodegradability of CIs at short time and at low cost. Therefore, a great benefit can be achieved for environment protection and petroleum industry.

KEYWORDS:
Corrosion inhibitors, biodegradability, correlation, physicochemical properties

INTRODUCTION

Oil & gas remain nowadays the main source of supply to cover energy demand, this industry consumes a big amount of materials made with steel (tubing, pipelines, well construction materials …etc), corrosion problems causing leaks are thus unavoidable [1-3].Companies use different strategies to minimizecorrosion reactions, one of which is the use of CIs[4], which act by forming a protective layer on the metal[5].Among all, oil&gas companies are the most important CIs consumer [6]. However, these products have the big disadvantage of being harmful to both human beings and environment [4, 5, 7]. Environmental considerationshand in hand with technical efficiency have led to a lot of research to develop green CIs[8]. Several studies had been carried out to develop eco-friendly CIs based on seed extracts[9],leaves[10] and other non-toxic natural compounds. It is worth to noting the huge volumes of CIs needed in the oil&Gas industry, this is why a serious economic and environmental study has to be done before using green CIs at large scale. Recently, many researchestargeted forthe prediction of chemical products environmental behaviour based on their physicochemical properties or on theirchemical composition [11-14].

Biodegradability is an essential parameter to be considered before introducing CIs into natural environment at large scale. However, biodegradability lab test is time consuming. To overcome this shortcoming, and to meet technical, economical, and environmental requirements, it is better to correlate the biodegradability of these products with their intrinsic properties at lab stage and to generalize subsequently the concept for swift and accurate product selection via consistent mathematical formulations, depending on the availability of intrinsic properties data. Thus, this study is devoted to provide a new vision for predicting biodegradability of CIs used in oil & gas industry based on their physicochemical properties.

MATERIALS AND METHODS

The twenty two (22)CIs commonly used are selected from a group of commercial products largely applied in Algerian oil&gas fields.These products contain lots of componentsfrom which, solvents, alcohols and other chemical products. Because the products are not pure; we have assessed our study on the classification and the study of CIs based on their active matter which belongs to the quaternary ammoniumgroup (10-60 % of active matter),or tothe fat amines with long hydrocarbon chains (20-50% of active matter)that are largely used to prevent foam formation. Their physicochemical properties are taken from their MSDSas shown in Table 1.

TABLE 1
Chemical family and physicochemical properties of the corrosion inhibitors

Product	Chemical Family of active matter	Viscosity (cSt)	pH	Flash Point (°C)	Density (g/cm^3)
1	Fat amines with long hydrocarbon chains	4,231	NA	57	0,92
2	Fat amines with long hydrocarbon chains	7,98	12,5	80	0,97
3	Quaternary Ammonium	2,27	NA	50	0,84
4	Fat amines with long hydrocarbon chains	NA	11,4	-18	1,1
5	Quaternary Ammonium	2,39	10,6	NA	0,89
6	Fat amines with long hydrocarbon chains	NA	9,5	27,2	0,87
7	Fat amines with long hydrocarbon chains	2,869	9,5	32	0,92
8	Fat amines with long hydrocarbon chains	5,494	NA	NA	0,95
9	Fat amines with long hydrocarbon chains	11,03	8,61	60	0,89
10	Fat amines with long hydrocarbon chains	7,6711	4,58	NA	1
11	Fat amines with long hydrocarbon chains	2,098	9,7	NA	0,87
12	Quaternary Ammonium	7,98	12,5	80	0,97
13	Fat amines with long hydrocarbon chains	21,52	5,19	100	1,07
14	Quaternary Ammonium	8,1038	8,8	62	1,02
15	Quaternary Ammonium	11,4	4,8	80	1
16	Quaternary Ammonium	7,947	NA	NA	0,99
17	Quaternary Ammonium	11,88	4	65	0,98
18	Quaternary Ammonium	4	4	65	1
19	Fat amines with long hydrocarbon chains	18,1	4,62	63	1,1
20	Fat amines with long hydrocarbon chains	NA	8,7	22,2	0,88
21	Fat amines with long hydrocarbon chains	NA		22	0,88
22	Fat amines with long hydrocarbon chains	NA	4,2	57,8	0,99

Biodegradability test. In our study the ready biodegradability of CIs are assessed using the standard ISO 9408 (1999) [15] equivalent to OECD 301 F (respirometry test), from the OCDE guideline (1992) [16],these tests are duplicated. This method is chosen by the authors to allow a generation of data in a reasonable time. The Biological Oxygen Demand (DBO) is determined for a period of 28 days using DBO-System with incubator-agitator (WTW OXITOP).

Mineral media are prepared from stock solutions:

1. 100 mL of solution A (8.50 g/L KH2PO4, 21.75 g/L K2HPO4, 33.40 g/L Na2HPO4 × 2H2O, 0.50 g/L NH4Cl),
2. 10 mL of solution B (27.50 g/L CaCl2),
3. 10 mL of solution C (22.50 g/L MgSO4 ×7H2O), and
4. 10 mL of solution D (0.25 g/L FeCl3 ×6H2O) are mixed, the volume is adjusted to 10 L with demineralised water, and the pH is adjusted to 7.4.

The used inoculum is brought from an activated sludge which is collected from the sewage plant or Waste Water Treatment Plant (WWTP) in Boumerdes city, Algeria, which is dedicated to the treatment of domestic waste water. The sample is diluted and aerated at room temperature until its use, within 24 hours.

The test material is dispersed directly in the final volume of medium (100 ml) to give a test concentration around 100 mg/L and then it is inoculated in the test flask with 30 mg/L dry weight of sludge.The samples are magnetically stirred and incubated under diffusing light at 22±1 °C. On day 28,all barometric data arecollected. It is important to indicate that the test duration is extended by two weeks for the chemical products that have a poor solubility as mentioned in the standard method.

The automatic barometric device,OxitopC (WTW, Weilheim) calculates the oxygen consumption.

Each sample container is related to a barometric system. This system is proportional to the amount of oxygen that is consumed by micro organisms.

The percentage of biodegradation is calculated via the OECD 301F guideline (OECD, 1992) [16].

RESULTS AND DISCUSSION

The generated experimental data are examined in order to predict under numerical correlation development the following target:

- The CIs environmental fate from their properties based on the biodegradability versus viscosity, flash points, pHand density. In details, the analysis is as follow:

Linear correlations are sought-after between corrosion inhibitors biodegradability and their physicochemical properties; the products are divided into four groups:

1. Biodegradable products
2. Non biodegradable products,
3. Quaternary ammonium
4. And fat amines.

This categorization assists us to find selective relationships in specific group or subgroup of products. The goodness of the fitting is assessed statistically as shown in Table 2, Table3, Table 4 and Table 5 : R (correlation coefficient), R^2 (Coefficient of de-

termination), SD (Standard Deviation), RMSE (Residual Mean Standard Error) and the slope.

TABLE 2
Statistical parameters calculated for Biodegradability vs Viscosity

	R	R^2	RMSE	Slope	SD
All Products	0.079	0.006	22.066	-0.311	5.492
Biodegradable products	0.024	0.000	7.739	0.034	5.309
Non biodegradable products	0.276	0.076	15.251	-0.579	6.554
Fat amines	0.150	0.022	30.364	-0.589	7.161
quaternary ammonium	0.512	0.262	6.316	1.039	3.578

Biodegradability vs Viscosity. For the case of viscosity versus biodegradability, there is no correlation except for the quaternary ammonium group which is possible to propose the following model:

$$B = 1.039\ (\mu) + 71.14 \quad (1)$$

A priori, this model would indicate that all quaternary ammonium corrosion inhibitors are biodegradable, the literature reports that quaternary ammonium compounds (QACs) are biologically degraded under aerobic conditions up to 90%[17, 18]. Furthermore, as indicated by Tezel, (2009)[19], The alkyl chain length also may have a decisive role in the fate and effect of QACs in the environment.

TABLE 3
Statistical parameters calculated for Biodegradability vs pH

	R	R^2	RMSE	Slope	SD
All Products	0.148	0.022	27.238	1.275	3.111
Biodegradable products	0.627	0.393	5.720	1.141	3.736
Non biodegradable products	0.295	0.087	16.090	1.741	2.674
Fat amines	0.299	0.089	27.117	2.681	2.966
quaternary ammonium	0.457	0.209	6.564	0.819	3.689

Biodegradability vs pH. Concerning pH-biodegradability relationship, there is no correlation except for the biodegradable products group, where the following model is proposed:

$$B = 1.141\ (pH) + 71.50 \quad (2)$$

Biodegradability vs Flash Point. For this case (Flash Point versus biodegradability), the whole products considered together presents a good correlation (r = 0.67) between Flash Point versus biodegradability .The flash point consideration of fat amines group also presents a good correlation with biodegradability (r = 0.62)

However, the weak point is that RMSE for those two tendencies are so high; 21.87 % for the products considered all together and 23.82 % for the fat amines group. The corresponding model is :

$$B \text{ all products} = 0.821\ (FP) + 9.03 \quad (3)$$

For the products considered all together and as follows for the fat amines group:

$$B \text{ Fat amines} = 0.682\ (FP) + 8.846 \quad (4)$$

TABLE 4
Statistical parameters calculated for Biodegradability vs flash point

	R	R^2	RMSE	Slope	SD
All Products	0.669	0.448	21.873	0.821	23.173
Biodegradable products	0.115	0.013	8.567	0.061	15.150
Non biodegradable products	0.508	0.258	13.649	-0.257	27.036
Fat amines	0.621	0.386	23.828	0.682	26.107
quaternary ammonium	0.462	0.213	8.551	0.346	11.496

TABLE 5
Statistical parameters calculated for Biodegradability vs density

	R	R^2	RMSE	Slope	SD
All Products	0.266	0.071	25.697	92.281	0.075
Biodegradable products	0.291	0.084	7.406	35.250	0.060
Non biodegradable products	0.431	0.185	14.218	69.610	0.092
Fat amines	0.339	0.115	28.240	112.873	0.086
quaternary ammonium	0.685	0.470	5.995	83.489	0.062

Biodegradability vs Density. For the study of density versus biodegradability, there is no correlation except for the quaternary ammonium group, this group presents a good correlation, where it is possible todevelop a mathematical model between density and biodegradability. The suggested model is as follow:

$$B \text{ quaternary ammonium} = 83.49\ (FP) + 2.12 \quad (5)$$

Case study. The previous developed models are applied to some CIs products to confirm the feasibility of the estimate tests biodegradability through these models without recur to laboratory biodegradability tests which varies according to the used method[20-22].

The physicochemical properties of products are shown in table 6.

The values of the physicochemical parameters of the corrosion inhibitors are integrated into different models developed above. The biodegradability results calculated using the model, linking

TABLE 6
Chemical family and physicochemical properties of the corrosion inhibitors

Product	Chemical family	Viscosity (cSt)	pH	Flash point (°C)	Density (g/cm^3)
01	quaternary ammonium	5	3	-20	1.05
02	quaternary ammonium	12	6	100	1.38
03	quaternary ammonium	50	5	63	1.3
04	fat amines	6	10	24	0.88
05	fat amines	250	6.6	100	1.04
06	fat amines	10	1.7	62	0.92
07	quaternary ammonium	25	9.5	100	1.00
08	quaternary ammonium	/	4.2	57.8	0.99
09	quaternary ammonium	86	8.8	/	1.02
10	quaternary ammonium	100	7	100	0.99
11	fat amines	/	12	100	1,04

TABLE 7
Estimated vs measured biodegradability

Chemical family Group	property	measured Biodegradability (%)	Estimated Biodegradability (%) (Eq.1)
Quaternary Ammonium	viscosity	Product 1: 64,92 Product 2: 92,84 Product 3: 63,76 Product 7: 50 Product 9: 37 Product 10: 84	76,33 83,60 123,09 97 160,5 175,04

biodegradability to viscosity, and those measured in the laboratory are summarized in Table 7.The following figure illustrates a comparison between the biodegradability values found experimentally and those evaluated by the model, where both generated data are relatively acceptable.

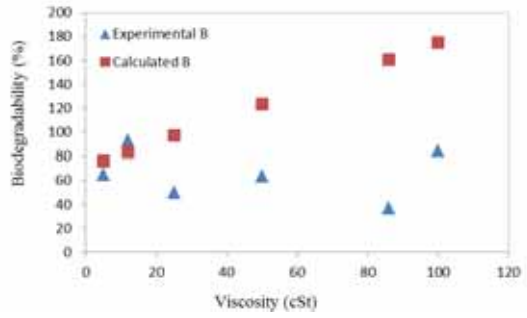

FIGURE 1
Experimental vs calculated biodegradability

The population is randomly distributed and there is no clear relationship between physicochemical parameters and biodegradability except for viscosity of CIs that does not exceed 25 cSt where a linear function between viscosity and biodegradability of quaternary ammonium based corrosion inhibitors is developed. Though biodegradability and viscosity of quaternary ammonium based corrosion inhibitors are related with a linear function with a boundary condition. According to Haus et al., (2004) [23], viscosity is found as a key parameter in predicting the ready biodegradability of mineral based oils.

From literature review, biodegradability prediction based on flash point, density or pH seems to be scarce.

It is always necessary to compare the results found with these models with others found before, but the major inconvenience is that the existing models in the literature are generally made on the basis of pure products, however,in the petroleum industry much of complex products are used in very large quantities, which necessitates the search for model predictionof biodegradability by group such as: corrosion inhibitor, biocides, surfactants, etc. In fact,with increasing degree of substitution and complexity of the structures, biodegradation in a screening test becomes less likely [22],which is in accordance with knowledge on generalrules of biodegradability for different classes of industrial chemicals [24].

Since, complex structures are described to be a problem for predictions [25], for CIs being very complex, it would perhaps be more appropriate to increase the incubation period of these products to 60 days as proposed by thecurrent REACH chemicals legislation [26](European Chemicals Agency, 2014a) and then use the generated data to predict biodegradability.

CONCLUSIONS

On the basis of experimental and statistical analysis, the following conclusions can be stated:

1) There is no clear relationship between physicochemical parameters and biodegradability except for viscosity of CIs that does not exceed 25 cSt.

2) Biodegradability and viscosity of quaternary ammonium based corrosion inhibitors are related with a linear function with a certain limitation.

3) Further experiments using an extended set of CIs and different laboratory techniques are required to confirm this conclusion and to look after other models predicting biodegradability based on

other physicochemical properties.

4) As indicated by Dick et al, (2016) [22], There is an obvious shortcoming in predicting models which are based on data from one specific test, because biodegradabilityvary when changing the used methods, through varying test duration, inoculums and product concentration.

5) The Use of different screening tests to generate experimental data will not solve definitely the problem, so that further improvements in these tests are required such as increasing incubation time to 60 days, especially for complex products such as corrosion inhibitors.

Nomenclature:
B: biodegradability
μ: viscosity
ρ: density
FP : Flash Point
R : correlation coefficient
R^2: Coefficient of determination
SD :Standard Deviation
RMSE:Residual Mean Standard Error

REFERENCES

[1] Osman, M.M., Shalaby, M.N.(2003) Some ethoxylated fatty acids as corrosioninhibitors for low carbon steel in formation water, Mater. Chem. Phys.77, p 261–269.

[2] Okafor, P.C., Liu, X., Zheng, Y.G.(2009) Corrosion inhibition of mild steel byethylamino imidazoline derivative in CO2-saturated solution, Corros. Sci. 51, p 761–768.

[3] Nešic´, S., Sun, W.(2010) 2.25 – Corrosion in acid gas solutions, in: J.A.R. Tony (Ed.),Shreir's Corrosion, Elsevier, Oxford, pp. 1270–1298.

[4] Raja, P.B. (2008) Gopalakrishnan, M.S, Natural Products as corrosion inhibitor for metals in corrosive media-A review.materials letters, p 62.

[5] Stringfellow, W.T., Domen, J.K, Camarillo, M.K.,Sandelin,W.L, Borglin, S.(2014)Physical, chemical, and biological characteristics of compounds used in hydraulic fracturing, Journal of Hazardous Materials, 275 37–54.

[6] Finšgar, M.,Jackson, J.(2014) Application of corrosion inhibitors for steels in acidic media for the oil and gas industry: A review, Corrosion ScienceVolume 86, September, Pages 17–41

[7] National Toxicology Program. (2011) Report on Carcinogens, 12th Ed., U.S. Department of Health and Human Services, Research Triangle Park, NC.

[8] Sitz, C., Frenier, W., Vallejo, C. (2012) Acid corrosion inhibitors with improved environmental profiles, in: SPE International Conference and Exhibition on OilfieldCorrosion, May 28–29, 2012, Aberdeen, UK, Society of Petroleum Engineers.

[9] Zucchi, F., Omar, I. (1985) Plant extracts as corrosion inhibitors of mild steel in HCl solutions, Surf. Technol. 24 391–399.

[10] El-Etre, A.Y.(2007) Inhibition of acid corrosion of carbon steel using aqueous extract ofolive leaves, J. Colloid Interface Sci. 314 578–583.

[11] Raymond J.W., Rogers,T.N.,Shonnard, D.R., Kline,A.A. (2001) review of structure-based biodegradation estimation methods, USA.

[12] Pizzo, F., Lombardo, A.,Manganaro, A., Benfenati,E. (2013) In silico models for predicting ready biodegradability underREACH: A comparative study, Science of the Total Environment463–464 161–168.

[13] Syaichurrozi, I., BudiyonoSumardiono, S. (2013) Predicting kineticmodel of biogas production and biodegradabilityorganic materials: Biogas production from vinasse at variation ofCOD/N ratio, Bioresource Technology 149 p 390–397.

[14] Jimenez, J., Gonidec, E., Cacho Rivero, J.A., Latrille, E., Vedrenne, F.,Steyer, J.P.(2014) Prediction of anaerobic biodegradability and bioaccessibility of municipal sludge by coupling sequential extractions with fluorescence spectroscopy:Towards ADM1 variables characterization, water research, 50, p 359- 372.

[15] ISO 9408:1999, Water quality -- Evaluation of ultimate aerobic biodegradability of organic compounds in aqueous medium by determination of oxygen demand in a closed respirometer.

[16] Oecd Guideline For Testing Of Chemicals Adopted By The Council On 17th July 1992

[17] Boethling, R.S. (1994) Environmental aspects of cationic surfactants. In J.Cross and E.J. and Singer (ed.), cationic surfactants: Analytical and Biological Evaluation, vol. 53. Marcel Dekker, Inc., New York, USA.

[18] Van Ginkel,C.G.(1996) Complete degradation of xenobiotic surfactants by consortia of aerobic microorganisms. Biodegradation,7: 151-164.

[19] Tezel, U.(2009) Fate And Effect Of Quaternary Ammonium Compounds In Biological Systems, A Dissertation Presented to The Academic Faculty In PartialFulfillment of the Requirements for the Degree Doctor of Philosophy in the School of Civil and Environmental Engineering, Georgia Institute of Technology.

[20] Painter H.A., Reynolds,P., Comber,S. (2003) Application of the headspace CO2 method (ISO 14 593) to the assessment of the ultimate biodegradability of surfactants: results of a calibration exercise, Chemosphere, 50 pp 29–38.

[21] Pedrazzani, R., Ceretti, E.,Zerbini, I., Casale, R., Gozio, E., Bertanza, G., Gelatti, U. (2012) Donato, F., Feretti, D., Biodegradability, toxicity and mutagenicity of detergents: Integrated experimental evaluations, Ecotoxicology and Environmental Safety, 84, 274–281.

[22] Dick, C., Rey, S. (2016)Boschung, A., Miffon,

F., Seyfried, M., Current limitations of biodegradation screening tests and prediction of biodegradability : a focus on fragrance substances. Environmental technology & innovation 5,pages 208-224.
[23] Haus, F.,Boissel, O., Junter,A. (2004) Primary and ultimate Biodegradabilities of mineral base oils and their relationships with oil viscosity, International Biodegradation Journal 54, 189-192.
[24] Painter, H.A.(1974) Biodegradability. Proc. R. Soc. Lond. Ser. B, 185, 149.
[25] Jenner, K.J., Kreutzer, G., Racine, P. (2011) Persistency assessment and aerobic biodegradation of selected cyclic sesquiterpenes present in essential oils. Environ. Toxicol. Chem., 30, 1096.
[26] European Chemicals Agency, (2014a). Guidance on information requirements and chemical safety assessment. Chapter R.7b: Endpoint specific guidance, version 2.0.

Received: **03.01.2017**
Accepted: **21.07.2017**

CORRESPONDING AUTHOR

Amel Begbeg
Sonatrach/R&D Center, 1th November Avenue, Boumedes, 35000, Algeria

e-mail: amelbegbeg@yahoo.fr

© by PSP Volume 26 – No. 10/2017 pages 5789-5796 Fresenius Environmental Bulletin

ADSORPTION BEHAVIOR OF 17*A*-ETHINYLESTRADIOL ONTO ACTIVATED SLUDGE DERIVED FROM MEMBRANE BIOREACTOR

Hai-Liang Song[1,2,*], Xiao-Li Yang[3], Tong-Qing Chen[3]

[1]School of Environment, Nanjing Normal University, Nanjing 210023, China
[2]School of Energy and Environment, Southeast University, Nanjing 210096, China
[3]School of Civil Engineering, Southeast University, Nanjing 210096, China

ABSTRACT

The adsorption behavior of 17α-Ethinylestradiol (EE2) onto activated sludge from a membrane bioreactor (MBR) was investigated. The effect of mixed liquor suspended solids (MLSS), sludge particle size and initial EE2 concentration on adsorption efficiency and the contributions of different sludge components to EE2 adsorption were discussed. Results showed that when initial EE2 concentrations were 1-500 $\mu g \cdot L^{-1}$, the time to reach adsorption equilibrium was 4h and the adsorption profiles matched both Langmuir and Freundlich isotherms. The EE2 adsorption rate displayed an inverse relationship with its initial concentration. With the increase of MLSS, the EE2 concentration in the sludge decreased remarkably. The total EE2 adsorption efficiency exhibited a linear correlation with MLSS concentrations. In addition, the EE2 adsorption effect decreased with the increase of sludge particle size. The contributions of each sludge component to EE2 adsorption were revealed to be positively correlated with their abundance. It was confirmed by reaction kinetics analysis that both adsorption and biodegradation contributed to the removal of EE2 in activated sludge system, and adsorption provided the prerequisite conditions for further biodegradation.

KEYWORDS:
17α-Ethinylestradiol, Adsorption, Biodegradation, Sludge components, Membrane bioreactor

INTRODUCTION

Steroid estrogens (SEs) may enter the aquatic environment via direct discharge of sewage or effluents from sewage treatment plants (STPs) [1]. The acknowledged principal SEs are naturally occurring endocrine disrupting compounds such as estrone (E1) and 17β-estradiol (E2), as well as the synthetic 17α-ethynylestradiol (EE2), which have 10^5-10^6 times higher activity than other suspected endocrine disrupting compounds, posing a serious risk to the reproductive and nervous system of various animal species including human even when their concentrations are as low as 1 ng/L[2]. Removal of estrogen compounds from the aqueous phase can be achieved through three pathways: biodegradation, adsorption onto solids and discharge with secondary effluent or excess sludge. Photodegradation is also an emerging technology of treating SEs in aqueous solution [3,4]. EE2 is more persistent than natural estrogens [5], and it is a kind of nonpolar and hydrophobic compound, has a higher octanol-water partition coefficient of 4.15 than E1 of 3.43 and E2 of 3.94 [6], so it can be strongly adsorbed onto activated sludge particles in wastewater treatment plant and might be an important way for EE2 removal in wastewater treatment systems [7]. Acting as the preamble of degradation process, adsorption played an important role in the biodegradation of EE2 [8].

The adsorption behavior of EE2 onto both activated and inactivated sludge was affected by pH, temperature, coexisting organic matters and so on [9]. The adsorption mechanisms of EE2 onto activated sludge are diverse due to different characteristics of sludge and usually being affected by environmental conditions. Ren et al. [10] and Xu et al. [11] investigated the thermodynamics of EE2 adsorption onto activated sludge biomass, and suggested that it was an exothermic process. Membrane bioreactor (MBR) may be well suited to remove EE2 via high adsorption because of the hydrophobic properties of activated sludge from MBR [12, 13], and providing the chance for further biodegradation. Therefore, this study was conducted to investigate the influence of the different properties of activated sludge, such as MLSS, particle size, sludge constituents (suspended solids, colloids, soluble materials), and the influence of initial EE2 concentration on adsorption behaviors of EE2. In addition, the adsorption effect was evaluated by the comparison experiment between EE2 adsorption of inactivated sludge and biodegradation of activated sludge. This study would be helpful for understanding the removal pathway of EE2.

MATERIALS AND METHODS

Reagents and chemicals. EE2 (purity > 98%) was purchased from Sigma-Aldrich, USA. Standard sample was dissolved in acetonitrile to prepare the stock solutions and further dilution was required to achieve target concentrations for the study. Chromatographic-grade methanol and acetonitrile were purchased from Chinese Pharmaceutical Group Chemical Reagent Co. Ltd. Remaining reagents were all analytical-grade. High-purity water was produced using a Milli-Q system (Millipore, USA).

Adsorption experiments. The activated sludge was taken from a MBR with the synthetic wastewater used as the influent. The MBR operated with a HRT of 12 h and a SRT of 30 d, and achieved the pollutants removal efficiencies with COD, TN and NH_4^+-N of 96%, 68% and 94%, respectively. As we know, both adsorption and biodegradation of activated sludge were contributed to EE2 removal. To avoid the influence of biodegradation, the activated sludge was heated at 121℃ for 30min to make it inactivated [14].

A series of adsorption experiments were performed as shown in Table 1. The influence of initial EE2 concentration, MLSS and particle size on adsorption efficiencies were investigated, and the contributions of sludge components were also evaluated. The different MLSS were obtained by diluting with ultrapure water. The particle sizes were changed by mechanical stirring and ultrasonic described by Duong et al. [15]. The sludge components were obtained according to aluminum sulfate flocculation separation method provided by Bouhabila et al. [16].

TABLE 1
The design of adsorption experiments

Initial EE2 concentration /(μg·L^{-1})	MLSS / (g·L^{-1})	Average particle size /μm	Components
1 10 100 200 500	3.97	248.9	complete sludge
100	1.50 2.53 2.90 3.97 5.86	248.9	complete sludge
100	3.97	248.9 227.7 195.2 186.3 163.8	complete sludge
100	3.97	248.9	suspended solids colloids soluble materials

The adsorption experiments were performed on a shaking bed (125 r/min) at 25℃. The sampling intervals were carefully determined on 5 min, 15min, 30 min, 1 h, 2 h, 4 h, 6 h, 24 h and 48 h after the spike of EE2.

Degradation experiment. In order to reveal the pathway of EE2 removal in the activated sludge system, the comparison experiments between adsorption and degradation were further conducted. The degradation experiment was operated with initial EE2 concentration of 100 μg·L^{-1}, MLSS of 5.86 g·L^{-1} and particle size of 248.9 μm.

Sample collection and pretreatment. For each sample, 10 - 100 mL mixed liquor was put into the glass centrifuge tube and centrifuged immediately at 3000 r/min for 5 min, and then filtrated through a pre-washed 0.7 μm glass fiber filter (GF/C, Whatman International Ltd., Maidstone, England) into a water phase and a sludge phase. Solid phase extraction (SPE; Caliper Company) was used to concentrate the samples which were under the detection limits. The C-18 SPE cartridge (Agilent Corporation) was preconditioned with 7 mL acetonitrile, 10 mL methanol and 10 mL water, with the loading rate of 10mL·min^{-1}. Afterwards, SPE cartridge was rinsed with 10 mL deionized water followed by 10 mL 10% methanol, and dried under nitrogen gas. Finally, samples were re-dissolved in 1 mL acetonitrile, and then be determined after being filtered through a glass fiber filter paper (0.22 μm).

The extraction procedure of EE2 from sludge samples followed the method described by wastewater examination methods (JSWA, 2002) [17]. Taking 50 mL mixed liquor sample as example. After decanting the supernatant, 40 mL of methanol/ acetate buffer (pH = 5) (9:1; v/v) was added to the precipitate, and it was shaken for 30 min. After centrifugation at 1800 r/min for 15 min, the supernatant was collected. Moreover, 40 mL of methanol/ acetate buffer (pH = 5) (9:1; v/v) was added to the precipitate, and it was shaken for 5 min. After centrifugation at 1800 r/min for 15 min, the supernatant was collected and mixed with the former supernatant. The mixture was then filtered through a glass fiber filter paper (0.22μm). After homogenized by sonication, SPE-HPLC analysis was carried out in the same procedure as the water phase described above. The sample recovery rate was 80.5-88.4%.

Analytical methods. EE2 concentrations were determined by HPLC (Shimadzu Corporation), which equipped with LC-20AB gradient pump, SIL-20A automatic sampler, SPD-20 ultraviolet detector, RF-10AXL fluorescence detector and LC solution chromatography workstation. Chromatographic separation was achieved on an Agilent Zorbax Extend-C18 column (250*4.6 mm, 5μm). Gradient elution was used in this study with a flow rate of 0.8

mL·min^{-1}. Beginning ratio of mobile phase water-acetonitrile was 55:45 (v/v); the ratio was changed linearly 50:50 (v/v) from 5-10 min, and then the ratio was increased linearly 55:45 (v/v) within 3 min and the system was continued at the same ratio for another 10 min. The UV detection wavelength was 200 nm; Column temperature was 30℃, injection volume was 20 μL, external standard method was used for calibration and peak area was used for quantitative in chromatography calibration system. Instrument detection limits was 5 μg·L^{-1} and method detection limits was 1 ng·L^{-1}.

MLSS and pH value were recorded according to Chinese NEPA standard methods [18]. Particle size distribution was determined by a BT-9300z Laser particle size analyzer (Dandong Baxter instrument co., LTD, China) with a measurement range of 0.02-760 μm.

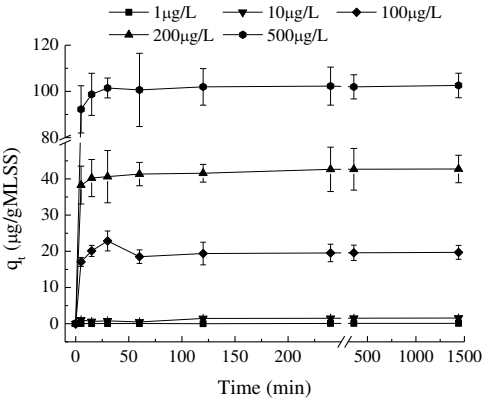

FIGURE 1
Adsorption of EE2 onto inactivated sludge with different initial EE2 concentrations.

RESULTS AND DISCUSSION

Influence of initial EE2 concentrations. Fig.1 showed the concentrations of EE2 in sludge with the initial EE2 concentrations of 1 μg/L, 10 μg/L, 100 μg/L, 200 μg/L and 500 μg/L, respectively. The time to reach adsorption equilibrium was 4 h for all the tested concentrations, and the removal efficiencies with five initial EE2 concentrations were 22.89%, 38.01%, 49.44%, 53.95% and 51.76%, respectively. The result has two implications: first, initial EE2 concentrations had little influence on adsorption equilibrium time, and second, the adsorption of EE2 was a rapid process. The adsorption rate of EE2 onto inactivated sludge biomass in the initial 5 min was 15.82%, 26.27%, 43.22%, 48.44% and 46.67% with increase of initial concentrations, which accounted for 69 - 90% of the equilibrium amount. Therefore, the adsorption of sludge can reduce EE2 concentrations in aqueous quickly, which is beneficial for the control of water ecological safety and the further biodegradation of EE2. Andersen et al. [6] and Braga et al. [19] found SEs adsorbed onto activated sludge reached 50 - 75% in primary sewage treatment.

At adsorption equilibrium, the adsorption amounts of EE2 onto sludge biomass with five initial EE2 concentrations were 0.17 μg/g, 2.00 μg/g, 19.54 μg/g, 42.64 μg/g and 102.29 μg/g, respectively. The adsorption capacity was positively correlated with initial EE2 concentration. It was because the higher initial EE2 concentration, the larger concentration difference between water phase and sludge phase, and the stronger adsorption capacity of sludge.

Data of EE2-removal and equilibrium EE2-concentration obtained from the isotherm studies were fitted to Langmuir and Freundlich isotherm equations as shown in Eqs (1) and (2), respectively.

The Langmuir isotherm has a theoretical basis, which relies on a postulated chemical or physical interaction (or both) between solute and vacant sites on the adsorbent surface, and it can be described as follows:

$$\frac{1}{q_e} = \frac{1}{q_{max} b C_e} + \frac{1}{q_{max}} \qquad (1)$$

Where, q_{max} is the maximum amount EE2 adsorbed onto inactivated sludge (μg·g^{-1}), qe is the amount of EE2 absorbed onto inactivated sludge at equilibrium (μg·g^{-1}), Ce is EE2 equilibrium concentration in liquid phase (μg·L^{-1}), b is a coefficient related to the affinity between EE2 and adsorbent.

Freundlich isotherm, on the contrary, has an empirical basis. The empirically derived Freundlich isotherm is defined as follows:

$$q_e = K_F C_e^{1/n} \qquad (2)$$

Where, qe and Ce have the same above-mentioned meaning, K_F and 1/n are Freundlich isotherm constants related to adsorption capacity and adsorption intensity, respectively.

Table 2 summarized the constants obtained from Langmuir and Freundlich isotherm. From Table 2, it was found that both Langmuir and Freundlich isotherm models fitted well with the adsorption of EE2, which indicated that the adsorption of EE2 occurs through combined mechanisms onto a heterogeneous surface.

TABLE 2
Comparison of the constants obtained from Langmuir and Freundlich isotherm at different EE2 concentrations

Langmuir isotherm			Freundlich isotherm		
q_{max}(μg/g)	B(L/μg)	R^2	K_F(L/g)	$1/n$	R^2
11.85	0.0239	0.9983	0.3323	1.1288	0.9974

K_d is the adsorption equilibrium constant, which also called distribution coefficient, and was usually used to reflect the function of adsorption, as indicated by Eq.3. [20]

TABLE 3
Summary of EE2 adsorption process evaluated by different kinetic models

	initial EE2 concentration (μg·L^{-1})	adsorption kinetic equation	adsorption rate K	R^2
intra-particle diffusion model	1	y = 0.0032x+0.0365	0.0032	0.6224
	10	y = 0.0592x+0.6368	0.0592	0.6882
	100	y = 0.1933x+16.8723	0.1933	0.9108
	200	y = 0.1051x+40.6095	0.1051	0.3328
	500	y = 0.5630x+95.2696	0.5630	0.5281
pseudo-first-order kinetic model	1	y = -0.0076x-2.2517	0.0076	0.5954
	10	y = -0.0137x-1.2011	0.0137	0.5838
	100	y = -0.0119x+1.5957	0.0119	0.7442
	200	y = -0.0222x+2.8963	0.0222	0.9612
	500	y = -0.0161x+2.9737	0.0161	0.7767
pseudo-second-order kinetic model	1	y = 10.2206x+257.3327	0.4059	0.9733
	10	y = 0.6178x+10.8812	0.0351	0.9886
	100	y = 0.0508x+0.1015	0.0254	0.9992
	200	y = 0.0234x+0.0310	0.0177	0.9998
	500	y = 0.0098x+0.0060	0.0160	1

TABLE 4
Comparison of the constants obtained from Langmuir and Freundlich isotherm at different MLSS

Langmuir isotherm			Freundlich isotherm		
q_{max}(μg/g)	B(L/μg)	R^2	K_F(L/g)	$1/n$	R^2
105.63	0.0039	0.9108	0.3927	1.0584	0.9079

TABLE 5
Summary of EE2 adsorption evaluated by the pseudo-second-order kinetic model

MLSS（g/L）	adsorption kinetic equation	adsorption rate K	R^2
1.5	y =0.0416x+0.3645	0.0047	0.9925
2.53	y =0.0508x+0.1015	0.0254	0.9992
2.9	y =0.0573x+0.4563	0.0072	0.9932
3.97	y =0.0788x+0.6552	0.0095	0.9897
5.86	y =0.0942x+0.9034	0.0098	0.9894

$$K_d = \frac{C_s}{C_w} \quad (3)$$

By calculating, the average logK_d of EE2 was 2.68 ± 0.14 at 25℃ in this study, which was consistent with the previous literature. Xu et al. [11] achieved the LogK_d of EE2 were 2.8 and 2.5 at 18℃ and 30℃, respectively. Andersen et al. [6] concluded that logK_d of EE2 was 2.77. The adsorption of EE2 in solution was a complicated process. The regression profiles of the adsorption process at different initial EE2concentrations was conducted with three kinetic models, including the intra-particle diffusion model [21], the pseudo-first-order kinetic model [11] and the pseudo-second-order kinetic model [22], see formula (4), (5), (6) .

$$q_t = k_p t^{0.5} \quad (4)$$

$$\frac{dq_t}{dt} = k_1(q_e - q_t) \quad (5)$$

$$\frac{dq_t}{dt} = k_2(q_e - q_t)^2 \quad (6)$$

Where, k_p for particle rate constant, μg·g^{-1}·min$^{-0.5}$; k_1 for adsorption pseudo-first-order reaction rate constant, μg·g^{-1}·min^{-1}; k_2 for adsorption pseudo-second-order reaction rate constant, g·μg^{-1}·min^{-1}; t for adsorption time, min; q_e, q_t for adsorption amount at adsorption equilibrium and adsorption time of t, respectively, μg·g^{-1}. The results of the kinetic regression were shown in Table 3.

From Table 3, the particle diffusion model cannot well describe the adsorption process with the regression line did not pass the origin, which indicated that the intra-particle diffusion was not the only adsorption rate-limiting step. The boundary layer diffusion of EE2, such as surface adsorption and liquid film diffusion, was also an important step of the adsorption process. They might be affected by the surface area of the inactivated sludge which mainly controlled by particle size, agitation velocity, adsorption temperature or solute concentration. Therefore, the adsorption process was the result of a variety of dynamic processes [23, 24].

The pseudo-first-order kinetics cannot describe the adsorption process of EE2 onto inactivated sludge with R^2 of 0.5838-0.9612. However, the pseudo-second-order kinetic model could best fit the adsorption of EE2 at different initial concentrations. Adsorption rate K was decreased with the increase of the initial EE2 concentrations. This might due to the higher initial EE2 concentration, more molecules collided possible with each other, and more time requirement. Feng et al. [9] also confirmed this when

they investigated the adsorption of EE2 onto the inactivated sludge.

Influence of MLSS. The influence of sludge concentration on the adsorption of EE2 was discussed and the adsorption process was expressed by Langmuir and Freundlich isotherm, and the isotherm constants were shown in Table 4. The results also indicated that the adsorption of EE2 at different MLSS could be well described by Langmuir and Freundlich isotherm.

Like the influence of initial concentrations of EE2, the pseudo-second-order adsorption kinetic model can also better describe the adsorption process of EE2 at different MLSS, as shown in Table 5.

Fig.2 showed the variation of EE2 adsorption capacity with different sludge concentration. It was seen that EE2 in unit sludge was dropped with the increase of MLSS, and the solid concentration effect was observed. This phenomenon may be due to the higher presence of tiny particles, which in the form of dissolved, large molecules or particles in the solution. A part of EE2 was adsorbed onto them and was still kept in solution as it was not easy to be removed by solid-liquid separation, and therefore resulted in the decrease of EE2 in solid phase [21]. Another possible reason was that EE2 segregation in water was reduced with MLSS increasing, and the actual specific surface area decreased, resulting in a decrease of adsorption capacity.

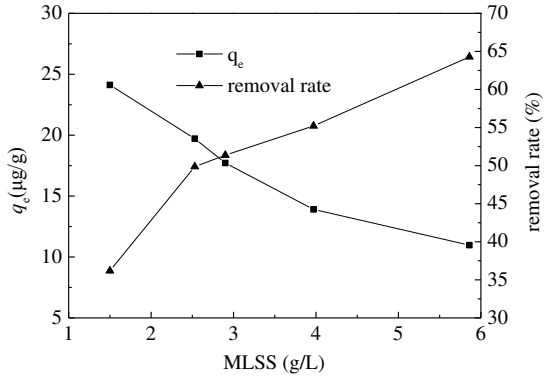

FIGURE 2
The influence of MLSS on EE2 adsorption capacity. (temperature: 25℃; agitation: 125 r·min^{-1}; initial concentration: 100μg·L^{-1}; pH: 7.0)

Although there was the solid concentration effect, the total adsorption removal rate of EE2 was increased with the increase of MLSS. The adsorption amount with MLSS of 5.86 g/L was about 1.78 times over that of 1.50 g/L. One-way ANOVA analysis indicated that the total EE2 adsorption rates displayed a linear correlation with MLSS concentrations, the correlation coefficient was 0.9504 ($p < 0.05$). Therefore, the higher MLSS was helpful to enhance EE2 adsorption effect. Thus, the extension of sludge age can not only reduce excess sludge, but also can greatly reduce the potential risk to the environment caused by micro-organic pollutants including SEs.

Influence of sludge particle size. Sludge particle size would affect the surface area of sludge directly, and further change the adsorption characteristics. Adsorption isotherms and kinetic models were used to characterize the adsorption of EE2 with different sludge particle sizes. It was also found that both Langmuir and Freundlich isotherm fitted well the adsorption of EE2, and pseudo-second-order kinetic model well described the adsorption process of EE2 (Regression coefficient $R^2 > 0.98$). The distribution coefficient logK_d decreased with the increase of particle size with the values of 2.93, 2.87, 2.73, 2.69 and 2.66, respectively. This was because the greater the particle size, the smaller the specific surface area, the less of adsorption point, and the decreased adsorption effect. Therefore, it can be concluded that MBR was superior in adsorption because of the smaller sludge particle size by air scouring for membrane fouling control in the systems.

Influence of sludge components. The main components of sludge can be classified into suspended solids, colloids and solutes according to their sizes. The sludge components would vary with different wastewater treatment processes and operation conditions. The contribution of sludge components on adsorption was evaluated for better understanding the adsorption effect. When MLSS concentration from MBR was 3.97 g·L^{-1}, the suspended solids, colloids and solutes were 3.49 g·L^{-1}, 0.38 g·L^{-1} and 0.10 g·L^{-1}, respectively, and they accounted for 87.8%, 9.6% and 2.6% of the total sludge. The suspended solids were the main ingredients of the sludge, and the proportion of colloids and solutes was smaller. MacNicol et al. [25] concluded that suspended solids accounted for 99%, colloids and solutes accounted for 1%. The relatively higher colloids in this research might be related to the system of MBR. MBR always operated with a long sludge age, a high MLSS and maintained at a lower sludge loading. Extracellular polymers (EPS), soluble microbial products (SMP) and some other microbial metabolites were produced in the process of biodegradation. These substances existed in the gel state around microbial cells or in dissolved state in the supernatant, increasing the colloids portion.

The concentrations of EE2 in the three components were 20.5 μg·g^{-1}, 37.8 μg·g^{-1} and 33.2 μg·g^{-1}, respectively, at adsorption equilibrium. The adsorption ability of colloids was greater than the other two components. It was seemed that the electric charge property of colloids make it easier to adsorb molecules in solution by electrostatic interactions, so as to improve its adsorption capacity. Because of the different contents of various components, the adsorption rate of EE2 onto suspended solids reached 54.5%, while which were 11.0% for colloids and

2.6% for solutes. Thus, the contributions of each sludge component on EE2 adsorption were positively correlated with their abundance.

Fate of EE2 in MBR. It was suggested that the removal of estrogens and its conjugates from wastewater in activated sludge processes mainly via adsorption and diffusion into activated sludge flocs and subsequent biodegradation by microorganisms [17, 26]. Therefore, the effect of adsorption was important not only for adsorption removal but also for the prerequisite conditions for biodegradation.

As indicated in Fig.3, about 60% of the spiked EE2 was transformed from water phase to sludge phase in 5 min, but the total amount of EE2 in the water phase and in the sludge phase was little different from the initial amount of EE2. No clear degradation of EE2 was observed in 4h and the degradation process presented a lag period. Following that, the concentrations of EE2 in both water phase and sludge phase decreased, and 91.9% of the initial spiked EE2 was removed in 48 h.

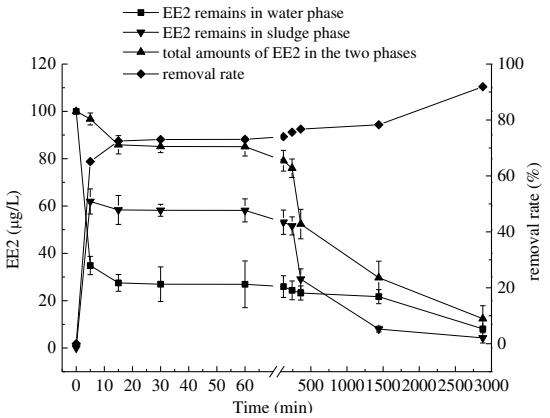

FIGURE 3
Concentration profiles of EE2 in degradation experiment.

In this study, first-order reaction kinetics was used to characterize both the biodegradation removal of EE2 (expressed by the variation of total amounts of EE2 in the two phases) and the total removal of EE2 (expressed by EE2 remains in water phase). The biodegradation of EE2 obeyed first-order reaction kinetics with degradation rate constant of $0.042h^{-1}$ when initial EE2 concentration of $100\mu g \cdot L^{-1}$.

As expected, the total removal of EE2 didn't obey the first-order kinetic model ($R^2 = 0.5221$), further indicating that EE2 removal was not only by biodegradation but also related to the adsorption of activated sludge. The total removal of EE2 by inactivated sludge (mainly adsorption) was 64.3%, as indicated in Fig.2, while which by activated sludge was 91.9%. The total removal of EE2 by activated sludge was much higher than that of inactivated sludge. In contrast, from Fig.4, one can see that the residual EE2 in activated sludge was much less than that of inactivated sludge at the equilibrium state. It was because the EE2 adsorbed onto activated sludge can be biodegraded continuously, and then the adsorption effect was enhanced in activated sludge process.

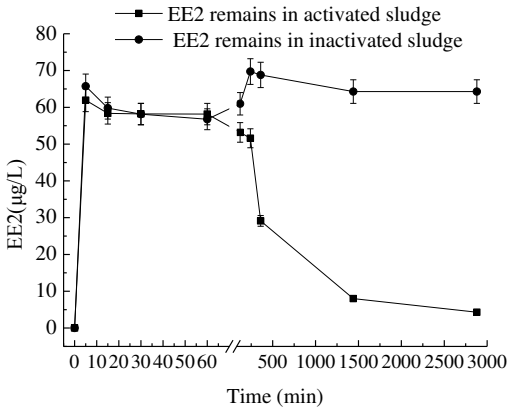

FIGURE 4
Concentration profiles of EE2 by adsorption onto inactivated and activated sludge.

CONCLUSIONS

Adsorption, as the preamble of degradation process, transferred EE2 from water phase to sludge phase and played an important role in the removal of EE2. The adsorption of EE2 onto inactivated sludge was a rapid process with the adsorption amount accounted for 69 - 90% of the equilibrium amount during initial 5 minutes. EE2 adsorption matched well both Langmuir and Freundlich isotherms at different initial EE2 concentrations, MLSS and particle sizes, and pseudo-second-order kinetic model could well described the adsorption profiles of EE2 onto inactivated sludge biomass. The initial concentrations were little related to the equilibrium time. The adsorption amount of EE2 by inactivated sludge was positive to the initial EE2 concentration while the adsorption rate displayed an inverse relationship with the initial concentrations. The adsorption capacity of EE2 by unit sludge decreased remarkably and the solid concentration effect was observed with the increase of MLSS. However, the total EE2 adsorption amount displayed a linear correlation with MLSS concentrations. The smaller sludge particle size was positive for the increase of adsorption equilibrium constant K_d and the enhancement of adsorption capacity. The adsorption ability of colloids was significantly greater than suspended solids and solutes because of the electric charge property of colloids.

ACKNOWLEDGEMENTS

The authors would like to acknowledge the financial support from National Natural Science Foundation of China (41571476), National Science and

Technology Support Project of China (2015BAL02B01), National Science and Technology Major Project of China (2017ZX07202004) and the Provincial Natural Science Foundation of Jiangsu, China (BK20141117).

REFERENCES

[1] Manickum, T. and John, W. (2014). Occurrence, fate and environmental risk assessment of endocrine disrupting compounds at the wastewater treatment works in Pietermaritzburg (South Africa). Science of the Total Environment. 468–469:584–597.

[2] Yang, X.L., Li, G.P., Chen, M., Shen, D.Q., Fu, D.F., Song, H.L. (2012). Occurrence and removal of steroid estrogens in three sewage treatment plants in Nanjing, China. Fresen. Environ. Bull., 21, 3836-3841.

[3] Liu, L.H., Li, Y., Zhang, H.H., Zhang, W.L. (2012). Photocatalytic degradation of 17a-ethinylestradiol using ZnO self-assembly microspheres. Fresen. Environ. Bull., 21, 2232-2237.

[4] Liu, X.L., Liu, B., Wu, F., Deng, N.S. (2003). Photodegradation of 17 alpha-ethynylestradiol in aqueous solution with Anabaena cylindrica under UV light. Fresen. Environ. Bull., 12, 690-694.

[5] Siegenthaler, P.F., Bain, P., Riva, F. and Fent, K. (2017). Effects of antiandrogenic progestins, chlormadinone and cyproterone acetate, and the estrogen 17α-ethinylestradiol (EE2), and theirmixtures: Transactivation with human and rainbowfish hormone receptors and transcriptional effects in zebrafish (Danio rerio) eleuthero-embryos. Aquatic Toxicology. 182:142–162.

[6] Andersen, H.R., Hansen, M., Kjølholt, J., Stuer-Lauridsen, F., Ternes, T., Halling-Sørensen, B. (2005). Assessment of the importance of sorption for steroidestrogens removal during activated sludge treatment. Chemosphere. 61:139-146.

[7] Cirja, M., Zuehlke, S., Ivashechkin, P., Hollender, J., Schaffer, V. and Corvini, P. (2007). Behavior of two differently radiolabelled 17 α-ethinylestradiols continuously applied to a laboratory-scale membrane bioreactor with adapted industrial activated sludge. Water Research. 41:4403-4412.

[8] Muller, M., Combalbert. S., Delgenès, N., Bergheaud, V., Rocher, V., Benoît, P., Delgenès, J., Patureau, D. and Hernandez-Raquet, G. (2010). Occurrence of estrogens in sewage sludge and their fate during plant-scale anaerobic digestion. Chemosphere. 81:65–71.

[9] Feng, Y., Zhang, Z., Gao, P., Su, H. and Yu, Y. (2010). Adsorption behavior of EE2 (17α-ethinylestradiol) onto the inactivated sewage sludge: Kinetics, thermodynamics and influence factors. Journal of Hazardous Materials. 175:970-976.

[10] Ren, Y.X., Nakano, K., Nomura, M., Chiba, N. and Nishimura, O. (2007). A thermodynamic analysis on adsorption of estrogens in activated sludge process. Water Research. 41:2341-2348.

[11] Xu, K., Willie, F Harper, Jr. and Zhao, D.Y. (2008). 17α-Ethinylestradiol sorption to activated sludge biomass: Thermodynamic properties and reaction mechanisms. Water Research. 42:3146-3152.

[12] Yi, T. and Harper, Jr, Willie, F. (2005). Mechanisms for removal of 17α-ethinylestradiol in bioreactors. Proc. 2005:78th Annual Water Environment Federation Technical Exposition and Conference, Washington, D.C., pp.5140-5153.

[13] Yi, T., Harper, Jr, Willie, F., Holbrook, R. David and Love, Nancy G.4. (2006). Role of Particle Size and Ammonium Oxidation in Removalof 17α-Ethinyl Estradiol in Bioreactors. Journal of environmental engineering. 11:1527-1529.

[14] Li, J.Z., Jiang, L., Liu, X., Lv, J.C. (2013). Adsorption and aerobic biodegradation of four selected endocrine disrupting chemicals in soilewater system. International Biodeterioration & Biodegradation. 76:3-7.

[15] Duong, C.N., Ra, J.S., Schlenk, D., Sang D. Kim, Hoon K. Choi and Sang Don Kim. (2010). Sorption of Estrogens onto Different Fractions of Sedimentand Its Effect on Vitellogenin Expression in Male Japanese Medaka. Arch Environ Contam Toxicol. 59:147-156.

[16] Bouhbaila, E.H., Aim, R.B. and Buisson, H. (2001). Fouling characterization in membrane bioreactors. Sep Puri Technol. 22-23:123-13.

[17] Hashimoto, T. and Murakami, T. (2009). Removal and degradation characteristics of natural and synthetic estrogens by activated sludge in batch experiments. Water Research. 43:573-582.

[18] China Environmental Protection Agency. (2002) The Monitoring Analysis Method of Water and Waste Water, 4th ed., China Environmental Science Press, Beijing.

[19] Braga, O., Smythe, G.A., Schafer, A.I. and Feitz, A,J. (2005). Fate of Steroid Estrogens in Australian Inland and Coastal Wastewater Treatment Plants. Environmental Science and Technology. 39, 9:3351-3358.

[20] Urase, T. and Kikuta, T. (2005). Separate estimation of adsorption and degradation of pharmaceutical substances and estrogens in the activate sludge process. Water Research. 39, 7:1289-1300.

[21] Voice, T.C., Rice, C.P. and Weber, W.J.Jr. (1983). Effect of solids concentrationon the sorptive partitioning of hydrophobic pollutants in aquatic systems. Environmental Science and Technology. 17, 9:513-518.

[22] Ho, Y.S. (2006). Review of second-order models for adsorption systems. Journal of hazardous materials.136:681-689.
[23] Mohan, S.V., Ramanaiah, S.V., Rajkumar, B. and Sarma P.N. (2007). Biosorption of fluoridefrom aqueous phase onto algal Spirogyra IOI and evaluation of adsorption kinetics. Bioresource Technology. 98:1006-1011.
[24] Khaled, A., Nemr, A.E., El-sikaily, A. and Abdelwahab, O. (2009). Removal of Direct N Blue-106 from artificial textile dye effluent using activated carbon from orange peel: Adsorption isotherm and kinetic studies. Journal of Hazardous Materials. 165, 1-3:100-110.
[25] MacNicol, R.D. and Beckett, P.H. (1989). The distribution of heavy metal between the principal components of digested sewage sludge. Water Research. 23, 2:199-206.
[26] Clara, M., Strenn, B., Saracevic, E., Kreuzinger, N. (2004). Adsorption of bisphenol-A, 17β-estradiole and 17α-ethinylestradiole to sewage sludge. Chemosphere. 56, 9:843-851.

Received: **11.01.2017**
Accepted: **25.07.2017**

CORRESPONDING AUTHOR

Hai-Liang Song
School of Environment, Nanjing Normal University, Nanjing 210023, China

e-mail: shlnjnu@163.com

© by PSP Volume 26 – No. 10/2017 pages 5797-5805 Fresenius Environmental Bulletin

EFFECT OF SIMULATED CORROSION ENVIRONMENT ON MECHANICAL PERFORMANCES OF SAND FIXATION BY HYDROPHILIC POLYURETHANE

Zhishui Liang[1], Zhiren Wu[2], Mohammad Noori[3,4], Lin Deng[1,*]

[1]School of Civil Engineering, Southeast University, Nanjing 210096, China
[2]Academy of Environmental Health and Ecological Security, Jiangsu University, Zhenjiang 212013, China
[3]International Institute for Urban Systems Engineering, Southeast University, Nanjing 210096, China
[4]California Polytechnic State University, San Luis Obispo, California CA 93405, USA

ABSTRACT

The utilization of new polymeric materials as sand-fixing agents has become very popular in desertification control. These materials have relatively better performance in protecting sand from wind and water erosion, but the durability in aggressive environments is highly important. Therefore, with this important factor in mind, a novel hydrophilic polyurethane has been developed and studied in this research which presents a significant effect on sand fixing. In this study, the aging performance under sunlight, corrosion behaviour under the conditions of acid, alkali, salt, freeze and thaw are considered. Specimens, consisting of sand-fixing bodies solidified by hydrophilic polyurethane (W-OH), were exposed to Xenon Lamp, freeze-thaw cycles and immersed in acidic, alkali, salt solutions. Mechanical properties of compressive strength and hardness were chosen as the indexes to evaluate the performance. The results demonstrated that in all conditions the loss rates for compressive strength and hardness of sand fixation body decreased with the increase of W-OH concentrations, the higher concentrations, and the bigger cohesion force were observed. The concentration of W-OH had a relatively large effect on hardness and comprehensive strength, the increased rates could reach 16% and 50%, respectively. When the specimens were exposed in simulation irradiation and immersed in the acid, and alkali solutions after 5 weeks, creep occurs in the surface and structure. The loss rate of hardness was relatively big exceeding 10% when the concentration of W-OH is 3%, while the loss rate is smaller and insignificant in the condition of 4% and 5% W-OH and salt solutions. Moreover, the loss rates of compressive strength also decreased less in all above conditions less than 5%, so the decrease in mechanical performance was negligible. However, the corrosion resistances were slightly different and the results demonstrated that the resistance to salt was higher compared with the one for acid and the resistance to alkali was the weakest. Moreover, loss rate of hardness in concentrations of 3%, 4% and 5% W-OH sand-fixing specimens were 6.5%, 5.2% and 4% after treatment of 50 freeze-thaw cycles, and the corresponding loss rate of compressive stress were respectively 10.2%, 6.5% and 4.9%, indicating that compressive strength was more sensitive in freeze-thaw condition. Therefore, when W-OH is used in sand fixation, its concentrations should be considered and selected to guarantee the effect and durability.

KEYWORDS:
Corrosion resistance; Hydrophilic polyurethane; Sand-fixing body; Hardness; Compressive strength

INTRODUCTION

In recent years, the global climate change and disturbance, or alterations, due to human activity, has continued to further desertification, land degradation, and consequently threatening the environmental safety, and sustainable development. These threats are causing adverse social, economic, political and institutional effects, [1-3]. According to "Desertification status bulletin in China" in 2014, the area of desertification has reached about 261.16 million square kilometers, accounting for 27.02% of the total land area. Thus, the area of desertification is very large and makes the ecological system fragile [4]. Therefore, the challenge of preventing desertification is difficult and the proposed plans have not yet offered any viable solutions

Desertification control has drawn great attention worldwide since the previous century and numerous measures have been proposed and implemented. Currently, the main measures for sand fixation are engineered products, vegetation, new materials and advanced solidification technologies [5-9]. As an efficient and effective measure, new protective materials have been widely used. In particular, bio and chemical materials have been developed and have become the focus of desertification control research. Chemical materials can form a sand-fixing layer on the surface of the sand resulting in water retention and solidification. These materials have char-

acteristics of simple formation process and remarkable effect on preventing sand from wind erosion [10-15]. However, most desertification regions have abominable conditions and organic materials are sensitive to aggressive environments, i.e. sunlight irradiation, acidification, alkalization, salinization and freeze thaw cycles. These harsh environmental factors can easily cause undesirable changes in physical, chemical, and mechanical characteristics of the protective materials [16-18]. For instance, for a material to be effective for sand fixation, its protective characteristics should not change under a large number of freeze and thaw cycles. Therefore, the durability and stability of the material and the consolidation layer are very important.

A type of composite organic polymer material (W-OH) that mainly contains hydrophilic polyurethane has been developed and studied as a sustainable chemical sand fixation material for preventing desertification [19] and saline-alkali soil erosion in cold regions [20, 21]. This material uses water as the curing agent and when it reacts with water, a flexible and porous gel is formed in 3~10 minutes [22, 23]. According to earlier research, reported in the literature, the W-OH solution has an excellent permeability on sand and the consolidation layer has reasonable mechanical strength and network structure [24, 25]. It also has a desirable performance for water, heat and fertilizers retention and for promoting vegetation growth. However, the limitation of durability and stability is still a significant problem for application. Thus, the study of corrosion behavior of consolidation layer in different aggressive environments has continued to attract considerable attention.

In this study, the sand fixation specimens with different concentrations of W-OH were exposed to simulated sunlight irradiation, immersed into acidic, alkali, and salt solutions for 5 weeks, and were subjected to freeze-thaw test for 50 cycles, in order to evaluate their compressive stress and hardness changes. Therefore, this research and the achieved results provide theoretical basis for evaluating and advancing W-OH durability and for providing guidelines for practical applications.

TABLE 1
The particle size distribution of sand in Qinghai Lake basin (in weight percent)

Grain size distribution(μm)	>350	350-250	250-150	150-100	<100
Percent (%)	2.04	17.96	51.44	26.91	1.65

MATERIALS AND METHODS

Sand and sand fixation material. The sand utilized in this study comes from the area around Qinghai Lake (99°36′-100°16′E, 36°32′-37°15′N). The region belongs to a semi-arid area where the annual average temperature is about -1.0~1.5℃, and the annual maximum temperature is 26℃ with the lowest temperature of -35.8℃. The average annual rainfall is about 300~400 mm and the annual average solar radiation reaches to 6,000~6,400 MJ/m^2 for one year [26, 27].

The particle size distribution is shown in Table 1.

W-OH utilized in this study is from Jiangsu JCK New Material Technology Co. Ltd. It has a color of faint yellow and its viscosity is about 300~600 mPa·s (20℃). The specific weight of this materials is about 1.18 g/cm^3. The main constituent materials include performed polymer (74%), toluene diisocyanate (10.5~11%), methyl ethyl ketone (15%) and sterically hindered amines (W-US 0.5%).

Sample preparation procedure. Specimens: Sand was placed into a cylindrical mold with a diameter of 5 cm and height of 10 cm. W-OH solution was prepared by adding W-OH into water. Then the solution with different concentrations (3, 4 and 5%) was sprayed on the surface of the sand specimens until the solution penetrated to the bottom and the entire sand sample was fixed in 10 minutes. The specimens were then placed in an electric oven with thermostat blast (DHG-9246A, manufactured by Shanghai Jing Hong Experimental Equipment Co., Ltd.) for one day to dry. The mold was then removed and the specimens were maintained for 28 days in the room condition to dry.

Simulation test methods. Simulated sunlight irradiation tests: To simulate solar outdoor exposure, the natural irradiation around Qinghai lake was used, which is about 6,000~6,400 MJ/m^2. The accelerated irradiation-testing machine (Solarbox 1500e, manufactured by CO.FO.ME.GRA) was used in this experiment. The irradiation setting was 0.55 W/m^2/340nm and the radiation power was measured according to ASTM G155. To simulate and accelerate weathering process [28], the irradiance between 290 ~1,100 nm was set 1000 W/m^2. Therefore, the total solar radiation emitted was about 3.6 MJ/m^2/h. The time needed to produce radiation corresponding to outdoor solar exposure in Qinghai Lake in one year is about 1667 h or 69 d. However, considering the limitation in the life cycle of the lamps, the test lasted for 35 d or the simulation time was equivalent to half year in Qinghai Lake.

The specimens were first placed in the test machine and the temperature was set at 65℃. The drying-wet cycle composed of 27 min dry phase, and 3 min flooding phase, respectively. The weight of the degraded sand and the hardness of W-OH sand-fixing layer were measured every week, in which hardness was measured by Yamanaka typed soil penetrometer (manufactured by Fujiwara Seisakusho of Japan) with the unit of mm (Fig. 1), and the compressive stress was tested by the AG–X plus universal

testing machine (manufactured by Shimadzu Corporation, Japan) following the standard of GB50107-2010 [25].

Freeze and thaw test: Freeze and thaw cycles were carried out using a climatic cabinet (MIT-683-1, manufactured by MARUI Company, Japan) in which the samples were totally immersed in water and were frozen to -20℃ for 3 h and then thawed to 20℃ for 1 h. This process was effectively similar to ASTM C666-75 for freeze and thaw [29]. After 10, 20, 30, 40 and 50 freeze-thaw cycles, the specimens were removed and kept at the room temperature until a constant weight were achieved, and then hardness and compressive stress tests were carried out.

Corrosion simulation test: The specimens were immersed into acidic, alkali, salt solutions with concentration of HCl, NaOH and NaCl being 0.01 and 0.1 mol/L. The hardness and compressive stresses were tested in 1, 2, 3, 4 and 5 weeks, respectively [30, 31].

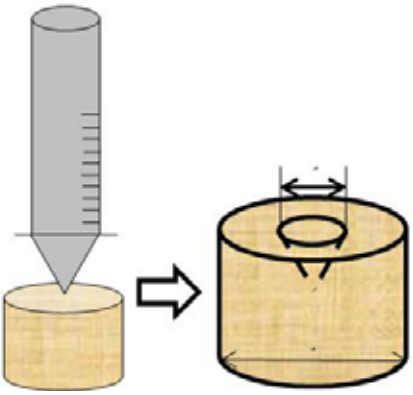

FIGURE 1
Schematic diagram of hardness test

RESULTS AND DISCUSSION

Effect of W-OH concentrations on mechanical performances. From Fig.2, it could be seen that concentration of W-OH had a relative large impact on both hardness and comprehensive strength of sand fixing body. Hardness increased from 21.5 to 25 mm from 3% to 5% with the increasing amplitude is about 16.3. Comprehensive strength increased from 0.36 to 0.72 MPa from 3% to 5% with the increased rate of 50%. While when the specimens were placed in the laboratory for 5 weeks without sunlight and without water immersion (25℃), the hardness and comprehensive strength almost wouldn't change (loss rates are less than 1%), this is because W-OH materials is stable in indoor conditions but sensitive to strong light (especially UV) and corrosion. So the adhesive effect of W-OH on sand particles still worked and the structure of sand fixing body still remains integrated and unchanged.

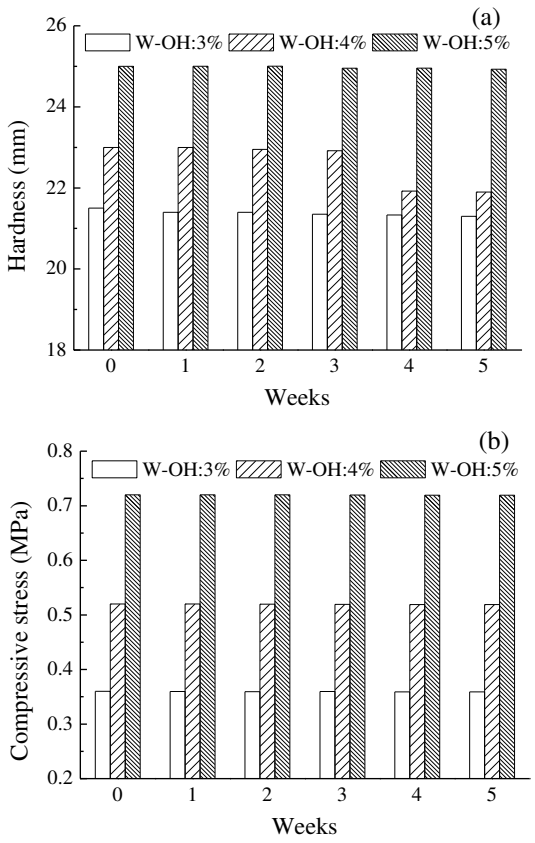

FIGURE 2
Effect of W-OH concentrations on mechanical performances: (a) Hardness; (b) Compressive strength

Effect of simulated sunlight irradiation on mechanical performances. In the condition of solar radiation, the W-OH would be degraded and the hardness and compressive stress of sand fixation body are decreased with time. The results showed that in the concentration of 3%, the hardness of W-OH sand-fixing specimens decreased from 21.5 to 19.1 mm with a loss rate of 11.1% after five-day solar radiation exposure (Fig. 3a), and the corresponding compressive stress decreased from 0.360 to 0.335 MPa with a loss rate of 7.0% (Fig. 3b). While the UV degradation resistance showed an increasing trend with the increase of concentrations of W-OH. Therefore, in concentration of 4% and 5%, the hardness and compressive stress had a smaller loss rate in the same exposure time, which are 5.8%, 3.2% and 4.3%, 2.0%, respectively.

This is due to the fact that W-US mainly contains HALS, one kind of UV stabilizer, which is capable of trapping the free radicals that have been formed and thereby interrupts the chain reaction of photo-oxidation. Under photo-oxidative conditions, W-US seizes free radical of peroxy and hydroxyl, and it largely transforms into the corresponding stable nitroxyl radical. The stable nitroxyl radical also reacts with free radical of alkyl to form stable alkyl

compound and therefore, degradation reaction is prevented [32]. Simultaneously, the nitroxyl radical transfers to form HALS and enters into cyclic mode of action and the velocity of degradation would be reduced (Fig. 4). Thereby, with extending radiation time, this degradation reduces, which results in inhibiting decreases of hardness and compressive stress with time. When the concentration of W-OH increases, the strength of the solid increases and the adhesive force between W-OH gel and sand particles increases. Furthermore, the concentration of W-OH also had effects on the mechanical properties as the content of HALS was less and the adhesive force between particles was less weak.

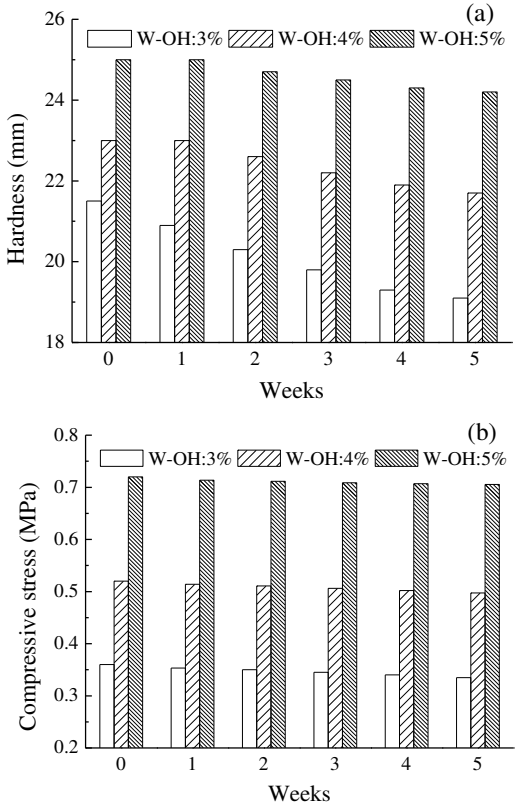

FIGURE 3
Effect of simulated sunlight irradiation on mechanical performances, (a) Hardness; (b) Compressive strength

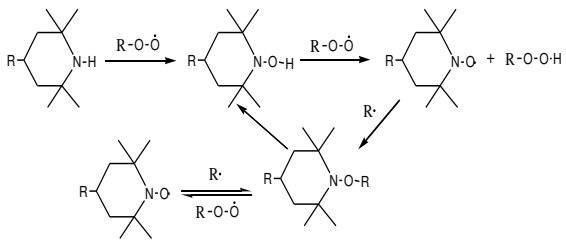

FIGURE 4
Functional mechanism of hindered amines

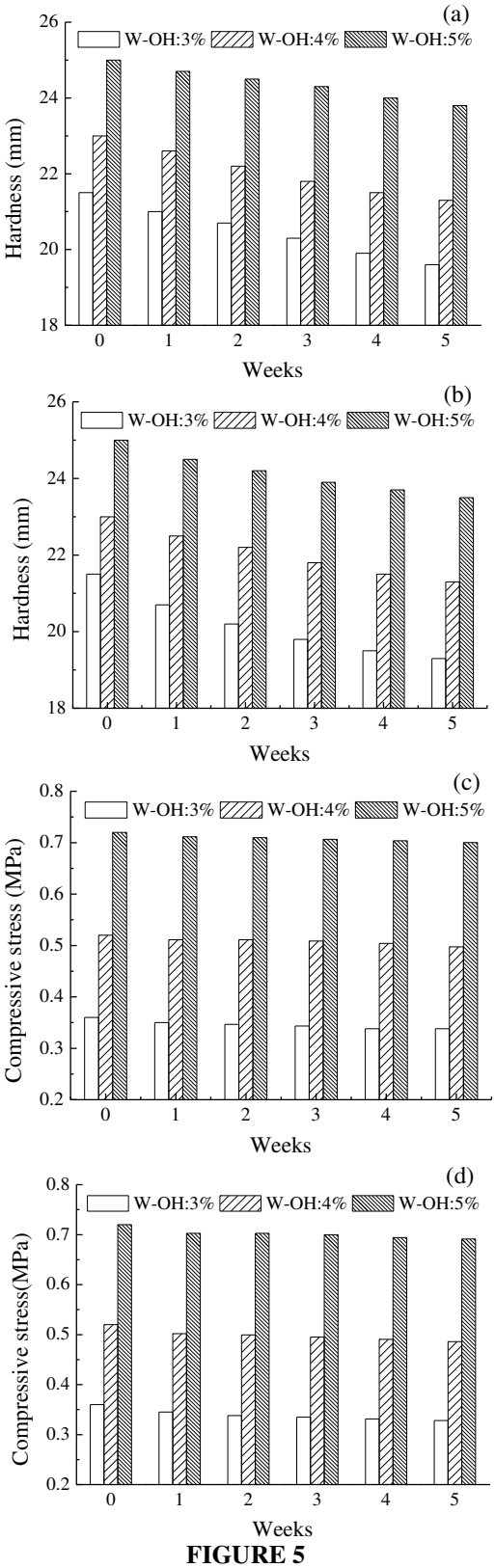

FIGURE 5
Effect of acidic corrosion on mechanical performances: (a) hardness in 0.01 mol/L HCl; (b) hardness in 0.1 mol/L HCl; (c) compressive strength in 0.01 mol/L HCl; (d) compressive strength in 0.1 mol/L HCl

Effect of acidic corrosion on mechanical performances. The molecular surface of W-OH initiated strand breaks under the action of H^+ when it is in acidic environment. This effect becomes more and more serious with an increase of acid concentration and corrosion time, thus, the hardness and compressive stress would be decreased. As shown in Fig. 5, corrosion in the first week was the most serious and the hardness and compressive stress of the W-OH sand-fixing specimen decreased greatly. With extending immersing time in acid solution, more and more acid penetrated into inner specimens, and the corrosion occurred from the outside to the inside, which resulted in further decrease of hardness and compressive stress. The hardness for a concentration of 3% W-OH sand-fixing specimen decreased from 21.5 to 19.6 mm with a loss rate of 8.8% when it was immersed in HCl solution at a concentration of 0.1 mol/L for 5 weeks. The corresponding compressive stress decreased from 0.36 to 0.3382 MPa.

The stronger the acidity was the more serious of the corrosion would be. When the concentration of HCl increased from 0.01 to 0.1 mol/L, the specimens was treated for 5 weeks, the hardness for a concentration of 3% W-OH sand-fixing specimen decreased to 19.3 mm, with a loss rate of 10.2%, and compressive stress decreased to 0.3282 MPa with a loss rate of 8.8%. The acid corrosion resistance of W-OH advanced with an increase of concentrations. It was then concluded that the strength of W-OH solid increased and the adhesive force between W-OH solution and sand particles increased, which resulted in improving difficulty for acidic solution penetrating into sand-fixing specimen and W-OH molecular. Thereby, the hardness for concentrations of 4% and 5% W-OH sand-fixing specimen decreased from 23.0 to 21.3 mm and from 25.0 to 23.8 mm with loss rates of 7.4% and 4.8%, respectively, when they were immersed in HCl solution at a concentration of 0.01 mol/L for 5 weeks. Moreover, the corresponding compressive stress decreased from 0.52 to 0.4974 MPa and from 0.72 to 0.7002 MPa, with loss rates of 4.3% and 2.7%. As acid increased to 0.1 mol/L and the specimens were treated for 5 weeks, the hardness for concentrations of 4% and 5% W-OH sand-fixing specimen decreased to 21.3 and 23.5 mm, with loss rates of 7.4% and 6%, and corresponding compressive stress decreased to 0.4861 and 0.6912 MPa, with a loss rate of 6.5% and 4.0%.

Loss rate of hardness was greater than that of compressive stress under same treatment, due to the fact that hardness is the surface strength and compressive stress is the entire strength, the effect of acidity on the surface is greater than that on the entire structure. Moreover, in acidic condition, the sand fixing layer is eroded and the adhesive-bonding is decreased, so the mechanical properties of sand fixing layer can be reduced. However, this type of polyurethane is not significantly sensitive to the acid solution as the decrease of mechanical strength is not dramatic [33].

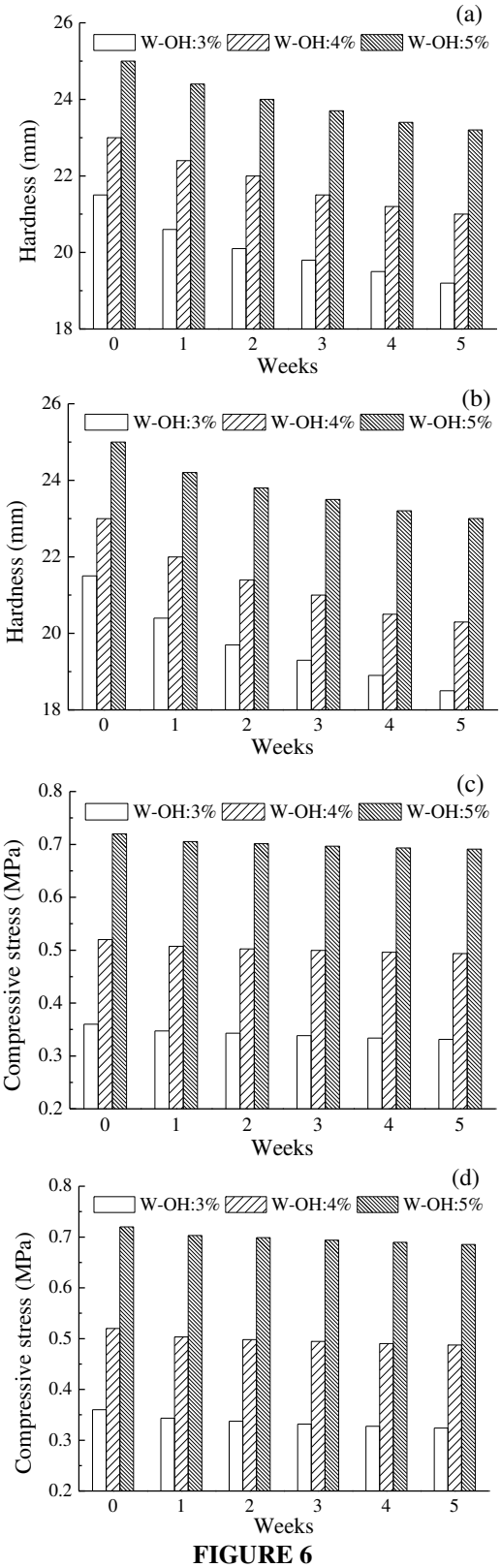

FIGURE 6

Effect of alkali corrosion on mechanical performances: (a) hardness in 0.01 mol/L NaOH; (b) hardness in 0.1 mol/L NaOH; (c) compressive strength in 0.01 mol/L NaOH; (d) compressive strength in 0.1 mol/L NaOH

Effect of alkali corrosion on mechanical performances. It is well known that the condition in desert is saline-alkaline, and the resistance of alkali corrosion for sand-fixing materials is an important evaluation factor for durability. Because of urethane bond in W-OH polymer molecules being attracted by OH^-, it initiated strand breaking. Decrease in adhesive force between W-OH solution and sand particle was presented by the decrease of hardness and compressive stress. Compared with the acidic corrosion, alkali corrosion was much greater. As shown in Fig. 6, corrosion in the first week was the most serious and the hardness and compressive strength of the W-OH sand-fixing specimens decreased most significantly With extending immersing time in alkali solution, more and more OH^- penetrates into inner specimens, and the corrosion proceeds from the outside to the inside, which resulted in further decrease of hardness and compressive stress. The hardness for a concentration of 3% W-OH sand-fixing specimen decreased from 21.5 to 19.2 mm with a loss rate of 10.7%, when they were immersed in NaOH solution at a concentration of 0.01 mol/L for 5 weeks. The corresponding compressive stress decreased from 0.36 to 0.3312 MPa, with a loss rate of 8.0%. The stronger the alkali was, and the more serious the corrosion was, as alkali increased to 0.1 mol/L and the specimen was treated for 5 weeks, the hardness for a concentration of 3% W-OH sand-fixing specimen decreased to 18.5 mm, with a loss rate of 14.0%, and compressive stress decreased to 0.3239 MPa, with a loss rate of 10.0%. The alkali corrosion resistance of W-OH advanced with concentration. It was concluded that the strength of W-OH gel increased and the adhesive force between W-OH gel and sand particles increased, which resulted in improving difficulty for OH^- penetrating into sand-fixing specimen and W-OH molecules. Thereby, the hardness for concentrations of 4% and 5% W-OH sand-fixing specimens decreased from 23 to 21 mm and from 25 to 3.2 mm, with loss rates of 8.7% and 7.2%, respectively. The corresponding compressive stress decreased to 0.4934 and 0.6912 MPa, with loss rates of 5.1% and 4.0%, when they were immersed in NaOH solution at a concentration of 0.01 mol/L for 5 weeks. As alkali increased to 0.2 mol/L and the specimens were treated for 5 weeks, the hardness for concentrations of 4% and 5% W-OH sand-fixing specimen decreased to 20.3 and 23.0 mm, with loss rates of 11.7% and 8%, and corresponding compressive stress decreased to 0.4876 and 0.6852 MPa, with a loss rate of 6.2% and 4.8%, respectively. Similar to acidic corrosion, loss rate of hardness was greater than that of compressive stress under the same condition, and the effect of alkali on the surface was greater than that on the entire structure.

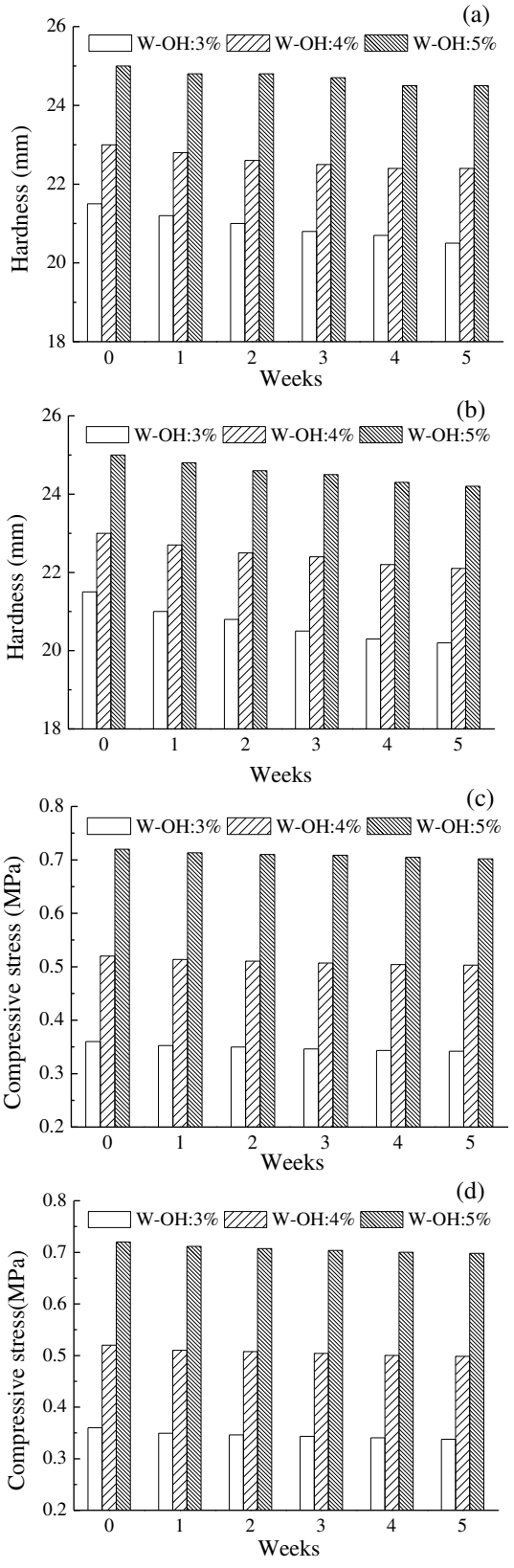

FIGURE 7

Effect of salt corrosion on mechanical performances: (a) hardness in 0.01 mol/L NaCl; (b) hardness in 0.1 mol/L NaCl; (c) compressive strength in 0.01 mol/L NaCl; (d) compressive strength in 0.1 mol/L NaCl.

Effect of salt corrosion on mechanical performances. Because of water evaporation, more and more salt was left, salt content in water accumulated greater and greater in desert. So the evaluation on salt corrosion of sand-fixing materials was also very important. By simulation experiments, W-OH sand-fixing specimens was immersed into NaCl solution at concentrations of 0.01 and 0.1 mol/L. The results demonstrate that W-OH had excellent salt corrosion resistance (Fig. 7). Even when immersed in NaCl solution at a concentration 0.2 mol/L for 5 weeks, rate of hardness loss was less than 6%, with 6.0% for W-OH 3%, 3.9% for W-OH 4% and 3.2% for W-OH 5%. The corresponding rate of compressive stress loss was 6.2%, 4.2% and 3.1%, respectively. The loss of hardness was almost the same with that of compressive stress.

Effect of freeze-thawing cycles on mechanical performances. Some deserts are distributed in the cold region, such as in the north western region of China, and the weather is characterized by drought, cold and great difference in temperature between day and night. The lowest temperature in these regions is up to -30℃. The adhesive force between sand-fixing material and sand particle decreases in freeze-thaw cycles which results in damaging the sand-fixing layer. Thereby, a sand-fixing material applied in these regions is necessary to have good performance under freeze-thaw cycles. The W-OH gel is a type of elastic material which has excellent freeze and deformability-resistance. It can be expanded or contracted with the change of external temperature, and it maintains a good adhesion with sand particles. By freeze-thaw test in laboratory environment, the performance of W-OH freeze-thaw resistance was studied. The results are shown in Fig. 8.

The hardness for a concentration of 3% W-OH sand-fixing specimen decreased from 21.5 to 20.1 mm with a loss rate of 6.5%, after 50 freeze-thaw cycles. Moreover, the corresponding compressive stress decreased from 0.36 to 0.3233 MPa, with a loss rate of 10.2%. With increase of W-OH concentration, the strength of W-OH gel increased and the adhesive force between W-OH gel and sand particles increased. Deformability also increased which results in advancement of freeze-thaw resistance. Therefore, the hardness for concentrations of 4% and 5% W-OH sand-fixing specimens decreased from 23 to 21.8 mm and from 25 to 24 mm with a loss rate of 5.2 % and 4%, respectively, and the corresponding compressive stress decreased to 0.4861 and 0.6844 MPa, with loss rates of 6.5% and 4.9% after treatment under 50 freeze-thaw cycles. Loss of compressive stress was greater than that of hardness under the same treatment, and the effect of freeze-thaw on the entire structure was greater than that on the surface.

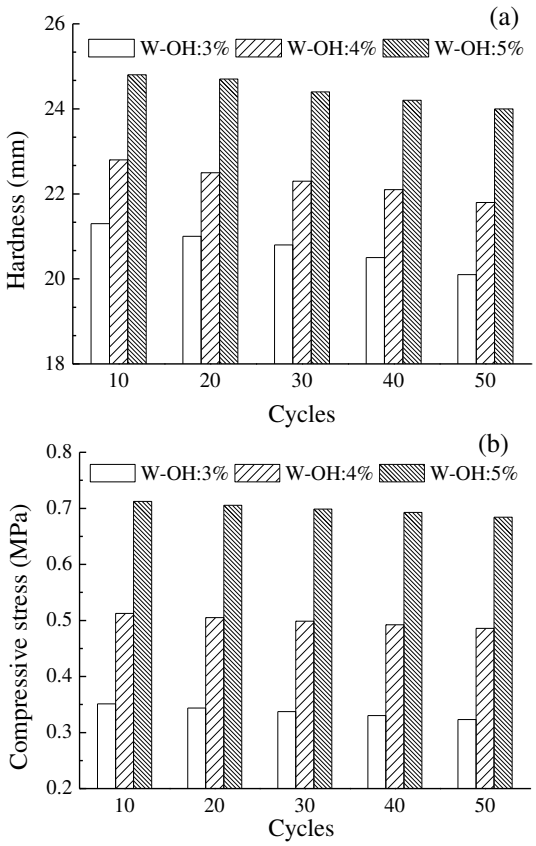

FIGURE 8
Effect of freeze-thawing cycles on mechanical performances: (a) hardness; (b) compressive strength

CONCLUSIONS

Corrosion experiments were carried out under simulated sunlight, acidic, alkali, salt and freeze-thaw conditions in order to evaluate the effectiveness of W-OH in different concentrations, and the hardness and compressive strength were the indexes. The following conclusions were drawn. With the increase concentrations of W-OH, hardness and comprehensive strength increased significantly with rate of 16% and 50% from 3% to 5%, respectively. One type of UV stabilizer-W-US in W-OH, which mainly contains HALS, is capable of trapping the free radicals and thereby interrupt the chain reaction of photo-oxidation. W-OH has excellent resistance against light/UV degradation. With extending radiation time, rate of degradation slows which results in inhibiting decrease of hardness and compressive stress further. Loss rate of hardness for concentrations of 3%, 4% and 5% W-OH sand-fixing specimens were respectively 11.1%, 5.8 % and 3.2% after UV radiation for 5 weeks. And the corresponding loss rate of compressive stress were respectively 7.0%, 4.3% and 2.0%. Moreover, with extending immersing time and increasing concentrations of acidic, alkali and salt solution, this corrosion is more and

more serious. Loss rate of hardness in 3% concentration of W-OH is much larger than that in 4% and 5% and compressive strength loss was similar, which showed that concentration was an important factor in evaluating the durability of sand fixing body. Furthermore, the loss rate of hardness is greater than that of compressive stress under same treatment, and the effect of acidic, alkali and salt corrosion on the surface is greater than that on the entire structure. The performance of W-OH resistance of acidic, alkali and salt corrosion demonstrates that it performs better under salt as compared with resistance under acidy environment. The resistance under alkali is the worst. W-OH gel is a type of elastic material, which has excellent freeze-resistance and deformability. It can be expanded or contracted with the change in external temperature and it is effective in maintaining adhesion with sand particles. With increase of W-OH concentration, the strength of W-OH solid increases and the adhesive force between W-OH solid and sand particles increases. Moreover, deformability also increases which results in increasing the freeze-thaw resistance. Loss of hardness for concentrations of 3%, 4% and 5% W-OH sand-fixing specimens is 6.5%, 5.2% and 4% after treatment of 50 freeze-thawing cycles. The corresponding loss rate of compressive stress is respectively 10.2%, 6.5% and 4.9%. Therefore, when W-OH is used in sand fixation, the concentration is an important factor to be considered in order to guarantee the comprehensive effect and durability.

ACKNOWLEDGEMENTS

This work was funded by the State Key Research Development Program of China (Grant No. 2017YFC0504505), the National Science & Technology Support Program (2013BAC05B02) and the Fundamental Research Funds for the Central Universities (KYLX15_0083).

REFERENCES

[1] Wrachien, D., Ragab, R., Giordano, A. (2006) Climate change, land degradation, and desertification in the Mediterranean environment. Desertification in the Mediterranean Region. A Security Issue. Springer Netherlands, p: 353-371.

[2] Lal, R. (2001) Soil degradation by erosion. Land Degradation & Development. 12(6), 519-539.

[3] Bestelmeyer, B.T., Okin, G.S., Duniway, M.C, Archer, S.R., Sayre, N.F., Williamson, J.C., Herrick, J.E. (2015) Desertification, land use, and the transformation of global drylands. Frontiers in ecology and the environment. 13(1SI), 28-36.

[4] Wang, T., Zhu, Z.D., Wu, W. (2002) Sandy desertification in the north of China. Science in China Series D: Earth Sciences, 45(1), 23-34.

[5] Li, S.Y., Tang, Q.L., Lei, J.Q., Wang, Y.D. (2015) An overview of non-conventional water resource utilization technologies for biological sand control in Xinjiang, northwest China. Environmental Earth Sciences, 73(2), 873-885.

[6] Hooke, J., Sandercock, P. (2012) Use of vegetation to combat desertification and land degradation: Recommendations and guidelines for spatial strategies in Mediterranean lands. Landscape and Urban Planning, 107(4), 389-400.

[7] Guo, Z.L., Huang, N., Dong, Z.B., Van Pelt, R.S., & Zobeck, T.M. (2014) Wind erosion induced soil degradation in Northern China: Status, measures and perspective. Sustainability, 6(12), 8951-8966.

[8] Cao, S.X., Zhang, J.Z., Chen, L., Zhao, T.Y. (2016) Ecosystem water imbalances created during ecological restoration by afforestation in China, and lessons for other developing countries. Journal of Environmental Management, 183, 843-849.

[9] Farshad, A., Deirdre, D. (2011) Combating desertification in Iran over the last 50 years: an overview of changing approaches. Journal of Environmental Management, 92(1), 1-13.

[10] Wang, Y.M., Cen, W.W. (2007) Experimental study on properties of a new chemical material in sand fixation. Bulletin of Soil and Water Conservation, 27(1), 108-111.

[11] Wang, H.J., Frits, P.D., Jin, Y.C. (2009) A win-win technique of stabilizing sand dune and purifying paper mill black-liquor, Journal of Environmental Sciences, 21(4), 488-493.

[12] Yang, J., Cao, H., Wang, F., Tan, T.W. (2007) Application and appreciation of chemical sand fixing agent-poly (aspartic acid) and its composites. Environmental Pollution, 150(3), 381-384.

[13] Zang, Y.X., Gong, W., Xie, H., Liu, B.L., Chen, H.L. (2015) Chemical sand stabilization: a review of material, mechanism, and problems. Environmental Technology Reviews, 4(1), 119-132.

[14] Ma, G.F., Ran, F.T., Feng, E.K., Dong, Z.B., Lei, Z.Q. (2015) Effectiveness of an eco-friendly polymer composite sand-fixing agent on sand fixation. Water, Air, & Soil Pollution, 226(7), 1-12.

[15] Gong, W., Zang, Y.X., Liu, B.L., Chen, H.L. Wu, F.S., Huang, R.H., Wang, S.K. (2016) Effect of using polymeric materials in ecological sand□ fixing of Kerqin Sandy Land of China. Journal of Applied Polymer Science, 133(43):44102(1-7).

[16] Yang, J., Wang, F., Tan, T.W. (2009) Controlling degradation and physical properties of chemical sand fixing agent poly (aspartic acid) by cross-linking density and composites. Journal of Applied Polymer Science, 111(3), 1557-1563.

[17] Boubakri, A., Guermazi, N., Elleuch, K.F.,

Ayedi, H.F. (2010) Study of UV-aging of thermoplastic polyurethane material. Materials Science and Engineering: A, 527(7): 1649-1654.
[18] Brožová, L., Holler, P., Kovářová, J., Jaroslav, S., Miroslava, T. (2008) The stability of polyaniline in strongly alkaline or acidic aqueous media. Polymer Degradation and Stability, 93(3): 592-600.
[19] Liang, Z.S., Wu, Z.R., Yang, C.Q., Yao, W.Y., Deng, L. (2016) Study on water resistance, anti-erosion and UV durability of Pisha sandstone solidified body. Yellow River, 38(6), 46-48. (in Chinese)
[20] Wu, Z.R., Gao, W.M., Liang, Z.S., Yang, W.W., Yang, C.Q., Xu, G. (2014) Study on prevention of saline alkali soil in Qaidam Basin with W-OH. Proceedings of the Sixth National Symposium on ecological restoration of soil and water conservation, Chengdu, 65-75.
[21] Min, M. (2006) The mechanism research on anti-seepage and anti-heave of the W-OH new canal material in cold region. Qinghai University.
[22] Wu, Z.R., Gao, W.M., Wu, Z.S., Iwashita, K., Yang, C.Q. (2011) Synthesis and characterization of a novel chemical sand-fixing material of hydrophilic polyurethane. Journal of the Society of Materials Science Japan, 60(7), 674-679.
[23] Gao, W.M., Wu, Z.R., Wu, Z.S. (2008) Kinetic study on solidification of the W-OH chemical sand-fixing material. Journal of Solution Chemistry. 2008, 37(8):1137-1148.
[24] Gao, W.M., Wu, Z.R., Wu, Z.S. (2012) Study of mechanism of the W-OH sand fixation. Journal of Environmental Protection, 3(9), 1025-1033.
[25] Liang, Z.S., Wu, Z.R. (2016) Performances and mechanism of sand fixation and growth promotion based on modified hydrophilic polyurethane. Transactions of the Chinese Society of Agricultural Engineering (CSAE), 32(22), 171-177.
[26] Deng, Z.W., Ni, S.X., Zhou, X.L., Zhang, H.L., Tu, Q.P. (2003) Calculation of possible direct solar radiation around Qinghai lake based on DEM. Plateau meteorology, 22(1), 92-96.
[27] Wang, Z.H., Huang, Z.F., Chen, Y., Xiao, H.B., Guan, Q. (2015) Research on variation of solar radiation over Yushu region of Qinghai Province from 1961 to 2010. Journal of Glaciology and Geocryology, 37(3), 692-700.
[28] Diepens, M., Gijsman, P. (2011) Outdoor and accelerated weathering studies of bisphenol A polycarbonate. Polymer degradation and stability, 96(4), 649-652.
[29] Klemm, A.J., Klemm, P. (1997) The effects of the alternate freezing and thawing cycles on the pore structure of cementitious composites modified by MHEC and PVA. Building & Environment. 32(6), 509-512.
[30] Huang, P.F., Bao, Y.W., Yao, Y. (2005) Influence of HCl corrosion on the mechanical properties of concrete. Cement and Concrete Research, 35(3), 584-589.
[31] Brozova, L., Holler, P., Kovarova, J., Kovářová, J., Stejskal, J., Trchová, M. (2008) The stability of polyaniline in strongly alkaline or acidic aqueous media. Polymer Degradation and Stability, 93(3), 592-600.
[32] Gao, W.M., Wu, Z.R., Wu, Z.S. (2012) Study on UV degradation resistance of a sand-fixing material by W-OH. Journal of the Society of Materials Science Japan, 61(8), 730-735.
[33] Khun, N.W., Liu, E. (2012) Tribological behavior of polyurethane immersed in acidic solution. Tribology Transactions, 55(4), 401-408.

Received: **12.01.2017**
Accepted: **26.07.2017**

CORRESPONDING AUTHOR

Lin Deng
School of Civil Engineering, Southeast University, Nanjing 210096, China

e-mail:dlwhu@163.com

© by PSP Volume 26 – No. 10/2017 pages 5806-5813 Fresenius Environmental Bulletin

NITROGEN MINERALIZATION VARIATION AMONG TREE SPECIES, INCUBATION METHOD AND INTRINSIC SOIL PROPERTIES

Soner Oktay[1], Huseyin Baris Tecimen[2,3,*]

[1]University Institute of Sciences 34116 Beyazıt İstanbul Turkey
[2]Soil Science and Ecology Dept., Faculty of Forestry, Istanbul University, 34473 İstanbul, Turkey
[3]Indian River Research and Education Center, Institute of Food and Agricultural Sciences, University of Florida, 34945, Fort Pierce, FL, USA

ABSTRACT

Evaluation of soil nitrogen mineralization under different tree species using various analytical methods under unique conditions (same climate, topography and soil genotype) were investigated to understand the tree effects on N mineralization. Tree species were introduced Monteri Pine (MP) and a native Oak-Beech mixed stand (OBM). A data matrix was formed from the parameters of tree species, period and incubation type, and we aimed to demonstrate how tree species induced changes in soil nitrogen mineralization under both laboratory and *in situ* conditions, and its relationship with intrinsic soil properties. The highest (26 mg N/kg/60 d – Tube; MP) and lowest (1.5 mg N/kg/60 d Bag; OBM) ammonium-N accumulation was detected April 2014 and June 2013, respectively. Mineral N accumulation (NH_4 + NO_3) was apparently 2 times higher at MP than OBM, while N mineralization was 1.4 times higher for MP than OBM. Ammonium-N values were 1.3 times higher with using the buried bag method than the tube method whilst we found 1.3 times higher nitrification with tube method than the buried bag method. Total N (R^2: 0.27; $p<0.005$) and organic C (R^2: 0.15; $p<0.005$) were positively related to ammonium-N accumulation, and there was also a positive relation with nitrate-N accumulation and pH (R^2: 0.20; $p<0.001$).

KEYWORDS:
Ammonium, Mineralization, Monteri Pine, Nitrate, Oak-Beech.

INTRODUCTION

Nitrogen budgets in soil are controlled by several agents such as microbial communities [1], climate [2], soil properties [3] and organic matter content [4]. The effect of plant species on soil nitrogen cycling and N mineralization was highly focused [5-9]. Mineral N (NH_4 + NO_3) is one of the most important nutrient element for plants and serve a determinant role on forest health and plant nutrition. Nitrogen mineralization under similar climatic conditions and edaphic factors but measured using different incubation methods have been investigated in the current study. Porosity and soil water saturation which are substantially efficient of soil N mineralization have been proved by Jensen et al. [10] who indicated contrasting net N mineralization vs denitrification at well aerated and highly dense soils, respectively. We sought correlation between nitrogen mineralization and soil properties such as; total nitrogen, organic carbon, pH, electrical conductivity and soil moisture for understanding their effects on N mineralization.

Nitrogen mineralization may be in part regulated by tree species and soil properties are subsequently then altered by tree species. Transplanted tree species introduced to any region as an exotic plant may generates unexpected outcomes in terms of biogeochemical cycling compared to native tree species. For example, lignin:N composition of leaf litter caused alteration of upper soil's physical, chemical and biological properties [11]. Tree species have considerable influence on nitrification by causing changes in upper soil with differences in the quantity and quality of litterfall decomposition by-products which in turn regulates microbial activity [12-14].

Within the current study, (i) the effects of tree species on soil nitrogen cycle; (ii) the nitrogen transformation under controlled (in vitro) and uncontrolled (in situ) conditions and; (iii) relations between nitrogen forms and other soil properties have been dwelled.

MATERIAL AND METHODS

The study the area is at cross section of 41°10'70" northern latitude and 28°59'00" eastern longitude near Istanbul Belgrade forest (Atatürk Arboretum). The study area is under the Mediterranean climate with dry summers according to Köppen-Geiger with the code Csa. Its altitude above sea level is

TABLE 1
Descriptive statistical data for soil properties per incubation type.

Tree Species	Incubation Type*	Measured Parameter	N	Min.	Max.	Mean	Std. Dev.
Oak-Beech	Ground	Total Nitrogen (%)	45	0.001	0.223	0.038	0.047
		Organic Carbon (%)	70	0.823	5.692	2.027	0.952
		pH	68	4.32	6.08	4.83	0.39
		EC µS/cm	68	35.7	348.0	92.6	49.8
	Tube	Total Nitrogen (%)	32	0.003	0.181	0.042	0.050
		Organic Carbon (%)	44	0.018	3.353	1.904	0.704
		pH	48	4.37	5.61	4.87	0.28
		EC µS/cm	48	40.3	333.4	99.8	48.7
	Bag	Total Nitrogen (%)	35	0.010	0.717	0.105	0.139
		Organic Carbon (%)	53	0.003	9.255	3.008	1.493
		pH	48	4.08	5.82	4.95	0.46
		EC µS/cm	48	64.0	722.0	162.7	118.0
Monteri Pine	Ground	Total Nitrogen (%)	44	0.001	0.395	0.049	0.069
		Organic Carbon (%)	69	0.367	7.043	2.318	1.348
		pH	60	4.24	5.66	4.83	0.27
		EC µS/cm	60	60.2	167.8	98.3	23.3
	Tube	Total Nitrogen (%)	35	0.008	0.225	0.049	0.058
		Organic Carbon (%)	44	0.169	4.408	2.208	0.891
		pH	50	4.35	5.96	4.80	0.29
		EC µS/cm	50	49.7	256.0	140.4	56.6
	Bag	Total Nitrogen (%)	35	0.002	0.371	0.108	0.105
		Organic Carbon (%)	53	1.241	6.395	3.114	1.298
		pH	50	4.15	5.40	4.70	0.28
		EC µS/cm	50	66.0	408.0	140.7	63.0

*Laboratory incubation samples were sub samples of ground samples so they are omitted here.

131 m and has a peneplain topography. The study site located at the ridge of a smooth hill, receiving 888 mm annual precipitation and annual average temperature is 13.4°C. Soil is formed on plyosen accumulation material and the texture is sandy clay.

Sampling area and sub-plots. The sampling plots are constituted from Monteri Pine (MP) and a native Oak-Beech mixed stands (OBM) in Istanbul Belgrade forest (Atatürk Arboretum). The plots were square shaped 50 × 50 m^2. Ten subsampling plots were taken from each stand for in situ incubations. The samplings were started in April 2013 and been continued until April 2014.

***In situ* and *in vitro* incubations.** Soil sampling was carried out from April 2013 to 2014 for field and laboratory incubation per 2 months from 20 cm depth of soil. Within the current study, we compared 3 different incubation methods which are: (i) Closed top cylinder method (expressed hereafter the "tube samples"), (ii) Buried bag method (expressed hereafter the "bag samples"), (iii) Laboratory incubations and the reference samples and we also took samples from the forest soils which are expressed hereafter the "ground samples". The sampling points were chosen to exclude the rhizosphere effect of trees. At the beginning of the study, 210 pvc tubes per sampling area (50 mm inner diameter and 250 mm length) were hand driven into the soil to collect 10 tripled sub samples at each sampling period. Per "closed top cylinder method" [15], at the first sampling date (10th of April 2013) the tops of the three pvc tubes at each sub-sampling plot were covered with stretch film that allows the gas transfer but prevents the entrance of water and left for *in situ* incubation for 60 days. Additionally, sealed soil bags were prepared and buried and incubated for 60 days per "buried bag method" [15]. Immediately after initiation of the in situ incubations, another 10 tripled ground sub samples as reference were taken from near the sub sampling points. Subsamples of soils were collected and stored in polyethylene bags until reaching the laboratory in a cooler (2-5 °C) to impede biological activity.

Soils from cores were composited in the laboratory for extraction and analysis (10 composite samples for the sampled area per incubation type). Coarse fractions from each soil sample were removed and fine fractions were saved for analysis. These soil samples provided the initial (t_o) concentrations of NH_4^+-N and NO_3^--N for the incubation. Then, 10 g equivalent soils were weighed to the plastic vials and covered with thin plastic wraps to allow gas exchange but minimize water loss, and incubated for 30 days at room temperature (21°C). Separate soil samples were used to determine gravimetric soil water content to calculate net soil weights subjected to mineral N content analyzes.

Mineral N (NH_4^+-N + NO_3^--N) and soil chemical analyzes. Net N mineralization was calculated by subtracting the initial quantity of soil inorganic-N from the post-incubation quantity of soil inorganic N. Similarly, net nitrification is calculated as the change in NO_3^--N pool size over the incubation period [15]. A well-mixed and 4 mm mesh sieved size 10-g dry-soil equivalent subsample was extracted

with 50 ml of 2 M KCl. The suspensions were shaken on a mechanical shaker for 1 h and centrifuged for 5 min. at 10 000 rpm. The filtered extracts were analyzed for NH_4^+-N and NO_3^--N with a Foss Fiastar 5000 Auto Analyzer system. Soil samples were air-dried and then the skeleton and coarse woody debris containing the roots were removed, ground and sieved through a 2 mm-sized mesh for soil analysis. Four soil samples were collected for soil physical analysis per plot. Separate soil sub-samples were oven-dried at 105ºC for 24 h (at hygroscopic moisture). The soil particle distribution was determined according to the Bouyoucous hydrometer method and soil texture composition measured using the International Particle Size Distribution triangle. Soil pH was determined in a suspension of 1:2.5 of sample in distilled water with pH meter. Soil organic carbon (SOC) was determined by Walkley-Black method, the total N with a Buchi Auto Kjeldahl Unit K-370.

The data collected from laboratory incubations were subjected to statistical evaluation. As much as the assumptions of normality and homogeneity of variances were met, then the ammonium-N and nitrate-N budgets were analyzed with ANOVA Tukey HSD, the data with unequal variance were subjected to Dunnett's T3 analysis. The significance levels were applied at $p<0.05$ and 0.01 in convenience. Analysis of variance and descriptive statistics were executed with anova and summary functions under Stats package version 3.2.2. in free software R statistical program version 3.2.2 and in Minitab statistical analysis software v17.

RESULTS

According to year round distribution of soil sampling, the lowest ammonium-N was detected in June-13 and the highest in April 14 period for both tree species. For the tube incubation method, ammonium-N in MP stand was 2.8 times higher than OBM stand at October 13 while it was 1.5 times higher in OBM stand than in MP stand in February 14 (Fig. 1). Amongst the incubation types, the highest NH_4^+-N was detected at laboratory incubations which are between 0.35 to 55 mg N/kg/60 d. The results of ground samples showed the similar synodical pattern during one year incubation period (Fig 1 NH_4^+-N Ground section). The 60-day mineral N accumulation values at bag incubations were 1.2 times higher than the tube incubation type.

The nitrate amount pattern indicated congruity between ground, tube and laboratory incubations while there was a contrast at buried bag incubations. Nitrate-N amounts for ground samples showed significant differences between tree species at all sampling periods (Fig. 2). When we compare incubation result, the nitrate-N accumulation at tube samples were 1.25 times higher than bag incubation type.

In total view of the results, the amounts of ammonium and nitrate have a contrasting progress along the annual period. From the point of this view, we may deduce that, ammonium amounts stimulate the increase of nitrate amounts (compare the Figs. 1 and 2).

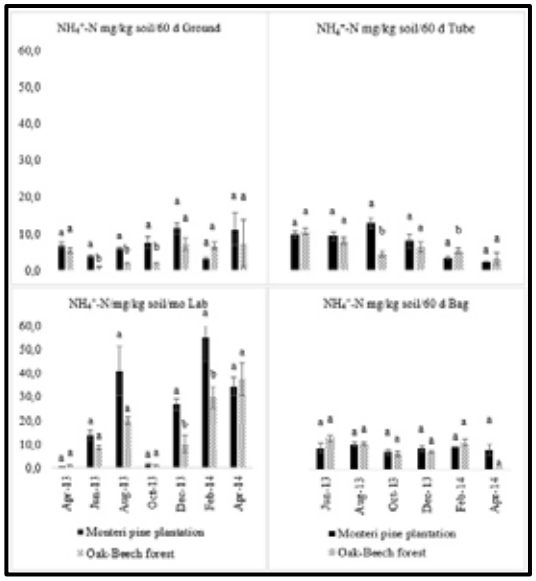

FIGURE 1
Comparison of ammonium-N distribution along incubation period per tree species with corresponding incubation types.

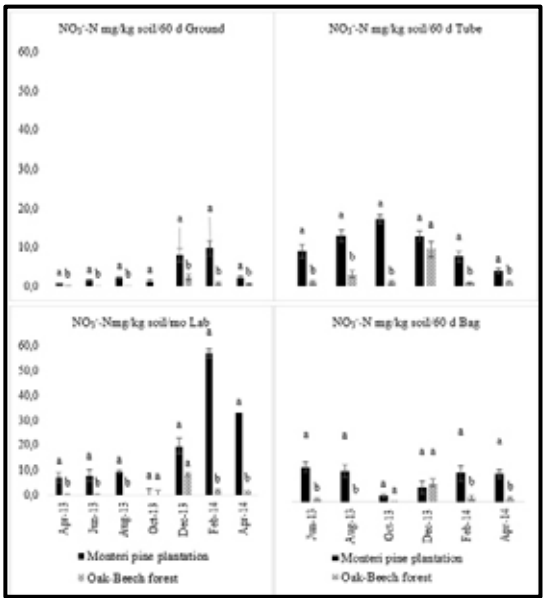

FIGURE 2
Comparison of nitrate-N distribution along incubation period per tree species with corresponding incubation types within t-test ($p<0.05$).

Ammonium-N mineralization and nitrification amounts were compared between tree species per

TABLE 2
NH_4^+-N mineralization amounts per incubation type mg/kg/60 d.

	Tube			Bag		
	Monteri	Oak-Beech	P value	Monteri	Oak-Beech	P value
Jun-Apr13	5,90	9,61	0,24	4,20	15,50	0,04
Aug-Jun13	10,88	14,97	0,17	13,30	20,70	0,01
Oct-Aug13	13,66	5,58	0,04	2,58	9,05	0,06
Dec-Oct13	-1,08	17,88	0,14	4,87	15,54	0,34
Feb14-Dec13	-15,10	-3,32	0,03	-17,01	9,59	0,12
Apr-Feb14	-0,31	-9,41	0,00	7,71	-19,51	0,00

TABLE 3
Nitrification amounts per incubation type mg/kg/60 d.

	Tube			Bag		
	Monteri	Oak-Beech	P value	Monteri	Oak-Beech	P value
Jun-Apr13	18.90	1.43	0.00	26.09	1.97	0.00
Aug-Jun13	23.29	6.19	0.00	21.48	0.19	0.00
Oct-Aug13	30.06	1.21	0.00	0.75	0.04	0.56
Dec-Oct13	41.05	38.23	0.79	13.51	23.84	0.33
Feb14-Dec13	-2.74	-2.34	0.94	16.64	-0.48	0.09
Apr-Feb14	-1.84	0.57	0.48	8.56	0.22	0.16

TABLE 4
Relation and p value table between ammonium and nitrate-N amounts and Nt, Corg and pH per incubation type at Monteri pine plot*.

		Ground		Tube		Bag		Laboratory	
		NH_4	NO_3	NH_4	NO_3	NH_4	NO_3	NH_4	NO_3
Nt	r^2	-0.025	-0.019	-0.015	0.060	0.147	0.232	0.024	-0.010
	p value	0.811	0.634	0.462	0.099	0.021	0.005**	0.180	0.431
Corg	r^2	-0.013	0.012	0.189	0.226	0.027	0.142	0.112	0.244
	p value	0.605	0.187	0.002**	0.001**	0.145	0.007**	0.005**	0.000***
pH	r^2	0.085	0.133	-0.022	0.204	-0.023	0.126	0.101	0.066
	p value	0.020*	0.003**	0.872	0.001**	0.747	0.014*	0.014*	0.040*

*The asterisks for p values imply that; *:p<0.05; **: p<0.005; ***: p<0.0005.

TABLE 5
Relation and p value table between ammonium and nitrate-N amounts and Nt, Corg and pH per incubation type at Oak-Beech plot*.

		Ground		Tube		Bag		Laboratory	
		NH_4	NO_3	NH_4	NO_3	NH_4	NO_3	NH_4	NO_3
Nt	r^2	0.122	0.124	0.268	-0.042	0.041	0.245	0.011	-0.022
	p value	0.012*	0.041*	0.002**	0.881	0.154	0.004**	0.231	0.717
Corg	r^2	0.147	0.068	0.146	-0.024	-0.013	-0.023	0.001	0.002
	p value	0.001**	0.046*	0.011*	0.701	0.523	0.954	0.304	0.115
pH	r^2	0.007	-0.024	-0.017	0.007	-0.024	0.067	-0.010	0.020
	p value	0.238	0.958	0.580	0.254	0.778	0.059	0.568	0.145

*The asterisks for p values imply that; *:p<0.05; **: p<0.005; ***: p<0.0005.

tube and bag incubation types and the results showed that; the mineralization amounts did not differ between tree species at tube incubations until January 14 – December 13 period. The buried bag incubations showed significant differences at first two incubation periods at OBM stand. We detected microbial immobilization of mineral N at both tube and bag incubation types at the periods following autumn for both tree species (Table 2).

The nitrification amount differences between tree species at both incubation types (tube and bag) were dramatic and the differences were significant with p values <0.000 (Table 3). The nitrification amounts initially were lower at both tree species and increased towards the middle of the observation period and then we observed some microbial immobilization of nitrate at both tree species for tube incubation type.

Soil properties such as total nitrogen, organic carbon and pH values presented relations with ammonium and nitrate-N at various significance. At MP stand, we found very strongly established positive relations between both ammonium and nitrate-N and organic carbon and pH. However, we detected significant relation only at bag incubation which is between nitrate-N and total nitrogen (Table 4). Adversely, there were significant relations between am-

monium and nitrate-N and total nitrogen for all incubation types (Table 5). Nonetheless, no significant relation between pH and ammonium and nitrate-N values has been detected.

DISCUSSION

The amounts of ammonium formation for a certain period reported by other studies vary due tree species, soil temperature, soil total nitrogen, soil organic carbon and soil microbial biomass. Kooch et al. [16] reported almost 7-fold higher net nitrogen mineralization (NNM) than our results under nitrogen fixing species (*Alnus subcordata*), while they could detect net microbial immobilization under oak species (*Quercus castaneifolia*). They attributed the difference to the tree species effect where alder species boosted the nitrogen pool in the soil and also difference between net ammonium-N formation to higher organic carbon content under the latter tree species. According to the study results of Urakawa et al. [17] daily ammonium-N formation is 0.26 mg/kg/day which is almost half of the results reached by Kooch et al. [16]. Arslan et al. [18] who made a comparative study like the current study under corresponding conditions found 0.41 mg NH_4^+-N kg/day accumulation under *Quercus robur* species while 0.2 mg NH_4^+-N kg/day under *Pinus pinea* and *Pinus brutia* which are the opposite ratios according to our results. The results obtained by Arslan et al. [18] were based upon the high carbon and nitrogen content in the soil which caused to high nitrogen mineralization potential of oak forests. From the studies stated above it can be extracted that, besides the tree species, one of the main factor responsible on NNM can be claimed as soil carbon and nitrogen contents [19]. The results found by other studies are generally higher than ours. This could also be caused from C:N ratio of the soils we investigated, which are between 28-53. Tree species charge to uppermost 0–10 cm layer owing to its higher nutrient content, higher microbial biomass and activity as well as the largest fine root biomass [20-25].

NNM is profoundly related to tree species, pH and organic matter in soil. According to Raath and Saayman [26] both release of ammonium and nitrate were higher at pH 7.3 than pH at 4.9. In contrast Cheng et al. [27] found relatively decline at N mineralization at higher pH at forest soil, attributing the decline to increased gross NH_4^+-N immobilization. Many studies have shown that increasing soil pH could enhance microbial activity and increase soil respiration [28-30]. In our study soil pH has revealed a strong relation with both ammonium-N and nitrate-N formations at Monteri Pine stand while no significant relation has been detected at Oak-Beech stand (Table 4 and 5). This might be attributed to the micro-climate induced differences. Slightly higher humidity content at Monteri Pine stands during the early and late summer periods (Fig. 3) might have been stimulated the microbial activity with the result of higher significance and better correlation (Table 4). This result also has been supported by De Boer et al. [31,32] who suggested that changes in nitrification rates were dominantly conducted by pH sensitive nitrifiers.

More light allowing structure of Monteri Pine stands with higher herbaceous plant accompany may explain the slightly higher total nitrogen and organic carbon content in soil (Table 1). Herbaceous understory provides a denser abandoned fine root in upper soil [33, 34]. Carbon content of soils is assumed to stimulate an excessive competition for available N in the soil, causing to create a strong competition for exchangeable NH_4^+-N, and thus reducing the ammonium-N content in the soil [35]. Even though, Yu et al. [36] stated that over accumulation of total nitrogen may be a suppressing agent, Yan et al. [37] found higher net N mineralization at forest litter when the N content is greater. Slightly higher soil total nitrogen content in Monteri pine soils with a higher ammonium and nitrate-N accumulation (Fig. 1 and 2) are in concordance with the previous researches.

Measuring sequential soil mineral nitrogen change in prevented (root uptake of N obstructed) and allowed soil permit to calculate net N mineralization, microbial immobilization and nitrogen leaching. Incubation procedures that cause to soil disturbance has been argued whether it provide a reliable or unreliable N-flux estimates in soils. According to Raison et al. [38] the sequential coring and *in situ* exposure techniques minimize the effects of the assay procedure on mineralization rates and appears to give a quantitative measure of N mineralization and uptake in surrounding undisturbed soil. The results on comparison of incubation methods showed that regardless of tree species, lower mineral nitrogen accumulation at ground samples were attributed to leaching. The values of ground samples provided us the year-round pattern of mineral nitrogen accumulation and removal. Besides, we reached to contrasting results concerned to mineral nitrogen accumulation values, when we compared the tube and bag incubation types (Table 2 and 3).

Jensen et al. [10] observed that NNM in meadow soils is in correlation with the soil moisture. They detected decreases NNM due to denitrification at clayey soils [10]. According to results obtained in this study, NNM and nitrification amounts have increased until October 13 from the beginning of the incubation periods. The difference should have been occurred from the blocked water content in sealed bag incubation while the excess water has been leaked at tube samples (Fig. 3). According to study executed on *Quercus robur* forest by Guntinas et al. [39], temperature and humidity are efficient on NNM to a specific extend such as they obtained the highest NNM at field capacity and over this level.

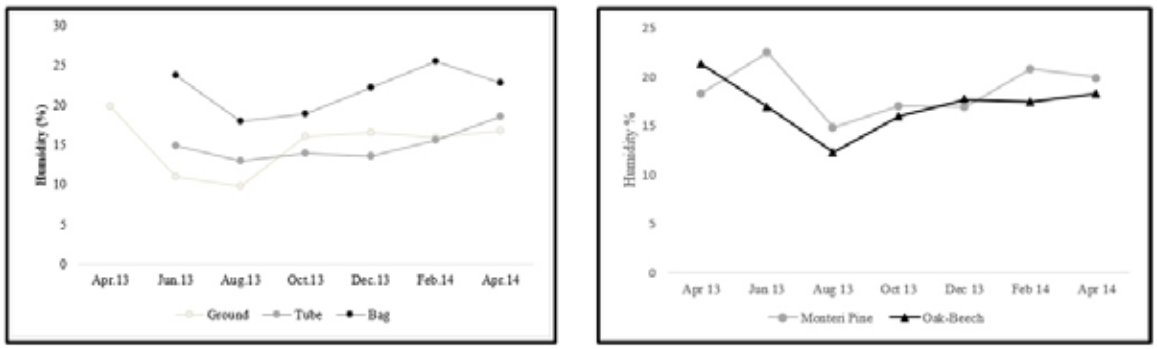

(a) (b)

FIGURE 3
Change of soil moisture according to incubation type (a) and according to tree species (b).

CONCLUSION

We can conclude that; ammonium and nitrate-N accumulation were significantly higher at Monteri pine plots than Oak-Beech plots, as well similar status at mineralization and nitrification amounts have been observed. The comparison of incubation type within the tree species, the results showed higher accumulation of nitrate-N at tube incubation types, while the opposite for ammonium-N accumulation. High regression between organic carbon, total nitrogen and ammonium-N vs nitrate-N took our results to think on differing microbial populations effects. In their study Taylor and Townsend [40] found that; nitrate bacteria in the soil environment can be claimed for their stimulated activity, because of organism specific substrates.

ACKNOWLEDGEMENTS

This study has been supported by Istanbul University Scientific Research Projects Executive Secretary within the project number 28424. The paper has been based on part of the data provided by MSci thesis of Soner OKTAY titled “Comparison of nitrogen mineralization at upper soil under different plant species in Atatürk Arboretum”. Special thanks to Mustafa KARADAĞ for his contribution to field and laboratory studies. We would like to thank to Dr. Alan L. Wright for his invaluable contributions to our manuscript and for language editorship.

REFERENCES

[1] Cookson, W.R., Abaye, D.A., Marschner, P., Murphy, D.V., Stockdale, E.A. and Goulding, K.W. (2005) The contribution of soil organic matter fractions to carbon and nitrogen mineralization and microbial community size and structure.Soil Biology and Biochemistry, 37(9), 1726-1737.

[2] Aponte, C., Marañón, T. and García, L.V. (2010). Microbial C, N and P in soils of Mediterranean oak forests: influence of season, canopy cover and soil depth. Biogeochemistry, 101(1-3), 77-92.

[3] Arnold, G., Van Beusichem, M.L. and Van Diest, A. (1994). Nitrogen mineralization and H+ transfers in a Scots pine (Pinus sylvestris L.) forest soil as affected by liming. Plant and soil, 161(2), 209-218.

[4] DeLuca, T.H., Zackrisson, O., Gundale, M.J. and Nilsson, M.C. (2008). Ecosystem feedbacks and nitrogen fixation in boreal forests. Science, 320(5880), 1181-1181.

[5] Binkley, D. and Valentine, D. (1991). Fifty-year biogeochemical effects of green ash, white pine, and Norway spruce in a replicated experiment. Forest Ecology and Management, 40(1), 13-25.

[6] Compton, J.E., Boone, R.D., Motzkin, G. and Foster, D.R. (1998). Soil carbon and nitrogen in a pine-oak sand plain in central Massachusetts: role of vegetation and land-use history. Oecologia, 116(4), 536-542.

[7] Ste-Marie, C. and Paré, D. (1999). Soil, pH and N availability effects on net nitrification in the forest floors of a range of boreal forest stands. Soil Biology and Biochemistry, 31(11), 1579-1589.

[8] Côté, L., Brown, S., Paré, D., Fyles, J. and Bauhus, J. (2000). Dynamics of carbon and nitrogen mineralization in relation to stand type, stand age and soil texture in the boreal mixedwood. Soil Biology and Biochemistry, 32(8), 1079-1090.

[9] Zhu, S.X., Chang, J., Ge, Y., Wang, H., Wang, F.Y., Zhang, J.M. and He, H.Z. (2012). Positive effects of plant species diversity on substrate nitrogen mineralization in a full-scale constructed wetland. Fresen. Environ. Bull., *21*(6b), 1689-1694.

[10] Jensen, L.S., McQueen, D.J., Ross, D.J. and Tate, K.R. (1996). Effects of soil compaction on

N-mineralization and microbial-C and-N. II. Laboratory simulation. Soil and Tillage Research, 38(3), 189-202.

[11] Scott, N.A. and Binkley, D. (1997). Foliage litter quality and annual net N mineralization: comparison across North American forest sites. Oecologia, 111(2), 151-159.

[12] Son, Y. and Lee, I.K. (1997). Soil nitrogen mineralization in adjacent stands of larch, pine and oak in central Korea. In Annales des sciences forestières (Vol. 54, No. 1, pp. 1-8). EDP Sciences.

[13] Wang, Z. and Fernandez, I. (1999). Soil type and forest vegetation influences on forest floor nitrogen dynamics at the Bear Brook Watershed in Maine (BBWM). In the Bear Brook Watershed in Maine: A Paired Watershed Experiment (pp. 221-234). Springer Netherlands.

[14] Compton, J.E. and Boone, R.D. (2002). Soil nitrogen transformations and the role of light fraction organic matter in forest soils. Soil Biology and Biochemistry, 34(7), 933-943.

[15] Hart, S.C., Stark, J.M., Davidson, E.A. and Firestone, M.K. (1994) Nitrogen mineralization, immobilization, and nitrification. In: Weaver, R. W., Angle, S., Bottomley, P., Bezdicek, D., Smith, S., Tabatabai, A. and Wollum, A., (Eds.), Methods of soil Analysis. Part 2. Microbiological and Biochemical Properties. Soil Science and Society of America, Madison, WI, USA, s. 985-1018.

[16] Kooch, Y., Rostayee, F. and Hosseini, S.M. (2016). Effects of tree species on topsoil properties and nitrogen cycling in natural forest and tree plantations of northern Iran. CATENA, 144, 65-73.

[17] Urakawa, R., Ohte, N., Shibata, H., Tateno, R., Hishi, T., Fukushima, K., Inagaki, Y., Hirai, K., Oda, T., Oyanagi, N., Nakata, M., Toda, H., Kenta, T., Fukuzawa, K., Watanabe, T., Tokuchi, N., Nakaji, T., Saigusa, N., Yamao, Y., Nakanishi, A., Enoki, T., Ugawa, S., Hayakawa, A., Kotani, A., Kuroiwa, M. and Isobe, K. (2015). Biogeochemical nitrogen properties of forest soils in the Japanese archipelago. Ecological Research, 30(1), 1-2.

[18] Arslan, H., Güleryüz, G., and Kırmızı, S. (2010). Nitrogen mineralisation in the soil of indigenous oak and pine plantation forests in a Mediterranean environment. European Journal of Soil Biology, 46(1), 11-17.

[19] Nourbakhsh, F. (2009). Can net nitrogen mineralization be estimated from short-term respiration rates?. Fresen. Environ. Bull., 18(5a), 732-736.

[20] Lõhmus, K., Truu, M., Truu, J., Ostonen, I., Kaar, E., Vares, A., Uri, V., Alam, S. and Kanal, A. (2006). Functional diversity of culturable bacterial communities in the rhizosphere in relation to fine-root and soil parameters in alder stands on forest, abandoned agricultural, and oil-shale mining areas. Plant and soil, 283(1-2), 1-10.

[21] Uri, V., Lõhmus, K., Kund, M., Tullus, H. (2008). The effect of land use type on net nitrogen mineralization on abandoned agricultural land: Silver birch stand versus grassland. Forest Ecology and Management 255, 226-233.

[22] Becker, H., Uri, V., Aosaar, J., Varik, M., Mander, Ü., Soosaar, K., Hansen, R., Teemusk, A., Morozov, G., Kutti, S. and Lõhmus, K. (2015). The effects of clear-cut on net nitrogen mineralization and nitrogen losses in a grey alder stand. Ecological Engineering, 85, 237-246.

[23] Uri, V., Lõhmus, K., Kiviste, A. and Aosaar, J. (2009). The dynamics of biomass production in relation to foliar and root traits in a grey alder (Alnus incana (L.) Moench) plantation on abandoned agricultural land. Forestry, 82(1), 61-74.

[24] Aosaar, J., Varik, M., Lõhmus, K., Ostonen, I., Becker, H. and Uri, V. (2013). Long-term study of above-and below-ground biomass production in relation to nitrogen and carbon accumulation dynamics in a grey alder (Alnus incana (L.) Moench) plantation on former agricultural land. European Journal of Forest Research, 132(5-6), 737-749.

[25] Varik, M., Aosaar, J., Ostonen, I., Lõhmus, K. and Uri, V. (2013). Carbon and nitrogen accumulation in belowground tree biomass in a chronosequence of silver birch stands. Forest Ecology and Management, 302, 62-70.

[26] Raath, P. J. and Saayman, D. (1996). Evaluation of an undisturbed-soil incubation method as an index of soil nitrogen availability in a limed and non-limed soil. South African Journal of Plant and Soil, 13(2), 35-41.

[27] Cheng, Y., Wang, J., Mary, B., Zhang, J. B., Cai, Z. C. and Chang, S. X. (2013). Soil pH has contrasting effects on gross and net nitrogen mineralizations in adjacent forest and grassland soils in central Alberta, Canada. Soil Biology and Biochemistry, 57, 848-857.

[28] Kemmitt, S.J., Wright, D., Goulding, K.W.T., Jones, D.L., (2006). pH regulation of carbon and nitrogen dynamics in two agricultural soils. Soil Biology and Biochemistry 38, 898-911.

[29] Aciego Pietri, J.C., Brookes, P.C., (2008). Relationships between soil pH and microbial properties in a UK arable soil. Soil Biology and Biochemistry 40, 1856-1861.

[30] Rousk, J., Brookes, P.C., Bååth, E., (2010). Investigating the mechanisms for the opposing pH relationships of fungal and bacterial growth in soil. Soil Biology and Biochemistry 42, 926-934.

[31] De Boer, W., Duyts, H. and Laanbroek, H. J. (1989). Urea stimulated autotrophic nitrification in suspensions of fertilized, acid heath soil. Soil Biology and Biochemistry, 21(3), 349-354.

[32] De Boer, W., Gunnewiek, P.K., and Troelstra, S.R. (1990). Nitrification in Dutch heathland soils. Plant and Soil, 127(2), 193-200.
[33] Cao, G., Tang, Y., Mo, W., Wang, Y., Li, Y. and Zhao, X. (2004). Grazing intensity alters soil respiration in an alpine meadow on the Tibetan plateau. Soil Biology and Biochemistry, 36(2), 237-243.
[34] Gonzalez, M., Augusto, L., Gallet-Budynek, A., Xue, J., Yauschew-Raguenes, N., Guyon, D., Trichet, P., Delerue, F, Niollet, S., Andreasson, F., Achat, D.L., Bakker, M.R. (2013). Contribution of understory species to total ecosystem aboveground and belowground biomass in temperate Pinus pinaster Ait. forests. Forest ecology and management, 289, 38-47.
[35] Vallejo, V. E., Gómez, M. M., Cubillos, A. M. and Roldán, F. (2011). Effect of land use on the density of nitrifying and denitrifying bacteria in the Colombian Coffee Region. Agronomía Colombiana, 29(3), 455-464.
[36] Yu, L., Wang, Y., Wang, Y. and Sun, S. (2016). Responses of soil respiration and its temperature sensitivity to soil temperature variation and simulated nitrogen deposition in subtropical mixed forest in Southwest, China. Fresen. Environ. Bull., 25, 4547-4560.
[37] Yan, E.R., Wang, X.H., Huang, J.J., Li, G.Y. and Zhou, W. (2008). Decline of soil nitrogen mineralization and nitrification during forest conversion of evergreen broad-leaved forest to plantations in the subtropical area of Eastern China. Biogeochemistry, 89(2), 239-251.
[38] Raison, R.J., Connell, M.J., and Khanna, P.K. (1987). Methodology for studying fluxes of soil mineral-N in situ. Soil Biology and Biochemistry, 19(5), 521-530.
[39] Guntinas, M.E., Leiros, M.C., Trasar-Cepeda, C. and Gil-Sotres, F. (2012). Effects of moisture and temperature on net soil nitrogen mineralization: A laboratory study. European Journal of Soil Biology, 48, 73-80.
[40] Taylor, P.G. and Townsend, A.R. (2010). Stoichiometric control of organic carbon–nitrate relationships from soils to the sea. Nature, 464(7292), 1178-1181.

Received: **19.01.2017**
Accepted: **31.07.2017**

CORRESPONDING AUTHOR

Huseyin Baris Tecimen
Soil Science and Ecology Dept., Faculty of Forestry, Istanbul University, 34473 İstanbul, Turkey

e-mail: hbarist@gmail.com

© by PSP Volume 26 – No. 10/2017 pages 5814-5823 Fresenius Environmental Bulletin

PHYSIO-BIOCHEMICAL AND NUTRITIONAL RESPONSES OF *ABELMOSCHUS ESCULENTUS* (L.) MOENCH (OKRA) UNDER MERCURY CONTAMINATION

Asiya Hameed[1], Tabasum Nazir Qadri[1], Mahmooduzzafar[1], Tariq Omer Siddiqi[1], Munir Ozturk[2,*], Volkan Altay[3], Parvaiz Ahmad[4]

[1]Botany Department, Hamdard University, New Delhi, India
[2] Botany Department & Centre for Environmental Studies, Ege University, Izmir, Turkey
[3]Biology Dept., Mustafa Kemal University, Antakya-Hatay, Turkey
[4]Botany Department, S.P. College, Srinagar, Kashmir, India and Department of Botany and Microbiology, College of Science, King Saud University, Riyadh, Saudi Arabia

ABSTRACT

The objective of this study was to evaluate the impact of $HgCl_2$ (0.05, 0.10, 0.50, 1 and 2 mM) on growth, pigment, biochemical attributes, nitrogen and phosphorous contents in *Abelmoschus esculentus*. The shoot and root length decreased by 36.12 and 36.26 percent respectively after post-flowering stage under 2 mM $HgCl_2$ application. Chl. *a* showed a maximum decrease of 63.90 percent at flowering stage when 2 mM $HgCl_2$ were applied to the experimental plants. Chl. *b*, total chl. and carotenoids also showed a significant decrease with an increase in the $HgCl_2$ concentration. $HgCl_2$ with 2 mM showed a maximum decrease of 83.52 and 20.60 percent in protein and sugar content respectively. The plants exposed to 2 mM $HgCl_2$ also showed an increase in the proline content (35.95%) during post-flowering stage. NR activity decreased during pre- as well as post-flowering stages at all stress levels. The nitrate, nitrogen and phosphorous values also decreased with an increase in the $HgCl_2$ concentration during all growth stages. The accumulation of Hg in roots was synergistic with increase in the concentration of Hg throughout the stages of growth. The maximum accumulation of 41.4 percent was observed at flowering stage under 2 mM $HgCl_2$ application.

KEYWORDS:
Mercury; accumulation; toxicity; growth; pigmentation; okra.

INTRODUCTION

Plants try to thrive under excessive noxious elements, which in higher concentrations are actually very toxic to living beings. Some of these are highly detrimental soil pollutants [1-10]. One of the heavy metals is mercury (Hg) which is non-degradable and with no beneficial role in the regulation of growth and development**.** It is toxic because of its mobility, bioaccumulation, methylation process and transport in the atmosphere [8, 11]. The estimated amount of Hg released into the atmosphere and water supply is approximately $2x10^4$ to $7x10^4$ tones/year. Naturally occurring mercury in soils is 0.003-4.6 mg kg^{-1} [12]. However the concentration of Hg ranging from 11500-14000 mg kg^{-1} of soil has been reported from the contaminated sites [13]. The estimated atmospheric Hg-emission was 2190 tons in the year 2000. The largest contribution to this emission was from Asian countries (67%) [14]. India ranks 2nd after China and the primary sources are fossil fuel burning and smelting industries [15].

Consumption of mercury-contaminated foods like fish, and other marine mammals, rice and rape grown on Hg polluted areas cause adverse effects on living beings [16, 17]. It adversely affects the human health leading to neurological, renal, cardiovascular, reproductive disorders [18].

Abelmoschus esculentus (L.) Moench, commonly known as ladies finger/okra, is a member of Malvaceae family. It is an annual, erect herb cultivated as a garden crop or a mixed field crop in tropical and sub-tropical regions of the world. India tops the list in its production followed by Nigeria, and Sudan. The area under okra cultivation in India is around 498 thousand hectares and the production lies around 5784 thousand tons a year [19]. This plant can be cultivated on any type of soil, but thrives best on well-manured loamy soil. The seeds are stimulant, cordial and antispasmodic [20], but the plant is also nutritionally important summer vegetable and an excellent source of potassium, calcium and unsaturated fatty acids. *In vitro* fresh watery extract of its seeds restrict growth of cancerous cell [21]. Some studies have been undertaken on this plant on water stress and gas exchange [22], but no report involving effects of Hg has been published uptill now. Therefore, present study was undertaken to evaluate the effects of Hg toxicity on growth, pigments, biochemical and nutritional responses of *A. esculentus* during different developmental stages.

MATERIALS AND METHODS

Sampling and preparation of samples. The experiments were carried out using earthen pots arranged in randomized block design and filled with 10 kg soil. Five healthy seeds were sown in each pot but, after germination only three healthy seedlings per pot were allowed to grow for twenty days. The application of different concentrations of $HgCl_2$ i.e., 0.05 mM, 0.10 mM, 0.50 mM, 1 mM and 2 mM was started after a growth period of 20 days. The control as well as $HgCl_2$ treated pots were irrigated with equal quantities of distilled water to avoid desiccation. The plants were sampled at pre-flowering, flowering and post-flowering stages. Shoot length was measured using a manual scale. The length from ground level to the upper most growing tip of the main axis was recorded, whereas for root length only measurements of the main taproot were recorded.

Determination of Chlorophyll. Fresh material (100 mg) was extracted in dimethyl sulphoxide (DMSO) and subsequently incubated at 65^0C for 40 min. Thereafter, 1 ml supernatant was vortexed with 2 ml DMSO and absorbance determined at 480, 510, 645, 663 nm using Beckman 640 D spectrophotometer against DMSO [23].

Estimation of Protein. The method of Bradford [24] was followed. Fresh plant material (0.5 g) was macerated using 1 ml phosphate buffer (pH 7.0) followed by centrifugation at 5000 x g for 10 min. Thereafter equal amount of 20% trichloroacetic acid (TCA) was added to the 0.5 ml of the supernatant and again centrifuged at 8000 x g for 15 min. The pellet was dissolved in 0.1 N NaOH (1 ml) and 5 ml Bradford reagent was added to it and absorbance recorded at 595 nm using the same spectrophotometer. The calculations were done using standard of bovine serum albumin.

Estimation of Sugar. Leaf sample (0.5 g) was extracted in hot 90 percent ethanol and extraction was repeated twice and supernatants were pooled together. Final volume was made to 25 ml with double distilled water (DDW). A known volume of extract was mixed with 1 ml phenol (5%) and 5 ml concentrated sulphuric acid and volume was made to 10 ml by DDW. The absorbance was measured at 485 nm [25].

Estimation of Proline. 300 mg of plant sample was extracted in 10 ml of aqueous sulfosalicylic acid (30%) and centrifuged at 9000 xg for 15 min. 2 ml of the supernatant was mixed with acetic acid and acid ninhydrin reagent. Samples were incubated for 1 h at 100 ^{0}C and the reaction was terminated by keeping the samples on ice. Proline was separated using toluene (4 ml) and read at 520 nm on UV-VIS spectrophotophometer against toluene [26].

Estimation of Nitrate. For estimation of nitrate 300 mg fresh plant samples were boiled in test tubes containing 50 mg charcoal and 10 ml DDW. The samples were filtered and volume was made to 50 ml by DDW. To 1 ml extract, 0.5 ml $CuSO_4$-$ZnSO_4$ solution, 0.25 ml hydrazine sulphate, 0.25 ml NaO_4 and 1.5 ml DDW were added and mixture kept in a water bath for 10 min at 33°C. Reaction was terminated in ice followed by the addition of 0.5 ml chilled acetone and 1 ml sulphanilamide and NED. Absorbance was recorded spectrophotometerically at 540 nm [27].

Nitrate Reductase Activity (NRA). NRA activity was determined according to Heuer and Plaut [28]. Leaf samples were infiltrated for 5 min under vacuum in 3 ml of phosphate buffer (0.2M, pH 6.8) containing 3 mM KNO_3. Vials with samples were transferred into a water shaker for 60 min at 33 ^{0}C and reaction was terminated by keeping vials on hot water bath for 5 min. To 0.2 ml aliquots, 1 ml of each sulphanilamide and NEDD (0.02%) were added and final volume was made up to 6 ml using DDW. After 20 min absorbance was determined spectrophotometrically at 540 nm.

Estimation of Nitrogen. Nitrogen content in the leaves was determined by the method of Linder [29]. 100 mg of finely powdered and thoroughly sieved leaves were taken in digestion tubes. 2 ml of conc. H_2SO_4 added to each test tube. Tubes were kept in ice for 15 min for cooling. 0.5 ml hydrogen peroxide (30%) was added drop wise and tubes left in the digester for 30 min's till the solution developed yellow colour. The tubes were again kept in ice for 5-10 mins for cooling. Again 3-4 drops of H_2O_2 were added in tubes and kept in digester for 15 mins till transparent clean solution was obtained. Volume of digested material was made up to 100 ml using DDW and 10 ml was mixed with 2 ml of NaOH (2.5 N), 1 ml of sodium silicate (10%) was added and the volume was made up to 50 ml using DDW. 0.5 ml of Nessler's reagent was added to 2 ml aliquots and volume made up to 10 ml with DDW, it was kept for 5 min for colour development and the absorbance read at 525 nm.

Estimation of Phosphorus. Phosphorous was estimated according to the method of Fiske and Subbarow [30]. 0.1 g oven dried (80 ºC) plant material was put into digestion tubes of 100 ml capacity, 2 ml of concentrated H_2SO_4 was added to each digestion tube containing 1.5 g potassium sulphate and 0.075 g selenium. After digestion volume was made up to 100 ml using DDW and 0.5 ml was mixed with 1 ml molybdate reagent and 0.4 ml 1, 2, 4-amino-napthol sulphonic acid and final volume was made up to 10 ml by using DDW. Samples

TABLE 1
Effect of different concentrations of $HgCl_2$ on the Root length and Shoot length (cm plant^{-1}) in *Abelmoschus esculentus* at three different growth stages.

		Preflowering	Flowering	Postflowering
Root length	**0.00**	23.540±0.852 (0.0)	24.560±0.935 (0.0)	26.420±1.003 (0.0)
	0.05	20.100±1.020 (14.61)	22.980±1.220 (6.43)	25.880±0.676 (2.04)
	0.10	19.160±1.576 (18.60)	19.420±0.886 (20.92)	23.680±0.417 (10.37)
	0.50	17.140±1.504 (27.18)	18.980±0.621 (22.71)	23.300±1.151 (11.80)
	1.0	17.060±1.176 (27.52)	17.320±1.003 (29.47)	18.920±0.952 (28.38)
	2.0	11.780±1.294 (49.95)	11.800±1.166 (51.95)	16.840±0.723 (36.26)
Shoot length	**0.00**	31.300±1.020 (0.0)	44.180±1.353 (0.0)	44.960±1.359 (0.0)
	0.05	28.260±1.015 (9.71)	44.165±0.970 (0.03)	30.800±1.166 (31.49)
	0.10	27.040±0.852 (13.61)	44.140±0.650 (0.09)	30.520±0.719 (32.11)
	0.50	24.660±0.833 (21.21)	36.340±0.599 (17.74)	29.980±0.483 (33.31)
	1.0	24.020±1.386 (23.25)	33.880±0.531 (23.31)	29.480±0.643 (34.43)
	2.0	23.700±1.166 (24.28)	30.340±1.001 (31.32)	28.720±0.445 (36.12)

P≤ 0.05

	CD at 5%				
S*	0.6028	T*	0.8525	SxT	1.4766

S* = Stages
T* = Treatments
SxT = Interaction

P≤ 0.05

	CD at 5%				
S*	0.5420	T*	0.7665	SxT	1.3276

S* = Stages
T* = Treatments
SxT = Interaction

The values (Mean ± SE) are based on five individual readings. Parentheses include percent variation.

were left for 5 min for colour development and absorbance recorded at 620 nm using Beckmann-DU 640B spectrophotometer. The amount of phosphate was calculated with the help of a calibration curve with a series of K_2SO_4 solutions treated with similar to that of aliquots, as given above. The phosphorous content was expressed in g^{-1} dry wt.

Estimation of Hg. 0.3 gm of dried root samples (80 ^{0}C) were digested in concentrated H_2SO_4 and $HClO_4$. The digested clear solution was diluted to 100 ml with DDW [31]. The mercury content was estimated using a flame atomic absorption spectrometer (Video 11, Thermo Jarrell Ash Corporation), using cathode lamp as a source and an air-acetylene flame. The measurements were made at 253.7 nm.

Statistical Analysis. Data presented is mean of five replications. It was statistically analyzed following ANOVA. Least significant differences were calculated at 0.05 percent level of significance. *P* values ≤ 0.05 were considered as significant.

RESULTS AND DISCUSSIONS

The results regarding the effect of $HgCl_2$ on root length in different cultivars of Okra are given in Table 1. $HgCl_2$ leads to a significant decrease in root length at all growth stages as compared to control. Maximum reduction of 49.95, 51.95 and 36.26 percent was recorded in 2 mM $HgCl_2$ application at preflowering, flowering and post-flowering stages respectively. Shoot length also showed a decrease 24.28, 31.32 and 36.12 percent at preflowering, flowering and post flowering stages respectively. The differences in the root and shoot lengths between the growth stages, treatments and their interactions were statistically significant over control. These findings fully corroborate with those of Lerda [32] for *Allium cepa.* The reason for this can be due to reduction in the rate of mitosis in the meristematic tissues. Sharma [33] has reported that there is an inhibition in the mobilization of nitrogen and phosphorous during germination and seedling growth of *Cucurbita* following mercury treatment. This inhibition in the seedling growth might be due to the fact that Hg has a strong affinity with -SH groups in living cells and is likely to form S-Hg-S bridges and thus affect the growth of seedlings.

A decrease in the chlorophyll content was recorded following an increase in the concentration of $HgCl_2$ at different growth stages. The maximum reduction in chl *a* and *b* was observed at flowering stage under all stress levels. Application of $HgCl_2$ showed a maximum reduction of 57.74 percent in chl. *a* at pre-flowering followed by 63.90 percent at the flowering stage. The effect was least during the post-flowering period **(25.66%)** (Table 2). Chl. *b* decreased by 19.78 and 44.38 percent at 0.05 mM and 2 mM $HgCl_2$ respectively at pre-flowering stage. A decrease of 59.88 percent at flowering stage and 31.21 percent at post-flowering stage in chl. *b* was recorded at 2 mM $HgCl_2$ (Table 2). Total chlorophyll content decreased under all stress levels and the maximum decrease was observed at 2 mM $HgCl_2$ after pre-flowering stage (Table 2). The results of the reduced chlorophyll content are in con-

firmation with the findings of Cho and Park [34]. A reduction in photosynthetic pigments due to mercury has been reported earlier as well in *Lemna trisulca* [35]. Moreover, similar findings have been published by Cho and Park [34], Nagajyoti et al. [36] and John et al. [37] in *Lycopersicum esculentus*, *Arachis hypogaea* and *Brassica juncea*. They report that heavy metals induce a reduction in the chlorophyll content. According to Stobart et al. [38] the activity of enzymes responsible for chlorophyll biosynthesis is down regulated under stress conditions. Other major reasons could be the photooxidative damage to chloroplast, reduction in size and density of chloroplasts, and deficiency of minerals like iron, magnesium and phosphorus [39, 40].

A significant increase in the carotenoid content was observed with an increase in the concentrations of $HgCl_2$. The maximum increase was 57.39, 44.20 and 35.65 percent respectively at preflowering, flowering and post-flowering stages with 2 mM $HgCl_2$ application (Table 2). The difference in the chlorophyll *a*, chlorophyll *b*, total chlorophyll and carotenoid contents among the stages, treatments and their interactions were statistically significant as compared to the control. Carotenoids have a special relevance as scavengers as reported by Demmig-Adams et al. [41] and they are responsible for the scavenging of toxic radicals and hence protect plants from oxidative damage [42]. Any loss in the carotenoid protection is followed by oxidation of the chlorophyll molecules and a quantitative reduction, which lead to a decrease in the photosynthetic ability of plants and thereby protective functions of carotenoids cannot be maintained. The ability of plants to bring modulation in the levels of carotenoids is essential for mitigation of abiotic stress effects through their role in protecting photosynthetic tissues from oxidation [43, 44].

TABLE 2
Effect of different concentrations of $HgCl_2$ on the chlorophyll '*a*', chlorophyll '*b*', total chlorophyll and carotenoid contents (mg g^{-1}FW) in *Abelmoschus esculentus* at three different growth stages.

		Preflowering	Flowering	Postflowering	P≤ 0.05
Chl '*a*'	**0.00**	0.762±0.010 (0.0)	0.967±0.004 (0.0)	0.300±0.025 (0.0)	CD at 5%
	0.05	0.741±0.011 (2.75)	0.866±0.017 (10.44)	0.273±0.030 (9.00)	S* 0.0142 T* 0.0201 SxT 0.0347
	0.10	0.678±0.002 (11.02)	0.722±0.061 (25.33)	0.260±0.009 (13.33)	S* = Stages T* = Treatments SxT = Interaction
	0.50	0.599±0.007 (21.39)	0.691±0.026 (28.54)	0.254±0.027 (15.33)	
	1.0	0.594±0.009 (22.04)	0.611±0.037 (36.81)	0.250±0.040 (16.66)	
	2.0	0.322±0.008 (57.74)	0.349±0.007 (63.90)	0.223±0.016 (25.66)	
Chl '*b*'	**0.00**	0.187±0.022 (0.0)	0.361±0.003 (0.0)	0.189±0.005 (0.0)	P≤ 0.05
	0.05	0.150±0.001 (19.78)	0.360±0.024 (0.27)	0.189±0.005 (0)	CD at 5%
	0.10	0.136±0.004 (27.27)	0.287±0.010 (20.49)	0.188±0.001 (0.52)	S* 0.0087 T* 0.0123 SxT 0.0213
	0.50	0.135±0.003 (27.80)	0.231±0.051 (36.01)	0.148±0.006 (21.69)	S* = Stages T* = Treatments SxT = Interaction
	1.0	0.115±0.007 (38.50)	0.152±0.003 (57.89)	0.147±0.002 (22.22)	
	2.0	0.104±0.003 (44.38)	0.145±0.008 (59.83)	0.130±0.002 (31.21)	
Total chl.	**0.00**	0.865±0.011 (0.0)	0.869±0.018 (0.0)	0.470±0.061 (0.0)	P≤ 0.05
	0.05	0.763±0.010 (11.79)	0.868±0.017 (0.11)	0.455±0.037 (3.19)	CD at 5%
	0.10	0.739±0.021 (14.56)	0.739±0.007 (14.95)	0.417±0.019 (11.27)	S* 0.0187 T* 0.0265 SxT 0.0458
	0.50	0.537±0.011 (37.91)	0.689±0.021 (20.71)	0.407±0.022 (13.40)	
	1.0	0.403±0.093 (53.41)	0.595±0.007 (31.53)	0.400±0.047 (14.89)	S* = Stages T* = Treatments SxT = Interaction
	2.0	0.400±0.008 (53.75)	0.563±0.021 (35.21)	0.387±0.006 (17.65)	
Carotenoids	**0.00**	0.239±0.002 (0.0)	0.332±0.043 (0.0)	0.166±0.026 (0.0)	P≤ 0.05
	0.05	0.336±0.001 (28.86)	0.402±0.031 (17.41)	0.202±0.036 (17.82)	CD at 5%
	0.10	0.412±0.002 (41.99)	0.438±0.054 (24.20)	0.205±0.008 (19.02)	S* 0.0200 T* 0.0283 SxT 0.0490
	0.50	0.432±0.002 (44.67)	0.561±0.087 (40.81)	0.236±0.010 (29.66)	S* = Stages T* = Treatments SxT = Interaction
	1.0	0.519±0.001 (53.94)	0.592±0.040 (43.91)	0.255±0.035 (34.90)	
	2.0	0.561±0.001 (57.39)	0.595±0.049 (44.20)	0.258±0.005 (35.65)	

The values (Mean ± SE) are based on five individual readings. Parentheses include percent variation.

TABLE 3
Effect of different concentrations of $HgCl_2$ on the Protein content (mg g^{-1}FW), Sugar content (mg g^{-1}FW) and Proline content (µg g^{-1}FW) in *Abelmoschus esculentus* at three different growth stages.

		Preflowering	Flowering	Postflowering	P≤ 0.05 CD at 5%
Protein content	**0.00**	18.764±0.415 (0.0)	21.960±0.050 (0.0)	15.166±0.544 (0.0)	**S*** 0.2479 T* 0.3506 SxT 0.6072
	0.05	18.724±0.548 (0.21)	13.726±0.164 (37.49)	10.084±0.552 (33.50)	S* = Stages T* = Treatments SxT = Interaction
	0.10	15.226±1.009 (18.85)	10.956±0.314 (50.10)	8.792±0.084 (42.02)	
	0.50	14.926±0.414 (20.45)	7.410±0.054 (66.25)	6.756±0.333 (55.45)	
	1.0	13.232±0.343 (29.48)	6.318±0.326 (71.22)	3.862±0.535 (74.53)	
	2.0	9.332±0.040 (50.26)	4.026±0.030 (81.66)	2.498±0.347 (83.52)	
Sugar content	**0.00**	15.612±0.627 (0.0)	13.684±0.761 (0.0)	10.648±0.293 (0.0)	P≤ 0.05 CD at 5%
	0.05	14.246±0.726 (8.74)	9.850±0.769 (28.01)	10.544±0.068 (0.97)	**S*** 0.7783 T* 1.1007 SxT 1.9065
	0.10	13.722±0.166 (12.10)	9.102±0.263 (33.48)	9.558±0.466 (10.23)	S* = Stages T* = Treatments SxT = Interaction
	0.50	11.212±0.715 (28.18)	8.884±0.114 (35.07)	9.292±0.541 (12.73)	
	1.0	10.904±0.188 (30.15)	8.374±0.112 (38.80)	8.786±0.167 (17.48)	
	2.0	9.846±0.210 (36.93)	7.846±0.459 (42.66)	8.454±3.591 (20.60)	
Proline content	**0.00**	3.382±0.222 (0.0)	9.446±0.120 (0.0)	14.594±0.348 (0.0)	P≤ 0.05 CD at 5%
	0.05	3.466±0.015 (2.42)	9.604±0.010 (1.64)	15.282±0.670 (4.50)	**S*** 0.1303 T* 0.1843 SxT 0.3191
	0.10	3.672±0.013 (7.89)	9.792±0.022 (3.53)	17.016±0.507 (14.2)	S* = Stages T* = Treatments SxT = Interaction
	0.50	3.738±0.012 (9.52)	9.820±0.014 (3.80)	22.434±0.017 (34.94)	
	1.0	4.020±0.019 (15.87)	10.868±0.012 (13.08)	22.596±0.124 (35.41)	
	2.0	4.410±0.014 (23.31)	10.916±0.010 (13.46)	22.786±0.010 (35.95)	

The values (Mean ± SE) are based on five individual readings. Parentheses include percent variation.

Protein content was found to be maximum at flowering stage as compared to pre-flowering and post-flowering stages. A significant decrease was observed in all stages of growth as the concentration of $HgCl_2$ increased. Maximum reductions were noticed to be 50.26, 81.66, and 83.52 percent with 2 mM $HgCl_2$ at pre-flowering, flowering and post-flowering stages respectively (Table 3). Reduced protein content in Hg treated plants may be due to enhanced oxidation rates induced by H_2O_2 and up-regulated proteolytic activity. ROS induced protein degradation and the enhanced proteolytic activity is widely accepted criteria for measuring the intensity of oxidative stress [45]. Metals interfere with sulfur containing amino acids and proteins resulting in decreased protein content [46]. Similar findings have been reported in duckweed [47] and *Brassica* [37].

Sugar content dropped markedly as a consequence of $HgCl_2$ treatments at all stages of the growth showing a maximum decrease of 42.66 percent with 2 mM $HgCl_2$ at flowering stage. A minimum decrease of 20.60 percent was observed after post-flowering stage at 2 mM $HgCl_2$ (Table 3). The decreased sugar content due to Hg stress corresponds to enhanced photosynthetic inhibition and heavy metals reduce carbon metabolism by reducing the activity of ribulose bisphosphate carboxylase as discussed by Stiborova et al. [48].

Proline content was observed to increase with increase in the concentrations of $HgCl_2$. The maximum increase of 35.95 percent was recorded with 2 mM $HgCl_2$ at post-flowering stage (Table 3), and minimum increase of 13.46 percent was observed at flowering stage. Metal induced accumulation of free proline is one of the key stress responses among plants [10]. Proline accumulation increases stress tolerance by maintaining osmoregulation, protecting enzymes and stabilizing protein synthesis [43, 44, 49, 50]. Our observations are concomitant with previous research reports by John et al. [37] and Ahmad et al. [10].

Results showing effect of $HgCl_2$ on nitrate content are presented in Figure 1. Nitrate content significantly decreased as the concentration of $HgCl_2$ increased during all stages of growth. The maximum reduction was observed with 2 mM $HgCl_2$ showing a decrease of 73.89 percent at pre-

TABLE 4
Effect of different concentrations of $HgCl_2$ on the nitrogen (mg g^{-1}DW) content, phosphorous (mg g^{-1}DW) content and Mercury content (ppm) in *Abelmoschus esculentus* at three different growth stages.

		Preflowering	Flowering	Postflowering	P≤ 0.05 CD at 5%					
Nitrogen content in leaves	**0.00**	67.200±1.166 (0.0)	79.800±0.748 (0.0)	90.200±0.748 (0.0)	**S***	0.9710	T*	1.3732	SxT	2.3784
	0.05	40.000±2.280 (40.47)	42.200±2.482 (47.11)	83.800±0.748 (7.09)	S* = Stages					
	0.10	36.800±0.748 (45.23)	32.600±4.176 (59.14)	78.600±1.356 (12.86)	T* = Treatments					
	0.50	36.800±0.748 (45.23)	30.600±2.15 (61.65)	76.000±1.095 (15.74)	SxT = Interaction					
	1.0	27.000±2.280 (59.82)	21.200±2.638 (73.43)	38.400±3.007 (57.42)						
	2.0	24.800±3.868 (63.09)	20.400±2.245 (74.43)	21.400±4.030 (76.27)						
Phospho-rous content in leaves	**0.00**	187.474±1.214 (0.0)	286.664±0.851 (0.0)	351.760±1.128 (0.0)	P≤ 0.05 CD at 5%					
	0.05	149.864±1.003 (20.06)	162.386±1.068 (43.35)	62.308±0.610 (82.28)	**S***	0.4788	T*	0.6771	SxT	1.1728
	0.10	77.180±1.170 (58.83)	65.928±1.232 (77)	26.336±0.558 (92.51)	S* = Stages					
	0.50	26.100±0.658 (86.07)	51.816±0.691 (81.92)	24.840±0.651 (92.93)	T* = Treatments					
	1.0	8.878±0.439 (95.26)	30.796±0.744 (89.25)	12.864±0.438 (96.34)	SxT = Interaction					
	2.0	3.904±0.313 (97.91)	18.258±0.516 (93.63)	9.538±0.348 (97.28)						
Mercury content in roots	**0.00**	107.7±0.553 (0.0)	132.2±0.728 (0.0)	237.1±2.405 (0.0)	P≤ 0.05 CD at 5%					
	0.05	113.7±0.595 (5.27)	152.6±1.073 (13.36)	248.2±0.607 (4.47)	**S***	0.5225	T*	0.7389	SxT	1.2798
	0.10	123.2±1.459 (12.58)	184.1±0.653 (28.19)	264.7±1.194 (10.42)	S* = Stages					
	0.50	132.3±0.747 (18.59)	194.1±1.146 (31.89)	282.5±1.256 (16.07)	T* = Treatments					
	1.0	158.6±0.694 (32.09)	212.4±0.963 (37.75)	314.0±0.989 (24.49)	SxT = Interaction					
	2.0	171.2±0.713 (37.09)	225.7±0.796 (41.42)	334.7±1.134 (29.16)						

The values (Mean ± SE) are based on five individual readings. Parentheses include percent variation.

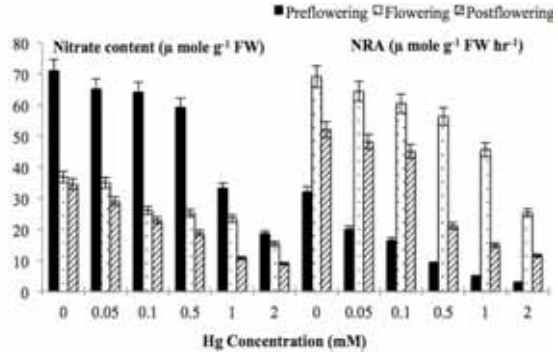

FIGURE 1
Effects on different concentrations of $HgCl_2$ on the nitrate (µ mole g^{-1} fr.wt.) and nitrate reductase activity (NRA) (µ mole g^{-1} fr.wt.hr^{-1}) content in leaves at three different growth stages.

flowering stage. Growing plants on the Hg supplemented medium has been reported to show reduced NO_3^- content in the leaves. This indicates that less NO_3^- accumulation in the leaves may be due to Hg induced reduction in NO_3^- transport from root to shoot. The activity of NR, the first enzyme of nitrate assimilation, is generally susceptible to stress conditions [51-54]. Hg induced enzyme inhibition may have resulted due to altered mobilization of nitrate between storage and the metabolic pool.

The nitrate reductase activity of the control plants increased upto flowering stage but decreased with the plant age. A marked decrease with increasing concentration of $HgCl_2$ was observed under all stress levels. The maximum reduction of 77.93 percent was recorded at 2 mM $HgCl_2$ at post-flowering stage (Figure 1). This reduction in nitrate reductase activity (NRA) by heavy metals is in close agreement with the reports of Buczek [55] and Hakeem et al. [56]. Stress induced down regulation of NRA activity may be due to a reduced supply of NADH and the destruction of chloroplast in addition of the reduced NO_3^- supply to the sites of enzyme synthesis. Metals interfere with the protein synthesis and share a strong affinity for functional -SH group of enzymes [57]. Similar inhibitory effect on NRA by Hg was also observed by Vyas and Puranik [58] in beans. The cytosolic concentration of nitrate has been reported to regulate the expression of NR genes, hence the activity [59]. So in the present study Hg induced reduction in NR activity might be

due to its impact on nitrate concentrations in the plant tissue.

A significant linear decrease of nitrogen content of leaf was observed with increasing concentrations of $HgCl_2$ at all growth stages (Table 4). Maximum reductions of 63.09, 74.43 and 76.27 percent were observed in pre-flowering, flowering and post-flowering stages respectively with 2 mM $HgCl_2$. The nitrogen metabolism impairment must be the primary determinant for the growth of plants grown under heavy metal stress. Decreased nitrogen content reported in our study due to Hg treatment corroborates with the finding of Buczek [55]. It seems that metal toxicity involves reduction in the mobilization of the endogenous nitrate, thus affecting the nitrogen metabolism. Generally heavy metals bind with free amino acids and form complexes that alter the initiation process of translation and thus drastically affect the enzyme synthesis and functioning of the cell [43, 44].

Phosphorous content of the leaves showed a gradual decline with respect to control at all growth stages. The maximum reduction of 97.91, 93.63 and 97.28 percent was observed with 2 mM $HgCl_2$ at pre-flowering, flowering and post-flowering stage respectively (Table 4). The differences in phosphorous content of leaf among the stages, treatments and their interactions were statistically significant over control. Effect of heavy metals on phosphorus can be attributed to phosphorous solubilizing micro-organisms and/or insufficient phosphorous uptake. The decrease in phosphorus content of the plants due to heavy metals is mainly due to the harmful effects on root colonization with arbuscular mycorrhizal (AM) fungi [60]. The heavy metals can also affect the phosphate solubilising activity as reported in the halophylic phosphobacteria [61].

The results related to the accumulation of Hg in the roots of *A. esculentus* at different growth stages are given in Table 4. The maximum accumulation of Hg in the roots was observed in post-flowering stage under all stress levels as compared to the pre and flowering stages. The maximum accumulation of 37.09, 41.42 and 29.16 percent was observed at pre-flowering, flowering and post-flowering stages respectively at 2 mM $HgCl_2$. Increased concentrations of mercury showed increased accumulation in the plant. This is more prominent in roots as compared to shoots as reported by Greger et al. [62]. These findings are also in conformity with the studies of Wang and Greger [63]. Lower accumulation of Hg in shoots as compared to the roots may be due to higher affinity of Hg for root tissues, resulting in maximal possible trapping of Hg within the roots [63]. This has been reported in *A. esculentus* as well by Wang and Greger [63]. In addition Hg has been reported to impede with water uptake by affecting plasma membrane aquaporins in higher plants and this effect of Hg on water transport can contribute towards a reduction in biomass accumulation as well as the dry weight of root and shoots [64].

CONCLUSION

Hg is dangerous for the plant growth and a mitigation of its stress is important for the growth and development of the plants in areas polluted by higher concentrations of this element. Present study confirmed that exposure of *A. esculentus* to $HgCl_2$ increases proline content and decreases chlorophyll, sugar, and protein content and NRA activity. In addition, N and P uptake is also hampered by $HgCl_2$ treatments. Future research studying the effects of mercury at the molecular level can be useful in understanding the mechanisms involved.

REFERENCES

[1] Ozturk, M. (ed) (1989). Plants and pollutants in developed and developing countries. Ege Univ. Press, Izmir, Turkey, 759 pp.

[2] Rodríguez, L., López-Bellido, F., Carnicer, A. and Alcalde, V. (2003). Phytoremediation of mercury-polluted soils using crop plants. Fresen. Environ. Bull., 12, 967-971.

[3] Ozturk, M., Yucel, E., Gucel, S., Sakcali, S. and Aksoy, A. (2008). Plants as biomonitors of trace elements pollution in soil. In: Prasad, M.N.V. (ed), Trace Elements: Environmental contamination, nutritional benefits and health ımplications. John Wiley and Sons, USA, pp. 723-744.

[4] Ozturk, M., Sakcali, S., Gucel, S. and Tombuloğlu, H. (2010). Boron and Plants. In: Ashraf et al. (eds), Plant Adaptation & Phytoremediation. Springer Verlag, Part 2, NY, USA, pp. 275-311.

[5] Ozturk, M., Memon, A.R., Gucel, S. and Sakcali, M.S. (2012). Brassicas in Turkey and their possible role in the phytoremediation of degraded habitats. In: Anjum, N.A. et al. (eds), The Plant Family Brassicaceae: Contribution Towards Phytoremediation. Springer Verlag, Environmental Pollution Book Series 21, NY, USA, pp. 265-288.

[6] Ahmad, P., Ozturk, M. and Gucel, S. (2012). Oxidative damage and antioxidants induced by heavy metal stress in two cultivars of mustard plants. Fresen. Environ. Bull., 21, 2953-2961.

[7] Jan, S. and Parray, J.A. (2016). Approaches to heavy metal tolerance in Plants. ISBN: 978-981-10-1692-9. Springer Science+Business Media Singapore.

[8] Jusufi, K., Stafilov, T., Vasjari, M., Korca, B., Halili, J. and Berisha, A. (2017). Measuring the presence of heavy metals and their bioavailability in potato crops around Kosovo's power

plants. Fresen. Environ. Bull., 26(2a), 1682-1686.
[9] Jusufi, K., Stafilov, T., Vasjari, M., Korca, B., Halili, J. and Berisha, A. (2016). Determination of heavy metals by ICP-AES in the agricultural soils surrounding Kosovo's power plants. Fresen. Environ. Bull., 25(5), 1313-1321.
[10] Divrikli, U., Saracoglu, S., Soylak, M. and Elci, L. (2003). Determination of trace heavy metal contents of green vegetable samples from Kayseri-Turkey by flame atomic absorbtion spectrometry. Fresen. Environ. Bull., 12(9), 1129-1131.
[11] Azevedo, R. and Rodriguez, E. (2012). Phytotoxicity of mercury in plants: A review. Journal of Botany, Article ID 848614.
[12] Steinnes, E. (1997). Mercury. In: Alloway, B.J. (ed.), Heavy metals in soils. Blackie academics and professional press, London, UK, 2nd edition, pp. 245-259.
[13] Neculita, C.M., Zagury, G.J. and Deschênes, L. (2005). Mercury speciation in highly contaminated soils from chlor-alkali plants using chemical extractions. Journal of Environmental Quality, 34(1), 255-262.
[14] UNEP United Nations Environmental Programme. (2008). The global atmospheric mercury assessment: Sources, Emissions and Transport.
[15] Kumari, R. (2011). Preliminary mercury emission estimates from non-ferrous metal smelting in India. Atmospheric Pollution Research, 2, 513-519.
[16] Pesko, M. and Kralova, K. (2012). Cadmium, nickel and mercury accumulation and some physiological and biochemical responses of hydroponically cultivated rapeseed (*Brassica napus* L.) plants. Fresen. Environ. Bull., 21(12), 3677-3686.
[17] Du, X., Zhu, Y.G., Liu, W.J. and Zhao, X.S. (2005). Uptake of mercury (Hg) by seedlings of rice (*Oryza sativa* L.) grown in solution culture and interactions with arsenate uptake. Environmental and Experimental Botany, 54(1), 1-7.
[18] Li, P., Feng, X. and Qiu, G. (2010). Methylmercury exposure and health effects from rice and fish consumption: A review. International Journal of Environmental Research and Public Health, 7, 2666-2691.
[19] IHD Indian Horticulture Database. (2011). nhb.gov.in/area-pro/database-2011.pdf.
[20] Prommakool, A., Sajjaanantakul, T., Janjarasskul, T. and Krochta, J.M. (2011). Whey protein-okra polysaccharide fraction blend edible films: tensile properties, water vapor permeability and oxygen permeability. Journal of the Science of Food and Agriculture, 91(2), 362-369.
[21] Khare, C.P. (2007). *Abelmoschus esculentus* (L.) Moench. In: Indian Medicinal Plants. A references work entry. Springer New York, pp. 1-1.
[22] Naveed, A., Khan, A.A. and Khan, I.A. (2009). Generation mean analysis of water stress tolerance in Okra (*Abelmoschus esculentus* L.). Pakistan Journal of Botany, 41(1), 195-205.
[23] Hiscox, J.D. and Israelstam, G.F. (1979). A method for extraction of chlorophyll from leaf tissue maceration. Canadian Journal of Botany, 57, 1332-1334.
[24] Bradford, M. (1976). A rapid and sensitive method for the quantification of microgram quantities of protein utilizing the principle of protein dye binding. Analytical Biochemistry, 72(1-2), 248-254.
[25] Dey, R.M. (1990). Method in plant biochemistry carbohydrates. Academic Press London 11.
[26] Bates, L.S., Waldren, R.P. and Teare, I.D. (1973). Rapid determination of free proline for water stress studies. Plant Soil, 39, 205-207.
[27] Grover, H.L., Nair, T.V.R. and Abrol, Y.B. (1978). Nitrogen metabolism of upper three leaf blades of wheat at different soil nitrogen levels, NR activity and contents of various nitrogenous constituents. Physiologia Plantarum, 42, 287-292.
[28] Heuer, Z. and Plaut, B. (1978). Reassessment of the in vivo assay for nitrate reductase in leaves. Physiologia Plantarum, 43, 306-312.
[29] Linder, R.C. (1944). Rapid analytical methods for some of the more common inorganic constituents of plant tissue. Plant Physiology, 19, 70-89.
[30] Fiske, C.H. and Subbarow, Y. (1925). Colorimetric determination of phosphorous. Journal of Biological Chemistry, 66, 375-400.
[31] Franson, M.A.H. (1998). Digestion of metals, HNO_3-HCl digestion. In: Standard methods for the examination of water and waste water. 20th Ed., American public health association Washington.
[32] Lerda, D. (1992). The effect of lead on *Allium cepa* L. Mutation Research Letters, 231, 80-92.
[33] Sharma, S.S. (1985). Effect of mercuric acetate on mobilization of N and P during germination and seedling growth of *Cicer arietinum*. Experientia, 41(1), 45-46.
[34] Cho, U.H. and Park, J.O. (2000). Mercury induced oxidative stress in tomato seedlings. Plant Science, 156, 1-9.
[35] Venanzi, G., Lupattelli, M., Pocceschi, N., Romano, B. (1989). Effect of heavy metals on some photosynthetic characteristics in *Lemna trisulca*. Rivista di Idrobiologia RIIDBN., 28(3), 247-254.
[36] Nagajyoti, P.C., Dinakar, N., Prasad, T.N.V.K.V., Suresh, C. and Damodharam, V. (2008). Heavy metal toxicity: Industrial effluent effect on groundnut (*Arachis hypogaea* L.)

seedlings. Journal of Applied Sciences Research, 4, 110-121.
[37] John, R., Ahmad, P., Gadgil, K. and Sharma, S. (2009). Heavy metal toxicity: effect on plant growth, biochemical parameters and metal accumulation by *Brassica juncea* L. International Journal of Plant Production, 3, 65-76.
[38] Stobart, A.K., Griffiths, W.T., Ameen-Bukhari, I. and Sherwood, R.P. (1985). The effect of Cd^{2+} on the biosynthesis of chlorophyll in leaves of barley. Physiologia Plantarum, 63(3), 293-298.
[39] Somashekaraiah, S.V., Padmaja, K. and Prasad, A.R.K. (1992). Phytotoxicity of cadmium ions on germinating seedlings of mung bean (*Phaseolus vulgaris*): Involvement of lipid peroxidation in chlorophyll degradation. Physiologia Plantarum, 85, 85-89.
[40] Benavides, M.P., Gallego, S.M. and Tomaro, M.L. (2005). Cadmium toxicity in plants. Brazilian Journal of Plant Physiology, 17(1), 21-34.
[41] Demmig-Adams, B., Gilmore, A.M. and Adams, I.I.I. W.W. (1996). In vivo functions of carotenoids in higher plants. Journal of the Federation of American Societies for Experimental Biology, 10, 403-412.
[42] Çakmak, I. and Marschner, H. (1992). Magnesium deficiency and light intensity enhances activities of **dismutase,** ascorbate peroxidase and glutathione reductase in bean leaves. Plant Physiology, 98, 1222-1227.
[43] Ahmad, P., Jhon, R., Sarwat, M. and Umar, S. (2008). Responses of proline, lipid peroxidation and antioxidative enzymes in two varieties of *Pisum sativum* L. under salt stress. International Journal of Plant Production, 2(4), 353-366.
[44] Ahmad, P., Jaleel, C.A., Salem, M.N., G. Nabi, G. and Sharma, S. (2010). Roles of enzymatic and non-enzymatic antioxidants in plants during abiotic stress. Critical Reviews in Biotechnology, 30(3), 161-175.
[45] Romero-Puertas, M.C., Palma, J.M., Gomez, M., del Rio, L.A. and Sandalio, L.M. (2002). Cadmium causes the oxidative modification of proteins in pea plants. Plant Cell & Environment, 25, 677-686.
[46] Somasundaram, R., Muthuchelian, K. and Murugesan, S. (1994). Inhibition of chlorophyll, protein, photosynthesis, nitrate reductase and nitrate content by vanadium in *Oryza sativa* L. Journal of Environmental Biology, 15(1), 41-48.
[47] Tripathi, R.D. and Smith, S. (1996). Effect of chromium (VI) on growth, pigment content, photosynthesis, nitrate reductase activity, metabolic nitrate pool and protein content in duckweed *Spirodela polyrrhiza* L. In: Yunus, M. (ed), ICPEP 96, Book of Abstracts 159.
[48] Stiborová, M., Ditrichová, M. and Březinová, A. (1987). Effect of heavy metal ions on growth and biochemical characteristics of photosynthesis of barley and maize seedlings. Biologia Plantarum, 29(6), 453-467.
[49] Ozturk, M., Turkyilmaz, B., Gucel, S. and Guvensen, A. (2011). Proline accumulation in some coastal zone plants of the Aegean region of Turkey. American Journal of Botany, 66(3), 307-312.
[50] Turkyilmaz, U.B., Guvensen, A., Dereboylu, E.A. and Ozturk, M. (2013). Variations in the proline and total protein contents in *Origanum sipyleum* L. from different altitudes of Spil Mountain, Turkey. Pakistan Journal of Botany, 45(SI), 571-576.
[51] Hewitt, E.J. and Nottan, B.A. (1979). Nitrate reductases: properties and possible mechanisms. Biochemical Society Transactions, 7, 629-633.
[52] Campbell, W.H. and Smarrelli, J. (1986). Nitrate reductase: biochemistry and regulation. In: Neyra, C.A. (ed), Biochemical basis of plant breeding. CRC press. Inc. Boca Raton Florida, pp 1-39.
[53] Ozturk, M., Gucel, S., Sakcali, S. and Baslar, S. (2013). Nitrate and edible plants in the Mediterranean Region of Turkey: An Overview. In: Umar, S. et al (eds), Nitrate in Leafy Vegetables-Toxicity and Safety Measures. I.K. International Public House Pvt. Ltd. New Delhi-Bangalore (India), pp. 17-51.
[54] Hakeem, K.H., Ahmad, A., Iqbal, M., Gucel, S. and Ozturk, M. (2011). Nitrogen efficient rice genotype can reduce nitrate pollution. Environmental Science and Pollution Research, 18, 1184-1193.
[55] Buczek, J. (1980). The nitrate reductase and nitrite reductase activities in cucumber seedlings as affected by divalent cations. Acta Physiologiae Plantarum, 3, 221-232.
[56] Hakeem, K.R., Ozturk, M., Sabir, M. and Akhtar, M.S. (2016). Nitrate and nitrogen oxides: sources, health effects and their remediation. Reviews of Environmental Contamination and Toxicology, 1-36.
[57] Prasad, D.D.K. and Prasad, A.R.K. (1987). Altered α-amino levullinic acid metabolism by lead and mercury in germinating seedling of Bajra. Journal of Plant Physiology, 127, 241-250.
[58] Vyas, J. and Puranik, R.M. (1993). Inhibition of nitrate reductase activity by mercury in bean leaf segments. Indian Journal of Plant Physiology, 1, 57-60.
[59] Tischner, R., Waldeck, B., Goyal, S.P. and Rains, W.D. (1993). Effects of nitrate pulses on the nitrate-uptake rate, synthesis of mRNA coding for nitrate reductase, and nitrate reductase activity in roots of barley seedlings. Plan-

ta, 189(4), 533-537.
[60] Omar, S.A. (1998). The role of rock-phosphate-solubilizing fungi and vesicular-arbuscular-mycorrhiza (VAM) in growth of wheat plants fertilized with rock phosphate. World Journal of Microbiology and Biotechnology, 14, 211-218.
[61] Ravikumar, S., Williams, P.G., Shanthy, S., Gracelin, N.A.A., Babu, S. and Parimala, P.S. (2007). Effect of heavy metals (Hg and Zn) on the growth and phosphate solubilising activity in halophilic phosphobacteria isolated from Manakudi mangrove. Journal of Environmental Biology, 28, 109-114.
[62] Greger, M., Wang, Y. and Neuschutz, C. (2005). Absence of Hg transpiration by shoot after Hg uptake by roots of six terrestrial plant species. Environmental Pollution, 134, 201-208.
[63] Wang, Y. and Greger, M. (2004). Clonal differences in mercury tolerance, accumulation, and distribution in willow. Journal of Environmental Quality, 33(5), 1779-1785.
[64] Zhang, W.H. and Tyerman, S.D. (1999). Inhibition of water channels by $HgCl_2$ in intact wheat root cells. Plant Physiology, 120(3), 849-858.

Received: **27.01.2017**
Accepted: **23.07.2017**

CORRESPONDING AUTHOR

Asiya Hameed
Botany Department, Hamdard University, New Delhi, India

e-mail: hameed901@gmail.com

© by PSP Volume 26 – No. 10/2017 pages 5824-5832 Fresenius Environmental Bulletin

ENVIRONMENTAL AND ECONOMIC CONDITIONING OF THE BREEDING OF DAIRY CATTLE

Andrzej Borusiewicz[1,*], Kamila Mazur[2]

[1]Higher School of Agribusiness in Lomza, 18402 Lomza, Poland
[2]Institute of Technology and Life Sciences, 05090 Falenty, Poland

ABSTRACT

The level of sustainability of animal production depends on the use of modern housing systems which ensure high productivity and quality of milk and meat, with the possibility of robotization of work, by simultaneously minimizing the negative impact on the environment, including energy inputs by using renewable energy sources and ensuring livestock animals' welfare. Livestock production, especially milk production, is a source of significant amounts of harmful gases such as carbon dioxide and ammonia. The main aim of the research was a multicriterial investigation of free-stall cattle barns for dairy cows taking into account sustainability of production. Twelve free-stall cattle barns were tested with boxed litter and non-litter systems, and with deep litter, four barns in each system. Original methodology was elaborated which allowed for the technological, economic and environmental assessment of cattle barns and their elements of infrastructure. The methodology scheme consisted of the following stages: stage 1 – choice of objects for research, stage 2 – characteristics of objects tested, stage 3 – identification of key elements characteristic of the objects tested which are helpful for technical, technological, quality and economic assessment, stage 4 – determination of these parameters, stage 5 – model of final assessment and choice of the best, most convenient technological-functional solutions, stage 6 – designing exemplary models.

The parameters obtained from tests allowed the selection of the best solutions, to be applied in new designs which comply with the requirements of standards, including welfare, environmental protection and minimization of energy inputs. Based on research results, three model proposals of functional-technological solutions for cattle barns were elaborated. The first proposed example was a free-stall boxed cattle barn with litter. The second best solution was a non-littered boxed cattle barn. The third model proposed was a cattle barn with deep litter. All three barns are considered to have very good microclimate parameters, by dint of the proper construction of the adjustable ventilation system. Also, investment costs and energy inputs could be at a level acceptable by investors thanks to high automation and robotization.

KEYWORDS:
sustainability, milk production, energy inputs, multi-criterial assessment, exploitation costs.

INTRODUCTION

Striving for sustainable animal production results primarily from the necessity of fulfilling EU and Polish law regulations which protect the environment. Concerning animal welfare, cattle and calves in particular, the regulations of the Ministry of Agriculture and Rural Development should be adhered to [20, 21, 22]. The idea of sustainable development is considered around the intensification of production while ensuring proper animal welfare conditions, and minimizing energy and labour inputs, which go together with the automation and robotization of technological treatments in milk and meat production [Fig.1].

According to research by Jankowiak and Bieńkowski, dairy and mixed types farms fulfil the relatively highest level of sustainable development, and farms with plant production have the lowest level of sustainability [31].

Directions of scientific-research activities for the future:

- analysis of state of the art and needs in the scope of technology and buildings in animal housing and production safety,
- research into minimizing economics inputs, including energetic inputs in milk and other animal materials production,
- research into environmental conditions in housing buildings and definition of directions for improving their state,
- complex elaboration and implementation of model solutions of livestock objects with different mechanization, automation and robotization level fulfilling particular criteria: economic, energetic, ecological, animal welfare and others.

Taking into account the problems mentioned above, an attempt was made to evaluate existing buildings for dairy cows in the scope of exploitation costs of buildings, machines and equipment, human labour inputs, energetic inputs and microclimate conditions.

Many researchers have dealt with exploitation and investment costs and labour inputs,

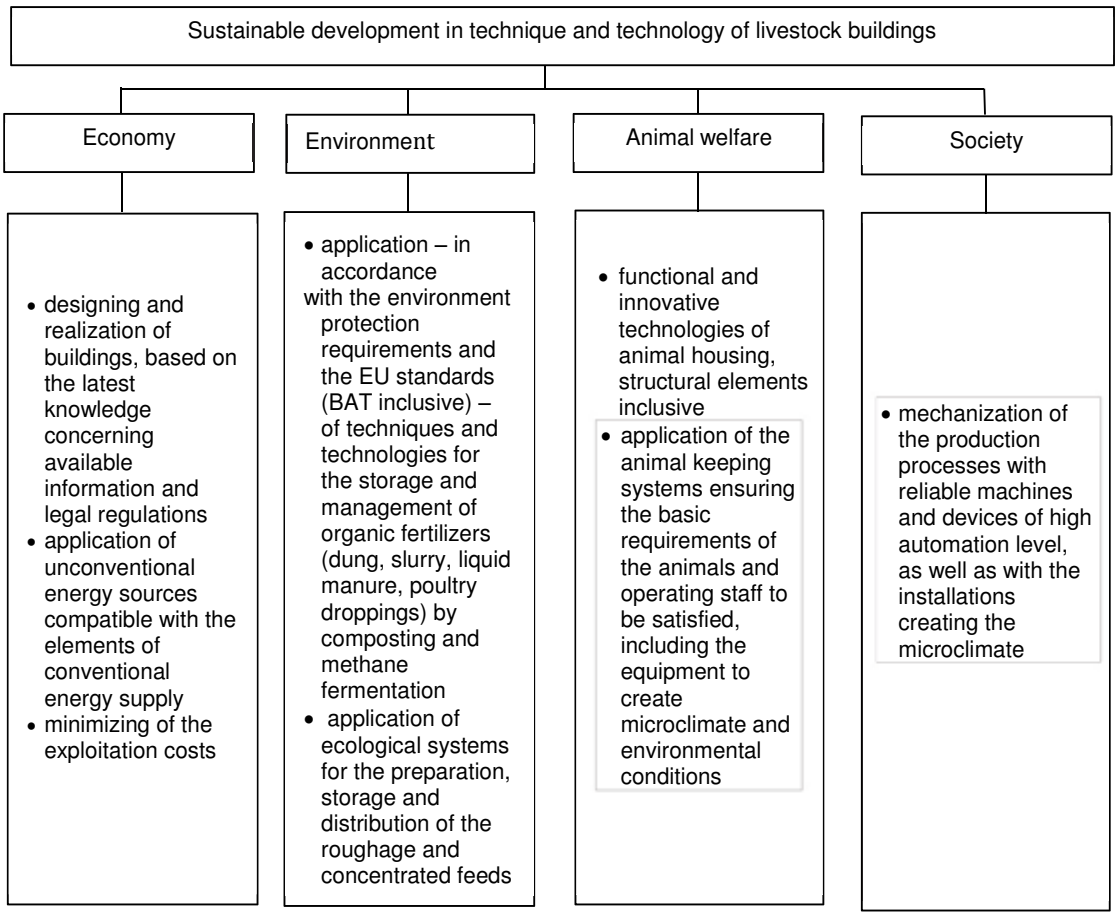

FIGURE 1
Elements shaping the development of a modern animal production system [24].

including mechanical and electrical energy inputs. Exploitation costs were tested by authors [18, 12, 16]. The questions connected with electrical energy inputs in milk production were discussed in publications by such researchers [30, 11, 16]. Costs of milk production and energetic inputs were also researched [7, 8, 9]. Labour inputs were tested, for example, by authors [29, 17, 13, 28].

Besides, many authors only describe housing systems or methods of designing functional- spatial solutions [4, 5, 24].

Microclimate and animal welfare were described by authors [15, 2, 3, 19].

Most authors present individual investigation's results of particular elements. But there is a lack of complex testing of constructional, technological-functional solutions of free-stall cattle barns in Poland.

The Scientific problem was formulated as three questions:

- how do technological solutions influence the mechanization level and energetic inputs in cattle barns?

- how do technological solutions influence the formation of microclimatic conditions in cattle barns?

- how do mutual relationships between elements of functional-technological solutions of cattle barns influence the costs in milk production?

The Main aim was a multi-criterial evaluation of free-stall cattle barns for dairy cows.

Detailed aims:

- evaluation of technological–functional elements of free-stall cattle barns for dairy cows,

- definition of the mechanization level of objects tested and the influence of housing systems on energetic inputs in milk production,

- definition of the evaluation model of technological–functional solutions in order to describe the most advantageous solutions,

- choice of the best solutions.

MATERIAL AND METHODS

The detailed scope of research included: technical, technological, qualitative and economic analysis.

- technical elements characterizing buildings tested (description of buildings, construction) such as: dimensions of resting, walking and feeding areas, manure corridors, cubage, ventilation, openings, mechanization of technological treatments in milk

production – machinery and equipment, including three robots for milking, feed scraping and cleaning of slatted floor;

- technological elements such as: labour inputs on four technological treatments (milking, milk cooling, feeding, manure removal, other works), electrical and mechanical energy inputs in milk production and mechanization level of cattle barns;
- qualitative assessment, including: microclimatic parameters such as temperature, relative humidity of air, amount of air exchange, amounts of greenhouse and harmful gases (carbon dioxide, ammonia), as well as illumination;
- calculation of investments in buildings, equipment and machines, investment costs, electrical energy costs, mechanical energy costs, labour costs and exploitation costs;
- evaluation of objects tested, and choice of the most advantageous solution taking account of limitations.

The field tests were conducted by the direct moderated interview method and photography of the working day, as well as the timing scheme directly on farms. The equations (1) to (9) show the method of these costs' calculation.

Twelve out of about forty cattle barns were chosen and tested, fulfilling the following preliminary criteria:

- at least 4th level of mechanization;
- average annual milk yield of herd above 6200 litres;
- number of animals above 39.

These cattle barns were in the loose housing system, with and without litter (4 with deep litter, 4 boxed with shallow litter, and 4 boxed with the slurry system and channels). The objects tested were described in the scope of technological-architectural solutions, including ways of mechanisation of four technological treatments (milking and milk cooling, forage preparing and feeding, manure removing and storaging, and other works).

Measuring microclimate parameters. Temperature and relative humidity of air, NH_3 and CO_2 concentration in 3-4 day periods in each barn in the animal area were measured. Temperature and relative humidity of the air outside the barn were also measured. Values (averages) from every 5 minutes were obtained.

The following apparatus was used to measure microclimatic conditions according to Polish Norm BN-86/880-03 [BN/86]:

- 4 thermo-, hygro-, barometers;
- 4 thermo - hygrometers with transfer to the data-concentrator were used, and all data were finally transported to a PC and elaborated in STATISTICA 10 PL;
- 4 gas multi-meters (ammonia, carbon dioxide concentrations, with infra-red sensors and with internal memories) MX6^{iBird} Industrial Scientific, thermo-anemometers TESTO, lux meter SONEL.

Exploitation costs were calculated according to Muzalewski's elaboration [16].

Twelve cattle barns for dairy cows in the loose housing system were surveyed and in field tested. These barns were located in Podlaskie, Mazovieckie and Varmia-Mazury provinces, and they were family farms. The number of cows was from 39 to 170 LU

Limitations to the choice of the best solution were the criteria for the final function as follows:

I Terminal investment's inputs

$$\mathbf{k}_{\text{invest.}} \leq \mathbf{k}_{\text{limit. invest.}} \text{ [PLN·LU}^{-1}\text{]} \quad (2)$$

II Permissible labour inputs on 4 technological treatments

$$\mathbf{n}_{\text{labour.}} \leq \mathbf{n}_{\text{limit. labour}} \text{ [working minutes· day}^{-1}\text{·LU}^{-1}\text{]} \quad (3)$$

III Permissible concentrations of harmful gases (CO_2 and NH_3)

$$\mathbf{S}_{CO2} \leq \mathbf{S}_{\text{limit. CO2}} \text{ [ppm]} \quad (4)$$

$$\mathbf{S}_{NH3} \leq \mathbf{S}_{\text{limit.NH3}} \text{ [ppm]} \quad (5)$$

IV Terminal energy inputs (electrical and mechanical)

$$\mathbf{e} \leq \mathbf{e}_{\text{limit.}} \text{ [kWh·day}^{-1}\text{·LU}^{-1}\text{ , HP·day}^{-1}\text{·LU}^{-1}\text{]} \quad (6)$$

The method of choice for the best solutions with the maintenance of all limitations is shown in the diagram below (Fig.2). All solutions were set in order of exploitations costs straining to minimum.

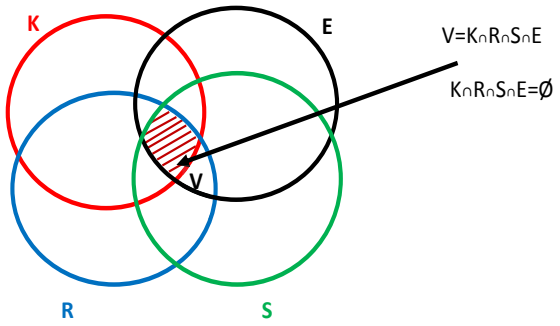

FIGURE 2
Choice of best solutions according to target function- exploitation costs.

Model of final multi-criterial evaluation. The final evaluation was made on the basis of the following target function – minimization of exploitation costs (1):

$$c_{eu} = \frac{C_m + C_{us}}{N} \rightarrow \text{minimum} \quad (1)$$

where: c_{eu} – unitary exploitation costs [PLN·year $^{-1}$·LU^{-1}]
C_m – costs of maintenance [PLN·year $^{-1}$]
C_u– cost of use [PLN·year $^{-1}$]
N – number of LU

Exploitation costs were calculated according to equations described by Gazzarin and Lips [9], as well as Muzalewski [16]

$$c_{eu} = \frac{C_m + C_{us}}{N} \text{ [PLN·LU}^{-1}\text{·year}^{-1}\text{]} \quad (7)$$

C_{eu} – unitary exploitation costs [PLN· year^{-1}]

C_m – costs of maintenance [PLN· year^{-1}]

C_{us} – costs of use [PLN· year^{-1}]

N – number of Livestock Units

Costs of maintenance. Costs of maintenance were the sum of amortization costs of buildings and machinery, and their insurance (eq.2)

$$C_m = \frac{C_{ib}}{T_b} + \Sigma\frac{C_{im}}{T_m} + C^b_{ins} + C^m_{ins} \text{ [PLN·year}^{-1}\text{]} \quad (8)$$

C_{ib} – investment costs of buildings [PLN]

T_b – the assumed stability of the building [number of years]

C_{im} – price (value) replacement of machinery or equipment [PLN]

T_m – the assumed stability of the machinery [number of years]

C^b_{ins} – insurance costs of building [PLN·year^{-1}]

C^m_{ins} – costs of insurance of machinery and equipment [PLN·year^{-1}]

Costs of usage.

$$C_u = C^b_{ee} + C^b_r + C^m_{ee} + C_{me} + C^m_r + C_L \text{ [PLN·year}^{-1}\text{]} \quad (9)$$

C_u – costs of usage [PLN·year^{-1}]

C^b_{ee} – costs of electrical energy of buildings [PLN·year^{-1}]

C^b_r – costs of repairs in buildings [PLN·year^{-1}]

C^m_{ee} – costs of electrical energy for machinery and equipment for mechanization [PLN·year^{-1}]

C_{me} – costs of mechanical energy [PLN·year^{-1}]

C^m_r – costs of repair of machinery and equipment [PLN·year^{-1}]

C_L – costs of labour inputs [PLN·year^{-1}]

Costs of electrical energy in buildings.

$$C^b_{ee} = (N^b_{eL} + N_{eV}) \cdot P_{kWh} \text{ [PLN·year}^{-1}\text{]} \quad (10)$$

N^b_{eL} – electrical energy usage for lighting of buildings [kWh·year^{-1}]

N_{eV} – electrical energy usage for ventilation [kWh·year^{-1}]

P_{kWh} – unitary price of electrical energy [PLN·kWh^{-1}]

$$C^b_r = R_b \cdot \frac{C_{ib}}{T_b} \text{ [PLN·year}^{-1}\text{]} \quad (11)$$

where: R_b = 0,2-0,5 – coefficient of repair costs

Costs of electrical energy for machinery and equipment.

$$C^m_{ee} = N_{ee} \cdot C_{kWh} \text{ [PLN·year}^{-1}\text{]} \quad (12)$$

N_{ee} – electrical energy inputs machinery and equipment [kWh· year^{-1}]

C_{kWh} – costs of 1 kWh of electrical energy [PLN·kWh^{-1}]

Costs of mechanical energy for machinery and equipment

$$C_{em} = N_{em} \cdot C_{em} \quad (13)$$

C_{em} – annual costs of mechanical energy [PLN·year^{-1}]

N_{em} – annual mechanical energy inputs [kWh·year^{-1}]

C_{em} – unitary costs of mechanical energy [PLN·kWh^{-1}]

Costs of repair of machinery and equipment

$$C^m_r = R^m_n \cdot \left(\frac{C_{im}}{T_m}\right) \text{ [PLN·year}^{-1}\text{]} \quad (14)$$

where: R^m_n = 0,2-1,1– coefficient of repair costs, depending on kind of machinery or equipment

Labour costs

$$C_L = N_L \cdot P_L \text{ [PLN·year}^{-1}\text{]} \quad (15)$$

N_L – labour inputs [working hour·year^{-1}]

P_L – cost of 1 working hour (labour) [PLN·hour^{-1}]

RESULTS AND DISCUSSION

The overall characteristics of the tested cattle barns are shown in table 1. Ways of mechanization in barns are shown in Table 2.

The annual average milk yield of cows was from 6200 litres to 9600 l of milk with extra class.

TABLE 1
Overall characteristics of farms tested.

No of barn	1	2	3	4	5	6	7	8	9	10	11	12
LU Breed	93 phf – cb simental 7300	87 phf – cb jersey	100 simental mont' beliarde phf – cb	100 phf – cb 9000	44 phf- cb 7000	81 phf- cb 7000	39 phf- cb 6500	144 phf- cb 7500	170 phf- cb	83 phf- cb	87 phf- cb	109 phf- cb
housing system	deep litter	deep litter	deep litter	deep litter	boxed, litter	boxed, litter	boxed, litter	boxed, litter	boxed, without litter	boxed, without litter	boxed, without litter	boxed, without litter
average milk yield	7300	8000	6200	9000	7000	7000	6500	7500	8500	9500	9600	9600

TABLE 2
Mechanization in barns tested.

No of barn	**Mechanization of main treatments**			
	1st treatment: milking and milk cooling Milking unit (type) Capacity of milk tank [dm^3]// Power vacuum aggregate /aggregate of milk tank [kWh]	**2nd treatment: preparing of feed and feeding**	**3rd treatment: manure removal and storage amount of litter kg·day^{-1}·LU^{-1}**	**4th treatment: other works**
1	FB 2x6(12) 6000// 3/ 4.2	feed mixer 17 m^3+ tractor 140 HP + loader; TMR	tractor 120 HP + loader, manure spreader 7	swinging cow brush, electric hoof knife
2	FB 2x4(8) 6700//2.2/ 4.2	feed mixer 10 m^3+ tractor 82HP + loader, TMR	tractor 82 HP + loader, manure spreader 5	electric hoof knife;
3	FB 2x5(10) 2500// 2.6/1.25	feed mixer 18m^3+ tractor 80HP + loader; TMR	tractor 120HP+ loader, manure spreader 6	2 swinging cow brush, electric hoof knife
4	FB 2x5(10) 8100/ 2.2/1.25	feed mixer 13m^3+ tractor 120HP+ loader; TMR	tractor loader 120HP, manure spreader 7	ventilator, electric hoof knife
5	FB 2x4(8) 1600//2.2/2	feed mixer 7m^3+ tractor 55HP+ loader; TMR	solid floor, manure scrapers, tractor 90 HP + loader ; 2	electric hoof knife
6	FB 2x5(10) 800// 2.2/1.25	tractor 100 HP + loader	solid floor, manure scrapers, tractor 100HP + loader; 2	electric hoof knife
7	FB 2x3(6) 2500//3.0/3.0	tractor 80HP + loader	solid floor in alleys, tractor 52HP + shovel; 2	electric hoof knife
8	Tandem 2x4(8) 2700/1500// 3.0/6.0 and 4.0	feed mixer 20m^3+ tractor - loader120HP ;TMR	solid floor, manure scrapers, tractor 100HP + loader; 2	electric hoof knife
9	2 milking robots 10000// 3.0/2.2	feed mixer 14 m^3+ tractor 95HP+ loader; TMR	deep slurry, robot-scraper, tractor 160 HP, slurry spreader	3 swinging cow brushes, electric hoof knife
10	VMS 5000// 3.0/2.2	feed mixer 11m^3+ tractor 110HP + loader, TMR	deep slurry, robot-scraper, tractor 74 HP, slurry spreader	swinging cow brushes, electric hoof knife
11	FB 2x4(8) 2600//3.0/1.5	feed mixer 12,5 m^3+ tractor 126HP + loader; TMR	slurry in channels, tractor 126HP + slurry spreader	electric hoof knife
12	FB 2x5(10) 4000// 2.6/4.0	feed mixer 12m^3+ tractor 75HP, loader TMR	slurry in channels tractor 77,2 HP +slurry spreader	electric hoof knife

Milking was done in milking parlours: herring-bone 2x4 (three barns), 2x3 (one barn), 2x5 (four barns), one 2x6 herring-bone, one tandem 2x4, and in two barns there were automatic systems. The power of milking pumps was 0.55 kW. Milk tanks had capacities from 1600 litres to 10 000 litres, and their power was from 1.25 kW to 6 kW. Roughage mixed with concentrates was fed by a feed mixer with capacities from 7 to 20 m^3. The feeders worked with tractors from 52 HP to 160 HP. In two cattle barns forage was fed directly by tractor and loader. Tractors cooperated with the loaders in ten cattle barns, and in two autonomous loaders with power from 60 HP to 100 HP, and they were used for loading forage onto the feed mixer. In two robotized cattle barns forage on the feeding table was pushed by a feed pusher - a kind of robot which can drive and push the forage in the direction of the feeding corridor. Natural manure from the deep litter system was removed by loaders and tractors.

TABLE 3
Microclimatic and building characteristics.

No of barn	Building construction	Cubage	Ventilation	Concentration/ average min.-max. [ppm]		Temperature/average min.-max outside	min. – max. inside	Relative humidity %	Relative humidity %
		$m^3 \cdot DJP^{-1}$	inflow//outflow	NH_3	CO_2	°C	°C	outside	inside
1	three bay construction with pillars	40.67	gravitational/windows//roof ridge gap	4.07 1-8.3	737.13 300-1400	22.87 16.7- 31.6	25.82 20.6-32.08	73.34 40.8-94.6	73.29 46.4-94.43
2	three bay construction with pillars	53.2	gravitational/windows//roof ridge gap	10	1360.29	18.52 16-23	18,29 14.33-23.7	83.38 71.5-93.6	79.54 59.3-95.57
3	three bay construction with pillars	68.41	gravitational/windows//roof ridge gap	3.23 1.67-6.6	715.2 400-1200	18.26 11.4-25.2	21.05 16.19-25.84	18.26 11.41-25.24	64.01 47.9-78.87
4	one room spaced without supporting pillars	126.1	gravitational/windows//roof ridge gap	1.82 0.75-3.4	626.47 475- 900	0.84 0.01-2	1.88 0.69-3.06	65.15 26.7-78.2	77.01 61.8 -81.17
5	two bay construction with pillars	107.8	gravitational/wall gaps//roof ridge gap	8.79 1-17	792.5 300-1733.3	22.36 15.08-34.24	23.92 19.95-26.80	73.86 38.6-96.7	73.30 54.35-86.40
6	three bay construction with pillars	51.02	gravitational/wall gaps// roof ridge gap	10.26 5-15	1313.42 770-2190	16.61 11.9-22.6	14.82 9.10-22.37	76.21 53.7-95.2	75.87 46.56-95.73
7	three bay construction with pillars	66.59	gravitational/windows//roof ridge gap	13.84 2-17	922.17 480-1810	20.28 11.5-29	21.41 17.47-25.43	62.38 26.80-97.5	70.92 35.90-94.47
8	three bay construction with pillars	42.25	gravitational/windows//roof ridge gap	4.5 1.3-7	941.70 500-1750	5.33 1.73-10.93	12.10 9.63-14.63	71.91 39- 90.3	58.48 36.90-69.37
9	three bay construction with pillars	70.64	gravitational/mobile curtains// roof ridge	11.97 0.6-20	845.50 472- 1380	23.07 16.80-	23.69 18.59-	48.14 18.4-67.6	58.31 21.28-
10	three bay construction with pillars	74.43	gravitational/windows// roof ridge gap	6.1 2.3-13.6	665.51 300-1500	18.32 12-23	17.60 13-21.03	59.25 38.10-91	66.47 46.97-83.5
11	one room spaced without supporting pillars	36.7	gravitational/windows//roof ridge gap	9.48 4-15	835.99 540-1400	15.50 11.6-19	14,4 9.83-18.83	81,21 51.7-93.8	73.70 45.82-89.98
12	one room spaced without supporting pillars	39.74	gravitational/windows//roof ridge gap	10.6 3.7-17.5	1500.89 920-1850	8.16 4.63-10.7	10.92 7.8-13.5	92.97 82.6-97.55	80.00 81-96.6

TABLE 4
Unitary labour inputs, investment costs, electrical and mechanical energy inputs.

No of barn	Unitary labour inputs working-minutes $day^{-1} \cdot LU^{-1}$	Unitary investment costs of technical equipment and building $PLN \cdot LU^{-1}$	Unitary electrical energy inputs kWh day^{-1} LU^{-1}	Unitary mechanical energy inputs HPh $day^{-1} \cdot LU^{-1}$
1	6.97	27 747.58	0.569	3.427
2	4.14	16 131.69	0.215	1.351
3	6.62	15 864.59	0.364	1.400
4	5.92	18 510.65	0.397	2.131
5	6.00	20 494.61	0.301	2.006
6	3.54	13585.15	0.257	1.235
7	7.25	22203.93	0.274	3.423
8	4.52	11556.69	0.400	1.170
9	0.78	22193.09	0.826	1.435
10	1.93	26648.38	0.816	1.282
11	3.54	16410.34	0.208	2.437
12	2.96	14992.86	0.269	1.88

In three cubicle cattle barns with litter manure was removed by a manure scraper with total power (longitudinal and cross scraper) from 4 kW (2 barns) to 4.5 kW directly on the manure plate. In one cubical, littered cattle barn, manure was removed by shovel installed on a tractor with 52 HP. Slurry from four non-littered cattle barns was stored in deep channels under a slatted floor and periodically applied on fields.

In addition, in two of the buildings there were robots for cleaning the slatted floors. Table 3 shows the constructional characteristic of the barns tested, The buildings tested were one-room spaced con-

structions or with pillars. The ventilation was gravitational, with the outlet of air by roof ridge gap.

Average ammonia concentration amounted to from 1.82 ppm in a cowshed with deep litter (number 4) to 13.84 in a boxed cattle barn with litter (number 7). The average carbon dioxide concentration amounted to from 626.47 ppm in a cattle barn with deep litter (number 4) to 1500.8 ppm in a cattle barn without litter (number 12). The average temperature inside almost all cattle barns (with the exception of one – with deep litter) did not exceed the recommended temperature of 25 °C.

Table 4 contains economic and energetic values measured in the cattle barns tested. The highest unitary investment costs of buildings and technical equipment for the mechanization of technological treatments were in a barn with deep litter (number 1) and amounted to 27,747.58 PLN·LU^{-1}. In second place, regarding unitary investments costs of equipment and building was cattle barn number 10, with three robots (one for milking, one feed-pusher, one floor scraper) and amounted to 26,648.38 PLN·LU^{-1}. The lowest unitary investment costs were in a boxed cattle barn with litter (number 8), and amounted to 11,556.69 PLN·LU^{-1}. Cattle barns which comply with requirements for the 1st criterion (unitary investment costs, both building and equipment ≤19 000 PLN·LU^{-1}) : 2, 3, 4 ,6, 8, 11 and 12.

Average unitary daily labour inputs amounted to from 0.78 for a robotised barn with robots for milking, feed pushing and removing manure from slatted floors, to 7.25 working-minutes·day^{-1}·LU^{-1} in a barn with the lowest number of cattle. In 7 barns they were below 5 working-minutes·day^{-1}·LU^{-1} (5th level of mechanization), and in 5 they did not exceed 10 working-minutes·day^{-1}·LU^{-1} (4th level of mechanization).The highest human labour inputs occurred for technological treatment, milking, and milk cooling. However, the lowest unitary daily labour inputs were in a cattle barn with two milking robots, and one feed pusher and a slatted floor cleaner robot (number 9), and amounted 0.88 working minutes·day^{-1} LU^{-1}. Cattle barns which comply with requirements for the 2nd criterion (average unitary daily labour inputs ≤ 4.6 working minutes ·day^{-1}·LU^{-1}): 2, 6, 8, 9, 10, 11 and 12.

Cattle barns which comply with requirements for the 3rd criterion (average ammonia concentration ≤ 10.9 ppm, average carbon dioxide concentration ≤ 1500.8 ppm): 1, 3, 4, 5, 6, 8, 10, 11 and 12.

Average electrical energy inputs for four technological treatments were from 0.208 kWh·day^{-1}·LU^{-1} (cowshed number 11) to 0.827 kWh·day^{-1}·LU^{-1} (number 9). Cattle barns which comply with requirements for the 4th criterion (unitary electrical energy inputs ≤ 0.40 kWh): 2, 3, 4, 5, 6, 7, 8, 11,12.

Average mechanical energy inputs amounted to from 1.172 HPh·day^{-1}·LU^{-1} (a boxed cattle barn with litter - number 8) to 3.427 HPh·day^{-1}·LU^{-1} (cowshed number 1) - Cattle barns which comply with requirements for the 4th criterion (average unitary daily mechanical energy inputs ≤ 2 HPh day^{-1}·LU^{-1}): 2, 3, 6, 8, 9,10 and 12.

TABLE 5
Unitary exploitation costs of building and equipment in growing order.

Number of barn	Large Unit	Unitary exploitation costs PLN·year^{-1}·LU^{-1}
6	81	1589.17
8	144	1710.98
2	87	1859.67
3	100	2036.24
12	109	2088.57
11	87	2190.69
7	39	2379.85
5	44	2504.66
9	170	2671.49
10	83	2887.15
4	100	3065.01
1	93	3519.88

Table 5 shows the final results of field research in barns. The best solutions were a boxed cattle barn with litter (number 8) and a boxed cattle barn without litter (number 12). They are barns which fulfilled all limitations. The robotized cattle barns (number 9 and 10) had the highest electrical energy inputs and investments costs, with the lowest human labour inputs.

Field tests showed that technological-functional solutions have an impact on investment costs, energy inputs and the environment.

There are many examples of publications with evaluations of each individual factor (costs of investments, exploitation costs, energy inputs, labour inputs, animal welfare). Methods for the planning of functional-technological solutions of cattle barns are multifarious. Nowadays, electronic media are used for planning the layout of cattle barns and also for cattle housing, including electronic control of microclimate conditions [27].

The lowest labour inputs among 12 cattle barns were in two buildings with robotic milking. According to Schick, the use of robots in comparison with traditional milking systems leads to significant reductions, and even halved labour inputs for its treatment [28, 18, 7, 10], and an observed meaningful reduction of human labour inputs in cattle barns with robotic milking. Sonck writes that labour inputs are reduced in robotic milking buildings (RMB) by about 37% to 66.1% [29]. According to de Koning, compared with the conventional twice daily milking, there is an average of 20%-30% reduction in total labour with robotic milking [13, 14]. Our tests showed reductions of 62 to 74% of labour inputs compared to traditional milking.

Burton and Turner indicated there are over one

hundred different gases and substances emitted from housing buildings for farm animals [2]. According to Polish regulations, concentrations of harmful gases should be at levels which should be safe for animals. For calves it should not exceed 3000 ppm of carbon dioxide and 20 ppm of ammonia [20, 21]. Average concentrations of both gases in the 12 cattle barns tested were below half of the values allowed by these regulations.

Ngwabie investigated the correlation between methane and ammonia emissions and the internal temperature of cowsheds. There was a high correlation (r=0.66) between these factors [19]. Dairy cattle are sensitive to heat stress because of the high metabolic heat production and feed intake associated with rumen fermentation and milk yield [3].

CONCLUSION

1. The best solutions which fulfilled all limitations were two boxed barns: with (number 8) and without litter (number 12. In the first barn the most important indicators which led to the final evaluation as the best solutions were as follows:

- investments costs 11556.69 PLN LU^{-1}, labour inputs 4.52 working-minutes day^{-1} LU^{-1} , electrical energy inputs 0.4 kWh day^{-1} LU^{-1}**,** mechanical energy inputs 1.17 HPh·day^{-1}·LU^{-1} and exploitation costs 1710.98 PLN $year^{-1}$ LU^{-1}. In the second barn (non-littered, boxed) investments costs amounted to 14992.86 PLN·LU^{-1}, labour inputs 2.96 working-minutes day^{-1}·LU^{-1}, electric energy inputs 0.4 kWh day^{-1} LU^{-1}**,** mechanic energy inputs 1.88 HPh·day^{-1} LU^{-1} and exploitation costs 2088.57 PLN·$year^{-1}$ LU^{-1}.

2. Although the best cattle barns (number 8 and 12) had large numbers of animals (144 LU and 170 LU respectively), the microclimate conditions, especially concentrations of harmful gases, temperature of the air and relative humidity, did not exceed the recommended values. This was because they had good ventilation solutions.

3. Robotising the main technological treatments in milk production led to low human labour inputs. In two robotised cattle barns with robots for milking, feed pushing and slatted floor cleaning there were low labour inputs observed, amounting to 0.78 and 1.93 working minutes ·day^{-1}·LU^{-1}.

4. Also, cleaning of slatted floors by robots led to relatively low concentrations of harmful gases NH_3 and CO_2, which amounted in these robotised barns (number 9 and 10) respectively to 11.97 ppm and 6.1 ppm for NH_3 and 845.5ppm and 665.5 ppm for CO_2, which is about or below half the recommended levels.

REFERENCES

[1] BN-86/880-03, Branch Norm "Microclimate in livestock buildings". *IBMER*, *Poland*, pp. 287.

[2] Burton, C.H., Turner, C. (2003) Manure Management: Treatment Strategies for Sustainable Agriculture. *Silsoe Research Inst., Bedford, UK*, pp. 450.

[3] Collier, R.J., Hall, L.W., Zimbleman, R.B. (2012) Quantifying Heat Stress and Its Impact on Metabolism and Performance. *Department of Animal Sciences University of Arizona*, pp. 68.

[4] DAAS (2001) Housing Design for cattle. Danish Recommendations, Third edition. *Danish Agricultural Advisory Center, Skejby, Denmark*, pp.122.

[5] Fernandez, M.E. (2008) Relationship between layout and timber structures in free-stall dairy cattle barns: influence of internal features. *Biosystems Engineering* 100, 266-280.

[6] Fiedorowicz, G., Mazur, K. (2011) Microclimate inside the buildings of free-stall cattle barns during spring-summer season. Part I, *Problems of Agriculture Engineering*, 1(71), ITP, Poland, 123-134.

[7] Freiberger, F., Klindtworht, K., Baumeister, J., Gierse, A., Lehman, B., Ohnesorge, M.,Harms, J., Wendl, G. (2005) Automatische Melken in modernen Milchviehställe. *KTBL, Darmstadt*, pp. 141.

[8] Gazzarin, C. (2011) Maschinenkosten ART– Bericht 747, *Tänikon* pp. 56.

[9] Gazzarin, C., Lips, M. (2013) Maschinenkosten, ART-Bericht 767, ISSN 1661-756, pp. 52.

[10] Hogeveen, H., Meijering, A. (2000) Robotic milking, *Proc. Int. Symp. Wageningen, The Netherlands, Wageningen Pers*, 201–211.

[11] Kocira, S., Kołtun, M. (2013) Energy inputs in the farms with balanced renewability of organic matter. *Problems of Agricultural Engineering*, 2(80), 99-106.

[12] Kocira, S., Sawa, J. (2005) Mechanization cost in farms of various economic size. *Agricultural Engineering* 6(66), 321-328.

[13] Koning, C.J.A.M. (2011a) Automatic milking – Common practice on dairy farms, Available form:http://citeseerx.ist.psu.edu/viewdoc/download?doi=10.1.1.464.8614 &rep=rep1&type=pdf.

[14] Koning, C.J.A.M. (2011b) Encyclopedia of Dairy Sciences, (Second Edition), 952–958, Available from: http://dx.doi.org/10.1016/B978-0-12-374407-4.00360-5.

[15] Lautner, M., Miller, A.M. (2003) Kühe lieben keine heißen Tage sondern kühlen Kopf, Nachrichtsblatt Besammungsbv Neustadt a. d. Aisch., 149: 23–25, in: Jaśkowski M. Urbaniak K. Olechnowicz J. (2005) Fertility disturbances caused by heat stress in cows – prophylactic measurements. *Życie Weter.,* 80 (1), 18–21.

[16] Muzalewski, A. (2010) Koszty eksploatacji maszyn. *ITP, Falenty, Poland*, 25, pp. 56.
[17] Næss, G., Bøe, K.E. (2011) Labour input in small cubicle dairy barns with different layouts and mechanization levels. *Biosystems Engineering* 110(2), 83- 89.
[18] Næss ,G., Stokstad, G. (2011) Dairy barn layout and construction: Effects on initial building costs. *Biosystems Engineering* 109(3), 196-202.
[19] Ngwabie, N.M., Jeppsson, K.H., Gustafsson, G., Nimmermark, S. (2011) Effects of animal activity and air temperature on methane and ammonia emissions from a naturally ventilated building for dairy cows. *Atmospheric Environment* 45(37), 6760-6768.
[20] Regulation (2010a) Rozporządzenie Ministra Rolnictwa I Rozwoju Wsi z dnia 28 czerwca w sprawie minimalnych warunków utrzymywania gatunków zwierząt gospodarskich, innych niż te, dla których normy ochrony zostały określone w przepisach UE, Dz.U. 2010, No 116, §778.
[21] Regulation (2010b) Rozporządzenie Ministra Rolnictwa I Rozwoju Wsi z dnia 15 lutego 2010 w sprawie wymagań i sposobu postępowania przy utrzymywaniu gatunków zwierząt gospodarskich, dla których normy ochrony zostały określone w przepisach UE, Dz. U, Nr 56, §344.
[22] Regulation (2013) In matter of technical conditions, which should comply agricultural buildings and their situating. Dz. U. No 74, §472, Ministry of Agriculture and Rural Development.
[23] Romaniuk, W., Overby, T. (2005) Housing systems for cattle, Handbook, Danish Agriculture Advisory Service, Institute for Building. *Mechanization and Electrification of Agriculture*, pp. 156
[24] Romaniuk, W. (2010) Current directions in the scope of building and technical equipment of modern cattle barns, (in Polish). *3rd Conference – Exhibition Cattle Farm, High School of Agribusiness*, November 20-21, Lomza, Poland, 23-25.
[25] Romaniuk, W., Rudnik, K., Biskupska, K. (2012) Formation of building objects and farmstead sites in the farms specialized in cattle raising – designing guidelines. *Engineering in Agriculture*, 5, pp. 152
[26] Romaniuk, W., Mazur, K., Rudnik, K., Biskupska, K. (2014) Complex evaluation of technological standards and building modules in cattle housing. *Engineering in Agriculture*, 17, pp 134.
[27] Samer, M., Loebsin, C., von Bobrutzki, K., Fiedler, M., Ammon, C., Berg, W., Sanftleben, P., Brunsch, R. (2011) A computer program for monitoring and controlling ultrasonic anemometers for aerodynamic measurements in animal buildings. *Computers and Electronics in Agriculture* 79(1), 1-12.
[28] Schick, M., Volet, M.R., Kaufmann, R. (2000) Modelling of time requirements and milking capacity in automatic milking systems with one or two milking stalls, 32-37. In: H. Hogeveen and A. Meijering (editors) *Robotic milking. Wageningen Pers, Wageningen*.
[29] Sonck, B.R. (1996) Labour organisation on robotic milking dairy farms, PhD thesis, *Wageningen Agricultural University*, pp. 201.
[30] Szulc, R. (2012) Results of operational research and functional solar system in the household. *Journal of Applications in Agricultrural,* 57(2), 171-174.
[31] Zegar, J.S. (editor). (2013) Z badań nad rolnictwem społecznie zrównoważonym (20). Wybrane zagadnienia zrównoważonego rozwoju rolnictwa, *IERGŻ*, ISBN 978-83-7658-431-7, pp. 217.

Received: **13.03.2017**
Accepted: **07.08.2017**

CORRESPONDING AUTHOR

Andrzej Borusiewicz
Higher School of Agribusiness in Lomza Faculty of Agriculture and Economy 18402 Lomza, Poland

e-mail: andrzej.borusiewcz@wsa.edu.pl

© by PSP Volume 26 – No. 10/2017 pages 5833-5840 Fresenius Environmental Bulletin

EXPERIMENTAL STUDY ON THE EFFECTS OF ULTRA-LOW SULFUR DIESEL FUEL TO THE EXHAUST EMISSIONS OF A FERRY

Murat Durmaz, Saliha Saadet Kalender, Selma Ergin*

Istanbul Technical University, Faculty of Naval Architecture and Ocean Engineering, Maslak 34469 Istanbul, Turkey.

ABSTRACT

Ship emissions have a significant contribution to the global emissions and have adverse effects to the environment and human health. This study investigates the effects of ultra-low sulfur diesel fuel on the gaseous and PM emissions of a ferry, experimentally. On-board emission measurements were carried out both for the main and auxiliary engines which are four-stroke medium speed diesel engines. The concentrations of NOx, SOx, CO, CO_2, O_2, PM and HC were measured for various engine loads. The shaft power measurements were also performed. The weighted emission factors, monthly and annual emissions of the ferry are calculated using the experimental data. The weighted emission factors of NOx, SOx, CO, CO_2, HC and PM emissions for the main engine are found to be 11.91 g/kWh, 0.10 g/kWh, 0.67 g/kWh, 611.14 g/kWh, 0.62 g/kWh and 0.079 g/kWh, respectively. For the auxiliary engine, the weighted emission factors of NOx, SOx, CO, CO_2 and HC are respectively, 13.01 g/kWh, 0.11 g/kWh, 2.19 g/kWh, 641.69 g/kWh and 1.31 g/kWh. The amount of emissions from the ferry is found to be maximum in the summer season. The results show that the emission factors are the major parameter in the emission inventory studies and should be defined carefully. It is seen that the ship emissions, especially SO_2 and PM emissions can be reduced substantially by using the ultra-low sulfur diesel fuel. Therefore, the sustainability of the maritime transport can be improved by utilizing the ultra-low sulfur diesel fuel for the propulsion of ships.

KEYWORDS:
ship emissions; emission measurements; ultra-low sulfur diesel; ferry; marine diesel engine; air pollution.

INTRODUCTION

Emissions generated by the maritime transport represent a significant contribution to the global emissions and they have adverse effects to the environment as well as human health [1-7]. The marine diesel engines are mostly used in the propulsion of the ships. The emissions are generated by the combustion of the fuel in these engines. The exhaust emissions of diesel engines primarily include carbon dioxide (CO_2), carbon monoxide (CO), sulphur oxides (SOx), nitrogen oxides (NOx), hydrocarbons (HC) and particulate matters (PM). CO, NOx and PM originate from engine technology whereas CO_2, SOx, heavy metals and further PM (sulphur compounds) become from fuel property [8]. Therefore, the sustainability of the shipping can be improved by utilizing the ultra-low sulfur diesel fuel for the propulsion [9, 10].

Due to the essential contribution of sea transport to global air pollution, ship based emissions have become a great concern in many studies recently. For example, Corbett et al. [3], Yau et al. [11] and Adamo et al. [12] were carried out detailed emission inventory studies for the merchant ships. Bilgili and Celebi [13] calculated the annual emissions of three different cargo ships by using annual cruise data. These studies show that maritime transport is the most energy efficient and clean mode of transport in terms of the load and distance transported. However, when the ships passing close to the shore, their emission can affect the human health and enviroment adversely. Ergin [14] calculated the exhaust emissions from ships sailing through Turkish Straits and Marmara sea using 2010 AIS data and national statistics. The number of ships passing through the Turkish Straits are respectively, 50871 and 46686 in 2010. The estimated emissions from these vessels were 56.49 ktonnes/year of NOx emissions, 18.57 ktonnes/year of SO_2 emissions, 2518.2 ktonnes/year of CO_2 emissions, and 18.57 ktonnes/year of PM emissions. In this study, the cost and benefit analysis of reducing emissions were also carried out for different scenarios. The results show that a substantial improvement in the air quality for Marmara region could be achieved by applying the ECA (Emission Control Area) emission limits for the ships passing through Turkish straits and Marmara region [15]. Also, Viana et al. [16] show that the implementation of ECA emission limits for ships in Bosphorous Strait would reduce the ship sourced PM and SO_2 ambient concentrations in Istanbul by 67% and 90%, respectively. Previous emission inventories of Marmara Sea were presented in the studies of Kesgin and Vardar [17] and Deniz and

Durmuşoğlu [18]. These studies show that the shipping activity in the Marmara Sea has increased substantially in the last fifty years and the ships in this region have a significant contribution to the local emissions.

In addition to emission inventory studies there are also experimental studies about ship emissions. However, there are a few number of experimental studies. For example, Winnes and Fridell [19] carrried out on board emission measurements at a product tanker by using HFO and MGO for various engine loads. Change of fuels and their effects on exhaust gas composition and emission factors were investigated. Uriondo et al. [20] compared the NOx mesurements of a marine diesel engine taken in the laboratory with the measurements taken during the operation of the ship at sea. Recently, Kowalski [21] examined the relation between exhaust emission of marine engine and malfunctions of a fuel pump such as fuel injection timing delay and fuel leakages in one of the fuel pump. As a result of measurements, fuel injection timing delay caused increase of CO_2 emissions and decrease of NOx emissions. CO emissions increase only at high engine loads. Fuel leakage in the fuel pump caused changes in CO emissions. CO_2 emissions increased and NOx emissions decreased, based upon the fuel leakage.

The main aim of this study is to investigate the effects of ultra-low sulfur diesel fuel on the gaseous and PM emissions of a ferry sailing at Marmara sea, experimentally. This study extends the previous works of authors ([22, 23]) by considering the effects of the ultra-low sulfur diesel fuel on the emissions of both the main and auxiliary engines, different engine loads, monhtly emissions of the ferry, annual emissions of the ferry and different emission factors. Therefore, this study presents an original research results and it has novelty. In the study, on-board measurements of NOx, SOx, CO, CO_2, HC and PM emissions of the main and auxiliary engines were carried out for various engine loads. In order to obtain the weighted emissions, the shaft power is also measured. The emission factors for different loads, the weighted emission factors, monthly emissions and annual emissions with different emission factors are presented and discussed. The results show that the ship emissions, especially SO_2 and PM emissions can be reduced substantially by using the ultra-low sulfur diesel fuel for the propulsion of the ships.

EXPERIMENTAL METHODOLOGY

The gaseous and particle emission measurements were carried out on a ferry sailing at Marmara Sea. The ferry was built in 2000 with a tonnage of 1600 GRT and it is 81 m long. Therefore, it should comply with the NOx emission limits, Tier I. She has two four-stroke medium speed main engines, each with 883 kW at rated speed of 750 rpm. The specific fuel consumption of the main engine is 198 g/kWh. On the other hand, the ferry has three four-stroke medium speed auxiliary engines, each with 175 kW at rated speed of 1500 rpm.

During the experimental study, the ultra-low sulfur diesel fuel (ULSD) were used in the main and auxiliary engines. Table 1 presents the fuel properties.

TABLE 1
Properties of the ultra-low sulfur diesel fuel

Fuel Property	
Density, kg/m^3	831.1
Water content, mg/kg	48
Sulfur, mg/kg	4.4
Cetan Index	58.6

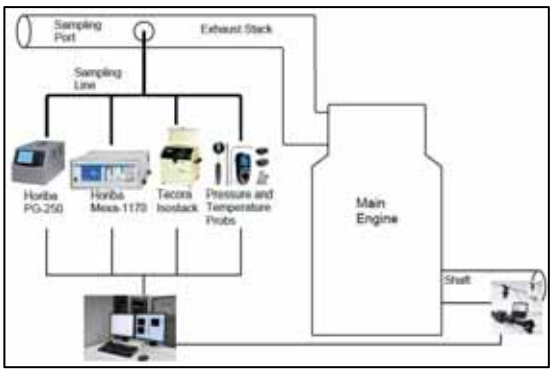

FIGURE 1
Experimental set-up

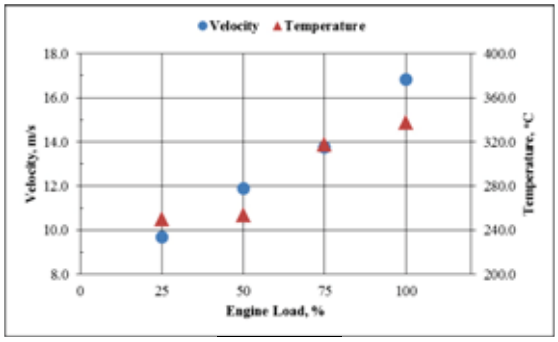

FIGURE 2
Exhaust temperatures and velocities for the main engine

The emission sampling was performed in the stacks of both main and auxiliary engines in the engine room at different engine loads. The measurements were done in accord with the IMO MARPOL Annex VI. E2 test cycle for the main engine and D2 test cyle for the auxiliary engine were employed [15].

Figure 2 presents the experimental set-up, schematically. The sampling port were placed after the turbocharger. The shaft power, exhaust temperature, exhaust humidity and differential pressure were measured. Furthermore, the ambient

pressure, temperature and humidity were also taken.

During the measurements, shaft power measurement system was monitored continuously. The engine brake power was measured on shaft by fixing strain gauges for different loads. Reduction gear losses were considered to be 5%.

The concentrations of NOx, SO_2, CO, CO_2 and O_2 were measured in raw exhaust gas using Horiba PG-250 gas analyser at the engine loads of 25%, 50% 75%, and 100% for the main engine and at the engine loads 10%, 25%, 50% and 75% for the auxiliary engine. According to D2 test cycle used for the auxiliary engine, the engine loads of 10%, 25%, 50%, 75% and 100% should be considered. During the measurements, it was not possible to load the auxiliary engine with 100% load. Therefore, the measurements for 100% load are absent for the auxiliary engine. Unburned HCs were measured by Horiba Mexa 1170. The particles were collected only for the main engine by using Tecora Isostack Basic Equipment. Particle mass was collected by using 47 mm glass-micro fibre filters that was analyzed gravimetrically, weighted before and after sampling using a micro balance in the laboratory. The sampling took around 30 minutes at nearly steady state conditions ensuring isokinetic flow rate. During the sampling, isokinetic deviation was around 10% that was acceptable value regarding the ISO 9096 standard [24].

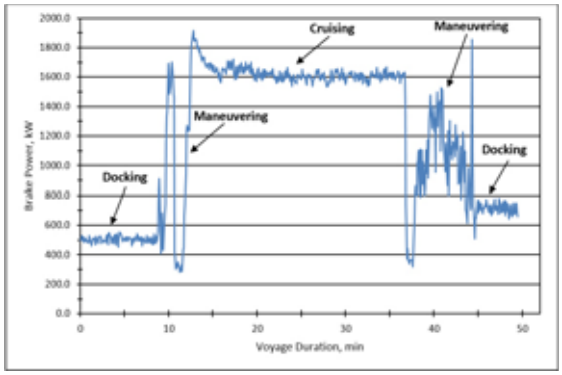

FIGURE 3
The voyage durations for different phases of a trip

The exhaust temperature and velocity distributions at different loads are shown in Figure 3. The temperarture and velocity values increases as the engine load increases. The samples at different loads were taken at the exhaust gas temperatures between 250°C and 350°C. The velocity values are between about 10 m/s and 17 m/s for the engine loads considered. The weighted emission factors for gas pollutants and particulate matters were calculated using the methodology given in IMO NOx Technical Code [15].

ESTIMATION OF THE EMISSONS

The annual emissions of the ferry were calculated by using bottom-up approach and the methodology given in Refs. [14, 25 and 26]. The ferry sails between Gebze and Yalova at Marmara Sea in Turkey. A trip of the ferry consists of two docking, two maneuvering and the cruising phases. The voyage durations for each phases of the trip are shown in Figure 3. As can be seen from the Figure that the total duration of a trip is about 50 minutes. Figure 3 also shows the measured shaft power for each phases of the trip. Firstly, the emissions for the docking, maneuvering and cruising phases of a trip were calculated, and then they are summed to find the total emissions for the trip.

The voyage numbers per month are given in Table 2. The ferry had a total of 8725 voyages or trips in 2015. There are 18 similar ferries sailing at the same route in this region. These information was taken from the ferry company, Istanbul Sea Buses Co., IDO. During the calculations, firstly, total emissions for the trip was multiplied with the voyage numbers per month to obtain the monthly emissions and then they are summed to obtain the annual emissions of the ferry. The annual emission calculations were also carried out by using the emission factors given in references [27, 28].

TABLE 2
The voyage numbers

Month	Voyage Number
January	646
February	575
March	710
April	714
May	748
June	720
July	833
August	835
September	763
October	751
November	717
December	713

RESULTS AND DISCUSSION

The measured emission factors of nitrogen oxides (NOx), sulfur dioxide (SO_2), carbon dioxide (CO_2), carbon monoxide (CO), hydracorbons (HC) and particulate matters (PM) for different loads are presented in Figures 4-9 for the main engine. The overall weighted emission factors are also showed in these figures.

It can be seen from Figure 4 that the measured NOx emission factors are between about 11.0 and 16.0 g/kWh. The emissions of NOx mainly depend on the engine combustion temperature, so, the emission values of NOx increase with the engine load.

However, NOx emissions are highest at 25% engine load due to the lean mixture of air/fuel ratio [29]. The overall weighted NOx emission factor is found to be 11.91 g/kWh which is just under the limit value 11.97 g/kWh set by the IMO regulations [15].

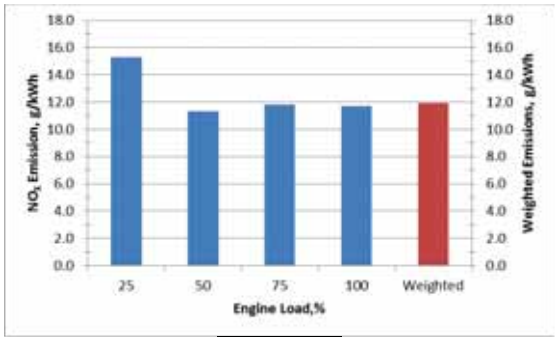

FIGURE 4
NOx emissions for the main engine

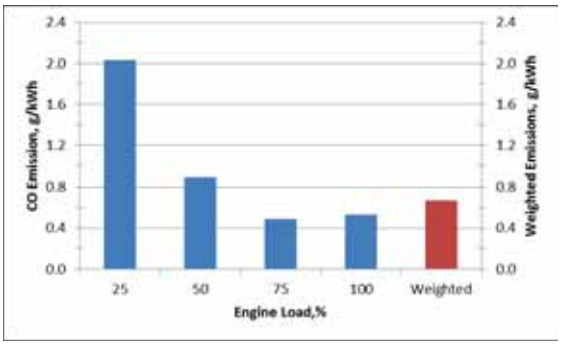

FIGURE 5
CO emissions for the main engine

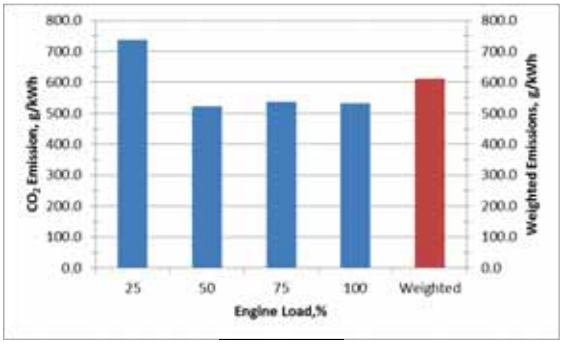

FIGURE 6
CO_2 emissions for the main engine

CO emissions occur as a result of incomplete combustion of fuel. Mostly they increase with engine load due to the lack of oxygen. As seen from Figure 5, the highest value of CO emission is at the engine load of 25%. This is due to the low temperatures in the combustion chamber which affect the fuel atomization [30]. The emissions of CO_2 and SO_2 are related to fuel properties [8]. However, there are some differences in the distributions of the emissions with this behavior as seen from Figure 6 and 7. The reason may be related to the performance of the engine at partial loads which is worse due to cold start up, inadequate atomization, low combustion temperature, heat losses from combustion chamber and etc. As can be seen from Figures 5-7, the overall weighted emission factors for CO, CO_2 and SO_2 are 0.67 g/kWh, 611.14 g/kWh and 0.10 g/kWh, respectively.

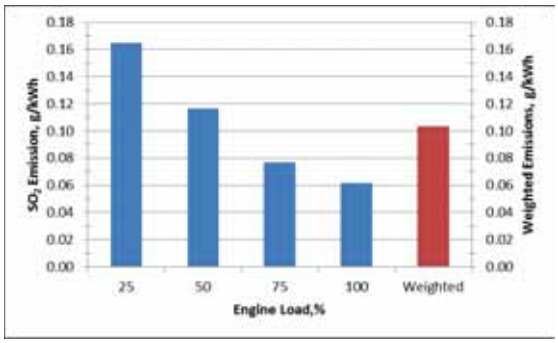

FIGURE 7
SO_2 emissions for the main engine

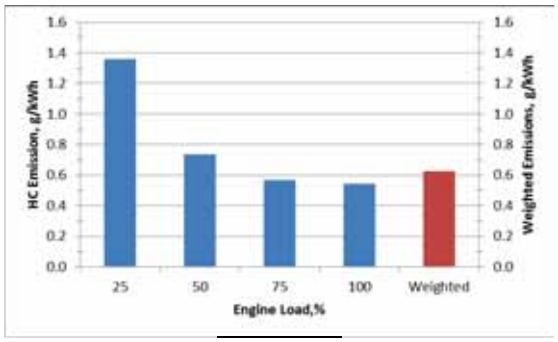

FIGURE 8
HC emissions for the main engine

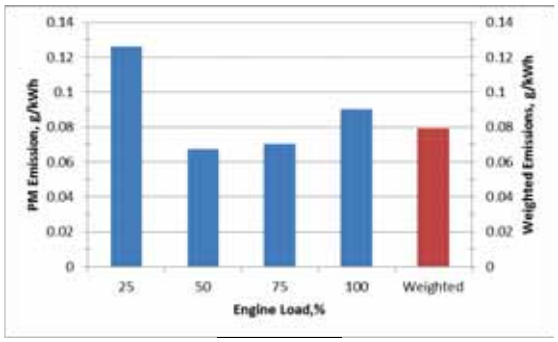

FIGURE 9
PM emissions for the main engine

In general, the emissions of unburned HC occur as a result of incomplete combustion of the hydrocarbon fuel [31]. The results presented in Figure 8 show that unburned HC emissions increase at partial loads. The overall weighted emission factor for the HC emission is obtained as 0.62 g/kWh.

Particulate matter emissions mostly depend on sulfur content in the fuel [32, 33, 34]. In this study, ultra-low sulfur diesel fuel is used. Therefore, the particulate emissions are quite low as seen from Figure 9. The overall weighted PM emission factor is obtained as 0.079 g/kWh. As can be seen from Figure 9, the highest PM emissions were observed at

the 25% engine load. This may be due to the low combustion efficiency that may influence the particle formation.

The uncertainty analysis of the measurements is carried out. The results show that the uncertainties of the gaseous emission measurements are in the range of 10-12%. The uncertainties in PM measurements are less than 13%.

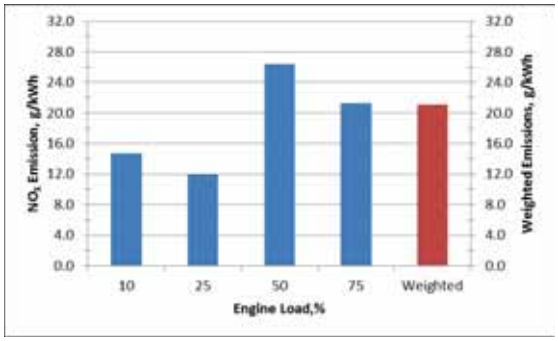

FIGURE 10
NOx emissions for the auxiliary engine

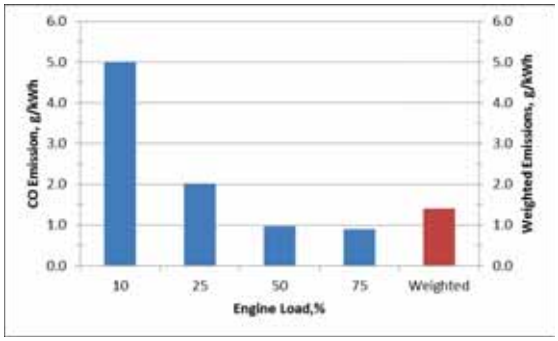

FIGURE 11
CO emissions for the auxiliary engine

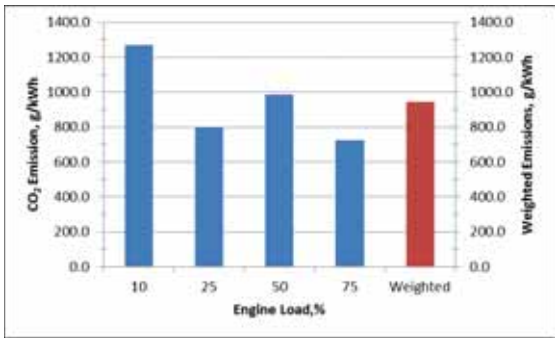

FIGURE 12
CO_2 emissions for the auxiliary engine

Figures 10-14 show the measured emission factors of the auxiliary engine for the engine loads of 10%, 25%, 50% and 75%. The overall weighted emissions are also presented in these Figures.

As can be seen from Figure 10, the NOx emission factors for different loads are between 14 and 21 g/kWh. The emissions of NOx mainly depend on the engine combustion temperature, so, the emission values of NOx increase with the engine load. The highest emission factor is about 27.0 g/kWh and occurs at the engine load of 50%.

Figure 11 shows CO emission factors of the auxiliary engine for different engine loads. The CO emission factors decrease as the engine load increases. The highest value of CO emission is at the engine load of 25%. This is as a result of the low temperatures in the combustion chamber which affect the fuel atomization. In general, the CO emissions occur as a result of incomplete combustion of fuel.

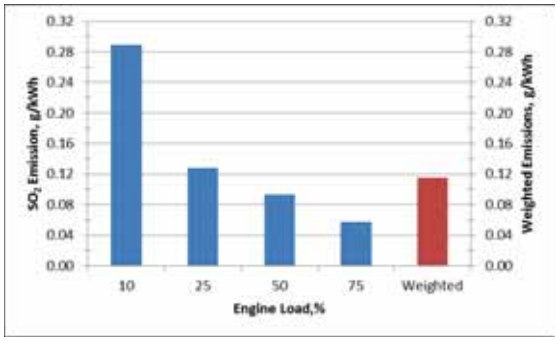

FIGURE 13
SO_2 emissions for the auxiliary engine

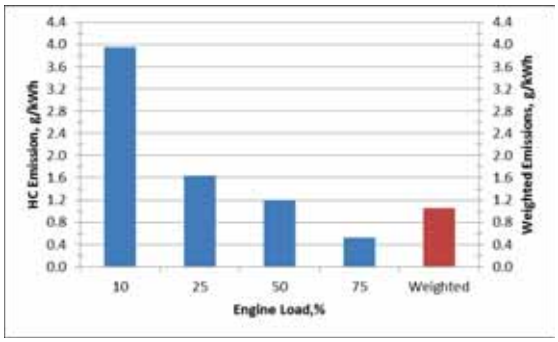

FIGURE 14
HC emissions for the auxiliary engine

In general, the emissions of CO_2 and SO_2 depends on the fuel properties. As seen from Figures 12 to 14, the CO_2, SO_2 and also HC emission factors decrease with increasing engine load. The highest values of emission factors occur at 10% engine load. Since, the combustion performance of the engine at partial loads is worse due to cold start up, inadequate atomization, low combustion temperature, heat losses from combustion chamber and etc.

The overall weighted NOx, SO_2, CO, CO_2 and HC emission factors of the auxiliary engine are obtained as 21.07 g/kWh, 0.12 g/kWh, 1.4 g/kWh, 942.75 g/kWh, and 1.05 g/kWh, respectively (see, Figures 10-14). Considering the operation profile of the ferry, the more realistic weighted emission factors can be calculated by modifying the weighting coefficients given for D2 test cycle from 0.1, 0.3, 0.3 and 0.3 to 0.3, 0.5, 0.15 and 0.05. In this case, the overall weighted emission factors for NOx, SO_2, CO, CO_2 and HC emissions are obtained as 13.01 g/kWh, 0.11 g/kWh, 2.19 g/kWh, 641.69 g/kWh and 1.31

g/kWh, respectively. Furthermore, the results show that the overall weighted NOx emission value (13.01 g/kWh) for the auxiliary engine is about 25% higher than the limit value (10.42 g/kWh) set by the IMO regulations [15].

The SO_2 and PM emissions both for the main and auxiliary engines are found to be quite low. This indicates that the sustainability of the maritime transport may be improved by using the ultra-low sulfur diesel fuel for the propulsion of the ships.

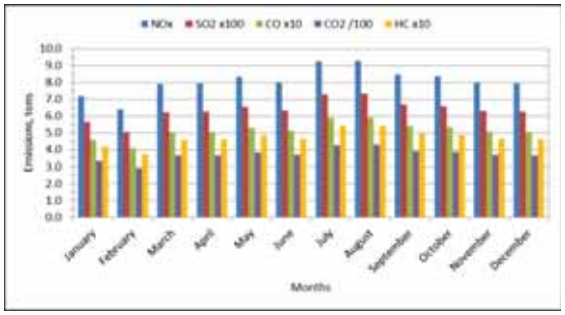

FIGURE 15
The monthly emissions of the ferry

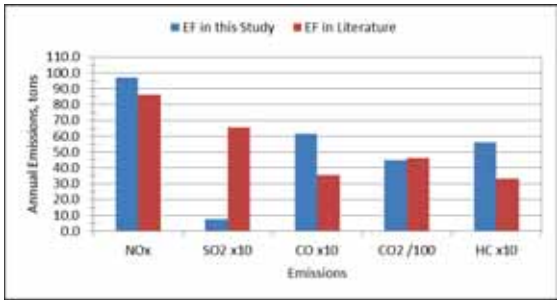

FIGURE 16
The comparison of the annual emissions of the ferry

Figures 15 and 16 present the estimated emissions of the ferry based on the experimental data of the main engine. The monthly emissions of the ferry for NO_X, SO_2, CO_2, CO and HC are presented in Figure 15. It can be seen that the highest emission values are obtained for the month of August. It can be said that the amount of emissions emitted from the ferry is highest for the summer season. This can be attributed mainly to the high voyage numbers during the summer season.

Figure 16 compares the annual emissions of the ferry obtained with the experimental emission factors of this study and the emission factors from the literature. The emissions of the ferry were calculated for NO_X, SO_2, CO_2, CO and HC emissions and the results are annually, 100.7 tonnes of NOx, 0,8 tonnes of SO_2, 4709.8 tonnes of CO_2, 6.8 tonnes of CO and 6.2 tonnes of HC. The annual CO_2 emissions per gross tonnage of the ferry is obtained as 2.95 tonnes/GT. According to the results presented in Figure 16, the annual NOx emissions is about 11 % higher than the results obtained using the emission factors available in the literature. Similarly, the CO and HC emissions are respectively, 42% and 41% higher than the results obtained with available emission factors. The annual CO_2 emissions are almost the same for both cases. On the other hand, the annual SOx emissions are quite high for the results obtained using the available emisson factors. The reason for this, the emission factor from the literature was for the fuel type with higher sulfur rate. The results show that the emission factors in the literature may give quite different emission values. Therefore, they should be used with care in emission inventory studies.

CONCLUSIONS

The effects of the ultra-low sulfur diesel fuel on the emissions of a ferry are investigated, experimentally. The NOx, SOx, CO, CO_2, HC and PM emissions from the main and auxiliary engines are measured on-board ferry sailing at Marmara Sea. The annual emissions of the ferry are estimated by using experimental emission factors and bottom-up approach. The overall weighted emission factors for NOx, SOx, CO, CO_2, HC and PM emissions from the main engine of the ferry are obtained as 11.91 g/kWh, 0.10 g/kWh, 0.67 g/kWh, 611.14 g/kWh, 0.62 g/kWh and 0.079 g/kWh, respectively. According to the results, the overall weighted NOx emission value for the main engine is just under the IMO limit value of 11.97 g/kWh. On the other hand, the overall weighted NOx emission value of 13.01 g/kWh for the auxiliary engine is higher than the limit value of 10.42 g/kWh. The SO_2 and PM emissions are obtained to be quite low. This is a result of using ultra-low sulfur diesel fuel for the engines. The results also indicate that the emissions at partial loads have the highest values. Furthermore, the uncertainty analysis are also carried out. The uncertainties of the emission measurements are obtained less than about 13%.

The monthly emissions of the ferry show that the highest emission values are obtained for August and for the summer season. This can be attributed mainly to the high voyage numbers during the summer season. The annual emissions of the ferry were obtained as 100.7 tonnes of NOx, 0.8 tonnes of SO_2, 4709.8 tonnes of CO_2, 6.8 tonnes of CO and 6.2 tonnes of HC. Comparisons between the annual emissions of the ferry and the results obtained using the available emission factors show that the estimations of the annual emissions can be quite different. Therefore, the emission factors for the emission inventory studies should be chosen carefully.

The study show that the emissions from ships may have an important impact on the public health and regional air quality in the Marmara Sea. Considering the increasing shipping activity at the Marmara sea, the ship emissions are becoming

dominant source of air pollution and the ship emissions should be reduced. Therefore, experimental studies on emissions are beneficial to foresee and reduce the impacts of ship emissions on the regional and global air quality.

The SO_2 and PM emissions both for the main and auxiliary engines are substantially reduced by using the ultra-low sulfur diesel fuel. Therefore, the sustainability of the maritime transport can be improved by using the ultra-low sulfur diesel fuel for the propulsion of ships.

ACKNOWLEDGEMENTS

The authors thank the ship owner company, IDO for their support on the experimental study. Also, masters, chief engineers and crew are thanked for their help during on-board measurements.

The study was partially supported by the Research Projects Coordination Unit (BAP), Istanbul Technical University, Turkey. The authors also thank them for the financial support.

REFERENCES

[1] Cofala, J., Amann, M., Heyes, C., Wagner, F., Klimont, Z., Posch, M., Schoepp, W., Tarasson, L., Whall, C. & Stavrakaki, A. (2007). Analysis of policy measures to reduce ship emissions in the context of the revision of the national emissions ceilings directive. *Laxenburg: International Institute for Applied Systems Analysis*.

[2] Cooper, D. (2001). Exhaust emissions from high speed passenger ferries. *Atmospheric Environment, 35*(24), 4189-4200.

[3] Corbett, J.J., Fischbeck, P.S., & Pandis, S.N. (1999). Global nitrogen and sulfur inventories for oceangoing ships. *Journal of Geophysical Research: Atmospheres (1984–2012), 104*(D3), 3457-3470.

[4] Corbett, J.J., & Koehler, H.W. (2003). Updated emissions from ocean shipping. *Journal of Geophysical Research: Atmospheres (1984–2012), 108*(D20).

[5] Corbett, J.J., Winebrake, J.J., Green, E.H., Kasibhatla, P., Eyring, V., & Lauer, A. (2007). Mortality from ship emissions: a global assessment. *Environmental Science & Technology, 41*(24), 8512-8518.

[6] Dalsøren, S.B., Eide, M., Endresen, Ø., Mjelde, A., Gravir, G., & Isaksen, I. S. (2008). Update on emissions and environmental impacts from the international fleet of ships. The contribution from major ship types and ports. *Atmospheric Chemistry and Physics Discussions, 8*(5), 18323-18384.

[7] Endresen, Ø., Dalsøren, S., Eide, M., Isaksen, I., & Sørgård, E. (2008). *The environmental impacts of increased international maritime shipping–Past trends and future perspectives.* Proc.of the Global Forum on Transport and Environment in a Globalising World, Guadalajara, Mexico, November.

[8] Entec (2002). Quantification of emissions from ships associated with ship movements between ports in the European Community. *Report for the European Commission. Entec UK Limited, Northwich, Great Britain*.

[9] Winebrake, J., Corbett, J., Green, E., Lauer, A., & Eyring, V. (2009). Mitigating the health impacts of pollution from oceangoing shipping: an assessment of low-sulfur fuel mandates. *Environmental Science & Technology, 43*(13), 4776-4782.

[10] Peksen, D.Y., Alkan, G., Bayar, S., Yildiz, M., & Elmas, G. (2016). LNG As Ship Fuel For SOx Emission Reduction Target In The Sea Of Marmara. *Fresen. Environ. Bull., 25*(5), 1406-1419.

[11] Yau, P.S., Lee, S.C., Corbett, J.J., Wang, C., Cheng, Y., & Ho, K.F. (2012). Estimation of exhaust emission from ocean-going vessels in Hong Kong. *Sci Total Environ, 431*, 299-306.

[12] Adamo, F., Andria, G., Cavone, G., De Capua, C., Lanzolla, A.M.L., Morello, R., & Spadavecchia, M. (2014). Estimation of ship emissions in the port of Taranto. *Measurement, 47*, 982-988.

[13] Bilgili, L., & Celebi, U.B. (2015). Emission Estimation Of Cargo Ships According To Ship Main Dimensions And Annual Emisson Footprint Calculation. *Fresen. Environ. Bull., 24*(3b), 1054-1062.

[14] Ergin, S. (2011). Controlling of Ship-Source Air Pollution, Final Report, Supported by Turkish Ministry of Environment and Urban Planning.

[15] IMO (2009). *Revised MARPOL Annex VI: Regulations for the Prevention of Air Pollution from Ships and NOx Technical Code 2008*: International Maritime Organization.

[16] Viana, M., Hammingh, P., Colette, A., Querol, X., Degraeuwe, B., Vlieger, I. d., & Van Aardenne, J. (2014). Impact of maritime transport emissions on coastal air quality in Europe. *Atmospheric Environment, 90*, 96-105.

[17] Kesgin, U. and Vardar, N. (2001). A study on exhaust gas emissions from ships in Turkish Straits. *Atmospheric Environment, 35*(10), 1863-1870.

[18] Deniz, C. and Durmuşoğlu, Y. (2008). Estimating shipping emissions in the region of the Sea of Marmara, Turkey. *Science of the total environment, 390*(1), 255-261.

[19] Winnes, H., & Fridell, E. (2009). Particle emissions from ships: Dependence on fuel type. *Journal of the Air & Waste Management Association, 59*(12), 1391-1398.

[20] Uriondo, Z., Grados, C.V.D., Clemente, M., Gutiérrez, J.M., & Martín, L. (2011). Effects of charged air temperature and pressure on NOx emissions of marine medium speed engines. *Transportation Research Part D: Transport and Environment, 16*(4), 288-295.

[21] Kowalski, J. (2014). An experimental study of emission and combustion characteristics of marine diesel engine with fuel pump malfunctions. *Applied Thermal Engineering, 65*(1), 469-476.

[22] Durmaz, M., Kalender, S.S. & Ergin, S. (2016). Bir feribottan yayılan emisyonların deneysel olarak incelenmesi, GIDB Dergi, Sayı:6 Yıl:2016 (in Turkish).

[23] Kalender, S.S., Durmaz, M. & Ergin, S. (2016). On-board measurements of emissions from a ferry, *Proc. of the 3rd Int. Conf.on Maritime Technology and Engineering, MARTECH 2016,* 4-6 July 2016, Lisbon, Portugal *745-749 Volume 2, ISBN 978-1-138-03000-8.*

[24] ISO9096 (2003). International Standards Organisation, ISO 9096, Stationary Source Emissions–Determination of concentration and mass flow rate of particulate material in gas-carrying ducts.

[25] Trozzi, C. (2010). Emission estimate methodology for maritime navigation. *Techne Consulting, Rome*.

[26] Van Aardenne, J., Colette, A., Degraeuwe, B., Hammingh, P., & De Vlieger, I. (2013). *The impact of int. shipping on European air quality and climate forcing* (Vol. 4).

[27] Ritchie, A., de Jonge, E., Hugi, C., & Cooper, D. (2005). European Commission Directorate General Environment, Service Contract on Ship Emissions: Assignment, Abatement, and Market-based Instruments. Task 2c–SO2 Abatement, Entec UK Limited, Cheshire, Northwich, UK.

[28] Smith, T.W.P., Jalkanen, J.P., Anderson, B.A., Corbett, J.J., Faber, J., Hanayama, S., O'Keefe, E., Parker,S., Johansson, L., Aldous, L., Raucchi, C., Traut, M., Ettinger, S., Nelissen, D., Lee, D.S., Ng, S., Agrawal A., Winebrake, J.J. Hoen, M., Chesworth, S. & Pandey, A. (2014). Third IMO GHG Study 2014. IMO, London.

[29] EPA (1999). Technical Bulletin, Nitrogen Oxides (NOx), Why and How They Are Controlled. *US Environmental Protection Agency Washington, DC*.

[30] EPA (2010). AP 42, Chapter 1: External Combustion Sources. *US Environmental Protection Agency Washington, DC, Fifth Edition, I*.

[31] Heywood, J.B. (1988). *Internal combustion engine fundamentals* (Vol. 930): McGraw-Hill New York.

[32] Merkisz, J., Kozak, M., Bielaczyc, P., & Szczotka, A. (2002). An investigation of influence of diesel fuel sulphur content on particulates emissions from direct injection common rail diesel vehicle. *Journal of KONES Internal Combustion Engines*(3-4).

[33] Singal, S., & Pundir, B. (1996). *Diesel fuel quality and particulate emissions: an overview* (0148-7191).

[34] Winnes, H., Moldanova, J., Anderson, M., & Fridell, E. (2014). On-board measurements of particle emissions from marine engines using fuels with different sulphur content. *Proceedings of the Institution of Mechanical Engineers, Part M: Journal of Engineering for the Maritime Environment*.

Received: **06.02.2017**
Accepted: **04.07.2017**

CORRESPONDING AUTHOR

Selma Ergin,
Istanbul Technical University, Faculty of Naval Architecture and Ocean Engineering, Maslak 34469, Istanbul, Turkey.

e-mail: ergin@itu.edu.tr

© by PSP Volume 26 – No. 10/2017 pages 5841-5848 Fresenius Environmental Bulletin

NATURAL ANTIOXIDANTS OF HUMIC AND FULVIC ACIDS AGAINST OXIDATIVE STRESS INDUCED BY HYDROGEN PEROXIDE: *IN-VIVO* STUDIES

Abd El-Moneim M R Afify*, Osama K Konswa

Department of Biochemistry, Faculty of Agriculture, Cairo University, p.12613, Gamma St., Giza, Cairo, Egypt

ABSTRACT

Fulvic acid (FA) and humic acid (HA) are formed through the degradation of organic substances by chemical and biological process. Fulvic acids and humic acid has been found to possess the highest activity as antioxidant scavenging. Treatments of humic acid at different concentrations with 10,50 ,100 and 150 mg/ Kg showed a significant differences in kidney function and liver function. The results exhibited a significant concentration-dependent manner of free radical scavenging activity as well as significant reduction of MDA level. The lowest lipid peroxidation has been reported with 150 mg/kg B.W. Humic acid and fulvic acid showed a significant decrease in the enzymes activity of glutathione peroxidase and superoxide dismutase indicating their direct protective effects against induced hydrogen peroxide. The antioxidant properties of the FA and HA partially support the health beneficial to enhance certain aspects of plant growth or mixed with fertilizers/chemicals.

KEYWORDS:
Fulvic acid, Humic acids, *In vivo* antioxidant scavenging capacity, kidney function, liver function.

INTRODUCTION

Humic substances are structurally complex large to macromolecules which occur in soils and natural waters as a consequence of the breakdown of plant and animal residues by microbial activity [1]. Oxidative stress occurs when pro-oxidant forces such as hydrogen peroxide oxygen radicals are believed to be a primary factor in various degenerative diseases, [2]. Some important antioxidant enzymes such as superoxide dismutase, catalase, glutathione peroxidase and glutathione reductase (GR) are involved in the reaction mechanism and work as antioxidants [3]. Humic acid is ubiquitous in the environment and has been found to influence physiological functions of aquatic organisms [4] as well as in soil [5]. The application fulvic acids as antioxidant substance has been described [6]. The main reason for the increasing attention devoted to humic acids can be explain by their antiviral, anti-inflammatory and estrogenic activities [7]. The potential of humic substances to form chelate complexes with heavy metals (such as cadmium) enable them to be used for the elimination of heavy metals from living organisms [8].

To prevent the damage caused by reactive oxygen specie, tissues had developed an antioxidant defense system that includes nonezymatic antioxidants (*e.g.*, glutathione, uric acid, bilirubin and vitamins C and E) and enzymatic activities such as superoxide dismutase, catalase and glutathione peroxidase [9-10].

Therefore, the objective of this work was to evaluate, *in vivo* superoxide ion ($O_2^{\bullet-}$), hydrogen peroxide (H_2O_2), scavenging capacity by humic acid and Fulvic acid against oxidative damage by administrated hydrogen peroxide to rats which affects prokaryotic growth and hydrolysis of specific components of the organic matter [12].

MATERIALS AND METHODS

Extraction and purification of humic and fulvic acids. (1) Extraction of humic substances. Extraction of humic acids was run according to the method described by [13] as follows: compost sample (25 gm) was taken and shaken with 500 ml of dispersion agent 0.5 N NaOH solution. The freshly prepared solution suspensions were left overnight and centrifuged and hence the supernatant contain humic and fulvic acids.

(2) Sepration of fulvic acid. The method described by [14] was followed for isolating and purifying humic acid. The extract of organic substances with alkali solution was adjusted first to pH 1.0 with H_2SO_4 conc. Then, it was allowed to stand 24 h to precipitate the humic acids. The supernatant contains the fulvic acids. The fulvic acid was then separated from the humic acid by centrifugation at 6000 rpm for 20 minutes. The supernatant contains the fulvic acid and the precipitate is identified as the humic

fraction of humus. The solution of fulvic acid passing through activated charcoal followed by elution of the charcoal. The solution was concentrated to small value by placing it inside an oven with a fan and left at room temperature. The concentrated solution was transferred to the membrane filter and electro dialyzed until the dialysate was free from chloride.

(3) Purification of Humic acid. The humic acid precipitate was washed several times with cold 0.05 N H_2SO_4 until the filtrate was colorless. The humic acid was re-dissolved in a small amount of 0.05 N NaOH solution, and then was transferred to a membrane filter. It was precipitated again by acidification to pH 1.0. The humic acid was transferred to cellophane bags and dialyzed against distilled water until the test for chloride in the distilled water outside the bags was negative [15] then humic acid was air-dried)

In order to reduce the ash content of the purified humic acid and to increase its purity, 10 g of the air dried humic acid were shaked with 100 ml of Khan's mixture (0.5 ml Conc. HCl + 0.5 ml HF 48% and 99 ml of H_2O) at room temperature for 42 hr after shaking, the acid mixture was centrifuged, the supernatant was removed, and the humic acid gel was dialyzed against distilled water until became Cl^- free. The precipitated humic acids gel was transferred to petri dishes and dried at room temperature (scrme 2,

The following scheme shows the separation of humic and fulvic were as flows (Scheme 1, 2, nd3):

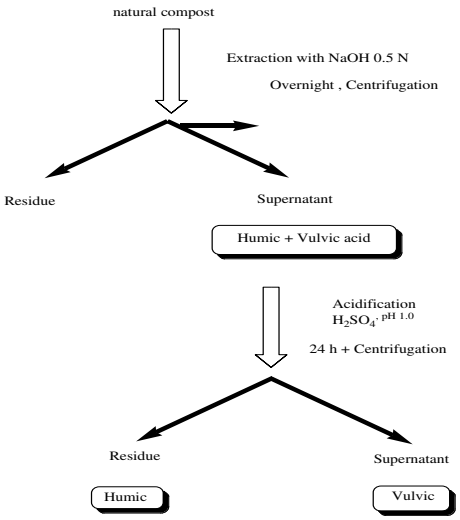

SCHEME 1
The separation of humic and fulvic

Structure of humic and vulvic acids are as follows:

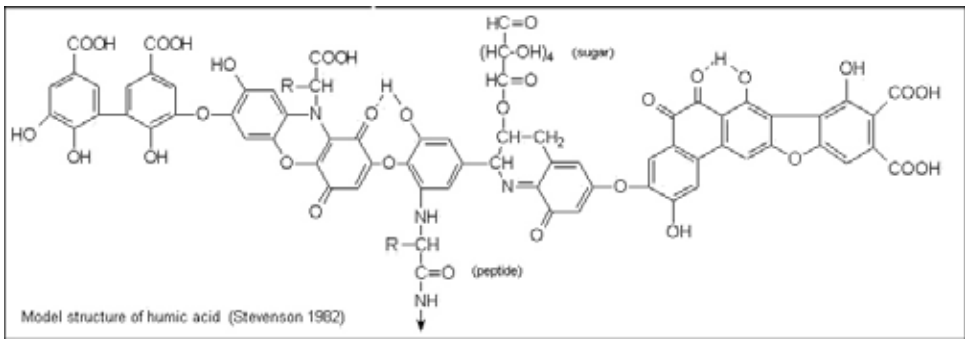

SCHEME 2
Humic acid structure

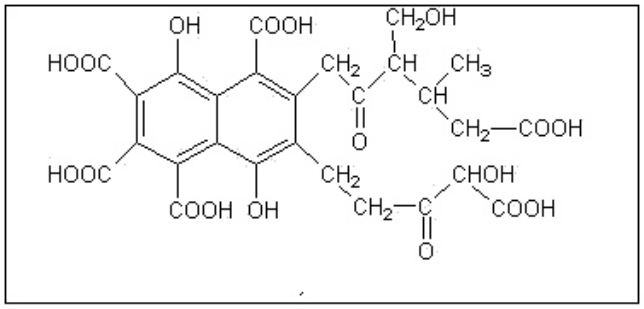

SCHEME 3
Fulvic acid structure

Hydrogen peroxide and superoxide radical Scavenging Activity. (1) Assay of superoxide radical scavenging activity. Superoxide radical scavenging activity was carried out according to [16] based on the inhibition of formazan formation. Each 3ml reaction mixture contained 50 mM sodium phosphate buffer (pH 7.6), 20 mg riboflavin, and 12mM EDTA, and 0.1 mg Nirobluetetrzolium (NBT) and 1ml sample solution. Reaction was started by illuminating the reaction mixture with different concentrations of sample extract (10,50,100 amd 150 µg/ml) for 90 s. Immediately after illumination, the absorbance was measured at 590 nm. The entire reaction assembly was enclosed in a box lined with aluminum foil. Identical tubes with reaction mixture were kept in the dark and served as blanks. The percentage inhibition of superoxide anion generation was calculated using the following formula:

$$\% \text{ Inhibition} = [(A_0 - A_1)/A_0] \times 100,$$

where A_0 is the absorbance of the control, and A_1 is the absorbance of the samples/standard.

(2) Determination of H_2O_2 scavenging capacity. The ability of humic and fulvic acids extracts to scavenge hydrogen peroxide was determined according to the method of [17].

***In vivo* Biological evaluation of humic acid and vulvic acid.** Rats Wistar used in this study were procured from the animal house olony at the National Research Centre (NRC), Egypt. All animals were housed under standard conditions of natural 12 h light and dark cycle with free access to food and water. All animal procedures were performed after approval from the Ethics Committee of The National Research Centre- Egypt and in accordance with the recommendations of the proper care and use of laboratory animals male rats (125-175 g) were divided into 9 groups (eight rats/ group). The first group represented the negative control, was administered 5% dimethylsulphoxide (DMSO). Groups two, three, four and five were treated with different concentrations of humic acid (10, 50 ,100 and 150 mg/Kg body weight). Groups six, seven, eight and nine were treated with analogous concentrations of fulvic acid. After four weeks rats were decapitated, samples were taken from various groups and prepared according to each method.

(1) Blood urea. It was estimated by the enzymatic method as described by [18].

(2) Serum creatinine. It was determined according to the method described by Faulkner and King (1976) [18].

(3) Determination of aspartate transaminase (AST) and alanine transaminase (ALT). Aspartate transaminase (AST) and alanine transaminase (ALT) were estimated according to the method described by [20].

***In-vivo* estimation of antioxidant enzymes activity.** Sprague - Dawley male rats (125-175 g) were divided into 11 groups (eight rats/ group). The first group represented the negative control, was administered 5% dimethylsulphoxide (DMSO). The second group, the positive control, was administered an oral dose of H_2O_2 + 5 % DMSO to induce oxidative damage. The single dose/week was 2 mL/Kg body weight. Groups three, four, five and six were treated with different concentrations of humic acid (10, 50, 100 and 150 mg/ Kg body weight). Groups seven, eight, nine and ten were treated with analogous concentrations of fulvic acid. Group eleven received an oral dose of Ascorbic acid 10 mg/ Kg body weight + 5% DMSO. After four weeks rats were decapitated, samples were taken from various groups and prepared according to each method.

TABLE 1
Superoxide Radical Scavenging Activity expressed as % inhibition.

Compound number	Superoxide scavenging activity 100 %			
	10 (µg/ml)	50 (µg/ml)	100 (µg/ml)	150 (µg/ml)
Ascorbic acid	64.82	90.73	99.74	100
Humic acid	28.05	36.77	60.01	67.12
Vulvic acid	32.51	42.91	67.89	79.00

TABLE 2
Hydrogen peroxide scavenging activity expressed as % inhibition.

Compound number	Hydrogen peroxide scavenging activity 100 %			
	10 (µg/ml)	50 (µg/ml)	100 (µg/ml)	150 (µg/ml)
Ascorbic acid	49.23	70.41	80.32	91.54
Humic acid	23.41	29.47	51.66	56.70
Vulvic acid	25.07	33.51	57.39	67.22

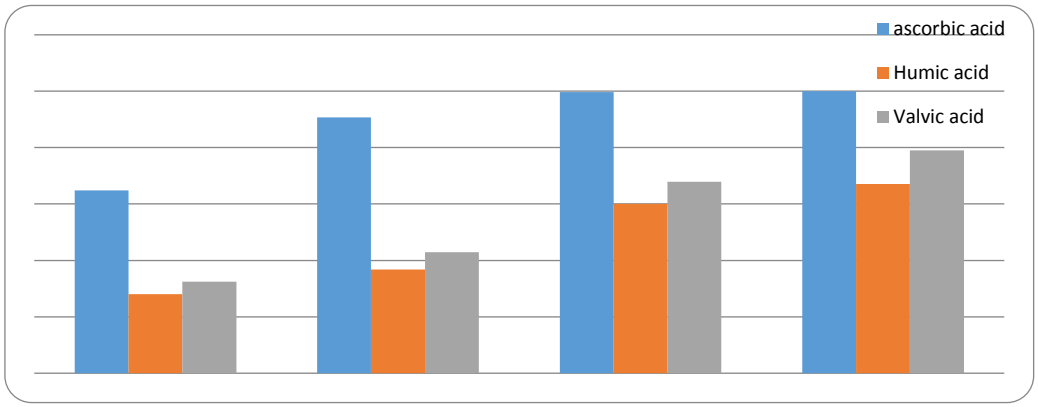

FIGURE 1
Humic and vulvic acid represent superoxide radical scavenging activity expressed as % inhibition

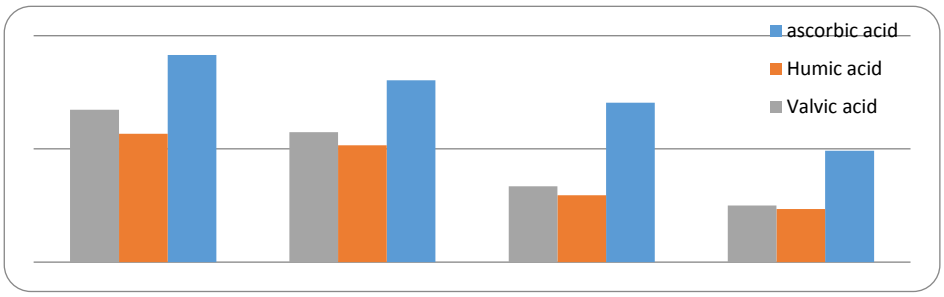

FIGURE 2
Humic and fulvic acid scavenge hydrogen peroxide expressed as % inhibition.

(1) Assay of Glutathione *peroxidase* (GPx) activity. Glutathione peroxidase was estimated by the method of [20].

(2) Assay of SOD activity. The activity of SOD was assayed by measuring its ability to inhibit the photochemical reduction of NBT using the method of [21].

(3) Lipid peroxidation assay (MDA contents). Fresh liver samples (200 mg) were homogenized in 2 ml of 0.1% (w/v) trichloroacetic acid (TCA), followed by centrifugation at 12,000×g for 20 min. The supernatant (1 ml) obtained was mixed with an equal volume of TCA (10%) containing 0.5% (w/v) TBA (or no TBA as the blank), and heated at 95°C for 30 min, then cooled in ice. The reaction product was centrifuged at 12,000×g for 15 min and the supernatant absorbance was measured at 400, 532 and 600 nm. The MDA equivalent was derived from the absorbance according to [22].

Statistical analysis. The results were analysed by an analysis of variance ($P < 0.05$) and the means were separated by Duncan's multiple range test. The results were processed by CoStat computer program (1986).
(Fig 2)

RESULTS

***In vivo* antioxidant activity of humic and vulvic acids.** The analysis of the fulvic acid and humic acids displays a scavenging activity compared to ascorbic acid reference compounds; although it was less efficient ($P<0.0001$). Scavenging activity of humic and vulvic acids were increased by increasing the concentration used in the experiments, by using 150 µg/ml for both compound. Superoxide scavenging activity represented by 79 and 76 for vulvic and humic compared to ascorbic acid (100 %) Table 2, Figure 1.

Hydrogen peroxide (H_2O_2) scavenging activity. The scavenging ability of various treatments with hydrogen peroxide is shown in Table 4 and illustrated in Figure 2 and used ascorbic acid as standards. It is noticed that all treatments are capable of scavenging hydrogen peroxide in an amount-dependent manner. The percentage of scavenging hydrogen peroxide is determined with 150 µg/ml of the humic acid and fulvic acid represented the highest scavenging activity expressed as % inhibition is as follows: humic acid (56.70%) and vulvic acid (67.22 %) against ascorbic acid standard at the same concentration (91.54%) (Table 1).

***In vivo* activity of antioxidant defense enzyme activities affected by administrated humic acid and fulvic acid under hydrogen peroxide oxidative stress.** Hydrogen peroxide-induced damage of liver cells results in oxidative damage through free-radical generation. In this work, the rats were treated with a single oral dose of hydrogen peroxide (2 ml/Kg body weight / week) to induce oxidative stress and liver damage. Humic acid and fulvic acid were evaluated for their protective effect against oxidative stress and induced liver damage in rats by estimating SOD, GPx activity as well as MDA levels. The results shown in Table 4 and illustrated in Figure 3 and Figure 4 revealed that, the administrated humic acid and fulvic acid showed a significant reduction in both enzymes indicating their protective effects against induced oxidative damage, *via* GPx and SOD defense enzymes modulation. Fulvic acid exhibited more potent protective activity at a dose of 150 mg/Kg.

The data also revealed a significant decrease in MDA level upon treatment with different concentrations of humic acid and fulvic acid. The best result was shown by Fulvic acid at a dose of 150 mg/Kg, which may be attributed to its higher antioxidant activity compared to humic acid. The data represented that, the humic acid and vulvic acid exhibited a significant concentration-dependent free radical scavenging activity as well as significant reduction of MDA level. Furthermore, both compounds, humic acid and fulvic acid, showed protective effect against lipid peroxidation in hepatic microsomes. This effect may be due to their inhibitory effect on inducible nitric oxide synthase and scavenging effect on peroxynitrite formation. The lowest MDA level was observed with compound fulvic acid at a dose of 150 mg/Kg b.w., Table 4 and Figure 4.

TABLE 3
Cytotoxicity effect of various concentrations of humic and fulvic acids on urea, creatinine and AST and ALT in rats

Compounds	Concentration mg/kg	Urea mg/dl	Creatinine mg/dl	AST U/ml	ALT U/ml
		Mean ± SE	Mean ± SE	Mean ± SE	Mean ± SE
Fulvic acid	10	$35.2^{d} \pm 0.88$	$1.08^{d} \pm 0.03$	$31.2^{d} \pm 1.3$	$21.2^{d} \pm 1.1$
	50	$39.2^{cd} \pm 1.25$	$1.16^{cd} \pm 0.08$	$32.1^{cd} \pm 1.4$	$23.8^{cd} \pm 1.6$
	100	$41.2^{bc} \pm 1.63$	$1.4^{bcd} \pm 0.08$	$37.4^{abc} \pm 2.3$	$22.9^{cd} \pm 2.0$
	150	$41.1^{bc} \pm 2.5$	$1.59^{bc} \pm 0.06$	$40.6^{ab} \pm 2.1$	$29.4^{ab} \pm 1$
Humic acid	10	$37.8^{cd} \pm 1.7$	$1.46^{bcd} \pm 0.18$	$35.3^{bcd} \pm 1.5$	$22.4^{cd} \pm 1$
	50	$42.5^{abc} \pm 2.8$	$1.57^{bc} \pm 0.11$	$37.1^{abc} \pm 1.2$	$25.6^{bcd} \pm 1$
	100	$44.8^{ab} \pm 1.68$	$1.71^{ab} \pm 0.14$	$40.4^{ab} \pm 1.8$	$27.2^{abc} \pm 1$
	150	$46.7^{a} \pm 2.04$	$2.1^{a} \pm 0.0.11$	$41.4^{a} \pm 1.63$	$31^{a} \pm 1.1$
Control negative		$40.1^{bcd} \pm 1.6$	$1.38^{bcd} \pm 0.28$	$36.2^{abcd} \pm 1.9$	$26.4^{abc} \pm 1$
$LSD_{0.05}$		4.870	0.4092	5.132	4.332

Each value represents the mean ± SE (Standard Error) and mean of three replicates; Values in the same column with the same letter are not significantly different at ($p \leq 0.05$)

TABLE 4
The antioxidant activity of compounds fulvic acids and humic substances against MDA formation, SOD and GPX in control and treated rats with H_2O_2 oxidative stress.

Compound	Concentration (mg/kg)	The measured parameters		
		SOD u/ml	GPX u/ml	MDA nmol/ mg protein
		Mean ± SE	Mean ± SE	Mean ± SE
Control (+)		$128.9^{a} \pm 31$	$5.69^{a} \pm 0.32$	$6.79^{a} \pm 0.3$
Control (-)		$35.77^{f} \pm 2.8$	$2.59^{d} \pm 0.26$	$3.5^{de} \pm 0.13$
Fulvic acid	10	$116.4^{ab} \pm 2$	$5.27^{ab} \pm 0.21$	$4.89^{b} \pm 0.24$
	50	$103.2^{abcd} \pm 2$	$4.72^{bc} \pm 0.35$	$4.02^{cd} \pm 0.23$
	100	$80.69^{cde} \pm 1$	$4.27^{c} \pm 0.2$	$3.88^{de} \pm 0.33$
	150	$70.97^{de} \pm 2$	$3.9^{c} \pm 0.18$	$3.27^{e} \pm 0.16$
Humic acid	10	$104.1^{abc} \pm 2$	$5.2^{ab} \pm 0.15$	$5.08^{b} \pm 0.07$
	50	$102.7^{abcd} \pm 3$	$4.7^{bc} \pm 0.25$	$4.65^{bc} \pm 0.23$
	100	$93.15^{bcd} \pm 2$	$4.2^{c} \pm 0.29$	$3.99^{cd} \pm 0.14$
	150	$86.71^{bcd} \pm 2$	$4.1^{c} \pm 0.12$	$3.82^{de} \pm 0.13$
Voltarine®	10	$63.31^{ef} \pm 3$	$3.01^{d} \pm 0.08$	$3.60^{de} \pm 0.28$
$LSD_{0.05}$		29.097	0.683	0.637

Each value represents the mean ± SE (Standard Error) and mean of three replicates; Values in the same column with the same letter are not significantly different at ($p \leq 0.05$)

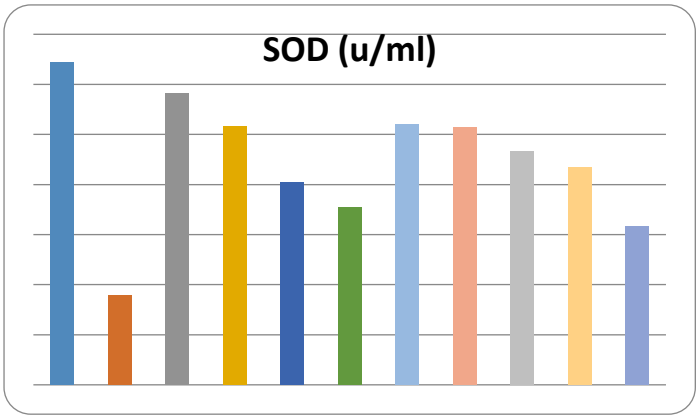

FIGURE 3
The modulating effect of administrated fulvic acids and humic substances on SOD activity under oxidative stress.

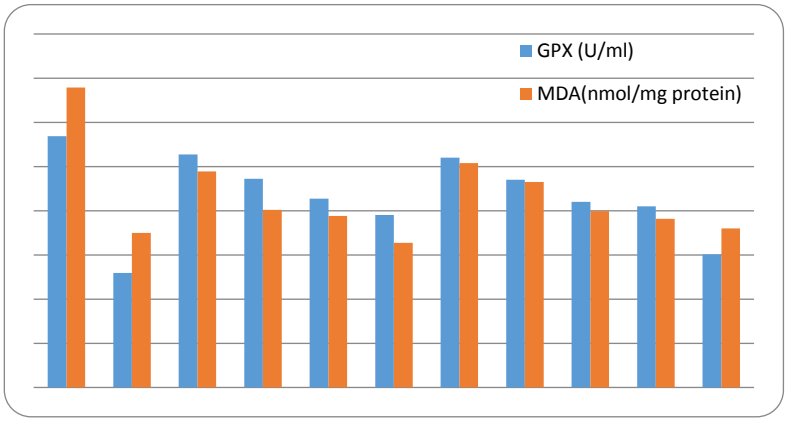

FIGURE 4
The modulating effect of administrated fulvic acids and humic substances on GPX activity and MDA formation under oxidative stress.

Effect of humic acid and vulvic acid on kidney and liver functions. The data obtained from Table 3 revealed that, humic acid and fulvic acid were tested for their possible effect on kidney and liver functions to assess their safety *in vivo* investigation. The results show that urea and creatinine levels as kidney function did not shows any significant toxicity when using fulvic acid with concentration of 10,50 ,100 and 150 mg/ Kg compared to negative control. On the other hand treatments of humic acid of different concentration with 10,50 and 100 mg/ Kg show significantly differences in kidney function Urea (mg/dl), Creatinine (mg/dl) and AST and ALT (U/ml) enzyme activities of the liver by using 150 mg/ Kg b.w. (46.7, 2.1, 41.4 and 31) respectively.

DISCUSSION

Vulvic and humic act as an antioxidant like other high molecular weight plant phenolics such as tannins [22-25]. The conversion of superoxide radical and H_2O_2 into more reactive species, e.g., hydroxyl radical, has been thought to be one of the unfavorable effects caused by superoxide radicals [9]. The results data was in accordance with [26] who found that, it has been known that phenolic hydroxyl group is the main active group which scavenges $OH^{\bullet}$ and favor's the encapsulation of the pro-oxidant iron species, which generates $OH^{\bullet}$ through the Fenton reaction [26]. This suggests that the phenolic hydroxyl group and metal-chelating ability by fulvic acid could explain the ROS scavenging activity observed.

Low concentrations of humic Acid, such as 25 and 50 µg/ml, reveal no increase induced lipid peroxidation compared to control conditions (28-29]. Also, the data reflected that at high doses of humic acid significantly affected the liver function and the kidney function that is may be due to the toxicity dose dependence of humic acid affecting the plasma membrane integrity and toxicity. Nevertheless, [30] reported that, the daily intake of humic acid by the average resident in these areas has been estimated to be as high as 400 mg. and has adversely affected the

health of inhabitants. Radioisotope tracing with iodinated humic acid in rats indicated that up to 60% of humic acid remained in the body 24 h after its administration. Humic acid disrupts intracellular calcium homeostasis and enhances the permeability of cell membranes to extracellular Ca^{+2}, resulting in sustained elevation of cytosolic Ca^{+2}/. These data was in accordance with [31], who found that, the antioxidant properties of fulvic acid explain some of the health beneficial effects of this compound since the excessive production of $O_2^{\bullet-}$, HOCl, H_2O_2, $OH^{\bullet}$, $ONOO^-$ and O_2 are involved in several pathologies. In addition, humic acid and fulvic compounds were able to prevent glutathione oxidation induced by H_2O_2 [28]. These results clearly indicated that SOD and GPx may play a role in the suppression of oxygen free radical formation in liver and kidney tissues and may be connected to the H_2O_2-induced increase in free radical generation or a decrease in amounts of protecting enzymes against lipid peroxidation. The decrease in SOD and GPx activity in the liver of H_2O_2 treated samples may indirectly cause oxidative DNA damage or mitochondrial damage in cells [32]. In accordance, the fulvic acids act as an antioxidant like other high molecular weight plant phenolics such as tannins. FA in vitro scavenged of $O_2^{\bullet-}$ and H_2O_2, in a concentration-dependent way. The presence of structural units O^- functionalized, including aromatic domains in fulvic acid, could explain their tendency to form molecular aggregates (hydrogen bridges, metal bridges and hydrophobic interactions) [33]. Treatments with humic acids in saline soils were associated with reduced soil electrical conductivity and reduced leakag as well as reducing potential as reported by double spraying with stimulator [34].

CONCLUSION

The antioxidant properties of humic and vularic acids explain some of the health beneficial effects which increase immune system function since the excessive production of free radicals are involved in several pathologies. Moreover, they could be a good candidate for use in pharmaceutical or food industries as an accessible source of natural antioxidants and for the improvement of food quality by retarding lipid oxidation. These substances may at times stimulate growth in both higher plants and soil microorganisms These compound could be applied directly to the soil or as a foliar spray, by itself or mixed with fertilizers/chemicals.

REFERENCES

[1] Jones, M.N. and Bryan, N.D. (1998) Colloidal properties of humic substances, Adv. Colloid and Interface Science**,** 78: 1-48.

[2] Li, Z.H., Zlabek, V., Velisek, J., Grabic, R., Machova, J., Kolarova, J., Li, P. and Randak, T. (2011) Acute toxicity of carbamazepine to juvenile rainbow trout (*Oncorhynchus mykiss*): Effects on antioxidant responses, hematological parameters and hepatic EROD. Ecotoxicology and Environmental Safety, 74, 319–327.

[3] Wang, C., Wang, Z., Peng, A., Hou, J. and Xin, W. (1996) Interaction between fulvic acids of different origins and active oxygen radicals. Sci. China C. Life Sci., 39, 267-275.

[4] Andersson, C., Abrahamson, A., Brunstrom, B. and Orberg, J. (2010) Impact of humic substances on EROD activity in gill and liver of three-spined sticklebacks (*Gasterosteus aculeatus*). Chemosphere, 81, 156–160.

[5] Gajdo.ova, D., Novotna, K., Prosek, P. and Havel, J. (2003) Separation and characterization of humic acids from Antarctica by capillary electrophoresis and matrix-assisted laser desorption ionization time of- flight mass spectrometry inclusion complexes of humic acids with cyclodextrins. J. Chromatogr. A., 1014, 117-127.

[6] Ueda, J., Ikota, N., Shinozuka, T. and Yamaguchi, T. (2004) Reactive oxygen species scavenging ability of a new compound derived from weathered coal. Spectrochim. Acta A. Mol. Biomol. Spectrosc., 60, 2487- 2492.

[7] Yamada, E., Ozaki, T. and Kimura, M. (1998) Determination and behavior of humic substances as precursors of trihalomethane in environmental water. Anal. Sci., 14, 327-332.

[8] Klocking, R. (1992) Humic substances in the global environment and implications in human health. Monopoli, p. 129.

[9] Halliwell, B. (2001) Role of Free Radicals in the Neurodegenerative Diseases: Therapeutic Implications for Antioxidant Treatment.Drugs Aging, 18, 685.

[10] Afify, A.E.M.M.R. Farahat, A.A., Al-Sayed, A.A., Mahfoud, N.A.M. (2014b) Antioxidant enzymes as well as oxidant activities involved in defense mechanisms against the root-knot, reniform and citrus nematodes in their host plants. International Journal of Biotechnology and Food Science, 2(6), 102-111.

[11] Stevenson F.J. (1982) Humus chemistry genesis, composition, reactions. 2nd Edition. F. J. Stevenson. ISBN: 978-0-471-59474-1 .

[12] Kononova, M.M. (1966) Soil Organic Matter. Pergmon Press, Oxford, London, Edinburgh, New York, 544 p.

[13] Chen, Y., Senesi, N. and Schnitzer, M. (1978) Chemical and physical characteristics of humic and fulvic acids extracted from soil of the Mediterranean region. Geoderma, 20(2), 87-104

[14] Beauchamp, C. and Fridovich, I. (1971) Superoxide dismutase: Improved assays and an assay applicable to acrylamide gels. Anal. Biochem. Review, 44: 276-287.

[15] Ruch, R.J., Cheng, S.J. and Klaunig, J.E. (1989) Prevention of cytotoxicity and inhibition of intracellular communication by antioxidant catechins isolated from Chinese green tea. Carcinogenesis, 10:1003–1008.
[16] Patton, C.J. and Couch, S.P. (1977) Spectrophoto- metric and kinetics investigation of the Berthelot Reaction for the determination of ammonia. Anal. Chem., 49: 464.
[17] Reitman, S.; Frankel, S. and Amer, J.A. (1957) Colorimetric method for the determination of serum glutamic oxalacetic and glutamic pyruvic transaminases. Clin. Pathology, 28: 56
[18] Faulkner, N.R. and King, J.W. (1976) Fundamental of clinical chemistry 2nd ed., Saunders Philadelphia, 994.
[19] Pagila, D.E. and Valentine, W.N. (1967) Studies on the quantitative and qualitative characterization of erythrocyte glutathione peroxidase J. Lab. Clin. Med., 70, 158.
[20] Hodges, D. M., DeLong, J.M.; Forney, C.F. and Prange, R.K. (1999) Improving the thiobarbituric acid-reactive-substances assay for estimating lipid peroxidation in plant tissues containing anthocyanin and other interfering compounds. Planta, 207: 604.
[21] Afify, A.E.M.M.R., Shalaby, E.A., El-Beltagi, H.S. (2011) Antioxidant activity of aqueous extracts of different caffeine products. Not Bot Horti Agrobo 39(2),117-123.
[22] Afify, A.E.M.M.R., Hossam, S.E.B., Samiha, M.A.E.S., Azza, A.O. (2012) Biochemical changes in phenols, flavonoids, tannins, vitamin E, carotene and antioxidant activity during soaking of three white sorghum varieties. Asian Pacific Journal of Tropical Biomedicine 2(3):203-209.
[23] Afify, A.E.M.M.R., Esawy, S.H., El-Hadidy, E.M. and Abdel-Salam, M.A.L. (2014a) Antioxidant content and cytotoxicity of Origanum syriacum L. Advances in Food Sciences 36(2), 58-64.
[24] Cos, P., Ying, L., Calomme, M., Hu, J.P., Cimanga, K., Van Poel, B., Pieters, L., Vlietinck, A.J. and Vanden Berghe, D. (1998) Structure-activity relationship and classification of flavonoids as inhibitors of xanthine oxidase and superoxide scavengers. J. Nat. Prod., 61:71-76
[25] Butkovic, V., Klasinc, L. and Bors, W. (2004) Kinetic study of flavonoid reactions with stable radicals. J. Agric. Food Chem., 52:2816-2820.
[26] Ho KJ, Liu TK, Huang TS,and Lu FJ (2003) Humic acid mediates iron release from ferritin and promotes lipid peroxidation in vitro: a possible mechanism for humic acid-induced cytotoxicity. Arch Toxicol., 77: 100–109.
[27] Topal, A. Alak, G., Atamanalp, M., Oruc, E., Ceyhun, S.B., Ucar, A., Arslan, H., Çelebi, F., Saglam Y.S. (2013) Effects of Humic Acid on Liver and Kidney Toxicity Induced by Cadmium in Brown Trout (Salmo trutta fario, L). Turkish Journal of Fisheries and Aquatic Sciences 13: 621-627
[28] Huang, T.S., Lu, F.J. and Tsai, C.W. (1995) Tissue distribution of absorbed humic acids. Environ Geochem Health, 17:1–4
[29] Yang, H.L., Lu, F.J., Wang, S.L. and Chiu, H.C. (1994) Humic acid induces expression of tissue factor by cultured endothelial cells: regulation by cytosolic calcium and protein kinase C. Thromb. Haemost., 71:325–330.
[30] Rodríguez N.C., Urrutia, E.C. Gertrudis, B.H., Chaverri, J.P. and Mejia, G.B. (2011) Antioxidant activity of fulvic acid: A living matter-derived bioactive compound. Journal of Food, Agriculture & Environment Vol.9 (3&4): 123-127.
[31] Karadeniz, A., Cemek, M. and Simsek, N. 2009. The effects of Panax ginseng and Spirulina platensis on hepatotoxicity induced by cadmium in rats. Ecotoxicology and Environmental Safety, 72: 231-235.
[32] Baigorri, R.; Zamarren˜o, A. M.; Fuentes, M.; González-Gaitano,. G.; Garcıa-Mina, J. M.; Almendros, G.; and González-Vila, F. J.. (2009) Complementary multianalytical approach to study the distinctive structural features of the main humic fractions in solution: gray humic acid, brown humic acid and fulvic acid. J. Agric. Food Chem., 57, 3266-3272.
[33] Aydin A, Kant C, Turan M (2012). Humic acid application alleviate salinity stress of bean (Phaseolus vulgaris L.) plants decreasing membrane leakage. Afr J Agric Res 7: 1073–1086.
[34] Kocira, A., Kocira, S., Zlotek, U., Kornas, R. and Swieca M. (2015) Effect of Nano-Gro preparation applications on yield components and antioxidant properties of common bean (Phaseolus vulgaris L.). Fresen. Environ. Bull. 24-11b: 4034-4041.

Received: **06.02.2017**
Accepted: **20.04.2017**

CORRESPONDING AUTHOR

Abd El-Moneim M R Afify
Department of Biochemistry
Faculty of Agriculture
Cairo University, p.12613
Gamma st., Giza, Cairo – EGYPT

E-mail: abdelmoneimafify@yahoo.com

© by PSP Volume 26 – No. 10/2017 pages 5849-5857 Fresenius Environmental Bulletin

OXIDATIVE STRESS RESPONSE AND CELL DEATH IN FISH INTESTINE DUE TO METRONIDAZOLE TOXICITY

Beyhan Gurcu[1,*], Yucel Basimoglu Koca[2], Sevinc Inan[3], Mehmet Ibrahim Tuglu[4]

[1]Celal Bayar University, School of Science and Letter, Department of Biology, Manisa, Turkey
[2]Adnan Menderes University, School of Science and Letter, Department of Biology, Aydın, Turkey
[3]Izmir University of Economics, Faculty of Medicine, Basic Medical Sciences, Izmir, Turkey
[4]Celal Bayar University, Faculty of Medicine, Department of Histology and Embryology, Manisa, Turkey

ABSTRACT

Metronidazole (MTZ) is commonly used as an antibiotic for enterozoa; however, its side-effects have not been fully characterized. In this study, the toxic effect of a dose and time-dependent MTZ application on morphology of the intestinal tissue of *Oncorhynchus mykiss* was examined.

Fish were exposed to 5, 10, and 20 mg/L of MTZ in the aquariums for 2, 4 and 8 days. Samples taken from the jejunum region of the small intestine were for Gomori Trichrome, NOS and TUNEL.

A slight toxic effect that started with a dosage of 5 mg/L for 2 days reached the maximum level with a dosage of 20 mg/L for 8 days. Erosion, oedema, inflammation, disintegration in the epithelium, and necrosis were detected at the tips of the villi. NOS staining had increased a great deal. Separately, a parallel TUNEL staining was monitored in the process of NOS staining practices.

The toxic effect that increased in proportion to the dosage and period had occurred due to oxidative damage and that the cells had been induced to die through apoptosis. It was thought that this toxic effect could be of significance because of food chain and needed to be investigated by means of advanced techniques.

KEYWORDS:
Metronidazole; Oxidative Stress; Cell Death; Fish; Intestine

INTRODUCTION

Toxic substances may distort animal physiology by causing stress in animals. These stress agents may even lead to the death of a living organism by affecting organs, tissues and cells. Fish are susceptible to acute and chronic environmental changes and generate a classical stress response in this respect. This stress response involves the changes in plasma glucocorticoids and catecholamines. Environmental changes may cause hypoxia, metabolic acidosis and alkalosis, hypotension, and hypoglycaemia [1-3]. In this sense, Metronidazole (MTZ: 1-[2-hydroxyethyl]-2-methyl-5-nitroimidazole), which is a compound of 5-Nitroimidazole, is an agent likely to pose a toxic effect. MTZ was accumulated in animals, fish farm water, and effluents from meat industries. Waters and wastewater have approximately 1 ~ 10 ng/L residual concentrations of MTZ. The toxic effects of MTZ on aquatic organisms, such as algae and daphnids, in low mg/L concentrations were shown [4]. MTZ is nonbiodegradable and highly soluble in water; thus it can accumulate in the aquatic environment. Elimination of MTZ from water systems is an important issue considering its toxicity, potential mutagenicity and carcinogenity [5]. Genotoxic effects of MTZ in fish have been shown with *Oreochromis niloticus*, not just for the intestines but also for other organs [6]. Clinically, biodegradation of certain popular antibiotics, such as ciprofloxacin, ofloxacin, and MTZ, is known to be highly important [7]. Moreover, It has been thought that MTZ continual entry into the environment may have significant, long-term effects on the stability of ecosystems because MTZ and its metabolites possess mutagenic, carcinogenic and toxic properties. For this reason, the application of MTZ in food-producing species is prohibited in developed countries. Measurement of MTZ in water, sediment and fish tissue samples by liquid chromatography-ion trap mass spectrometry (LC-MS/MS) showed the highest concentrations in water, sediment and tissue were 136.2 ng L(-1), 12.0 ng g(-1) and 1.5 ng g(-1), respectively [8].

Although MTZ is considered to be a rodent mutagenic and carcinogenous, it is a clinically important antibiotic used in the treatment of infections caused by anaerobic bacteria and protozoa [9, 10]. Separately, MTZ is also said to have a negative effect on beneficial bacteria within a biofilter. The biological filtration in aquariums is the transformation of nitrate into nitrogen gas, which is the final stage of the nitrogen cycle, and this process is executed by anaerobic bacteria. MTZ accumulation in water as the result of not changing the aquarium water after its usage inhibits the occurrence of nitrogen gas and leads to nitrate accumulation. Nitrate taken in orally is swallowed by being transformed into nitrite by the bacteria in the mouth and then changed into Nitric Oxide (NO) within the stomach [11]. It is reduced to

NO within the circulation system and in tissues, depending on hypoxia, anoxia and acidosis by being transformed into nitrite that has a rather reactive and toxic effect [12] rapidly within the gastrointestinal system [13, 14].

NO is synthesized through L-Arginine, a semi-essential amino acid catalysed by the NOS enzyme [15]. NOS has three isoforms; neuronal NOS (nNOS, NOS 1), inducible NOS (iNOS, NOS 2) and endothelial NOS (eNOS, NOS 3). A Ca^{2+} /calmodulin-dependent enzyme, eNOS, is activated as the result of the temporary rise of the intracellular Ca^{2+} concentration within physiological boundaries through various stimulators and leads to NO synthesis in essential amounts. iNOS is functionally independent of Ca^{2+} and can generate a high amount of NO. It is found particularly within smooth muscle cells and macrophages, apart from endothelial cells [2, 3, 16].

NO is a powerful molecule that plays a role within the intracellular and intercellular messenger system in every aspect of life [17]. It has two functional characteristics: (1) the antioxidant effect over the detoxification of reactive oxygen metabolites, and (2) exhibiting a free radical activity through the formation of redox couples. NO forms NO_2 and $ONOO^-$ (peroxynitrite) by interacting with O_2^- and forms $ONOO^-$ and a conjugated acid referred to as ONOOH (peroxynitrose acid) by interacting with O_2^- (superoxide anion). These formed molecules are the compounds that are far more toxic than NO [18], and they can modify the structural proteins through the nitrozilation of the sulfhydryl groups in proteins [19, 20]. This phenomenon is the case considered among the indirect effects of NO, ensuring a long-term effect. It has been shown that there is a relationship between both histologic and biochemistry parameters on oxidative stress where there were alterations in iNOS and eNOS staining similar to alterations in superoxide dismutase, catalase and malondialdehyde levels [21].

Long periods of exposure of cells to nitric oxide donors at high concentrations cause necrosis (cell death) through necrotic and apoptotic mechanisms [22]. Necrosis is often observed as cell swelling and then decomposition in the plasma membrane. On the other hand, in apoptosis, the cell membrane is strong. The density of the nuclear chromatin increases, while the DNA is enzymatically broken down and a budding process occurs at the cell surface. Then, phosphatidylserines come out into the open over the cell membrane and are phagocytosed by cell macrophages [23]. Depending on the amount of S-nitrozilation occurring in the cell, apoptosis is either stimulated or inhibited [24, 25]. NO shows several effects, such as enhancing cytotoxicity and DNA damage under oxidative stress and affecting the enzymes containing iron sulphide, impairing the mitochondrial respiration and thus triggering apoptosis.

Apoptosis in living cells is a cell death mechanism that plays a role both in eliminating unwanted or unnecessary cells and in tissue homeostasis throughout the whole biological process. However, apoptosis is an essential biochemical mechanism for a healthy maintenance of vitality. The apoptosis mechanism in a cell is conducted in two ways. One of these originates extracellularly and through the tumour necrosis factor superfamily members and their receptors, such as cell surface death receptors, while the other is apoptosis originating intracellularly and is conducted through mitochondrial means [26, 27]. Cell surface death receptors are the members of the transmembrane proteins belonging to the Tumour Necrosis Factor Receptor (TNFR) superfamily. These receptors are found within the cysteine rich domains recurring in extracellular regions. Death receptors carry protein chains referred to as "death domains" in the inner part of the cytoplasm.

Death domains, when ligandly bound to death receptors, stimulate the apoptotic mechanism and transmit the stimulus occurring extracellularly into the intracellular region [28]. Oxidative stress in a living organism that occurs rather intensely and repeatedly exceeds the detoxification and endurance capacity of the trabecular meshwork cells, leading to pathologies resulting in destruction of cytoskeleton structures, decrease of viscousness/tenacity, as well as cell losses and finally cell death [29]. Eventually, loss of cell-matrix viscousness affects the cell cycle, ceases growth and stimulates apoptosis.

The effects of MTZ practices on intestinal tissue are not clear because MTZ has not been studied on healthy samples. The relationship between the possible damage and the oxidative stress effect mechanism has not been evaluated. In light of the above mentioned information, the oxidative stress occurring in healthy fish exposed to MTZ will be evaluated according to the dosage, and the damage-based mechanisms will be associated in the way that they involve apoptosis.

MATERIALS AND METHODS

Oncorhynchus mykiss/Rainbow trout (*O. mykiss*) is a species preferred in aquaculture due to its characteristics, such as high adaptability and feed conversion capability, ability to tolerate high water temperatures (26ºC) and the oxygen content dissolved at lower levels, as well as their egg capacity through artificial methods along with their short incubation period and their resistance to diseases.

All experiments were conducted in accordance with the animal research protocol of Ege University Ethical Committee (2011-038).

The salmon/trout species, referred to as *O. mykiss,* were purchased from the trout breeding farms and brought to the laboratory with controlled environmental conditions and were kept at 12-hour

light and 12-hour dark photoperiods for 10 days in glass aquariums (100x30x50 cm) containing stabilized tap water at a constant temperature of (19±2°C) to allow for environmental adaptability. The fish were separated into three groups: positive (cyclophosphamide (CP)-Baxter, Malta), negative (Serum physiologic) and control application groups. The fish of the application group were also separated into three groups, each of which was respectively subjected to MTZ mixed into the aquarium water in the form of 5, 10, and 20 mg/L for 2, 4 and 8 day durations. Next, a small intestine dissection was performed on the fish belonging to each group (n=10) subjected to MTZ at different doses, and the tissue samples were taken from the jejunum region.

Histological examination. The tissue samples were taken and evaluated with a 10% of buffered neutralized formalin for 24-48 hours. In the wake of the dehydration process by means of alcohol, they were made pellucid with xylol and then were embedded in paraffin, and then 5 µm of sections were taken from the tissues and were spread over the laminae with lysine. Sections were stained with Gomori Trichrome (GT) [30] histochemistry and eNOS, iNOS immunohistochemistry and TUNEL. The preparations were examined under a Leica (DM 4000B) bright field microscope, and their images were taken via an Olympus (DP 71) camera at various magnifications, and then they were evaluated for scoring in a digital environment.

Immunohistochemical stains. In order to determine the oxidative damage immunohistochemically, eNOS (1:100 diluted, SCBT, sc-654, St. Louis, USA) and iNOS (1:100 diluted, SCBT, sc-651, St. Louis, USA) immunohistochemistry were applied. After the sections were deparaffinized in the incubators at 60˚C, the pellucidity process with xylol was performed. Next, rehydration through the decreasing alcohol series was performed, and they were subsequently kept waiting in distilled water. 3% H_2O_2 was applied to the sections with 0.5% of trypsin solution. The sections were washed by means of phosphate buffer solution (PBS) and were treated with the blocking solution. The sections incubated with primary antibodies and washed through PBS were stained with anti-hydrogen peroxidase secondary antibody. The sections washed through PBS once again and then were stained with Diaminobenzidine tetrahydrochloride (DAB) to identify the visibility of the immunohistochemical reaction. After background staining was performed through Mayer's Hematoxylin, the sections washed with distilled water were closed by means of the closure/mounting medium [31].

TUNEL. The TUNEL (Terminal deoxynucleotidyl transferase mediated dUTP nick end labeling) (1:100 diluted, Millipore, S7101, Temecula, CA) method was applied to determine apoptotic cells. After the sections taken onto the laminae with lysine had been deparaffinized in the incubator of 60˚C, the pellucidity process with xylol was performed. In the wake of practicing rehydration with the decreasing alcohol series, the tissues were treated with physiological saline solution. The tissues were subsequently subjected to the process with 20 µg/ml of proteinase K. Following the washing process through PBS, the endogenous peroxidation was blocked with 3% hydrogen peroxide. After 4% paraformaldehyde, the treatment with the equilibrium buffer was performed. The sections then were subjected to incubation with TdT enzyme. In the wake of the peroxidase practice of anti-dioxygen, DAB staining was performed. Washing processes were performed at intervals with PBS washing solution. The background staining was performed by means of Mayer's Hematoxylin, and the sections were closed via Entellan. The preparations were examined under a Leica (DM 4000B) bright field microscope, their images taken via an Olympus (DP 71) camera at various magnifications, and then they were evaluated for scoring in a digital environment [32].

Statistical analysis. Immunohistochemical staining was scored as 1: no or weak staining, 2: moderate staining, 3: moderate-strong staining, 4: strong staining and 5: very strong staining. The results were evaluated by using the mean+SD of one-way ANOVA statistical method and Graphpad program. The statistical significance was accepted as $p < 0.05$ [32].

RESULTS

Even at higher doses and during long periods of time, there was no death or macroscopic pathology observed in other organs. The small intestine that constitutes a broad occlusion/absorption surface of the gastrointestinal system is composed of 4 layers as mucosa, sub-mucosa, muscular layer and serosa.

In GT staining, the small intestine mucosal epithelium in the control groups was of simple cylindrical epithelial structures, the boundaries of which were prominent and comprised of microvillus at the surfaces facing the lumen, as well as having almost-basal oval nuclei. The connective tissue cells showed a GT positive reaction and the intraepithelial lymphocytes with small, oval and dark-coloured nucleus were scattered amidst the epithelium. The lamina propia mucosa was of a ligament structure, and GT positivity was observed on the muscular part. The tunica muscularis covers a wide area, being circular internally and longitudinal externally (Figure 1 A). Cell death in the form of necrosis, as well as dilations and degradations, depending on the dosage and time of the samples exposed to MTZ, were observed at

the tips of the villi, which face the lumen. The degradation, on the other hand, was in the form of the integration and breakdown of the villi at the tips and then in the form of taking a smooth shape. Separately, there was dissociation in the epithelium, deterioration in the basal membrane and a decrease in the sub-mucosal region along with the lamina propria. There was a lymphocytic infiltration in the mucosal epithelium and lamina propria. In all the regions, there was a decrease in GT staining compared to the control group (Figure 1 C-D). Among the villi, there were viscosities/adherences in the microvilli (Figure 2, (+) Control). It was also observed in the positive control group to which CP was applied, and some damage similar to that of the control group was observed.

When the experimental groups were compared with the negative control groups, it was determined that the damage in question had started during the 5 mg/L of MTZ dosage for 2 days and that it came close to the positive control group by increasing in time and dosage. This damage occurred in the form of a slight degeneration of the villi heading towards necrosis, and the process had taken place by starting from the cell infiltration in the submucosal layer towards the cell death in the muscular layer. GT staining was diminished in relation to the pathology (Figure 1). As the oxidative stress indicator/marker, there was a basal staining in the controls in the eNOS staining, which was more prominent in the sub-epithelial and connective tissues (ligaments). It was also observed in the muscular and connective tissues in the inter-epithelial areas, in particular during the stainings that increased in every area in the positive samples to which CP was applied. On the other hand, MTZ groups had higher staining than the control group but decreased staining according to CP application in the form of increasing dosage. eNOS staining diminished in the connective tissue, particularly in the necrotic regions at high doses (Figure 2).

As another marker/indicator of oxidative stress, there was less basal staining in iNOS staining compared to that in eNOS staining. It also occurred in the muscular and connective tissues, in particular during the stainings that increased in every area in the positive samples to which CP was applied. In MTZ groups, staining was higher than that of the control group but decreased according to the CP application in the form of increasing dosage. iNOS staining was diminished in the connective tissue, particularly in the necrotic regions at high doses. This staining was denser in the muscular tissue when compared with eNOS. With a lower dose of MTZ, eNOS was stained more than iNOS (Figure 2). It was also found in the control groups and was located up to the tips of the villi in the TUNEL staining for apoptosis, one of the

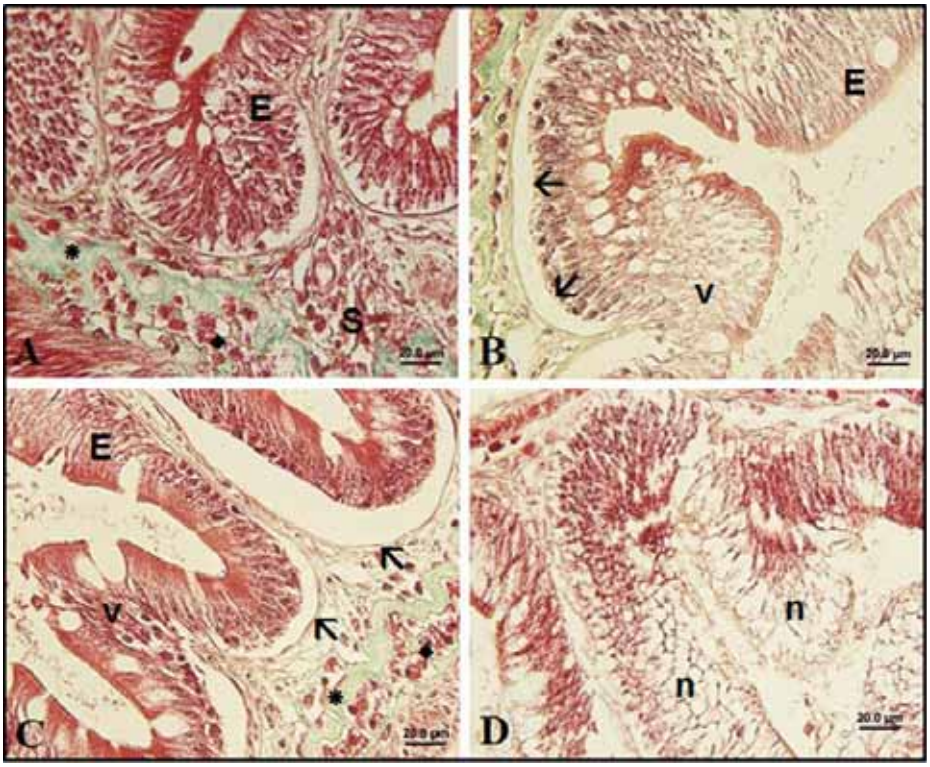

FIGURE 1

The effect of MTZ on the intestine depending on dose and time. E; cili columnar epitelium with cilia, v; villus, S; submucosae, ❋; str. compactum, ◆; str. granulosum, n; necrosis of epithelia, →; defects of basal part of epithelia. A: Control (-), B: Control (+), C: MTZ 5 mg/L days 2, D: MTZ 20 mg/L days 8. Staining: Gomori trichrome (Bar: 20 µ).

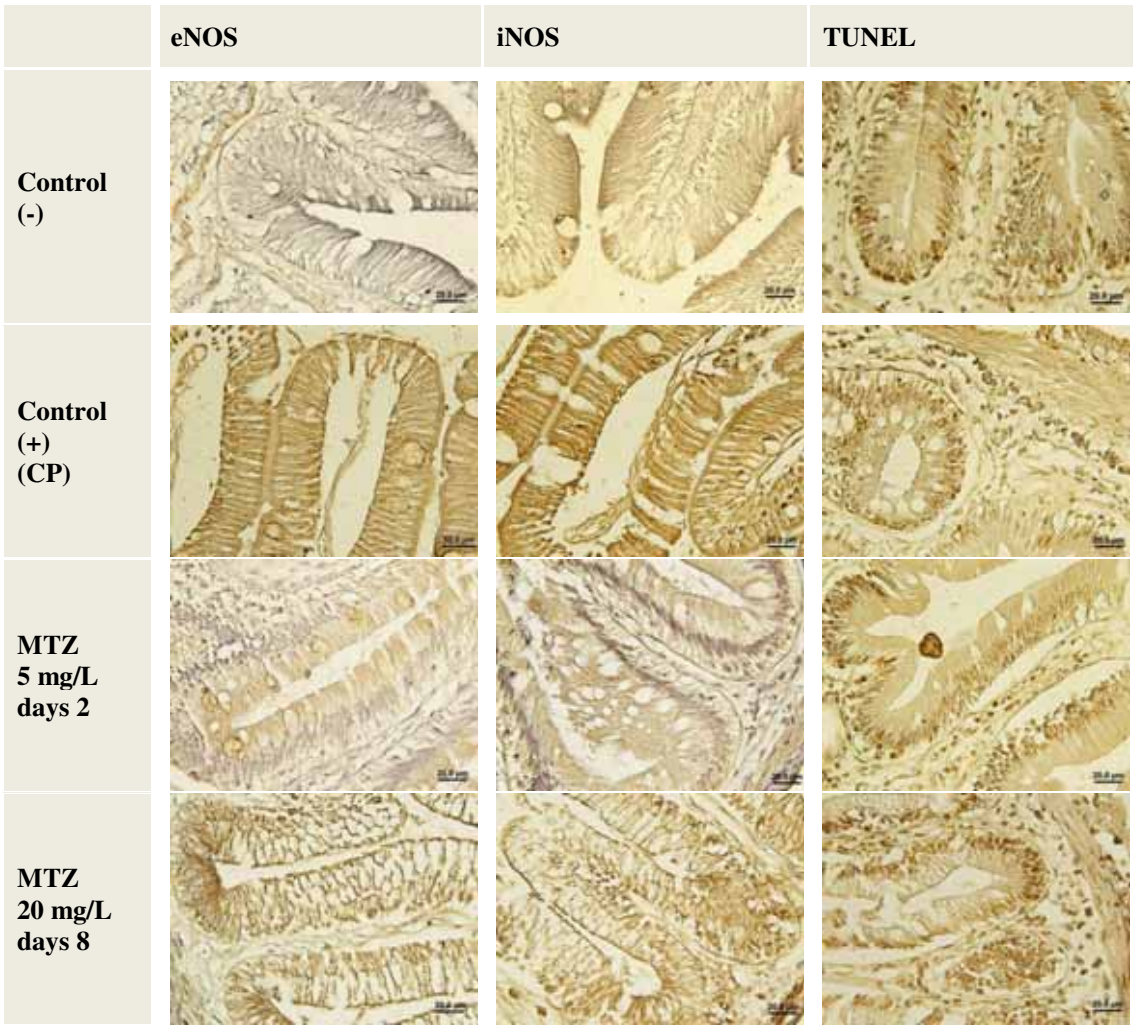

FIGURE 2
Immunocytochemistry of *O. mykiss* intestine after MTZ application. Histopathologic alterations due to MTZ depending on dose and duration can be observed due to oxidative stress (NOS) and apoptotic cell death (TUNEL) (Bar: 20 µ).

mechanisms of cell death. However, in the positive samples to which CP was applied, TUNEL positivity was less in the necrotic regions at the villus tips.

In MTZ practices, staining was higher than in the control group but decreased according to the CP application in the form of increase with dosage and was also observed in the epithelium and connective tissues. The TUNEL positive cells observed at the bases of the villi but less in the epithelium were distributed heterogeneously. Villus bases at high doses were compared to low doses, and more apoptotic cells in the connective tissue were found as well (Figure 2).

During the scoring performed for eNOS, iNOS and TUNEL markers/indicators in the fish intestine subjected to the effect of MTZ for 2 days, a similar sham case at 5 mg doses was determined, where quite a significant increase ($p<0.001$) at 10 and 20 mg doses similar to CP was also found. Similar results were also achieved on the 4th and 8th days (Figure 3, 4, 5).

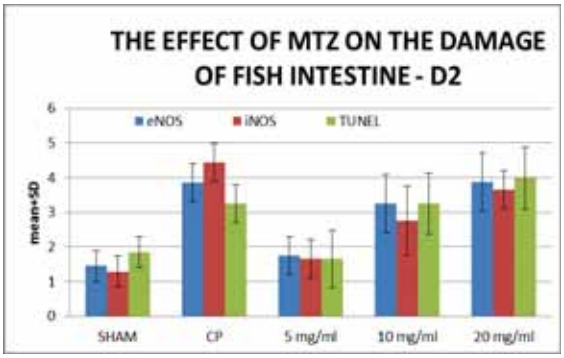

FIGURE 3
Scoring of two days application of MTZ with pathologic parameters. There were significant ($p<0,001$ including *eNOS*: Sham vs CP, Sham vs MTZ20, MTZ5 vs MTZ20; *iNOS* and *TUNEL*: Sham vs CP, CP vs MTZ5, MTZ5 vs MTZ20) alterations due to dosage, between sham and CP application controls.

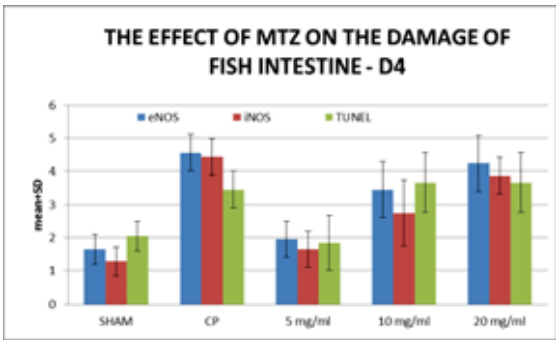

FIGURE 4
Scoring of four days application of MTZ with pathologic parameters. There were significant (p<0,01 including *eNOS* and *iNOS*: Sham vs CP, Sham vs MTZ20, CP vs MTZ5; p<0,05 including *TUNEL*: Sham vs CP, CP vs MTZ5) alterations due to dosage, between sham and CP application controls.

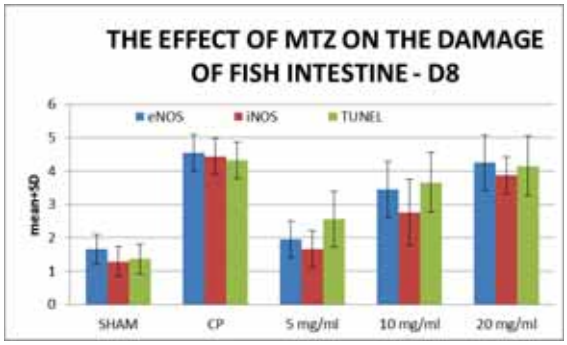

FIGURE 5
Scoring of eight days application of MTZ with pathologic parameters. There were significant (p<0,01 including *eNOS* and *iNOS*: Sham vs CP, Sham vs MTZ20, CP vs MTZ5; *TUNEL*: Sham vs CP, Sham vs MTZ20) alterations due to dosage, between sham and CP application controls.

DISCUSSION

The agents used for therapeutic purposes are potentially harmful. It is reported that the increasing nitrate rate has a negative effect on aquatic organisms, such as infection, various physiological stresses, stimulation of the immune system and tissue injury. Separately, nitrate is also reported to cause the development of renal failure and the failure in the oxygen-carrying capacity within the bloodstream [3, 33, 34]. While the corticotrophin releasing factor, cortisone and the secretion of ACTH increase under acute stress conditions, it may also lead to the secretion of reactive oxygen metabolites, such as cytokines, chemokines, growth factors, arachidonic acid and nitric oxide, when the central immune system cell population is activated. In this study, the toxic effects of MTZ used as an antibiotic was examined, and the presence of its association with the oxidative stress was shown. The increasing free radicals were found to have driven a cell to death through apoptosis.

NO is an important molecule that plays a role within the intracellular and extracellular messenger system that exits in all living organisms, extending from bacteria to mammals. NO acts as a mediator in the activation of cGMP synthesis over signal pathways, in the changes occurring in cytosolic Ca^{2+} concentration and in protein-kinase activation [20]. NO has an anti-oxidant effect over the detoxification of reactive oxygen metabolites, as well as free radical activity with the formation of redox couples. When cells are confronted with this medium, their response, depending on the dose and time period, is death through either necrotic or apoptotic mechanisms [22]. In our study, we investigated the relationship between the damage that occurred in the intestines on which MTZ was applied and these mechanisms. It was determined that the damage had occurred through oxidative stress, whereas in the areas where the damage was serious, the regions which were necrotically moderate, the cells were determined to have died through apoptotic mechanisms.

While inflammation and erosion in damaged intestines, particulary the epithelium, was monitored, integrations were observed at the tips of the villi and vacuoles in the epithelium [35, 36]. Similar forms of these findings detected through indomethacin were also observed via the MTZ practice. While MTZ provides tissue health with an immunomodulator effect, some damage occurs along with the dosage increase. The oxidative stress and ROS level on a basal level in intestines showed an antioxidant effect in normal doses in healthy rats. Such an effect, however, was shown on a different level in the intestines during the MTZ administration, and oxidative stress occurred.

In a study conducted previously, similar oxidative damage occurred in the intestines through the titanium dioxide nanoparticle (TiO_2 NP) practice and showed histopathological changes similar to those in our study. In this sort of damage, the findings in the intestines also indicate erosion in the villi, integration and mucosal vacuoles [37]. On the other hand, in another study, when high doses of indomethacin were used, an increasing toxic effect depending on the dose and time period was also observed, in addition to which this toxic effect was said to be likely to occur in mammals as well [38]. In this sense, the findings in our study also seem to be significant for mammals.

One of the findings obtained in fish intestines with the toxic effect is related to cells using apoptotic mechanisms. The moderate reaction in the cell injury due to oxidative stress is apoptosis, and in a former study, apoptotic cells were encountered in the intestines that underwent gastroenteritis, along with the findings determined in our study [39]. More promi-

nent in the epithelial cells, apoptotic cells were detected also in the Goblet cells and in the connective tissue both in the former study and in ours.

In the previous study, several apoptotic figures were found, such as vascular dilatation, ruptured enterocytes, mucosal desquamation, as well as cell roundnesses--which are characteristic changes--eosinophilic cytoplasm, chromatin condensation and apoptotic particles, which were also found in our findings. Immunohistochemistry revealed that caspase 3 was positive in these cells, the morphology of which was identified above. In the previous study, apoptotic cells in small quantities were also determined in the control groups [39]. That those necrotic regions depended on high doses of antibiotics is different from what was observed in our study and changes our interpretation of apoptosis. The TUNEL staining we used as an indicator/marker was lower in some regions, and this was attributed to the death of cells through necrosis. Some results obtained from chromaffin cells in culture are examples of cases where necrosis is confused with apoptosis. In this study, we showed that signals regarding cell death, which originate from different sources, develop different forms of death. It was found that the free radicals caused apoptotic cell death through NOS activation, whereas the super oxide formation over peroxynitrite led to necrotic cell death. The major difference between these two types of cell death is ATP due to mitochondrial activation, in other words, the state of energy. However, what regulates this relationship is the effect dose and time period of the oxidative factor [40, 41]. A similar mechanism can also be considered to occur in the intestinal tissue.

In conclusion, the damage inflicted by MTZ application on the intestinal tissue and the extent of this phenomenon are presented. These results are becoming quite important in terms of human and environmental health, which are important issues for the quality of life and economic benefit of the public.

REFERENCES

[1] Barton, B.A., Iwama, G.K. (1991). Physiological changes in fish from stress in aquaculture with emphasis on the response and effects of corticosteroids. Annual Review of Fish Diseases 991, 3-26.

[2] Wendelaar Bonga, S.E. (1997). The stress response in fish. Physiological Reviews 77, 591–625.

[3] Fabbri, E., Capuzzo, A., Moon, T.W. (1998). The role of circulating catecholamines in the regulation of fish metabolism: An overview. Comparative Biochemistry and Physiology Part C, 20, 177-192.

[4] Farzadkia, M., Esrafili, A., Baghapour, M.A., Shahamat, Y.D., Okhovat, N. (2014). Degradation of metronidazole in aqueous solution by nano-ZnO/UV photocatalytic process. Desalination and Water Treatment 52, 4947-4952.

[5] Farzadkia, M., Bazrafshan, E., Esrafili, A., Yang, J. K., Shirzad-Siboni, M. (2015). Photocatalytic degradation of Metronidazole with illuminated TiO2 nanoparticles. Journal of Environmental Health Science and Engineering 21, 13-35.

[6] Cavaş, T., Ergene-Gözükara, S. (2005). Genotoxicity evaluation of metronidazole using the piscine micronucleus test by acridine orange fluorescent staining. Environmental Toxicology and Pharmacology 19, 107-11.

[7] Gürcü, B., Koca, Y.B., Özkut, M., Tuğlu, M.İ. (2016). Matrix changes due to the toxic effects of metronidazole in intestinal tissue of fish (Onchorhynchus mykiss). Chemosphere 144, 1605-10.

[8] Wagil, M., Maszkowska, J., Białk-Bielińska, A., Caban, M., Stepnowski, P., Kumirska, J. (2015). Determination of metronidazole residues in water, sediment and fish tissue samples. Chemosphere 119, 28-34.

[9] Bendesky, A., Menéndez, D., Ostrosky-Wegman, P. (2002). Is metronidazole carcinogenic?. Mutation Research 511, 133-44.

[10] Ezzeldin, E. (2012). Pharmacodynamic and pharmacokinetics of metronidazole in protein malnourished rats. African Journal of Pharmacy and Pharmacology 6, 2982-2993.

[11] Chang, N.B. (2011). Making a Progress to Speed up the Nitrification and Denitrification Processes in Novel Biosorption Activated Media: Can Archaea be in Concert with Anammox?. Journal of Bioprocessing and Biotechniques. 1, 2.

[12] Yarube, I.U. (2011). Nitrate-induced oxidative stress and the effects of dietary antioxidant vitamins C, E and A: insights from experimental and clinical studies. Bayero Journal of Pure and Applied Sciences 4, 69-79.

[13] Lundberg, J.O., Weitzberg, E., Gladwin, M.T. (2008). The nitrate-nitrite-nitric oxide pathway in physiology and therapeutics. Nature Reviews. Drug Discovery 7, 156-67.

[14] Weitzberg, E., Hezel, M., Lundberg, J.O. (2010). Nitrate-Nitrite-Nitric Oxide Pathway: Implications for Anesthesiology and Intensive Care. Anesthesiology 113, 1460-1475.

[15] Ribeiro, M.O., Antunes, E., de Nucci, G., Lovisolo, S.M., Zatz, R. (1992). Chronic inhibition of nitric oxide synthesis. A new model of arterial hypertension. Hypertension 20, 298-303.

[16] Omer, N., Rohilla, A., Rohilla, S., Kushnoor, A. (2012). Nitric Oxide: Role in Human Biology. International Journal of Pharmaceutical Sciences and Drug Research 4, 105-109.

[17] Brüne, B. (2003). Nitric oxide: NO apoptosis or

turning it ON?. Cell Death and Differentiation 10, 864–869.
[18] Pacher, P., Beckman, J.S., Liaudet, L. (2007). Nitric oxide and peroxynitrite in health and disease. Physiological Reviews, 87, 315-424.
[19] Kone, B.C. (2006). S-nitrosylation: targets, controls and outcomes. Current Genomics 7, 301-310.
[20] Kasprowicz, A., Szuba, A., Volkmann, D., Baluska, F., Wojtaszek, P. (2009). Nitric oxide modulates dynamic actin cytoskeleton and vesicle trafficking in a cell type-specific manner in root apices. Journal of Experimental Botany 60, 1605-17.
[21] Kumral, Z.N., Sener, G., Ozgur, S., Koc, M., Suleymanoglu, S., Hurdag, C., Yegen, B.C. (2016). Regular exercise alleviates renovascular hypertension-induced cardiac/ endothelial dysfunction and oxidative injury in rats. Journal of Physiology and Pharmacology 67, 45-55.
[22] Oset-Gasque, M.J., Fuentes, M.P., Vicente, S., Figueroa, S., Pérez-Rodríguez, R., González, M.P. (2004). Mitochondrial mechanisms involved in nitric oxide (NO)-induced apoptosis in bovine chromaffin cells in primary culture. Cell Biology of the Chromaffin Cell R. Borges & L. Gandía Eds. Instituto Teófilo Hernando, Spain 167-174.
[23] Bal-Price, A., Brown, C. (2000). Nitric-oxide-induced necrosis and apoptpsis in PC12 cells Mediated by mitochondria. Journal of Neurochemistry 75, 1455-1464.
[24] Mannick, J.B. (2007). Regulation of apoptosis by protein S-nitrosylation. Amino Acids 32, 523-526.
[25] Bey, E.A., Reinicke, K.E., Srougi, M.C., Varnes, M., Anderson, V.E., Pink, J.J., Li, L.S., Patel, M., Cao, L., Moore, Z., Rommel, A., Boatman, M., Lewis, C., Euhus, D.M., Bornmann, W.G., Buchsbaum, D.J., Spitz, D.R., Gao, J., Boothman, D.A. (2013). Catalase abrogates β-lapachone-induced PARP1 hyperactivation-directed programmed necrosis in NQO1-positive breast cancers. Molecular Cancer Therapeutics 12, 2110-20.
[26] Elmore, S. (2007). Apoptosis: a review of programmed cell death. Toxicologic Pathology 35, 495-516.
[27] Dhanasekaran, D.N., Reddy, E.P. (2008). JNK signaling in apoptosis. Oncogene 27, 6245-51.
[28] Ashkenazi, A., Dixit, V.M. (1998). Death receptors: Signaling and modulation. Science 281, 1305-1308.
[29] Zhou, L., Li, Y., Yue, B.Y. (1999). Oxidative stress affects cytoskeletal structure and cell-matrix interactions in cells from an ocular tissue: the trabecular meshwork. Journal of Cellular Physiology 180, 182-9.
[30] Bancroft, J.D., Cook, H.C. (1994). Manual of histological techniques and their diagnostic application. Churchill Livingstone, New York 457.
[31] Inan, S., Ozturkcan, S., Vatansever, S., Ermertcan, A.T., Zeybek, D., Oksal, A., Giray, G., Muftuoglu, S. (2006). Histopathological and ultrastructural effects of glycolic acid on rat skin. Acta Histochemica 108, 37-47.
[32] Ozbilgin, K., Boz, B., Tugyan, K., Inan, S., Vatansever, S. (2012). RHAMM Expression in the Rat Endometrium during the Estrous Cycle and following Implantation. Journal of Reproduction and Infertility 13, 131-7.
[33] Shimura, R., Ma, Y.X., Ijiri, K., Nagaoka, S., Uchiyama, M. (2004). Nitrate toxicity on visceral organs of Medaka fish, Oryzias latipes: aiming to raise fish from egg to egg in space. Biological Sciences in Space 18, 7-12.
[34] Camargo, J.A., Alonso, A., Salamanca, A. (2005). Nitrate toxicity to aquatic animals: a review with new data for freshwater invertebrates. Chemosphere 58, 1255-67.
[35] Filaretova, L.P., Bagaeva, T.R., Morozova, O.Y., Zelena, D. (2014). A wider view on gastric erosion: detailed evaluation of complex somatic and behavioral changes in rats treated with indomethacin at gastric ulcerogenic dose. Endocrine Regulations 48, 163-72.
[36] Hayashi, S., Kurata, N., Yamaguchi, A., Amagase, K., Takeuchi, K. (2014). Lubipros-tone prevents nonsteroidal anti-inflammatory drug-induced small intestinal damage by suppressing the expression of inflammatory mediators via EP4 receptors. The Journal of Pharmacology Experimental Therapeutics 349, 470-9.
[37] Federici, G., Shaw, B.J., Handy, R.D. (2007). Toxicity of titanium dioxide nanoparticles to rainbow trout (Oncorhynchus mykiss): gill injury, oxidative stress, and other physiological effects. Aquatic Toxicology 84, 415-30.
[38] Lovy, J., Speare, D.J., Wright, G.M. (2007). Pathological effects caused by chronic treatment of rainbow trout with indomethacin. Journal of Aquatic Animal Health 19, 94-8.
[39] Ronza, P., Bermúdez, R., Losada, A.P., Robles, A., Quiroga, M.I. (2011). Mucosal CD3ε+ cell proliferation and gut epithelial apoptosis: implications in rainbow trout gastroenteritis (RTGE). Journal of Fish Diseases 34, 433-43.
[40] Vicente, S., Pérez-Rodríguez, R., Oliván, A.M., Martínez Palacián, A., González, M.P., Oset-Gasque, M.J. (2006). Nitric oxide and peroxynitrite induce cellular death in bovine chromaffin cells: evidence for a mixed necrotic and apoptotic mechanism with caspases activation. Journal of Neuroscience Research 84, 78-96.

[41] Merino, J.J., Roncero, C., Oset-Gasque, M.J., Naddaf, A., González, M.P. (2014). Antioxidant and protective mechanisms against hypoxia and hypoglycaemia in cortical neurons in vitro. International Journal of Molecular Sciences 15, 2475-93.

Received: **20.04.2017**
Accepted: **07.08.2017**

CORRESPONDING AUTHOR

Beyhan Gurcu
Celal Bayar University, School of Science and Letter, Department of Biology, Manisa-Turkey

e-mail: byhgurcu@gmail.com

© by PSP Volume 26 – No. 10/2017 pages 5858-5864 Fresenius Environmental Bulletin

A CASE STUDY: TREND ANALYSIS OF TOTAL ANNUAL RAINFALLS ON EASTERN ANATOLIA REGION IN TURKEY

Serkan Senocak[1,*] , Muhammed Fatih Emek[2]

[1]Atatürk University, Engineering Faculty, Civil Engineering Department, 25240 Erzurum, Turkey
[2]12th Regional Directorate of Highways, 25070 Erzurum, Turkey

ABSTRACT

In this study, a possible trend that may be occurring is being investigated, and the trend being investigated is the total annual rainfalls fall in Eastern Anatolia Region of Turkey. For this reason, Mann-Kendall test, Spearman's Rho test and Sen's slope method was applied to total annual rainfall data collected from 38 rainfall observation stations.

According to the study results; there has been a significant decrease in rainfall in 4 observation stations: Baskil, Dogansehir, Ercis and Sivrice, with 95% confidence level. There is a 10% significance level, that Agin and Elazig have also seen decreasing trends in rainfall. According to Sen's slope method there has been a a decrease observed in 28 stations, also there has been no significant increase in rainfall being observed in 10 other observation stations. There is a general increasing trend in rainfall that dominates Eastern Anatolia Region's northern parts, while a decreasing trend is occurring in the southern and western region. These results could be due to regional climate changes and are consistent with projections related to climate change phenomena.

KEYWORDS:
Eastern Anatolia Region; Trend analysis, Mann–Kendall test, Spearman's rho test, Sen's slope method

INTRODUCTION

Knowledge of trends and variations in current and historical hydro-climatological variables has become pertinent to the future development and sustainable management of water resources in a given region especially within the context of global warming, water and energy cycles and the increasing demand for water due to population and economic growth [1, 2, 3]. Rainfall, is one of indicators of climate change, and a principal element of the hydrological cycle. Being able to detect trends in precipitation time series yields important information when it comes to understanding the climate.

Many researchers have analyzed variability and trends in rainfall across the world. Fluctuations of precipitation in Europe has been analyzed using a series of annual areal precipitation sums described in a different study [4].

Trend within a 64 year period (1929-1993) of rainfall at 96 stations was examined in Turkey [5]. The overall result indicated that the trend in precipitation is a downward one, nonetheless, there are few stations that showed increasing trend. Annual extreme precipitation for short duration rainfalls (SDR), which ranges from 5 to 60 minutes, was studied using the Adana city station and Black Sea Region of Turkey in order to find possible trends [6, 7].

This study, determined the trend of the annual total rainfalls by using Mann-Kendall test and Spearman's rho test which are nonparametric methods and the trend slopes were determined by using the Sen's slope test, with the data that was obtained from the precipitation stations in Eastern Anatolia Region.

MATERIALS AND METHODS

The study area and data. Turkey is located at the eastern corner of southern Europe, and is one of the five regions selected by the Intergovernmental Panel on Climate Change (IPCC) for rainfall and environmental studies. Eastern Anatolia Region, is the roof of Turkey, and is the highest and most rugged region of Turkey and it has a triangular shape. The region contains 21% of the land mass of Turkey, is 163.000 km², and the widest region among the 7 geographical regions in Turkey. In the Eastern region of Anatolia, the elevation of the mountains exceeds 2500-3000 m. Coldest temperatures range from -30°C to -38°C and are usually observed in the mountainous area of the east, and snow may lie on the ground 120 days of the year.

In order to analyze the trend in rainfall in the Eastern Anatolia Region, total annual rainfall records from 38 stations operated by Turkish State Meteorological Service (TSMS) were used in this study. Further, the data collected from the 38 precipitation stations, is between the years 1960 and 2013 in order to try and find possible trends. Keban Precipitation Station and Baskale Precipitation Station draw the most attention, of the 38 precipitation stations being

considered because they are 808 and 2286 meters above the sea level respectivily. In the Figure 1, the station numbers of the 38 stations being used for evaluation in this study is shown, and the data being used is shown in Table 1.

Methods. Since the rainfall trend analysis is based on long-term examination, obtaining data on a monthly or a seasonal basis will not affect the result of the analysis. The trend can be linear or curvilinear. However, the most significant characteristic to look for in the rainfall trend is that it is consistent with both conditions.

It can be discovered using statistical tests whether a considerable decrease or an increment (trend) increase has occurred in the measured values over the course of time. Since the hydrological magnitudes (precipitation, flow) have a characteristic that changes randomly over time, researching a continuous decreasing or increasing inclination requires the use of specific methods [8].

Mann – Kendall test. Mann-Kendall test is a statistical testing method that is commonly used in defining the trend of the time series in hydrology and climatology fields and it is recommended by the World Meteorological Organization (WMO). Mann-Kendall test has been used to determine trend analysis in several studies. The Mann-Kendall statistic S is given as:

$$S = \sum_{k=1}^{n-1} \sum_{j=k+1}^{n} \mathrm{sgn}(x_j - x_k) \quad (1)$$

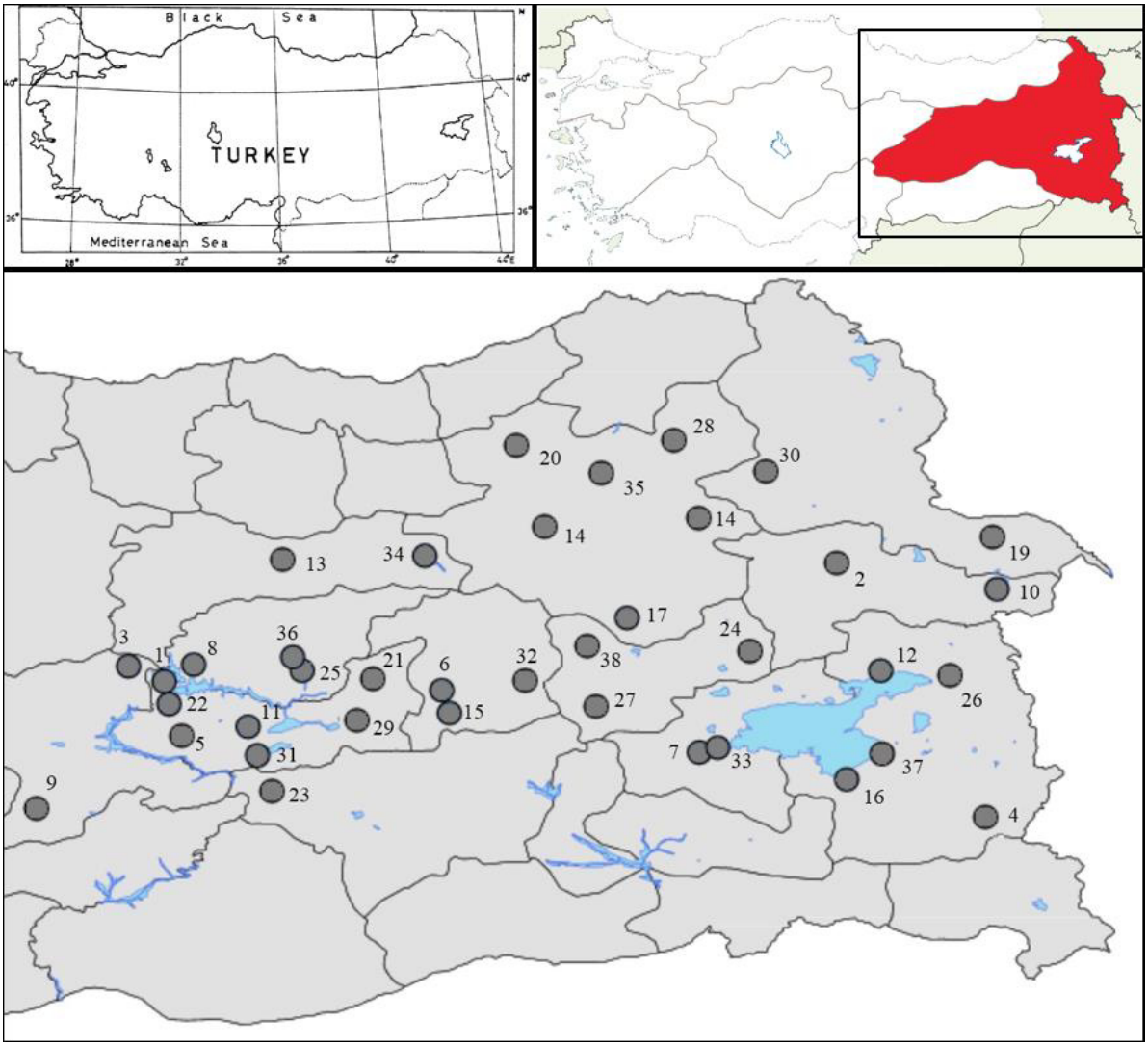

FIGURE 1
Map of rainfall

TABLE 1
Station locations and record duration (listed in alphabetical)

		Positions			
		Longitude	Latitude	Elevation	
	Stations	(E)	(N)	(m)	Record Duration
1	Agin	38,72	38,94	900	1979–2013 (35)
2	Agri	43,05	39,73	1646	1960–2013 (54)
3	Arapgir	38,49	39,04	1211	1964–2010 (47)
4	Baskil	38,83	38,57	1300	1979–2013 (35)
5	Baskale	44,02	38,04	2286	1964–2013 (50)
6	Bingol	40,50	38,88	1177	1963–2013 (51)
7	Bitlis	42,16	38,47	1785	1965–2010 (46)
8	Cemisgezek	38,91	39,05	953	1969–2013 (45)
9	Dogansehir	37,89	38,09	1223	1965–2013 (49)
10	Dogubeyazıt	44,09	39,55	1725	1963–2009 (47)
11	Elazig	39,26	38,64	989	1960–2013 (54)
12	Ercis	43,34	39,02	1678	1965–2013 (49)
13	Erzincan	39,49	39,75	1216	1960–2013 (54)
14	Erzurum	41,19	39,95	1758	1960–2008 (49)
15	Genc	40,55	38,73	1250	1980–2013 (34)
16	Gevas	43,12	38,29	1694	1982–2013 (32)
17	Hinis	41,69	39,37	1715	1964–2011 (48)
18	Horasan	42,17	40,04	1540	1969–2013 (45)
19	Igdir	44,05	39,92	856	1960–2013 (54)
20	Ispir	40,99	40,48	1223	1965–2011 (47)
21	Karakocan	40,04	38,94	1090	1980–2013 (34)
22	Keban	38,74	38,79	808	1963–2013 (51)
23	Maden	39,40	38,23	1100	1980–2010 (31)
24	Malazgirt	42,53	39,13	1540	1963–2013 (51)
25	Mazgirt	39,60	39,02	1400	1982–2013 (32)
26	Muradiye	43,76	38,99	1706	1964–2013 (50)
27	Mus	41,50	38,75	1322	1964–2013 (50)
28	Oltu	41,99	40,55	1312	1966–2013 (48)
29	Palu	39,93	38,69	869	1966–2013 (48)
30	Sarikamis	42,59	40,33	2092	1963–2013 (51)
31	Sivrice	39,31	38,45	1240	1979–2013 (35)
32	Solhan	41,05	38,96	1366	1965–2013 (49)
33	Tatvan	42,28	38,50	1687	1965–2013 (49)
34	Tercan	40,39	39,78	1429	1964–2013 (50)
35	Tortum	41,54	40,30	1576	1963–2013 (51)
36	Tunceli	39,54	39,10	981	1964–2013 (50)
37	Van	43,35	38,47	1675	1960–2013 (54)
38	Varto	41,44	39,17	1510	1977–2010 (34)

The application of trend test is done using a time series x_i that is ranked from $i = 1,...,n-1$ and x_j, which is ranked from $j = i+1,...,n$. Each of the data point in x_i is taken to be a reference point which is compared to the rest of the data points x_j so that, where

$$\mathrm{sgn}(\theta) = \begin{cases} 1 \ \ if \ \ \theta > 0 \\ 0 \ \ if \ \ \theta = 0 \\ -1 \ if \ \ \theta < 0 \end{cases} \quad (2)$$

It has been documented that when $n \geq 8$, the statistic S is approximately normally distributed with the mean.

$E(S) = 0$

The variance statistic is given as:

$$Var(S) = \frac{n(n-1)(2n+5)\sum_{i=1}^{q} t_p(t_p-1)(2t_p+5)}{18} \quad (3)$$

The test statistics Z is computed as:

$$Z = \begin{cases} \frac{S-1}{\sqrt{Var(S)}}, & S > 0 \\ 0, & S = 0 \\ \frac{S+1}{\sqrt{Var(S)}}, & S < 0 \end{cases} \quad (4)$$

Z here follows a standard normal distribution. A positive (negative) value of Z signifies an upward (downward) trend. A significance level α is also utilized for testing either an upward or downward monotone trend (a two-tailed test). If Z is greater than $Z_{\alpha/2}$ where α depicts the significance level, then the trend is considered to be significant.

Spearman's Rho test. A quick and simple test is the Spearman's rank correlation test to determine whether a correlation exists between two classifications of the same series of observations. In this test, there is a significant trend only if the correlation between time steps and rainfall observations is found to be significant. Account of the test statistic Z based on r_s was not presented here, since it can easily be found in any statistical books.

TABLE 2
Station locations and record duration (listed in alphabetical)

		Mann–Kendall			Spearman's Rho			Sen's Slope
	Stations	*Z*	α=0,05	α=0,1	**Z**	α=0,05	α=0,1	*Q*
1	Agin	-1,704	-	↓	-1,717	-	↓	-3,49
2	Agri	-0,813	-	-	-0,828	-	-	-0,78
3	Arapgir	-1,174	-	-	-1,305	-	-	-2,33
4	Baskil	-2,073	↓	↓	-1,984	↓	↓	-3,58
5	Baskale	-0,435	-	-	-0,539	-	-	-0,57
6	Bingol	-0,796	-	-	-0,809	-	-	-1,36
7	Bitlis	-1,042	-	-	-0,965	-	-	-2,97
8	Cemisgezek	0,538	-	-	-0,636	-	-	-0,82
9	Dogansehir	-2,086	↓	↓	-2,216	↓	↓	-2,97
10	Dogubeyazit	1,101	-	-	1,061	-	-	1,15
11	Elazig	-1,895	-	↓	-1,790	-	↓	-1,66
12	Ercis	-2,250	↓	↓	-2,158	↓	↓	-3,14
13	Erzincan	-0,254	-	-	-0,251	-	-	-0,24
14	Erzurum	0,086	-	-	0,221	-	-	0,05
15	Genc	-1,156	-	-	-0,984	-	-	-3,74
16	Gevas	-0,892	-	-	-0,894	-	-	-2,70
17	Hinis	0,364	-	-	0,331	-	-	0,54
18	Horasan	0,655	-	-	0,731	-	-	0,71
19	Igdir	0,962	-	-	0,894	-	-	0,67
20	Ispir	1,229	-	-	1,369	-	-	1,21
21	Karakocan	0,000	-	-	-0,189	-	-	-0,07
22	Keban	-1,267	-	-	-1,361	-	-	-1,48
23	Maden	-1,360	-	-	-1,500	-	-	-5,57
24	Malazgirt	0,244	-	-	0,171	-	-	0,28
25	Mazgirt	-0,211	-	-	-0,157	-	-	-1,11
26	Muradiye	0,803	-	-	0,925	-	-	1,11
27	Mus	-0,435	-	-	-0,516	-	-	-0,74
28	Oltu	0,693	-	-	0,652	-	-	0,67
29	Palu	-1,467	-	-	-1,450	-	-	-2,17
30	Sarikamis	-0,211	-	-	-0,171	-	-	-0,33
31	Sivrice	-2,031	↓	↓	-1,998	↓	↓	-4,48
32	Solhan	-0,233	-	-	-0,381	-	-	-0,22
33	Tatvan	-1,595	-	-	-1,596	-	-	-3,61
34	Tercan	-0,368	-	-	-0,334	-	-	-0,44
35	Tortum	-0,812	-	-	-0,950	-	-	-0,88
36	Tunceli	-1,121	-	-	-1,200	-	-	-2,83
37	Van	0,358	-	-	0,244	-	-	0,32
38	Varto	0,000	-	-	-0,089	-	-	-0,05

The test statistics r_s is computed as:

$$r_s = 1 - 6\left[\sum_{i=1}^{n}(R(x_i)-i)^2\right]/(n^3-n) \quad (5)$$

For $n>30$, the distribution of r_s will be normal, so that the normal distribution tables can be used. In this case, the test statistic r_s is computed by

$$Z = r_s\sqrt{n-1} \quad (6)$$

If $|Z| > Z_\alpha$ at a significance level of α; then the null hypothesis of no trend (in other words, values of observations are identically distributed) is rejected.

Sen's estimator of slope. If a linear trend is present, the true slope (change per unit time) can be estimated by using a simple non-parametric procedure. In computational procedures, the slope estimates of *N* pairs of data are first computed by

$$Q_i = \frac{x_j - x_k}{j-k} \quad (7)$$

for $i = 1,\ldots,N$; where x_j and x_k are data values at times j and k ($j>k$); respectively. The median of these *N* values of *Qi* is Sen's estimator of slope. If there is only one datum in each time period,

$$N = n.(n-1)/2 \quad (8)$$

Where *n* is the number of time periods. If *N* is odd, then Sen's estimator is computed by

$$Q_{median} = Q_{(N+1)/2} \quad (9)$$

and if is even, then Sen's estimator is computed by

$$Q_{median} = \left[Q_{N/2} + Q_{(N+2)/2}\right]/2 \quad (10)$$

The detected value of Q_{median} is tested by a two-sided test at the 100(1-α)% confidence interval and true slope may be obtained by the non-parametric test.

RESULTS AND DISCUSSION

In this trend analysis, the aim was to evaluate the annual areal precipitation amounts using the date from the stations. The annual areal precipitations of each station has been analyzed with Mann-Kendall

test, Spearman's Rho test and the Sen's inclination method and the results obtained are in Table 2 [9].

According to Mann–Kendall and Spearman's Rho trend analysis results; existence of significant trend is observed at 4 of 38 rainfall observation stations those being Baskil, Dogansehir, Ercis and Sivrice, annual total rainfalls is at 95% confidence level. For 90% confidence level, the decreasing trends were observed in Agin, Baskil, Dogansehir, Elazig, Ercis and Sivrice rainfall observation stations, as shown in Figure 2.

The inclination of the trend in these stations becomes significant following the analysis if a considerable trend exists. The Sen's inclination method has been used in order to define the inclination of the trend. As a result of the analyses carried out with Sen's inclination method using the data obtained from the 38 precipitation stations; it has been observed that the inclination was an increasing one at 10 precipitation stations and a decreases one at the 28 stations. It is showed that the increase occurred generally in northern located stations of the Eastern Anatolia Region. Trends in Baskil, Dogansehir, Ercis and Sivrice are shown in Figures 3-6 (for 95% confidence level).

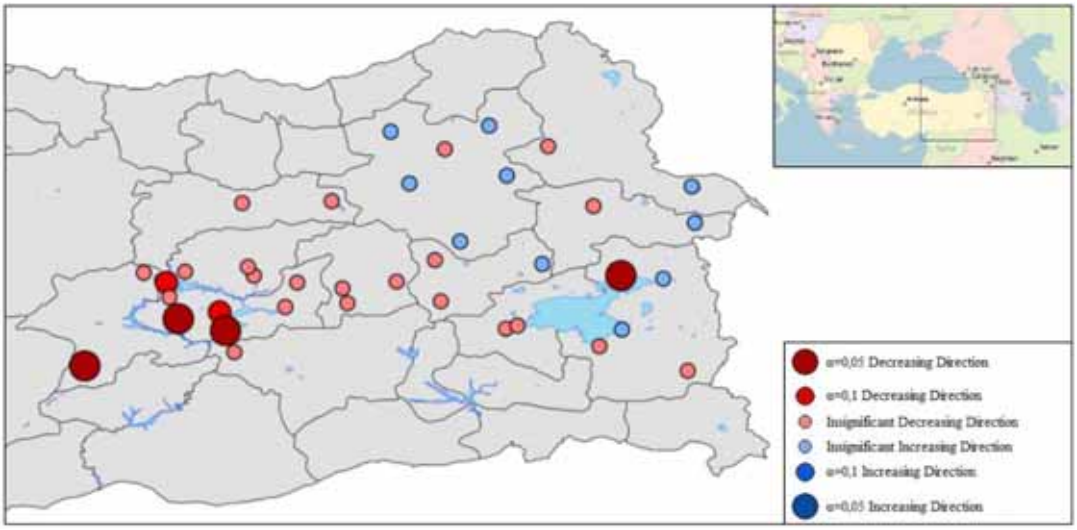

FIGURE 2
Results of Mann–Kendall and Spearman's Rho trend analysis.

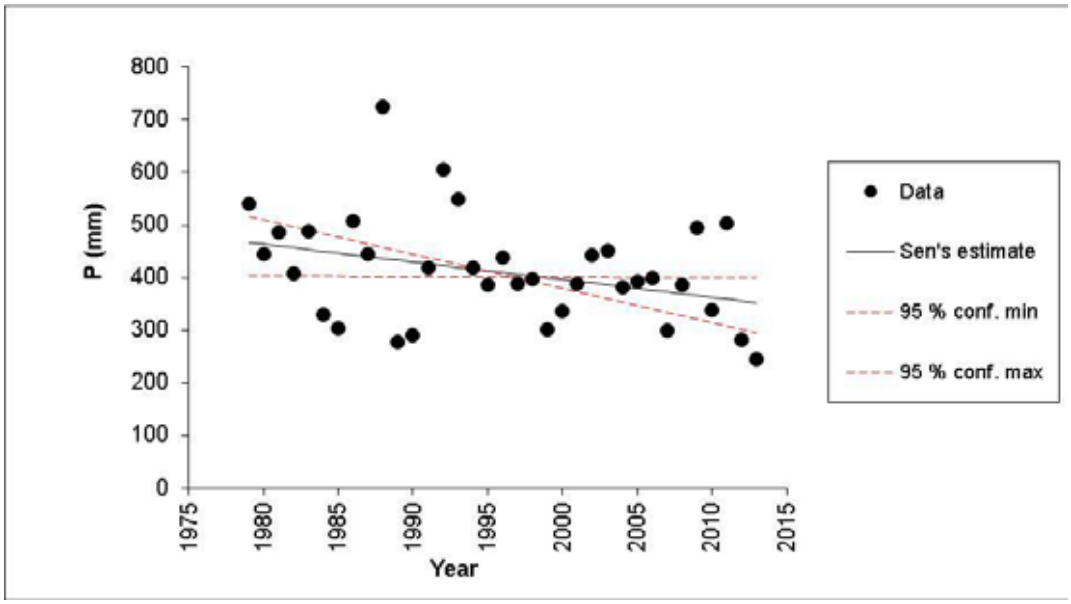

FIGURE 3
Trend analysis results for Baskil station.

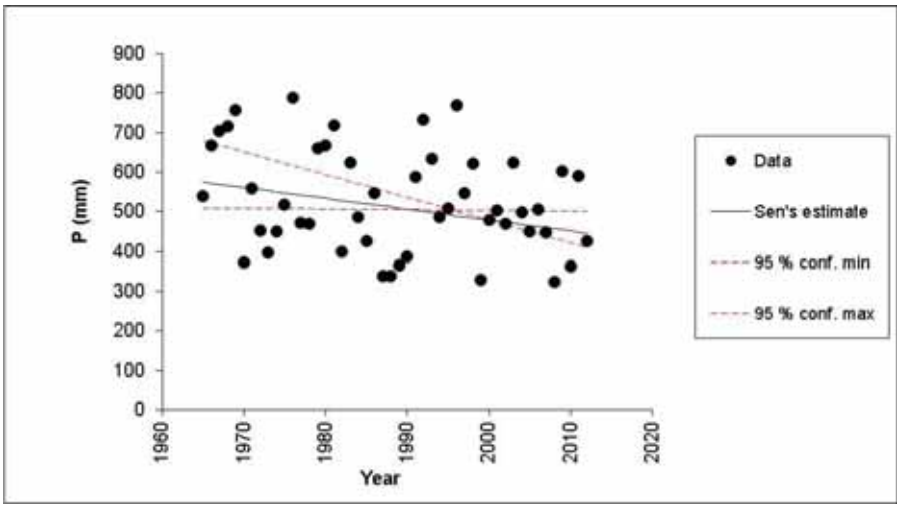

FIGURE 4
Trend analysis results for Dogansehir station

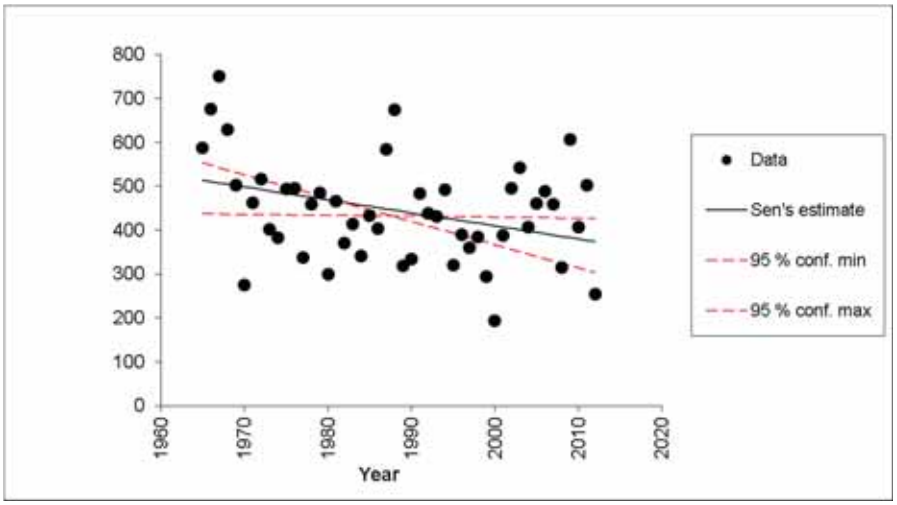

FIGURE 5
Trend analysis results for Ercis station

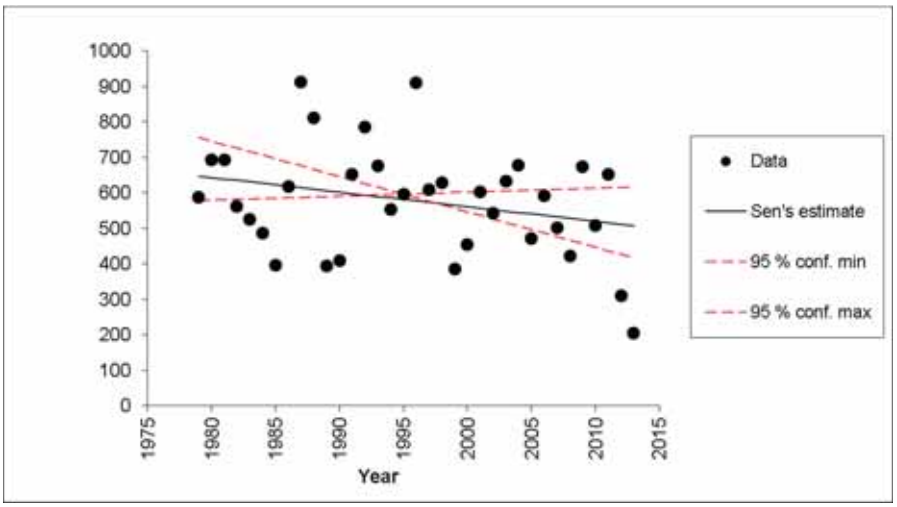

FIGURE 6
Trend analysis results for Sivrice station

CONCLUSIONS

In Eastern Anatolia Region, which is the widest geographical region in Turkey, the precipitations usually occur in form of snow and irregular rainfall, which causes the flow regime to become irregular. The precipitations being in the form of snow make it an important factor in the rivers if they will flow rapidly in the spring or not. Moreover, the high elevations and the steep slopes of the region create a potential for hydroelectricity.

The highest precipitation with an average of 1247,7 mm occurs in Bitlis, and the lowest in Iğdır with the average of 258,4 mm. In addition, the highest precipitation value was observed in Tunceli with a total of 1992,8 mm in 1967, the lowest value was observed in Igdir station with 114,5 mm in 1970. When evaluated on average, between the years 1960 and 2013, the highest average yearly precipitation occurred with an average of 796,6 mm is in 1967 and the minimum precipitation with an average of 313,2 mm was in 2013.

According to Mann-Kendall trend analysis and Spearman's Rho trend analysis results; existence of the significant trend was observed at 4 of 38 units rainfall Baskil, Dogansehir, Ercis and Sivrice, annual total rainfalls at 95% confidence level. For 90% confidence level, decreasing significant trend was observed at Agin, Baskil, Dogansehir, Elazig, Erciş and Sivrice stations. According to the Sen's slope method a decreasing tendency occurred at 28 observation stations, also an increasing but not significant tendency happened at 10 observation station is determined.

The stations which show an increasing inclination are generally located in the northern area of the Eastern Anatolia Region. However, the increases in these stations do not constitute a significant trend.

The results of the analyses performed by Mann-Kendall test and Spearman's rho test for the total annual precipitations has shown that there has been significant decrease in the trend at the same stations, with the confidence interval between 90% and 95%. According to these results, the province of Elazig and its surroundings is under risk, since it shows a significant decreasing rainfall tendencies.

REFERENCES

[1] Cannarozzo, M., Noto, L.V. and Viola, F. (2006) Spatial distribution of rainfall trends in Sicily (1921-2000). Phys Chem Earth, 31(18), 1201–1211.

[2] Oguntunde, P.G., Friesen, J., De Giesen, N.V. and Savenije, H.H.G. (2006) Hydroclimatology of the Volta river basin in west Africa: trends and variability from 1901 to 2002. Phys Chem Earth, 31, 1180-1188.

[3] Oguntunde, P.G., Abiodun, B.J., Lischeid, G. (2011) Rainfall trends in Nigeria, 1901-2000. Journal of Hydrology, 411, 207-218.

[4] Brazdil, R. (1992) Fluctuation of Atmospheric Precipitation in Europe. GeoJournal, 27, 275-291.

[5] Partal, T. and Kahya, E. (2006) Trend analysis in Turkish precipitation data. Hydrol Process, 20, 2011-2026.

[6] Acar, R. and Senocak, S. (2008) Detection of statistically significant trends in the short duration rainfalls (SDR) of Adana city. EGU General Assembly 2008: IS22-HS2.1 Session on Climate, Water and Health, Vienna/Austria.

[7] Senocak, S., Acar, R. and Sengul, S. (2012) Annual extreme Short Duration Rainfall (SDR) trends in Black Sea Region of Turkey. Fifth International Conference on Water Observation and Information System for Decision Support (BALWOIS 2012), Ohrid, Republic of Macedonia

[8] Helsel, D.R. and Hirsch, R.M. (1992) Statistical methods in water resources. Elsevier Science Ltd.

[9] Emek, M.F. (2014) Trend analysis of annual and monthly rainfalls on Eastern Anatolia Region in Turkey. Graduate School of Natural and Applied Sciences, Ataturk University.

Received: **17.02.2017**
Accepted: **11.07.2017**

CORRESPONDING AUTHOR

Serkan Senocak
Department of Civil Engineering
Engineering Faculty
Ataturk University
25240 Erzurum – TURKEY

E-mail: ssenocak@atauni.edu.tr

© by PSP Volume 26 – No. 10/2017 pages 5865-5872 Fresenius Environmental Bulletin

SCREENING OF HYDROLYTIC ENZYME PRODUCTION AND FATTY ACID METHYL ESTERS (FAME) ANALYSIS OF THERMOPHILIC BACTERIA FROM HOT SPRINGS

Meral Yilmaz Cankilic[1,*], Emine Celikoglu[1], Umut Celikoglu[2]

[1]Department of Biology, Faculty of Science, Anadolu University, Eskisehir, Turkey
[2]Department of Chemistry, Faculty of Science, Anadolu University, Eskisehir, Turkey

ABSTRACT

Extremophilic enzymes can function with high efficiency under extreme conditions. Thermophilic bacteria constitute an important source in terms of these extremophilic enzymes. The isolation and identification of these bacteria and enzymes are very important for industrial applications. Many methods are used for the identification of microorganisms. The Fatty Acid Methyl Esters (FAME) analysis that enables the comparison of the methylated fatty esters of microorganisms in addition to 16S rRNA-based molecular identification also takes a significant place in the taxonomy. In this study, we examined the hydrolytic enzyme (protease, amylase, and lipase) production ability of our 65 thermophilic isolates, and the FAME analysis of some isolates was performed. As a result of the study, 42 thermophilic isolates exhibited a weak or strong protease, amylase and lipase activity. However, 23 isolates showed no activities for these enzymes when cultured on skim milk, starch, and tributyrin agar. The fatty acid analysis data showed the presence of 35 different fatty acids in 18 bacteria strains examined. 16:0 fatty acid was found in all strains. As a result of the analyses carried out based on the fatty acid profiles, it was determined that the bacteria strains were divided into 12 phenotypic groups, but these data did not match the genotypic analysis results exactly.

KEYWORDS:
Hydrolytic Enzymes, FAME, Balikesir, Kutahya, Thermophilic

INTRODUCTION

The enzymes, such as amylase, protease, lipase, laccase, nuclease, and polymerase, obtained from bacteria, actinomycetes, and fungi are used in almost all areas of the industry, molecular studies and bioremediation processes [1-6]. Plant or animal-derived enzymes do not exhibit a very high catalytic activity when compared to microbial enzymes. Therefore, microbial enzymes have great advantages in terms of not creating unwanted side products, being more stable and cheaper. Protease constitutes 60% of commercial enzymes, and it is widely used in the leather industry, food industry, pharmaceutical industry and bioremediation processes. Amylase is the other commercial enzyme responsible for the digestion of the starch used as food and food additives, and it makes up 25% of commercial enzymes. Furthermore, starch is used as a substrate for ethanol production. The importance of amylolytic enzyme increases because ethanol is used as a starting material for fuel additives or chemicals [7]. Thermophilic and hyperthermophilic enzymes are widely used in the process of decomposition in the starch industry [8]. The other enzyme, lipase converts ester via the hydrolysis of fats and fatty acids. Lipases have specificity in terms of the chain length of the fatty acid, the degree of saturation, the position of fatty acids and the physical condition of the substrate [9]. Lipases isolated from various microorganisms including bacteria, fungi, yeasts, and actinomycetes are resistant to organic solvents [10, 11].

The lipid analysis is widely used both in ecologic and taxonomic studies. The species and types of microorganisms can be determined by comparing the diversity of fatty acid profiles, content, fatty acid type and the amount of microorganisms with the microorganisms, of which fatty acids profiles have been previously defined. For this purpose, previously created reference data are used [12-15]. However, there is also literature showing that these data are not sufficient [16, 17].

MATERIALS AND METHODS

Thermophilic isolates. Thermophilic isolates were obtained from Balikesir (Sindirgi, Gure, and Havran) and Kutahya (Eynal) hot springs in February and August 2014. These isolates were identified based on the 16S rRNA gene sequences [18].

TABLE 1
Protease, amylase, and lipase activity scores of thermophilic isolates

Isolates	Protease Activity	Amylase Activity	Lipase Activity
S1 (*Geobacillus thermoparaffinivorans)*	-	++	+
S2 (*Geobacillus thermoleovorans)*	+	-	-
S5 (*Geobacillus thermoparaffinivorans)*	-	+	+
S6 (*Geobacillus thermoleovorans)*	+	-	-
SY2 (*Geobacillus thermoparaffinivorans)*	-	++++	++
SY4 (*Geobacillus thermoparaffinivorans)*	-	++	+
G2 (*Brevibacillus thermoruber)*	+	-	-
G3 (*Bacillus licheniformis)*	++	++	-
G5 (*Aneurinibacillus thermoaerophilus)*	-	+	-
G8 (*Bacillus licheniformis)*	+++	++++	-
G9 *(Bacillus licheniformis)*	++	++	-
GY1 *(Anoxybacillus* **sp.***)*	-	++	-
GY2 (*Anoxybacillus* **sp.***)*	-	++	-
GY5 *(Anoxybacillus* **sp.***)*	-	++++	-
H3 *(Anoxybacillus flavithermus)*	++	-	-
H4 *(Anoxybacillus flavithermus)*	+++	-	-
H5 *(Anoxybacillus flavithermus)*	++	-	-
H6 *(Bacillus* **sp.***)*	++	-	-
H8 *(Anoxybacillus flavithermus)*	++++	-	-
H10 *(Anoxybacillus flavithermus)*	++++	-	-
H11 *(Brevibacillus thermoruber)*	+	-	-
H13 *(Anoxybacillus flavithermus)*	++	-	-
E2 *(Geobacillus thermoleovorans)*	+	+	-
E3 *(Geobacillus thermoleovorans)*	+	++	-
E4 *(Geobacillus thermoleovorans)*	-	-	+
E6 *(Geobacillus kaustophilus)*	-	++	-
EY2 *(Bacillus sonorensis)*	++	++++	-
EY4 *(Bacillus sonorensis)*	+++	+	-
EY5 *(Bacillus sonorensis)*	++	++	-
EY6 *(Bacillus sonorensis)*	+++	++++	-
EY7 *(Bacillus sonorensis)*	+++	++	-
EY8 *(Bacillus sonorensis)*	++	++	-
EY9 *(Bacillus sonorensi)*	+	-	-
EY10 *(Bacillus sonorensis)*	++++	-	-
EY12 *(Bacillus licheniformis)*	++	++++	-
EY14 *(Bacillus licheniformis)*	-	+++	-
EY15 *(Geobacillus* **sp.***)*	-	++	-
EY16 *(Bacillus licheniformis)*	-	+++	-
EY17 *(Geobacillus* **sp.***)*	+	-	-
EY18 *(Aeribacillus pallidus)*	-	-	++
EY19 *(Geobacillus thermoparaffinivorans)*	-	++	+
EY21 *(Bacillus licheniformis)*	-	+	-

-: No activity +: 0-10 mm ++: 10-20 mm +++: 20-35 mm ++++: >35 mm

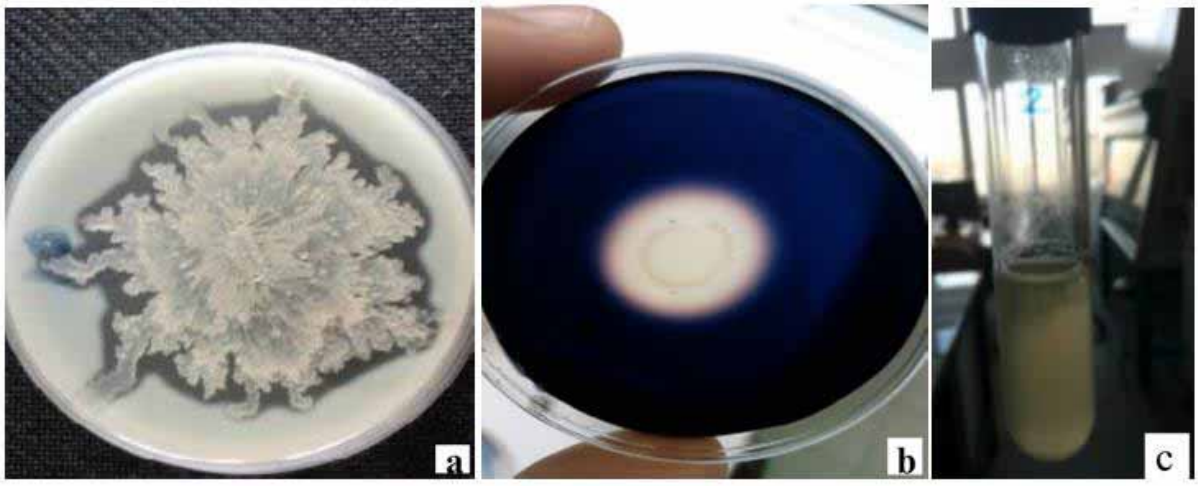

FIGURE 1
Plate photograph of a) Protease positive isolate b) Amylase positive isolate c) Lipase positive isolate

Screening of protease, amylase and lipase activity of thermophilic isolates. For the screening of protease, amylase and lipase activity, the isolates were streaked on the Modified Basal Medium (MM) that contained (per liter): 1 g glucose, 2.5 g yeast extract and 14 g agar–agar supplemented with 6.2 g/L skim milk, [19, 20] modified starch and tributyrin agar containing (per liter): starch/tributyrin 10.0; peptone 5.0; yeast extract 5.0; 14 g agar–agar, respectively, and incubated at 55 °C for 24-48 h. To observe the amylolytic activity, Gram's iodine solution was added to the modified starch agar petri dish following incubation. For each enzyme screening method, a clear zone around the isolates indicated a positive result, while no clear zone indicated a negative result. The zone diameter obtained was recorded in mm.

FAME (Fatty Acid Methyl Esters) Analysis. The extraction and analysis of the fatty acid methyl ester (FAME) profiles of thermophilic isolates were performed according to the method described in the manufacturer's manual (Sherlock Microbial Identification System version 4.0, MIDI, Inc., Newark, DE, USA). Firstly, the isolates were grown on TSA (Tryptic Soy Agar, SIGMA) at 55 °C for 24 h. Then, for the extraction of whole lipids from the isolates, 40 mg of culture were transferred to a Teflon-lined, screw-cap test tube and mixed with 1 ml of saponification solution containing 3.75 M NaOH in MeOH:H_2O (1:1). The test tubes were vortexed and placed in a 100 °C water bath for 5 min, then, again vortexed and placed in a 100 °C water bath for 25 min. Following the incubation period, the test tubes were cooled immediately. Then, 2 ml of methylation solution containing 6.00 M HCl:MeOH (1:0.85) were added, vortexed and incubated in a water bath for 10 min at 80 °C and immediately rinsed with cool tap water. Afterwards, 1.25 ml of the extraction solution, which is hexane:methyl-tert butyl ether (1:1), were added to the extract. In order to remove acidic residual reagents, 3 ml of the washing solution containing 0.3 M NaOH were added and gently mixed for 5 min [21]. Finally, the organic phase was transferred from the glass tube to a vial for the gas chromatography (GC) analysis using an Agilent Technologies 6890N gas liquid chromatograph with a G2614A autosampler and a 6783 injector.

RESULTS

Cultural identification. 65 pure thermophilic bacteria were identified as genotypic-based according to the ARDRA (Amplified Ribosomal DNA Restriction Analyses) profiles and partial 16S rRNA gene sequencing. As a result of the identification, it was determined that the isolates obtained made up 20 different ARDRA profiles. Furthermore, it was determined by the partial 16S rRNA gene sequencing that the isolates were the members of *Geobacillus, Bacillus, Brevibacillus, Aneurinibacillus, Anoxybacillus, Aeribacillus* species (Table 1) [18].

Protease, Amylase and Lipase Enzyme Profile Determination. According to the screening of the protease, amylase and lipase enzymes of our thermophilic bacteria, 42 thermophilic isolates exhibited a weak or strong protease, amylase, and lipase activity (Table 1; Figure 1). However, 23 isolates exhibited no activity for these enzymes when cultured on skim milk, starch, and tributyrin agar.

The isolates labeled with EY10, H8, and H10 exhibited the highest protease activity (Figure 2). These isolates were identified as *Bacillus sonorensis* (EY10) and *Anoxybacillus flavithermus* (H8, H10) (Table 1) [18].

Isolates labelled with EY2, G8, EY6 and EY12 exhibited the highest amylase activity (Figure 3) and these isolates were identified as *Bacillus sonorensis* (EY 2, EY6) and *Bacillus licheniformis* (G8, EY12) (Table 1) [18]. Our isolates showed weak lipase activity (Figure 4). Isolate has the highest lipase activity was identified as *Aeribacillus pallidus* (EY18) (Table 1) [18].

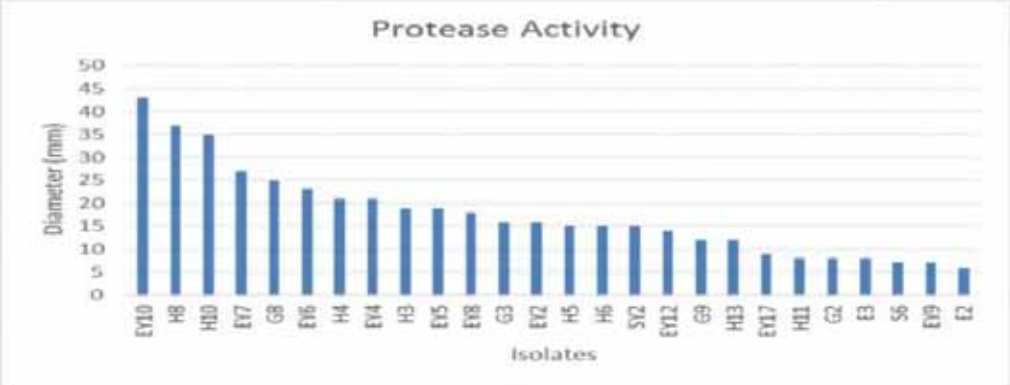

FIGURE 2
Protease activity of thermophilic isolates

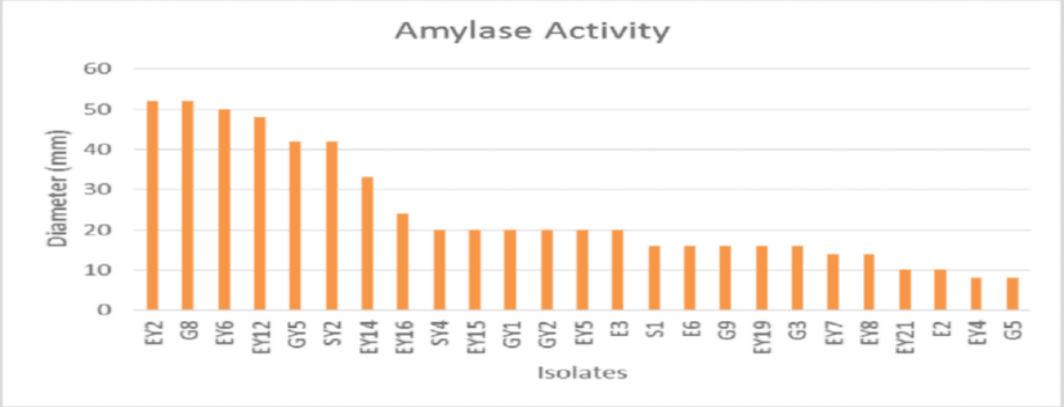

FIGURE 3
Amylase activity of thermophilic isolates

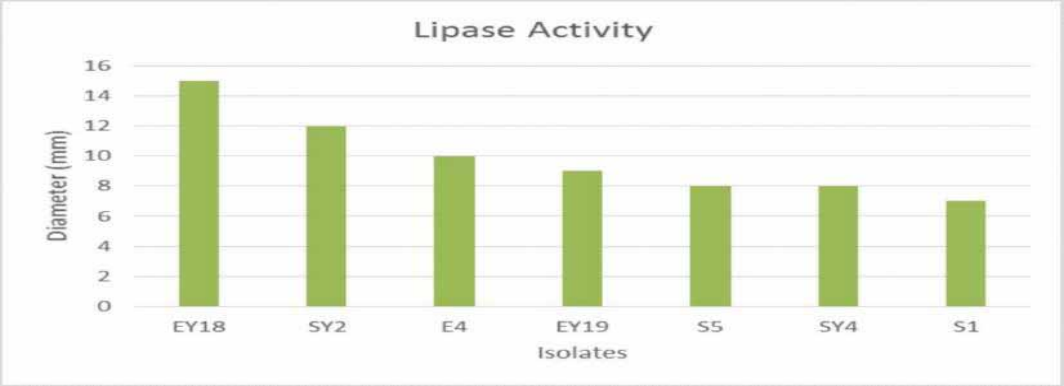

FIGURE 4
Lipase activity of thermophilic isolates

TABLE 2
Fatty acid concentration of the thermophilic isolates obtained from Sindirgi

	Fatty Acid Concentration (%)		
Fatty Acid	**S2 isolate**	**S5 isolate**	**SY5 isolate**
14:0	10.63	10.92	-
14:0 ISO	-	-	0.59
15:0 ISO	-	-	37.02
15:0 ANTEISO	-	-	27.51
16:0	50.67	47.60	3.30
16:0 ISO	-	-	3.43
16:1 w7c	7.37	7.90	-
17:0 ISO	-	-	14.47
17:0 ANTEISO	-	-	13.02
18:0	10.18	9.27	0.67
18:1 w7c	15.52	17.56	-
19:0 CYCLO w8c	5.63	6.75	-

FAME Analysis of Some Isolates. In this study, the FAME analysis was applied to 18 thermophilic isolates. These isolates were selected according to their different ARDRA profiles [18]. The fatty acid profiles of the isolates are presented in Tables 2-5.

The isolates were divided into 12 different phenotypic groups according to their fatty acid profiles (Tables 2-5). 35 different fatty acids were determined to belong to all isolates. 16: 0 fatty acid was present in all isolates. 15: 0 ISO, 15: ANTEISO 0, 16: 0 ISO, 17: 0 ISO and 17: 0 ANTEISO were common in most of them.

TABLE 3
Fatty acid concentration of the thermophilic isolates obtained from Gure

	Fatty Acid Concentration (%)				
Fatty Acid	**G1**	**G2**	**G5**	**G9**	**GY4**
10:0	-	0.34	-	-	-
12:0 ALDE	-	-	-	-	-
13:0 ISO	-	0.82	0.24	-	-
13:0 3OH	-	-	1.21	-	-
14:0	2.39	0.90	1.08	-	-
14:0 ISO	1.15	0.69	0.90	-	-
14:0 3OH	3.29	-	-	-	-
15:0 ISO	60.84	61.59	60.70	36.56	60.13
15:0 ANTEISO	3.07	15.95	3.58	24.35	14.02
16:0	2.00	3.59	3.67	8.33	6.81
16:0 ISO	3.73	1.88	4.34	3.83	1.64
16:1 ISO H	-	-	0.69	-	-
16:1 w5c	-	-	0.64	-	-
16:1 w7c	7.31	-	0.97	-	-
17:0	-	-	-	-	-
17:0 ISO	5.44	10.72	9.59	13.37	12.13
17:0 ANTEISO	1.39	2.76	1.51	11.25	2.81
17:1 ANTEISO A	1.98	-	-	-	-
ISO17:1w5c	7.40	-	-	-	-
ISO17:1w9c	-	-	1.35	-	-
18:0	-	0.77	-	2.30	2.47
18:0 3OH	-	-	-	-	-
18:1 2OH	-	-	-	-	-
18:1 w7c	-	-	-	-	-
19:0 CYCLO w8c	-	-	-	-	-
20:1 w7c	-	-	-	-	-
Unknown	-	-	-	-	-

TABLE 4
Fatty acid concentration of the thermophilic isolates obtained from Havran

	Fatty Acid Concentration (%)			
Fatty Acid	**H4**	**H6**	**H7**	**H13**
11:0 ISO	-	-	0.43	-
13:0 ISO	1.12	-	0.43	-
13:0 3OH	-	-	1.57	0.98
14:0	5.47	-	1.06	1.44
14:0 ISO	1.30	-	0.98	0.56
15:0 ISO	53.98	31.23	67.13	55.16
15:0 ANTEISO	7.11	26.24	3.29	3.91
16:0	9.06	13.54	3.65	11.10
16:0 ISO	3.00	3.41	3.07	2.84
16:1 ISO H	-	-	0.47	-
16:1 w5c	-	-	0.50	-
16:1 w7c	5.46	-	0.70	0.97
17:0 ISO	4.80	10.39	7.36	10.06
17:0 ANTEISO	3.25	11.65	1.13	1.89
17:1 ANTEISO A	1.58	-	-	-
17:1 ANTEISO B	-	-	7.48	6.89
ISO 17:1 w5c	1.63	-	-	-
ISO 17:1 w9c	-	-	0.75	0.92
18:0	2.25	3.54	-	3.27

TABLE 5
Fatty acid concentration of the thermophilic isolates obtained from Eynal

	Fatty Acid Concentration (%)					
Fatty Acid	**E4**	**E6**	**EY5**	**EY12**	**EY18**	**EY21**
10:0	-	-	-	-	0.25	-
14:0	-	-	-	-	3.43	-
14:0 ISO	-	-	-	-	0.77	0.60
15:0 ISO	31.83	34.17	36.23	38.81	19.50	37.62
15:0 ANTEISO	26.29	22.52	27.39	30.00	8.77	24.47
16:0	5.53	6.89	8.18	3.82	14.29	3.58
16:0 ISO	4.62	4.06	3.72	3.50	10.88	4.22
16:1w7c alcohol	-	-	-	-	1.44	-
16:1 w11c	-	-	-	-	6.09	-
17:0 ISO	16.79	18.66	12.87	12.89	8.56	16.61
17:0 ANTEISO	14.94	13.70	11.61	10.98	21.40	12.30
17:1 ISO I	-	-	-	-	1.38	-
ISO 17:1 w10c	-	-	-	-	2.02	-
18:0	-	-	-	-	0.90	0.61
18:1 w9c	-	-	-	-	0.32	-

E4, E6, EY5, EY12, EY21, SY5, G2, G9 and GY4 isolates had a more saturated fatty acid composition than the others.

11:0 ISO fatty acid was found only in the isolate labeled with H7. Moreover, this isolate was identified to be *Aneurinibacillus* according to the 16 S rRNA sequence analysis, and it had 67.13% of 15:0 ISO.

16:1 w7c alcohol, 16:1 w11c, 17:1 iso I, iso 17:1 w10c, and 18:1 w9c fatty acids were found only in EY18 isolate. The majority of the fatty acids of this isolate were composed of 15:0 ISO (% 19.50), 16:0 (% 14.29), 16:0 ISO (% 10.88), and 17:0 ANTEISO (% 21.40) fatty acids.

DISCUSSION

As a result of this study, the protease, amylase and lipase enzyme production capacities of 65 thermophilic bacteria isolates obtained in the previous study were investigated in the media containing a suitable substrate. It was concluded that 42 isolates produced amylase, protease or lipase enzymes, while 23 isolates could not produce any of these enzymes. It was determined that the thermophilic isolates with the capacity to produce these specified enzymes were the members of *Bacillus* and *Anoxybacillus* species.

Bacillus sp. bacteria are very important microorganisms for industrial applications. The types of this species produce the enzymes and metabolites that are widely used in many areas such as medicine, pharmacology, and agriculture. There are numerous studies on the production of commercial enzymes by these bacteria and the purification of these enzymes from these bacteria [21-25].

Similarly to our study, 311 thermophilic bacteria were isolated from the hot water samples taken from certain geothermal sources in Afyonkarahisar, Denizli, Kütahya and Manisa provinces. The molecular diagnosis of 24 strains in total was performed with the 16S rRNA sequence analysis as a few strains with the highest protease, amylase and lipase activity among the isolates and a strain for each not producing these enzymes. Accordingly, the isolates were defined at the species and type level as *Geobacillus* sp., *Geobacillus kaustophilus*, *Geobacillus thermoleovorans*, *Geobacillus lituanicus*, *Geobacillus stearothermophilus*, *Bacillus licheniformis*, *Thermus* sp., *Thermus thermophilus*, *Anoxybacillus flavithermus* and *Pseudoxanthomonas taiwanensis* [26].

As a result of the isolation study conducted in 42 different thermal sources in 6 provinces of Turkey, it was reported that 451 thermophilic bacilli were isolated, and 67 of these isolates had a high amylase activity. As a result of the 16S rRNA sequence analysis, it was determined that these isolates belonged to *Geobacillus* species [27].

The determination of a potential source for the large-scale, cheap production of lipase, amylase and protease enzymes, which have a great industrial importance, as a result of the enzymatic activity screening has become promising for future projects.

Furthermore, the FAME analyses of these isolates representing different ARDRA groups were performed. It has been reported that thermophilic bacteria have a high level of saturated fatty acids, to keep membrane function stable at high temperatures [28]. Upon comparing the fatty acid composition obtained, 70% of them were saturated. The greater length of the carbon chain and branching fatty acids increases the membrane stability and therefore causes the higher boiling point of the lipid. Most of our isolates have long and branching fatty acids, and thus they can survive at high temperatures.

11:0 ISO fatty acid was found only in the isolate labeled with H7. In the other study investigating the fatty acids profiles of *Aneurinibacillus* genus, 15:0 ISO fatty acid was found to be the major fatty acid. Similarly, in our study, H7 labeled isolate was identified to be *Aneurinibacillus,* and it had 67.13% of 15:0 ISO [29].

16:1 w7c alcohol, 16:1 w11c, 17:1 iso I, iso 17:1 w10c and 18:1 w9c fatty acids were found only in EY18 isolate. The majority of the fatty acids of this isolate were composed of 15:0 ISO (% 19.50), 16:0 (% 14.29), 16:0 ISO (% 10.88), and 17:0 ANTEISO (% 21.40) fatty acids. In our study, the EY18 isolate was identified to be *Aeribacillus pallidus,* and the fatty acid composition of the isolate was consistent with the literature [30].

According to the FAME analysis results, it was verified that most of our isolates had the types of fatty acids frequently encountered in thermophilic isolates. However, the fatty acid profiles obtained were not directly compatible with the identification results we obtained. According to the fatty acid analysis results, the isolates were gathered under 12 different phenotypic groups. However, they were not compatible with the results of the 16S rRNA sequence analysis. For example, while the FAME profiles of the isolates coded E4, E6, EY5, and EY12 (Table 5) are similar to each other, they have different identification results (Table 1). Similarly, it is observed in Tables 3 and 5 that the isolates coded G9, EY12 and EY21 have different FAME profiles although their identification results are the same, and in Table 4, it is observed that the isolates coded H4 and H13 have different FAME profiles although they have the same identification results. From here, we can infer that the FAME analysis may not be sufficient alone for the identification of thermophilic bacteria. This result is also supported by the similar literature [16, 17].

ACKNOWLEDGEMENTS

The authors would like to thank Anadolu University Research Project Department, Project No 1403F100 and 1705F332.

REFERENCES

[1] Pandey, A., Selvakumar, P., Soccol, C.R. and Nigam, P. (1999) Solid state fermentation for the production of industrial enzymes. Current science. 77(1), 149-162.

[2] Pantazaki, A., Pritsa, A. and Kyriakidis, D. (2002) Biotechnologically relevant enzymes from *Thermus thermophilus*. Applied microbiology and biotechnology. 58(1), 1-12.

[3] Zhang, S.B., Zhang, D.Y., Liu, Y., Luo, X.W., Cheng, F.X., Luo, Y.H., Cheng, J.E., Ma, X.M. (2009) Degradation characteristics and pathway of fenpropathrin by *Rhodopseudomonas* sp. strain PSB07-6. Fresen. Environ. Bull., 18, 2060–2065.

[4] Nadaroglu, H., Kalkan, E. and Celebi, H. (2014) Equilibrium, kinetic and thermodynamic studies on adsorption of Reactive Black 5 dye by laccase modified-red mud from aqueous solutions. Fresen. Environ. Bull., 23, 70-83.

[5] Sarre, A., Okvist, M., Klar, T., Moe, E. and Timmins, J. (2014) Expression, purification and crystallization of two endonuclease III enzymes from *Deinococcus radiodurans*. Acta Crystallographica Section F: Structural Biology Communications. 70(12), 1688-1692.

[6] Muthumari, G.M., Thilagavathi, S. and Hariram, N. (2016) Industrial Enzymes: Lipase Producing Microbes from Waste Volatile Substances. International Journal of Pharmaceutical Sciences and Research. 7(5), 2201.

[7] Elleuche, S., Schroder, C., Sahm, K. and Antranikian, G. (2014) Extremozymes--biocatalysts with unique properties from extremophilic microorganisms. Current Opinion in Biotechnology. 29, 116-123.

[8] Anitori, R.P. (2012) Extremophiles: Microbiology and Biotechnology: Horizon Scientific Press.

[9] Abbas, H., Hiol, A., Deyris, V. and Comeau, L. (2002) Isolation and characterization of an extracellular lipase from *Mucor* sp strain isolated from palm fruit. Enzyme and Microbial Technology. 31: 968-975.

[10] Sharma, R., Chisti, Y. and Banerjee, U.C. (2001) Production, purification, characterization, and applications of lipases. Biotechnology Advances. 19, 627-662.

[11] Gunasekaran, V. and Das, D. (2005) Lipase fermentation: progress and prospects. Indian Journal of Biotechnology. 4, 437-445.

[12] Goldfine, H. (1972) Comparative aspects of bacterial lipids. Advances in Microbial Physiology. 8, 1-58.

[13] Shaw, N. (1974) Lipid composition as a guide to the classification of bacteria. Advances in Applied Microbiology. 17, 63-108.

[14] Lechevalier, M.P. (1977) Lipids in bacterial taxonomy - a taxonomist's view. CRC critical Reviews in Microbiology. 5, 109-210.

[15] Bobbie, R.J. and White, D.C. (1980) Characterization of benthic microbial community structure by high-resolution gas chromatography of fatty acid methyl esters. Applied and Environmental Microbiology. 39, 1212-1222.

[16] Surve, V.V., Patil, M.U. and Dharmadhikari, S.M (2012) FAME and 16S rDNA sequence analysis of halophilic bacteria from solar salterns of Goa: A comparative study. International Journal of Scientific and Research Publications. 2(8), 209.

[17] Cordova-Kreylos, A.L., Fernandez, L.E., Koivunen, M., Yang, A., Flor-Weiler, L. and Marrone P.G. (2013) Isolation and characterization of *Burkholderia rinojensis* sp. nov., a non-*Burkholderia cepacia* complex soil bacterium with insecticidal and miticidal activities. Applied and Environmental Microbiology. 79, 7669-7678.

[18] Celikoglu, E. and Yilmaz Cankilic, M. (2016) Prokaryotic diversity of hot springs in Balikesir and Kutahya, Turkey. Applied Ecology and Environmental Research. 14, 429-440.

[19] Perez Borla, O., Davidovich, L.A. and Roura, S.I. (2010) Isolation and characterization of proteolytic microorganisms from fresh and fermented cabbage. LWT - Food Science and Technology. 43, 298-301.

[20] Mazzucotelli, C.A., Ponce, A.G., Kotlar, C.E. and Moreira, M.R. (2013) Isolation and characterization of bacterial strains with a hydrolytic profile with potential use in bioconversion of agroindustrial by-products and waste. Food Science and Technology (Campinas). 33, 295-303.

[21] Ferreira, A.M., Wait, R., Nobre, M.F. and da Costa, M.S. (1999) Characterization of glycolipids from *Meiothermus* spp. Microbiology (Reading, England). 145 (Pt 5), 1191-1199.

[22] Ferrero, M.A., Castro, G.R., Abate, C.M., Baigori, M.D. and Sineriz, F. (1996) Thermostable alkaline proteases of *Bacillus licheniformis* MIR 29: isolation, production and characterization. Applied Microbiology and Biotechnology. 45, 327-332.

[23] Declerck, N., Machius, M., Joyet, P., Wiegand, G., Huber, R. and Gaillardin, C. (2003) Hyperthermostabilization of *Bacillus licheniformis* α-amylase and modulation of its stability over a 50 ℃ temperature range. Protein Engineering. 16, 287-293.

[24] Schallmey, M., Singh, A. and Ward, O.P. (2004) Developments in the use of *Bacillus* species for industrial production. Canadian Journal of Microbiology. 50, 1-17.

[25] Voigt, B., Schweder, T., Becher, D., Ehrenreich, A., Gottschalk, G., Feesche, J., Maurer, K.H. and Hecker, M. (2004) A proteomic view of cell physiology of *Bacillus licheniformis*. Proteomics. 4, 1465-1490.

[26] Akdas, H. (2013) Bazi jeotermal kaynaklardan termofilik bakterilerin deizolasyonu ve endustriyel oneme sahip enzimlerin belirlenmesi, Suleyman Demirel Universitesi Fen Bilimleri Enstitusu, Isparta - Turkiye.

[27] Cihan, A.C., Ozcan, B. and Cokmus, C. (2009) Characterization of thermostable α-glucosidases from newly isolated *Geobacillus* sp. A333 and thermophilic bacterium A343. World Journal of Microbiology and Biotechnology. 25, 2205-2217.

[28] Marr, A.G. and Ingraham, J.L. (1962) Effect of temperature on the composition of fatty acids in *Escherichia coli*. Journal of Bacteriology. 84, 1260-1267.

[29] Lee, K.C., Kim, K.K., Eom, M.K., Kim, J.S., Ko, S.H. and Lee, J.S. (2014) *Aneurinibacillus* sp. nov., isolated from mountain soil. International Journal of Systematic and Evolutionary Microbiology. 64, 3792-3797.

[30] Yasawong, M., Areekit, S., Pakpitchareon, A., Santiwatanakul, S. and Chansiri, K. (2011) Characterization of thermophilic halotolerant *Aeribacillus pallidus* TD1 from Tao Dam Hot Spring, Thailand. International Journal of Molecular Sciences. 12, 5294-5303.

Received: **20.02.2017**
Accepted: **11.07.2017**

CORRESPONDING AUTHOR

Meral Yilmaz Cankilic
Anadolu University,
Faculty of Science,
Department of Biology,
Yunusemre Campus,
Eskisehir – TURKEY

E-mail: meralyilmaz@anadolu.edu.tr

© by PSP Volume 26 – No. 10/2017 pages 5873-5881 Fresenius Environmental Bulletin

RAPID DETERMINATION OF NITROGEN IN OVERLYING RIVER WATER DURING INTERMITTENT AERATION USING INTERVAL PARTIAL LEAST SQUARES AND NEAR-INFRARED SPECTROSCOPY

Jian Huang[1,2], Xiong Zhang[1], Hua Zhang[1], Qing-ye Sun[2,*], Xian-huai Huang[1], Xiao-kun Yu[1], Zhao-liang Wu[1]

[1]Key Laboratory of Anhui Province of Water Pollution Control and Wastewater Reuse, Anhui Jianzhu University, Hefei, 230601, P.R. China
[2]School of Resources and Environmental Engineering, Anhui University, Hefei, 230601, P.R. China

ABSTRACT

Near-infrared spectroscopy analysis was used in combination with interval partial least squares method to rapidly determine the total nitrogen, ammonia nitrogen, nitrite nitrogen in overlying water during intermittent aeration. Near-infrared spectroscopy was used to obtain absorbance data of water samples. Interval partial least squares was used to choose spectral region and establish calibration models (interval partial least squares calibration model) of total nitrogen, ammonia nitrogen and nitrite nitrogen. The full-spectrum was 4000-12500cm^{-1} divided into 20 sub-intervals with interval partial least squares method. The best spectral region of total nitrogen, ammonia nitrogen and nitrite nitrogen were respectively 7432-7824 cm^{-1}, 10465-10860 cm^{-1} and 7854-8250cm^{-1}. The interval partial least squares calibration models were established in the selected sub-interval. The established calibration models are capable of better predictions. The interval partial least squares calibration model of total nitrogen indicated that prediction coefficient of the prediction value and actual value is 0.9554, with the root mean square error of prediction being 0.1147. The interval partial least squares calibration model of ammonia nitrogen showed that correlation coefficient of the prediction value and actual value is 0.9651, with the root mean square error of prediction being 0.05437.The interval partial least squares calibration model of nitrite nitrogen showed that correlation coefficient of the prediction value and actual value is 0.9616, with the root mean square error of prediction being 0.03688. The results indicated that the proposed method was rapid, accurate, non-polluted, and reliable in determining the concentration of total nitrogen, ammonia nitrogen and nitrite nitrogen in overlying river water during biological nitrogen removal.

KEYWORDS:
near-infrared spectroscopy, interval partial least squares, intermittent aeration, overlying water

INTRODUCTION

Excessive nitrogen is the main reason for the pollution of river water. Nitrogen can make river water black, odorous and eutrophic [1-3]. Continuous aeration technology is usually used to remove nitrogen from polluted river [4]. The concentration of ammonia nitrogen decreased in continuous aeration process, which was achieved by biological nitrification reaction. However, the concentration of nitrate and nitrite nitrogen increased in the process of continuous aeration. The removal efficiency of total nitrogen was not satisfactory [5-8]. Therefore, the technique and method of nitrogen removal are researched and developed in polluted river.

Rapid determination of nitrogen is very important for regulating and controlling biological nitrogen removal process in polluted river. However, chemical method for detecting nitrogen consumes considerable time and may cause secondary pollution [9]. Near-infrared spectroscopy technology has attracted much attention because it has advantages of rapid determination, low cost, and zero-pollution [10-11]. Recently, near infrared spectroscopy combined with chemometrics has been widely used in many fields [12-13], such as agriculture, medicine, chemical industry and so on [14-16].

Currently, quantitative correlation has been found between the spectral data and the component content [17-19]. Partial least squares (PLS) is a common quantitative analysis of component content based on near-infrared spectral data [20-23]. However, in the range of full spectral region, calibration model of component content is established with PLS. The prediction ability of calibration model was affected by the over-lapping spectral bands, or even the background noise in full spectral region. So these interfering regions should be excluded to establish a better calibration model [24-25]. In order to reduce these interferences, spectral region should be carefully selected before establishing calibration model.

Interval partial least squares (iPLS) is a novel chemometric method based on PLS method [26]. Compared with PLS, it can select the spectral region

and exclude background noise [27]. The best spectral region was selected by dividing the full-spectrum into several sub-intervals with iPLS. The optimal calibration model was established with iPLS [28-29]. Some studies have identified that calibration model established with iPLS can improve the prediction by selecting spectral region [30-32]. However, there is little research on quick determination of nitrogen using near-infrared spectroscopy combined with iPLS.

In order to achieve effective biological nitrogen removal in polluted rivers, intermittent aeration process is developed in this study. The intermittent aeration was achieved in overlying water, the removal of total nitrogen in polluted rivers can be achieved. The intermittent aeration process developed can achieve the purpose of real nitrogen removal. In addition, near-infrared spectroscopy was used to obtain absorbance data of water samples. The iPLS was used to select spectral region and establish calibration models (iPLS calibration models) of total nitrogen, ammonia nitrogen, nitrite nitrogen. Furthermore, the calibration models were tested against the prediction values (by iPLS calibration model) and actual values (by chemical method). The method developed in this study provides new technology for quick determination of nitrogen concentration in polluted river.

EXPERIMENTAL MATERIALS AND ANALYTICAL METHODS

Sample collection and experimental method. *Shiwuli River*, located at the southwest of Hefei city, China, is a major pollution source of *Chaohu Lake*. It runs through Hefei city. The concentration of pollutants was higher in this river. Sediment samples were taken with gravity cylinder sediment sampler. Sediment is collected at a depth of 30 cm. All the samples are shielded from sunshine and taken back to lab at 4 ℃.The overlying water was also collected simultaneously. The sampling spot is shown in Figure 1.

The plexiglass reactor was adopted to simulate the river system. The length of the reactor is 21 cm, the width is 20 cm and the height is 51 cm. The sediment and overlying water are kept at 9 cm and 27 cm in depth. The position of aeration is 5 cm above the top of sediment. The dissolved oxygen was kept at 5.5 mg·L^{-1} with float-type flow meter.

Experimental method and equipment. Near-infrared spectral data are measured with a near infrared spectrometer (Bruker, Germany), which scans 4000-12500 cm^{-1} with 32 scans and resolution of 8 cm^{-1}. Total nitrogen is analyzed by *alkaline potassium persulfate digestion ultraviolet spectrophotometric* method; ammonia nitrogen is analyzed by *nessler's reagent spectrophotometry* method; Nitrate nitrogen and Nitrite nitrogen are analyzed by *spectrophotometric* method.

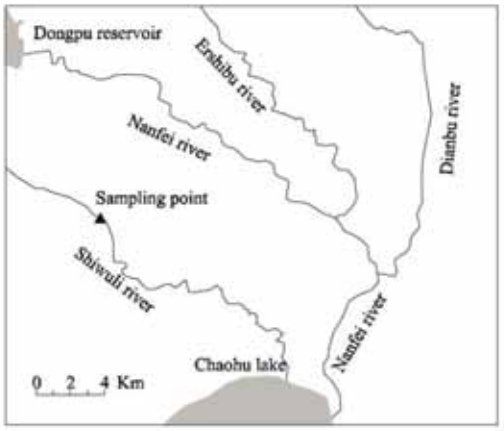

FIGURE 1
Sampling site in *Shiwuli* River

Establishment of interval partial least squares (iPLS) model. The experiment lasted for 138 d and a sample was taken every day. The 138 water samples were centrifuged and filtered with 0.45 um filter membrane. After pretreatment, the 138 water samples were analyzed by near-infrared spectrometer to obtain spectral data. In addition, the concentrations of ammonia nitrogen, total nitrogen and nitrite nitrogen of the water samples were also analyzed by traditional chemical method to obtain the actual value. The spectral data and actual values of 116 water samples were used as calibration set to establish calibration models. In addition, the spectral data and actual values of 22 water samples were used as test set to test the established calibration model.

Evaluation index of model. The root mean square error of cross validation (RMSECV) and the correlation coefficient (R^2) were used to evaluate the accuracy of the calibration models. Root mean square error of prediction (RMSEP) and the correlation coefficient (R^2) were used to test the performance of the calibration models. They were defined as Eq. (1)-(3) [33-35].

$$R^2 = 1 - \frac{\sum_{i=1}^{n}(y_i - y_i')^2}{\sum_{i=1}^{n}(y_i - \overline{y})^2} \quad (1)$$

$$\mathrm{RMSECV} = \sqrt{\frac{\sum_{i=1}^{n}(y_i - y_i')^2}{n-1}} \quad (2)$$

$$\mathrm{RMSEP} = \sqrt{\frac{\sum_{i=1}^{n}(y_i - y_i')^2}{m-1}} \quad (3)$$

Where y_i was the actual value, $y_i$was the prediction value, $\overline{y}$ was the average of actual value, n is the number of calibration set, and m is the number of test set.

RESULTS AND ANALYSIS

Change of nitrogen concentration in intermittent aeration period. The changes of total nitrogen, ammonia nitrogen, nitrate nitrogen and nitrite nitrogen were shown in Figure 2. It can be seen that all the nitrogen indexes in the overlying water were effectively removed in intermittent aeration process.

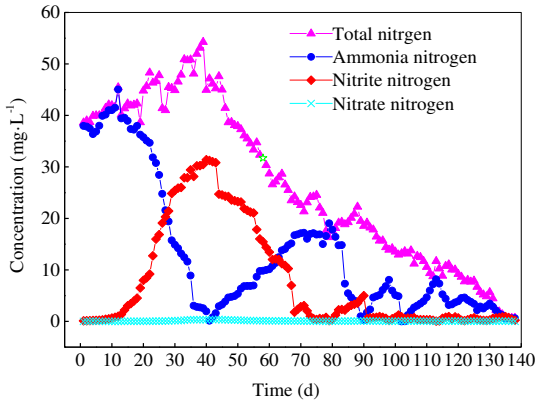

FIGURE 2
Changes of nitrogen in intermittent aeration process

From Figure 2, it can be seen that total nitrogen increased from 38.6 mg·L^{-1} to 54.25 mg·L^{-1} because nitrogen released from the sediment during the first 38 d. After 38 d, total nitrogen decreases from 54.25 mg·L^{-1}to 0.64mg·L^{-1} because denitrification occurred during intermittent aeration. Ammonia nitrogen slowly increased in the first 12 d due to transformation of organic nitrogen in the condition of non-aeration. However, ammonia nitrogen decreased from 45.04 mg·L^{-1} to 0.57 mg·L^{-1} after 12 d because nitrification reaction occurred in the condition of aeration. Nitrite nitrogen gradually increased in the first aeration and gradually decreased later. However, the concentration of nitrate nitrogen was lower and kept at 0-0.37 mg·L^{-1} during the whole intermittent aeration reaction.

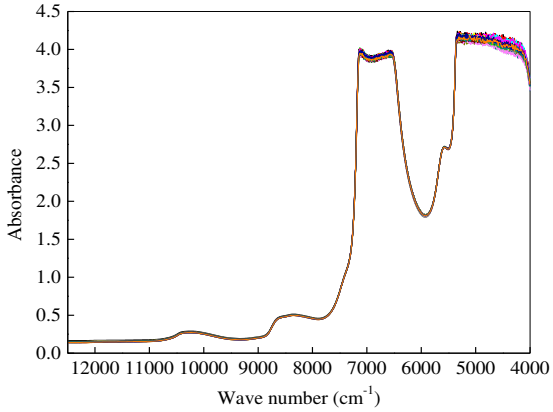

FIGURE 3
Raw near-infrared spectra of water samples

Establishment of iPLS calibration model. The near-infrared spectra of 116 water samples were shown in Figure 3. The 2203 spectra data were recorded with near-infrared spectrometer in full-spectra range of 4000-12500 cm^{-1}. All the spectral data were used to establish the iPLS calibration model. However, the accuracy of model was affected by background noises in raw spectra. Therefore, these 2203 raw spectral data were divided into several sub-intervals, and local regression model were established for every sub-interval. The optimal sub-interval was selected with R^2 and RMSECV of local regression model. The local regression model established in optimal sub-interval was the optimal model.

In this study, these 2203 raw spectral data were divided into 20 sub-intervals. The first 19 sub-intervals included, apiece, 110 raw spectral data, and the 20th sub-interval contained 113 raw spectra data. In this study, the R^2, RMSECV and RMSEP of calibration models were shown in Table 1.

TABLE 1
Root mean square error and correlation coefficient of calibration set and test set

Project	Calibration set		Test set	
Numbers of sample	116		22	
Parameter	Correlation coefficient	Root mean square error of cross validation	Correlation coefficient	Root mean square error of prediction
Total nitrogen	0.9574	0.08309	0.9554	0.11470
Ammonia nitrogen	0.9706	0.04709	0.9651	0.05437
Nitrite nitrogen	0.9687	0.03129	0.9616	0.03688

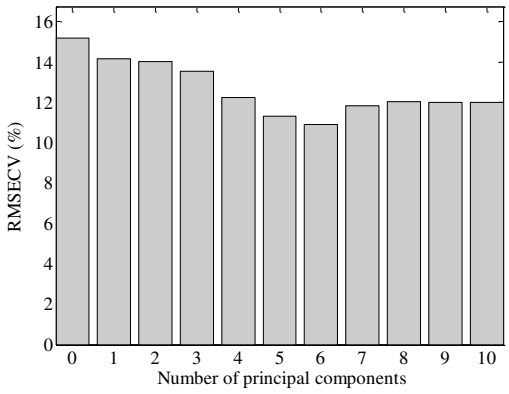

FIGURE 4
RMSECV of the PLS model of total nitrogen in full-spectrum

Establishment of iPLS calibration model of total nitrogen. Figure 4 showed that RMSECV changed with different number of principal component when the PLS model of total nitrogen was established using PLS method in the full-spectrum. It can be seen from Figure 4, RMSECV was minimum when the number of principal component was 6.

Therefore, the minimum RMSECV was 10.91% during establishing PLS method of total nitrogen in the full-spectrum.

Figure 5 indicated that full-spectrum was divided into 20 sub-intervals with iPLS method. The curve in Figure 5 was raw near-infrared spectrum of water sample. The dotted line represented the lowest RMSECV establishing of PLS model of total nitrogen in full-spectrum. The number in each histogram showed the optimal principal component number of each sub-interval. The height of each histogram indicated RMSECV of each sub-interval. It can be seen from Figure 5, the RMSECV was the lowest in the 12th sub-interval compared with the full-spectrum. Therefore, the spectral information in 12th sub-interval was the best. So the 12th sub-interval was the best interval to establish iPLS calibration model of total nitrogen.

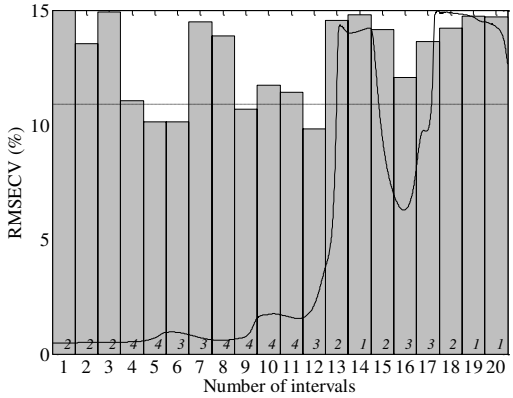

FIGURE 5
RMSECV of each sub-interval in establishing iPLS calibration model of total nitrogen

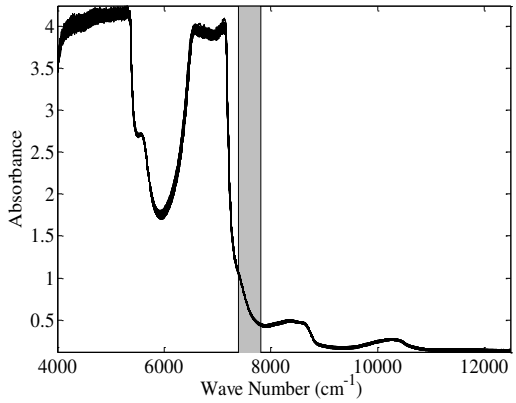

FIGURE 6
Optimal wave number establishing iPLS calibration model of total nitrogen

In Figure 6, the gray column was the optimal sub-interval selected in full-spectrum. The wave number of the optimal sub-interval was 7432-7824 cm^{-1}. The calibration model of total nitrogen was established using the optimal sub-interval, as shown in Figure 7. It can be seen from Figure 7, the R^2 between calibration value and actual value of total nitrogen was 0.9574, with the RMSECV being 0.08309.

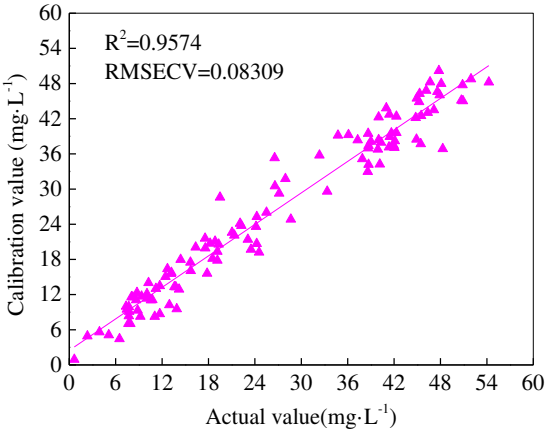

FIGURE 7
iPLS calibration model of total nitrogen

Establishment of iPLS calibration model of ammonia nitrogen. Figure 8 indicated that RMSECV changed with different number of principal component when the PLS model of ammonia nitrogen was established using PLS method in the full-spectrum. As illustrated in Figure 8, RMSECV was the smallest when the number of principal component was 5, RMSECV was the smallest, 10.88%. So the minimum RMSECV was 10.88% when PLS method of ammonia nitrogen was established in the full-spectrum.

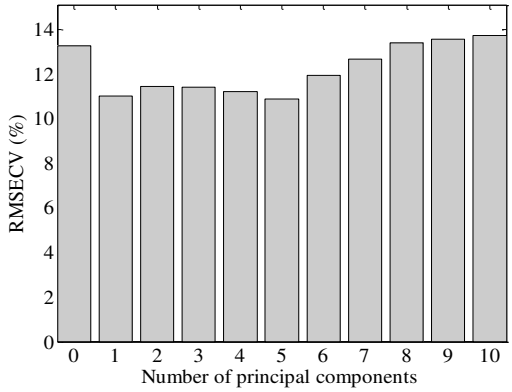

FIGURE 8
RMSECV of each sub-interval in establishing iPLS calibration model of ammonia nitrogen

Figure 9 showed that full-spectrum was divided into 20 sub-intervals with iPLS method. The curve in Figure 9 was raw near-infrared spectrum of water sample. The dotted line represented the lowest RMSECV when PLS model ammonia nitrogen was established in full-spectrum. The numbers in each histogram showed the optimal principal component number of each sub-interval. The height of each histogram indicated RMSECV of each sub-interval. It can be seen from Figure 9, the RMSECV was the lowest in the 5th sub-interval. Therefore, the spectral information in 5th sub-interval was the best. So the 5th sub-interval was the best interval to establish

iPLS calibration model of ammonia nitrogen.

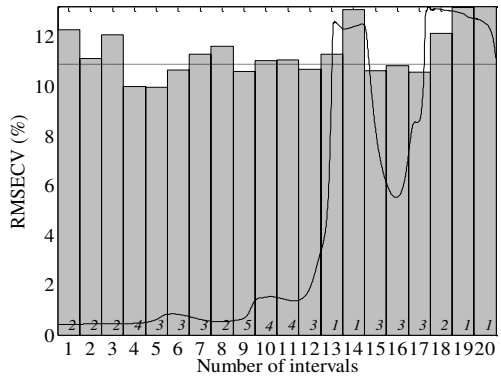

FIGURE 9
RMSECVof each sub-interval in establishing iPLS calibration model of ammonia nitrogen

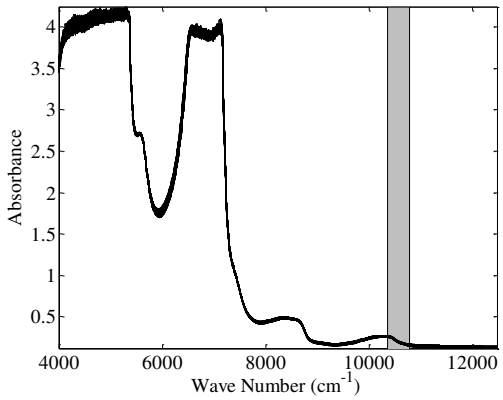

FIGURE10
Optimal wave number establishing iPLS calibration model of ammonia nitrogen

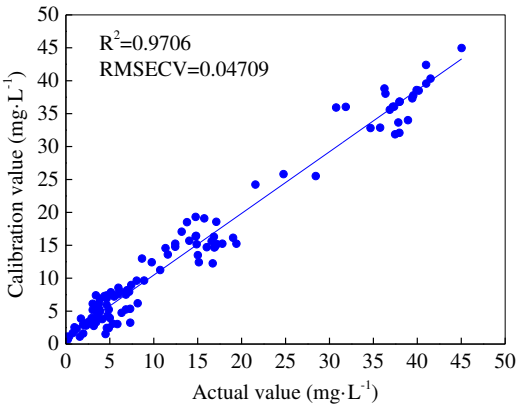

FIGURE 11
iPLS calibration model of ammonia nitrogen

In Figure 10, the gray column was the optimal sub-interval selected in full-spectrum. The wave number of the optimal sub-interval was 10465-10860 cm^{-1}. The calibration model of ammonia nitrogen was established using the optimal sub-interval, as shown in Figure 10. It can be seen from Figure 11, the R^2 between calibration value and actual value of ammonia nitrogen was 0.9706, with the RMSECV being 0.04709.

Establishment of iPLS calibration model of nitrite nitrogen. Figure 12 indicated that RMSECV changed with different number of principal component when the PLS model of nitrite nitrogen was established using PLS method in the full-spectrum. As illustrated in Figure 12, when the number of principal component was 6, RMSECV was the smallest, 9.18%. So the minimum RMSECV was 9.18% when PLS method of nitrite nitrogen was established in the full-spectrum.

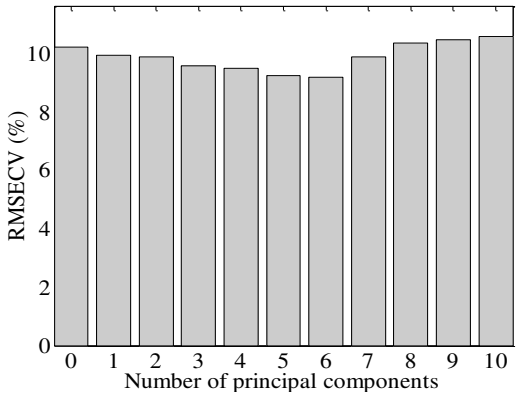

FIGURE 12
RMSECV of each sub-interval in establishing iPLS calibration model of nitrite nitrogen

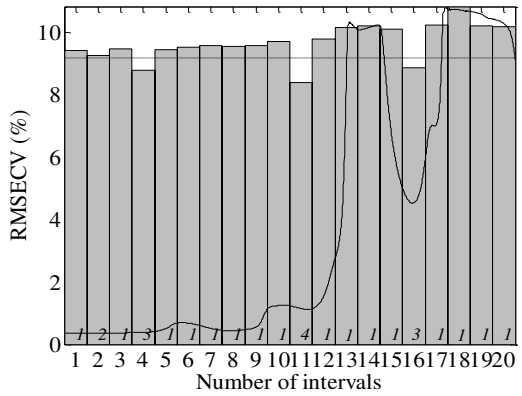

FIGURE 13
RMSECV of each sub-interval in establishing iPLS calibration model of nitrite nitrogen

Figure 13 showed that full-spectrum was divided into 20 sub-intervals with iPLS method. The curve in Figure 13 was raw near-infrared spectrum of water sample. The dotted line represented the lowest RMSECV establishing PLS model of nitrite nitrogen in full-spectrum. The numbers in each histogram showed the optimal principal component number of each sub-interval. The height of each histogram indicated RMSECV of each sub-interval. It can be seen from Figure 13, the RMSECV was the lowest (9.18%) in the 11th sub-interval compared with the full-spectrum. Therefore, the spectral information in 11th sub-interval was the best. So the 11th sub-interval was the best interval to establish iPLS calibration model of nitrite nitrogen.

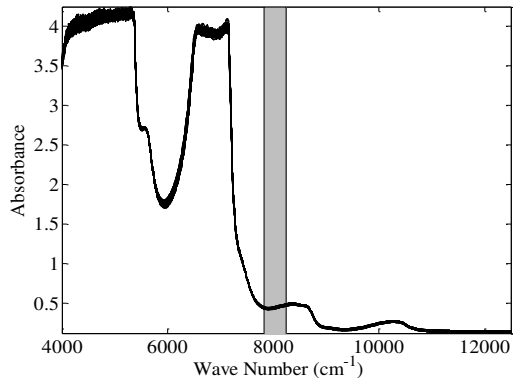

FIGURE 14
Optimal wave number establishing iPLS calibration model of nitrite nitrogen

In Figure 14, the gray column was the optimal sub-interval selected in full-spectrum. The wave number of the optimal sub-interval was 7854-8250 cm^{-1}. The calibration model of nitrite nitrogen was established using the optimal sub-interval, as shown in Figure 14. As shown in Figure 15, the R^2 between calibration value and actual value of nitrite nitrogen was 0.9687, with the RMSECV being 0.03129.

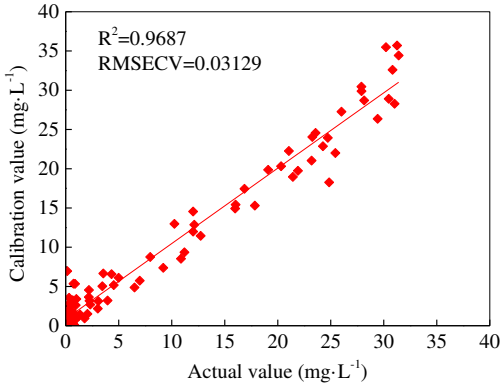

FIGURE15
iPLS calibration model of nitrite nitrogen

Test of iPLS calibration model of total nitrogen, ammonia nitrogen and nitrite nitrogen. The near-infrared spectral data of 22 water samples of test set were measured with near-infrared spectroscopy. These spectral data were used as input of iPLS calibration models of the total nitrogen, ammonia nitrogen and nitrite nitrogen. The predicted concentrations of the total nitrogen, ammonia nitrogen and nitrite nitrogen were predicted by iPLS calibration model. Correspondingly, the actual values of the total nitrogen, ammonia nitrogen and nitrite nitrogen were measured by chemical method. The test results were shown in Figure 16, Figure 17, Figure 18 respectively. Figure 16-18 illustrated that the R^2 of prediction value and actual value were 0.9554, 0.9651 and 0.9616 respectively, with RMSEP being 0.1147, 0.05437 and 0.03688. The results indicated that the prediction value and actual value had a good correlation. It showed that the calibration model of total nitrogen, ammonia nitrogen and nitrite nitrogen are able to accurately predict the concentrations of total nitrogen, ammonia nitrogen and nitrite nitrogen.

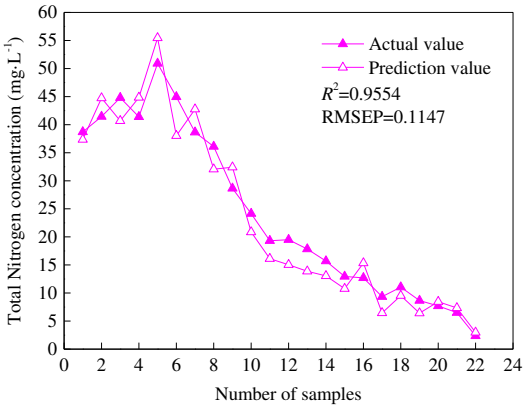

FIGURE 16
Test result of iPLS calibration model of total nitrogen

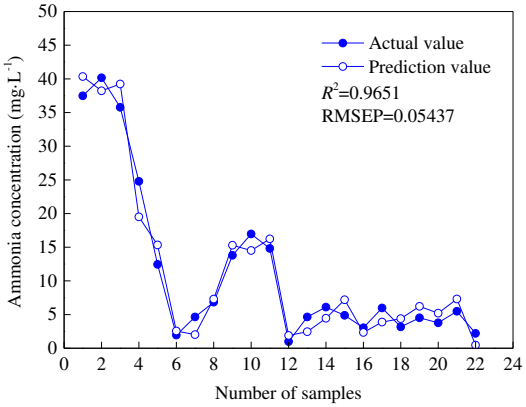

FIGURE 17
Test result of iPLS calibration model of ammonia nitrogen

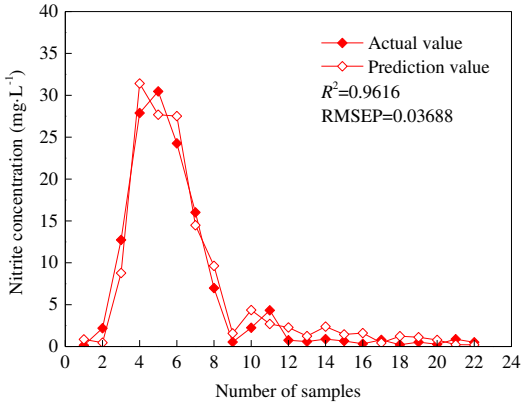

FIGURE 18
Test result of iPLS calibration model of nitrite nitrogen

CONCLUSIONS

The iPLS calibration models were established with the combination of iPLS method and the near-infrared spectroscopy. The optimal sub-interval was

firstly selected, and major interference in near-infrared spectrum was eliminated with iPLS method. The wave number of the optimal sub-interval was 7432-7824 cm^{-1}, 10465-10860 cm^{-1} and 7854-8250 cm^{-1} respectively.

The iPLS calibration model of total nitrogen, ammonia nitrogen and nitrite nitrogen showed that the R^2 of calibration value and actual value were 0.9574, 0.9706 and 0.9687, with the RMSECV being 0.08309, 0.04709 and 0.03129. It showed that the calibration models had higher accuracy.

The iPLS calibration model of total nitrogen, ammonia nitrogen and nitrite nitrogen were tested by test set. The R^2 of prediction value and actual value were 0.9554, 0.9651 and 0.9616 respectively, with root mean square error of prediction (RMSEP) being 0.1147, 0.05437 and 0.03688. This indicated that iPLS calibration models can better predict the concentrations of the total nitrogen, ammonia nitrogen and nitrite nitrogen during intermittent aeration treatment of the overlying water. The proposed method was accurate, rapid, non-polluted and cost-effective, so it had good application prospects to monitor the total nitrogen, ammonia nitrogen and nitrite nitrogen in water.

ACKNOWLEDGEMENTS

The work was supported by the Key Projects to Support the Talent for Colleges of Anhui Province (gxyqZD2017059), Research Projects of Visiting Scholars for Excellent Young and Backbone Talents both at Home and Abroad for Colleges of Anhui Province (gxfx2017054), Major Science and Technology Program for Water Pollution Control and Treatment of China (2014ZX07405-003-03).

REFERENCES

[1] Small, G.E., Cotner, J.B., Finlay, J.C., Stark, R.A., Sterner, R.W. (2014) Nitrogen transformations at the sediment–water interface across redox gradients in the Laurentian Great Lakes. Hydrobiologia,731, 95-108.

[2] Li, J.Z., Wu, H.X., Jiang, W., Yuan, X.Y., Liu, B.W. (2015) Pollution characteristics and ecological risk assessment of sediment from malodorous rivers in Nanjing city. Resources Environmental in the Yangtze Basin, 24, 1913-1919.

[3] Qing, X.Y., Ren, Y.F., Lv, Z.Q., Wang, X.K., Pang, R., Deng, R., Meng, L., Ma, H.Y. (2015) Characteristics of Total Nitrogen and Total Phosphorus Pollution and Eutrophication Assessment of Secondary River in Urban Chongqing. Environmental Science, 36, 2446-2452.

[4] Cao, Q.Q., Yu, L.J., Xue, J.P. (2015) Review on city polluted river reaeration techniques. Environmental Engineering, 33, 1-5.

[5] Yu, G.W., Lei, H.Y., Liu, G.L., Bai, T., Liu, K.S., Chen, R.W. (2007) Research on the characteristics of sediment release in a heavily polluted tidal river and control technologies. Acta Scientiae Circumstantiae, 27, 1476-1484.

[6] Sommer, S., Gier, J., Treude, T., Lomnitz, U., Dengler, M., Cardich., Dale, A.W. (2016) Depletion of oxygen, nitrate and nitrite in the Peruvian oxygen minimum zone cause an imbalance of benthic nitrogen fluxes. Deep Sea Research Part I Oceanographic Research Papers, 112, 113-122.

[7] Zhang, X.X., Li, A., Szewzyk, U., Ma, F. (2016) Improvement of biological nitrogen removal with nitrate-dependent Fe(II) oxidation bacterium Aquabacterium parvum, B6 in an up-flow bioreactor for wastewater treatment. Bioresource Technology, 219, 624–631.

[8] Basset, N., Katsou, E., Frison, N., Malamis, S., Dosta, J., Fatone, F. (2016)Integrating the selection of PHA storing biomass and nitrogen removal via nitrite in the main wastewater treatment line. Bioresource Technology, 200,820-829.

[9] Huang, J., Huang, S., Zhang, H., Huang, X.H., Zhang, Y., Wang, M., Zhu, J., Wang, K. (2015) Near infrared spectroscopy analysis of inorganic nitrogen in shortcut nitrification-denitrification based on interval partial least square. China Environmental Science, 35, 2014-2020.

[10] Ma, H.L., Wang, J.W., Chen, Y.J., Cheng, J.L., Lai, Z.T. (2017) Rapid authentication of starch adulterations in ultrafine granular powder of Shanyao by near-infrared spectroscopy coupled with chemometric methods, Food Chemistry, 215, 108-115.

[11] Munawar, A.A., Hörsten, D.V., Wegener, J.K., Pawelzik,E., Mörlein, D. (2016) Rapid and non-destructive prediction of mango quality attributes using Fourier transform near infrared spectroscopy and chemometrics, Engineering in Agriculture. Environment & Food, 9,208-215.

[12] Mariani, N.C., da Costa, R.C.D., de Lima, K.M., Nardini, V., Cunha, J.L.C., Teixeira, G.H. (2014) Predicting soluble solid content in intact jaboticaba [*Myrciaria jaboticaba*, (Vell.) O. Berg] fruit using near-infrared spectroscopy and chemometrics. Food Chemistry, 159, 458-462.

[13] Niu, X.Y., Zhao, Z.L., Jia, K.J., Li, X. (2012) A feasibility study on quantitative analysis of glucose and fructose in lotus root powder by FT-NIR spectroscopy and chemometrics. Food Chemistry, 133,592-597.

[14] Ning, L., Chen, J.M., Pan, T., Yao, L.J., Han, Y., Yu, J. (2016) Near-infrared spectroscopy combined with equidistant combination partial

least squares applied to multi-index analysis of corn. Infrared Physics & Technology, 76, 648-654.

[15] Kang, Q., Ru, Q.G., Liu, Y., Xu, L., Wang, Y., Zhang, Y., Li, H., Zhang, Q., Wu, Q. (2015) On-line monitoring the extract process of Fufang Shuanghua oral solution using near infrared spectroscopy and different PLS algorithms. Spectrochimica Acta Part A: Molecular and Biomolecular Spectroscopy, 152, 431-437.

[16] Melendez-Pastor, I., Almendro-Candel, M.B., Jose, N.P., Gomez, L., Lillo, M.G., Hernandez, E.I. (2013) Monitoring urban wastewaters' characteristics by visible and short wave near-infrared spectroscopy, Water, 2026-2036.

[17] Arrieta, M.P., López, J., López, D., Kenny, J.M., Peponi, L. (2016) Development of flexible materials based on plasticized electrospun PLA-PHB blends: structural, thermal, mechanical and disintegration properties. European Polymer Journal, 73, 433-446.

[18] Li, Y., Fan, Q., Liu, S., Wang, L. (2011) Simultaneous analysis of moisture, active component and cake structure of lyophilized powder for injection with diffuse reflectance FT-NIR chemometrics. Journal of Pharmaceutical & Biomedical Analysis, 55,216-219.

[19] Heitmann, A.P., Patrício, P.S.O., Coura, I.R., Pedroso, E.F., Souza, P.P., Mansur, H.S., Mansur, A. Oliveira, L.C.A. (2016) Nanostructured niobium oxyhydroxide dispersed Poly (3-hydroxybutyrate) (PHB) films: highly efficient photocatalysts for degradation methylene blue dye. Applied Catalysis B Environmental, 189, 141-150.

[20] Zhu, X.L., Lu, W.Z. (2014) Research and application progress of near infrared spectroscopy analytical technology in China in past five years. Spectroscopy and Spectral Analysis, 34, 2595-2605.

[21] Borràs, E., Ferré, J., Boqué, R., Mestres, M., Aceña, L.,Calvo, A.,Busto, O. (2016) Prediction of olive oil sensory descriptors using instrumental data fusion and partial least squares (PLS) regression. Talanta, 155, 116-123.

[22] Hosseinpour, S., Aghbashlo, M., Tabatabaei, M., Khalife, E. (2016) Exact estimation of biodiesel cetane number (CN) from its fatty acid methyl esters (FAMEs) profile using partial least square (PLS) adapted by artificial neural network (ANN). Energy Conversion & Management, 124, 389-398.

[23] Pérez-Rodríguez, M., Horák-Terra, I., Rodríguez-Lado, L., Matinez, C.A. (2016) Modelling mercury accumulation in minerogenic peat combining FTIR-ATR spectroscopy and partial least squares (PLS). Spectrochimica Acta Part A Molecular & Biomolecular Spectroscopy, 168, 65-72.

[24] Ferrão, M.F., Viera, M.D.S., Pazos, R.E.P., Fachini, D., Gerbase A.E., Marder, L. (2011) Simultaneous determination of quality parameters of biodiesel/diesel blends using HATR-FTIR spectra and PLS, *i*PLS or *si*PLS regressions. Fuel, 90, 701-706.

[25] Rahman, A., Kondo, N., Ogawa, Y., Suzuki, T., kanamori, K. (2016) Determination of K value for fish flesh with ultraviolet–visible spectroscopy and interval partial least squares (iPLS) regression method. Biosystems Engineering, 141, 12-18.

[26] Norgaard, L., Saudland, A., Wagner, J., Nielsen, J.P., Munch, L., Engelsen, S.B. (2000) Interval partial least-squares regression (iPLS): a comparative chemometric study with an example from near-infrared spectroscopy. Applied Spectroscopy, 54, 413-419.

[27] Huang, F.R., Li, S.P., Yu, J.H., Zheng, S.F., Chen, Z. (2011) Determination of cholesterol and triglyceride in serum based on interval partial least squares by near-infrared spectrum. Chinese Journal of Spectroscopy Laboratory, 28, 2774-2778.

[28] Li, X.L., Sun, C.J., Luo, L.B., He, Y. (2015) Determination of tea polyphenols content by infrared spectroscopy coupled with iPLS and random frog techniques. Computers & Electronics in Agriculture, 112, 28–35.

[29] Mahanty, B., Yoon, S.U., Kim, C.G. (2016) Spectroscopic quantitation of tetrazolium formazan in nano-toxicity assay with interval-based partial least squares regression and genetic algorithm. Chemometrics and Intelligent Laboratory Systems, 154, 16-22.

[30] Suhandy, D., Yulia, M., Ogawa, Y., kondo, N. (2013) Prediction of L-Ascorbic acid using FTIR-ATR terahertz spectroscopy combined with interval partial least squares (iPLS) Regression. Engineering in Agriculture, 6, 111-117.

[31] Borin, A., Poppi, R.J. (2005) Application of mid infrared spectroscopy and iPLS for the quantification of contaminants in lubricating oil. Vibrational Spectroscopy, 37, 27-32.

[32] Pereira, A.F.C., Pontes, M.J.C., Neto, F.F.G., Santos, S.R.B., Galvão, R.K.H., César, M. (2008) NIR spectrometric determination of quality parameters in vegetable oils using iPLS and variable selection. Food Research International, 41, 341-348.

[33] Xu, L., Li, W.H., Yang, Y., Yan, G.B., Shuai, L., Zhao, Q. (2016) Rapid determination of the intracellular PHA content during the enhanced biological phosphorus removal using NIR spectroscopy based on the modified PLS methods.China Environmental Science, 36, 1426-1434.

[34] Khulal, U., Zhao, J.W., Hu, W.W., Chen, Q. (2017) Intelligent evaluation of total volatile basic nitrogen (TVB-N) content in chicken meat by an improved multiple level data fusion model. Sensors & Actuators B Chemical, 238, 337-345.
[35] Zhang, W., Li, X., Shen, D.H., Teglio, A. (2016) R^2 and idiosyncratic volatility: Which captures the firm-specific return variation. Economic Modelling, 55, 298-304.

Received: 22.02.2017
Accepted: 23.07.2017

CORRESPONDING AUTHOR

Qing-ye Sun
School of Resources and Environmental Engineering, Anhui University, Jiulong Road 111, Hefei, 230601, P. R. China

e-mail: sunqingye@ahu.edu.cn

© by PSP Volume 26 – No. 10/2017 pages 5882-5890 Fresenius Environmental Bulletin

THE HIDDEN FRAGMENTATION AFTER LAND CONSOLIDATION IN TURKEY

Muge Kirmikil[1,*], S Tulin Akkaya Aslan[1], Kemal S Gundogdu[1] , Ismet Arici[2]

[1]Department of Biosystems Engineering, Uludag University, Bursa, Turkey
[2]Emeritus

ABSTRACT

It is accepted that inheritance is the primary cause of land fragmentation. The inheritance law is the leading significant cause of fragmentation or shrinking of land. Inheritance laws applied in most countries facilitate or demand the subdivision of holdings into equal parts among all heirs or in some countries among only sons.

Intense fragmentation or shrinking of agricultural land is a significant problem in Turkey. Inheritance law in Turkey prescribes equal distribution of agricultural land which is subject to heritage. When there are disputes towards the inheritance distribution, the new owner's submission of deed is not done. This situation brings out the truth that an agricultural land which seems as one piece is used by more than one person in reality.

In this study, it is aimed to evaluate public and hidden joint ownership in the areas where land consolidation is done. As study field, the data related to Bursa-Karacabey Plain villages were used where the most intensive agricultural activities are done in Turkey. In the study area, in order to determine joint ownership which is off the record Ismetpasa, Beylik and Yenisaribey villages are chosen and survey study was applied. After land consolidation in this study area, heirs wanted to own agricultural lands even if the plots are small and joint because the lands gained value, production became easier and yields increased, and alternative production opportunities arose. As a result, it was concluded that, after land consolidation hidden joint ownership is still going on in parcels, real joint ownership condition is mostly not recorded to registry of deeds.

KEYWORDS:
Inheritance law, land consolidation, one-way ANOVA test, ownership, Turkey

INTRODUCTION

Agricultural land fragmentation, also known as pulverization, parcellisation and scattering [1], is defined in the literature as the situation in which a single farm or ownership consists of numerous spatially separated parcels [2, 3, 4] which may be small in size and have irregular shapes [5].

[2] characterise land fragmentation as a fundamental rural spatial problem concerned with farms that are poorly organised at locations across space. Similarly, many authors [6, 7, 8] consider land fragmentation as a serious obstacle to optimal agricultural development because it hinders mechanisation, causes inefficient production and involves large costs to alleviate the adverse effects, resulting in a reduction in farmers' net incomes.

Land fragmentation is evident in many areas throughout the world. In particular, whilst land fragmentation has been closely associated with Europe and Mediterranean countries [8, 9] it is a topic that has been studied in many other countries and regions around the world [10, 11, 12, 13, 14, 15, 16].

Although the causes of land fragmentation vary from country to country and from region to region, there is general agreement that there are four main factors that trigger fragmentation: inheritance; population growth; land markets; and historical/cultural perspectives [1, 2, 17, 18, 19]. Other factors noted in more specific situations include: social and administrative decrees [1]; long-established cultivation; shortages of land and nucleated settlement; the piecemeal conversion of forests and moorland to arable land [20]; and the privatization transition process, e.g. in ex-eastern block and central European countries [4].

The size of landholdings gradually decreases when they are fragmented into parcels. This process becomes more problematic when a fragmented landholding is further fragmented into several parcels at the same time. This is a typical phenomenon, which is attributed to equal sub-division of different qualities of land parcels, for example, irrigated and non-irrigated, comprising a landholding among household heirs. Besides getting each land parcel smaller and smaller over the time, such land fragmentation leads to physical dispersion of parcels [17].

Land fragmentation also results in low efficiency in irrigation water management because of the irregular shape of numerous plots, and also causes time loss in travel and inconvenience in agricultural management [12]. Land consolidation is one of the main instruments to counteract the ongoing

fragmentation of the agrarian structure and to shape the spatial structure of rural areas. The aim of land consolidation is to improve the economic conditions for agricultural and forestry activity pursued on farms by improving the spatial structure of farms, such as by decreasing the number of separate plots that compose farms, and improving the location of arable plots relative to dwellings [21, 22, 23].

The excessive fragmentation or dispersion of landholdings is a major problem in Turkey. This is a consequence of demographic pressure on land resources, as well as the laws of inheritance and endowment of patrimony. Consequently, farmland in Turkey is divided into small farms, scattered over numerous non-contiguous plots in which mechanized agriculture is not used extensively. Farming activities such as sowing, planting, tillage, maintenance and harvesting require sufficient road systems to access the plots. In areas where land consolidation has not been implemented, farmers must travel long distances to reach their plots, resulting in lost time and increased expenditures for fuel oil and depreciation [23].

In Turkey, 23.2% of the population resides in towns and villages. Although the percentage of those living in rural areas seem to have decreased compared to previous years, the total sum accounts to 20 million people [24, 25]. According to the latest agriculture census (TS2001) there were 3 million agricultural enterprises in Turkey. Within the scope of farmer register system (FRS) there were approximately 2.3 million agricultural enterprises, according to the assessments in 2011 [26]. Throughout Turkey there are approximately 30 million parcels and 40 million joint sharers. The continued fragmentation of parcels and continuous downsizing of enterprises lead to a decline in yield and productivity in agriculture, and inadequate social development [27, 28]. This manifests a socioeconomic problem that involves soil-human relationships and all physical factors in the countryside [29]. A partial solution to this problem entails enlargement of parcels and enterprises [30].

The fact that ownership structure is fragmented, and lands are small and dispersed in Turkey moves agribusiness away from being economical [31]. Furthermore, owing to such reasons as increase in cost of irrigation projects, and decrease in irrigation rate, expected rural development cannot be realized and agricultural productivity cannot be increased [32].

With land consolidation, on the one hand, agricultural land is reshaped and new working conditions are brought about [24]. On the other hand, a new ownership structure and new joint tenancy premises are emerging. Land consolidation enables both better working conditions for producers, and realization of activities to the benefit of local farmers and public such as land leveling, a new rural landscape, and renewal of farm roads, irrigation and drainage systems, and village settlement [22, 23, 33, 34]. Land consolidation studies are done according to land consolidation of institution regulations by General Directorate of Rural Services until the year 2005 on the fields where irrigated farming is implemented. In agricultural reform areas, in accordance with law no. 3083, the studies of land consolidation is carried out by General Directorate of Agricultural Reform. Soil Conservation and Land Utilization Act came into force in 2005. With this law, in agricultural reform areas according to law no. 3038 and in other areas according to law no. 5403 land consolidation is continued to be implemented [35, 36]. In recent years (2014-2015) tendered land consolidation projects instead of provisions of law no. 3083 are being tendered according to provisions of law no. 5403.

There are two different joint ownerships are in question according to Turkish Civil Code. These are, joint tenancy (joint partnership, joint-owned property) and collective ownership (joint property, co-ownership). Joint tenancy is defined as more than one person is having an immovable property together in certain interest ratio that is not in fact divided into. In collective ownership co-partners have no defined interests and right of each one embraces whole of the goods included in partnership. The difference of collective ownership from joint tenancy; in collective ownership interests are undefined but in joint tenancy interests are defined. In collective ownership co-partners have to act together in order to take any action. However in joint tenancy co-partners can take an action independent from each other [37].

Owing to the inheritance law in Turkey, fragmentation continues after land consolidation as there are no preventive measures against land fragmentation. Because of the disputes among the heirs about division or the size of the parcel shrinks below 2 ha, heirs continue to use the parcel commonly. In land registers the land appears to be a single piece, as a result of an informal agreement among heirs; the land can belong to more than one party. Owing to land consolidation these parcels are appealing to use which transforms into a well geometrical shape and has common usage facilities like roads, irrigation and drainage facilities.

As a result, enterprises further downsize, investment in land by appropriation further decreases, modernization of enterprises is obstructed, it is not possible to make investments by taking out loans, inheritance conflicts among family members increase, youth wishing to engage in agriculture are anxious about the future, and villages are deserted.

The aim of this study was to examine the change in land ownership pre- and post- consolidation in "Ismetpasa, Beylik, and Yenisaribey" villages of Karacabey, Bursa, where land consolidation was completed between the years 1990 and 2000s. In

these areas, land consolidation studies were done according to the land consolidation of institution regulations by General Directorate of Rural Services. In this way, it was attempted to reveal positive and negative changes in ownership after land consolidation projects.

MATERIALS AND METHODS

To determine and analyze the change in ownership structure in land consolidation areas, villages of Ismetpasa, Beylik, and Yenisaribey within the borders of Karacabey, Bursa were selected.

The survey study was administered in February 2012 in the research area and constitutes the primary data of the study. Besides, examination of owner structure data in the records obtained from Land Registry Office, Karacabey Irrigation Association, General Directorate of State Hydraulic Works, and Chamber of Agriculture was a significant data source. Furthermore, secondary data were obtained from the results of existing scientific studies that had been carried out on the same field for analyzing ownership structure.

Stratified random sampling method was employed to determine the number of questionnaires to be given in the survey study. Stratified random sampling method has two aims. The first one is to increase the accuracy of estimations about the population, and the second one is to enable enterprises, of different qualities, in the population to be represented in the best way [38]. To determine the enterprises comprising sample for the study that would be carried out in the villages of Karacabey Plain, the following equation(1) proposed by Neyman [39].

$$n = \frac{(\sum N_h S_h)^2}{(N^2 * D^2) + \sum N_h S_h^2} \quad (1)$$

Where, $D^2 = \frac{d^2}{z^2}$

In the formula;
n: number of samples,
N: total number of enterprises
N_h: number of enterprises in h^{th} stratum
S_h: standard deviation of h^{th} stratum
d: permissible margin of error
z: t value in confidence interval

The 95% confidence level and 10% margin of error was used in determining the sample size for enterprises located in the villages in the plains of Karacabey. The formula (2) was used to partition sample size into strata [39]. As a result of the calculations, the survey study was carried out with a total of 152 people. The responses concerning the causes and effects of hidden fragmentation in land consolidation, number-percent allocation, and differences according to villages were analyzed using one-way ANOVA test [40] with SPSS (Statistical Package for the Social Sciences) software package. Differences that were statistically significant according to ANOVA test results were evaluated.

$$n_h = \frac{N_h}{N} \quad (2)$$

RESULTS AND DISCUSSION

Ownership data obtained from Karacabey Land Registry Office were analyzed and joint parcel use is presented in Figure 1. These values are those that were declared to the registry office. According to Figure 1, the percentage of solely owned parcels is 81% in Beylik, 53.7% in Ismetpasa, and 49.8% in Yenisaribey. The percentage of jointly owned parcels is 66.2% in Beylik, 46.3% in Ismetpasa and 50.2% in Yenisaribey.

Parcels that are registered as solely owned or shared by few can be, in practice, shared by more owners. Because the registry records of heritage and changes in property cannot be carried out or postponed because of various reasons. For example, as parcels smaller than 2 ha cannot be divided legally, these parcels are used jointly or shared out and used among heirs but their land registration cannot be done.

The results of the survey reveal that sole or joint parcel use is very different from land registers (Figure 2). As can be seen, percentage of villagers who are the title owners of all the lands cultivated is 10% in Beylik Village, 26% in Ismetpasa Village, and 28% in Yenisaribey Village. In other words, 90% of the lands in Beylik, 74% of the lands in Ismetpasa, and 72% of the lands in Yenisaribey are jointly used. This situation reveals that on the one hand with the negative effect of caused by heritage law, family lands cultivated by producers are not devolved to their names.

One-Way ANOVA test was employed to study the difference between the questions (Table 1) concerning causes and results of joint ownership in the study area. In the Levene test table (Table 2), which was performed for homogeneity of variances, equality of variances was not obtained when significance value of Levene statistic was less than 0.05. Following this step, significance values that met the requirements in ANOVA table were studied. The results of the questions having significant differences according to ANOVA test are given in Table 3.

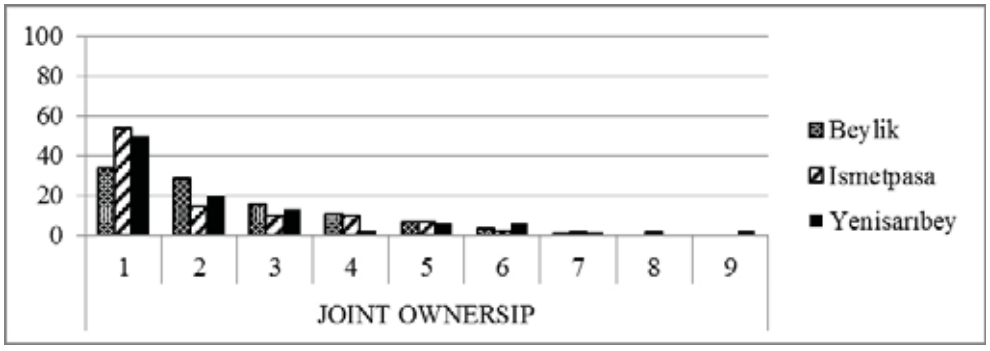

FIGURE 1
Joint Ownership in the Study Area According to Land Registers (%)

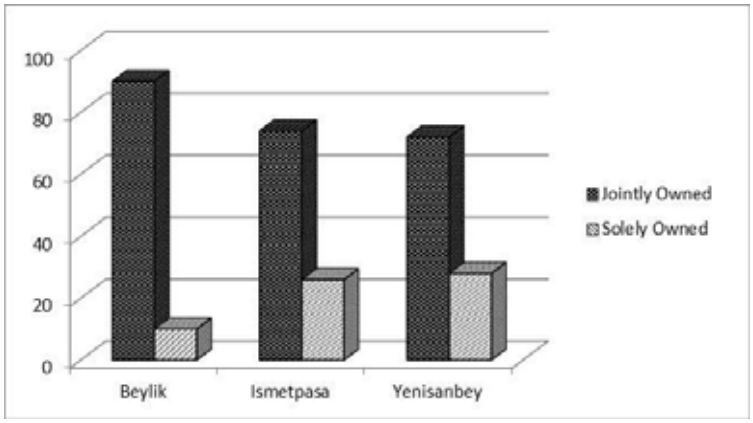

FIGURE 2
Joint Ownership in the Study Area According to Survey Results (%)

TABLE 1
Survey Question

Abbreviation	Survey Question	Abbreviation	Survey Question
Q3	Is all lands' title of deed you cultivate belongs to your name?	**Q19**	How far are your parcels' to each other?
Q5	Do you rent your land?	**Q20**	Are there any new lands purchased after land consolidation?
S6	Can you cultivate all of the parcels you have?	**Q21**	Is there any land selling after land consolidation?
Q7	After land consolidation to whom lands belong to?	**Q22**	How do you assess your income level after land consolidation?
Q8	The parcels you have taken on you after land consolidation, before land consolidation to whom they were belonged to?	**Q23**	To whom do you agree to turn over the enterprise?
Q9	Do you have a land that you do not use (abandoned)?	**Q24**	Are there any shared lands to your children after land consolidation?
Q10	The lands you cultivate	**Q26**	Is there any land fragmentation again after land consolidation?
Q11	How do you use your joint-owned property?	**Q27**	Do you concern long-term investment to your own land?
Q12	Do you have inherited land?	**Q28**	Do you invest to the lands that you do not have the title of deed on you?
Q13	Title of deeds of inherited lands devolved to heirs?	**Q29**	Is there any share outs that off the record on your name on your land?
Q14	How is the working conditions on land of agricultural production?	**Q31**	Is joint-owned property on your lands cause to uneasiness?
Q15	Is the income you obtain enough?	**Q34**	How joint-owned affects the usage of credit?
Q16	Do you cultivate second crop?	**Q35**	How joint-owned affects cultivation of land in a best way?
Q17	Do you do husbandry?	**Q36**	How hidden joint ownership affects continuity of production?
Q18	How far is your agricultural lands' distance to the village?		

TABLE 2
Levene's Test Results

	Levene Statistic	df1	df2	Significance		Levene Statistic	df1	df2	Significance
Q3	15.204	2	136	.000	**Q19**	.943	2	134	.392
Q5	8.503	2	136	.000	**Q20**	15.697	2	136	.000
Q6	7.858	2	136	.001	**Q21**	.785	2	137	.458
Q7	6.907	2	133	.001	**Q22**	.516	2	135	.598
Q8	.234	2	133	.792	**Q23**	.577	2	137	.563
Q9	3.513	2	136	.033	**Q24**	3.596	2	137	.030
Q10	1.473	2	134	.233	**Q26**	.135	2	134	.874
Q11	4.691	2	131	.011	**Q27**	12.146	2	135	.000
Q12	.218	2	134	.804	**Q28**	2.699	2	80	.073
Q13	.124	2	83	.884	**Q29**	42.205	2	81	.000
Q14	2.193	2	134	.116	**Q31**	8.751	2	64	.000
Q15	8.655	2	137	.000	**Q34**	8.631	2	61	.001
Q16	30.093	2	136	.000	**Q35**	1.285	2	57	.285
Q17	101.831	2	136	.000	**Q36**	2.355	2	58	.104
Q18	.536	2	136	.586					

TABLE 3
One-Way ANOVA test results

		Sum of Squares	Degrees of Freedom	Mean Square	F	Significance (p)
Q14	**Between Groups**	6.950	2	3.475	3.904	.023
	Within Groups	119.284	134	.890		
	Total	126.234	136			
Q16	**Between Groups**	2.366	2	1.183	5.598	.005
	Within Groups	28.742	136	.211		
	Total	31.108	138			
Q17	**Between Groups**	6.077	2	3.038	14.906	.000
	Within Groups	27.722	136	.204		
	Total	33.799	138			
Q19	**Between Groups**	4.991	2	2.496	5.327	.006
	Within Groups	62.775	134	.468		
	Total	67.766	136			
Q27	**Between Groups**	1.571	2	.785	3.292	.040
	Within Groups	32.205	135	.239		
	Total	33.775	137			
Q29	**Between Groups**	3.858	2	1.929	10.553	.000
	Within Groups	14.808	81	.183		
	Total	18.667	83			
Q34	**Between Groups**	1.052	2	.526	3.689	.031
	Within Groups	8.698	61	.143		
	Total	9.750	63			
Q36	**Between Groups**	1.776	2	.888	4.295	.018
	Within Groups	11.994	58	.207		
	Total	13.770	60			

Differences between the responses to the answers among 3 villages were determined according to significance values produced by ANOVA test. As significance levels of working conditions in the lands (Q14 p= 0.023 < 0.05), planting second crop (Q16 p= 0.005 < 0.05), livestock raising (Q17 p= 0.001 < 0.05), distance between parcels (Q19 p= 0.006 < 0.05), long term investment in the lands owned (Q27 p= 0.040 < 0.05), unregistered joint ownership (Q29 p= 0.001 < 0.05), the effect of hidden joint ownership on loan usage (Q34 p= 0.031 < 0.05), and the effect of hidden joint ownership on continuity of production (Q36 p= 0.018 < 0.05) are less than 0.05, there is statistically significant difference between the villages in terms of these issues.

According to the survey results, it was found that fragmentation continues even after the land consolidation. Fragmentation does not cause multiplication of parcel numbers however it reveals itself jointly usage on parcel. The main reason of this joint ownership is the unofficial division as a result of heritage. The point in question why joint ownership cannot be abolished is the oldest family member is still alive even s/he does not engage in farming and does not allow sharing of land, a quite number of shareholders, unanimity that cannot be achieved while doing transactions and sharing, heirs do not want to deal with this case because of the small size of lands, conflicts between heirs and the passion to have land in rural areas even though the heirs live in the cities. When inherited lands are searched in the study field, it is seen that most of the lands are inherited from the eldest in the family but because of various reasons they are not devolved to land registry office. According the survey results, 72%, 65%, and

80% of the lands are not devolved to the registry office, respectively in Beylik, Ismetpasa, and Yenisaribey. Three reasons were identified for the lack of sufficient devolve percentage: 1) there are conflicts of heritage share among the family members, 2) the heirs cannot gather because they reside off the village and 3) the small parcels less than 2 ha cannot be divided legally.

Although land consolidation is conducive to agricultural development, particularly small farmers may perceive it as interference in their internal matters leading to their reduced benefit [2]. The easy and flexible policies for land transactions such as leasing-in, leasing-out, buying and selling of land could also help to reduce the land fragmentation. As such policies have also proved to be successful in China and Japan [17,18]. Further, the extension agents should play an active role in dissemination of suitable sustainable technologies to the different category of farmers aiming for further reducing the inefficiency [41].

Another important issue is the process of further fragmentation. Land inheritance is generally a key driver of land use [42]. As per the law of inheritance, individuals separating from a farm household may get a few tiny parcels of land as their share from the paternal property. They would still like to have these because without them they are vulnerable to the risk of starvation, as alternative income opportunities are scarce. Moreover, the greed for paternal land is reinforced by a lack of progressive tax on inherited land. Irrespective of their landholding size or economic status, eligible household members want to have a share from their paternal property, as it does not incur any cost to them [17]. In countries where the equal inheritance system has been applied for centuries, i.e. where land is not passed down to a single heir but to all heirs in equal shares, the situation is particularly critical. In these countries, the process of land fragmentation continues at an exponentially increasing rate. The tools for land-ownership defragmentation, i.e. the farmland sales market and land consolidation programs, cannot keep up with this pace. Therefore, within a few decades, the symptoms of extreme farmland fragmentation will be seen in countries and regions where the phenomenon has not yet occurred. In regions where these problems currently exist, they will become significantly more acute [43].

Hidden joint ownership brings some problems. Land ownership is obstructed especially because there is no young generation willing to live in a village and engage in farming, and the uncertainties related to heritage in the long term is still a consideration. These causes serious impediments in the long term investments and plans of these lands. According to the survey results, 86% of the farmers expressed that they did not consider long term investments. The reasons were that the eldest member of the family (title owner) does want to engage in farming activities and does not allow the sharing of land, being a land owner is considered as reassurance and is prestigious, parcels have multi sharers, it is thought that shareholders not engaged in farming might demand for invested land in the future, bank credit is not supplied because of not having a property for his/her name. Especially when bank credit is needed for investment to the land the banks do not provide loans if all of the shareholders do not approve of the investment.

Hidden joint ownership affects cultivation of land in the best way [12, 44]. According to the survey result of the current study, as shareholders cannot act independently they refrain from investment and they cannot cultivate crops as they want, which causes decreases in the income levels and affects the crop production in a negative way [45]. Continuity of hidden joint ownership results in cultivation of land in a small sizes and this eventually raises the need for land consolidation study on the same area in a short time. The difficulties in the use of property cause land owners to lose interest in farming activities and abandon the joint-owned land.

As seen in the survey results, the fragmental lands are combined and their shapes are fixed, improving the production and working conditions. Under these conditions hidden and public ownership cannot be hampered. After land consolidation, heirs wanted to own agricultural lands even if the plots are small and joint because the lands gained value, production became easier and yields increased, and alternative production opportunities arose. After the land consolidation, fragmentation and shrinkage of the lands continue. This in turn emerges a number of social problems besides the inefficient use of lands. In this case, land consolidation is inadequate on its own while promoting sustainable production. Along with land consolidation, property problems have to be handled.

In Turkey while the number and ratio of people who engage in farming keeps decreasing persistently, the number of land owners is also decreasing. Agricultural lands divided by heritage reached such small size that cannot supply subsistence of a family, it causes desolation of lands and an intense domestic migration takes place. Uneasiness caused by public and hidden joint ownership accelerates the desolation of land.

Since the main subsistence of people living in rural areas is farming, it is urgently needed that fragmentation and shrinkage of land be stopped in the first place. To maximize enterprise of land, precautions should be taken, that is parcel sizes should be increased and protected to provide sufficient conditions for sustainable production.

In Turkey, related articles in Civil Code, altered on 15 May 2014 with The Law Amending the Law on Soil Conservation and Land Use, causes fragmentation of agricultural lands. The aim of this law is to

enlarge the plots and hence the farm sizes by eliminating the shareholders not involved with farming activities. This is achieved by paying these unattended shareholders for their land and enterprises and allocating the land and the facilities to the shareholders currently engaged in the farming business.

This Law, from the date 15 May 2014, while preventing drop of parcel sizes below a certain size, the minimum land size is determined depending on the region and district. It is foreseen that enterprises' land existence by inheritance should not drop below minimum land size. With this Law it is also aimed to establish land acquisition offices that can realize land alteration. On the date of issue of Law it is foreseen that conveyancing of agricultural lands which have not shared yet among heirs, should be completed according to previous act of law. After the date of issue, lands which will be subject of inheritance will be dependent on to the Law's provisions. This situation can be seen as a factor diminishing the effect of Law. As it is explained above, if the implementation is carried out with multi-purposed land consolidation, it will contribute to the solution of property related problems and reforming the production and working conditions. The program should be implemented in such a way that the land acquisition offices should be found in advance to realize purchase and sale transactions and these offices should play an active role during land consolidation studies. In agricultural production, it is not enough for enterprises to have a land size that provides subsistence. The system should be supported by various incentives to increase the production and to solve the marketing problems. Venture, difficulty and devotion in agricultural production, living conditions and social problems should be considered holistically, and incentives should also be devoted to producers to improve the social aspects.

ACKNOWLEDGEMENTS

This research was supported by Uludag University Scientific Research Projects Unit. (BAP). Project No: UAP(Z)-2012/13

REFERENCES

[1] Bentley, W. (1987) Economic and ecological approaches to land fragmentation: In defence of a much-maligned phenomenon. Annual Review of Anthropology, 16, 31–67.

[2] King, R. & Burton, S. (1982) Land fragmentation: Notes on a fundamental rural spatial problem. Progress in Human Geography, 6(4), 475–494.

[3] McPherson, M.F. (1982) Land fragmentation: A selected literature review. Development discussion paper no. 141. Harvard Institute for International Development, Harvard University.

[4] Van Dijk, T. (2003) Dealing with central European land fragmentation. Delft: Eburon.

[5] Demetriou D., Stillwell J. and See L. (2013) A new methodology for measuring land fragmentation. Computers, Environment and Urban Systems 39, 71–80.

[6] De Lisle, D. (1982) Effects of distance on cropping patters internal of the farm. Annals of Association of American Geographers, 72(1), 88–98.

[7] Jabarin, A.S. and Epplin, F.M. (1994) Impacts of land fragmentation on the cost of producing wheat in the rain-fed region of northern Jordan. Agricultural Economics, 11(2–3), 191–196.

[8] Karouzis, G. (1971) Time-wasted and distance travelled by the average Cypriot farmer in order to visit his scattered and fragmented agricultural holding. Geographical Chronicles: Bulletin of the Cyprus Geographical Association, 1(1), 39–58.

[9] Falah, G. (1992) Land fragmentation and spatial control in the Nazareth metropolitan-area. Professional Geographer, 44(1), 30–44.

[10] Goland, C. (1993) Field scattering as agricultural risk management – A case-study from Cuyo-Cuyo, Department of Puno, Peru. Mountain Research and Development, 13(4), 317–338.

[11] Kjelland, M., Kreuter, U., Clendenin, G., Wilkins, R., Ben, X., Afanador, G., Grant, W. (2007) Factors related to spatial patterns of rural land fragmentation in Texas. Environmental Management, 40(2), 231–244.

[12] Nguyen, T., Cheng, E.J. and Findlay, C. (1996) Land fragmentation and farm productivity in China in the 1990s. China Economic Review, 7(2), 169–180.

[13] Ram, K.A., Tsunekawa, A., Sahad, D.K. and Miyazaki, T. (1999) Subdivision and fragmentation of land holdings and their implication in desertification in the Thar Desert, India. Journal of Arid Environments, 41(4), 463–477.

[14] Soltow, L. (1983) Land fragmentation as an index of history in the Virginia military district of Ohio. Explorations in Economic History, 20(3), 263–273.

[15] Verry, E.S. (2001) Land fragmentation and impacts to streams and fish in the Central and Upper Midwest. In Proceedings of the society of American foresters, 2000 national convention (pp. 38–44). National Convention of the Society American-Foresters.

[16] Wan, G.H. and Cheng, E.J. (2001) Effects of land fragmentation and returns to scale in the

Chinese farming sector. Applied Economics, 33(2), 183–194.
[17] Niroula, G., and Thapa, G. (2005) Impacts and causes of land fragmentation, and lesson learned from land consolidation in South Asia. Land Use Policy, 22, 358–372.
[18] Tan, S., Heerink, N. and Qu, F. (2006) Land fragmentation and its driving forces in China. Land Use Policy, 23, 272–285.
[19] Van Hung, P., MacAulay, G. and Marsh, S. (2007) The economics of land fragmentation in the North Vietnam. The Australian Journal of Agricultural and Resource Economics, 51, 195–211.
[20] Grigg, D. (1980) Population growth and agrarian change: An historical perspective. Cambridge: Cambridge Univ. Press.
[21] Kupiduraa A., Luczewski M., Homec R. and Kupiduraa P. (2014) Public perceptions of rural landscapes in land consolidation procedures in Poland. Land Use Policy 39(2014) 313–319.
[22] Pasakarnis, G. and Maliene, V. (2009) Land Readjustment for Sustainable Rural Development 5th International Vilnius Conference EURO Mini Conference "Knowledge-Based Technologies and Or Methodologies for Strategic Decisions of Sustainable Development" (KORSD-2009) September 30–October 3, 2009, Vilnius, Lithuania, 169–174.
[23] Yaslioglu, E., Akkaya Aslan, S.T., Kirmikil, M., Gundogdu, K.S. and Arici, I. (2009) Changes in farm management and agricultural activities and their effect on farmers' satisfaction from land consolidation: The case of Bursa-Karacabey-Turkey. European Planning Studies 17(2), 327-340.
[24] Arici, I. and Akkaya Aslan, S.T. (2014) Arazi Toplulastirmasi Planlama ve Projelemesi, Dora Yayinlari, ISBN: 978-605-4798-49-0 Pp.237 (in Turkish).
[25] Akkaya Aslan, S.T., Gundogdu, K.S., Yaslioglu, E., Kirmikil, M. and Arici, I. (2007) Personal, physical and socioeconomic factors affecting farmers' adoption of land consolidation, Spanish Journal of Agricultural Research 5(2), 204-213.
[26] Anonymous (2015) T.C. Gida Tarim ve Hayvancilik Bakanligi 2015 Yili Performans Programi, Ankara Pp.116 (in Turkish).
[27] Cevik, B. and Tekinel, O. (1988) Sulama Projelerinde Arazi Toplulastirmasinin Yeri, Onemi ve Yararlari, DSI Genel Mudurlugu, Teknoloji Dairesi Baskanligi, Sulama Projelerinde Arazi Toplulastirmasi Semineri Notlari, Çukurova Universitesi Basimevi, Adana (in Turkish).
[28] Schupbach, B., Zgraggen, K. and Szerencsits, E. (2008) Incentives for low-input land-use types and their influence on the attractiveness of landscapes, Journal of Environmental Management, 89(3), 222-233.
[29] Bochard, K., Kotter, T., Schaefer, G. and Schaloske M. (1990) Landentwicklung in Rheinland-Pfalz, Untersuchungen uber kunftige Zielsetzungen und Aufgabenschwerpunkte fur die Entwicklung des landlichen Raumes, Institut fur Stadebau, Bodenordnung und Kulturtechnik der Universitat Bonn, Pp.156 (in German).
[30] Aereboe, F. (2013) Allgemeine landwirtschaftliche Betriebslehre, ISBN: 3846021024, EAN: 9783846021026, Paperback. Salzwasser-Verlag GmbH, Pp.720 (in German).
[31] Todorova, S.A. and Lulcheva, D. (2005) Economic and Social Effects of Land Fragmentation on Bulgarian Agriculture. Journal Central European Agriculture, 6 (4), 555-562.
[32] Yaganoglu, A.V., Okuroglu, M. and Hanay, A. (2000) Arazi Toplulastirilmasi. Atatürk Universitesi Ziraat Fakultesi, Ders Yayinlari No:159, Erzurum, Pp.169 (in Turkish).
[33] Anonymous (2009) Tarim Arazilerinin Korunmasi, Kullanilmasi ve Arazi Toplulastirmasina İliskin Tüzük, Official Gazette, no. 27298 (in Turkish).
[34] Yaslioglu, E., Arici, I., Kuscu, H, Gundogdu, K.S, Akkaya Aslan, S.T. and Kirmikil, M. (2008) Adoption factors of irrigation systems whose projects are synchronized with land consolidation. Kuwait Journal Sci. Eng. 35(2A), 1-10.
[35] Anonymous (2005) Toprak Koruma Ve Arazi Kullanimi Kanunu, Official Gazette, no.25880 (in Turkish).
[36] Anonymous (2007) Toprak Koruma Ve Arazi Kullanimi Kanununda Degisiklik Yapilmasi Hakkinda Kanun, no. 26429 (in Turkish).
[37] Anonymous (2001) Türk Medeni Kanunu, Kanun Numarasi: 4721, Ankara (in Turkish).
[38] Günes, T. ve Arikan, R. (1988) Tarim Ekonomisi İstatistigi, Ankara Üniversitesi Ziraat Fakültesi, no. 1049, Ankara Üniversitesi Basimevi, Ankara Pp. 293 (in Turkish).
[39] Yamane, T. (1967) Elementary Sampling Theory. Prentice Hall Inc. Englewood Cliffs. NT. Pp.404.
[40] Field, A. (2005) Discovering Statistics using SPSS Statistics, SAGE Publications Ltd, 2005-Pp.856.
[41] Manjunathaa, A.V., Anikc, A.R., Speelmand, S. and Nuppenaua, E.A. (2013) Impact of land fragmentation, farm size, land ownership and crop diversity on profit and efficiency of irrigated farms in India, Land Use Policy 31, 397–405.
[42] Gibson, M.A. and Gurmu, E. (2011) Land inheritance establishes sibling competition for marriage and reproduction in rural Ethiopia. PNAS 108, 2200–2204.
[43] Sklenicka, P., Janovska, V., Salek M., Vlasak, J. and Molnarova, K. (2014) The Farmland

Rental Paradox: Extreme land ownership fragmentation as a new form of land degradation, Land Use Policy, 38, 587–593.
[44] Zhang, L., Huang, J. and Rozelle, S. (1996) Land policy and land use in China. Paper presented at OECD Conference on Agricultural Policies in China, Paris, 12–13 December 1996.
[45] Rahman S. and Rahman, M., (2009) Impact of land fragmentation and resource ownership on productivity and efficiency: The case of rice producers in Bangladesh, Land Use Policy, 26(1), 95-103.

Received: **22.02.2017**
Accepted: **27.06.2017**

CORRESPONDING AUTHOR

Muge Kirmikil
Department of Biosystems Engineering
Uludag University
Bursa – TURKEY

E-mail: muge@uludag.edu.tr

© by PSP Volume 26 – No. 10/2017 pages 5891-5899 Fresenius Environmental Bulletin

ASSESSMENT OF SULPHUR EFFICIENCY OF DURUM AND BREAD WHEAT GENOTYPES

Halil Erdem[1,*], Mustafa Bulent Torun[2]

[1]Gaziosmanpasa University, Faculty of Agriculture, Soil Science and Plant Nutrition Department, Tokat, Turkey
[2]Cukurova University, Faculty of Agriculture, Soil Science and Plant Nutrition Department, Adana, Turkey

ABSTRACT

A greenhouse experiment has been carried out to evaluate the effects of sulphur (S) applications on shoot dry matter, spad value, S and nitrogen (N) concentrations of 35 bread and 18 durum wheat cultivars. Plants were grown with a control and 100 ppm S soil treatments. Shoot dry matter of durum (63%) and bread (74%) wheat cultivars significantly increased ($P<0.01$) with S application and the difference in S efficiency between wheat varieties was significant. Sulphur and N concentrations of shoot were also increased with S application. The S applications in bread wheat cultivars slightly affected the N concentrations of shoot, whereas N concentrations of durum wheat cultivars significantly varied ($P<0.01$) with S application. The results revealed that S deficiency lead to a significant decline in shoot dry matters of wheat cultivars, and deficiency can be eliminated by S application during planting.

KEYWORDS:
Sulphur, durum wheat, bread wheat, efficiency, N:S ratio, spad value

INTRODUCTION

Sulphur (S), one of the six macro nutrients in soil is essential for crop growth and has many common physiological functions with nitrogen (N) [1-2-3]. Sulphur deficiency was showed up at very early growth stages of winter cereals that causes a significant reduction in yield components [4]. Several studies [5-6] have shown that S fertilization may increase the efficiency of N use. Salvagiotti et al. [6] indicated that yield increase is associated with the increasing N efficiency of crops. The lack of adequate S limits plant growth and results in severe reduction in agricultural production throughout the world [7].

Depletion of S deposition from the industrial sources and the use of fertilizers contain lower rate of S led to significant S deficiencies in soils. Despite depletion and importance of S as an essential element for plant growth, S-containing fertilizers have not been used for wheat crops before 1980s [8]. Although S requirement of wheat is low [9], S deficiency in agricultural soils significantly affects the yield, quality of winter wheat [10-11], and some of the yield components [12-13-14].

The application of S has significantly affects the wheat yield and some of the yield components [15-16]. The S application increases grain protein concentration, particularly at low N fertilizer rates [17] and affects the wheat N:S ratio [10]. The increasing N:S ratio with N application in case of S deficiency can reduce crop yield [18-19]. The interaction between N and S revealed that an optimum plant-available N:S ratio in soil was needed to avoid yield restrictions in many plants [20-21]. Therefore, optimum crop yields cannot be obtained without balancing the N:S ratio in soil [19-22].

Sulphur efficiency is the ability of a plant to maintain good growth on S-limited conditions [16-23]. The S efficiency value was used to determine the tolerance to S deficiency. Assessment of genotypic variation in tolerance to other nutrient deficiency can be determined by the use of S efficiency calculated with considerations for the growth of the whole shoot. Some genotypes are more resistant to low S conditions and their growth may not be affected by S supply. Ahmad et al. [24] indicated that S content displayed 6–8-fold differences among the genotypes grown under S-insufficient conditions. Since limited reports could be found on potential differences among durum and bread wheat varieties on S uptake and utilization, this greenhouse experiment was designed to determine the effects of S-application on growth, spad value, S efficiency, S and N concentrations and N:S ratio in shoots of bread and durum wheat genotypes.

MATERIALS AND METHODS

A greenhouse experiment was conducted with 35 bread and 18 durum wheat cultivars with the application of two different S doses (0 and 100 mg S kg^{-1}). Seeds of durum (*Triticum durum*) and bread wheat (*Triticum aestivum*) cultivars were sown in plastic pots containing 1.75 kg soil, and grown under greenhouse conditions at the University of Cukurova Adana, Turkey. The extractable S concentration of soils used in pot experiment was 12.2 mg SO_4-S kg^{-}

[1], soil was clay loam-textured, $CaCO_3$ content was 11.2%, pH was 8.02 and organic matter content was 1.1%. The analysis of chemical and physical properties of soils were carried out using standard methods described by Bloem et al. [25], Bouyoucous [26], Klute et al. [27] and Jackson [28], respectively.

Fifteen seeds were sown in each pot, and the seedlings were thinned to seven per pot after the emergence. Before potting, the soil was homogeneously treated with a basal application of 300 mg N kg^{-1} in a form of $Ca(NO_3)_2.4H_2O$, 100 mg P kg^{-1} in KH_2PO_4 form, 2.5 mg Fe kg^{-1} in Fe-EDTA form and 2 mg Zn kg^{-1} in $ZnCl_2$ form. Two doses of S (0 and 100 mg S kg^{-1}) in the form of $CaSO_4.2H_2O$ were applied. Pots were sustained almost at field capacity, and distilled water was used in irrigations.

Plant growth was observed, and spad values were recorded with a chlorophyll meter as an indication of S-deficiency symptom (Minolta Spad 502). SPAD value is usually linked to chlorophyll concentration of plants [29], and increases with increasing chlorophyll content. SPAD measurement on leaves was performed just below the youngest full-grown leaf. Harvest time was determined based on symptom intensity.

Plants were harvested at 46th day of growth. Harvested plants were washed, dried at 70 ºC for 48 hours and dry weights were determined. Dry samples were milled, and became ready for laboratory analysis. Shoot samples were treated with H_2O_2-HNO_3 acid mixture and burned in a microwave (Mars X-Press) for S-analysis. Following the digestions, S was analyzed by using Inductively Coupled Plasma-Atomic Emission Spectrometry (ICP-AES; Jobin Yvon) device at 182.562 nm wavelength [30]. Nitrogen was analyzed by Kjeldahl method [31].

Sulphur efficiency of wheat varieties were calculated as;

SE (%) = (dry matter yield at S0 conditions/dry matter yield at S100 conditions)*100 [24].

Standard variance analyze techniques were used to assess the significance of treatment means. The data presented in the tables are mean values of replications. The homogeneities of bread and durum wheat varieties in response to S0 (0 mg S kg^{-1}) and S100 (100 mg S kg^{-1}) treatments in terms of dry matter yield, spad value, S and N concentrations and N:S ratios were determined by the Duncan`s test at 0.05 probability level. The differences for S0 and S 100 applications were compared using the paired t-test. The statistical analyses were performed with SPSS version 21.

RESULTS AND DISCUSSION

Shoot dry matter yield, S efficiency and Spad value. The responses of 35 bread and 18 durum wheat cultivars to two sulphur (S) doses on shoot dry matter yield and spad values were presented in Table 1 and 2. Significant positive shoot dry matter yield responses (either $P<0.01$ or $P<0.05$) of S application were obtained for bread and durum wheat cultivars. Whereas, Zhao et al. [10] observed that S mainly affected the number of grains per ear, and other yield components were less affected by S application. Since S application increased the shoot N concentrations of most of wheat varieties, dry matter yield increase might be associated with the increased N efficiency of wheat cultivars. The improvements in crop yield for oilseed rape, barley, rice, durum and bread wheat, sugar beet and grass [12-16-4-33-34] have been reported from different countries.

Average shoot dry matter yield of bread wheat cultivars in control treatment was 0.60 g plant^{-1}, and increased to 1.04 g plant^{-1} with S100 application. The yield increase in bread wheat cultivars with S application was average 74% and the highest yield increases were obtained for Sultan, Bayraktar, Aytin, Yildiz and Kutluk varieties as 90%, 89%, 85%, 85% and 84%, respectively. The lowest dry matter yield increase (47%) was occurred at Seri cultivar (Table 1). Although dry matter yield increased up to 77% with the addition of 100 mg S kg^{-1}, Kirac variety yielded the lowest dry matter in both S0 and S100 doses, and dry matter significantly ($P<0.01$) differed from all other 34 bread wheat varieties evaluated. The results indicated a distinct difference on responses to S application among the varieties of the same species. The variation of dry matter yield of different varieties in S-deficient soil was related to the ability of a plant to maintain good growth on S-limited condition which is known as S efficiency [24].

The results revealed that resistance of wheat species to S deficiency was different even among the different varieties of the same species. Hawkesford [35] also stated that crops have various abilities to respond to S-deficiency stress which is the goal for the genetic improvement of S-utilization efficiency studies. Average S efficiency in bread wheat varieties was 58% and it was 62% for the durum wheat varieties (Table 1 and 2). The difference in S efficiency between durum and bread wheat varieties was significant. Balint et al. [36] indicated significant genotypic variations in growth and sulfur efficiency among 84 canola germplasm which is particularly sensitive to low S supply in soils. The lowest S efficiency value (53%) of bread wheat varieties was obtained for Sultan and Bayraktar while the highest value (68%) was for Seri variety. The lowest S efficiency of durum wheat varieties was 52% for Altintas and the highest value was 78% for Yelken and Selcuklu varieties. The relationship between S concentrations of seeds and the S-efficiency values of durum and bread wheat varieties was not significant (Figure 1). The results showed that factors such as S absorption capacity of species, S use efficiencies and

the rate of S transport in plant other than S concentration of seeds are active in the resistance of durum and bread wheat varieties. Similarly, Barutcular et al. [37] indicated that genotypes, environmental factors and their interactions significantly affects the quality traits of wheat. Therefore, S supply may not always correct the S deficiency due to the effects of agronomic, environmental and economic factors. However, cultivation of S-efficient genotypes may substitute to S fertilizer application in some edaphic environments [24].

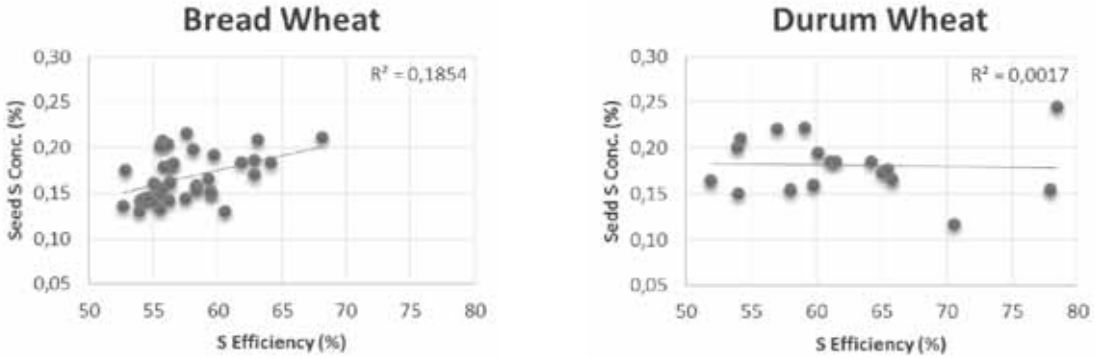

FIGURE 1
Relationship between S concentrations of durum and bread wheat varieties and S efficiency

TABLE 1
Effects of S treatments on dry matter production (g plant^{-1}), S-efficiency and spad value in bread wheat varieties.

Genotypes	Dry Weight (g plant^{-1})			S Efficiency (%)	Increase (%) in dry weight by S	Spad Value		
	S 0	S 100	t-test			S 0	S 100	t-test
Golia	0,55^{bcd}	0,99^{bcd}	**	56	80	22^{abcd}	44^{ab}	**
Bal Atilla	0,63^{fghi}	1,05^{cde}	**	60	68	24^{bcdefgh}	45^{abcd}	*
Dogu 88	0,59^{cdefghı}	1,08^{cdef}	**	55	82	20^{a}	44^{abc}	**
Sultan	0,60^{defghı}	1,14^{efg}	*	53	90	21^{ab}	46^{abcde}	**
Bayraktar	0,60^{defghı}	1,14^{efg}	**	53	89	19^{a}	44^{a}	**
Sonmez	0,56^{bcd}	1,01^{bcd}	*	56	80	23^{bcde}	49^{defghı}	**
Aytin	0,54^{abc}	1,00^{bcd}	**	54	85	25^{cdefghı}	48^{cdefghı}	**
Katea	0,57^{bcde}	0,99^{bcd}	**	58	72	26^{efghıij}	55^{j}	**
Kutluk	0,56^{bcde}	1,04^{bcde}	**	54	84	27^{hıijk}	53^{ij}	**
Yildiz	0,53^{a}	0,98^{abc}	**	54	85	22^{abc}	50^{efghı}	**
Suzen	0,60^{defghı}	1,01^{bcd}	**	59	69	28^{ijk}	51^{ghı}	**
Soyer	0,59^{cdefgh}	0,98^{abc}	*	60	67	24^{bcdefgh}	47^{abcdefg}	**
Dagdas	0,63^{fghi}	0,98^{abc}	**	64	56	28^{ijk}	53^{ij}	**
Atay	0,59^{cdefgh}	1,01^{bcd}	*	58	71	24^{bcdefgh}	50^{fghı}	**
Bagci	0,59^{cdefgh}	1,01^{bcd}	**	58	71	24^{bcdefgh}	48^{cdefghı}	**
Yakar	0,56^{bcde}	0,98^{abc}	**	58	74	25^{cdefghı}	49^{defghı}	**
BDME 00/55	0,60^{defghı}	1,06^{cde}	**	56	77	24^{bcdefg}	52^{hıij}	**
BDME 02/01	0,66^{i}	1,06^{cde}	*	63	59	27^{ghıijk}	49^{defghı}	*
Gerek	0,58^{bcdefgh}	1,05^{cde}	*	55	82	24^{bcdefgh}	47^{abcdefg}	**
Izgi	0,62^{efghı}	1,11d^{efg}	**	56	79	26^{efghıij}	49^{defghı}	**
Aksel	0,60^{defghı}	1,08^{cdef}	**	56	79	25^{cdefghı}	50^{efghı}	**
BDME 0014	0,59^{cdefghı}	1,05^{cde}	**	56	78	23^{bcdef}	49^{defghı}	*
Bezostaja	0,6d^{efghı}	1,07^{cdef}	**	56	78	24^{bcdefgh}	51^{fghı}	**
Demir	0,66^{i}	1,20^{f}	**	56	80	25^{cdefghı}	48^{bcdefgh}	**
Konya	0,65^{ıı}	1,09^{cdefg}	*	60	68	26^{defghıij}	49^{defghı}	**
Kirac	0,50^{a}	0,88^{a}	**	57	77	29^{ijk}	47^{abcdefg}	**
Altay	0,63^{hıi}	1,14^{efg}	**	56	79	25^{cdefghı}	49^{efghı}	**
Goksu	0,58^{bcdefgh}	1,00^{bcd}	*	58	74	25^{cdefghı}	49^{efghı}	**
Pehlivan	0,67i	1,18^{fg}	**	56	77	26^{defghıij}	48^{cdefghı}	**
Kinaci	0,57^{bcdefg}	0,92^{ab}	*	62	62	26^{efghıij}	50^{efghı}	**
Karahan	0,58^{bcdefgh}	1,07^{cdef}	**	55	83	27^{hıijk}	50^{efghı}	**
Seri	0,63^{ghı}	0,92^{ab}	*	68	47	27^{fghıijk}	50^{fghı}	**
Zencirci	0,62^{fghı}	0,99^{bcd}	*	63	59	26^{efghıij}	49^{efghı}	**
Ikizce	0,63^{fghı}	0,99^{bcd}	*	63	58	27^{hıijk}	47^{abcdef}	**
Cetinel	0,65^{ıı}	1,07^{cdef}	**	61	65	30^{k}	50^{fghı}	**
Mean	**0,60**	**1,04**		**58**	**74**	**25**	**49**	

*P<0.05; **P<0.01; ±: Standard Error

TABLE 2
Effect of S treatments on dry matter production (g plant^{-1}), S-Efficiency and spad value in durum wheat varieties.

Genotypes	Dry Weight (g plant^{-1})			S Efficiency (%)	Increase (%) in dry weight by S	Spad Value		
	S 0	S 100	t-test			S 0	S 100	t-test
Gokgol	0,64^{cd}	0,99^{cde}	**	65	54	30^{bcde}	50^{bc}	**
Yelken	0,63^{cd}	0,81^{ab}	ns	78	28	29^{bcde}	53^{cd}	**
Vatan	0,63^{cd}	0,95^{bcde}	**	66	52	28^{abcd}	51^{bcd}	**
Mirzabey	0,60^{cd}	0,93^{abcd}	**	64	56	31^{cdef}	50^{bc}	**
Durnadili	0,72^{d}	1,21^{f}	**	59	69	33^{ef}	51^{bc}	**
Zenit	0,67^{cd}	1,10^{ef}	**	61	64	27^{abc}	49^{b}	**
Altintas	0,57^{abcd}	1,10^{def}	**	52	93	29^{bcde}	53^{bcd}	**
Yilmaz	0,68^{d}	0,96^{cde}	*	71	42	29^{bcde}	51^{bcd}	**
Kiziltan	0,52^{abc}	0,87^{abc}	**	60	66	27^{abcd}	55^{d}	*
C-1252	0,56^{abcd}	0,97^{bcde}	**	58	72	31^{cdef}	53^{cd}	**
Altin	0,57^{abcd}	0,95^{bcde}	**	60	67	31^{def}	58^{e}	**
Meram	0,56^{abcd}	1,04^{de}	**	54	85	24^{a}	51^{bcd}	**
Cakmak	0,62^{cd}	0,95^{abcde}	**	66	53	26^{ab}	51^{bcd}	**
Kunduru	0,66^{cd}	1,08^{def}	**	61	63	30^{bcde}	51^{bcd}	**
Selcuklu	0,61^{cd}	0,78^{a}	**	78	27	38^{g}	52^{bcd}	**
Fırat-93	0,59^{bcd}	1,04^{de}	**	57	75	26^{ab}	45^{a}	**
Balcali2000	0,45^{ab}	0,83^{abc}	**	54	85	28^{abcd}	50^{bc}	**
Kiziltan	0,44^{a}	0,82^{ab}	**	54	85	28^{abcd}	53^{bcd}	*
Mean	**0,60**	**0,96**		**62**	**63**	**29**	**52**	

*P<0.05; **P<0.01; ±: Standard Error

TABLE 3
Effect of S treatments on S and N concentration (%) and N:S ratio bread wheat varieties.

Genotypes	S Concentrations (%)			N Concentrations (%)			N/S Ratios		
	S 0	S 100	t-test	S 0	S 100	t-test	S 0	S 100	t-test
Golia	0,10^{e}	0,44^{k}	**	3,25^{cdefg}	3,74^{defghı}	*	32^{a}	9^{a}	**
Bal Atilla	0,09^{abcd}	0,38^{hıij}	**	3,18^{bcdef}	3,63^{cdefghı}	*	37^{bcdefg}	10^{abcde}	**
Dogu 88	0,09^{abcd}	0,30^{ab}	**	3,41^{efghı}	3,09^{a}	ns	40^{efgh}	10^{cdef}	**
Sultan	0,09^{abcd}	0,32^{abcde}	**	3,85^{jk}	3,28^{abc}	ns	45^{i}	10^{bcdef}	*
Bayraktar	0,09^{abcd}	0,28^{a}	**	2,97^{ab}	3,16^{a}	*	34^{abc}	11^{defg}	**
Sonmez	0,09^{abcd}	0,33^{bcdefgh}	**	3,42^{efghı}	3,63^{bcdefghı}	ns	39^{defgh}	11^{defg}	**
Aytin	0,09^{bcde}	0,32^{abcde}	**	3,69^{ij}	3,45^{abcdef}	ns	42^{ghı}	11^{defg}	**
Katea	0,09^{abcd}	0,36^{defghı}	**	3,11^{abcd}	3,63^{bcdefghı}	ns	35^{abcde}	10^{bcdef}	**
Kutluk	0,09^{cde}	0,39^{ij}	**	3,58^{hıi}	3,36^{abcd}	ns	39^{defgh}	9^{ab}	**
Yildiz	0,09^{cde}	0,37^{fghıi}	**	3,16^{abcde}	3,65^{cdefghıi}	ns	34^{abcd}	10^{abcde}	**
Suzen	0,08^{abc}	0,36^{efghıi}	**	2,99^{ab}	3,65^{cdefghıi}	*	36^{abcdef}	10^{abcde}	**
Soyer	0,09^{cde}	0,31^{abcd}	**	3,58^{hıi}	3,87^{fghıi}	ns	39^{defgh}	12^{gh}	**
Dagdas	0,09^{abcd}	0,32^{abcdef}	**	3,43^{efghı}	4,39^{j}	*	39^{defgh}	14^{h}	*
Atay	0,09^{abcd}	0,37^{fghıi}	**	2,88^{a}	3,77^{efghıi}	*	33^{abc}	10^{bcdef}	**
Bagci	0,09^{cde}	0,32^{abcdefg}	**	3,15^{abcde}	3,43^{abcdef}	ns	35^{abcd}	11^{bcdef}	**
Yakar	0,09^{cde}	0,36^{efghıi}	**	3,39^{efghıi}	3,92^{ghıi}	*	36^{abcdef}	11^{cdef}	**
BDME 00/55	0,09^{abcd}	0,33^{abcdefg}	**	3,45^{fghıi}	3,62^{cdefghıi}	ns	39^{cdefgh}	11^{defg}	**
BDME 02/01	0,08^{abc}	0,34^{bcdefghı}	**	3,02^{abc}	3,69^{cdefghıi}	ns	37^{bcdefg}	11^{cdef}	**
Gerek	0,08^{abc}	0,31^{abcd}	**	3,63^{ıij}	3,50^{abcdefg}	ns	43^{hıi}	11^{defg}	**
Izgi	0,08^{ab}	0,36^{defghıi}	**	3,02^{abc}	3,46^{abcdef}	ns	38^{bcdefgh}	10^{abcd}	**
Aksel	0,09^{bcde}	0,34^{bcdefgh}	**	3,29^{cdefgh}	3,71^{cdefghıi}	ns	37^{abcdef}	11^{defg}	**
BDME 0014	0,10^{de}	0,35^{cdefghı}	**	3,91^{k}	3,63^{cdefghıi}	ns	40^{fghı}	10^{abcde}	**
Bezostaja	0,09^{cde}	0,29^{ab}	**	3,36^{defgh}	3,48^{abcdef}	ns	36^{abcdef}	12^{fgh}	**
Demir	0,09^{abc}	0,30^{abc}	**	2,89^{a}	3,19^{ab}	*	34^{ab}	10^{cdef}	**
Konya	0,10^{de}	0,30^{abc}	**	3,35^{defghı}	3,47^{abcdef}	ns	35^{abcd}	11^{efg}	**
Kirac	0,12^{f}	0,35^{cdefghıi}	*	4,03^{k}	4,07^{ij}	ns	34^{abc}	12^{fgh}	*
Altay	0,08^{abc}	0,31^{abc}	**	2,93^{ab}	3,40^{abcde}	**	34^{abcd}	11^{defg}	**
Goksu	0,09^{bcde}	0,35^{cdefghıi}	**	3,53^{ghıi}	3,97^{hıi}	ns	39^{defgh}	11^{efg}	**
Pehlivan	0,08^{a}	0,31^{abc}	**	3,41^{efghıi}	3,32^{abcd}	ns	45^{ıi}	11^{defg}	**
Kinaci	0,09^{bcde}	0,39^{ıij}	**	3,38^{efghıi}	3,98^{hıi}	*	37^{bcdefg}	10^{bcdef}	**
Karahan	0,10^{cde}	0,37^{ghıi}	**	3,05^{abc}	3,54^{abcdefgh}	*	32^{a}	9^{abcde}	**
Seri	0,09^{cde}	0,42^{jk}	**	3,23^{bcdef}	4,01^{ıij}	*	35^{abcd}	10^{abcde}	**
Zencirci	0,09^{abc}	0,36^{defghıi}	**	2,93^{a}	3,63^{cdefghıi}	**	34^{abcd}	10^{bcdef}	**
Ikizce	0,09^{bcde}	0,42^{jk}	**	3,37^{defghı}	3,83^{fghıi}	ns	37^{bcdefg}	9^{abc}	**
Cetinel	0,09^{cde}	0,33^{abcdefg}	**	3,09^{abcd}	3,52^{abcdefgh}	ns	34^{abcd}	11^{bcdef}	**
Mean	**0,09±0,008**	**0,35±0,004**		**3,31±0,03**	**3,62±0,03**		**37±0,38**	**11±0,13**	

*P<0.05; **P<0.01;±: Standard Error

TABLE 4
Effects of S treatments on S and N concentrations (%) and N:S ratio durum wheat varieties

Genotypes	S Concentrations (%)			N Concentrations (%)			N/S Ratios		
	S 0	S 100	t-Test	S 0	S 100	t-test	S 0	S 100	t-test
Gokgol	0,09^{a}	0,37^{ab}	*	3,56^{a}	3,67^{ab}	ns	40^{cdef}	10^{def}	**
Yelken	0,10^{abcd}	0,43^{cdef}	**	3,69^{ab}	4,18^{bcdef}	ns	36^{abcd}	10de	**
Vatan	0,10^{ab}	0,53^{h}	**	4,24^{cdef}	3,65^{ab}	*	44^{fgh}	7^{a}	**
Mirzabey	0,10^{abc}	0,39^{bc}	**	4,09^{cde}	3,90^{abcde}	ns	41^{cdefg}	10^{def}	**
Durnadili	0,11^{bcd}	0,45efg	**	3,51^{a}	4,33^{def}	*	33^{ab}	10^{cd}	**
Zenit	0,09^{a}	0,36^{ab}	**	3,96^{bc}	3,35^{a}	*	45^{gh}	9de	**
Altintas	0,10^{abc}	0,34^{a}	**	4,52^{f}	3,40^{a}	*	46^{h}	10^{def}	**
Yilmaz	0,12^{cde}	0,42^{cde}	**	4,35^{cdef}	4,30^{def}	ns	37^{abcd}	10^{def}	**
Kiziltan	0,12^{cde}	0,39^{bc}	**	4,50^{f}	4,27^{cdef}	*	38^{bcde}	11^{f}	**
C – 1252	0,10^{abcd}	0,40^{bcd}	**	4,03^{cd}	3,88^{abcde}	ns	40^{cdef}	10de	**
Altin	0,11^{bcd}	0,38^{abc}	**	3,65^{ab}	3,79^{abcd}	ns	34^{ab}	10^{def}	**
Meram	0,10^{abc}	0,39^{abc}	**	4,37^{def}	3,70^{abc}	*	44^{efgh}	10de	**
Cakmak	0,10^{abcd}	0,41^{cde}	*	3,65^{ab}	4,40^{ef}	**	36^{abc}	11^{ef}	**
Kunduru	0,09^{ab}	0,35^{ab}	**	3,67^{ab}	3,72^{abc}	ns	39^{bcde}	11^{ef}	**
Selcuklu	0,13^{f}	0,48^{fg}	**	4,27^{cdef}	4,59^{fg}	ns	32^{a}	10de	**
Firat-93	0,10^{abcd}	0,47^{efg}	**	4,31^{cdef}	3,76^{abcd}	*	41^{defgh}	8^{bc}	**
Balcali2000	0,12^{ef}	0,57^{h}	**	4,60^{f}	4,36^{ef}	ns	38^{bcde}	8^{ab}	**
Kiziltan	0,12^{def}	0,44^{defg}	**	4,43^{ef}	4,53^{f}	ns	38^{bcd}	10^{def}	**
Mean	**0,11**	**0,42**		**4,08**	**3,99**		**39**	**10**	

*P<0.05; **P<0.01;±: Standard Error

The mean dry matter yield of durum wheat was 0.60 g plant^{-1} and the yield increased to 0.96 g plant^{-1} with S100 application. The highest yield increase in durum wheat cultivars were obtained for Altintas (93%), Meram (85%), Kiziltan (85%) and Balcali 2000 (85%). The lowest yield increase was obtained for Selcuklu and Yelken varieties as 27% and 28%, respectively (Table 2). Durnadili variety yielded significantly higher (P<0.01) dry matter with both S0 and S100 applications as compared to the rest of the durum wheat varieties. The increase in dry matter yield of bread wheat varieties with the application of S were higher compared with the durum with varieties (Table 1 and 2). Taureau et al. [38] observed yield increase in wheat with S application at 183 field trials in France. Zhao et al. [39] and Ercoli et al. [40] also reported significant yield increase in durum wheat with the S application.

Under sufficiency of other nutrients and S-deficiency conditions, the chlorophyll concentration of leaves could be accepted as a good indicator of S deficiency in plants [41]. The spad value of leaves significantly increased (P<0.01) with the S application in bread and durum wheat varieties (Table 1 and 2). Zhao et al. [10] observed a decline in spad value whereas spad value increased with the application of adequate S. The average spad value of in S0 was 25 for bread, and it was 29 for durum wheat varieties. The spad value increased up to 49 for bread wheat and 52 for durum wheat varieties with S100 application (Table 1 and 2). Pagani and Echeverria [41] and Szulc et al. [42] also reported that spad value of corn leaves decreased in case of S deficiency and increased with the S fertilization. Sulphur application increased the chlorophyll and protein concentration of tomato leaves [43]. The lowest spad values for bread wheat varieties in S-deficient conditions were obtained for Bayraktar (19), Dogu 88 (20) and Sultan (21) varieties. However, the dry matter yields of these varieties were almost 0.60 g plant^{-1} which is the average yield value for bread wheat. The lack of a yield response despite the appearance of S-deficiency (lower spad values) might be due to the uptake and translocation of S mineralized late in the season symptoms [44].

Shoot S and N concentrations and N:S ratio. The S and N concentrations and N:S ratio of bread and durum wheat varieties have been presented in Table 3 and 4. There was a significant (P<0.01) increase in the total S concentrations in bread and durum wheat cultivars with increasing S applications. The average shoot S concentration of bread wheat varieties was 0.09% with S0 and it was increased to 0.35% with S100 applications (Table 3 and 4). Kour et al. [16] also reported significant increase in S uptake of mustard with 30, 45 and 60 kg S ha^{-1} applications. The highest shoot S concentration (0.12%) among bread wheat varieties was obtained in Kirac variety with S0, whereas dry matter yield of above ground biomass for Kirac variety was the lowest among all. The Golia variety contained the highest shoot S concentration (44%) with the S100 application (Table 3). Shivaya et al. [45] indicated that S concentration in wheat seed with S0 dose was 0.103% and increased to 0.126% when 45 kg S ha^{-1} applied. In durum wheat varieties, the average shoot S concentration in S0 was 0.11%, and the concentration increased to 0.42 with the S100 treatment. The higher S application significantly increased the shoot S and seed S concentrations [33]. The S concentrations in shoot for Selcuklu (0.13%) variety with S0 and Balcali (0.57%) variety with S100 treatments

were significantly different among durum wheat varieties (Table 4).

The effects of S addition on N use efficiency of wheat varieties have not been thoroughly explained. Campbell [46], Mendel [47] and Swamy et al. [48] explained the effects of S fertilization on N use efficiency were consequence of changes in whether recovery efficiency, internal efficiency, or both. The authors concluded that due to the role of S in the nitrate reductase and nitrite reductase involved at N metabolism, the deficiency of S could lower N assimilation of plants. The effects of S application on N concentrations of above ground biomass both for bread and durum wheat varieties were variable, and N concentration was significantly increased or decreased depending on the variety (Table 3 and 4). Inal et al. [12] reported similar results for the changes in N concentration of a durum and a bread wheat variety after the addition of 10, 20, 30 and 40 mg S kg^{-1}. The N concentrations in above ground biomass for twenty eight of bread wheat varieties have slightly increased with the addition of 100 mg S kg^{-1} (Table 3). The increases of N were mostly nonsignificant except in Zencirci and Altay varieties. The average N concentration was 3.31% with S0 and increased to 3.62% with S 100 treatment (Table 3). Whereas, N concentration was slightly decreased in Doğu 88, Sultan, Aytin, Kutluk, Gerek, BDME-0014 and Pehlivan varieties. The N concentrations of durum wheat varieties with S0 doses ranged from 3.51% and 4.60% and the mean concentration was 4.08%. The N concentration of Cakmak variety was significantly increased with the addition of S, whereas N concentration of Meram variety was significantly reduced (Table 4). Salvagiotti et al. [49] indicated that positive interaction between N and S is due to the greater N use efficiency of wheat varieties. Therefore, addition of S increases the N as well as biomass and grain yield in wheat.

The N:S ratio in the above ground biomass of a crop is an important indication of its S requirement particularly for wheat intended for bread making as compared to the other wheat varieties [50]. In this study, N:S ratios of above ground biomass were generally decreased by the S treatments, and increased by increasing the N rate (Table 3 and 4). Bergmann [51] stated that N:S ratio might vary depending on plant species even for the different parts of the same plant. The critical N:S ratio for deficiency in wheat grain was reported as 17:1 [10] whereas the critical N:S value for wheat leaves was 15:1 [18]. The N:S ratio for both bread and durum wheat varieties were greater than the critical threshold value of 15:1. Randall et al. [52] also stated that the ratio of >15 is associated with S deficiency in wheat. Large N:S ratios (>15) were obtained in the S0 treatments for all bread and durum wheat varieties, whereas the values were significantly decreased ($P<0.01$ or $P<0.05$) with S100 mg S kg^{-1} application. The average N:S ratio of bread wheat varieties ranged from 37 (for S0) to 11 (S100 mg S kg^{-1}) and similarly the N:S ratio in durum wheat varieties decreased from 39 to 10 with the addition of 100 mg S kg^{-1} (Table 3 and 4). The good correlation between spad value of wheat leaves and N:S ratio supports the idea that N:S ratio of above ground biomass could be used as an apparent indicator of the S status in the bread and durum wheat varieties.

CONCLUSIONS

The results revealed that S deficiency in wheat varieties can be corrected by fertilization and dry matter yield of bread and wheat varieties increases with the S application. However, responses of bread and durum wheat varieties even for the same plant species significantly differ from each other. Therefore, identification and cultivation of S efficient genotypes as in zinc and nitrogen efficient genotypes could efficiently use the soil S and produce higher yields compared to the non-efficient genotypes.

The increase in yield was affected by N and S metabolism of wheat varieties. The efficiency of bread wheat varieties increased with increased S application. The measurement of leaf spad value in greenhouse conditions reflected the S use efficiency of wheat varieties. The N:S rate of above ground biomass might be used as a reliable parameter to understand the S use status of wheat varieties.

ACKNOWLEDGEMENTS

The authors are grateful to Prof. Dr. Hikmet and Prof. Dr. Selim Eker for their critical reviews and editing of the manuscript.

REFERENCES

[1] Marschner, H. (1997) Sulfur supply, plant growth, and plant composition. In: Marschner, H. (Ed.) Mineral nutrition of higher plants, London: Academic Press, 261-265.

[2] Salvagiotti, F. and Miralles, D.J. (2007) Wheat development as affected by nitrogen and sulfur nutrition. Australian Journal of Agricultural Research, 58, 39-45.

[3] Niewiadomska, A., Barlog, P., Borowiak, K. and Wolna-Maruwka, A. (2015) The effect of sulphur and potassium fertilisation on the nitrogenase and microbial activity in soil under broad bean (Vicia faba L.) cultivation. Fresen. Environ. Bull., 24, 723-732.

[4] Haneklaus, S., Fleckenstein, J. and Schnug, E. (1995) Comparative studies of plant and soil analysis for the sulphur status of oilseed rape and winter wheat. Z. Pflanzenernahr. Bodenkd. 158, 109-111.

[5] Jarvan, M. and Adamson, A. (2005) Effect of sulphur applied as top dressing on yield of winter wheat (Triticum aestivum). Transactions of Estonian Agricultural University, 220, 66-68 (in Estonian, with English abstract).
[6] Salvagiotti, F. and Miralles, D.J. (2008) Radiation interception, biomass production and grain yield as affected by the interaction of nitrogen and sulfur fertilization in wheat. Eur. J. Agron. 28, 282–290.
[7] Mascagni, H.J. Jr., Harrison, S.A. and Padgett, G.B. (2008) Influence of sulfur fertility on wheat yield performance on alluvial and upland soils. Commun. Soil Sci. Plant Anal. 39, 2133–2145.
[8] Pacyna, S. (2005) Bedeutung des Schwefels fur den Ferredoxin- und Lehhamoglobin-Gehalt sowie die Energieversorgung in N2-fixierenden Leguminosen. Bonner Agrikulturchemische Reihe, Bonn (in German); 173 p.
[9] Eriksen, J., Thorup-Kristensen, K. and Askegaard, M. (2004) Plant availability of catch crop sulphur following spring incorporation. J. Plant Nutr. Soil Sci. 167(5), 609–615.
[10] Zhao, F.J., Salmon, S.E., Withers, P.T.A., Monaghan, J.M., Evans, E.J., Shewry, P.R. and McGrath, S.P. (1999) Variation in the bread-making quality and rheological properties of wheat in relation to sulphur nutrition under field conditions. J. Cereal Sci. 30, 19–31.
[11] Jarvan, M., Edesi, L. and Adamson, A. (2009) The effect of sulphur fertilization on yield, quality of protein and baking properties of winter wheat. Agraarteadus (Journal of Agricultural Science), 20, 8-15 (in Estonian, with English summary).
[12] Inal, A., Gunes, A., Alpaslan, M., Adak, M.S., Taban, S. and Eraslan, F. (2006) Diagnosis of sulfur deficiency and effects of sulfur on yield and yield components of wheat grown in Central Anatolia, Turkey. Journal of Plant Nutrition, 26, 1483-498.
[13] Khan, B.A., Haq, I. and Ahmad, E. (2003) Wheat response to sulphur application. Sarhad Journal of Agriculture, 19, 225-228.
[14] Atak, M., Ilhan, E., Erayman, M., Dilbirligi, M., Eren, A.H., Arslan, M. and Celiktas, N. (2015) Identification of SSR and EST markers associated with waterlogging tolerance in bread wheat. Fresen. Environ. Bull., 24(11), 3649-3656.
[15] Girma, K., Mosali, J., Freeman, K.W., Raun, W.R., Martin, K.L. and Thomason, W.E. (2005) Forage and grain yield responses to applied sulfur in winter wheat as influenced by source and rate. Journal of Plant Nutrition, 28, 1541-1553.
[16] Kour, S., Arora, S., Jalali V.K., Bali, A.S. and Gupta, M. (2014) Direct and residual effect of sulphur fertilization on yield, uptake and use efficiency in Indian mustard and succeeding rice crop. Journal of Plant Nutrition, 37, 2291–2301.
[17] Gooding, M.J. and Davies, W.P. (1997) Wheat Production and Utilization. CAB Int., Wallingford, UK.
[18] Blake-Kalff, M.M.A., Zhao, F.J., Hawkesford, M.J. and McGrath, S.P. (2001) Using plant analysis to predict yield losses caused by sulphur deficiency. Ann. Appl. Biol. 138, 123–127.
[19] Karamanos, R.E., Goh, T.B. and Flaten, D.N. (2007) Nitrogen and sulphur fertilizer management for growing canola on sulphur sufficient soils. Can. J. Plant Sci. 87, 201–210.
[20] Janzen, H.H. and Bettany, J.R. (1984) Sulfur nutrition of rapeseed. 1. Influence of fertilizer nitrogen and sulfur rates. Soil Sci. Soc. Am. J. 48, 100-107.
[21] Bailey, L.D. (1986) The sulphur status of eastern Canadian prairie soils: Sulphur response and requirements of alfalfa (*Medicago sativa L.*), rape (*Brassica napus L.*) and barley (*Hordeum vulgare L.*). Can. J. Soil Sci. 66, 209-216.
[22] Salvagiotti, F., Ferraris, G., Quiroga, A., Barraco, M., Vivas, H., Prystupa, P., Echeverria, H. and Boem, F.H.G. (2012) Identifying sulfur deficient fields by using sulfur content; N: S ratio and nutrient stoichiometric relationships in soybean seeds. Field crops research, 135, 107-115.
[23] Gourley, C.J.P., Allan, D.L. and Russelle, M.P. (1994) Plant nutrient efficiency: A comparison of definitions and suggested improvement. Plant and Soil, 158(1), 29-37.
[24] Ahmad, A., Khan, I., Anjum, N.A., Abrol, Y.P. and Iqbal, M. (2005) Role of sulphate transporter systems in sulphur efficiency of mustard genotypes. Plant Science, 169, 842–846.
[25] Bloem, E., Haneklaus, S. and Schnug, E. (2002) Optimization of a method for soil sulphur extraction. Comm. In Soil Sci. And Plant Anal. 33(1-2), 41-51.
[26] Bouyoucous, G.J. (1952) Hydrometer method improved for making particle size at analysis of soil. Argon. J. 54(5), 464-465.
[27] Klute, A., Campbell, G.S., Jackson, R.D., Mortland, M.M. and Nielsen, D.R. (1986) Methods of soil analysis. Part 1. Physical and Mineralogical Methods (Second edition). Madison, Wisconsin USA.
[28] Jackson, M.L. (1964) Soil chemical analysis. Englewood Cliffs, New Jersey.
[29] Schaper, H. and Chacko, E.K. (1991) Relation between Extractable Chlorophyll and Portable Chlorophyll Meter Readings in Leaves of Eight Tropical and Subtropical Fruit-Tree Species. Journal of Plant Physiology, 138(6), 674–677.
[30] Zhao, F.J. and McGrath, S.P. (1994) Soil extractable sulphate and organic sulphur and their

availability to plant. Plant and Soil 164, 243–250.
[31] Bremner, J.M. (1965) Total nitrogen in C.A. Block et al. (ed.) Methods of soil analysis. Part 2. Agronomy 9: 1149-1178. Am. Soc. Of Argony., Inc. Madison, Wisconsin, USA.
[32] Thomas, S.G., Hocking, T.J, Bilsborrow, P.E., Thomas, S.G., Hocking, T.J. and Bilsborrow, P.E. (2003) Effect of sulphur fertilisation on the growth and metabolism of sugar beet grown on soils of differing sulphur status. Field Crops Research 83: 223–235.
[33] Ercoli, L., Lulli, L., Arduini, I., Mariotti, M., Masoni, A. (2011) Durum wheat grain yield and quality as affected by S rate under Mediterranean conditions. Eur. J. Agron. 35, 63–70.
[34] De Bona, F.D., Fedoseyenko, D., Wirén, N. and Monteiro, F.A. (2011) Nitrogen utilization by sulfur-deficient barley plants depends on the nitrogen form. Environmental and Experimental Botany 74: 237– 244.
[35] Hawkesford, M. J. (2000) Plant responses to sulphur deficiency and the genetic manipulation of sulphate transporters to improve S-utilization efficiency. Journal of Experimental Botany, 51(342), 131-138.
[36] Balint, T., Rengel, Z. and Allen, D. (2008) Australian canola germplasm differs in nitrogen and sulfur efficiency. Australian Journal of Agricultural Research,59, 167–174.
[37] Barutcular, C., Yildirim, M., Koc, M., Akinci, C., Tanrikulu, A., El-Sabagh, A., Saneoka, H., Ueda, A., Islam, M.S., Toptas, I., Albayrak, O. and Tanrikulu, A. (2016) Quality traits performance of bread wheat genotypes under drought and heat stress conditions. Fresenius Environmental Bulletin, 25(10), 1-7.
[38] Taureau, J.C., Thevenet, G., Bordeaux, J. L. and De Froberville, G. (1987) Reponse des cultures a la fertilisation soufree. Perspectives Agricoles 111, 22-44.
[39] Zhao, F.J., McGrath, S.P., Blake-Kalff, M.M.A., Link, A. and Tucker, M. (2002) Crop responses to sulphur fertilization in Europe. The International Fertiliser Society, Proceedings 504.
[40] Ercoli, L., Arduini, I., Mariotti, M., Lulli, L. and Masoni, A. (2012) Management of sulphur fertiliser to improve durum wheat production and minimise S leaching. Europ. J. Agronomy 38: 74– 82.
[41] Pagani, A. and Echeverria, H.E. (2012) Influence of sulfur deficiency on chlorophyll-meter readings of corn leaves. J. Plant Nutr. Soil Sci., 175: 604–613.
[42] Szulc, P., Bocianowski, J. and Rybus-Zajac, M. (2012) The effect of soil supplementation with nitrogen and elemental sulphur on chlorophyll content and grain yield of maize (zea mays L.). Zemdirbyste=Agriculture, 99(3), 247-254.
[43] Marschner, H. (1995) Mineral nutrition of higher plants. Academic Press, London, p. 45.
[44] Withers, P.J.A. and Sinclair, A.H. (1994) Sulphur Nutrition of Cereals in the UK: Effects on Yield and Grain Quality, HGCA Research Review No. 30. London: Home- Grown Cereals Authority.
[45] Shivaya, Y.S., Prasada, R. and Pala, M. (2014) Effect of Levels and Sources of Sulfur on Yield, Sulfur and Nitrogen Concentration and Uptake and S-Use Efficiency in Basmati Rice. Communications in Soil Science and Plant Analysis, 45, 2468–2479.
[46] Campbell, W.H. (1999) Nitrate reductase structure, function and regulation: bridging the gap between biochemistry and physiology. Annual Review of Plant Physiology and Plant Molecular Biology 50, 277–303.
[47] Mendel, R. (1997) Molybdenum cofactor of higher plants: biosynthesis and molecular biology. Planta 203, 399–405.
[48] Swamy, U., Wang, M., Tripathy, J.N., Kim, S.K., Hirasawa, M., Knaff, D.B. and Allen, J.P. (2005) Structure of spinach nitrite reductase: implications for multi-electron reactions by the iron–sulfur: siroheme cofactor. Biochemistry 44, 16054–16063.
[49] Salvagiotti, F., Castellarin, J.M., Miralles, D.J. and Pedrol, H.M. (2009) Sulfur fertilization improves nitrogen use efficiency in wheat by increasing nitrogen uptake. Field Crops Research, 113(2), 170-177.
[50] Griffiths, M.W., Kettlewell, P.S. and Hocking, T.J. (1995) Effects of foliar-applied sulphur and nitrogen on grain growth, grain sulphur and nitrogen concentrations and yield of winter wheat. The Journal of Agricultural Science, 125(3), 331-339.
[51] Bergmann, W. (1992) Nutritional disorders of plants: Developments, Visual and analytical diagnosis. VCH publishers Inc., 303 N. W. 12th Avenue, Deerfield, Beach, Florida 33444-1705. USA.
[52] Randall, P.J., Spencer, K. and Freney, J.R. (1981) Sulfur and nitrogen fertiliser effects on wheat. I. Concentrations of sulfur and nitrogen and the nitrogen to sulfur ratio in grain, in relation to the yield response. Aust. J. Agric. Res. 32, 203–212.

Received: **27.02.2017**
Accepted: **27.07.2017**

CORRESPONDING AUTHOR

Halil Erdem
Gaziosmanpasa University,
Faculty of Agriculture,
Soil Science and Plant Nutrition Department,
Tokat – TURKEY

E-mail: erdemh@hotmail.com

© by PSP Volume 26 – No. 10/2017 pages 5900-5910 Fresenius Environmental Bulletin

RAW KENAF BAST FIBER AS A GREEN BIOADSORBENT FOR CATIONIC AND ANIONIC DYES

Ridwan Shamsudin[1], Azlan Kamari[2,*], Hanisom Abdullah[1]

[1]Department of Biology, Faculty of Science and Mathematics, Universiti Pendidikan Sultan Idris, 35900, Tanjong Malim, Perak, Malaysia
[2]Department of Chemistry, Faculty of Science and Mathematics, Universiti Pendidikan Sultan Idris, 35900, Tanjong Malim, Perak, Malaysia

ABSTRACT

The overall aim of this study was to evaluate the effectiveness of raw Kenaf Bast Fiber (KBF) to remove methylene blue (MB), rhodamine B (Rh. B), congo red (CR) and methyl orange (MO) dyes from aqueous solutions and simulated wastewater using batch adsorption system. The effects of solution pH, initial dye concentration and adsorbent dosage on removal of dyes were investigated. The adsorption capacity of raw KBF for MB, Rh. B, CR and MO was greatly influenced by initial dye concentration and amount of adsorbent dosage. The best pH value for adsorption of CR, MO and Rh. B was recorded at pH 2.0, while the maximum adsorption for MB was obtained at pH 6.0. The equilibrium data were analyzed by the Langmuir and Freundlich isotherm models. The adsorption of cationic and anionic dyes onto raw KBF was best described by the Freundlich isotherm model. Scanning Electron Microscope (SEM) and Fourier Transform Infrared Spectrometer (FTIR) were used to characterize raw KBF. Interaction with dyes has changed the surface morphology and shifted the wavenumbers of functional groups present in raw KBF. In multi-dye system, MB was the dye most removed by raw KBF. Overall, results from this study highlight the great potential of raw KBF as a natural bioadsorbent for the removal of toxic dyes in wastewater.

KEYWORDS:
adsorption, dyes, kenaf bast fiber, wastewater treatment

INTRODUCTION

Dyes are defined as aromatic organic compounds that possess unique abilities to colorize other substances [1]. Dyes have very complex structure and therefore they are difficult to degrade biologically in the environment [2]. Generally, colored wastewater originates from many industries such as textile, cosmetics, plastics, food processing, carpets, rubbers, dye manufacturing, paper and pulp, tannery and paint [3]. It has been estimated that the global wastewater discharged from textile industries can reach more than 1 million liter annually [4]. Colored wastewater is easily detected especially in aquatic system because it is highly visible even at very low concentrations [5]. Toor et al. [6] stated that even at 0.005 mg/L dye is already visible for human eyes.

Untreated colored wastewater may affect the aquatic communities by reducing the photosynthetic activity [7]. The presence of dyes will reduce the penetration of sunlight into aquatic ecosystem [8]. In addition, dyes can also enter the food web and cause adverse effects to human, if consumed [9]. It is clear that dyes could impose an acute and/or chronic effect towards human, animals and plants if discharged into water bodies. Therefore, preventive actions must be taken to overcome the aforementioned issues.

Adsorption is known as an effective technique to remove contaminants such as dyes and heavy metals in wastewater [10]. Activated carbon has been extensively used as an adsorbent for adsorption in wastewater treatment [4]. This scenario can be related to its high surface area and excellent adsorption capacity [11]. However, the application of activated carbon in wastewater treatment as an adsorbent has several drawbacks especially in large scale treatment system due to its high cost. Besides, the process to alienate contaminants from the exhausted activated carbon and the regeneration of used activated carbon are technically challenging and add up more to a treatment plant operational cost [4,11]. Therefore, activated carbon may not be an economic adsorbent especially for undeveloped and developing countries that practice small-scale wastewater treatment facilities.

In recent years, the integration of natural materials particularly lignocellulosic materials in many sectors has attracted environmental researchers' attention. Within Malaysia context, kenaf fiber is one of the lignocellulosic materials planted massively in east cost of peninsular Malaysia. Saba et al. [12] mentioned that kenaf is a cost-effective fiber plant and has environmental friendly properties. Like other natural fibers, kenaf is classified as renewable energy and do not have negative impacts on the environment due to its ability to self-degrade[13].

To the best of our knowledge, data on the adsorption and characterization studies of raw KBF in the removal of dyes have not been published. In the last 15 years, research studies on kenaf fiber have focused on kenaf core fiber (KCF) and modified kenaf fiber (MKF). As discussed by Ong et al. [14], there are only several studies have compared the removal

of both cationic and anionic dyes by certain adsorbents. Hence, in the present study the adsorption behavior of cationic (MB and Rh. B) and anionic (Cr and MO) dyes onto raw KBF was investigated in both single- and multi-dye batch experiments.

MATERIALS AND METHODS

Preparation of adsorbent. Raw KBF, which was obtained from the outer part of kenaf stalks (MR grade), was used in this study. The raw KBF was supplied by Malaysian National Kenaf and Tobacco Board, Kubang Kerian, Kelantan. The raw KBF biomass was ground using a laboratory mill and washed several times using distilled water followed by deionized water. The material was dried in an oven at 60 °C for 7 days. The dried KBF was then sieved using an American Society for Testing and Materials (ASTM) standard to obtain uniform size particles of 1.0 mm before being used.

Preparation of stock solution. Methyl orange (MO) and rhodamine B (Rh. B) were purchased from Bendosen Laboratory Chemicals, while congo red (CR) and methylene blue (MB) were acquired from Merck Chemicals. Dye solutions (10 mg/L) were prepared by adding specific amount of dyes powder into deionized water. These stocks solutions were then diluted into desired concentrations prior to use.

Batch adsorption studies. The fundamental adsorption studies for MB, Rh. B, CR and MO were carried out by batch experiments. Several experimental parameters, namely solution pH, initial dye concentration and adsorbent dosage were studied in order to evaluate their effects on anionic and cationic dyes uptake by raw KBF. In this research, the effect of solution pH was studied in the range between 2.0 to 8.0 as suggested by Santhi et al. [15]. pH 8.0 was chosen as the highest pH value based on results obtained from preliminary study of which there was no significant effect in dyes adsorption at solution pH higher than 8.0. To obtain the desired pH value, 0.05 mol/L of HCl and 0.05 mol/L of NaOH were added to dyes solution. The pH was measured using a Thermo Scientific Orion 2-Star pH meter. The effect of initial dye concentration was studied at the concentrations of 2.5, 5.0, 7.5, 10.0 and 20.0 mg/L, while the effect of adsorbent dosage was studied at the rates of 0.025, 0.050, 0.100 and 0.200 g.

The adsorption capacity of MO and MB onto raw KBF at equilibrium was calculated using equation (1):

$$q_e = \left(\frac{C_o - C_e}{W} \right) V \quad (1)$$

where q_e is the amount of dye adsorbed by raw KBF (mg/g), C_o is the initial concentration of dye (mg/L), C_e is the equilibrium concentration of dye (mg/L), W is the weight of the raw KBF (g), and V is the volume of dye solution (L). Meanwhile, the percentage of removal (%) was computed using equation (2):

$$\text{Removal (\%)} = \left(\frac{C_o - C_e}{C_o} \right) \times 100 \quad (2)$$

On the other hand, three experimental conditions namely volume of dye solution (50 mL), time of contact (60 mins) and rotation speed (100 rpm) were set at constant. The dye solutions were agitated using a Protech 720 Orbital Shaker. Dye free blanks were used as controls. After adsorption experiment, the dye solutions were filtered through Filtre Fioroni (125 mm) filter paper. The residual dye concentration was measured using an Agilent Cary 60 UV-Visible Spectrophotometer. Experiments were conducted in triplicates and average values (with respective standard error of average) were reported.

Effectiveness study. The effectiveness of raw KBF to remove dyes was further evaluated in multi-dye system using a simulated dye wastewater. For this study, 0.1 g of raw KBF adsorbent was added into 50 mL of 5 mg/L multi-dye solution containing MB, Rh. B, CR and MO. The adsorption studies were conducted at pH 2.0 and 6.0, optimum pH values obtained from single-dye adsorption system.

Characterization studies. Another focus of the present study was on the characteristics of raw KBF. Several analytical techniques such as Scanning Electron Microscopy (SEM) and Fourier Transform Infrared Spectroscopy (FTIR) were applied to investigate the physical and chemical characteristics of raw KBF, before and after interaction with the contaminants. Meanwhile, surface area and pore diameter of raw KBF was analyzed by Brunauer-Emmett-Teller (BET) and Barrett, Joyner and Halenda (BJH) techniques, respectively.

MATERIALS AND METHODS

Adsorption studies. Effect of solution pH. In dyes adsorption, the solution pH plays a very critical role because the varies in pH could altered the properties of the adsorbents and the structure of the dyes [16,17]. The results for effect of solution pH on the adsorption capacity and removal percentage of MB, Rh. B, CR and MO by raw KBF are displayed in Fig. 1.

From Fig. 1(a), the adsorption of CR and MO onto raw KBF was performed well at pH 2.0. The adsorption capacity and the removal percentage of both dyes were at the highest at pH 2.0 and decreased when the pH was adjusted to a higher pH value. At pH 2.0, the adsorption capacity of raw KBF for CR and MO was 2.45 and 0.71 mg/g, meanwhile the removal percentage was 98.55 and 28.54 %, respectively. This observation is similar to the reports by

Elmoubarki et al. [16], of which the adsorption of anionic dyes was optimum at low pH values. Moreover, the optimum pH of CR removal at pH 2.0 is in agreement with Reddy et al. [18] that used Jujube seed as an adsorbent. The trend for adsorption capacity could be related to the ionization process that occurred at low pH values which has contributed to strong electrostatic attraction between ionized functional groups of the adsorbent and anionic dyes. On the other hand, when the solution pH increased, the adsorption system has more negatively charged sites consequently anionic dye uptake was diminished due to electrostatic repulsion [19,20].

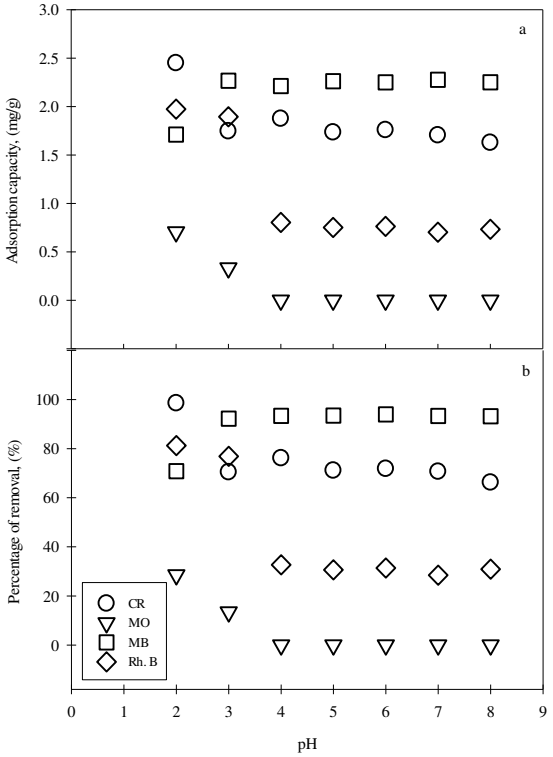

FIGURE 1
Effect of solution pH on the adsorption capacity (a) and percentage of removal (b) of CR, MO, MB and Rh. B by raw KBF

In the case of MB, the adsorption capacity and removal of MB increased as the pH of the solution increased. When the pH increased from pH 2.0 to 3.0, the adsorption capacity and the percentage of removal increased from 1.71 to 2.27 mg/g and 70.87 to 92.22 %, respectively. Previous studies suggested that at low pH, more H^+ and H_3O^+ ions are available and directly increased the positive charge density on the adsorbent surface that consequently reduced the dyes uptake [21]. Apparently, an excess of H^+ ions and MB cations competed for active sites on the surface of raw KBF. This competition creates electrostatic repulsion between positive charged of MB cations and positively chargedsurface that significantly decreased the dye uptake onto the adsorbent. At pH higher than pH 3.0 however, the surface of the adsorbent was deprotonated and therefore favorable for MB binding [22].There was no significant effect in MB uptake as the pH increased to pH 8.0. Similar trends were observed by Lim et al. [23] and Tan et al. [24] that have used breadnut peel and activated maize cob powder to remove cationic dyes.

In contrast, another cationic dye namely Rh. B exhibited a different adsorption behavior onto raw KBF. The uptake of Rh. B by raw KBF was higher within pH 2.0-3.0 and started to decrease at pH 4.0 and remained constant thereafter. The adsorption capacity decreased from 1.97 to 0.80 mg/g (Fig. 1(a), while the removal percentage decreased from 81.27 to 32.67 % when the pH was altered from pH 2.0 to 4.0 (Fig. 1(b)). This scenario can be related to the formation of different structure of Rh. B in aqueous solution particularly at different pH values. As discussed by Motahari et al. [25] and Li et al. [26], Rh. B exists as small cations at pH lower than 4.0 while at higher pH Rh. B exists as larger zwitterions. This statements explained the effect of solution pH in the removal of Rh. B onto raw KBF of which at lower pH values, the smaller formed of cationic Rh. B diffused easily onto KBF while at higher pH values, the adsorption capacity and removal efficiency decreased due to inaccessibility of larger zwitterionic Rh. B to enter the pore of raw KBF.

As a conclusion, both anionic (CR and MO) and cationic dyes (MB and Rh. B) dyes had shown optimum performance at different solution pH. Generally, the highest uptake of MB occurred at pH near to neutral (alkaline pH) and the removal of CR, MO and Rh. B by raw KBF was best at very acidic solution. This phenomenon was greatly influenced by the presence of ions in the aqueous solution and the molecular structure of the dyes.

Effect of initial dye concentration. The adsorption capacity and removal efficiency of an adsorbent is also influenced by initial concentration of contaminants [4,27]. The effect of varying initial dye concentration on the adsorption capacity and the percentage of dyes removal by raw KBF are shown in Fig. 2. From Fig. 2(a) The adsorption capacities for CR, MO, MB and Rh. B were increased from 1.22 to 9.27, 0.09 to 1.28, 1.11 to 9.52 and 1.00 to 3.851 mg/g, respectively as the initial dye concentration was increased from the lowest (2.5 mg/L) to the highest (20 mg/L) initial concentration. The increase in adsorption capacity for both anionic and cationic dyes at higher concentrations can be related to the stronger driving force at higher initial dye concentrations which is needed to overcome the resistance of mass transfer towards the removal of dyes molecule between aqueous phase and solid phase [28]. This situation can also be described as at higher initial dyes concentrations, the interactions between dyes and the adsorbent became stronger that leads to higher adsorption capacity [2].

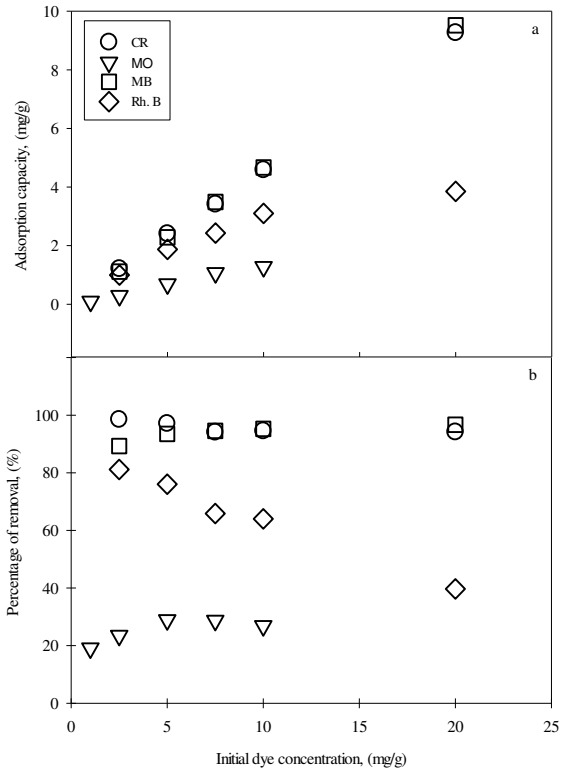

FIGURE 2
Effect of initial dye concentration on the adsorption capacity (a) and percentage of removal (b) of CR, MO, MB and Rh. B by raw KBF

However, the removal percentage for dyes showed different trends when the initial dyes concentration was increased. As presented in Fig. 2(b), the removal of CR and MB was not really affected of which CR removal decreased slightly from 98.52 to 94.20 %, while removal percentage of MB increased slightly from 89.29 to 96.70 %. This observation can be explained by the fact that the available active sites on raw KBF provided was sufficient enough for CR and MB adsorption even at higher concentration (20 mg/L). A slight increment in MB removal percentage was also reported by Gong et al. [8] when granular kohlrabi peel was used as an adsorbent for MB. In the case of MO adsorption, removal percentage was increased slightly from 19.07 to 26.84 % as the initial metal concentration increased from 1.0 to 10.0 mg/L. A different trend was obtained for Rh.B. The removal of Rh. B decreased from 81.16 to 39.68 %. The decrease in Rh. B removal percentage delineates the limitation of adsorbent active sites at higher Rh. B concentration as suggested by Mahmoud et al. [2]. This phenomenon also can be associated to the competition among the Rh. B molecules for the fixed adsorption sites [29].

Overall, the adsorption capacity and the removal percentage of investigated dyes strongly influenced by the initial dyes concentration. This was because there are significant relationships between initial dye concentration and number of active sites available on the adsorbent.

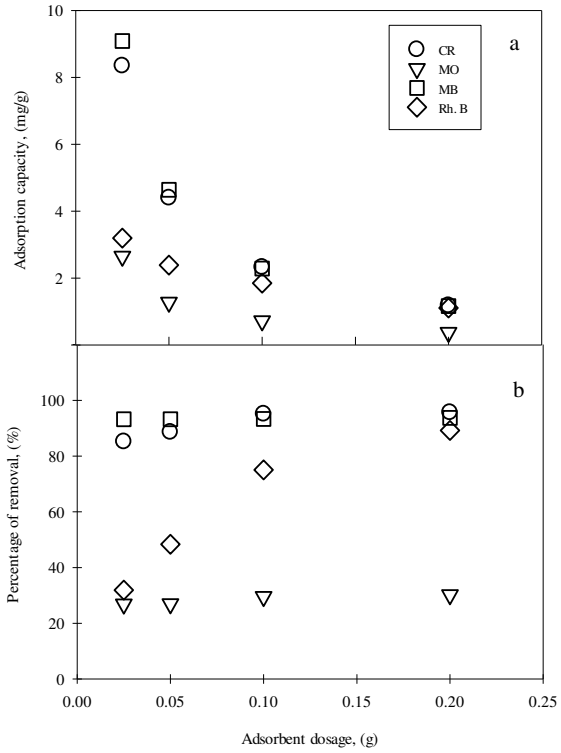

FIGURE 3
Effect of adsorbent dosage on the adsorption capacity (a) and percentage of removal (b) of CR, MO, MB and Rh. B by raw KBF

Effect of adsorbent dosage. Adsorbent dosage is another critical parameter that should be considered in designing an effective adsorption system. Firstly, the amount of adsorbent dosage is directly proportional towards the availability of the active binding sites. Secondly, the amount of adsorbent used gives direct effect on wastewater treatment plant operational cost.

As shown in Fig. 3(a), the adsorption capacity for all dyes increased when the adsorbent dosage was reduced from 0.200 to 0.025 g. The adsorption capacity of CR, MO, MB and Rh. B increased from 1.18 to 8.35, 0.37 to 2.65, 1.16 to 9.09 and 1.11 to 3.20 mg/g, respectively. This finding can be explained by the fact that at high adsorbent dose, the active sites available on the adsorbent became unsaturated [21,30]. Therefore, these active sites might not be fully utilized for dyes adsorption [31].

In terms of removal percentage, the uptakes of MB kept constant at range of 93.0 % while the uptake of CR, MO and Rh. B increased from 85.20 to 95.66, 26.87 to 30.22 and 31.91 to 89.20 % as the raw KBF dosage was increased from 0.025 to 0.200 g, respectively. The behavior of MB removal could be due to amount of raw KBF at 0.025 g might not the minimum dosage for the removal of MB at these experimental conditions. Meanwhile, the trends of removal percentage for CR, MO and Rh. B could be explained in terms of at higher dose, more adsorption sites are readily available for dyes binding.

Adsorption isotherms. Isotherm studies described the relationship between the quantity of solutes adsorbed and the concentration of the solute when equilibrium was reached [32]. Furthermore, adsorption isotherms provide information on how adsorbent and adsorbate interact to each other [33,34]. In this study, dye equilibrium adsorption isotherms were expressed by means of the Langmuir and Freundlich isotherm models.

Langmuir isotherm model known as an important and most applied model that assumes contaminants form a monolayer on the adsorbents [35]. This model describes maximum adsorption occurs at fixed homogenous site that formed saturated monolayer at the exterior surface of the adsorbent [36], where one molecule of adsorbate bound to one specific active site in the surface of adsorbent. In addition, Langmuir isotherm also assumes that all the adsorption sites of the adsorbent are exact and energetically equivalent [29]. The linear form of the Langmuir isotherm can be expressed as equation (3) [37]:

$$\frac{C_e}{q_e}=\frac{C_e}{Q}+\frac{1}{Qb} \qquad (3)$$

where $C_e$is the equilibrium concentration of dye (mg/L),q_e is the amount of dye adsorbed per unit weight of adsorbent at equilibrium concentration (mg/g), Q is the maximum adsorption at monolayer (mg/g), and b is the Langmuir constant related to the affinity of binding sites (mL/mg) as well as a measurement of the energy of adsorption. The values of Q and b can be calculated from linear plot of C_e/q_e against C_e.

As forFreundlich isotherm model, the adsorption process could occur at any sites of the adsorbent due to randomly distribution of active sites and their energies [38]. Freundlich isotherm model is an empirical equation based on the adsorption at multilayer heterogeneous surface [39]. The linear form of the Freundlich isotherm model is given as equation (4) [40]:

$$\log q_e = \log K_F + \frac{1}{n}\log C_e \qquad (4)$$

where n is the Freundlich constant that representing adsorption intensity and K_F (mg/g) related to the adsorption capacity. The linear plot of log q_e against log C_e gives values of n and K_F.

The equilibrium adsorption data of MB, Rh. B, CR and MO onto raw KBF were better fitted by Freundlich compared to Langmuir isotherm model. Therefore, the maximum adsorption capacity was expressed based on Freundlich isotherm model (K_F) as depicted in Table 1. Another important parameter that should be considered in adsorption study is separation factor, (R_L). This dimensionless constant was derived from the Langmuir isotherm model and can be used to evaluate the suitability and the effectiveness of an adsorbent for decontamination of effluent [27]. The separation factor, (R_L) could be expressed as equation (5) [41]:

$$R_L = \frac{1}{1+bC_o} \qquad (5)$$

where C_o is the initial concentration of dye (mg/L) and b is the Langmuir constant (L/mg). Based on R_L values the isotherm shape of an adsorption process can be categorized into four systems [41]: (1) $R_L = 0$ (irreversible), (2) $0 < R_L < 1$ (favorable), (3) $R_L = 1$(Linear) and (4) $R_L > 1$(unfavorable).

The R_L values calculated at different concentrations of CR, MO, MB and Rh. B lie between 0 and 1 suggested that the adsorption of dyes studied onto raw KBF was favorable. The applicability of raw KBF for dye removal was further evaluated in terms of Freundlich isotherm constant (n) values. The n values obtained were in the range of 1 to 10 suggesting that the removal of dyes by raw KBF was favorable. Meanwhile, the low value of b computed from the Langmuir equation reflects strong affinity of raw KBF towards dyes.As presented in Table 2, the adsorption capacities of raw KBF for cationic and anionic dyes studied were comparable to other selected low-cost adsorbents.

Effectiveness study. It is known that real wastewater contains a number of toxic contaminants, not a single contaminant. Therefore in this study adsorption experiments were also performed in multi-dye systems in order to examine the ability of raw KBF to treat wastewater. The results for dyes uptake by raw KBF in simulated wastewater at pH 2.0 and pH 6.0 are shown in Table 3.

TABLE 1
Freundlich and Langmuir isotherm constants for adsorption of CR, MO, MB and Rh. B onto raw KBF

Dyes	Freundlich				Langmuir		
	K_F (mg/g)	1/n	n	R^2	Q_{max} (mg/g)	b (L/mg)	R^2
CR	6.83	0.54	1.84	0.9463	13.16	1.31	0.6044
MO	7.76	1.22	0.82	0.9910	2.43	0.05	0.5343
MB	22.48	2.08	0.48	0.9985	3.20	1.20	0.8587
Rh.B	1.57	0.61	1.65	0.9738	4.38	0.61	0.9966

TABLE 2
Comparison of maximum adsorption capacity estimated for dyes from Freundlich isotherm model for selected adsorbents

Adsorbents	K_F				Reference
	CR	MO	MB	Rh. B	
Kenaf bast fiber	6.83	7.76	22.48	1.57	Present study
Acid treated kenaf fiber char	-	-	10.88	-	[2]
Bagasse fly ash	8.16	-	-	-	[42]
Banana peels	0.05	1.73	1.34	0.39	[43]
Orange peels	0.65	2.20	1.75	1.01	
Berrechid raw clay	-	0.11	19.96	-	[16]
Safi raw clay	-	0.29	37.03	-	
Bottom ash	-	0.338	-	-	[44]
De-oiled soya	-	3.16	-	-	
Cashew nut shell	1.36	-	-	-	[45]
Chemically treated *Acacia nilotica* leaf	-	-	-	1.97	[15]
Coir pith carbon	3.82	-	-	-	[46]
Date palm leaves	-	-	2.03	-	[47]
Garlic peel	-	-	7.88	-	[48]
Luffa cylindrica fiber	-	-	16.00	-	[49]
Meranti sawdust	-	-	12.14	-	[50]
Peanut husk	-	-	16.65	-	[51]
Peanut shell	0.11	-	-	-	[52]
Raw *Posidonia oceanica* fiber	-	-	1.20	-	[53]
Spent tea leaves	-	-	6.43	-	[54]
Sugarcane bagasse	-	-	3.70	-	[55]
Tamarind fruit shell	3.48	-	-	-	[18]
Yellow passion fruit shell	-	-	0.40	-	[56]

TABLE 3
Single- and multi-dye system at pH 2.0 and pH 6.0

Dyes	Single-dye system		Multi-dye system	
	Adsorption capacity, Q (mg/g)	Removal efficiency (%)	Adsorption capacity, Q (mg/g)	Removal efficiency (%)
Solution pH 2.0				
CR	2.449	98.55	0	0
MO	0.705	28.54	0.420	16.95
MB	1.712	70.87	2.382	96.26
Rh. B	1.974	81.27	1.058	42.75
Solution pH 6.0				
CR	1.758	71.83	0	0
MO	0	0	0	0
MB	2.250	93.96	2.374	100
Rh. B	0.763	31.39	0.940	39.59

At both solution pH values, the adsorption of MB was higher in multi-dye as compared to in single-dye system. On the other hand, CR is the most affected dyes in multi-dye system in where the removal of CR was zero at both pH solutions studied. The competition between CR, MO, MB and Rh. B has resulted in a very low anionic dyes (CR and MO) uptake by raw KBF. Higher molecular weight of CR (696.68 g/mol) as compared to MB (319.86 g/mol) and Rh. B (479.02 g/mol) also one of the relevant factors that hinder CR uptake by raw KBF. In addition, the greater molecule size of CR as compared to other dyes has reduced the affinity of raw KBF towards CR. As a result, no CR adsorption was observed in the present study. In the case of MO and Rh. B, the adsorption of both dyes decreased in multi-dye system. Specifically, the removal of Rh. B decreased significantly in multi-dye system at both pH values. Meanwhile, the adsorption of MO was only occurred at pH 2.0 due to MO characteristics as an anionic dye. Generally, it can be concluded that the reduction of MO and Rh. B uptake in multi-dye system was strongly influenced by the competition effect between molecules of Rh. B, MB, CR and MO for binding site on KBF.

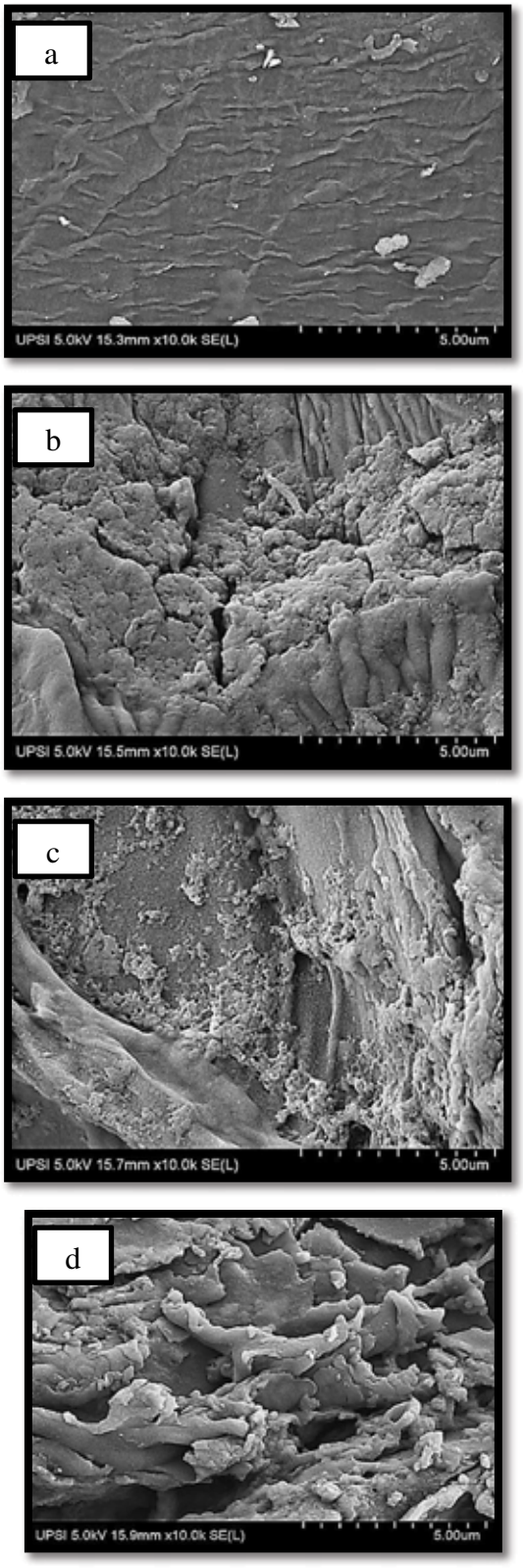

FIGURE 4
SEM micrograph images of raw KBF before adsorption (a) and after adsorption of CR (b), MO (c), MB (d) and Rh. B (e)

Characterization study. Surface area and pore diameter analyses. The BET surface area and average pore diameter of raw KBF were determined as 2.08 m^2/g and 1.17 Å, respectively. It is interesting to note that the BET surface area of raw KBF was higher than coconut shell (0.40 m^2/g) [42], sawdust of beech (1.08 m^2/g), linden (1.22 m^2/g) and poplar (0.89 m^2/g) [43], as well as modified chitosan beads (0.27 m^2/g) [44]. Meanwhile, raw KBF is categorized as micropores based on the guideline set by International Union of Pure and Applied Chemistry (IUPAC) for total porosity classification.

SEM analysis. SEM images for raw KBF after interaction with cationic and anionic dyes are shown in Fig. 4. The surface of raw KBF upon adsorption of CR and MO dyes did not change significantly, where the groove texture of raw KBF (Fig. 4(a)) still could be clearly seen (Figs. 4(b) and 4(c). This observation supports the low anionic dyes adsorption onto raw KBF as reported earlier in adsorption study. On the other hand the surface morphology of raw KBF formed lump-like structure following MB adsorption (Fig. 4(d)), meanwhile interaction with Rh. B turned a groove texture of KBF into a bean-like texture (Fig. 4(e)).

FTIR analysis. Following dyes adsorption, there were insignificant changes in the wavenumbers of raw KBF as shown in Fig. 5. The data indicated that possible similar mechanisms for dyes uptake by raw KBF. For example, the absorption bands of hydroxyl group shifted from 3344 cm^{-1} to 3342 cm^{-1} for CR and 3390 cm^{-1} for MO. Meanwhile, MB and Rh. B had similar wavenumbers observed at 3339 cm^{-1}. At the same time, the absorption intensity was changed as well. In addition, N-H binding vibration that represents amine group shifted to 1645 cm^{-1}, 1640 cm^{-1}, 1634 cm^{-1} and 1645 cm^{-1} after binding with CR, MO, MB and Rh. B, respectively. The wavenumbers changed for both functional groups indicated their involvement in dyes uptake. On the other hand, the wavenumbers for carboxylic groups exhibited insignificant change, which consequently

suggest that carboxylic functional groups may not involve directly in dye adsorption. In addition, the small changes in wavenumbers after the interaction of CR and MO can be related to the lower adsorption capacity of this dye onto raw KBF. In conclusion, it can be suggested that the main functional groups involved in dyes uptake by KBF were hydroxyl and amine groups.

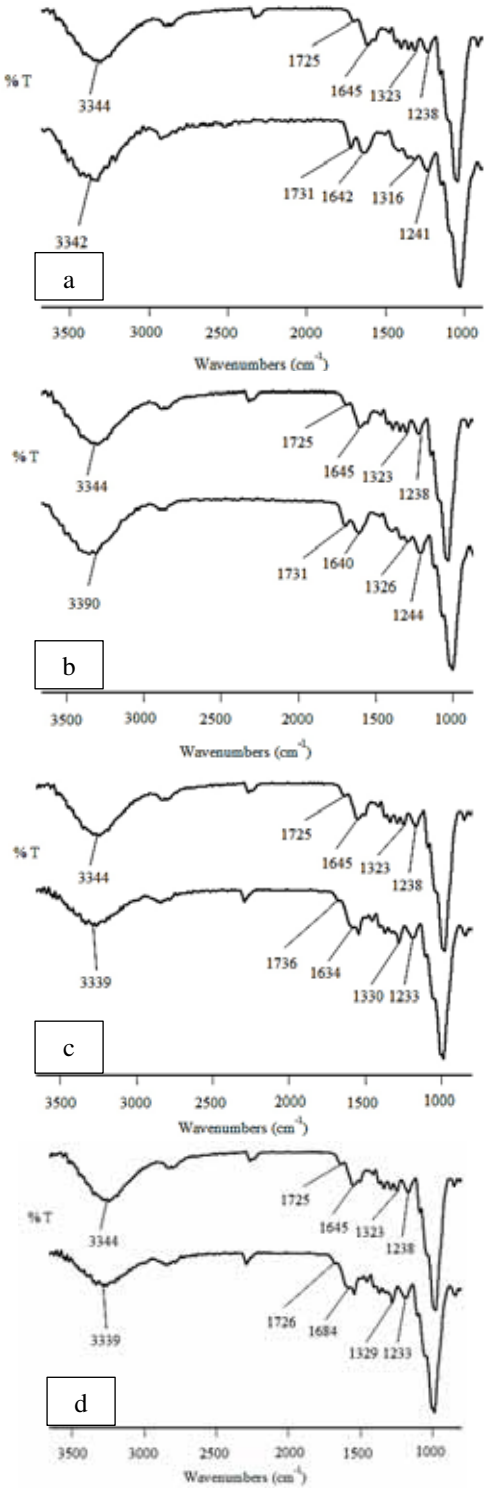

FIGURE 5
The FTIR spectra of raw KBF before adsorption (upper line) and after interaction with CR (a), MO (b), MB (c) and Rh. B (d)

CONCLUSION

Overall, results from this study highlight excellent capacity of raw KBF to adsorb CR, MO, MB and Rh. B in specific experimental conditions. The application of raw KBF to remove anionic dyes was best performed at low pH values, while the removal of cationic dyes was maximum in basic media. The maximum adsorption capacity based on Freundlich isotherm model indicated that raw KBF has great adsorption capacity as compared to other natural adsorbents. Kenaf is cultivated and available in large quantities at low-cost especially in Asian countries. It has great potential to be an alternative candidate to expensive activated carbon for wastewater treatment in developing countries.

ACKNOWLEDGEMENTS

The authors would like to Mr. Bisyr Asfar Ahmad Bakhtiar, Mr. Mohd Zurin Mahmood, Mr. Ibrahim Saidin and Mr. Hashimi Ma'ani for their technical assistance.

REFERENCES

[1] Bhattacharyya, R. and Ray, S.K. (2015). Removal of congo red and methyl violet from water using nano clay filled composite hydrogels of poly acrylic acid and polyethylene glycol. Chem. Eng. J. 260: 269-283.

[2] Mahmoud, D.K., Salleh, M.A.M., Karim, W.A.W.A., Idris, A. and Abidin, Z.Z. (2012). Batch adsorption of basic dye using acid treated kenaf fibre char: Equilibrium, kinetic and thermodynamic studies. Chem. Eng. J. 181-182: 449-457.

[3] Chen, H., Zhao, J. and Dai, G. (2011). Silkworm exuviae - A new non-conventional and low-cost adsorbent for removal of methylene blue from aqueous solutions. J. Hazard. Mater. 186: 1320-1327.

[4] Bharathi, K.S. and Ramesh, S.T. (2013). Removal of dyes using agricultural waste as low-cost adsorbents: A review. Appl. Water Sci. 3: 773-790.

[5] Zheng, Y., Yu, S., Shuai, S., Zhou, Q., Cheng, Q., Liu, M. and Gao, C. (2013). Color removal and COD reduction of biologically treated textile effluent through submerged filtration using hollow fiber nanofiltration membrane. Desalination. 314: 89-95.

[6] Toor, M., Jin, B., Dai, S. and Vimonses, V. (2014). Activating natural bentonite as a cost-effective adsorbent for removal of Congo-red in wastewater, J. Ind. Eng. Chem. 21: 653-661.

[7] Hossain, M.A. and Alam, M.S. (2012). Adsorption kinetics of Rhodamine-B on used

black tea leaves. Iran. J. Environ. Heal. Sci. Eng. 9: 1-7.

[8] Gong, R., Zhang, X., Liu, H., Sun, Y. and Liu, B. (2007). Uptake of cationic dyes from aqueous solution by biosorption onto granular kohlrabi peel. Bioresour. Technol. 98: 1319-1323.

[9] Doğan, M., Abak, H. and Alkan, M. (2009). Adsorption of methylene blue onto hazelnut shell: Kinetics, mechanism and activation parameters. J. Hazard. Mater. 164: 172-181.

[10] Savci, S. (2017). Study of malachite green adsorption by waste ash using a batch method. Fresen. Environ. Bull., 26:1026-1032.

[11] Rangabhashiyam, S., Anu, N., Giri Nandagopal, M.S. and Selvaraju, N. (2014). Relevance of isotherm models in biosorption of pollutants by agricultural byproducts. J. Environ. Chem. Eng. 2: 398-414.

[12] Saba, N., Jawaid, M., Hakeem, K.R., Paridah, M.T., Khalina, A. and Alothman, A.Y. (2015). Potential of bioenergy production from industrial kenaf (*Hibiscus cannabinus* L.) based on Malaysian perspective. Renew. Sustain. Energy Rev. 42: 446-459.

[13] Basri., M.H.A., Arifin, A., Nasima, J., Hazandy, A.H. and Khalil, A. (2014). Journey of kenaf in Malaysia: A Review, Sci. Res. Essays. 9: 458-470.

[14] Ong, S.A., Ho, L.N., Wong, Y.S. and Zainuddin, A. (2013). Adsorption Behavior of Cationic and Anionic Dyes onto Acid Treated Coconut Coir, Sep. Sci. Technol. 48: 2125-2131.

[15] Santhi, T., Leena, A. and Manonmani, S. (2014). A comparative study of microwave and chemically treated Acacia nilotica leaf as an eco friendly adsorbent for the removal of rhodamine B dye from aqueous solution. Arab. J. Chem. 7: 494-503.

[16] Elmoubarki, R., Mahjoubi, F.Z., Tounsadi, H., Moustadraf, J., Abdennouri, M., Zouhri, A., El Albani, A. and Barka, N. (2015). Adsorption of textile dyes on raw and decanted Moroccan clays: Kinetics, equilibrium and thermodynamics. Water Resour. Ind. 9: 16-29.

[17] Qu, J., Zhang, Q., Xia, Y., Cong, Q. and Luo, C. (2014). Synthesis of carbon nanospheres using fallen willow leaves and adsorption of Rhodamine B and heavy metals by them. Environ. Sci. Pollut. Res. Int. 22: 1408-1419.

[18] Somasekhara Reddy, M.C., Sivaramakrishna, L. and Varada Reddy, A. (2012). The use of an agricultural waste material, Jujubaseeds for the removal of anionic dye (Congo red) from aqueous medium. J. Hazard. Mater. 203: 118–127.

[19] Mahmoodi, N.M., Hayati, B., Arami, M. and Lan, C. (2011). Adsorption of textile dyes on Pine Cone from colored wastewater: Kinetic, equilibrium and thermodynamic studies. Desalination 268: 117-125.

[20] Shu, J., Wang, Z., Huang, Y., Huang, N., Ren, C. and Zhang, W. (2015). Adsorption removal of Congo red from aqueous solution by polyhedral Cu_2O nanoparticles: Kinetics, isotherms, thermodynamics and mechanism analysis. J. Alloys Compd. 633: 338-346.

[21] Pua, F.L., Sajab, M.S., Chia, C.H., Zakaria, S., Rahman, I.A. and Salit, M.S.(2013). Alkaline-treated cocoa pod husk as adsorbent for removing methylene blue from aqueous solutions. J. Environ. Chem. Eng. 1: 460-465.

[22] Kumar, K.Y., Muralidhara, H.B., Nayaka, Y.A., Balasubramanyam, J. And Hanumanthappa, H. (2013). Low-cost synthesis of metal oxide nanoparticles and their application in adsorption of commercial dye and heavy metal ion in aqueous solution. Powder Technol. 246: 125-136.

[23] Lim, L.B.L., Priyantha, N., Tennakoon, D.T.B., Chieng, H.I., Dahri, M.K. and Suklueng, M. (2014). Breadnut peel as a highly effective low-cost biosorbent for methylene blue: Equilibrium, thermodynamic and kinetic studies, Arab. J. Chem.

[24] Tan, K.A., Morad, N., Teng, T.T., Norli, I. and Panneerselvam, P. (2012). Removal of Cationic Dye by Magnetic Nanoparticle (Fe_3O_4) Impregnated onto Activated Maize Cob Powder and Kinetic Study of Dye Waste Adsorption. APCBEE Procedia. 1: 83-89.

[25] Motahari, F., Mozdianfard, M.R. and Salavati-Niasari, M. (2015). Synthesis and adsorption studies of NiO nanoparticles in the presence of H2acacen ligand for removing Rhodamine B in wastewater treatment. Process Safety Environ. Protect. 93: 282-292.

[26] Li, L., Liu, S. and Zhu, T. (2010). Application of activated carbon derived from scrap tires for adsorption of Rhodamine B. J. Environ. Sci. 22(8): 1273-1280.

[27] Coelho, G.F., Gonçalves Jr., A.C., Tarley, C.R.T., Casarin, J., Nacke, H. and Francziskowski, M.A. (2014). Removal of metal ions Cd (II), Pb (II), and Cr (III) from water by the cashew nut shell *Anacardium occidentale* L.Ecol. Eng. 73: 514-525.

[28] Fomina, M. and Gadd, G.M. (2014). Biosorption: current perspectives on concept, definition and application. Bioresour. Technol. 160: 3-14.

[29] Kyzas, G.Z., Lazaridis, N.K. and Mitropoulos, A.C. (2012). Removal of dyes from aqueous solutions with untreated coffee residues as potential low-cost adsorbents: Equilibrium, reuse and thermodynamic approach. Chem. Eng. J. 189-190: 148-159.

[30] Wang, M., Fu, J., Zhang, Y., Chen, Z., Wang, M., Zhu, J., Cui, W., Zhang, J. and Xu, Q. (2015). Removal of Rhodamine B, a Cationic Dye From Aqueous Solution Using

Poly(cyclotriphosphazene-co-4,4′-sulfonyldiphenol) Nanotubes. J. Macromol. Sci. Part A. 52: 105-113.
[31] Alencar, W., Acayanka, E. and Lima, E. (2012). Application of Mangifera indica (mango) seeds as a biosorbent for removal of Victazol Orange 3R dye from aqueous solution and study of the biosorption mechanism. Chem. Eng. J. 209: 577-588.
[32] Zhang, Z.,Hara, I.M.O., Kent, G.A. and Doherty, W.O.S. (2013). Comparative study on adsorption of two cationic dyes by milled sugarcane bagasse. Ind. Crop. Prod. 42: 41-49.
[33] Abdel Salam, O.E., Reiad, N.A. and ElShafei, M.M. (2011). A study of the removal characteristics of heavy metals from wastewater by low-cost adsorbents. J. Adv. Res. 2: 297-303.
[34] Yargıç, A.Ş., Yarbay Şahin, R.Z., Özbay, N. and Önal, E. (2015). Assessment of toxic copper(II) biosorption from aqueous solution by chemically-treated tomato waste. J. Clean. Prod. 88: 152-159.
[35] Kamari, A., Yusoff, S.N.M., Abdullah, F. and Putra, W.P. (2014). Biosorptive removal of Cu(II), Ni(II) and Pb(II) ions from aqueous solutions using coconut dregs residue: Adsorption and characterisation studies. J. Environ. Chem. Eng. 2: 1912-1919.
[36] Igberase, E., Osifo, P. and Ofomaja, A. (2014). The adsorption of copper (II) ions by polyaniline graft chitosan beads from aqueous solution: Equilibrium, kinetic and desorption studies. J. Environ. Chem. Eng. 2: 362-369.
[37] Langmuir, I. (1916). The constitution and fundamental properties of solids and liquids. Part I. Solids. J. Am. Chem. Soc.38: 2221-2295.
[38] Bazargan-Lari, R., Zafarani, H.R., Bahrololoom, M.E. and Nemati, A. (2014). Removal of Cu(II) ions from aqueous solutions by low-cost natural hydroxyapatite/chitosan composite: Equilibrium, kinetic and thermodynamic studies. J. Taiwan Inst. Chem. Eng. 45: 1642-1648.
[39] Yuvaraja, G., Krishnaiah, N., Subbaiah, M.V. and Krishnaiah, A. (2014). Biosorption of Pb(II) from aqueous solution by Solanum melongena leaf powder as a low-cost biosorbent prepared from agricultural waste. Colloids Surf. B. Biointerfaces. 114: 75-81.
[40] Freundlich, H.M.F. (1906). Uber Die adsorption in Lasungen. J. Phys. Chem.57: 385-470.
[41] Hall, K.R., Eagleton, L.C., Acrivos, A. and Vermeulen, T. (1966). Pore-and solid-diffusion kinetics in fixed-bed adsorption under constant-pattern conditions. Ind. Eng. Chem. Fund.5(2): 212-223.
[42] Mall, I.D., Srivastava, V.C., Agarwal, N.K. and Mishra, I.M. (2005). Removal of congo red from aqueous solution by bagasse fly ash and activated carbon: Kinetic study and equilibrium isotherm analyses. Chemosphere 61: 492-501.
[43] Annadurai, G., Juang, R.S. and Lee, D.J. (2002). Use of cellulose-based wastes for adsorption of dyes from aqueous solutions. J. Hazard Mater. 92: 263-274.
[44] Mittal, A., Malviya, A., Kaur, D., Mittal, J. and Kurup, L. (2007). Studies on the adsorption kinetics and isotherms for the removal and recovery of methyl orange from wastewaters using waste materials. J. Hazard. Mater. 148: 229-240.
[45] Senthil Kumar, P., Ramalingam, S., Senthamarai, C., Niranjanaa, M., Vijayalakshmi, P. and Sivanesan, S. (2010). Adsorption of dye from aqueous solution by cashew nut shell: studies on equilibrium isotherm, kinetics and thermodynamics of interactions. Desalination 261(1-2), 52-60.
[46] Namasivayam, C. and Kavitha, D. (2002). Removal of congo red from water by adsorption onto activated carbon prepared from coir pith, an agricultural solid waste. Dyes Pigments 54: 47-58.
[47] Gouamid, M., Ouhrani, M.R. and Bensaci, M.B. (2013). Adsorption equilibrium, kinetics and thermodynamics of methylene blue from aqueous solutions using date palm leaves. Energy Proc. 36: 898-907.
[48] Hameed, B.H. and Ahmad, A.A. (2009). Batch adsorption of methylene blue from aqueous solution by garlic peel, an agricultural waste biomass. J. Hazard. Mater. 164(2-3): 870-875.
[49] Demir, H., Top, A., Balköse, D. and Ulkü, S. (2008). Dye adsorption behaviour of Lufta cylindrica fibers. J. Hazard. Mater. 153(1-2): 389-394.
[50] Ahmad, A., Rafatullah, M. and Sulaiman, O. (2009). Scavenging behaviour of meranti sawdust in the removal of methylene blue from aqueous solution. J. Hazard. Mater. 170: 357-365.
[51] Song, J., Zou, W., Bian, Y., Su, F. and Han, R. (2011). Adsorption characteristics of methylene blue by peanut husk in batch and column modes. Desalination 265(1-3): 119-125.
[52] Abbas, A., Murtaza, S., Shahid, K., Munir, M., Ayub, R. and Akber, S. (2012). Comparative Study of Adsorptive Removal of Congo Red and Brilliant Green Dyes from Water Using Peanut Shell. Middle-East J. Sci. Res. 11: 828-832.
[53] Ncibi, M.C., Mahjoub, B. and Seffen, M. (2007). Kinetic and equilibrium studies of methylene blue biosorption by *Posidonia oceanica* (L.) fibres. J. Hazard. Mater. 139(2): 280-285.
[54] Hameed, B.H. (2009). Spent tea leaves: a new non-conventional and low-cost adsorbent for removal of basic dye from aqueous solutions. J. Hazard. Mater. 161(2-3): 753-759.
[55] Gusmão, K., Gurgel, L., Melo, T. and Gil, L. (2013). Adsorption studies of methylene blue

and gentian violet on sugarcane bagasse modified with EDTA dianhydride (EDTAD) in aqueous solutions: Kinetic and equilibrium aspects. J. Environ. Manage. 118: 135-143.

[56] Pavan, F.A., Lima, E.C., Dias, S.L.P. and Mazzocato, A.C. (2008). Methylene blue biosorption from aqueous solutions by yellow passion fruit waste. J. Hazard. Mater. 150(3): 703-712.

Received: **27.02.2017**
Accepted: **26.07.2017**

CORRESPONDING AUTHOR

Azlan Kamari
Department of Chemistry, Faculty of Science and Mathematics, Universiti Pendidikan Sultan Idris, 35900, Tanjong Malim, Perak, Malaysia

e-mail: azlkam@yahoo.co.uk

© by PSP Volume 26 – No. 10/2017 pages 5911-5916 Fresenius Environmental Bulletin

EFFECT OF THREE ENVIRONMENTAL FACTORS ON POTENTIAL NITRIFICATION RATES OF RIPARIAN SEDIMENT

Xiaohong Zhou*, Chunzi Wen, Yimin Li

School of the Environment and Safety Engineering, Jiangsu University, Zhenjiang, Jiangsu, 212013, China

ABSTRACT

Nitrification is the crucial nitrogen biogeochemical cycles processing in various freshwater ecosystem. This processing was effected by various environmental factors. However, the effect of environmental factors on potential nitrification rates (PNRs) of riparian sediment are yet not known until now. This aims of this study to investigate the influence processing of three environmental factors on PNRs variation for riparian sediment using the single factor incubations experiment. The results shown that (1) PNRs obviously varied with the pH values changes in cultivation systems and the peak of PNRs was detected in pH7.5 cultivation group; (2) PNRs showed a significantly increasing trend with the cultured temperature increased from 10 to 28℃, whereas, PNRs showed an obvious decline when temperature was exposed to 37℃; (3) The PNRs rapidly increased when ammonia concentration increasing from 10 to 50 mg·L^{-1}, whereas, it significantly decreased when ammonia concentration increased to 100 mg·L^{-1}. Therefore, the maximum value of PNRs was detected in the cultivation environment with a temperature of 28℃, pH of 7.5 and ammonia concentration of 50 mg·L^{-1}, respectively.

KEYWORDS:
Potential nitrification rates, sediment, pH, temperature, ammonia

INTRODUCTION

Nitrogen (N) is an important nutrient for primary producers, including plants and phytoplankton. However, with the development of industrial, agriculture and urbanization, enormous N were anthropogenic produced in recent decades all over the world. Superfluous N enters the various freshwater ecosystem resulting in eutrophication for lakes, rivers and ponds [1-2]. Therefore, it is one of the fundamental topic for freshwater ecosystem to understanding the N-cycling processing and their mechanisms.

Nitrification, as for a crucial process and underpinning for N transfer among water, sediment and plants/phytoplankton, plays a critical role in N biogeochemical cycle of freshwater ecosystem [3-4]. In this process, microbial oxidation ammonia into nitrate via nitrite [5-10]. Generally speaking, nitrification could be divided two step, one is the ammonia oxidation, the other is nitrite oxidation [11]. Ammonia oxidation is conversion ammonia into nitrite [7]. As for the the first and rate-limiting step for nitrification [12], it was derived and carried out by two groups of microorganisms, ammonia oxidizing bacteria (AOB) and ammonia oxidizing archaea (AOA) [7, 13-15]. Nitrite oxidation were carried out by nitrite-oxidizing bacteria for the conversion of nitrite to nitrate [15].

It has been shown that nitrification could be influenced by a variety of environmental parameters in freshwater ecosystem. For example, Lyu et al. [16] reported that pH, salinity and ammonia concentration, temperature has obvious influence on nitrification for Yellow River delta wetland sediment. Zheng et al. [17] also found that PNRs were effected by temperature and salinity in Yangtze Estuary intertidal sediments. However, previous studies mainly focused on the oceans, estuaries and wetland ecosystem, little information is known about the environmental factors on the nitrification for the riparian sediment of river ecosystem. Therefore, the primary goal of this study was to quantify and confirmed the influence of three environmental factors on PNRs of the riparian sediments of ancient canal, Zhenjiang, China, which is the urban river with frequent human activities.

MATERIALS AND METHODS

Experimental design. Potential nitrification rates (PNRs) were measured through the single factor incubations experiment. The environmental factors included pH, temperature and ammonia concentration. And the lever of each environmental factors were shown in Table 1. Sediment samples using in this study were collected from three different sites of the ancient canal riparian of Zhenjiang, China.

Thirty-three 250mL Erlenmeyer flask containing 100 mL culture solution (3 replicates × 3 pH

TABLE 1
Experimental groups and culture environment of each group

Environmental factors	Treatment groups	Culture environment and culture volume (100 mL)
pH	6.5	Ammonia concentration,50 mg·L^{-1}; Temperature, 28℃; pH, 6.5
	7.5	Ammonia concentration,50 mg·L^{-1}; Temperature, 28℃; pH, 7.5
	8.5	Ammonia concentration,50 mg·L^{-1}; Temperature, 28℃; pH, 8.5
Temperature (℃)	10	Ammonia concentration,50 mg·L^{-1}; pH, 7.5; Temperature, 10℃;
	20	Ammonia concentration,50 mg·L^{-1}; pH, 7.5; Temperature, 20℃;
	28	Ammonia concentration,50 mg·L^{-1}; pH, 7.5; Temperature, 28℃;
	37	Ammonia concentration,50 mg·L^{-1}; pH, 7.5; Temperature, 37℃;
Ammonia concentration (mg·L^{-1})	10	Temperature, 28℃; pH, 7.5; Ammonia concentration,10 mg·L^{-1};
	20	Temperature, 28℃; pH, 7.5; Ammonia concentration, 20 mg·L^{-1};
	50	Temperature, 28℃; pH, 7.5; Ammonia concentration, 50 mg·L^{-1};
	100	Temperature, 28℃; pH, 7.5; Ammonia concentration, 100 mg·L^{-1};

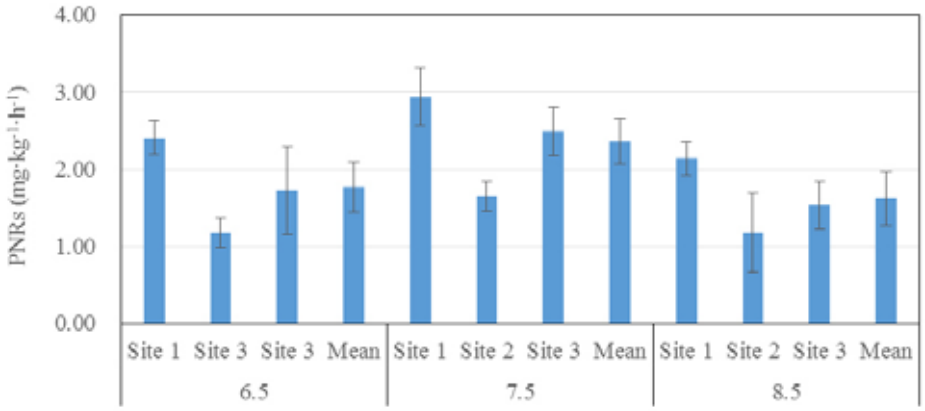

FIGURE 1
Effect of pH on potential nitrification rates

treatments groups+ 3 replicates × 4 temperature treatments groups+3 replicates × 4 ammonia concentration treatments groups) were randomly assigned. 15g fresh soil was put into those vessel, respectively. Then, the suspension was incubated in dark at designed temperature (see Table1) with continuous shaking at 180 rpm. Subsamples were taken at 0, 24 and 48 h after incubation. Then, the nitrate was quickly analysis.

Physicochemical analysis. Ammonium (NH_4^+-N) and nitrate (NO_3^--N) of culture solution were measured with the indophenol blue and phenol disulfonic acid methods, respectively [18]. pH of culture solution was measured using the PHS-3C digital pH meter (INESA Scientific Instrument Co., Ltd., China). To determine the sediment water content, sediments were dried until a constant weight was achieved.

PNRs calculation. The PNRs were calculated based on the changes in nitrate concentrations with time in this study according to the method of our previously research [15]. The PNRs were calculated using Eq. (1).

$$PNRs = \frac{(C_2 - C_1) \times (V_2 - V_1)}{t \times m \times k} \quad (1)$$

where C_1 and C_2 is the initial and final nitrate concentration (mg/L), V_1 and V_2 is the volume of culture solution and sediment moisture (L); 't' is the incubation time (h), m is the weight (kg) and k is the water coefficient of sediment samples.

Statistics analysis. Statistical analyses were performed using SPSS 19.0. One-way ANOVA was performed to determine significant differences among the different groups in the same lever for three environmental factors, with significant levels at P<0.05 or 0.01 for all the analyses.

RESULTS AND DISCUSSION

Effect of pH on PNRs. pH is the key factor to influence the nitrogen cycle microbial. Previous research found that pH above 8.5 or less than 5.8 will inhibit anammox activity [19-20], ultimately, might be effect the nitrification. In our research, the values of PNRs ranged from 1.18 to 2.41, 1.65 to 2.95 and 1.18 to 2.14 mg·kg^{-1}·h^{-1}, respectively, with an average number of 1.77, 2.36 and 1.62 mg·kg^{-1}·h^{-1} in pH values of 6.5, 7.5 and 8.5 cultivation groups, indicated the PNRs obviously varied with the pH change in cultivation systems (Fig 1). In

TABLE 2
Statistics results of values of PNRs (mg·kg^{-1}·h^{-1})

Treatment groups		Average	Minimum	Maximum	S.D[1)]	CV (%)[2)]
pH	6.5	1.77	1.18	2.41	0.62	34.77
	7.5	2.36	1.65	2.95	0.66	27.77
	7.5	1.62	1.18	2.14	0.49	30.05
Temperature	10	1.92	1.13	2.56	0.72	37.65
	20	2.54	1.59	3.10	0.83	32.61
	28	3.01	2.04	3.88	0.92	30.67
	37	2.65	1.36	3.62	1.16	43.88
Ammonia concentration	10	1.53	1.18	1.87	0.35	22.70
	20	2.15	1.65	2.68	0.51	23.93
	50	2.63	1.81	3.21	0.73	27.84
	100	1.95	1.18	2.95	0.90	46.33

[1)] S.D.: standard deviation; [2)] CV: coefficients of variation.

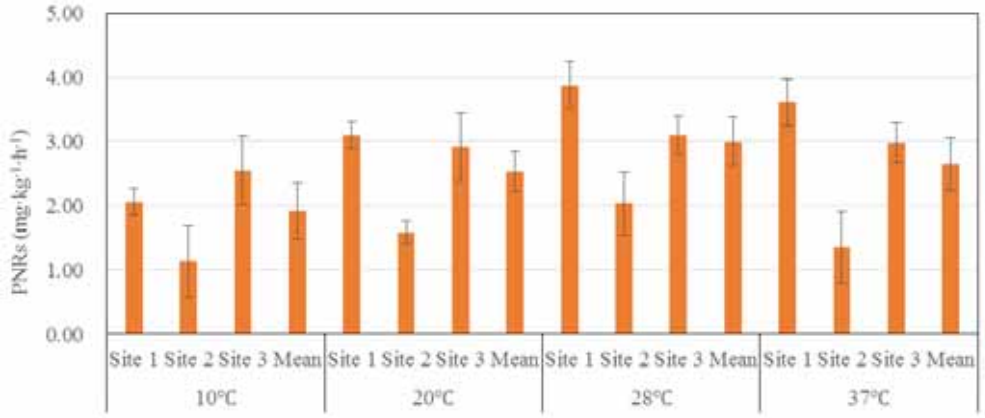

FIGURE 2
Effect of temperature on potential nitrification rates

addition, the order of PNRs was pH7.5> pH6.5> pH8.5, whereas, coefficient of variation (C. V) of PNRs was pH6.5> pH 8.5> pH7.5 (Table 2). One-way ANOVA analysis result found that a significant difference of PNRs between pH7.5 and pH 8.5 groups (P<0.05), whereas, not significant difference was found between pH 6.5 and pH 7.5 (P>0.05), and pH 6.5 and pH 8.5 groups (P>0.05) (Table 3). Princic et al. [21] reported that the optimal pH is between 6.5 and 8.5 for nitrification. Sun et al. [22] also reported that the nitrification rate would rapidly decreases when the pH is below 6 or above 8. Chen et al. [23] also reported that the optimal pH range were 7.0-7.5 for ammonia nitrogen degradation by heterotrophic nitrification by bacterium *Shinella zoogloeoides* sp. CPZ 56. Our research also confirmed the maximal PNRs values in the 7.5 pH cultivation groups, indicated that more strong nitrification in pH 7.5 cultivation environment.

TABLE 3
***P*-value of One-way ANOVA analysis between different pH groups**

pH groups	6.5	7.5	8.5
6.5	/		
7.5	0.065	/	
8.5	0.616	0.022	/

TABLE 4
***P*-value of One-way ANOVA analysis between different temperature groups**

Temperature groups	10°C	20°C	28°C	37°C
10°C	/			
20°C	0.080	/		
28°C	0.012	0.095	/	
37°C	0.059	0.666	0.208	/

Effect of temperature on PNRs. In our study, the PNRs was significantly effected by temperature (Fig. 2). The PNRs values ranged from 1.13 to 2.56 mg·kg^{-1}·h^{-1}, from 1.59 to 3.10 mg·kg^{-1}·h^{-1}, from 2.04 to 3.88 mg·kg^{-1}·h^{-1} and from 1.36 to 3.62 mg·kg^{-1}·h^{-1}, respectively, with the average values of 1.92, 2.54, 3.01 and 2.65 mg·kg^{-1}·h^{-1} in 10, 20, 28 and 37°C cultivation groups, indicated the PNRs obviously varied with the temperature change in cultivation systems (Table 2). PNRs showed a significantly increasing trend when temperature of cultured environment was increased from 10 to 28 °C. The peak of PNRs was detected in 28°C cultivation group, which was 1.57, 1.19 times higher than the in 10 and 20°C cultivation groups, respectively, indicated more strong nitrification in 28°C experimental group. However, PNRs showed an obvious

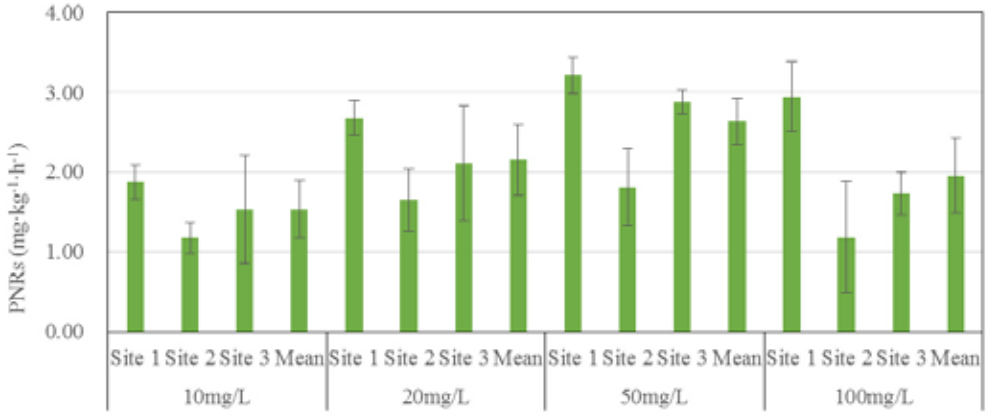

FIGURE 3
Effect of ammonia concentration on potential nitrification rates

decline when temperature was exposed to 37℃ (Fig. 2). Besides, The C.V of PNRs order was 37℃>10℃>20℃>28℃ (Table 2). One-way ANOVA analysis result found that a significant difference of PNRs among four temperature groups (P<0.05) and between 10℃ and 28℃ experimental groups (P<0.05), whereas, not significant difference was found between others any two groups (P>0.05) (Table. 4). Our research results were consistent with the previous findings. For example, Seitzinger et al. [24] reported that temperature increase would lead to an increase of nitrification rate. Chen et al. [23] also found that the optimal temperature range were 30-35℃ for ammonia nitrogen degradation by heterotrophic nitrification by bacterium *Shinella zoogloeoides* sp. CPZ 56 and the ammonia nitrogen degradation rate could reach 96% in a temperature range of 30-35℃. Those results indicated that temperature is an important factor in regulating nitrification activity and rate. The main reason might be the temperature could influence the abundance, diversity and community structure of nitrogen cycle microorganism, resulting in PNRs obviously varied with the temperature changes. Numerous studies have verified the temperature could strong effect microbial biological processing [25]. For example, Jing and Lin [26] reported that denitrifying bacteria are more abundant in spring and summer compared with fall and winter in wetland sediments. Picard et al. [27] found that 30 °C is the suitable temperature and temperature under 5 °C might restrict N biological processes. Chen et al. [23] reported that temperature plays an important role in the growth and reproduction of microorganisms and temperature could effect the liquid crystal structure of the microbial film and the synthesis and activity of enzymes and proteins. Our research was consistent with the previous findings. In this study, the PNRs were peak in the 28 ℃ cultured environment and it obvious declined when temperature under or higher 28 ℃.

TABLE 5
P-value of One-way ANOVA analysis between different ammonia concentration groups

Ammonia concentration	10 mg·L^{-1}	20 mg·L^{-1}	50 mg·L^{-1}	100 mg·L^{-1}
10 mg·L^{-1}	/			
20 mg·L^{-1}	0.104	/		
50 mg·L^{-1}	0.003	0.206	/	
100 mg·L^{-1}	0.149	0.616	0.065	/

Effect of ammonia concentration on PNRs. Ammonia is the important substrates for nitrogen cycle microorganism, including to ammonia-oxidizing archaea and bacteria, etc. [28], thus, their concentration in environmental samples would obviously effect the nitrification process. For example, Zhou et al. [15] reported that abundance of ammonia-oxidizing archaea were negatively correlation with ammonia concentration in riparian surface sediment. However, Yang et al., [28] found that the abundance of ammonia-oxidizing archaea was a positive correlation with NH_4^+-H in both water and sediment samples. These conclusions shown that the influence of ammonia to nitrifying bacteria and nitrification process were very complicated. In this study, the mean values of PNRs rapidly increased when ammonia concentration were increased from 10 to 50 mg·L^{-1}, and PNRs reached to a maximum value of 2.63 mg·kg^{-1}·h^{-1} in ammonia concentration of 50 mg·L^{-1}, which were 1.72 and 1.22 times times higher than in 10 and 20 mg·L^{-1} ammonia concentration cultivation groups, respectively. However, it significantly decreased when ammonia concentration increased to 100 mg·L^{-1} (Fig 3). A similar result was obtained by Lyu [29] who observed the strongest nitrification in the Yellow River delta wetland when ammonia concentration is 50 mg·L^{-1}. These results show that the ammonia concentration obviously affected the PNRs values. Besides, the C. V order of PNRs was 100 mg·L^{-1}>50 mg·L^{-1}> 20 mg·L^{-1}>10 mg·L^{-1} in our

study (Table 2). In addition, One-way ANOVA analysis result found that a significant difference of PNRs among four ammonia concentration (P<0.05) and between 10 and 50 mg·L^{-1} experiment groups, whereas, not significant difference was found between other any two groups (P>0.05) (Table. 5). Chen et al. [23] also found that the optimal initial ammonia nitrogen concentration was 50 mg/L for ammonia nitrogen degradation by heterotrophic nitrification by bacterium *Shinella zoogloeoides* sp. CPZ 56, and the ammonia nitrogen degradation rate could reach 100% in the 50 mg/L ammonia nitrogen concentration. This confirms our research results.

CONCLUSION

In summary, this study measured the potential nitrification rates (PNRs) of riparian sediment through the single factor incubations experiment. And the results demonstrated the PNRs were obviously effected by pH, temperature and ammonia concentration to a certain degree. The peak of PNRs was detected in 28℃, pH7.5 and 50 mg·L^{-1} ammonia concentration cultivation group, respectively, indicated more strong nitrification in such cultivation environment. These results shed light on the understanding of the suitable environmental conditions for potential nitrification rates and N cycling in sediment of freshwater ecosystems.

ACKNOWLEDGEMENTS

This study was supported by the China Postdoctoral Science Foundation (grant # 2012T50464), and Jiangsu province water conservancy science and technology project (grant # 2016050), and Jiangsu Collaborative Innovation Center of Technology and Material of Water Treatment.

REFERENCES

[1] Yoshinaga, I., Amano, T., Yamagishi, T., Okada, K., Ueda, S., Sako, Y., Suwa, Y. (2011) Distribution and Diversity of Anaerobic Ammonium Oxidation (Anammox) Bacteria in the Sediment of a Eutrophic Freshwater Lake, Lake Kitaura, Japan. *Microbes and environments,* 26(3): 189–197.

[2] Wu, F.P., Wang, Y.C., Xia, C., Huo, J.Y., Wei, B.G (2016) Sorption of ammonia nitrogen on suspended sediments in Lanzhou section of the yellow river, China. *Fresen. Environ. Bull.*, 25(1): 4-13.

[3] Liu, Y., Zhang, J., Zhang, X., Xie, S. (2014) Depth-related changes of sediment ammonia-oxidizing microorganisms in a high-altitude freshwater wetland. *Applied microbiology and biotechnology*, 98(12):5697-5707.

[4] Li, S.P., Sun, S.J., Chen, P.Z. (2016) Construction of a complex denitrifying bacterial flora and its application in rural domestic sewage. *Fresen. Environ. Bull.*, 25(11): 4760-4766.

[5] Cao, H., Li, M., Hong, Y., Gu, J.D (2011) Diversity and abundance of ammonia-oxidizing archaea and bacteria in polluted mangrove sediment. *Systematic and Applied Microbiology*, 34(7): 513–523.

[6] Damashek, J., Casciotti, K.L., Francis, C.A (2016) Variable Nitrification Rates Across Environmental Gradients in Turbid, Nutrient-Rich Estuary Waters of San Francisco Bay. *Estuaries and Coasts,* 39(4):1050–1071.

[7] French, E., Kozlowski, J.A., Mukherjee, M., Bullerjahn, G., Bollmann, A. (2012) Ecophysiological Characterization of Ammonia-Oxidizing Archaea and Bacteria from Freshwater. *Applied and Environmental Microbiology*, 78 (16): 5773–5780.

[8] Dang, H.Y., Li, J., Chen, R. P., Wang, L., Guo, L.Z., Zhang, Z.N., Klotz, M.G.(2010) Diversity, Abundance, and Spatial Distribution of Sediment Ammonia-Oxidizing Betaproteobacteria in Response to Environmental Gradients and Coastal Eutrophication in Jiaozhou Bay, China. *Applied and Environmental Microbiology*, 76(14):4691-4702.

[9] Tanner, C.C., Kadlec, R.H., Gibbs, M.M., Sukias, J.P.S., Nguyen, M.L. (2002) Nitrogen processing gradients in subsurface-flow treatment wetlands-influence of wastewater characteristics. *Ecological Engineering*, 18(4): 499-520.

[10] Wu, J., Zhang, J., Jia, W.L., Xie, H.J., Gu, R.R., Li, C. (2009) Impact of COD/N ratio on nitrous oxide emission from microcosm wetlands and their performance in removing nitrogen from wastewater. *Bioresource Technology*, 100(12): 2910-2917.

[11] Zhou, X.H., Wang, G.X. (2010) Nutrient concentration variations during *Oenanthe javanica* growth and decay in the ecological floating bed system. *Journal of Environmental Sciences*, 22(11):1710-1717.

[12] Kowalchuk, G.A., Stephen, J.R. (2001) Ammonia-oxidizing bacteria: a model for molecular microbial ecology. *Annual review of microbiology*, 55(1): 485-529.

[13] He, J.Z., Shen, J.P., Zhang, L.M., Zhu, Y.G., Zheng, Y.M., Xu, M.G., Di, H. J. (2007) Quantitative analyses of the abundance and composition of ammonia-oxidizing bacteria and ammonia-oxidizing archaea of a Chinese upland red soil under long-term fertilization practices. *Environmental Microbiology,* 9(9): 2364–2374.

[14] Könneke, M., Bernhard, A.E., dela Torre, J.R., Walker, C.B., Waterbury, J.B., Stahl, D. A. (2005) Isolation of an autotrophic ammonia-oxidizing marine archaeon. *Nature*, 437(7058):

543–546.
[15] Zhou, X.H., Li, Y.M., Zhang, J.P., Liu, B., Wang, M.Y., Zhou, Y.W., Lin, Z.J., He, Z.L (2016) Diversity, abundance and community structure of ammonia-oxidizing archaea and bacteria in riparian sediment of Zhenjiang ancient canal. *Ecological Engineering,* 90:447–458.
[16] Lyu, Y.H., Bai, J., Jiang, Y. (2008) Nitrification intensity and influencing factors of the Yellow River delta wetland. *Transactions of Oceanology and Limnology*. 2: 26-30. [Chinese]
[17] Zheng, Y.L., Hou, L.J., Newell, S., Liu, M., Zhou, J,L., Zhao, H., You, L.L., Cheng, X.L. (2014) Community Dynamics and Activity of Ammonia-Oxidizing Prokaryotes in Intertidal Sediments of the Yangtze Estuary. *Applied and Environmental Microbiology,* 80(1):408–419
[18] Bao, S.D (1981) Soil Agricultural Chemical Analysis. *China Agricultural Press, Beijing,* 42–49 (Chinese)
[19] Jin, R.C., Yang, G.F., Yu, J.J., Zheng, P. (2012) The inhibition of the anammox process: a review. *Chemical Enginering journal,* 197(29): 67–79.
[20] Waki, M., Yasuda, T., Suzuki, K., Komada, M., Abe, K. (2015) Distribution of anammox bacteria in a free-water-surface constructed wetland with wild rice (*Zizania latifolia*). *Ecological Engineering,* 81:165–172.
[21] Princic, A., Mahne, I., Megusar, F., Paul, E.A., Tiedje, J.M. (1998) Effects of the pH and oxygen and ammonium concentrations on the community structure of nitrifying bacteria from wastewater. *Applied and Environmental Microbiology,* 64(10): 3584-3590.
[22] Sun, Z.S., Ke, Q., Chen, Y.X., (2001) Mechanism of biodenitrification of SBR and its effecting factors. *China Biogas* 19: 16-19
[23] Chen, P.Z., Li, S.P., Zheng, X.Q., Ren, T.Z., Wang, L.G. (2016) Heterotrophic nitrification by bacterium *Shinella zoogloeoides* Sp. CPZ56. *Fresen. Environ. Bull.*, 25(8): 3017-3022.
[24] Seitzinger, S.P. (1988) Denitrification in freshwater and coastal marine ecosystems: Ecological and geochemical significance, *Limnolgy oceanography*, 33:702–724.
[25] Hill, D.T., Payton, J.D. (2000) Effect of plant fill ratio on water temperature in constructed wetlands. *Bioresource Technology*, 71(3):283-289.
[26] Jing, S.R., Lin, Y.F., (2004) Seasonal effect on ammonia nitrogen removal by constructed wetlands treating polluted river water in southern Taiwan. *Environmental Pollution,* 127(9):291-301.
[27] Picard, C.R., Fraser, L.H., Steer, D. (2005) The interacting effects of temperature and plant community type on nutrient removal in wetland microcosms. *Bioresource Technology*, 96(9):1039-1047.
[28] Yang, J.Y., Wang, W.L., Zhao, L.Y., Wang, J.Z., Zhu, C., Shao, Y. (2017) Abundance of ammonia-oxidazing archaea among eight lakes and reservoirs at different trophic states. *Fresen. Environ. Bull.*, 26(1a): 803-809.
[29] Lyu, Y.H. (2007) Ecological characteristic of nitrifying bacteria and nitrification in the Yellow River delta wetland [Master dissertation]. *Ocean university of China*. [Chinese]

Received: **28.02.2017**
Accepted: **27.07.2017**

CORRESPONDING AUTHOR

Xiaohong Zhou
School of the Environment and Safety Engineering
Jiangsu University Zhenjiang, Jiangsu, 212013-P. R. CHINA

e-mail: xhzhou0214@163.com

© by PSP Volume 26 – No. 10/2017 pages 5917-5928 Fresenius Environmental Bulletin

HYDROLOGICAL RESPONSES TO ECOLOGICAL MANAGEMENT OF THE LOESS HILLY-GULLY AREA, CHINA

Erjia Liu[1,2,3], Xiaoli Zhang[1,2,3,*], Xiaoping Zhang[4,5], Zhidong Luo[1,6], Aijuan Wang[6], Zhiguang Li[6]

[1]Forestry College, Beijing Forestry University, Beijing 100083, China
[2]Key Laboratory of Precision Forestry, Beijing Forestry University, Beijing 100083, China
[3]Provincial Key Laboratory of Forestry Cultivation and Conservation, Beijing Forestry University, Beijing 100083, China
[4]State Key Laboratory of Soil Erosion and Dry land Farming in Loess Plateau, Institute of Soil and Water Conservation, Chinese Academy of Sciences and Ministry of Water Resources, Yangling 712100, Shanxi, China
[5]Institute of Soil and Water Conservation, Northwest A & F University, Yangling 712100, Shanxi, China
[6]Soil and Water Conservation Monitoring Center of the Ministry of Water Resources, Beijing100053, China

ABSTRACT

The Loess Plateau is known as one of the most severe soil erosion sites in the world. Over the last six decades, soil and water conservation measures have been implemented on the Loess Plateau, China, including the construction of terraces and warping dams, vegetation restoration, and the 'Grain for Green Program', resulted in the land cover change. In this study, we focused on analysing the variation characteristics of streamflow-sediment behaviours and quantitatively calculating the effects of climate changes and human activities on annual streamflow and sediment load in the upper reaches of the Beiluo River of the Loess Plateau with extensive vegetation restoration. The daily hydrological data over the period of 1963-2011 were summed to assess the variation characteristics. The non-parametric Mann–Kendall test, Spearmen method and Pettitt's test were used to identify trends and shifts in hydrological factors. Moreover, the relative changes of the streamflow and sediment load were analysed around the change points. To further confirm the calculation results of the impacts of climate change and anthropogenic activities on annual streamflow and sediment load, the double-mass curve, correction coefficient methods and empirical hydrologic methods based on precipitation were used. The results showed that under the background of precipitation with no significant trend, both the streamflow and sediment load had a significant negative trend ($P<0.01$) with an average annual rate of -0.26 mm/a and -172 t/km^2·a. The annual streamflow decreased related to decreasing high flow (5%) in the flood season in subsequent years, whereas an increase in low flow (95%) was identified in the non-flood season. Two change points were detected in 1979 and 2002 for streamflow and sediment yield annually and in the flood season at the significance levels of $p<0.05$ and $p<0.01$, respectively, mostly because of the change point of the high flow in the flood season. Compared with PI (1963-1979), the dimension of the induction in the average sediment load was greater than the streamflow. The extreme ratio and the coefficient of variation about them in different periods after the change point also changed. Meanwhile, the streamflow for 5% and 50% decreased in PII (1980-2002) and PIII (2003-2011), respectively, and increased for 95%. The extent of the reduction in sediment load was greater than that of streamflow with the periods altered, and the changes in sediment load were negative. It was estimated that human activities including the underlying surface changes and conservation measures in PII accounted for 38.2% and 51.4% of the changes in streamflow and sediment load, respectively. In PIII, the effects reached 74.7% and 86.7%, respectively. The great improvement in the ecological environment on the Loess Plateau has already revealed the advantages of biological treatments in reducing flood volumes and compensating streamflow on a regional scale. The results can provide theoretical basis for water resource management and water and soil conservation for the administrators.

KEYWORDS:
The change of streamflow and sediment load; Ecological restoration; Contribution; The Loess hill-gully area

INTRODUCTION

The Loess Plateau, an important agricultural area of China located in the middle reaches of the Yellow River basin, is characterized by a heavily fragmented landscape and severe soil erosion, with sediment yields exceeding 3×10^4 to 4×10^4 t·km^{-2}·a^{-1} in several drainage basins over recent decades [1,2]. The heavily fragmented landscape and severe soil erosion have resulted in the loss of soil nutrients and agricultural land and damage to local ecological security and social economic development [3]. Most of the sediment yield was caused by the intensification of land use induced by the increasing population, leading to sedimentation in the lower river

[1,4,5,6,7]. To ensure ecological safety, numerous integrated soil conservation measures have been adopted to extenuate inappropriate and unreasonable land use with the aim of controlling the soil erosion and increasing the water supply comprehensively, including through the construction of terraces and sediment-trapping dams and a modest effort to replant trees and improve grass during the 1970s [3,8]. The engineered projects can significantly and immediately induce the flow of streamflow, weaken the magnitudes and peaks of high flow, and decrease sediment deposition [9-12]. However, if sediment-trapping dams are not properly maintained, they may become abandoned dams and lose effectiveness. The "Grain for Green Program" initiated by the government in 1999 has been widely adopted on a massive scale to improve vegetation cover. This project differs from the former by its lack of an extensive series of engineering works. The conversion from the comprehensive soil and water conservation project to the "Grain for Green" project is actually an intensified process of ecological management. The vegetation cover of the Loess Plateau underwent an increasing period (1981-1989), a relatively stable period (1990-1998), a rapidly declining period (1999-2001), and a rapidly increasing period (2002-2006), resulting in great improvement of the ecological environment, and ecological efficiency is gradually materializing [13-15].

Stable hydrological regime plays an important role in maintaining aquatic biodiversity and river ecological function integrity[16]. The hydrological cycle through which precipitation is transferred to river streamflow and groundwater recharge is being affected by climate change, however, the effects differ by terrain, geomorphology conditions, soil, geological properties, rainfall characteristics and management practices. Such changes influence the hydrological processes of basins by altering both the balance between rainfall and evaporation and the runoff response of the area. Among these climatic factors, rainfall and Potential Evapotranspiration are the main drivers because they control the total evapotranspiration [8, 17]. In the Loess Plateau, most of the precipitation occurs during May to October in some form of short-duration, high-intensity rainfall. Several reaches show that the region has suffered from the reduction of precipitation with the increase in temperature [18-20]. The impact of human activities on the hydrological regime is spatially identical in different regions. These changes have influenced the flow of water and sediment transport, functioned greatly in retaining sediment and streamflow, reduced the streamflow frequency and the frequency of the hyperconcentrated flow, and increased the streamflow distribution uniformity [5,7,9,11,21-22]. Human activities have resulted in land use change, of which impacts are manifested by changes in evaporation/transpiration performance, the infiltration characteristics of soil, the convection of moisture, albedo, heat and net radiation; ultimately, land use change affects the water balance and hydrological cycle. The comprehensive effects of climatic variability and human activities still influence the gathering of regional streamflow and sediment transport in the Loess Plateau. Therefore, it is very important for the optimization of ecological management to understand the relationships between climatic factors, human activities and the hydrological regime.

Recently, many studies on the middle Yellow River basin focused on the changes in streamflow and sediment transport under the influence of climate change and ecological management have found that the management measures have resulted in streamflow reduction, effectively impeding sediment yields [3-5,9,11,23-31]. These studies also found differing results about the hydrological regime among basins. It is not clear how the hydrological regime changed concurrently with the implementation of different ecological management projects. Meanwhile, although the streamflow and sediment load have decreased significantly on a large scale, the response mechanism of the streamflow and sediment load with ecological recovery remain to be discussed. The upper reaches of the Beiluo catchment is a typical region of the Loess hilly and gully region with the centralized source of concentrated coarse sediment. In 1999, in response to the "Grain for Green" program, Wuqi made breakthroughs in environmental construction and was recognized as the first county of the "Grain for Green" programme [32]. It is a typical region with sufficient time series data, and many investments in watershed management have been implemented on this basin for the purpose of examining the effect of vegetation restoration on the change in streamflow and sediment load. Many studies in this region have studied climate change, human activities, and soil erosion. Additionally, some studies have been conducted on the responses of streamflow and sediment to the ecological management in the region. However, there is no consistent conclusion among the previous studies of hydrological processes, thus demonstrating the complexity of the hydrological process in this basin.

To contribute to evaluating the regional ecological environmental effect of the changes in land cover and the soil and water conservation measures in the past half century, minimizing the economic costs associated with floods and droughts, helping managers make rational decisions on strategies for ecological construction, and guiding the future preservation of sustainable water resources in the basin, the purposes of this study were as follows: (1) to detect the trends and change points of annual streamflow and sediment load in the upper Beiluo catchment from 1963 to 2011; (2) to find the extent of change in streamflow and sediment load by daily duration curves; and (3) to assess the relative contribution of a climatic factor (precipitation) and human

activities to the variation in streamflow and sediment load.

STUDY AREA AND METHODS

The study site. The upper reaches of the Beiluo catchment is a secondary tributary of the Yellow River located in the region between E107°38′57″-108°32′49″E and N36°33′33″-37°24′27″ with the Wuqi gauge station as the outlet of the catchment (Figure 1). The drainage area of the catchment is approximately 3408 km^2 (12.7% of the whole Beiluo catchment), while the length of the main channel is approximately 275 km with an average gradient of 1.6‰. The catchment belongs to a semi-arid climate. The annual average precipitation was 418 mm from 1963 to 2010, of which 71.6% occurred from May to October. The region is characterized by high intensity rainstorms, loess soil, fragmented terrain, crisscrossing galleys, steep slopes and intensive human activities, which have contributed to severe soil erosion and a plentiful sediment load. To control the severe soil erosion, a series of soil conservation measures have been adopted since the 1950s. Through the recent lasting ecological construction, this region has formed secondary vegetation with deciduous broad-leaved forests and shrub-grasslands [33].

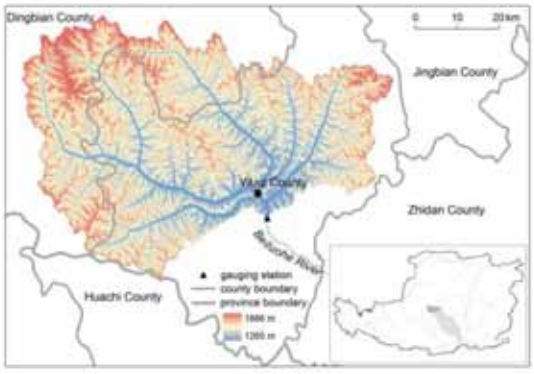

FIGURE 1
Location of the study area and hydrological station in the upper reaches of the Beiluo catchment

The daily streamflow and sediment load data of the Wuqi hydrologic station used in this study were obtained from the Water Resources Committee of the Yellow River Conservancy Commission of China. The daily precipitation data of Wuqi, Dingbian, Zhidan, Huachi, and Huanxian were obtained from the State Meteorology Bureau of China. All of the data were from 1963 to 2011. The data used in this study were checked by the corresponding agencies to guarantee their quality. The annual precipitation and precipitation erosivity [34] were computed by a Thiessen polygon.

Methods. Trends analysis. The Mann-Kendall (MK) method is widely used to test trends in hydrological and climatological time series, and it has been used for trend detection as a result of its robustness for distributed and censored data [35-37]. Therefore, this method can be used to determine whether a significant trend exists for the hydro-meteorological series time. The Mann-Kendall test statistic, S, is calculated using the following formula:

$$S = \sum_{k=1}^{n=1} \sum_{j=k+1}^{n} \mathrm{sgn}(x_j - x_k), k < j < n \quad (1)$$

$$\mathrm{sgn}(\theta) = \begin{cases} +1, x_j - x_k > 0 \\ 0, x_j - x_k = 0 \\ -1, x_j - x_k < 0 \end{cases} \quad (2)$$

where n is the data set record length and x_j and x_k are the values in periods j and k (j>k), respectively.

The Mann–Kendall test has two parameters of importance to trend detection. These parameters are the significance level, which indicates the trend's strength, and the slope magnitude estimate, which indicates the direction as well as the rate of change. Under the null hypothesis that there is no trend in the data, for n>0 the distribution of the statistics of S is approximately normally distributed with the mean and variance of the following:

$$\mathrm{var}(S) = \frac{n(n-1)(2n+5)}{18} \quad (3)$$

A positive value of Z indicates an upward trend, whereas a negative value represents a downward trend in the data. The null hypothesis is rejected at a significance level of α if $|Z| > Z_{(1-\alpha/2)}$, where $Z_{(1-\alpha/2)}$ is the value of the standard normal distribution with a probability of exceedance of $\alpha/2$. The standard test statistic, Z, is computed as follows:

$$z = \frac{S}{[\mathrm{var}(S)]^{0.5}} \quad (4)$$

If a linear trend is present, the magnitude of the trend is estimated using a nonparametric median-based slope method proposed by Sen [38] and extended by Hirsch et al. [39]:

$$\beta = Median\left[\frac{x_j - x_k}{j-k}\right] \quad (5)$$

where 1<j<k<n.β is the median of all possible combinations of pairs for the whole data series.

Change point analysis. In this study, the Nonparametric Pettit test [40] was used to test the change point in the hydrological and precipitation time series. The Pettit statistic, $U_{t,N}$ [41], was calculated using the following formula:

$$U_{t,N} = U_{t-1,N} + \sum_{j=1}^{N} \mathrm{sgn}(x_j - x_k) \quad (6)$$

$$\mathrm{sgn}(\theta)=\begin{cases}+1, x_j - x_k > 0\\ 0, x_j - x_k = 0\\ -1, x_j - x_k < 0\end{cases} \quad (7)$$

where N is the number of observed data series and x_j and x_k are the values in periods j and k (j>k), respectively.

The test statistic counts the number of times a member of the first sample exceeds a member of the second sample. The null hypothesis of Pettit's test is the absence of a changing point. The test statistic KN and significance test of dependent probability (p) are computed as follows:

$$K_t = Max_{1\le t\le N} |U_{t,\ N,}| \quad (8)$$

$$p \cong 2\exp\{-6(K_N^2)/(N^3+N^2)\} \quad (9)$$

Estimates of anthropogenic impact on hydrological factors. The location of the basin determined the atmospheric circulation patterns and climate type, further determining the amount of streamflow and sediment load and their spatial and temporal characteristics. Increasing human activities can change the components and the energy distribution of the streamflow, which influences the process of streamflow and sediment transport. Separating the effects of climate from all factors on the change in mean streamflow and sediment yield can contribute to understanding the hydrological responses to vegetation restoration and their driving forces in a catchment on the Loess hilly-gully area. A double-mass curve [42], correction coefficient methods [43] and empirical hydrologic methods [44] are usually used to estimate the effect of climate and human activities on the hydrological behaviour of a basin. In this study, we used the three methods to interactively inspect the calculation results.

RESULTS AND DISCUSSION

Trends in annual hydrological factors. The trends in streamflow and sediment load were tested using the Mann-Kendall non-parametric test and Spearman method. As shown in Table 1, there was a decreasing trend of the annual streamflow and sediment load at the significance level of p<0.01. The average annual streamflow and sediment load were 34.3 mm and 13.9×10^3 t·km^{-2} in the 1960s compared with 18.2 mm and 3.1×10^3t/km^2 in the 21st century, respectively. The average rates for precipitation, streamflow, sediment load were -1.21 mm, -0.26 mm, 172 t/km^2 per year, respectively. These results are consistent with the findings that afforestation and integrated soil conservation projects have some decreasing effects on streamflow and sediment yield [3, 7-9, 11, 21].

TABLE 1
Results of trend tests for streamflow and sediment load modulus in catchment

Method	Streamflow depth		Sediment load modulus	
	Statistics	significance	statistics	significance
Spearman	-0.38	**	-0.42	**
Mann-Kendall	-2.75	**	-3.05	**

Note: ** indicates significance level of 0.01.

To further describe the trend of streamflow and sediment load, the exceedance deciles for streamflow and sediment were used in the analysis. The results are summarized in Tab 2. Significant trends were indicated for 61.54% of the streamflow records. In total, 7 of 39 streamflow series were identified in the catchments with significant upward trends, and 15 of 39 streamflow records show significant downward trends. The trend tests of streamflow for high-frequency events indicated significant upward trends annually and in the flood season but non-significant downward trends in the non-flood season. The streamflow for low-frequency events exhibited a significant upward trend in the non-flood season but no significant upward trends in the flood season. For the Q_5:Q_{50} series, the records indicate a significant downward trend of the wet index variability, apart from the non-flood season record, showing that a decreasing magnitude of high flow. However, the trend tests for the Q_{95}:Q_{50} records indicate significant upward trends of the dry index variability, showing an increasing magnitude of low flow. All data series of the sediment load indicate a significant download trend with the exception of high-frequency events and the Q_{95}:Q_{50}.

Change points of hydrological factors. Mutation refers to the sequence of data affected by a factor, leading to the data from a steady-state transition to another stable state. As shown in Fig.2, two change points were detected in 1979 and 2002 for streamflow and sediment load in annual and flood season at the significance levels of p<0.05 and p<0.01, respectively. It took two years for hydrological factors to show a statically significant change after the Grain for Green Program. The delay in hydrological response was related to the lag effect and cumulative effect of ecological management measures. It should be noted that catchment response time was mainly dependent on the extent of vegetation change and rate of tree growth[45]. The viewpoint also showed that the

TABLE 2
Results of trend tests for streamflow, and sediment load in the catchment

Record	Streamflow			sediment load		
	Annual	May-October	November-April	annual	May-October	November-April
Q5	-3.22**	-3.57**	-1.30^{NS}	-4.23**	-3.59**	-6.08**
Q10	-2.83**	-3.34**	-0.10^{NS}	-4.39**	-3.99**	-7.04**
Q20	-2.24*	-2.53*	-0.81^{NS}	-5.35**	-3.40**	-6.87**
Q30	-2.80**	-1.9 ^{NS}	-2.82**	-5.66**	-3.28**	-6.57**
Q40	-2.67**	-1.69^{NS}	-4.10**	-5.22**	-3.22**	-6.32**
Q50	-2.76**	-2.30*	-2.69**	-4.83**	-2.85**	-5.93**
Q60	-2.77**	-2.31*	-1.47^{NS}	-5.19**	-2.78**	-4.57**
Q70	-1.16^{NS}	-1.58^{NS}	-0.08^{NS}	-4.90**	-2.61**	-3.94**
Q80	0.05^{NS}	-1.11^{NS}	2.09*	-3.89**	-2.05*	-3.20**
Q90	2.40*	-0.30 ^{NS}	4.17**	-3.26**	-1.91 ^{NS}	-2.94**
Q95:	3.92**	0.36 ^{NS}	4.26**	-2.92**	-1.85 ^{NS}	-2.60**
Q5:Q50	-2.44*	-3.39**	1.41^{NS}	-4.70**	-2.39**	-5.00**
Q95:Q50	4.83**	2.06*	4.96**	-2.62**	1.76 ^{NS}	-4.50**

Note: ** and * indicate significance level of 0.01 and 0.05, NS indicates that significance level exceeds 0.05.

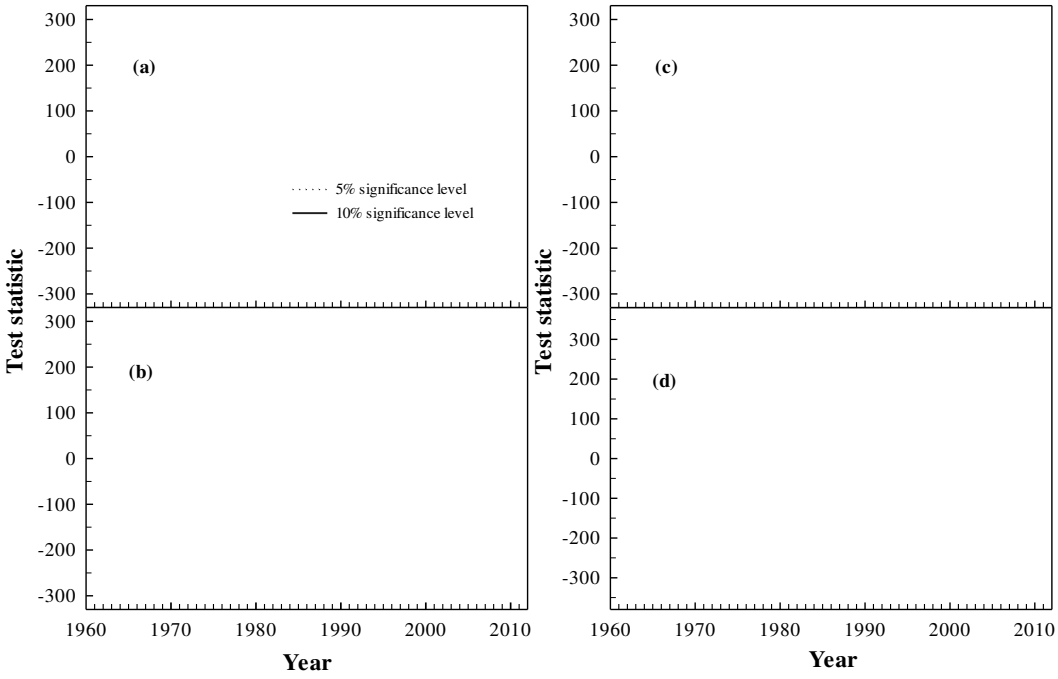

FIGURE 2
Pettit test for detecting change point in (a) annual streamflow, (b) flood season streamflow, (c) annual sediment load and (d) flood season sediment load. The horizontal lines in each graphic represent the significance levels of 1% (dotted) and 5% (solid).

time to reach a statistically significant change in streamflow and sediment load happened, when the accumulated area of artificial vegetation coverage exceeded about 20% [27,46].The results of the change point test for all data series are summarized in Table 3. Change points were detected in 20 of 39 tests, and most of these change points were detected in the annual and non-flood season streamflow records. High-frequency streamflow change points were detected in 1980, 1991 and 2002 in annual and flood season records. The low-frequency streamflow data show change points in 1977, 1983 and 1998 in the annual and non-flood season records but no change point in the flood season. No change points were detected in the Q_5:Q_{50} data. Two change points were found in 1985 and 1999 in the annual data and in 1997 and 2001 in the non-flood season data, but only one point was found in 2002 in the flood season for the Q_{95}:Q_{50} records. For the sediment load, change points between 1988 and 2002 were detected in all records.

According to the processes of soil and water conservation on the Loess Plateau, considering the distribution characteristics of the sequential streamflow, sediment load data and other study results [24,28,30,47,48], the data could be divided into PI (baseline period from 1963 to 1979), PII (the period of the effect on soil and water conservation from 1979 to the change point of 2002) and PIII ("Grain for Green" period from 2003 to 2011) to analyse the degree of evolution of the hydrological regime.

TABLE 3
Change point detection results for runoff and sediment in the catchment

Record	Streamflow			sediment load		
	Annual	May-October	November-April	annual	May-October	November-April
Q5	2002*	2002**	NS	1988**,2002**	2002**	1992**
Q10	1991*	2002**	NS	1991**	2002**	1991**
Q20	2002*	NS	NS	1991**	1991**,2002**	1991**
Q30	1980*	NS	1978**	1991**	1991**	1987**
Q40	1991*,2002**	NS	1979**,1999**	1988**	1991**	1992**
Q50	1990*,2002**	NS	1979*,1997**	1988**	1990**	1994**
Q60	1998**	NS	NS	1991**	1990**	1994**
Q70	1998*	NS	NS	1991**	1989**	1994**
Q80	NS	NS	1983**	1993**	1989**,2004*	1994**
Q90	1977**	NS	1983**	1994**	1989**,2004*	1994**
Q95:	1977**	NS	1977**	1993**	1988*	1994**
Q5:Q50	NS	NS	NS	1999*	2002*	1994**
Q95:Q50	1985**,1999*	2002*	1977**,2001*	1993**	1993**	1994**

Note: ** and * indicate a significance level of 0.01 and 0.05, respectively, and NS indicates that the significance level exceeds 0.05.

TABLE 4
Annual statistical values of hydrological factors

Theme	PI (1963-1979)			PII (1980-2002)			PIII (2003-2011)		
	average	Max/Min	C_V	average	Max/Min	C_V	average	Max/Min	C_V
streamflow/ mm	31.2	3.7	0.39	28.2	5.8	0.54	16.0	1.8	0.20
sediment load/ 10^3t.km^{-2}	11.5	12	0.67	10.1	32	1.17	1.7	23	0.85

Hydrological characteristics before and after change point. The mean values, extreme ratio and coefficient of variation in the pre-change point and post-change point periods were calculated to investigate the changes in streamflow and sediment load. Table 4 summarizes the data on their characteristics. The mean annual streamflow values pre- and post-change point were 31.2 mm, 28.2 mm and 16 mm, showing a reduction in different periods. Compared with PI, the mean annual streamflow decreased by 9.6%, 48.7% in PII and PIII, respectively. Accordingly, the dimension of the induction in the average sediment load was greater than the streamflow. The extreme ratio and the coefficient of variation in the annual streamflow and sediment load in different periods after the change point also changed. It can be noted that compared with PI, the extreme ratio and coefficient of variation of the streamflow increased in the PII, whereas they decreased in PIII. The extreme ratio and coefficient of variation in streamflow increased by 56.8% and 38.5% in the PII, whereas they decreased by 51.4% and 48.7% in the PIII. However, compared with PI, the extreme ratio and the coefficient of variation in the sediment load increased. In PII, the changes are inconsistent with the expected impact of soil and water conservation. The reason is that a rainstorm occurred on August 30 and 31 in 1994 in Wuqi and Zhidan [3,49]. Although the yearly precipitation was 490 mm, the streamflow was an unbelievable 88 mm, and sediment load was up to 59325 t·km^{-2}, which had a great effect on the extreme ratio and the coefficient of variation. This indicates that the effect of integrated measures on high-intensity rainstorms is relatively small. However, the observed changes in PIII can be explained by the fact that forests and pastures gradually act as a buffer in reducing peak streamflow and supplying dry flow. Simultaneously, because of the increased zero-sediment days, the effect on decreasing soil erosion was more obvious. This also showed that ecological management can reduce streamflow more than sediment load [28].

To analyse the effects of water and soil conservation, daily streamflow and sediment load duration curves in the pre-change point and post-change point periods were derived in figure 3. The slope curve of FDC is a sign of the hydrogeological and soil texture conditions in the region[3,8]. For the streamflow, the slopes of FDC show little difference between 10% and 85% but steeper slopes in 0%～10% and 85%～100% in the three periods. Because of the increased number of zero-sediment days, large relative variability in the daily sediment load occurred with steeper slopes period by period in the FDC. The relative change in streamflow and sediment load, defined as the difference in the pre-change point and post-change point divided by the change point ($Q_{after} - Q_{before}$)/Q_{before}), was calculated in different periods for high (exceeding 5% of the time), median (exceeding 50% of the time) and low (exceeding 95% of the time) streamflow and sediment load. Compared with PI, the streamflow decreased period by period in 5% and 50%, and the extent of change increased greatly. The streamflow in PII decreased with -21.7% and -4.4% in the 5% and 50% percentiles and further decreased with -42.4% and -23.8% in PIII. Meanwhile, the low flow of the 95% percentile increased with 107.6% in PII and 138.1% in PIII.

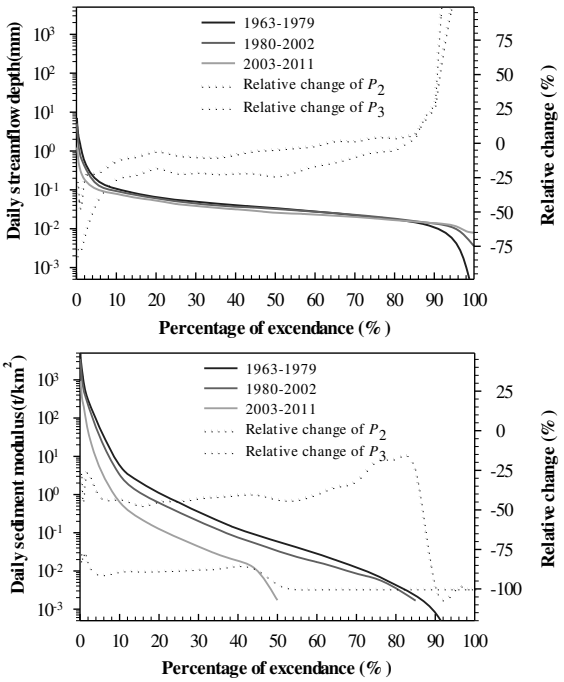

FIGURE 3
Duration curves of streamflow and sediment during 1963-1979, 1980-2002, and 2003-2009

In summary, larger percentage changes in the streamflow regime were observed in PIII than in PII. It was reported that the area of vegetation restoration was not large enough in PII [50], so the engineering measures worked by intercepting the sediment load and releasing the streamflow, leading to the high flow and median flow decreasing in PII. Due to not proper maintenance, engineering measures, especially the check dams, lost functions gradually in early 1980s [8,49,51]. So the effects of engineering measures became small and the increasing of vegetation cover became great during PIII. Liu et al. [52] indicated that the change of vegetation coverage lead to the change of low flow. The implementation of "Grain for Green" project increased the evapotranspiration and canopy interception, leading to precipitation supplemented to the streamflow by surface streamflow little but to deep soil and groundwater systems relatively great[53-54]. The area of vegetation cover increased and community functional diversity established after 30 years' vegetation succession also improved the soil structure including soil permeability and water holding capacity. They promoted the supply of slope soil streamflow to the river streamflow, resulting in the low flow increased[55].This showed the alterations in vegetation cover can notably alter low flow by influencing base-flow composition[56-57].

The sediment load decreased with -41.9% and -43.4% in the 5% and 50% percentiles in PII and further to -91.1% and -97.1% in PIII. The number of zero-sediment load days increased with each period. The extent of reduction in sediment load was greater than that of streamflow with the periods altered, and the change in sediment load was negative. The results above indicate that the water and soil conservation measures and the "Grain for Green" project reflect a great ecological effect in decreasing flood volumes, compensating streamflow, and reducing erosion and sediment transport [5,27,45].

The factors influencing hydrological regime. The change of meteorological factor. The water balance depends on a stable climate system. Changes in the streamflow and sediment processes in a catchment are closely related to precipitation and potential evapotranspiration. Generally, regional patterns of changes in hydroclimate are complex and uncertain, with both regional increases and decreases in precipitation and PET [58]. Climate variability is the dominate environment factor for hydrological regime changes in the study area.To fully understand the potential effect of climatic changes on hydrological factors, the Mann–Kendall and Pettitt's tests were applied to calculate the annual precipitation (P) and potential evaporation (PET), and the results are shown in Table 5. Precipitation exhibited an insignificant ($p<0.05$) decreasing trend over the last 50 years. The average annual precipitation was 429.9 mm in the 1960s, compared with 401.3 mm in the 21st century. Correspondingly, no change point was detected ($p<0.05$) in the annual precipitation. Similar results in trends and change point analysis were found in the flood season and the non-flood season. As for annual PET, no trend was identified in the catchments at the 0.05 level of significance. Although precipitation and PET had no significant downward trend, conversely, the streamflow and sediment load significantly decreased over the same time period. It was referred that the changes in regional precipitation and PET were insufficient for the significant decline in hydrological regimes in this region. These analyses show that for the streamflow and sediment load, the significant decrease over the six decades was not influenced by only climatic factors. The finding also indicates that the anthropogenic impact on streamflow and sediment load reduction was bigger than the climatic factors.

TABLE 5
Results of trend and change point for precipitation and PET in different periods

Period	Precipitation		PET	
	Z statistic	Change point	Z statistic	Change point
May-October	-0.62^{NS}	NS	-0.12^{NS}	NS
November-April	-1.86^{NS}	NS	-0.18^{NS}	NS
Annual	-1.12^{NS}	NS	-0.16^{NS}	NS

Note: NS indicate that significance level exceeds 0.05.

TABLE 6
Annual statistical values of meteorological factors

Theme	PI (1963-1979)			PII (1980-2002)			PIII (2003-2011)		
	average	Max/Min	C_V	average	Max/Min	C_V	average	Max/Min	C_V
Precipitation / Mm	430.1	2.6	0.25	408.8	2.2	0.21	385.3	1.6	0.19
PET / Mm	1783.8	1.5	0.08	1787.3	1.3	0.09	1788.6	1.2	0.05

TABLE 7
Cumulative areas adopted by major soil and water conservation practices and corresponding percentage area from 1950 to 2006.

Management Measures	Cumulative area in different periods					
	1950-1959	1960-1969	1970-1979	1980-1989	1990-1999	1999-2006
Terrace (km^2)	1.36	17.72	42.94	67.48	101.90	132.23
Afforestation (km^2)	26.24	82.81	143.82	277.41	420.89	754.53
Pasture (km^2)	0.68	6.48	18.06	84.18	134.62	342.84
Sediment-Trapping Dams	0.34	5.11	9.88	9.88	9.88	9.88
Cumulative conservation area (km^2)	28.63	112.12	214.70	438.95	667.29	1239.49
Percentage area (%)	0.84	3.29	6.3	12.88	19.58	36.37

To fully understand the nature of streamflow changes, it is necessary to determine precipitation and PET variations. The mean values, extreme ratio and coefficient of variation of precipitation, and PET in the three periods were analysed. The extreme ratio and the coefficient of variation meteorological factors were a key measure of the inter-annual variability of the hydrological cycle. In Table 6, the mean, extreme ratio and coefficient of variation of the annual precipitation exhibited insignificant changes between PI and PII, but a decline in PIII was identified. The mean annual PET basically had no change during different periods. It can be noted that compared with PI, the extreme ratio and coefficient of variation of PET decreased by 9.6% in PII and by 48.7% in PIII.

Implementation of soil and water conservation measures. Numerous soil and water conservation measures through various government-sponsored programmes and environmental governance movements have been adopted in the Loess Plateau[49]. The cumulative area and percentage of area treated by management actions in this basin are listed in Table 7 [8,47,48]. The upper of Beiluo River Catchment has been subjected to many measures, including the construction of terraces, sediment-trapping dams, and fish-scale pits, horizontal trenches and the planting of trees and pasture. The engineering projects can significantly and immediately intercept more hill-slope surface streamflow and sediment load into the mainstream river, weaken high-flow magnitudes and peaks, and decrease sediment deposition[9,51]. Hydrological regime regulation is an important vegetation ecosystem service. It is involved in natural processes, such as regional climate circulation, the hydrological cycle, soil conditions, and other natural processes[59,60]. The improvement of vegetation cover reduced the surface streamflow and the frequency of the hyperconcentrated flow, enhancing the infiltration characteristics by increasing precipitation interception and evapotranspiration.

Prior to the 1960s, the implementation of management action was slow, and it significantly accelerated after the 1970s. In particular, the cumulative area with conservation measures has increased rapidly since 1999. The control area of sediment-load dams has not changed since 1970. Meanwhile, it was reported that more than 80% of sediment-trapping dams were destroyed by fierce rainstorms in early 1980s[8], so they may become abandoned dams and lose effectiveness. This indicates that the effect of engineering works greatly weakened during PIII. With the implementation of the strict policy of the Grain for Green Program, afforestation and pasture areas grew rapidly, but engineering measures increased slowly. By 2006, the cumulative area under conservation was 1239.49 km^2, and different types of conservation measures covered 36.67% of the territory. From 1999 to 2006, 572.2 km^2 of the territory was to be protected, including 30.33 km^2 of terrace, 333.64 km^2 of forest, and 208.22 km^2 of pasture. The effect of afforestation measures on regulating hydrological regime was more and more significant during PIII. Certainly, it can be inferred that the vegetation coverage exceeded about 20%, the article vegetation played an important role in inducing streamflow discharge and decreasing sediment deposition[23,27].

Effects of climate change and human activities on streamflow and sediment load. The double-mass curve, correction coefficient methods and empirical hydrologic methods were used to evaluate the effect of variable climate and human activities on the change in streamflow and sediment load, as shown in Tab 8. All three methods are built on the basis of the relationship of precipitation to stream

TABLE 8
The impacts of climate change and human activities on streamflow and sediment

Period	The impacts of human activities on streamflow/%				The impacts of human activities on sediment load/%			
	Correcting coefficient	Dual-mass curve	Hydrological modelling	mean	Correcting coefficient	Dual-mass curve	Hydrological modelling	mean
1980-2002	46.9	35.7	31.9	38.2	78.8	48.6	26.8	51.4
2003-2011	76.0	76.3	71.8	74.7	87.7	94.3	78.2	86.7

flow and erosion by precipitation to sediment load. By using the actual streamflow and sediment load data in PII and PIII and climate conditions to evaluate the difference between observation and calculation, the effects of soil conservation measures and the "Grain for Green" project on the change of streamflow and sediment load were investigated. The three methods can corroborate each other for more reliable results. The correction coefficient method is optimal for evaluating the effect of human activities on streamflow; however, the optimal estimation for the effect on sediment load is obtained by the double-mass curve. This may be due to the difference in the fitting equation. The average annual streamflow in PI and PII were found to be 31.2 mm/a and 28.2 mm/a, respectively. The sediment loads were 11.5×10^3 t/km^2·a and 10.1×10^3 t/km^2·a, respectively. With the comprehensive measures of soil and water conservation over the 20 years, the average annual streamflow decreased by 3 mm, and the contribution of human activities was 38.2%. The average annual sediment load decreased by 1.4×10^3 t/km^2·a, and the contribution of human activities was 51.4%. The measures of the "Grain for Green" programme have been a key factor to the environmental improvement, with the average annual streamflow and sediment load 16.0 mm and 1.7×10^3 t/km^2·a in PIII, respectively. Compared with PI, they decreased by 15.2 mm and 9.6×10^3 t/km^2·a, respectively. The contributions of human activities were 74.7% and 86.7%, respectively. Although increasing population, the development of urbanization and exploitable resources comprise the cause for the increase in sediment load, large-scale vegetation restoration plays a key function in decreasing flood volumes and compensating streamflow and reducing erosion and sediment transport[8,50,51].

CONCLUSIONS

In this study, the upper reaches of the Beiluo catchment are regarded as a characteristic "Grain for Green" project in the Loess hilly and gully region, China. Streamflow and sediment load data from 1963 to 2011 were used to investigate the hydrological responses to the LUCC. There was no significant pattern of change in annual precipitation. Both the streamflow and sediment load had a negative trend at a significance level of $P<0.01$, mostly because of decreasing high flow (5%) in the flood season in subsequent years. Pettitt's test and the distributed characteristics of the sequential data provided two change points in 1979 and 2002, respectively.

Compared with PI (1963-1979), the mean annual streamflow decreased by 9.6%, 48.7% in PII and PIII, respectively, but the dimension of the induction in the average sediment load was greater than the streamflow. The extreme ratio and the coefficient of variation about them in different periods after the change point also changed. The analysis of the flow duration curves indicated that the daily streamflow slopes showed little difference between 10% and 85% but steeper slopes in 0%～10% and 85%～100% in the three periods. Because of the increased number of zero-sediment days, large relative variability occurred with steeper slopes period by period in the daily sediment load. Compared with PI, the streamflow for 5% and 50% decreased by 21.7% and 4.4% in PII, whereas it increased by 107.6% for 95%. The suspended sediment load decreased more significantly by 41.9% and 43.4% for 5% and 50% and no suspended sediment days almost constant for 95%. In PIII, the streamflow further decreased by 42.4% and 23.8% for 5% and 50%, while the suspended sediment load decreased by 91.1% and 97.1%. For 95%，streamflow rose by 138.1%, and no sediment days increased.

The effects of climate change and human activities can lead to the decrease of streamflow, but the contribution rate differs; it was 61.8% and 38.2% in PII, respectively. Meanwhile, the effects of climate and human activities on the change in sediment load were 25.3% and 74.7%, respectively. They accounted for 48.6% and 51.4% of the streamflow decrease in PIII, respectively. As for the decrease in sediment load, they contributed 13.3% and 86.7%, respectively. With the double-mass curve, correction coefficient methods and empirical hydrologic methods aimed to investigate the effect of human activities and climate change on the changes in streamflow and sediment load, the result could overestimate the contribution rate of human activities. Among these three methods, only precipitation and non-precipitation were separated, but increased evapotranspiration caused by the rising temperatures was not considered, which could result in the decrease of the streamflow and the capacity for the sediment transport. Meanwhile, the results may be not precise

for the cyclical changes of climate, such as precipitation.

ACKNOWLEDGEMENTS

This study is supported by the National Natural Science Foundation of China (Grant Nos. 41230852, 41101265), and the funding from the Chinese Academy of Science (KZZD-EW-04-03; KZCX2-XB3-13).Thanks are given to two anonymous reviewers for their constructive comments.

REFERENCES

[1] Shi, H., Shao M. (2000) Soil and water loss from the Loess Plateau in China. *J. Arid Environ. 45*, 9-20.

[2] Zhang, X., Walling, D.E., Quine, T.A., Wen.A. (1997) Use of reservoir deposits and caesium-137 measurements to investigate the erosional response of a small drainage basin in the rolling loess plateau region of China. *Land Degrad. Dev. 8*, 1-16.

[3] Tang, K. (1993) The changes of erosion, runoff and sediment in the Yellow River. Beijing: Science China Press. (in Chinese)

[4] Zheng, F., He, X., Gao, X., Tang, K. (2005) Effects of erosion patterns on nutrient loss following deforestation on the Loess Plateau of China. *Agr. ecosyst. environ.*, *108*, 85-97.

[5] Fu, B., Qiu Y., Wang, J., Chen, L. (2002) Effect of land use change on the runoff and erosion for a Gully Catchment of the Loess Plateau, China. *Acta Geographica Sinica.* 57, 717-722. (in Chinese)

[6] Xu, J. (1998) A study of physico-geographical factors for formation of hyperconcentrated flows in the Loess Plateau of China. *Geomorphology*; *24*, 245-255.

[7] Shi, C., Dian, Z., You, L. (2002) Changes in sediment yield of the Yellow River basin of China during the Holocene. *Geomorphology*. *46*, 267-283.

[8] Ran, D., Liu, L., Zhao, L. (2000) The soil conservation practices and streamflow and sediment load changes in the Hekou-Longmen region of middle reaches of Yellow River. Yellow River Water Conservancy Press: Zhengzhou, China. (in Chinese)

[9] Yao, W., Li, Z., Kang, L. (2005) The effects of controlling soil erosion on environment on the Loess Plateau. *Science and Technology Press*: Beijing, China. (in Chinese)

[10] Wang, Y., Fu, B., Chen, L., Gao, Y. (2011) Check dam in the Loess Plateau of China: engineering for environmental services and food security. *Environ. sci. technol.*, *45*, 10298-10299.

[11] Xu, X., Zhang, H., Zhang, O. (2004) Development of check-dam systems in gullies on the Loess Plateau, China. *Environ. Sci. Policy*, *7*, 79-86.

[12] Ran, L., Lu, X., Xin, Z., Yang, X. (2013) Cumulative sediment trapping by reservoirs in large river basins: a case study of the Yellow River basin. *Global Planet. Change. 100*, 308-319.

[13] Zhang, B., Wu, P., Zhao, X. (2011) Detecting and analysis of spatial and temporal variation of vegetation cover in the Loess Plateau during 1982-2009.*Transactions of the CSAE*. *27*, 1982-2009. (in Chinese)

[14] Xin, Z., Xu, J.X. (2007) The responses of spatiotemporal variation of vegetation cover to climate in the Loess Plateau. *Progress in Natural Science*. *17*, 770-778. (in Chinese)

[15] Sun, G., Zuo, C., Liu, S., Liu, M., McNulty, S.G., Vose, J.M. (2008) Watershed evapotranspiration increased due to changes in vegetation composition and structure under a subtropical climate. *Journal of the American Water Resources Association* . *44*, 1164–1175.

[16] Smakhtin, V. (2001) Low flow hydrology: a review. *Journal of Hydrology.* 240: 144

[17] Gao, C., Yu, X. (2000) Review on researches of water conservation forests. *Journal of Beijing Forestry University. 22*, 78-82. (in Chinese)

[18] Yao, Y.B., Wang, Y.R., Li, Y.H., Zhang, X.Y. (2005) Climate warming and drying and its environmental effects in the Loess Plateau. *Resources science*. *27*, 146-152. (in Chinese)

[19] Cheng, L.X., Zhu, W.Q., Wang, W., Zhou, X., Li, W. (1998) Studies on climate change in china in recent 45years. *Acta Meteorological Sinica*. *56*, 257-271. (in Chinese)

[20] Li, Z.C., Wei, Z.G., Wen, J., Fu, R. (2008) Analyses on climate variation characteristics over the Loess Plateau in recent 50 years. *Journal of Arid and Resources and Environment. 22*, 57-62. (in Chinese)

[21] Zhao, F.F., Zhang, L., Xu, Z.X., Scott, D.F. (2010) Evaluation of methods for estimating the effects of vegetation change and climate variability on streamflow. *Water Resources Research*. *46*, W03505.

[22] Xu, J.X., Sun, J., (2004c) Effect of erosion control measures on sediment delivery ratio. Advance in Water Science, *15(1)*:29-34.

[23] Zhu, H.F., Kang, M.Y., Zhao, W.W., Guo, W.W. (2008) Effect of human activities on flood season runoff in water and soil conservation region. *Advances in Water Science. 3*, 400-406. (in Chinese)

[24] Zhang, X., Zhang, L., Zhao, J., Rustomji, P., Hairsine, P. (2008) Responses of streamflow to changes in climate and land use/cover in the Loess Plateau, China. Water Resour. Res. *44*, doi:10.1029/2007WR006711.

[25] Zhao, G., Tian, P., Mu, X., Jiao, J., Wang, F., Gao, P. (2014) Quantifying the impact of climate variability and human activities on streamflow in the middle reaches of the Yellow River basin, China. *J. Hydrol. 519*, 387-398.

[26] Gao, Z., Fu, Y., Li, Y., Liu, J., Zhang, X. (2012) Trends of streamflow, sediment load and their dynamic relation for the catchments in the middle reaches of the Yellow River over the past five decades. *Hydrol. Earth Syst. Sci. 16*, 3219-3231.

[27] Cai, Q. (2001) Soil erosion and management on the Loess Plateau. *J. Geogr. Sci. 11*, 53-70.

[28] Mu, X., Zhang, L., McVicar, T.R., Basang, C. (2007) Analysis of the impact of conservation measures on streamflow regime in catchments of the Loess Plateau, China. *Hydrol. Process. 21*, 2124-2134.

[29] Wan, L., Zhang, X., Ma, Q., Zhang, J., Ma, T., Sun, Y. (2013) Spatiotemporal characteristics of precipitation and extreme events on the Loess Plateau of China between 1957 and 2009. *Hydrol. Process*. doi: 0.1002/hyp.9951.

[30] Mu, X., Basang, C., Zhang, L., Gao, P., Wang, F., Zhang, X. (2007) Impact of soil conservation measures on runoff and sediment in Hekou-Longmen region of the Yellow River. *Journal of Sediment Research. 2*, 36-41. (in Chinese)

[31] Zhao, G., Mu, X., Tian, P., Wang, F., Gao, P. (2013) Climate changes and their impacts on water resources in semiarid regions: a case study of the Wei River basin, China. *Hydrol. Process.s 27*, 3852-3863.

[32] Yang, G., Ding, G.D., Zhao, T.N., Sun, B. (2005) Study on benefits of soil and water conservation about returning cropland to forest in the Loessy Hilly Region of North Shaanxi-Take Wuqi country in Shaanxi province as an example. *Bulletin of Soil and Water Conservation. 26*, 20-23. (in Chinese)

[33] Qin, W., Zhu, Q.K., Liu, G.Q., Zhang, Y. (2010) Regulation effects of runoff and sediment of ecological conservation in the upper reaches of Beiluo River. *Journal of Hydraulic Engineering. 47*, 1325-1332. (in Chinese)

[34] Zhang, W.B., Xie, Y., Liu, B.Y. (2002) Rainfall erosivity using daily amounts. *Scientia Geographica Sinica.*, *22*, 705- 711. (in Chinese)

[35] Mann, H.B. (1945) Nonparametric tests against trend. *Econometrica: Journal of the Econometric Society* DOI, 245-259.

[36] Kendall, M. (1975) *Rank correlation methods*. Griffin: London, UK.

[37] Yue, S., Pilon, P., Cavadias, G. (2002) Power of the Mann–Kendall and Spearman's rho tests for detecting monotonic trends in hydrological series. *J. hydrol. 259*, 254-271.

[38] Sen, PK.. (1968) Estimates of the regression coefficient based on Kendall's tau. Journal of the American Statistical Association. *63*, 1379–1389.

[39] Hirsch, R.M., Alexander, R.B., Smith, R.A. (1991) Selection of methods for the detection and estimation of trends in water quality. Water Resources Research. *27*, 803–813.

[40] Pettitt, A. (1979) A non-parametric approach to the change-point problem. Applied statistics, *28*, 126-135.

[41] Kiely, G., Albertson, J.D., Parlange, M.B. (1998) Recent trends in diurnal variation of precipitation at Valentia on the west coast of Ireland. Journal of Hydrology. *207*, 270–279.

[42] Zhang, S.H., Liu, S.X., Mo, X., Shu, C., Zheng, C., Hou, B. (2010) Impacts of precipitation variation and soil and water conservation measures on runoff and sediment yield in the Wuding River Basin, middle reaches of the Yellow River. *Journal of Beijing Forestry University. 4*, 161-16. (in Chinese)

[43] Smakhtin, V.U.A. (1999) Concept of Pragmatic Hydrological Time Series Modeling and Its Application in South African Context. Ninth South African National Hydrology Symposium.

[44] Chen, X.H., Liu, M.N., Hu, R.X. (1997) The Analysis of descent and distribution of water and sediment at the middle reaches of the Yellow River. *Hydrology. 1*, 9-23. (in Chinese)

[45] Wei, X.H., Li, W.H., Zhou, G.Y., Liu, S.R., Sun, G. (2005) Forests and streamflow-Consistence and complexity. Journal of Natural Resources. *5*, 761-770. (in Chinese)

[46] Scott, D.F., Smith, R.E. (1997) Preliminary empirical models to predict reductions in total and low flows resulting from afforestation. Water SA. *23(2)*:134-140.

[47] Gao, P., Mu, X.M., Li, R., Wang, W. (2009) Analyses on trend and driving force of runoff and sediment load in the Wuding River. *Journal of Sediment research. 5*, 22-28. (in Chinese)

[48] Zhang, X.P., Zhang, L., Wang, Y., Mu, X. (2009) Tempo-spatially responses of the annual streamflow to LUCC in the middle reaches of Yellow River. *Science of Soil and Water Conservation. 7*, 19-26. (in Chinese)

[49] Yao, W., Xu, J., Ran, D. (2011) Analysis and evaluation of the water sand changing regime in catchments of Yellow River basin. In. Zhengzhou: Yellow River Water Conservancy Press. 24-37. (in Chinese)

[50] Zhang, J..J., Zhang, T.T., Zhang, X.P. (2016) Streamflow Regime Variations Following Ecological 649 Management on the Loess Plateau, China. Forests, *7(1)*, 1-6.

[51] Yan, R., Zhang, X.P., Yan, S.J., Zhao, W.H. (2016) The vegetation restoration in the Beiluo River Basin from 1995 to 2014 and their distribution on the landform. Journal of Northeastern University. *Natural Science. 37(11)*, 1598-1603. (in Chinese)

[52] Liu, W.F., Wei, X.H., Fan, H.B., Guo, X.M.,

Liu Y.Q., Zhang, M.F., Li, Q. (2015) Response of flow regimes to deforestation and reforestation in rain-domained large watersed of subtropical China. Hydrological Process. *29(24)*: 503-5015.

[53] Yang, Z., Zhou, Y., Wenninger, J. (2012) Uhlenbrook S. The causes of flow regime shifts in the semi-arid Hailiutu River, Northwest China. Hydrology and Earth System Sciences, *16(1)*: 87-103.

[54] Schneider, C, Laize, C.I, Masey, S, Smakhtin, V. (2011) Streamflow trends and climat linkages in the Zagros Moutains, Iran. Climatic Change, *104(2):* 31-338.

[55] Zhang, M.F., Wei, X.H. (2014) Alteration of flow regimes caused by large-scale foest disturbance: a case study from a large watershed in the interior of British Columbia, Canada. Ecohydrology. *7(2)*:544-566.

[56] Wei, X.H., Liu, W.F., Zhou, P.C. (2013) Quantifying the relative contributions of forest change and cliamtic variability to hydrology in large watersheds: a critical review of research methods. Water. *5(2)*: 728-746.

[57] Zhang, S., Kang, L., Wei, Y. (2010) Research of the impact of human activities on streamflow and sediment load in the middle reaches of Yellow River. Yellow River Water Conservancy Press: Zhengzhou, China.

[58] Milly, P.C., Dunne, K.A., Vecchia, A.V. (2005) Global pattern of trends in streamflow and water availability in a changing climate. *Nature 438*, 347-350.

[59] Nunez, D., Nahuelhual L., Oyarzun C. (2006) Forestes and water: the value of native temperate forests in supplying water for human consumption. Ecological Economics. *58(3)*: 606-616.

[60] Jiapaper, G.L., Chen, X., Bao, A. (2011) M.A comparision of methods for estimating fractional vegetation cover in arid regions. Agricultural and Forest Meteorology. *151(12)*: 1698-1710.

Received: **01.03.2017**
Accepted: **29.07.2017**

CORRESPONDING AUTHOR

Xiaoli Zhang
Forestry College, Beijing Forestry University, Beijing 100083, China

e-mail: zhang-xl@263.net

© by PSP Volume 26 – No. 10/2017 pages 5929-5935 Fresenius Environmental Bulletin

SOLAR ENERGY AS HEAT SOURCE FOR ENHANCING EXCESS SLUDGE REDUCTION

Wei Zheng[1,2,*], Qi-Di Mao[1], Wei Zhang[2], Bing-Zheng Li[1], Xiao-Fang Guo[1]

[1]School of Environment and safety, Taiyuan University of Science and Technology, Taiyuan 030024, P.R. China
[2]Key Laboratory of Renewable Energy Electric-Technology of Hunan Province, Changsha University of Science & Technology, 410076, P.R. China

ABSTRACT

The characteristics and role of solar energy as heat source for enhancing excess sludge reduction were investigated. TS and TVS removal were 36.9% and 44% (summer), 29.3% and 27.5% (autumn), and 18.5% and 24.8% (winter), respectively.

The average temperatures inside and outside the reactor in summer, autumn, and winter on sunny day were 46.3 °C and 28.3 °C, 43.5 °C and 26.1 °C, and 25 °C and 15.3 °C, respectively; On rainy day, the average temperatures inside and outside the reactor were 38.9 °C and 26.4 °C, 28.5 °C and 22.4 °C, and 16.8 °C and 12.8 °C, respectively. The average temperatures inside the reactor in summer, autumn, and winter on sunny day were higher than those outside, and the relationship between the temperatures was 18.3 °C, 17.4 °C, and 9.7 °C, respectively; On rainy day, the relationship was 12.1 °C, 6.1 °C, and 4.1 °C, respectively.

KEYWORDS:
solar energy; excess sludge; minimization; anaerobic digestion; thermophilic digestion

INTRODUCTION

The activated sludge process is the most widely used biological treatment for municipal wastewater worldwide [1-3]. The major byproduct of this process is excess sludge, which entails serious disposal problem for treatment plants. The main treatment of the excess sludge presently employed in China depends on the landfill operation after coagulation filtration. The problem is disposing the excess sludge through this operation is ineffective because it occupies a vast land area. Costs associated with the treatment of excess sludge may also account for 25% to 65% of the total plant operation cost [4, 5]. Anaerobic digestion is employed worldwide for treating excess sludge before final disposal [6]. Mesophilic anaerobic digestion needs lower energy than thermophilic anaerobic digestion. However, the latter is usually characterized by higher growth rate of microorganisms, lower hydraulic retention times, and higher deactivation of pathogenic organisms [7]. Previous studies showed that the enhanced hygienization effect of the thermophilic process complies with the EU policy for eliminating pathogens originating mainly from humans and animals [8-11]. Although thermophilic anaerobic digestion performs better, additional energy is required to heat the digester [10, 12, 13]. This process needs high energy consumption. The Chinese government and municipal wastewater treatment plants face two challenges in disposing excess sludge. The amount of excess sludge requiring treatment and disposal is increasing, and the treatment charge remains high.

Temperature is important for thermophilic anaerobic digestion in determining the rate of digestion, and it affects the cost of sludge treatment. How to reduce the cost is critical to the government and wastewater treatment plants. Solar energy has many advantages, such as availability and low cost, and thus can provide abundant renewable energy (thermal) [14]. However, previous studies on treating excess sludge using solar energy mainly focus on drying and improvement of dewaterability [15-21]. The present study investigated the economical and environmental energy—solar energy—as heat source to enhance the excess sludge reduction during different seasons (summer, autumn and winter), sludge retention time (SRT) (10 and 20 days), and the relationship between temperatures during different seasons and weather.

MATERIALS AND METHODS

Source of waste activated sludge (WAS). The WAS used in this study was obtained from the secondary sedimentation tank of a municipal wastewater treatment plant in Changsha, China. The sludge was concentrated by settling at 4 °C for 24 h, further filtered through a 1 × 1 mm metal sieve, and then stored at 4 °C for later use. The main characteristics of the sludge after filtration are shown in Table 1.

Experimental setup and operation. Figure 1 shows the experimental equipment; the volume of sludge tank (1) was 20.4 L. Twenty liters excess sludge was added into the sludge tank. The sludge

retention time was kept at a constant agitation rate of 140 rpm for 10 and 20 days. Sample was collected and analyzed at 8:00 daily. The temperature inside and outside the reactor was collected at 8:00, 12:00, 16:00, and 20:00, generating the average temperature of one day.

Analytical methods. The values of TS, TVS, TCOD, SCOD, NH_4^+-N, and SP were determined according to standard methods [22]. The pH was determined using a Multiline 330i pH meter standardized by employing buffer solutions of different pH values. The temperature was measured using a thermometer.

RESULTS AND DISCUSSION

The characteristics of sludge used in this study were V=20 L, TS=8.2 g L^{-1}, TVS=5.3 g L^{-1} (summer); TS=14 g L^{-1}, TVS=8 g L^{-1} (autumn); and TS=16.4 g L^{-1}, TVS=8.3 g L^{-1} (winter). The reactor was mixed at 140 rpm during the entire experiment.

Figure 2 shows the SRT on sludge reduction during different seasons. TS and TVS all decreased gradually as time increased at different seasons (Figs. 2a and 2b). TS and TVS decreased from 8.2 and 5.3 g L^{-1} to 5.2 and 3 g L^{-1} (summer), 14 and 8 g L^{-1} to 9.9 and 5.8 g L^{-1} (autumn), and 16.4 and 8.3 g L^{-1} to 13.4 and 7.1 g L^{-1} (winter) at a SRT of 10 days. The removal rate of TS and TVS were 36.9% and 44% at a SRT of 10 days in summer. During the same SRT, TS and TVS removal rate were only 29.3% and 27.5% for autumn, and 18.5% and 24.8% for winter, respectively (Fig. 2c). TS and TVS removal were more pronounced in summer than in autumn and winter. Previous study showed that less-temperature-tolerant microorganisms at high temperature undergo cell lysis and then release thermostable enzymes; these released enzymes can enhance sewage sludge degradation [23, 24]. Increasing SRT can improve TS and TVS removal significantly (Fig. 2d).

TABLE 1
The characteristics of the filtered excess sludge

Parameters	Values
pH	6.9 ± 0.1
SCOD (Soluble Chemical Oxygen Demand) (mg/L)	220-550
TCOD (Total Chemical Oxygen Demand) (mg/L)	8000-14000
TS (Total Solids) (g/L)	7-17
TVS (Total Volatile Solids) (g/L)	4-9
NH_4^+-N (mg/L)	80-160
SP (Soluble phosphate) (mg/L)	10-50

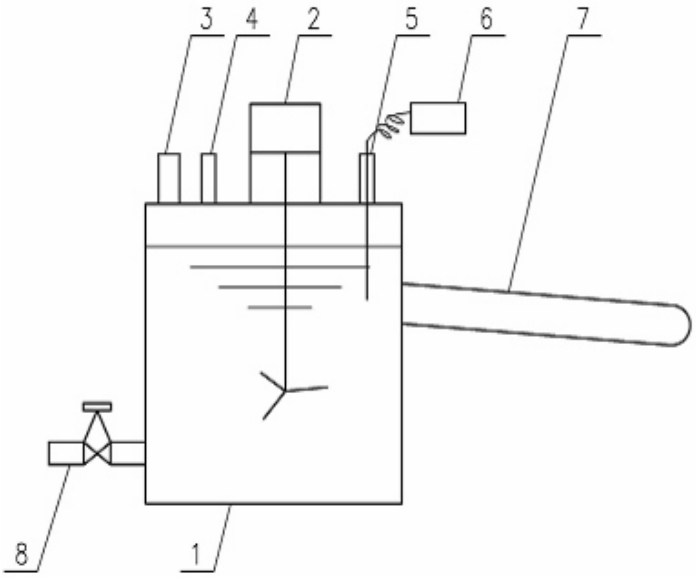

FIGURE 1
Schematic diagram of experimental equipment
1-the sludge tank; 2-agitator; 3-sludge inlet; 4-gas outlet; 5-temperature detector; 6-temperature display panel; 7-vacuum tube; 8-sludge outlet

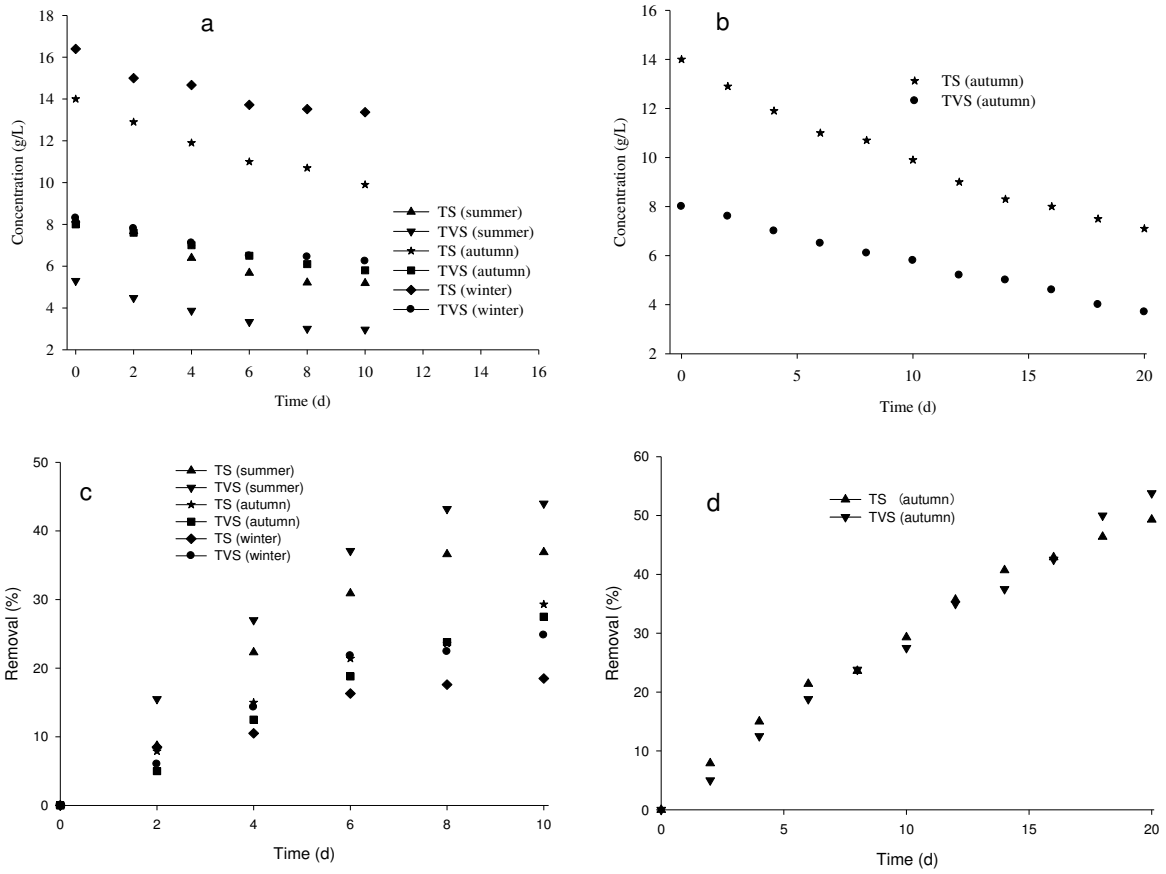

FIGURE 2
Effect of sludge retention time on sludge reduction
(a: 10 days; b: 20 days; c: TS, TVS removal; d: TS, TVS removal)

Figure 3 shows the variations of SCOD, TCOD, and NH_4^+ during different seasons. The concentration of TCOD decreased gradually during the digestion period in winter (Fig. 3c). However, the concentration of TCOD decreased gradually first then exhibited moderate variation after six days in summer (Fig. 3a) and eight days in autumn (Fig. 3b). Sludge digestion needs short time at high temperature. On the contrary, the concentration of SCOD and NH_4^+ increased gradually as digestion time increased during different seasons. Previous studies revealed that a large amount of particulate organics in sludge flocs, including lipids, carbohydrates, proteins and nucleic acid, was transferred into the supernatant during sludge digestion [23, 25]. Carbohydrates and proteins are two of the most predominant organic matters in EPS, which compose a large proportion of SCOD in the supernatant. The proteins ultimately converted to low molecule organic acid, ammonia, and carbon dioxide [26, 27]. Thermophilic digestion leads to the microorganisms' dead, releasing the organic matters to the supernatant. The variations of SCOD/TCOD in summer were significantly higher than in autumn and winter (Fig. 3c). For example, the maximum SCOD/TCOD was 0.647 in summer, 0.195 in autumn, and 0.141 in winter. The research demonstrated that thermostable enzymes can be released by cell lysis because of less-temperature microorganisms' death; the released enzymes further enhance sludge degradation.

Previous study showed that high temperature is advantageous to the volatile suspended solid removal ratio [13]. Fig. 4 shows the variations of temperature inside and outside the reactor during different seasons (summer, autumn, and winter). The maximum, minimum, and average temperature outside the reactor in summer was 32 °C-37 °C, 25 °C-30 °C and 28.5 °C-33.5 °C, respectively.

The average temperature of the reactor was 34 °C-53 °C, with temperatures higher than 50 °C maintained for five days. Furthermore, the maximum, minimum, and average temperature outside the reactor as well as the average temperature of the reactor in autumn and winter was 19 °C-32 °C, 17 °C-20 °C, 18 °C-26 °C, and 23 °C-49 °C and 12 °C-26 °C, 7 °C-13 °C, 10 °C-18 °C, and 14 °C-28 °C, respectively. The average temperature of the reactor in summer was higher than those in autumn and winter were. The removal ratio of TS and TVS in summer was higher than those in autumn and winter were (Fig. 2c).

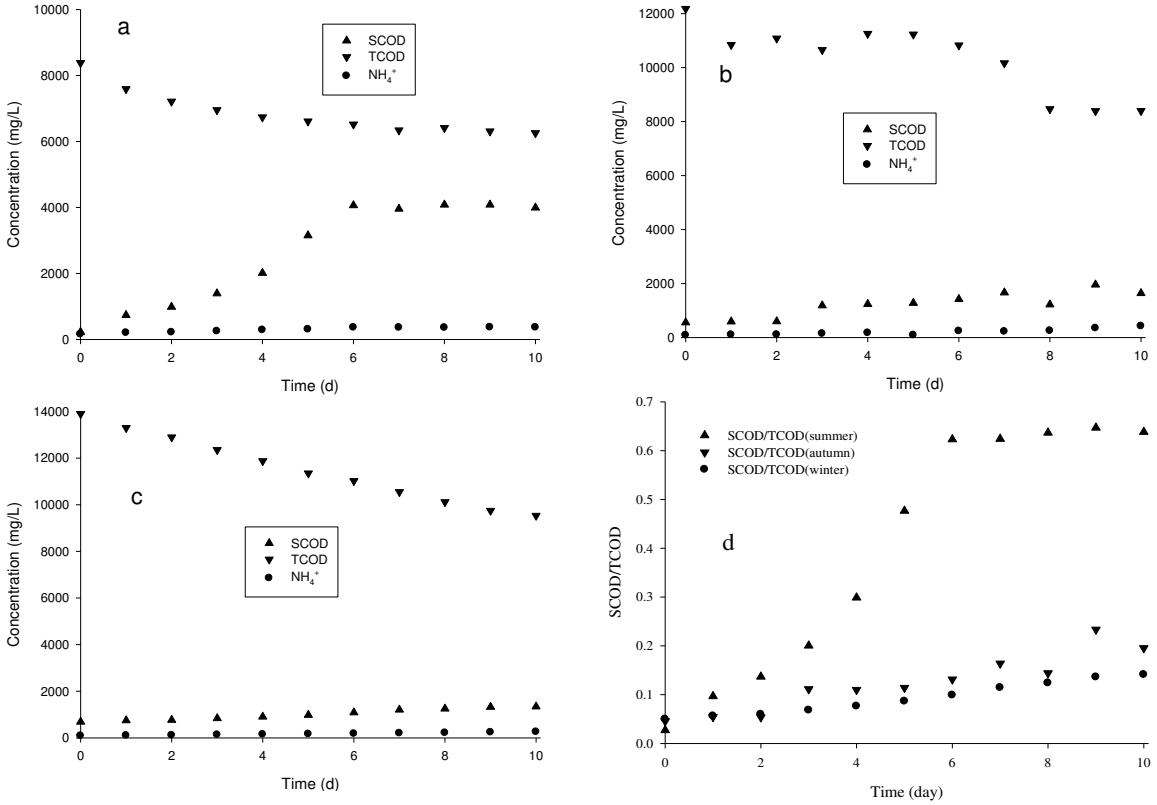

FIGURE 3
Variations of SCOD, TCOD, NH_4^+, and SCOD/TCOD during different seasons (a: summer; b: autumn; c: winter; d: SCOD/TCOD)

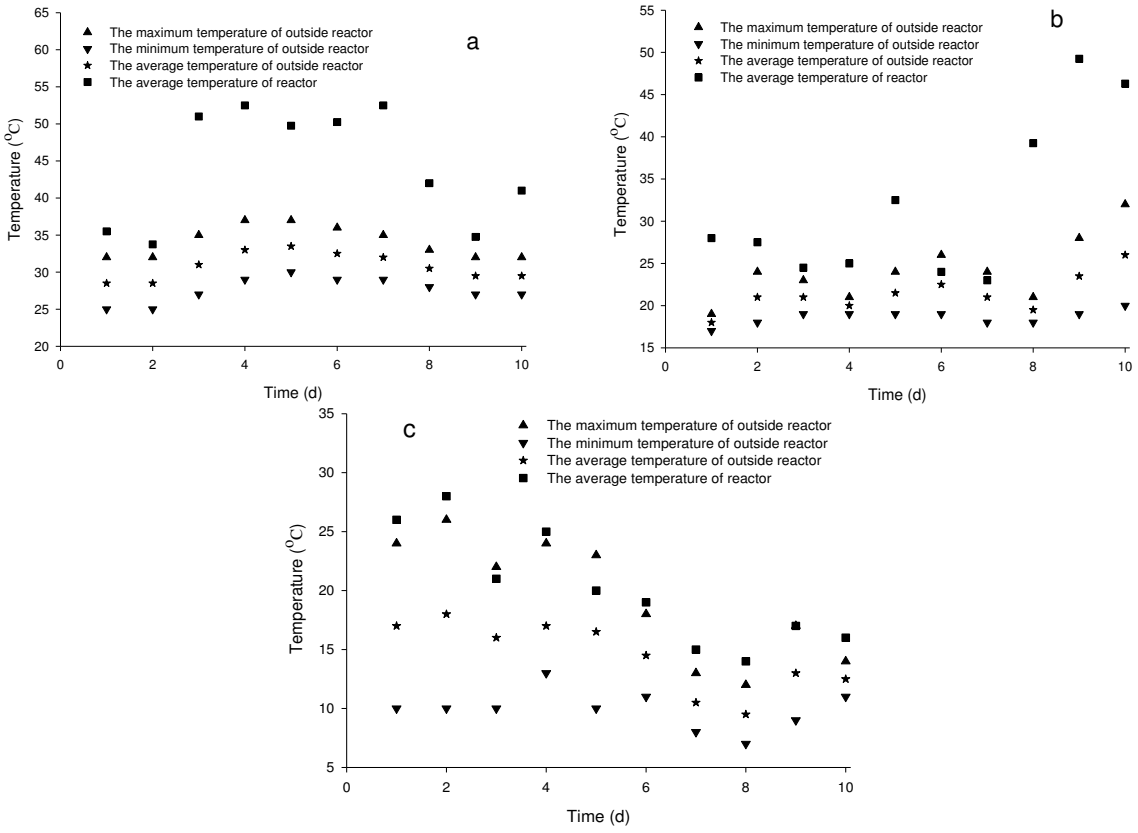

FIGURE 4
Variations of temperature during different seasons (a: summer; b: autumn; c: winter)

Temperature was one of the critical parameters for anaerobic excess sludge digestion because the growth rates double with approximately every 10°C increase. Figure 5 and Table 2 show the relationship between the average temperature inside and outside the reactor during different seasons and weather. The symbol Y, x and R in equations denote the average temperature inside the reactor, the average temperature outside the reactor and correlation coefficient, respectively. The temperature in summer and autumn was high and the fluctuation was great; therefore, the correlation coefficient was low. The average temperature inside and outside the reactor in summer, autumn, and winter on a sunny day were 46.3 °C and 28.3 °C, 43.5 °C and 26.1 °C, and 25 °C and 15.3 °C, respectively; On a rainy day, the average temperatures were 38.9 °C and 26.4 °C, 28.5 °C and 22.4 °C, and 16.8 °C and 12.8 °C, respectively. On both sunny and rainy day, the average temperature inside the reactor was higher than that outside the reactor across the three seasons. The average temperatures were 18.3 °C (summer), 17.4 °C (autumn), and 9.7 °C (winter) on a sunny day and 12.1 °C (summer), 6.1 °C (autumn), and 4.1 °C (winter) on a rainy day. The average temperatures inside the reactor in summer, autumn, and winter on a sunny day were higher than those outside, and the relationship between the temperatures was 18.3 °C, 17.4 °C, and 9.7 °C, respectively; on a rainy day, the relationship was 12.1 °C, 6.1 °C, and 4.1 °C, respectively.

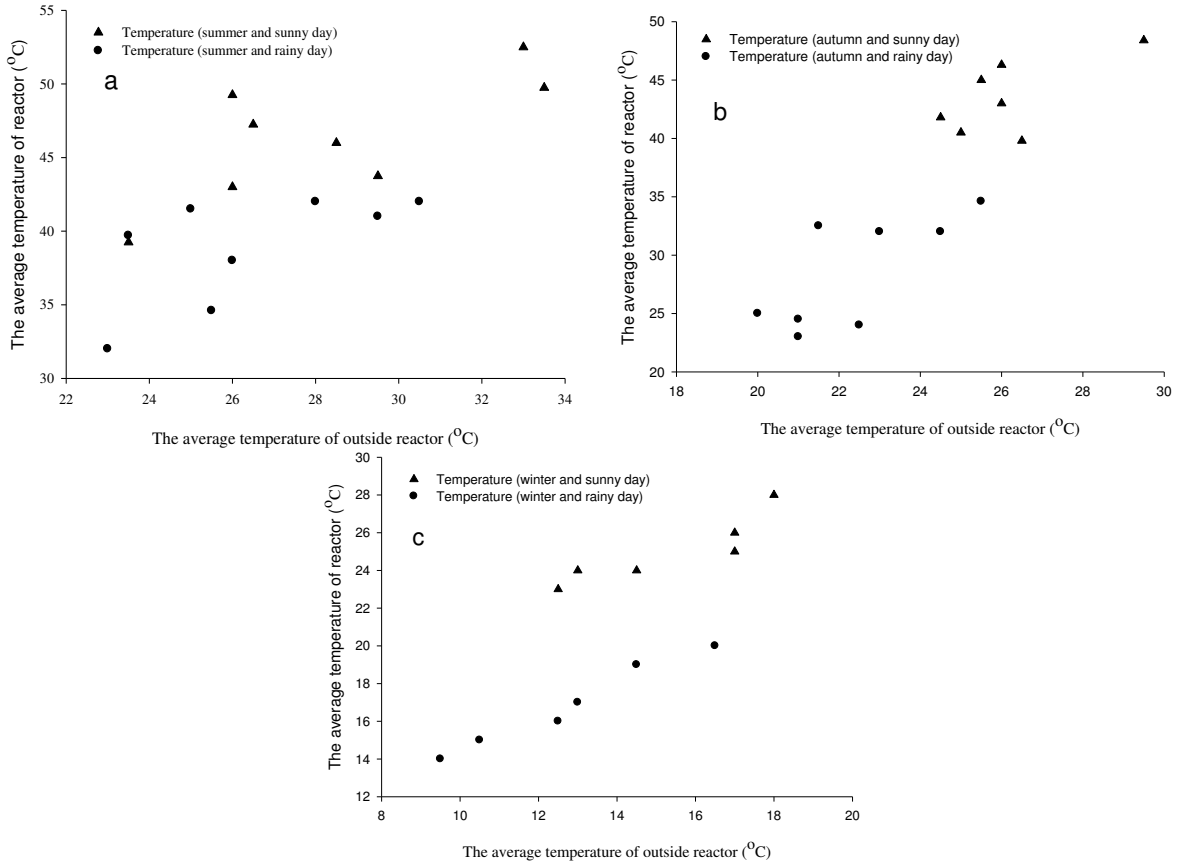

FIGURE 5
Relationship between temperatures inside and outside the reactor during different seasons and weather (a: summer; b: autumn; c: winter)

TABLE 2
Relationship between temperatures inside and outside the reactor during different seasons and weather.

	summer	autumn	winter
Sunny day	Y=0.8791x+21.4553 R=0.7292	Y=1.2649x+10.4757 R=0.6507	Y=0.6894x+14.4286 R=0.8928
Rainy day	Y=0.8848x+15.5129 R=0.6440	Y=1.8492x-12.9269 R=0.7374	Y=0.8897x+5.4892 R=0.9848

CONCLUSIONS

The results of this study showed that enhancing excess sludge reduction could be achieved with solar energy as heat source. TS and TVS removal were 36.9% and 44% for summer, 29.3% and 27.5% for autumn, and 18.5% and 24.8% for winter. The average temperatures inside and outside the reactor in summer, autumn and winter on sunny day were 46.3 °C and 28.3 °C, 43.5 °C and 26.1 °C, and 25 °C and 15.3 °C, respectively; on rainy day, the average temperatures were 38.9 °C and 26.4 °C, 28.5 °C and 22.4 °C, and 16.8 °C and 12.8 °C, respectively.

ACKNOWLEDGEMENTS

This research was supported by the Undergraduate Innovation and Training Program Fund of Shanxi Province (No. 2014265), Key Laboratory of Renewable Energy Electric-Technology of Hunan Province (No. 2014ZNDL009).

REFERENCES

[1] Zhang, G.M., Zhang, P.Y., Yang, J.M. and Chen, Y.M. (2007) Ultrasonic reduction of excess sludge from the activated sludge system. J. Hazard. Mater. 145, 515–519.

[2] Coma, M., Rovira, S., Canals, J. and Colprim, J. (2013) Minimization of sludge production by a side-stream reactor under anoxic conditions in a pilot plant. Bioresour. Technol. 129, 229–235.

[3] Wang, D.B., Zeng, G.M., Chen, Y.G. and Li, X.M. (2015) Effect of polyhydroxyalkanoates on dark fermentative hydrogen production from waste activated sludge. Water Res. 73, 311–322.

[4] Wei, Y.S., Van Houten, R.T., Borger, A.R., Eikelboom, D.H. and Fan, Y.B. (2003) Comparison performances of membrane bioreactor and conventional activated sludge process on sludge reduction induced by Oligochaete. Environ. Sci. Technol. 37, 3171–3180.

[5] Song, K., Zhou, X., Liu, Y.Q., Xie, G.J., Wang, D.B., Zhang, T.T., Liu, C.S., Liu, P., Zhou, B.B. and Wang, Q.L. (2016) Improving dewaterability of anaerobically digested sludge by combination of persulfate and zero valent iron. Chem. Eng. J. 295, 436–442.

[6] Gavala, H.N., Yenal, U., Skiadas, I.V., Westermann, P. and Ahring, B.K. (2003) Mesophilic and thermophilic anaerobic digestionof primary and secondary sludge. Effect ofpre-treatment at elevated temperature. Water Res. 37, 4561–4572.

[7] Zabranska, J., Stepova, J., Wachtl, R., Jenicek, P. and Dohanyos, M. (2000) The activity of anaerobic biomass in thermophilic and mesophilic digesters at different loading rates. Water Sci. Technol. 42, 49–56.

[8] Watanabe, H., Kitamura, T., Ochi, S. and Ozaki, M. (1997) Inactivation of pathogenic bacteria under mesophilic and thermophilic conditions. Water Sci. Technol. 36, 25–32.

[9] Rojas Oropeza, M., Cabirol, N., Ortega, S., Castro Ortiz, L.P. and Noyola, A. (2001) Removal of fecal indicator organisms and parasites (fecal coliforms and helminth eggs) from municipal biologic sludge by anaerobic mesophilic and thermophilic digestion. Water Sci. Technol. 44, 97–101.

[10] Kim, M., Ahn, Y.H. and Speece, R.E. (2002) Comparative process stability and efficiency of anaerobic digestion; mesophilic vs. thermophilic. Water Res. 36(17), 4369–4385.

[11] Ge, H.Q., Jensen, P.D. and Batstone, D.J. (2010) Pre-treatment mechanisms during thermophilic-mesophilic temperature phased anaerobic digestion of primary sludge. Water Res. 44, 123–130.

[12] Song, Y.C., Kwon, S.J. and Woo, J.H. (2004) Mesophilic and thermophilic temperature co-phase anaerobic digestion compared with single-stage mesophilic- and thermophilic digestion of sewage sludge. Water Res. 38(7), 1653–1662.

[13] Zheng, W., Li, X.M., Li, B.Z., Xu, H.Y. and Guo, Y.B. (2014) Enhancing the hydrolysis of excess sludge using thermophilic *Bacillus* sp. Hnu under different oxygen supply conditions. J. Serb. Chem. Soc. 78, 1135–1147.

[14] Hou, Y., Vidu, R. and Stoeve, P. (2011) Solar energy storage methods. Ind. Eng. Chem. Res. 50(15), 8954–8964.

[15] Haralambopoulos, D.A., Biskos, G., Halvadakis, C. and Lekkas, T.D. (2002) Dewatering of wastewater sludge through a solar still. Renew. Energ. 26(2), 247–256.

[16] Salihoglu, N.K., Pinarli, V. and Salihoglu, G. (2007) Solar drying in sludge management in Turkey. Renew. Energ. 32, 1661–1675.

[17] Slim, R., Zoughaib, A. and Clodic, D. (2008) Modeling of a solar and heat pump sludge drying system. Int. J. Refrigeration 31, 1156–1168.

[18] Mathioudakis, V.L., Kapagiannidis, A.G., Athanasoulia, E., Diamantis, V.I., Melidis, P. and Aivasidis, A. (2009) Extended dewatering of sewage sludge in solar drying plants. Desalination. 248(1-3), 733–739.

[19] Tokumura, M., Katoh, H., Katoh, T., Znad, H.T. and Kawase, Y. (2009) Solubilization of excess sludge in activated sludge process using the solar photo-Fenton reaction. J. Hazard. Mater. 162, 1390–1396.

[20] Bennamoun, L. (2012) Solar drying of wastewater sludge: A review. Renew. Sust. Energ. Rev. 16(1), 1061–1073.

[21] Liu, C.G., Lei, Z.F., Yang, Y.N., Wang, H.F. and Zhang, Z.Y. (2013) Improvement in settleability

and dewaterability of waste activated sludge by solar photocatalytic treatment in Ag/TiO2-coated glass tubular reactor. Bioresour. Technol. 137, 57–62.

[22] APHA. (1998) Standard Methods for the Examination of Water and Wastewater, 20th ed. American Public Health Association, Washington, DC.

[23] Li, X.S., Ma, H.Z., Wang, Q.H., Matsumoto, S., Maeda, T. and Ogawa, H.I. (2009) Isolation, identification of sludge-lysing strain and its utilization in thermophilic aerobic digestion for waste activated sludge. Bioresour. Technol. 100(9), 2475–2481.

[24] Liu, S.G., Zhu, N.W., Li, L.Y. and Yuan, H.P. (2011) Isolation, identification and utilization of thermophilic strains in aerobic digestion of sewage sludge. Water Res. 45, 5959–5968.

[25] Liu, S.G., Song, F.Y., Zhu, N.W., Yuan, H.P. and Cheng, J.H. (2010) Chemical and microbial changes during autothermal thermophilic aerobic digestion (ATAD) of sewage sludge. Bioresour. Technol. 101(24), 9438–9444.

[26] Ji, R. and Brune, A. (2005) Digestion of peptidic residues in humic substances by an alkali-stable and humic-acid-tolerant proteolytic activity in the gut of soilfeeding termites. Soil Biol. Biochem. 37(9), 1648–1655.

[27] Yang, Q., Luo, K., Li, X.M., Wang, D.B., Zheng, W., Zeng, G.M. and Liu, J.J. (2010) Enhanced efficiency of biological excess sludge hydrolysis under anaerobic digestion by additional enzymes. Bioresour. Technol. 101, 2924–2930.

Received: **09.03.2017**
Accepted: **19.07.2017**

CORRESPONDING AUTHOR

Wei Zheng
School of Environment and Safety,
Taiyuan University of Science and Technology,
Taiyuan 030024 – P.R. CHINA

E-mail: zhwstar2016@163.com

© by PSP Volume 26 – No. 10/2017 pages 5936-5941 Fresenius Environmental Bulletin

SEASONAL CHANGES IN ANTIOXIDANT DEFENCE SYSTEM ON BROWN TROUT *(SALMO* SP.) IN MUNZUR STREAM

Erkan Can[1,*], Nuran Cikcikoglu-Yildirim[2], Devrim Erdogan[1]

[1]Fisheries Faculty, Department of Aquaculture, Munzur University, Tunceli, Turkey
[2] Engineering Faculty, The Department of Environmental Engineering, Munzur University, Tunceli, Turkey

ABSTRACT

The aim of the present study was to evaluate the oxidant and antioxidant status of the indigenous brown trout (*Salmo* sp.) caught from Munzur stream (Tunceli, Turkey) at different seasons in different tissues. Glutathione peroxidase (GPx), catalase (CAT), superoxide dismutase (SOD), total antioxidant status (TAS) and total oxidant status (TOS) levels were measured. These measurements were read in a microplate reader using commercial kits with ELISA method. At the end of the study, significant variations of oxidative stress biomarkers were observed between seasons and tissues. The results of this study show that oxidative stress responses in tissues of *Salmo* sp. are sensitive to the tissues and the seasons in relation to the contaminants, climatic parameters and reproductive period in Munzur stream. The selected parameters are in valuable biomarkers for monitoring of water systems since at molecular levels they give an early warning signal of xenobiotics on aquatic organisms. It was concluded that the measurement of antioxidants biomarkers known such as SOD, CAT and GSH-Px activities, TAS and TOS levels may also be promising indicators of an oxidant impact on aquatic organisms.

KEYWORDS:
Salmo sp, TAS, TOS, SOD, GSH-Px, CAT, Munzur Stream.

INTRODUCTION

Free radicals and other reactive oxygen species (ROS) are generated by all aerobic cells [1].To minimize the negative effects of ROS, fish like other vertebrates possess an antioxidant defense system. Main enzymatic actors in this system are SOD (superoxide dismutase), CAT (catalase), GSH-Px (glutathione peroxidase) [2, 3, 4]. They are involved in detoxification and stress tolerance, being first line of defense against reactive oxygen species (ROS) [2]. Furthermore, TAS (Total Antioxidant Status) is a quantitative measurement which represents the total contribution from a wide range of antioxidant molecules [5]. The reactive oxygen species, which are produced under usual oxidative damage, can be eliminated by the body's antioxidant system [2]. Numerous studies have been focused on fish antioxidant enzymes [6, 7, 8, 9, 10, 11]. Increased antioxidant defence in some fish species has been related to pollutants or chemical exposure [12, 13, 14].

A rare fish species inhabited the Munzur River is the wild brown trout belonging to the genus salmo, may be distinguished by their brownish-yellow colour with dark and red spots on olive background. Trout that lives in great number in the Munzur River became one of the most preferred and caught fish because of its unique aroma and makes up an important economic value for the region [15]. It is commonly known red spotted trout with high economic value in Munzur Stream where is an important water supply in Turkey and its cultivating studies are ongoing by catching them from the wild.

FIGURE 1
Munzur trout (*Salmo sp.)*

It is also known that in aquatic ecosystems, seasonal and daily changes in dissolved oxygen and temperature are environmental variables that are likely to influence oxidative processes [16]. Degradation of spawning habitats and river damming are endangering wild brown trout populations [17], and there is a need for good management practices for the conservation of stocks in the East Anatolian Region of Turkey. To fulfil this task, it is necessary to achieve a sound knowledge of the biology of these species [18], and aims to assess the seasonal changes in the oxidant and antioxidant status of gill, muscle and liver. Some of the main enzymatic actors used bioindicator are SOD, CAT, GSH-Px, [2, 3]. It was

also investigated that whether TAS and TOS is a quantitative measurement and promising indicators which represents the total contribution from a wide range of antioxidant molecules or not in the present study.

MATERIALS AND METHODS

Experiments were conducted on the Central Labotatuaries of R&D (Fisheries and Environment) in University of Munzur, Turkey in 2014.

Sampling sites. Fish (five specimens for each group) were caught from the Munzur stream (between the coordinates of 39° 9' 2.01'' north - 39° 29' 21.93" east and 39° 10' 1.09'' North- 39° 27' 59.91'' east) on seasonal basis, then, they were transported to laboratory.

Physico-chemical analysis. The water parameters (temperature, salinity, pH and dissolved oxygen) were measured by YSI Professionals Plus at the sampling area where the fish caught on time.

Preparation of samples. Captured fishes were placed in plastic bags and dissected purposed tissues. The blood in the tissues was removed by treating them with 0.9% of NaCl, after then, tissues are divided into the groups to determine the levels of enzymatic activity. Firstly, the samples have been weighed and homogenized by adding PBS buffer (salt solution buffered with phosphate) at a rate of 1/5 w/v and using homogenizer with ice. The homogenized samples have been centrifuged for 15 min in a refrigerated centrifuge at 17 000 rpm the supernatants obtained were immediately put in deep freeze at -80 C and kept there until their analyses.

SOD, CAT and GSH-Px enzym activities. The activities of SOD, CAT and GSH-Px enzymes were analyzed by using the Cayman Chemical Superoxide Dismutase Assay Kit (Catalog No: 706002) (Cayman Chemical Company) at 450 nm, the Cayman Chemical Catalase Assay Kit (Catalog No: 707002; Cayman Chemical Company) and the Cayman Chemical Glutathione Peroxidase Assay Kit (Catalog No: 703102; Cayman Chemical Company) by a microplate reader (Thermo scientific multiscan®).

TAS and TOS levels. TAS and TOS levels were analyzed by using Total Antioxidant Status (TAS) Assay Kits and Total Oxidant Status (TOS) Assay Kits (Rel Assay Diagnostics, Turkey) by a microplate reader (Thermo scientific multiscan®) by aproving to the cataloque of producer company.

Statistical analyze. All data were analized by SPSS-15 software for Windows (SPSS Inc., Chicago, IL, USA). (Multiple Regression Analysis and AN(C)OVA).

RESULTS

Some oxidative stress parameters (SOD, CAT, GSH-Px activities and TAS and TOS levels) determined in gill, liver and muscle tissues of indigenous brown trout (*Salmo* sp.) caught from Munzur stream (Tunceli, Turkey) at different seasons.

Fish sizes and water parameters on the sampling area. Total lengths of fish used in the study were 31.30±2.39 cm. The water parameters (temperature, salinity, pH and dissolved oxygen) were shown in Table 1. The mean water temperatures of the Munzur Stream changed between 4.10 and 14.10 ◦C. The pH values ranged from 8.29 to 8.69 over all the sesons. Dissolved oxygen concentrations were detected between 9.81 mg l^{-1} and 12.88 mg l^{-1}. The lowest salinity value was found in spring. The salinity changed between 0.13 and 0.29 °C (Table 1).

TABLE 1
Water paramaters on the sampling area

Seasons	Temperature (°C)	Dissolved Oxygen (mg l^{-1}).	Salinity (ppt)	pH
Spring	5.80	11.91	0.13	8.29
Summer	14.10	9.81	0.28	8.35
Autumn	11.30	11.20	0.29	8.62
Winter	4.10	12.88	0.19	8.69

TAS and TOS levels. Changes of TAS concentration in liver and muscle among the four investigated seasons were found statistically significant ($p<0.05$) but there was no significant differences were found in gill ($p>0.05$). The differences of TAS levels were found statistically significant at all seasons when compared to three tissues ($p<0.05$) (Table 2).

The TAS levels reached its maximum level in liver tissue in summer (3.608 mmol/L). The lowest TAS levels were found in gill in winter season (2.540 mmol/L) (Table 2).

TOS levels were found to be statistically unsignificant in spring and winter when compared tissues ($p>0.05$) but were found significant in summer and autumn ($p<0.05$). Changes of TOS levels in muscle were unsignificant except summer ($p>0.05$). There was no significant differences were found in gill and liver when compared to seasons except autumn ($p>0.05$). The highest TOS levels were determined in gills and liver in autumn (Table 3).

TABLE 2
TAS levels (mmol/L) of indigenous brown trout (*Salmo* sp.) caught from Munzur stream (Tunceli, Turkey) at different seasons.

Seasons	Muscle	Gill	Liver
Spring	2.905±0.175^{ABb}	2.670±0.149^{Aa}	3.039±0.045^{Ab}
Summer	3.149±0.362^{Bab}	2.617±0.085^{Aa}	3.608±0.468^{Bb}
Autumn	2.768±0.119^{ABa}	2.574±0.183^{Aa}	3.109±0.250^{ABb}
Winter	2.608±0.328^{Ba}	2.540±0.046^{Aa}	3.190±0.183^{ABb}

A,B,C: Different letters in same column show statistical importance of values among seasons in same tissue (p<0.05).
a,b,c : Different letters in same line show statistical importance of values among tissues in same season (p<0.05).

TABLE 3
TOS levels (µmol/L) of indigenous brown trout (*Salmo* sp.) caught from Munzur stream (Tunceli, Turkey) at different seasons.

Seasons	Muscle	Gill	Liver
Spring	26.494±2.487^{Aa}	28.092±5.628^{Aa}	26.391±2.763^{Aa}
Summer	22.135±4.027^{Bb}	26.192±1.133^{Aa}	28.179±0.953^{Aa}
Autumn	27.717±1.111^{Ab}	41.077±2.855^{Ba}	38.360±1.776^{Ba}
Winter	28.216±0.939^{Aa}	28.521±0.864^{Aa}	30.933±2.843^{Aa}

A,B,C: Different letters in same column show statistical importance of values among seasons in same tissue (p<0.05).
a,b,c: Different letters in same line show statistical importance of values among tissues in same season (p<0.05).

TABLE 4
SOD activities (U/ml) of indigenous brown trout (*Salmo* sp.) caught from Munzur stream (Tunceli, Turkey) at different seasons.

Seasons	Muscle	Gill	Liver
Spring	0.043±0.01^{Ba}	0.048±0.01^{Ba}	0.19±0.03^{Ab}
Summer	0.029±0.01^{ABa}	0.025±0.01^{Aa}	0.24±0.02^{Ab}
Autumn	0.025±0.01^{Aa}	0.070±0.02^{Cb}	0.23±0.01^{Ac}
Winter	0.025±0.01^{Aa}	0.038±0.01^{ABa}	0.21±0.04^{Ab}

A,B,C: Different letters in same column show statistical importance of values among seasons in same tissue (p<0.05).
a,b,c : Different letters in same line show statistical importance of values among tissues in same season (p<0.05).

TABLE 5
GSH-Px activities (nmol/dk/ml) of indigenous brown trout (*Salmo* sp.) caught from Munzur stream (Tunceli, Turkey) at different seasons

Seasons	Muscle	Gill	Liver
Spring	78.95±16.00^{Aa}	75.45±3.26^{Aa}	82.70±9.96^{Aa}
Summer	183.27±20.44^{Ba}	142.91±16.52^{Ba}	206.82±23.30^{Ba}
Autumn	55.61±4.26^{Aa}	59.98±12.85^{Aa}	92.96±20.08^{Aa}
Winter	52.33±4.63$^{A\ a}$	51.32±5.18^{Aa}	53.67±4.26^{Aa}

A,B,C: Different letters in same column show statistical importance of values among seasons in same tissue (p<0.05).
a,b,c: Different letters in same line show statistical importance of values among tissues in same season (p<0.05).

TABLE 6
CAT activities of indigenous brown trout (*Salmo* sp.) caught from Munzur stream (Tunceli, Turkey) at different seasons.

Seasons	Muscle	Gill	Liver
Spring	20.40±4.90^{Aa}	31.02±3.68^{Aa}	23.25±6.37^{Aa}
Summer	28.90±4.60^{Ba}	32.80±3.69^{Aa}	30.45±5.74^{Ba}
Autumn	26.72±1.20^{Ba}	23.10±2.13^{Ba}	24.12±3.78^{Aa}
Winter	22.52±5.35^{Aa}	34.70±5.03^{Aa}	27.92±5.21^{Ba}

A,B,C: Different letters in same column show statistical importance of values among seasons in same tissue (p<0.05).
a,b,c: Different letters in same line show statistical importance of values among tissues in same season (p<0.05).

The activities of SOD. Changes of SOD activities in liver among the four investigated seasons were found statistically unsignificant (p>0.05) but SOD activeties of gill and muscle were significant (p<0.05). SOD activities in muscle were unsignificant (p>0.05) but not in gill and liver when compared seasons (p<0.05). The highest SOD activities were found in liver in summer (Table 4).

The activities of GSH-Px. GSH-Px activities were increased in summer ($p<0.05$). The highest GSH-Px activities were found in all tissues in summer. Unsignificant differences were found between the tissues at all seasons ($p>0.05$).(Table 5).

The activities of CAT. CAT activities of indigenous brown trout (*Salmo* sp.) were significantly increased in muscle and liver in summer ($p<0.05$). Differences of CAT activities were found statistically unsignificant at all seasons when compared to three tissues ($p>0.05$). CAT activities were increased in summer in muscle and liver ($p<0.05$) (Table 6).

DISCUSSION

The reactive oxygen species, which are produced under usual oxidative damage, can be eliminated by the body's antioxidant system [2]. SOD, CAT and GPx are three main antioxidant enzymes [19]. SOD is an oxidoreductase and it provides the first defense against oxidative stress. SOD greatly accelerates the conversion of O_2 to water and H_2O_2. The efficacy of SOD relies on its co-operation with CAT and GPx [16, 20]. Gabryelak et al. [21] and Palace and Klaverkamp [22] suggested that antioxidant defense enhancement in fishes during the spring and summer compared to colder winter months. But, Ronisz et. al., [23] reported no correlation between activities of GPx and CAT and water temperature. In the present study, SOD increased in liver especially in summer period. The highest activity of GSH-Px was determined in summer, as well and our results are similar to the results from Gabryelak et al., [21] and Palace and Klaverkamp [22]. CAT activities of indigenous brown trout (*Salmo* sp.) were significantly increased in muscle and liver in summer ($p<0.05$). CAT activities were increased in summer in muscle and liver ($p<0.05$). In another study,[9] reported that an increase in the main liver antioxidant enzyme activities did not relate to increased temperature however it was changed in autumn. At this period it was suggested that the fishes are experiencing oxidative stress. This is the period prior to spawning, whereas, this is the season which temperature drops rapidly, a daylight decreases and rainfall increases, all factors that may cause stress in the fishes, and alter the status of the antioxidants potentially [9]. The same researchers reported that the activities of SOD, CAT and GPx were higher in livers than gills, these findings are similar to ours especially activities of SOD and GSH-Px in liver were found higher than the other tissues at all seasons.

As it is known free radicals and other reactive oxygen species (ROS) are generated by all aerobic cells [1] and to minimize the negative effects of ROS, fish like other vertebrates possess an antioxidant defense system. Some of the main enzymatic actors in this system are SOD, CAT, GSH-Px [2, 3]. At the same time, TAS is a quantitative measurement which represents the total contribution from a wide range of antioxidant molecules [5, 24]. The highest TAS values was found in the liver at all seasons while the lowest of TAS was found in the gills. TOS levels were increased in the gill and in the liver in autumn, while it reached to the lowest levels in muscle tissue in summer. The results of this study show that oxidative stress responses in tissues of *Salmo* sp. are sensitive to the tissues and the seasons in relation to the contaminants, climatic parameters and reproductive period in Munzur stream and these findings are similar to the study from Gabbott, [25] and Aras et. al., [9]. Therefore, it was recommended to be measured such parameters included TAS and TOS which represent the total distribution of antioxidants.

It was concluded that the measurement of antioxidants biomarkers known such as SOD, CAT and GSH-PX activities, TAS and TOS levels may also be promising indicators of an oxidant impact on aquatic organisms. The selected parameters are in valuable biomarkers for monitoring of water systems, since at molecular levels they give an early warning signal of xenobiotics on aquatic organisms which help to preclude their negative effects. This approach, used in this study has an important potential for usage in routine monitoring or assessments researches of all others aquatic environments as recorded by Danabas et. al., [26]. Munzur trout is an indigenous species that the culture studies are ongoing. The findings obtained from this study will also be used as a reference and will shed light on future studies in related to the studies with this fish species and others. The enzyme activities of oxidant and antioxidant vary according to the seasons but also they were affected by location, gender, age, date, sexual maturity, contaminants, climatic parameters and reproductive period. Therefore, regular monitoring and evaluation are recommended [27], and the researches should be focused on similar studies considering age, size, gender etc to explore unknowns.

ACKNOWLEDGEMENTS

This study was funded by a grant from the University of Munzur Scientific Research and Project Office (Project number: MFTUB013-13).

REFERENCES

[1] Winston, G.W., Di Giulio, R.T. (1991) Prooxidant and antioxidant mechanisms in aquatic organisms, Aquat. Toxicol. 19, 137–161.
[2] Halliwell, B., Gutteridge, J.M.C. (1999) Free radicals in biology and medicine. Oxford: Oxford University Press.
[3] Bayir, A. (2005) The investigation of seasonal

changes in antioxidant enzyme activities, serum lipids, lipoproteins and hematological parameters of siraz fish (*Capoeta capoeta umbla*) living in Hinis Stream (Murat Basin). PhD Thesis, Ataturk University, Erzurum, Turkey.

[4] Demirbas, S., Acar, O. (2017) Physiological and Biochemical Defense Reactions of *Arabıdopsis Thaliana* to *Phelipanche Ramosa* Infectıon and Salt Stress. Fresen. Environ. Bull., 26, 2275-2268.

[5] Prior, R.L., Cao, G. (1999) In vivo total antioxidant capacity: comparison of different analytical methods. Free Radic. Bio. Med. , 27, 1173–1181. *doi*: 10,1016/S0891-5849(99)00203-8.

[6] Özmen,İ. Atamanalp, M. Bayır, A. Sirkecioğlu, A.N., Cengiz, M. (2007) The effects of different stressors on antioxidant enzyme activities in the erythrocyte of rainbow trout (*Oncorhynchus mykiss* W., 1792) Fresen. Environ. Bull., 16 (8), 922-927.

[7] Reyes-Becerril, M., Tovar-Ramírez, D., Ascencio-Valle, F., Civera-Cerecedo, R., Gracia-López, V., Barbosa-Solomieu, V. (2008) Effects of dietary live yeast *Debaryomyces hansenii* on the immune and antioxidant system in juvenile leopard grouper *Mycteroperca rosacea* exposed to stress. Aquaculture. 280, 39-44.

[8] Orun, I., and Talas, Z.S. (2008). Antioxidative role of sodium selenite against the toxic effect of heavy metals (Cd^{2+}, Cr^{3+}) on some biochemical and hematological parameters in the blood of rainbow trout (Oncorhynchus mykiss Walbaum, 1792). Fresen. Environ. Bull., 17, 1242–1246.

[9] Aras, N.M., Bayır, A., Sırkecıoglu, A.N., Bayır, M., Aksakal, E., Halıloglu, H.I. (2009) Seasonal changes in antioxidant defence system of liver and gills of *Salmo trutta caspius*, *Salmo trutta labrax* and *Salmo trutta macrostigma*, J. Fish Biol. 74, 842–856.

[10] Orun, I., Talas, Z.S., Alkan, A. (2011) Modulating effect of selenium on gills of fish exposed to heavy metals. Fresen. Environ. Bull., 20, 04-108.

[11] Uncumusaoglu, A.A., Sengul, U. and Akkan T., (2016) Environmental Contamination of Heavy Metals in The Yaglidere Stream (Giresun), Southeastern Black Sea. Fresen. Environ. Bull., 25(12), 5492-5498.

[12] Lemaire, P., Fo¨rlin, L., Livingstone, D.R. (1996) Responses of hepatic biotransformation and antioxidant enzymes to CYP1A-inducers (3-methylcholanthrene, bnaphthoflavone) in sea bass (*Dicentrarchus labrax*), dab (*Limanda limanda*) and rainbow trout (*Oncorhynchus mykiss*). Aquat. Toxicol. 36, 141–160.

[13] Li, X., Liu, Y., Song, L., Liu, J. (2003) Responses of antioxidant systems in the hepatocytes of common carp (*Cyprinus carpio* L.) to the toxicity of microcystinLR. Toxicon. 42, 85–89.

[14] Souza, D.M, Martins, A.C, Jensen, L, Wasielesky, J., Monserrat, J.M, Garcia, L.O. (2014) Effect of temperature on antioxidant enzymatic activity in the Pacific white shrimp *Litopenaeus vannamei* in a BFT (biofloc technology) system. Mar. Freshw. Behav. Physiol., 47: 1–10.

[15] Kayım, M., Öksüz, A., Özyılmaz, A., Kocabaş, M., Can, E., Kızak, V., Ateş, M. (2011) Proximate composition, fatty acid profile and mineral content of wild brown trout (*Salmo trutta* sp.) from Munzur River in Tunceli, Turkey, Asian J. Chem. 23, 3533-3537.

[16] Parihar, M.S., Javeri, T., Hemnani, T., Dubey, A. K., Prakash, P. (1997) Responses of superoxide dismutase, glutathione peroxidase and reduced glutathione antioxidant defenses in gills of the freswater catfish (*Heteropneustes fossilis*) to short-term elevated temperature. J. Therm. Biol. 22 (2), 151-156.

[17] Alp, A., Kara, C., Buyukcapar, H.K. (2005) Age, growth and diet composition of the resident brown trout, *Salmo trutta macrostigma* Dumeril 1858, in Firniz Stream of the River Ceyhan, Turkey. Turk. J. Vet. Anim. Sci. 29, 285–295.

[18] Gortazar, J., de Jal´on, D.G., Alonso-Gonz´alez, C., Vizca´ıno, P., Baeza, D., Marchamalo, M. (2007). Spawning period of a southern brown trout population in a highly unpredictable stream. Ecol. Freshw. Fish, 16, 515–527.

[19] Wilhelm Filho, D. (1996) Fish antioxidant defences – a comparative approach. Brazilian Braz J. Med. Biol. Res. 29, 1735–1742.

[20] Pandey, S., Parvez, S., Sayeed, I., Haque, R., Bın-hafeez, B., Raısuddın, S. (2003) Biomarkers of oxidative stress: a comparative study of river Yamuna fish Wallago atto. Sci. Total Environ. 309: 105-115.

[21] Gabryelak, T., Piatkowska, M., Leyko, W., Peres, G. (1983) Seasonal variations in the activities of peroxide metabolism enzymes in erythrocytes of freshwater fish species. Comp. Biochem. Physiology. 75, 383-385.

[22] Palace, U.P., Klaverkamp, J.F. (1993) Variation of hepatic enzymes in three species of freshwater fish from precambrian shield lakes and the effect of cadmium exposure. Comp. Biochem. Physiology. 104, 147-154.

[23] Ronisz, D., Joakim Larsson, D.G., Förlin, L. (1999) Seasonal variations in the activities of selected hepatic biotransformation and antioxidant enzymes in eelpout (*Zoarces viviparus*). Comp. Biochem. Physiology. 124, 271-279.

[24] Can, E., Kurtoğlu, İ.Z., Benzer, F., Erişir, M., Kocabaş, M., Kızak, V., Kayım, M., Çelik H. T. (2012). The Effects of different dosage of kefir on growth performances and antioxidant system in the blood and liver tissues of Çoruh trout (*Salmo coruhensis*). Turkish J. Fish. Aquatic

Sci. 12, 277-283.
[25] Gabbott, P.A., (1983) Developmental and seasonal metabolic activities in marine molluscs. In, The Mollusca, Vol. 2. Environmental Biochemistry Andphysiology, edited by P. W. Hochachka, Academic Press, New York, pp. 165-217.
[26] Danabas, D., Cikcikoglu Yildirim, N., Yildirim, N., Oztufekci Onal, A., Uslu, G., Unlu, E., Danabas, S., Ergin, C., Tayhan, N. (2015) Changes in antioxidant defence system in gills of *Capoeta umbla* caught from Uzuncayir Dam Lake, Turkey, Biochem. Syst. Ecol., 63:72-79.
[27] Polat, N. and Akkan, T. (2016) Assessment of Heavy Metal and Detergent Pollution in Giresun Coastal Zone, Turkey. Fresen. Environ. Bull., 25(8), 2884-2890.

Received: **09.03.2017**
Accepted: **10.07.2017**

CORRESPONDING AUTHOR

Erkan Can
Fisheries Faculty, Department of Aquaculture, Munzur University, TR62000, Tunceli, Turkey.

e-mail: ecanengineer@gmail.com

© by PSP Volume 26 – No. 10/2017 pages 5942-5941 Fresenius Environmental Bulletin

OPTIMIZING FENTON PROCESS FOR OLIVE MILL WASTEWATER TREATMENT USING RESPONSE SURFACE METHODOLOGY

Farzaneh Doosti, Reza Ghanbari, Hamzeh Ali Jamali*, Hamid Karyab

Department of Environmental Health Engineering, School of Public Health, Qazvin University of Medical Sciences (QUMS), Qazvin, Iran

ABSTRACT

The effect of factors affecting the Fenton process including H_2O_2/Fe^{2+} ratio, pH and reaction time on the removal of BOD_5, COD, color and total phenolic compounds from olive mill wastewater as well as variations of the BOD5/COD ratio was investigated using central composite design and response surface methodology. The ranges of H_2O_2/Fe^{2+} ratio, pH and reaction time were considered as 4.64-11.36, 2.32-5.68 and 9.6-110.4 min, respectively.

Based on ANOVA and regression results, the high values of the obtained R^2 (0.86-0.99) indicated that removal of the contaminants could be defined by the polynomial quadratic model and there was a good agreement between the model prediction and experimental data. The removal efficiencies of BOD_5, COD, color and total phenolic compounds were 87%, 93.8%, 42.85% and 70.4%, respectively. Also, measuring the BOD_5/COD ratio showed that this value increased from 0.16 to 0.44 after the process. Therefore, response surface methodology is a powerful tool for optimizing the Fenton process during olive mill wastewater treatment. Increased BOD_5/COD ratio indicated that the Fenton process, as a pre-treatment, could prepare the wastewater for complementary biological treatment by reducing the level of toxic and recalcitrant contaminants.

KEYWORDS:
Olive mill wastewater, Fenton process, optimization, central composite design (CCD), phenolic compounds

INTRODUCTION

Due to the nutritional and antioxidant as well as cosmetic and health properties of olive oil, the demand for its consumption has been increased around the world. As a result, the industries associated with its production and processing have been significantly grown [1]. High consumption of water in olive oil extraction stages results in a significant amount of olive mill wastewater (OMW) [2]. Extracting each liter of olive oil leads to nearly 2.5 L of wastewater [3]. Controlling wastewater contamination is highly essential for all kinds of creatures, whether those living in water or profiting from it [4]. One of the major environmental problems in the food industry is the treatment of the wastewater produced by olive oil production industries. Such wastewater contains organic compounds such as polyphenolic macromolecules that are highly toxic to the environment [5]. Chemical properties of olive oil mill wastewater depend on various factors including weather conditions, cultivation conditions and type of extraction process [2, 6]. Olive mill wastewater contains high concentrations of BOD_5 (23-100 g/l), COD (40-220 g/l), phenolic compounds (1.4-14.3 g/l) and suspended solids (190 g/l) (2, 6-8). The common methods for managing such wastewater include the use of evaporative ponds and landfill of solids, ultrafiltration, reverse osmosis, ion exchange and adsorption of different materials. These treatment techniques convert the contamination from iquid into solid phases and are not appropriate for reducing wastewater toxicity [7, 10]. Furthermore, the biological methods used for these wastewaters include aerobic and anaerobic digestion. The aerobic treatment is very efficient, but the use of these processes is limited due to the high cost of aeration. Limitation of the anaerobic digestion for this type of wastewater is caused by phenolic compounds and organic acids, which prevent the activity of the methanogenic bacteria [6]; thus, efficient and sustainable treatment of such wastewater cannot be achieved using only a single process [10]. Radical production systems provide a scientific solution for improving the biodegradability of such wastewater [11]. Among these processes, the Fenton process is economically more cost-effective. The advantages of this process include high efficiency, simplicity and possibility of decomposing various compounds [12]. The Fenton oxidative process is considered as a technique for chemical oxidation and coagulation of organic compounds [13]

"One factor at a time" method that is utilized conventionally in multivariate analysis sewage treatment procedure is done in a such way that one of the variables is altered at a time while others hold constant and, then, its influences on the dependent variable are scrutinized, which is expensive and time-consuming [14]. Moreover, in this type of optimization, the mutual effects between the variables

are not taken into consideration. The statistical design of the experiments is a useful technique to obtain the statistically significant models that are useful for a process with the minimum number of tests; furthermore, in such designs, the interactive effects of the variables are investigated, so the parameters used in the multivariate systems can be optimized. The central composite design (CCD) provides useful data for the interactive and multiple effects of the variables in the linear and curve forms, respectively [15, 16].

In previous studies, olive mill wastewater treatment has been performed using the Fenton process and, then, the removal level of COD, color, total phenolic compounds and aromatic compounds have been investigated [17]. However, none of these studies have pointed to the changes in the BOD_5/COD ratio. In the present research, in addition to investigating the treatability of the biological pretreated wastewater of this industry, the variation rate of the BOD_5/COD ratio was studied. Besides, the optimal conditions for treating this wastewater was determined using the CCD with three independent variables (factors) including pH, H_2O_2/Fe^{2+} ratio and reaction time, and five dependent variables (responses) of BOD_5, COD, color, total phenolic compounds and BOD_5/COD ratio.

MATERIALS AND METHODS

Wastewater. The wastewater consumed in the present research was provided from an olive oil mill factory in Gilan Province, Iran, and was kept at 4°C after being transferred to the laboratory. The required samples were directly provided from the factory's wastewater effluent and were biologically treated.

Materials. In the Fenton process, 35% hydrogen peroxide and 99.5% $FeSO_4.7H_2O$ were used, which were provided by Arman SINA Corporation, Iran, and Merck & Co., Germany, respectively. Furthermore, sulfuric acid and NaOH for pH adjustment, iron chloride, magnesium sulfate, calcium chloride and phosphate buffer for BOD measurement, mercury sulfate, potassium dichromate, silver sulfate and potassium hydrogen phthalate for COD measurement, and ammonium hydroxide, 4-aminoantipyrine, potassium ferricyanide and solid phenol for measuring the total phenolic compounds were provided by Merck & Co., Germany.

Equipment. The equipment used in the present study included a BOD meter (Model: OxiTopIS6, WTW Company, Germany), a COD reactor from HACH Company, USA, spectrophotometer (Model: T80, PG Instruments Ltd.), a CONSORT multimeter (Model: C863T, Belgium) for pH measurement and a Fhiller Scientific mixer (Model: HS-10 Digital) equipped with temperature and round control.

Fenton oxidation process. The Fenton process tests were carried out in a Pyrex batch reactor with the volume of 1 L and a magnet inside. Adjusting pH was performed by H_2SO_4 and NaOH 1 N. The total sample size in each test was 500 ml. For this purpose, first, the wastewater sample was transferred to the reactor and, then, iron sulfate ($FeSO_4.7H_2O$) and hydrogen peroxide (H_2O_2) were added. The sample was placed on the mixer equipped with the temperature and round control (25°C and 250 rpm). The required samples were taken from the reactor by a pipette at certain intervals. In order to stop the process reactions, the 1 N NaOH quenching solution was used and, then, the analyses were performed.

Analysis of OMW samples. Analyses of BOD_5, COD and total phenolic compounds were performed based on the instructions provided in the standard methods for the examination of water and wastewater [18]. Furthermore, in order to determine the color level, the sample was first diluted and passed through the 0.45µm filter. Afterwards, its absorption rate was determined at the wavelength of 288 nm using spectrophotometry technique [17, 19].

Experimental design and data analysis. A full-factorial design including all the possible orders of factors is a powerful tool for understanding complicated processes and describing linear quadratic and mutual effects in multifactor systems. The response surface method is an experimental technique used for multiple regression analyses by the data obtained from the appropriate experiments designed to solve the multivariate equations at the same time. In the present study, a limited range of each independent variable was obtained using the preliminary experiments done at the ambient temperature.

The experimental runs were carried out with different values of three independent variables, including reaction time, pH and H_2O_2/Fe^{2+} ratio, for the simultaneous coverage of a range of variables in order to eliminate COD, BOD_5, total phenol, color and variations of the BOD_5/COD ratio in the CCD. To describe the effects of pH, reaction time and H_2O_2/Fe^{2+} ratio on the removal of BOD, COD, TP, color and variations of BOD_5/COD ratio, the experiments were performed in a batch reactor. The coded values of the process variables were obtained using Equation (1):

$$xi = \frac{Xi - Xic}{\Delta Xi} \quad (1)$$

where x_i, X_i, X_{ic} and ΔXi indicate the coded value of the i^{th} studied variable, the actual value of the i^{th} studied variable, the actual value of X_i at the central point of the studied area and the difference between the real value of X_i and its value at the

central point (step size), respectively.

TABLE 1
Dependent variables and their range for studying response surface.

Variables	Unit	Coded values (surfaces)				
		1.68	1	0	-1	-1.68
Reaction time	min	110.4	90	60	30	9.6
pH	-	5.68	5	4	3	2.32
H_2O_2/Fe^{2+} ratio	-	11.36	10	8	6	4.64

The range and levels of the independent variables are presented in Table 1. The responses were estimated using the quadratic polynomial model as follows:

$$Y = \beta 0 + \sum_{i=1}^{k} \beta i.\, xi + \sum_{i=1}^{k} \beta ii.\, xi^2 \sum_{ii\le j}^{k} \sum_{j}^{k} \beta ij.\, xi.\, xj + \cdots e \quad (2)$$

where (Y) is the response, x_i and x_j are the variables, k is the number of independent variables, β_0 is the constant factor, β_j, β_{jj} and β_{ij} are the constants of interactive, linear and quadratic effects, respectively, and e_i is the random error.

For the regression analysis of the data obtained from the experiments and estimating the constant of the regression equation, Design Expert 7.1 software was used. The equations were validated using analysis of variance (ANOVA). The significance of each term of the equation estimates the fitness of each effective factor in the process. Further, the 2D diagrams (contour) were drawn to determine the interactive effects of each factor on the responses. After running ANOVA, the modified model was obtained by eliminating the terms that were not significant at 95% confidence level. Afterwards, by setting the factor in the "in range" mode and the response variables in the "maximum" mode, the numerical optimization was carried out.

The quality of fitness of the polynomial model was determined using the coefficient of determination (R^2) and the adjusted R-squared (R^2_{Adj}). The statistical significance was controlled by AP ratio and p-values.

RESULTS AND DISCUSSION

Table 2 represents the results of the physical and chemical characteristics of the effluent (treated wastewater samples) of the factory used in the present study.

TABLE 2
Characteristics of wastewater used in this study.

Parameter	Unit	Value
BOD_5	mg/l	2210 ±25
COD	mg/l	13600 ±30
pH	-	6.9 ±0.6
Total phenolic compounds	mg/l	557±15
Temperature	°C	20.7±0.4
BOD_5/COD ratio	-	0.16±0.05

In total, 20 tests with 5 iterations at the central point were designed in order to study the effects of the three independent variables of reaction time, pH and H_2O_2/Fe^{2+} ratio, shown as A, B and C, respectively, on the dependent variables (responses), removal percentage of BOD_5, COD, total phenol, color and variations of the BOD_5/COD ratio and to optimize them using the CCD. Table 3 shows the design matrix of the tests, actual values and values predicted by the quadratic model.

TABLE 3
Design matrix of tests using CCD method in Fenton process with actual and predicted results.

No.	Run	Time (A)	pH (B)	H_2O_2/Fe (C)	Removal efficiency %								BOD_5/COD	
					BOD_5		COD		TP		Color			
					Actual	Predicted	Actual	Predicted	Actual	Predicted	Actual	Predicted	Actual	Predicted
1	4	30	3	6	63	58.07	50	49.56	54	53.19	10	9.95	0.12	0.13
2	11	90	3	6	84	85.32	77	75.21	64	62.65	28	26	0.11	0.094
3	10	30	5	6	37	28.42	32	30.95	31	32.1	12	14.18	0.25	0.23
4	12	90	5	6	40	41.67	40	43.6	50	53.56	31	33.23	0.165	0.19
5	17	30	3	10	95	84.05	36	33.58	65	62.21	20	19.06	0.015	0.002
6	9	90	3	10	66	65.3	45	47.22	55	54.67	25	24.11	0.1	0.11
7	6	30	5	10	93	82.4	40	42.97	50	52.12	22	29.29	0.02	0.023
8	16	90	5	10	54	49.65	42	43.61	55	56.59	32	33.34	0.13	0.13
9	7	9.6	4	8	44	60.37	46	47.12	55	55.6	15	12.96	0.17	0.18
10	1	110.4	4	8	59	55.75	72	69.22	69	67.31	33	33.22	0.24	0.23
11	18	60	2.32	8	87	91.6	53	55.01	68	71.51	25	27.93	0.045	0.045
12	13	60	5.68	8	45	53.52	40	36.32	60	55.39	44	39.25	0.15	0.15
13	3	60	4	4.64	43	44.78	48	48.38	34	32.89	13	12.21	0.18	0.18
14	14	60	4	11.36	62	73.34	37	34.96	43	43.02	21	19.96	0.01	0.013
15	20	60	4	8	93	85.79	89	92.36	65	69.11	44	42.55	0.45	0.45
16	19	60	4	8	93	85.79	90.13	92.36	68	69.11	41	42.55	0.42	0.45
17	15	60	4	8	73	85.79	89.87	92.36	69.5	69.11	42	42.55	0.45	0.45
18	8	60	4	8	82	85.79	93.11	92.36	71	69.11	40	42.55	0.42	0.45
19	2	60	4	8	86	85.79	95.42	92.36	69.5	69.11	45	42.55	0.47	0.45
20	5	60	4	8	90	85.79	96.34	92.36	71.5	69.11	43	42.55	0.48	0.45

TABLE 4
Results of ANOVA for response parameters.

Responses	Final equations	P	PLOF	R^2	Adj. R^2	Pred.R^2	AP	S.D.	CV	PRESS
BOD_5	85.79- 11.32B+8.49C-11. 5AC-9.8A^2-9.45C^2	0.0034	0.1356	0.86	0.73	0.14	8.3	10.76	15.49	6948.16
COD	92.36+6.57A-5.55B-3.00C-3.25AB-3AC+7BC-12.09A^2-16.51B^2-17.92C^2	<0.0001	0.3432	0.99	0.98	0.94	25.19	3.45	5.69	633.24
TP	69.11+3.48A-3.79B+3.01C+ 3AB-4.25AB+2.75BC-2.71A^2-2B^2-11.02C^2	<0.0001	0.1684	0.96	0.93	0.79	17.89	3.12	5.34	573.71
Color	42.55+6.02A3.36B+2.3C+0.75AB-2.75AC+0.5BC- 6.88A^2-3.17B^2-9.36C^2	<0.0001	0.0878	0.97	0.94	0.8	16.04	2.87	9.81	522.67
BOD_5/COD ratio	0.45+0.016A+0.029B-0.049C+ 0.036AC-0.019BC-0.086A^2-0.12B^2-0.12C^2	<0.0001	0.7851	0.99	0.98	0.97	31.33	0.021	9.65	0.014

The mathematical equations were obtained using the results predicted by the model so that each dependent variable (Y) was a function of A, B and C. Then, by adding a constant number, the first-order effects (A, B, C), mutual effects (AB, AC, BC) and quadratic effects (A^2, B^2, C^2) were evaluated based on Equation (2). ANOVA was performed to assess the goodness of fit. Then, by eliminating the terms that were not statistically significant at 95% confidence level in the first ANOVA, the equations were modified. The final equations of the removal efficiency of BOD_5, COD, TP, color and BOD_5/COD ratio, which were respectively Y_1, Y_2, Y_3, Y_4 and Y_5, were calculated based on the quadratic polynomial model shown in Table 4.

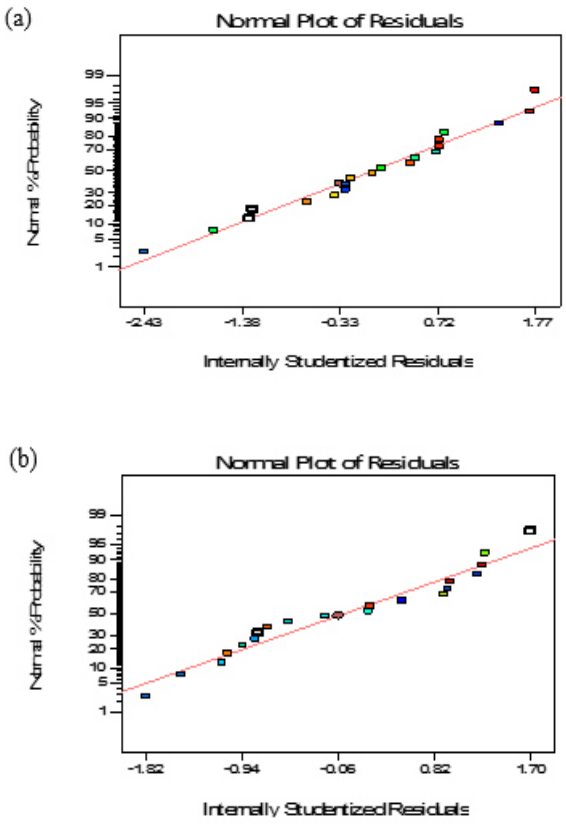

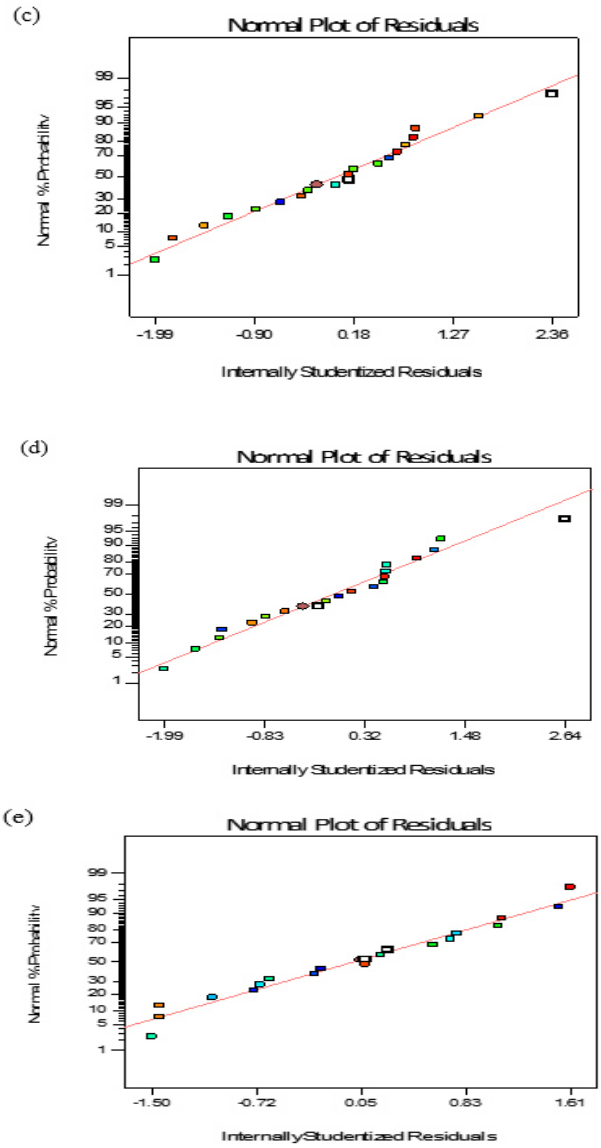

FIGURE 1
Normal % probability versus studentized residuals for removing a- BOD_5, b- COD, c- TP, d- color and e- variations of BOD_5/COD ratio.

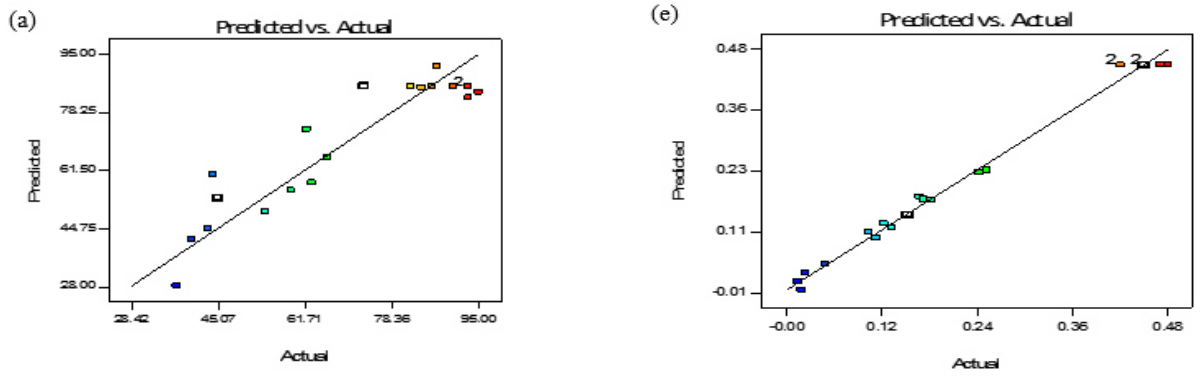

FIGURE 2
Predicted versus actual values for removing a- BOD_5, b- COD, c-TP, d-color and e- variations of BOD_5/COD ratio.

At the confidence level of 95%, the p-values were significant for all the models obtained for the five studied responses. Lack of fit test determines the data variations in the fitted model so that it is significant in the case that the model is not fitted properly [20]. Thus, according to Table 4, the test was not significant in all the variables and the data were fit to the obtained model. The quality of fit of the quadratic polynomial model is expressed by R^2. The high values of R^2 (above 0.8) in all the responses indicated high reliability of the obtained removal efficiencies. Therefore, there was good consistency between the actual data and the data predicted by the model. A desirable agreement between R^2 and Adj.R^2 (adjusted R^2) is essential. Pred.R^2 is the prediction of the model so that the closer the value to 1, the more accurate the model's prediction of responses would be. According to Table 4, all of these coefficients, except for BOD, were higher than 0.8 and, thus, desirable [21]. Adequate precision is the index for measuring the "signal to noise ratio"; in fact, A.P compares the predicted values in the design with the average predicted error. The values above 4 for this ratio indicate the model's adequacy. Accordingly, in all the responses of Table 4, these ratios were above 4, which indicated the adequate signal [16]. Coefficient of variation (C.V) describes the reproducibility of the model so that if the CV value were lower than 10%, it could be estimated as the standard error value. On this basis, as shown in Table 4, the CV for all the variables, except for BOD, was less than 10 and, thus, the model can be considered reproducible [16]. PRESS stands for the predicted residual error sum of squares and is used to assess models' predictive ability so that the smaller the PRESS value, the better the model's predictive ability would be.

Equality of variance and normal distribution of the residuals are the basic assumptions of ANOVA. In this section, some of the assumptions of the pro-

posed model are tested. The normal distribution diagram shows if the residuals follow the normal distribution. If the points are located on a straight line, the assumption of normal data distribution can be accepted. Figure 1 (a-e) shows the probability distribution of the residuals for the studied responses. In these diagrams, it can be seen that the residuals were almost located on a straight line; thus, the assumption of the residuals' normal distribution for the models was valid [22, 23].

Figure 2 (a-e) shows the comparison of the values predicted by the model with the values obtained from the experiment. These diagrams show a satisfactory agreement between the predicted data and the data obtained from the experiments. Thus, according to this diagram, the precision of the model was sufficient for predicting the model's performance.

Figure 3 (a-e) shows the response values predicted for each experiment by the model versus the studentized residuals. In this plot, the points were randomly distributed and followed no certain pattern (especially the megaphone pattern). Consequently, the assumption of the equality of variances was confirmed for the model [22, 23].

The response surface diagrams drawn by the software indicated a 2D view of the removal level of the contaminants.

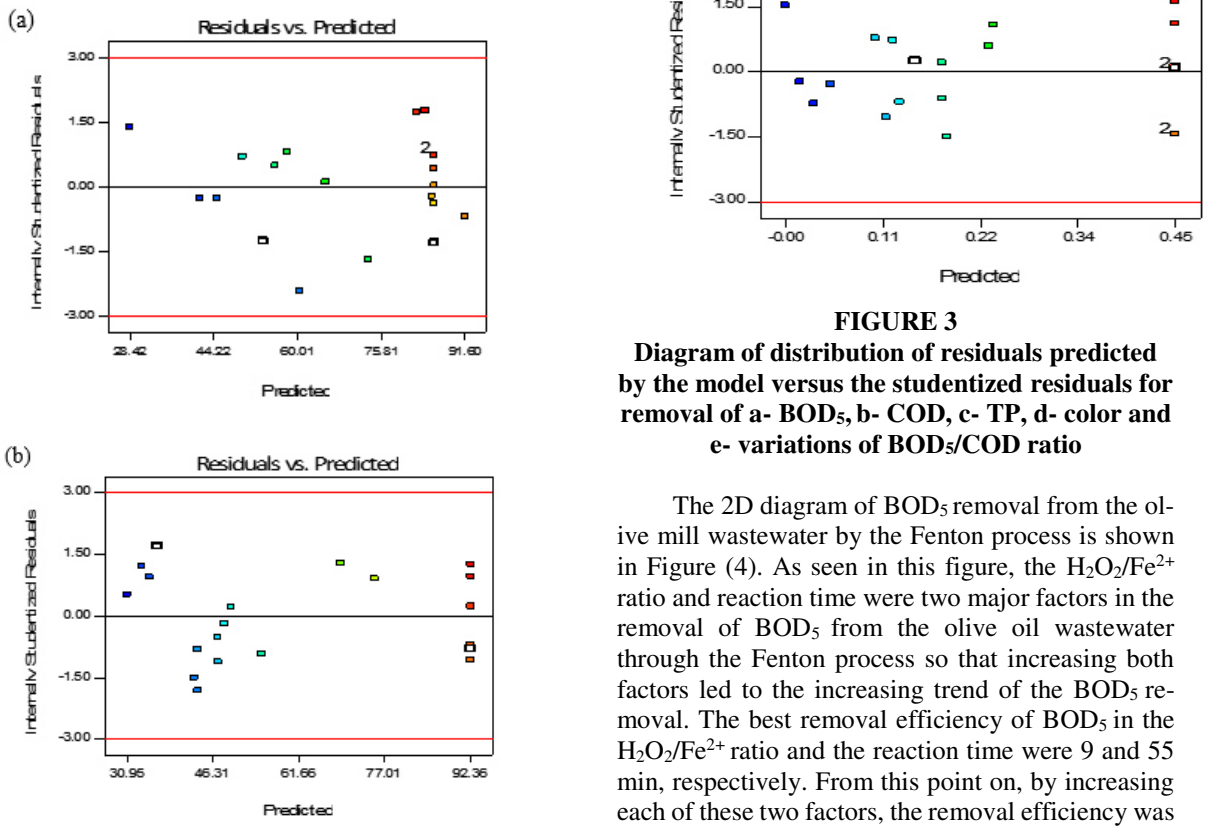

FIGURE 3
Diagram of distribution of residuals predicted by the model versus the studentized residuals for removal of a- BOD_5, b- COD, c- TP, d- color and e- variations of BOD_5/COD ratio

The 2D diagram of BOD_5 removal from the olive mill wastewater by the Fenton process is shown in Figure (4). As seen in this figure, the H_2O_2/Fe^{2+} ratio and reaction time were two major factors in the removal of BOD_5 from the olive oil wastewater through the Fenton process so that increasing both factors led to the increasing trend of the BOD_5 removal. The best removal efficiency of BOD_5 in the H_2O_2/Fe^{2+} ratio and the reaction time were 9 and 55 min, respectively. From this point on, by increasing each of these two factors, the removal efficiency was reduced so that, at the reaction time of 110.45 min and H_2O_2/Fe^{2+} ratio of 6, the removal efficiency reached 35%. Ahmadi et al. reported that with the

concentration of hydrogen peroxide similar to the one in the present research, hydrogen peroxide was completely consumed on the first hour of the reaction and removal of the contaminants was stopped. Therefore, the consumption time was dependent on the initial value of H_2O_2 used in the experiments [17]. They also reported that, at the initial concentration of 0.2 M, hydrogen peroxide was completely consumed after 1-2 h and, at the initial concentration of above 0.5 M, the complete consumption occurred after 8 h [24]. In the present research, the removal efficiency of BOD_5 reached its maximum value (89%) after the reaction time of almost 55 min. Furthermore, H_2O_2 was completely consumed during this period, but after this time, the removal of BOD_5 had a decreasing trend.

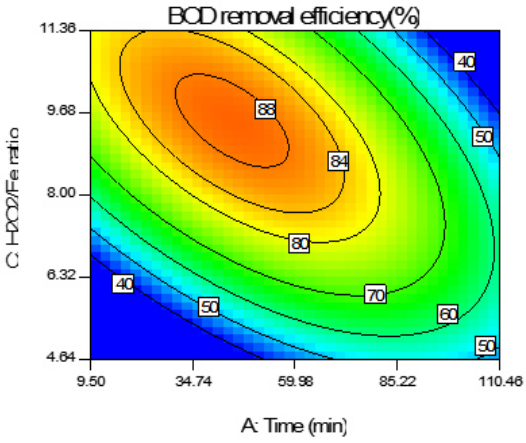

FIGURE 4
Contour plot for removal of BOD_5.

The diagrams in Figure 5 (a, b & c) show the interactive effects of the two factors on the removal of COD while keeping the other factor at the middle level. The obtained elliptic curves indicated the significant effects of the factors on the removal of COD. According to Figure (5-a), by increasing both factors of reaction time and pH, the emoval efficiency of COD was increased so that at the pH of 2.3 and reaction time of 9.6 min, there was no removal of COD. The maximum removal efficiency was obtained at the reaction time of 60 min and pH of 4. From this point on, by increasing both factors, the removal efficiency of COD had a decreasing trend. These results were compatible with those of the previous study done on the removal of COD from coking wastewater industry [25]. The efficiency of the Fenton process was strictly influenced by pH. Moreover, these results were consistent with those of recent reports stating that the optimal pH for the Fenton process is independent from the nature of wastewater and is about 3-5 [26, 27]. In the Fenton process, excessive increase of pH resulted in the elimination of Fe^{2+} ion from the catalytic cycle and formation of $Fe(OH)_3$, leading to a reduction in the efficiency of the process. Furthermore, at very low pH, Fe^{2+} slowly reacts with hydrogen peroxide and, as a result, production of the hydroxide radical is reduced [28].

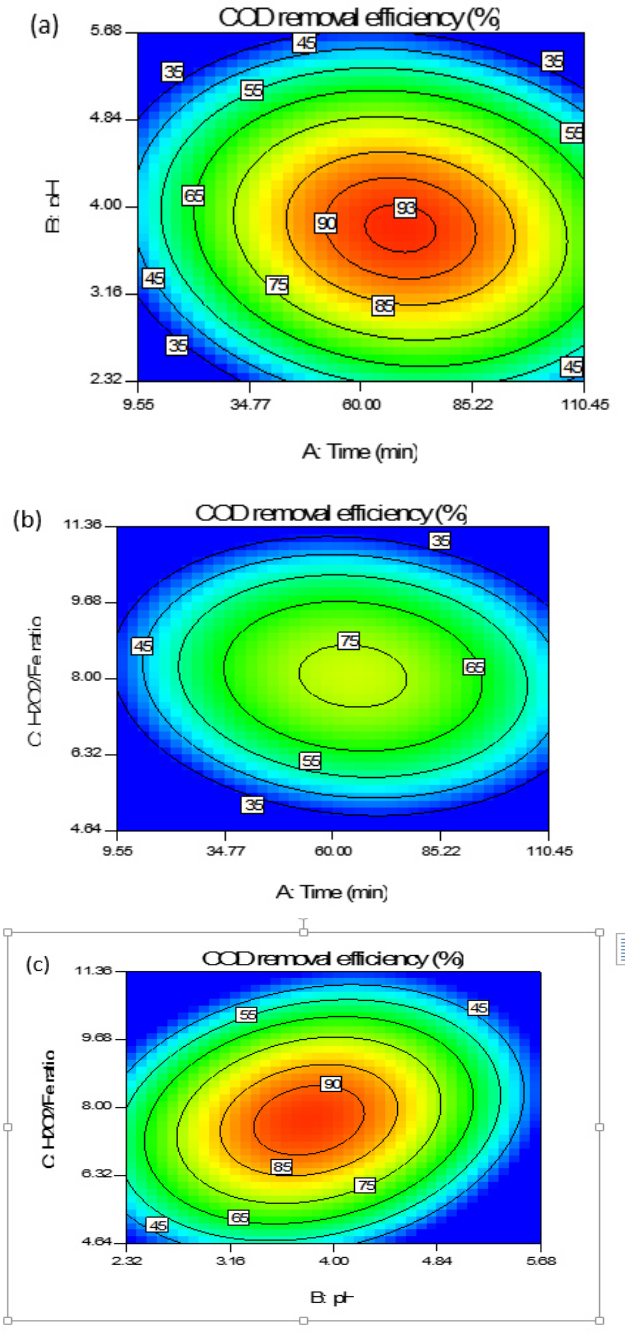

FIGURE 5
Contour plot for removal of COD.

Figure (5-b) shows the mutual effect of two factors of reaction time and H_2O_2/Fe^{2+} ratio on the removal efficiency of COD. This diagram is also elliptic, indicating the significant effect of these two factors on the removal of COD by the process. Accordingly, increasing both factors led to the increasing trend of the removal efficiency of COD so that, at the reaction time of 60 min and H_2O_2/Fe^{2+} ratio of 8, the removal efficiency of COD was at its maximum

level (94%). From this point on, by increasing both factors, the removal efficiency was reduced. The minimum removal efficiency was obtained at the reaction time of 69 min and H_2O_2/Fe^{2+} ratio of 10. Bensalah Nasr et al. reported that, at high molar ratios of hydrogen peroxide to iron salt, the hydroxyl radicals were formed slowly and the removal rate of COD remained constant. They also obtained the removal efficiency of 86% at the H_2O_2/Fe^{2+} molar ratio of [5]/[0.4] and reaction time of 20 min [2], while at lower H_2O_2/Fe^{2+} molar ratio and optimal reaction time of 60 min, the removal efficiency of COD was 94%.

Figure (5-c) shows the interactive effects of both factors of pH and H_2O_2/Fe^{2+} ratio on the removal of COD. As seen in this figure, increasing the value of both factors led to the increasing trend of the removal efficiency of COD so that this trend reached its maximum level (94%) at the point with the pH of 3.5 and H_2O_2/Fe^{2+} ratio of 8. From this point on, by increasing both factors, the removal efficiency of COD was decreased. The minimum removal efficiency of COD was 10% at the pH of 5.68 and H_2O_2/Fe^{2+} ratio of 6. According to the reports provided by Kallel and Neyens, high values of H_2O_2 produced more hydroxyl radicals, leading to the improvement of the COD removal efficiency, but the excessive concentration of H_2O_2 was not recommended because the excessive amount of hydrogen peroxide had adverse effects and prevented the formation of hydroxyl radicals besides reducing the removal efficiency of COD [25, 29]. Furthermore, the excessive amount of H_2O_2 scavenged hydroxyl radicals and had adverse effects on the decomposition process [29]. In the present study, in the case of high volumes of hydrogen peroxide as well as the H_2O_2/Fe^{2+} molar ratios of above 8, the removal efficiency of COD had a decreasing mode.

Figure (6-a) shows the interactive effects of reaction time and pH on the removal of the total phenol. According to this figure, the removal curves of the total phenol were elliptic as other curves, indicating the significant effect of both factors on the removal of the total phenol by the Fenton process. The minimum and maximum removal efficiencies of total phenol were obtained 33% at the reaction time of 10 min and pH of 5 and 72% at the reaction time of 60 min and pH of 2.8, respectively. From this point on, the removal efficiency of total phenol was reduced by increasing both factors. Removal of the phenolic compounds was affected by the reaction time more than other variables so that increasing the reaction time led to the increased removal level. As reported by Kallel, destruction of the phenolic compounds was initiated slowly and, then, the concentration of the phenolic compounds was reduced rapidly [25]. Also, Kang reported that decomposition of the contaminants by the Fenton process depends on the level of accessibility to the iron ions involved in the formation of hydroxyl radicals. The bivalent iron ions are produced even after complete consumption of hydrogen peroxide. Thus, some of the organic acids or acidic radicals might be involved in its production [30].

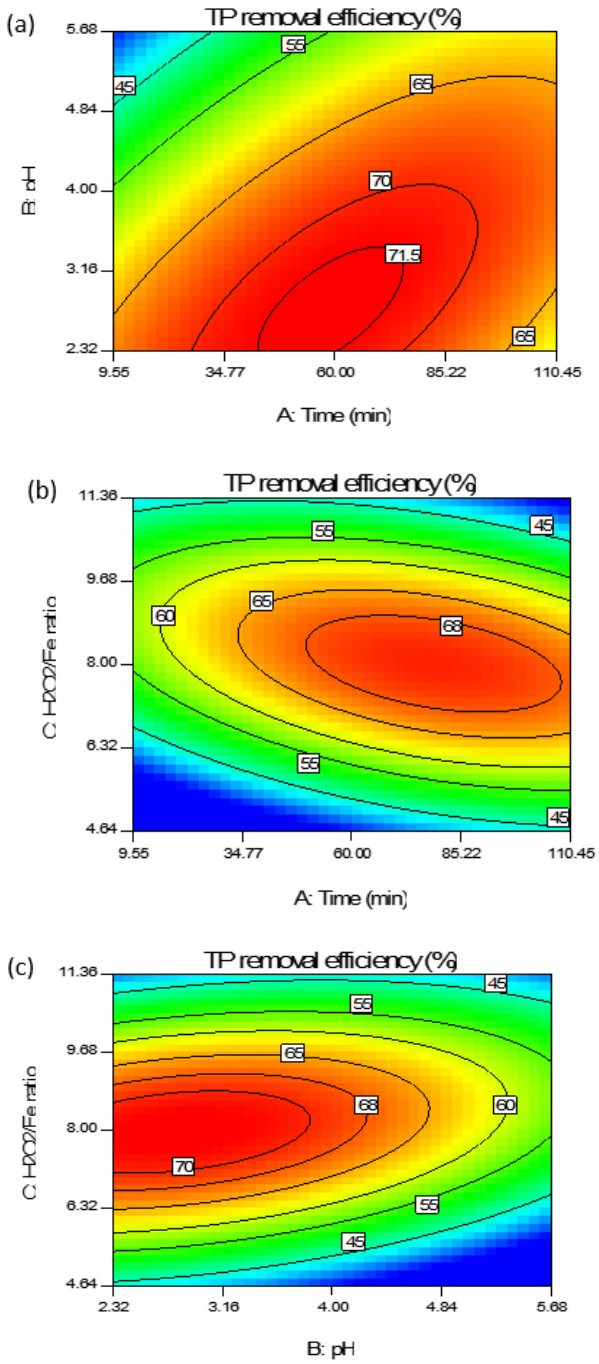

FIGURE 6
Contour plot for removal of TP.

Figure (6-b) shows the interactive effects of reaction time and H_2O_2/Fe^{2+} ratio. According to this figure, the minimum level of removal of total phenol was obtained at the reaction time of 9.6 min and H_2O_2/Fe^{2+} ratio of 6, while the maximum level was 71% at the reaction time of 60 min and H_2O_2/Fe^{2+} ratio of 8. Hydroxyl radicals were not formed in the

absence of the iron ions; thus, the phenolic compounds were not removed. At low concentrations of the iron ions, removal of the phenolic compounds was relatively low [17]. According to the report by Beltran et al., removal of the phenolic compounds did not occur with consuming only H_2O_2 and in the absence of the iron ions [31]. Therefore, the optimal H_2O_2/Fe^{2+} ratio plays a very effective role in the removal of phenolic compounds.

Figure (6-c) shows the interactive effects of pH and H_2O_2/Fe^{2+} ratio on the removal of total phenol. According to this figure, the effect of the H_2O_2/Fe^{2} ratio was more than that of pH. By increasing the H_2O_2/Fe^{2+} ratio from 6 to 8, the removal efficiency of the total phenol was increased so that the minimum and maximum removal efficiencies of total phenol were 36% at the H_2O_2/Fe^{2+} ratio of 6 and pH of 5.68 and 71.5% at the pH of 2.8 and H_2O_2/Fe^{2+} ratio of 8. However, after this point on, the removal efficiency had a reverse trend. According to Kallel's report, Kuo examined 5 different types of wastewater and observed that the most appropriate pH for the Fenton process was 3.5; further, he showed that at the pH of 2-4, the maximum amount of $Fe(OH)^{+}$ was formed and the activity of $Fe(OH)^{+}$ was higher than Fe^{2+} in the Fenton process [25, 26].

Figure (7-a) shows the interactive effects of reaction time and pH on the removal percentage of color. The minimum removal efficiency of color was 7% at the pH of 2.3 and reaction time of 9.6 min. The formed elliptic curves indicated the effect of both factors on the removal of color. According to this figure, the maximum removal efficiency of color was at the reaction time of 70 min and pH of 4.5, while from this point on, the increase in both factors led to the reduced removal efficiency of color. According to the obtained results, the minimum efficiency was related to the removal of color so that the maximum obtained efficiency was 95.43%. Ahmadi et al. also reported that the Fenton process had no identical performance in the decomposition of all the contaminants and its effect on the discoloration of the olive mill wastewater was limited [17].

However, this process had high efficiency in the removal of color from the wastewater of the textile, palm oil production industries and decolorization of Reactive Yellow B-4RFN dye [16, 17,32]. Thus, the removal rate of color from wastewater depends on the type and nature of the dye in the wastewater, and this process might have different efficiencies for the removal of various colors.

Figure (7-b) shows the interactive effects of reaction time and H_2O_2/Fe^{2+} ratio on the removal of color. According to this figure, both factors affected the removal of color. The minimum removal efficiency at the reaction time of 9.6 and H_2O_2/Fe^{2+} ratio of 4.64 was 11.5%. By increasing both factors, the removal efficiency of color was increased, but the effect of H_2O_2/Fe^{2+} ratio was more than that of the reaction time. The removal efficiency reached its maximum value (44%) at the reaction time of 60 min and H_2O_2/Fe^{2+} ratio of 8. However, from this point forward, the removal efficiency of color was reduced by increasing both factors. In the study conducted by Kallel et al., regarding the increased concentration of the organic complexes of iron in the solution, the black color of the olive oil wastewater reappeared in the tests after 2-3 h of the reaction time. Also in this study, the best removal efficiency of color occurred after 1 h of reaction time [25].

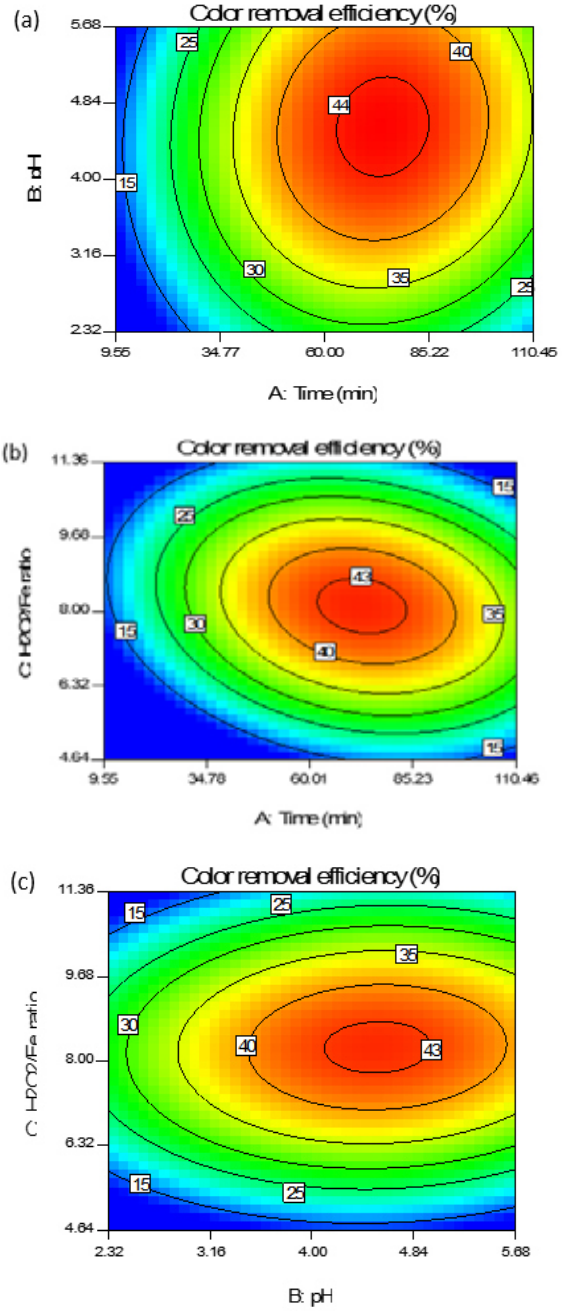

FIGURE 7
Contour plot for removal of color.

Figure (7-c) shows the interactive effects of pH and H_2O_2/Fe^{2+} ratio on the removal of color. According to this figure, both factors had significant effects

on the removal efficiency of color, but the effect of H_2O_2/Fe^{2+} ratio was more than that of pH. The best removal efficiency of color (96.36%) was obtained at pH of 4.5 and H_2O_2/Fe^{2+} ratio of 8. From this point on, increasing both factors led to the reduction in the removal efficiency of color.

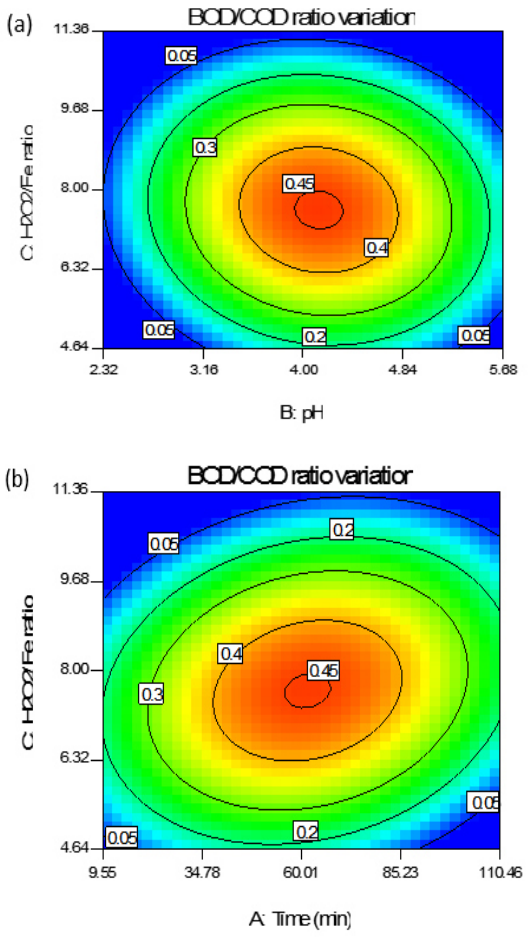

FIGURE 8
Contour plot for BOD_5/COD ratio variations.

Figure (8-a) shows the interactive effects of pH and H_2O_2/Fe^{2+} ratio on the BOD_5/COD ratio variations. According to this figure, the concentric circles indicated the significant effect of both factors on the improvement of the BOD_5/COD ratio. By increasing both factors of pH and reaction time, the BOD_5/COD ratio was increased, but after a certain level, this ratio was reduced by increasing one of the factors. The maximum BOD_5/COD ratio was obtained at the pH of 4 and H_2O_2/Fe^{2+} ratio of 6.5.

Figure (8-b) demonstrates the interactive effects of reaction time and H_2O_2/Fe^{2+} ratio. Accordingly, the elliptic shape of the curves indicated the significant effects of these two factors on the studied response. According to this figure, by increasing both factors, the BOD_5/COD ratio was improved, but this trend continued up to a certain extent and, then, it was reversed. The maximum BOD_5/COD ratio was obtained at the reaction time of 60 min and H_2O_2/Fe^{2+} ratio of 7.

The low BOD_5/COD ratio in the output wastewater of the factory indicated non-biodegradability of this wastewater; thus, the biodegradability feature of the wastewater can be improved using the Fenton process.

Process optimization. In order to optimize the process factors in the removal of the studied responses, in the numerical optimization section of the software mentioned above, all the three factors of reaction time, pH and H_2O_2/Fe^{2+} ratio were set in the "in range" mode and the four studied responses were set in the "maximize" mode. In this mode, the optimal conditions for reaction time, pH and H_2O_2/Fe^{2+} ratio were obtained equal to 66.81 min, 3.83 and 8, respectively. The removal efficiency of BOD_5, COD, total phenol, color and BOD_5/COD ratio variations was obtained equal to 87%, 93.8%, 70.4%, 42.85% and 0.44%, respectively. Under these conditions, the desirability was 92.8%.

To confirm the agreement between the results obtained by the model and laboratory experiments, three additional experiments were performed under optimal conditions. The obtained results are shown in Table 5.

The results obtained from the tests under the optimal conditions predicted by the model showed a good agreement between the results estimated by the model and the actual values.

TABLE 5
Laboratory results of verification under optimal conditions obtained by the model.

Optimal conditions: **Reaction time: 66.81** **pH: 3.83** **H_2O_2/Fe^2 ratio: 8**	**Responses**				
	Removal efficiency of BOD_5(%)	Removal efficiency of COD(%)	Removal efficiency of total phenol (%)	Removal efficiency of color(%)	Variations of BOD_5/COD ratio
Experimental value	89.2	95.3	73.1	43.4	0.45
Model prediction	86.94	93.82	70.4	42.85	0.44
Error	2.26	1.48	2.7	0.55	0.01
Standard deviation (SD)	±1.2	±0.73	±1.32	±0.15	±0.004

CONCLUSION

According to the results of the present research, the Fenton process affects the removal of the contaminants from the olive mill wastewater; thus, it is considered as an efficient and powerful technique for the pre-treatment of this type of wastewater. Furthermore, at certain values of the studied factors, the BOD_5/COD ratio can be increased so that the biodegradability is increased; consequently, the biological processes can be used for the additional treatment of this type of wastewater. The CCD and response surface method are also appropriate for designing the tests, predicting the results and determining the optimal conditions in order to exploit the Fenton process for olive oil wastewater treatment.

ACKNOWLEDGEMENTS

This paper is partially the result of a Master's thesis approved in Qazvin University of Medical Sciences (QUMS).The authors wish to acknowledge the Vice Chancellery for Research of QUMS for the financial support of Research Project No. IR.QUMS.REC.1395.137.

REFERENCES

[1] Ochando-Pulido, J.M., Hodaifa, G., Victor-Ortega, M.D., Rodriguez-Vives, S., Martinez-Ferez, A. (2013) Reuse of olive mill effluents from two-phase extraction process by integrated advanced oxidation and reverse osmosis treatment. Journal of Hazardous Materials 263, 158-67.

[2] Bensalah, N., Bedoui, A., Gadri, A. (2004) Fenton treatment of olive oil mill wastewater-Applicability of the method and parameters effects on the degradation process. journal of envirenment sciences 16(6), 942-4.

[3] Galiatsatou, P., Metaxas, M., Arapoglou, D., Kasselouri-Rigopoulou, V. (2002) Treatment of olive mill waste water with activated carbons from agricultural by-products. Waste Management 22(7), 803-12.

[4] Uğurlu, M. (2005) Removal of some inorganic compounds from papare mill effluents by the electrocoagulation methods. Fresen. Environ. Bull. 14(4) 319-325.

[5] Jamil, R., Kamil, R., Karrine, A. (2014) Advanced oxidation of olive mill wastewater OMW by an oxidative free-radical process induced with zero valent iron. journal of Food research 3, 70-82.

[6] Ochando-Pulido, J.M., Victor-Ortega, M.D., Hodaifa, G., Martinez-Ferez, A. (2015) Physicochemical analysis and adequation of olive oil mill wastewater after advanced oxidation process for reclamation by pressure-driven membrane technology. Science of The Total Environment 503–504, 113-21.

[7] Kestioğlu, K., Yonar, T., Azbar, N. (2005) Feasibility of physico-chemical treatment and Advanced Oxidation Processes (AOPs) as a means of pretreatment of olive mill effluent (OME). Process Biochemistry 7, 2409-16.

[8] Mantzavinos, D., Kalogerakis, N. (2005) Treatment of olive oil mill effluents part I. organic matter degradation by chemical and biological processes- an overview. Environmental International 31, 289-95.

[9] Zouari, N. (1998) Decolourization of olive oil mill effluent by physical and chemical treatment prior to anaerobic digestion. chemical Technology Biotechnology 73, 297–303.

[10] Michael, I., Panagi, A., Ioannou, L.A., Frontistis, Z., Fatta-Kassinos, D. (2014) Utilizing solar energy for the purification of olive mill wastewater using a pilot-scale photocatalytic reactor after coagulation-flocculation. Water Research 60:28-40.

[11] Baldrian, P., Zervakis, G., Merhautová, V., Ntougias, S., Ehaliotis, C., Nerud, F. (2006) The use of Hydroxyl-radical-generating systems for the treatment of olive mill wastewater. Folia Microbial 51(4), 337-41.

[12] Hodaifa, G., Ochando-Pulido, J.M., Rodriguez-Vives, S., Martinez-Ferez, A. (2013) Optimization of continuous reactor at pilot scale for olive-oil mill wastewater treatment by Fenton-like process. Chemical Engineering Journal 220, 117-24.

[13] Apostolos G. Vlyssides, Haralampos N. Loukakis, Panagiotis K. Karlis, Elli Maria P. Barampouti and Sofia T. Mai (2004) Olive mill wastewater detoxification by appiying pH related fenton oxidation process. Fresen. Environ. Bull. 13(6), 501-505.

[14] Yang, K., Guo, J., Liao, Y., Liu, H., Wang, Y. (2017) Optimization of photo – fenton process with diatomite – supported α- Fe_2O_3 for treatment of dimethyl phthalate using respoponse surface methodology. Fresen. Environ. Bull. 26(2a), 1477-1484.

[15] Mohajeri, S., Aziz, H.A., Isa, M.H., Zahed, M.A., Adlan, M.N. (2010) Statistical optimization of process parameters for landfill leachate treatment using electro-Fenton technique. Journal of Hazardous Materials 176(1–3), 749-58.

[16] Saeed, M.O., Azizli, K., Isa, M.H., Bashir, M.J.K. (2015) Application of CCD in RSM to obtain optimize treatment of POME using Fenton oxidation process. Journal of Water Process Engineering 12(8), 7-16.

[17] Ahmadi, M., Vahabzadeh, F., Bonakdarpour, B., Mofarrah, E., Mehranian, M. (2005) Application of the central composite design and

response surface methodology to the advanced treatment of olive oil processing wastewater using Fenton's peroxidation. Journal of Hazardous Materials 123(1–3),187-95.
[18] APHA. (2005) Standard Methods for the Examination of Water and Wastewater, APHA-AWWA-WPCF.;washington, D.C, USA.
[19] Sigge, G., Britz, J., Fourie, P., Barnardt, C., Strydom, R. (2002) Combining UASB technology and advanced oxidation processes (AOPs) to treat food processing wastewaters. Water Sci Technology 45(10), 329-34.
[20] Ghafari, S., Aziz, H.A., Isa, M.H., Zinatizadehd, A.A. (2009) Application of response surface methodology (RSM) to optimize coagulation–flocculation treatment of leachate using poly-aluminum chloride (PAC) and alum. Journal of Hazardous Materials 163, 650-6.
[21] Noordin. M., Venkatesh, V., Sharif, S., Elting, S., Abdullah, A. (2004) Application of response surface methodology in describing the performance of coated carbide tools when turning AISI 1045 steel. Mater Process Technology 145(1), 46-58.
[22] Behbahani, M., Moghadam, M.A., Arami, M. (2011) Techno-economical evaluation of fluoride removal by electrocoagulation process: optimization through response surface methodology. Desalination 271, 209–218.
[23] Montgomery DC., Runger GC., Hubele NF. (2011) Engineering Statistics. John Wiley & Sons Inc, USA.
[24] Rivas, F.J., Beltran, F.J., Gimeno, O. Frades, J. (2001) Treatment of olive oil mill wastewater by Fenton's reagent. Food Chem. 49, 3285–91.
[25] Peng, R., Yu, P., Luo, Y. (2016) A comparative study of fenton and electrofenton treatment for COD removal from coking industry wastewater. Fresen. Environ. Bull. 25(10), 3987-3992.
[26] Kallel, M., Belaid, C., Boussahel, R., Ksibi, M., Montiel, A., Elleuch, B. (2009) Olive mill wastewater degradation by Fenton oxidation with zero-valent iron and hydrogen peroxide. Journal of Hazardous Materials 163(2–3), 550-4.
[27] Kuo, WG. (1992) Decolorizing dye wastewater with Fenton's reagent. Water Research 26(7):881-6.
[28] Parsons, S. (2004) Advanced oxidation processes for water and wastewater treatment: IWA.
[29] Neyens, E., Baeyens, J. (2003) A review of classic Fenton's peroxidation as an advance oxidation technique. Hazard Mater.;98:33-50.
[30] Kang, N., Lee, D., Yoon, J. (2002) Kinetic modeling of Fenton oxidation of phenol and monochlorophenols. Chemosphere 47, 915–24.
[31] Beltran-Heredia, J., Torregrosa, J., Dominguez, J., Peres, J. (2001) Oxidation of *p*-hydroxybenzoic acid by UV radiation and by TiO_2/UV radiation: comparison and modelling of reaction kinetic. Journal of Hazardous Materials 83(3), 255-264.
[32] Gao, A., Peng. Z., Wang W., Li, F. (2017) Online monitoring of decolorization kinetics of reactive yellow B-4RFN in fenton process. Fresen. Environ. Bull. 26(5), 3415-3421.

Received: **14.03.2017**
Accepted: **05.07.2017**

CORRESPONDING AUTHOR

Hamzeh Ali Jamali
Department of Environmental Health Engineering, School of Public Health, Qazvin University of Medical Sciences (QUMS), Qazvin, Iran

e-mail: hajamali@qums.ac.ir

© by PSP Volume 26 – No. 10/2017 pages 5954-5964 Fresenius Environmental Bulletin

EFFECTS OF SOIL ENVIRONMENTAL FACTORS ON VEGETATION COMMUNITIES IN THE DEGRADED TARIM RIVER WETLAND

Peng Dong[1], Ming Li[1], Jiyuan Jiang[1], Jun Zhang[1], Qiling Chen[1,*], Yaojun Zhu[2]

[1]Xinjiang Academy of Agricultural and Reclamation Science, Shihezi City, Xinjiang Province, China
[2]Research Institute of Wetland, Chinese Academy of Forestry, Beijing, China

ABSTRACT

The distribution of wetland vegetation is significantly influenced by soil environmental factors. Few studies have been conducted on the restoration processes used on the degraded wetlands of the Tarim River. We surveyed the vegetation communities of the Tarim River Basin, and their responses to soil environmental factors using two methods of indicator species classification (TWINSPAN): detrended correspondence analysis (DCA) and detrended canonical correspondence analysis (DCCA) ordination. Results showed that Tarim River wetland species were limited, the community structure was simple, and there were no endemic species. There were only 34 plant species in the study area, and 12 families were represented by only 1 species. Wetland flora in the Tarim River Basin consisted mainly of herbaceous plants, with only a few shrub and tree species. These results show that the degradation of the Tarim River wetland is severe. The vegetation community was divided into 4 formations using TWINSPAN, and 3 formations using DCA. Both methods showed clear distribution boundaries, and the DCA also provided a good reflection of the vegetation and soil environment. The DCCA ordination showed that the distribution of vegetation in the study area was affected by a combination of elevation, salinity, and soil moisture. Pairwise correlations also showed that vegetation diversity was significantly correlated with elevation. Therefore, we suggest that the process of restoring the degraded wetland cannot solely rely on restoring the hydrological conditions in the Tarim River Basin, as topography and soil salinity must also be taken into account. These results should be integrated into the vegetation restoration and management plans of the Tarim River wetland and could be important for the ecological management of the Tarim River Basin.

KEYWORDS:
Tarim River; vegetation community; TWINSPAN; DCA; DCCA;

INTRODUCTION

Wetlands are well-known biodiversity hotspots [1]. Wetlands are among the most productive ecosystems on Earth. As well as providing a diverse array of important ecosystem services, they are fundamental to the maintenance of the water cycle and the control of water flow that refills aquifers [2]. Wetland plants play an important role in the stability of wetland ecosystems [3], but are very sensitive to environmental changes, such that the degradation of wetlands manifests initially through the vegetation [4]. The plant community is a significant component of and a primary producer in wetland ecosystems, and maintains various physical processes and biological functions of the ecosystem. The structure, function, and ecological characteristics of the wetland ecosystem reflect the basic and functional features of the ecological environment of the wetland.

Researchers in China have studied plant community features and species diversity in different wetland types [5], especially in arid and semiarid regions, and have reported that wetlands make a significant contribution to the protection of biodiversity. Studies on species diversity in desert oasis wetlands in arid and semiarid regions have gained increasing attention [6,7]. Soil is a living terrestrial matrix and is one of the most important environmental conditions affecting the distribution of vegetation communities and plant survival. The interaction of wetland plants and the environment was thought to occur via the relationship between individual wetland species and the environment. This inter-species relationship emphasized the need for research into wetland vegetation community ecology. Recently, ecologists have attempted to explore the factors that control plant species distribution and variation in vegetation communities [8]. The study of wetland vegetation communities is important for wetland protection, restoration, and reconstruction [9].

Xinjiang is a typical arid region in China, which contains various types of wetlands that are severely degraded. In the early 1950s, the total wetland area in this region was reduced from 2.8 million to 1.48 million hm^2. The Tarim River in Xinjiang is considered to be a world-famous inland river, is one

of the key areas for biodiversity conservation and global climate change research in China, and has distinct regional characteristics and environmental issues that are well recognized on a global scale. Over the past 50 years, the Tarim River wetland has undergone significant changes, where rivers and lakes have dried up, water tables have declined, ecosystem diversity has been depleted, and desertification processes have intensified. The Tarim River has therefore become a hotspot for ecological research in China. Many studies have been conducted on the effects of groundwater on vegetation, the effects of ecological water conveyance, and the relationship between the distribution of vegetation and the environment [10].

Quantitative ecology, including classification and ordination, has advanced research into wetland community ecology, and has become an essential tool for modern vegetation ecology, as it presents the relationship between vegetation and the environment using the sequence theory of community ecology [11]. Since the 1930s, numerous studies have been conducted on the relationship between the vegetation community and environmental factors [12, 13, 14]. However, because of the complexity of soil environmental factors within the Tarim River wetland, information regarding the restoration of the degenerated wetland in the Tarim River Basin is lacking.

Therefore, the objectives of this study were to (1) identify the effects of soil environmental factors on both vegetation types and the classification of vegetation types; and (2) demonstrate the strength of the dependence of wetland vegetation types on the quantitative variables of the soil environment. To achieve this, a quantitative study of vegetation and soil environment factors was conducted on the Tarim River wetlands using a multivariate analysis. Wetland vegetation communities were classified using the Two-Way Indicator Species Analysis (TWINSPAN). Detrended correspondence analysis (DCA) and detrended canonical correspondence analysis (DCCA) were used to sort and analyze the responses of wetland vegetation to soil environmental factors within the study area. This study provides a scientific basis for the management and restoration of vegetation and habitat in the Tarim River Basin.

MATERIALS AND METHODS

Experimental design. Study area. The Tarim River is located in the hinterland of Eurasia between 34° 55′–43° 08′ N and 73° 10′–94° 05′ E (Fig. 1). The river is isolated from the ocean in a region with a typical temperate continental climate, undulating topography in the Southern Desert, mountainous ranges in the northwest, and a central highland zone. The total area of the river basin is 1,026,000 km^2 (including an area outside China of 23,400 km^2). The river basin experiences a dry climate, scarce precipitation, intensive evaporation, excessive sand and dust storms, a long duration of sunshine, and an abundance of light and heat radiation. The annual maximum daily temperature is generally above 25°C, with an annual average temperature of 10.7°C. The average annual precipitation is between 17.4 and 42.8 mm, strong evaporation is between 1125 and 1600 mm, and there is a high frequency of windy weather, with a maximum wind speed of 40 m/s [15]. The water in the river basin is mainly sourced from glacial/snow melt, which accounts for 48.2% of the total water volume [16].

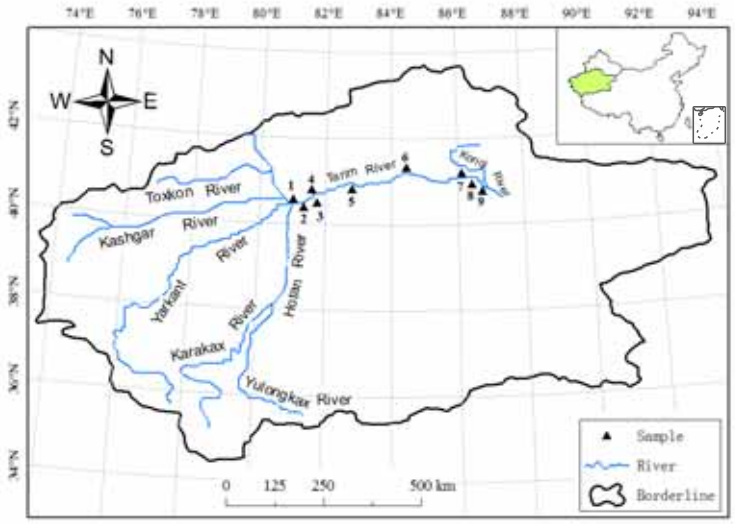

FIGURE 1
Location of quadrats in the 9 study areas of the Tarim River Basim

TABLE 1
Plant associations with structural features of a typical degraded wetland

Study area	Community number	Plant community	Elevation (m)	Coverage	Number of Companions	Number of canopy layers
I	1	Ass. *Lycium ruthenicum* & *Phragmites australis*	1041	83%	5	3
	2	Ass. *Halocnemum strobilaceum*	1017	48%	1	2
	3	Ass. *Tamarix ramosissima* & *Phragmites australis*	1022	88%	3	3
	4	Ass. *Phragmites australis* & *Eleocharis dulcis*	1018	100%	5	1
	5	Ass. *Phragmites australis*	1012	82%	1	2
II	6	Ass. *Phragmites australis*	1024	76%	7	1
	7	Ass. *Salicornia europaea*	1023	81%	2	2
	8	Ass. *Phragmites australis* & *Salicornia europaea*	1025	73%	3	3
	9	Ass. *Herba suaedae*	1024	59%	2	1
	10	Ass. *Tamarix ramosissima* & *Salicornia europaea*	1023	86%	5	3
	11	Ass. *Phragmites australis* & *Halocnemum strobilaceum*	1018	83%	2	2
III	12	Ass. *Populus euphratica*	989	15%	3	1
	13	Ass. *Phragmites australis*	997	95%	3	1
	14	Ass. *Populus euphratica* & *Tamarix ramosissima*	998	91%	2	3
IV	15	Ass. *Halostachys caspica* & *Phragmites australis*	1007	62%	2	3
	16	Ass. *Tamarix ramosissima* & *Phragmites australis*	1004	78%	2	3
	17	Ass. *Phragmites australis*	1002	87%	3	2
	18	Ass. *Populus euphratica* & *Phragmites australis*	1007	91%	5	3
	19	Ass. *Lycium ruthenicum* & *Phragmites australis*	1007	80%	1	3
V	20	Ass. *Tamarix ramosissima* & *Glycyrrhiza inflata*	971	95%	7	3
	21	Ass. *Apocynum venetum*	969	33%	2	1
	22	Ass. *Lycium ruthenicum*	971	46%	2	1
	23	Ass. *Halimodendron halodendron*	969	95%	5	2
	24	Ass. *Populus euphratica* & *Tamarix ramosissima*	977	80%	0	1
	25	Ass. *Tamarix ramosissima*	965	57%	1	2
VI	26	Ass. *Populus euphratica* & *Halimodendron halodendron*	921	53%	2	3
	27	Ass. *Populus euphratica* & *Tamarix ramosissima*	919	69%	1	2
	28	Ass. *Populus euphratica* & *Glycyrrhiza inflata*	925	100%	6	2
	29	Ass. *Populus euphratica* & *Phragmites australis*	917	95%	3	3
VII	30	Ass. *Populus euphratica*	863	95%	3	2
	31	Ass. *Hexinia polydichotoma*	858	26%	1	1
	32	Ass. *Phragmites australis* & *Apocynum venetum*	857	61%	1	2
	33	Ass. *Tamarix ramosissima* & *Lycium ruthenicum*	856	90%	6	3
VIII	34	Ass. *Karelinia caspia* & *Alhagi sparsifolia*	863	36%	2	2
	35	Ass. *Tamarix ramosissima* & *Karelinia caspia*	963	63%	2	2
	36	Ass. *Halostachys caspica* & *Halocnemum strobilaceum*	865	97%	4	2
	37	Ass. *Karelinia caspia*	859	72%	2	2
IX	38	Ass. *Apocynum venetum*	864	66%	3	2
	39	Ass. *Licorice* & *Phragmites australis*	861	78%	2	2

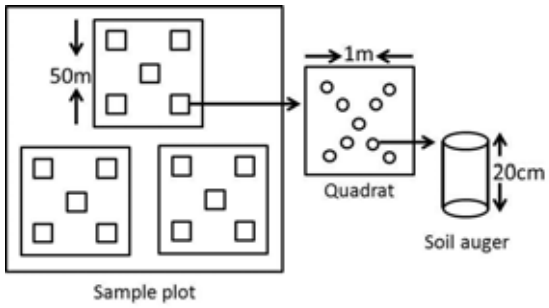

FIGURE 1
Sampling methods of vegetation communities and soil

Data collection. (1) Survey design. This study selected 39 typical degraded wetland sites in 9 study areas (Fig. 1), located at four distinct areas of the Tarim River Basin, in July 2014. Between 2 and 6 vegetation communities were selected in each study area, which was perpendicular to the riparian zone. For each vegetation community, three fixed (50 m × 50 m) quadrats were established, for a total of 117 quadrats, to directly observe the structure and composition of the tree layer. Within each quadrat, three 5 m × 5 m sample observations were made to measure the structure and composition of the shrub layer, and three 1 m × 1 m sample observations were made to measure the structure and composition of the herb

layer, for a total of 351 samples. The indicators used were species composition, number of individuals, and vegetation coverage. The number of individuals was calculated using a statistical method, and vegetation coverage was calculated using a projection method (Table 1).

(2) Soil parameters. Soil samples were collected from each community (39) in July 2014 at a depth of 0–20 cm [17, 18, 19] (Fig. 2). Three replicate soil samples were taken from each community and tested for soil water content, soil organic matter content, total salt concentration, pH, available nitrogen, soil available phosphorous, and available kalium. Soil samples were transported to the lab to remove any visible plant residues and invertebrates. Soil moisture content was calculated using the average of the soil moisture monitor record data. Soil pH was measured by suspending soil in a 1:2.5 solution of distilled water. Salt content was expressed as conductivity and was measured using a conductivity meter (soil:water = 1:5). Available nitrogen was measured using the alkaline hydrolysis nitrogen diffusion method with alkali N. Olsen P was extracted using 0.5 M $NaHCO_3$ (pH = 8.5) at a 20:1 extract:soil ratio for 0.5 h. The P concentration in the extracts was determined using Mo-Sb colorimetry [20]. Available K was extracted using 1 M NH_4OAc (pH = 7) at a 10:1 extract:soil ratio for 0.5 h. The K concentration in the extracts was determined using flame photometry [21]. To estimate the organic matter content, the Walkley–Black method was used, which involved oxidizing organic substances using 10 ml of $K_2Cr_2O_7$ in 20 ml of H_2SO_4 at 96% at the temperature reached during the sudden dilution of the sulfuric acid [22]. Each soil index was measured three times, and the three measurements were combined to give a final average for each index. The results of the vegetation survey and soil parameters were used in the classification and ordination analyses.

Data analysis. (1) Numerical vegetation classification. The environmental gradient and the relationship between species and samples were interpreted using TWINSPAN with WinTWINS 2.3 software. The Plant Community Classification (PCC) method is one of the most advanced methods currently available, because of the absence of artifacts in the analysis. A matrix of 39 × 34 represented the Importance Values (see below) from 39 quadrats and 34 species. The results established an arborescence in the fourth classification results. Classification using WinTWINS software was conducted by importing the data matrix containing the species importance values. Four levels of classification were set for each species importance value: 5, 30, 50, and 70 (the importance values ranged from 0 to 85.9). Four levels of weight value were also set: 1, 1, 1, and 2 (the lowest level of 0-5 was not included). Classification groups were set with a minimum of 3 and a maximum of 6. In each division, the maximum indicator species was 7 [23].

(2) Statistical analysis. All data conformed to the assumptions of equal variance and normality. The unimodality of data was tested using detrended correspondence analysis (DCA) and detrended canonical correspondence analysis (DCCA) [24]. Then, unconstrained and constrained ordination (DCA and DCCA) was performed using CANOCO for Windows, version 4.5 [25]. The significance of the DCCA results was tested using the Monte Carlo method. Pairwise correlations of variables were calculated using PAST software, version 2.03 [26].

(3) Calculation of indicators. The Importance Values of trees, shrubs, and herbs were calculated as follows:

$$IV = (RFE + RHI + RCO)/300 \quad (1)$$

where IV is the Importance Value, RFE is the relative frequency, RHI is the relative height, and RCO is the relative coverage. A matrix of 39 vegetation plots × 34 species importance values was constructed.

Shannon-Wiener Diversity Index - Species Diversity Index formula [27]:

$$H = -\sum_{i=1}^{s}\left(P_i \times Ln\, P_i\right) \quad (2)$$

where P_i is the number of species, i, which is proportional to the total number of all species in a community, namely $P_i = N_i/N$ (where N_i represents the number of species, i), n represents the total number of individuals across all species, and S represents the number of species communities.

RESULTS

Floristic composition. Across the 39 sample communities, 34 plant species were recorded (Table 2), belonging to 32 genera, and 18 families. Among the 34 species, there were 8 monocotyledon species from 8 genera, in 4 families, and 26 dicotyledon species from 24 genera, in 14 families. This indicates that dicotyledons comprised a significant proportion of the plant communities. There were 6 species from the families Chenopodiaceae and Asteraceae, which accounted for 17.65% and 17.65% of total species count, respectively. There were 4 species from the family Poaceae, accounting for 11.76% of total species count, and 2 species each from the families Cyperaceae, Salicaceae, and the sub-family Papilionaceae. Among all families, 12 were represented by only 1 species, accounting for 66.67% of the total family count. This indicates that vegetation in the degraded wetlands in the study areas was not dominated by one species or family.

TABLE 2
Percentage of plant species in the study area

Class	Family	Number of genera	Percentage of genera (%)	Number of species	Percentage of species (%)
Monocotyledon	Poaceae	4	12.50	4	11.76
	Cyperaceae	2	6.25	2	5.88
	Juncaceae	1	3.13	1	2.94
	Solanaceae	1	3.13	1	2.94
subtotal	4	8	25.00	8	23.53
Dicotyledon	Salicaceae	2	6.25	2	5.88
	Rosaceae	1	3.13	1	2.94
	Portulacaceae	1	3.13	1	2.94
	Amaranthaceae	1	3.13	1	2.94
	Primulaceae	1	3.13	1	2.94
	Chenopodiaceae	5	15.63	6	17.65
	Scrophulariaceae	1	3.13	1	2.94
	Asteraceae	6	18.75	6	17.65
	Tamaricaceae	1	3.13	1	2.94
	Caryophyllaceae	1	3.13	1	2.94
	Haloragaceae	1	3.13	1	2.94
	Leguminosae	1	3.13	1	2.94
	Apocynaceae	1	3.13	1	2.94
	Papilionaceae	1	3.13	2	5.88
subtotal	14	24	75.00	26	76.47
Total	18	32	100	34	100

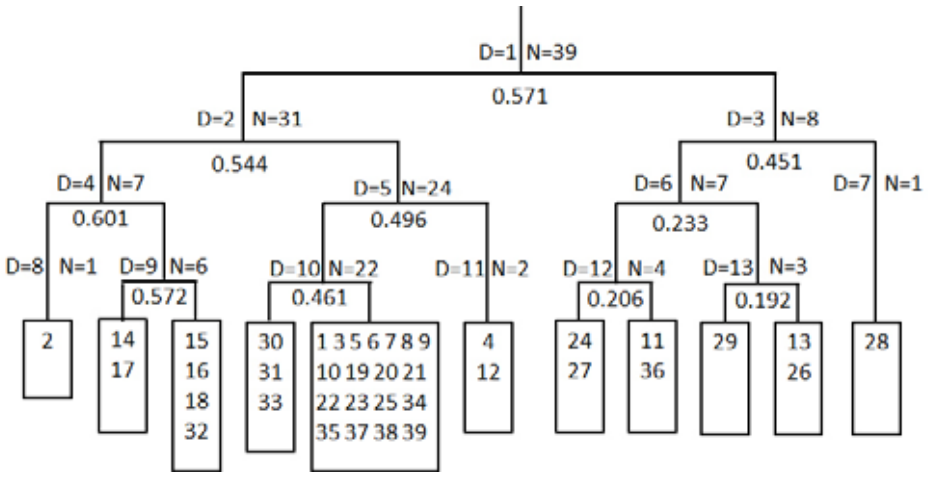

FIGURE 3
TWINSPAN classification of vegetation communities in the Tarim River Basin

Plant types in the study areas included trees, shrubs, annual herbs, and perennial herbs. Herbaceous plants were the most abundant, with 24 species accounting for 70.59% of the total species count, including 11 annual and 13 perennial herb species. There were 8 shrub species and 2 tree species, accounting for 23.53% and 5.88% of the total species count, respectively.

TWINSPAN classification of the vegetation communities. The importance of the value data matrix obtained from TWINSPAN produced a classification tree of the fourth classification results. This showed a conclusive division of the associated species in the degraded Tarim wetland vegetation community, which was divided into 11 groups. The degraded Tarim River wetland was divided into 4 formations as follows (Fig. 3):

Formation I: *Halostachys caspica* + *Salicornia europaea*. Included samples 2, 14, 15, 16, 17, 18, and 32, with an eigenvalue of 0.601. The samples showed that soil water content, salt content, and unit weight were relatively high. Associated with *Kalidium foliatum*, *Halocnemum strobilaceum*, *Suaeda glauca*, *Lycium ruthenicum*, and other halobiont vegetation.

Formation II: *Lycium ruthenicum* + *Alhagi sparsifolia* + *Phragmites australis*. Included all of the other samples not in formations I, III, or IV, with

an eigenvalue of 0.496. Dominant species were semi-desert vegetation. Soil nutrient content and pH value were higher than normal.

Formation III: *Populus euphratica*. Included samples 11, 13, 24, 26, 27, 29, and 36, with an eigenvalue of 0.233. Higher vegetation coverage and lower salt content.

Formation IV: *Populus euphratica* + *Glycyrrhiza inflata*. Included sample 28 only, with an eigenvalue of 0.451. Moderate terrain. Higher vegetation coverage and lower salt content.

DCA ordination. DCA ordination reflects the distribution of communities along major environmental gradients, prioritizes the environmental factors that significantly affect communities, and assigns them to axes in order of priority. According to the DCA, the length of the gradient of the first axis was 4.148. Datasets of all the vegetation types proved to be strongly unimodal. DCA was selected as a method for indirect gradient analysis [24]. According to the indirect analysis, 15.5% of the variance in the species-environment correlation was explained by the first axis, and an additional 15.5% by the second axis (Table 3). The sampling distribution of the two axes of cumulative contribution was 31%, with a correlation coefficient of 0.254. The eigenvalues of the first two short axes were 0.599 (first axis) and 0.479 (second axis). Remarkably, the two axes were positively correlated, and sequence diagrams show that the species distribution was related to soil environmental factors.

The DCA scattergrams of quadrat, community, and soil environment data show 3 distinct groups of samples (Fig. 4), where 10 advantaged species were selected from 34 species artificially: Formation I: *Populous euphratica*, relatively high altitude area, lower soil salinity, and requiring only groundwater supply; no flooding. Formation II: *Lycium ruthenicum*, *Phragmites australis*, and *Sparsifolia*; relatively high soil nutrient content, and lower soil salinity; temporarily water-covered area. Formation III: *Halostachys caspica*, *Salicornia europaea,* and halophytic vegetation; a large amount of salinized area; often water-covered area.

The classification and ordination of vegetation communities along the ecological gradient coincided with the actual distribution of communities in the Tarim River Basin. TWINSPAN and DCA both showed clear distribution boundaries.

Relationship between environmental factors and vegetation. The species type importance value matrix, soil environmental factors, and the elevation matrix was selected and applied using Indirect Gradient Analysis. DCCA was applied to analyze the relationship between the species and environmental factors. The direct analysis of background variables using DCCA showed higher correlations between species and environment (Table 4), reaching 89.5%, 63.6%, 57.8%, and 59.7% for the four axes. The first axis of the species-environment correlation explained 30.4% of the variance, and an additional 15.6% was explained by the second axis. DCCA ordination results were significant (Monte Carlo test: $F = 3.323$, $p = 0.002$), which is the highest obtainable value available with this software. The remaining unexplained variance may be the result of other factors that were not considered, such as anthropogenic factors and groundwater level. We did not measure these, as they are related to artificial influences rather than natural conditions. Figure 5 shows strong correlations between the soil environment indices with arrangement according to elevation, salt, and soil water (elevation was positive with soil water, salt, organic matter and available P; and negative with available N, available K, and pH).

The DCCA ordination showed that the distribution of vegetation in the river basin was affected by a combination of elevation, salt, and soil moisture, as well as soil water content in the third (Table 5). The correlation indices between these three variables and the first axis were −0.4961, −0.4561, and −0.3844, respectively. These results indicate that elevation was the most important factor affecting the distribution of vegetation, and soil moisture in the third status only, which may have been affected by the hydrological data in this study.

TABLE 3
Variation explained by species-environment variables using unconstrained ordination (DCA)

Axes	1	2	3	4	Total inertia
Eigenvalues	0.599	0.479	0.277	0.207	5.345
Lengths of gradient	4.148	3.333	3.044	2.387	
Species-environment correlations	0.696	0.788	0.595	0.575	
Cumulative percentage variance of species data	11.2	20.2	25.2	29.2	
of species–environment relation	15.5	31.0	0	0	
Sum of all eigenvalues					5.345
Sum of all canonical eigenvalues					1.638

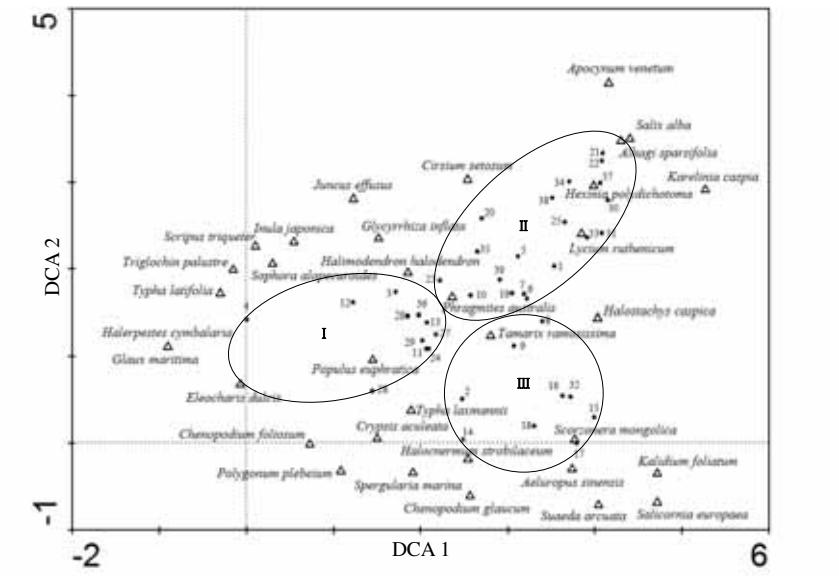

FIGURE 4
Scattergram of detrended correspondence analysis of elevation and soil environmental factors
Note: ●: survey quadrats; △: advantaged vegetation.

TABLE 4
Variation owing to species-environment factors by constrained ordination (DCCA)

Axes	1	2	3	4	Total inertia
Eigenvalues	0.389	0.184	0.085	0.046	3.780
Lengths of gradient	2.393	1.700	1.338	1.369	
Species-environment correlations	0.895	0.636	0.578	0.597	
Cumulative percentage variance of species data	10.3	15.1	17.4	18.6	
of species–environment relation	30.4	46.0	0	0	
Sum of all eigenvalues					3.780
Sum of all canonical eigenvalues					1.138
Summary of Monte Carlo test					
Test of significance of first canonical axis: eigenvalue = 0.389					
F-ratio = 3.323					
P-value = 0.002					

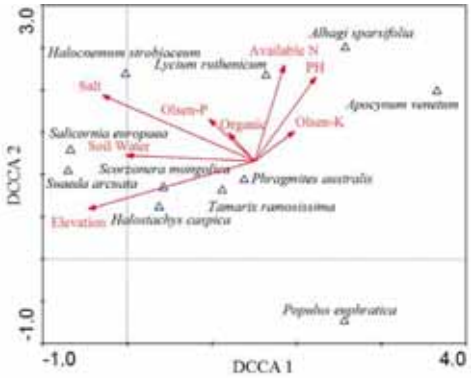

FIGURE 5
Scattergram of detrended canonical correspondence analysis of elevation and soil environmental factors. Solid lines with arrows: environmental factors. Quadrat extension cord with an arrow indicates the length of the vertical distance plots, correlating between the size of the environmental factors. Angle arrow connection with the ordination axis indicates the magnitude of the correlation between environmental factors and the ordination axis. The direction of the arrow links to the factors development trend.

TABLE 5
Correlation coefficients between soil environmental factors and detrended canonical correspondence analysis axes

Axes	Axis 1	Axis 2	Axis 3	Axis 4
PH	0.1807	0.2199	0.2053	0.0131
Salt	-0.4561	0.1764	0.2701	-0.0298
Organic matter	-0.0791	0.0743	0.3812	-0.2856
Available N	0.0864	0.2521	0.2210	-0.4591
Olsen-P	-0.1377	0.1112	0.1492	-0.3678
Available K	0.1181	0.0773	0.3507	-0.3022
Soil water content	-0.3844	0.0174	-0.0653	0.1692
Elevation	-0.4961	-0.1231	-0.1487	0.1106

TABLE 6
Pairwise correlations between vegetation diversity, and soil environmental factors

	PH	Salt	Organic matter	Available N	Olsen-P	Olsen-k	Elevation	Soil Water content	Diversity index
PH	1	0.037*	0.928	0.920	0.495	0.732	0.307	0.511	0.186
Salt	−0.334	1	0.062	0.313	0.288	0.113	0.860	0.009**	0.094
Organic matter	−0.015	0.302	1	0**	0**	0**	0.567	0.394	0.351
Available N	−0.017	0.166	0.588	1	0**	0**	0.016	0.607	0.529
Olsen-P	−0.113	0.174	0.757	0.716	1	0**	0.429	0.600	0.458
Olsen-k	−0.057	0.258	0.874	0.805	0.767	1	0.491	0.899	0.763
Elevation	−0.168	0.029	0.095	−0.382	−0.130	−0.114	1	0.016*	0.004**
Soil Water content	0.197	0.411	−0.231	−0.191	−0.080	−0.270	0.381	1	0.519
Diversity index	0.007	0.184	−0.302	0.011	−0.134	−0.225	−0.448	−0.087	1

Note: Upper triangle: p values; lower triangle: correlation coefficients. Significant p values ($p < 0.05$) and high correlation values (> 0.5 or < -0.5).

The pairwise correlations of soil environment indices, elevation, and vegetation diversity index (Table 6) supported the visible patterns of the scattergrams. The close relationship between soil environmental factors validated the DCCA results to a certain extent. In most cases, pH, elevation, and soil water were negatively correlated. A positive and significant relationship was observed between organic matter, available nitrogen, available P, and available K, all the value is $p = 0$ ($p < 0.01$). Elevation significantly influenced the surface vegetation diversity index, with a correlation coefficient of 0.448 ($p = 0.004$).

DISCUSSION

Of the 39 sample plots and 34 plant species, 12 families were represented by only 1 species each, accounting for 66.67% of the total family count. This indicated that plant species of the degraded wetland in the Tarim River Basin were limited, the community structure was simple, and there were no endemic species. Endemic genera and species can be a better reflection of the original characteristics of regional flora [6]. The vegetation of the degraded wetland in the study area was not dominated by one species or family. Wetland flora in the Tarim River Basin consisted of mainly herbaceous plants, with only a few shrub and tree species. This concurs with research of wetland plants in the Yangguan Nature Reserve of Dunhuang [28], and shows that the Tarim River wetland is in a severe state of degradation.

TWINSPAN provides objective and reasonable in-depth classification results, and takes the combination of biotope characteristic indicator species into account. TWINSPAN classified 11 community types and 4 formations, which was in agreement with research on the middle reach of the Tarim River by Li [23]. The DCA generated 3 ecological formations, projecting the environment-ray to three directions. The results from the DCA were equivalent to the formation levels produced by TWINSPAN. Both results were in good agreement in relation to sample 28. This quadrat was located in the middle reaches of the Tarim River and was in the community dominated by *P. euphratica* and *G. inflata*. As identified by TWINSPAN, *G. inflata* is an infrequent species in this quadrat of the study region, while the *P. euphratica* community is the single dominant species in sample 28. The difference in classification results may be a result of the distribution of mutually related vegetation, as smaller distributions were associated with other vegetation in mutual relationships, thereby explaining the lower frequency of *G. inflata*.

In addition, the classification and ordination of vegetation communities along the ecological gradient coincided with the actual distribution of communities in the Tarim River Basin.

The relationship between vegetation and soil environment was divided into three vegetation communities in the Tarim River Basin: diffuse water halophyte community (abundant), diffuse water semi-desert community (occasional), and desideratum ground water supply *P. euphratica* community (rare). The vegetation communities were closely correlated with distribution and ecological gradients. In this study, a soil depth of 0–20 cm was used for analysis [17, 18, 19]; as in the degrading Tarim river wetland ecosystem, herbaceous plants (with shallow roots) were the most abundant plant type, accounting for over 70% of all species. It is likely that the numbers of species and individuals of herbaceous plants changed substantially as the wetland ecosystem of the Tarim River Basin degraded. Herbaceous plants were mainly affected by characteristics of surface layer soil, while trees and shrubs root deeper; however, the numbers of species and individuals changed little to not at all over the course of this study, as the growth of seedlings are also greatly influenced by surface layer soil. Qi et al (2016) showed that most of the nutrients and soil organic matter were distributed in the topsoil at a depth of 0–20 cm, and that this was favorable for seed germination and seedling survival. Many studies indicate that soil water and elevation are the most important factors in vegetation distribution [29,30]. Other studies regarding the Tarim River have also shown that that the soil, water, and gradients of salt compounds were key factors influencing spatial distribution patterns of plant communities [31]. However, other studies have yielded different results. Josu et al (2011) showed that vegetation in the topsoil showed a trend with age of vegetation and pH, whereas in deeper soil layers, these factors seemed to limit succession. In this study, the DCCA ordination showed that the distribution of vegetation in the study region was affected by a combination of elevation, salt, and soil moisture, as well as soil water in the third. However, the correlation analysis showed that vegetation diversity was not correlated with any other factors, except elevation. These differences may be related to experimental field and hydrological data, as some of the experimental fields periodically diffuse water, so that soil water is largely transient. As such, sampling the soil water status for the whole experimental period was not possible, resulting in disparate results. However, the DCCA ordination results can be changed by the addition of hydrological data, such as groundwater level. As the hydrological data was not available from the river authority, we were unable to include this data in our analysis. Nevertheless, there was evidence of vegetation growth (halophytes *Salicornia europaea, Halostachys caspica, Halocnemum strobilaceum,* and *Suaeda arcuata*) in high salt-concentrated areas, highlighting the importance of salinity [32]. Likewise, soil salinity was generally higher in the Tarim River wetland. Therefore, this study shows that the restoration of degraded wetlands cannot rely solely on the restoration of hydrological conditions in the Tarim River, as topography and soil salinity must also be taken into account. These results should be integrated into the vegetation restoration and management plans of the Tarim River wetland, and could be important for the ecological management of the Tarim River Basin.

CONCLUSIONS

In the present study, the plant species in the study area of the Tarim River were limited, the community structure was simple, and there were no endemic species. There were only 34 plant species in the study areas, and 12 families were represented by only 1 species each. Wetland flora in the Tarim River Basin consisted of mainly herbaceous plants, with only a few shrub and tree species. This shows that the degradation of the Tarim River wetland is severe.

The classification and ordination of vegetation communities along the ecological gradient coincided with the actual distribution of communities in the Tarim River Basin. TWINSPAN divided samples into 4 formations, and showed the vegetation along the soil moisture gradient. DCA divided samples into 3 formations, and reflected the relationships between plant distribution and soil environmental factors. TWINSPAN and DCA both showed clear distribution boundaries, whilst DCA also provided a good reflection of the vegetation and soil environment.

The DCCA ordination showed that the distribution of vegetation in the region was affected by a combination of elevation, salt, and soil moisture, as well as soil salinity (which was generally higher in the Tarim River wetland). Therefore, the restoration of these degraded wetlands cannot rely solely on restoring hydrological conditions in the Tarim River, as topography and soil salinity must also be taken into account.

REFERENCES

[1] Ward, J., Tockner, K., Arscott, D. and Claret, C. (2002) Riverine landscape diversity. Freshwater Biology, 47(4), 517-539.

[2] Melendez-Pastor, I., Navarro-Pedreno, J., Gomez, I. and Koch, M. (2010) Detecting drought induced environmental changes in a Mediterranean wetland by remote sensing. Applied Geography, 30(2), 254-262.

[3] Sen, C. (2017) Impact of soil factors and management systems on pasture vegetation in

Tekirdag, Turkey. Fresen. Environ. Bull., 26(4), 2903-2913.
[4] Watt, S.C.L., Garcia-Berthou, E. and Vilar, L. (2007) The influence of water level and salinity on plant assemblages of a seasonally flooded Mediterranean wetland. Plant Ecology, 189(1), 71-85.
[5] Zhang, X.R., Cao, Y.G., Bai, Z.K., Wang, J.M., Zhou, W. and Ding, X. (2016) Relationships between vegetation coverage and soil properties on the reclaimed dump of opencast coal mine in loess plateau, China. Fresen. Environ. Bull., 25(11), 4767-4776.
[6] Cheng, L.X., Chen, K.L. and Wang, S.P. (2013) Plant diversity of the Xiaopo Lake Wetland in the basin of the Qinghai Lake. Wetland Science, 11(4), 460-465.
[7] Dai, X.L., Dong, Z.B. and Xie, J.P. (2013) Characteristics and sustainable utilization of Yangguan Wetland in Dunhuang. Environment & Sustainable Development, 12(6), 101-104.
[8] He, M.Z., Zheng, J.G., Li, X.R. and Qian, Y.L. (2007) Environmental factors affecting vegetation composition in the Alxa Plateau, China. Journal of arid environments, 69(3), 473-489.
[9] Zhang, H.B., Meng, H.J., Liu, X.D., Zhao, W.J. and Wang, X.P. (2012) Vegetation characteristics and ecological restoration technology of typical degradation wetlands in the middle of Heihe river basin, Zhangye city of Gansu province. Wetland Science, 10(2), 194-199. (Chinese)
[10] Chen, Y.N., Xu, C.C., Chen, Y.P., Liu, Y. and Li, W. (2013) Progress, Challenges and prospects of Eco-Hydrological studies in the Tarim River Basin of Xinjiang, China. Environmental Management, 51(1), 138–153.
[11] Dwire, K.A., Kauffman, J.B. and Baham, J.E. (2006) Plant species distribution in relation to water-table depth and soil redox potential in montane riparian meadows. Wetlands, 26(1), 131-146.
[12] Guisan, A., Weiss, S.B. and Weiss, A.D. (1999) GLM versus CCA spatial modeling of plant species distribution. Plant Ecology, 143(1), 107-122.
[13] Hettrich, A. and Rosenzweig, S. (2003) Multivariate statistics as a tool for model-based prediction of floodplain vegetation and fauna. Ecological modelling, 169(1), 73-87.
[14] Koning, C.O. (2005) Vegetation patterns resulting from spatial and temporal variability in hydrology, soils, and trampling in an isolated basin marsh, New Hampshire, USA. Wetlands, 25(2), 239-251.
[15] Rumbaur, C., Thevs, N., Disse, M., Ahlheim, M., Brieden, A., Cyffka, B. and Halik, U. (2015) Sustainable management of river oases along the Tarim River (SuMaRiO) in Northwest China under conditions of climate change. Earth System Dynamics, 6(1): 83.
[16] Chen, Y.N., Li, W.H., Xu, C.C. and Hao, X.M. (2007) Effects of climate change on water resources in Tarim River Basin, Northwest China. Journal of Environmental Sciences, 19(4), 488-493.
[17] Alday, J.G., Marrs, R.H. and Martinez-Ruiz, C. (2011) Vegetation succession on reclaimed coal wastes in Spain: the influence of soil and environmental factors. Applied Vegetation Science, 14(1), 84-94.
[18] Wang, Y., Qiao, J., He, C., Wang, Z., Luo, W. and Sheng, L. (2015) Towards multi-level biomonitoring of nematodes to assess risk of nitrogen and phosphorus pollution in Jinchuan Wetland of Northeast China. Ecotoxicology, 24(10), 2190-2199.
[19] Qi, G., Chen, H., Zhou, L., Wang, X., Zhou, W., Qi, L. and Dai, L. (2016) Carbon stock of larch plantations and its comparison with an old-growth forest in northeast China. Chinese Geographical Science, 26(1), 10-21.
[20] Watanabe, F.S. and Olsen, S.R. (1965) Test of an ascorbic acid method for determining phosphorus in water and NaHCO3 extracts from soil. Soil Science Society of America Journal, 29(6), 677-678.
[21] Oliveira, V., Ludwick, A.E. and Beatty, M.T. (1971) Potassium removed from some Southern Brazilian soils by exhaustive cropping and chemical extraction methods. Soil Science Society of America Journal, 35(5), 763-767.
[22] Del Suolo, S.I.S. (1985) Metodi normalizzati di analist del suolo. Edagricole, Bologna.
[23] Li, T., Yin, L.K. and Yan, C. (2003) Quantitative classification and ordination analysis on vegetation in the middle reaches of Tarim River. Arid Land Geography, 26(2), 173-179. (Chinese)
[24] Leps, J. and Smilauer, P. (2003) "Multivariate analysis of ecological data using CANOCO," Cambridge university press.
[25] Braak, C.J.F. and Smilauer, P. (2012) Canoco reference manual and user's guide: software for ordination, version 5.0. Biometris.
[26] Hammer, R., Harper, D.A.T. and Ryan, P.D. (2001) PAST: Paleontological Statistics Software Package for education and data analysis. Palaeontolia Electronica 4.
[27] Sun, Y. X., Yan, C., Wei, Y., Xu, H. AND Yao, Y. L. (2017) Influence of topsoil addition on species diversity and aboveground biomass of plant community on the damaged mined land in Altay, China. Fresen. Environ. Bull., 26(3), 2214-2220.
[28] Dai, X.L., Zhao, T.W., Ma, S.S., Liu, X.W., Yang, J.W., Ma, H.T. and Xie, J.P. (2016) Community characteristics and species diversity of wetland plants in the Yangguan nature reserve of

Dunhuang. Journal of Landscape Research, 8(2), 55-58.
[29] Capon, S.J. (2005) Flood variability and spatial variation in plant community composition and structure on a large arid floodplain. Journal of Arid Environments, 60(2), 283-302.
[30] Lite, S.J., Bagstad, K.J. and Stromberg, J.C. (2005) Riparian plant species richness along lateral and longitudinal gradients of water stress and flood disturbance, San Pedro River, Arizona, USA. Journal of Arid Environments, 63(4), 785-813.
[31] Zhang, Y.M., Chen, Y.N. and Zhang, X.L. (2004) Plant communities and their interrelations with environmental factors in the lower reaches of Tarim river. Acta Geographica Sinica, 59(6), 903-910. (Chinese)
[32] Al-Taisad, W.A. (2016) The effect of soil properties on characteristics of halopeplis perfoliata community in the coastal environment in eastern Saudi Arabia. Fresen. Environ. Bull., 25(12), 5819-5829.

Received: **14.03.2017**
Accepted: **01.08.2017**

CORRESPONDING AUTHOR

Qiling Chen
Xinjiang Academy of Agricultural
and Reclamation Science,
Shihezi Xinjiang 832000 – CHINA

E-mail: 48570766@qq.com

© by PSP Volume 26 – No. 10/2017 pages 5965-5970 Fresenius Environmental Bulletin

INDOOR AIR QUALITY: THE SAMPLES OF SAFRANBOLU BULAK MENCILIS CAVE

Mehmet Cetin[1,*], Hakan Sevik[2], Ahmet Saat[3]

[1]Kastamonu University, Faculty of Engineering and Architecture, Department of Landscape Architecture, 37150, Kastamonu, Turkey
[2]Kastamonu University, Faculty of Engineering and Architecture, Department of Environmental Engineering, 37150, Kastamonu, Turkey
[3]Kastamonu University, Faculty of Engineering and Architecture, Department of Landscape Architecture, 37150, Kastamonu, Turkey

ABSTRACT

Visiting caves is an increasingly important tourism activity today. Because of this trend, caves draw thousands of people every year. However, visiting caves can lead to some serious health problems. For example, the concentration of harmful gases, including carbon dioxide (CO_2), may exceed the critical level during the visit of a group of tourists. Within the outline of this research, Safranbolu Bulak Mencilis Cave was chosen, which has a high potential for visit by cavers and tourists. The purpose of this research on cave's air quality is to measure the amounts of CO_2 and particulate matter. The research was conducted in June 2016 during a visit to the cave with 25-meter intervals using an average from portable air measurement devices in various corners. Starting at the entrance of the cave, the study concluded that the amount of CO_2 increased rapidly: from 50 meters inside the cave entrance it was 1,200 ppm, and increased to 2500 ppm at150 meters inside. The amount of particulate matter in the caves was determined to reduce progressively the deeper into the cave. These results indicate that when the tourists' visits occur, the indoor air quality may change and some health problems may arise, especially from the effect of rising amounts of CO_2. This may cause headaches, dizziness, throat and nose irritation, sneezing, coughing, and tears.

KEYWORDS:
Air quality, Safranbolu Bulak Mencilis Cave, Carbon dioxide (CO_2), Particulate Matter, Indoor air, Sustainability

INTRODUCTION

Caves are natural underground spaces among the rocks extended in such a way that they allow the entrance of humans. They are formed throughout thousands of years and have unique visual richness. Thus, they have much importance as sites for recreation and tourism activities. They have especially become important elements of tourism in Turkey, and have been studied in this context [1-10]. Aydoğdu and Sevik [5], for example, studied Mantar cave in Turkey.

Visitors are not checked or prepared for cave visits in any way. Many of the caves are only protected to preserve natural formations. However, there might be factors in caves open to visitors that may be threatening for human health. One such factor is poisonous gases that may exist in the indoor air of caves and have negative influences on human health. Indoor air quality in caves, which are limited environments, is shaped by many factors and may contain dangerous elements.

Many studies have investigated the influence of indoor air quality in indoor environments other than caves. Indoor building areas are especially more CO_2dense than outdoor areas [11-14]. These studies focus on the effects of human air health on the air quality. Kotzias and Pilidis [11] studied indoor air quality for building design. They discussed information on indoor environmental quality issues at the European level, taking into account the energy saving requirements for new and old buildings, and suggest actions to be taken in the years ahead to achieve healthy and resource efficient buildings. There are positive signs from science and politics regarding improvement in indoor air quality; efforts are being made to adopt the relevant industry regulations that are required for a proper domestic market and to raise consumers' awareness about environmentally sensitive products. The study shows that air quality certification of buildings would be very positive, similar to energy performance certification. Sakellaris et al. [12] took ionic PAH compositions and PM samples. Strong emission sources were found to affect the interior of buildings. Sabaziotis et al.'s [13] indoor air quality studies were conducted in the winter of 2011 in three housing units in Kozani, Greece. These studies show that residences in the city center offered higher concentrations than outside areas near the city center and the downtown residences. All mean indoor carbonyl concentrations were higher than those outdoor, except for hexanal inresidences. In addition, Cimino-Reale's study [14] makes it clear that genomic methodologies are suitable for modulating large biological processes and biochemical effects by exposing them to complex environmental conditions. They measured compounds indoors, and found the highest concentration of CO_2 for two of the

three tested houses, and formaldehyde for one of the three examined houses.

This study deals with the quantities of CO_2 and particulate matter, which are the primary components of indoor air quality for caves, in Safranbolu Bulak Mencilis cave. With the measurements made in the cave within the scope of the study, the change in the quantities of CO_2 and particulate matter (0.3 µm, 0.5 µm, and 5.0 µm) was monitored and interpreted throughout the depths of the cave.

MATERIALS AND METHODS

This study was conducted in Bulak Mencilis Cave, which is located within the boundaries of Safranbolu district. Mencilis cave is situated in Bulak village of Karabük province in the Western Black Sea Region of Turkey. It is 10 km northeastofthe central district of Karabük. Different measurements were carried out to measure the total length of the cave. Some sources state that it is 6,052 meters while others say that it is 2,725 meters. Taking the assumption that total length is over 6 km as a basis, it is possible to say that it is the 4th largest cave in Turkey [15].

This study was conducted in the section of the Mencilis cave open to visitors. This section starts with a large gallery and extends horizontally. Measurements with taken at a rate of one measurement per 25 meters starting from the external section and conducted until a depth of 350 meters.

TABLE 1
Changes in CO_2 and particulate matter in Mencilis Cave

Location	*CO_2*	*$PM_{0.3}$*	*$PM_{0.5}$*	*PM_5*
Entrance	980	22498	7148	166
25 m	570	13453	5438	61
50 m	1270	30380	7759	97
75 m	1540	30615	7896	85
100 m	1570	26386	6158	39
125 m	2340	19919	5693	83
150 m	2700	13625	5150	104
175 m	2650	10036	3614	114
200 m	2600	5818	2173	80
225 m	2585	5638	1916	58
250 m	2575	5522	1815	26
275 m	2590	5615	1516	35
300 m	2620	5622	1026	41
325 m	2650	5465	1578	56
350 m	2720	5326	1507	76

Analyses of temperature and CO_2 measurements were performed using "Extech EA80 Indoor Air Quality Meter", and particulate matter measurements were performed using the 3-channel "Lighthouse 3013" particulate counter. Particulate matter concentrations were measured for three different sizes: 0.3 µm ($PM_{0.3}$), 0.5 µm ($PM_{0.5}$), and 5 µm (PM_5).

RESULTS

The external temperature outside the cave was measured to be 20.5°C, while the temperature ranged from 14.8°C to 15.2°C inside the cave. Therefore, no assessments were made regarding the temperature values. Table 1 shows CO_2 and particulate matter values.

To increase the understandability of the values in the table, we created graphics for each parameter. Figure 1 shows the changes in CO_2 quantity.

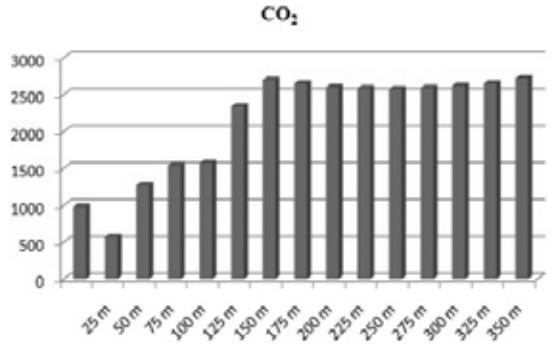

FIGURE 1
The changes in the CO_2 quantity depending on the depth inside Mencilis Cave

Figure 1 shows that CO_2 quantity is lower than 1,000 ppm outside the cave and in the entrance to cave. However, it rapidly increases depending on the depth inside the cave, reaching 1,270 ppm at 50 meters, 1,540 ppm at 75 meters, 1,570 ppm at 100 meters, 2,340 ppm at 125 meters, and 2,700 ppm at 150 meters. At this depth, the cave follows a horizontal course and CO_2 quantity ranges from 2,575 to 2,720 ppm. Figure 2 gives the changes in particulate matter quantity.

Table 1 and Figure 2 show that small size particulate matter quantity inside the cave decreases, especially after 100 meters. There are 22,498 particulates at a size of 0.3 m outside the cave, while this number is 26,386 at 100 meters and decreases decrease afterwards. However, the number remains stable at 5,600 after 200 meters. The quantity of particulate matter with a size of 0.5 m follows a similar course. There are 7,148 particulates outside the cave. The number reaches 6,158 at 100 meters and decreases afterwards, reaching below 2,000 after 200 meters. However, though the quantity of particulate matter with a size of 5.0 m is lower inside the cave than outside, it does not show a significant change. The number is 166 outside the cave and ranges from 26 to 114 throughout the cave.

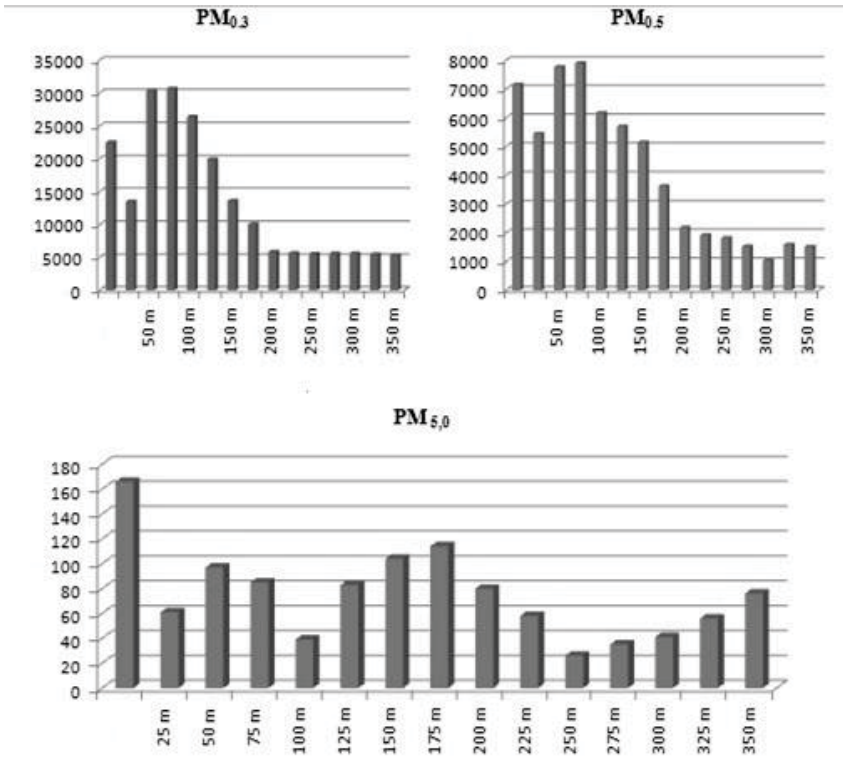

FIGURE 2
The change in the quantity of particulate matter in Mencilis Cave depending on the depth

DISCUSSION

In Turkey, caves are particularly associated with cave tourism, and the studies dwelling on caves mostly concentrate on tourism potential [4, 16-21]. There are almost no studies focusing on indoor air quality in Turkish caves, and only a limited number of studies dealing with determination of indoor air quality in caves around the world [22-30].

Sanna et al. [26] studied temperature, relative humidity, and carbon dioxide in caves; and Aydogdu and Sevik [5] conducted studies to determine temperature, CO_2, and relative humidity in caves. James [31] studied Lava Tubes and Bayliss caves in Australia in terms of temperature, relative humidity, and carbon dioxide and radon gases; Osborne [32] studied indoor air quality and carbon dioxide quantity in the air of the caves in Australia.

Previous studies heavily dwelled on indoor air quality of caves are open to touristic activities in terms of temperature, relative humidity, and carbon dioxide values. Kim et al. [33] report in their study titled "*A Study on the Changes of Air Quality the Baekryong Cave in Pyeonchang*" that the most important elements determining the indoor air quality for humans and microbiological sustainability inside the caves are temperature, relative humidity, and carbon dioxide.

The present study shows that CO_2 quantity in Mencilis cave exceeds the 1500 ppm limit from 75 meters on. High CO_2 quantities in closed areas is one of the parameters having much influence on human health. CO_2 is one of the gases rapidly changing in concentrations as a result of human metabolic activities in indoor environments. Of the air inhaled from the normal atmosphere, 21% is O_2 and 0.033% is CO_2. However, of the air exhaled from the lungs, 16-17% is O_2 and 4% is CO_2. This change leads to a rapid increase in CO_2quantities, particularly closed areas where there are collective activities [34,35].

As a result of the increase in carbon dioxide in the environment, people may experience fatigue, difficulty in perception, and sleepiness [36]. A quantity of CO_2in an environment over 1000 ppm can cause headaches, vertigo, fatigue, concentration disruptions, and smelling disorders; sores in the throat and nose, sneezing, coughing, and lacrimation occur when it is over 1500 ppm [37,38]. According to the EPA, the maximum acceptable carbon dioxide rate for indoor environments is 800 ppm, and 1000 ppm at most in environments with large numbers of people [39].

Recently, it has been found that the indoor air quality of the closed areas in the studies is almost the same as that of the cave [11-14,40]. As the influence of CO_2 in closed areas on human health is well-known, many studies dealing with CO_2quantity in closed areas have been conducted [41,42]. However, there are only a limited number of studies dwelling on the determination of CO_2quantity in caves. These limited number of studies report that CO_2 quantity in caves is far above the threshold value, and thus

threatens human health. The present study found out that CO_2quantities in Mencilis cave reach up to 2,720 ppm. Aydoğdu and Sevik [5] reported that CO_2 quantities in Mantar cave exceed 1,100 ppm from the entrance and do not fall below this rate inside the cave. Previous studies also indicate that CO_2 quantities in caves may reach fatal levels. Fraser initiated the measurement of carbon dioxide in Wellington caves in 1958. Fraser's measurements detected carbon dioxide at a rate of 13.5% inside the cave [32].

The present study also focused on the quantity of particulate matter. The quantity of particulate matter is one of the most important parameters constituting indoor air quality. An excess in the quantity of particulate matter leads to disorders and it may cause serious problems for persons with upper respiratory disorders, elderly people, and children [43,44]. Particulate matter is defined as a suspension consisting of fine solid or liquid matter inside a gas that emerge as a result of activities such as wind, sea, volcanoes, and anthropogenic activities. The sources and composition of particulate matter in nature are rather complicated. A considerable amount of particulate matters in the troposphere is anthropogenic, consisting of sulfate, ammonium, nitrate, sodium, chlorine, trace metals, matters with carbon, soil elements, and water [45].

The threshold values of particulate matter concentration have been specified by regulations in many parts of the world, including but not limited to the European Union, due to its potential health and environmental impacts. Responding to these threatening impacts of particulate matter on human health and the environment, including the climate and many ecosystems, there is an increase in the number of studies dwelling on particulate matter [46-50].

The present study showed that the quantity of particulate matter inside the cave is less than in the external environment. We believe that this result is associated with the relative humidity inside the cave. As a matter of fact, Aydogdu and Sevik [5] report that relative humidity inside caves may reach 100%. Such an increase in the rate of humidity in the air may lead to a reduction in the quantity of particulate matter.

CONCLUSIONS

In the present study, the most remarkable values were obtained from measuring CO_2 in Mencilis cave. The CO_2 quantity inside the cave is 4 to 5 times more than that of the external environment and reaches up to 2,720 ppm. Previous studies report that CO_2 levels rapidly increase, particularly in crowded environments [51-55]. This situation may cause problems, particularly during group visits. Long-time visits may reduce indoor air quality inside caves, leading to headaches, vertigo, sore in throats and nose, sneeze, cough, and lacrimation. This is particularly problematic for people with upper respiratory disorders, asthma, and so on. Hence, visitors should be warned in this matter.

Similar studies should be conducted, particularly for caves with long galleries. The measurements should be varied to include gases that are important for health. These prospective results should be compiled to be presented in cave introduction brochures. The results should be given on warning plates before entrance to caves to prevent possible health problems.

REFERENCES

[1] Ulusan, Y. and Batman, O. (2010) Alternatif Turizm Çeşitlerinin Konya Turizmine Etkisi Üzerine Bir Araştırma. Selçuk Üniversitesi Sosyal Bilimler Enstitüsü Dergisi. 23, 244-260.

[2] Yazgan, Ş. and Kadanalı, E. (2012) Ağrı İlinin Kırsal Turizm Potansiyelinin Değerlendirilmesi. Karamanoğlu Mehmetbey Üniversitesi Sosyal ve Ekonomik Araştırmalar Dergisi. 14(22), 5-10.

[3] Cetin, M., Sevik, H. and Isınkaralar, K. (2017) Changes in the Particulate Matter and CO_2Concentrations Based on the Time and Weather Conditions: The Case of Kastamonu. Oxidation Communications. 40(1-II), 477-485.

[4] Arpacı, Ö., Zengin, B. and Batman, O. (2012) Karamanın Mağara Turizmi Potansiyeli ve Turizm Açısından Kullanılabilirliği. Karamanoğlu Mehmetbey Üniversitesi Sosyal ve Ekonomik Araştırmalar Dergisi. 14(23), 59-64.

[5] Aydogdu, A. and Sevik, H. (2015) Indoor Air Quality: The Samples of Ilgarini and Mantar Caves. I. Eurasia InternationalTourism Congress: Current Issues, Trends, and Indicators (EITOC-2015).Proceedings Vol: II. 28-30 May 2015. Konya, Turkey. 95-104.

[6] Cetin, M. and Sevik, H. (2016) Evaluating the recreation potential of Ilgaz Mountain National Park in Turkey. Environmental Monitoring and Assessment. 188(1), 52.

[7] Cetin, M. and Sevik, H. (2016) Chapter 5: Assessing Potential Areas of Ecotourism through a Case Study in Ilgaz Mountain National Park. In: Tourism-From Empirical Research Towards Practical Application. Eds: Leszek Butowski, InTech, 81-110.

[8] Cetin, M. (2017) Change in Amount of Chlorophyll in Some Interior Ornamental Plants. Kastamonu University Journal of Engineering and Sciences 3(1), 11-19.

[9] Cetin, M. (2016) Sustainability of urban coastal area management: A case study on Cide. Journal of Sustainable Forestry. 35(7), 527-541.

[10] Cetin, M., Adiguzel, F., Kaya, O. and Sahap, A. (2016) Mapping of bioclimatic comfort for po-

tential planning using GIS in Aydin. Environment, Development and Sustainability. in press. 1-16.
[11] Kotzias, D. and Pilidis, G. (2017) Building design and indoor air quality - experience and prospects. Fresen. Environ. Bull., 26(1), 323-326.
[12] Sakellaris, I.A., Tolis, E.I., Saraga, D.E. and Bartzis, J.G. (2017) VOCs, PAHs and IONs measurements in an office environment in the vicinity of a small industry. Fresen. Environ. Bull., 26(1), 292-300.
[13] Sabaziotis, V., Galinos, K., Missia, D., Kalimeri, K.K., Tolis, E.I. and Bartzis, J.G. (2017) Indoor air quality in residences at the city of Kozani, Greece: effects of the house location. Fresen. Environ. Bull., 26(1), 255-262.
[14] Cimino-Reale, G., Collotta, A.,Sarigiannis, D. A., and Marafante, E. (2008) Toxicogenomic study of indoor and outdoor air chemical mixtures. Fresen. Environ. Bull., 17(9b), 1485-1491.
[15] Özdemir, Ü. (2005) Mencilis Cave. Doğu Coğrafya Dergisi10(13), 135-150
[16] Sever, R. (2008) Polat Mağarası ve Turizm Potansiyeli. Doğu Coğrafya Dergisi. 13(19), 251-266
[17] Yeşil, P., Yeşil, M. and Yılmaz, H. (2008) Jeolojik Miras Alanlarının Alternatif Turizm Kapsamında Değerlendirilmesi: Ballıca Mağarası Örneği. Atatürk Üniversitesi Ziraat Fakültesi Dergisi. 39(2), 241-248.
[18] Albükrek, M., Aytan, A., Taylan, M.S., Usuloğlu, T. and Sıvacıoğlu, A. (2012) Bartın-Kastamonu Küre Dağları Milli Parkı Mağaralarının Biyoçeşitlilik ve Turizm Potansiyeli-Yönünden Değerlendirilmesi. Kastamonu'nun Doğal Zenginlikleri Sempozyumu, 16-17 Ekim, 2012, Kastamonu,12.
[19] Aydoğdu, A. (2012) Kastamonu'nun Doğal Zenginliklerinin Turistik Ürün Bakış Açısı ile İrdelenmesi. Kastamonu'nun Doğal Zenginlikleri Sempozyumu, 16-17 Ekim, 2012, Kastamonu,18.
[20] Öcal, T. and Özcan, F. (2013) Çamlık Mağaraları ve Turizm Potansiyeli. Marmara Coğrafya Dergisi. 28, 423-443.
[21] Özşahin, E., Kaymaz, Ç.K. (2014) Gilindire (Aynalıgöl) Mağarasının Turizm Potansiyeli (Aydıncık, Mersin). Doğu Coğrafya Dergisi. 19(31), 145-166.
[22] Cetin, M. (2015) Evaluation of the sustainable tourism potential of a protected area for landscape planning: a case study of the ancient city of Pompeipolis in Kastamonu. Int. J. Sust. Dev. World. 22 (6), 490
[23] Cetin, M. (2015) Using GIS analysis to assess urban green space in terms of accessibility: case study in Kutahya. Int. J. Sust. Dev. World. 22 (5), 420
[24] Cetin, M. (2015) Determining the bioclimatic comfort in Kastamonu City. Environmental Monitoring and Assessment. 2015; 187 (10), 640.
[25] Smith, S.L. and Telling, J.P. (2004) UBSS expedition to northern Thailand 2003: Breaking the bad air barrier. Proc. University Speology Society. 23(2), 87-95.
[26] Sanna, L., Arca, A., Ventura, A., Zara, P. and Duce, P. (2007) Carbon flux and climate change effects on Capo Caccia karst ecosystem. Advances in Climate Science Second Annual Conference on climate change, scenarios, impacts and policies, Sardinia, Italia.
[27] Linan, C., Vadillo, I. and Carrasco, F. (2008) Carbon dioxide concentration in air within the Nerja Cave (Malaga, Andalusia, Spain). International Journal of Speology. 37(2), 99-106.
[28] Badino, G. (2009) The legend of carbon dioxide heaviness. Journal of Cave and Karst Studies. 71(1), 100–107.
[29] Whitaker, T., Jones, D., Baldini, J.U.L. and-Baker, A.J. (2009) A high-resolution spatial survey of cave air carbon dioxide concentrations in Scoska Cave (North Yorkshire, UK): implications for calcite deposition and re-dissolution. Cave and Karst Science. 36(3), 85-92.
[30] Freitas, de C.R. (2010) The role and importance of cave microclimate in the sustainable use and management of show caves. Acta Carsologica. 39(3), 477–489.
[31] James, J.M. (2010) Air Quality Measurements in the Undara Lava Tubes. Proceedings 14th International Symposium on Vulcanospeleology. Undara, Australia,77-80.
[32] Osborne, R.A.L. (2001) Karst geology of Wellington caves: a review. Helictite. 37(1), 3-12.
[33] Kim, T.H., Kong, D.Y., Choi, D.W., Lim, J.D., Yu, Y.W., Cho, J.H. and Yeon, U. (2012) A study on the changes of air quality the baekryong cave in Pyeonchang (natural monument number 260). Journal of Korean Nature. 5(3), 237-241.
[34] Bulgurcu, H., İlten, N. and Coşkun, A. (2003) Okullarda İç Hava Kalitesi Problemleri ve Çözümler. Ulusal Tesisat Mühendisliği Kongresive Sergisi.VI, 15-18.
[35] Cetin, M. and Sevik, H. (2016)Measuring the Impact of Selected Plants on Indoor CO_2 Concentrations. Polish Journal of Environmental Studies.25(3), 973-979.
[36] Cetin M. (2016) Determination of bioclimatic comfort areas in landscape planning: A case study of Cide Coastline. Turkish Journal of Agriculture-Food Science and Technology. 4(9), 800-804.
[37] Ercan, M.S. (2012) Yeşile Pusulanız "Çevre Göstergesi. In: Uluslararası Yapıda Tesisat Teknolojisi Sempozyumu. Bildiriler Kitabı, 30 Nisan-Mayıs, 2012, İstanbul, 169-175.
[38] Sevik, H., Cetin, M. and Isinkaralar, K. (2016)

Bazı İç Mekan Süs Bitkilerinin Kapalı Mekanlarda Karbondioksit Miktarına Etkisi. Düzce Üniversitesi Bilim ve Teknoloji Dergisi. 4, 493-500.

[39] Cetin M. and Sevik H. (2016) Change of air quality in Kastamonu city in terms of particulate matter and CO_2 amount. Oxidation Communications.39(4-II), 3394–3401.

[40] Cetin, M. (2016) A Change in the Amount of CO_2 at the Center of the Examination Halls: Case Study of Turkey. Studies on Ethno-Medicine.10(2), 146-155.

[41] Baysan, S. (1999) Bina İçi Hava Kalitesinin İnsan Sağlığına Etkileri. Marmara Üniversitesi, Marmara Coğrafya Dergisi. 2, 224-236.

[42] Güllü, G. and Menteşe, S. (2007) İç Ortam Havasında Biyoaerosol Düzeyler VIII. In: Ulusal Tesisat Mühendisliği Kongresi. İç Hava Kalitesi Sempozyumu, Temmuz, 2007, İzmir.

[43] Aricak, B. (2016) The Damping Effect of Forest Vegetation in Reducing the Amount of Particular Matter and Noise Resulting from Highway Trafficking. KÜBAP. 01/2015, 20.

[44] Cetin, M. (2016) Changes in the amount of chlorophyll in some plants of landscape studies. Kastamonu University Journal of Forestry Faculty. 16(1), 239-245.

[45] Özdemir, H., Borucu, G., Demir, G., Yigit, S. and Namik A.K. (2010) Examining the Particulate Matter ($PM_{2.5}$ ve PM_{10}) Pollution on the Playgrounds in Istanbul. Ecology. 20(77), 72-79.

[46] Basar, P., Okyay, P., Ergin, F., Cosan, S. and Yildiz, A. (2005) Air Pollution in Aydin City Between 1997-2004. Adnan Menderes Üniversitesi Tıp Fakültesi Dergisi.6(3),11-15.

[47] Karaca, F., (2008) Evaluation of Statistical Distribution Characteristics of the Metallic Compositions of $PM_{2.5}$ andPM_{10} Particles in Büyükçekmece Watershed Atmosphere. Ecology. 17(68), 33-42.

[48] Doğan, F. and Kitapçıoğlu, G. (2007) Comparing air pollution in Izmir according to years. Ege Journal of Medicine. 46(3), 129-133.

[49] Yatkın, S. and Bayram, A. (2007) The Air Borne Particulate Matter Pollution in Izmir. Dokuz Eylül Üniversitesi Mühendislik Fakültesi Fen ve Mühendislik Dergisi. 9(2), 15-27.

[50] Sevik, H., Karakas, H. and Senöz, E. (2013) Evaluation of air quality in terms of the amount of carbon dioxide in black sea region. International Journal of Engineering Science & Research Technology. 2(2), 805-809.

[51] Isinkaralar, K., Cetin, M., Icen, H.B. and Sevik, H. (2015) Indoor Quality Analysis of CO_2 For Student Living Areas. In: The International Conference on Science, Ecology and Technology I (ICONSETE'2015 – Vienna)August 25-28, 2015, Vienna, Austria, 123.

[52] Fernandez-Cortes, A., Calaforra, J.M. and Sanchez-Martos, F. (2006) Spatiotemporal analysis of air conditions as a tool for the environmental management of a show cave. Atmospheric Environment. 40(38), 7378–7394.

[53] Cetin, M., Topay, M., Kaya, L.G. and Yilmaz, B. (2010) Biyoiklimsel Konforun Peyzaj Planlama Sürecindeki Etkinliği: Kütahya Örneği. Süleyman Demirel Üniversitesi Orman Fakültesi Dergisi. 1(1), 83–95.

[54] Sevik, H., Cetin, M. and Belkayali, N.(2015)Effects of Forests on Amounts of CO_2: Case Study of Kastamonu and Ilgaz Mountain National Parks. Pol.J.Environ.Stud. 24(1), 253-256.

[55] Sevik, H., Cetin, M., Guney, K. and Belkayali, N. (2017). The Influence of House Plants on Indoor CO_2. Polish Journal of Environmental Studies. 26(4), 1643-1651.

Received: **26.03.2017**
Accepted: **07.08.2017**

CORRESPONDING AUTHOR

Mehmet Cetin
Kastamonu University, Faculty of Engineering and Architecture, Department of Landscape Architecture, 37150, Kastamonu, Turkey

e-mail: mcetin@kastamonu.edu.tr

© by PSP Volume 26 – No. 10/2017 pages 5971-5979 Fresenius Environmental Bulletin

OCCURRENCE OF PHARMACEUTICAL AND PERSONAL CARE PRODUCTS (PPCPS) IN THE AFRICAN AQUATIC ENVIRONMENT: A BRIEF REVIEW FOR THE FUTURE OF ENVIRONMENT

Yongbum Kwon, Do Gyun Lee*

Department of Environmental Engineering, Incheon National University, Incheon 22012, South Korea

ABSTRACT

Little is known about the current contamination levels of pharmaceutical and personal care products (PPCPs) in Africa countries. This review summarized the occurrence of PPCPs within the aquatic environment in Africa. Twenty five PPCPs belonging several categories, such as antibiotics, steroids/hormones, analgesics/anti-inflammatory drugs, antiepileptic drugs, blood lipid regulators, stimulant, antimicrobial agents, synthetic musks/fragrances, insect repellants and sunscreen UV filters, were detected in the African aquatic environment including surface water, groundwater, wastewater, and sediments. Among 8 African countries including South Africa, Senegal, Cote d'Ivoire, Chana, Nigeria, Kenya, Tanzania, and Zambia, a wide variety of PPCPs were more detected in South Africa and Nigeria than others. This may be due to the different degree of attention regarding the occurrence of PPCPs in different African countries. It is the first short review on summarizing the studies on the occurrence of PPCPs in the African aquatic environment, which would provide helpful information for efficient management of water resources and the environment in African countries.

KEYWORDS:
Pharmaceuticals; personal care products; human health; aquatic environment; African countries

INTRODUCTION

For the past decades, the detection of pharmaceuticals and personal care products (PPCPs) in the aquatic environment have been widely reported because of the advances in analytical techniques [1-4]. PPCPs have been usually released using daily personal products including hand soap, shampoo, skin lotion and perfume as well as medication including analgesics and antibiotics [5]. In addition, the continuous uses of PPCPs from agriculture, household, and hospital have also contributed to some amounts of their input [6]. The occurrence of PPCPs in the aquatic environment could cause endocrine disruption, acute/chronic toxicity, and microbial antibiotic resistance when aquatic organisms are exposed to PPCPs through various pathways [7-9]. Several studies have reported the occurrence and potential environmental impact of PPCPs in African countries including South Africa, Kenya, Nigeria and Zambia [10-12]. As many of PPCPs are still included in the list of non-regulated chemicals, developed countries including US and EU have strived to robustly establish regulations for the management and treatment of PPCPs [13,14]. However, in developing countries in Africa, such PPCP regulations as discharge guidelines and standards has not yet been established due to lack of awareness of the potential risk of PPCPs to human health and aquatic habitat and the African countries are currently confronted with such environmental issues [5,12].

In this review, we aim to summarize the occurrence of a wide range of PPCPs in the aquatic environment in African countries and to help citizens and policy-makers to increase awareness of PPCP occurrence and adverse effects for the robust establishment of regulation for PPCPs.

CLASSIFICATION OF PPCPS

Pharmaceutical and Personal Care Products (PPCPs) includes wide range of organic compounds used on a daily basis for various purposes as shown in Table 1 (for pharmaceuticals: antibiotics, steroids/hormones, analgesics, anti-inflammatory drugs, antiepileptic drugs, blood lipid regulators, β-blockers, stimulant, contrast media, artificial sweeter and cytostatic drugs; for personal care products: antimicrobial agents, sun-screen agents, fragrances, disinfectants, preservation, synthetic musk and insect repellants) [15-18]. Antibiotics, such as sulfamethoxazole, trimethoprim and ampicillin are essential medication for both humans and animals to treat bacterial contamination and are among the most prescribed group of pharmaceuticals due to their wide uses in residential area and livestock agriculture [19]. Especially, a group of sulfonamides which include sulfamethoxazole, sulfadiazine and sulfadimethoxine are

the most broadly used antibiotics [3]. For instance, sulfamethoxazole was ranked within top 5 antibiotic agents prescribed in U.S. 2013 [20]

TABLE 1
List of general pharmaceutical and personal care products [19,34,54]

PPCPs	Groups	Compounds	
Pharmaceuticals	Antibiotics	Erythromycin	Sulfamethoxazole
		Ciprofloxacin	Chloramphenicol
		Trimethoprim	Ampicillin
		Sulfadiazine	Nalidixic acid
		Clarithromycin	Sulfadimethoxine
		Norfloxacin	
	Steroids & Hormones	Estrone (E1)	Estradiol (E2)
		Ethinyl estradiol (EE2)	Estriol
		17- β-estradiol	Norethisterone
		Norgestrel	Testosterone
	Analgesics and anti-inflammatory drugs	Diclofenac	Naproxen
		Ibuprofen	Ketoprofen
		Paracetamol	Aspirin
		Acetaminophen	Acetylsalicylic acid
		Hydrocortisone	Triamcinolone
	Antiepileptic drugs	Carbamazepine	Primidone
	Blood lipid regulators	Clofibrate	Gemfibrozil
		Bezafibrate	
	β-blockers	Metoprolol	Propanolol
	Stimulant	Caffeine	
	X-ray contrast agents	Diatrizoate	Iopromide
		Iomeprol	Iopamidol
	Artificial sweeter	Cyclamate	Saccharin
		Aspartame	
	Cytostatic drugs	Ifosfamide	Cyclophosphamide
Personal Care Products	Antimicrobial agents / Disinfectants	Triclosan	Triclocarban
	Synthetic musks / Fragrances	Galaxolide (HHCB)	Toxalide (AHTN)
		Acetophenone	Indole
		Isoborneol	Isoquinoline
		Nitromusks	
		3-methyl-1(H)-indole (Skatole)	
		Methyl salicylate (tri) ethyl citrate	
	Insect repellants	N,N-diethyl-m-toluamide (DEET)	
	Preservatives	Parabens	
	Sunscreen UV filters	2-ethylhexyl-4-trimethoxycinnamate(EHMC)	
		4-methyl-benzilidine-camphor(4MBC)	
		Benzophenone	
	Artificial sweetener	Acesulfame	Sucralose
	Cosmetic	Propylparaben	
	Flame retardants	Polybrominated diphenyl ethers (PBDEs)	

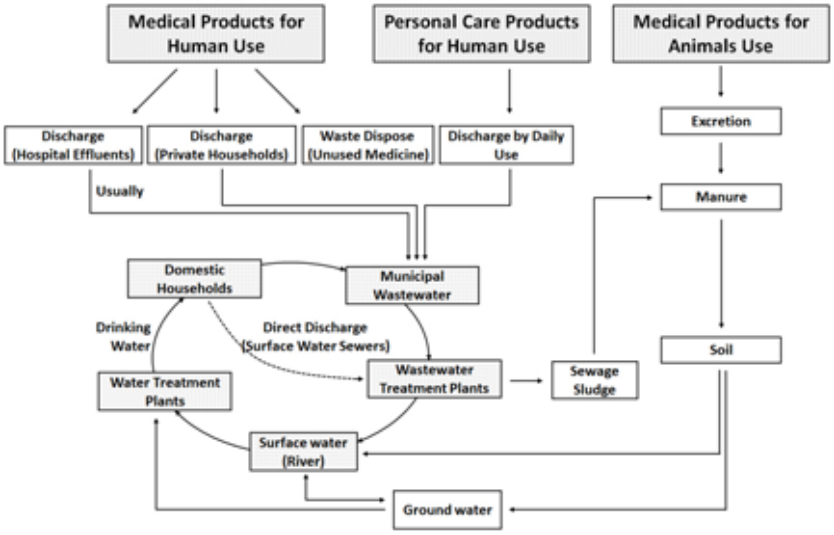

FIGURE 1
Possible pathways of PPCPs in the aquatic environment (adapted from Ellis 2006 and Heberer 2002)

SOURCES AND PATHWAYS OF PPCPS TO THE ENVIRONMENT

The main source of PPCPs into the aquatic environment is effluents from sewage treatment plants (STPs) [21,22], although the large portion of PPCPs in wastewater could be treated by a STP such as sedimentation, flocculation and active sludge system [23,24]. Loading of pharmaceuticals can initiate from hospital effluents, the discharge from private households, waste disposal of unused medication, and even the release of medical products for animal use. Then, the pharmaceuticals are collected into municipal wastewater and treated in STPs. However, due to the limited removal of pharmaceuticals through STP process with varying degree of natural attenuation, some quantity of pharmaceuticals are discharged into the receiving water bodies [25]. Then, pharmaceuticals could cause subsequent contamination particularly to the water supply bodies [26]. As shown in Figure 1, personal care products, such as hair care products, skin lotions, soap, cosmetics, tooth pastes and body wash, also have similar pathways as pharmaceuticals.

A study reported that occurrence of PPCPs in urban groundwater are closely related to landfill contamination and its leachate [25]. Moreover, a recent study investigated that humans could be possibly exposed to plants and food crops irrigated with treated wastewater or amended with biosolids containing PPCPs [27]. Verlicchi and Zambello [28] reported that the sludge-amended soil contained the most critical compounds including estradiol, ciprofloxacin, ofloxacin, tetracycline, caffeine, triclosan and triclocarban. Octanol-water partition coefficient (log K_{ow}) can be a good parameter to predict the behavior of PPCPs. The compounds with the high values of log K_{ow}, such as gemfibrozil (log K_{ow} 4.77), estradiol (log K_{ow} 4.01), galaxolide (log K_{ow} 5.9), triclosan (log K_{ow} 4.76) and tonalide (log K_{ow} 5.7) are hydrophobic, while PPCPs with low log K_{ow}, such as paracetamol (log K_{ow} 0.46), caffeine (log K_{ow} -0.07), norfloxacin (log K_{ow} -1.03) and ciprofloxacin (log K_{ow} 0.28) are hydrophilic [29,30]. As a result, PPCPs have been extensively detected in soil, surface water, groundwater, and even in drinking water [31]. More extensive studies on the biodegradability, adsorption and absorption, persistence, conjugation and de-conjugation of PPCPs are required to predict the fate and pathways in the environment [32].

TABLE 2
List of PPCPs detected in 8 African countries reviewed in this study

PPCPs	Groups	Compounds	Chemical Structure	Location
Pharmaceuticals	Antibiotics	Erythromycin	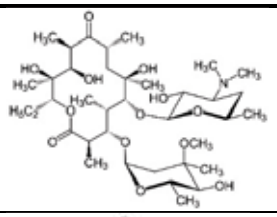	Surface water Groundwater
		Sulfamethoxazole	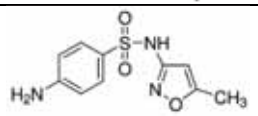	Surface water River Groundwater
		Ciprofloxacin	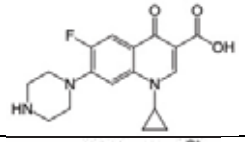	Wastewater Surface water Sediments
		Chloramphenicol	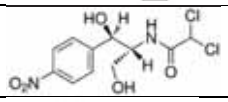	Surface water Groundwater
		Trimethoprim	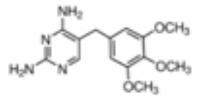	Surface water Groundwater
		Sulfadiazine	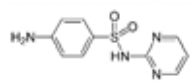	Surface water Groundwater
		Ampicillin	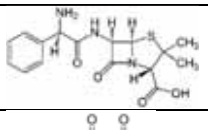	Wastewater Surface water Sediments
		Nalidixic acid	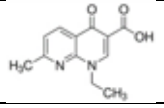	Wastewater Surface water Sediments

PPCPs	Groups	Compounds	Chemical Structure	Location
	Steroids & Hormones	Estrone (E1)	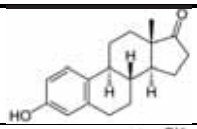	Surface water Groundwater
		Estradiol (E2)	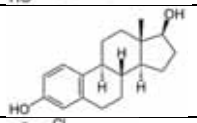	Surface water Groundwater
	Analgesics and anti-inflammatory drugs	Diclofenac	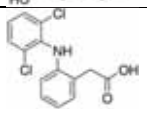	Wastewater Surface water Groundwater Sediments
		Ibuprofen	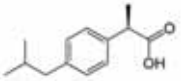	Wastewater Surface water, River Groundwater, Sediments
		Naproxen	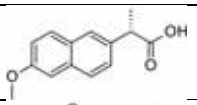	Surface water Groundwater
		Ketoprofen	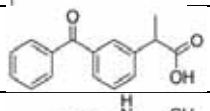	Wastewater Surface water Sediments
		Paracetamol	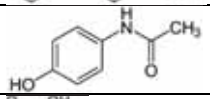	River
		Aspirin	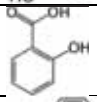	Wastewater Surface water
	Antiepileptic drugs	Carbamazepine	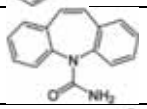	Surface water Groundwater
	Blood lipid regulators	Clofibrate	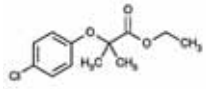	Surface water Groundwater
	Lipid regulators	Bezafibrate	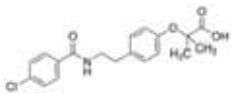	Wastewater Surface water Groundwater, Sediments
	Stimulant	Caffeine	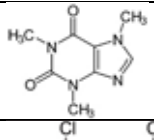	Surface water Groundwater
Personal Care Products	Antimicrobial agents	Triclosan	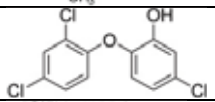	Groundwater
	Synthetic musks / Fragrances	Galaxolide (HHCB)	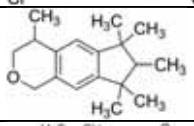	River Groundwater
		Toxalide (AHTN)	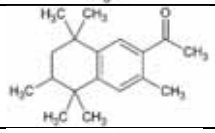	River Groundwater
	Insect repellants	N,N-diethyl-m-toluamide (DEET)	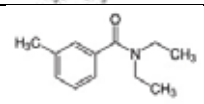	Groundwater
	Sunscreen UV filters	2-ethylhexyl-4-trimethoxycinnamate (EHMC)	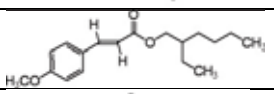	River Groundwater
	Flame retardants	Polybrominated diphenyl ethers (PBDEs)	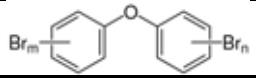	Lake Sediments

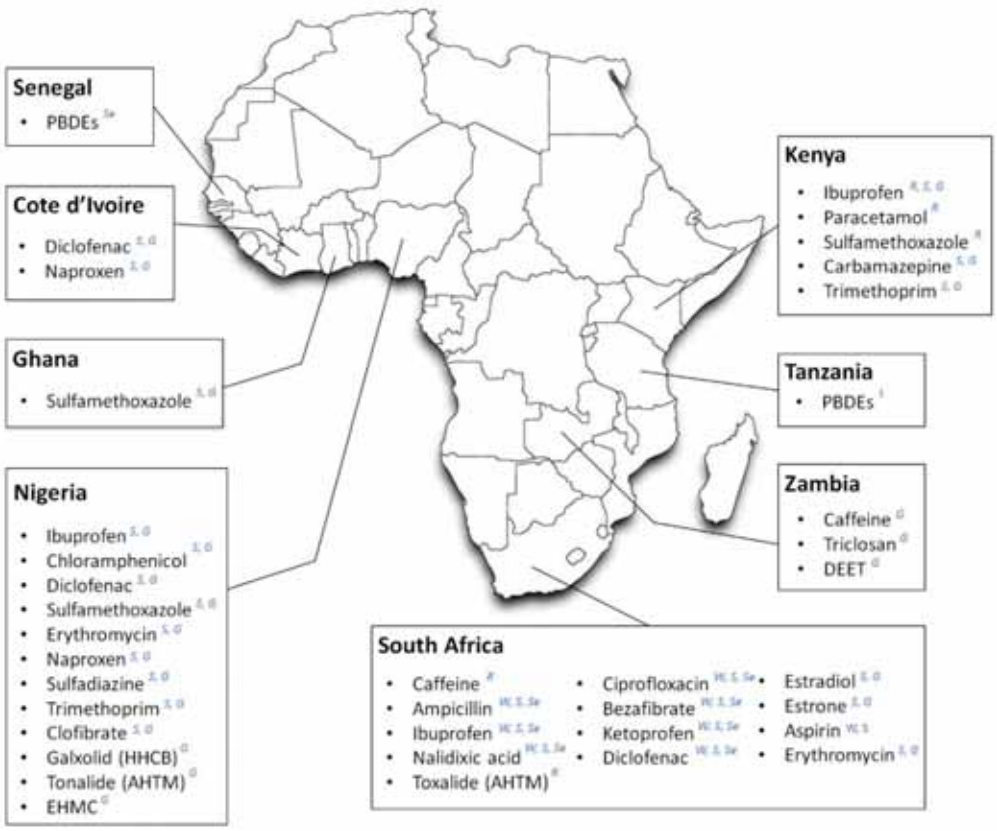

W: Wastewater, *S:* Surface water, *R:* River, *L:* Lake, *G:* Groundwater, *Se:* Sediments

FIGURE 2
Occurrence of PPCPs in the aquatic environment in Africa

IMPACTS TO HUMAN HEALTH

Humans could be potentially exposed to PPCPs through daily use of medications as well as personal care products [33]. Although human exposure to PPCPs through the atmospheric environment is limited due to their low volatility [34], inhalation or dietary intake can be routes of potential human exposure to PPCPs [35]. Thus, PPCPs can be found in urine samples, blood samples, and even human breast milk [34]. Although there is the concrete evidence that PPCPs entering the aquatic environment through several possible pathways can cause harmful effects in human health, drugs including hormone substance, birth control pills and other medications remaining in the aquatic environment could have potential risks for human [36,37]. Antibiotics that are used to kill or inhibit the growth of bacteria are one of the most frequently detected compounds and the excessive use of antibiotics may lead to negative effects in aquatic organisms such as algae and daphnids, and even in human [38]. Residual antibiotics could be persistently circulate in the aquatic environment and be accumulated eventually in the human body [39]. PPCPs remaining in fish as either parent compounds or their metabolites may lead to toxic effects on human health after consumption of fish [40]. Some hormones such as estrone (E1) and estradiol (E2), which were also detected in South Africa may disrupt hormonal system or cause other adverse health effects as endocrine disrupting compounds (EDCs) [19]. For instance, several studies have reported that exposure to EDCs may cause sexual maturation, adult obesity, breast cancer, emotional disorder, physical illness and disordered eating [41-43].

OCCURRENCE OF PPCPS IN AFRICAN COUNTRIES

This paper reviewed the occurrence of 25 PPCPs in the aquatic environment in 8 African countries including South Africa, Senegal, Cote d'Ivoire, Chana, Nigeria, Kenya, Tanzania, and Zambia (summarized in Table 2). As shown in Figure 2, 25 compounds have been detected in these countries and belonged to 11 categories including antibiotics, steroids/hormones, analgesics/anti-inflammatory drugs, antiepileptic drugs, blood lipid regulators, stimulant, antimicrobial agents, synthetic musks/fragrances, insect repellants and sunscreen UV filters. Particularly, it appeared

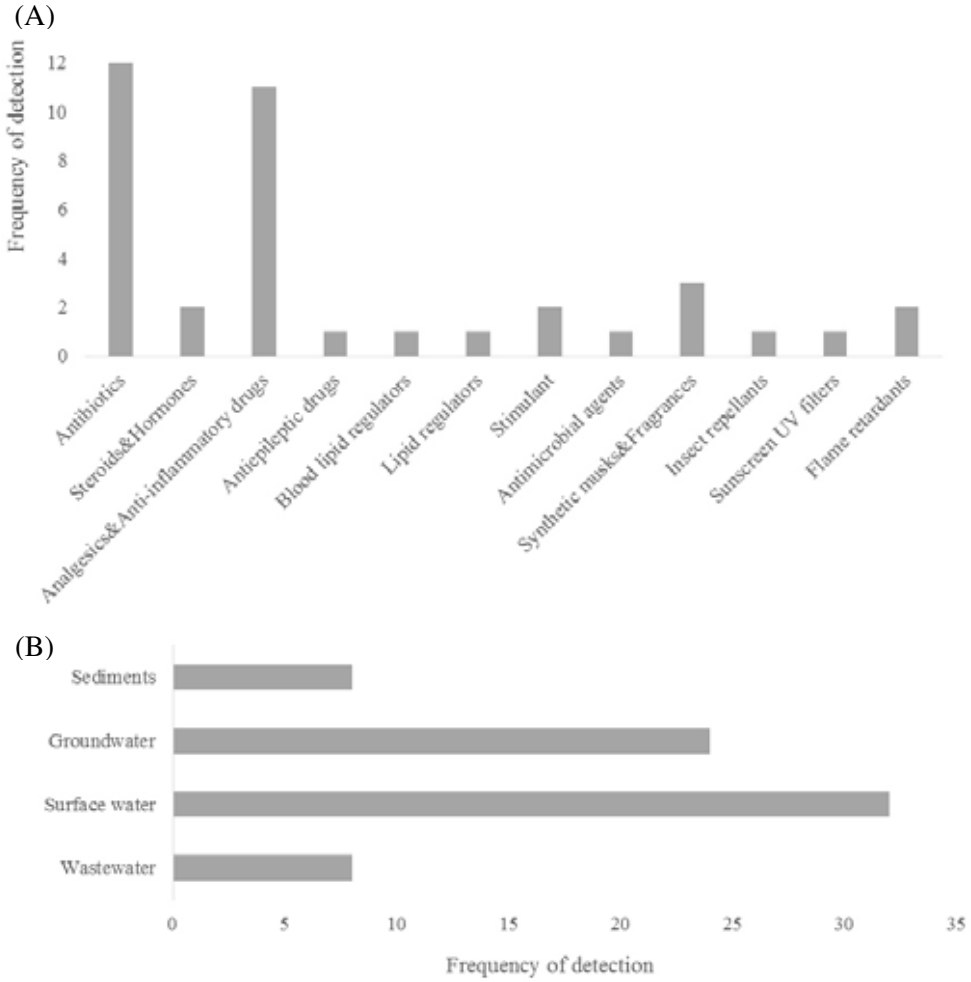

FIGURE 3
(A) Frequencies of detection of different types of PPCPs in the African aquatic environment; (B) Frequencies of detection of PPCPs in different water bodies in African countries.

that a wide range of PPCPs were detected in South Africa and Nigeria, while PBDEs (fire retardants) and sulfamethoxazole (an antibiotic) were observed in Senegal, Ghana and Tanzania. diclofenac and naproxen (analgesics/anti-inflammatory drugs) were mainly detected in Cote d'Ivoire [12]. As shown in Figure 3, antibiotics, analgesics/anti-inflammatory drugs are two major categories of PPCPs detected in African countries. The reason that the more PPCPs occurred especially in South Africa and Nigeria may be due the difference in the number of researches related to the detection of PPCPs. Thus, if the more researches for the detection of PPCPs are performed in other African countries, the chance of detecting PPCPs that may occur would be higher.

The detection of 25 PPCPs in African countries was observed in wastewater, groundwater, sediments and surface water such as rivers and lakes. In Kenya, sulfamethoxazole and trimethoprim (antibiotics), ibuprofen and paracetamol (analgesics and anti-inflammatory drugs) were frequently detected in river water [10,12]. In Zambia, the occurrence of caffeine, triclosan and *N*,*N*-diethyl-meta-toluamide (DEET) were observed in groundwater [6]. Interestingly, the median concentration of DEET was five times higher in the wet than in the dry season, suggesting that DEET was more mobile in the rainy season and can be useful as a wastewater indicator in African water bodies. A wide range of PPCPs were detected in surface water and groundwater in South Africa and Nigeria [10-12,44]. Particularly, estrogenic hormones such as estrone (E1) and estradiol (E2) were detected in surface water as well as groundwater in South Africa [12]. The occurrence of PPCPs were mostly prevalent in shallow wells located in low cost housing area due to the localized vulnerability associated with inadequate well protection, sanitation, and household waste disposal. In addition, galaxolide (HHCB) and toxalide (AHTM) which are used as synthetic musks and fragrance were observed in surface water and groundwater. It is also known that sediments were contaminated by antibiotics (ampicillin, ciprofloxacin and nalidixic acid), analgesics/anti-inflammatory drugs (ibuprofen, ketoprofen and diclofenac), and a blood lipid regulator (bezafibrate) [11,45]. Figure 3 indicates

that the frequency of detection of PPCPs in surface water was higher than other water bodies and sediments. It is also common that antibiotics and hormones in the aquatic environment have been frequently detected in developed countries including U.S. and Europe [18,46-53]. On the other hand, the absence of general PPCPs which have been commonly detected in the developed countries may be due to the limited availability and affordability of general PPCPs in African countries. However, the possibility that PPCPs may be naturally attenuated during transport to the aquatic environment cannot be also excluded.

CONCLUSIONS

The release and occurrence of PPCPs via diverse pathways to the aquatic environment from numerous pollution sources can result in adverse effects in humans and the environment. In this review, we summarized the detection of PPCPs in the African aquatic environment. Twenty five compounds belonging to various groups of PPCPs were detected in surface water, groundwater, wastewater and even in sediments, indicating that there could be the potential risks to human and aquatic organisms. As compared with the developed countries, there is still a lack of information about the contamination levels of PPCPs in the African countries.

Furthermore, it is also important to prepare for establishing the regulations for PPCPs in African countries in order to control the contamination of PPCPs. In U.S., the regulations for several PPCPs the assessment of environmental risks from pharmaceuticals were established in 1969 by U.S. Food and Drug Administration (U.S.FDA) and the regulations for the pharmaceutical industry to manage the discharges from air and water has been required by U.S. EPA since 1998 [34]. In addition, the first guideline for Environmental Risk Assessment of Human Medicines has been issued for the PPCP regulations by European Union (EU) in 2006. In Australia, Switzerland and China have established the regulations for PPCPs [34].

Therefore, for the first step in fully understanding contamination sources, fate and transport of a wide range of PPCPs, and their toxic impacts on human health and aquatic ecosystems, it is required to broadly investigate the occurrences of PCPPs in the African aquatic environment.

ACKNOWLEDGEMENTS

This work was supported by Incheon National University Research Grant in 2015.

REFERENCES

[1] Rahman, M., Yanful, E., Jasim, S. (2009) Endocrine disrupting compounds (EDCs) and pharmaceuticals and personal care products (PPCPs) in the aquatic environment: implications for the drinking water industry and global environmental health. Journal of Water and Health 7: 224-243.

[2] Farré, M., Kantiani, L., Petrovic, M., Pérez, S., Barceló, D. (2012) Achievements and future trends in the analysis of emerging organic contaminants in environmental samples by mass spectrometry and bioanalytical techniques. Journal of Chromatography A 1259: 86-99.

[3] Sui, Q., Cao, X., Lu, S., Zhao, W., Qiu, Z., Yu, G. (2015) Occurrence, sources and fate of pharmaceuticals and personal care products in the groundwater: a review. Emerging Contaminants 1: 14-24.

[4] Lee, D.G. (2015) Removal of a synthetic broad-spectrum antimicrobial agent, triclosan, in wastewater treatment systems: A short review. Environmental Engineering Research 20: 111-120.

[5] Babatunde, B., Kika, P., Ugoeze, K., Nwanchukwu, N., Sikoki, F., Udeala, O. (2016) Ecotoxicity potentials of residual paracetamol and personal care products (PPCPS) in household waste at the University of Port Harcourt, Nigeria. Journal of Environmental and Analytical Toxicology 2016.

[6] Sorensen, J., Lapworth, D., Nkhuwa, D., Stuart, M., Gooddy, D., Bell, R., Chirwa, M., Kabika, J., Liemisa, M., Chibesa, M. (2015) Emerging contaminants in urban groundwater sources in Africa. Water Research 72: 51-63.

[7] de García, S.O., Pinto, G.P., Encina, P.G., Mata, R.I. (2013) Consumption and occurrence of pharmaceutical and personal care products in the aquatic environment in Spain. Science of the Total Environment 444: 451-465.

[8] Fent, K., Weston, A.A., Caminada, D. (2006) Ecotoxicology of human pharmaceuticals. Aquatic Toxicology 76: 122-159.

[9] Luo, Y., Guo, W., Ngo, H.H., Nghiem, L.D., Hai, F.I., Zhang, J., Liang, S., Wang, X.C. (2014) A review on the occurrence of micropollutants in the aquatic environment and their fate and removal during wastewater treatment. Science of the Total Environment 473: 619-641.

[10] Matongo, S., Birungi, G., Moodley, B., Ndungu, P. (2015) Pharmaceutical residues in water and sediment of Msunduzi River, KwaZulu-Natal, South Africa. Chemosphere 134: 133-140.

[11] Agunbiade, F.O., Moodley, B. (2016) Occurrence and distribution pattern of acidic pharmaceuticals in surface water, wastewater, and sediment of the Msunduzi River, Kwazulu□ Natal, South Africa. Environmental Toxicology

and Chemistry 35: 36-46.
[12] Olarinmoye, O., Bakare, A., Ugwumba, O., Hein, A. (2016) Quantification of pharmaceutical residues in wastewater impacted surface waters and sewage sludge from Lagos, Nigeria. Journal of Environmental Chemistry and Ecotoxicology 8: 14-24.
[13] Breton, R., Boxall, A. (2003) Pharmaceuticals and personal care products in the environment: regulatory drivers and research needs. QSAR and Combinatorial Science 22: 399-409.
[14] Gibson, K. (2010) Pharmaceuticals and personal care products (PPCPs): disposal, scientific, and regulatory challenges. Environmental Quality and Management 20: 39-48.
[15] Yang, X., Flowers, R.C., Weinberg, H.S., Singer, P.C. (2011) Occurrence and removal of pharmaceuticals and personal care products (PPCPs) in an advanced wastewater reclamation plant. Water Research 45: 5218-5228.
[16] Edwards, M., Topp, E., Metcalfe, C., Li, H., Gottschall, N., Bolton, P., Curnoe, W., Payne, M., Beck, A., Kleywegt, S. (2009) Pharmaceutical and personal care products in tile drainage following surface spreading and injection of dewatered municipal biosolids to an agricultural field. Science of the Total Environment 407: 4220-4230.
[17] Reyes-Contreras, C., Hijosa-Valsero, M., Sidrach-Cardona, R., Bayona, J.M., Bécares, E. (2012) Temporal evolution in PPCP removal from urban wastewater by constructed wetlands of different configuration: a medium-term study. Chemosphere 88: 161-167.
[18] Ferguson, E.M., Allinson, M., Allinson, G., Swearer, S.E., Hassell, K.L. (2013) Fluctuations in natural and synthetic estrogen concentrations in a tidal estuary in south-eastern Australia. Water Research 47: 1604-1615.
[19] Esplugas, S., Bila, D.M., Krause, L.G.T., Dezotti, M. (2007) Ozonation and advanced oxidation technologies to remove endocrine disrupting chemicals (EDCs) and pharmaceuticals and personal care products (PPCPs) in water effluents. Journal of Hazardous Materials 149: 631-642.
[20] Centers for Disease Control Prevention (2016) Outpatient antibiotic prescriptions-United States, 2013.
[21] Daughton, C.G., Ternes, T.A. (1999) Pharmaceuticals and personal care products in the environment: agents of subtle change? Environmental Health Perspectives 107: 907.
[22] Lee, D.G., Roehrdanz, P.R., Feraud, M., Ervin, J., Anumol, T., Jia, A., Park, M., Tamez, C., Morelius, E.W., Gardea-Torresdey, J.L. (2015) Wastewater compounds in urban shallow groundwater wells correspond to exfiltration probabilities of nearby sewers. Water Research 85: 467-475.
[23] Jiang, J.-Q., Zhou, Z., Sharma, V. (2013) Occurrence, transportation, monitoring and treatment of emerging micro-pollutants in waste water—a review from global views. Microchemical Journal 110: 292-300.
[24] Lee, D.G., Zhao, F., Rezenom, Y.H., Russell, D.H., Chu, K.-H. (2012) Biodegradation of triclosan by a wastewater microorganism. Water Research 46: 4226-4234.
[25] Ellis, J.B. (2006) Pharmaceutical and personal care products (PPCPs) in urban receiving waters. Environmental Pollution 144: 184-189.
[26] Suárez, S., Carballa, M., Omil, F., Lema, J.M. (2008) How are pharmaceutical and personal care products (PPCPs) removed from urban wastewaters? Reviews in Environmental Science and Bio/Technology 7: 125-138.
[27] Wu, X., Dodgen, L.K., Conkle, J.L., Gan, J. (2015) Plant uptake of pharmaceutical and personal care products from recycled water and biosolids: a review. Science of the Total Environment 536: 655-666.
[28] Verlicchi, P., Zambello, E. (2015) Pharmaceuticals and personal care products in untreated and treated sewage sludge: occurrence and environmental risk in the case of application on soil—a critical review. Science of the Total Environment 538: 750-767.
[29] Ratola, N., Cincinelli, A., Alves, A., Katsoyiannis, A. (2012) Occurrence of organic microcontaminants in the wastewater treatment process. a mini review. Journal of Hazardous Materials 239: 1-18.
[30] Kim, J.-W., Ishibashi, H., Yamauchi, R., Ichikawa, N., Takao, Y., Hirano, M., Koga, M., Arizono, K. (2009) Acute toxicity of pharmaceutical and personal care products on freshwater crustacean (*Thamnocephalus platyurus*) and fish (*Oryzias latipes*). The Journal of Toxicological Sciences 34: 227-232.
[31] Hu, X., Zhou, Q., Luo, Y. (2010) Occurrence and source analysis of typical veterinary antibiotics in manure, soil, vegetables and groundwater from organic vegetable bases, northern China. Environmental Pollution 158: 2992-2998.
[32] Heberer, T. (2002) Tracking persistent pharmaceutical residues from municipal sewage to drinking water. Journal of Hydrology 266: 175-189.
[33] Lu, Y., Yuan, T., Wang, W., Kannan, K. (2011) Concentrations and assessment of exposure to siloxanes and synthetic musks in personal care products from China. Environmental Pollution 159: 3522-3528.
[34] Liu, J.-L., Wong, M.-H. (2013) Pharmaceuticals and personal care products (PPCPs): a review on environmental contamination in China. Environment International 59: 208-224.
[35] Grassi, M., Rizzo, L., Farina, A. (2013)

Endocrine disruptors compounds, pharmaceuticals and personal care products in urban wastewater: implications for agricultural reuse and their removal by adsorption process. Environmental Science and Pollution Research 20: 3616-3628.
[36] Cabello, F.C. (2006) Heavy use of prophylactic antibiotics in aquaculture: a growing problem for human and animal health and for the environment. Environmental Microbiology 8: 1137-1144.
[37] Brausch, J.M., Rand, G.M. (2011) A review of personal care products in the aquatic environment: environmental concentrations and toxicity. Chemosphere 82: 1518-1532.
[38] Thiele□Bruhn, S. (2003) Pharmaceutical antibiotic compounds in soils–a review. Journal of Plant Nutrition and Soil Science 166: 145-167.
[39] Kümmerer, K., Al-Ahmad, A., Mersch-Sundermann, V. (2000) Biodegradability of some antibiotics, elimination of the genotoxicity and affection of wastewater bacteria in a simple test. Chemosphere 40: 701-710.
[40] Mottaleb, M.A., Bellamy, M.K., Mottaleb, M.A., Islam, M.R. (2015) Use of LC-MS and GC-MS Methods to Measure Emerging Contaminants Pharmaceutical and Personal Care Products (PPCPs) in Fish. Journal of Chromatography and Separation Techniques 6: 1.
[41] Patton, G.C., Viner, R. (2007) Pubertal transitions in health. The Lancet 369: 1130-1139.
[42] Hamilton, A.S., Mack, T.M. (2003) Puberty and genetic susceptibility to breast cancer in a case–control study in twins. New England Journal of Medicine 348: 2313-2322.
[43] Lomenick, J.P., Calafat, A.M., Castro, M.S.M., Mier, R., Stenger, P., Foster, M.B., Wintergerst, K.A. (2010) Phthalate exposure and precocious puberty in females. The Journal of Pediatrics 156: 221-225.
[44] Arukwe, A., Myburgh, J., Langberg, H.A., Adeogun, A.O., Braa, I.G., Moeder, M., Schlenk, D., Crago, J.P., Regoli, F., Botha, C. (2016) Developmental alterations and endocrine-disruptive responses in farmed Nile crocodiles (*Crocodylus niloticus*) exposed to contaminants from the Crocodile River, South Africa. Aquatic Toxicology 173: 83-93.
[45] Bayen, S. (2012) Occurrence, bioavailability and toxic effects of trace metals and organic contaminants in mangrove ecosystems: a review. Environment International 48: 84-101.
[46] Arikan, O.A., Rice, C., Codling, E. (2008) Occurrence of antibiotics and hormones in a major agricultural watershed. Desalination 226: 121-133.
[47] Kolpin, D.W., Skopec, M., Meyer, M.T., Furlong, E.T., Zaugg, S.D. (2004) Urban contribution of pharmaceuticals and other organic wastewater contaminants to streams during differing flow conditions. Science of the Total Environment 328: 119-130.
[48] Kolpin, D.W., Furlong, E.T., Meyer, M.T., Thurman, E.M., Zaugg, S.D., Barber, L.B., Buxton, H.T. (2002) Pharmaceuticals, hormones, and other organic wastewater contaminants in US streams, 1999-2000: a national reconnaissance. Environmental Science and Technology 36: 1202-1211.
[49] Kasprzyk-Hordern, B., Dinsdale, R.M., Guwy, A.J. (2009) The removal of pharmaceuticals, personal care products, endocrine disruptors and illicit drugs during wastewater treatment and its impact on the quality of receiving waters. Water Research 43: 363-380.
[50] Tamtam, F., Mercier, F., Le Bot, B., Eurin, J., Dinh, Q.T., Clément, M., Chevreuil, M. (2008) Occurrence and fate of antibiotics in the Seine River in various hydrological conditions. Science of the Total Environment 393: 84-95.
[51] Vieno, N.M., Härkki, H., Tuhkanen, T., Kronberg, L. (2007) Occurrence of pharmaceuticals in river water and their elimination in a pilot-scale drinking water treatment plant. Environmental Science and Technology 41: 5077-5084.
[52] Brix, R., Postigo, C., González, S., Villagrasa, M., Navarro, A., Kuster, M., de Alda, M.J.L., Barceló, D. (2010) Analysis and occurrence of alkylphenolic compounds and estrogens in a European river basin and an evaluation of their importance as priority pollutants. Analytical and Bioanalytical Chemistry 396: 1301-1309.
[53] Noppe, H., Verslycke, T., De Wulf, E., Verheyden, K., Monteyne, E., Van Caeter, P., Janssen, C.R. (2007) Occurrence of estrogens in the Scheldt estuary: a 2-year survey. Ecotoxicology and Environmental Safety 66: 1-8.
[54] Jjemba, P.K. (2006) Excretion and ecotoxicity of pharmaceutical and personal care products in the environment. Ecotoxicology and Environmental Safety 63: 113-130.

Received: **23.03.2017**
Accepted: **25.07.2017**

CORRESPONDING AUTHOR

Do Gyun Lee
Department of Environmental Engineering, Incheon National University, 119 Academy-ro, Incheon, 22012, South Korea.

e-mail: dlee31@inu.ac.kr

© by PSP Volume 26 – No. 10/2017 pages 5980-5986 Fresenius Environmental Bulletin

THE STUDY OF THE UPSTREAM SLOPE OF A SIPHON SPILLWAY ON ITS DISCHARGE COEFFICIENT USING FLOW3D SOFTWARE

Amir Abbas Kamanbedast[*,1], Ali Assareh[1]

1-Department of Water Science and Engineering, Ahvaz Branch, Islamic Azad University, Ahvaz, Iran

ABSTRACT

In many projects for supplying water and energy, such as dams, the flow rate of water must be controlled to achieve this goal. To that end, a special structure, called the dam's spillway, is used to discharge the surplus water. In other words, this technique is used when the size of the dam is inadequate for storing the surplus water and avoiding the risk of flooding. Dam spillways are complex and diverse equipment, and it is very important for designers to understand the hydraulic behavior of this equipment and to be able to analyze specific physical parameters by changing the angle of the slope above the siphon spillway in the KWPTI (Khuzestan water and power authority) laboratory. In this research, the governing equations were solved by the finite volume discrimination method (flow 3D software), and the standard K-ε model was used to estimate the turbulent flow. A structured grid was used to fit the irregular boundaries, and the volume of fluid (VOF) method was used to solve the complex free-surface problem. The free surface, velocities, and pressures on the siphon spillway were obtained by the numerical simulation of the turbulence. The results of the numerical method were in good agreement with the experimental results that were obtained. The results of the tests that were conducted in this research indicated the discharge coefficient decreased as the angle of the slope increased.

KEYWORDS:
Siphon spillway, discharge coefficient, upstream slope, flow 3D, physical model

INTRODUCTION

Generally, spillways are designed to discharge extra water or flood waters that exceed the capacity of the reservoir. Spillways also are used in directional dams to bypass or redirect the flow of water that exceeds the system's capacity. Most dams that have been damaged or destroyed were designed inappropriately and did not have suitable spillway capacity. In fact, if dams' spillways were computed and designed appropriately, the surrounding area would not be damaged by their structural instability and by floods. Spillways are structures that are used in canals for measurement water and many other applications. Thus, significant efforts have been made to increase the accuracy of the flow measurements associated with such structures. Ogee spillways are the most common and inexpensive spillways with high capability of flow. These spillways are used extensively in directional dams due to their high hydraulic efficiency Kamanbedast, [12]. Ogee spillway: A weir is defined as an obstruction over which water must flow in an open channel, and weirs are used as an indirect method for obtaining the flowrate of water based on the geometry of the weir and the water pressure at the crest of the weir King and Brater, [17] Ogee spillways are of reservoir dams spillways, as discussed in this paper. These spillways are commonly used in dams. One of major types of dam spillways is siphon spillways. As the name implies, the operation of such a spillway is based on siphon physics. Any siphon spillway has a maximum flowrate to discharge different volumes of water, which is computed with the following equation. As observed from above equation, the coefficient of the flowrate has a direct relationship with the output flowrate and has an important role. In this paper, we have reported the results of our investigation and analysis of the relationship between upstream changes in slope and the final arc angle of siphon spillways on the flow rate coefficient, which has a direct relationship with the maximum flow rate. Most siphon spillways consist of five main components, i.e., an inlet, an upper leg, a throat or control section, a lower leg, and an outlet. A siphon-breaker air vent also is provided to control the siphon action of the spillway so that it will cease operation when the reservoir water level is drawn down to normal level. Otherwise, the siphon continues to operate until air enters the inlet. The inlet is generally placed well below the normal reservoir water level to prevent entrance of ice and other debris. The major benefit of a siphon spillway is that it is capable of passing the total design flow rate upon a partial increase of upstream water level. Another benefit of such spillways is their automation process, since their good performance requires no mechanical machines

or stimulators. However, their costs are greater than those of other spillways. Siphon spillways operate based on siphon laws, with reduced pressure causing the flow of water downward from behind the dam (Figure 1).

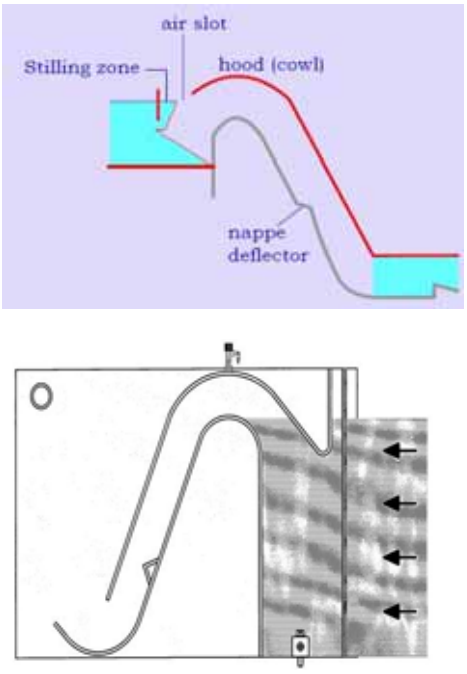

FIGURE 1
Schematic of a siphon spillway

Head [11] showed that there were differences between siphons by comparing one working with black water, which operated only based on active-inactive conditions, and one with an air control vent, which automatically controlled the flow rate to reach a fixed water level. Kamanbedast and Gholizade [14] by the study of siphon spillway investigate the spillway's angles in downstream and modeled the overhead flow of a siphon spillway in a numerical basis in three dimensions for different geometries using 3D Flow model, and he solved the Navier–Stokes equations with the K-ε model. Gramathy et al [10] made an experimental model of a siphon spillway such that the spillway's cross sectional area increased upon closing to spillway outlet (divergent outlet) and pressure decreases in center line. Dornarck et al. [8] made a physical model of the Oker dam in the laboratory and studied the operation of an air valve and flow rate control through air flow, and they also computed the minimum opening diameter, the cross-sectional area of the air inlet, and the local loss coefficient of an aerator valve at different levels of water in the reservoir. Aigner et al. [4] suggested a simple method to compute and manage adjustment and control steps associated with a siphon spillway. Kamanbedast A.A. [13]. Investigate of Discharge Coefficient for the Morning Glory Spillway Using Artificial Neural Network. Abbasi S., and Kamanbedast, A.A. [1] investigated the effect of changes in dimension and the hydraulics of stepped spillways for maximization of energy dissipation. They were among the first researchers to use flow3D to obtain a solution based on the method for the flow analysis of stepped spillways. Aydin, M.C., Ozturk, M. and Yucel, A. [5] Evaluate siphon side weir by physical modeling and numerical on a straight open channel.

Rostami, H. et al. [19] investigate labyrinth spillways and showed that increasing the weir hydraulic head ratio (Hd/P) would decrease the discharge coefficient (C_d). Rouzegar, J. et al. [20] find out that the increase in length of spillway and number of zigzag will increase the flow rate.

METHODS AND MATERIALS

Dimensional analysis and extraction of dimensionless numbers. In this research, Buckingham theory was used for dimensional analysis. First, these relationships allowed us to reduce the number of variables, and, second, they allowed us to use the results for all modes. The following points must be considered for the dimensional analysis of flow, i.e., repetitive variables should have all of the dimensions of the related variables. Select a variable as repetitive variable that can be measured in the laboratory with acceptable accuracy (e.g., the diameter of a tube or a pipe). It is beneficial to select one of repetitive variables from the fluid's features, and, if no such variables are available, use the acceleration of gravity parameter as a repetitive variable. Select one of the repetitive variables from the flow's features. Considering the above-mentioned points, the following relationship was developed using variables:

$$f(Cd, \mathrm{Fr}, \mathrm{Su},, H, L, Q) = 0$$

Parameters of this research are as follows:
C_d: coefficient of spillway; Q: spillway flow; S_d: downstream slope; H_0: the height of water over the spillway; L: length of the spillway; and V: velocity of water over the spillway

Considering the above relationships, parameters were obtained as follows:
In this research, we ignored the parameters that included Weber and Reynolds numbers due to lack of intervention in order to simplify and reduce number of tests and observed parameters. Performing a series of tests on these models, the following parameters were considered as follows:

$$Cd = f(Su, fr)$$

The authors used the hydraulic laboratory of Khuzestan Water and Power Industry Higher Education and Research Complex to obtain the calibration results presented in this paper; the characteristics of the equipment were as follows:

FIGURE 2
7.5-m flume that was set up and used in the laboratory

TABLE 1
Variables and number of tests

N	Descriptions	Variables
1	Flow rate 5,10,15,20,25 m^3/h	5
2	Spillway	1
3	Upstream slope	4
4	Total tests	20

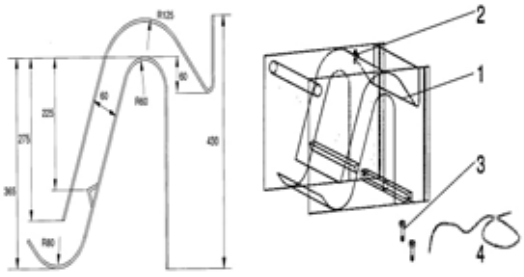

FIGURE 3
Siphon spillway designed and built in the laboratory

7.5-m flume with a 30-cm width and a 45-cm height; made in Germany by Gunt Company, equipped with a flow rate meter and pitot tube to read input flow rate of the flume with details mentioned under the image (Fig. 2).

A level gauge was used to measure depth and water surface elevation of canal flow. It also was used to measure depth and water surface elevation in all spots of canal flow. The spillway profile of this device was coordinated with the standard spillway profile. The spillway was made of PVC, to do this and also to reach research and educational goals, an Ogee spillway was set up in the laboratory flume, and it was fastened to the base plate. Note that this spillway could be used without the base plate. To conduct the desired research, first, it was described with a physical model, and the Ogee spillway and discharge coefficient were computed with five different flow rates. Then, this process was repeated with different upstream slope in addition to the natural state of the spillway; then, the required processing was performed. We were able to determine the relationship between the discharge coefficient with relative slope and the height of the water in the spillway and Froude number. All of the tests that were performed are listed in Table 1 and Figure 3.

Using the control valve for input flow rate and reading the flow rate meter that was embedded in the flume, we observed a flow rate of 5 m3/hr, and, after a few minutes when the flow conditions became stable, the depth of fluid in the upstream portion of the spillway and the depth of water in the spillway were measured and sited in Table 2. Then, we increased the flowrate to10 m3/hr, and after the flow conditions stabilized, we repeated the same process and sited the results. We repeated this processes for flow rates of 15, 20, and 25 m3/hr and sited the results in Table 2.

TABLE 2
Upstream slope changes (30^0)

Sd	Su	Q(l/s)	$H_{(m)}$	$A_{(m2)}$	Cd	$V_{(m/s)}$	Fr	$H_{(cm)}$	$h_{(cm)}$
		6.67	0.317	0.008	0.345	0.860	0.487	40.750	2.730
		5.56	0.314	0.008	0.295	0.733	0.417	40.400	2.670
30	0	4.44	0.308	0.007	0.243	0.597	0.344	39.750	2.620
		3.33	0.300	0.007	0.188	0.455	0.265	39.000	2.580
		2.22	0.293	0.007	0.128	0.307	0.182	38.100	2.550
		6.67	0.317	0.008	0.345	0.854	0.483	40.800	2.750
		5.56	0.314	0.008	0.295	0.733	0.415	40.350	2.685
30	15	4.44	0.308	0.007	0.243	0.597	0.342	39.650	2.640
		3.33	0.300	0.007	0.188	0.455	0.265	39.000	2.580
		2.22	0.294	0.007	0.128	0.303	0.179	38.350	2.580
		6.67	0.317	0.008	0.355	0.838	0.484	40.900	2.800
		5.56	0.314	0.008	0.294	0.711	0.406	40.300	2.750
30	25	4.44	0.308	0.007	0.243	0.591	0.340	39.800	2.650
		3.33	0.300	0.007	0.187	0.451	0.265	39.100	2.600
		2.22	0.292	0.007	0.128	0.301	0.181	38.300	2.600
		6.67	0.321	0.008	0.328	0.824	0.464	41.100	2.850
		5.56	0.314	0.008	0.291	0.699	0.397	40.500	2.800
30	30	4.44	0.308	0.008	0.243	0.569	0.326	40.000	2.750
		3.33	0.300	0.008	0.188	0.435	0.252	39.250	2.700
		2.22	0.293	0.008	0.123	0.295	0.174	38.500	2.650

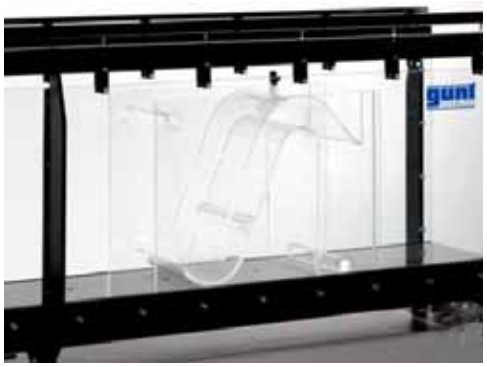

FIGURE 4
Siphon spillway used in the experiments

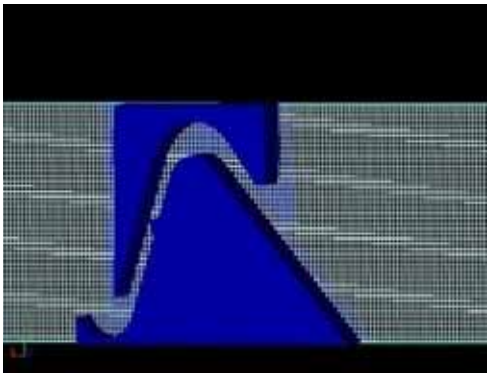

FIGURE 5
Siphon spillway used in the software

FIGURE 6
Images from the model

Flow 3D software – Standard $k-\varepsilon$ Turbulence Model. Also in the present study, the $k-\varepsilon$ model was used to simulate the flow turbulence characteristics. This model is the most extensively-used, two-equation model because it is easy to understand and its proper applicability in programming. In this model, the turbulent field is defined in terms of two variables, i.e., 1) the kinetic energy of turbulent flow (k) and2) the collapse rate of turbulent kinetic energy (ε). Values of k and ε can be obtained from the following semi-experimental equations:

That turbulent viscosity (μ_t) is related to the length of large scaling for turbulent flow. For modeling the flow algorithm, flow3D software and AutoCAD were used simultaneously. Fig. 4, 5.

In this research, tests were performed using a physical model at a flowrate of 25 to 250 l/min over the siphon spillway with different upstream and downstream angular modes (Figure 6, 7).

Conceptions related to each of upstream angles should be inserted in a table with fixed angle distal arch and graphs related to discharge coefficient changes, upstream slope. Then, changing duct angle continues the operation in accordance with Figure 6 and inserts it in the related table.

RESULTS AND DISCUSSION

The results of the analysis of the experimental data are presented in figures and tables. As mentioned, the above physical model was used for five flow rates between 8 and 24 m^3/hr and four upstream angles; the results are presented in Table 3. After acquiring the data in 20 different modes, we observed and analyzed conditions in the following modes (Diagram 1; Table 3.

Investigating the effect of upstream slope (Su) on the discharge coefficient (C_d). Diagram 1 shows that increases of the upstream slope in the siphon spillways resulted in decreases of the flow rate coefficient with mild slope.

Investigating downstream slope (Sd) on discharge coefficient (C_d). Diagram 2, shows that increasing the downstream slope in siphon spillways resulted in increases of the flow rate coefficient with sharp slope.

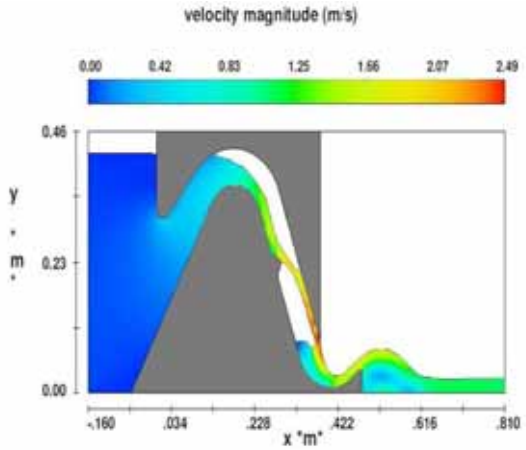

FIGURE 7
Simulation of the spillway with 3Dflow model

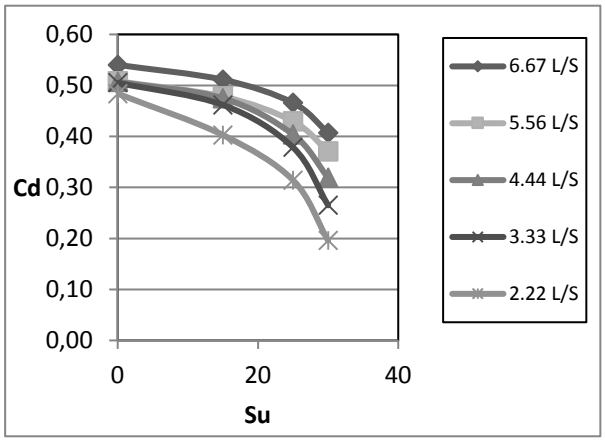

DIAGRAM 1
Effect of changes in the upstream slope on the flow rate coefficient

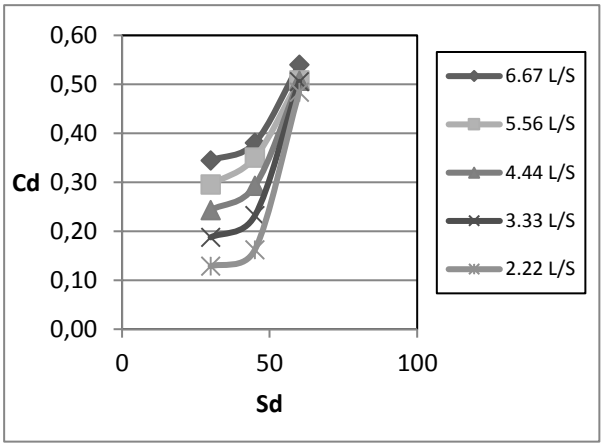

DIAGRAM 2
Effect of downstream slope on flow rate coefficient

TABLE 3
Upstream slope changes in flow3D

Test-Name	Q(m3/hr)	S-Upstream	A	H(cm)	H2(cm)	C_d-flow3D-1	C_d-model	Error%
S0-Q24	24	0	0.007	41.1	2.1	0.34	0.345	2.7877
S0-Q30	30	0	0.007	41.9	2	0.43	-	-
S0-Q36	36	0	0.007	42.65	2.1	0.52	-	-
S15-Q24	24	15	0.007	41.15	1.8	0.33	0.342	1.9946
S15-Q30	30	15	0.007	42	2.2	0.42	-	-
S15-Q36	36	15	0.007	42.8	3	0.51	-	-
S30-Q24	24	30	0.007	41.4	1.5	0.32	0.328	-1.8796
S30-Q30	30	30	0.007	42.05	2.7	0.4	-	-
S30-Q36	36	30	0.007	42.85	3	0.5	-	-
S45-Q24	24	45	0.007	41.55	2	0.3	-	-
S45-Q30	30	45	0.007	42.15	2.2	0.39	-	-
S45-Q36	36	45	0.007	42.9	3	0.48	-	-

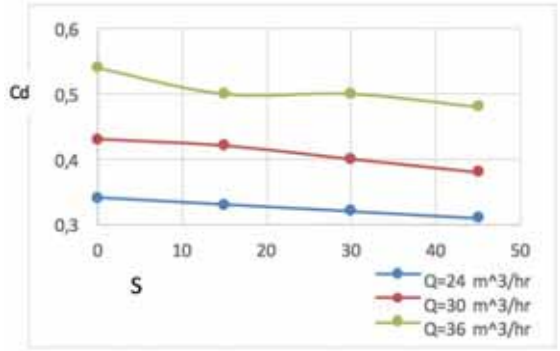

DIAGRAM 3
Impact of changes in the upstream slope on the discharge coefficient

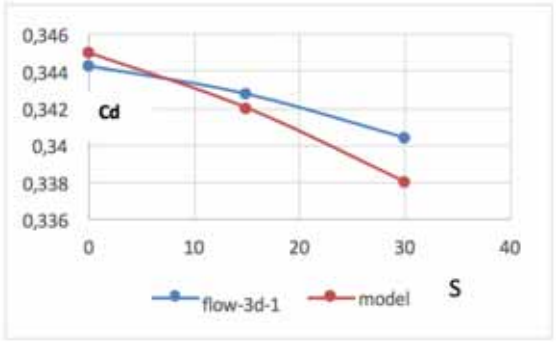

DIAGRAM 4
Comparison of Cd-Su in the model's results and the experimental results

As mentioned earlier, at a constant flow rate with an increase in the upstream slope of the siphon spillway, the discharge coefficient decreases due to the ease of moving water in the upstream portion of the overflow. However, as the flow rate is increased, it was obvious that the flow rate increased from the discharge because the overflow connection increased at fixed geometric conditions. This was observed in the physical model. Diagram 3.

It should be noted that the results provided by the mathematical model and the experimental results also are compared in Diagram 4. Also, according to

the calculations in Table 3, the calculation error was negligible.

CONCLUSIONS

Conclusions that can be drawn from this research by assessing and analyzing the results presented in the above tables and figures are as follows. In this research, the significant and effective parameters that affect the discharge coefficient of a siphon spillway were determined. This was done by using dimensional analysis and by performing about 20 tests on a siphon spillway with certain geometrical features and a range of slopes. These studies produced following results:

1. In general, it may be concluded that, in siphon spillways, the flow rate coefficient decreases as the upstream slope angle increases.
2. The slope increases when the angle is more than 45°, and there was a sharper slope in changing the angle between 20° to 45°.

ACKNOWLEDGEMENTS

This paper is taken from the research, of water science and engineering, Ahvaz Branch, Islamic Azad University (IAU), and also the authors would like to special thanks to Office of Researches and Standards of Khuzestan Water and Power Authority which helped us in research process of this paper.

REFERENCES

[1] Abbasi, S. & Kamanbedast, A.A (2012). Investigation of effect of changes in dimension and hydraulic of stepped spillways for maximization energy dissipation. World Applied Sciences Journal, 18(2), 261-267.
[2] Abrishmi, J. (1995) Handbook of open channel hydraulic. Publish, 3th Mashhad, Iran.
[3] Ghafourian, A., Jahromi, H. M., & Bajestan, M. S. (2011). Hydraulic of siphon spillway by physical and computational fluid dynamics.
[4] Aigner, D., & Horlacher, H. B. (2007, July). Investigation of Aerated Siphon. In Proceedings Of The Congress-International Association For Hydraulic Research (Vol. 32, No. 1, p. 312).
[5] Aydin, M.C., Ozturk, M. and Yucel, A. (2015) Experimental and numerical investigation of self-priming siphon side weir on a straight open channel. Flow Measurement and Instrumentation, 45, 140-150.
[6] Boatwright, J. D. (2014). Air-regulated siphon spillways: Performance, modeling, design, and construction (Doctoral dissertation, Clemson University).
[7] Davies, B., Larson, M., & Wright, G. (1999). Fool Hollow Spillway Rehabilitation Project. In WRPMD'99: Preparing for the 21st Century (pp. 1-10).
[8] Dornack, S., & Horlacher, H. B. (1999, August). Hydraulic model experiments for the siphon spillway of the Oker Dam. In 28th IAHR Congress.
[9] Erfanain-Azmoudeh, M. H., & Kamanbedast, A. A. (2013). Determine the appropriate location of aerator system on gotvandoliadam's spillway using Flow 3D. American-Eurasian Journal of Agricultural & Environmental Sciences, 13(3), 378-383.
[10] Gramathy, G. and Robinson, K. (1970) Siphon Spillway, Thesis, California Institute of Technology.
[11] Head, C.R. (1975) Low-head air-regulated siphons, J. Hydraulics Division, ASCE. 101 (HY3), 329-345.
[12] Kamanbedast, A. (2013) Handbook of hydraulic structures engineering. Published in Islamic Azad University, Ahvaz, Iran.
[13] Kamanbedast, A.A. (2012) The Investigation of Discharge Coefficient for the Morning Glory Spillway Using Artificial Neural Network, World Applied Sciences Journal, 17(7): 913-918.
[14] Kamanbedast, A. and Gholizade, B. (2012). The study of siphon spillway Hydraulic by Modeling (physical and software), Journal of Applied Sciences Research, 8(5): 2548-2553, 2012.
[15] Kamanbedast, A.A, & Ghahremani, A. (2014). Evaluation of Scour Around Bridge Pile in Flood with Hec-Ras Software. Journal of River Engineering, 2.
[16] Kamanbedast, A. A., Mousavi, S. R., & Barati, A. (2014). The effect of number and angle of guide piers on hydraulic behavior of morning glory spillway with square inlet. Advances in Environmental Biology, 2377-2384.
[17] King, H.W. and Brater, E.F. (1963) Handbook of Hydraulics, 5th Edition, McGraw-Hill Book Company, New York.
[18] Houichi, L., Ghassan, I., & Achour, B. (2009). Experimental comparative study of siphon spillway and over-flow spillway.
[19] Rostami, H., Heidarnejad, M., Purmohammadi, M. H., Kamanbedast, A., & Bordbr, A. (2016). An Experimental Study Into Discharge Coefficient Of Labyrinth Weirs With Rectangular-Shaped Plans. Fresen. Environ. Bull., 25(12), 5138-5144.
[20] Rouzegar, J., Kamanbedast, A. A., Masjedi, A., Heidarnejad, M., & Bordbar, A. (2017). The Experimental Investigation Of Flow Hydraulics In Zigzag Morning Glory Spillways. Fresen. Environ. Bull., 26(3), 2389-2396.

[21] Tadayon, R. and Ramamurthy, A.S. (2012) Discharge Coefficient for Siphon Spillways. Journal of Irrigation and Drainage Engineering, 139(3), 267-270.

Received: **01.04.2017**
Accepted: **30.07.2017**

CORRESPONDING AUTHOR

Amir Abbas Kamanbedast
Department of Water Science and Engineering,
Ahvaz Branch,
Islamic Azad University
Ahvaz – IRAN

E-mail: ka57_amir@yahoo.com

© by PSP Volume 26 – No. 10/2017 pages 5987-5990 Fresenius Environmental Bulletin

STUDY ON SYNTHESIS OF LUBRICATING OIL ADDITIVES OF SULFIDE ESTER

Miao Changqing*, Chen Yongkui, Ma Xin, Zhang Wei

College of Chemistry and Chemical Engineering, Xinxiang University, Xinxiang, China

ABSTRACT

In this paper, sulfur-containing lubricating oil additive is prepared by sulfur-cured corn oil and corn oil ethyl ester. Results showed that the additive reduced friction and wear in the specimen contaminated lubricants. There were also indications that the frictional process, when coupled with the additive induced a structural change in the soot particles within the contact zones, contributing to the improved tribological performance.

KEYWORDS:
Lubricating oil, additive; Tribofilm; Tribochemistry;

INTRODUCTION

Ionic liquids (ILs) are low-temperature molten salts exhibit liquid at or near room temperature which usually composed of organic cations and inorganic anions [1-4]. Ionic liquids have a wide range of applications because of their interesting and remarkable properties, such as no-volatility, no-flammability, low vapor pressure, good dissolving properties, high thermal stability and chemical stability. Ionic liquids, as steel/steel, steel/ aluminum, steel/copper, steel/monocrystalline silicon, steel/ceramic, ceramic/ceramic etc. friction lubricants, have excellent anti-friction and anti-wear performance whether at room temperature or high temperature, high or low loads [5-7]. For these reasons, some researchers have begun to focus on the application of ionic liquids in lubrication field. Liu et al. [8] first reported the tribological properties of ionic liquids as novel versatile lubricants in 2001. In that study, imidazolium tetrafluoroborate was prepared and showed excellent friction reduction and anti-wear properties when used as lubricant for different friction pairs. Since then, more and more people began to study the tribological properties and action mechanisms of ionic liquids as lubricating oil additives [9-12]. Qu et al. [13] found that oil-miscible ionic liquid trihexyltetradecylphosphonium bis(2-ethylhexyl) phosphate as lubricating additive can improve the anti-friction and anti-wear abilities of base oil under both room and elevated temperature. The results also showed that the ionic liquid significantly outperformed zinc dialkyldithiophosphate (ZDDP) in the 100 °C tests. It is known that ZDDP is the traditional lubricant additive to improve the tribological performance of base oil, but ZDDP is the main source of ash and easy to poison the catalysts. Moreover, the electrochemical reaction between ZDDP and some metal bearings is one of the main causes of metal corrosion when ZDDP used as lubrication additive [14]. Therefore, ionic liquids can make up the shortcomings of ZDDP and become good alternative lubricant additives. Wang and co-workers [15] synthesized two ionic liquids gels by grinding multiwall carbon nanotubes in 1-butyl-3-methylimidazolium tetrafluoroborate and 1-butyl-3-methylimidazolium hexafluorophosphate ionic liquids and investigated their physical and tribological properties. The results demonstrated that these ILs gels possess high conductivity and excellent tribological performance. The mechanism of friction reducing and anti-wear abilities is the tetrafluoroborate and hexafluorophosphate anions react with metal atoms to form a tribolchemical reaction film to prevent direct contact of the friction pairs [16].

The intention of this work is to investigate synthesis of sulfur-containing lubricating oil additive and is trying to find out the best synthesis condition of lubricating oil additive. The present work aims to evaluation of performance lubricating oil additive.

MATERIALS AND METHODS

Material. Sublimed sulfur, Zinc phosphate (chemical purity); Corn oil (Longevity Flower, 600 ml, palmitic acid 8%-12%, stearic acid 2%-5%, pleic acid 19%-49%, lindeic acid36%-64%) corn oil ethyl ester (purchased in the United States), Differential Scanning Calorimetry (DSC200F3, Shanghai), Multifunctional Friction and Wear Tester (MFT-3000, USA).

Experiment procedure. Synthesis of a mixture of corn oil and corn oil was added into the three-necked flask in a certain proportion. Calcium phosphate was used as the catalyst and N_2 is used as the shielding gas. The sulfur content was 6%, the reaction temperature was 160 ℃, reaction time was 5 h, The product was filtered by filtration.

The tribological properties of lubricating oil additives were analyzed on the four-ball friction and wear tester according to the standard method GB 3142-82. The friction and wear tests were conducted at the ambient temperature, test duration of 30 min, applied load of 392 N and rotary speed of 1500 rpm. The test balls with a diameter of 12.7 mm and hardness of HRC 60+1 were made of GCr15. The friction coefficient automatically recorded by the computer connected to the four-ball tester and the wear scar diameters (WSD) of the three lower balls were measured via an optical microscope at an accuracy of 0.01 mm. Moreover, each test was performed three times and the average WSD were calculated. Before and after each test, the oil box and balls were washed in petroleum ether and dried in air.

RESULTS AND DISCUSSION

Characterization of the lubricating oil additives. The chemical structures of the products lubricating oil additives were characterized by FTIR analysis. The resulting spectra are shown in Fig. 1. As far as lubricating oil additives ionic liquid is concerned, the strong absorption peak at 3633 cm^{-1} corresponds to stretch vibration of O-H, which demonstrates that the presence of water and consistent with the water-absorbing of lubricating oil additives ionic 1iquid. The peaks at 3135, 2985 and 2880 cm^{-1} are assigned to stretching vibration of C-H and 1741 cm^{-1} corresponds to C=O. Besides, the characteristic peak is at about 861 cm^{-1}, indicating that lubricating oil additives was successfully synthesized.

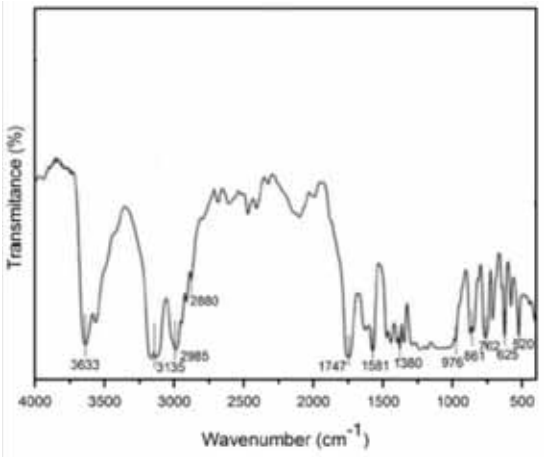

FIGURE 1
Fourier transforms infrared analysis spectra of the lubricating oil additives

Tribological properties of the lubricating oil additives. Effect of loading on tribological properties. The tribological properties of lubricating oil additives were analyzed on the four-ball friction and wear tester according to the standard method GB 3142-82. Variation of the friction coefficient of lubricating oil additives with load at a sliding speed of 1.0 m/s is shown in Fig. 2. It is seen that friction coefficient of lubricating oil additives increased with the load increasing firstly, and then decreases with the load when the applied load is higher than 150 N. Adding the nano-Zn presents the same trend. The friction increased with nano-Zn added.

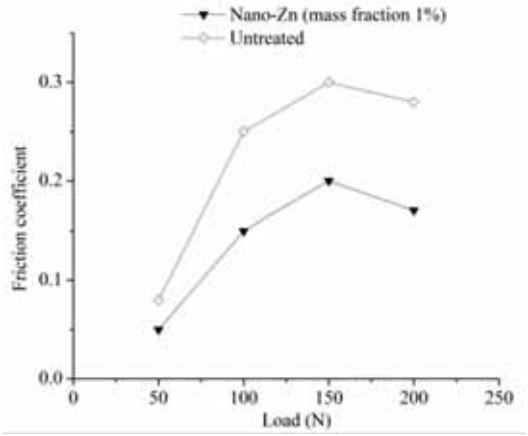

FIGURE 2
Variation of friction coefficient with load for the lubricating oil additives (sliding speed: 1.0 m/s).

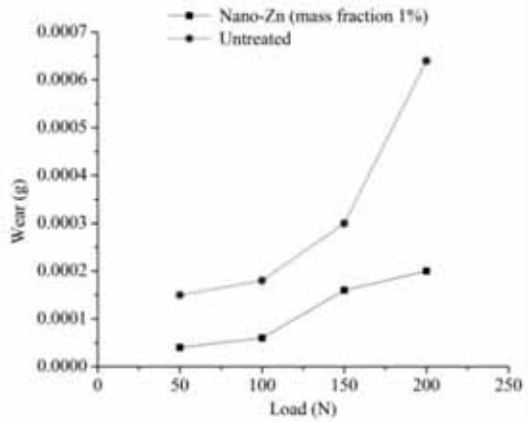

FIGURE 3
Changes of wear with load for the lubricating oil additives (sliding speed: 1.0 m/s).

Fig. 3 shows changes of the wear of the lubricating oil additives with load under a sliding speed of 1.0 m/s. It is seen that the wear of the untreated and the lubricating oil additives added nano-Zn slowly increase with the load firstly and then rapidly increase when the load is higher than 150 N. In contrast, the wear of nano-Zn treated composite always slowly increases with the load, and keeps the lowest under the load from 50 to 200 N.

Effect of mass fraction of nano-Zn and particle diameter on tribological properties. Effect of nano-Zn content and particle diameter on the tribological properties of lubricating oil additives is shown in Figure 4. It is shown that the two kinds of

nano-Zn (particle size were 50 and 100 nm) enhanced tribological properties of lubricating oil additives. As can be seen that the use of 50 and 100 nm particle sizes of the nano-enhanced Zn powder, wear and friction factor of lubricating oil additives are increased.

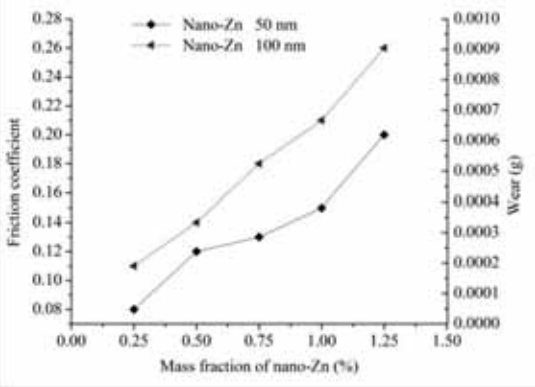

FIGURE 4
Effect of nano-Zn content and particle diameter on the tribological properties of lubricating oil additives (1.0 m/s, 200 N)

CONCLUSIONS

Sulfur-containing lubricating oil additive is prepared by sulfur-cured corn oil and corn oil ethyl ester. Results showed that the additive reduced friction and wear in the specimen contaminated lubricants. There were also indications that the frictional process, when coupled with the additive induced a structural change in the soot particles within the contact zones, contributing to the improved tribological performance.

Nano-Zn is effective to decrease friction coefficient of lubricating oil additives. The two kinds of nano-Zn (particle size were 50 and 100 nm) enhanced tribological properties of lubricating oil additives.

ACKNOWLEDGEMENTS

The authors acknowledge the financial support provided by the Innovation Funds of Xinxiang University (Grant No. 15ZB01)

REFERENCES

[1] Wang, Y. and Guo, J.S. (2016) Preparation and Characterisation of Ionic Liquid Polymer Modified Silica and Its Application in Degradation of Methyl Orange. Oxid Commun 39, 1251-1262.

[2] Wadhia, K. and Dando, T.R. (2009). Environmental Toxicity Testing Using The Microbial Assay For Risk Assessment (Mara). Fresen. Environ. Bull., 18, 219-225.

[3] Özyurt, M. and Deveci, E.Ü. (2004) Conversion Of Agricultural And Industrial Wastes For Single Cell Protein Production And Pollution Potential Reduction: A Review. Fresen. Environ. Bull., 13, 693-699.

[4] Lin, M., Hou, Z.B., Yao, S., Wang, Z.X. and Song, H. (2017) Synthesis and Physicochemical Properties of New Tropine-based Chiral Dication Ionic Liquids. J Mol Liq 225, 217-223.

[5] Chatel, G., Naffrechoux, E. and Draye, M. (2017) Avoid the PCB Mistakes: A More Sustainable Future for Ionic Liquids. J Hazard Mater 324, 773-780.

[6] Robles, P.A., Morales, J.W. and Cisternas, L.A. (2016) Modeling of Liquid-liquid Equilibrium for Binary and Ternary Systems Containing Ionic Liquids with the Hexafluorophosphate Anion using the ASOG Method. Fluid Phase Equilibr 429, 119-126.

[7] Zhang, X., Su, D., Xiao, L.F. and Wu, W. (2017) Immobilized Protic Ionic Liquids: Efficient Catalysts for CO_2 Fixation with Epoxides. J CO_2 Util 17, 37-42.

[8] Ye, C., Liu, W. and Chen, Y. (2001) Room-temperature Ionic Liquids: a Novel Versatile Lubricant. Chem Commun 33, 2244-2245.

[9] Fan, M.J., Liang, Y.M., Zhou, F. and Liu, W.M. (2012) Dramatically Improved Friction Reduction and Wear Resistance by in Situ Formed ILs. RSC Adv 2, 6824-6830.

[10] Wang, Z., Xia, Y. and Liu, Z. (2012) Conductive Lubricating Grease Synthesized using the Ionic Liquid. Tribol Lett 46, 33-42.

[11] Yao, M., Pan, M., Liang, Y., Zhou, P. and Xia, Y. (2010) Imidazolium Hexafluorophospate ILs as High Temperature Lubricants for Steel-steel Contacts. Wear 268, 67-71.

[12] Qu, M.N., Yao, Y.L., He, J.M., Ma, X.R., Liu, S.S., Feng, J. and Hou, L.G. (2016) Tribological Performance of Functionalized Ionic Liquid and Cu Microparticles as Lubricating Additives in Sunflower Seed Oil. Tribol Int 104, 166-174.

[13] Qu, J., Luo, H.M., Chi, M.F., Ma, C., Blau, P.J., Dai, S. and Viola, M.B. (2014) Comparison of an Oil-miscible Ionic Liquid and ZDDP as a Lubricant Anti-wear Additive. Tribol Int 71, 88-97.

[14] Spikes, H.A. (2004) The History and Mechanism of ZDDP. Tribol Lett 17, 469-489.

[15] Fan, X.Q. and Wang, L.P. (2015) Ionic Liquids Gels with in Situ Modified Multiwall Carbon Nanotubes Towards High-performance Lubricants. Tribol Int 88, 179-188.

[16] Minami, I. (2009) Ionic Liquids in Tribology. Molecules 14, 2286-2305.

Received: **02.04.2017**
Accepted: **28.07.2017**

CORRESPONDING AUTHOR

Miao Changqing
College of Chemistry and Chemical Engineering, Xinxiang University, 453003, Xinxiang, China

e-mail: 13569827510@163.com

© by PSP Volume 26 – No. 10/2017 pages 5991-5998 Fresenius Environmental Bulletin

EFFECT OF SUPER-ABSORBENT POLYMER (SAP) ON BASALT FIBER ENGINEERED CEMENTITIOUS COMPOSITE

Qiang Du*, Jing Wei, Jing Lv

Institute of Construction Engineering and Economics, Chang'an University, Xi'an 710064, China

ABSTRACT

This paper reports on tests conducted to investigate the effect of SAP addition on the properties of basalt fiber engineered cementitious composites (BF-ECC). The fresh properties, autogenous shrinkage, compressive strength, flexural strength, splitting tensile strength and elastic modulus with five SAP additions of 0%, 0.1%, 0.2%, 0.4% and 0.6% were studied, respectively. Experimental results show that the use of basalt fibers has little influence on the compressive strength but results in significant improvement on flexural strength and splitting tensile strength, however, reduces elastic modulus of ECC mixtures. The workability and mechanical strength all decrease with an increase in SAP content, while slight increase in strength can be observed when SAP content is 0.1%. Accounting for the hydration process of cement particles with gradual release of water, the strength decrease ratio is lowered as curing age prolongs. With respect to autogenous shrinkage, SAP addition achieves excellent autogenous shrinkage reduction as expected. However, this reduction becomes non-significant when SAP exceeds 0.4%.

KEYWORDS:
Super-absorbent polymers; Basalt fiber; Fresh property; Mechanical properties; Autogenous shrinkage.

INTRODUCTION

In recent years, engineered cementitious composites(ECC) are widely produced as fiber reinforced cementitious materials in construction industry due to the benefits derived from its large tensile ductility and intrinsic crack width control capacity [1]. However, it is known that autogenous shrinkage will occur as the hydration process of cementitious materials with low water-to-cement (W/C) ratios [2]. Consequently, early-age cracking will appear in hardened cement-based materials. Therefore, the long-term durability of cement-based materials is adversely affected. In order to relieve the autogenous shrinkage of cementitous materials, using SAP as internal curing agent has been proposed and applied as an efficient method [3, 4].

SAP is a group of polymeric materials that has the capacity of absorbing a significant amount of liquid from the surrounding environment and to retain it within its structure without dissolving [5]. Generally, it is utilized in the fields such as agriculture, pharmaceutical, biomedical engineering, et al. [6]. In 2001, Jensen and Hansen firstly introduced SAP as a means for internal water curing of cementitious materials to mitigate autogenous shrinkage. Then, plenty of researches were focused on studying the performance of cementitious materials containing SAP. The results of these studies have proven that the autogenous shrinkage can be greatly reduced by adding SAP into cementitious materials [7-10]. In addition, the workability decreased as less water is available in the matrix itself due to the uptake if mixing water by SAP [11-12]. Some investigations were conducted regarding the influence of SAP on the mechanical properties. The majority of the tests showed that the addition of SAP results in a decrease in mechanical properties [13-16], in particular at early age caused by higher total porosity [17, 18]. However, several publications demonstrated an increment in mechanical properties [19, 20].

From the foregoing review, most literature about SAP is concerning concrete. However, there are many existing researches about the properties of ECC containing SAP. The most recent report appears to be Yao et al. [21], which is about incorporating SAP in ECC. The results showed that SAP can improve tensile strain capacity and flexural deflection of ECC matrix, but reduce the compressive strength and have a negative effect on tensile strength. In addition, it was verified that the incorporation of SAP effectively mitigate the autogenous shrinkage of PVA-ECC.

Nowadays, the growing attention is focused on the development of sustainable composites with natural fibers and the basalt fiber engineered cementitious composites (BF-ECC) are the most interesting ones. Basalt fiber is a new kind of high-performance inorganic fiber which is characterized by high temperature resistance and better tensile strength and failure strain [22]. In particular, the basalt fibers do

not contain any other additives in a single producing process, which makes additional advantage in cost [23]. Tang and Yang incorporated basalt fiber as reinforcing material for cementitious composites. They found that the basalt fiber as an enhanced component has a very good flexural strength enhancement effect. Moreover, the fibers still connect the two sections in some broken cross-sections under the electron microscopic observation and are being helpful in preventing cracking [24]. As mentioned before, the usage of SAP is supposed to reduce the autogenous shrinkage of BF-ECC. However, the multifactorial effect of SAP in BF-ECC on hardened mechanical properties was not examined.

In view of the above facts, this paper aims to investigate the effect of different SAP content on the mechanical properties and autogenous shrinkage in BF-ECC. For this purpose, the fresh properties are determined with flow table test first. Then, the strength property tests including compressive strength, flexural strength, splitting tensile strength and elastic modulus are conducted at different ages to evaluate the strength development under various SAP dosages. In addition, the measurement of autogenous shrinkage is recorded to assess the effectiveness of SAP materials for internal curing of BF-ECC.

MATERIALS AND METHODS

Test materials. All mixtures prepared for this study were composed of ordinary Portland cement(PC), class I fly ash (FA), fine sand with the maximum grain size of 118μm, tap water and a polycarboxylate-based high range water reducer (HRWR). The chemical and physical properties of PC and FA are shown in Table 1. The basalt fiber was added in the content of 1% by total volume and the geometric specifications and mechanical properties of basalt fiber are given in Table 2. SAP is a kind of copolymer of acrylamide and sodium acrylate with an average particle size of 75 μm. The scanning electron microscopy(SEM) image of basalt fiber and SAP in dry state, as shown in Fig.1 and Fig.2, were obtained on "Hitachi S-4800" instrument with the voltage of 3.0 KV.

Mix proportions. Six mixtures were designed and prepared in this research and all mixtures were set with constant water-binder ratio(W/B) of 0.32 in order to study the effects of SAP without interference in the results. The dosages of SAP were 0%, 0.1%, 0.2%, 0.4% and 0.6% by weight of total binder materials, which are widely accepted within the usual dosage. Considering the absorption characteristic of SAP used in this study in cement paste solution, the amount of extra water and HRWR are added to satisfy the mortar workability, as listed in Table 3. The SAP was mixed with other dry materials without being pre-wetted.

TABLE 1
Chemical and physical properties of cement and fly ash.

	Cement	FA
Chemical composition (wt.%)		
SiO_2	21.08	66.43
Al_2O_3	5.48	19.05
Fe_2O_3	3.93	4.42
CaO	62.27	3.08
MgO	1.78	1.25
SO_3	2.65	0.28
R_2O	0.52	—
Loss on ignition	1.63	3.09
Physical properties		
Water required (%)	—	93.2
Specific gravity(g/cm³)	3.12	2.32
Retained on 45 μm (%)	4.2	4.3

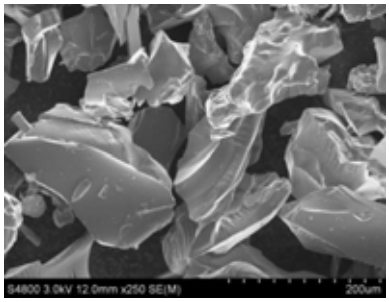

FIGURE 1
The SEM micrograph of SAP in dry state

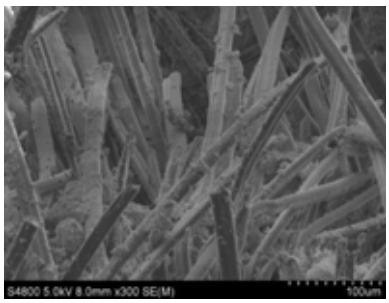

FIGURE 2
The SEM micrograph of basalt fiber

TABLE 2
Properties of Basalt fiber.

Length (mm)	Length-diameter ratio	Young's modulus (GPa)	Elongation (%)	Tensile strength (MPa)	Density (g/cm³)
12	750	100	4	2800	2.68

TABLE 3
Mix proportion of BF-ECC(kg/m^3).

ID	Basalt fiber	Cement	FA	Sand	Water	HRWR	SAP	Slump flow (mm)
ECC	0	526	526	684	337	8.5	0	185
ECC-0	26.9	526	526	684	337	10.6	0	175
ECC-0.1	26.9	526	526	684	345	10.6	1.05	170
ECC-0.2	26.9	526	526	684	354	10.6	2.1	165
ECC-0.4	26.9	526	526	684	371	10.6	4.2	155
ECC-0.6	26.9	526	526	684	388	10.6	6.3	145

TABLE 4
The experimental testing results

Mixture	Compressive strength (MPa)			Flexural strength (MPa)			Splitting tensile strength (MPa)			Elastic modulus (GPa)		
	3d	28d	56d	3d	28d	56d	3d	28d	56d	3d	28d	56d
ECC	16.8	33.7	39.6	3.6	6.1	7.2	1.97	3.57	4.28	13.2	24.3	25.9
ECC-0	16.5	34.2	39.2	4.6	8.0	8.7	2.31	4.66	5.49	12.9	23.4	25.2
ECC-0.1	15.9	34.5	40.3	4.2	8.2	9.1	2.20	4.71	5.52	11.8	23.3	25.4
ECC-0.2	14.2	31.8	38.9	3.8	7.9	8.5	1.99	4.25	5.37	10.7	21.6	24.1
ECC-0.4	12.6	30.7	37.6	3.5	7.4	8.2	1.86	4.11	5.18	9.8	19.9	22.6
ECC-0.6	10.7	28.9	36.5	3.1	6.6	7.5	1.78	3.89	4.89	8.5	18.2	20.3

Mixtures preparation. To produce the mixtures in this study, the mixing procedure was as follows: cement, FA, sand and SAP were put into mixer of 60L capacity. Then the mixer was started and all dry ingredients were mixed for initial 2 min before the addition of water and HRWR. The fibers were added gradually in two minutes later and mixed for further 4 min to ensure a homogeneous distribution in cement paste. Finally, 90 s break followed by a high-speed mixing until the mixture had a well workability. The mixture was then cast into molds and demoulded after 24 h. After demoulding, all mixtures for mechanical property tests were cured at room temperature until testing. Especially, the mixtures for autogenous shrinkage were sealed in molds and stored properly to the designed age.

The fresh cement pastes were immediately poured into moulds after completing the mixing process, and then all mixtures were put on the vibrating table to vibrate for 1-2 min. The mixtures were demolded after 24 h and then immersed in water for curing with the temperature of 20±3℃ until the age of 3 days. After that, the mixtures were stored in laboratory environment of 25℃ until testing.

Test method. (1) Flow table test. Considering the absorptivity of SAP, the incorporation of SAP can affect the workability of cement mixture. The effect of SAP on fresh properties of mixture can be measured by flow table test according to BS EN 1015-3 [25]. As mixing procedure completed, the truncated conical mould was filled with cement mortar in two layers, and each was compacted with a tamper striking for 15 times. After raising the mould, the flow table was started to jolt for 15 times followed by measuring the diameter of spread mortar with a caliper. The value of flow table test in this study was determined to be 180±5mm. The amount of HRWR was adjusted and determined by the flow table test value to ensure the workability of mixture.

(2) Mechanical properties and autogenous shrinkage test. In order to study the effect of SAP on mechanical properties of mixtures, compressive strength test, flexural strength test, splitting tensile strength and elastic modulus test were conducted. All mixtures adopted to mechanical properties test were at age of 7 days, 28 days and 56 days, and the result for each mixture was based on the test data of at least three mixtures. Compressive strength test was performed on "YA-300" compression machine with loading capacity of 300 kN. Cylinder mixtures with dimension of 100 mm×200 mm were determined in this study and loaded at a constant rate of 0.3 MPa/s according to ASTM C39/39M [26]. Using the same machine, splitting tensile test was carried out on 100 mm×200 mm cylinder mixtures with constant displacement rate of 1.2 MPa/min following ASTM C496/C496M [27]. Beam mixtures measuring 100 mm×100 mm×400 mm were prepared for three-point loading test under a loading rate of 1.0 MPa/min using "WDW3030" electronic universal testing machine, which was in accordance with ASTM C78/C78M [28]. Elastic modulus test was conducted at a constant rate of 250kPa/s for cylinder mixtures of 200 mm in length and 100 mm in diameter according to C469/C469M [29]. Each specimen was loaded three times during the test and the result was an average result of these loadings. Data presented in Table 4 shows the results of tests.

The autogenous shrinkage was determined by

using the corrugated tubes and a dilatometer according to ASTM C 1698-09. Three mixtures were prepared to be measured for each mixture. The specimen length at the time of final setting which was obtained from the corresponding Vicat needle test was measured as the initial value, and the length of 1, 3, 7, 14, 28, 56 and 90d were recorded.

RESULTS AND DISCUSSION

The test results are presented in Table 4.

Compressive strength. The compressive test results for fibrous and non-fibrous mixtures with different SAP contents at the age of 3, 28 and 56 days, respectively, are shown in Fig. 3. As seen in the figure, no obvious variation can be observed on compressive strength with addition of basalt fiber. The maximum strength loss for fibrous mixtures was obtained in mixtures with 0.6% SAP at the age of 3 days, which could be attributed to the higher water content of SAP particles at early age. The overall results of the compression test show that the compressive strength decreased with increasing SAP dosage, while slight increase could be seen when the SAP content is 0.1%.

In 28-day mixtures, the compressive strength losses were approximately 7% for 0.2% SAP, 10.2% for 0.4% SAP and 15.9% for 0.6% SAP when compared to the control mixtures. As curing age prolongs, the lower strength decrease ratio could be observed with SAP addition. In 56-day mixtures, the compressive strength losses were 1.8% for 0.2% SAP, 5.1% for 0.4% SAP and 7.8% for 0.6% SAP. It is understandable that SAP has positive effect on hydration process of cement particles due to the gradual release of water. However, the discontinuous pores caused by the swelling of SAP particles resulted in the reduction of strength.

Flexural strength. Fig.3 shows the effects of different SAP additions on the flexural strength at the age of 3 days, 28 days and 56 days, respectively. The figure demonstrates that the flexural strength of each mixtures has a clear tendency to decrease with the increase of SAP addition and this reduction is more pronounced compared to that of compressive strength.

As seen in Fig.4, it is evident that the basalt fiber can improve the flexural strength due to the fiber bridge. Compared to the non-fibrous mixtures, the increase in the strength of the mixture containing basalt fiber in varied ages were approximately 27.8% for 3 days, 31.1% for 28 days and 20.8% for 28 days. When the SAP addition was 0.1%, the presence of SAP increases the flexural strength compared with ECC-0. While the flexural strength of 3-days aged, 28-days aged and 56-days aged mixtures with addition amount of 0.2% SAP decreased by approximately 0.8MPa, 0.1MPa and 0.2MPa from the value of the control mixtures. When the amount of SAP was increased to 0.4%, the strength of the mixtures decreased by 1.1MPa, 0.6MPa and 0.5MPa at the age of 3 days, 28 days and 56 days, respectively. After SAP addition exceeded 0.6%, the reduction of flexural strength in fibrous mixtures was 1.5MPa at 3 days, 1.4MPa at 28 days and 1.2MPa at 56 days. As mentioned before, presence of SAP could produce pores in the matrix after giving up the internal curing water, which leads to strength degradation. However, a milder decrease could be observed in flexural strength at later age and this was contributed to the continuous hydration process. It was worth noting that the flexural strength value of non-fibrous mixtures at 56 days was lower than that of fibrous mixtures with 0.6% SAP at the age of 28 days and 56 days. This fact indicated that the flexural strength of mixtures is more affected by incorporation of basalt fiber than SAP addition.

Splitting tensile strength. The results shown in Fig.5 can be used to assess the effects of the SAP dosage on the splitting tensile strength of mixtures. The tendency for the change in splitting tensile strength is similar with flexural strength.

Results in Fig.5 indicate that the presence of basalt fiber can improve the splitting tensile strength compared with non-fibrous mixtures. At the age of 3 days, 28 days and 56 days, the splitting tensile strength increased 17%, 31% and 28%, respectively. However, after adding SAP into mixtures, the strength decreased. When SAP content was 0.1%, a slight increase was observed in the splitting tensile strength at the age of 28 days and 56 days when compared to the ECC-0. With the increased SAP addition, the splitting tensile strength decreased continuously. For instance, the average splitting tensile strength with 0.2% SAP addition was 86.1% at 3rd day, 91.2% at 28th day and 97.8% at 56th day of the control mixtures strength, which was further reduced to 80.5% at 3rd day, 88.2% at 28th day and 94.4% at 56th day, respectively with 0.4% SAP addition. When the SAP addition was up to 0.6%, the splitting tensile strength values were 1.78MPa at 3 days, 3.89MPa at 28 days and 4.89MPa at 56 days. In particular, the splitting tensile strength of fibrous mixtures with 0.6% SAP at 28 days was 9.0% greater than non-fibrous mixtures at 28 days without SAP addition.

Elastic modulus. The effect of SAP addition on elastic modulus of mixtures is plotted in Fig.6. For non-fibrous mixtures at 3 days, only approximately 54.3% of the stiffness at 28 days was achieved but then the stiffness increased rapidly with age. There was an obvious trend of reduction in elastic modulus by adding basalt fiber and SAP to the mixtures.

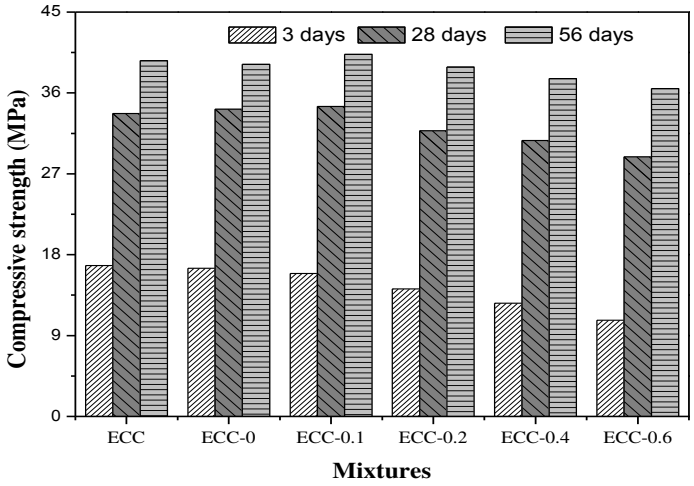

FIGURE 3
Compressive strength of ECC mixtures at different ages

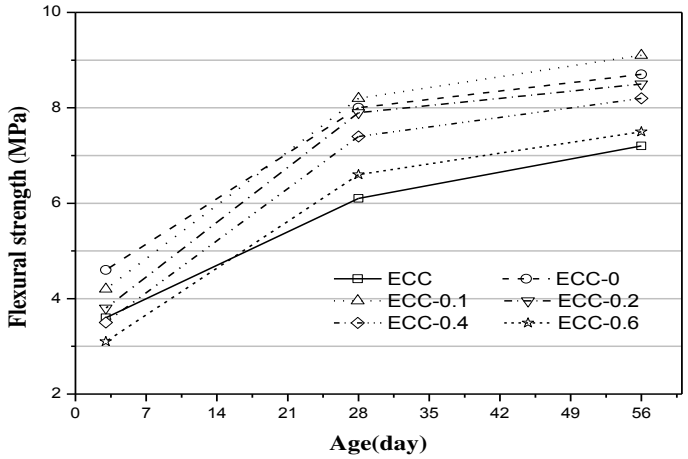

FIGURE 4
Flexural strength of ECC mixtures at different ages

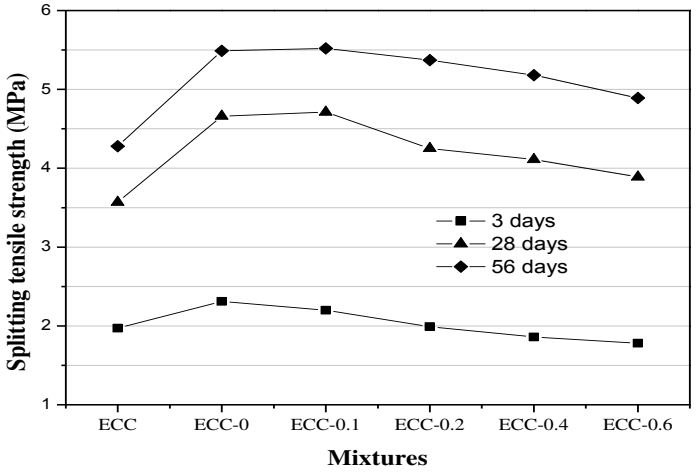

FIGURE 5
Splitting tensile strength of ECC mixtures at different ages

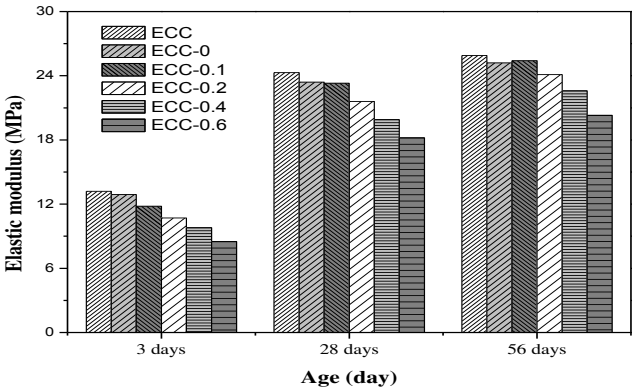

FIGURE 6
Elastic modulus of ECC mixtures at different ages.

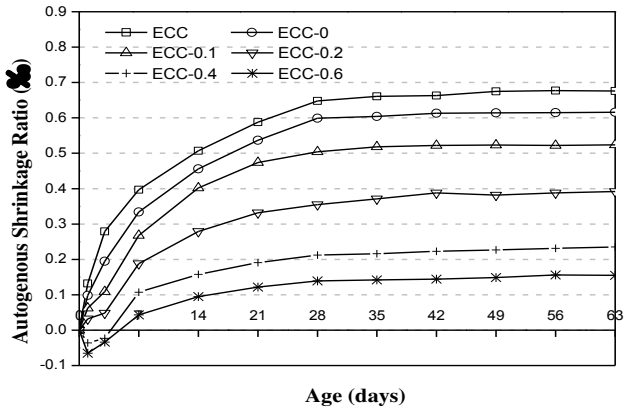

FIGURE 7
Autogenous shrinkage of ECC mixtures at different ages

Compared to the non-fibrous mixtures, the results revealed 2.3% at 3 days, 3.7% at 28 days and 2.7% at 56 days of elastic modulus loss with basalt fiber. It can be observed that the mixtures with basalt fiber had slightly less rigidity in comparison to the non-fibrous mixtures, which might be associated with the additional porosity caused by fiber content.

SAP contents of 0.1% and 0.2% resulted in a reduction in elastic modulus value of fibrous mixtures by approximately 8.5% and 17% at 3 days, 0.4% and 7.7% at 28 days, 0.8% and 4.4% at 56 days, respectively, compared to the ECC-0. When the SAP addition increased to 0.4% and 0.6%, the elastic modulus values between 9.8 and 8.5MPa at 3 days, 19.9 and 18.2 MPa at 28 days, 22.6 and 20.3 MPa at 56 days were achieved. This could be explained by the increasing porosity after SAP particle swelling, which led to loss in stiffness, with increasing SAP contents [30].

Autogenous shrinkage. The effects of the basalt fiber and replacement ratio of SAP on the autogenous shrinkage of ECC mixtures are shown in Fig.7. The deformations were supposed to be zero at the moment of final setting time and the measurements were conducted until the age of 63 days. In addition, positive and negative proportions represent the shrinkage and expansion deformations, respectively.

For control mixtures with a water-cement ratio of 0.32, the hydration process resulted in obvious autogenous shrinkage especially at early age. This was caused by the fact that the absolute volume of cement and water in the fresh cement paste decreases when the cement hydrates. However, the fly ash used in this study relatively mitigated the autogenous shrinkage as the amount of cement was lowered, which was described in previous study [8]. At addition of 1% by volume of BF-ECC, the basalt fibers were found to have some positive effect on autogenous shrinkage while the shrinkage ratio decreased by 0.5% compared with control mixtures.

As clearly seen in Fig.7 and as expected, all ECC mixtures with SAP addition showed lower autogenous shrinkage at different ages and this reduction was enhanced with increasing SAP dosage. For ECC mixtures, the 0.1% SAP of binder materials led to a 15.9% reduction in autogenous shrinkage at 28 days compared to that of ECC-0, while the 0.2% SAP addition showed a 41% reduction at 28 days. This indicated that with double amount of additional

water introduced into mixtures, the 0.2% SAP addition was more effective to mitigate the autogenous shrinkage. Since the slope of autogenous shrinkage ratio curves represented the shrinkage development rate of mixtures, it could be obtained that the minor shrinkage (even expansion) occurred after the initial setting time and followed by a fastest shrinkage development until 7 days. This is different from the control mixtures with remarkable autogenous shrinkage at very early age. After 7days, the autogenous shrinkage ratio curves became gentler and then gradually subsided until the age of 63 days. When SAP addition exceeded till 0.4%, the reduction of autogenous shrinkage is significant and approximately four times higher than that of ECC-0.1. It is evident that the expansion can be observed in the figure. This phenomenon can be ascribed to the modification of portlandite formation by the presence of superabsorbent polymers and ettringite crystallisation. The average autogenous shrinkage of mixtures with 0.6% SAP was close to ECC-0.4 at 63 days, which means that at high SAP dosage situation, the mitigation of autogenous shrinkage was reduced with the increase of SAP.

CONCLUSIONS

This paper revealed the effect of different SAP additions on properties of BF-ECC at 3 days, 28 days and 56 days, respectively. The following conclusions can be drawn from the experimental results and discussions.

1. The addition of SAP leads to the loss in workability due to the absorption of mixing water. Based on the value of flow table test, the extra water is provided to reach the aspired workability.

2. In accordance with the results, it is clear that the SAP addition affects the mechanical properties of mixtures, with increasing SAP contents being increasingly effective. The deterioration of the matrix can be observed in terms of reduced compressive strength, flexural strength, splitting tensile strength and elastic modulus. However, it should be noted that the effects of SAP addition of 0.1% are found to result in slight increase of the mechanical properties of mixtures.

3. The lower strength decrease ratio of mixtures can be observed at later ages (28 and 56 days) compared with early age (3 days), accounting for the hydration process of cement particles with gradual release of water.

4. Addition of basalt fiber significantly increases the flexural strength and splitting tensile strength but decreases the elastic modulus.

5. The incorporation of SAP significantly reduces the autogenous shrinkage of ECC mixtures and this reduction is enhanced with increasing SAP addition. However, when SAP exceeds 0.4%, the changes of autogenous shrinkage become non-significant.

ACKNOWLEDGEMENTS

This work was supported by China National Research Fund (51379015); Shaanxi Research Fund (2013KW13-01, 2016JM5044); Shaanxi Construction Technology Project (JQ201501); Central Universities Fund (310823172001, 310823170213, 310823170648).

REFERENCES

[1] Li, V.C., Wu, C., Wang, S., Ogawa, A. and Saito, T. (2002) Interface tailoring for strain-hardening Polyvinyl Alcohol-Engineered Cementitious Composite(PVA-ECC). ACI Mater J, 99, 463-72.

[2] Zorla, E., Ipbuker, C., Gulik, V., Kovaljov, S., Kiisa, M., Biland, A. and Tkaczyk, A.H. (2016) Optimization of Basalt Fiber in Concrete Composite for Industrial Application in Estonia. Fresen. Environ. Bull., 25, 355-364.

[3] Dogan, M. and Alkan, M. (2004) Some physicochemical properties of perlite as an adsorbent. Fresen. Environ. Bull., 12, 251-257.

[4] Andres, A., Velasco, M.D, M.F., Cox, A., Ruiz, C., Viguri, J.R. and Irabien, J.A. (2002) Treatment of foundry sludges by stabilization/solidification with cement and siliceous binders. Fresen. Environ. Bull., 11, 849-853.

[5] Soliman, A.M. and Nehdi, M.L. (2013) Effect of partially hydrated cementitious materials and superabsorbent polymer on early-age shrinkage of UHPC. Constr Build Mater, 41,270-275.

[6] Buchholz, F. and Graham, A. (1998) Modern Superabsorbent Polymer Technology. John Wiley & Sons.

[7] Assmann, A. and Reinhardt, H.W. (2013) The use of Superabsorbent Polymers to Mitigate Shrinkage of Concrete. International Conference on Creep, 301-307.

[8] Snoeck, D., Jensen, O.M. and Belie, N.D. (2015) The influence of superabsorbent polymers on the autogenous shrinkage properties of cement pastes with supplementary cementitious materials. Cem Concr Res, 74, 59-67.

[9] Mechtcherine, V., Dudziak, L., Schulze, J. and Staehr, H. (2006) Internal curing by Super Absorbent Polymers (SAP)- effects on material properties of self-compacting fibre-reinforced high performance concrete, In: Jensen, O.M., Lura, P. and Kovler, K. (eds.), International RILEM Conference on Volume Changes of Hardening Concrete: Testing and Mitigation, RILEM Proceedings PRO 052, RILEM Publications S.A.R.L, Bagneux (France); 87-96.

[10] Igarashi, S. and Watanabe, A. (2006) Experimental study on prevention of autogenous deformation by internal curing using super-absorbent polymer particles, in: Jensen, O.M., Lura, P. and Kovler K. (eds.), International RILEM Conference on Volume Changes of Hardening Concrete: Testing and Mitigation, RILEM Proceedings PRO 052, RILEM Publications S.A.R.L, Bagneux (France); 77-86.
[11] Schrofl, C., Mechtcherine, V. and Gorges, M. (2012) Relation between the molecular structure and the efficiency of superabsorbent polymers (SAP) as concrete admixture to mitigate autogenous shrinkage. Cem Concr Res, 42, 865-873.
[12] Snoeck, D., Schaubroeck, D., Dubruel, P. and Belie, N.D. (2014) Effect of high amounts of superabsorbent polymers and additional water on the workability, microstructure and strength of mortars with a water-to-cement ratio of 0.50. Constr Build Mater, 72, 148-157.
[13] Wang, F.Z., Zhou, Y.F. and Liu, Z.C. (2009) Autogenous Shrinkage of Concrete with Super-Absorbent Polymer. ACI Mater J, 106, 123-127.
[14] Craeye, B., Geirnaert, M. and Schutter, G.D. (2011) Super absorbing polymers as an internal curing agent for mitigation of early-age cracking of high-performance concrete bridge decks. Constr Build Mater 25, 1-13.
[15] Lam, H. and Hooton, R.D. (2005) Effects of internal curing methods on restrained shrinkage and permeability. In: Persson, B., Bentz, D. and Nilsson, L.-O. (eds.) Proc. 4th int. sem. on self-desiccation and its importance in concrete technology. Lund, (Sweden): Lund University; 210-228.
[16] Esteves, L.P., Cachim, P. and Ferreira, V.M. (2007) Mechanical properties of cement mortars with superabsorbent polymers. Adv Constr Mater, 2, 451-462.
[17] Pourjavadi, A., Fakoorpoor, S.M., Hosseini, P. and Khaloo, A. (2013) Interactions between superabsorbent polymers and cement-based composites incorporating colloidal silica nanoparticles. Cem Concr Compos, 37, 196-204.
[18] Mechtcherine, V., Dudziak, L. and Hempel, S. (2009) Mitigating early age shrinkage of ultra-high performance concrete by using super absorbent polymers (SAP). In: Tanabe, T., Sakata, K., Mihashi, H., Sato, R., Maekawa, K., Nakamura, H. Creep, shrinkage and durability mechanics of concrete and concrete structures – CONCREEP-8. London, UK: Taylor & Francis Group; 847-853.
[19] Klemm, A.J. and Sikora, K.S. (2013) The effect of Superabsorbent Polymers (SAP) on microstructure and mechanical properties of fly ash cementitious mortars. Constr Build Mater, 49, 134-143.
[20] Hasholt, M.T., Jensen, O.M., Kovler, K. and Zhutovsky, S. (2012) Can superabsorent polymers mitigate autogenous shrinkage of internally cured concrete without compromising the strength? Constr Build Mater, 31, 226-230.
[21] Yao, Y., Zhu, Y. and Yang, Y. (2012) Incorporation superabsorbent polymer (SAP) particles as controlling pre-existing flaws to improve the performance of engineered cementitious composites (ECC). Constr Build Mater 28, 139-145.
[22] Wei, B., Cao, H. and Song, S. (2010) Tensile behavior contrast of basalt and glass fibers after chemical treatment. Mater Des, 31, 4244-4250.
[23] Sim, J. and Park, C. (2005) Characteristics of basalt fiber as a strengthening material for concrete structures. Compos B Eng, 36, 504-512.
[24] Tang, M. and Yang, H. (2010) Basalt fiber reinforce cement-based composites materials. Concrete, 5, 76-78.
[25] BS EN 1015-3, Methods of test for mortar for masonry,1999.
[26] ASTM C39/C39M, Standard Test Method for Compressive Strength of Cylindrical Concrete mixtures, 2010.
[27] ASTM C496/C496M, Standard Test Method for Splitting Tensile Strength of Cylindrical Concrete mixtures, 2004.
[28] ASTM C78 / C78M, Standard Test Method for Flexural Strength of Concrete (Using Simple Beam with Third-Point Loading), 2010.
[29] ASTM C469/C469M, Standard Test Method for Static Modulus of Elasticity and Poisson's Ratio of Concrete in Compression, 2010.
[30] Beushausen, H. and Gillmer, M. (2014) The use of superabsorbent polymers to reduce cracking of bonded mortar overlays. Cem Concr Compos, 52, 1-8.

Received: **02.04.2017**
Accepted: **11.07.2017**

CORRESPONDING AUTHOR

Qiang Du
Institute of Construction Engineering
and Economics,
Chang'an University,
Xi'an 710064 – CHINA

E-mail: Q.Du@chd.edu.cn

© by PSP Volume 26 – No. 10/2017 pages 5999-6003 Fresenius Environmental Bulletin

CATALYTIC TREATMENT OF OILFIELD WASTEWATER BASED ON RESPONSE SURFACE METHOD

Hai-xiang Zhang[1], Yang Li[2], Zhan-dong Li[1,3,*], Cang-ming Ma[4], Shu-xin Zhang[1], Hao Shi[1], Mi Tian[1], Haotian Dai[4], Wei Li[1]

[1]College of Petroleum Engineering Institute, Northeast Petroleum University, Daqing 163318, China
[2]Daqing Vocational College, Daqing 163255, China
[3]Energy Research Institute of the Lower Saxon, Clausthal University of Technology, 38640 Goslar Germany
[4]College of Earth Sciences Institute, Northeast Petroleum University, Daqing 163318, China

ABSTRACT

In this paper, catalytic wet oxidation is adopted to treat oilfield wastewater. Central composite design (CCD), an experimental design for response surface methodology (RSM), was used to create a set of 30 experimental runs needed for optimizing of the operating conditions. Temperature, catalyst quality, reaction time and oxidant dosage are examined factors. The experimental results show that catalytic wet oxidation could effectively reduce COD removal by 98.37%. Catalytic wet oxidation process is possibly suitable for a primary treatment for oilfield wastewater.

KEYWORDS:
Oilfield wastewater; Removal efficiency; COD removal; Response surface method;

INTRODUCTION

A large amount of oil-field wastewater is produced from oil exploitation, storage, transportation, oil dehydration and reuse processes [1]. Environmental contamination by petroleum increases enormously and becomes a serious problem worldwide, so it should be treated using a suitable method before discharging into environment. Oilfield wastewater is typically hard to be treated due to its characteristics of high COD, low BOD, high toxicity, and difficult removing dissolved oil [2]. Oilfield wastewater is a complex mixture of oil, water, suspended and dissolved solids. It may contain high mineral salt concentrations, heavy metals, naturally occurring radioactive elements, and chemical additives used in drilling and operating the well (surfactants, biocides, pH controlling agents, etc.) [3]. Of the oilfield wastewater constituents, polycyclic aromatic hydrocarbons (PAH), phenols, heavy metals, and radioactive elements are of particular environmental concern [4]. Different physicochemical methods were developed for oilfield wastewater treatments, including hydrocyclone separation [5], membrane filtration and electrodialysis [6], coagulation and flocculation, and electrochemical processes [7]. However, to meet environmental standards for discharged wastewater, more efficient and environmentally safe technologies are required.

Nowadays oil-field wastewater is generally treated with physicochemical methods of flotation [8], coagulation, sedimentation, micro-electrolysis and advanced oxidation processes [9]. Although various processes are used in oil-field wastewater treatment, there are still some problems remaining in these processes, such as high energy consumption, low processing efficiency, loud operation noise and secondary pollution [10].

Advanced oxidation processes (AOPs) are becoming increasingly attractive due to their numerous applications, particularly in the treatment of wastewaters containing refractory and/or toxic compounds [11]. AOPs provide efficient pollutants degradation rather than their simple transfer to another phase, as occurs with other processes, such as coagulation/flocculation, filtration and adsorption, among others. Particularly, catalytic heterogeneous AOPs are a very important research topic due to the interest of supporting an active phase (e.g. a noble metal) on a structured matrix, avoiding the need of downstream units for catalyst separation and recovery, as occurs in homogeneous processes [12-14]. However, one of the main challenges of catalytic heterogeneous AOPs is the quest for efficient catalysts that are simultaneously stable and without (metallic) active phase losses from the support [15].

Gold catalysts have been the focus of attention, particularly in the removal of pollutants from water by wet peroxide oxidation (WPO) [16], due to their low leaching. Recent studies refer to gold on carbon [17], on Ti and Fe oxides [18]. To the best of our knowledge, Au on Al_2O_3 was never tested before for the heterogeneous catalytic wet oxidation of dissolved organics with hydrogen peroxide, and that is the purpose of this paper.

EXPERIMENTAL

Characteristics of oilfield wastewater are listed in Table 1. Hydrogen peroxide solution with mass

fraction of 35% served as the oxidant.

TABLE 1
Features of the oilfield wastewater

Parameter	Concentration
COD (mg/l)	3780
Phenols (mg/l)	48
Oil (mg/l)	1146
pH	6.7
Turbidity (NTU)	358
Total organic carbon (TOC)	11400
Suspended solid (mg/l)	305

Apparatus and method. All the experiments were performed in a batch reactor. As shown in Fig.1, the apparatus includes feed system, preheater, reactor, condenser, gas-liquid separator and back-pressure regulator. WPO of oilfield wastewater was carried out in a 0.5 L batch autoclave. Firstly, water, oilfield wastewater (concentration was 5000 mg/L) was put into the reactor, and then the system was flowed by nitrogen to remove the air within the system; the valves around the reactor were closed when the air was removed entirely. Liquid samples (ca.10 mL) were periodically withdrawn from the reactor and analyzed.

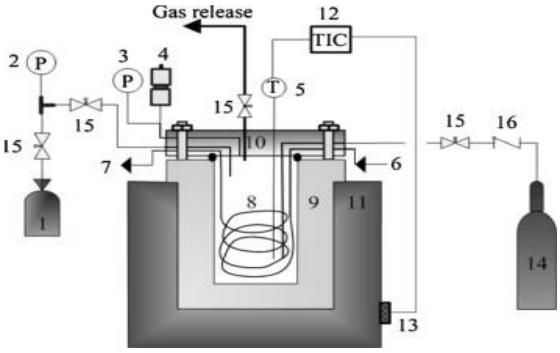

FIGURE 1
Schematic diagram of the batch reactor (1) gas bag; (2) low-pressure gauge; (3) high-pressure gauge; (4) safety valve; (5) thermocouple; (6) cooling water inlet; (7) cooling water outlet; (8) cooling coil; (9) kettle; (10) kettle cover; (11) electric heater; (12) temperature controller; (13) power source; (14) nitrogen cylinder; (15) needle valve; (16) check valve.

Analytical methods. The diluted wastewater and COD of the collected liquid are measured by potassium dichromate method of Chinese Standard 11914-89.

Experimental design. The central composite design, an experimental design for RSM, was used to create a set of designed experiments by MINITAB software (version 17). In this paper, the central composite design is selected for 4 factors, i.e., temperature (A), reaction time (B), catalyst quality (C) and oxidant dose (D).

Table 2 shows the levels of original and coded factors using central composite design. Table 3 shows central composite design and response value.

TABLE 2
Factor level

Factor level	-2	-1	0	1	2
A (temperature)/°C	260	280	300	320	340
B (reaction time) /min	60	90	120	150	180
C (catalyst quality) /g	40	80	120	160	200
D (oxidant dose) /mg/L	100	150	200	250	300

TABLE 3
Central composite design and response value

RunOrder	A	B	C	D	COD removal (%)
1	1	1	-1	1	89.39
2	-1	1	-1	1	82.24
3	1	1	-1	-1	85.07
4	0	0	0	0	93.81
5	0	0	0	0	95.01
6	-1	1	-1	-1	95.68
7	1	-1	-1	-1	85.85
8	1	1	1	1	96.37
9	1	-1	1	1	92.95
10	1	1	1	-1	94.03
11	-1	1	1	1	95.88
12	-1	1	1	-1	96.84
13	1	-1	-1	1	86.89
14	0	0	0	0	96.08
15	-1	-1	-1	1	88.09
16	-1	-1	1	-1	98.37
17	-1	-1	-1	-1	85.43
18	-1	-1	1	1	87.14
19	1	-1	1	-1	80.28
20	0	0	0	0	98.35
21	0	0	0	0	88.01
22	2	0	0	0	96.99
23	0	-2	0	0	85.43
24	0	0	0	-2	85.71
25	0	0	-2	0	85.13
26	0	0	0	2	85.7
27	0	0	0	0	95.51
28	0	2	0	0	85.89
29	0	0	2	0	85.67
30	-2	0	0	0	85.91

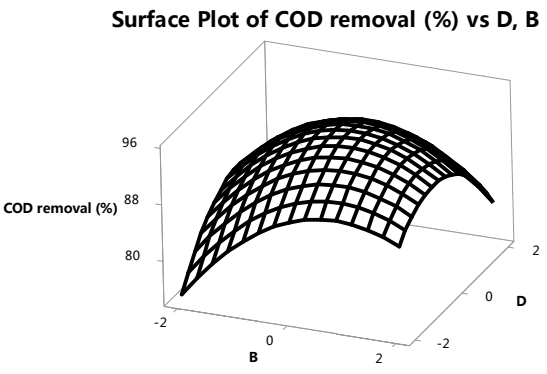

FIGURE 1
Response surface for COD removal as a function of reaction time and oxidant dose

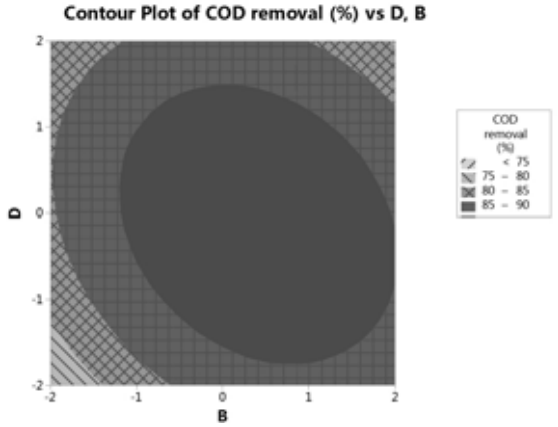

FIGURE 2
Contour plots for COD removal as a function of reaction time and oxidant dose

RESULTS AND DISCUSSION

Response surface analysis. It is seen that in Fig.1 and Fig.2, COD removal increases when reaction time and oxidant dose increases. And the change is very significant, while the surface trend is steeper.

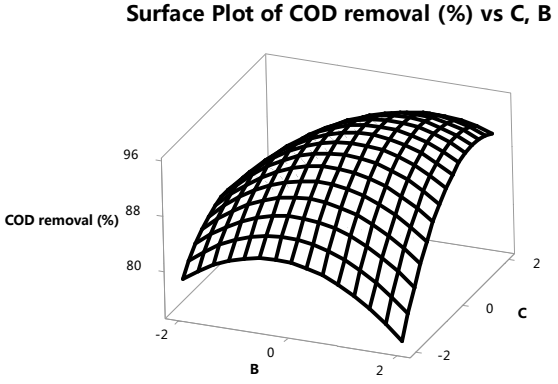

FIGURE 3
Response surface for COD removal as a function of reaction time and catalyst quality

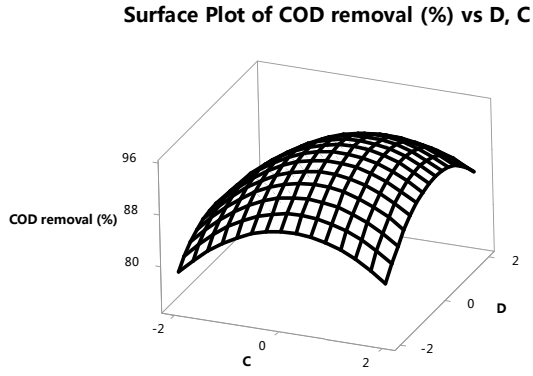

FIGURE 4
Response surface for COD removal as a function of oxidant dose and catalyst quality

For Fig.3, COD removal increases when reaction time and catalyst quality increases. COD removal has little change trend when reaction time increases from 60 to 180 min. When catalyst quality is up to 200 g, COD removal is about 96%.

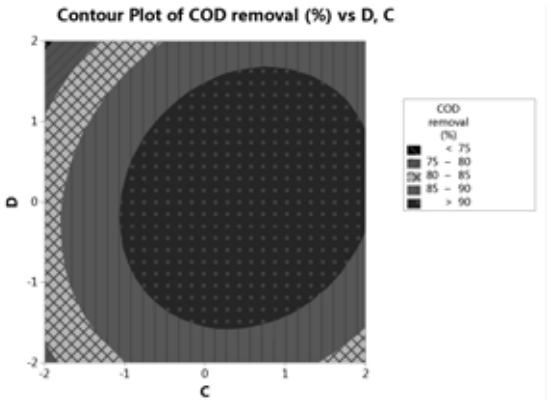

FIGURE 5
Contour plots for COD removal as a function of oxidant dose and catalyst quality

It is seen that in Fig.4 and Fig.5, COD removal increases when catalyst quality and oxidant dose increases. Au on Al_2O_3 catalyst shows good characteristics. The change is very significant, while the surface trend is steeper.

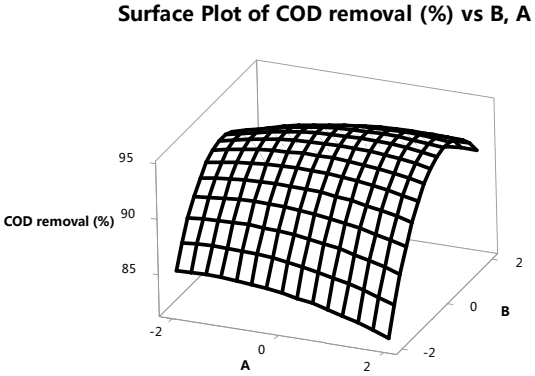

FIGURE 6
Response surface for COD removal as a function of reaction time and temperature

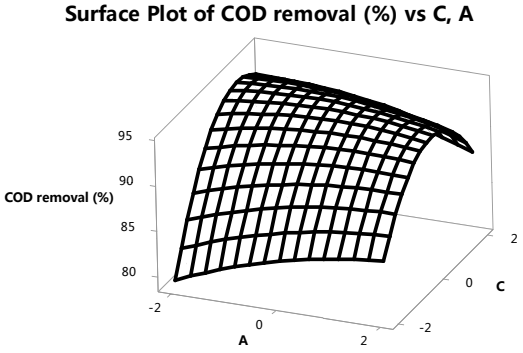

FIGURE 7
Response surface for COD removal as a function of temperature and catalyst quality

For Fig.6, it is seen that COD removal increases when reaction time increases. At this time, function of reaction time and temperature is weak. When reaction time is up to 90 min, temperature is 280°C, and COD removal is 94.03%.

From Fig.7, it is seen that COD removal increases when temperature increases. At this time, function of temperature and catalyst quality is strong. When temperature is rising from 260 to 340°C, catalyst quality is rising from 40 to 200 g, COD removal is rising from 80% to 95%.

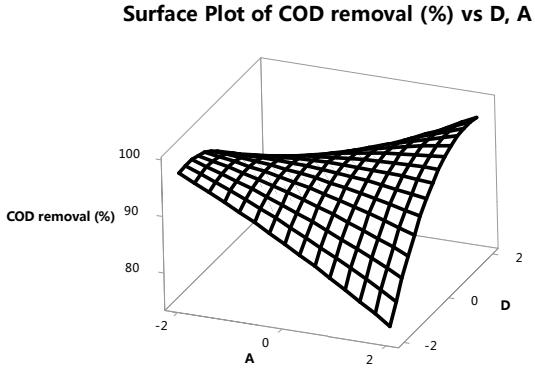

FIGURE 8
Response surface for COD removal as a function of temperature and oxidant dose

For Fig.8, COD removal is up to 98.37% when temperature is 260°C and oxidant dose is 100 g. COD removal increases when oxidant dose increases. At this time, oxidant dose plays a main role in increasing the COD removal.

CONCLUSIONS

In this paper, catalytic wet oxidation is adopted to treat oilfield wastewater. Central composite design (CCD), an experimental design for response surface methodology (RSM), was used to create a set of 30 experimental runs needed for optimizing of the operating conditions. Temperature, catalyst quality, reaction time and oxidant dosage are examined factors. The interaction was examined. The experimental results show that catalytic wet oxidation could effectively reduce COD removal by 98.37%. Au on Al_2O_3 catalyst shows good characteristics. Catalytic wet oxidation process is possibly suitable for a primary treatment for oilfield wastewater.

REFERENCES

[1] Feng, C.T., Wang, J. (2015) Treatment of Oily Wastewater via Supercritical Water Gasification (SCWG). Oxid Commun, 38(3), 1384.
[2] Zhang, L.S., Feng, Y., Li, G.H. (2015) Oily Wastewater Treatment via Alkali Catalytic Gasification.Oxid Commun, 38(3), 1401.
[3] Zhang, M., Zhao, B.L., Hu, L., Li, T.T., Qiang, X.L. (2016) Recent Advances in Oily Wastewater Treatment. Oxid Commun, 39(4), 3415.
[4] Cheng, Y., Guo Y. (2016) Efficient Degradation of High Concentration Oily Wastewater by Metal-organic Framework. Oxid Commun, 39(4), 3424.
[5] Xu, J., Li, S. (2016) Catalytic Properties of Ti/CeO2 on Oily Wastewater Treatment via Supercritical Water Gasification. Oxid Commun, 39(4), 3430.
[6] Mo, Z., Hu, S., Hu D. (2016) Study on Oily Wastewater Treatment via Catalytic Oxidation with Chlorine Dioxide Addition. Oxid Commun, 39(4), 3462.
[7] Li, P., Zhao, D., Zhang, Y., Sun, L., Zhang, H., Lian, M., Li, B. (2015) Oil-field wastewater treatment by hybrid membrane-aerated biofilm reactor (MABR) system. Chemical Engineering Journal, Volume 264, 595-602
[8] Guo, C., Chen, Y., Chen, J., Wang, X., Zhang, G., Wang, J., Cui, W., Zhang, Z. (2014) Combined hydrolysis acidification and bio-contact oxidation system with air-lift tubes and activated carbon bioreactor for oilfield wastewater treatment. Bioresource Technology, Volume 169, 630-636
[9] Hu, Y., Wang, D., Zhang, C., Wang, Z., Chen, M., Li, Y. (2013) An interval steady-state multimedia aquivalence (ISMA) model of the transport and fate of chloridion in a surface flow constructed wetland system treating oilfield wastewater in China. Ecological Engineering, Volume 51, 161-168
[10] Zha, S., Gusnawan, P., Zhang, G., Liu, N., Lee, R., Yu, J. (2016) Experimental study of PES/SiO2 based TFC hollow fiber membrane modules for oilfield produced water desalination with low-pressure nanofiltration process. Journal of Industrial and Engineering Chemistry, Volume 44, 118-125
[11] Moreira, F.C., Boaventura, R.A.R., Brillas, E., Vilar, V.J.P. (2017) Electrochemical advanced oxidation processes: A review on their application to synthetic and real wastewaters. Applied Catalysis B: Environmental, Volume 202, 217-261
[12] Jasim, S.Y., Saththasivam, J. (2017) Advanced oxidation processes to remove cyanotoxins in water. Desalination, Volume 406, Pages 83-87
[13] Tezcanlı Güyer, G., Nadeem, K., Dizge, N. (2016) Recycling of pad-batch washing textile wastewater through advanced oxidation processes and its reusability assessment for Turkish textile industry. Journal of Cleaner Production, Volume 139, 488-494
[14] Zhang, Y., Zhuang, Y., Geng, J., Ren, H., Xu, K., Ding, L. (2016) Reduction of antibiotic resistance genes in municipal wastewater effluent

by advanced oxidation processes. Science of The Total Environment, Volume 550, Pages 184-191

[15] Bethi, B., Sonawane, S.H., Bhanvase, B.A., Gumfekar, S.P. (2016) Nanomaterials-based advanced oxidation processes for wastewater treatment: A review. Chemical Engineering and Processing: Process Intensification, Volume 109, 178-189

[16] Marino, T., Molinari, R., García, H. (2013) Selectivity of gold nanoparticles on the photocatalytic activity of TiO2 for the hydroxylation of benzene by water. Catalysis Today, Volume 206, 40-45

[17] Carabineiro, S.A.C., Chen, X., Martynyuk, O., Bogdanchikova, N., Avalos-Borja, M., Pestryakov, A., Tavares, P.B., Órfão, J.J.M., Pereira, M.F.R., Figueiredo, J.L. (2015) Gold supported on metal oxides for volatile organic compounds total oxidation. Catalysis Today, Volume 244, 103-114

[18] Chang, Y.C., Chen, D.H. (2009) Catalytic reduction of 4-nitrophenol by magnetically recoverable Au nanocatalyst. J Hazard Mater. 165(1-3):664.

ACKNOWLEDGEMENTS

The authors are grateful for the financial support by Petro China Innovation Foundation (2016D-5007-0212), the University Sci-tech Innovation teams in Heilongjiang Province (2009td08) and Natural Science Foundation of China (51490650); Graduate Innovative research projects of Northeast Petroleum University (YJSCX2015-011NEPU)

Received: **02.04.2017**
Accepted: **11.07.2017**

CORRESPONDING AUTHOR

Zhan-dong Li
College of Petroleum Engineering Institute, Northeast Petroleum University, Daqing 163318, China

e-mail: lizhandong8888@outlook.com

© by PSP Volume 26 – No. 10/2017 pages 6004-6006 Fresenius Environmental Bulletin

STUDY ON ANTIBIOTIC WASTEWATER TREATMENT BY NEODYMIUM COORDINATION POLYMER CATALYST

Xu Jingyi*, Zhou Zipeng

Henan Polytechnic Institute, Nanyang 473009 P. R. China

ABSTRACT

In this paper, neodymium coordination polymer is prepared to treat antibiotic wastewater. Catalyst dose, hydrogen peroxide dose, temperature and other factors that affect the performance degradation of antibiotic wastewater is studied. The optimized conditions are present: temperature is 60°C, H_2O_2 dose is 1.25 mg/L, and catalyst amount is 300 mg.

KEYWORDS:
Antibiotic wastewater; catalytic oxidation; H_2O_2; Chemical oxygen demand (COD)

INTRODUCTION

Contemporary populations of enteric bacteria, when compared with those from the preantibiotic era, display a higher tolerance in their nonspecific responses to several antibiotics [1-3]. The increase in antimicrobial resistance, observed in a bacterial population, may result from the clonal selection of organisms that tolerate sublethal antimicrobial doses and that present greater fitness under conditions of selective pressure, or from the spreading of resistance genetic determinants through horizontal gene transfer. The most plausible hypothesis is that, in the natural environment, both mechanisms are responsible for the dynamics of the bacterial population. In different environments, bacteria are expected to experience distinct selective pressures for antibiotic resistance and, hence, distinct patterns of antibiotic resistance acquisition and evolution. Urban wastewater treatment plants represent important reservoirs of human and animal commensal bacteria in which antibiotic resistance determinants and/or organisms persist in the final effluent and are released to the environment [4-8]. More recently, neodymium (Nd) organic complexes and coordination polymers have shown interesting catalysis effect on some organic polymerisation reactions, which has subjected to further investigations [9-12]. This contribution deals with Nd coordination polymers with propionate and succinate ligands. A neodymium propionate complex with a one-dimensional (1D) structure has previously been reported [13].

In this study, antibiotic wastewater was treated by $Nd_2(C_3H_5O_2)_6(H_2O)_3 \cdot 3H_2O$ and hydrogen peroxide. The experimental results of antibiotic wastewater were treated by $Nd_2(C_3H_5O_2)_6(H_2O)_3 \cdot 3H_2O$ and hydrogen peroxide was reported. The feasibility of the technology as a pre-treatment to reduce toxic organic compounds was examined. The effects of the amount of catalyst, the amount of hydrogen peroxide and temperature on the removal efficiency of COD were investigated.

MATERIALS AND METHODS

Materials and reagents. Antibiotic wastewater used in this study was obtained from an antibiotic industry producing amoxicillin of Zhengzhou. The characteristics of antibiotic wastewater are summarized in Table 1.

TABLE 1
Characteristics of antibiotic wastewater

Parameter	Value
Amoxicillin (mg/L)	190
Chemical oxygen demand (COD) (mg/L)	860
Biochemical oxygen demand (BOD) (mg/L)	90
pH	6.7
Total phosphorus (TP) (mg/L)	10
Cl^- (mg/L)	12
Turbidity (NTU)	55
NO_3^-–N (mg/L)	9

Hydrogen peroxide (35% w/w) was purchased from Jilin, China.

Preparation of eodymium coordination polymer. $Nd_2(C_3H_5O_2)_6(H_2O)_3 \cdot 3H_2O$ was synthesized at room temperature by dissolving freshly prepared $Nd(OH)_3$ with propionic acid. Neodymium nitrate hexahydrate (0.88 g, 2.0 mmol) was dissolved in 10 mL deionized water. To the above solution, 2.0 mL concentrated ammonia solution was added to precipitate neodymium(III) ions as $Nd(OH)_3$. The precipitation was washed with deionized water for three times to remove the excess ammonia and then was dissolved in 2.0 mL of concentrated propionic acid and 10.0 mL of deionized water. Colorless crystalline product was formed in three weeks after slow evaporation with 86% yield. Formula: $C_{18}H_{42}O_{18}Nd_2$

(FW = 835.0), Anal. Calc. C, 25.88; H, 5.06. Found: C, 25.83; H, 5.13%.

RESULTS AND DISCUSSION

Effect of H_2O_2 dose on COD removal. The effect of concentration on antibiotic wastewater degradation within the range of hydrogen peroxide 0.5 mg/L-1.25 mg/L is investigated. The result is presented in Fig. 1. As can be seen in Fig. 2, adding H_2O_2 can increase COD removal. H_2O_2 displayed high oxidation activity in the antibiotic wastewater treatment. 92% of COD was removed when H_2O_2 dose was 1.25 mg/L.

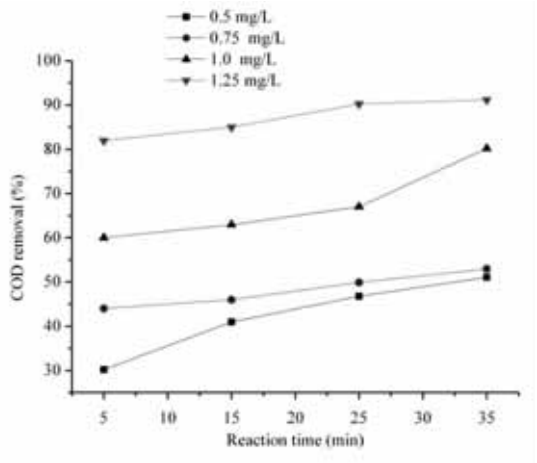

FIGURE1
Effect of H_2O_2 dose on COD removal

Effect of temperature on COD removal. Fig. 2 showed COD removal in the antibiotic wastewater degradation at temperature of 30-60°C. Approximately COD removal is 96% (Fig. 2), adding H_2O_2 and $Nd_2(C_3H_5O_2)_6(H_2O)_3$•$3H_2O$ after 40 min reaction.

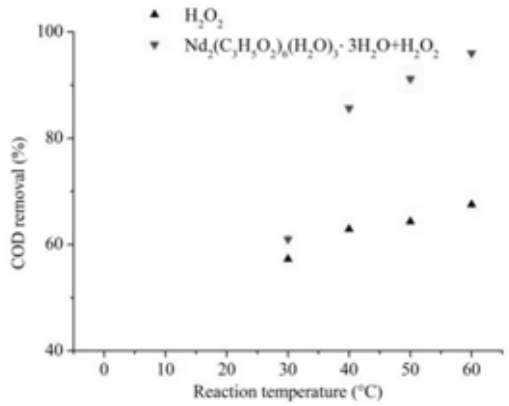

FIGURE 2
Effect of temperature **on COD removal**

Effect of catalyst on COD removal. The results are presented in Fig. 3. As it is expected, rising catalyst dose can increase COD removal. COD removal reached 96% after 40 min at 60°C. Therefore, catalyst had a significant impact on the oxidation of antibiotic wastewater.

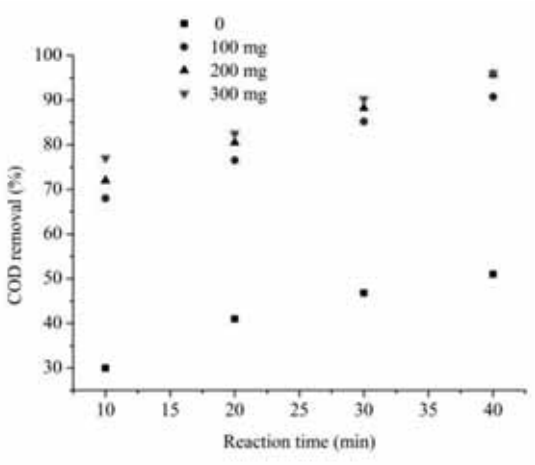

FIGURE 3
Effect of catalyst dose on COD removal

CONCLUSIONS

In conclusion, we reported a novel neodymium coordination polymer $Nd_2(C_3H_5O_2)_6(H_2O)_3$• $3H_2O$ was synthesized with propionate. Furthermore, it is used to treat antibiotic wastewater, knowledge of the impact of the operating conditions such as the amount of catalyst, H_2O_2 dosage, temperature is required. Experimental results indicated that 96% COD was removed after 40 min reaction. Adding a catalyst significantly improved the COD removal.

REFERENCES

[1] Wang, G.P., Zhang, X. and Si, G.C. (2015) Antibiotic Wastewater Treatment via Advanced Oxidation Process. Oxid Commun 38, 1436-1442.

[2] Yang, R.H. and Zhu, J.Z. (2017) The Preparation If Fe-Al-C Mico-Electrolysis Filler And Coupling With H_2o_2 For Treatment Sf Methyl Orange Simulated Wastewater. Fresen. Environ. Bull. 26, 2486-2494.

[3] Yang, K., Guo, J.W., Liao, Y., Liu, H. and Wang, Y. (2017) Optimization Of Photo-Fenton Process With Diatomite -Supported Alpha-Fe2o3 For Treatment Of Dimethyl Phthalate Using Response Surface Methodology. Fresen. Environ. Bull. 26, 1477-1484.

[4] Vaizogullar, A.I., Ugurlu, M., Ayyildiz, A., Yilmaz, S.I. and Chaudhary, A.J. (2017) TiO_2, WO_3, AND V_2O_5, Supported On Activated Carbon: Preparation, Structural And Catalytic Behaviour In Photocatalytic Treatment Of Phenol And Lignin From Olive Mill Wastewater.

Fresen. Environ. Bull. 26, 3529-3541.
[5] Stenstrom, T.A., Okoh, A.I. and Adegoke, A.A. (2016) Antibiogram Of Environmental Isolates Of Acinetobacter Calcoaceticus From Nkonkobe Municipality, South Africa. Fresen. Environ. Bull. 25, 3059-3065.
[6] Lévesque, C., Piché, L., Larose, C. And Roy, P.H. (1995) PCR Mapping of Integrons Reveals Several Novel Combinations of Resistance Genes. Antimicrob Agents Chemother 39, 185-191.
[7] Elmolla, E.S. and Chaudhuri, M. (2012) The Feasibility of Using Combined Fenton-SBR for Antibiotic Wastewater Treatment. Desalination 285, 14-21.
[8] Behera, S.K., Kim, H.W., Oh, J.E. And Park, H.S. (2011) Occurrence and Removal of Antibiotics, Hormones and Several Other Pharmaceuticals in Wastewater Treatment Plants of The Largest Industrial City of Korea. Sci Total Environ 409, 4351-4360.
[9] Scales, N., Zhang, Y.J., Bhadbhade, M., Karatchevtseva, I., Kong, L.G., Lumpkin, G.R. And Li, F. (2015) Neodymium Coordination Polymers with Propionate, Succinate and Mixed Succinate–oxalate Ligands: Synthesis, Structures and Spectroscopic Characterization. Polyhedron 102, 130-136.
[10] Yuan, L.F., Li, J., Liu, R.P., Liu, B., Guo, H. And Zhang, F.X. (2013) A Novel 2D Sandwich Layered Neodymium Coordination Polymer Based on 2,2′-bipyridyl-4,4′-dicarboxylate Ligand. Inorganica Chimica Acta 404, 197-200.
[11] Nicholls, J.L., Bacsa, J. And Fogg, A.M. (2010) Synthesis and Crystal Structure of A Neodymium Coordination Polymer with 2,6-anthraquinonedisulfonate. Particuology, 8, 221-224.
[12] Wei, P.R., Wu, D.D., Zhou, Z.Y., Li, S.L. And Mak, T.C.W. (1997) Lanthanide Coordination Polymers with Dicarboxylate-like Ligands: crystal structures of polymeric neodymium(III) and erbium(III) complexes with flexible double betaines. Polyhedron 16, 749-763.
[13] Yang, L.R., Liu, L., Wu, L.Z., Xu, Z.H. And Wang, L.C. (2014) Isomorphous and Isostructural Lanthanide Coordination Polymers Based on 2-(4-chlorobenzoyl) Benzoic Acid: Synthesis, Structure, Characterization, and Luminescent Properties. Dyes Pigments 111, 176-184.

Received: **03.04.2017**
Accepted: **11.07.2017**

CORRESPONDING AUTHOR

Xu Jingyi
Henan Polytechnic Institute, Nanyang 473009 P. R. China

e-mail: 2402065969@qq.com

© by PSP Volume 26 – No. 10/2017 pages 6007-6016 Fresenius Environmental Bulletin

THE EFFECTS OF LAND USE CHANGE ON SOIL LOSS AND CARBON STOCK AMOUNTS

Sezgin Hacisalihoglu*, Mehmet Misir, Nuray Misir, Zafer Yucesan, Ercan Oktan, Selcuk Gumus, Ugur Kezik

Karadeniz Technical University, Faculty of Forestry, 61080 Trabzon, Turkey

ABSTRACT

Owing to the land use change, vegetation cover, ecosystem functions and soil properties are affected and changing. Such a change on the land use forms is also the fact in this study area. The main purpose in this study was to determine the effects of land use change on the soil properties, soil loss and carbon stock. As a result, the land use change caused significant (P<0.001) alteration in soil loss (0.6 t/ha/yr in forest, 3.6 t/ha/yr in pasture). Soil carbon (150.4 t/ha in pasture, 174.3 t/ha in forest) and total carbon stock amounts (151.1 t/ha in pasture, 202.4 t/ha in forest) have also changed significantly (P<0.001). As well as soil organic matter, pH and EC in forest were found significantly different (P<0.01) in land use groups. According to the land use scenario which was established by utilizing the average values obtained in the research, it is expected that there will be about 2.1 t/ha/yr of soil loss amount per year in this area and about 15% of this is caused from the forest area and about 85% from the pasture. In other words, the effect of pasture lands on total soil loss is about 6 times higher than the forest lands.

KEYWORDS:
Land use change, Soil loss, Carbon stock, Oriental beech

INTRODUCTION

The war between man and the natural environment, under various land use, continues without losing momentum. Environmental problems have increased due to the urbanization in parallel with the development of the industry and technology [1, 2]. At the forefront of today's most important environmental problems are the global warming, climate change and land degradation [3,4]. These problems are significantly affected by the land use [5, 6]. Therefore, the concept of land use change is vital in environmental and ecological assessments [7, 8].

The land use term is mostly expressed by human activities and it is at the center of ecosystem function and dynamics [9]. The ecological, sociological and economic structure of a region is the most important parameter that determines the land use and its affects [10, 11]. There is a strong relationship between land use pattern and vegetation type and soil fertility, erosion sensitivity, carbon binding potential and other soil characteristics [12, 6, 13, 14, 15, 16].

Soil which is classified as non-renewable natural resource, can heal itself over time [17, 18]. Conversion of agricultural land to pastureland or open areas into forests in a basin also increases soil and water quality [19]. Natural transition process and plantation activities play an important role in improving the area where land use changed. It has been determined that positive changes in soil quality indicators (bulk density, aggregate stability, organic matter content) increased with the abandonment of an active farming area to its natural state [20].

Carbon stock potential of the soils has also an important effect on environmental problems [21]. It is also an important parameter in reducing the soil loss [22]. Soil erosion is also considered as a variable of determining land use change [23]. Generally, under the same ecological conditions, annual soil loss in a hectare is expected to be highest in the treated agricultural land, then in the pasture, and at least in the forested area, depending on the plant cover. A land, used as a pasture, can be turned into a forest area after years if the ecological conditions are suitable. This may increase the carbon-binding potential and reduce the susceptibility of the soils to erosion [24]. By the plantation efforts, carbon stock of the soils can be increased and soil erosion can be reduced. The physical, chemical and biological properties of the soils may be changed in a positive way by planting a damaged area with conifer species. In this way, the carbon stock potential can be increased and the susceptibility to soil erosion can also be reduced [25].

There have been major changes on the land use forms from past to present in Turkey. Despite the increase in forest area, half of them are considered as unproductive due to degradation caused by human activities such as illegal cutting, grazing and unplanned using for many years. This study was carried out to understand and determine the situation in the study area. The study area where the study took place was used as a cropland until 1970s. With time, with the loss of the fertility, the croplands have been abandoned, some of which have been turned into pasture

and some of which have been turned into forest (with the plantation studies in the 1980s). The main purpose of this research is to determine the effects of the land use change on the basic soil properties, soil loss amounts and carbon stock amounts.

MATERIALS AND METHODS

Study area. The study area is placed in the Middle Eastern Black Sea Region of Turkey in the village Goksu Unye, Ordu (40°53`36" N - 36°57`77" E, Elevation: between 1200 m - 1300 m asl) (Figure 1). The main aspect of the study areas is shady and study areas extend in the north to northeast aspect direction.

There are two different land use types in the study area (Figure 2). The main tree species in the forested (which have been planted in 1970s and are about 35-45 years old nowadays) area is the oriental beech (*Fagus orientalis* Lipsky.) and there are also pasture areas which are mostly over grazed and unfavorable.

The study area is located within the *Fagetum* zone according to Mayr's forest zone [26] classification. The indicator tree of this zone is the *Fagus orientalis* Lipsky. (Oriental beech) which is spread out mostly in Caucasus, Northern Iran, Turkey and North-East Europe. In Turkey, it stretches from the Istranca mountains in the west to the Georgia border in the east in a narrow and expanding belt and is usually located between 0 to 1800 m above the sea level.

Climate data (1970-2015) was obtained from the nearest meteorological station (Unye) to the study area. This data was interpolated into the study area conditions [27] and a climate diagram was created according to Walter [28]. In accordance with Walter climate diagram, the study area is related to the humid oceanic climate type. There is no water shortage in the environment and no dry period is observed throughout the year (Figure 3). In addition, the study area is "semi-humid" according to De Martonne [29] climate classification and is in “B3 Humid” climate type according to Thornthwaite [30].

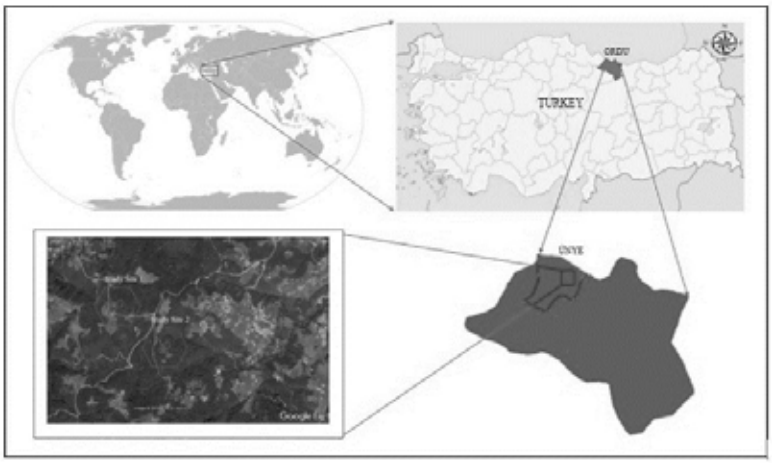

FIGURE 1
Study area and study sites.

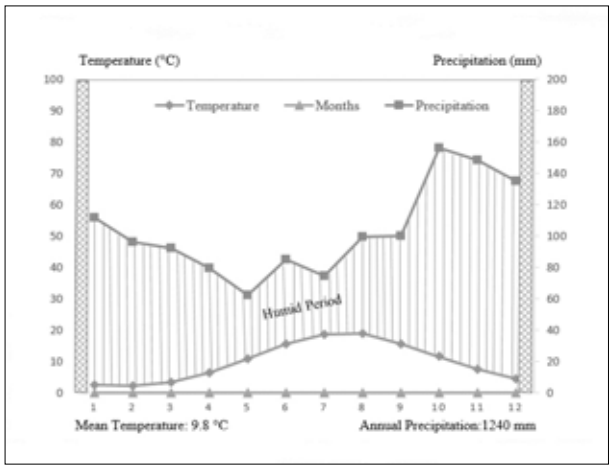

FIGURE 3
Walter climate diagram of the research area.

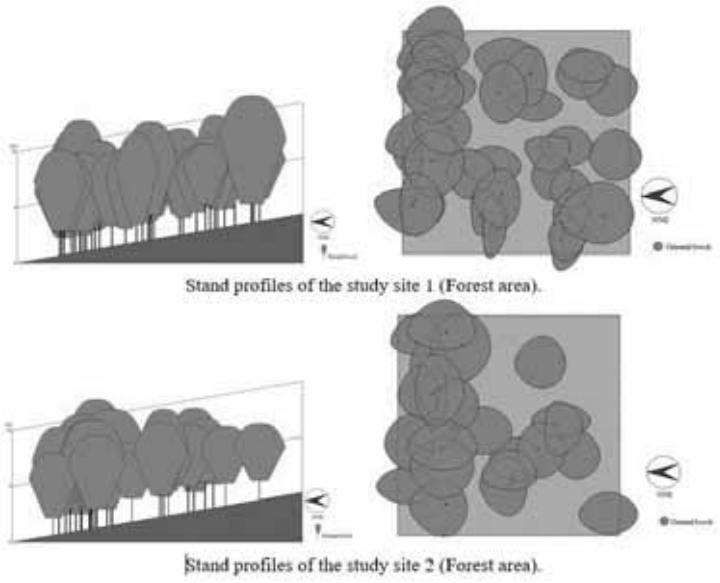

FIGURE 4
Stand structures of the study sites.

The topography in the research area is usually rough terrain where the hilly terrain changes frequently. Especially in the south of the study area are extremely steep slopes. Geological characteristics of the study area and its surroundings are represented by volcanic and sedimentary rocks of the middle - upper Eocene, and clastics and carbonates [31].

Data collection. Stand Structure. The stand profiles taken from forested area were determined and painted by using the "ARGUS Forstplanung" simulation program [32]. Vertical stand profiles were used to determine the canopy closure in each sample plot (20 m x 20 m). Slope, aspect, distribution of trees in the coordinate axis (x, y), diameter at breast height (*DBH*), tree height, crown width and living crown height were measured in sampling plots to quantify canopy closure. Height characteristics were measured with Vertex Forester device. All trees were classified as either dominant or suppressed trees using the classification of IUFRO [33].

Canopy closure was about 70-80 % and more homogenous in the study site 1 (Figure 4). However, the percentage of gaps in the canopy is much higher in study site 2 than study site 1. Canopy closure was about 50-60 % in study site 2 (Figure 4). Mean *DBH* was 11.8 cm in study site 1 and 12.0 cm in study site 2. Both trees in two sample stands were of >8 cm *DBH*. So, sample stands had entered to pole stage with *DBH* values ranging from 8.0 to 19.9 cm.

Soil Sampling. Two study sites were identified in the study area (Figure 1). Both study sites were

divided into two different types of land use including forest and pasture. Two sample plots (55m x 55 m) were taken from each study site (one in the forest and one in the pasture). Two soil profiles were opened in each sample plots (two in the forest and two in the pasture). In this way, totally 8 soil profiles were opened and 40 soil samples were taken and pooled in every plot from 5 different soil depth stages for further analysis. Physical, chemical and hydrological analyses were carried out on each soil sample in the laboratory.

Altitude above sea level (asl) was assessed with an altimeter and the bedrock was derived from the existing geological maps [31]. Landscape position, surface roughness and landform were recorded at sight. Surface stoniness (%), slope (%), aggregate classes etc. were assessed in each study site respectively according to [34]. The slope exposition, measured in degrees relative to N with a compass. Permeability and the other hydraulic soil specifications were determined according to Saxton et al. [35]. Soil depth was measured in each soil profile. Soil texture according to Bouyoucos hydrometer method [36] and organic matter content depend on Walkley-Black wet oxidation method [37] were determined in the laboratory.

Soil Loss Predicting with the ABAG (Allgemeine Boden Abtrags Gleichung). *ABAG* is the international version (where the values are turned in to metric system and adapted to the European conditions) of the simulation model *USLE* (Universal Soil Loss Equation) [38] used to determine the soil loss amounts according to Schwertmann et al. [39].

Most of the erosion assessments performed in North America and around the world during the past two decades have used the USLE. This model was derived empirically from approximately 10,000 plot-years of data [38] and may be used to calculate erosion at any point in a watershed that experiences net erosion. The USLE is written as follows (1):

$$A = R \times K \times L \times S \times C \times P \quad (1)$$

where A is the average annual soil loss (t/ha per year), R the rainfall erosivity factor, K the soil erodibility factor, L the slope length factor, S the slope steepness factor, C the cover management factor and P is the supporting practice factor. Climate erosivity is represented by R and can be estimated from the rainfall intensity and amounts data which were taken from Dogan and Gücer [40]. The soil erodibility monograph has been used to predict the K value [39]. The topography and hydrology effects on soil loss are characterized by the L and S factors. For direct USLE applications, a combined LS factor was evaluated for each land cell [38]. Land use and management are represented by P and can, with some difficulty, be inferred using remote sensing combined with ground-trusting.

Carbon Stock. Two sample plots (each plot (20x20 m) within the soil sample plots (55 m X 55 m) covers an area of 400 m^2) were taken from planted oriental beech stands in each study site. Two woody debris quadrats (1x1 m) were randomly located within both forest and pasture areas in each study site. Species type and diameter at breast height (*DBH*) were recorded for every living tree (*DBH* ≥8 cm, height ≥1.3 m) in sample plots. It was also planned to measure tree height and *DBH* of every dead standing tree (*DBH*≥5 cm, height ≥1.3 m) within the sample plots. But there was no standing dead tree in sample plots. In each quadrat (1x1 m), all plants including seedlings (height ≤1.3 m), saplings, shrubs, herbs and woody species were destructively harvested. In destructive sampling, the vegetation in each area is cut and weighed (fresh weight), and subsamples of parts of the vegetation are taken, weighed fresh in the field, and weighed again after oven-drying. Biomass of each ground vegetation component was oven-dried during 72 h at 65 °C, to calculate dry biomass and carbon content on an area basis.

In each sample plot, four samples of litter, consisting of leaves, fruits, buds, barks, branches and twigs (*DBH*<1cm) were sampled using 25 cm x 25 cm metal quadrats. The four quadrats were systematically distributed in each 400 m^2 plot. All material of litter was collected inside the quadrats. To minimize contamination with mineral soil, the samples were soaked and washed in water. All components of litter were oven-dried during 48 h at 65°C and weighed, analyzed for carbon content.

To estimate belowground biomass and carbon stock we used the roots directly measured in sample plots. The roots were separated in three groups (fine, small and coarse). The carbon stock of fine (0-2 mm), small (2-5 mm) and coarse (5< mm) roots were assessed in two soil profiles plots. The roots were separated from the soil by soaking in water and then gently washing them over a series of sieves with mesh sizes of 2 and 5 mm. The roots were sorted into diameter classes 0-2 mm, 2-5 mm and 5 mm < root classes. The roots from each sizes category were oven-dried at 65 °C for 24 h, weighed, analyzed for carbon content.

The carbon stock was estimated for living trees, woody debris, roots and litter in forested area. The living tree biomass C stock was obtained directly using algorithmic C equation for oriental beech [41] (2).

$$LTC = 0.025672 \times DBH^{2.775} \quad (2)$$

In the equation *LTC* is living tree carbon stock and *DBH* is diameter at breast height (cm). Soil carbon stock expressed in t ha^{-1} were calculated for the soil depth intervals 0–10 cm, 10–30 cm, 30-60 cm, 60-90 cm and 90–120 cm. Soil organic carbon stock (SOCS) was computed as the product of three variables, BD, soil sampling depth (cm) and carbon concentration (C%) calculated as a function of OM (%).

SOCS (t ha^{-1}) was estimated as follows (3, 4):

$$C\ \% = 0.58 \times OM \quad (3)$$

and

$$SOCS = BD \times C\ \% \times D \quad (4)$$

In the equation *OM* is organic matter, *BD* is soil bulk density (g cm^{-3}), and *D* is soil sampling depth (cm) [42].

Statistical methods. Associations among the variables were analyzed. The compatibility with normal distribution of all variables analyzed was evaluated using the Kolmogorov–Smirnov test. Results are expressed as means ± SD (Standard deviation). Statistical analyses were performed with SPSS version 23.0 software package [43]. Differences between groups were established by Student's *t* -test for normally distributed values and by Mann-Whitney *U*-test for nonparametric values. Pearson's correlation coefficient was searched to examine the relation between normally distributed variables. Spearman's correlation coefficient was used for non-normally distributed values. Statistical significance was defined as *P* was <0.05.

RESULTS AND DISCUSSION

Many different variables have been measured and determined to obtain the requirements of the used soil loss predicting model, the carbon stock and stand structure profiles.

The negative effects of the human activities on the soil loss event [44, 45] are also effective in the study area. According to the measurement results the average slope is about 19 % in the sample plots. It is well known that a positive and strong correlation exists between the slope gradient, slope length and soil loss [38, 46, 47].

Soil hydro-physical properties including soil texture (sand, silt, clay), permeability, bulk density and surface stoniness were found non-significant between forest and pasture area (P>0.05). However, organic matter, electrical conductivity (EC) and soil acidity pH were statically significant (P<0.01). In addition, some important soil function indicators like soil loss, soil carbon and total carbon were found statistically significant among the groups (Table 1, Figure 5). In other words, according to the results, there is a significant statistical relationship (P <0.001) between the soil carbon stock and total carbon stock due to land use. There is also a significant statistical relationship (P <0.001) between the soil loss and land use (Table 1).

There is also a significant negative correlation between the predicted soil loss amounts and organic matter content in the study area (r= - 0.88, P<0.01, A3). Organic matter contents of the sampled soils are in average 2.5 % in forest land and 2.2 % in pasture land (Table 1). It is known that organic matter content of the top soils has a very positive effect on the physical, chemical, hydrological soil characteristics. There is also a positive relation with the organic matter content and soil and total carbon stock (r=0.976 and r=0.981, P<0.001) respectively.

Predicted soil loss amounts in the study are in average 0.6 t/ha/yr in forest land and 3.6 t/ha/yr in pasture land (Table 1, Figure 5). Erskine et al. [48] determined close soil loss values (3.3 t/ha/yr in pasture area and 7.1 t/ha/yr in agricultural area) in their study. Mahmoudzadeh et al. [49] have also reported the soil loss amounts in their study as 3.1 t/ha/yr in agricultural land, 2.2 t/ha/yr in pasture land and 0.8 t/ha/yr in forest land.

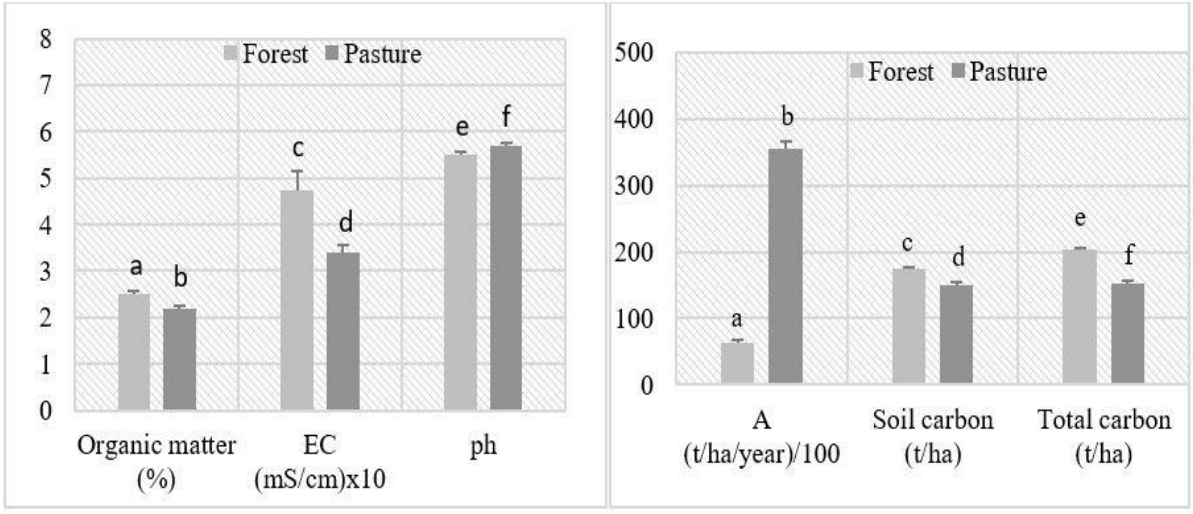

FIGURE 5
Some soil characteristics according to the land use groups.

TABLE 1
Average values of some soil characteristics according to land use groups (n=8, mean ± SD).

Variables	Forest	Pasture	P value
Sand (%)	55.1±6.8	53.3±8.0	*NS*
Silt (%)	20.5±1.1	23.9±3.0	*NS*
Clay (%)	24.3±6.1	22.8±5.0	*NS*
Organic Matter (%)	2.5±0.1	2.2±0.1	*P*<0.001
EC (mS/cm)	47.3±4.2	33.9±1.8	*P*<0.01
pH (H_2O)	5.5±0.1	5.7±0.1	*P*<0.01
Permeability (cm/hr)	19.7±7.8	19.1±8.3	*NS*
Bulk Density (gr/cm^3)	1.5±0.03	1.4±0.01	*NS*
Surface Stoniness (%)	44.5±8.1	49.9±2.9	*NS*
A (t/ha/year)	0.6±0.1	3.6±0.1	*P*<0.001
Soil C (t/ha)	174.3±2.0	150.4±4.9	*P*<0.001
Total C (t/ha)	202.4±2.9	151.1±4.9	*P*<0.001

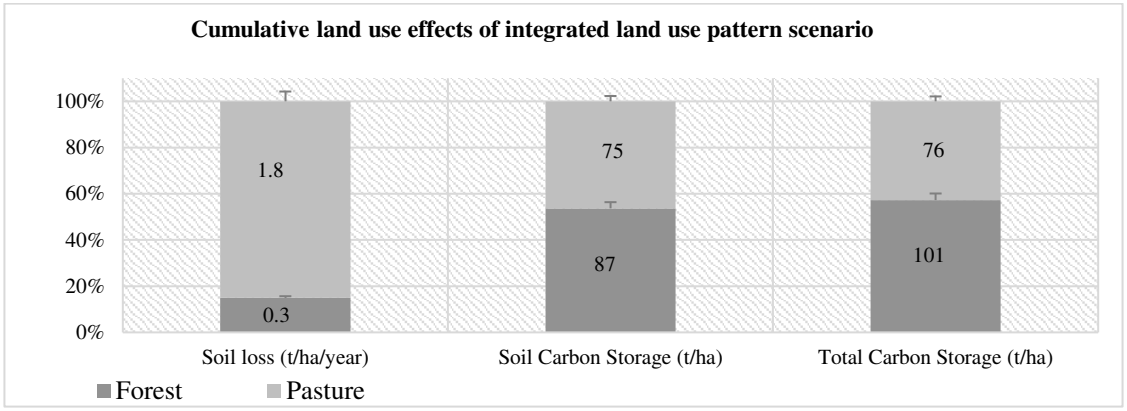

FIGURE 6
The amount of soil loss, soil carbon and total carbon in 1 hectare integrated land.

TABLE 2
The parameters used in the scenario.

Land use	Forest (0.5 ha) (1)	Pasture (0.5 ha) (2)	∑ (1.0 ha) (1+2)	Forest effects (%)	Pasture effects (%)
Soil loss (t/ha/year)	0.3	1.8	2.1	15	85
Soil Carbon Stock (t/ha)	87	75	162	54	46
Total Carbon Stock (t/ha)	101	76	177	57	43

The soil loss values in forest lands in the study area are quite low beside the values in pasture lands. But the average soil loss amounts in the forest lands are higher than expected [46, 50]. The predicted soil loss in forest area is negligible erosion in terms of soil erosion sensitivity classes [51].

These values indicate that the ecological conditions will turn in to natural structure in the forest lands, in time. But it is not the fact in pasture lands, because of the over grazing and non-protective soil loss trends which also affects the land use and plant cover. Golosov et al. [52] reported that the soil loss amounts decreased 3.2 t/ha/yr in the forests lands and increased 0.7 t/ha/yr in pasture lands in a period of 32 years.

It is determined in this study that the soil carbon stock amounts in the forest lands are in average 174.3 t/ha and 150.4 t/ha in pasture lands (Table 1, Figure 5). Wasak and Drewnik [53] found the soil organic carbon stock values are 63.5 t/ha in a forest area and 47.5 t/ha in a pasture area.

It is known that soils represent the most important long-term organic carbon (OC) reservoir which is mostly based on the organic matter [54,55]. The results in this study confirm this knowledge (Table 1). Total carbon stock (soil + biomass) is higher in the forest lands and lower in pasture lands as expected. This situation in the pasture lands is because of the very low biomass.

An integrated land use scenario was established by utilizing the average values obtained in the research (Table 1, Figure 5). In this scenario (totally 1 ha), it is assumed that 50% of the area is pasture and 50% is forest (Table 2).

In this case, it is expected that there will be about 2.1 tons of soil loss per year in this area (Table 2). It is observed that about 15% of this soil loss amount is coming from the forest area and about 85% from the pasture. In other words, the effect of pasture lands on total soil loss is about 6 times higher than the forest lands (1.8 / 0.3) (Figure 6). Erskine et al. [48] was pointed that soil loss in pasture lands is 3-5 times higher than in forest lands.

In such an area, the amount of carbon stock in the soils is about 162 t/ha, while the total carbon stock amount (soil + biomass) is 177 t / ha. The effect of forest area on soil carbon storage is 54% (87 t / ha) whereas the effect of pasture is 46% (75 t /ha). Similarly, the total carbon storage effect of the forest land is 57% (101 t/ha), while the pasture land effect is 43% (76 t/ha) (Figure 6). This difference can be explained by the scarcity of biomass.

CONCLUSIONS

In this study, it has been found that soil loss by erosion, soil carbon stock and total carbon stock in a unit area are significantly affected by vegetation cover depending on land use change. And there is a trend of positive change in soil characteristics in areas converted into forest by plantation. Previous studies have reported that the soil loss amount by erosion in forest area tends to decrease over time while reverse trend exist in pasture and open areas [52]. This indicates that, in the long run, soil quality increases in the forest area and will may decrease in the pasture area.

Land use and soil characteristics are the main factors determining and affecting soil loss by erosion. However, rainfall regime included climatic factors is the most important parameter that is effective in soil loss in hilly areas. In addition, in this study, soil organic matter, soil acidity and electrical conductivity were significantly affected by changes in the amount of plant biomass in the unit area, while no significant change in the basic hydro-physical properties of the soil was observed due to land use over a period of 30-40 years. Soil organic matter, soil acidity and electrical conductivity are classified into important soil quality indicators [56]. Therefore, in the coming period, it is obvious that the quality of the forest land in this region will increase further. And according to created scenario, it is observed that differences in soil loss and organic matter accumulation is due to the litter and plant cover in the forest area. This effect is at the lowest level in pasture areas that are open to excessive and irregular grazing.

As a result, the process of healing is continuing in these areas, which were used for agricultural purposes until 1970s and then abandoned (some of them have been turned into the pasture and some have been turned into forest by plantation). The recovery process in forest areas is progressing much faster. Especially soil loss and total carbon storage values support this result. This process is progressing more slowly in pasture areas. It is considered that the improvement process in these areas will accelerate the recovery process.

ACKNOWLEDGEMENTS

This study was investigated with the transportation support of the Unye Forest Directorate and with the technical and laboratory support of the Karadeniz Technical University Faculty of Forestry. A special thanks to Hasan Fahri Gunkur for their efforts in the land and laboratory works.

APPENDIX

TABLE 3
Correlations between some variables.

Soil Characteristics	Sand (%)	Silt (%)	Clay (%)	Organic Matter (%)	EC (Ms/cm)	pH
Sand (%)	*					
Silt (%)	-0.810*	*				
Clay (%)	-0.714*	0.262*NS*	*			
Organic Matter (%)	-0.095 *NS*	-0.381*NS*	0.619*NS*	*		
EC (Ms/cm)	-0.476 *NS*	-0.833*	0.119*NS*	0.786*	*	
pH	-0048 *NS*	0.524 *NS*	-0.643*NS*	-0.881**	-0.762*	*
Permeability (cm/hr)	0.976***	-0.690*NS*	-0.762*	-0.167 *NS*	0.357*NS*	0.047 *NS*
Bulk Density (gr/cm^3)	0.903 **	-0.638*NS*	-0.861**	0.157 *NS*	0.347*NS*	0.009 *NS*
Surface Stoniness (%)	-0.723*	0.552 *NS*	0.667 *NS*	-0.317 *NS*	-0.333 *NS*	0.160 *NS*
A (t/ha/yr)	0.238 *NS*	0.333 *NS*	-0.762*	-0.880**	-0.643*NS*	0.857**
Soil C (t/ha)	0.138 *NS*	-0.564*NS*	0.115*NS*	0.976***	0.786*	-0.838 **
Total C (t/ha)	0.157 *NS*	-0.618*NS*	0.119*NS*	0.981***	0.786*	-0.861**

Soil Characteristics	Permeability (cm/hr)	Bulk Density (gr/cm^3)	Surface Stoniness (%)	A (t/ha/yr)	Soil C (t/ha)	Total C (t/ha)
Sand (%)						

Silt (%)						
Clay (%)						
Organic Matter (%)						
EC (Ms/cm)						
pH						
Permeability (cm/hr)	*					
Bulk Density (gr/cm^3)	0.902 **	*				
Surface Stoniness (%)	-0.711*	-0.883**	*			
A (t/ha/yr)	0.357 *NS*	0.252 *NS*	-0.119 *NS*	*		
Soil C (t/ha)	0.066 *NS*	0.331*NS*	-0.458*NS*	-0.690*	*	
Total C (t/ha)	0.075 *NS*	0.327 *NS*	-0.481 *NS*	-0.690 *	0.991 ***	*

NS: Correlation is non-significant., *****: Correlation is significant at the 0.05 level, ******: Correlation is significant at the 0.01 level, *******: Correlation is significant at the 0.001 level.

REFERENCES

[1] Shankar, B.S., Balasubramanya, N. and Maruthesha, R.M. T. (2008) Impact of industrialization on groundwater quality – a case study of Peenya industrial area, Bangalore, India. Environ Monit Assess. 142, 263-268.

[2] Ejaro, S.P. and Abdullahi, U. (2013). Spatio-temporal Analyses of Land Use and Land Cover Changes in Suleja Local Government Area, Niger State, Nigeria. Journal of Environment and Earth Science. 3(9), 72-83.

[3] Costanza, R. and Jorgensen, S.E. (2002) Understanding and Solving Environmental Problems in the 21st Century. Elsevier, First edition. ISBN: 0-08-044111-4.

[4] IUCN (International Union for Conservation of Nature). (2015) Land Degradation and Climate Change The multiple benefits of sustainable land management in the drylands. Technical Reports. CH-1196 Gland, Switzerland.

[5] Wu, J. (2008) Land Use Changes: Economic, Social, and Environmental Impacts. Agricultural & Applied Economics Association. JEL Classifications: Q24, Q28. Choices and the Agricultural& Applied Economics Association.

[6] Li, L., Wang, Y. and Liu, C. (2014) Effects of land use changes on soil erosion in a fast-developing area. Int. J. Environ. Sci. Technol. 11, 1549-1562.

[7] Wu, S., Mickley, L.J., Kaplan, J.O. and Jacob, D.J. (2012) Impacts of changes in land use and land cover on atmospheric chemistry and air quality over the 21st century. Atmos. Chem. Phys., 12, 1597-1609.

[8] Uriarte, M., Rivera, L.W., Zimmerman, J.K., Aide, T.M., Power, A.G. and Flecker, A.S. (2004) Effects of land use history on hurricane damage and recovery in a neotropical Forest. Plant Ecology 174: 49-58.

[9] DeFries, R.S., Asner, G.P. and Houghton, R. (2004) Trade-offs in Land-Use Decisions: Towards a Framework for Assessing Multiple Ecosystem Responses to Land-Use Change (pp. 1-9). American Geophysical Union.

[10] Axinn, W.G. and Ghimire, D.J. (2011) Social Organization, Population, and Land Use. AJS. July; 117(1), 209–258.

[11] Fu, B; Zhang, L., Xu, Z., Zhao, Y., Wei, Y. and Skinner, D. (2015) Ecosystem services in changing land use. J Soils Sediments.15, 833–843.

[12] Sariyildiz, T., Savaci, G. and Kravkaz, I.S. (2015) Effects of tree species, stand age and land-use change on soil Carbon and nitrogen stock rates in northwestern Turkey. iForest 9: 165-170.

[13] Lech-hab, K.B.H., Issa, L.K., Raissouni, A., Arrim, A.E., Tribak, A.A. and Moussadek, R. (2015) Effects of Vegetation Cover and Land Use Changes on Soil Erosion in Kalaya Watershed (North Western Morocco). International Journal of Geosciences, 6, 1353-1366.

[14] Meng, H.Q., Fu, B.J. and Yang, L.Z. (2001) Effects of land use on soil erosion and nutrient loss in the Three Gorges Reservoir Area, China. Soil and Management.17, 288-291.

[15] Twesigye, C.K., Onywere, S.M., Getenga, Z.M., Mwakalila, S.S. and Nakiranda, J.K. (2011) The Impact of Land Use Activities on Vegetation Cover and Water Quality in the Lake Victoria Watershed. The Open Environmental Engineering Journal, 4, 66-77.

[16] Schoenholtz, S.H., Van Miegroet, H., and Bruger, J.A. (2000) A review of chemical and physical properties as indicators of forest soil quality: challenges and opportunities, For. Ecol. Manage., 138, 335-356.

[17] Aide, T.M., Zimmerman, J.K., Herrera, L., Rosario, M. and Serrano, M. (1995) Forest recovery in abandoned tropical pastures in Puerto Rico. Forest Ecology and Management 77, 77-86.

[18] Benayas, J.M.R, Martins, A., Nicolau, J.M. and Schulz, J.J. (2007) Abandonment of agricultural land: an overview of drivers and consequences. CAB Reviews: Perspectives in Agriculture, Veterinary Science, Nutrition and Natural Resources.2:057.

[19] Gellis, A.C., Webb, R.M.T., McIntyre, S.C. and Wolfe, W.J. (2006) Land-use effects on erosion, sediment yields, and reservoir sedimentation: a

case study in the lago loiza basin, puerto rico. Physical Geography, 27(1), 39-69

[20] Cerda, A., Burguet, M., Keesstra, S., Prosdocimi, M., Di Prima, S., Brevik, E., Novara, A., Jordan, A. and Tarolli, P. (2016) The impact of agriculture terraces on soil organic matter, aggregate stability, water repellency and bulk density. A study in abandoned and active farms in the Sierra de Enguera, Eastern Spain. Geophysical Research Abstracts Vol. 18, EGU2016-18104.

[21] Plante, A. and Conant, R.T. (2014) Soil organic matter dynamics, climate change Effects. Global Environmental Change Volume 1 of the series Handbook of Global Environmental Pollution. 317-323pp.

[22] Wei W., Chen L., Fu B., Huang Z., Wu D. and Gui L. (2007) The effect of land uses and rainfall regimes on runoff and soil erosion in semi-arid loess hilly area, China. Journal of Hydrology, 335, 247–258.

[23] Bakker, M.M., Govers, G., Kosmas, C., Vanacker, V., Oost, K.v. and Rounsevell, M. (2005) Soil erosion as a driver of land-use change. Agriculture, Ecosystems and Environment 105, 467–481.

[24] FAO (Food and Agriculture Organization of the United Nations) (2001) Soil carbon sequestration for improved land management. Chapter 2, The evaluation of soil carbon storage and main Changes, 13pp.World Soil Resources Reports, 96.

[25] Zhiyanski, M., Glushkova, M., Ferezliev, A., Menichetti, L. and Leifeld, L. (2015) Carbon storage and soil property changes following afforestation in mountain ecosystems of the Western Rhodopes, Bulgaria. iForest 9, 626-634.

[26] Atalay, I., Efe, R. and Ozturk, M. (2014) Ecology and Classification of Forests in Turkey. Procedia- Social and Behavioral Sciences. 120, 788-805.

[27] Cepel, N. (1995) Orman Ekolojisi. I.U. Yayın No. 3S86, Orman Fak. Yay. No.433. ISBN 975-404-398-1. I.U. Basimevi ve Film Merkezi, Istanbul 1995. XXl+536 s.

[28] Walter, H., Harnickell, E. and Mueller-Dombois, D. (1975) Climate-diagram maps of the individual continents and the ecological climatic regions of the earth. Berlin: Springer-Verlag. 36p. with 9 maps.

[29] De Martonne, E. (1926) Areisme et indice artidite. Comptes Rendus de L'Acad Sci, Paris, 182, 1395–1398.

[30] Thornthwaite, C.W. (1948) An Approach toward a Rational Classification of Climate. Geographical Review, 38(1), 55-94.

[31] MTA (Maden Tetkik ve Arama Genel Mudurlugu). (2015) Turkiye Yeralti Kaynaklari (Illere Gore). Yer Bilmleri ve Kültür Serisi-5, Edition 2, Ankara.

[32] Staupendahl, K. (2003) Tree Draw for Windows, ARGUS Forstplanung, Gottingen.

[33] Yucesan, Z., Ozcelik, S. and Oktan, E. (2015) Effects of thinning on stand structure and tree stability in an afforested oriental beech (Fagus orientalis Lipsky) stand in northeast Turkey. J. For. Res., 26(1), 123-129.

[34] Kartieranleitung, B. B. (1994). Bodenkundlische Kartieranleitung, 4. Auflage E.

[35] Saxton, K.E., Rawls, W.J., Romberger, J.S. and Papendick, R.I. (1986) Estimating generalized soil-water characteristics from texture. Soil Sci. Soc. Amer. J., 50(4):1031-1036.

[36] Bouyoucos, G.J. (1962) Hydrometer Method Improved for Making Particle Size Analyses of Soils. Agronomy Journal, 54, 464-465.

[37] Allison, L.E. (1965) Organic Carbon: Walkley-Black Method. In: Methods of Analysis. Agronomy Monographs No: 9, Part 2. American Society Agronomy, Madison, Wisconsin, USA,1367-1378 pp.

[38] Wischmeier, W.H. and Smith, D.D. (1978) Predicting Rainfall Erosion Losses, A Guide to Conservation Planning, USDA, Supersedes Agriculture Handbook No.282, Washington.

[39] Schwertmann, U., Vogl, W. and Kainz, M. (1990) Bodenerosion durch Wasser: Vorhersage des Abtrags und Bewertung von Gegenmassnahmen, Ulmer Verlag, Stuttgart.

[40] Dogan, O. and Gucer, C. (1976) Su Erozyonunun Nedenleri – Olusumu ve Universal Denklem ile Toprak kayiplarinin Saptanmasi, Ankara.

[41] Erkut, S. (2013) Capacity of carbon stock in pure beech stands of Giresun Forest District Directorate Akkuş Forest Enterprise, Msc Thesis, Karadeniz Technical University Institute of Natural Sciences, p. 45.

[42] Guo, L.B. and Gifford, R.M. (2002) Soil carbon stocks and land use change: a meta-analysis, Glob. Chang. Biol., 8: 345–360.

[43] SPSS Inc. (2016) SPSS version 23.0 User's Guide. Chicago, IL USA.

[44] Bermudez, F.L., Diaz, A.R., Fernandez, H.M. and Fernandez, J.M. (1998) Vegetation and soil erosion under a semi-arid Mediterranean climate: a case study from Murcia (Spain), Geomorphology, 24: 51-58.

[45] Lasanta, T., Garcia-Ruiz, J.M., Perez-Rontomo, C. and Sancho-Marcean, C. (2000) Runoff and sediment yield in a semi-arid environment: the effect of land management after farmland abandonment, Catena 38(4), 265-278.

[46] Aydemir, H. (1973) Bolu Masifinde Araziden Faydalanma Bicimlerinde Yüzeysel Akisla Su Kaybi ve Toprak Tasinması Uzerine Arastirmalar, Ormancilik Arastirma Enstitusu Yayinları, Teknik Bülten, Seri No.54, Ankara.

[47] Hacisalihoglu, S., Kalay, H.Z., Sariyildiz, T. and Oktan, E. (2006) Quantitative Determination of Soil Loss and Runoff in Different Land Use Typs and Slope Classes in a Semi-Arid Area in Turkey, Fresen. Environ. Bull., 15, 1299-1306.

[48] Erskine, W.D., Mahmoudzadeh, A. and Myers, C. (2002) Land use effects on sediment yields and soil loss rates in small basins of Triassic sandstone near Sydney, NSW, Australia. Catena 49, 271-287.

[49] Mahmoudzadeh, A., Erskine, W.D. and Myers, C. (2002) Sediment yields and soil loss rates from native forest, pasture and cultivated land in the Bathurst area, New South Wales. Australian Forestry 65(2), 73-80.

[50] Hacisalihoglu, S. (2010) Variations of measured and simulated soil-loss amounts in a semiarid area in Turkey, Environmental Monitoring and assessment, 165: 255-262.

[51] Bera, A. (2017) Assessment of soil loss by universal soil loss equation (USLE) model using GIS techniques: a case study of Gumti River Basin, Tripura, India. Model. Earth Syst. Environ. 3, 29.

[52] Golosov, V., Gusarov, A., Litvin, L., Yermolaev, O., Chizhikova, N., Safina, G. and Kiryukhina, Z. (2017) Evaluation of soil erosion rates in the southern half of the Russian Plain: methodology and initial results. Proc. IAHS, 375, 23-27.

[53] Wasak, K. and Drewnik, M. (2015) Land use effects on soil organic carbon sequestration in calcareous Leptosols in former pastureland – a case study from the Tatra Mountains (Poland). Solid Earth, 6, 1103-1115.

[54] Schimel, D.S. (1995) Terrestrial Ecosystems and the Carbon-Cycle, Glob. Change Biol., 1, 77–91.

[55] Tarnocai, C., Canadell, J.G., Schuur, E.A.G., Kuhry, P., Mazhitova, G., and Zimov, S. (2009) Soil organic carbon pools in the northern circumpolar permafrost region, Global Biogeochem. Cy., 23, 11 pp.

[56] Veum, K.S., Sudduth, K.A., Kremer, R.J. and Kitchen, N.R. (2015) Estimating a Soil Quality Index with VNIR Reflectance Spectroscopy. Soil Sci. Soc. Am. J. 79, 637-649.

Received: **04.04.2017**
Accepted: **10.08.2017**

CORRESPONDING AUTHOR

Sezgin Hacisalihoglu
Karadeniz Technical University
Faculty of Forestry
61080 Trabzon – TURKEY

E-mail: sezgin@ktu.edu.tr

© by PSP Volume 26 – No. 10/2017 pages 6017-6027 Fresenius Environmental Bulletin

EFFECT OF GLUCOSE AS CO-METABOLISM SUBSTRATE ON THE BIODEGRADATION OF DICHLOROPHENOLS

Zhirong Sun[1,*], Jiangyang Li[1], Jinwei Zhang[1], Jianguang Wang[1], Xueyun Wang[1], Xiang Hu[2]

[1]National Engineering Laboratory for Advanced Municipal Wastewater Treatment and Reuse Technology, Beijing University of Technology, Beijing 100124, P. R. China.
[2]College of Chemical Engineering, Beijing University of Chemical Technology, Beijing, 100029, P.R. China.

ABSTRACT

In this study, co-metabolism biodegradation of DCPs was investigated, with glucose as co-metabolism substrate and four DCPs including 2,3-dichlorophenol (2,3-DCP), 2,5-dichlorophenol (2,5-DCP), 3,4-dichlorophenol (3,4-DCP) and 3,5-dichlorophenol (3,5-DCP) as target pollutants. The results showed that glucose could accelerate the biodegradation process of DCPs due to the reasons that glucose could enhance the microorganisms' adaptability towards DCPs as a co-metabolism substrate in the activated sludge and speed up the acclimation process of DCPs high-efficiency degradation strains, which indirectly improved the biodegradation rate of DCPs in activated sludge. Through 80 days of acclimatization, the microorganisms were able to degrade 6.5 mg L^{-1} 2,3-DCP, 7.5 mg L^{-1} 2,5-DCP, 6.3 mg L^{-1} 3,4-DCP and 7.2 mg L^{-1} 3,5-DCP in different bioreactors, respectively. With the stepwise improvement of glucose feed concentration, the biodegradation rate of DCPs changed gradually. The glucose influent concentrations of 1000 mg L^{-1}, 1200 mg L^{-1}, 1000 mg L^{-1} and 1200 mg L^{-1} were selected as optimal experimental value, respectively. Under these conditions, biodegradation concentrations of 2,3-DCP, 2,5-DCP, 3,4-DCP and 3,5-DCP with the initial concentration of 15 mg L^{-1} reached up to 11.6 mg L^{-1}, 12.3 mg L^{-1}, 11.5 mg L^{-1} and 10.6 mg L^{-1}, correspondingly. Combination with DCPs structure and effect of each DCP on microorganisms, results also demonstrated that the *meta*- and *para*-substituted CPs were of greater toxicity than the *ortho*-substituteds'.

KEYWORDS:
dichlorophenol; co-metabolism; glucose; biodegradation.

INTRODUCTION

Chlorophenols (CPs) have been widely used as industrial synthesis intermediates for dyes, preservative, disinfectant and pesticides [1]. However, due to their high toxicity and the effect of carcinogenicity as well as low biological degradability, CPs are considered be one class of the notorious hazardous organic compounds that are of great concern for human health and ecological system when they are discharged into soil, urban wastewater and surface water [2-4]. EPA of The United States, European Community (EC) and China national environmental monitoring center have already listed a variety of CPs as priority pollutants, such as 2-monochlorophenol (2-CP), 2,4-dichlorophenol (2,4-DCP) [5, 6].

In recent decades, a variety of techniques such as physical, chemical, photocatalytic and electrochemical technology have been proposed for the treatment of CPs with small-scale process level in the lab [7]. Comparing with abovementioned techniques, co-metabolic biodegradation with advantages of low investment, good governance effect, no secondary pollution and environmental sustainability has attracted much attention and now is emerging to be an advanced and effective method. It has been reported that using an easily assimilated carbon source as co-metabolism substrate is benefit for CPs to be dechlorinated and mineralized by microorganisms. Usually, easily degradable carbon sources can stimulate microbial growth and thus more key enzymes concerning metabolism are available to attack and decompose CPs [8-10]. The previous research had certified that it was advisable to gain simultaneous removal of 4-CP and phenol in lab-scale bioreactors under the conditions of different temperatures. Pentachlorophenol (PCP) as the single carbon and energy source could be mineralized by some certain aerobic stains, and better co-metabolic degradation effect can be obtained when glucose, acetic acid, and formic acid were respectively chosen as growth substrates in horizontal-flow anaerobic immobilized biomass (HAIB) reactors [2, 6, 11].

The concentration of conventional substrates and their proportions relative to target pollutants also perform a significant role in the co-metabolic conversion and degradation of CPs. Exerting co-metabolism by addition of the right amount of multiple matrixes is helpful for the microorganisms growth, but excessive growth substrates might arouse a competitive inhibitory result towards biodegradation of refractory compounds. For example, the 4-CP biodeg-

radation rate could be optimized by adjusting the ratio of 4-CP and sodium glutamate. High growth substrate concentrations may cause carbon catabolite repression and lead to pausing of the microbial degradation. Therefore, appropriate dosage of growth substrate played an important role on co-metabolism [9, 12].

DCPs are one kind of toxic chlorophenol pollutants that commonly present in various kinds industrial effluents. The relationship between the toxicity and substituent group of CPs have been concluded, and the toxicity of DCP isomerides mainly relied on their chlorinated degree and the substitutions away from the ortho-position. In this work, the co-metabolic biodegradation of 2,3-DCP, 2,5-DCP, 3,4-DCP and 3,5-DCP in sequencing batch reactor (SBR) under aerobic conditions was investigated when glucose was selected as a co-metabolic substrate. The dosage of glucose was optimized to obtain optimal degradation efficiency of each DCP. The results revealed that the glucose with appropriate dosage could accelerate the acclimation process of DCP degrading bacterium. It could also be proved that the *meta*- and *para*-substituted CPs are of greater toxicity than the *ortho*-substituteds according to the different toxicity intensity of DCP showed by biological indicator of acclimation process.

EXPERIMENTAL

Chemicals. DCPs (Beijing Chem Service Inc.) including 2,3-DCP, 2,5-DCP, 3,4-DCP and 3,5-DCP were selected as objective processed objects. All chemicals used in the research containing DCPs, mineral salts (Beijing Reagent Co.) and glucose (Beijing Chemical Works) were of analytical grade. All aqueous solutions were prepared with ultrapure water (Millipore-Q system, 18.2 MΩ·cm). The chemical structures of selected DCPs used in the experiments were described in Fig. 1.

Experimental facility. The schematic diagram of the experimental apparatus was described in Fig. 2. The SBR system contained a cylindrical organic glass as sample port (260 mm in height and 140 mm in bottom diameter) and a mechanical stirrer to the mixture of sludge. The rotameter was located between aeration diffuser and the air pump to adjust aeration rate. The total volume of SBR was 4 L, but its effective volume was set in 3 L for preventing overflow. Two peristaltic pump were used to keep continuous feeding via the top of the reactor and pump the effluent to drain tank, respectively. The research was implemented under the condition of normal pressure and temperature.

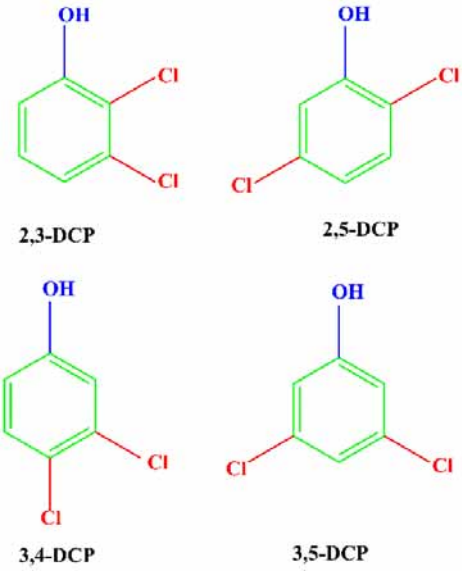

FIGURE 1
Chemical structures of selected DCPs used in the research

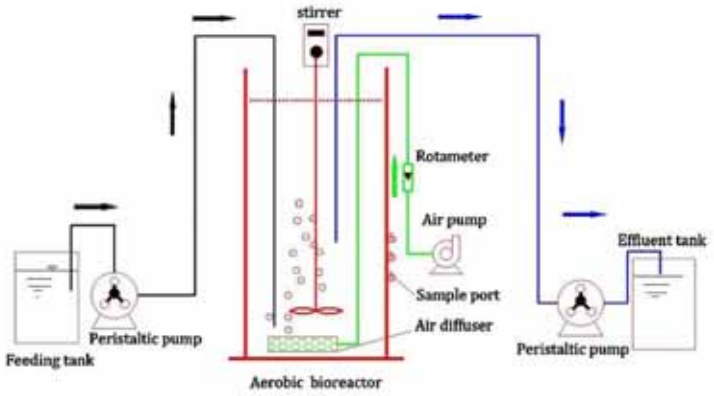

FIGURE 2
A schematic diagram of the activated sludge bioreactor in experimental studies

TABLE 1
Basic characteristic of tested sludge

pH	MLSS (mg L^{-1})	SVI (ml g^{-1})	MLVSS (mg L^{-1})	SV (%)
7.4	4557	115.58	3919	86

TABLE 2
Composition of mineral salts

Compound	Concentration (mg L^{-1})
$FeSO_4$	20
NH_4Cl	20
K_2HPO_4	10
$CaCl_2 \cdot 2H_2O$	2
$KH_2PO_4 \cdot 3H_2O$	30
$MgSO_4 \cdot 7H_2O$	8
$CuSO_4 \cdot 5H_2O$	25
$ZnSO_4 \cdot 7H_2O$	0.0003
$MnCl_2 \cdot 2H_2O$	0.00012
$Na_2MoO_4 \cdot 2H_2O$	0.00012
KI	0.00006
H_3BO_4	0.00003
$CoCl_2 \cdot 6H_2O$	0.00015
$FeCl_3 \cdot 6H_2O$	0.0015

All SBRs had the same structure and mode of operation. Each reactor ran two cycles one day and operated a 12 hrs cycle in sequence with 20 min of feeding both water and substrates, 10 hrs aerobic aeration (mechanical agitation of 300 r min^{-1}), 30 min settling, 10 min dewatering and 60 min idling.

Seed sludge and wastewater composition. This study used mixed bacterium in SBRs. Activated sludge culture was taken from the secondary sedimentation tank of wastewater treatment plant in Beijing, China. The basic characteristic of tested sludge was shown in Table 1.

Taking 2,3-DCP as example to instruct wastewater composition. The required synthetic wastewater was made up of glucose, various concentrations of 2,3-DCP and some mineral salts [13, 14] (Table 2). Glucose was viewed as main carbon source and the ratio of carbon, nitrogen and phosphorus kept at 100/10/5 in the influent to avoid the N and P to become restricted nutrients. Influent COD (chemical oxygen demand) fluctuated within the range of 500 mg L^{-1} to 600 mg L^{-1} during the acclimation stage. Each DCP was disposed individually in the same way.

Experimental procedure. Taking 2,3-DCP as example to discuss the detailed acclimation processes. 2,5-DCP, 3,4-DCP and 3,5-DCP were dealt respectively in the same way.

The experiments contain test and control groups. In the test group, glucose was regarded as main carbon source with influent concentration between 500 mg L^{-1} and 600 mg L^{-1}, and 2,3-DCP was stepwise added into the reactor with feed concentration gradient of 1 mg L^{-1} (from 1 to 10 mg L^{-1}) at intervals of around 7 days. In the control group, 2,3-DCP was used as single carbon source with influent concentration of 200 mg L^{-1} that accorded with concentration of carbon source one period in sewage treatment plant. Through 80 days of acclimation, degrade abilities of the acclimatized microorganisms in different SBRs for 2,3-DCP, 2,5-DCP, 3,4-DCP and 3,5-DCP were 6.5 mg L^{-1}, 7.5 mg L^{-1}, 6.3 mg L^{-1} and 7.2 mg L^{-1}, respectively.

Then the influence of the glucose feed concentration was investigated. The activated sludge that acclimated for 80 days with ability to degrade 2,3-DCP of 6.5 mg L^{-1} were inoculated into six SBRs (1#--6#) and the sludge concentration was 4500 mg L^{-1} in each reactor. The glucose feed concentration was successively 500 mg L^{-1}, 800 mg L^{-1}, 1000 mg L^{-1}, 1200 mg L^{-1}, 1500 mg L^{-1} and 1800 mg L^{-1} from SBR 1# to 6#, and the concentrations of 2,3-DCP were 15 mg L^{-1} for all reactors.

Sludge retention time (SRT) was controlled in 8 days, and an appropriate volume of mixed liquor was drained out in the last 10 minutes of aeration phase. According to different experiment requirements, reaction temperature was adjusted at T = 15±1 °C, 25±1 °C or 35±1 °C, and pH was adjusted at 7.15-7.5. Dissolved oxygen (DO) concentration was controlled at more than 3 mg L^{-1} by adjusting flow meter. Supernatant liquor was drained at volume exchange rate of 50%. The specific settings were shown in Table 3.

Analytical methods. Taking 100 ml mixed liquid from SBR and using the constant weight method to analyze mixed liquor suspended solids (MLSS). The liquid supernatants obtained by centrifugation was used to COD analyses with potassium dichromate method based on digestion and colorimetric analysis. High efficiency liquid chromatography (HPLC waters-2489) equipped with C-18 column (Atlantis) was used for DCPs concentration analyses. The mobile phase consisted of a mixed solvent of methanol and water (7/3, v/v) and its flow velocity was 0.2 mL min^{-1} in HPLC. The variations of DO and pH were monitored with WTW Analyzer (Multi3420) equipped with a temperature probe.

In order to exclude the influence of sludge adsorption on DCPs, the mixture samples from the initial and end of one period were eluted repeatedly until DCP content could not be detected. By detecting the DCP concentration in the eluent, the results represented the initial and effluent concentration of DCP respectively. The degradation efficiency of DCP was computed from the following equation:

$$Degradation\ efficiency\ (\%) = \frac{C_0 - C_1}{C_0} \times 100\%$$

Where C_0 was the initial concentration of DCP and C_1 represented the DCP effluent concentration after one period. According to determination, volatile DCPs in the process of experiments were negligible.

RESULTS AND DISCUSSION

Comparison of COD degradation efficiency. It was reported that the chlorinated phenolic compounds which owned *meta*- or *para*-substituent had stronger toxicity than those had *ortho*-substituents' [15, 16]. In this research, 2,3-DCP was treated as representative in the comparison of COD removal degradation during sludge domestication stage.

TABLE 3
Parallel experiments in the domestication stage and comparative trials with glucose feed concentration as variation

Stage	Group	Influent concentration (mg L^{-1})					Temp (°C)
		2,3-DCP	2,5-DCP	3,4-DCP	3,5-DCP	glucose	
Acclimatization	Test	0-10	0-10	0-10	0-10	500	25±1
	Control	200	200	200	200	--	25±1
Comparative trials with different influent glucose concentration	1#	15	15	15	15	500	
	2#	15	15	15	15	800	
	3#	15	15	15	15	1000	15±1
	4#	15	15	15	15	1200	25±1
	5#	15	15	15	15	1500	35±1
	6#	15	15	15	15	1800	

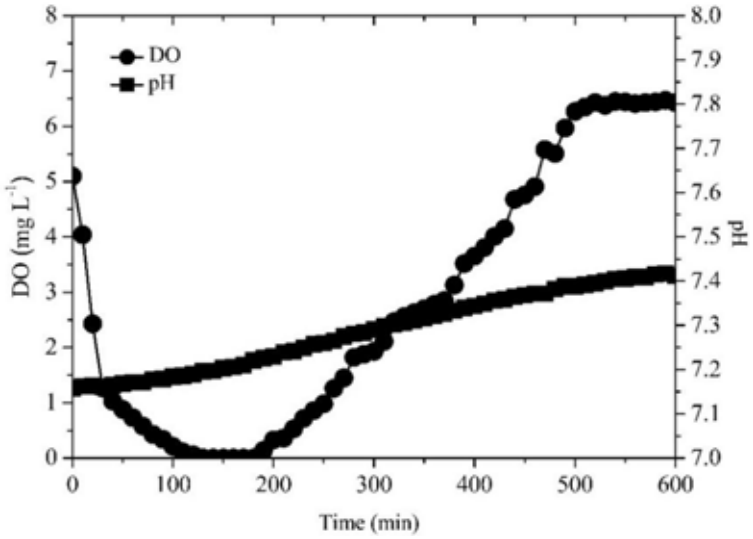

FIGURE 3
The variations of DO and pH within one period in the test SBR: 2,3-DCP as target pollutant

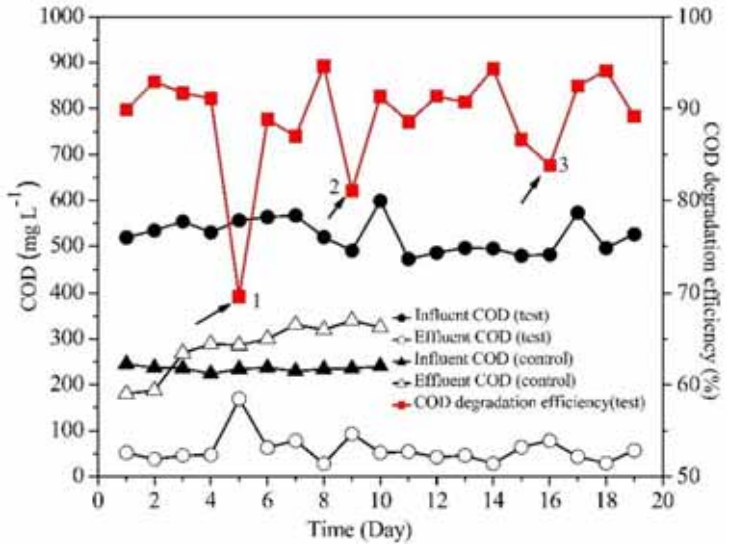

FIGURE 4
The comparison of COD degradation efficiency in the control and test SBRs: 2,3-DCP as target pollutant

As shown in Fig. 3, in the test group, DO fell sharply in the initial stage of aeration operation (0-180 min) on account of the consuming of matrix by the microorganisms via a series of biochemical reaction in SBR. About 300 min later, DO rose gradually until the whole mixture recovered back to aerobic condition (DO>3 mg L^{-1}). In the meantime, pH ranged from 7.15 to 7.5, which was suitable for the growth of microorganisms. So it was unnecessary to adjust pH in the whole reaction process.

In the control group, 2,3-DCP with influent concentration of 200 mg L^{-1}, equivalent to 240 mg L^{-1} influent COD which accorded with concentration of carbon source in sewage treatment plant every cycle, was looked upon as the single carbon source. As shown in Fig. 4, although the activated sludge had no ability to degrade 2,3-DCP in short term, the effluent COD declined and kept at a high level of 160 mg L^{-1} in the initial stage (in 4 days) probably due to the absorption of 2,3-DCP by activated sludge and achieved adsorption saturation along with the continuous running. As a result of 2,3-DCP not degraded actually, COD degradation rate kept in low level, less than 50%. On account of the long-standing strong toxic environment and shortage of available external carbon source, the microbes started to split and lead to the effluent COD rising more than 200 mg L^{-1} in the liquid supernatant after 4 days. Even it appeared phenomenon of turbidity and the effluent COD was a little higher than the influent because of desorption of 2,3-DCP.

In the test group, the COD degradation efficiency appeared fluctuation from down to up as the reactor ran continuously to the stable state. At the points, such as the point 1, 2, 3 (Fig. 4) that 2,3-DCP was feed, the COD degradation rate descended due to the strong toxicity of 2,3-DCP that inhibited the microbial metabolic activity to a certain extent [17, 18]. However, according to the whole process, COD degradation efficiency remained stable and was more than 85%, illustrating the important role of glucose on resisting toxicity of 2,3-DCP for activated sludge.

In a general way, the growth matrix was usually easy to degrade and could stimulate microbial metabolism to a certain extent in the co-metabolism process and availed to treating CPs pollutants [19, 20]. The energy produced from catabolism of growth substrate was benefit for CPs decomposing and could promote the detoxification and degradation of CPs so as to improve operation efficiency of the system and treatment effect. Cobos-Vasconcelos reported that phenol as primary substrate had effect on removal of 2-CP, 4-CP, 2,4-DCP, 2,6-DCP in batch and fed-batch cultures [21]. Wang also studied the additive phenol and sodium glutamate as carbon source to maximize the co-metabolism of 4-chlorophenol by researching *Pseudomonas putida* ATTCC 49451 [22, 23].

Therefore, the approach of using glucose as co-metabolism substrate was more suitable for degradation of 2,3-DCP and its isomers.

The difference of COD degradation. Glucose was not only a substrate that may be utilized by microbial metabolism but also induced the key enzymes for microbial stress metabolism [24]. With the stepwise enhancement of DCP feed concentration, on one hand, microorganisms used energy from decomposing glucose to degrade DCP, on the other hand, gluconic stress protection could ease toxicity of DCP so as to slow the inhibition of DCP on microorganisms.

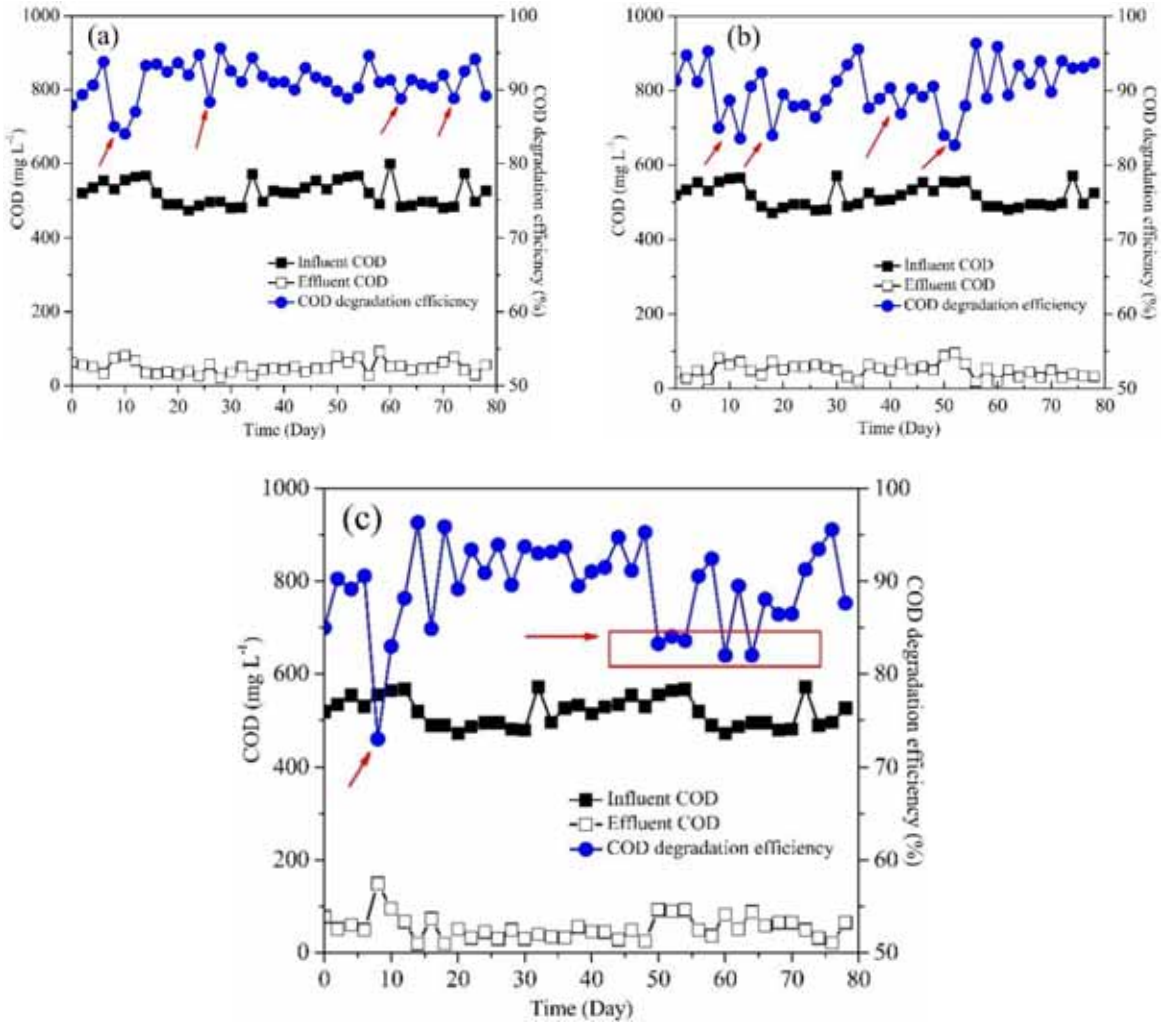

FIGURE 5
The variations of COD degradation efficiency towards test SBRs: 2,5-DCP as target pollutant (a), 3,4-DCP as target pollutant (b) and 3,5-DCP as target pollutant (c)

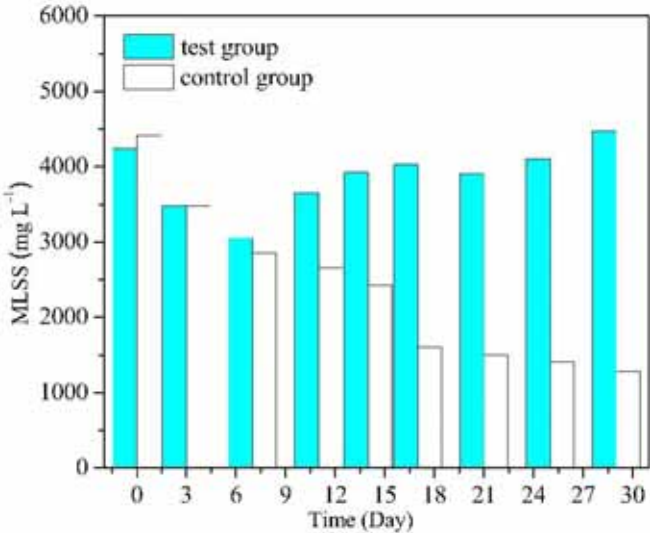

FIGURE 6
The comparison of MLSS in the control and test SBR: 2,3-DCP as target pollutant

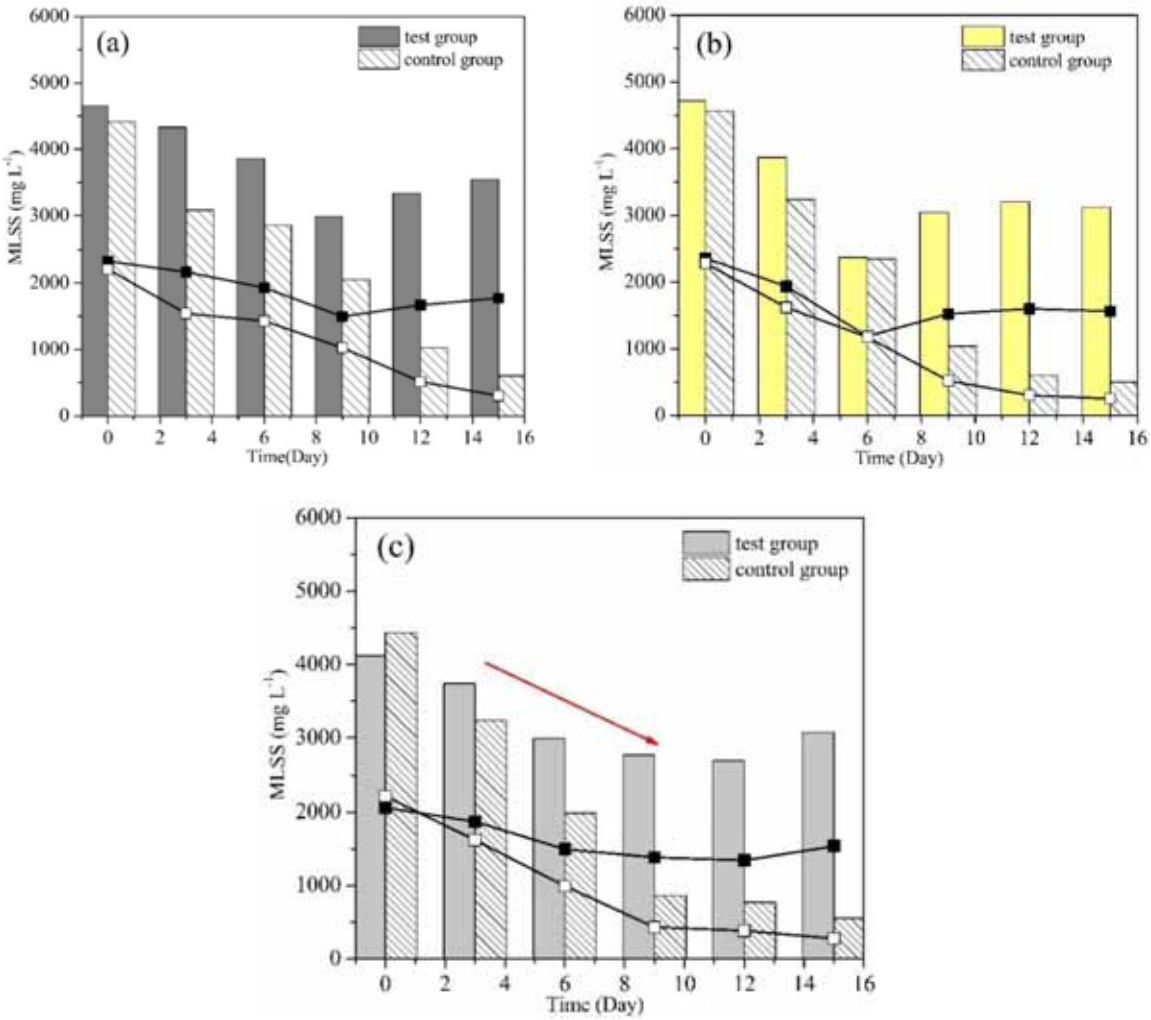

FIGURE 7
The comparison of MLSS in the control and test SBRs: 2,5-DCP as target pollutant (a), 3,4-DCP as target pollutant (b) and 3,5-DCP as target pollutant (c)

Variations of COD degradation efficiency in the acclimatization process using glucose as co-metabolism carbon source for 2,5-DCP, 3,4-DCP and 3,5-DCP were depicted in Fig. 5. It can be found that the microbes could adapt to the initial concentration of DCP (1 mg L^{-1}), which ensured COD degradation efficiency to maintain at a high state, mostly over 90% (with 10 days). With the DCP feed concentration stepwise increasing, COD degradation efficiency appeared fluctuation obviously in the process of domestication, like those points marked in Fig. 5. Effluent COD transformed from down to up, even more than 150 mg L^{-1}, and then restored the stability less than 50 mg L^{-1}. The microbes needed more energy to dispose DCP so that energy from glucose metabolism was insufficient to resist DCP toxicity and support DCP biodegraded fully. The reasons that included toxicity of DCP and inhibition of key enzymes activities leaded to COD degradation efficiency declining dramatically.

The curves in Fig. 5 (a), (b) and (c) were similar but not identical, indicating the different COD degradation processes of the DCPs. For Fig. 5(c), the lowest point of removal rate was at around 70%, and the whole process shew greater fluctuation, for instance 96% to 80% (from 48 to 52 days). Perhaps for different DCP isomers, the relative position of substituent group leaded to different toxicity, which indirectly gave rise to difference of COD degradation during domestication process [25, 26]. With comparison and analysis among the structure of DCPs, that the *meta*- and *para*-substituted CPs were of greater toxicity than the *ortho*-substituteds has been reported [27].

The variations of MLSS. According to Fig. 6, the microorganisms existing in the activated sludge were inhibited or killed due to strong toxicity of 2,3-DCP, which resulted in a sharp drop towards MLSS in the control group, from 4500 mg L^{-1} down to less than 1000 mg L^{-1} within 15 days. However, MLSS of the test group started to decline in the initial stage

of reaction because the microorganisms were in adaptive phase (within 10 days). About 10 days later, the microbes were acclimatized to adapted co-substrates conditions and the MLSS began to rise gradually and recovered to normal treatment concentration about 18 days later with the reactor ran continuously. Thus it can be seen that microorganisms in the test group were more suitable for degradation of 2,3-DCP than that in control group.

It can be seen from Fig. 7 that the MLSS in all SBRs declined, and the MLSS in the control groups also had a sharp drop within 15 days. As shown from Fig. 7 (b), the MLSS was inferior to 2000 mg L^{-1} on the 6th day. And in Fig. 7 (c), a linear decrease of MLSS was presented from the 1th to the 9th day. During the process of experiments, massive activated sludge turned black and floated in the supernatant and was drained as effluent. This suggested that massive microorganisms could not bear the toxicity of DCP when they lacked easily degradable carbon source, for example glucose. It can also be found that the MLSS in Fig. 7 (c) to recovered the most slowly to normal level during the same domestication cycles. It follows that the 3,5-DCP had stronger toxic effects on activated sludge and was more difficult to be degraded than other DCPs.

The relationship between 2,3-DCP biodegradation efficiency and glucose feed concentration. As shown in Fig. 8, 2,3-DCP degradation rate changed apparently with different glucose feed concentration through one cycle of reaction. As glucose feed concentration increased from 500 mg L^{-1} to 1000 mg L^{-1} stepwise, the 2,3-DCP degradation efficiency gradually went up from 41% to nearly 80%, corresponding to the degradation concentration of 11.6 mg L^{-1}. This was because when glucose feed was 500 mg L^{-1}, the microbes mainly used glucose to ease toxicity and growth, and only a small amount of glucose was utilized to induce key enzyme [28]. The microbes needed to produce a series of enzymes for instance microbial oxygenase enzymes, e. g which was utilized to degrade both growth matrix level 1 and 2. Since the level 2 growth matrix tended to be some pollutants which was not easy to degrade, microorganisms had priority over using glucose than 2,3-DCP. Further increase the glucose feed concentration more than 1200 mg L^{-1}, the 2,3-DCP degradation concentration was down to 7 mg L^{-1}. It confirmed that excessive substrates inhibited the degradation process due to the energy consuming for glucose degradation. So 1000 mg L^{-1} was the appropriate glucose feed concentration to get better degradation rate under the condition of 15 mg L^{-1} 2,3-DCP influent.

Even if concentration of glucose increased gradually, 2,3-DCP degradation rate (not over 5 mg L^{-1}) was not significantly improved due to the low enzymes activity at 15 °C. When the SBR temperature was set at 35 °C, the maximum biodegradation concentration slightly decreased to 10.5 mg L^{-1}. But the maximum degradation rate point between 75% and 80% had a tendency to move forward in 800 mg L^{-1} glucose feed. The main reason might be that most key enzymes on the microorganisms were inhibited, at the same time, a part of key enzymes bearing higher temperature could be used for co-metabolism all the same [29].

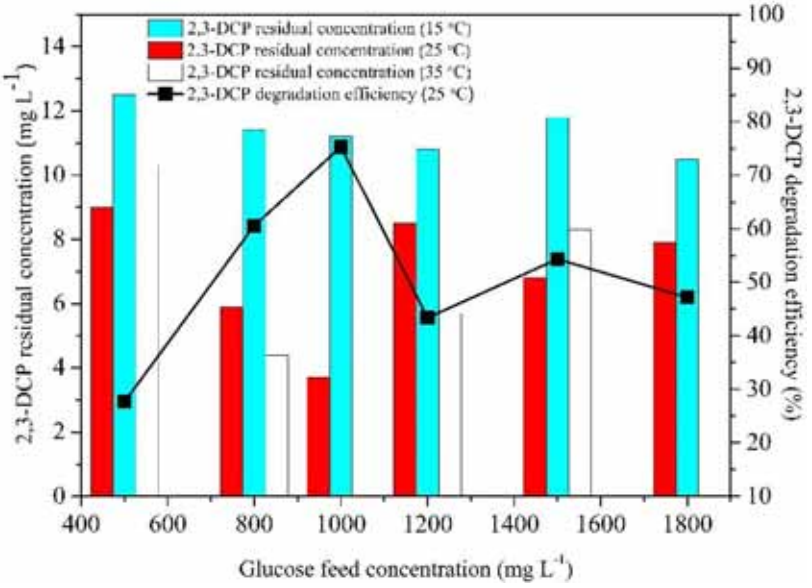

FIGURE 8
The variation of 2,3-DCP biodegradation efficiency with the stepwise improvement of glucose feed concentration under different temperature

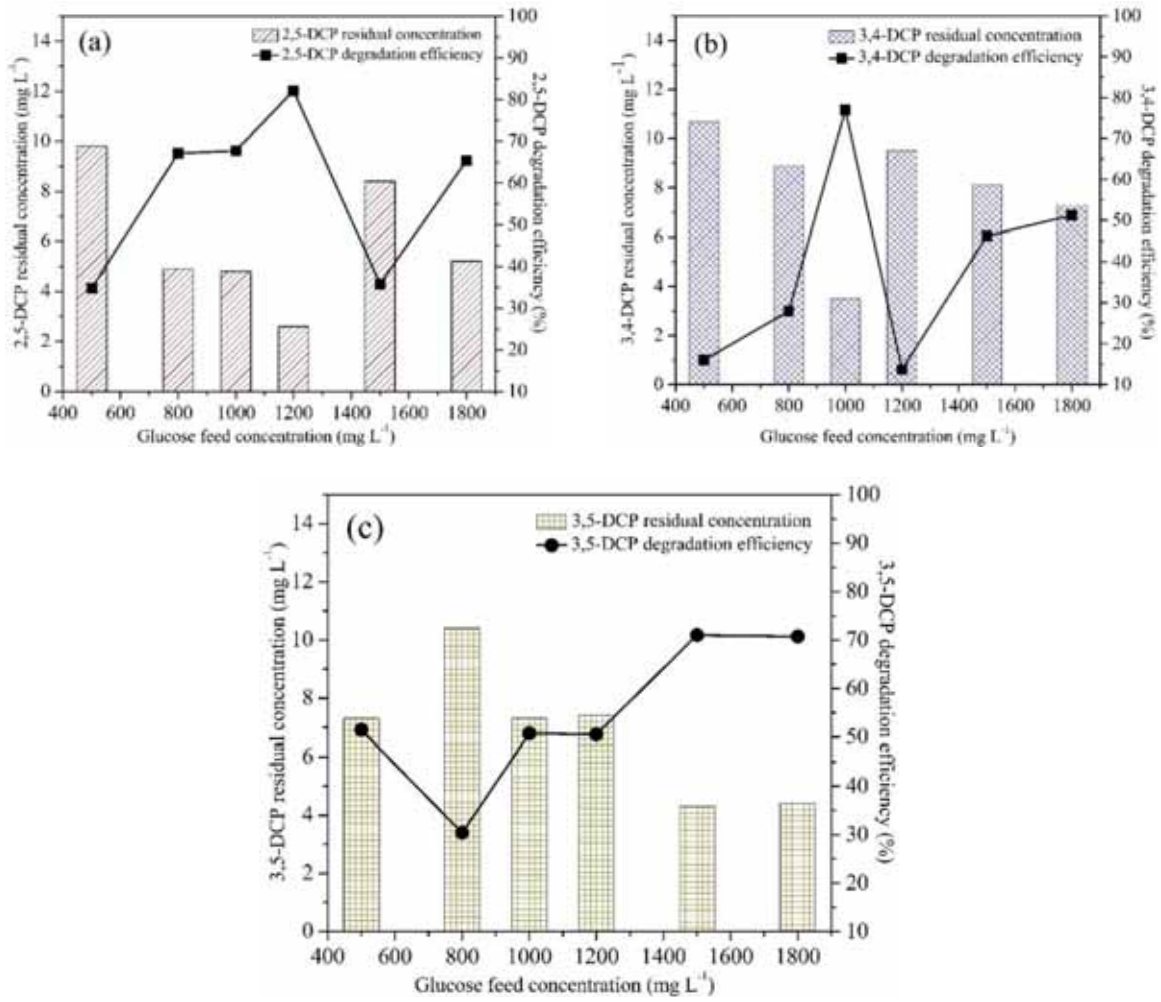

FIGURE 9
The relationship between other DCPs biodegradation efficiency and glucose feed concentration under the condition of 25 °C: 2,5-DCP as target pollutant (a), 3,4-DCP as target pollutant (b) and 3,5-DCP as target pollutant (c)

The other DCPs biodegradation. The 2,5-DCP, 3,4-DCP and 3,5-DCP degradation situations at 25 °C were described in Fig. 9. The 2,5-DCP degradation efficiency gradually went up from 34% to 82% as glucose feed concentration increased from 500 mg L^{-1} to 1200 mg L^{-1} stepwise. When glucose feed concentration was over 1200 mg L^{-1}, there was an obvious descent in 2,5-DCP degradation efficiency for the reason that excess of growth substrates might gave rise to a competitive inhibitory effect on degradation of target compounds. There was a little distinction for 2,5-DCP, 3,4-DCP and 3,5-DCP degradation efficiency with changed glucose feed concentration.

The similar curves appeared in 3,4-DCP and 3,5-DCP reduction and the best influent points on glucose were respectively 1000 mg L^{-1} and 1200 mg L^{-1}. The 3,4-DCP degradation efficiency in Fig. 9(b) was gradually arousing up from 28.7% to 77% as glucose feed concentration increased from 500 mg L^{-1} to 1000 mg L^{-1} stepwise. Similarly, the reduction result of 3,5-DCP in Fig. 9(c) was gradually arousing up from 51% to 71% as glucose feed concentration increased from 500 mg L^{-1} to 1200 mg L^{-1} stepwise. It worked out that getting maximum biodegradation rate on 3,5-DCP need more glucose feed concentration. It also has been confirmed that the *meta*- and *para*-substituted CPs were of greater toxicity than that of *ortho*-substituteds [30, 31].

CONCLUSIONS

DCPs had strong toxicity towards microorganisms and activated sludge from Wastewater Treatment Plant hardly had the ability to biodegrade DCPs when DCPs were treated as unique carbon source. The research results showed that glucose as a co-metabolism substrate could enhance the microorganisms' adaptability in wastewater environment containing DCP, and speed up acclimation process of each DCP high-efficiency degradation strains, which

thus indirectly improved the biodegradation rate of each DCP in the activated sludge.

Through 80 days of acclimatization, research results have confirmed that microorganisms were able to degrade 6.5 mg L^{-1} 2,3-DCP, 7.5 mg L^{-1} 2,5-DCP, 6.3 mg L^{-1} 3,4-DCP and 7.2 mg L^{-1} 3,5-DCP respectively in different bioreactors. With the stepwise improvement of glucose feed concentration, DCP degradation efficiency changed apparently and the addition of appropriate dosage of glucose would obtain optimal co-metabolism effect on each DCP. The glucose influent concentrations of 1000 mg L^{-1}, 1200 mg L^{-1}, 1000 mg L^{-1} and 1200 mg L^{-1} were deemed as optimal experimental value, respectively, under these conditions, biodegradation concentrations of 2,3-DCP, 2,5-DCP, 3,4-DCP and 3,5-DCP with the initial concentration of 15 mg L^{-1} reached up to 11.6 mg L^{-1}, 12.3 mg L^{-1}, 11.5 mg L^{-1} and 10.6 mg L^{-1}, correspondingly. Comparative analysis on the structure of each DCP, the strength of toxicity on activated sludge and optimal influent dosages of glucose were as a result of different substituent position, when one DCP was selected as target pollutant. The study turned out that the *meta*- and *para*-substituted CPs were of greater toxicity than the *ortho*-substitutes', like that 3,5-DCP had stronger toxic effects on activated sludge and was more difficult to be degraded than other DCPs.

ACKNOWLEDGEMENTS

The work was supported by National Natural Science Foundation of China (51478014, 51278006), Cultivation Fund for Beijing New Century Hundred, Thousand and Ten Thousand Talents Project.

REFERENCES

[1] Peng, Y., Chen, J., Lu, S., Huang, J., Zhang, M., Buekens, A., Li, X. and Yan, J. (2016) Chlorophenols in Municipal Solid Waste Incineration: A review. Chem. Eng. J., 292: 398-414.

[2] Limam, I., Limam, R.D., Mezni, M., Guenne, A., Madigou, C., Driss, M.R., Bouchez, T. and Mazeas, L. (2016) Penta- and 2,4,6-tri-chlorophenol biodegradation during municipal solid waste anaerobic digestion. Ecotox. Environ. Safe, 130: 270-278.

[3] Menale, C., Nicolucci, C., Catapane, M., Rossi, S., Bencivenga, U., Mita, D.G. and Diano, N. (2012) Optimization of operational conditions for biodegradation of chlorophenols by laccase-polyacrilonitrile beads system. Journal of Molecular Catalysis B: Enzymatic, 78: 38-44.

[4] Oh, W., Lim, P., Seng, C. and Sujari, A.N.A. (2012) Kinetic modeling of bioregeneration of chlorophenol-loaded granular activated carbon in simultaneous adsorption and biodegradation processes. Bioresource Technol., 114: 179-187.

[5] Xiangchun, Q., Hanchang, S., Yongming, Z., Jianlong, W. and Yi, Q. (2003) Biodegradation of 2,4-dichlorophenol in an air-lift honeycomb-like ceramic reactor. Process Biochem., 38: 1545-1551.

[6] Ziagova, M., Kyriakou, G. and Liakopoulou-Kyriakides, M. (2009) Co-metabolism of 2,4-dichlorophenol and 4-Cl-m-cresol in the presence of glucose as an easily assimilated carbon source by Staphylococcus xylosus. J. Hazard. Mater., 163: 383-390.

[7] Song, X., Shi, Q., Wang, H., Liu, S., Tai, C. and Bian, Z. (2017) Preparation of Pd-Fe/graphene catalysts by photocatalytic reduction with enhanced electrochemical oxidation-reduction properties for chlorophenols. Applied Catalysis B: Environmental, 203: 442-451.

[8] Chen, Y., He, J., Wang, Y., Kotsopoulos, T.A., Kaparaju, P. and Zeng, R.J. (2016) Development of an anaerobic co-metabolic model for degradation of phenol, m-cresol and easily degradable substrate. Biochem. Eng. J., 106: 19-25.

[9] Zhao, J., Chen, X., Bao, L., Bao, Z., He, Y., Zhang, Y. and Li, J. (2016) Correlation between microbial diversity and toxicity of sludge treating synthetic wastewater containing 4-chlorophenol in sequencing batch reactors. Chemosphere, 153: 138-145.

[10] Moussavi, G., Ghodrati, S. and Mohseni-Bandpei, A. (2014) The biodegradation and COD removal of 2-chlorophenol in a granular anoxic baffled reactor. J. Biotechnol., 184: 111-117.

[11] Damianovic, M.H.R.Z., Moraes, E.M., Zaiat, M. and Foresti, E. (2009) Pentachlorophenol (PCP) dechlorination in horizontal-flow anaerobic immobilized biomass (HAIB) reactors. Bioresource Technol., 100: 4361-4367.

[12] Wang, Y., Tan, C., Zhuang, S., Zhai, P., Cui, Y., Zhou, Q., Zhang, H. and Fei, Z. (2014) In vitro and in silico investigations of the binding interactions between chlorophenols and trypsin. J. Hazard. Mater., 278: 55-65.

[13] Cobos-Vasconcelos, D.D.L., Santoyo-Tepole, F., Juarez-Ramirez, C., Ruiz-Ordaz, N. and Galindez-Mayer, C.J.J. (2006) Cometabolic degradation of chlorophenols by a strain of Burkholderia in fed-batch culture. Enzyme Microb. Tech., 40: 57-60.

[14] Salmeron-Alcocer, A., Ruiz-Ordaz, N., Juarez-Ramirez, C. and Galindez-Mayer, J. (2007) Continuous biodegradation of single and mixed chlorophenols by a mixed microbial culture constituted by Burkholderia sp., Microbacterium phyllosphaerae, and Candida tropicalis. Biochem. Eng. J., 37: 201-211.

[15] Mubarik, S., Saeed, A., Athar, M.M. and Iqbal, M. (2016) Characterization and mechanism of

the adsorptive removal of 2,4,6-trichlorophenol by biochar prepared from sugarcane baggase. J. Ind. Eng. Chem., 33: 115-121.
[16] Baggi, G., Bernasconi, S., Zangrossi, M., Cavalca, L. and Andreoni, V. (2008) Co-metabolism of di- and trichlorobenzoates in a 2-chlorobenzoate-degrading bacterial culture: Effect of the position and number of halo-substituents. Int. Biodeter. Biodegr., 62: 57-64.
[17] Huang, L., Gan, L., Zhao, Q., Logan, B.E., Lu, H. and Chen, G. (2011) Degradation of pentachlorophenol with the presence of fermentable and non-fermentable co-substrates in a microbial fuel cell. Bioresource Technol., 102: 8762-8768.
[18] Kim, Y., Murugesan, K., Schmidt, S., Bokare, V., Jeon, J., Kim, E. and Chang, Y. (2011) Triclosan susceptibility and co-metabolism – A comparison for three aerobic pollutant-degrading bacteria. Bioresource Technol., 102: 2206-2212.
[19] Moussavi, G., Ghodrati, S. and Mohseni-Bandpei, A. (2014) The biodegradation and COD removal of 2-chlorophenol in a granular anoxic baffled reactor. J. Biotechnol., 184: 111-117.
[20] Guo, W., Guo, S., Yin, R., Yuan, Y., Ren, N., Wang, A. and Qu, D. (2015) Reduction of 4-chloronitrobenzene in a bioelectrochemical reactor with biocathode at ambient temperature for a long-term operation. J. Taiwan Inst. Chem. E., 46: 119-124.
[21] Van Aken, P., Van den Broeck, R., Degreve, J. and Dewil, R. (2015) The effect of ozonation on the toxicity and biodegradability of 2,4-dichlorophenol-containing wastewater. Chem. Eng. J., 280: 728-736.
[22] Monsalvo, V.M., Mohedano, A.F., Casas, J.A. and Rodriguez, J.J. (2009) Cometabolic biodegradation of 4-chlorophenol by sequencing batch reactors at different temperatures. Bioresource Technol. 100: 4572-4578.
[23] Wang, S., Loh, K. and Chua, S.S. (2003) Prediction of critical cell growth behavior of Pseudomonas putida to maximize the cometabolism of 4-chlorophenol with phenol and sodium glutamate as carbon sources. Enzyme Microb. Tech., 32: 422-430.
[24] Frascari, D., Zanaroli, G. and Danko, A.S. (2015) In situ aerobic cometabolism of chlorinated solvents: A review. J. Hazard. Mater., 283: 382-399.
[25] Nzila, A. (2013) Update on the cometabolism of organic pollutants by bacteria. Environ. Pollut., 178: 474-482.
[26] Ekman, A., Campos, M., Lindahl, S., Co, M., B Rjesson, P.L., Karlsson, E.N. and Turner, C. (2013) Bioresource utilisation by sustainable technologies in new value-added biorefinery concepts – two case studies from food and forest industry. J. Clean Prod., 57: 46-58.
[27] Albrecht, R., Perissol, C., Ruaudel, F., Petit, J.L. and Terrom, G. (2010) Functional changes in culturable microbial communities during a co-composting process: Carbon source utilization and co-metabolism. Waste Mange., 30: 764-770.
[28] Xie, S., Liu, J., Li, L. and Qiao, C. (2009) Biodegradation of malathion by Acinetobacter johnsonii MA19 and optimization of cometabolism substrates. J Environ Sci (China), 21: 76-82.
[29] Sari, A.A., Tachibana, S. and Itoh, K. (2012) Determination of co-metabolism for 1,1,1-trichloro-2,2-bis(4-chlorophenyl) ethane (DDT) degradation with enzymes from Trametes versicolor U97. J. Biosci. Bioeng., 114: 176-181.
[30] Prasse, C., Stalter, D., Schulte-Oehlmann, U., Oehlmann, J. and Ternes, T.A. (2015) Spoilt for choice: A critical review on the chemical and biological assessment of current wastewater treatment technologies. Water Res., 87: 237-270.
[31] Dixit, V. and Yadav, R.A. (2015) DFT-B3LYP computations of electro and thermo molecular characteristics and mode of action of fungicides (chlorophenols). Int. J. Pharmaceut, 491: 277-284.

Received: **05.04.2017**
Accepted: **25.07.2017**

CORRESPONDING AUTHOR

Zhirong Sun
National Engineering Laboratory for Advanced Municipal Wastewater Treatment and Reuse Technology,
Beijing University of Technology
100 Pingleyuan, Chaoyang District,
Beijing 100124 – P.R. CHINA

E-mail: zrsun@bjut.edu.cn

© by PSP Volume 26 – No. 10/2017 pages 6028-6034 Fresenius Environmental Bulletin

STUDY ON COKING WASTEWATER TREATMENT BY CATALYTIC SUPERCRITICAL WATER OXIDATION

Dong Xu*, Peifeng Wang, Rui Yang

College of Geomatics and Municipal Engineering, Zhejiang University of Water Resources and Electric Power, P.R. China

ABSTRACT

The removal effects of main toxic organic pollutants in coking wastewater by catalytic supercritical water oxidation (CSCWO) treatment process were investigated. The experimental results indicate that the degradation rates of the main pollutants in the coke wastewater increased with the increase of temperature, pressure, and oxidation coefficient (OC). Results showed that the most suitable conditions for CSCWO of coke wastewater are 470°C, 20 MPa, OC=5, catalyst dose 400 mg and residence time of 9 min. After treating the coke plant wastewater by CSCWO with above conditions, the main pollutants in the treated coke wastewater were degraded to a low level.

KEYWORDS:
Coke wastewater; Supercritical water; Catalytic oxidation; Pollutant removal rate

INTRODUCTION

Water pollution attributing to coking wastewater pollutants has appeared to be a globally serious issue in recent years, and this issue is much more obvious in China, where coal plays a very important role in the country's economic development and is treated as major energy resources [1-4]. Coking wastewater contains complex organic and inorganic contaminants, most of the containments are normally toxic, mutagenic and carcinogenic [5-7], once the coking wastewater without effective treatment is discharged into the river, and it will have severe and long-term impacts on environment and ecology [8].

Supercritical water oxidation (SCWO) has been proposed as a promising technology for complete destruction of waste that are rich in hazardous organic pollutants, such as sewage sludge, military wastes and variety of industrial wastes [9-11]. It is well known now that supercritical water behaves as an intermediate between its gaseous and liquid states and exhibits high diffusivity and good heat-transporting properties. The particular properties of SCW make the oxidation reaction occurring generally in a single fluid phase without transfer limitation in water/oxygen/organic mixture. In this way, the process involves a complete elimination of the target organic molecules to mainly water and carbon dioxide in SCW with excess oxygen in an extremely fast rate [12]. Furthermore, the low dielectric constant of SCW tremendously reduces the solubility of inorganic compounds (e.g. salts, oxides) and results in an efficient separation from water [13]. The process is being developed as an alternative to incineration since there is virtually no formation of NOx as results of the relatively lower operating temperature. Besides, dioxins and other undesired incineration by-products are normally not observed in SCWO process [14].

The SCWO process takes advantage of the unique SCW properties, where complex hydrocarbons are rapidly oxidized in SCW medium with >99% removal efficiency, producing liquid water, benign gases like CO_2 and N_2, and minor amounts of inorganic salts (depending on the feedstock composition). Such advantages potentially place SCWO as the technology to replace incineration, with added advantages: (i) zero toxic emissions, (ii) no ash formation (landfill issues), (iii) no predrying of waste is required. On the treatment hierarchy scale SCWO replaces the two most undesirable approaches namely landfill and disposal (incineration with no heat recovery) [15]. Furthermore, SCWO is highly exothermic, producing enough energy to make it self-sustaining in addition to production of green electricity [16].

MATERIALS AND METHODS

Experiment method and equipment. The experiment equipment is shown in Figure 1.

During the experiment, it compress the air in the steel bottle to the air preheat or with the air compressor. At the same time, through the high pressure liquid plunger pump, it infuses the simulation wastewater into the liquid preheated.

The gas, liquid raw material after the pretreatment mix well is sent into the reaction device. After the reaction, the mixture is sent the gas –liquid separation device after cooling. After the separation, the gas comes into the back pressure valve, through the

valve controlling the system pressure stably, the liquid is emission continuous.

Analysis method. The total organic content (TOC) in the sample was measured by a commercial TOC analyzer (EURO TECH, ET 1020A).

RESULTS AND DISCUSSION

Effect of different temperature on coking wastewater degradation. Effect of temperature on degradation rate of the coking wastewater is shown in Figure 2 and 3. From 390℃ to 470℃, with the increase of the temperature, the degradation rate of the coking wastewater obviously increases. TOC concentration of the coking wastewater obviously decreases with the increase of the temperature.

Effect of different reaction pressure on coking wastewater degradation. Fig. 4 and Fig.5 shows the effect of different reaction pressure on TOC removal and TOC concentration. When reaction pressure rises from 4 to 20 MPa, TOC removal demonstrated an imperceptible improvement. At 9 min, reaction pressure rises from 4 to 20 MPa, TOC removal increased from 86.1 to 98%.

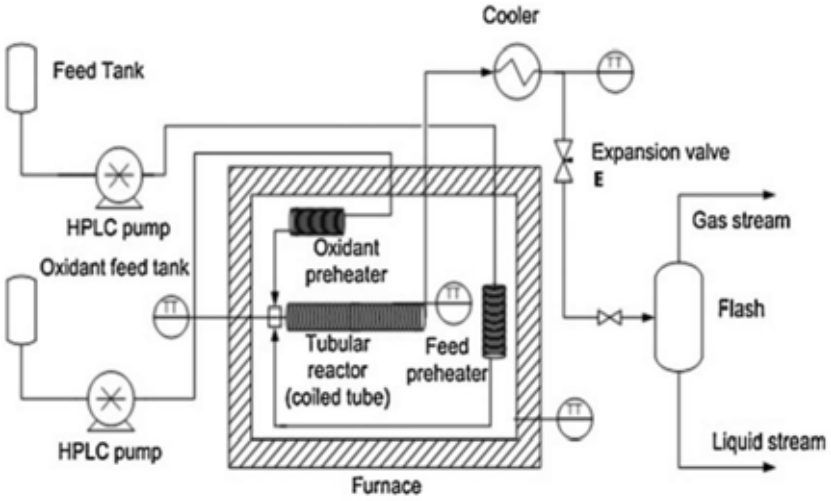

FIGURE 1
Schematic diagram of the SCWO apparatus

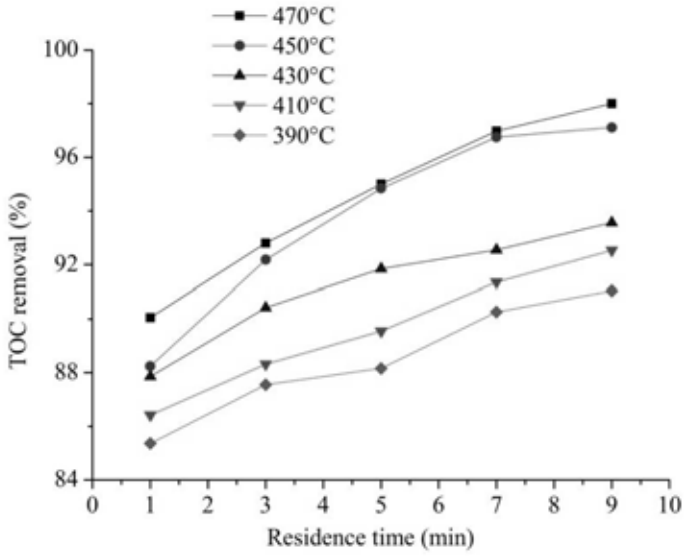

FIGURE 2
Effect of different temperature on TOC removal

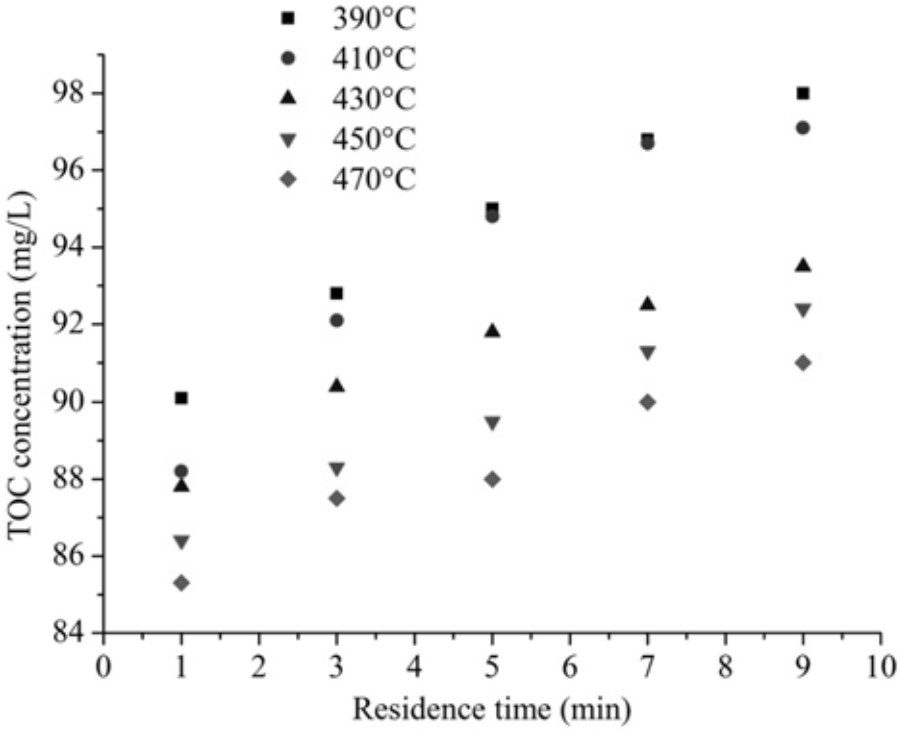

FIGURE 3
Effect of different temperature on TOC concentration

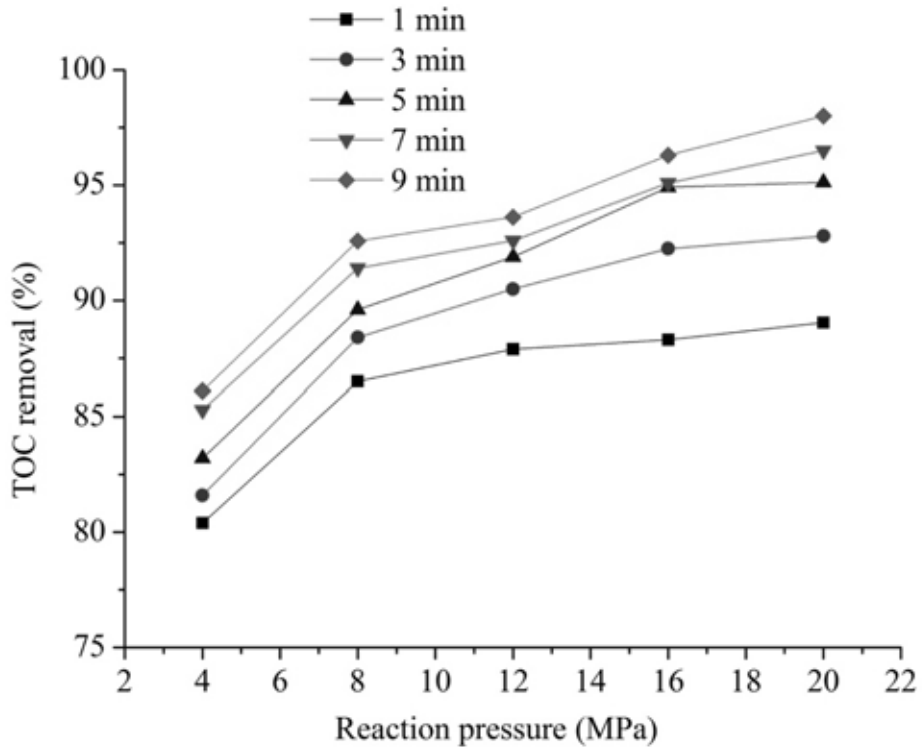

FIGURE 4
Effect of different reaction pressure on TOC removal

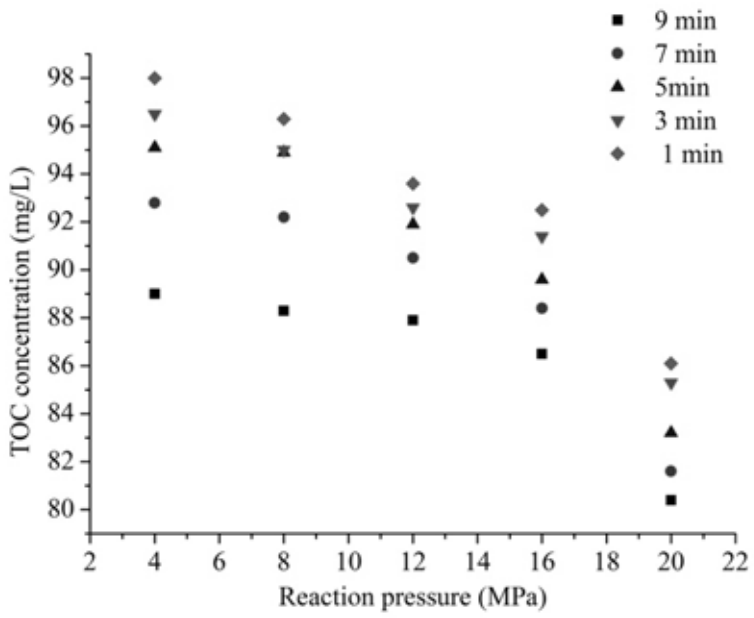

FIGURE 5
Effect of different reaction pressure on TOC concentration

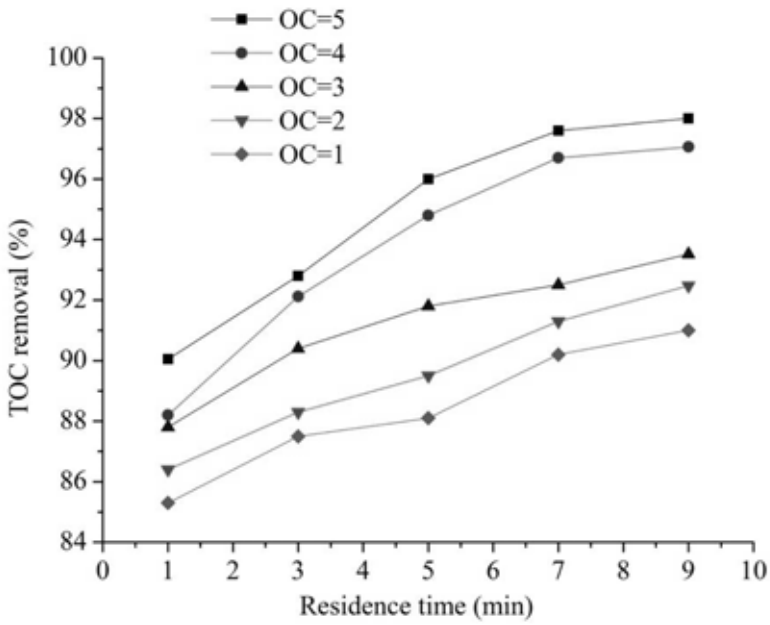

FIGURE 6
Effect of oxidation coefficient (OC) on TOC removal

Effect of oxidation coefficient (OC) on coking wastewater degradation. The variation of TOC and TOC removal versus OC are shown in Fig. 5 and 6. In the range of OC < 4, a significant improvement of TOC removal was observed by increasing OC. In the range of OC > 4, however, enhancement on TOC removal from OC is very limited. A maximum TOC removal of 98% was found at 470 °C and OC of 5, and the corresponding TOC at this point was 98 mg/L. At OC = 1, it also resulted in high TOC removal (85.3%). It indicates that, the presence of O_2 greatly improved the conversion of the contaminants. Even at lower oxygen concentration, a significant improvement on TOC removal can still be obtained.

Effect of catalyst on coking wastewater degradation. The variation of TOC and TOC removal versus catalyst dose are shown in Fig. 8 and 9. A significant improvement of TOC removal was observed by increasing catalyst dose. A significant reducement of TOC concentration was observed by increasing catalyst dose. When catalyst dose is 400 mg, TOC removal is 99.2%, it increased by 11.2% compared with not adding the catalyst.

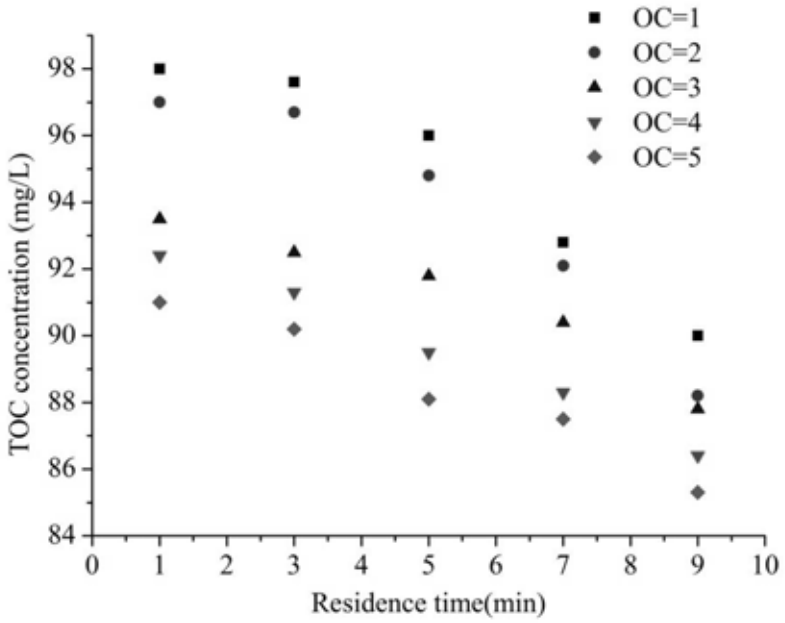

FIGURE 7
Effect of oxidation coefficient (OC) on TOC concentration

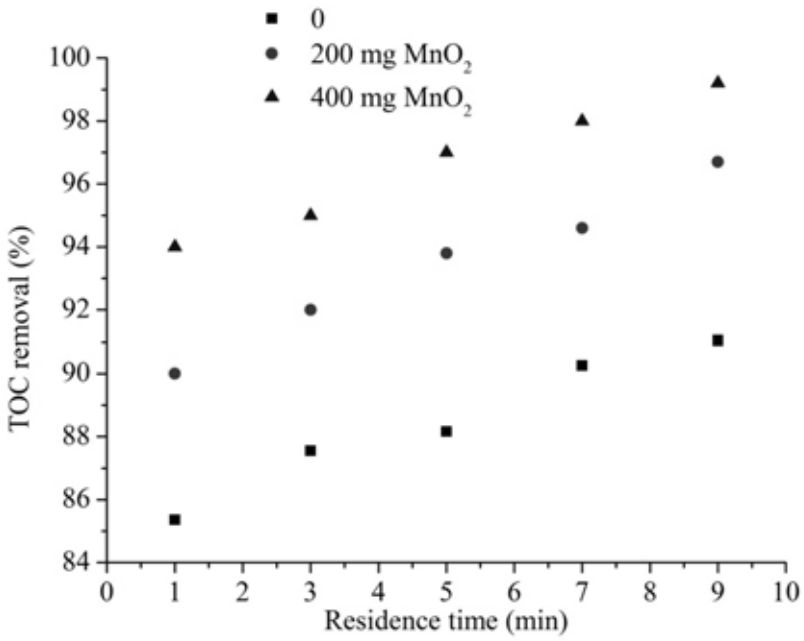

FIGURE 8
Effect of catalyst on TOC removal

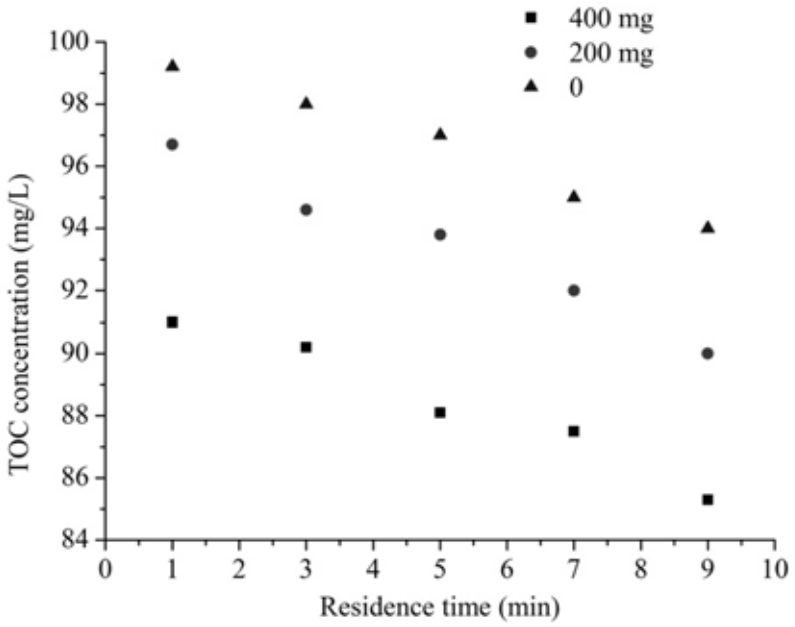

FIGURE 9
Effect of catalyst on TOC concentration

CONCLUSIONS

The active component is MnO_2. It adopts the equal volume to produce the good catalytic performance, and the effect of the catalytic oxidation in the coking wastewater is studied, the conclusion is as following:

On the basis of testing the coking wastewater, it makes sure the suitable process condition is that the most suitable conditions for CSCWO of coke wastewater are 470°C, 20 MPa, OC=5, catalyst dose 400 mg and residence time of 9 min. After treating the coke plant wastewater by CSCWO with above conditions, the main pollutants in the treated coke wastewater were degraded to a low level. TOC removal can reach to 99.2%, so it can reach to the emission standard of GB 8978-1996.

REFERENCES

[1] Gu, Q.Y., Sun, T.C. and Zhao, W.G. (2015) Study on the Electrochemical Oxidation Treatment of Coking Wastewater by DSA Anode. Oxid Commun, 38, 328-338.

[2] Tian G. L. (2016) Study on Coking Wastewater Treatment via Electrochemical Oxidation. Oxid Commun, 39, 2738-2742.

[3] Shokri, A., Mahanpoor, K. and Soodbar, D. (2016) Degradation of 2-nitrophenol from petrochemical wastewater by UV/$NiFe_2O_4$/Clinoptilolite process. Fresen. Environ. Bull., 25, 500-508.

[4] Peng, R.C., Yu, P. and Luo, Y.B. (2016) A comparative study of Fenton and electro-Fenton treatment for COD removal from coking industry wastewater. Fresen. Environ. Bull., 25, 3987-3992.

[5] Zhen S.C. (2015) Supercritical Water Gasification (SCWG) of Coking Wastewater. Oxid Commun, 38, 1464-1469.

[6] Bazrafshan, E., Biglari, H. and Mahvi, A.H. (2012) Phenol removal by electrocoagulation process from aqueous solutions. Fresen. Environ. Bull., 21, 364-371.

[7] Chu, L.B., Wang, J.L., Dong, J., Liu, H.Y. and Sun X.L. (2012) Treatment of coking wastewater by an advanced Fenton oxidation process using iron powder and hydrogen peroxide. Chemosphere, 86, 409-414.

[8] Jin, X.W., Li, E.C., Lu, S.G., Qiu, Z.F. and Sui Q. (2013) Coking wastewater treatment for industrial reuse purpose: Combining biological processes with ultrafiltration, nanofiltration and reverse osmosis. Journal of Environmental Sciences, 25, 1565-1574.

[9] Yan, Q., Hou, Y., Luo, J., Miao, H. and Zhang, H. (2016) The exergy release mechanism and exergy analysis for coal oxidation in supercritical water atmosphere and a power generation system based on the new technology. Energy

Conversion and Management, 129, 122-130.
[10] Bai, H. and Dai, W. Y. (2016) Alkaline Cleaning Solution Wastewater Treatment via Combined Coagulation and Supercritical Water Oxidation Processes. Oxid Commun, 39, 2722-2777.
[11] Benjumea, J.M., Sanchez-Oneto, J., Portela J.R. and Martinez de la Ossa E.J. (2017) Temperature control in a supercritical water oxidation reactor: Assessing strategies for highly concentrated wastewaters. Journal of Supercritical Fluids, 119, 72-80.
[12] Gong, Y.M., Guo, Y., Wang, S.Z. and Song, W.H. (2016) Supercritical water oxidation of Quinazoline: Effects of conversion parameters and reaction mechanism. Water Research, 100, 116-125.
[13] Liu, K., Zhang, Z.Y. and Zhang, F.S. (2016) Advanced degradation of brominated epoxy resin and simultaneous transformation of glass fiber from waste printed circuit boards by improved supercritical water oxidation processes. Waste Management, 56, 423-430.
[14] Zhu, Z.L., Xu, H., Jiang, D.F., Mao, X.P. and Zhang, N.Q. (2016) Influence of temperature on the oxidation behaviour of a ferritic-martensitic steel in supercritical water. Corrosion Science, 113, 172-179.
[15] Zhu, Z.L., Xu, H., Jiang, D.F., Yue, G.Q., Li, B.R. and Zhang, N.Q. (2016) The role of dissolved oxygen in supercritical water in the oxidation of ferritic–martensitic steel. Journal of Supercritical Fluids, 108, 56-60.
[16] Xu, D.H., Huang, C.B., Wang, S.Z., Lin, G.K. and Guo, Y. (2015) Salt deposition problems in supercritical water oxidation. Chemical Engineering Journal, 279, 1010-1022.

Received: **06.04.2017**
Accepted: **10.07.2017**

CORRESPONDING AUTHOR

Dong Xu
College of Geomatics and Municipal Engineering
Zhejiang University of Water Resources and Electric Power
Hangzhou 310018 – P.R. CHINA

Email: xudong99888@126.com

© by PSP Volume 26 – No. 10/2017 pages 6035-6042 Fresenius Environmental Bulletin

LEVELS OF CHLORINATED PESTICIDES IN HUMAN ADIPOSE TISSUE FROM BAGHDAD/ IRAQ

Mahmoud A Alawi*, Firas T Al-Tameemi, Sana'a Al-Aqqad

The University of Jordan, Department of Chemistry, Amman-11942, Jordan

ABSTRACT

Twenty human adipose tissue samples which were gathered from different hospitals in Baghdad/Iraq were analyzed for thirteen different chlorinated pesticide using gas chromatography with electron capture detector (^{63}Ni). Total concentration of all analyzed Organochlorine pesticides (OCP) in adipose tissue samples were 343.9±21.27 µg/kg. The *p,p'*-DDT concentrations were below the limit of detection however the *p,p'*-DDE levels were found the most abundant OCP in all analyzed samples with mean concentrations 83.86±3.87 µg/kg . The results of this study show that the concentrations of OCPs in human adipose tissues from Iraq were within the levels or lower than the values reported from other countries.

KEYWORDS:
Adipose tissues, Iraq, Organochlorine pesticides, GC-ECD.

INTRODUCTION

Chlorinated pesticides have raised global concern due to their persistence in the environment, impact on non-target organisms, and bioaccumulation in the humans and animals via food chain especially in lipid rich tissues and body fluids, such as adipose tissue [1, 2] and mother milk [3, 4]

Pesticides are substances or mixture of substances meant for attracting, repelling, seducing, and then destroying, or mitigating any pest [5]. The most common use of pesticides is as plant protection products, which in general protect plants from damaging influences such as weeds, plant diseases or insects [6]. This use of pesticides is so common that the term pesticide is often treated as synonymous with plant protection product, although it is in fact a broader term, as pesticides are also used for non-agricultural purposes. The lipid-rich tissues act as depots or reservoirs by virtue of physiochemical interactions of cellular components with them [7]. Thus, analysis of lipid-rich tissues indicates the magnitude of exposure and diffusion in the environment [8, 9].

The major risk of Organochlorine pesticides to human health is the increasing infertility of men, and the potential increased risk of breast cancer in women. A study on infertile men found increased levels of DDT metabolites in patients' blood [10]. Similar statistical work on women in New York found a significant increased risk of breast cancer in those with higher DDE levels in their adipose tissue [11].

The direct measurement of the chlorinated pesticides levels in human adipose tissue samples is a good indicator to show the extent of exposure to the polluted chemicals and to evaluate the health hazards. In general, after the American invasion in Iraq in 2003 and according to the UNEP report (2005), the Iraqi environment was expected to be polluted with different chemicals, especially the chlorinated pesticides [12]. This report was about Al Suwaira Pesticide Warehouses. Al Suwaira is located to the south of Baghdad. Approximately 100 cubic meters of waste pesticides are present in the warehouses and these are unsafe to use or even enter and will remain in that condition unless decontaminated, says the report. After March 2003, it was looted leading to containers being smashed and pesticides being spread around the buildings.

It is known that OCPs (not all pesticides) have been banned in Iraq since 1978 [11], but one has also to notice that: 1) the half life time for OCPs is very long and there was accumulation along the 70 years of use. 2) as mentioned above, there was a source of contamination of ca. 100 m^3 of pesticides in Al-Suwaira warehouse nearby Baghdad which was looted and smashed leading to contaminations. Therefore we expect that the Iraqi environment and the human body are contaminated with OCPs.

There are limited data of Organochlorine pesticide contamination levels in human body in Iraq. Al-Omar *et al.,* (1985) [14] studied the Organochlorine pesticide levels in human milk samples from Baghdad. Due to this, the results of the present study are considered important in terms of providing baseline data from different sources of OCP contamination in Iraq for future studies.

The objective of this study is to measure the human body burden through measuring the concentrations of chlorinated pesticides in human adipose tissues samples gathered from Baghdad/Iraq using gas chromatography with the Electron Capture Detectors (ECD), and then the potential influence of age, sex, smoking habits, and type of food consumption on the concentration of chlorinated pesticides will be investigated.

TABLE 1
Participants data

Participants	Sex	Age	Body weight	Smoker/non smoker	Food type
sample 1	Male	50 years	50 kg	Yes	meat
sample 2	Male	23 years	85 kg	Yes	vegetarian
sample 3	Male	35 years	106 kg	NO	vegetarian & meat
sample 4	Female	22 years	45 kg	NO	vegetarian
sample 5	Female	29 years	69 kg	NO	vegetarian
sample 6	Female	22 years	55 kg	NO	vegetarian & meat
sample 7	Male	60 years	72 kg	NO	meat
sample 8	Male	48 years	78 kg	Yes	meat
sample 9	Female	33 years	87 kg	NO	vegetarian
sample 10	Female	21 years	92 kg	NO	vegetarian
sample 11	Female	28 years	56 kg	NO	vegetarian & meat
sample 12	Male	54 years	60 kg	Yes	meat
sample 13	Female	32 years	65 kg	NO	vegetarian & meat
sample 14	Female	26 years	47 kg	NO	vegetarian & meat
sample 15	Female	16 years	65 kg	NO	meat
sample 16	Female	60 years	67 kg	NO	vegetarian & meat
sample 17	Male	19 years	90 kg	NO	vegetarian & meat
sample 18	Male	39 years	73 kg	NO	meat
sample 19	Female	15 years	45 kg	NO	vegetarian
sample 20	Female	15 years	75 kg	NO	vegetarian

MATERIALS AND METHODS

Sampling and sample locations. Twenty adipose tissue samples combined with questionnaires about many factors (age, weight, job, smoking, working) were gathered from patients in cooperation with competent physicians and nurses from three different hospitals (Al-Kadhimiya, Al-Yarmouk and Al-Kindy hospital), in Baghdad/Iraq.

Samples were collected with the help of surgeons from patients performing surgery in the above mentioned hospitals. Adipose tissue samples were obtained from the patients after getting their permission in the period January - February 2014. All samples were stored at -20

^{o}C until analysis. Information like sex, age, body weight etc. is listed in Table 1. The mean age of the monitored population was 32.4 years (range 15-60). Divided according to sex, the mean age for females was 26.6 years (range 15-60), and for males was 41 years (range 19-60).

Chemicals and Reagents. Chlorinated pesticides standards: α -HCH, ß-HCH, Heptachlor, Heptachlor-epoxide, Aldrin, Dieldrin, Endrin, *p,p`*-DDT, *o,p`*-DDT, *p,p`*-DDD, *o,p`*- DDD, *p,p`*-DDE and HCB (All standards of 97% - 99% purity) were purchased from Dr. Ehrenstorfer (Augsburg, Germany). The chemicals used for extraction were purchased as follows: Florisil 60, 100 mesh (Riedel-de Haën, Germany), Florisil was activated by heating at 550 °C for 5 hours. After cooling in a dessicator, it was mixed with de-ionized water to give (3% w/w) mixture. This mixture was shaken for 15 minutes and kept overnight in a closed container prior to use. Anhydrous sodium sulfate, extra pure for analysis (Sheung-city Gyonggi – do Korea). Dichloromethane, HPLC-grade was purchased from Janssen Chimica, (Belgium), *n*-Hexane, ACS grade, >95% was purchased from TEDIA, (USA). Petroleum ether, ACS grade, 95% was purchased from Carlo Erba, (Italy).

Sample Extraction and Clean-Up. Human adipose tissue samples were extracted according to the method of Alawi *et al.,* 1991 [15] with slight modification. One gram of each homogenized adipose tissue sample was extracted in a Soxhlet apparatus for 4 hours using 180 ml of petroleum ether. The solvent was then evaporated using the rotary evaporated at 40º C and 40 mbar to ca. 3 ml.

A glass column (30 x 1.6 cm) was filled as follows: 25 g of Florisil (3% w/w deionized water) was filled into the column then 1 cm of anhydrous sodium sulfate was added. This column was washed with 100 mL petroleum ether. The residues from the extraction step were added to the column and eluted with 60 mL dichloromethane and 240 petroleum ether. The eluates were evaporated at 40º C and 100 mbar to ca. 1ml, then to dryness using a gentle stream of nitrogen. The residues were dissolved in 1.0 mL n-hexane containing 1 µg/ml internal standard (Isodrin), and then 1 µl was injected onto the GC/ECD column [8].

GC Analysis. Gas chromatograph (GC) (Varian, model) was used for the analysis of OC- pesticides. GC was equipped with split- splitless injector, ^{63}Ni-ECD (electron capture detector), and a fused silica capillary column ZPB-5 (nonpolar, 30 m x 0.25 mm, 0.25 µm film thickness). The GC was interfaced with computer for further integration, calibration, and calculation.

GC/ECD operating conditions :Split ratio: 1:10, Injector temperature: 250 °C, Oven temperature program: 150°C (5 min.), 150-220°C (14 °C/min), 220°C (20 min.), 220-250 °C (20°C/min.) and 250 °C (10 min).Detector temperature: 300°C.

Carrier gas: He, (99.999% purity).Carrier gas flow rate: 1.1 ml/min. Make up gas: Argon-methane 95:5% (99.999% purity).Make up gas flow rate: 25 ml/min.

Each sample was analyzed in triplicate (weighing, Soxhlet extraction and Florisil column clean up) and each extract was injected onto the GC/ECD-column three times. For each 5 samples, a chromatogram of the standard mixture was produced. Then the relative peak areas (RPA) for each compound with the IS, in the unknown chromatogram and the standard mixture chromatogram were calculated, then a comparison was made between RPA for the standard and RPA for the unknown with concentration in the standard mixture to calculate the concentration in the unknown as follows:

Concentration of (X), unknown sample =

$$\frac{\text{Concentration of (X) in the standard x (RPA) unknown}}{\text{(RPA) standard in the mixture}}$$

Method Validation. Linear Range. For the calculation of the performance data, a calibration was carried out at with five concentration levels (100, 200, 400, 750 and 1000 µg/L) of the chlorinated pesticides. From the resulting calibration curves, the regression coefficients were calculated, characterizing the linearity of the calibration function. The regression coefficients were between 0.992 and 0.997, indicating a good linearity of the calibration function in this concentration range.

TABLE 2
Peak number in the chromatogram, Retention time (t_R), Limit of detection (LOD) and Limit of quantitation (LOQ) for the studied chlorinated pesticides

Peak No.	Pesticides	Retention time [min]	LOD (µg/kg)	LOQ (µg/kg)
1	α-HCH	8.3	2.3	7.67
2	HCB	8.5	2.8	9.33
3	β-HCH	9.0	11.1	37.00
4	Heptachlor	10.3	4.3	14.33
5	Aldrin	11.0	2.4	8.00
6	Heptachlor epoxide	12.0	2.5	8.33
7	*p,p'*-DDE	13.6	11.1	37.00
8	Dieldrin	13.7	3.4	11.33
9	*o,p'*-DDD	13.9	21.9	73.00
10	Endrin	14.5	5.3	17.67
11	*o,p'*-DDT	15.2	19.2	64.00
12	*p,p'*-DDD	15.4	21.1	70.33
13	*p,p'*-DDT	17.0	22.4	74.67

Detection Limits and Limits of Quantitation. The limits of detection (LODs) and limits of quantitation (LOQs) were determined for chlorinated pesticides as shown in Table 2. The calculated LODs represent the lowest concentration levels at which the target compounds could be detected with a signal-to-noise ratio of 3 and found to be in the range 2.3 – 22.4 µg /kg for the studied pesticides. The LOQs were determined as signal-to-noise ratio of 10 and found to be in the range from 7.67– 74.67µg /kg for the chlorinated pesticides. LODs, LOQs and the corresponding retention times of the studied compounds are shown in Table 2.

Recoveries. Three samples, each of one gram sheep adipose tissue blank sample were spiked with the chlorinated pesticides standard mixture to give the concentrations of 100, 500 and 1000 µg/kg. These samples were mixed thoroughly and extracted, cleaned-up and analyzed according to the above mentioned method. The recovery tests were done in triplicate at different times. The average recoveries of chlorin6ted pesticides were found between 87 and 116%. All recoveries were found to lie within the acceptable range for trace analysis of 80-120 % [14].

Instrument Precision of Chlorinated Pesticides. The precision of the instrument was measured through the injection of standard solutions (100, 500, 1000 µg/L) each three times. The coefficients of variation (CV) were found to be less than the acceptable limit value for trace analysis (CV <15%) [15], these results mean that the method have a good instrument precision.

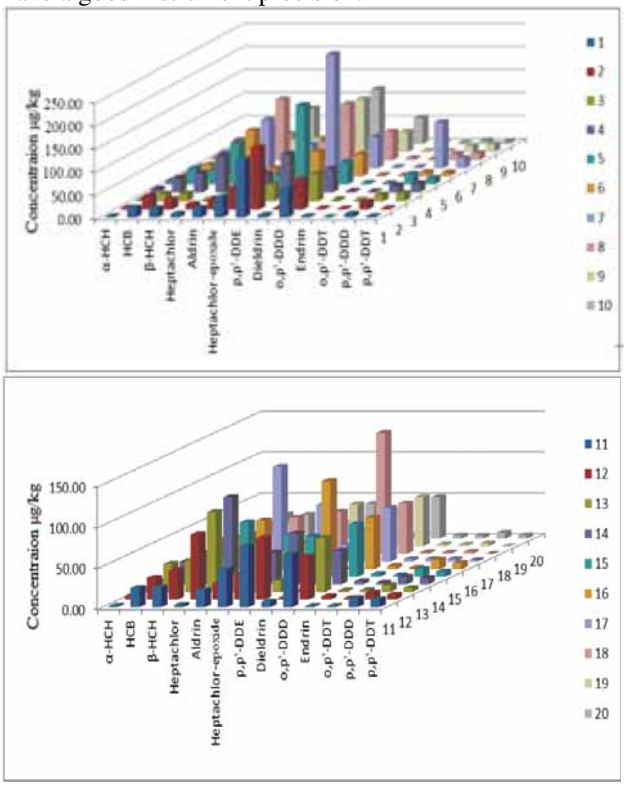

FIGURE 1
Concentrations of chlorinated pesticides in human adipose tissue samples 1-10 and 11-20

TABLE 3
Concentration (average ± standard deviation) of the individual pesticides in the studied 20 samples in [µg/kg]; total concentration in each sample; average total concentration for all samples, and the average concentration of each pesticide in all samples.

Sam-ple #	α - HCH	HCB	β-HCH	Hepta-chlor	Al-drine	H-chlor epox-ide	*p,p'*-DDE	Dieldrin	*o,p*-DDD	En dri n	*o,p'*-DDT	*p,p'*-DDD	*p,p'*-DD T	∑All pesti-cides
1	2.89± 0.16	21.56± 0.95	20.68± 1.03	8.61 ± 0.64	20.98± 1.63	41.93± 1.06	119.19 ±4.60	5.79 ± 0.09	60.21 ± 9.31	< d. L	< d.L	< d.L	< d.L	301.84 ±19.47
2	3.75± 0.55	28.03± 3.78	20.27± 0.62	11.86± 1.30	22.14± 2.51	46.39± 3.94	129.67 ±5.75	< d.L	63.58± 4.59	< d. L	< d.L	< d.L	< d.L	325.92 ±23.04
3	2.58± 0.35	14.36± 1.68	14.98± 1.75	< d.L*	15.86± 1.34	43.51± 0.23	35.21± 3.04	12.03±0. 23	58.27± 2.71	< d. L	< d.L	< d.L	< d.L	196.80 ±11.33
4	7.80± 0.41	31.31± 0.53	41.32± 2.27	79.18 ±0.52	31.62± 4.30	40.73± 1.60	83.50 ±6.38	13.95±1. 55	51.69 ±6.89	< d. L	< d.L	< d.L	< d.L	381.11 ±24.45
5	7.24± 0.65	34.49± 5.11	30.76± 3.52	89.78± 9.85	29.10± 3.04	20.68± 1.94	161.48 ±8.80	3.98±0.5 8	48.49± 4.09	< d. L	< d.L	22.35± 2.84	< d.L	448.35 ±37.58
6	3.48± 0.39	25.01± 0.79	26.95± 2.61	99.12± 11.75	17.31± 0.40	29.43± 0.62	53.38± 5.45	5.32±0.0 6	47.85± 1.21	< d. L	< d.L	< d.L	< d.L	307.85 ±23.28
7	4.33± 0.59	33.38± 2.64	30.60± 1.75	104.94 ±9.68	18.39± 1.19	50.09± 6.85	237.06 ±7.54	< d.L	67.27± 8.31	< d. L	< d.L	99.76± 5.82	< d.L	645.82 ±44.37
8	3.90± 0.44	43.85± 6.34	39.87± 4.12	121.84 ±3.96	14.06± 1.57	40.16± 5.38	112.10 ±1.48	11.91±1. 14	61.43± 4.44	< d. L	< d.L	< d.L	< d.L	449.60 ±28.87
9	3.55± 0.37	20.64± 0.65	27.26± 3.42	26.68± 2.18	29.59± 4.39	11.64± 1.33	109.52 ±6.86	< d.L	43.65± 5.98	< d. L	< d.L	< d.L	< d.L	272.53 ±25.18
10	5.12± 0.35	31.76± 2.46	22.27± 3.22	77.07± 2.29	18.87± 1.11	42.45± 4.72	118.73 ±3.57	< d.L	56.80± 1.23	< d. L	< d.L	< d.L	< d.L	373.07 ±18.98
11	< d.L	23.63± 0.85	24.49± 1.60	< d.L	20.79± 1.42	46.25± 0.26	75.27± 0.60	6.95±0.2 5	64.98± 0.63	< d. L	< d.L	< d.L	< d.L	262.36 ± 5.61
12	5.03± 0.08	26.95± 0.32	35.98± 0.55	80.16± 0.99	20.30± 0.19	31.98± 0.60	75.29± 1.01	< d.L	52.61± 2.03	< d. L	< d.L	< d.L	< d.L	328.60 ± 5.77
13	4.88± 0.59	34.54± 0.85	38.82± 4.11	97.76± 8.68	21.19± 1.51	60.15± 8.37	13.78± 1.58	< d.L	65.97± 8.86	< d. L	< d.L	< d.L	< d.L	337.09 ±34.55
14	4.88± 0.61	27.98± 0.67	32.18± 1.73	102.11 ±3.38	14.70± 1.33	39.21± 3.29	62.50± 6.72	11.22±0. 40	40.93± 3.18	< d. L	< d.L	< d.L	< d.L	335.71 ±21.31
15	3.29± 0.44	29.52± 2.03	25.93± 2.65	66.86± 5.03	21.95± 1.19	51.37± 7.67	49.30± 4.82	6.34±0.6 7	64.41± 6.61	< d. L	< d.L	< d.L	< d.L	318.97 ±31.11
16	7.62± 0.45	36.05± 2.05	39.61± 0.81	59.70± 1.46	22.46± 0.48	30.60± 1.23	108.10 ±1.69	< d.L	62.79± 1.59	< d. L	< d.L	< d.L	< d.L	366.93 ± 9.76
17	4.31± 0.02	27.37± 2.70	22.52± 1.20	116.17 ±3.86	23.40± 1.56	69.35± 0.70	19.54± 0.83	39.10±0. 76	65.70± 0.15	< d. L	< d.L	< d.L	< d.L	387.46 ±11.78
18	3.42± 0.29	24.49± 2.14	23.29± 2.51	44.28± 0.48	16.35± 0.73	51.59± 2.75	< d.L	143.44± 8.56	61.79± 6.69	< d. L	< d.L	< d.L	< d.L	368.63 ±24.15
19	4.89± 0.31	30.40± 2.68	28.14± 0.00	6.78±0 .45	18.92± 0.06	51.49± 2.28	16.33± 1.89	44.86±0. 44	60.59± 6.42	< d. L	< d.L	< d.L	< d.L	262.40 ±14.53
20	4.53± 0.19	29.83± 0.75	29.26± 0.18	10.77± 0.18	20.36± 2.32	42.63± 0.69	13.47± 0.92	5.09±0.3 8	51.13± 4.64	< d. L	< d.L	< d.L	< d.L	207.07 ±10.25
Av-erage	4.61 ±0.38	28.77 ±1.99	28.76 ±1.98	66.87 ±3.70	20.92 ±1.61	42.08 ±2.78	83.86 ±3.87	23.84 ±1.16	57.51 ±4.48	< d. L	< d.L	6.11 ± 0.43	< d.L	**∑aver age 343.90 ±21.27**

*< d.L = under detection limit

RESULTS AND DISCUSSION

In this study, thirteen of the chlorinated pesticides have been determined in human adipose tissue samples collected from different regions of Baghdad/Iraq.

Comparing the concentration of studied thirteen compounds, one notice that the α-HCH was found in the range from below detection limit (sample 11) to7.8 µg/kg (sample 4). HCB was found in the concentration range between 14.36 µg/kg (sample 3) and 43.85 µg/kg (sample 8). β-HCH was found in the concentration range between 14.36 µg/kg (sample 3) and 41.32 µg/kg (sample 4). Heptachlor was found in the concentration range between below detection limit (samples 3 and 11) and 121.84 µg/kg (sample 8). Aldrine was found in the concentration range between 14.06 µg/kg (sample 8) and 31.62 µg/kg (sample 4). Heptachlor epoxide was found in the concentration range between 11.64 µg/kg (sample 9) and 69.35 µg/kg (sample 17). *p,p'*-DDE was found in the concentration range between below detection limit (sample 18) and 237.06 µg/kg (sample 7).

Dieldrin was found in the concentration range between below detection limit (samples 2, 7, 9,10,12,13 and 16) and 143.44 µg/kg (sample 18). *o,p'*-DDD was found in the concentration range between 40.93 µg/kg (sample 14) and 67.27 µg/kg (sample 7). *p,p'*-DDD was found at 22.35 and 99.79 µg/kg in two samples 5 and 7. Endrin, *o,p'*-DDT and *p,p'*-DDT were found below detection limit in all human adipose tissue samples. All previous results are presented in Figures 1 and Table 3.

Of the thirteen individual studied pesticides, 10 were detected in at least 10 % of all samples (n = 20); their frequencies of detection are shown in Figure 2. Five pesticides; HCB, *β*-HCH, Aldrin, Heptachlor epoxide, *o,p'*-DDD were found with frequency of almost 100%, followed by α-HCH, *p,p'*-DDE, were presented in 95% of the studied samples. Heptachlor was detected in 90%, Dieldrin in 60%, *p,p'*-DDD in 10% of the studied human adipose tissue samples.

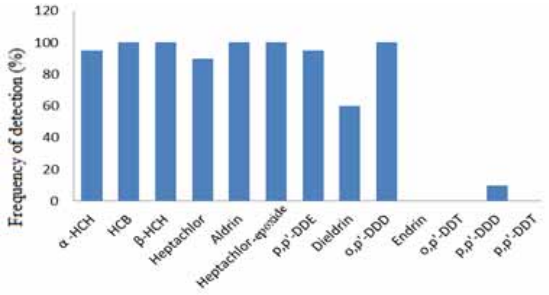

FIGURE 2
Percent frequency of individual congeners of the chlorinated pesticides detected in all human adipose tissue samples (n = 20)

The total concentration of all studied pesticides in all samples was ranged between 197 and 646 µg/kg.

Although α-HCH comprises the majority of HCH technical mixture, ranging from 55 to 80 % [17], the mean concentration of *β*-HCH was detected at high mean concentration (14.36 – 41.32 µg/kg) due to its greater persistency compared to other HCH isomers [18]. In this study, HCH concentrations were lower than those of DDTs in human adipose tissue samples of Iraq males and females (see Table 4), due to greater bioaccumulation potential of DDTs than HCHs [16]. A similar pattern is also found in the level of total HCHs for all countries mentioned in Table 4.

TABLE 4
Comparison of average concentrations (µg/kg) of DDTs, HCHs and HCB of Iraqi participants with those reported from other countries.

country	n*	Sex	Sampling year	Total DDT_s	Total HCH_s	HCB	References
		8 Male		162	27	28	
Iraq	20	12 Female	2014	135	36	30	This paper
Korea	53	Female	2008-2009	250	12	9	Moon *et al., 2012* [19]
Japan	10	Female	2003-2004	1300	900	35	Kunisue *et al.* 2007 [20]
Singapore	88	Female	2004-2006	640	190	20	Tan *et al*., 2008 [21]
The Czech Republic	98	5 Male & 93 female	2007	616	24		Pulkrabova' *et al.,* 2009 [22]
Italy	12	9 Male & 3 Female	2005-2006	2040	74	152	Schiavone *et al.,* 2010 [23]
Turkey	25	Infertile men	2002-2007	681	342	125	Cok *et al*., 2010
	21	fertile men		556	265	100	[24]
Mexico	80	60 Male & 20 Female	2008	2589	72	n.d	Waliszewski *et al*., 2010 [25]
		21 Male		10060	938	446	Alawi & Ababneh 1991
Jordan	32	11 Female	1990	12800	1715	710	

n* : Number of samples

Although the sampling campaign was different among investigated countries, the overall mean concentrations of the DDTs in human adipose tissues of Iraqi participants were the lowest among all countries mentioned in Table 4; for the HCHs the Iraqi samples show the third lowest concentration after Korea and the Czech Republic while the concentration of HCB in the Iraqi samples show also the third lowest concentration after Korea and Singapore. This low concentration of the studied OCPs could be attributed to two factors. First the stop of use of all chlorinated pesticides in Iraq since 1978, and the second factor is the stop of using pesticides in the past one and half decade due to the war.

The main objective of this study was to measure the levels of human contamination with OCPs and it was not expecting that these contaminants are interring the human body from the local environmental contaminations, but as known the main source of the body burden is the food contaminations. Therefore we are surprised to find low levels of OCPs in the Iraqi adipose tissues which meansthat the imported (no local production during the war) have low levels of OCPs. *p,p'*-DDT was found in all studied human adipose tissue samples at a concentration below the lower limit of detection, but *p,p'*-DDE was found among the most abundance pesticides with a mean concentration of 83.86±3.87 µg/kg. In several other studies (Table 4), much higher concentrations (5-10 times more) were found with higher mean concentration [2; 26 – 27]. DDE, the primary metabolite of DDT, is rarely excreted from the body [28]; thus, the association between age and *p,p'*- DDE could be explained by the fact that DDE levels increase when DDT is metabolized.

Levels of some pesticides such as heptachlor and *p,p'*-DDE were highest among the oldest participants in our study, which is a common finding [29 – 31] and probably due to the longer period of exposure to the bioaccumulating chlorinated pesticides. Also the concentrations of OCPs in the Iraqi environment during the 1960s and 1970s were higher than they are today, leading to much higher body burdens in older people.

There is no correlation found between concentrations of HCB and HCHs with other variables like sex, but the concentration of the DDTs was found a little bit higher in males compared with females (Table 4)

Many persistent compounds can still be detected in samples of the human body decades after they are banned. For example, DDT_s was banned in Iraq in 1978 [15] but its breakdown products DDE and the insecticide DDT are still detected in the human adipose tissue samples because its estimated half life time in the environment is 2-15 years [32].

CONCLUSIONS

In summary, the results of this study show that the concentrations of chlorinated pesticides in human adipose tissues from Iraq are within the levels or lower than the values reported from other countries. The highest concentration of the chlorinated pesticides was in sample 7 because the patient lives in Al-amil-district adjacent area of agricultural land is exposed often to spraying pesticides. Finally, we found that there is a relationship between the concentration of chlorinated pesticides and the place where the patient lives. There is no correlation between concentrations of chlorinated pesticides and with other variables like sex, smoking and meal type in the human adipose tissue samples.

ACKNOWLEDGEMENT

The authors would like to thank the Deanship for Academic Research at the University of Jordan. Also thanks are due to Dr. Ibrahim Tarawneh and Dr. Sharif Arar for their valuable help.

Compliance with Ethical Standards. Informed consent was obtained from all individual participants included in the study.

The protocol of this research project has been approved by a constituted Ethics Committee of the institutions within which the samples were collected.

Declaration of interest. The authors report no declaration of interest regarding the publication of this manuscript.

REFERENCES

[1] Alawi, M., Ababneh, M. (1991) Residue Analysis of Chlorinated Pesticides in Jordanian Human Adipose Tissues. Analytical Letters (1991) 24 (10): 1897-1911.

[2] Alawi, M., Tamimi, S., and Jaghabir, M. (1999) Storage of organochlorine pesticides in human adipose tissues of Jordanian males and females. Chemosphere 38(12): 2865-2873.

[3] Alawi, M.A., Al-Antary, T.M, Estityha, H., Al-Aqqad, S., and Al-Oqlah, K. (2013) Comparative Study for Chlorinated Pesticides in Mother Milk from Jordan in Four Studies between 1993 and 2003 Fresen. Environ. Bull., 22(1A): (279-285).

[4] Alawi, M.A., AlAntary, T.M., Estityha, H., Al-Aqqad, S. (2015) Chlorinated pesticides residues in human breast milk from southern Jordan: Comparative study between 2008 and

2012. Fresen. Environ. Bull., 24: 4512-4518.

[5] US Environmental Protection Agency (July 24, 2007), what is a pesticides epa.gov. Retrieved on September 15, 2007.
[6] WHO (1989) Public health impact of pesticides used in agriculture, Report of WHO/UNEP working group, WHO, Geneva.
[7] Mussalo-Rauhamaa, H. (1991) Partitioning and levels of neutral organochlorine compounds in human serum, blood cells, and adipose and liver tissue. Science of the Total Environment 103: 159–175.
[8] Adeshima, F., and Todd, E.L. (1991) Exposure assessment of chlorinated pesticides in the environment. Journal of Environmental Science and Health, A 26: 139–153.
[9] Sasaki, K., Ishizaka, T., Suzuki, T., Takeda, M., and Uchiyama, M. (1991) Accumulation levels of organochlorine pesticides in human adipose tissue and blood. Bulletin of Environmental Contamination and Toxicology 46: 662–669.
[10] Pines, A., Cusoc, S., Ever-Hadani, P., and Ron, M. (1987) Some organochlorine insecticide and polychlorinated biphenyl blood residues in infertile males in the general Israli population of the middle 1980s. Arch. Environ. Contam. Toxicology 16: 587- 597.
[11] Wolff, M.S., Toniolo, P.G., Lee, E.W., Rivera, M., and Dublin, N. (1993) Blood levels of organochlorine residues and risk of breast cancer. J. Nat. Cancer Inst. 85: 648.
[12] United Nations Environment Programme, Toxic Sites in Iraq to be Made Safe, Geneva/Nairobi, 10 November 2005.
[13] Shalli, A.K., AL-Saadi, S.H., and AL-Okaily, A.K. (1980) Status of resistance of anopheline mosquitoes in Iraq, A.V. manoucher. 40: 535-540.
[14] Al-Omar, M., Tawfiq, S.J., Al-Ogaily, N. (1985) Organochlorine residue levels in human milk from Baghdad. Bulletin of Environmental Contamination and Toxicology 35(1): 65-67.
[15] Alawi, M.A., and Ababneh, M. (1991) Residue analysis of Chlorinated pesticides in Jordanian human adipose tissues. Analytical Letters 24(1):1897-1911.
[16] Gonzalez, G., Herrador, A.M., and Asuero, A.G. (2010) Intra-laboratory assessment of method accuracy (trueness and precision) by using validation standards. Talanta 82: 1995-1998.
[17] Willett, K.L., Ulrich, E.M., and Hites, R.A. (1998) Differential toxicity and environmental fates of hexachlorocyclohexane isomers. Environ Sci Technol. 32: 2197–2207.
[18] Loganathan, B.G., and Kannan, K. (1994) Global organochlorine contamination trends: an overview. Ambio, 23: 187–191.
[19] Moon, H.B., Duk, H.L., Yoon, S.L., Minkyu, C., Hee-Gu, C., and Kurunthachalam, K. (2012) Polybrominated diphenyl ethers, polychlorinated biphenyls, and organochlorine pesticides in adipose tissues of Korean women. Arch Environ Contam Toxicol. 62: 176–184.
[20] Kunisue, T., Takayanagi, N., Isobe, T., Takahashi, S., Nose, M., and Yamada, T. (2007) Polybrominated diphenyl ether and persistent organochlorines in Japanese human adipose tissue. Environ Int. 33: 1048-1056.
[21] Tan, J., Li, Q.Q, Loganath, A., Chong, T.S., Xiao, M., Obbard, J.P. (2008), Multivariate data analyses of persistent organic pollutants in maternal adipose tissue in Singapore**.** Environ Sci Technol. 42: 2681-2687.
[22] Pulkrabova, J., Hradkova, P., Hajšlova, J., Poustka, J., Napravnikova, M., and Polaĉek, J. (2009) Brominated flame retardants and other organochlorine pollutants in human adipose tissue samples from the Czech Republic. Environ Int. 35, 63-68.
[23] Schiavone, A., Kannan, K., Horii, Y., Focardi, S., and Corsolini, S. (2010) Polybrominated diphenyl ethers, polychlorinated naphthalenes and polycyclic aromatic musks in human fat from Italy: comparison to polychlorinated biphenyls and organochlorine pesticides. Environ Pollunt. 158: 599-606.
[24] Cok, I., Durmaz, T.C., Durmaz, E., Satıroglu, M.H., Kabukcu, C. (2010) Determination of organochlorine pesticide and polychlorinated biphenyl levels in adipose tissue of infertile men. Environmental Monitoring and Assessment 162 (1-4): 301-309.
[25] Waliszewski, S.M., Valencia, Q.R., Corona, C.A., Herrero, M., Sanchez, K., Aguirre, H., Aldave, I.A., Gomez, A.S., and Villalobos, P.R. (2010) Comparison of organochlorine pesticide levels in human adipose tissue of inhabitants from Veracruz and Puebla, Mexico. Arch Environ Contam Toxicol. 58: 230–236.
[26] Focardi S, Fossi C, Leonzio C, and Romei R. (1986) PCB hexachlorobenzene, and organochlorine insecticides in human fat in Italy. Bull Environ Contam Toxicol. 36: 644-650.
[27] Waliszewski, S.M., Aguirre, A.A., Infanzon, R.M., Rivera, J., Aguirre, A., and Infanzon, R. (1998) Time trend of organochlorine pesticide residues in human adipose tissue agriculture in Veracruz (Mexico) 1988-1997 survey. Sci. Total Environ. 221: 201-204.
[28] ATSDR (1992), Toxicological Profile for *4, 4-*DDT, 4, 4 -DDE, 4, 4-DDD. Agency for Toxic Substances and Disease Registry, Atlanta, GA, USA.
[29] Laden, F., Neas, L.M., Spiegelman, D., Hankinson, S.E., Willett, W.C., Ireland, K., Wolff, S., Hunter, D.J. (1999) Predictors of plasma concentrations of DDE and PCBs in a

group of U.S. women. Environ Health Perspect 107: 75–81.
[30] Glynn, A.W., Granath, F., Aune, M., Atuma, S., Darnerud, P.O., Bjerselius, R., Vainio, H., and Weiderpass, E. (2003) Organochlorines in Swedish women: determinants of serum concentrations. Environ Health Perspect. 111: 349–355.
[31] Vaclavik, E., Tj_nneland, A., Stripp, C., Overvad, K., Philippe, W.J. and RaaschouNielsen, O. (2006) Organochlorines in Danish women: predictors of adipose tissue concentrations. Environ Res. 100: 362–370.
[32] US Environmental Protection Agency (1989) Environmental Fate and Effects Division, Pesticide Environmental Fate One Line Summary: DDT (*p, p'*). Washington, DC.

Received: **10.07.2017**
Accepted: **21.07.2017**

CORRESPONDING AUTHOR

Mahmoud A Alawi
The University of Jordan, Department of Chemistry, Amman-11942, Jordan

e-mail: alawima@ju.edu.jo

© by PSP Volume 26 – No. 10/2017 pages 6043-6048 Fresenius Environmental Bulletin

AN ESTIMATION OF SOME PLANT TRAITS WITH THE REMOTE SENSING METHOD IN THE NARBON BEAN (*VICIA NARBONENSIS* L.)

Yasar Ozyigit*

Akdeniz University Korkuteli Vocational High School, Antalya, Turkey

ABSTRACT

The aim of this study was to estimate some biochemical and biophysical properties of plants such as chlorophyll content, water content and plant height at the seedling stage, using spectral reflectance values in the narbon bean (*Vicia narbonensis* L). The study was carried out in greenhouse conditions and in plastic pots. Seven nitrogen treatments (0, 5, 10, 15, 20, 25, 30 kg.da^{-1}) were applied and the experiment was designed in randomized plots with 3 replications. The reflectance measurements were taken using a portable spectroradiometer measuring the wavelength range of 325-1075 nm of the electromagnetic spectrum. A portable chlorophyll meter was also used to determine chlorophyll content. According to results of the study, good relationships were recorded between plant traits and spectral reflectance value. In particular, there was a linear relationship (r=0.68) between chlorophyll content and red region reflectance of spectrum. The results have shown that spectral reflectance data could be used to estimate especially the chlorophyll content at the seedling stage of the narbon bean.

KEYWORDS
Chlorophyll, narbon bean, plant height, remote sensing, water content,

INTRODUCTION

The biochemical and biophysical properties of plants (such as nutrient and chlorophyll content, plant height, leaf area) have a considerable potential for resistance to environmental conditions. Moreover, these characteristics directly affect the yield in plants. Therefore, it is very important that these are determined early in crops.

Chemical analyses are carried out in the laboratory to determine the biochemical contents of plants. For example, the chlorophyll concentration of green leaves is usually determined by extraction from leaf samples and subsequent spectrophotometric measurements [1]. However, all traditional laboratory analyses are generally expensive and time-consuming methods [2, 3, 4]. Laboratory analysis may also result in environmental pollutants through the use of chemicals [5]. Furthermore, to be able to determine the biophysical status of plants it is necessary to take measurement from many samples in many areas. As these measurements are also very time-consuming, there is a need for new methods to be developed which can provide results in a shorter time and at a lower cost.

The spectral properties of leaves and canopies are affected by the biochemical and biophysical characteristics of the plant species [6, 7]. In recent years, there have been increased efforts to obtain information about plants using their optical properties, such as the function of leaves, the structural biochemicals and water content [8]. The reflectance properties in the visible and near infrared regions of the electromagnetic spectrum are affected by interactions between leaf molecules (protein, cellulose, lignin) and solar radiation. The absorbance, transmittance and reflectance properties of short wavelength solar radiation (280-2800 nm) are also affected by the biochemical, morphological and anatomic components of the plant leaves. Therefore, changes in the concentrations of absorptive chemicals provide a basis for changes in plant absorbance, transmittance, and reflectance [9]. These features help to determine the biochemical and biophysical traits of plants with the use of remote sensing systems.

Remote sensing systems are rapid and non-destructive methods to determine plant traits. Remote sensing is the acquisition of information about an object without making physical contact with the object. In recent years, remote sensing has been used in a variety of applications including agriculture and forestry [10, 11]. Light energy reflectance can be measured in one or more wavelengths with remote sensing systems. These systems have been used to estimate plant and soil characteristics in many studies [12, 13, 14, 15, 16, 17].

In the present study, the spectral reflectance measurements of the narbon bean (*Vicia narbonensis* L) were analyzed to estimate chlorophyll content, water content and plant height at the seedling stage.

MATERIALS AND METHODS

Greenhouse experiment. This greenhouse experiment was carried out with seven treatments (0, 5, 10, 15, 20, 25, 30 kg.da^{-1} nitrogen) and the experiment was designed in randomized plots with 3 replications. Nitrogen fertilizer doses were applied using ammonium nitrate. At the first stage, soil (strong alkali, loam, and low organic matter) was uniformly packed into plastic pots 20 cm in diameter, and ammonium nitrate fertilizers were mixed into the soil in each pot. Narbon bean seeds were sown with 4 seeds per pot and after emergence of the seedlings, they were were thinned to one plant per pot.

Measurements. A Minolta SPAD-502 (Osaka, Japan) hand-held chlorophyllmeter was used to take chlorophyll meter readings (SPAD values) and the readings were repeatedly taken on 5 leaves of each plant at the 8-leaf stage.

After the chlorophyllmeter readings, reflectance measurements were taken on the same leaves using a hand held portable spectroradiometer (FieldSpec Handheld Pro FR, Analytical Spectral Devices, Boulder, USA) with a wavelength range of 325-1075 nm of the electromagnetic spectrum [18]. The reflectance measurements were taken using a plant probe attached to the spectroradiometer in contact with leaves. A 100-W halogen lamp mounted on the plant probe was used as the light source and reflectance readings were made from a 1cm diameter area. For each plant sample, 5 replicate spectra were collected and the average spectrum of these 5 replicates was used as the data of this plant sample. A white reference panel measurement was made before each of the 5 measurements. All spectral data were stored in a portable computer.

Finally, the height of the seedlings (cm) was determined by measuring the length from the neck of the root to the terminal bud with a tape measure. The measured seedlings were then clipped individually at ground level with scissors and dried in a forced- air oven at 65°C for 48 hours to determine the dry weight, and thus, the water content (%).

Statistical Analysis. The spectral reflectance values were transformed into ASCII format using ASD ViewSpec Pro software (ASD, Inc., Boulder, CO). Stepwise multiple linear regression was then applied to the transformed data using MINITAB statistics software. Stepwise regression is the repeated application of multiple regression, each time removing the weakest correlated variable. The variables finally remaining are those which best explain the distribution. The only requirements are that the data are normally distributed (or rather, that the residuals are), and that there is no correlation between the independent variables (known as collinearity) [19]. Although the spectroradiometer measurements were made between 325nm and 1075 nm wavelengths, the evaluation of the results was limited to the range of 400-900 nm because the data were very noisy at wavelengths shorter than 400 nm and longer than 900 nm because of instrument and/or atmospheric noise [20, 21]. In regression analysis, the data obtained from the spectral reflectance measurements were classified into 5 broad wavebands of blue (400-500 nm), green (501-600 nm), red (601-700 nm) and near infrared (NIR, 700-900 nm). Significant wavelengths which were associated with plant traits were determined at the end of the analysis and regression equations were calculated using the selected wavelengths.

RESULTS AND DISCUSSION

The relationship between leaf chlorophyll content and spectral reflectance. The regressions between chlorophyll content (CHL) and the spectral reflectance values are shown in Table 1. The maximum number of selected wavelengths was fixed at 12 to avoid problems of overfit. For each spectral region, 4 different models were formed. The results of the study showed that the highest regression coefficient (R) values were found to be in the red region with 0.68, in the NIR region with 0.67 and in the green region with 0.66. The lowest R value was determined in the blue region with 0.46.

Leaf chlorophyll concentration is an important variable to understand the physiological properties of plants [22] especially in photosynthesis [23, 24] and nitrogen status [25]. Chlorophyll molecules provide the energy needed to fuel the photosynthetic reactions, by absorbing light. However, energy is not absorbed completely by chlorophyll pigments. A small amount (typically <5%) is re-emitted as a double-peaked spectrum of chlorophyll fluorescence in the visible to near infrared wavelengths (approximately 650 nm-820 nm) [17]. Chlorophyll is the main plant constituent determining the reflectance in the visible region of the spectrum, so optical remote sensing techniques have great potential in providing information on canopy chlorophyll and N content. [26]. Cho et al. [27] recorded significant relationships between observed and predicted total leaf chlorophyll content in the red region (600-700 nm) of spectrum in various crops and indigenous tree species. Natural chlorophyll fluorescence (CF) occurs when red and far-red light is emitted from photosynthetic green plant tissues in response to photosynthetically active radiation [28]. The results of the current study are similar to those of previous reports.

TABLE 1
The prediction models and R values for chlorophyll content (CHL) and spectral reflectance values

	Regression Equation	R
Blue Region (400-500 nm)	CHL = 51.27-(46.3*R402 nm)-(131.4*R418 nm)+(43*R425nm)–(182*R426nm) +(443*R433nm) –(615*R434nm)+(578*R435 nm) +(235*R447nm) +(424*R480nm) +(980*R488nm)–(880*R495nm)–(890*R498nm)	0.46
Green Region (501-600 nm)	CHL= 66.09+(357*R555nm)+(2588*R534nm)+(1126*R540nm)-(1782*R539nm) -(3223*R550nm)+(5449*R456nm)+(5337*R549nm)-(3452*R545nm) -(3496*R548nm)-(1703*R541nm)-(704*R533nm)-(544*R553nm)	0.66
Red Region (601-700 nm)	CHL=71.44-(1367*R700nm)+(1399*R699nm)-(502*R604nm) +(2154*R636nm) -(1818*R632nm)+(999*R609nm)-(1688*R628nm)-(1710*R653nm) +(802*R690nm) +(1396*R650nm)-(658*R658nm) +(817*R647nm)	0.68
NIR Region (701-900 nm)	CHL=51.7-(1363*R711nm)+(2080*R819nm)-(4212*R821nm)+(3129*R707nm) -(2053*R706nm)+(2032*R814nm)-(1581*R786nm)+(1731*R796nm) -(687*R703nm) +(1638*R709nm)-(1522*R714nm)+(734*R717nm)	0.67

Note: R letters in the tables describe the reflectance. For example, R402 nm shows value of reflectance in 402 nanometer.

The chlorophyllmeter provides an alternative method for the measurement of relative leaf chlorophyll levels that overcomes the disadvantages of chemical analysis. It is an inexpensive, hand-held device based on two light-emitting diodes and a silicon photodiode receptor, that measures leaf transmittance in the red (650 nm; the measuring wavelength) and infrared (940 nm; a reference wavelength used to adjust for non-specific differences between samples) regions of the electromagnetic spectrum [29]. During the last decade, the use of chlorophyllmeters has greatly increased in agriculture research to determine the chlorophyll concentration of plants such as maize [30], cotton [31], wheat [32] and barley [33]. Although chlorophyllmeters provide rapid and non-destructive measurements of chlorophyll concentration [34], one of the most important disadvantages of this device is the small measuring area (about 13 mm^2) [35]. Although the chlorophyll content of the plants can be determined with a chlorophyllmeter without time-consuming laboratory analysis, it requires 30 or more readings to be taken from representative plants in each area of interest, which can be time-consuming for large fields that have spatial variations [36]. Therefore, remote sensing systems have certain advantages compared to chlorophyllmeters, such as an extensive measurement area (e.g. 10 mm diameter with plant probe) and measurements can be taken at numerous wavelengths (according to the device, 751 or 2125).

The relationship between water content and spectral reflectance. The estimation equations of the relationships between water content (WC) and spectral reflectance are shown in Table 2. According to the results in the table, there was a weak relationship between leaf water content and spectral reflectance. While the highest relationships were determined in the NIR region and the red region with 0.42 and 0.41 respectively, weak relationships were calculated in the green (0.36) and blue regions (0.25) of the spectrum.

TABLE 2
The prediction models and R values for water content (WC) and spectral reflectance values

	Regression Equation	R
Blue Region (400-500 nm)	WC = 87.0+(34.0*R406nm)-(55.6*R407nm)-(38.7*R416nm)-(20.3*R417nm)	0.25
Green Region (501-600 nm)	WC = 81.79-(143*R507nm)-(185*R509nm)+(334*R510nm)+(1273*R580nm) -(619*R581nm)-(753*R587nm)-(2013*R590nm)+(5718*R591nm) -(5904*R592nm) +(2699*R593nm)-(885*R594nm)+(428*R599nm)	0.36
Red Region (601-700 nm)	WC= 81.73+(309*R666nm)-(1103*R652nm)-(2172*R649nm) +(2828*R651nm) +(1042*R674nm)+(78*R679nm)-(2164*R659nm)+(1106*R646nm) -(1169*R634nm) +(1338*R640nm)-(815*R665nm)+(666*R647nm)	0.41
NIR Region (701-900 nm)	WC = 79.25+(89*R701nm)-(1296*R704nm)+(833*R707nm)+(1993*R710nm) -(1575*R711 nm)+(1013*R712nm)-(2180*R716nm)+(1382*R718 nm) +(1301*R720nm)-(2992*R721nm) +(2333*R724nm)-(948*R725nm)	0.42

Note: R letters in the tables describe the reflectance. For example, R406 nm shows value of reflectance in 406 nanometer.

TABLE 3
The prediction models and R values for plant height (PH) and spectral reflectance values

	Regression Equation	R
Blue Region (400-500 nm)	PH=38,43-(33*R435nm)+(421*R433nm)+(154*R402nm)-(741*R449nm) +(107,1*R415nm)+(189,4*R421nm)-(347*R480nm)+(174*R499nm) -(1031*R489nm) +(638*R497nm)+(99,5*R418nm)+(236*R491nm)	0.55
Green Region (501-600 nm)	PH=36,33-(665*R506nm)+(558*R504nm)-(1177*R501nm)+(738*R522nm) -(748*R553nm)+(62*R525nm)+(1531*R539nm)-(1314*R537nm)-(1419*R520nm) +(480*R511nm)+(1181*R513nm)+(607*R531nm)	0.53
Red Region (601-700 nm)	PH=18,63-(3192*R667nm)+(726*R684nm)+(734*R666nm)+(1490*R678nm) +(62*R661nm)-(278*R610nm)+(647*R620nm)+(3469*R630nm)-(1499*R608nm) -(1136*R635nm)+(650*R603nm)-(1646*R629nm)	0.54
NIR Region (701-900 nm)	PH=-17,9+(3009*R767nm)-(419*R772nm)+(5541*R776nm)-(2478*R804nm) + (4944*R799nm)+(3403*R846nm)-(4177*R816nm)-(2100*R771nm) -(5529*R775nm)-(1899*R829nm)+(1089*R880nm)-(1330*R853nm)	0.52

Note: R letters in the tables describe the reflectance. For example, R435 nm shows value of reflectance in 435 nanometer.

In plants, the spectral values of the near and mid-infrared regions of the electromagnetic spectrum can be used to estimate crop water status remotely. As water absorption is strong in these regions, the reflectance at 950–970 nm has proved to be particularly useful for the estimation of plant water status [37]. Furthermore, water strongly absorbs radiation at 970 nm, 1200 nm, 1450 nm, 1930 nm, and 2500 nm bands, and these wavelengths can be used to estimate leaf water content remotely [37, 38]. According to the study results, the highest relationships were determined in the NIR region and red regions, but the regression coefficient of the obtained result was low. The reason for this was that the maximum measurement value of the spectroradiometer used in the study was 900 nm, so data could not be obtained at larger wavelengths.

The relationship between plant height and spectral reflectance. When the relationships between plant height and reflection values were examined, the R values were observed to be close to each other in different regions (Table 3). The most important associations were determined in the blue region and the regression coefficient value was calculated as 0.55. The blue region was followed by the red zone with 0.54, and the regression coefficients of the green and NIR regions were 0.53 and 0.52, respectively.

Morphological and biochemical characteristics are significant determinants of photosynthetic activity and nutrient cycling in plant canopies [39]. Vegetation height is an important measurement for ecological and environmental application such as screening plant biodiversity, conservation planning, fire modeling and biomass estimation [40]. In some remote sensing studies, significant relationships have been recorded between spectral reflectance values and plant height. For example, Choubey and Choubey [41] determined a linear relationship between spectral reflectance and rice plant height (r= 0.97), for band 1 (450–520 nm) reflectance values. Thenkabail et al. [42] also found that the accuracy in estimating plant height could be improved by using reflectance in narrow spectral wavebands in the red and NIR regions (R2 = 0.64). Payero et al. [43] compared 11 vegetation indices in order to estimate grass (*Festuca arundinacea*) and alfalfa (*Medicago sativa*) plant height, and good relationships were reported between plant height and vegetation indices, especially in the NDVI. The results of the current study are similar to those of previous reports.

CONCLUSIONS

A rapid estimate of the foliar chemistry and growth traits of plants is quite important, and the reflectance spectrum of green plants is considerably affected by their biochemical and biophysical properties. Relationships between spectral reflectance values and some plant features were determined in the present study. The results of this study demonstrated the potential of using spectral reflectance data to estimate the foliar chemistry and growth traits, especially chlorophyll content and plant height, in the narbon bean (*Vicia narbonensis* L.)

REFERENCES

[1] Uddling, J., Gelang-Alfredsson, J., Piikki, K. and Pleijel, H. (2007) Evaluating the relationship between leaf chlorophyll concentration and SPAD-502 chlorophyll meter readings. Photosynthesis Research, 91: 37-46.
[2] Kokaly, R.F. and Clark, R.N. (1999) Spectroscopic determination of leaf biochemistry using band-depth analysis of absorption features and stepwise multiple linear regression. Remote Sensing of Environment, 67(3): 267-287.
[3] Graeff, S., Steffens, D. and Schubert, S. (2001) Use of reflectance measurements for the early

detection of N, P, Mg, and Fe deficiencies in corn (*Zea mays* L.). Journal of Plant Nutrition and Soil Science, 164: 445–450.

[4] Li, B., Liew, W. and Asundi, A.K. (2006) Pre-visual detection of iron and phosphorus deficiency by transformed reflectance spectra. Journal of Photochemistry and Photobiology, B: Biology, 85: 131-139.

[5] Zhao, D., Starks, P.J., Brown, M.A., Phillips, W.A. and Coleman, S.W. (2007) Assessment of forage biomass and quality parameters of bermudagrass using proximal sensing of pasture canopy reflectance. Grassland Science, 53: 39-49.

[6] Roelofsen, H.D., Van Bodegom, P.M., Kooistra, L. and, Witte, J-P.M. (2013) Trait estimation in herbaceous plant assemblages from in situ canopy spectra. Remote Sensing, 5: 6323–6345.

[7] Cervena, L., Lhotakova, Z., Kupkova, L., Kovarova, M. and Albrechtova, J. (2014) Models for estimating leaf pigments and relative water content in three vertical canopy levels of Norway spruce based on laboratory spectroscopy. In Proceedings of the 34th EARSeL Symposium 2014, Warsaw, Poland, 16–20 June 2014; Zagajewski, B., Kycko, M., Reuter, R. (eds.) EARSeL and University of Warsaw: Warsaw, Poland, 2014; pp. 6.1–6.8.

[8] Asner, G.P. (1998) Biophysical and biochemical sources of variability in canopy reflectance. Remote Sensing of Environment, 64: 134-53.

[9] Ritchie, G.L. (2003) Use of ground-based canopy reflectance to determine radiation capture, nitrogen and water status, and final yield in wheat. M.S. thesis. (Unpublished) Utah State University, Logan. 122 pp.

[10] Wright, D.L., Rasmussen, V.P. and Ramsey, R.D. (2005) Comparing the use of remote sensing with traditional techniques to detect nitrogen stress in wheat. Geocarto International, 20: 63-68.

[11] Ozyavuz, M., Satir, O. and Bilgili, B. C. (2011) A change vector analysis technique to monitor land-use/land-cover in the Yildiz Mountains, Turkey. Fresen. Environ. Bull., 20(5), 1190-1199.

[12] Gitelson, A.A. and Merzlyak, M.N. (1996) Signature analysis of leaf reflectance spectra: algorithm development for remote sensing of chlorophyll. Journal of Plant Physiology, 148: 494–500.

[13] Datt, B. (1999) A new reflectance index for remote sensing of chlorophyll content in higher plants: tests using Eucalyptus leaves. Journal of Plant Physiology, 154: 30–36.

[14] Singh, S.K., Hoyos-Villegas, V., Ray, J.D., Smith, J.R. and Fritschi, F.B. (2013) Quantification of leaf pigments in soybean (Glycine max (L.) Merr.) based on wavelet decomposition of hyperspectral features. Field Crops Research, 149: 20–32.

[15] Demirel, K., Genc, L., Bahar, E., Inalpulat, M., Smith, S. and Kizil, U. (2014) Yield estimate using spectral indices in eggplant and bell pepper grown under deficit irrigation. Fresen. Environ. Bull., 23(5): 1232-1237.

[16] Leone, A. P., Leone, N., Rampone, S. (2013) An Application of vis-NIR reflectance spectroscopy and Artificial Neural Networks to the Prediction of soil Organic Carbon content in Southern Italy. Fresen. Environ. Bull., 22(4b): 1230-1238.

[17] Atherton, J., Nichol, C.J. and Porcar-Castell, A. (2016) Using spectral chlorophyll fluorescence and the photochemical reflectance index to predict physiological dynamics. Remote Sensing Environment, 176: 17–30.

[18] Albayrak, S. (2008) Use of reflectance measurements for the detection of N, P, K, ADF and NDF contents in sainfoin pasture. Sensors, 8: 7275-7286.

[19] Urrutia, J.D., Tampis, R.L., Mercado, J., Baygan, A.V.M. and Baccay, E.B. (2016) Modeling the Philippines' Real Gross Domestic Product: A Normal Estimation Equation for Multiple Linear Regression. AIP Conference Proceedings 1707, 050016; doi: 10.1063/1.4940848 (http://dx.doi.org/10.1063/1.4940848)

[20] Han, L. and Rundquist, D.C. (2003) The spectral responses of *Ceratophyllum demersum* at varying depths in an experimental tank. International Journal of Remote Sensing, 24(4): 859-864.

[21] Lin, Y. and Liquan, Z. (2006) Identification of the spectral characteristics of submerged plant *Vallisneria spiralis*. Acta Ecologica Sinica, 26(4): 1005-1011.

[22] Lu, X. and Peng, H.C. (2015) Predicting cherry leaf chlorophyll concentrations based on foliar reflectance spectra variables. Journal of the Indian Society of Remote Sensing, 43(1): 109-120.

[23] Buttery, B.R. and Buzzell, R.I. (1977) The relationship between chlorophyll content and rate of photosynthesis in soybeans. Canadian Journal of Plant Science, 57: 1-5.

[24] Etinski, M., Petkovic, M. and Ristic, M.M. (2013) A study of the low-lying singlet and triplet electronic states of chlorophyll a and b. Journal of Serbian Chemical Society, 78: 1775–1787.

[25] Yuan, Z., Ata-Ul-Karim, S.T., Cao, Q., Lu, Z., Cao, W., Zhu, Y. and Liu, X. (2016) Indicators for diagnosing nitrogen status of rice based on chlorophyll meter readings. Field Crops Research, 185: 12-20.

[26] Clevers, J.G.P.W. and Gitelson, A.A. (2013) Remote estimation of crop and grass chlorophyll and nitrogen content using red-edge bands

on Sentinel-2 and-3. International Journal of Applied Earth Observation and Geoinformation, 23: 344–351.
[27] Cho, M.A., Ramoelo, A. and Skidmore, A. (2014) Exploring various spectral regions for estimating chlorophyll from ASD leaf reflectance using prospect radiative transfer model. In: Geoscience and Remote Sensing Symposium (IGARSS), 2014 IEEE International. IEEE, 2014. p. 4754-4757.
[28] Zarco-Tejada, P.J., Pushnik, J.C., Dobrowski, S. and Ustin, S.L. (2003) Steady-state chlorophyll a fluorescence detection from canopy derivative reflectance and double-peak red-edge effects. Remote Sensing of Environment, 84(2): 283-294.
[29] Ling, Q., Huang, W. and Jarvis, P. (2011) Use of a SPAD-502 meter to measure leaf chlorophyll concentration in *Arabidopsis thaliana*. Photosynthesis Research, 107(2): 209-214.
[30] Argenta, G., Silva, P.R.F.D. and Sangoi, L. (2004) Leaf relative chlorophyll content as an indicator parameter to predict nitrogen fertilization in maize. Ciencia Rural, 34(5): 1379-1387.
[31] Muharam, F.M., Bronson, K.F., Maas, S.J. and Ritchie, G.L. (2014) Inter-relationships of cotton plant height, canopy width, ground cover and plant nitrogen status indicators. Field Crops Research, 169: 58-69.
[32] Islam, M.R., Haque, K.S., Akter, N. and Karim, M.A. (2014) Leaf chlorophyll dynamics in wheat based on SPAD meter reading and its relationship with grain yield. Scientia Agriculturae, 8(1): 13-18.
[33] Zhao, B., Liu, Z., Ata-Ul-Karim, S.T., Xiao, J., Liu, Z., Qi, A., Ning, D., Nan, J. and Duan, A. (2016) Rapid and nondestructive estimation of the nitrogen nutrition index in winter barley using chlorophyll measurements. Field Crops Research, 185: 59-68.
[34] Fu, X.Y., Mo, W.P., Zhang, J.Y., Zhou, L.Y., Wang, H.C. and Huang, X.M. (2014) Shoot growth pattern and quantifying flush maturity with SPAD value in litchi (*Litchi chinensis* Sonn.). Scientia Horticulturae, 174: 29-35.
[35] Netto, A.T., Campostrini, E., Oliveira, J.G.D. and Yamanishi, O.K. (2002) Portable chlorophyll meter for the quantification of photosynthetic pigments, nitrogen and the possible use for assessment of the photochemical process in *Carica papaya* L. Brazilian Journal of Plant Physiology, 14(3): 203-210.
[36] Daughtry, C.S.T., Walthall, C.L., Kim, M.S., De Colstoun, E.B. and McMurtrey, J.E. (2000) Estimating corn leaf chlorophyll concentration from leaf and canopy reflectance. Remote Sensing of Environment, 74(2): 229-239.
[37] Poças, I., Rodrigues, A., Gonçalves, S., Costa, P.M., Gonçalves, I., Pereira, L.S. and Cunha, M. (2015) Predicting grapevine water status based on hyperspectral reflectance vegetation indices. Remote Sensing, 7(12): 16460-16479.
[38] Seelig, H.D., Hoehn, A., Stodieck, L.S., Klaus, D.M., Adams, III W.W. and Emery, W.J. (2008) The assessment of leaf water content using leaf reflectance ratios in the visible, near-, and short-wave-infrared. International Journal of Remote Sensing, 29(13): 3701-3713.
[39] Serbin, S.P., Singh, A., McNeil, B.E., Kingdon, C.C. and Townsend, P.A. (2014) Spectroscopic determination of leaf morphological and biochemical traits for northern temperate and boreal tree species. Ecological Applications, 24(7): 1651-1669.
[40] Petrou, Z.I., Tarantino, C., Adamo, M., Blonda, P. and Petrou, M. (2012) Estimation of vegetation height through satellite image texture analysis. In Proceedings of the International Archives of the Photogrammetry, Remote Sensing and Spatial Information Sciences, XXII ISPRS Congress, Melbourne, 25: 321-326.
[41] Choubey, V.K. and Choubey, R. (1999) Spectral reflectance, growth and chlorophyll relationships for rice crop in a semi-arid region of India. Water Resources Management, 13(2): 73-84.
[42] Thenkabail, P.S., Smith, R.B. and De Pauw, E. (2000) Hyperspectral vegetation indices and their relationships with agricultural crop characteristics. Remote Sensing of Environment, 71(2): 158-182.
[43] Payero, J.O., Neale, C.M.U. and Wright, J.L. (2004) Comparison of eleven vegetation indices for estimating plants height of alfalfa and grass. Applied Engineering in Agriculture, 20(3): 385-393.

Received: **11.04.2017**
Accepted: **07.08.2017**

CORRESPONDING AUTHOR

Yasar Ozyigit
Akdeniz University, Korkuteli Vocational High School, Horticulture Program, Antalya – TURKEY

E-mail: ozyigit@akdeniz.edu.tr

© by PSP Volume 26 – No. 10/2017 pages 6049-6057 Fresenius Environmental Bulletin

EFFECT OF FLOC RECYCLING ON GROWTH AND CHARACTERISTICS OF FLOCS FORMED BY POLYMERIC ALUMINIUM CHLORIDE

Wei Wei[1,*], Jia Zhu[2], Chaosheng Zhang[1], Yongfeng Cao[1]

[1]School of Civil Engineering, Guangzhou University, Guangzhou, China
[2]Department of Building and Environmental Engineering, Shenzhen Polytechnic, Shenzhen, China

ABSTRACT

Floc recycling flocculation (FRF) derived from traditional flocculation (TF) is a controversial, but widely used, technology to enhance the removal efficiency of contaminants. In this study, the effect of floc recycling on zeta potential, residual turbidity and floc characteristics was made via a comparison between FRF and TF with a series of polymeric aluminium chloride doses. Compared with TF, the high coagulant dosage caused higher zeta potential in FRF, and the residual turbidity was optimized by charge neutralization and deteriorated at the high dosage of coagulant. The floc growth and physical characteristics were analysed with pictures captured by a high speed imaging system. The results showed that, by FRF, larger flocs were formed, and the formation rate was improved. However, floc recycling weakened the strength of flocs at low coagulant dosage ($\leq$ 0.008 mmol.L^{-1}), but strengthened flocs at high doses ($\geq$ 0.01mmol.L^{-1}). Floc size recovery was better at charge neutralization and worsened above 0.015mmol.L^{-1}. The fractal dimension of final flocs in FRF was superior to that in TF at low dosage, and the concentration of small flocs following FRF was much less than TF.

KEYWORDS:
Floc recycling flocculation; Floc growth; Charge neutralization; Isoelectric point; Morphology

INTRODUCTION

Flocculation is one of the most widely applied physical/chemical technologies in water treatment for the separation of solids from liquid. Generally, aggregation of colloidal substances involves species being hydrolyzed by aluminum or ferric salt coagulants [1]. The mechanism by which flocculation occurs is potentially affected by floculant concentration. At low dosages, charge neutralization is the probable dominant mechanism of colloid destabilization [2]. However, when charge reversal occurs, the colloids restabilize. Alternatively, where the dosage is high enough to create plenty of amorphous precipitation for enmeshing small particles, a mechanism known as sweeping is the main cause of flocculation [3].

Final floc characteristics, including size, morphology, strength and size distribution, all directly affect the solid-liquid separation process. It is universally accepted that the growth of flocs is determined by random collisions between colloidal particles resulting in nonlinear characteristics. Fractals are commonly used to describe the nonlinear mechanisms of geometrically irregular objects with self-similarity and scale-invariance structures and have been applied in the structural description of nanoparticle agglomerates [4], asphaltene aggregates [5, 6] and proteins [7]. The morphology of flocs is described by a fractal dimension defined by the exponential relationship between mass (M) and characteristic length (R) shown in equation 1 [8, 9].

$$\mathrm{M(L)} \propto R^{D_f} \qquad (1)$$

Image analysis, settling and light scattering are the main methods for the determination of fractal dimensions [9], with the former currently more broadly applied due to the rapid development of digital camera technology.

Floc breakdown is a problem because it interferes with the course of floc growth. The two modes of floc rupture classified as surface erosion and large-scale fragmentation are common behaviors of flocs due to the local high shear generated in flocculation systems [10]. Floc break down results in an increase of small particles and associated reduction in the removal efficiency of colloids. The breakage resitance capacity of a floc is determined by its structure, formation mechanism and internal attractive and repulsive forces. Additionally, the reaggregation ability of post-breakage small flocs is another important property which determines whether the breakage is reversible or not. Consequently, floc breakage factor (FB_f), floc strength factor (FS_f) and floc recovery factor (FR_f), as defined by equations 2, 3 and 4, have been used frequently to characterise flocs [10-13].

$$FB_f = \frac{d_a - d_b}{d_a} \times 100\% \qquad (2)$$

$$FR_f = \frac{d_c - d_b}{d_a - d_b} \times 100\% \qquad (3)$$

$$FS_f = \frac{d_b}{d_a} \times 100\% \qquad (4)$$

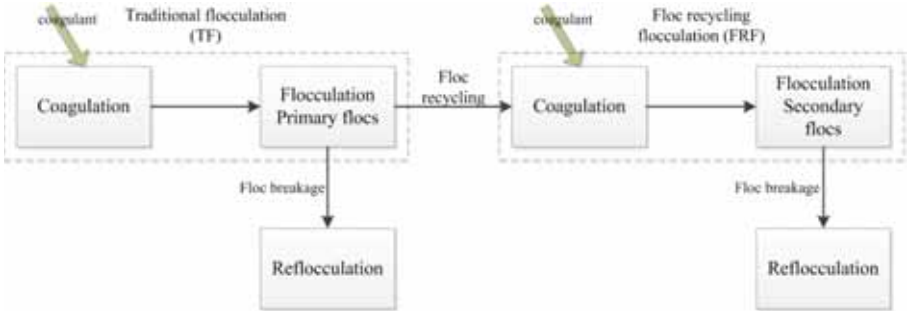

FIGURE 1
Schematic flow diagram of the application of floc recycling.

where d_a is the size of the floc plateau before breakage, d_b is the floc size after the breakage, and d_c is the steady-state floc size after regrowth.

Floc recycling flocculation (FRF) derives from traditional flocculation which was recorded as early as 1873 [14], involving returning floc sediments to raw water and conducting a new flocculation cycle after rapid mixing (Fig.1). The efficiency of FRF application and its mechanism of action have been strongly debated for many years and until recent years, many research applications reported that it reduced coagulant dosages and improved flocculation efficiency [15-18]. Suggestions of mechanistic action included enhancement of collision opportunities due to increased floc concentration and the full utilization of unsaturated adsorption. Alternately, Fu et al. argued that recycled flocs have compact structures with huge specific surface areas to induce contact flocculation [19] while Guan et al. reported that, after recycling, some aluminum species exposed due to the raw alum sludge unentirely enclosed by particles can become to be activated sites when the rapid mixing introduced [20]. Delichatsios and Probstein analysed the theoretical model of floc recycling and elucidated the kinetic equation of initial particle removal rate [21], however, this research failed to take the effect of floc breakage into account which is an obvious consequence of FRF. For now, studies focusing on regrowth of broken flocs under various conditions have proved that their recovery capacity is linked to flocculation mechanism and coagulant dosage [22-25]. At low dosage, the flocs formed by PACl tended to reversibility, and irreversibility at high dosage. Therefore, this gives rise to the question, when the flocs recycle into the raw water system, how it changes the aggregation strategy of colloidal particles. It will explain the performance of FRF from a viewpoint of basis study.

This study aims to significantly enhance flocculation theory and the application of FRF via elucidation of how the introduction of flocs to raw water affects the aggregation of colloidal particles. Polymeric aluminum chloride (PACl) was used as the coagulant to treat colloidal suspensions of tap-water and kaolin. The subsequent effects on floc formation, strength, recoverability, fractal structure and size distribution were measured by an established high speed imaging system.

MATERIALS AND METHODS

Materials and suspension preparation. Colloidal stock suspensions were prepared from kaolin particles (100 g) suspended in deionized water (1 L) with high speed stirring (2 hr, 1000 rpm). The pH was adjusted to 8.5 with NaOH (0.5 mol·L^{-1}) and the supernatant decanted into polyethylene reserve tanks following overnight standing.

The kaolin particle size distribution was determined by a particle size analyzer (S3500, Microtrac, USA) to within the range from 1 to 10 μm.

The test water was prepared via a dilution of the stock suspension with tap water of temperature = 20.8~25.9°C, pH = 7.6±0.3, alkalinity = 8.4~15.9 mg $CaCO_3$·L^{-1}. The pH was adjusted to 7.9±0.05 by the addition of NaOH solution (0.5 mol·L^{-1}) and HCl (2 mol·L^{-1}), and alkalinity was adjusted by adding 0.5 mmol·L^{-1} $NaHCO_3$. The turbidity (2100Q, Hach, USA) of the prepared suspension was tested to be 40±2 NTU.

Commercially available polyaluminium chloride with 30% Al_2O_3 content and 70–75% basicity was used as the coagulant.

TF/FRF jar test. Jar test experiments were performed by an equipment of High speed imaging system for flocculation monitoring which was the same to that of previous research[26].

To model TF, the system was mixed rapidly for 120s at 300rpm followed by a 15min flocculation phase at 70rpm and finally a 10 min settlement period with no agitation. Water samples were collected from 3 cm below the liquid surface for a residual turbidity measurement by portable turbidimeter. Subsequently, a 60s rapid breakage stage at 300rpm followed by a 15 min recovery phase at 70rpm and a 10 min settlement with no mixing were performed to test the FB_f, FS_f and FR_f, using formulae 2, 3 and 4. The residual turbidity was measured again.

For the FRF experiment, flocs gathered from

the parallel TF experiment prior to breakage and recovery were poured into a reactor pre-loaded with suspension before an analogous mixing procedure to that described above was repeated.

PACl dosages of: 0.005, 0.008, 0.010, 0.015, 0.020, 0.030, 0.040, 0.060, 0.080, 0.100, 0.150, 0.200 mmol·L^{-1} were added at 60s during the rapid mixing stage to assess their effect on flocculation. After 50s from dosing of coagulant, zeta potential was measured by a zeta potential analyzer (90Plus Zeta, Brookhaven, USA). To investigate the effect of floc recycling on zeta potential, the water sample collected at 50s after the addition of flocs in the FRF experiment was also measured.

Image acquisition and analysis. Photographs were acquired twice per min during breakage period and once per minute during slow mixing and analysed as follows.

Background subtraction and binarization using image-pro plus software (Media Cybernetics, USA) were used to assess floc size and size distribution. According to the software documentation, the diameter of a single floc was defined by the average length of secants measured at 2 degree intervals passing through the object's centre. The maximum diameter-area power law relationship was applied for the assessment of the fractal dimension of single floc which is defined by formula 4.

$$\text{fractal dimension} = \frac{\log A}{\log L} \quad (5)$$

Where A and L are the projected floc area and maximum diameter of flocs, respectively. The slope of logA − logL is considered to be the fractal dimension. Lower fractal dimension values represent looser and linearly structured flocs, while higher values imply compact, circular structures.

To investigate the change of floc morphology following breakage, the reversibility of morphology is defined by the morphology recovery factor (MR_f) which is calculated as follows.

$$MR_f = \frac{D_c - D_b}{D_a - D_b} \times 100\% \quad (6)$$

Where D_a, D_b and D_c are the fractal dimension of terminal flocs captured after growth, breakage and recovery, respectively.

RESULTS AND DISCUSSION

Effect of floc recycling on zeta potential and residual turbidity. The variation of zeta potential and residual turbidity at increasing PACl dosage in TF and FRF is shown in Fig 2. For TF with PACl only, a rapid increase of zeta potential to 0 mV and a decrease of residual turbidity were observed clearly with increasing coagulant doses below 0.015 mmol·L^{-1}. This implies that charge neutralization was the main mechanism of floc formation. The zeta potential switched from negative to positive charge at a dosage of 0.02mmol·L^{-1} and continued to increase gradually with PACl dosage above this point while the residual turbidity remained approximately constant indicating an increasing domination of sweep flocculation in floc formation.

For FRF in the absence of PACl, the zeta potential of the colloid rose above the original kaolin suspension which was close to -30 mV (Fig 2a) suggesting that the addition of primary flocs neutralized part of negative charge attached to the colloid. Compared to flocs formed by charge neutralization, the neutralization capacity of flocs formed by excess charge neutralization is stronger.

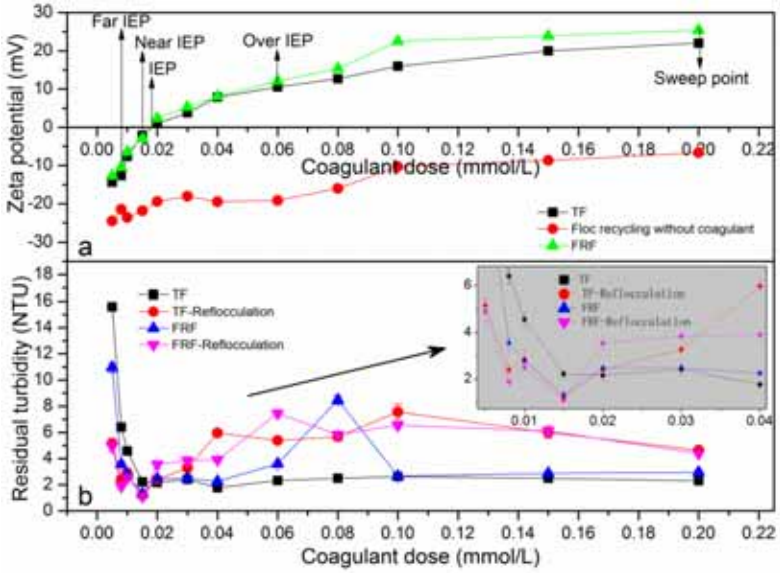

FIGURE 2
Variations of the (a) zeta potential in the condition of TF, Floc recycling without coagulant and FRF and (b) residual turbidity by TF, FRF and their Reflocculation with different coagulant dosage.

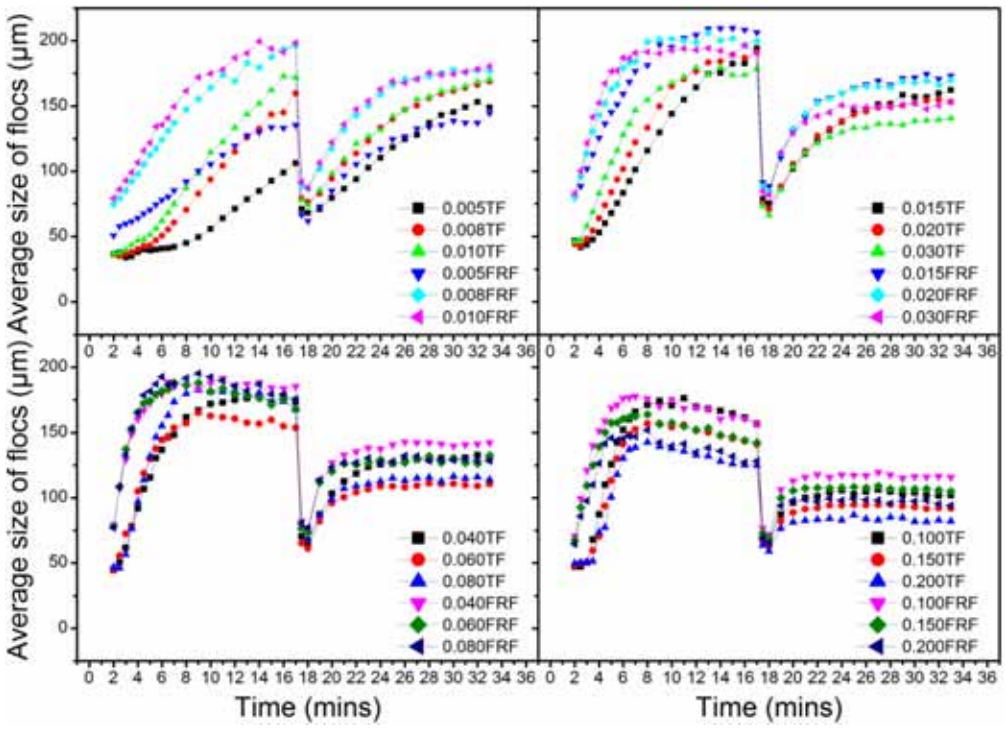

FIGURE 3
Comparison of growth and regrowth after breakage between TF and FRF.

But it seems that there is no benefit for aggregation of flocs after adding PACl. Because the zeta potential of FRF was larger than that of TF at dosages over 0.015mmol·L^{-1} which would hinder further floc growth. Under these conditions, it can be seen from (Fig. 2b) that the residual turbidity during FRF presented an upward trend which was worse than the TF until the coagulant dose rose to 0.10 mmol·L^{-1}. However, increasing the dose further caused a reduction of residual turbidity. This could be attributed to the precipitation of amorphous Al hydroxide at the high dosage, where the sweep flocculation occupied the mechanism of flocs formation completely. A similar situation was observed with the residual turbidity of regrowth after breakage during TF and FRF. At the other condition of dosage less than 0.015 mmol·L^{-1}, the zeta potential of FRF was found to be nearly the same as that of TF which indicated the system was in charge neutralization zone. The optimization of residual turbidity comparing to TF was observed in FRF, as well as the floc regrowth after breakage.

That the breakage and regrowth of flocs formed at low coagulant dosage optimizes the effluent quality has been confirmed by this study in agreement with previously published research [27, 28]. Except the double concentration of particles, the characteristic change of secondary flocs by the properties of primary flocs described above will be investigated in the following texts as the main causation leading to the observed variation in residual turbidity after floc recycling (Fig 2b).

With respect to the above analyses of variation in zeta potential and residual turbidity, coagulant doses of 0.008, 0.015, 0.060 and 0.200 mmol·L^{-1} were denoted as the far isoelectric point (IEP), near IEP, over IEP and sweep point respectively in terms of the colloid charge state.

Effect of floc recycling on flocs growth. Floc size during formation and breakage under TF and FRF at increasing PACl dosage is shown in Fig 3. The mean floc diameter during floc recycling was consistently larger under FRF than TF regardless of the coagulant dose.

Generally, the flocs grew rapidly following coagulant addition until a steady-state size distribution was reached, a process accelerated by higher floc growth rates. As can be seen in Fig 3, during TF, the steady state was not reached during the initial 15min of flocculation when the system was charge neutral (<0.015 mmol·L^{-1}), however, it was reached before 15 min in the FRF experiments. For example, when the PACl dosage was at far and near IEP, steady states with mean diameters of 193.58 μm and 197.19 μm were reached by 16 min and 13 min respectively under FRF compared with unsteady state diameters of 144.99 μm and 174.59 μm under TF. With the increasing of coagulant dosage, the maximum floc size was found to be 157.18 μm at 8 min in TF and 188.32 μm at 7 min in FRF when the charge state was over IEP, and 137.15 μm at 6.5 min and 141.51 μm at 4.5 min when it was sweep point.

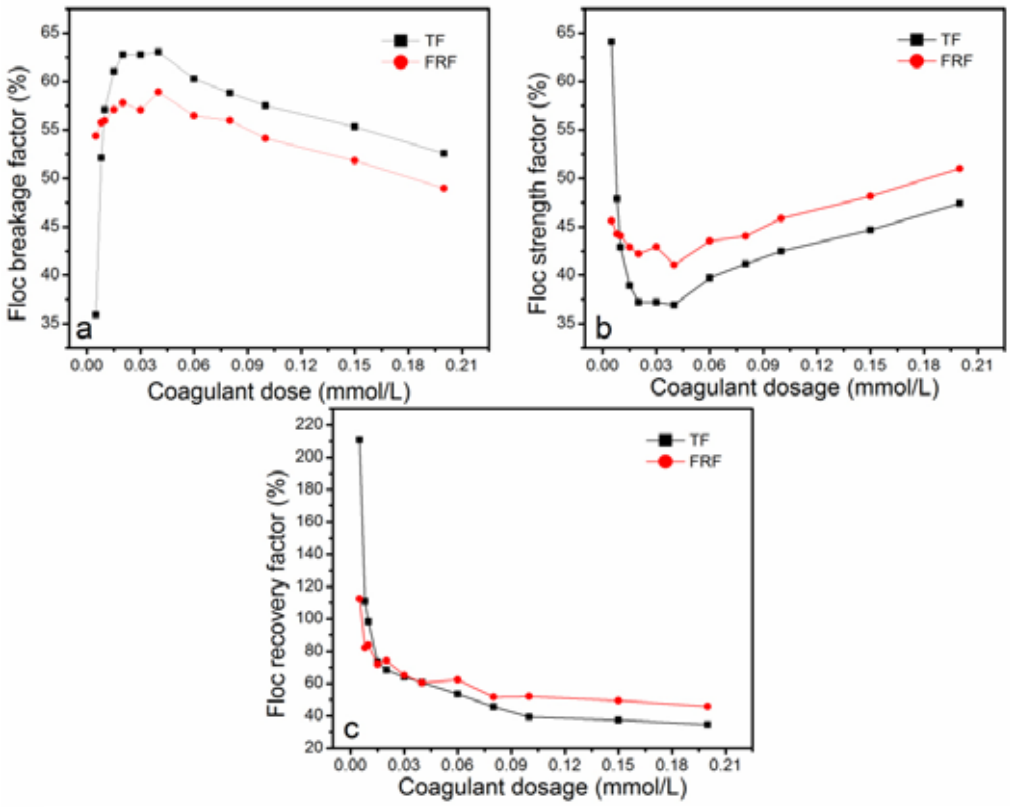

FIGURE 4
The effects of coagulant dose on (a) breakage factor, (b) strength factor and (c) size recovery factor under TF and FRF.

These results suggest that, after FRF, larger, steadier flocs are obtained more quickly independent of coagulant dose, indicating that floc recycling enhances floc formation.

Effect of floc recycling on floc strength and reversibility. Flocs were characterized according to Eqs. (2), (3) and (4) to determine floc regrowth at 70 rpm for 15 min following a floc breakage period at a shear rate of 300rpm for 1min. As shown above, a new stable steady-state floc size was reached quickly once the recovery phase was introduced, but the recovery level differed depending on coagulant dosage.

The effect of floc recycling on the properties of flocs under different coagulant doses is shown in Fig. 4. These results showed that the strength factor declined rapidly with initially increasing coagulant dose before slowly increasing at doses above 0.05 mmol·L^{-1}, which was opposite to the breakage factor as expected intuitively. More specifically, the breakage factor of at the far IEP was higher withFRF than TF (55.76% vs. 52.1%),but lower at near IEP, over IEP and the sweep point (57.09% vs. 61.04%, 56.44% vs. 60.27%, 48.99% vs. 52.57%, respectively). Contrastingly, the strength factor of FRF was lower at the far IEP and higher at the other charge states. These findings may be attributed to the larger floc size under FRF. At low coagulant dosage, Van Der Waals force is the main force inducing the cohesion of colloidal particles. Regardless of the operation of flocs, that aggregation mode between colloids did not change after FRF. Also, an increase of floc size generally leads to a decrease of floc strength [10, 29]. Due to both two reasons, larger flocs will be easily broken by natural turning. However, at high coagulant dosage, particles are connected by formation of amorphous metal hydroxide. After floc recycling without coagulant dosing the small flocs deposited by precipitates could adsorb high concentrations of colloids by electrostatic forces, and then form secondary flocs with more complex internal force structures after coagulant dosing potentially explaining the resistance of secondary flocs to breakage.

As suggested by Jarvis et al. [30], when higher dosages were used, broken flocs could not fully connect with other flocs at the breakage points as the chemical bonds were broken. Yu et al. also believed that, after breakage, the broken flocs have fewer potential points for connecting with each other than during the aggregation of primary flocs. With increasing dosage, the FR_f decreased rapidly to charge neutralization and then fell more slowly at doses above 0.015 mmol·L^{-1} (Fig. 4b). During charge neutralization, the FR_f with FRF was lower than with TF, which could be explained by invalid active sites of primary flocs. However, the result

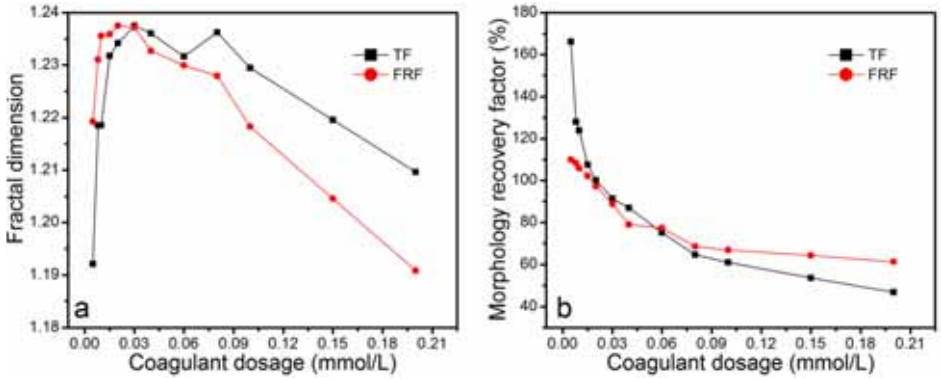

FIGURE 5
(a) Fractal dimension and (b) MR_f of final flocs by TF and FRF.

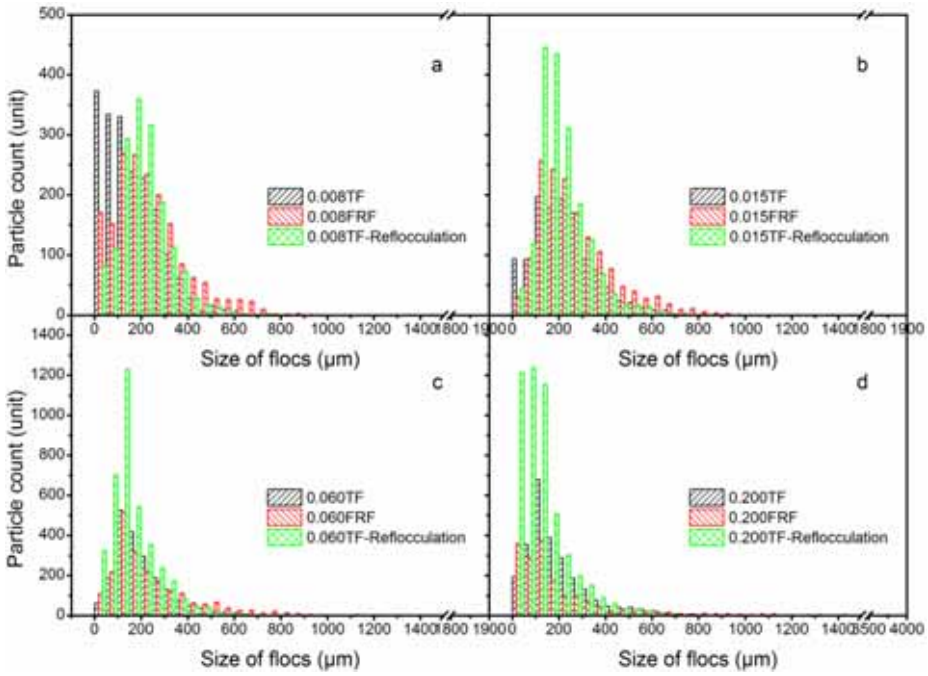

FIGURE 6
Final floc size distributions by TF, FRF and Reflocculation of TF at the (a) far IEP, (b) near IEP, (c) over IEP and (d) sweep point.

was inverted at dosages from 0.02 to 0.20mmol·L^{-1}. This may be due to the adsorption of colloids on small flocs mentioned in the previous paragraph. For example, the final floc sizes of TF and FRF at the sweep point was close, whilst the steady-state size of FRF after breakage phase was greater than that of TF (Fig.3).

Effect of floc recycling on floc structure. The fractal dimension of flocs influences the floc density, with a lower value indicating a more open structure and lower effective density. From the results shown in Fig. 5a, fractal dimension of FRF was higher than that of TF at low coagulant dosage (<0.02 mmol·L^{-1}), but lower when the coagulant dosage was more than 0.02 mmol·L^{-1}. As the flocs regrow, the morphology recovery, expressed by MR_f and calculated by Eq. (6), is shown in Fig. 5b. The results suggest that the MR_f is fully reversible with FRF and TF if charge neutralization dominates the coagulation mechanism, with a sharp degradation in morphology recovery by floc recycling.The MR_f values for FRF at dosages between 0.02 and 0.06 mmol·L^{-1} were slightly lower than those of TF, before becoming increasingly higher at dosages of more than 0.06 mmol·L^{-1}. The reversibility of morphology may result in the higher fractal dimension after FRF at low dosage.

Effect of floc recycling on floc size distribution. Effluent quality is significantly affected by the size distribution of the final flocs, especially the small flocs with poor removal efficiency. There is a popular belief that for the similar floc densities, the settling velocity is slower for the smaller flocs [32, 33].

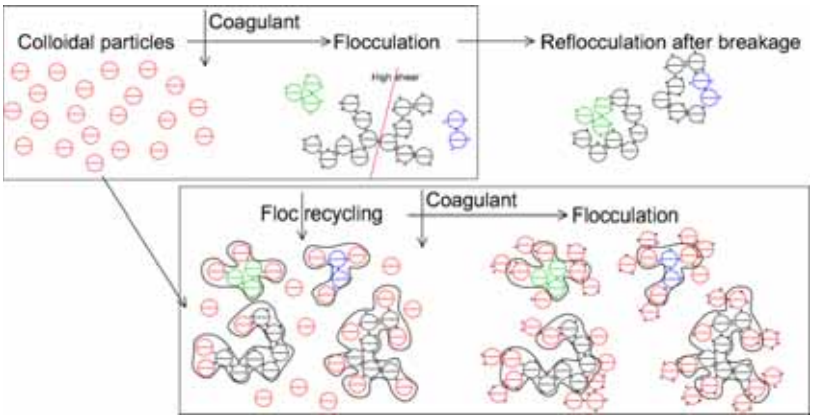

FIGURE 7
Mechanism of FRF at low coagulant dosage.

The size distribution of final flocs for TF, FRF and regrowth of TF after breakage in the four charge states are shown in Fig. 6. The results suggest that, the size distribution of secondary flocs was obviously the widest ranging among the three cases, regardless of the charge state involved. Additionally, when flocculation was conducted by charge neutralization (Fig. 6a and Fig. 6b), the count of small flocs (< 50 µm) by FRF and regrowth of TF was far less than by TF which caused the improvement of residual turbidity. In contrast, for secondary flocs and regrown flocs after breakage, the count of flocs larger than 200 µm at the far IEP and 100 µm at the near IEP was greater than for primary flocs. However, at the over IEP and sweep point, the number of secondary flocs (< 50 µm) was higher than the primary flocs, causing a deterioration of residual turbidity, and the secondary flocs larger than 100 µm was fewer. This means that floc recycling gives a diverse size distribution at different charge states.

DISCUSSION AND MECHANISMS

In this study, residual turbidity was similar between FRF and regrowth following TF. To investigate the origins of this similarity, we studied the effects of primary floc recycling on secondary flocculation via investigation of growth, structure and size distribution of flocs.

It is very likely that the floc variability between FRF and TF is due to the interactions among the broken recycled flocs, the colloidal particles in raw water and the coagulant dose. The mechanism which has been reported for explaining the phenomenon of floc regrowth after breakage can also enhance the understanding of FRF. As can be seen in Fig. 7, at low dosages of coagulant, numerous tiny flocs with uneven positive charge are produced by the breakage of primary flocs. Once the tiny flocs collide with colloidal particles, migration of partial charge occurs which slightly reduces the Zeta potential. After the second dosing of coagulant, polynuclear hydroxyl complex ions attach to the surface of the colloids and tiny flocs, destablizing the colloids and increasing active sites on microflocs. During the growth of secondary flocs, the colloidal particles and tiny flocs can aggregate with each other. However, the more significant interactions are between tiny flocs with open structure which act as condensation nuclei for accelerating the rate of floc growth with the colloidal particles and some microflocs resulting in lower residual turbidity. Hence, the morphology of secondary flocs becomes more compact with higher fractal dimensions which restrict the reversibility of flocs.

At a high dosage of coagulant, amorphous aluminum hydroxide deposits on the surface of colloids forming primary flocs, exhibiting low morphological recovery following breakage. During FRF, the loose precipitates adsorb and swallow some colloidal particles, creating the surfaces of broken flocs covered by colloids. Subsequently, following second coagulant dosing, aluminum precipitate appeared and partially deposited on the surface of flocs and colloids once again. This creates flocs with complex internal mechanical structures which maybe the main reason why the secondary flocs presented higher breakage resistance. However, it also blocks the aggregation of secondary flocs, therefore, many microflocs cannot be trapped leading to a deterioration in residual turbidity. As the effective contact decreases, the flocs grow depend on the un-deposited parts of the colloidal surface or mechanical collision and show a loose morphology with a lower fractal dimension.

It is particularly necessary to point out that the results involving reversibility of primary floc breakage in this study only partially agree with the previous research. Many researchers hypothesise that, by charge neutralization, the broken Al-flocs could fully regrow to the level before breakage which was not the same as we observed at the near IEP. However, the floc morphology was more compact implying that the optimization of residual turbidity at low dosage is significantly relevant to not only the larger size but also the superiority of floc morphology, as

higher effective density facilitates the settlement of flocs. In addition, the relationship of floc strength between FRF and TF did not reverse at the near IEP either, but rather after the far IEP. It is possible that the surface properties of flocs changed after floc recycling. Yu et al. considered that floc regrowth after breakage relies on the chemical characteristics of the floc surface which has changed from that of primary flocs [31]. James and Healy proposed that the surface charge alteration is attributed to the coverage of colloid particles by metal hydroxide gels and precipitates [34, 35]. Hence, it can be assumed that the deposition of amorphous aluminum hydroxide was present before complete charge neutralization was achieved, before or after floc recycling. That was the inevitable result by transition of flocs formation mechanism from charge neutralization to enmenshment with the increasing of coagulant dosage. If such a condition (precipitates appear in the charge neutralization) arises, the weaker the bonding in the precipitate or between gel and colloids surface than the electrostatic force between colloidal particles can explain why the relationship reversed before the near IEP.

CONCLUSIONS

Comparisons of a series of experimental procedures with different coagulant doses were performed to assess the effect of floc recycling on zeta potential, residual turbidity and floc properties.

1. The residual turbidity was optimized at the stage of charge neutralization and deterioration out of it, same as the performance of reflocculation after TF.
2. Floc recycling without coagulant partially neutralized the negative charge and the primary flocs formed by higher dosing had higher neutralization capacities which probably hindered the aggregation of secondary flocs at the same coagulant dosage.
3. Floc recycling accelerated the formation of secondary flocs and changed their properties. The average size of secondary flocs was larger than that of primary flocs.
4. The secondary flocs formed at lower coagulant doses had a tendency to be lower strength, lower breakage reversibility, better structure and fewer small particles than primary flocs. On the contrary, the secondary flocs formed at higher coagulant dosage had a reverse tendency.

These results suggest that a low dose of coagulant with FRF is the advisable course for flocculation. To understand the effect of floc recycling deeply, an investigation on the change of surface chemical characteristic should be carried out.

ACKNOWLEDGEMENTS

This research was supported by the National Natural Science Foundation of China (51478274) and Foundation for Distinguished Young Talents in Higher Education of Guangdong, China (2014kqncx105).

REFERENCES

[1] Gregory, J. (2006) Particles in water : properties and processes. Boca Raton, FL: Taylor & Francis.
[2] Snodgrass, W.J., Clark, M.M., O'Melia C.R. (1984). Particle formation and growth in dilute aluminum(III) solutions: Characterization of particle size distributions at pH 5.5. Water Research. 18(4), 479-488.
[3] Lu, S., Pugh, R.J., Forssberg, E. (2005) Interfacial separation of particles: Elsevier.
[4] de Martín, L., Fabre. A., J. Ommen, R.V., (2014) The fractal scaling of fluidized nanoparticle agglomerates. Chemical Engineering Science. 112(0), 79-86.
[5] Rahmani, N.H.G., Dabros, T., Masliyah, J.H., (2005) Fractal structure of asphaltene aggregates. Journal of Colloid and Interface Science. 285(2), 599-608.
[6] Gmachowski, L., Paczuski, M. (2011) Fractal dimension of asphaltene aggregates determined by turbidity. Colloids and Surfaces A: Physicochemical and Engineering Aspects. 384(1 – 3), 461-465.
[7] Peng, X., Qi, W., Wang, M., Su, R., He, Z. (2013) Backbone fractal dimension and fractal hybrid orbital of protein structure. Communications in Nonlinear Science and Numerical Simulation. 18(12), 3373-3381.
[8] Vahedi, A., Gorczyca, B. (2011) Application of fractal dimensions to study the structure of flocs formed in lime softening process. Water Research. 45, 545-556.
[9] Bushell, G. (2002) On techniques for the measurement of the mass fractal dimension of aggregates. Advances in Colloid and Interface Science. 95(1), 1-50.
[10] Jarvis, P., Jefferson, B., Gregory, J., Parsons, S.A. (2005) A review of floc strength and breakage. Water Research. 39(14), 3121-3137.
[11] Sun, J., Qin, L., Li, G., Kang, Y. (2013) Effect of hydraulic conditions on flocculation performances and floc characteristics in Chinese herbal extracts by chitosan and chitosan hydrochloride. Chemical Engineering Journal. 225(0), 641-649.
[12] François, R.J. (1987) Strength of aluminium hydroxide flocs. Water Research. 21(9), 1023-1030.

[13] Yukselen, M.A., Gregory, J. (2004) The reversibility of floc breakage. International Journal of Mineral Processing. 73(2-4), 251-259.
[14] Rudolfs, W., Gehm, H.W. (1937) Chemical Coagulation of SewageVI.Clarifying Value of Return Sludge. Sewage Works Journal. 9(1), 22-33.
[15] Xi, B., Zhao, Y., Zhang, L., Xia, X., Luan, Z., Peng, X., Lv, W. (2013) Return chemical sludge employed in enhancement of phosphate removal from wastewater. Desalination and Water Treatment. (ahead-of-print), 1-9.
[16] Jiang, S.J., Long, X.Y., Zhang, Y., Wang, P.F. (2012) Pilot Study of Yangtze River Water Treatment in the Winter by Sludge Return. Applied Mechanics and Materials. 209-211, 1915-1922.
[17] Liu, S., Liang, T. (2004) Return sludge employed in enhancement of color removal in the integrally industrial wastewater treatment plant. Water Research. 38(1), 103-110.
[18] Chu, W. (1999) Lead metal removal by recycled alum sludge. Water Research. 33(13), 3019-25.
[19] Fu, P., Sun, L., Wang, S., Jiang, C., Wang, J. (2009) Application of enhanced coagulation process by sludge refluxing to the wastewater recycling treatment. Industrial Water Treatment. 29(4), 38-41.
[20] Guan, X., Chen, G., Shang, C. (2005). Re-use of water treatment works sludge to enhance particulate pollutant removal from sewage. Water Research. 39(15), 3433-3440.
[21] Delichatsios, M.A., Probstein, R.F. (1975) Scaling Laws for Coagulation and Sedimentation. Journal (Water Pollution Control Federation). 47(5), 941-949.
[22] Barbot, E., Dussouillez, P., Bottero, J.Y., Moulin, P. (2010) Coagulation of bentonite suspension by polyelectrolytes or ferric chloride: Floc breakage and reformation. Chemical Engineering Journal. 156(1), 83-91.
[23] Yu, W., Gregory, J., Campos, L.C. (2011) Breakage and re-growth of flocs: Effect of additional doses of coagulant species. Water Research. 45(20), 6718-6724.
[24] Zhou, Z., Yang, Y., Li, X., Wang, W., Wu, Y., Wang, C., Luo, J. (2014) Coagulation performance and flocs characteristics of recycling presonicated condensate sludge for low-turbidity surface water treatment. Separation and Purification Technology. 123(0), 1-8.
[25] Yu, W., Gregory, J., Liu, H., Qu, J. (2014) Investigation of the property of kaolin – alum flocs at acidic pH. Colloids and Surfaces A: Physicochemical and Engineering Aspects. 443(0), 177-181.
[26] Wei, W., Li, X., Zhu, J., Du, M. (2015) Characteristics of flocs formed by polyaluminum chloride during flocculation after floc recycling and breakage. Desalination and Water Treatment. 56(4), 1110-1120.
[27] Yu, W., Li, G., Xu, Y., Yang, X. (2009) Breakage and re-growth of flocs formed by alum and PACl. Powder Technology. 189(3), 439-443.
[28] Yu, W., Gregory, J., Campos, L., Li, G. (2011) The role of mixing conditions on floc growth, breakage and re-growth. Chemical Engineering Journal. 171(2), 425-430.
[29] Bache, D.H., Rasool, E., Moffat, D., McGilligan, F.J. (1999) On the strength and character of alumino-humic flocs. Water Science and Technology. 40(9), 81-88.
[30] Jarvis, P., Jefferson, B., Parsons, S.A. (2005) Breakage, Regrowth, and Fractal Nature of Natural Organic Matter Flocs. Environmental Science & Technology. 39(7), 2307-2314.
[31] Yu, W., Gregory, J., Campos, L.C. (2010) Breakage and re-growth of flocs formed by charge neutralization using alum and poly-DADMAC. Water Research. 44(13), 3959-3965.
[32] Slavik, I., Müller, S., Mokosch, R., Azongbilla, J.A., Uhl, W. (2012) Impact of shear stress and pH changes on floc size and removal of dissolved organic matter (DOM). Water Research. 46(19), 6543-6553.
[33] Boller, M., Blaser, S. (1998) Particles under stress. Water Science and Technology. 37(10), 9-29.
[34] James, R.O., Healy, T.W. (1972) Adsorption of hydrolyzable metal ions at the oxide—water interface. I. Co(II) adsorption on SiO2 and TiO2 as model systems. Journal of Colloid and Interface Science. 40(1), 42-52.
[35] James, R.O., Healy, T.W. (1972) Adsorption of hydrolyzable metal ions at the oxide—water interface. II. Charge reversal of SiO2 and TiO2 colloids by adsorbed Co(II), La(III), and Th(IV) as model systems. Journal of Colloid and Interface Science. 40(1), 53-64.

Received: **13.04.2017**
Accepted: **26.07.2017**

CORRESPONDING AUTHOR

Wei Wei
School of Civil Engineering, Guangzhou University, Guangzhou, China

e-mail: weiweihit@hotmail.com

© by PSP Volume 26 – No. 10/2017 pages 6058-6063 Fresenius Environmental Bulletin

RESPONSE OF SOIL ENZYMES TO VOLATILE ORGANIC COMPOUNDS EMITTED FROM CREOSOTE-TREATED WOOD

Arkadiusz Telesinski[1,*], Krystyna Cybulska[2], Michal Strek[1], Maciej Platkowski[1], Martyna Snioszek[1], Robert Biczak[3]

[1]Department of Plant Physiology and Biochemistry, West Pomeranian University of Technology in Szczecin, Słowackiego 17, 71-434 Szczecin, Poland
[2]Department of Chemistry, Microbiology and Biotechnology of Environment, West Pomeranian University of Technology in Szczecin, Słowackiego 17, 71-434 Szczecin, Poland
[3]Department of Biochemistry and Ecotoxicology, Jan Długosz University in Częstochowa, Armii Krajowej Av. 13/15, 42-200, Częstochowa, Poland

ABSTRACT

This paper presents the comparison of changes in the enzyme activities involved in carbon, phosphorus, and nitrogen cycle in soil exposed to volatile organic compounds (VOCs) emitted from creosote-treated wood. The laboratory experiment was carried out on two soil samples: loamy sand (C_{org} 8.71 g kg^{-1}, pH_{KCl} 6.36) and sandy loam (C_{org} 10.92 g kg^{-1}, pH_{KCl} 6.81). The soil samples were incubated with ground sleepers impregnated with creosote. After 21 days of incubation, in the soil samples the activities of dehydrogenases, catalase, β-glucosidase, *o*-diphenol oxidase, lipase, acid phosphomonoesterase, alkaline phosphomonoesterase, phosphodiesterase, phosphotriesterase, inorganic pyrophosphatase, urease, nitrate reductase, and proteases were determined. VOCs emitted from the creosote-treated wood significantly changed activities most of the soil enzymes. Increase in activity was found for dehydrogenases (in both soil types) and lipase (in loamy sand). The highest inhibition was observed for inorganic pyrophosphatase, nitrate reductase, and proteases. Calculated values of resistance index showed that among the measured enzymes involved in carbon, phosphorus, and nitrogen cycle, dehydrogenases, inorganic pyrophosphatase, and proteases were the most sensitive to VOCs, respectively.

KEYWORDS:
creosote, soil enzymes, volatile organic compounds (VOCs), resistance index, cluster analysis, principal component analysis

INTRODUCTION

Creosote is a wood-preserving product obtained by fractional distillation of crude coal tar produced by high-temperature carbonization of bituminous coal [1]. It is composed of approximately 85% polycyclic aromatic hydrocarbons (PAH), 10% phenolic compounds, and 5% *N*-, *S*-, and *O*-heterocyclics [2]. The relative concentrations of volatile organic compounds (VOCs) and polycyclic aromatic hydrocarbons (PAHs) differ in the composition of tar used and variations in the distillation process [3]. Gallego et al. [1] reported that the main components of the vapors released from the creosote-treated wood were naphthalene, toluene, *m*+*p*-xylene, ethylbenzene, *o*-xylene, isopropylbenzene, benzene, and 2-methylnaphthalene. Recently, special attention is being paid to VOCs since these compounds are found in about two-thirds of the total contaminated areas. Additionally, eight species of VOCs are listed on the top 100 toxic substances priority chart published by the Agency for Toxic Substances and Disease Registry [4].

The enzymes produced by soil microorganisms are involved in the catalytic transformation of organic pollutants and it is a crucial step in their biodegradation [5]. The VOCs degradation involves oxygenase, dehydrogenase, and ligninolytic enzymes. The fungal ligninolytic enzymes consist of lignin peroxidase, laccase, and manganese peroxidases [6].

The activity of enzymes is also one of the markers of changes occurring in the soil environment with the effect of natural and anthropogenic factors, especially organic xenobiotics [7]. The changes in soil enzymatic activities are among the earliest signals indicating the changes in the intensity of environmental life processes because multiple chemical compounds assume a toxic or mutagenic character following the metabolic transformations occurring in the living organisms [8].

In this paper, we characterize the impact of VOCs emitted from the creosote-treated wood on the activity of different enzymes involved in carbon, phosphorus, and nitrogen cycles in two different soils: loamy sand and sandy loam.

MATERIALS AND METHODS

The tests were performed on two soil materials collected from the topsoil of Brunic Arenosol in Agricultural Experimental Station in Lipnik (53°24'N, 14°28'E) and from the topsoil of Gleyic Chernozem in the Gumieniecka Plain (53°41'N, 14°47'E), in the West Pomeranian District, Poland. According to the classification of the United States Department of Agriculture, it was soil with a granulometric composition of loamy sand and sandy loam. Some of the soil properties are presented in Table 1.

TABLE 1
Properties of soils used in experiment

Properties	Loamy sand	Sandy loam
Organic carbon (g kg^{-1})	8.71	10.92
Total nitrogen (g kg^{-1})	0.83	1.03
Hydrolytic acidity (mmol(+) kg^{-1})	13.02	11.81
Cation exchangeable bases (mmol(+) kg^{-1})	10.50	13.39
Cation exchange capacity (mmol(+) kg^{-1})	23.52	25.20
pH in 1 M KCl	6.36	6.81

The soil collected from the field was air dried and then sieved through a sieve (2 mm mesh diameter). The soil was divided into samples of 0.5 kg weight and their moisture content was brought down to 60% of the maximum water capacity. The prepared soil samples were placed on 200 mm diameter Petri dishes in tightly closed desiccators of 15 dm^3 volume half filled with chopped railroad ties saturated with creosote oil. The reference points were soil samples stored in desiccators without shavings of railroad ties. The samples were incubated for 21 days. After 21 days, the samples were analyzed for the activity of enzymes involved in the metabolism of carbon compounds: dehydrogenases (EC 1.1.1.x) [9], catalase (EC 1.11.1.6) [10], *o*-diphenol oxidase (EC 1.10.3.1) [11], β-glucosidase (EC 3.2.1.21) [12], and lipase (EC 3.1.1.3) [13]; phosphorus compounds: acidic phosphomonoesterase (EC 3.1.3.2) and alkaline phosphomonoesterase (EC 3.1.3.1) [14], phosphodiesterase (EC 3.1.4.1) [15], phosphotriesterase (EC 3.1.8.1) [16], and inorganic pyrophosphatase (EC 3.6.1.1) [17]; and nitrogen compounds: urease (EC 3.5.1.5) [18], nitrate reductase (EC 1.6.6.1) [19], and proteases (EC 3.4.4.x) [20].

Deionized water purified using the HLP Smart 2000 demineralizer (manufactured by Hydrolab, Poland) with a mean appropriate conductivity of 0.15 $\mu S \cdot cm^{-1}$ and a surface tension of 72.3 $mN \cdot m^{-1}$ at 25°C was used for the preparation of solutions needed for analyzes. UV-1800 spectrophotometer (Shimadzu) was used for the spectrophotometric analyzes.

The results obtained were used to calculate the index of enzymatic resistance (RS) to effect of VOCs according to the formula developed by Orwin and Wardle [21]:

$$RS = 1 - \frac{2|D|}{C + |D|}$$

where C is the soil resistance under natural conditions (not exposed to VOCs) and P the resistance of soil exposed to VOCs; D = C−P.

The results were processed using Statistica 12.5 software (StatSoft, Inc.). The homogeneous groups were identified using Tukey's test at a significance level of $P<0.05$. The enzymatic resistance indices to the VOCs were described using the hierarchical cluster analysis (CA) applying Ward's method and Euclidean distance. Enzymatic responses to VOCs were compared using principal component analysis (PCA). CA and PCA were conducted by exploring multidimensional data sets.

RESULTS AND DISCUSSION

The results of the experiment indicate that soil exposed to VOCs emitted from creosote-treated wood produced different levels of enzyme activities. Among the enzymes involved in the carbon cycle, statistically significant increase in the activity of DHA (48.11%) and Lip (24.48%) in loamy sand and in the activity of DHA (14.50%) and CAT (12.99%) in sandy loam were observed compared to the control (Table 2). As reported by Praveen-Kumar and Tarafdar [22], an increased DHA activity in the soil can prove the accelerated metabolism of soil microorganisms, mainly bacteria and actinomycetes. The activity of dehydrogenases in soil is related to the activity of several enzymes or enzymatic systems commonly found in soil microorganisms [9] and the active DHA are present in soil as an integral part of the intact microbial cells [23]. Przybulewska et al. [24] showed an increase in the number of bacteria and actinomycetes in the soil as well as a decline in the number of fungi under the influence of *o*-xylene. An increase in the number of bacteria and decrease in the number of fungi in the soil contaminated with creosote was confirmed in the study conducted by Blakely et al. [25]. In turn, Stręk and Telesiński [26] showed an increase in the DHA activity in the first seven days following the creosote introduction into the sandy soil at a dose of 50 $g \cdot kg^{-1}$. In the further part of the experiment, creosote showed an inhibiting activity for the enzyme. Moreover, the activity of *o*-DPO was reduced compared to the control during the whole 28-day experiment. This study also found statistically significant loss in the *o*-DPO activity affected by VOCs, both in loamy sand (19.07%) and sandy loam (18.54%), as well as the Gluc activity in sandy loam (12.39%).

When analyzing the changes in the activity of enzymes involved in phosphorus compounds

TABLE 2
Activity of soil enzymes exposed to VOCs emitted from creosote-treated wood

Enzyme	Loamy sand		Sandy loam	
	Control	VOCs	Control	VOCs
Enzymes of carbon cycle				
DHA (mg TPF kg^{-1} DM h^{-1})	1.06 b	1.57 a	1.31 b	1.50 a
Gluc (mg *p*-NP kg^{-1} DM h^{-1})	89.95 a	92.06 a	94.44 a	82.74 b
CAT (mg H_2O_2 kg^{-1} DM h^{-1})	140.75 a	148.82 a	162.60 b	183.73 a
o-DPO (mg OC kg^{-1} DM h^{-1})	27.68 a	22.40 b	32.41 a	26.40 b
Lip (mg *p*-NP kg^{-1} DM h^{-1})	24.51 b	30.51 a	28.08 a	28.52 a
Enzymes of phosphorus cycle				
Pac (mg *p*-NP kg^{-1} DM h^{-1})	67.99 a	67.97 a	79.46 a	69.96 b
Pal (mg *p*-NP kg^{-1} DM h^{-1})	217.86 a	167.77 b	212.18 a	147.00 b
PD (mg *p*-NP kg^{-1} DM h^{-1})	5.00 a	4.89 a	5.89 a	4.65 b
PT (mg *p*-NP kg^{-1} DM h^{-1})	15.87 a	16.58 a	17.89 a	17.14 a
IPP (mg PO_4^{3-} kg^{-1} DM h^{-1})	151.53 a	111.90 b	191.22 a	108.03 b
Enzymes of nitrogen cycle				
Ure (mg N-NH_4 kg^{-1} DM h^{-1})	79.42 a	67.43 b	85.49 a	71.45 b
NR (µg N-NO_2^- kg^{-1} DM h^{-1})	2.47 a	1.68 b	2.00 a	1.34 b
Prot (mg Tyr kg^{-1} DM h^{-1})	26.30 a	15.09 b	40.20 a	21.46 b

Values denoted with the same letters in line do not differ statistically at $P<0.05$

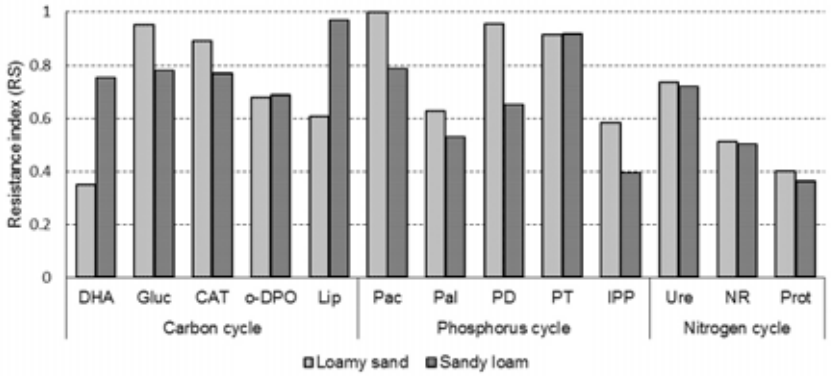

FIGURE 1
Resistance indices of enzyme activities in soil exposed to VOCs emitted from creosote-treated wood

metabolism, it was found that VOCs in loamy sand caused statistically significant inhibition of the activity of Pal (22.99%) and IPP (26.15%). In turn, activity of all examined enzymes except PT in sandy loam was subject to decrease under the influence of VOCs. The observed inhibition of activity for Pac, Pal, PD, and IPP was 11.96%, 30.72%, 21.05%, and 43.50%, respectively (Table 2). Changes in the activity of soil phosphatases could show the disturbances in hydrolyze compounds of organic P and transform them into inorganic P forms, which can be assimilated by plants and microorganisms [27]. Decrease in alkaline phosphomonoesterase could indicate some dysfunctions in the metabolism of microorganism, because this enzyme has not been detected in plants and it is mainly produced by soil bacteria and soil microorganisms other than arbuscular mycorrhizal fungi [28].

The activity of examined enzymes involved in the metabolism of nitrogen compounds, i.e., urease, nitrate reductase, and proteases, decreased in both soils under the influence of VOCs, and compared to the control this decrease in loamy sand was 15.10%, 31.98%, and 42.62%, and in sandy loam it was 16.42%, 33.00%, and 46.62%, respectively (Table 2). An inhibition of the activity of enzymes involved in the nitrogen cycle under the influence of variety of oil products was reported by many authors [23, 31–33].

It was found based on the calculated values of resistance index that among the enzymes involved in carbon metabolism, the most sensitive to VOCs in loamy sand was DHA (RS 0.35), while in sandy loam it was *o*-DPO (RS 0.69). However, in the case of enzymes involved in phosphorus cycle both in loamy sand and sandy loam, the lowest RS values were found in the activity of IPP (0.58 and 0.39, respectively). Among the enzymes involved in the metabolism of nitrogen compounds, in both soils, the lowest RS values were observed for Prot activity, in the loamy sand it was 0.40 and in the sandy loam it was 0.36 (Figure 1).

According to Griffiths and Philippot [32] and Orwin and Wardle [21], soil resistance values can be used to determine the analyzed ecosystem's sensitivity to various stressors. Soil resistance indicators

provide information about the status of soil environments contaminated with organic compounds, including hydrocarbons [33, 34]. There is a general scarcity in the published data about the influence of volatile organic compounds on soil resistance, and the results of this study can increase our knowledge about the resistance of soil contaminated with creosote.

Nannipieri et al. [35] reported that the interpretation of the effect of any pollutant on soil enzyme activities is problematic because of the limitations of the enzyme assays currently used (as already discussed) and the presence of direct and indirect effects on the target enzyme. For example, the inhibition of enzyme activity by a pollutant may be masked by the growth of surviving microorganisms with the expression of genes codifying the enzyme; the microbial growth may be due to the use of microbial debris (derived from microbial cells killed by the pollutant) by the surviving microorganisms [36].

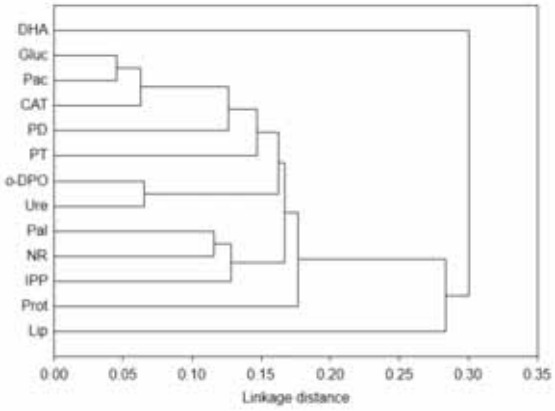

FIGURE 2
Similarities in the responses of enzyme activities in soil exposed to VOCs emitted from creosote-treated wood

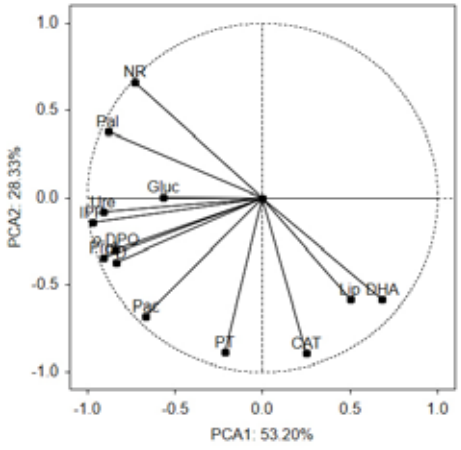

FIGURE 3
Principal component analysis for responses of enzyme activities in soil exposed to VOCs emitted from creosote-treated wood

For this reason, the responses of the tested enzymes to VOCs emitted from creosote-treated wood were confirmed by cluster analysis involving Ward's method and principal component analysis.

The results of cluster analysis involving Ward's method are presented in a dendogram in Figure 2. A high degree of similarity was observed between Gluc, Pac, and CAT, between *o*-DPO and Ure, and between Pal and NR, whereas Lip was the most significantly differed compared to remaining enzymes.

TABLE 3
Pearson product-moment correlation coefficients between responses of enzyme activities in soil exposed to VOCs emitted from creosote-treated wood.

Enzyme	PCA1	PCA2
DHA	0.68	-0.59
Gluc	-0.57	0.01
CAT	0.25	-0.90
o-DPO	-0.84	-0.30
Lip	0.50	-0.58
Pac	-0.67	-0.68
Pal	-0.88	0.38
PD	-0.84	-0.37
PT	-0.22	-0.88
IPP	-0.97	-0.14
Ure	-0.91	-0.08
NR	-0.73	0.66
Prot	-0.91	-0.34

PCA was carried out to establish the relationships between the response of soil enzymes to VOCs. Eigen values from PCA indicated that the first two principal components accounted for 81.53% of the variance of data (PC1: 53.20% and PC2: 28.33%; Figure 3). IPP, Ure, Prot, Pal, and *o*-DPO had a major negative effect on PC1 (−0.97, −0.91, −0.91, −0.88, and −0.84, respectively), while CAT and PD had a major negative effect on PC2 (−0.90 and −0.88, respectively). However, the PC1 was the most positively correlated with DHA (0.68) and the PC2 with NR (0.66) (Table 2).

CONCLUSION

We showed that VOCs emitted from creosote-treated wood affected the enzymatic activity of the soil. The biggest changes occurred in the activity of enzymes involved in the metabolism of nitrogen compounds. Among all examined enzymes, the most frequently observed effect was activity reduction. A stimulating effect of VOCs was only reported for dehydrogenases and lipase. Moreover, more changes in the enzymatic activity were noted in sandy loam compared to loamy sand.

ABBREVIATIONS

CAT, catalase; DHA, dehydrogenases; Gluc, β-glucosidase; IPP, inorganic pyrophosphatase; Lip, lipase; NR, nitrate reductase; *o*-DPO, *o*-diphenol oxidase; Pac, acid phosphomonoesterase; Pal, alkaline phosphomonoesterase; PD, phosphodiesterase; Prot, proteases; Ure, urease

REFERENCES

[1] Gallego, E., Roca, F.J., Perales, J.F., Guardino, X., Berenguer, M.J. (2008) VOCs and PAHs emissions from creosote-treated wood in a field storage area. Science of the Total Environment 402, 130-138.

[2] Simarro, R., González, N., Bautista, L.F., Molina, M.C. (2013) Assessment of the efficiency of *in situ* bioremediation techniques in a creosote polluted soil: Change in bacterial community. Journal of Hazardous Materials 301, 17-26.

[3] Grant, R.J., Muckian, L.M., Clipson, N.J.W., Doyle, E.M. (2007) Microbial community changes during the bioremediation of creosote-contaminated soil. Letters in Applied Microbiology 44, 293-300.

[4] Biswas, B., Sarkar, B., Rusmin, R., Naidu, R. (2015) Bioremediation of PAHs and VOCs: Advances in clay mineral–microbial interaction. Environment International 85, 168-181.

[5] Huang, P.M. (2004) Soil mineral-organic matter-microorganism interactions: fundamentals and impacts. Advances in Agronomy 82, 391-472.

[6] Haritash, A., Kaushik C. (2009) Biodegradation aspects of polycyclic aromatic hydrocarbons (PAHs): a review. Journal of Hazardous Materials 169, 1-15.

[7] Bielińska, E.J., Mocek-Płóciniak, A. (2010) Impact of ecochemical soil conditions on selected heavy metals content in garden allotment vegetables. Polish Journal of Environmental Studies 19(5), 895-900.

[8] Filipek-Mazur, B., Tabak, M., Gorczyca, O. (2014) Enzymatic activity of soils exposed to transportation pollutants, located along road No. 957. Journal of Ecological Engineering 15(4), 145-149.

[9] Thalmann, A. (1968) Zur Methodik der Bestimmung der Dehydrogenaseaktivität im Boden mittels Triphenyltetrazoliumchlorid (TTC). Landwirtschaftliche Forschung 21, 249-258 (In German).

[10] Johnson, J.I., Temple, K.L. (1964) Some variables affecting measurement of catalase activity in soil. Soil Science Society of America Proceedings 28, 207-209.

[11] Perucci, R., Casucci, C., Dumonet, S. (2000) An improved method to evaluate the *o*-diphenol oxidase activity of soil. Soil Biology and Biochemistry 32(8-9), 1927-1933.

[12] Eivazi, F., Tabatabai, M.A. (1988) Glucosidases and galactosidases in soils. Soil Biology and Biochemistry 20, 601-606.

[13] Margesin, R., Feller, G., Hämmerle, M., Stegner, U., Schinner, F. (2002) A colorimetric method for determination of lipase activity in soil. Biotechnology Letters 24, 27-33.

[14] Tabatabai, M.A., Bremner, J.M. (1969) Use of p-nitrophenyl phosphate for assay soil phosphatase activity. Soil Biology and Biochemistry 1(4), 307-310.

[15] Browman, M.G., Tabatabai, M.A. (1978) Phosphodiesterase activity of soils. Soil Science Society of America Journal 42, 284-290.

[16] Eivazi, F., Tabatabai, M.A. (1977) Phosphatases in soils. Soil Biology and Biochemistry 9, 167-172.

[17] Dick, W.A., Tabatabai, M.A. (1978). Inorganic pyrophosphatase activity of soils. Soil Biology and Biochemistry 10, 59-65.

[18] Kandeler, E., Gerber, H. (1988) Short-term assay of soil urease activity using colorimetric determination of ammonium. Biology and Fertility of Soils 6, 68-72.

[19] Abdelmagid, H.M., Tabatabai, M.A. (1987) Nitrate reductase activity of soils. Soil Biology and Biochemistry 19, 421-427.

[20] Ladd, I.N., Butler, J.H.A. (1972) Short-term assay of soil proteolytic enzyme activities using proteins and dipeptide derivates as substrates. Soil Biology and Biochemistry 4, 19-30.

[21] Orwin, K.H., Wardle. D.A. (2004) New indices for quantifying the resistance and resilience of soil biota to exogenous disturbance. Soil Biology and Biochemistry 36, 1907-1912.

[22] Praveen-Kumar, J.C., Tarafdar (2003) 2,3,5-Triphenyltetrazolium chloride (TTC) as electron acceptor of culturable soil bacteria, fungi and actinomycetes. Biology and Fertility of Soils 38, 186-189.

[23] Lipińska, A., Wyszkowska, J., Kucharski, J. (2015) Diversity of organotrophic bacteria, activity of dehydrogenases and urease as well as seed germination and root growth *Lepidium sativum*, *Sorghum saccharatum* and *Sinapis alba* under the influence of polycyclic aromatic hydrocarbons. Environmental Science and Pollution Research 22, 18519-18530.

[24] Przybulewska, K., Wieczorek, A., Krzywy-Gawrońska, E., Zaręba, N., Turała, A. (2012) Effect of environmental contamination with orthoxylen on the number of soil micr-oorganisms. In: Musialik-Piotrowska, A., Rutkowski, J.D. (Ed-s.) Air protection – chosen problems. PZITS, Wrocław, 247-251 [In Polish].

[25] Blakely, J.K., Neher, D.A., Spongberg, A.L.

(2002) Soil invertebrate and microbial communities, and decomposition as indicators of polycyclic aromatic hydrocarbon contamination. Applied Soil Ecology 21, 71-88.
[26] Stręk, M., Telesiński, A. (2016) The effect of calcium peroxide on the activity on some oxidoreductases in soil contaminated with creosote. Chemistry. Environment. Biotechno-logy 19, 7-11 [In Polish].
[27] George, T.S., Gregory, P.J., Hocking, P., Richardson, A.E. (2008) Variation in root-associated phosphatase activities in wheat contributes to the utilization of organic P substrates in vitro, but does not explain differences in the P-nutrition of plants when grown in soil. Environmental and Experimental Botany 64, 239-249.
[28] Piotrowska-Długosz, A., Wilczewski, E. (2014) Soil phosphatase activity and phosphorus content as influenced by catch crops cultivated as green manure. Polish Journal of Environmental Studies 23(1), 157-165.
[29] Guo, H., Yao, J., Cai, M., Qian, Y., Guo, Y., Richnow, H.H., Blake, R.E., Doni, S., Ceccanti, B. (2012) Effects of petroleum contamination on soil microbial numbers, metabolic activity and urease activity. Chemosphere 87(11), 1273-1280.
[30] Ma, J., Shen, J., Liu, Q., Fang, F., Cai, H., Guo, C. (2014) Risk assessment of petroleum-contaminated soil using soil enzyme activities and genotoxicity to *Vicia faba*. Ecotoxicology 23(4), 665-673.
[31] Stręk, M., Telesiński, A. (2016) Comparison of selenite (IV) and selenate (VI) effect on some oxidoreductive enzymes in soil contaminated with spent engine oil. Plant Soil and Environment 62(4), 157-163.
[32] Griffiths, B.S., Philippot, L. (2013) Insights into the resistance and resilience of the soil microbial community. FEMS Microbiology Reviews 37(2), 112-129.
[33] Kaczyńska, G., Borowik, A., Wyszkowska, J. (2015) Soil dehydrogenases as an indicator of contamination of the environment with petroleum products. Water Air and Soil Pollution 226(11), 372.
[34] Wyszkowska, J., Borowik, A., Kucharski, J. (2015) Response of *Avena sativa*, microorganisms and enzymes to contamination of soil with diesel oil. Plant Soil and Environment 61(11), 483-488.
[35] Nannipieri, P., Ascher, J., Ceccherini, M.T., Landi, L., Pietramellara, G., Renella, G. (2003) Microbial diversity and soil functions. European Journal of Soil Science 54, 655-670.
[36] Nannipieri, P., Giagnoni, L., Landi, L., Renella, G. (2011). Role of phosphatase enzymes in soil. In: Bünemann, E.K., Oberson, A., Frossard, E. (Eds.), Phosphorus in action. Springer-Verlag, Berlin, Heidelberg, pp. 215-243.

Received: **10.08.2017**
Accepted: **20.08.2017**

CORRESPONDING AUTHOR

Arkadiusz Telesinski
Department of Plant Physiology and Biochemistry, West Pomeranian University of Technology in Szczecin, Słowackiego 17, 71-434 Szczecin, Poland

e-mail: arkadiusz.telesinski@zut.edu.pl

© by PSP Volume 26 – No. 10/2017 pages 6064-6070 Fresenius Environmental Bulletin

EVALUATION OF ECOLOGICAL TOLERANCE AND REQUIREMENTS OF EXOTIC CONIFERS IN THE URBAN LANDSCAPE OF BURSA

Nilufer Seyidoglu Akdeniz, Elvan Ender, Murat Zencirkiran*

Department of Landscape Architecture, Faculty of Agriculture, University of Uludag, 16 059 Gorukle, Bursa, Turkey

ABSTRACT

Plants are alive landscape elements showing lively, dynamic, decorative, aesthetic and functional features and they are actively used both in urban and rural landscape applications. Effective compositions can be created by using a combination of native and exotic (foreign originated) plants in urban landscaping instead of being content just with native species. In this study, exotic conifers that appear in the urban landscape of Bursa, which has a rich diversity due to its location and ecologic situation, is determined in detail with their potentials and their evaluation in terms of their ecological tolerance (frost, drought, and salt tolerance) and ecological requests (soil properties, light requirements). As a result of the evaluation, 17 genera belonging to 5 families, 46 species and 72 cultivars have been found to be used in the urban landscape of Bursa. Many of the exotic conifers were determined to be resistant to urban conditions and had high environmental tolerance

KEYWORDS:
Ecological requests, urban landscape, ecological resistance.

INTRODUCTION

Urbanisation is a global phenomenon with a higher rate in developing nations. It has brought immense benefits to human society and resulted in higher living standards. In addition to this, social, economic opportunities and urbanization cause people living in rural areas to settle in cities [1]. However, it has also caused a large scale negative impact on the global environment including increased pressure on native biodiversity, unprecedented increase in production of waste and pollution [2] and environmental problems have increased worldwide along with an increase of urbanization [3]. Due to human influences, the quality of urban landscapes and land use is often impaired.

On the other hand, green spaces have been one of the key components of urban landscapes and play an important role in improving the quality of life of city-dwellers. They are capable of shaping the image of a city and provide biological diversity and several other benefits such as improved climate, hygiene, aesthetics, recreational opportunities, environmental protection and biodiversity, while they also help meet the social, spiritual and psychological needs of urban people [3, 4]. Plants (especially trees and shrubs) are the most important materials to be used while forming living green spaces or liveable green spaces. However, the importance of green spaces in urban areas is due to their role in aspects of urban life [5]. Some functions of plants especially trees in urban areas are ecological, economical, aesthetical and social. Trees play a crucial role as providers of ecosystem services, which enhance human well-being directly and indirectly [6, 7, 8]. Meanwhile, plants are examined under different groups such as native, exotic, naturalized and of unknown origin in terms of their origin. The diversity in the origins of the species is important for landscaping and it allows the emergence of different applications. Enhancement of biodiversity in urban ecosystems can have a positive impact on the quality of life and educate urban dwellers, thus ultimately facilitate the preservation of biodiversity also in natural ecosystems [9].

Species diversity also provides greater security against environmental changes and stochastic events, including pest invasions, by increasing the potential for adaptation and survival. Urban biodiversity, in particular, increases the amount of exposure that city residents have to a wide spectrum of nature, which is an important element in stimulating people's desire to support conservation. Additionally, evidence suggests a range of positive psychological and physiological effects are present when people interact with areas high in biodiversity [10].

Urban trees deliver measurable benefits to urban environmental quality and residential quality of life. They reduce urban heat stress, building energy use, atmospheric carbon dioxide (CO_2), rainfall runoff, flooding, noise levels, and wind speed, and remove air pollutants. Trees cooling effects in urban areas will become more important given the impact of climate change [11]. The speed of climate change is expected to exceed the ecological amplitude for adaptation of many tree species. Air temperature is expected to increase in southern Europe between 2 and 3^{o}C before 2050, recent research suggests that climate change will result in extreme inter annual

variability in terms of heat and cold waves. These extreme events can have a great ecological importance in tree species survival [12].

Accordingly, when selecting trees for urban landscapes, planners must prioritise stress resistance and climate adaptation above aesthetic appeal and functional aspects [13]. The selection of tree species for urban sites should consider the adaptability to the environmental site conditions, functions of the tree, and low costs of propagation, production, establishment, and management. Functions of the tree include benefits to people and aesthetic quality of the site. However, little is known about which tree characteristics are relevant to perception and how they are associated with tree's aesthetics. Furthermore, within tree species composition in urban sites, there is a troubling conflict between the aesthetic preference for visual uniformity and the ecological need for species diversity. In the face of climate change, the importance of species diversity is growing even more, as higher temperatures and longer periods of drought increase the vulnerability of urban trees to pests and diseases [11].

This study was carried out in order to ensure the sustainable use of the plant in the urban landscape of Bursa which closely feels the pressure of urbanization and climate change. For this purpose, exotic woody plant species and landscape characters used in the urban landscape have been identified and ecological tolerances of these plants (soil, light, temperature, etc.) have been tried to be exhibited.

MATERIAL AND METHODS

Research material and study area. Our study was focused on Bursa, one of the biggest cities of Turkey. The province Bursa, which is subject to the study, is located in Susurluk basin in the south of Marmara Region 39° 35'- 40° 40' north latitude and 28° 10'- 30° 00' east longitude. It has a land area of 1 104 301 ha (Figure 1). Uludag, which is the most significant elevation of the Marmara Region, is located within the boundaries of Bursa. Iznik and Uluabat lakes, which are located within the boundaries of the province, constitute the two major freshwater lakes. Although plains of Bursa shows the general characteristics of the Mediterranean type of climate, the region has a low mean temperature and a high annual precipitation whose distribution by months is also partly regular compared to the Mediterranean Region. According to De Mortanne drought index equation, summer months are dry and autumn and spring months are less humid (Table 1) [14, 15]. The material of the study consists of exotic conifers located within the boundaries of the province Bursa.

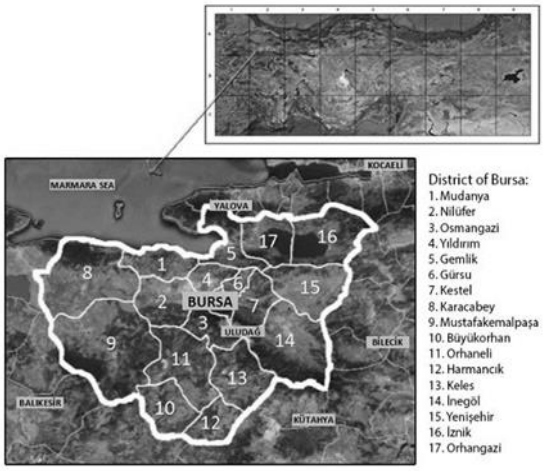

FIGURE 1
Research area

TABLE 1
Bursa climate in last 65 years*.

Average temperature (°C)	14.5
Maximum temperature (°C)	43.8
Minimum temperature (°C)	-19.2
Precipitation (total-mm)	695.1

*Turkey, General directorate of meteorology data 2016.

Method. This study, which was carried out in order to identify exotic conifers species, consisted of two phases which are observation phase and analysis and evaluation phase. In the first phase of the study (observation phase), streets, traffic islands, small bazaar squares, small and large scaled squares and parks, garden houses in Bursa and its counties have been seasonally examined in line with the current site plan and the species of the conifers used for landscaping of the mentioned places have been identified and their dendrological features have been defined. [8, 10, 11, 13, 14, 15, 16, 17] The exotic conifers species are evaluated as follows [18, 19]: trees: short trees (up to 10m of height), medium-sized trees (from 10 to 18 m of height), large trees (over 18 m of height), giant trees (over 50 m of height); shrubs: large shrubs (over 3 m of height), medium-sized shrubs (from 1.5 to 3 m of height), short shrubs (from 1 to 1.5 m of height), dwarf shrubs (from 0.3 to 0.75 m of height), prostrate (creeping) shrubs.

In the second phase of the study (analysis and evaluation phase), ecological tolerances (soil properties, light requirements, frost tolerance, drought tolerance, and salt tolerance) of the identified exotic conifers on the study area have been revealed [18, 19, 20, 21, 22, 23, 24, 25]. As a result of this evaluation, recommendations have been developed for the use of exotic conifers in urban landscape of Bursa.

TABLE 2
Plant species, varieties and cultivars of exotic conifers used in urban landscape in Bursa.

Genus	Species, varieties and cultivars
Cupressus	*Cupressus sempervirens* L. (var. *Pyramidalis), Cupressus arizonica* Woodall (cv: '*Glauca'*, 'Glauca Compacta','Glauca Pyramidalis'), *Cupressus goveniana* GORD., *Cupressus macrocarpa* GORD. (C. lambertiana GORD.) (cv: 'Goldcrest', 'Wilma')
Chamaecyparis	*Chamaecyparis lawsoniana* (MURR.)PARL.(cv: 'Alumii', 'Aureavariegata', 'Ellwoodii', 'Elwood's Gold', 'Stricta', 'Lutea', 'Minima Glauca'), *Chamaecyparis pisifera* (SIEB & ZUCC.) ENDL. (cv: Filifera', 'Filifera Aurea', 'Nana', 'Boulevard', 'Squarrosa Aurea Nana'), *Chamaecyparis obtusa* (SIEB & ZUCC.)ENDL (cv: 'Nana Gracilis'), *Chamaecyparis nootkatensis* (D.DON) SPACH (cv: 'Pendula')
Thuja	*Thuja orientalis* L. (*Biota orientalis* (L.) ENDL.) (cv: 'Compacta', 'Compacta Aurea', 'Pyramidalis', 'Pyramidalis Aurea', 'Elegantissima'), *Thuja occidentalis* L. (cv: 'Pyramidalis', 'Rheingold', 'Smaragd', 'Sunkist', 'Holmstrup', 'Danica', 'Tiny Tim'), *Thuja plicata* D.DON (*T. lobbii* HORT. ex GORD) (cv: 'Aurea', 'Zebrina')
Juniperus	*Juniperus chinensis* L. (cv: 'Albovariegata','Aurea', 'Blue Alps', 'Columnaris', 'Kaizuka', 'Spartan', 'Stricta', 'Pfitzeriana', 'Pfitzeriana Glauca') *Juniperus comminus* L. (cv: 'Green Carpet', 'Hibernica', 'Oblonga Pendula', 'Repanda'), *Juniperus conferta* PARL. (*J. litoralis* MAXIM.), *Juniperus drupacea* LABILL., *Juniperus virginiana* L. (cv: 'Canaertii', *a* 'Cupressifolia', 'Grey Owl', 'Hillii'), *Juniperus horizontalis* MOENCH. (cv: 'Alpina', 'Bar Harbor', 'Blue Chip', 'Glauca'), *Juniperus procumbens* SIEB.ex.MIQ (cv: 'Nana'), *Juniperus foetidissima* Willd., *Juniperus scopulorum* SARG (cv: 'Skyrocket')
Calocedrus	*Calocedrus decurrens* (TORR.) FLORIN (cv: 'Aureovariegata')
Cupressocyparis	*Cupressocyparis leylandii* (DALLIM &Jacks.)DALLIM.
Abies	*Abies concolor* (GORD.)LINDL., *Abies alba* MILLER
Cedrus	*Cedrus libani* Link., *Cedrus atlantica* MANETTI. (cv: '*Glauca*', '*Glauca* Pendula'), *Cedrus deodora* G. DON. (cv: 'Aurea', Pendula')
Picea	*Picea orientalis* (L.) Link., *Picea excalsa* LINK (*P. Abies* (L.)KARSTEN), *Picea omorika* (PANCIC) PURKYNE, *Picea pungens* ENGELM. (cv: '*Glauca*', 'Hoppsii', 'Globosa'), *Picea glauca* (MOENCH) VOSS.(*P.alba* LINK) (var. *albertiana* 'Conica')
Pinus	*Pinus brutia* TENORE, *Pinus griffithii* Mc.Clelland., *Pinus nigra* subsp. *pallasiana* (var.*pyramidata*), *Pinus pinaster* AIT (*P. maritima* POIR.), *Pinus strobus* L., *Pinus mugo* TURRA (*P. mughus* Scop) (var. *pumilia*)
Pseudotsuga	*Pseudotsuga menziesii* (MIRB.) FRANCO
Taxus	*Taxus baccata* L (.cv: 'Fastigiata', *' Aurea*)
Cryptomeria	*Cryptomeria japonica* D.DON (cv: 'Elegans', 'Globosa Nana')
Metasequoia	*Metasequoia glyptostroboides* HU & CHENG.
Sequia	*Metasequoia glyptostroboides* HU & CHENG.
Taxodium	*Taxodium distichum* (L.) RICH.
Ginkgo	*Ginkgo biloba* L.

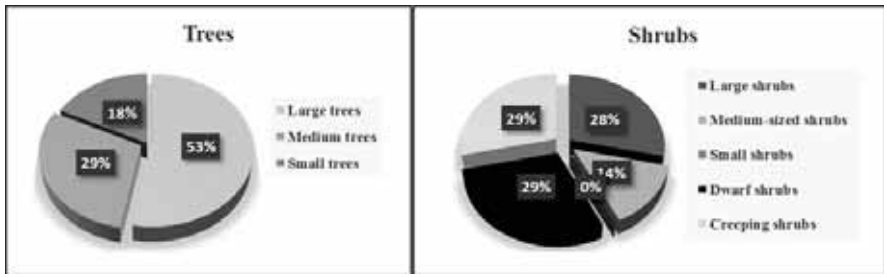

FIGURE 2
Application rates of exotic coniferous plants in Bursa.

RESULTS

Evaluation of exotic conifers in terms of species. In Bursa 17 genus, 46 species and 72 cultivars in 5 families belonging to Gymnospermae subdivision have been identified. It has been observed that 23 of these species are located in Cupressaceae family, 17 in Pinaceae family, 1 in Ginkgoaceae family, 1 in Taxaceae family and 4 in Taxodiaceae family (Table 2). Analyses on the application rates of exotic coniferous plants have indicated that tall trees dominate the urban landscape (46.55%). Medium-sized trees follow this group with 25.86% and short trees with 15.52%. On the other hand, when shrubs are analysed, it has been detected that the highest rate belongs to large shrubs, and dwarf and prostrate (creeping) shrubs has the lowest share with 3.45 %. Short shrubs are not preferred for landscaping (Figure 2). When the distribution of the plants used in the urban landscape by genus and species examined, it has been identified that the family containing the highest amount of genus is Cupressaceae with 35.29%. Pinaceae, Taxodiaceae, Taxaceae and Ginkgoaceae families follow this family with 29.41, 23.53 and 5.88%. When the distribution of species examined, it has been observed that the families are rich in diversity. Cupressaceae family includes the highest amount of species with 48.89%. Pinaceae and Taxodiaceae families follow the Cupressaceae family with 37.78 and 8.89%. Families containing the least amount of species are Taxaceae and Ginkgoaceae with 2.22 % (Figure 3). It has been observed that a large number of cultivars of exotic coniferous plants appear in the landscape of Bursa and cultivars belonging to species are stated in Table 3.

TABLE 3
Cultivar distribution according to species.

Genus	Species	Cultivar (%)	Genus	Species	Cultivar (%)
Cupressus	*C. sempervirens*	1,39	Juniperus	*J. chinensis*	12,5
	C. arizonica	4,17		*J. comminus*	6,94
	C, macrocarpa	2,78		*J. virginiana*	5,56
	C. lawsoniana	9,72		*J. horizontalis*	5,56
	C. pisifera	6,94		*J. procumbens*	1,39
Chamaecyparis	*C. obtusa*	1,39		*J. scopulorum*	1,39
	C. nootkatensis	1,39	Picea	*P. pungens*	*2,78*
	T. orientalis	6,94		*P. glauca*	*1,39*
Thuja	*T. occidentalis*	9,72	*Pinus*	*P. nigra*	*1,39*
	T. plicata	2,78		*P. mugo*	*1,39*
Taxus	*T. baccata*	*2,78*	*Cryptomeria*	*C. japonica*	*2,78*
Cedrus	*C. atlantica*	*2,78*	*Calocedrus*	*C. decurrens*	*1,39*
	C. deodora	*2,78*			

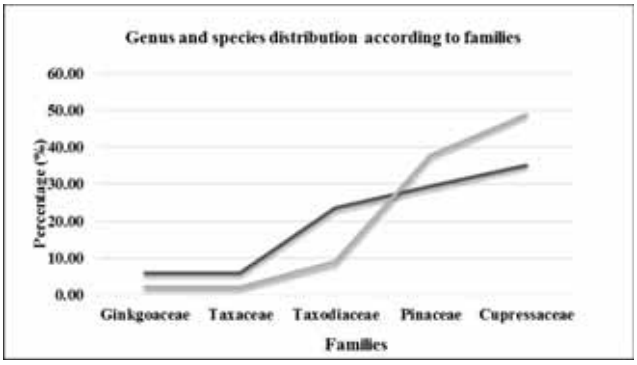

FIGURE 3
Distribution of species and genus in coniferous plants according to families.

These cultivars are found to be mostly of *Juniperus, Thuja, Chamaecyparis* and *Cupressus* species. According to the evaluation made on the basis of the species among the cultivars used in urban landscape, the highest rate belongs to the cultivars of the species *J. chinensis* (12.50%). *C. lawsoniana* and *T. occidentalis* (9.72%), *T. orientalis* and *J. communis* (6.94%), *J. virginiana* and *J. horizontalis* (5.56%) and *C. arizonica* (4.17%) follow *J. chinensis.* On the other hand, species not having any cultivars and being represented by single species such as *Abies concolor*, *Picea orientalis*, *Pinus grifittii*, *Pseudotsuga menziesii*, *Metasequoia glyptostroboides*, *Sequoia sempervirens*, *Taxodium distichum* and *Ginkgo biloba* are found out to be used in urban landscape.

Evaluation of exotic conifers in terms of ecological tolerance and requirements. Exotic conifers that were determined were grouped in terms of ecological requirements (soil and light) and ecological tolerance of plants were evaluated for resistance to drought, frost and salt. The results obtained on the evaluation of soil properties, soil texture class, mass class and pH are given in Table 4. It is determined that 36.89% of the detected plants liked sandy soil, 54.1% of them wanted good drainage and 51.79% of them had good growth in acidic soil.

A classification is made according to light requests of exotic conifers, and 37.60% of the conifers need full sun, 26.09% need sun, 30.43% need partshade, 5.80% of them need shade (Figure 4).

Ecological tolerances of exotic conifers were examined in terms of frost, drought, salt resistance and air pollution (Table 5). 81.40% of the determined exotic conifers were resistant to frost, and 67.44% showed higher durability to drought. Only 32.56% of the detected conifers were found to be salt tolerant (Figure 5)

TABLE 4
Soil properties of exotic conifers in Bursa.

Soil properties		Frequencies (%)
Soil texture	sandy	36,89
	clay	27,18
	loamy	35,92
Soil mass	well-drained	54,1
	moist	40,98
	wet	4,92
pH	acidic	51,79
	neutral	7,14
	alkaline	41,07

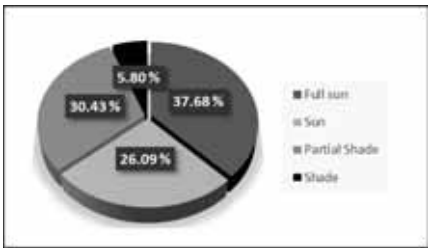

FIGURE 4
Light requirements of exotic conifers in Bursa.

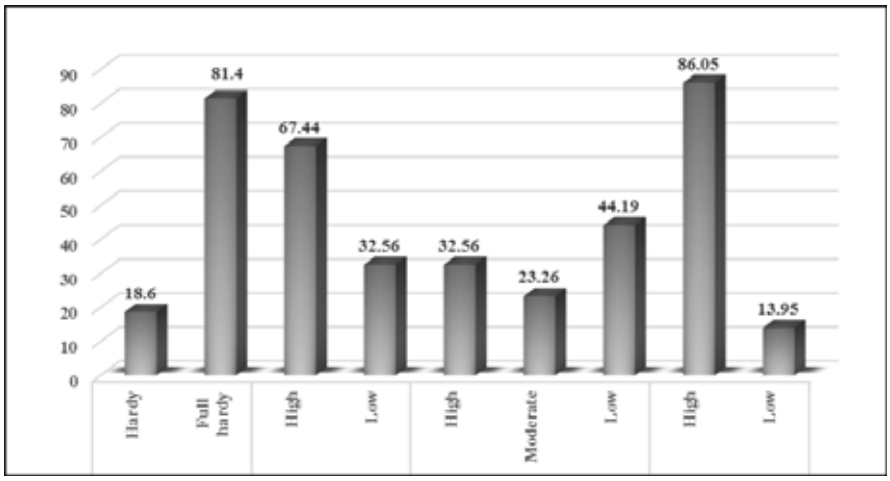

FIGURE 5
Distribution of ecological tolerance (%) of exotic conifers in Bursa.

TABLE 5
Ecological tolerance of exotic conifers in Bursa.

Plant name	Ecological tolerance								
	frost		drought		salt		air pollution		
	hardy (-5 °C) – (-15°C)	full hardy (down to -15 °C)	high	low	high	moderate	low	high	low
Abies alba		*	*				*		*
Abies concolor		*	*				*	*	
Calocedrus decurrens		*	*		*			*	
Cedrus atlantica		*	*				*	*	
Cedrus deodora		*	*				*	*	
Cedrus libani		*		*			*		*
Chamaecyparis lawsoniana		*	*			*		*	
Chamaecyparis nootkatensis		*		*			*		*
Chamaecyparis obtusa		*	*				*		*
Chamaecyparis pisifera		*	*				*	*	
Cryptomeria japonica		*		*			*	*	
Cupressoscyparis leylandii		*	*			*		*	
Cupressus arizonica	*		*		*			*	
Cupressus goveniana	*			*	*			*	
Cupressus macrocarpa	*		*		*			*	
Cupressus sempervirens	*		*			*		*	
Ginkgo biloba		*	*			*		*	
Juniperus chinensis		*	*			*		*	
Juniperus comminus		*	*			*		*	
Juniperus conferta		*	*		*			*	
Juniperus drupacea		*	*				*	*	
Juniperus foetidissima	*		*			*		*	
Juniperus horizontalis		*	*		*			*	
Juniperus procumbens		*	*		*			*	
Juniperus scopulorum		*	*				*	*	
Juniperus virginiana		*	*		*			*	
Metasequoia glyptostroboides		*		*			*	*	
Picea excelsa		*		*		*		*	
Picea glauca		*	*				*	*	
Picea omorika		*		*			*	*	
Picea orientalis		*		*	*			*	
Picea pungens		*		*	*			*	
Pinus brutia	*		*				*	*	
Pinus griffithii		*	*				*	*	
Pinus mugo		*		*	*			*	
Pinus nigra		*	*		*			*	
Pinus pinaster	*		*		*			*	
Pinus strobus		*		*			*		*
Sequoia sempervirens	*			*			*		*
Taxodium distichum		*	*			*		*	
Taxus baccata		*		*		*		*	
Thuja occidentalis		*		*	*			*	
Thuja orientalis		*	*				*	*	

DISCUSSION AND CONCLUSION

Plants contributing to urban aesthetics and ecology in the creation of liveable cities are one of the most indispensable elements in landscape design. Also, the history, identity, cultural characteristics and geography of cities may have an impact on plants in cities [5]. Aesthetic and functional characteristics of plants are of great importance as they improve and enrich their environment with their appearance. On the other hand, Steiner [26] has stated that planning with nature can improve the quality of urban settlements for people, plants and animals, and enhance ecosystem services. Both native and exotic plant species and their number vary depending on geographic location, soil type, economic structure, land use, climate and local governments [17, 27, 28, 29].

The impact of the vast fertile lands of Bursa plain, of the semi-terrestrial and Mediterranean climate type that starts from high altitudes and is seen up to the coastal areas, on the diversity is inevitable. Both in the city centre and at the counties of Bursa it is observed that several exotic species are used in many areas such as official institutions, home gardens, open green spaces and parks. It is seen that especially in urban landscaping, medium-sized coniferous tree species which are included in the species *Juniperus, Cupressus, Chamaecyparis* and *Thuja* are used dominantly. This situation is in compliance with Jim [27] and Yilmaz and Irmak [17]. Hence, Jim [27] and Yilmaz and Irmak [17] stated that the plant species used in the cities and their application rates vary depending on the area, geographic location, the history of the city, local governments and individual preferences. According to Foresman et al. and Lister, 'Urban ecosystems represent the most complex mosaic of vegetative land cover and multiple land uses of any landscape' which may be because they are formed by human design [16].

Good planning and governance practices for greater urban tree diversity do exist across the globe. Enhanced tree diversity has become integrated in Singapore green infrastructure planning, while cities such as Copenhagen and Denmark try to get away from a tradition of using only a few, dominating tree species, such as elm and lime [13]. On the other hand, poor planning and governance practices lead to the emergence of some problems. For example, more than 1.8 million cedar trees were planted on the periphery of Tokyo, Japan, decades ago and today, during their pollination in spring, they have turned this mega-city into the allergy capital of the World with three million allergic residents in Tokyo [30].

Many studies have reported that the number (and proportion) of exotic species tends to increase along the urban–rural gradient, moving towards the urban centre. There are concerns that exotic species will out-compete native species and therefore urban landscapes with too many exotic species will not function well in terms of providing ecosystem services even though they are diverse [16].

The stressful urban environment (e.g. exposure to heat, low air humidity, periods of drought, high soil pH, limited soil volume, de-icing salt and other pollutants), together with the predicted climate-change-related increases in average temperature and more frequent heat waves and droughts in some areas during summer create challenges. On the other hand, the argument for the use of exotic species often refers to fluctuating environmental conditions, which are expected to increase under climate change. Under such conditions it is suggested that exotic species have a better chance to cope with these fluctuations than native species. There are also suggestions that compromises should be made and that natural sites should be established that mainly contain natives, whereas semi-natural and artificial sites could accommodate both [16].

The results reveal that Bursa urban landscape has a rich diversity in terms of the exotic plants used in design. Indeed, it has been evaluated that exotic conifers determined in city scape are compatible with different soil structures. On the other hand, it has been determined that most of those species have a good performance standing on frost, drought and salt. The importance of increasing the proportion of species, which are resistant to adverse conditions as a result of climate change in the city scape, was observed. In this context, for the elimination of the deficiencies and creating public awareness for sustainable landscape areas, measures to be taken by the local governments are inevitable.

REFERENCES

[1] Wei, W., Shi, P., Zhou, J., Li, C., and Xie, B. (2017). Analysıs Of Urban Expansion And Landscape Patterns In Arid Inland: A Case Study Of Liangzhou District In Northwest China. Fresen. Environ. Bull., 26 (6):3880-3885.

[2] Bhardwaj, B.M. and Singh, S. (2015). Air Pollution Tolerance of Ornamental Trees in Industrial City. Hortflora Research Spectrum, 4 (3):185.

[3] Öztürk S. and Bozdoğan, E. (2015). The Contribution Of Urban Road Trees On Improving The Air Quality In An Urban Area. Fresen. Environ. Bull., 24 (5a):1822-1829.

[4] Hepcan, S. (2013). Analyzing the Pattern and Connectivity of Urban Green Spaces: a Case Study of Izmir, Turkey. Urban Ecosystems, 16, 279.

[5] Bekçi, B., Cengiz,C. and Cengiz, B. (2012). Evaluating Urban Biodiversiy In Terms Of User Preferences: Urban Residential Landscapes In Bartın (Turkey). Fresen. Environ. Bull., 21 (6b):1626-1635.

[6] Cervantes-camacho, M., Schondube, J.E., Castıllo, A. and Macgregor-Fors, I. (2014). How Do People Perceive Urban Trees? Assessing Likes and Dislikes in Relation to the Trees of a City. Urban Ecosystems, 17, 761.
[7] Escobedo, F. and Chacalo, A. (2008). Reduction in Atmosphere Pollution Due to the Urban Trees in Mexico City (Descontaminación Atmosférica Por El Arbolado Urbano De La Ciudad De México). Interciencia, 33, 29.
[8] Grahn, P. and Sıigsdotter, U.A. (2003). Landscape Planning and Stress. Urban Forestry & Urban Greening, 2, 1.
[9] Nielsen,A.B., Bosch Van Den, M., Maruthaveeran, S. and Bosch Van Den, C.K. (2014). Species Richness in Urban Parks and İts Drivers: a Review of Emprical Evidence. Urban Ecosystems, 17, 305.
[10] Bourne, K.S. and Conway, T. M. (2014). The Influence of Land Use Type and Municipal Context on Urban Tree Species Diversity. Urban Ecosystems, 17, 329.
[11] Gerstenberg, T. and Hofmann, M. (2016). Perception and Preference of Trees: a Psychological Contibution to Tree Species Selection in Urban Areas. Urban Forestry & Urban Greening, 15, 103.
[12] Mayoral, C., Stimberck, R., Gonzalez, M.S., Rafael, C. and Pardos, M. (2015). Dynamics of Frost Tolerance during Regeneration in Mixed (Pine – Oak - Juniper) Mediterranean Forest. Trees, 29, 1893.
[13] Sjöman, H., Ostberg, J. and Buhler, O. (2012). Diversity and Distribution of the Urban Tree Population in Ten Major Nordic Cities. Urban Forestry & Urban Greening, 11, 31.
[14] Zencirkiran, M. (2004). Plant Species to Be Used in the City of Bursa Landscape and Identification of Domestic and Foreign Origin Plant Can Be Used for This Purpose. Uludag Univ Research Project No 2002/24, 2004.
[15] Zencirkiran, M. (2009). Determination of Native Woody Landscape Plants in Bursa and Uludag. African Journal Biotecnology, 8, 5737.
[16] Morgenroth, J., Ostberg, J., Bosch Van Den, K., Hauer, R., Sjöman, H., Chen, W. and Jansson, M. (2016). Urban Tree Diversity—Taking Stock and Looking Ahead. Urban Forestry& Urban Greening, 15, 1.
[17] Yilmaz, M. and Irmak, M.A: (2004). Evaluating Plant Materials Used in Open-green Areas in Erzurum. Ecology, 13, 9.
[18] Anonymous (1999). The Hillier Manual of Trees and Shrubs. Pocket Edition. David and Charles Book.
[19] Zencirkiran, M. (2013). Landscape Plants I (Gymnosperms Plants - Gymnospermae). Nobel Publisher, Ankara.
[20] Brickell, C. (1994). The Royal Horticultural Society Gardeners' Encyclopedia of Plants and Flowers. New Edition. Dorling Kindersley, London, 640 p.
[21] Davis, P.H. (1965-1988) Flora of Turkey and the East Aegean Islands. Edinburgh University Press. Vols 1-10, Edinburgh.
[22] Dirr, M.A. (1992). Manual of Woody Landscape Plants: Their Identification, Ornamental Characteristics, Culture, Propagation and Uses. Varsity Press.
[23] Günay, R. (2001). Bursa City Flora. Uludag Univ. Graduate School of Natural and Applied Science, M. Sc. Thesis, Bursa.
[24] Orcun, E. (1972). Dendrology. Vol. I. Coniferous Trees and Shrubs, Ege Univ Fac of Agric, Publication No: 196, Izmir.
[25] Pamay, B. (1992). Plant Material I: Trees and Shrubs. Uycan Press, Istanbul.
[26] Steiner, F. (2011). Landscape Ecological Urbanism: Origins and Trajectories. Landscape and Urban Planning, 100, 333.
[27] Jim, C.Y. (1987). The Status and Prospects of Urban Trees in Hong Kong, Landscape Urban Plan, 14, 1.
[28] Jim, C.Y. and Liu, H.T. (1997). Storm Damage on Urban Trees in Guangzhou, China. Landscape and Urban Planning. 38, 45.
[29] Talarchek, C.M. (1990). Urban Forest of New Orleans: an Explanatory Analysis of Relationships. Urban Goegraphy, 1, 65.
[30] Asgarzadeh, M., Vahdati, K., Lotfi, M., Arab, M., Babaei, A., Soufi, M. and Rouhani, G. (2014). Plant Selection Method for Urban Landscapes of Semi-arid Cities (A Case Study of Tehran). Urban Forestry & Urban Greening, 13, 450.

Received: **18.04.2017**
Accepted: **19.07.2017**

CORRESPONDING AUTHOR

Murat Zencirkiran
Department of Landscape Architecture, Faculty of Agriculture, University of Uludag, 16 059 Gorukle, Bursa, Turkey.

e-mail: mzencirkiran@uludag.edu.tr

© by PSP Volume 26 – No. 10/2017 pages 6071-6077 Fresenius Environmental Bulletin

INFLUENCE OF STORED PRODUCT INSECTS ON PLANTING CHICKPEA SEEDS

Tawfiq M Al Antary[1,*], Talal A Thalji[2]

[1]Plant Protection Department, School of Agriculture, University of Jordan, Amman, 11942, Jordan
[2]Horticulture and Field Crops Department, School of Agriculture, University of Jordan, Amman, 11942, Jordan

ABSTRACT

Seeds samples of five cultivars of chickpea were collected from stores of farms from different locations in Jordan during 2014 and 2015 to evaluate the biological factors including stored product insects on the plant production. Purities, viability and germination % of chickpea seeds of the samples were examined according to the international standards seed germination was ranged from 60 to 100% and seeds viability between 25 and 100% relying on the chickpea cultivar and the location of seed gathering. The correlation between viability % and seed germination% was medium positively. The seed purity % was ranged between 92 and 100% in all chickpea cultivars. Number of holes resulted from the activity of the attacked insects in all examined chickpea seeds of the Turkey and Balady were significantly less than the other cultivars. The most common insects in the seeds samples of all the five cultivars from different sites of Jordan were *Rhyzopertha dominica* followed by *Anthrenus museorum, Bruchus rufimanus, and Sitophilus granaria*, and from Amman governorate wasC *allosobruchus chinenensis, B.rufimanus, B.quingnegntlatus, C.macutals, B.lentis, Trogoderma granarium, and B.pisorum.*Several agricultural measures were concluded and recommended to avoid insect infestation and to get high quality of chickpea seeds to be cultivated.

KEYWORDS:
Chickpea, Seeds cultivars, Germination, Viability, Purity, and Chickpea .Stored insects.

INTRODUCTION

Chickpea (*Cicer arietinum*) is an old legume that has been grown in most world countries. It is an important crop grown in Asia, Africa and the Middle East countries particularly Jordan [5, 26]. It is planted in Jordan in high land with total production of 3729 tones and 33220 tons annually in average in the last ten years [25].

Chickpea contain protein 20%and three times more than in wheat or maize or rice. It does have amino acids such as lestin and treptofan, and also contains 61% carbohydrates and4-4.5% lipids [6]. In Jordan and some other Arab countries, chickpea can be sold and eaten as green chickpeas called "Hamleh". In addition, their dried seeds can be eaten in the famous "Homous" dish and "Falafel" by Jordanians daily or at least weakly.Dried chickpea seeds must be stored for several months to provide citizens with the required amounts [1]. During storing the seeds of chickpea for several months, they might be attacked by several beetles and weevils. Dried seeds might have significant quantitative and qualitative losses due to pests infestation, particularly insects.These insect pests might cause physical and chemical changes in the chickpea seeds such as holes, bad odor, unacceptable appearance and size and increase in temperature and humidity, leading to more infestation by other pests such as fungi and bacteria [21, 15]. The insect pests might kill embryos and produce punctured seeds and undesirable flour[4, 13]. In addition, seeds might be contaminated with dead insects molting skins, posses hair, and attacked insects are potential to transmit diseases causals [1, 17].

It is the aim of this study to find influence of chickpea seeds stored in the farms conditions when being attacked with stored product insects, particularly beetles and weevils infesting several cultivars. In addition, it is very useful to report the different beetles and weevil attacking the stored seeds of chickpeas which will be helpful to protect stored seeds by using several integrated pest management practices in chickpea stores.

MATERIALS AND METHODS

Chickpea seeds sampling. (1) Stores in farms. During 2014 and 2015, random samples of chickpea seeds from different locations from stores of farmers in Jordan were collected. The locations from which the collected seeds were farms cultivated with chickpea by the farmers of Jordan. These samples were put in brown bags of paper, carried to the laboratory of School of Agriculture in the University of Jordan, placed at room conditions and then taken for the needed tests. Temperatures in farm stores where they were collected were ranged between 5-

40°c and % of relative humidity were ranged between 40-85%.

The replications of the collected samples for each of the cultivars were ranged between 4 to 6 replicates. For three biological health seed tests, 2-3 kgs were sampled from the large stored amounts of chickpea seeds for each location were mixed separately and placed in obvious labeled bags containing code numbers, locations of collections and then kept at room temperature until insect examination. % of relation humidity in stored room were ranged between 40 to 70% and temperatures were 22± in average. Samples of chickpea seeds were collected from Amman the capital of Jordan and Madaba in the middle of Jordan and Shoubak in the south, and Mafrak and Irbid in the north of the country.

(2) Amman governorate. Samples of chickpea seeds were randomly gathered from governorate of Amman, the capital from various store houses of farms for several years extended between 2010 and 2016. The other needed requirements were described as above in materials and methods (1).

Seeds germination tests. Samples of chickpea of fifty grams were taken. There were four replicates of samples. All impurities in each replicate particularly weeds seeds other crops seeds, small stones and small earth masses, gravel particles and other impurities were removed and weighed, according to the international standards, [13, 18, 4]. The tested seeds were dipped for 24 hour in tap water to determine the germination %. Four hundred of the impregnated chickpea with the four replications were taken and then divided into four groups [4].There were 100 seeds per group. These seeds were placed into a plastic dish lined with moistened filter paper. The dish was then covered with muslin cloth to minimize drying opportunity and placed in the lab at room conditions. Temperature in the lab was in average of 25±2°c and percent of relative humidity was of 60±5. These seeds were evaluated after five days[13, 4]. The germinated seeds were grouped according to several workers [14, 4] to healthy, not healthy and dead ones. To confirm the first counting, the seeds were revaluated and recounted after fourteen days of the start [14, 4]. The germination % of tested seeds were recalculated adopting the following formula [2].

% seed germination = Normal seedlings/Total number of seedsX100

and then the average of the four replicates was obtained.

Purity of seeds test. Fifty grams from each chickpea samples were taken with four replicates and weighed. The weed seeds, other crop seeds, gravel particles and small stones, and other impurities were removed. The pure chickpea seeds were then reweighed [13, 18, 2]. The % of seeds purity were calculated according to the following formula [4].

% of seed purity= Weight of seeds before removing impurities/Weight of seeds after removing impurities X 100.

Viability of seeds test. This examination was carried out according to the work of several authors [13, 2, and 4].The chickpea seeds were placed onto moistened filter paper with tap water, for two days period to test viability of seeds, under the room conditions. The % of germinated seeds were taken by the calculation of the seeds with emerged embryos. The examination was repeated but after one week period to get the normal seed germination.

Number of seeds holes. From each chickpea cultivar, fifty grams from each replicate were separately and randomly considered. The taken seeds were placed into a glass Petri dish with 10 cm in diameter to count the number of holes in all seeds made by the infested insects by bare eyes and sometimes under the binocular dissecting microscope particularly when needed [2, 4]. Total number of punctures (holes) and means numbers of holes per one seed were calculated. The experimental design was randomly completely design (RCD). The differences between means for number of holes for all examined seeds and per one seed for all the five chickpea cultivars were got using one way analysis of variance (F test) and LSD test.

Beetles and weevils of chickpea seeds in five cultivars. From each chickpea cultivars, fifty grams were separately and randomly transferred into glass Petri dish from that sample gathered between 2014 and 2015 from all regions of Jordan and those gathered from Amman governorate between 2010 and 2016. There were four replications at least from each examined cultivar for insect evaluation [2, 4]. The found stored chickpea insect were separated and also counted for each species. Several keys were adopted to confirm or identity weevils and beetles which normally infested seeds of stored legumes [5, 17,24,6] In addition to confirm and identify insects infesting chickpea seeds but normally infest seeds of stored cereals, the key of Pfadt [20] was adopted. The experimental design was the completely randomized design (CRD) in all experiment [4]. Moreover, the differences between the number of each insect species for the five tested chickpea cultivar or the Balady cultivar in the governorate of Amman were detected using one way analysis of variance (F-test) and the LSD test.

RESULTS

Viability of seeds. Seeds viability % of chickpea were ranged between 25 and 100%, depending on the source of collection, the period of storing in store house of farms, and the cultivars are shown in Table 1. The northern sites of Jordan especially from Mafrak and Irbid with viability % ranged between 80 and 95%. Chickpea collected from stores in the middle region in Jordan particularly Amman and Madaba were ranged between 25 to 100% viability. The southern sites of Jordan particularly from Karak, Shoubak, and Tafila were ranged between 60 to 95% viability. Hindi cultivar was the lowest in viability; it was 25% from Amman location. Local cultivar, Balady was ranged between 80 to 100% viability. Balady from Madaba was the greatest in viability % (100%), Mexico in Irbid (97%) followed by Turkey in Amman (95%) (Table 1).

Germination of seeds. Seeds germination% of chickpeas were ranged between 60 to 100 (Table 1). The correlation between viability % and germination % was positively medium (r^2= 0.57) (Table 2). Generally, germination % for that sample collected from the northern, middle and southern locations of Jordan were about similar (Table 1). The lowest germination in all sites was 10% for Hindi cultivar from Amman sites (Table 1).

Purity of seeds. Chickpea seeds purity percentages were ranged from 98 to 100 in all cultivars collected from all locations in different parts of Jordan (Table 1). Purity percentages of chickpea seed collected from all locations of Jordan were relatively high and did not differ significantly (Table 1). The correlation coefficient between purity and viability was positively weak (r^2=0.156) (Table 2). The correlation coefficient between seeds germination % and seeds purity% was positively poor (r^2=0.025) (Table 2).

TABLE 1
Percentages of purity%, germination% and viability% for chickpeas seeds of several cultivars collected from different locations of Jordan in 2014 and 2015.

Sample no.	Sample source	Cultivar	Percentage %		
			Purity	Germination	Viability
7	Amman	Turkey	100%	90%	95%
8	Amman	Turkey	100%	95%	95%
9	Amman	Turkey	100%	90%	70%
10	Amman	Turkey	100%	100%	75%
11	Amman	Turkey	100%	98%	90%
12	Amman	Turkey	98%	100%	75%
13	Amman	Hindi	100%	60%	25%
14	Amman	Hindi	99%	65%	35%
21	Madaba	Balady	99%	85%	100%
22	Madaba	Balady	98%	90%	98%
23	Madaba	Balady	100%	95%	97%
30	Madaba	Balady	99%	85%	90%
31	Madaba	Balady	98%	80%	90%
38	Karak	Balady	99%	100%	90%
39	Karak	Balady	99%	100%	95%
40	Karak	Turkey	100%	99%	90%
41	Karak	Turkey	98%	100%	95%
44	Shoubak	Balady	99%	100%	95%
45	Shoubak	Balady	98%	99%	90%
52	Tafella	Turkey	100%	95%	60%
53	Tafella	Turkey	98%	98%	65%
58	Shoubak	Balady	99%	100%	90%
59	Shoubak	Balady	100%	95%	80%
78	Madaba	Balady	99%	85%	100%
79	Madaba	Balady	98%	85%	98%
82	Madaba	Balady	100%	99%	100%
83	Madaba	Balady	98%	98%	99%
105	Mafrak	Turkey	100%	95%	90%
106	Mafrak	Turkey	99%	90%	93%
121	Irbid	Mexico	99%	99%	97%
122	Irbid	Mexico	98%	97%	80%
123	Irbid	Syria	100%	85%	90%
124	Irbid	Syria	98%	80%	85%

TABLE 2
Values of correlation coefficient (r^2) between germination%, viability% and purities% for chickpeas seeds collected from different sources in Jordan during 2014 and 2015.

Variables	Correlation coefficient (r^2)
Seeds germination% vs seeds viability %	0.57
Seeds purity% vs seeds germination %	0.025
Seeds purity% vs seeds viability	0.156

TABLE 3
Means numbers of holes caused by several stored product insects in five chickpeas cultivars collected from different locations in Jordan in 2014 and 2015.

Chickpeas cultivar	No. of holes ± ISE	
	All seeds in 50g	Per seed
Mexico	27 ± 4.1 a	0.54 ± 0.07 a
Turkey	10 ±1.9 c	0.20 ± 0.02 c
Balady	13 ± 2.2 c	0.26 ± 0.03 c
Hindi	30 ± 5.2 a	0.60 ± 0.08 a
Syria	18 ± 2.9 b	0.36 ± 0.05 b

Means in columns sharing the same letter do not differ significantly at 5% using LSD test.

TABLE 4
Means numbers of stored product insects for live check peas cultivars seeds collected from different locations in Jordan in 2014 and 2015.

Chickpeas cultivars	No. of counted insects / cultivar ± SE				
	Rhyzopertha dominica	*Sitophilus oryzae*	*Sitophilus granaria*	*Tribolium castaneum*	*Oryzaephilus surinamensis*
Mexico	**7.3 ± 0.16 a**	**0.0 ± 0.0 b**	**0.0 ± 0.0 c**	**0.0 ± 0.0 b**	**0.0 ± 0.0 c**
Turkey	**1.2 ± 0.15 b**	**0.2 ± 0.12 a**	**0.80 ± 0.39 a**	**0.3 ± 0.02 a**	**0.09 ± 0.01 b**
Balady	**0.8 ± 0.05 c**	**0.0 ± 0.0 b**	**0.8 ± 0.04 a**	**0.0 ± 0.0 b**	**0.3 ± 0.03 a**
Hindi	**0.6 ± 0.04 c**	**0.1 ± 0.09 a**	**0.3 ± 0.02 b**	**0.2 ± 0.01 a**	**0.2 ± 0.02 a**
Syria	**1.5 ± 0.20 b**	**0.0 ± 0.0 b**	**0.0 ± 0.0 c**	**0.0 ± 0.0 b**	**0.0 ± 0.0 c**
Chickpeas cultivars	**No. of counted insects / cultivar ± SE**				
	Bruchus rufimanus	*Cryptolestes ferrugineus*	*Anthrenus museorum*	*Anthrenus verbasci*	
Mexico	**0.0 ± 0.0 b**	**7.0 ± 0.2 a**	0.0 ± 0.0 b	0.0 ± 0.0 c	
Turkey	**0.0 ± 0.0 b**	**0.0 ± 0.0 b**	**0.0 ± 0.0 b**	1.0 ± 0.02 b	
Balady	**0.0 ± 0.0 b**	**0.0 ± 0.0 b**	**0.0 ± 0.0 b**	1.3 ± 0.08 a	
Hindi	**0.2 ± 0.0 a**	**0.0 ± 0.0 b**	**0.1 ± 0.01 a**	2.5 ± 0.1 a	
Syria	**0.0 ± 0.0 b**	**0.0 ± 0.0 b**	**0.0 ± 0.0 b**	1.5 ± 0.09 a	

Means in columns sharing the same letter do not differ significantly at 5% level using LSD test

TABLE 5
Means numbers of 2 stored product insects for Balady cultivar from Amman governorate in Jordan between 2014 and 2015.

Insect species	No. of counted insects ± SE
Callosobruchus maculates	9.4 ± 0.34 c
Callosobruchus chinensis	14.1 ± 0.14 a
Bruchus rufimanus	11.2 ± 0.38 b
Bruchus quingnegntlatus	12.1 ± 0.39 b
Bruchus incarnates	7.5 ± 0.31 c
Bruchus pisorum	6.3 ± 0.31 d
Bruchus lentis (ervri)	8.5 ± 0.33 c
Trogoderma granarium	5.6 ± 0.33 c

Means in columns sharing the same letter do not differ significantly at 5% level using LSD test.

Holes in seeds. Table 3 shows the means numbers of holes in the five cultivars of chickpea seeds collected from different locations in Jordan during the period between 2015 and 2016, which done by different beetles and weevils in all seeds and per seed. Number of counted holes in all tested seeds in the Hindi cultivar and followed by Mexico, but without different significances (Table 3). Turkey cultivar had holes in all seeds was significantly less than the other cultivars, followed by Balady but without significant differences. Moreover, means numbers of holes per seed in the five cultivars had similar trend as described in case of numbers of holes in all seeds (Table 3).

Stored chickpeas insects. (1) Different regions in Jordan. Table 4 shows means numbers of seven insect species in the tested five chickpea cultivars seeds collected from different locations in Jordan between 2015 and 2016. The highest common insect species in the chickpea seeds samples of the five cultivars was *Rhyzopertha dominica*, the lesser grain borer, followed by *Antherus muserun*, the large faba bean beetle *Bruchus rufimanus* and then *Sitophilus granarium* (Table 4). The mexico cultivar was significantly infested by *Rhyzopertha dominica* (7.3) with a greater mean compared with the other cultivars infestation (Table4). Hindi cultivar (0.8) was significantly the least infested with the previous mentioned borer without significant differences, with the Balady cultivar (0.6), followed by Turkey and Syria cultivars. However, the other insects namely *Sitophilus oryzae, Sitophilus granaria, Tribolium castaneum, Oryzaephilus surinamensis, Bruchus rufimanus, Cryptolestes ferrugineus, Anthrenus museorum* and *A.rerbasci* had attacked the various chickpea cultivars but in a few numbers (Table 4).

(2) Governorate of Amman. Means number of eight stored product insects separated from Balady cultivar from governorate of Amman between 2010 and 2016 are shown in Table (5). The most common insect in the seeds samples of chickpea of the Balady cultivar was significantly *Callosobruchus chinensis*, followed by *Bruchus rufimanus* and *B.quingnegntlatus* without significant differences, *Challosobruchus maculates*, *B.lentis* (evri) and *Trogoderma granarium* without significant differences and then *Bruchus pisorum* which was the least significantly.

DISCUSSION

Stored products grains including cereals and legumes might be attacked by several species of insects and then followed by bacteria and fungi infection leading to deteriorate these stored comedies particularly when stored for long time [1, 17, 10].
Classic methods such as the use of pesticides and fumigants are still globally in use to reduce insect infestation affecting stored products [15, 4] to avoid losses in grains, bad quality and contamination commodities with dead insects, molting skins. Some stored product insects might infest chickpea pods and move to the stored seeds [1, 5]. Among the attacked insects, bruchids cause substantial loss during storage [1, 23]. Stored chickpea seeds must protected from the direct and indirect attack by insects to reduce the caused damage qualitatively and quantitatively [1, 5] particularly when insects density increased to population outbreaks, If bins and grain stores left unchecked regularly. This might increase in micro environmental temperatures and relative humidity which lead to insect development and fungi infection[8, 1, 17]. Abnormal chickpea seed particularly those broken or small or shrunk or infested with insects, should be separated from healthy ones, because their viability and germination might be very low. It is necessary that post harvested seeds should be kept and stored in well established and prepared storages, clean, free of insects, water content with less than 12% and other needed measures for grain storing [27, 2, 4]. However, chickpea seeds infested with stored product insects in the present investigation in some cases were low in their vigor. Some Jordanian workers on other stored grains found similar results on wheat [3], barley [2]and lentil [4]. In this study, beetles and weevils and their mobile and immobile stages might move from grown plants in the field or to the stored chickpea seeds [3, 4]. Biological factors such as purity, viability, seed germination and pests are important in seed technology. It is important to select the chickpeas seeds to meet successfully the previous mentioned factors which are urgently needed in the agricultural steps [12, 3, 4]. Insects may transfer cultivation from country to another country through packing and sold. Beetles and weevils attacking harvesting, chickpea seeds may reach any part of the world through the previous mentioned practices, leading to important postharvest loss in the stored production [16, 3,4]. In this study, flour such as *Tribolum castaneum* which normally attacked non healthy cereal seeds, but in this study it was found infesting stored chickpea seeds in few numbers [20, 22, 2]. The third group is usually infesting legume stored seeds. Of these are *B.rufimanus, C.ferrugineus, A.museorum,* and *A.verbasci* but attacked the five cultivars of chickpeas seeds collected from different locations in Jordan in few numbers, and *callosobruchus chinensis*, *C.maculatus, B.quingnegnthlatuns, B.rufimanus, B.incarnatus, B.pisorum, B.lentis,* and *T.granarim* in Balady cultivar of chickpea seeds collected from Amman governorate. The beetles which normally infest seeds of legume members are named bruchids. These insects complete their cycles in and on seeds of legumes such as the studied chickpeas, faba bean, beans, peas

and lentils resulting in small and large holes and powdered products [11, 17, 6, 4] Seeds of Turkey and Balady chickpea cultivars from this study have shown the least in numbers of holes in all seeds and per seed under the present experimental conditions. These obtained results might be used in agricultural extension to adopt the cultivation of these two chickpea cultivars by the Jordanian farmers. Moreover, agronomist particularly crop breeder asked to conduct research with economic entomologies in the purpose of finding new chickpea cultivars suit Jordanian conditions, with high production and less attack with field and stored pests.

The primary categorized stored product insects and the Brunched insects might complete their life cycle within stored chickpea seeds destroying the embryos, decreasing seeds germination and viability as reported by several workers [1, 3, 4]. In addition, these insects might cause holes in the healthy stored seeds leading other or secondary pests to attack damaging the seeds qualitatively and quantitatively [19, 3,4].

In conclusion, cooperation between agronomic and entomologists are needed to improve the local chickpea cultivars concerning production of high quality and quantity chickpea seeds and to tolerate pests particularly stored insects. Local chickpea seeds with great standards are needed to get high viability and germination, and great yield. Stores for chickpea seeds should be cleaned, prepared, and insects controlled to be ready for storing the seeds which should be harvested after well ripened, separated from unhealthy seeds, crushed, broken, weed seeds, impurities, stones and well insects controlled to avoid insects and diseases infection in store houses. Regular monitoring for relative humidity and temperature for stored seeds should be considered.

ACKNOWLEDGEMENTS

Thanks for the Deanship of Scientific Research of the University of Jordan for supporting financially this research. The authors also would like to thank Eng Wa'ad Abu Helalah for her help in the laboratory work and typing this paper.

There are no conflicts of interest between the authors.

REFERENCES

[1] Al-Antary, T.M. and Al Momany, A. (1990) Pests of Home and Garden, the 1st edition. Al Dar Al Ar abiah for Publication and Distribution, Cairo.360 pp.

[2] Al Antary,T.M. and Thalji, T.(2015) Effect of stored product insects on viability of farm's barely seeds stored for planting in Jordan. Advances in Environmental Biology 9(23):338-344.

[3] Al Antary,T.M. and Thalji, T.(2016) Biological factors affecting seeds of wheat cultivars stored for cultivation with emphasis on stored product insects. Entomologia Generalis, 35(4):307-315.

[4] Al Antary, T.M. and Thalji, T. (2017) Biological factors affecting seeds of lentil cultivars stored for planting with emphasis on grain legumes beetles and weevils. Advances in Environmental Biology 11(3):52-57.

[5] Al-Momany, A. and Al-Antary, T.M. (2008) Pests of Home and Garden, the 2nd edition. Jordan University Publication, Amman. 518 pp.

[6] Benish, C. (2016) German Beefle Fanna-kertier. De.photo overview Bruchidae (seed Beetles of Germany).https://www.kerbtier.de/enindex.html.

[7] Bhalla, S., Gupta, K., Lal, B. and Kupar, M.(2008) Efficacy of various nonchemicals methods against pulse beetle, *Callosobruchus maculates* (Fab). Diver, Crop Prot. 41:12-15.

[8] Dunkel, F. (1988) The relationship of insects to deterioration of stored grain by fungi. Internat. J.Food Microbiology 7:887-244.

[9] Gandhi, N. and Pillai, S. (2011) Control of *Ryzopertha dominoca* (Coleeptera: Bosirichidae) by pulverized leaves of *Punice granatum* (Lythraveae) and *Mueeaya koeniqi* (Rutaccae). Internat. Journal of Agricultural Biology 13(4):535-540.

[10] Haile, A.(2015) Eco-friendly management of chickpea storage pest, *Callosobruchus chinensis* L. (Coleoplern: Bruchidae) under laboratory conditions in Eritrea. Journal of Stored Products and Postharvest 6(8):66-71.

[11] Howe, R. and Currie, J. (1964) Some laboratory observations on the rates of development, mortality and oviposition of several species of Bruchidae breeding in stored pulses. Bull. Entom. Research 55:437-477.

[12] Igncimuthu, S. and Prakash, S. (2006) Agrobacterium- mediated transformation of chickpea with a-amylase inhibitor gene for insect resistance. J. Biosci. 31(3): 339-345.

[13] International Seed Testing Association (ISTA) (1999), International Rules for Seed Testing, Rules. Zurich. 333 pp.

[14] Klys,M.(2012) Emigration activity of the sawtoothed grain beetle *Oryzeaphilus surinamensis* L. (Coleoptera: Silvanidae) in various environmental temperature. Journal of Plant Protection Research 52(4):397-400.

[15] Loganathan, M., Jayas, D., Fields, P. and White, N.(2011) Low and high temperature for the control of cowpea beetle, *Callosobruchus maculates* (F.) (Coleoplera: Bruchidae) in chickpea. Journal of stored Product Research 47:244-248.

[16] Lund, F. and Frisyad, J. (2003) *Penicillium verrucosum* in wheat and barley indicates presence of Orchratoxin A.J. of Applied Microbiolog 95:1117-1123.
[17] Masson, L. and McDonough,N. (2011) Biolog, behavior, and ecology of stored grain and legume insects. Publication from Kansas University, USA. www.ksre.ksu.edu, 14pp.
[18] Mathur, S. and Kongsdal, O.(2003) Common Laboratory Seed Health Testing Methods for Detecting Fungi. International Seed Testing Association, Zurich. 425 pp.
[19] Neelhirajan S., Karunakram, S., Jayas, D. and White, N. (2007) Detection Techniques for Stored Product Insects in Grain - Int. Fd. Control 18: 157-162.
[20] Pfadt, R. (1978) Fundamental of Applied Entomology, 3rd edition. McMillan Publishing Co. Inco., New York. 798 pp.
[21] Philips, T. and Throne, J.(2010) Biorational approaches to manage stored products. Annual Review of Entomology 55:375-397.
[22] Saxena, B. and Saxena, R. (2011) Nutritional changes in stored chickpea, *Cicer arietinum* in relation to bruchid damage. Journal of Stored Products and Postharvest Research 2(5):110-112.
[23] Sing, K., Malhorta, R., Halila, H., Knights, E. and Verma, M. (1994) Current status and future strategy in breeding chickpea for resistance to biotoc and abiotic. Enphytica 73:137-149.
[24] Sprinivasan, R. (2014) Insects and mite pests on vegetable legumes: a field guide for identification and management. AVRDC-Publication No.14,778.92pp.
[25] Statistics Department (2016) General Statistics Department, Amman, Jordan.
[26] Tesfu, F. (2011) Evaluation of *Parthenium hysterophrus*powder against *callosobruchus chinensis* L.(Coleoptere: Bruchidae)on chickpea under laboratory condition. M.Sc Thesis, Addis Ababa University, Elhiopia.
[27] Thalji, T. and Al Momany, A. (2015) Effect of Fungi on viability farmers wheat seeds stored for planting in Jordan. – Jordan Journal of Agriculture Sciences 12(2):347-362.

Received: **18.04.2017**
Accepted: **18.08.2017**

CORRESPONDING AUTHOR

Tawfiq M Al Antary
Plant Protection Department,
School of Agriculture,
University of Jordan
Amman, 11942 – JORDAN

E-mail:tawfiqalantary@yahoo.com.

© by PSP Volume 26 – No. 10/2017 pages 6078-6084 Fresenius Environmental Bulletin

SOIL CARBON MINERALIZATION IN *ARBUTUS ANDRACHNE* AND *CUPRESSUS SEMPERVIRENS* GROWING ON THE DIFFERENT ELEVATIONS

Ilay Cevik, Husniye Aka Sagliker*

University of Osmaniye Korkut Ata, Faculty of Science and Letters, Department of Biology, Osmaniye, 80000-Turkey

ABSTRACT

In this study, it was determined carbon (C) and nitrogen (N) contents (%) at shoots, leaves and soil samples of *Arbutus andrachne* L. and *Cupressus sempervirens* L. growing naturally on the two different elevations (250 m and 1000 m) of Zorkun plateau of Osmaniye. It was also studied the carbon mineralization (28°C, 30 days) of soil samples at the same elevations. C mineralization of these soils was determined by CO_2 respiration method. There was no significant difference between 250 m and 1000 m of *Arbutus andrachne* L. in terms of view of C mineralization values ($P > 0.05$) at the end of 30 days of incubation experiments. In contrast to *Arbutus*, carbon mineralization value of *Cupressus sempervirens* L. soil at 1000 m was statistically higher than 250 m ($P = 0.001$). C mineralization ratio of *Arbutus* at 250 m was significantly higher than the other plant and elevation soils ($P < 0.05$). These findings exhibited that C mineralization of both plants might vary depending on the elevation difference.

KEYWORDS:
Arbutus andrachne; carbon mineralization; elevation; *Cupressus sempervirens*

INTRODUCTION

Mineralization of soil organic carbon expressed also as soil respiration is known the decomposition of the organic carbon in soil by microorganisms into carbon dioxide [1]. Soil respiration is an important parameter reverberating the level of microbial activity, soil organic matter (SOM) content and its decomposition [2, 3]. It reflects the capacity of soil and supports soil vita including all of plants and soil organisms [3] and is affected by variations of vegetation type, altitude, topographic position, soil organic matter, temperature and soil humiditiy [4-6]. The plant biomass together with soil respiration is also under the influence of some ecological factors like altitude, temperature and humidity conditions. Although the plant biomass production decreases by increasing altitude [7], the higher amounts of total organic carbon happens because of a lower microbial activity [8], which is due to the colder soil temperatures occurring at higher elevations [9, 10]. The increase of altitude in high-frigid forest causes a decrease in the average temperature, but the temperature fluctuation increases [11]. Differences in environmental factors such as drying and wetting plus freezing and thawing cycles and water content at freezing contributed to variation in the aggregates formation and stability of soil aggregates along the altitudinal gradient. Higher altitudes with colder and wetter climate tended to benefit the formation and stability of macro-aggregates [8]. The quality of litter indirectly affects soil aggregation by altering microbial activity [12]. Different plant litters affecting the microbial community also contribute to changes of soil properties [13]. It has been reported that soils of coniferous dominated forest ecosystems are acid and beneficial to the reproduction of fungi [14, 15], with more fungal hyphae being released as a binding agent. All these factors surrounding the different organisms and soils are individually important. All of the biological durations in the environment influence microorganisms, either positively or negatively [16, 17]. Soil microbial diversities and their activities were impressed by different tree kinds [18, 19]. There are differences between soils under evergreen tree and the soils under decidious tree in these studies.

In this study, it was determined C and N content (%) of shoots, leaves and soils of *Arbutus andrachne* L. (Ericaceae) and *Cupressus sempervirens* L. (Cupressaceae) growing naturally on the two different altitudes (250 m and 1000 m) in Zorkun plateau (Osmaniye) of Eastern Mediterranean Region of Turkey. Soil organic carbon mineralization (28°C, 30 days) was comparatively measured both two different plants and 250 m and 1000 m elevations.

MATERIALS AND METHODS

Study Site Characteristics. This study was carried out at two different altitudes (250 m and 1000 m) in the Zorkun Plateu of Osmaniye (Fig.1).

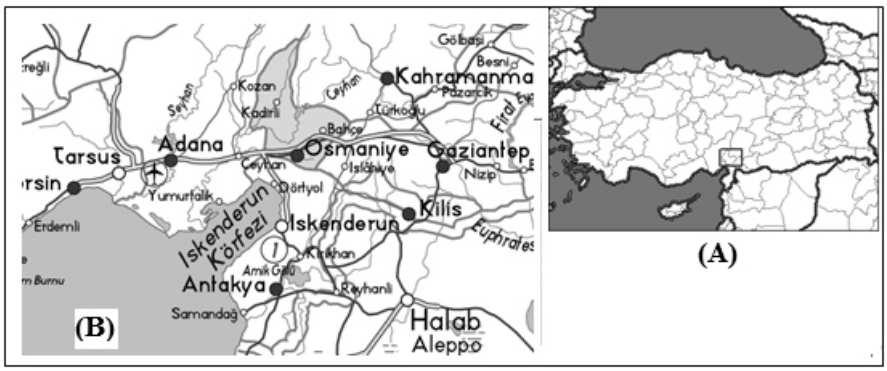

FIGURE 1
The location of Osmaniye (A) and the zoomed image of Osmaniye in Turkey map

TABLE 1
Some physical and chemical characteristics of *Arbutus andrachne* L. soils at the different Elevations (250 m and 1000 m; mean ± standard error; n = 3)

Arbutus andrachne							
Characteristics	**250 m**			**1000 m**			**P**
Sand (%)	65.3	±	3.79	56.4	±	3.77	0.172
Loam (%)	13.9	±	8.89	22.4	±	2.09	0.409
Clay (%)	20.8	±	5.86	21.2	±	1.72	0.945
Texture type	Sandy clay loam (SCL)						
Field capacity (%)	25.8	±	0.36	43.6	±	0.55	0.000*
pH	6.75	±	0.24	7.10	±	0.04	0.224
$CaCO_3$ (%)	8.66	±	0.29	3.17	±	0.22	0.000*
C (%)	2.73	±	0.18	3.34	±	0.20	0.086
N (%)	0.27	±	0.00	0.24	±	0.00	0.003*
C/N	9.99	±	0.57	13.7	±	0.79	0.019*

* express significant difference between two different altitudes at the $P < 0.05$.

TABLE 2
Some physical and chemical characteristics of *Cupressus sempervirens* L. soils at the different elevations (250 m and 1000 m; mean ± standard error; n = 3)

Cupressus sempervirens							
Characteristics	**250 m**			**1000 m**			**P**
Sand (%)	63.5	±	5.06	72.4	±	0.83	0.156
Loam (%)	22.7	±	3.19	16.3	±	0.12	0.116
Clay (%)	13.8	±	1.91	11.3	±	0.77	0.282
Texture type	Sandy loam (SL)						
Field capacity (%)	37.8	±	0.56	38.6	±	1.40	0.603
pH	6.96	±	0.07	6.98	±	0.08	0.831
$CaCO_3$ (%)	20.2	±	0.32	19.7	±	0.50	0.385
C (%)	3.71	±	0.34	5.19	±	0.39	0.044*
N (%)	0.28	±	0.00	0.23	±	0.10	0.013*
C/N	13.4	±	1.22	16.4	±	1.01	0.134

* express significant difference between two different altitudes at the $P < 0.05$

Mediterranean climate conditions are dominated in Osmaniye with some minor differences in mountainous and plains. Summers are generally hot and arid, winters are warm and rainy in Osmaniye [20]. While the average and the highest temperatures are 18.2º C and 42.8 °C, respectively, rainfall period is more than the other months in the winter and autumn months, the average annual rainfall is 767.6 mm [20].

Taking of Samples. The research materials were leaves, branches and soils taken from 0-20 cm depth of two different trees (*Arbutus andrachne* L. and *Cupressus sempervirens* L.) which naturally grow at two different elevations (250 m and 1000 m) in Zorkun Plateau of Osmaniye. All samples belonging to leaves, branches and soils of *Arbutus andrachne* and *Cupressus sempervirens* used as material and sampled from both 250 m and 1000 m altitudes were collected on 06 February 2013.

Physical and Chemical Analysis of Samples. Soil texture, pH and $CaCO_3$ content (%) were measured by hydrometer method [21], InoLab pH meter [22] and Scheibler calcimeter, respectively [23]. Field capacity (%) was determined by vacuum pump with 1/3 atmosphere pressure [24]. Total N contents (%) and organic C content (%) of soil and

TABLE 3
C, N and C/N ratios (%) in the shoots and leaves of *Arbutus andrachne* L. and *Cupressus sempervirens* L. at the two different elevation gradients (250 m and 1000 m; mean ± standard error; n = 3)

		Arbutus andrachne			*Cupressus sempervirens*		
Parts	Elements	250 m	1000 m	P	250 m	1000 m	P
Shoots	C (%)	45.9±0.88	44.1±1.68	0.383	46.6±0.83	45.3±0.61	0.278
	N (%)	0.57±0.03	0.80±0.04	0.011*	0.57±0.04	0.80±0.01	0.087
Leaves	C (%)	44.8±0.47	49.0±2.24	0.141	47.0±0.57	45.8±1.30	0.472
	N (%)	1.33±0.08	1.66±0.07	0.036*	1.12±0.03	0.70±0.05	0.002*

* express significant difference between two different altitudes at the $P < 0.05$

leaf specimens of both species were determined by the modified Kjeldahl method and Anne method, respectively [25]. The carbon mineralization of two different plant soils at the two altitudes (250 m and 1000 m) was monitored under controlled conditions (28 °C, 80% of field capacity) by CO_2 respiration method for 30 days [26].

Statistical Analysis. General Linear Model was used to determine the significant differences between both two plants (*Arbutus andrachne* and *Cupressus sempervirens*) and two altitudes (250 m and 1000 m) from the point of view of carbon mineralization over incubation time [27]. For each of the above mentioned analyses, 3 repetitive measurements were made for comparisons. Results were offered as mean ± standard error in the all tables and the figures. $P < 0.05$ was a significant value statistically.

RESULTS AND DISCUSSION

Plant and Soil Charactestics. The study included comparatively work on some physical and chemical characteristics of soils of *Arbutus andrachne* L. and *Cupressus sempervirens* L. growing on the two different altitudes (250 m and 1000 m) in the Zorkun plateau of Osmaniye and its soil microbial activity via carbon mineralization. The some soil properties of the *Arbutus* and *Cupressus* at the 250 m and 1000 m altitudes were separately presented in Table 1 and Table 2.

While *Arbutus* had a soil textured sandy clay loam (SCL) at both altitudes, *Cupressus* was loamy sand (LS) at 250 m and sandy loam (SL) at 1000 m. A significant difference of field capacities of *Arbutus* soils was observed between two different elevation gradients ($P = 0.000$), but it did not change between the same altitudes of *Cupressus* soils ($P > 0.05$). Soil pH was not affected by the altitude difference in both plant soils ($P > 0.05$). $CaCO_3$ contents (%) of *Arbutus* soils decreased significanty from 250 m (8.66) to 1000 m (3.17, $P = 0.000$), but it was not significant between *Cupressus* soils ($P > 0.05$). While organic C concentrations (%) of *Arbutus* soils were not significant between two elevations ($P > 0.05$, Table 1), it's N contents and C/N ratios varied significantly between them ($P = 0.003$ and $P = 0.019$, respectively). There was a significant difference between *Cupressus* soils at the two different elevation gradients in terms of organic C and nitrogen concentrations ($P = 0.044$ and $P = 0.013$, respectively). C/N ratio did not vary between two *Cupressus* soils ($P > 0.05$, Table 2).

Although a similar trend occurred for C contents in the shoots and leaves of both *Arbutus* and *Cupressus*, it was not significant between the 250 m and 1000 m elevation gradients ($P > 0.05$, Table 3). N contents in the shoots and leaves of *Arbutus* located in the 250 m were significantly lower than 1000 m ($P = 0.011$ and $P = 0.036$, respectively). However, leaf N content of *Cupressus* located in the 1000 m (0.70%) was lower than 250 m (1.12%, $P = 0.002$). There was a significant relationship between soil chemical properties and different elevation.

Soil composition also changed with elevation differences. Some researchers found in their study that Pearson correlation coefficient analysis showed significantly negative correlation ($P < 0.01$, $P < 0.05$) of clay, silt, bulk density, particle density, pH and cation exchange capasity whereas positive correlation of sand and organic carbon ($P < 0.01$) with altitude [28]. Hence, these findings suggest the altitudinal variations in soil physico-chemical properties. These altitude differences might affect climatic variables such as especially temperature and precipitation [29]. In our study, the soil field capacity, $CaCO_3$, C and N contents (%) and C/N ratio of the *Arbutus andrachne* showed significant difference between 250 m and 1000 m altitudes. The content of all these characteristics increased with increasing elevation. *Cupressus sempervirens* soils were significant between two different altitudes in terms of C and N contents (%). Soil C content (%) of 1000 m was higher (5.19) than 250 m (3.71), but soil total N content was significantly lower in 1000 m. Our findings were supported by some researchers [30-34]. They were presented in their studies that soil carbon concentration increased together with rising altitude. The alteration in elevation gradients impresses soil organic matter and its content by controlling soil water balance, elevational temperature, soil erosion, species and biomass production of the native vegetation [35-37]. The varying climatic conditions at the high altitudes might be obligating the significant differences on

soil organic matter decomposition against to its storage. Some study results showed that soil organic matter and carbon contents increased with altitude in different localities like Tuscan Volcanic Plateau of California, Chugach Mountains of South-Central Alaska and Kazdagı of Turkey, respectively [36, 38, 39]. Both N contents of *Arbutus* leaves and shoots were significantly higher at 1000 m than 250 m elevation opposite to N contents of *Cupressus* leaves and shoots. These results reflected to normally variety of nutrient element status between two different plant species and temperature degrees in the presence of different altitudes (250 m and 1000 m). Higher environment like 1000 m is recognized by high solar radiation, low temperature and rapid temperature changes [40]. Temperature is the most considerable constraint factor for nitrogen turnover in the soil from the others [39]. Lower environment like 250 m is known by the higher temperature and different humidity conditions. These varying factors affect each plant and its performance in this altitude. The height, structure and physiology of each plant change with the changing climatic and environmental properties together with elevation. Soil characteristics and plant diversity are also affected by these factors in the different altitudes [41].

Soil Carbon Mineralization. At the end of incubation period (30 days), a great difference was observed between *Arbutus* located in 250 m and 1000 m from the point of view of soil organic carbon mineralization (P = 0.001, Fig. 2).

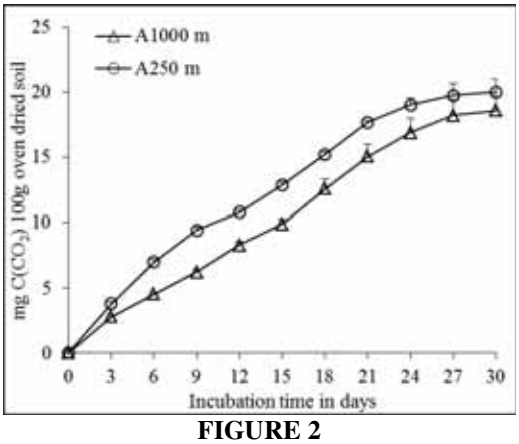

FIGURE 2
Cumulative carbon mineralization (mean ± standard error; *n* = 3) at the different incubation times (30 days) under the controlled laboratory conditions (28°C, 80 % of field capacity) in soils of *Arbutus andrachne* L. (A) growing on 250 m and 1000 m elevations

Cumulative C mineralization showed a significant difference between two elevation gradients of *Cupressus* at the P = 0.003 significance level. Microbial activity increased with increasing altitude in *Cupressus* soil. There were also significant differences between *Arbutus* and *Cupressus* at the both 250 m and 1000 m (P = 0.000 and P = 0.015, respectively), but this difference was not observed in between both two across altitudes and plants (P > 0.05, Fig. 2-3).

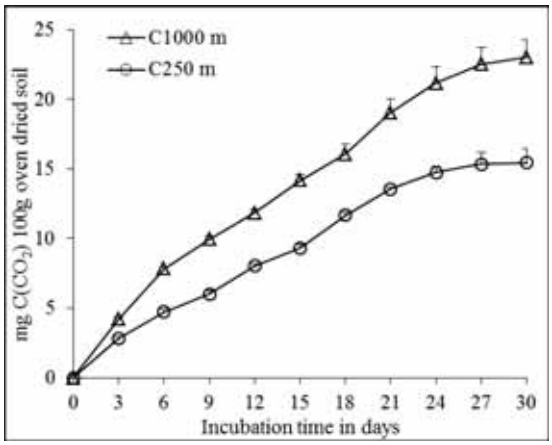

FIGURE 3
Cumulative carbon mineralization (mean ± standard error; *n* = 3) at the different incubation times (30 days) under the controlled laboratory conditions (28°C, 80 % of field capacity) in soils of *Cupressus sempervirens* L. (C) growing on 250 m and 1000 m elevations

C mineralization of *Cupressus* was the greatest at the 1000 m elevation while this value was high at *Arbutus* growing on the 250 m. The soil microbial activity of both *Arbutus* and *Cupressus* affected from the elevation difference, but two plants showed different sensitivity to the elevation difference. These results might be explained with both tree litter quality differences between elevations and different plant composition and also having significant impact on some soil characteristics of the changes in altitude [31, 33, 36, 42]. A research result showed that mean annual air and soil temperatures decreased approximately 0.5 °C with every 100 m increase in elevation result [43]. It means that air and soil temperatures and organic matter decomposition amount decline with increasing altitude [32], but this sitiation was not current for soil carbon mineralization of *Cupressus* growing on Zorkun Plateu of Osmaniye. It can be associated with organic matter quality of vegetation [44] and the strong stoichiometric homeostasis [45] of soil microorganisms at the 1000 m. All these differences showed that soil organic C mineralization was affected by differences of plant type, elevation and the other climatic factors.

Carbon Mineralization Ratios of The Soils. Carbon mineralization ratio of *Arbutus* soils was not affected by the elevation difference (P > 0.05, Fig. 4) while there was a significant difference between 250 m and 1000 m altitudes for *Cupressus* soils (P = 0.011). It might be proposed that microorganisms

living in *Arbutus* soil were stable and showed similar tendency in both 250 m and 1000 m elevations than soil microorganisms of *Cupressus* in the light of this result.

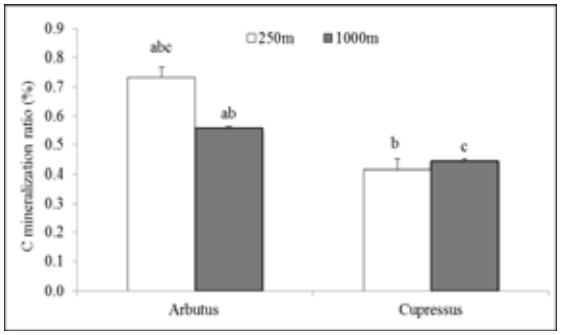

FIGURE 4
C mineraization ratios (mean ± standard error; *n* = 3) of *Arbutus andrachne* L. and *Cupressus sempervirens* L. soils at the different elevations (250 m and 1000 m). Different letters (a, b, c) represent significant differences between both plants and elevations (P < 0.05)

C mineralization ratio of *Arbutus* at the 1000 m altitude was significantly higher than *Cupressus* at the same altitude (P = 0.009). No great difference was observed between two plants at the 250 m altitude (P > 0.05, Fig. 4). Soil microorganisms of *Cupressus* living at 250 m showed similar behaviour with soils at both 250 m and 1000 m of *Arbutus*. It was a remarkable result for microorganisms in *Cupressus* soil that they adapted to 1000 m altitude better than 250 m. Soil microbial composition and activity was affected by various tree characteristics [18, 19] and their different litter qualities [39], changes in soil environment like soil moisture, pH and temperature [16]. Varieties in the litter qualities of decidious and coniferous plants, compounds of different plants and climatic systems directly affected to the soil micbial activities [46-48]. Similar results were observed in this study results by observing C mineralization.

CONCLUSIONS

C mineralization and its ratio at Zorkun plateau of Osmaniye prominently increased with increasing elevation in *Cupressus* soil. These parameters were more stable in *Arbutus* soils and their microbial activity. These differences between *Arbutus* and *Cupressus* might be caused from having the different tolerance limits to ecological factors of own environment, different soil characteristics and also different organic matter quality.

ACKNOWLEDGEMENTS

We thank Professor Cengiz DARICI for assistance in the execution of the Project and also Meric Simsek for English check. This project numbered OKUBAP-2015-PT3-009 was funded by Research and Application Center in Osmaniye Korkut Ata University.

REFERENCES

[1] Sheng-Xuan, G., D., Wei, Tao, Z. (2015) Soil Organic Carbon Mineralization along an Altitudinal Gradient in a Natural Spruce Forest, China, Adv. J. Food Sci. Technol. 8: 337-342.
[2] Merino, C., Godoy, R., Matus, F. (2016) Soil enzymes and biological activity at different levels of organic matter stability, J. Soil Sci. Plant Nutr. 16: 14-30.
[3] Parkin T.B., Doran, J.W., Franco-Vizcaíno, E. (1996) Field and Laboratory Tests of Soil Respiration, in Methods For Assessing Soil Quality. Madison, 231-245.
[4] Garten, C.T., Huston, M.A., Thoms, C.A. (1994) Topographic variation of soil nitrogen dynamics at Walker Brance Watershed, Tennessee, Forest Sci. 40: 497-512.
[5] Powers, R.F. (1990) Nitrogen mineralization along an altitudinal gradient: interactions of soil temperature, moisture, and substrate quality, Forest Ecol. Manag. 30: 19-29.
[6] Zengin, E., Aka Sağlıker, H., Darıcı, C. (2008) Carbon Mineralization of *Acacia cyanophylla* Soils under the Different Temperature and Humidity Conditions, Ekoloji. 69: 1-6.
[7] Zianis D., Mencuccini, M. (2005) Aboveground net primary productivity of beech (Fagus moesiaca) forest: a case study of Naousa forest, northern Greece, Tree Physiol. 25: 713-722.
[8] Jia, J., Yu, D., Zhou, W., Zhou, L., Bao, Y., Meng, Y., Dai, L. (2015) Variations of soil aggregates and soil organic carbon mineralization across forest types on the northern slope of Changbai Mountain, Acta Ecol. Sin. 35: 1-7.
[9] Blume, E., Bischoff, M., Reichert, J.M., Moorman, T., Konopka, A., Turco, R.F. (2002) Surface and subsurface microbial biomass, community structure and metabolic activity as a function of soil depth and season, Appl. Soil Ecol. 20: 171–181.
[10] Xu, M., Li, X., Cai, X., Li, X., Christie, P., Zhang, J. (2014) Soil microbial community structure and activity along a montane elevational gradient on the Tibetan Plateau, Eur. J. Soil Biol. 64: 6-14.
[11] Liu, Q. (2002) Ecological Research on Subalpine Coniferous Forests in China, Sichuan University Press, Chengdu, 33-35.

[12] Abiven, S., Menasseri, S., Angers, D., Leterme, P. (2007) Dynamics of aggregate stability and biological binding agents during decomposition of organic materials, Eur. J. Soil Sci. 58: 239–247.
[13] Salinas, N., Malhi, Y., Meir, P., Silman, M., Cuesta, R.R., Huaman, J. (2011) The sensitivity of tropical leaf litter decomposition to temperature: results from a large-scale leaf translocation experiment along an elevation gradient in Peruvian forests, New Phytol. 189: 967-977.
[14] Xu, G.H., Zheng, H.Y., Zhang, D.S., Lu, Y.B., Li, Y.K., Zhang X.S. (1984) The research of ecological distribution of soil microbial and its biochemical characteristics in nature reserve forest at north slope of Changbai Mountain, Acta Ecol. Sin. 4: 207-223.
[15] Xue, L., Kuang, L.G., Chen, H.Y., Tan, S.M. (2003) Soil nutrients, microorganisms and enzyme activities of different stands, Tu Rang Xue Bao 40: 280-285.
[16] Nagendran, N.A., Deivendran, S., Prabavathi, S. (2014) Diversity of Soil Microbes under Different Ecosystem Landuse Patterns, J. Appl. Environ. Microbiol. 2: 90-96.
[17] Zeden, H., (1993) The economic value of microbial diversity, Biotech. Appl. Microbiol. 43: 178-185.
[18] Bauhus, J., Pare, D., Cote, L. (1998) Effects of tree species stand age and soil type on soil microbial biomass and its activity in a southern boreal forest, Soil Biol. Biochem. 30: 1077-1089.
[19] Billore, S.K., Ohsawa, M., Numata, M., Okano, S. (1995) Microbial biomass nitrogen pool in soils from a warm temperate grassland and from deciduous and evergreen forest in Chiba Central Japan, Biol. Fertil. Soils. 19: 124–128.
[20] Üçeçam D., Hayli, S. (2004) Osmaniye İlinde Yerfıstığı Tarımı ve Önemi, Fırat Ü. Sosyal Bl. Drg. 14: 67-92.
[21] Bouyoucos, G.S. (1951) A recalibration of the hydrometer for mohing mechanical analysis of soil, Agron. J. 43: 434-438.
[22] Jackson, M.L. (1958) Soil Chemical Analysis. Prentice-Hall, Inc., Englewood Cliffs, NJ, 1-50.
[23] Allison L.E., Moodie, C.D. (1965) Carbonate, J. Am. Soc. Agron. 9: 1379-1396.
[24] Demiralay, I. (1993) Toprak Fiziksel Analizleri. Atatürk Üniversitesi Ziraat Fakültesi Yayınları, Erzurum, 53-58.
[25] Duchaufour, P. (1970) Precis de pedologie. Masson et C^{le}, Paris, 101-102.
[26] Schaefer, R. (1967) Characteres et evolution des activites microbiennes dans une chaine de sols hidromorphes mesotrophiques de la plaine d'Alsace, Rev. Ecol. Biol. Sol 4: 567-592.
[27] Kleinbaum, D.G., Kupper, L.L., Muller, K.E., Nizam, A. (1998) Applied Regression Analysis and Other Multivariable Methods. Duxbury Press, California, 111-115.
[28] Wani, S.A., Najar, G.R., Akhter, F., Wani, M.S., Mir, S.A. (2017) Altitudinal variations of soil physico-chemical properties in pear orchards of district Pulwama under temperate Jammu and Kashmir, India, Int. J. Chem. Stud. 5: 162-166.
[29] Lockeretz, W., Sheares, G., Kohl, D.H. (1981) Organic farming in the corn belt, Sci., 211: 540-547.
[30] Bolstad, P.V., Vose, J.M. (2001) The effects of terrain position and elevation on soil C in the southern Appalachians, in Assessment Methods for Soil Carbon. Lewis Publishers, Boca Raton, 45-51.
[31] Charan, G., Bharti, V.K., Jadhav, S.E., Kumar, S., Acharya, S., Kumar, P., Gogoi, D., Srivastava, R.B. (2013) Altitudinal variations in soil physico-chemical properties at cold desert high altitude, J. Soil Sci. Plant Nutr. 13: 267-277.
[32] Garten, C.T., Post, W.M., Hanson, P.J., Cooper, L.W. (1999) Forest soil carbon inventories and dynamics along an elevation gradient in the southern Appalachian Mountains, Biogeochem. 45: 115-145.
[33] Griffiths, R.P., Madritch, M.D., Swanson, A.K. (2009) The effects of topography on forest soil characteristics in the Oregon Cascade Mountains (USA): Implications for the effects of climate change on soil properties, Forest Ecol. Manag. 257: 1-7.
[34] Trumbore, S.E., Chadwick, O.A., Amundson, R. (1996) Rapid exchange between soil carbon and atmospheric carbon dioxide driven by temperature change, Sci. 272: 393-396.
[35] Davis, J., Schober, A., Bahn, M., Sveinbjornsson, B. (1991) Soil carbon and nitrogen turnover at and below the elevational treeline in northern Fennoscandia, Arct. Alp. Res. 23: 279-286.
[36] Sevgi, O., Tecimen, H.B. (2009) Physical, chemical and pedogenetical properties of soil in relation with altitude at Kazdagi upland black pine forest, J. Environ. Biol. 30: 349-354.
[37] Tan, Z.X., Lal, R., Smeck, N.E., Calhoun, F.G. (2004) Relationships between Surface Soil Organic Carbon Pool and Site Variables, Geoderma. 121: 185-187.
[38] Alexander, B.E., Mallory, J.I., Colwell, W.L. (1993) Soil- elevation relationships on a volcanic plateau in southern Cas-cade Range, Northern California, USA, Catena. 20: 113-128.
[39] Sveinbjiirnsson, B., Davis, J., Abadie, W., Butler, A. (1995) Soil Carbon and Nitrogen Mineralization at Different Elevations in the Chugach Mountains of South-Central Alaska, U.S.A., Arct. Alp. Res. 27: 29-37.
[40] Streb, P., Shang, W., Feierabend, J., Bligny, R. (1998) Divergent strategies of photoprotection

in high-mountain plants, Planta. 207: 313-324.
[41] Hutchins, R.L., Hill, J.D., White, E.H. (1976) The influence of soil and microclimate on vegetation of forested slopes in eastern Kentucky, Soil Sci. 121: 234-241.
[42] Saeed, S., Barozai, M.Y.K., Ahmad, A., Shah, S.H. (2014) Impact of Altitude on Soil Physical and Chemical Properties in Sra Ghurgai (Takatu mountain range) Quetta, Balochistan, Int. J. Sci. Engin. Res. 5: 730-735.
[43] Li-xia, Y., Jian-jun, P., Shao-feng, Y. (2006) Predicting dynamics of soil organic carbon mineralization with a double exponential model in different forest belts of China, J. Forest. Res. 17: 39-43.
[44] Qi, G., Wang, Q., Zhou, W., Ding, H., Wang, X., Qi, L., Wang, Y., Li, S., Dai, L. (2011) Moisture effect on carbon and nitrogen mineralization in topsoil of Changbai Mountain, Northeast China, J. Forest Sci., 57: 340–348.
[45] He, X., Hou, E., Liu, Y., Wen, D. (2016) Altitudinal patterns and controls of plant and soil nutrient concentrations and stoichiometry in subtropical China, Sci. Rep. 6: 242-261.
[46] Moore, T.R. (1980) The nutrient status of subarctic woodlands soils, Arct. Alp. Res. 12: 147-160.
[47] Boga, T., Aka Sagliker, H., Cenkseven, S. (2017) The first effect of *Eucalyptus camaldulensis* leaves and eucalyptol additions on soil carbon mineralization, Fresen. Environ. Bull. 26: 1052-1060.
[48] Mao, D., Wang, Z., Wu, C., Zhang, C., Ren, C. (2014) Topsoil carbon stock dynamics in the songnen plain of northeast China from 1980 to 2010, Fresen. Environ. Bull. 23a: 533-541.

Received: **24.04.2017**
Accepted: **14.07.2017**

CORRESPONDING AUTHOR

Husniye Aka Sagliker
University of Osmaniye Korkut Ata, Faculty of Science and Letters, Department of Biology, Osmaniye, 80000-Turkey

e-mail: hasagliker@osmaniye.edu.tr

© by PSP Volume 26 – No. 10/2017 pages 6085-6092 Fresenius Environmental Bulletin

EFFECTS OF ZINC AND UREA AS FOLIAR APPLICATION ON NUTRITIONAL PROPERTIES AND GRAIN YIELD IN BARLEY (*HORDEUM VULGARE L. CONV. DISTICHON*) UNDER SEMI ARID CONDITION

Mehmet Yagmur[1,*], Digdem Arpali[2], Fusun Gulser[3]

[1]Ahi Evran University, Faculty of Agriculture, Department of Field Crops, Kirsehir, Turkey
[2]Yuzuncu Yil University, Faculty of Agriculture, Department of Field Crops, Van, Turkey
[3]Yuzuncu Yil University, Faculty of Agriculture, Department of Soil Science, Van, Turkey

ABSTRACT

This current study was conducted to evaluate the effects of different rates of urea and zinc on grain yield and some important grain mineral contents in barley (*Hordeum vulgare L. conv. Distichon* cv. Tokak 157/37). The experimental design was a randomized complete block (RCB), arranged as split-plot with two doses of urea (0, 20 kg ha^{-1}) (main plots) and five zinc doses (0, 0.5, 1.0, 2.0 and 4.0 kg ha^{-1}) (subplots) with 3 replicates. The recorded agronomic parameters were grain yield (kg ha^{-1}), plant height (cm), spike length (cm), seeds spikes^{-1}, 1000 kernel weight (g), seeds weight spike^{-1}and grain mineral contents (N, P, Zn and Fe). When used solely, either urea or zinc significantly increased grain yield and all measured parameters. Besides, the use of the combined higher zinc doses with the urea (20 kg urea ha^{-1}+4 kg Zn ha^{-1}, 20 kg urea ha^{-1}+2 kg Zn ha^{-1}) increased grain yield (3.49 t ha^{-1} and 3.64 t ha^{-1}). These yields were not statistically different between each other, suggesting that 20 kg urea ha^{-1} + 2 kg Zn ha^{-1} application dose would be sufficient for higher grain yield. Moreover, the foliar application of urea and zinc affected the protein content and grain mineral contents (N, Zn and Fe) when sprayed at boot stage of barley. To conclude, zinc & urea treatment via foliar will maintain better quality and higher quantity barley grains under under semi arid conditions.

KEYWORDS:
Barley, Grain yield, Nutritional properties, Urea, Zinc

INTRODUCTION

Barley is considered as the most important cereal crops in the semi arid region of Turkey. Barley (Hordeum vulgare L. conv. Distichon) has been grown for malting but also it can be grown for human food and animal feed where sufficient carbohydrate sources are not available, such as corn in many ecological conditions.

Zinc is essential to life, playing an important role in biological processes of all living organisms (humans, animals, and plants). Zinc an essential mineral for the proper functioning of our daily intake. It is also used as the food supplement and biofortification of cereals. Zinc is an important part of cellular metabolism as well as the catalytic activity of enzymes [1]. Zinc is crucial for cell division, protein synthesis, the immune system and growth. Moreover it is known that zinc influences on basic plant life processes, such as nitrogen metabolism and photosynthesis.

Zinc deficiency in soil appears to be the most widespread and frequent micronutrient deficiency problem in field crops, resulting in severe losses in all grain yield components and mineral contents of grain and other plant parts. Zinc deficiency has been a major nutritional problem mostly in cereal growing areas in many countries, and the lack of zinc in the soil reduces grain yields as well as the resistance of crops to diseases [2]. Zinc deficiency in soils, especially arid and semi-arid regions, occurs in the calcareous soils, necessitating enrichment of these soils in terms of zinc minerals [3]. Zn-deficient arable lands in Turkey are about 14 million hectares [4].

The grown plants in low zinc soils have lower protein content due to low the rate of protein synthesis [5]. For this reason, zinc deficient arable lands have to be fertilized with zinc fertilizer to have higher yields. Zinc deficiency in plants is removed by using various methods with zinc fertilization [6]. Zinc fertilization is mostly applied to the soil, seeds and also foliar applications are common in worldwide. In general, soil application of Zn is recommended for plant growth. Zinc application to soil in high amount of zinc therefore this method is quite costly. There are also some reports of applying Zn to crop through foliar spray [7]. The foliar application of Zn has the advantage that much smaller quantities of Zn are needed compared to soil application.

The sufficient urea for crop growth has become an essential aspect for high crop yield [8]. Urea fertilizer is applied as a nitrogen source to soil or via foliar for optimum plant growth and improve protein

synthesis. Recently, it has been suggested that foliar uptake of urea for optimal growth and protein contents of cereals. Availability of nitrogen late in the season, when soil moisture content and root uptake is often low, is especially necessary for increasing grain protein content [9]. Studies conducted in this respect were obtained success like as in wheat, foliar urea application at the end of tillering increased the grain number per m^{-2}, dry matter yield, grain yield, harvest index and total nitrogen uptake [10]. Similarly, Salwau [11] observed that foliar application of 6% (w/v) urea at booting stage led to a higher wheat grain yield as compared with soil urea application. The risk of damage appears to be less with urea than with other forms of nitrogen fertilizer solution because urea has a low salt index and, therefore, desiccation of leaf cells through osmosis is reduced [12]. Khan et al. [13] reported that low (4 %) urea solution was applied as foliar spray had higher grain yield. The higher concentrations of urea spray were not found to be useful and economical as it declined the grain yield by 25 % or even more probably due to its toxicity.

Recently, erratic rainfall due to climatic changes may cause to drought stress during grain filling periods in cereals, therefore the application of urea and zinc via foliar may have a positive effect on increasing of the grain zinc content and grain crude protein. There has been a limited study in the barley production with the use of the combined zinc with the urea in zinc-deficient soils. Above mentioned reasons, the present study was carried out at Van ecological condition to examine the effects of zinc & urea treatment via foliar on two rowed barley in respect of grain yield and nutrient contents at marginal experimental area being fairly low zinc content (generally about 0.52 ppm).

MATERIALS AND METHODS

Experimental area. This study was conducted in a field condition of the eastern of Turkey (Van province) (38°-55' N; 42° – 05' E, 1725 m above sea level).

Plant material. A barley cultivar (*Hordeum vulgare* L. conv. *Distichon* cv. Tokak 157/37*)* was used as a seed material that has environmental tolerance compared to other barley varieties, moreover it has higher yields in poor soil conditions in province of Van.

Climatic description. Table 1. illustrates the climatic data of the experimental region. During the experiment, from October to July in 2009-2010 years, rainfall was observed higher in the autumn and winter seasons compared to the data belonging to long term period (1954-2010).

The properties of the experimental soil. In the analysis of soil, the texture was determined by Bouyoucous' hydro-metric method, pH value in 1/2.5 soil/water suspension, lime by calcimetric methods, organic matter by the modified Walkley Black method, salt content by Richards, total nitrogen by Kjeldahl method, available phosphorous by the method of Olsen, potassium by extracted with 1 N neutral ammonium acetate, total elements by atomic absorption spectrophotometry (AAS) [14].

Table 2 shows the chemical and physical characteristics of experimental soil. Experiment soil was low in organic matter, nitrogen and alkaline, sandy-clay loam texture, rich in potassium and calcium content, medium phosphorus and low zinc content [15].

TABLE 1
Climatic data of Van province in 2009-2010 years and long term (LTM).

	Rainfall (mm)		Temperature (^{0}C)		Moisture (%)	
Months	LTM*	2009-2010	LTM	2009-2010	LTM	2009-2010
September	15.4	16.0	16.3	9.5	55.2	48.9
October	49.6	45.9	10.3	12.6	63.2	46.8
November	47.5	91.1	4.3	4.3	67.0	61.1
December	32.1	34.8	-1.1	2.0	69.0	63.6
January	41.9	51.6	-3.6	0.1	69.0	63.4
February	35.4	71.1	-3.5	1.4	64.0	65.6
March	46.2	38.3	0.5	5.8	57.0	58.9
April	57.5	46.3	7.0	8.4	50.0	62.2
May	40.5	69.8	13.0	13.3	44.0	61.2
June	16.8	41.0	17.8	19.8	41.0	43.6
July	5.5	-	22.0	24.0	43.0	34.3
Total Rainfall	323.4	505.9	-	-	-	-
Average	-	-	7.5	9.2	56.58	55.41

TABLE 2
The experimental soil properties.

Depth (cm)	Lime (%)	pH	Salinity (m^s/cm)	Organic matter (%)	P (ppm)	N (%)	K (ppm)	Zn (ppm)	Fe (ppm)
0-20	4.7	8.20	276	0.98	6.79	0.069	214	0.60	6.93
20-40	4.9	8.19	266	0.81	5.51	0.057	229	0.52	7.52

Methods. The design of the experiment was randomized complete block (RCB), arranged as split-plot with two (2) doses of urea (main plots) and five (5) different doses of zinc fertilizer (subplots) treatments with 3 replicates with a total number of 30 plots. Area of each plot was 6.0 m^{-2} (1.20 m^{-1} x 5 m^{-1} each one).

Sowing and agricultural applications. Barley cultivar (Tokak 157/37) seeds were sown on October 15, 2009. Cleaned seeds were hand-drilled at 5 cm (4-5 cm) soil depths. The distance between each row was 20 cm (500 seeds m^{-2}). Each plot was sown 3 meters away each other due to limit the mixing of treatments. Plots were fertilized at seeding time with 150 kg ha^{-1} di-ammonium phosphate (18 % N and 46 % P_2O_5) and 250 kg ha^{-1} ammonium sulphate (21 % N) was applied at tillering stage. In this current study was conducted to determine the effect of five different zinc rates (0, 0.5, 1.0 and 2.0 and 4.0 kg Zn ha^{-1}). In this study $ZnSO_4 \cdot 7H_2O$ (21.0 % Zn) was used as a source of zinc (Zn). Urea (45 % N) doses were 0 kg N ha^{-1} and 20 kg N ha^{-1}. The volume of spray was 1000 L ha^{-1} using a precision sprayer with constant pressure of 0.4 MPa. The sprays of zinc and urea treatments were applied at booting stage (Zadoks growth stage, ZGS 43-45) [16] about 05-08 p.m. The control plots were sprayed with tap water. Grain yield (kg ha^{-1}), plant height (cm), spike length (cm), seeds $spikes^{-1}$, seeds weight $spike^{-1}$, 1000 kernel weight (g), grain crude protein (%) and grain N (%) and some mineral contents (P, Zn and Fe ppm) were evaluated.

Plant Measurements. The following agronomic traits were recorded: Plants were harvested at the beginning of July 2010. Plant height was measured as the height of the tallest culm of approximately 15 plants from the soil surface to the tip of the spike, awns excluded. Spike length was measured from the base of the spike to the tip of the apical spikelets, excluding awns on the same plants at physiological maturity. Grains were threshed by hand, and seeds $spike^{-1}$ and seed weight $spike^{-1}$ were calculated based on $spike^{-1}$. Thousand seeds weight in g, measured as the average of 4 samples of 100 kernels per plot. Grain yield (t ha^{-1}) were measured at harvest time. Four central rows were harvested and they were air dried and weighed it on a digital scale accurate to 0.1 g to record grain yield which were calculated per hectare basis.

Grain mineral analysis. Grain materials were analysed based on [15] and AOAC [17] as following: Grains were cleaned and washed with pure water, dried at 70 ^oC and finally ground. Nitrogen content in grain was analysed by using of the Kjeldahl method. Available phosphorous by the method of Olsen. Some plant nutrient (Fe, Zn) were analysed by using flame atomic absorption spectrophotometer apparatus with graphite furnace (AAS). The crude protein was found by the formulae N x 6.25 (1/0.16 = 6.25) to convert the analysed nitrogen content into crude protein content.

Statistical analysis. The obtained data were analysed statistically (analysis of variance) for significant differences. These analyses were performed by the procedure of MSTATc statistical package. Means were grouped in Duncan Multiple Comparison Test ($P<0.05$).

RESULTS AND DISCUSSION

Grain Yield and Some Grain Yield Components. Means of grain yield and some yield components are shown in Table 3. Foliar application of urea and zinc treatments significantly enhanced grain yield and grain yield components compared to control. In other words, data analysis showed that foliar application of urea and zinc affected positively all measured parameters. These effects were found higher than those of unfertilized control plots on the mentioned parameters.

When we evaluate the positive effects of zinc and urea applications on yield and yield traits separately, it was found that the foliar application of urea increased plant height, but this has not been found to be a statistically significant. Besides, the increasing of zinc rates positively changed plant height in barley. Furthermore, the combined zinc with urea fertilizer significantly increased plant height and the highest plant height was obtained with 63.9 cm by the highest zinc dose with urea via foliar applied plot. (U_1Zn_4) (Table 3).

As important yield traits, spike length was affected significantly by urea and the zinc fertilization. The longest spike length with 12.3 cm was obtained by the foliar application of urea (20 kg ha^{-1}). On the other hand, the shortest spike length was obtained in unapplied urea plots. The increased zinc doses increased spike length in dose dependent manner. It

was found that there was a significant urea and zinc interactions on spike length. The highest spike length was obtained with 14.39 cm by the combined dose of 20 kg urea ha^{-1} and 4 kg zinc ha^{-1} via foliar. Besides the shortest spike length 8.43 cm was obtained in control treatment. The combined urea and zinc fertilizer were found to be more effective on spike length in comparison when used solely, either urea or zinc.

The number of seeds per spike were affected significantly by foliar urea and zinc application. Likewise, the combined effect of urea (N) and zinc (Zn) on number of seeds per spike were also significant. The maximum number of seeds 27.4 per spike was obtained by 20 kg urea ha^{-1} and 4 kg zinc ha^{-1} foliar treatment. It was 17.17 in control plot which was the lowest number of seeds per spike.

The foliar application of Zn fertilizer had positive and considerably high effect on spike length and number of seed per spike compared to control plots. It could be explained by the fact that zinc deficiency affects the development of plants by lowering enzyme activity [18]. Similarly improvement in different grain yield components with an increase in Zn levels could be attributed to adequate Zn supply that might have affected the metabolic and enzymatic activity [19]. Also, Yilmaz et al. [20] demonstrated that the effect of Zn on grain yield was higher than biomass. These results indicate that the importance of Zn nutrition for grain set is greater than for vegetative growth. It was reported that anther and pollen seed development in zinc deficient wheat plants were largely impaired, more likely, due to the reduced levels of indole acetic acid and proteins [21, 22].

It was observed in the study that seeds weight per spike significantly were increased by urea via foliar (Table 3). The measured data showed that plots supplied with urea had the maximum seeds weight per spike with 1.00 g. The lowest seeds weight per spike was obtained in control plot. Similarly, the increased zinc doses up to 4.0 kg ha^{-1} increased seeds weight per spike. The same increase was seen in combined urea (N) and zinc (Zn) application without statistical significance.

It is known that thousand grain weight is an important yield components, which is mostly determined by genetic potential. Nevertheless, it was observed in the study that the foliar application of urea significantly increased thousand grain weight (Table 3). Similarly the increasing of zinc doses increased thousand grain weights. Combined effect of urea (N) and zinc (Zn) tended to increase thousand grain weights compared to control without any statistical significance. In other study, the foliar spray of 4% urea solution yielded heavier seeds compared to control (water spray). This may be due to the provision of nitrogen through urea spray which might have enhanced accumulation of assimilates in the grains and thus resulting in heavier grains in wheat [13]. It was reported that 1000 grain weight and spike length increased by foliar application of zinc fertilizer compared with the control. Therefore, the increase of 1000 grain weight and spike length can be the cause of high grain yield as compared to the control [23].

TABLE 3
Foliar application of zinc and nitrogen on some yield traits.

		Plant Height (cm)	Spike Length (cm)	Seeds $Spikes^{-1}$	Seeds Weight $Spike^{-1}$	1000 Seeds Weight (g)	Grain Yield (T ha^{-1})
Urea	U_0	58.1	10.38 b	19.91 b	0.84 b	43.57 b	2.83 b
	U_1	59.5	12.35 a	24.54 a	1.00 a	46.10 a	3.22 a
	F Value	1.95 ^{ns}	95.50*	66.05*	70.85*	1131.03**	20.65*
Zinc	Z_0	57.1 b***	8.74 d	18.46 d	0.83 c	42.51 c	2.65 d
	Z_1	58.2 ab	11.06 c	21.03 c	0.87 bc	44.25 bc	2.85 c
	Z_2	58.6 ab	11.85 bc	23.11 b	0.90 b	44.58 abc	3.05 b
	Z_3	58.9 ab	12.17 ab	23.98 ab	0.99 a	46.00 ab	3.24 a
	Z_4	60.9 a	12.99 a	24.55 a	1.01 a	46.83 a	3.35 a
	F Value	3.45*	54.87**	59.35**	17.82**	7.62**	43.61**
Urea and zinc Interactions	U_0Zn_0	56.9 ^{b}	8.43 h	17.17 g	0.75	41.03	2.61 e
	U_0Zn_1	57.9 b	9.78 fg	19.00 f	0.79	42.66	2.65 de
	U_0Zn_2	58.8 b	10.97 ef	20.90 de	0.81	43.00	2.86 cd
	U_0Zn_3	58.9 b	11.14 de	20.83 def	0.91	44.66	3.00 bc
	U_0Zn_4	58.0 b	11.59 cde	21.66 cd	0.92	46.50	3.06 bc
	U_1Zn_0	57.4 b	9.06 gh	19.76 ef	0.90	44.0	2.70 de
	U_1Zn_1	58.6 b	12.35 bcd	23.06 c	0.95	45.83	3.06 bc
	U_1Zn_2	58.3 b	12.74 bc	25.33 b	1.00	46.16	3.23 b
	U_1Zn_3	59.0 b	13.21 ab	27.13 a	1.06	47.33	3.49 a
	U_1Zn_4	63.9 a	14.39 a	27.43 a	1.10	47.16	3.64 a
	F Value	3.04*	3.78*	5.11**	0.14^{ns}	0.76 ^{ns}	4.59*

ns: not significant, * $P < 0.05$; ** $P < 0.01$, ***different letters indicate means significantly different (Duncan Multiple Comparison test).

Grain yield was tended to increase in the foliar applied urea fertilizer. The highest grain yield was obtained from the foliar application of urea in comparison only water sprayed plots (Table 3). The increasing of zinc doses increased grain yield in the dose dependent manner. The higher grain yields (3.24 t ha^{-1} and 3.35 t ha^{-1}) were obtained in the respective higher zinc application doses (Zn_3 and Z_4, Table 3). Since these yields were not statistically different between each other, it can be suggested that 2 kg ha^{-1} zinc application dose would be sufficient for higher grain yield. On the other hand, the control plot produced the lowest grain yield in average 2.65 t ha^{-1}. As results of this study, it was found that significant urea and zinc interactions on grain yield. Barley produced higher grain yields (3.49 t ha^{-1} and 3.64 t ha^{-1}) in the use of the combined the highest zinc doses with the urea via foliar (U_1Zn_3 and U_1Zn_4, Table 3). These yields were not statistically different between each other, therefore, 20 kg urea ha^{-1} +2 kg Zn ha^{-1} application dose would be sufficient for high grain yield. On the other hand, the control plot produced the lowest grain yield. Another expression, plots not supplied with any urea and zinc showed the lowest grain yield in average 2.61 t ha^{-1}. It was demonstrated that foliar applied urea at different plant growth stages had different effects on grain yield such as mean grain yield response to foliar urea was optimized by applications during ear emergence. Effects of urea via foliar on grain yield may be more pronounced in drought years or late season of vegetative growth where uptake of soil applied urea may be restricted, or in situations where rooting, or root efficiency is restricted where take all disease is a problem [24, 25]. The application time in the current study is similar to their findings. The increase in grain yield with increasing urea and zinc doses could be ascribed to more productive number of seeds per spike, the higher seeds weight per spike and spike length. Similar findings were reported by many studies in rice [26, 27] and in wheat [28].

Grain chemical contents: Means of crude protein and mineral contents of barley seed are presented in Table 4. Data analysis confirmed that the grain protein content was significantly affected by urea. The foliar applied urea had positive and significantly high effects on grain protein content that was obtained with 12.19 % compared to control (10.63 %) (Table 4). Even, zinc application increased significantly grain protein over control. The higher grain protein (11.39, 11.47, 11.70 and 11.92 %) were obtained respective higher zinc application doses (Zn_1, Zn_2, Zn_3 and Zn_4, Table 4). These were not statistically different between each other, suggesting that 0.5 kg ha^{-1} (Zn1) zinc application dose would be sufficient for higher grain protein content. Whereas, the control plot produced the lowest grain protein in average of 10.56 %. Moreover, it was found that significant urea and zinc interactions on grain protein ratio. The higher grain protein content (12.47 and 12.66 %) was obtained in the higher doses of zinc with added urea (U_1Zn_3 and U_1Zn_4, Table 4) without statistical significance between each other. On the other hand, the lowest protein content (9.26 %) was observed in the control plot. It resulted that combined urea and zinc was obtained more effective on grain protein ratio compared to alone zinc and urea applied plots. The recent studies showed the foliar applied urea between anthesis and late milk development was most likely to have the most effects on grain protein. Besides, the applied urea at the right time to plants, foliar application of urea would be more effective on grain protein content than granular nitrogen [25]. In many plants grown in zinc deficient soils have low protein contents. Besides, many studies about the effects of zinc on protein showed positively higher affects. It could be explained by the fact that zinc applied to plants increased grain protein due to the higher rate of protein synthesis in plants [29]. Likewise, zinc has been shown to have a significantly increased grain protein and enhanced grain zinc contents, while the reduced grain phosphorus concentration [30]. Nitrogen efficiency was more essential for zinc absorptions and uptakes in cereals. Since zinc has a direct effect on the increase of protein in grains, the deficiency of this element in crops would reduce the grain protein and thus amino acids could not be accumulated [31]. The increase of total nitrogen uptake induced by zinc application was confirmed on its primary effect on main physiological processes related to nutrients uptake [5]. The availability of nitrogen can affect the chlorophyll content of the leaves which is positively correlated with leaf nitrogen content and its allocations into seeds [32].

Data analysis showed that urea and zinc affected significantly grain nutrients (N, P, Zn and Fe). The content of each mineral in the grain was affected differently by urea and zinc treatments. N content in barley grain was significantly affected with the foliar applied urea and zinc, compared to those of their controls. Even, it was found that urea and zinc interactions affected significantly grain nitrogen content (Table 4). The results when evaluated for grain phosphorus contents, the grain phosphorus content was affected significantly by the foliar application of urea. On the contrary, the applied the increasing zinc doses decreased grain phosphorus content in dose dependent manner but this was not statistically different. Even, it was found that significant urea and zinc interactions on grain phosphorus content (Table 4). The higher P contents were determined with 3.54 and 3.47 ppm from U_1Zn_1 and U_1Zn_2 respectively. But these P contents were not significantly different.

TABLE 4
Foliar application of zinc and nitrogen on some plant nutrients.

		Crude Protein (%)	N (%)	P (ppm)	Zn (ppm)	Fe (ppm)
Urea	U_0	10.63 b***	1.70 b	2.74 b	21.91b	85.68
	U_1	12.19 a	1.95 a	3.28 a	26.37 a	94.61 a
	F Value	47.29*	45.03*	51.62*	140.93**	133.55**
Zinc	Z_0	10.56 b	1.69 c	3.12^{ns}	18.47 d	71.96 d
	Z_1	11.39 a	1.82 b	3.02	21.77 c	92.26 b
	Z_2	11.47 a	1.83 ab	3.05	24.30 b	108.85 a
	Z_3	11.70 a	1.87 ab	3.00	27.33 a	92.66 b
	Z_4	11.92 a	1.90 a	2.85	28.85a	85.00 c
	F Value	11.87**	11.93**	1.01 ns	71.76**	67.29**
Urea and zinc Interactions	U_0Zn_0	9.26 d	1.48 d	2.79 cd	15.02 f**	58.00 e**
	U_0Zn_1	10.78 c	1.73 c	2.50 d	20.19 e	92.06 bcd
	U_0Zn_2	10.97 c	1.76 c	2.64 cd	23.18 cd	97.66 b
	U_0Zn_3	10.93 c	1.74 c	2.90 bcd	25.60 c	94.00bc
	U_0Zn_4	11.19 bc	1.79 c	2.85cd	25.58 c	86.66 cd
	U_1Zn_0	11.86 ab	1.90 b	3.44 ab	21.91 de	85.92 cd
	U_1Zn_1	12.01 ab	1.92 ab	3.54 a	23.34 cd	92.45 bcd
	U_1Zn_2	11.97 ab	1.91 b	3.47 a	25.42 c	120.03 a
	U_1Zn_3	12.47 a	1.99 ab	3.11abc	29.06 b	91.33 bcd
	U_1Zn_4	12.66 a	2.03 a	2.85 cd	32.17 a	83.33 d
	F Value	4.18*	4.30*	4.90**	4.54*	21.07**

ns: not significant, * $P < 0.05$; ** $P < 0.01$, ***different letters indicate means significantly different (Duncan Multiple Comparison test).

The zinc contents in grain changed between 21.91 and 26.37 ppm in the dose manner. It was found that the applied urea had higher zinc content (26.37 ppm) compared to control (21.91 ppm). Similarly the increasing of zinc levels significantly increased grain zinc content. The higher grain zinc contents (27.33 and 28.85 ppm) were determined from respective higher zinc application doses (2.0 and 4.0 kg ha^{-1} Table 4). These higher zinc levels in grain were not statistically different between each other, suggesting that 2.0 kg ha^{-1} zinc application dose would be sufficient for grain zinc contents. Besides foliar application of combined zinc with urea increased grain zinc content. The highest zinc content in grain (32.17 ppm) was obtained by the highest zinc concentration with added urea. On the other hand, the control plots produced the lowest grain zinc content in average 15.02 ppm.

Many reports showed about zinc fertilization has great effects on zinc content. Zinc application via foliar was observed to be more effective in grain Zn increase and grain Zn recovery compared to other applications [8]. Yılmaz et al. [20] reported that zinc fertilizers could increase grain Zn concentration up to three- or fourfold. Similarly, Habib [23] reported that foliar application of (Zn) at tillering and heading stage increased Zn concentration up to 50.9 from 12.17 mg kg^{-1}. The remobilization of Zn from leaves to grain contributed to the Zn content of grain. Thus foliar applied zinc that easily moves to corn grain should be adopted as a practice for agronomic biofortification of corn [30]. Similarly, Haslett et al. [34] reported that transport of Zn in phloem from leaves to the stem, lower leaves and roots is substantial. It was concluded that zinc was highly mobile in phloem. Enrichment of wheat grain with zinc was maximized when plants were supplied sufficiently with nitrogen fertilizers [35]. Similarly, Shivay et al. [36] reported that foliar applied Zn-coated urea fertilizer significantly increased both grain yield and grain zinc contents in spring wheat. In addition, enrichment of barley grain with zinc fertilizations also produces bigger roots and shoots during their early growth. Greater root mass would be beneficial in later growth stages for nutrients and water uptake when plants face water shortage in case of early drought periods that are fairly often during springs in semi-arid areas [37]. In the study, observed zinc content in grain was below unhealthy levels. Zinc concentration in wheat grain should be < 34 mg kg^{-1} for it to be suitable for human consumption [38].

As it appeared from the result of the experiment in this research, the foliar applied urea significantly increased iron contents in grain. Additionally, it was found that the lower zinc levels increased grain iron content but this zinc effect on iron content was lost with higher zinc doses. But grain iron levels was significantly higher at all amount of zinc levels compared to control. The highest iron content (120.0 ppm) in barley grain was obtained from the foliar application of 1.0 kg Zn ha^{-1} and 20 kg N ha^{-1}. Habib [23] reported that foliar application of (Zn) at tillering and heading stage increased Fe concentration compared with control (from 84.93 to 123.7 mg kg^{-1}). Their findings are similar to our results.

CONCLUSION

The higher grain yields (3.49 t ha^{-1} and 3.64 t ha^{-1}) were obtained the respective higher zinc with combination of urea doses (20 kg urea ha^{-1} + 2 kg Zn ha^{-1}; 20 kg urea ha^{-1} + 4 kg Zn ha^{-1}) without statistical significance between each other. Therefore, 20 kg urea ha^{-1} + 2 kg Zn ha^{-1} application dose would be sufficient for high grain yield. Also, the foliar application of urea and zinc solutions enhanced the protein content and grain mineral contents (N, Zn and Fe) when sprayed at boot stage. The foliar application of urea increased grain phosphorus content. On the contrary, zinc treatment decreased grain phosphorus content. To conclude, zinc & urea treatment via foliar will maintain better quality and higher quantity barley grains or other cereals under under semi arid conditions.

REFECENCES

[1] Ahmad, M.S., Khan, Z.I., Ahmad, K., Batool, A.I., Hamid, S., Sher, M.I., Noorka, R., Hayat, Z., Bashir, H., Sohail, M., Ejaz, A., Sheikh, Z., Muneeb, A., Mehmood, N., Muqaddas, H., Zubair, F., Amjad, N., Taj, F.N., Iqbal, S. and Batool, F. (2017) Accretion and dispersion of heavy metals in a vegetable grown in contaminated soil with sewage water: a matter of great concern and community health consequences. Fresen. Environ. Bull. 26(7), 4345-4349.

[2] Graham, R.D. and Welch R.M. (1996) Breeding for staple food groups with high micronutrient density: long term sustainable agricultural solutions to hidden hunger in developing countries. In: Workshop on Food Policy and Agricultural Technology to Improve Diet Quality and Nutrition, Annapolis, MD, IFPRI, Washington, DC.

[3] Takkar, P.N. and Walker C.D. (1993) The distribution and correction of zinc deficiency, 151-166. In: A.D. Robson (ed.), Zinc in Soils and Plants. Kluwer Academic Publishers, Dordrecht, The Netherlands.

[4] Eyupoglu, F., Kurucu, N., Talaz, S. and Canisag, U. (1994) Status of plant available micronutrients in Turkish soils (in Turkish), pp. 25-31. In: Soil and Fertilizer Research Institute Annual Report, 1993. Report No. 118, Ankara, Turkey.

[5] Potarzycki, J. and Grzebisz W. (2009) Effect of zinc foliar application on grain yield of maize and its yielding components. Plant Soil Environ. 55(12), 519-527.

[6] Sun, J., Ma, J., Zhu, M., Yuan, Z. and Yao, J. (2016) Effects of nitrogen application on the soil microbial activity, enzyme activities and properties and their relationships in a maize field. Fresen. Environ. Bull. 25(3), 852-861.

[7] Slaton, N.A., Normal, R.J. and Wilson, J.C.E. (2005) Effect of zinc source and application time on zinc uptake and grain yield of flood-irrigated rice. Agronomy Journal 97, 272 –278.

[8] Mao, H., Zhanga, T., Wanga, Z. and Lia, M. (2016) Improvement of zn and fe concentrations in maize grains as influenced by zn application in loess plateau, China. Fresen. Environ. Bull., 25(6), 2145-2153.

[9] Alkier, A.C., Racz, J.G. and Soper, R.J. (1972) Effects of foliar- and soil- nitrate-nitrogen level on the protein content of Neepawa wheat. Can J Soil Sci. 52, 301-309.

[10] Sarandon, S.J. and Gianibelli, M.C. (1990) Effect of foliar urea spraying and nitrogen application at sowing upon dry matter and nitrogen distribution in wheat (*Triticum aestivum* L.). Agronomie 10, 183-189.

[11] Salwau, M.I.M. (1994). Effect of Soil and Foliar Application of Nitrogen Levels on Yield and Yield Components of Wheat (*Triticum aestivum* L.). Field Crop Abst. 49, 2192.

[12] Gray, R.C. (1977). Foliar fertilisation with primary nutrients during the reproductive stage of plant growth. Proc. Fert. Soc., London no. 164.

[13] Khan, P., Memon, M.Y., Imtiaz, M. and Aslam, M. (2009) Response of wheat to foliar and soil application of urea at different growth stages. Pak. J. Bot. 41(3), 1197-1204.

[14] Kacar, B. (1994) Chemical analysis of plant and soil. III. Soil analysis. University of Ankara, Faculty of Agri-culture, Ankara, Turkey.

[15] Kacar, B. (1984) Plant nutrition application guide. Ankara University, Agricultural Faculty Number. 900, Ankara, 140 pp

[16] Zadoks, J.C., Chang, T.T. and Konzak, C.F. (1974) A decimal code of the growth stages of cereals. Weed Res. 14, 415-421.

[17] Helrich, K. (Ed.) (1990) Official Methods of Analysis of the Association of Official Analytical Chemists. Washington, DC.

[18] Pandey, N., Gupta, M. and Sharma, C.P. (2001) Zinc efficiency affects pollen structure and viability in green gram (*Vigna radiate* L. cv T-44). Geophytology 28, 31-34.

[19] Hafeez, B., Khanif, Y.M., Samsuri, A.W., Radziah, O., Zakaria, W. and Saleem, M. (2010) Evaluation of rice genotypes for zinc efficiency under acidic flooded condition. In 19th World Congress of Soil Science, Soil Solutions for a Changing World 1-6 August 2010, Brisbane, Australia.

[20] Yilmaz, A., Ekiz, H., Torun, B., Gultekin, I., Karanlik, S., Bagci, S.A. and Cakmak, I. (1997) Effect of different zinc application methods on grain yield and zinc concentration in wheat cultivars grown on zinc-deficient calcareous soils. Journal of Plant Nutrition 20, 4-5.

[21] Cakmak, I., Marscher, H. and Bangerth, F. (1989) Effect of zinc nutritional status on

growth, protein metabolism and levels of indole-3-acetic acid and other phytohormones in bean (*Phaseolus vulgaris* L.). J Exp Bot. 40, 405-412.

[22] Brown, P.H., Cakmak, I. and Zhang, Q. (1993) Form and function of zinc in plants, pp. 93- 106. In: Robson, A.D. (ed.), Zinc in Soil and Plants. Kluwer Academic Publishers, Dordrecht, The Netherlands.

[23] Habib, M. (2009) Effect of foliar application of Zn and Fe on wheat yield and quality. African J Biotechnol. 8, 6795–6798.

[24] Dampney, P.M.R., Salmon, S.E., Greenwell, P. and Pritchard, P.E. (1995) Management of breadmaking wheat: Effects of extra nitrogen on yield, grain and flour quality. Research Report 109, London, 166 pp.

[25] Turley, D.B., Sylvester-Bradley, R. and Dampney, P.M.R. (2001) Foliar-applied nitro-gen for grain protein and canopy management of wheat. Research Review No. 47, HGCA -Pp 36.

[26] Hakoomat, A., Hasnain, Z., Shahzad, A.N., Sarwar, N., Qureshi, M.K., Khaliq, S. and Qayyum, M.F. (2014) Nitrogen and zinc interaction improves yield and quality of submerged basmati rice (*Oryza sativa* L.). Not Bot Horti Ag. 42 (2), 372-379.

[27] Yashbir, S.S. and Prasad, R. (2012) Zinc-coated urea improves productivity and quality of basmati rice (*Oryza sativa* l.) under zinc stress condition, Journal of Plant Nutrition 35 (6), 928-951.

[28] Khattak, S.G., Dominy, P.J. and Ahmad, W. (2016) Effect of Zn as soil addition and foliar application on yield and protein content of wheat in alkaline soil. J Natn Sci Foundation Sri Lanka 43(4), 303 – 312

[29] Marschner, H. (1995) Mineral Nutrition of Higher Plants. 2 Ed. Academic Press.

[30] Zeidan, M.S. (2001) Response of wheat plants (*Triticum aestivum* L) to different methods of Zinc fertilization in reclaimed soils of Egypt. Plant Nutrition - Food Security and Sustainability of Agro-ecosystems (Eds. Horst, W.J., Schenk**,** M.K., Bürkert**,** A., Claassen**,** N., Flesa, H., Frommer, W.B., Goldbach, H., Olfs, H.W., Römheld, V., Sattelmacher, B., Schmidhalter, U., Schubert**,** S., von Wirén**,** N., Wittenmayer**,** L.) Kluwer, Dordrecht**,** The Netherlands, pp: 1048-1049.

[31] Palmgren, M.G., Clemens, S., Williams, L.E., Kramer, U., Borg, S., Schjorring, J.K. and Sanders, D. (2008) Zinc biofortification of cereals: problems and solutions. Trends in Plant Science 13, 464-473.

[32] Xue, Y.F., Yue, S.C., Zhang, Y.Q., Cui, Z.L., Chen, X.P., Yang, F.C., Cakmak, I., McGrath, S.P., Zhang, F.S. and Zou, C.Q. (2012) Grain and shoot Zn accumulation in winter wheat as affected by nitrogen management. Plant and Soil 261, 153-163.

[33] Schluter, U., Mascher, M., Colmsee, C., Scholz, U., Brautigam, A., Fahnenstich, H. and Sonnewald, U. (2012) Maize source leaf adaptation to nitrogen deficiency affects not only nitrogen and carbon metabolism but also control of phosphate homeostasis. Plant Physiology 160, 1384-1406.

[34] Haslett, B.S., Reid, R.J. and Rengel, Z. (2001) Zinc mobility in wheat: Uptake and distribution of Zn applied to leaves or roots. Annals of Botany 87, 379-386.

[35] Cakmak, I. (2010) Biofortification of cereals with zinc and iron through fertilization strategy. In: 19th World Congress of Soil Science, Brisbane.

[36] Shivay, Y.S., Prasad, R. and Rahal, A. (2008) Relative efficiency of zinc oxide and zinc sulphate-enriched urea for spring wheat. Nutrient Cycling in Agroecosystems 82, 259-264.

[37] Rengel, Z. (2001). Genotypic differences in micronutrient use efficiency in crops. Communication in Soil Science and Plant Analysis, 32: 1163–1186.

[38] Andersson, A. and Pettersson, O. (1981) Cadmium in Swedish winter wheat. Swed. J. Agr. Res. 11, 49-55.

Received: **24.04.2017**
Accepted: **23.07.2017**

CORRESPONDING AUTHOR

Mehmet Yagmur
Ahi Evran University Faculty of Agriculture
Department of Field Crops Kirsehir – TURKEY

E-mail: mehmetyag@yahoo.com.

© by PSP Volume 26 – No. 10/2017 pages 6093-6103 Fresenius Environmental Bulletin

SEDIMENTS CHARACTERISTICS AND HEAVY METALS DISTRIBUTION OF A VERY SHALLOW PROTECTED COASTAL LAGOON, PROKOPOS LAGOON, MEDITERRANEAN SEA WESTERN GREECE

Dimitrios Katsaros[1], Dionisios Panagiotaras[2], Nikolaos Kontopoulos[3], Pavlos Avramidis[3,*]

[1]Decentralised Administration of Peloponnese, Western Greece & Ionian (APD-DEPIN), N.E.O. Patron-Athinon 158, 264 42 Patras, Greece
[2]Technological Educational Institute (T.E.I.) of Western Greece, Department of Mechanical Engineering, Laboratory of Chemistry, M. Alexandrou 1, 263 34 Patras, Greece
[3]University of Patras, Department of Geology, Laboratory of Sedimentology, 265 04 Rio-Patras, Greece

ABSTRACT

In this study we present sedimentological and geochemical parameters in order to evaluate the environmental status of an internationally protected shallow coastal lagoon, Prokopos Lagoon, Western Greece. Six gravity cores with sediment depth up to 0.70 m l were collected and analyzed for K_2O, CaO, Na_2O, MgO Fe_2O_3, MnO, Al_2O_3, P_2O_5, TOC, V, Cr, Zn, Ni, Cu, Cd, Pb. In addition the clay, sand and silt content were determined and the mean size (Mz), sorting (σ), skewness (Sk) and kurtosis (KG) values were deduced. The lagoon's sediments are composed mainly of fine silt to medium sand. The clay content of the samples ranges from 0.76 % to 6.73 % and the average values of the silt and sand content are 50.20 % and 42.56 % respectively. The geochemical evaluation indicates that mainly the terrigenous input of the surrounding catchment materials controlling inter –element and grain size association. The Cr, Ni, Cu and Zn affiliated in the aluminosilicates fraction identifying their primarily detrital origin. Fe and Mn is representative of the oxides/hydroxides group and thus Cd is associated with this fraction of the sediments. The calculation of three geochemical indices (the enrichment factor - EF, contamination factor - CF and index of geo-accumulation - I_{geo}) were used in order to distinguish between affected and unaffected sampling sites. The EF values calculated for Cd showing significant enrichment in some sampling sites while the CF values for Cd, Cr, Cu, Pb and Zn are indicative for a low contamination. Cr and Ni exceed the Toxicity Screening Values (TSVs) and Threshold Effect Level (TEL) according to sediment quality guidelines for metals. Nevertheless, the Zn, Cd, Cu and Pb average concentration values are bellow the Toxicity Screening Values (TSVs) and the Threshold Effect Level (TEL). By contrast, Cr and Ni exceed the TSVs and TEL values in the Prokopos lagoon sediments. The study of sediment geochemical characteristics can be considered as a baseline for future monitoring in accordance to the European Union Directives and for any future engineering interventions for the lagoon environmental maintenance and conservation.

KEYWORDS:
Geochemistry, coastal sedimentology, lagoons, pollution indices, Prokopos Greece

INTRODUCTION

Lagoon environment affected as a result of intensive agriculture activities, overexploitation of the water resources and urbanization [1, 2]. The anthropogenic input of pollutants is concentrated to the lagoon sediments and threats the aquatic ecosystems [3, 4]. Sea level fluctuations, storm and river flooding as well as human activities also affect the lagoon environment [5].

The geochemical investigation of lagoon bottom sediments can often delineate changes in the chemical, biological, and physical conditions of the environment [6, 7, 8, 9]. For example, Mn and Fe change their chemical forms and concentrations according to the redox condition [10, 11], while distribution profiles of some bio-elements such as Ca, P and Si, are sensitively affected by biological activity [12, 13]. However, metals' enrichment factors, pollutions indices and statistical analysis have been developed in order to define sediment quality assessment [14, 15, 16, 17].

In this study we use the enrichment factor (EF), the contamination factor (CF) and the index of geo-accumulation (I_{geo}) in order to find enrichments or depletions at the metals distribution in sediment samples collected from the Prokopos Lagoon, Western Greece [18]. Moreover this study can be consider as a baseline for future monitoring in accordance to the European Union Directives and for any future engineering interventions for the lagoon environmental maintenance and conservation. This is of a great environmental and social importance because of the significant and substantially development of inner waters fishery and fish

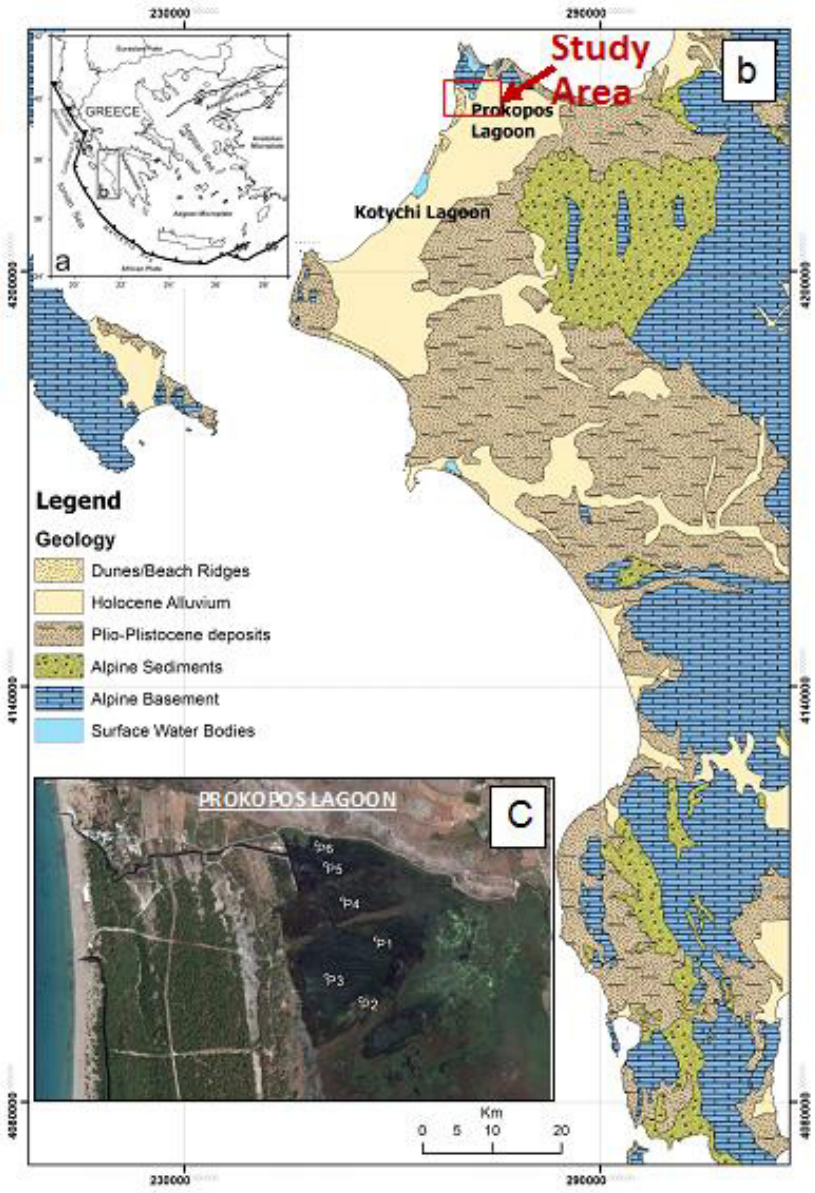

FIGURE 1

(a) General map of Greece, (b) Simplified geological map of the surrounding area of Prokopos Lagoon and western Peloponnese and (c) the sites of the coring P1, P2, P3, P4, P5 and P6 of the study area

farming in the region of Western Greece as well as for the touristic development of the study area.

MATERIALS AND METHODS

Study area. In the western Peloponnese are located the most important coastal ecosystems of Greece, the lagoons Kotychi [19], Pappas [20], Gialova [21], Kaifa [22] and Prokopos (Figure 1). The study area is the Prokopos Lagoon which is located at the prefecture of Western Greece (Figure 1). The Prokopos lagoon is situated approximately 35 km south-west of Patras in the Peloponnese, Greece. It is one of the most important ecological Greek areas, with international significance as it is listed in the Natura 2000 European Community Network with code GR232001 as a Special Protected Area (SPA) and Site of Community Importance (SCI) with code GR233007.

It is a very shallow lagoon with a maximum depth of 1 m. It is a brackish lagoon with a surface area fluctuating between 1km^2 and 4km^2 in summer and winter respectively, and is connected with the sea by a 2.5 km canal. A number of small rivers and streams supply the protected area with freshwater; and as it cannot reach the sea due to the sand dunes, it stays in the area forming a large brackish wetland consisting of lagoon and marshes (Figure 1). It has an average declared fish production of 25 t/year (50% eels, 45% mullet, 5% bass) so it is used as an extensively fish farm.

TABLE 1
Results of sedimentological analysis of the Prokopos Lagoon sediments

Depth	Clay	Silt	Sand	Mean	Sorting	Skewness	Kurtosis	Mean	Sorting	Skewness	Kurtosis	Color
(m)	%	%	%	Φ	Φ	Φ	Φ					
Gravity Core P1												
0	0.76	11.84	87.4	1.72	1.52	0.403	1,304	Medium Sand	Poorly Sorted	Very Fine Skewed	Leptokurtic	5Y 4/2
0.2	8.66	61.08	30.25	5.58	2.48	0.02	0.794	Coarse Silt	Very Poorly Sorted	Symmetrical	Platykurtic	7.5Y 4/1
0.32	4.74	45.4	49.86	4.29	2.69	0.161	0.889	Very Coarse Silt	Very Poorly Sorted	Fine Skewed	Platykurtic	7.5Y 4/2
0.46	7.83	59.33	32.84	5.43	2.75	-0.133	0.776	Coarse Silt	Very Poorly Sorted	Coarse Skewed	Platykurtic	7.5Y 4/2
Gravity Core P2												
0	4.76	51.01	44.23	4.6	2.46	0.108	0.969	Very Coarse Silt	Very Poorly Sorted	Fine Skewed	Mesokurtic	7.5Y 4/3
0.2	8.74	57.49	33.76	5.33	2.86	-0.1	0.771	Coarse Silt	Very Poorly Sorted	Symmetrical	Platykurtic	7.5Y 4/2
0.35	4.01	40.79	55.19	4.06	2.55	0.273	0.927	Very Coarse Silt	Very Poorly Sorted	Fine Skewed	Mesokurtic	7.5Y 4/2
Gravity Core P3												
0	3.26	40.64	56.1	3.98	2.32	0.343	0.995	Very Fine Sand	Very Poorly Sorted	Very Fine Skewed	Mesokurtic	7.5Y 3/1
0.15	4.48	36.99	58.54	3.7	2.81	0.391	0.827	Very Fine Sand	Very Poorly Sorted	Very Fine Skewed	Platykurtic	7.5Y 4/2
0.3	3.54	32.85	63.61	3.49	2.55	0.433	0.979	Very Fine Sand	Very Poorly Sorted	Very Fine Skewed	Mesokurtic	7.5Y 4/1
0.4	2.83	28.54	68.63	3.34	2.5	0.397	0.978	Very Fine Sand	Very Poorly Sorted	Very Fine Skewed	Mesokurtic	7.5Y 4/1
Gravity Core P4												
0	3.08	43.64	53.28	3.82	2.25	0.091	1,133	Very Fine Sand	Very Poorly Sorted	Symmetrical	Leptokurtic	7.5Y 3/2
0.15	3.98	50.3	45.72	4.82	1.94	0.377	1,009	Very Coarse Silt	Poorly Sorted	Very Fine Skewed	Mesokurtic	7.5Y 3/2
0.3	2	28.03	69.96	3.03	2.31	0.339	0.978	Very Fine Sand	Very Poorly Sorted	Very Fine Skewed	Mesokurtic	7.5Y 3/2
0.45	10.02	68.35	21.64	5.93	2.62	-0.206	1,038	Coarse Silt	Very Poorly Sorted	Coarse Skewed	Mesokurtic	5Y 5/1
0.55	11.1	58.14	30.75	5.79	2.89	-0.27	0.754	Coarse Silt	Very Poorly Sorted	Coarse Skewed	Platykurtic	2.5Y 5/2
0.7	4.78	47.77	47.44	4.48	2.69	0.09	0.869	Very Coarse Silt	Very Poorly Sorted	Symmetrical	Platykurtic	10Y 4/1
Gravity Core P5												
0	2.17	32.64	65.19	3.15	2.26	0.262	0.97	Very Fine Sand	Very Poorly Sorted	Fine Skewed	Mesokurtic	7.5Y 3/2
0.12	7.5	64.66	27.83	5.38	2.78	-0.155	0.85	Coarse Silt	Very Poorly Sorted	Coarse Skewed	Platykurtic	7.5Y 3/2
0.27	21.38	78.47	0.15	7.89	1.36	-0.002	0.959	Fine Silt	Poorly Sorted	Symmetrical	Mesokurtic	7.5Y 4/1
0.38	19.76	80.06	0.17	7.79	1.37	0.016	0.933	Fine Silt	Poorly Sorted	Symmetrical	Mesokurtic	7.5Y 4/1
0.47	17.24	82.74	0.02	7.66	1.37	-0.004	0.92	Fine Silt	Poorly Sorted	Symmetrical	Mesokurtic	10Y 4/1
0.55	19.81	79.7	0.49	7.74	1.43	0.018	0.929	Fine Silt	Poorly Sorted	Symmetrical	Mesokurtic	10Y 4/1
Gravity Core P6												
0.16	2.91	54.55	42.55	3.99	2.37	-0.065	1	Very Fine Sand	Very Poorly Sorted	Symmetrical	Mesokurtic	2.5Y 5/2
0.21	5.12	65.84	29.04	4.81	2.59	-0.058	1,008	Very Coarse Silt	Very Poorly Sorted	Symmetrical	Mesokurtic	2.5Y 5/2
0.32	3.59	36.96	59.46	3.75	2.69	0.336	0.834	Very Fine Sand	Very Poorly Sorted	Very Fine Skewed	Platykurtic	7.5Y 4/1

Sampling and grain size analysis. In order to estimate the spatial distribution of sediment characteristics six gravity corers (P1, P2, P3, P4, P5, P6) were taken and sediments samples were collected from a maximum depth of 0.70 m bellow the lagoon bottom (Figure 1). Positioning was achieved with a hand held GPS (accuracy 3 m). All samples were analyzed for their grain size distribution. Material coarser than 4 Φ was dry sieved, while fine grained material >4 Φ was analyzed using Malvern Mastersizer 2000. Moment measures were calculated using GRADISTAT V.4 [23] and based on Folk (1974) nomenclature [24], and finally grain size distribution was calculated.

Sediments colour was identified using a Minolta CM-2002 hand held spectrophotometer. To access the interrelation between the grain size analysis, the major and trace elements and the total organic carbon, Principal Components Analysis (PCA) applied in order to distinguish factors with common geochemical characteristics. Statistical analyses were performed using the SPSS 17.0 software package.

Geochemical analysis. Approximately 1g ± 0.1mg of sample was digested with 2.35 mL of 65% HNO_3 and 7 mL of HCl (aqua regia) in a microwave digestion system (Berghof speedwave MWS-3+). The temperature digestion protocol was as follows: at 145°C for 5 min, at 170°C for 10 min and at 170°C for 15 min. The resulting solutions were cooled for 30 minutes and diluted to 10 mL with distilled water. The clear solutions were analyzed on a Thermo Scientific iCAP 6000 ICP OES. The operating conditions were: nebulizer gas flow rates: 0.5 l/min; auxiliary gas flow: 0.5 l/min; plasma gas flow: 15 l/min; pump rate: 45 rpm; ICP RF power: 1100 W.

Aliquots of an ICP commercially multi-element standard solution (100 mg/L Merck) containing the analyzed elements, was used in the preparation of calibration solutions. Working standard solutions were prepared by dilution of the stock standard solutions to the desired concentration in 1% HNO_3. The ranges of the calibration curves (6 points) were selected to match the expected concentrations for all the elements of the samples analysed by ICP-OES. The correlation coefficient R^2 obtained for all cases was 0.999. The detection limits were calculated as the concentrations of an element given by the standard deviation of a series of ten consecutive measurements of blank solutions. The quality control was performed using soil samples from BIPEA's proficiency testing scheme A15 to ascertain the accuracy of the measurements.

Replicate analyses performed in order to estimate the precision of the elements determination. For all elements studied the precision was better than ±5%. The Total Organic Carbon (TOC) content was determined according to Wakley-Black titration method modified by Gaudette et al. (1974) [25].

RESULTS AND DISCUSSION

Sedimentological analysis. Based on the grain size analyses of the sediment samples, the mean size (Mz) ranged from 1.72 to 7.89 Φ, with an average value of 4.83 Φ, indicating that the lagoon's sediments are composed mainly of fine silt to medium sand (Table 1). The analysis of the moment measures showed that the sediments are characterized by poorly to very poorly sorted (σ), and range from 1.36 to 2.89 Φ, by an average value of 2.32 Φ (Table 1).

This can be interpreted by the existence of very weak currents into the lagoon and the low wave action that prevails in it. The skewness of the analyzed sediments ranged from coarse skewed to very fine skewed (Sk = –0.27 to 0.3 Φ), with an average value of 0.12 Φ (Table 1). The calculation of kurtosis displays a fluctuation from very platykurtic to leptokurtic values (KG= 0.75 to 1.30 Φ).

Inter-element geochemical association. The geochemical analysis of six gravity cores from the study area is presented in Table 2. The concentrations of the elements in the Upper Continental Crust (UCC) and the average shale's composition are also reported. The mean values of Zn, Cu, Pb, Cr and V are bellow than the average shale values reported by Turekian and Wedepohl (1961) (Table 2) [26]. The Ni and Cd average values are above of that reported for shale's by Turekian and Wedepohl (1961) [26]. The Fe_2O_3, Al_2O_3, Na_2O, K_2O, MgO and MnO are depleted, while CaO and P_2O_5 are enriched relative to the shale values reported by Turekian and Wedepohl (1961) [26].

TOC profiles of the sediments analyzed showing variation ranging from 0.00% to 9.49%. Elevated TOC values are observed at P3, P4 and P5 core locations for the surface sediment samples (Table 2). TOC is related to the primary biological production and represents that the biological fraction controlled by precipitation and temperature [27, 28]. By contrast, the Al_2O_3, K_2O and Fe_2O_3, commonly associate with the detrital fraction of the sediments and their distribution controlled by weathering, runoff, and erosion within the catchment, representing the terrigenous input of the surrounding lagoon area [29, 30]. The clay fraction of the sediments showing a tendency to increase with depth in cores P4 and P5 indicating the input of fine grain materials during the past.

A model of tree factors accounts for 83.77% of the total variance (Table 3). Factor 1 (53.87%) can be clearly identified as the 'terrigenous aluminosilicates' factor, showing high loadings for Al, Fe, K, V, Cr, Ni, Cu and Zn (Table 3). Most of the heavy metals are mainly represented in this factor, identifying their primarily detrital origin. Aluminosilicates are concentrated in the silt and clay fraction, which shows positive loading in Factor 1. Factor 1 is negatively loaded in Ca and the sand fraction, implying its antipathetic relation to autochthonous biogenic carbonates, which are coarse-grained. TOC, P_2O_5, Na, Mg, Cu and Pb are loaded in Factor 2 (20.13%). Factor 2 corresponding to the 20.13% of the total variance (Table 3), thus represents the organic fraction of the sediments which scavenge effectively some metals, eventually in the form of sulfides [27, 31]. The presence of Cu and Pb in factor 2 indicating that TOC is a good carrier, for both elements, in the analyzed samples. In addition Na and Mg related with salinity and authigenic input [32, 33]. Factor 3 (9.77%) is positively loaded in Mn, Fe, and Cd representing the hydroxides and/or oxides group (Table 3). The presence of Fe and Cd in this factor explained both their terrigenous origin and their association with the Mn-oxyhydroxides phases [34, 35].

Sediment quality assessment. In order to assess metals background enrichments or depletions

TABLE 2
Geochemical analysis of the Prokopos Lagoon sediments. Upper Continental Crust (UCC) and Shales values are also reported

Elements	Al_2O_3	CaO	Fe_2O_3	K_2O	MgO	MnO	Na_2O	P_2O_5	TOC	Cd	Cr	Cu	Ni	Pb	V	Zn
Units	%	%	%	%	%	%	%	%	%	mg/kg	mg/kg	mg/kg	mg/kg	mg/kg	mg/kg	mg/kg
Detection limit	0.047	0.011	0.005	0.12	0.001	0.001	0.214	0.018	-	0.001	0.006	0.006	0.001	0.005	0.005	0.001
Depth(m)																
Gravity Core P1																
0	4.51	16.93	1.86	0.39	1.84	0.05	0.88	0.83	-	0.37	40.6	19.97	50.72	19.41	23.34	32.31
0.2	6.06	10.75	3.77	0.49	1.33	0.08	0.38	0.16	4.51	0.72	75.92	21.31	103.71	19.72	36.11	40.5
0.32	3.05	19.27	2.56	0.33	1.2	0.13	0.29	0.13	4.33	0.5	47.26	11.48	64.46	9.13	20.16	25.35
0.45	5	7.27	3.74	0.78	1.47	0.07	0.37	0.12	2.74	0.71	87.91	23.79	117.17	12.97	42.02	47.1
Gravity Core P2																
0	3.85	7.06	2.66	0.47	1.57	0.04	0.99	0.65	-	0.52	55.43	26.4	70.01	20.16	30.26	40.42
0.2	5.18	8.17	4.3	0.57	1.39	0.09	0.46	0.16	3.69	0.82	95.06	24.98	129.21	14.22	43.03	47.34
0.35	2.35	18.59	2.2	0.33	1.08	0.1	0.35	0.1	3.48	0.43	42.58	10.63	57.62	4.86	19.16	22.2
0.53	3.82	15.85	2.68	0.51	1.12	0.09	0.38	0.12	3.36	0.52	50.84	12.66	71.23	9.49	30.01	26.73
Gravity Core P3																
0	4.1	4.22	2.69	0.54	1.34	0.03	1.04	0.74	7.96	0.5	53.23	19.5	67.54	19.68	25.11	41.06
0.15	4.57	10.2	3.43	0.45	1.28	0.08	0.55	0.18	3.65	0.62	62.6	17.35	89.73	16.03	29.38	38.13
0.3	2.26	16.97	1.78	0.25	0.86	0.08	0.25	0.09	2.56	0.32	32.14	6.44	45.88	5.39	13.42	17.67
0.4	3.88	14.95	1.99	0.35	1.06	0.07	0.39	0.11	3.11	0.36	35.61	10.85	54.46	11.48	23.93	22.9
Gravity Core P4																
0	2.65	9.03	2.23	0.5	1.41	0.03	1.26	0.49	8.23	0.42	45.91	22.61	55.39	16.93	21.57	30.57
0.15	4.11	7.16	4.08	0.63	1.38	0.08	0.94	0.2	-	0.77	72.41	21.21	96.39	17.56	32.17	42.7
0.3	4.96	13.68	3.46	0.59	1.32	0.08	0.67	0.17	6.48	0.64	62.64	14.42	73.75	10.22	30.64	32.59
0.45	4.17	13.45	1.82	0.49	1.17	0.06	0.38	0.08	2.85	0.27	47.66	11.25	58.81	13.09	20.43	26.45
0.55	6.71	8.21	4.48	0.8	1.42	0.06	0.45	0.1	3.85	0.86	83.89	21.73	135.12	14.6	43.43	43.16
0.7	7.81	13.88	2.91	0.51	1.32	0.09	0.55	0.13	4.36	0.49	49.7	15.26	75.8	22.18	32.54	30.4
Gravity Core P5																
0	3.6	7.8	1.95	0.59	1.47	0.03	1.78	0.56	9.49	0.37	43.32	23.5	48.8	17.27	23.64	30.99
0.2	7.4	1.31	2.93	0.73	1.24	0.01	0.58	0.09	3.78	0.44	71.78	20.28	113.39	21.99	44.65	48.02
0.35	6.32	0.22	3.64	1.01	1.44	0.02	0.44	0.06	2.33	0.49	115.48	24.32	123.68	16.81	60.52	52.53
0.45	4.17	13.45	1.82	0.49	1.17	0.06	0.38	0.08	n.a	0.27	47.66	11.25	58.81	13.09	20.43	26.45
0.55	6.76	0.23	4.02	1.05	1.57	0.02	0.51	0.09	2.36	0.69	117.97	27.92	162.08	20.39	55.33	60.22
Gravity Core P6																
0	3.43	17.35	1.19	0.33	1.99	0.03	1.35	0.38	-	0.26	22.2	12.69	31.25	16.3	14.62	23.5
0.16	3.29	25.23	1.12	0.22	1.26	0.06	0.52	0.13	4.44	0.21	17.88	7.28	27.59	11.23	10.84	14.87
0.25	2.83	23.05	1.61	0.3	0.98	0.06	0.42	0.08	3.15	0.27	27.69	7.18	41.36	7.16	14.08	15.9
0.32	4.04	12	2.74	0.54	1.15	0.06	0.44	0.12	3.85	0.51	52.99	13.21	85.17	11.23	28.87	34.08
Average	4.48	11.71	2.73	0.53	1.33	0.06	0.63	0.23	3.64	0.5	57.72	17.02	78.12	14.54	29.25	33.86
Min	2.26	0.22	1.12	0.22	0.86	0.01	0.25	0.06	2.33	0.21	17.88	6.44	27.59	4.86	10.84	14.87
Max	7.81	25.23	4.48	1.05	1.99	0.13	1.78	0.83	9.49	0.86	117.97	27.92	162.08	22.18	60.52	60.22
UCC[1]	15.2	4.2	5.00[a]	3.4	2.2	0.08[b]	3.9	-	-	0.098	35	25	20	20	60	71
Shales[2]	15.11	3.09	6.75	3.2	2.49	0.11	1.29	0.16	-	0.3	90	45	68	20	130	95

1. UCC: [52]
2. Shales: [26]. The Al_2O_3, CaO, Fe_2O_3, K_2O, MgO, MnO, Na_2O and P_2O_5 concentrations calculated using the appropriate molar ratio
a: Calculated after the results given by [52] for Fe 3.50%
b: Calculated after the results given by [52] for Mn 600 ppm
n.a.: Not analyzed
-: Not reported

in the Prokopos Lagoon sediments, we employ three geochemical indices, the enrichment factor, the contamination factor and the index of geo-accumulation. However, other techniques and heavy metal pollution indices can be applied in order to assess the quality of soils and fresh waters [36, 37].

Enrichment Factor (EF). The calculation of the EF values contacted using the following equation 1 [1]:

$$EF = (C_{sample} / C_{Al\ sample}) / (C_{standard} / C_{Al\ standard}) \quad (1)$$

where C_{sample} is the concentration of the element and $C_{Al\ sample}$ is the concentration of Al in the sample. The Al normalization is utilized because concentrations of most elements show correlation with Al_2O_3. The selected reference sample is usually an average crust or a local background sample [38, 39, 40]. Average shale values are used as the standard in our study [26].

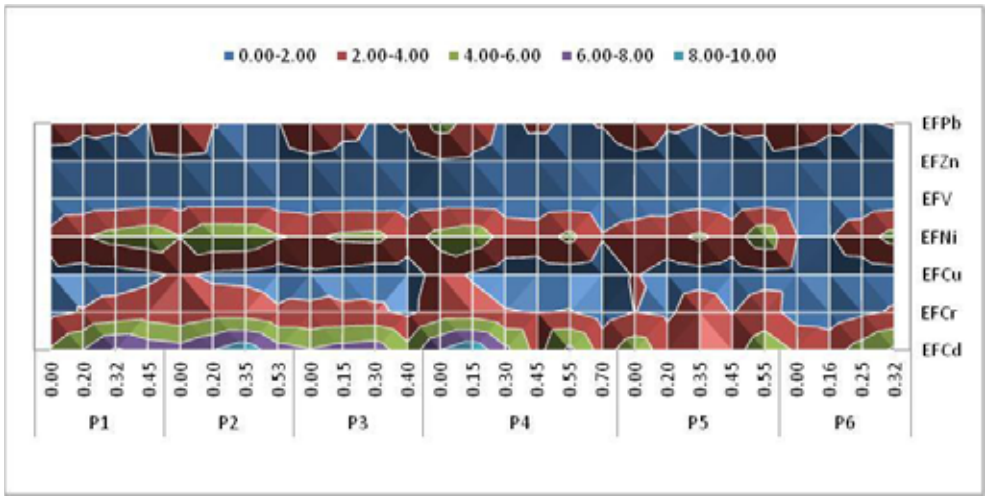

FIGURE 2
Enrichment Factors (EF) calculated for Zn, V, Pb, Ni, Cu, Cr and Cd in the Prokopos lagoon sediments

TABLE 3
Factor loadings and communalities of the PCA applied for all variables in the Prokopos lagoon sediments

n=27	F1 (53.87%)	F2 (20.13%)	F3 (9.77%)	Communality
K_2O	0.932	-	-	0.883
CaO	-0.849	-0.333	-	0.840
Na_2O	-	0.884	-0.221	0.834
MgO	0.503	0.677	-	0.718
Al_2O_3	0.769	-	-	0.599
P_2O_5	-0.175	0.903	-	0.850
Fe_2O_3	0.828	-	0.511	0.950
MnO	-0.414	-0.478	0.673	0.853
TOC	-0.180	0.304	-0.172	0.154
V	0.967	-	-	0.941
Cr	0.964	-	0.143	0.957
Zn	0.951	0.212	0.117	0.962
Ni	0.944	-0.143	0.232	0.966
Cu	0.800	0.529	-	0.924
Cd	0.690	-	0.656	0.907
Pb	0.587	0.596	-0.127	0.717
Clay	0.824	-0.373	-0.299	0.907
Mz	0.803	-0.460	-0.322	0.960
Silt	0.665	-0.490	-0.453	0.888
Sand	-0.727	0.478	0.431	0.943

-: absolute value <0.100

According to the EF criterion the sediments for the elements Pb, Ni and Cr characterized as for moderate enrichment, while V, Zn and Cu shows depletion to mineral enrichment. In the case of Cd, sediments are showing significant enrichment in the P1, P2 and P4 sampling sites, especially for the 0.15 m, 0.32 m and 0.35 m sediment horizons (Figure 2). The enrichment factor for the elements studied, except that of V is well above 1 (Figure 2). This is indicative of the source input of fine grain materials from the surrounding catchment area. In this case the EF>1 could be interpreted as enrichments caused by anthropogenic activities [41].

Contamination Factor (C^i_f). The C^i_f values for the Prokopos lagoon sediments were deduced from the equation 2 [42, 18]:

$$C_f^i = \overline{C_{0-1}^i} / C_n^i \quad (2)$$

Where $\overline{C_{0-1}^i}$ is the mean content of the substance i from at least 5 sample sites, and C_n^i is the pre-industrial reference level for the substance. The pre-industrial reference level (Table 4) determined from various European and American lakes is given by Håkanson (1980) [42].

The contamination factor of Cd, Cr, Cu, Pb and Zn calculated for the surface horizon (0.00 m) and the deep sediment layer (0.45 m) is below than 1 (C^i_f<1; Figure 3) indicating a low contamination [42]. The elements Zn, Cu and Pb are enriched in the surface sediment horizon in comparison to the deep sediment layers. By contrast Cd and Cr shows depletion to the surface samples, while they are enriched in the deep horizon (Figure 3).

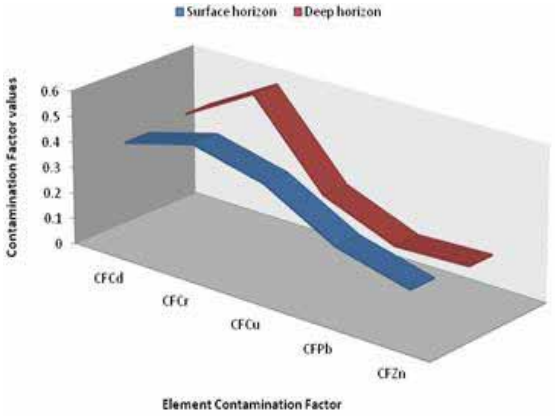

FIGURE 3
Element Contamination Factor (CF) for Cd, Cr, Cu, Pb and Zn in the sediments at Prokopos lagoon

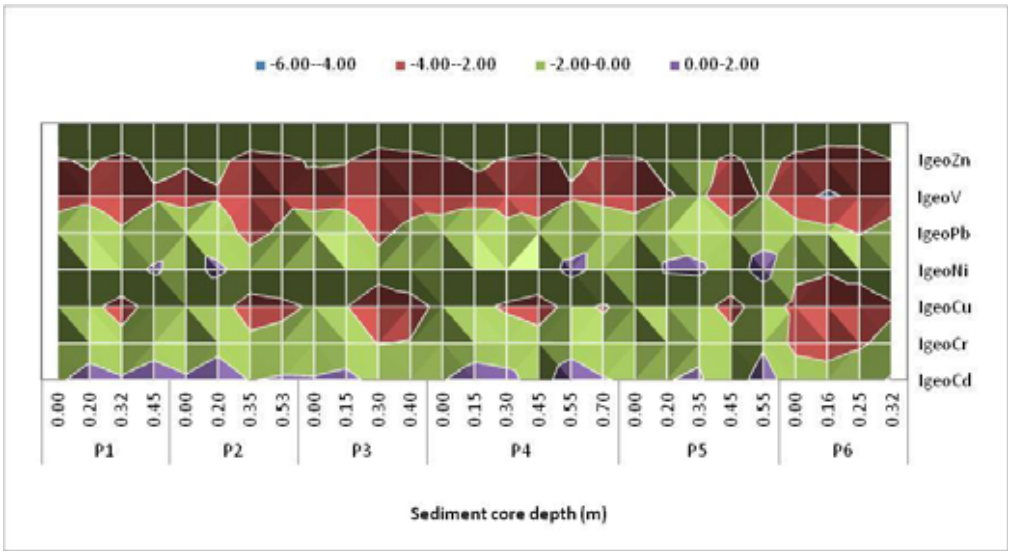

FIGURE 4
Index of geo-accumulation (I_{geo}) for Zn, v, Pb, Ni, Cu, Cr and Cd calculated for the Prokopos lagoon sediments

TABLE 4
Comparative data of Prokopos lagoon sediments with other areas in Greece. UCC, average Shales, Pre-industrial reference levels, Threshold Effect Level (TEL) values and Toxicity Screening Values (TSVs) for metals are also reported

Element	Fe_2O_3	MnO	Fe	Mn	Zn	Cu	Pb	Ni	Cr	V	Cd	Reference
Unit	%	%	%	mg/kg	mg/kg	mg/kg	mg/kg	mg/kg	mg/kg	mg/kg	mg/kg	
Prokopos lagoon, mean	2.73	0.06	1.91*	464.70*	33.86	17.02	14.54	78.12	57.72	29.25	0.5	This study
Prokopos lagoon, range	1.12-4.48	0.01-0.13	0.78-3.13*	77.45-1006.85*	14.87-60.22	6.44-27.92	4.86-22.18	27.59-162.08	17.88-117.97	10.84-60.52	0.21-0.86	This study
Messolonghi lagoon	3.37	0.08*	2.36*	630	60	20	16	84	101	75	-	[33]
Koumoundourou lake	0.83	0.02*	0.58*	155	83	21	53	28	58	23	-	[49]
Aetoliko lagoon	5.96*	0.11*	4.17	837	122.2	88	-	75.6	140	-	-	[53]
Kleisova lagoon	2.34*	0.07*	1.64	562	29	13	-	62	-	-	-	[35]
Rhodia lagoon	4.04*	0.11*	2.83	867	72	37	36	124	231	112	-	[48]
Tsoukalio lagoon	4.52*	0.15*	3.16	1191	76	31	26	131	274	108	-	[48]
Logarou lagoon	6.78*	0.12*	4.74	922	105	44	25	221	302	153	-	[48]
Tsopeli lagoon	5.69*	0.09*	3.98	665	100	48	26	168	295	129	-	[48]
UCC	5.00*	0.08*	3.5	600	71	25	20	20	35	60	0.098	[52]
Shales	6.75*	0.11*	4.72	850	95	45	20	68	90	130	0.3	[26]
Threshold Effect Level (TEL) in sediment quality guidelines for metals	-	-	-	-	123	35.7	35	18	37.3	-	0.6	[51]
Pre-industrial reference level	-	-	-	-	175	50	70		90	-	1	[42]
Toxic-response factor	-	-	-	-	1	5	5		2	-	30	[42]
Toxicity Screening Values (TSVs) for Freshwater sediments	-	-	-	-	124	25.2	35.3	18.7	20.2	-	0.991	[50]
Toxicity Screening Values (TSVs) for Marine or Estuarine sediments	-	-	-	-	142	28.7	41.3	19.5	25	-	1.31	[50]

*: Calculated concentrations using the appropriate molar ratio.
-: not reported.

Index of geo-accumulation (I_{geo}). The I_{geo} calculated using the following equation 3 [43, 18]:

$$I_{geo} = \log_2 [C_n / (1{,}5\ B_n)], \quad (3)$$

where C_n is the measured concentration in the sediment for the metal n, B_n is the background value for the metal n and the factor 1.5 is used because of possible variations of the background data due to lithological variations. However, several researchers

have used the previous expression using regional backgrounds and on the less than 63–65 μm sediment fraction [44, 45].

In this study, I_{geo} has been calculated using global average shale data from Turekian and Wedepohl (1961) [26], because they refer to the bulk concentrations and are naturally very rich in fine grain sizes [46, 47]. In addition we do not establish a local baseline value because pollution effects may extend to a considerable variation in depth, while the selection of the low concentration samples for baseline averaging is best done by inspection of the metal trends in the lower core.

In respect to the geo-accumulation index calculated the I_{geo} values are ≤0 for the majority of the samples analyzed, showing unpolluted features for the Prokopos lagoon sediments. However, the Igeo values for Cd are indicative of the class 1 Müller (1979) [43], ($0<I_{geo}\leq1$), showing unpolluted to moderately polluted features in the subsurface sediment horizons in sampling sites P1, P2, P3 and P4. In addition, the deep horizon at the P4 and P5 sampling sites shows high loadings with respect to Cd concentration (Figure 4). The Ni shows unpolluted to moderately polluted features in P1, P2, P4 and P5 sampling location especially in the subsurface and deep sediment horizons (Figure 4). The most affected samples are of the P1, P2, P3, P4 and P5 sampling sites with respect to the Cd and Ni concentrations, while P6 sampling site shows unpolluted features with respect to the I_{geo} values calculated for the Zn, V, Pb, Ni, Cu, Cr and Cd.

The geochemical evaluation of the Prokopos lagoon sediments shows the same features in comparison to other studies in Greece (Table 4). The contamination factor calculated for Cd, Cr, Cu, Pb and Zn in the sediments collected from the Prokopos lagoon area, are comparable with that reported for the Messolonghi, Rodia, Tsoukalio, Logarou, Tsopeli lagoons, and Koumoundourou Lake sediments in Greece [48, 49, 33]. In addition the Zn, Cd, Cu and Pb average values in the Prokopos lagoon sediments are below the Toxicity Screening Values (TSVs) reported by McDonald and Ingersoll (2010) [50], while Cr and Ni exceed the TSVs concentrations in a factor about three. The same geochemical patterns are observed for Zn, Cd, Cu, Pb, Cr and Ni using the Threshold Effect Level (TEL) in sediment quality guidelines for metals reported by Burton (2002) [51] (Table 4).

CONCLUSIONS

The Prokopos lagoon sediments are composed of fine silt to medium sand with the mean size (Mz) ranges from 1.72 Φ to 7.89 Φ. They are poorly to very poorly sorted with an σ average value of 2.32 Φ, due to the weak currents and the low wave action in the lagoon. The sediments raging from coarse skewed to very fine skewed (Sk = –0.27 Φ to 0.3 Φ), while the kurtosis varied from 0.75 Φ to 1.30 Φ indicating a very platykurtic to leptokurtic character. The Al_2O_3, K_2O, Fe_2O_3, V, Cr, Ni, Cu, Zn associate with the detrital fraction of the sediments. The Cu and Pb relation with the organic fraction indicates that TOC is a good carrier for both elements in the Prokopos lagoon sediments. By contrast, Na and Mg concentrations are related to salinity and authigenic input following the water evaporation-precipitation cycles due to the regional climatic conditions. The sediment quality evaluation with respect to the EF values indicate that the elements Pb, Ni and Cr are moderate enriched and V, Zn and Cu are depleted. An exception for Cd occurs showing a significant enrichment in the P1, P2 and P4 sampling sites. However, Zn, Cu and Pb are enriched in the surface sediment horizon in comparison to the deep sediment layers. By contrast Cd and Cr show depletion to the surface and enrichment in the deep sediments layers using the CF criterion. The I_{geo} values calculated for Cd are $0<I_{geo}\leq1$, showing unpolluted to moderately polluted features in the P1, P2, P3, P4 and P5 sampling sites. The P6 sampling site shows unpolluted features with respect to the I_{geo} values calculated for the Zn, V, Pb, Ni, Cu, Cr and Cd. The concentrations of Cr and Ni in the Prokopos lagoon sediments are above than the TSVs and TEL values, while Zn, Cd, Cu and Pb average values are depleted compared to the TSVs and TEL values according to the sediment quality guidelines for metals.

ACKNOWLEDGEMENTS

The authors would like to express their thanks to the Management Body of Kotychi - Strofylia National Park for the permission of sampling and the field campaign.

REFERENCES

[1] Reimann, C. and de Caritat, P. (2005) Distinguishing between natural and anthropogenic sources for elements in the environment: Regional geochemical surveys versus enrichment factors. Science of the Total Environment, 337, 91–107.

[2] Bellucci L.G., Giuliani, S., Mugnai, C., Frignani, M., Paolucci, D., Albertazzi, S. and Ruiz Fernandez, A.C. (2010) Anthropogenic metal delivery in sediments of Porto Marghera and Venice lagoon (Italy). Soil Sediment Contamination International Journal, 19, 42–57.

[3] Sestinova, O. and Findorakova, L. (2017). Assesment of eastern Slovakia sediments genotoxicity and phytotoxicity using screening tests: Chromotests and phytotoxkit. Fresen. Environ. Bull., 26, 2454-2462.

[4] Zafiri, C., Marazioti, C.E., Kornaros, M., Angelopoulos, K. and Lyberatos, G. (2009). The deterioration of the environmental state of the shallow Koutavos lagoon in Kefalonia, Greece. Fresen. Environ. Bull., 18, 935-947.
[5] Duck, R. and Silva, J.F. (2012) Coastal lagoons and their evolution: A hydromorphological perspective. Estuarine, Coastal and Shelf Science, 110, 2-14.
[6] Wu, Z., Geng, J. and Huang, L. (2015). Heavy metal contamination in sediments and mangroves from Maowei gulf, south China. Fresen. Environ. Bull., 24, 1091-1097.
[7] Eken, D.M. and Akman, B. (2017). Evaluation of pollution from rivers in northeastern Mediterranean region: Heavy metals. Fresen. Environ. Bull., 26, 4845-4850.
[8] Young, S.M., Pitawala, A. and Ishiga, H. (2013) Geochemical characteristics of stream sediments, sediment fractions, soils, and basement rocks from the Mahaweli river and its catchment, Sri Lanka. Chemie der Erde-Geochemistry, 73, 357– 371.
[9] Jirsa, F., Gruber, M., Stojanovic, A., Odour Omondi. S., Mader, D., Körner, W. and Schagerl, M. (2013) Major and trace element geochemistry of Lake Bogoria and Lake Nakuru, Kenya, during extreme draught. Chemie der Erde-Geochemistry, 73, 275– 282.
[10] Davison, W. (1993) Iron and manganese in lakes. Earth-Science Reviews, 34, 119–163.
[11] Stumm, W. and Morgan, J.J. (1996) Aquatic Chemistry: New York, John Wiley & Sons, pp.1022.
[12] Riley, J.P. and Chester, R. (1983) Chemical Oceanography. London, Academic Press, pp. 414.
[13] Horne, A.J. and Goldman, C.R. (1994) Limnology, 2nd edition. New York: McGraw-Hill, pp. 627.
[14] Salomons, W. and Forstner, U. (1984) Metals in the hydrocycle. Springer-Verlag, Berlin-Heidelberg, pp. 349.
[15] Caeiro, S., Costa, M.H. and Ramos, T.B. (2005) Assessing heavy metal contamination in Sado estuary sediment: An index analysis approach. Ecological Indicators, 5, 151–169.
[16] Wang, L., Li, Y., Yu, L., Lv, X., Wang, X. and Feng, M. (2016). Distribution assessment and statistical analysis of sediment heavy metal pollution in the Shaying river basin, China. Fresen. Environ. Bull., 25, 2909-2918.
[17] Huang, Y., Zhang, D., Li, Y., Xu, Z., Yuan, S. and Wang, L. (2015). Heavy metals sorption on river sediments: kinetics, equilibria and relative selectivities. Fresen. Environ. Bull., 27, 2792-2799.
[18] Abrahim, G.M.S. and Parker, R.J. (2008) Assessment of heavy metal enrichment factors and the degree of contamination in marine sediments from Tamaki Estuary, Auckland, New Zealand. Environmental Monitoring and Assessment, 136, 227–238.
[19] Avramidis, P., Bouzos, D., Antoniou, V. and Kontopoulos, N. (2008) Application of grain size trend analysis and spatiotemporal changes, as a tool for lagoon management. Case study the Kotychi lagoon western Greece. Geologica Carpathica, 59, 261-268.
[20] Papatheodorou, G., Avramidis, P., Fakiris, E., Christodoulou, D. and Kontopoulos, N. (2012) Bed diversity in the shallow water environment of Pappas lagoon in Greece. International Journal of Sediment Research, 27, 1-17.
[21] Avramidis, P., Iliopoulos, G., Kontopoulos, N., Panagiotaras, D., Barouchas, P. and Nikolaou, K. (2015) Depositional environments, sediment characteristics and environmental assessment of an internationally protected shallow Mediterranean lagoon, Gialova lagoon – Navarino bay, Greece. Earth and Environmental Science Transactions of The Royal Society of Edinburgh, 105, 189-206.
[22] Christia, C., Papastergiadou, E., Papatheodorou, G., Geraga, M. and Papadakis, E. (2014) Seasonal and spatial variations of water quality, substrate and aquatic macrophytes based on side scan sonar, in an eastern Mediterranean lagoon (Kaiafas, Ionian Sea). Environmental Earth Sciences, 71, 3543–3558.
[23] Blott, S.J. and Pye, K. (2001) Gradistat: A grain size distribution and statistics package for the analysis of unconsolidated sediments. Earth Surface Processes and Landforms, 26, 1237-1248.
[24] Folk, R.I. (1974) Petrology of sedimentary rocks. Hamphill Austin Texas, pp. 182.
[25] Gaudette, H., Flight, W., Toner, L. and Folger, D. (1974) An inexpensive titration method for the determination of organic carbon in recent sediments. Journal of Sedimentary Petrology, 44, 249-253.
[26] Turekian, K.K. and Wedepohl, K.H. (1961) Distribution of the elements in some major units of the earth's crust. Geological Society of America Bulletin, 72, 175-192.
[27] Calvert, S.E. and Pedersen, T.F. (1993) Geochemistry of recent oxic and anoxic marine sediments: Implications for the geological record. Marine Geology, 113, 67-88.
[28] Sampei, Y., Matsumoto, E., Tokuoka, T. and Inoue, D. (1997) Changes in accumulation rate of organic carbon during the last 8000 years in sediments of Nakaumi Lagoon, Japan. Marine Chemistry, 58, 39–50.
[29] Mügler, I., Gleixner, G., Günther, F., Mäusbacher, R., Daut, G., Schütt, B., Berking, J., Schwalb, A., Schwark, L., Xu, B., Yao, T.,

Zhu, L. and Yi, C. (2010) A multi-proxy approach to reconstruct hydrological changes and Holocene climate development of Nam Co, Central Tibet. Journal of Paleolimnology, 43, 625-648.

[30] Haenssler, E., Nadeau, M.J., Vött, A. and Unkel, I. (2012) Natural and human induced environmental changes preserved in a Holocene sediment sequence from the Etoliko Lagoon, Greece: New evidence from geochemical proxies. Quaternary International, 308–309, 89–104.

[31] Horowitz, A.J. (1991) A primer on sediment-trace element chemistry, 2nd ed., Lewis Publishing Company, Chelsea, Michigan, pp. 136.

[32] Parker, A.G., Goudie, A.S., Stokes, S., White, K., Hodson, M.J., Manning, M. and Kennet, D. (2006) A record of Holocene climate change from lake geochemical analyses in southeastern Arabia. Quaternary Research, 66, 465–476.

[33] Karageorgis, A.P., Sioulas, A., Krasakopoulou, E., Anagnostou, C.L., Hatiris, G.A., Kyriakidou, H. and Vasilopoulos, K. (2012) Geochemistry of surface sediments and heavy metal contamination assessment: Messolonghi lagoon complex, Greece. Environmental Earth Sciences, 65, 1619–1629.

[34] Varnanas S.P., Panagiotaras D. and Wolff G.A. (2001) Biogeochemical processes at the sediment – water interface in a Northeastern Atlantic abyssal locality (Porcupine Abyssal Plain). Progress in Oceanography, 50, 223- 243.

[35] Papatheodorou, G., Hotos, G., Geraga, M., Avramidou, D. and Vorinakis, T. (2002) Heavy metal concentrations in sediments of Klisova lagoon (Southeast Mesolonghi – Aetolikon Lagoon complex), W. Greece. Fresen. Environ. Bull., 11, 951-956.

[36] Lu, S., Teng, Y., Wang, Y., Wu, J. and Wang, J. (2015) Research on the ecological risk of heavy metals in the soil around a Pb–Zn mine in the Huize County, China. Chinese Journal of Geochemistry, 34, 540–549.

[37] Rajkumar, H., Madhuri, S.R. and Naval, K. (2015) Integrated approach of heavy metal pollution indices and complexity quantification using chemometric models in the Sirsa Basin, Nalagarh valley, Himachal Pradesh, India. Chinese Journal of Geochemistry, 34, 620–633.

[38] Chatterjee, M., Silva, F.E.V., Sarkar, S.K., Sella, S.M., Bhattacharya, A., Satpathy, K.K., Prasad, M.V.R., Chakraborty, S. and Bhattacharya, B.D. (2007) Distribution and possible source of trace elements in the sediment cores of a tropical macrotidal estuary and their ecotoxicological significance. Environment International, 33, 346–356.

[39] Liu, W.H., Zhao, J.Z., Ouyang, Z.Y., Soderlund, L. and Liu, G.H. (2005) Impacts of sewage irrigation on heavy metal distribution and contamination in Beijing, China. Environment International, 31, 805–812.

[40] Blaser, P., Zimmermann, S., Luster, J. and Shotyk, W. (2000) Critical examination of trace element enrichments and depletions in soils: As, Cr, Cu, Ni, Pb, and Zn in Swiss forest soils. Science of the Total Environment, 249, 257–280.

[41] Acquavita, A., Predonzani, S., Mattassi, G., Rossin, P., Tamberlich, F., Falomo, J. and Valic, I. (2010) Heavy metal contents and distribution in coastal sediments of the gulf of Trieste (Northern Adriatic Sea, Italy). Water Air and Soil Pollution, 211, 95-111.

[42] Håkanson, L. (1980) An ecological risk index for aquatic pollution control: A sedimentological approach. Water Research, 14, 975–1001.

[43] Müller, G. (1979) Schwermetalle in den sedimenten des Rheins-Veranderungenseit 1971. Umschau 79:778-783.

[44] Subramanian, V. and Mohanachandran, G. (1990) Heavy metals distribution and enrichment in the sediments of Southern East coast of India. Marine Pollution Bulletin, 2, 324-330.

[45] Sahu, K.C. and Bhosale, U. (1991) Heavy metal pollution around the island city of Bombay, India. Part I: quantification of heavy metal pollution of aquatic sediments and recognition of environmental discriminants. Chemical Geology, 91, 263-283.

[46] Rubio, B., Nombela, M.A. and Vilas, F. (2000) Geochemistry of major and trace elements in sediments of the Ria de Vigo (NW Spain): an assessment of metal pollution. Marine Pollution Bulletin, 40, 968–980.

[47] Harikumar, P.S. and Jisha, T.S. (2010) Distribution pattern of trace metal pollutants in the sediments of an urban wetland in the southwest coast of India. International Journal of Engineering Science and Technology, 2, 840-850.

[48] Karageorgis, A.P. (2007) Geochemical study of sediments from the Amvrakikos gulf lagoon complex, Greece. Transitional Waters Bulletin, 3, 3-8.

[49] Karageorgis, A.P., Katsanevakis, S. and Kaberi, H. (2009) Use of enrichment factors for the assessment of heavy metal contamination in the sediments of Koumoundourou lake, Greece. Water Air and Soil Pollution, 204, 243-258.

[50] MacDonald, D.D. and Ingersoll, C.G. (2010) Tools for assessing contaminated sediments in freshwater, estuarine, and marine ecosystems. In Sedimentology for Aqueous Systems, Cristiano Poleto and Sussane Charlesworth Eds, pp. 205. Wiley –Blackwell, John Wiley & Sons, Ltd.

[51] Burton, Jr.G.A. (2002) Sediment quality criteria in use around the world. Limnology, 3, 65–75.

[52] Taylor, S.R. and McLennan, S.M. (1985) The Continental Crust: its Composition and Evolution. Blackwell, Oxford pp. 312.

[53] Dassenakis, M., Krasakopoulou, E. and Matzara, B. (1994) Chemical Characteristics of Aetoliko Lagoon, Greece, after an Ecological Shock. Marine Pollution Bulletin, 28, 427-433.

Received: **17.05.2017**
Accepted: **01.08.2017**

CORRESPONDING AUTHOR

Pavlos Avramidis
University of Patras, Department of Geology, 265 04 Rio-Patras, Greece

e-mail: p.avramidis@upatars.gr

© by PSP Volume 26 – No. 10/2017 pages 6104-6111 Fresenius Environmental Bulletin

A CONTRIBUTION TO CHEMICAL CONTAMINATION OF GROUNDWATER

Sonja Ketin[1,*], Predrag Dasic[2], Vera Vukanic[3],Tatjana Jaksic[4], Predrag Vasic[4]

[1]University of Novi Sad, Faculty of Technical Science, Environmental Engineering, Trg Dositeja Obradovica 6, Novi Sad, Serbia
[2] High Technical Mechanical School for Professional Studies, Radoja Krstica Street No19, 37240 Trstenic, Serbia
[3]State University of Novi Pazar, Department of Biomedical Sciences, Faculty of Biology, Vuka Karadzica bb, Novi Pazar 36300, Serbia
[4]University of Pristine, Kosovska Mitrovica, Faculty of Science and Mathematics, Kosovska Mitrovica, Lole Ribara Street No29, Kosovska Mitrovica 38220, Serbia

ABSTRACT

The paper presents chemical analysis of groundwater after sudden release of substances. Construction of monitoring was setting on 4 locations, two in the vicinity of City complex process systems. Measuring apparatuses were placed in the vicinity of complex process systems area at the depth of 50m. Result of chemical analysis presents organic substances, halogen hydrocarbon, aromatic hydrocarbon (benzene, toluene and xilene), phenol and other chemical substances. Review of chosen gas chromatograms for benzene, toluene and xylene, low-chlorate hydrocarbons, polychlorinated biphenyls (PCB) and poly aromatic hydrocarbons polycyclic aromatic hydrocarbons (PAH) was presented.

KEYWORDS:
chemical analyses, groundwater, monitoring

INTRODUCTION

Groundwater pollution is one of the most dangerous forms of contaminating the natural environment. Pollution of groundwater is very difficult or impossible to clean, especially if the contamination of organic origin. It is enough to express the fact that the pollution caused by hydrocarbons uselessness million times larger quantities of water in relation to the initial pollution. Yet the nature of the event processes, which in a certain way reduce the initial concentration of pollutants, so it comes to cleansing groundwater to some extent. The dangers of pollutants groundwater can come from various sources, ranging from industrial waste water, municipal water settlements, waste water in agriculture and other human activities that threaten surface water and water reservoirs. This paper presents the risk of pollution caused by a sudden release of hazardous and toxic pollutants in the country after the accident situations. The main concern in the protection of groundwater against pollution must have a preventive character, taking the necessary measures to prevent harmful impacts. The monitoring plan and regular analysis of the results enables timely response [1-5].

EXPERIMENTAL

Construction of monitoring was setting on 4 locations, two in the vicinity of City complex process systems. On each location four piezometers of varying depths were drilled through which underground water samples were collected for chemical analysis to determine the actual situation at this time of the pollution state of underground waters and, in future, monitor pollution emission from these industrial plants. In the first phase of monitoring, piezometers and chemical analyses were done by the Institute for Health Protection, which are taken as starting/reference parameters, called "zero analysis". These results will be presented in a separate chapter in this report and are named “zero analysis”. The second phase is anticipated to go on for the next two years. Every three months samples will be taken from the piezometers for chemical and microbiological analysis. The aim of these investigations is to determine the quality of underground waters, that is, determine the degree of pollution and potential of this locality for bioremediation, i.e. self-purification. Bioremediation processes are basically physical and chemical, chemical and microbiological-biochemical. Sorption characteristics depend on both the type and quality of the soil (content of humus, sand, clay, granulation…) and type of chemical in question. Sorbing on the land is regulated by kinetics of degradation processes.

Location number 1 is located some 100 m from the fence of the complex process systems. On location 1, 2, 3and 4 the project anticipated construction of 4 piezometers, depths: 45m, 25m, 15m and 7m. HDPE (Polyethylene High Density) pipes, 160 mm in diameter, were built in the piezometers. Around the filter part quartz granulate 1-3 mm was poured in. Above it, a clay tampon was made and the space between the pipes and walls of the hole above the clay tampon was filled with drilled material. All piezometers were washed with pure water

by a pump followed by air-lift piezometer compression until the water was completely clear. Also piezometers were secured by protective metal caps and locks (Fig1).

RESULTS AND DISCUSSION

During the last year, as measuring testing of pollutants have been observed, the concentration is still high. Spreading of the pollutants still lasts, in our opinion beside everything decreasing of concentration hydrocarbons from the crude oil and the BTEX (benzene, toluene, ethylbenzene and xylene) group you can see optimistic result. Exemption of this is high sudden jump of concentration of the toluene is last circle of sampling. Supposition is that it is the result of fresh pollution. Measuring contents of the PCB substances were under line of detection for ECD (1,2-dichlorethane). Casual appearance of PAH is expectable and their concentration is variable, what bring us the problem in sampling concentration. Appearance of chlorinated hydrocarbons is unstable intensity. For now, we do not know, how can it be possible transformation of some chlorinated hydrocarbons, because we still do not know their precursor on this location?

The results of these examinations indicate an increased organic content in the water. The concentrations of ammonia ions are increased. There is also evidence of the presence of pyralene type substances. Concentration of halogenated hydrocarbons, especially 1,2-dichlorethane are considerably high. The 45m sample showed an increased content of hydrocarbons originating from petrol. At all depths aromatic hydrocarbon (BTX) are present (Fig2). Phenol concentrations are very high, as was the ace with the previous sample. Moreover, at all depth the presence of mercury was noted.

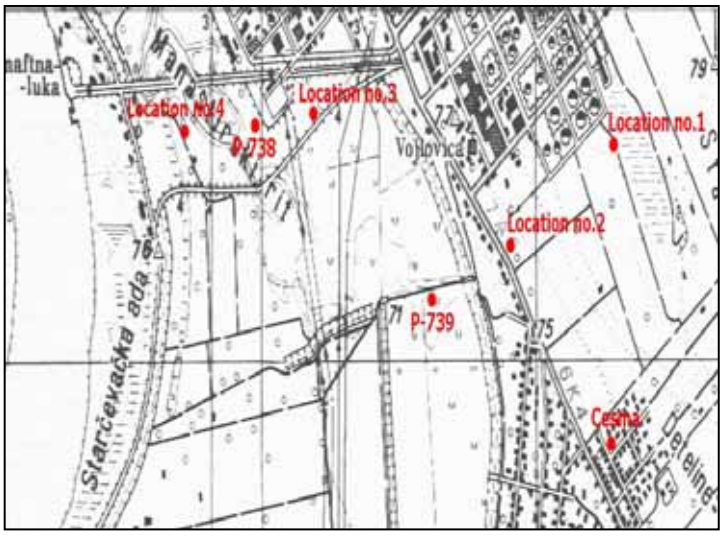

FIGURE 1
Sketch of locations

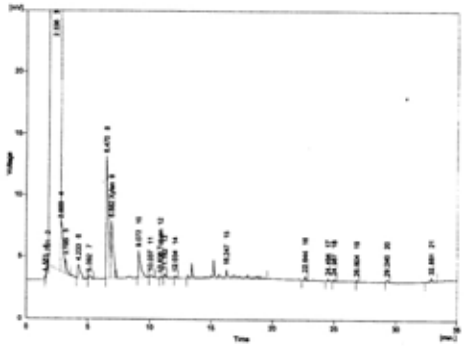

FIGURE 2
Review of chosen gas chromatograms for benzene, toluene and xylene

TABLE 1
Result of chemical analysis taken from piezometric on location No.1

Sampling point		PA-1/7		PA-1/15		PA-1/25		PA-1/45	
Temperature (air)	^{O}C	34.8	-7.0	32.7	-7.0	32.7	-7.0	32.7	-7.0
Temperature (water)	^{O}C	23.2	9.0	23.2	10.8	23.2	12.0	23.2	11.2
pH value		6.5	7.61	6.64	7.72	6.59	7.62	6.36	7.64
Turbidity (descriptive)		clear	turbid	clear	turbid	clear	turbid	clear	turbid
Turbidity	(NTU)	0	35.24	0	27.44	0	5.72	0	6.05
Oxygen Dissolved, O_2	(mg/L)	7.33	8.1	6.55	7.2	4.22	2.8	3.88	5.9
Saturated with oxygen	(%)	86.03	70.1	76.88	64.9	49.53	25.9	45.54	53.6
Redox potential	(mV)	359	475	320	469	346	456	354	459
Conductivity	(mS)	1405	1378	781	1092	522	1024	745	938
COD	(mg O_2/l)	55.1	84.0	9.18	315.0	12.46	142.8	15.68	88.2
BOD	(mg O_2/l)	5.1	9.6	< 3	< 3	< 3	45.0	< 3	24.0
TOC	(mg/l)	4.62		3.92		3.86		3.38	
$KMnO_4$ demand	(mg/l)	256	30.0	7.6	26.6	6.3	49.0	11.1	25.6
Nitrates	(mg/l)	0.14	1.55	1.75	1.07	2.09	1.31	1.16	2.32
Nitrites	(mg/l)	0.01	< 0.005	< 0.005	< 0.005	< 0.005	< 0.005	< 0.005	< 0.005
Ammonia ion	(mg/l)	1.74	1.1	0.08	1.97	0.02	1.32	0.16	1.12
Phosphates	(mg/l)	0.3	0.04	0.08	0.16	0.04	0.30	0.08	0.16
Dissolved iron	(mg/l)	8.72	8.96	<0.05	4.33	<0.05	0.56	0.28	1.57
Manganese	(mg/l)	1	0.96	< 0.02	0.27	< 0.02	0.16	< 0.02	0.72
Lead	(mg/l)	< 0.0020	< 0.0020	< 0.0020	< 0.0020	< 0.0020	0.80	< 0.0020	0.85
Total hydrocarbons	(mg/l)	0.132	< 0.005	< 0.005	< 0.005	< 0.005	< 0.005	< 0.005	< 0.486
PAH (total)	(mg/l)	< 0.005	< 0.0002	< 0.005	<0.0004	< 0.005	< 0.0002	< 0.005	0.0004
Naphthalene	(mg/l)	<0.005	< 0.002	<0.005	< 0.002	<0.005	< 0.002	<0.005	< 0.002
Fluorene	(mg/l)	< 0.005	< 0.0004	< 0.005	0.0004	< 0.005	< 0.0004	< 0.005	0.0004
Phenanthrene	(mg/l)	< 0.005	< 0.0002	< 0.005	< 0.0002	< 0.005	< 0.0002	< 0.005	< 0.0002
Fluoranthene	(mg/l)	< 0.005	< 0.0007	< 0.005	< 0.0007	< 0.005	< 0.0007	< 0.005	< 0.0007
Pyren	(mg/l)	<0.005	< 0.0008	<0.005	< 0.0008	<0.005	< 0.0008	<0.005	< 0.0008
Benzo(a)anthracene	(mg/l)	< 0.005	< 0.0005	< 0.005	< 0.0005	< 0.005	< 0.0005	< 0.005	< 0.0005
Chrysene	(mg/l)	< 0.005	< 0.0004	< 0.005	< 0.0004	< 0.005	< 0.0004	< 0.005	< 0.0004
Benzo(a)pyrene	(mg/l)	< 0.005	< 0.0009	< 0.005	< 0.0009	< 0.005	< 0.0009	< 0.005	< 0.0009
Benzene	(µg/l)	19.1	2.0	22	7.8	11	6.2	81.3	9.8
Toluene	(µg/l)	925	9.3	562	15.6	324	3.2	318	10.1
Xylene	(µg/l)	22	<1.0	13.5	<1.0	1	<1.0	30	<1.0
Ethylbenzene	(µg/l)	13.2	<1.0	4.1	<1.0	<1.0	<1.0	27.3	<1.0
1,2-dichlorbenzene	(µg/l)	11.6	<0.5	13.2	<0.5	18.4	<0.5	22.5	<0.5
1,2-dichloethane	(µg/l)	20.5	183.0	50.1	461.0	85.2	265.0	1300	407.0
Chloroform	(µg/l)	< 5	1.7	164.04	6.0	< 5	2.7	443.2	1.6
Trichloethylene	(µg/l)	< 0.1	< 0.08	14	<0.08	0.39	<0.08	20.01	<0.08
Tetrachloroethylene	(µg/l)	0.023	< 0.005	6.83	< 0.005	0.37	< 0.005	21.7	0.009
PCB	(mg/l)	< 0.001	< 1.0	< 0.001	1.9	< 0.001	< 1.0	< 0.001	< 1.0
Phenol	(mg/l)	<0.0005	125.0	<0.0005	62.0	<0.0005	8.0	<0.0005	68.0

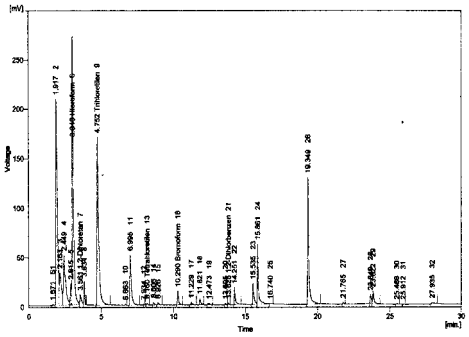

FIGURE 3
Review of chosen gas chromatogram for low-chlorinated hydrocarbons

On this location exits trend of reduce concentration of some contaminant in previous period of examination. Extremely high jump of the chlorinated derivate coincides with results of piezometric on same location. Samples at all depths are characterized by high conductivity. Mercury pollution is present but to a lesser extent than at location No.1. Organic substance strain is considerable (Table 1). Contamination by chlorinated hydrocarbon derivate is also present, as well as by phenol derivatives (Fig3). PCB presence was noted.

TABLE 2
Result of chemical analysis taken from piezometric on location No. 2

Sampling point		PA-2/7		PA-2/15		PA-2/25		PA-2/45	
Temperature (air)	^{O}C	34	-6.6	35.1	-6.5	33.8	-6.4	33.8	-6.6
Temperature (water)	^{O}C	23.2	11.3	23.2	11.7	23.2	12.1	23.2	12.5
pH value		6.83	7.58	6.68	7.92	6.73	7.63	6.54	7.56
Turbidity (descriptive)		clear	turbid	clear	turbid	clear	turbid	clear	turbid
Turbidity	(NTU)	0	1.23	0	2.19	0	9.98	0	2.66
Oxygen Dissolved, O_2	(mg/L)	8.22	5.9	7.11	4.7	4.22	5.0	2.77	7.3
Saturated with oxygen	(%)	96.48	53.8	83.45	43.2	49.53	46.4	32.51	68.4
Redox potential	(mV)	373	465	374	423	377	439	374	454
Conductivity	(mS)	3450	30.92	1800	30.18	858	30.14	683	30.51
COD	(mg O_2/l)	64.3	2570	9.18	1318	18.63	1061	14.22	1076
BOD	(mg O_2/l)	6.4	50.3	7.2	83.8	8.4	155.1	5.2	29.3
TOC	(mg/l)	3.22	8.5	3.84	17.0	2.96	20.0	3.55	7.1
$KMnO_4$ demand	(mg/l)	354	19.9	15.5	33.2	6.6	237.1	6.3	12.6
Nitrates	(mg/l)	0.33	7.75	0.93	2.14	1.92	1.97	1.38	0.18
Nitrites	(mg/l)	0.017	0.196	0.018	< 0.005	< 0.005	< 0.005	0.005	< 0.005
Ammonia ion	(mg/l)	< 0.02	< 0.02	< 0.02	0.73	0.14	1.26	0.05	1.67
Phosphates	(mg/l)	0.16	0.06	0.05	0.39	0.03	0.16	0.04	0.03
Dissolved iron	(mg/l)	0.09	< 0.05	0.16	2.20	0.09	3.49	<0.05	0.23
Manganese	(mg/l)	0.05	0.93	0.61	0.67	< 0.02	0.13	< 0.02	0.59
Lead	(mg/l)	< 0.0020	< 0.0020	< 0.0020	< 0.0020	< 0.0020	< 0.0020	< 0.0020	< 0.0020
Mercury	(µg/l)		0.15		0.26		0.16		0.22
Total hydrocarbons	(mg/l)	0.024	< 0.005	0.079	< 0.005	0.027	0.285	0.048	0.103
PAH (total)	(mg/l)	< 0.005	< 0.0002	< 0.005	< 0.0002	< 0.005	< 0.0002	< 0.005	0.0013
Naphthalene	(mg/l)	<0.005	< 0.002	<0.005	< 0.002	<0.005	< 0.002	<0.005	< 0.002
Fluorene	(mg/l)	< 0.005	< 0.0004	< 0.005	< 0.0004	< 0.005	< 0.0004	< 0.005	< 0.0004
Phenanthrene	(mg/l)	< 0.005	< 0.0004	< 0.005	< 0.0004	< 0.005	< 0.0004	< 0.005	< 0.0004
Fluoranthene	(mg/l)	< 0.005	< 0.0007	< 0.005	< 0.0007	< 0.005	< 0.0007	< 0.005	< 0.0007
Pyrene	(mg/l)	<0.005	< 0.0008	<0.005	< 0.0008	<0.005	< 0.0008	<0.005	0.0009
Benz(a)anthracene	(mg/l)	< 0.005	< 0.0005	< 0.005	< 0.0005	< 0.005	< 0.0005	< 0.005	< 0.0005
Chrysene	(mg/l)	< 0.005	< 0.0004	< 0.005	< 0.0004	< 0.005	< 0.0004	< 0.005	< 0.0004
Benzo(a)pyrene	(mg/l)	< 0.005	< 0.0009	< 0.005	< 0.0009	< 0.005	< 0.0009	< 0.005	< 0.0009
Benzene	(µg/l)	<1.0	<1.0	<1.0	<1.0	<1.0	<1.0	12.6	<1.0
Toluene	(µg/l)	<1.0	<1.0	<1.0	<1.0	<1.0	<1.0	46.8	<1.0
Xylene	(µg/l)	<1.0	<1.0	<1.0	<1.0	<1.0	<1.0	<1.0	<1.0
Ethylbenzene	(µg/l)	<1.0	<1.0	<1.0	<1.0	<1.0	<1.0	<1.0	<1.0
1,2-dichlorbenzene	(µg/l)	5.8	<0.5	10.0	<0.5	<18.2	<0.5	20.5	<0.5
1,2-dichloethane	(µg/l)	18.5	455.0	25.3	36.1	40.5	147.0	1020	580.0
Chloroform	(µg/l)	35.2	<1.0	22.5	5.0	28.5	3.9	1238.2	1.4
Trichloroethylene	(µg/l)	< 0.1	0.16	< 0.1	0.10	< 0.1	< 0.08	38.42	< 0.08
Tetrachloroethylene	(µg/l)	< 0.02	<0.005	< 0.02	<0.005	< 0.02	<0.005	37.8	<0.005
PCB	(mg/l)	<0.001	<1.0	<0.001	<1.0	<0.001	4.4	<0.001	<1.0
Phenol	(mg/l)	< 0.0005	180	< 0.0005	150.0	0.0042	130.0	< 0.0005	75.0

TABLE 3
Result of chemical analysis taken from piezometric on location No. 3

Sampling point		PA-3/7		PA-3/15		PA-3/25		PA-3/45	
Temperature (air)	^{O}C	38.2	-4.0	43.5	-4.0	32.6		32.6	
Temperature (water)	^{O}C	23.2	12.0	23.2	12.4	23.2		23.2	
pH value		6.55	7.01	6.53	7.64	6.78		6.46	
Turbidity (descriptive)		clear	turbid	clear	turbid	clear	turbid	clear	turbid
Turbidity	(NTU)	0	16.35	0	21.54	0	344	0	127
Oxygen Dissolved, O_2	(mg/L)	5.3	5.7	7.1	6.5	6.2	2.6	5.8	2.9
Saturated with oxygen	(%)	62.21	52.8	83.45	60.7	72.77	24.5	68.08	27.4
Redox potential	(mV)	387	398	368	387	350	-127	359	-71
Conductivity	(mS)	3580	27.51	3840	28.40	6040	11.25	17710	12.69
COD	(mg O_2/l)	13.8	4410	36.6	6120	13.7	1190	0	41200
BOD	(mg O_2/l)	<3	46.1	<3	146.0	<3		<3	449.2
TOC	(mg/l)	4.88	93.0	3.56	8.0	3.48	99.5	4.46	269.0
$KMnO_4$ demand	(mg/l)	28.4	33.5	32.6	249.7	19.3	246.5	35.4	150.1
Nitrates	(mg/l)	1.93	0.72	< 0.04	3.34	1.39	5.22	1.79	5.22
Nitrites	(mg/l)	0.005	< 0.005	< 0.005	< 0.005	< 0.005	< 0.005	0.019	< 0.005
Ammonia ion	(mg/l)	< 0.02	< 0.02	0.27	0.76	1.14	6.08	1.87	5.62
Phosphates	(mg/l)	0.01	0.21	0.29	0.57	0.16	0.61	0.04	0.39
Dissolved iron	(mg/l)	0.15	0.98	0.12	1.42	0.05	0.28	<0.05	1.17
Manganese	(mg/l)	0.49	< 0.02	0.1	< 0.02	0.03	< 0.02	0.05	< 0.02
Mercury			< 0.0020		< 0.0020		< 0.0020		< 0.0020
Lead	(mg/l)	< 0.0020	0.27	< 0.0020	<0.10	< 0.0020	0.18	< 0.0020	0.98
Total hydrocarbons	(mg/l)	0.021	< 0.005	0.265	0.243	0.695	0.613	0.096	1.719

Sampling point		PA-3/7		PA-3/15		PA-3/25		PA-3/45	
PAH (total)	(mg/l)	< 0.005	< 0.0002	0.07	< 0.0002	< 0.005	0.008	< 0.005	< 0.0002
Naphthalene	(mg/l)	< 0.005	< 0.002	0.05	< 0.002	< 0.005	< 0.002	< 0.005	< 0.002
Fluorine	(mg/l)	< 0.005	< 0.0004	0.02	< 0.0004	< 0.005	< 0.0004	< 0.005	< 0.0004
Phenanthrene	(mg/l)	< 0.005	< 0.0004	0.005	< 0.0004	< 0.005	< 0.0004	< 0.005	< 0.0004
Fluoranthene	(mg/l)	< 0.005	< 0.0007	< 0.005	< 0.0007	< 0.005	< 0.0007	< 0.005	< 0.0007
Pyrene	(mg/l)	< 0.005	< 0.0008	< 0.005	< 0.0008	< 0.005	0.008	< 0.005	< 0.0008
Benz(a)anthracene	(mg/l)	< 0.005	< 0.0005	< 0.005	< 0.0005	< 0.005	< 0.0005	< 0.005	< 0.0005
Chrysene	(mg/l)	< 0.005	< 0.0004	< 0.005	< 0.0004	< 0.005	< 0.0004	< 0.005	< 0.0004
Benzo(a)pyrene	(mg/l)	< 0.005	< 0.0009	< 0.005	< 0.0009	< 0.005	< 0.0009	< 0.005	< 0.0009
Benzene	(µg/l)	<1.0	<1.0	68.2	<1.0	503.3	<1.0	24.9	<1.0
Toluene	(µg/l)	53.4	<1.0	240	<1.0	1100	4.1	566	<1.0
Xylene	(µg/l)	<1.0	64.5	<1.0	92.9	<1.0	575.0	21.1	134.0
Ethylbenzene	(µg/l)	11.2	<1.0	<1.0	<1.0	<1.0	<1.0	4.8	<1.0
1,2-dichlorbenzene	(µg/l)	15. 2	<0.5	22.0	3.6	14.6	17.5	27.6	<0.5
1,2-dichloethane	(µg/l)	120	12.5	155	172.0	180	266.0	130	528.0
Chloroform	(µg/l)	672.2	4.1	270.71	71.6	237.39	624.0	58.79	110.0
Trichloroethylene	(µg/l)	24.02	0.71	7.63	24.40	15.2	8.77	4.76	3.05
Tetrachloroethylene	(µg/l)	14.2	<0.005	0.05	0.022	1.37	0.089	2.42	<0.005
PCB	(mg/l)	<0.001	2.5	<0.001	<1.0	<0.001	<1.0	<0.001	<1.0
Phenol	(mg/l)	< 0.0005	73.0	0.0035	95.0	< 0.0005	350.0	< 0.0005	60.0

TABLE 4
Result of chemical analysis taken from chosen locations in the direction of village

Sampling point		P-738		P-739		Cesma
pH value		6.6	7.85	6.87	7.54	6.69
Turbidity (descriptive)		clear	turbid	clear	turbid	clear
Turbidity	(NTU)	0	12.46	0	4.58	0
Oxygen Dissolved, O_2	(mg/L)	3.8	7.2	2.9	5.1	6.7
Saturated with oxygen	(%)	44.60		34.04		78.64
Redox potential	(mV)	367	320	358	401	404
Conductivity	(mS)	700	26.55	1329	28.67	558
COD	(mg O_2/l)	0	1238	0	819	0
BOD	(mg O_2/l)	<3	14.2	<3	9.4	<3
TOC	(mg/l)	3.22	4.0	4.55	9.5	3.88
$KMnO_4$ demand	(mg/l)	12.6	31.6	60.1	60.1	2.5
Nitrates	(mg/l)	0.12	0.66	0.2	0.89	0.42
Nitrites	(mg/l)	< 0.005	< 0.005	0.005	< 0.005	0.007
Ammonia ion	(mg/l)	1.87	6.84	0.77	4.18	0.17
Phosphates	(mg/l)	0.06	0.05	0.04	0.51	0.06
Dissolved iron	(mg/l)	23	17.25	1.03	0.82	3
Manganese	(mg/l)	0.21	0.13	0.07	0.21	0.06
Lead	(mg/l)	< 0.0020	< 0.0020	< 0.0020	< 0.0020	< 0.0020
Total hydrocarbons	(mg/l)	0.023	< 0.005	0.141	< 0.005	0.031
PAH (total)	(mg/l)	< 0.005	< 0.0002	< 0.005	< 0.0002	< 0.005
Naphthalene	(mg/l)	< 0.005	< 0.0020	< 0.005	< 0.0020	< 0.005
Fluorine	(mg/l)	< 0.005	< 0.0004	< 0.005	< 0.0004	< 0.005
Phenanthrene	(mg/l)	< 0.005	< 0.0004	< 0.005	< 0.0004	< 0.005
Fluoranthene	(mg/l)	< 0.005	< 0.0007	< 0.005	< 0.0004	< 0.005
Pyrene	(mg/l)	< 0.005	< 0.0008	< 0.005	< 0.0008	< 0.005
Benz(a)anthracene	(mg/l)	< 0.005	< 0.0005	< 0.005	< 0.0005	< 0.005
Chrysene	(mg/l)	< 0.005	< 0.0004	< 0.005	< 0.0004	< 0.005
Benzo(a)pyrene	(mg/l)	< 0.005	< 0.0009	< 0.005	< 0.0009	< 0.005
Benzene	(µg/l)	6.7	<1.0	25.2	<1.0	<1.0
Toluene	(µg/l)	<1.0	<1.0	972	<1.0	<1.0
Xylene	(µg/l)	<1.0	<1.0	18	<1.0	<1.0
Ethylbenzene	(µg/l)	<1.0	<1.0	<1.0	<1.0	<1.0
1,2-dichlorbenzene	(µg/l)	<1.0	<0.5	<1.0	<0.5	<1.0
1,2-dichloethane	(µg/l)	<1.0	1.1	36	2.2	<1.0
Chloroform	(µg/l)	<5	0.6	20.59	0.8	<5
Trichloroethylene	(µg/l)	< 0.1	0.26	< 0.1	0.41	< 0.1
Tetrachloroethylene	(µg/l)	< 0.02	0.005	0.51	0.006	< 0.02
PCB	(mg/l)	<0.001	<1.0	< 0.001	1.4	< 0.001
Phenol	(mg/l)	<0.0005	332.0	0.0028	288.0	0.0014

The examination results indicate enormous electrolytic conductivity of samples at all depths. At depths of 25 and 45 meters, an increased concentration of ammonia ions was noted, as well as the organic substance strain. The appearance of pyralene substances is worrying, although their concentrations are low. Chlorinated hydrocarbons and phenol derivatives are the main polluters at this location

(Table 2). This location also shows evidence of mercury pollution. Location No. 3 is specific for the high concentration of chlorinated derivate of hydrocarbons (Table 3). High concentration of chloroform leads us to the process of chlorinated humic substances. During the time, the third sampling is come to the increased concentration of hydrocarbons from group BTEX. High concentration is obvious.

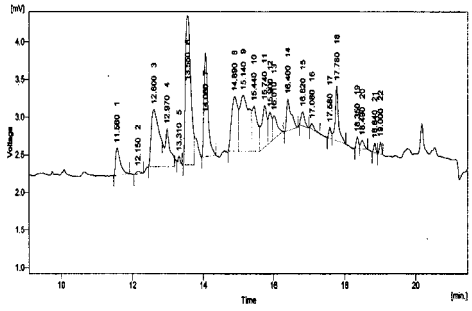

FIGURE 4
Review of chosen gas chromatogram for PCB

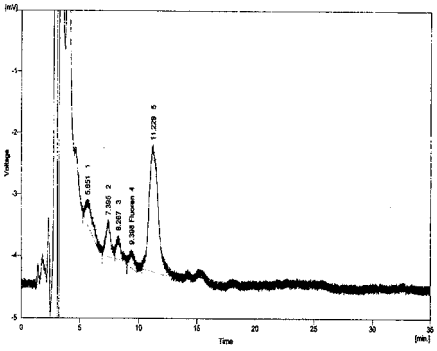

FIGURE 5
Review of chosen gas chromatogram for poly nuclear aromatic hydrocarbons PAH

Examinations shows that has been a migration of pollution towards populated areas. Increased concentrations of ammonia ions, mercury, iron… were detected. The presence of PCB, halogen hydrocarbon derivatives and phenol was observed (Fig4). The results indicate an urgent need to undertake measures of further pollution spread. It's been stressed out that near this contaminated area, in the direction of underground waters, is an inhabited area where part of the population uses well water for drinking. As far as we know, the water quality in these wells is not defined. Since the health of these people is at stake, we select 3 wells in use under. Parameters that would be determined would be same as parameters on locations 1, 2, 3, and 4. Calculated values show us that the well P-739 is most endangered object (Table 4). If we by this occasion, conductivity see as one who marks pollution, we can see similarly with examination of piezometrics. Under current circumstances it would be very brave supposition to talk about pollution migration. High conductivity, existing of total hydrocarbons source from oil, BTEX, also like chlorinated hydrocarbons, lead us to think about pollution moves to populated village(Fig5). Figure 2, 3,4 and 5 shows gas chromatograms for benzene, toluene and xylene; low-chlorinated hydrocarbons; PCB and poly nuclear aromatic hydrocarbons PAH.

From the biological indicators of the quality of surface waters, commonly examined following: microbiological composition of the water and hydrobiological water quality. A large number of underground water containing bacteriological contamination. Because of its importance to human health, the content of bacteria and other microorganisms. Water is the most important sanitary and hygienic quality indicator water. In natural and waste water can be present various microorganisms - bacteria, viruses, protozoa. Microbiological assay, however, generally include only certain indicator microorganisms that indicate the occurrence of pollution, and sometimes to its origin [6]. As an indicator microorganisms apply coliform bacteria, which, however, are not specific indicators of fecal pollution [7]. Therefore, in addition to total coliform additionally tested bacteria and thermotolerant coliforms - fecal coliform (A typical example of *Escherichia coli* - *Escherichia coli*), streptococci and enterococci and fecal origin (*Enterococcus*), as well as the sulfato-reducing clostridia (*Clostridium perfringens*). Analyzes of physic-chemical and microbiological composition of the water very useful indicators of the current status of the water body, but do not show long-term picture of the observed ecosystem. Therefore, in order to assess the long-term status of the water bodies apply different methods of hydrobiological characterization water, among which are indices of diversity, biotic indices, saprobioticke methods assess the quality of the habitat and the like [8].

CONCLUSION

We came to a conclusion that the underground water in the vicinity of main piezometers is polluted. At the complex process systems area results of these tests indicate a higher amount of organic substance in the water. The amount of reduction produce such as ammonium ion has also been increased. The amount of halogen hydrocarbon is very high as well. In a sample taken at the depth of 45m there is a high amount of hydrocarbon, originating from oil. There is aromatic hydrocarbon at all depths (benzene, toluene and xylene). The amount of phenol is high, whereas the amount of mercury is low. Tests have proven that substances

of pyralene type are also present. Samples at all depths have high specific conductivity. Results of the tests performed in the vicinity of complex process systems area shown enormous electrolytic conductivity of samples at all depths. At 25m and 45m we found a high amount of reduction produce of the ammonium ion type, as well as organic and pyralene substance load. Even though the amounts of these substances are low, these indicators are worrying. Chlorinated hydrocarbons and phenol derivatives represent the main pollutants. On the basis of the provided information, it is obvious that we are dealing with a long-term pollution of the environment. As a solution to this huge problem, a number of foreign projects have been implemented and proved that the soil pollution could be successfully dealt with. Due to the level of pollution, there is a necessity for the continual implementation of projects for the remedying of contaminated soil. Depending on the used technology, these projects contribute to the adequate reduction of pollution [9-19].

REFERENCES

[1] Ketin, S., Sacirovic, S., Plojovic, S., Skrijelj, R. and Biocanin, R. (2014). Method for comparison of the maximum range of chemical pollutation, Russian Journal of General Chemistry, 84(13), 2677-2680.

[2] Biocanin, R., Stefanov, S. and Urosevic, S. (2012). Modeling of pollutants in the air in terms of fire on dumps, Ecological Chemistry and Engineering S-chemia inzynieria ekologicznas, 19(4), 609-616.

[3] Beskoski, V.P., Gojgic-Cvijovic, G.D., Milic, J.S., Ilic, M.V., Miletic, S.B., Jovancicevic, B.S. and Vrvic, M.M. (2012). Bioremediation of soil polluted with crude oil and its derivatives: microorganisms, degradation pathways, technologies. Hem. Ind., 66(2) 275-289.

[4] Rajicevic, V., Lalevic, B., Dabic, D., Kikovic, D., Jovanovic, Lj., Niksic, M., Zastita materijala, (2007), Microorganisms in soil and water bioremediation, 48(2), 49-52

[5] Tzai-Tang, T., Chih-Ming, K., Tzung-Yuh,Y., Shu-Hao, L. and Hua-Yi., C., (2009). Remediation of fuel oil-contaminated soils by a three-stage treatment systems, Environmental Engineering science, 26(3), 651-659.

[6] U.S. EPA (1978). Bacteriological Methods in Water Quality Control Programs, Training Manual, EPA 430/1-78-014. Office of Water Program Operations, Cincinnati, OH, USA.

[7] Fewtrell, L. and Bartram, J. (2001). Water Quality; Guidelines, Standards and Health: Assessment of risk and risk management for water related infectious disease.IWA Publishing, London, UK http://www.who.int/water_sanitation_health/dwq/iwaforeword.pdf

[8] Knoben, R.A.E., Roos, C. and Van Oirschot, M.C.M. (1995).Vol3: Biological Assessment Methods for Watercourses, UN/ECE Task Force on Monitoring & Assessment Biology Assessment

[9] US EPA, (1990). Engineering Bulletin, Slurry Biodegradation, EPA, 540 2 90016.

[10] US EPA (1996). A Citizens Guide to Bioremediation, EPA, 542 F 96 007.

[11] US EPA (1998). Innovative Site Remediation Technology, Design and Application, Vol 10, l.1., Bioremediation, EPA, 542 B 97 004.

[12] US EPA (2001). A Citizens Guide to Bioremediation, EPA, 542 F 01 001.

[13] Ketin, S., Imamovic, M., Nikolic, D. and Biocanin,R. (2015). Technology for the Remediation of Soil, Bulgarian Journal of Agricultural Science, Agricultural Academy, 21(5), 935-939.

[14] Hu, Y., Dong, Z. and Liu,G.(2017). Characterization and quality of groundwater in Huaibei, China, Fresen. Environ. Bull., 26(4), 2541-2550.

[15] Duan, Z. and Fan, G. (2017). Research on the main factors of influencing the infiltration-reducing effect with cement permeating river sediment, Fresen. Environ. Bull., 26(5), 3231-3239.

[16] Ennaceur, S. (2017). Levels and distribution pattern of organ chlorine Pesticides and polychlorinated biphenyls in main edible fishes and benthic invertebrates collected from red sea in Saudi Arabia, Fresen. Environ. Bull., 26(5), 3430-3438

[17] Filiz, N. and Kucuksezgin, F. (2008). Composition and distribution of organ chlorine pesticide residues in surface sediments from Gediz and Bajircay rivers (Eastern Aegean), Fresen. Environ. Bull., 17, 744-755.

[18] Zeng, Y., Lai, Z., Yang, W. and Gu, B. (2017). Multivariate statistical analysis of heavy metals in water from the Pearl River watershed, south china, Fresen. Environ. Bull., 26(5), 3350-3357.

[19] Polat, N. and Akkan, T. (2016). Assessment of heavy metal and detergent pollution in Giresun coastal zone, Turkey, Fresen. Environ. Bull., 25, 2884-2890.

Received: **18.05.2017**
Accepted: **21.07.2017**

CORRESPONDING AUTHOR

Sonja Ketin
University of Novi Sad
Faculty of Technical Science
Environmental Engineering Department
Novi Sad 21000 – SERBIA

E-mail: ketin.sonja@gmail.com

© by PSP Volume 26 – No. 10/2017 pages 6112-6120 Fresenius Environmental Bulletin

A CALIBRATED HYDROLOGICAL MODEL FOR ALIBEYKÖY WATERSHED IN ISTANBUL, TURKEY INCORPORATING LID IMPLEMENTATION

Sezar Gulbaz[1], Cevza Melek Kazezyilmaz-Alhan[1,*], Rouhollah Nasirzadeh Dizaji[1], Mehmet Dikici[1]

[1]Istanbul University, Engineering Faculty, Civil Engineering Department, 34320 Avcılar, Istanbul, Turkey

ABSTRACT

Increase in urbanization adversely affects our water resources. Therefore, new solution techniques related to the protection of drinking watersheds should be investigated to avoid present and future problems such as floods, droughts, and pollution. In this study, a hydrological model for Alibeyköy Watershed is developed by using Environmental Protection Agency Storm Water Management Model (EPA SWMM). The model is calibrated by using the rainfall and flow data obtained from the stations in the area. Then, Low Impact Development (LID) type of storm water Best Management Practices (BMPs) is implemented into the model in areas nearby the main streams to reduce adverse impacts of urbanization such as flood in Alibeyköy Watershed. Finally, several LID types' scenarios such as bioretentions, vegetative swales, permeable pavements, and infiltration trenches are simulated to observe the influence of LID Implementation on peak flow rate causing flood.

KEYWORDS:
Best Management Practices, Low Impact Development, Flood Control, Watershed Modeling.

INTRODUCTION

Water resources, their protection and regulation are essential to meet drinking water demand and to prevent hazards such as flood events and contamination. Therefore, exploring and evaluating the results of human activities with direct influence on water resources and hazardous events are of concern for researchers in the hydrology area. Protection of both surface water and ground water for sustainable life is one of the essential and crucial topics of current and past decade. Freshwater is a fundamental and an irreplaceable resource for retaining environmental sustainability of human survival and social development [1, 2]. Supplying sufficient amount of good quality water for the entire population of the planet is the general objective that must be met. For this purpose, the hydrological, biological and chemical functions of ecosystems have to be preserved. In order to control and improve water supply and quality, the behavior of water resources system needs to be investigated.

Urbanization results in an increase in impervious surfaces areas and enhanced proportion of impervious surface areas results in shorter delay time between inception of precipitation and peak flow rate. Thus, overall hydraulic performance of a catchment basin is affected by urbanization [3]. Total storm water runoff volume rises in receiving water leading to flooding, and the degradation of instream ecosystem status [4, 5]. In addition, excessive storm water runoff affects also flooding potential of highways, parking lots and buildings. Furthermore, excess runoff accelerates pollutant transport and causes water pollution in water resources. In reaching solutions to minimize the aforementioned problems, a number of researchers have been working on monitoring and modeling studies related to the storm water runoff [6, 7]. For example, storm water control measures (SCMs) is suggested to obtain better water quality through forested watershed stream hydrograph fractions comprised of surfaces runoff, shallow interflow and groundwater surge [8]. Seveso catchment in the Lombardy Region in Italy is modelled and calibrated by using the EPA SWMM to observe the impacts of green roof implementation on peak runoff rates and runoff volumes [9].

Characteristics like area, imperviousness, slope, land cover and land use of sub-catchments are fundamental factors for controlling storm water runoff quantity and quality. According to these characteristics, different techniques can be taken into account in selecting the optimum scenario for rural and urban runoff management [10]. Recently, the cost efficiency of Low Impact Development Best Management Practices (LID-BMPs) implementation has been dramatically received much recognition as storm water management and a comprehensive land use planning technique to assist planners and decision-makers for evaluating and mitigating urban runoff impacts on hydrology and water quality and pollutant loadings to streams [11, 12, 13, 14]. This approach has been suggested as an alternative to storm water design [15], and research on individual LID practices such as green roof, permeable pavement,

infiltration trenches, bioretention cells, vegetative swales and rainwater cisterns has been gained attention [16, 17, 18, 19]. There are successful experimental studies related to hydrological performances of LID in the literature [20, 21, 22, 23, 24, 25].

The aim of this study is to investigate the effects of the LID type of BMPs implementation on the surface water quantity by a calibrated hydrological model for Alibeyköy watershed. For this purpose, first, a hydrological model for Alibeyköy watershed is developed with the EPA SWMM. Then, for calibration of the model, flow rate and rainfall data are measured by installing a flow meter and a rain gauge into the field site. Simulations are carried out first for current conditions of the watershed. Then, the simulations are repeated by increasing the impervious areas from 20% to 40%. Four types of LIDs, i.e., bioretention, permeable pavement, vegetative swales, and infiltration trench, are incorporated into the model and the possible effects of LIDs on surface runoff are observed. Thus, impacts of rapid urbanization and LID implementation as a possible solution are analyzed.

MATERIALS AND METHODS

EPA SWMM. Environmental Protection Agency Storm Water Management Model (EPA SWMM) is a hydrological simulation model for the surface runoff developing on a watershed during a storm [26, 27]. The quantity and quality of surface runoff on each subcatchment; the flow rate, the depth, and the concentration in each conduit and junction can be calculated by EPA SWMM. Input data for the watershed profile is composed of width, slope, area, and percent perviousness-imperviousness for each subcatchment; length, cross section, height, and slope for each conduit; and elevation for each junction. The outputs from the program are change of flow rate (hydrograph) and change of concentration (pollutograph) through time, while the change of the rainfall intensity through time (hyetograph) is given as input to the program. In order to calculate flow rate, EPA SWMM solves the continuity and momentum equations for flood routing. One can select kinematic, diffusion, or dynamic wave options according to the characteristics of the considered catchment. The most general form of the flood routing equations is the dynamic wave equations which describe unsteady non-uniform flow. Kinematic wave equations can be derived from the dynamic wave equations by neglecting both inertial and pressure terms in the momentum equation, whereas diffusion wave equations are obtained by ignoring only the inertial terms. In order to calculate infiltration, EPA SWMM uses three methods, namely the Green-Ampt Method, the Integrated Horton Method and the SCS Curve Number Method. Furthermore, EPA SWMM is capable of assessing the hydrological impacts of LID to storm water management systems. Several Low Impact Development (LID) types such as bioretention, infiltration trench, porous pavement, rain barrel and vegetative swale, can be modeled with EPA SWMM.

Study Area: Alibeyköy Watershed. Alibeyköy Watershed is located on the European Continental side of Istanbul in Turkey. It has a drainage area of 161 km^2 and supplies an important portion of Istanbul's drinking water. There are 10 streams which gather overland flow generated over the basin. These streams are Cebeci stream, Bogazkoy stream, Bolluca stream, Kocaman stream, Ciplak stream, Ayvali stream, Elmali stream, Gulgen stream, Malkoc stream, Ciftepinar stream. The land morphology of the great part of the watershed is in the form of sandy clay loam. The altitude of the watershed is between 30-170 m in the topographic boundaries. Alibeyköy Watershed area is composed of 23% of agricultural and pasture land, 15% of residential and industrial areas, 60% of forest and 2% of dam area. However, there is a great potential of population growth due to the new developments of infrastructures in the basin. These new infrastructures include third Bosphorus Bridge, third airport of Istanbul and finally Canal Istanbul project. Therefore, high urbanization is expected within the next 10 years and these changes will have negative effects on the ecosystem in the future, if no action is taken. In Fig. 1, the boundary of Alibeyköy Watershed and Alibeyköy Dam are shown.

Data Collection. Flow rate and rainfall data need to be measured on the watershed in order to calibrate Alibeyköy Watershed model in EPA SWMM. A rain gauge (Fig. 2 (a)) is set up on the watershed in order to measure rainfall data in terms of volume each time rainfall occurs. And, a flow meter (Fig. 2 (b)) is set up close to the downstream of the main stream in the Alibeyköy Watershed. The rainfall data is continuously collected by automatic data logger and flow rate is measured during rainfall events.

Model Development. In order to determine the input parameters for the hydrological model in EPA SWMM, topographical map of the modeled area, cross-sectional area of the main stream and soil properties of the study area are used. The watershed area is divided into 24 subcatchments by using the topographical maps of the Alibeyköy Watershed. Slope, area, and width are defined as input data for each subcatchment. Using topographical maps, main channels, which collect the surface runoff generated over the watershed, are determined and introduced into the program as conduits. Length, cross sectional area, roughness, and start-end points of conduits are defined as input data for conduits. All conduits have trapezoidal cross sections and a total number of 46 conduits are formed. Each link is connected with

junctions which are described by invert elevation and maximum depth. And 46 junctions and one outlet are defined into the Alibeyköy Watershed model.

A rain gauge is defined in the model which reads rainfall data in terms of intensity, volume, or cumulative precipitation with identified time series. Infiltration is calculated with the Green-Ampt method chosen within the program. Green-Ampt infiltration parameters, which are suction head and hydraulic conductivity, are defined according to the soil type. In Fig. 3, the hydrological model of Alibeyköy Watershed modelled by using EPA SWMM is shown.

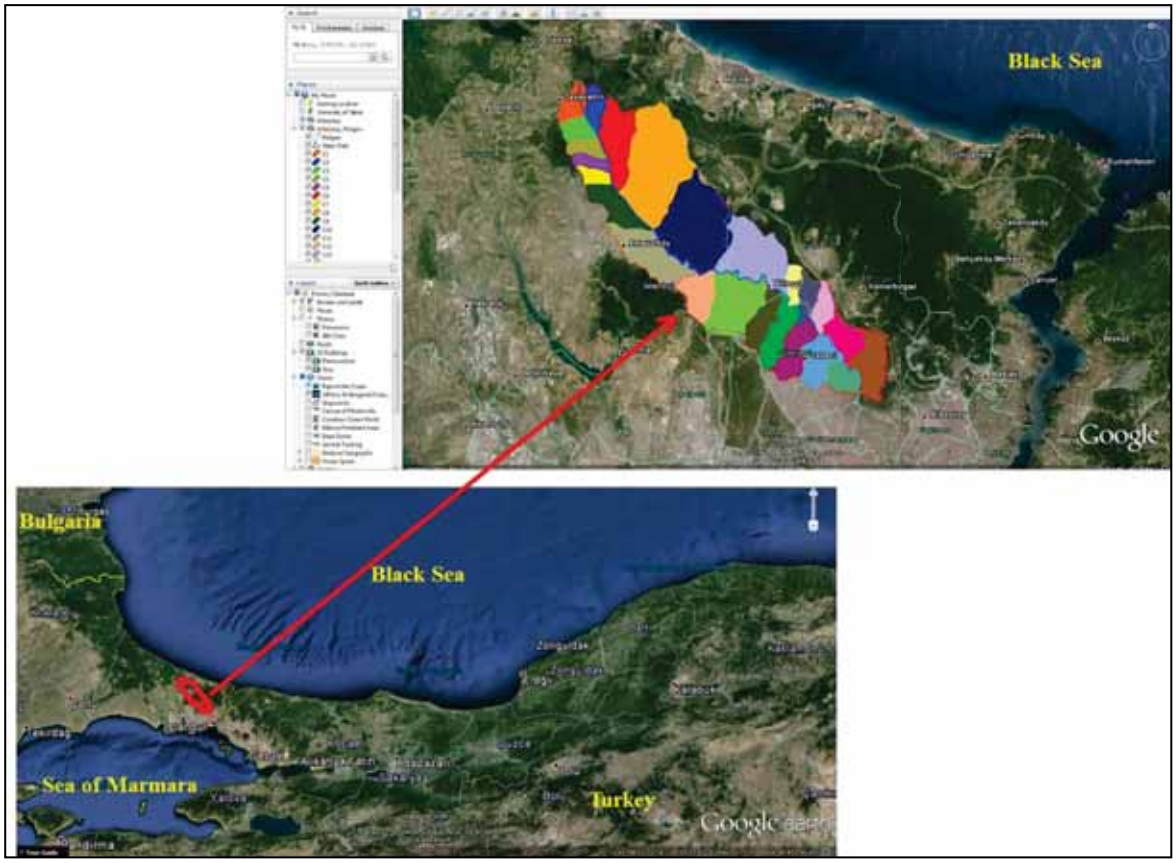

FIGURE 1
General view of Alibeyköy Watershed and subcatchments (Retrieved from Google Earth).

(a) **(b)**

FIGURE 2
General view of rain gauge (a) and flow meter (b) in Alibeyköy Watershed.

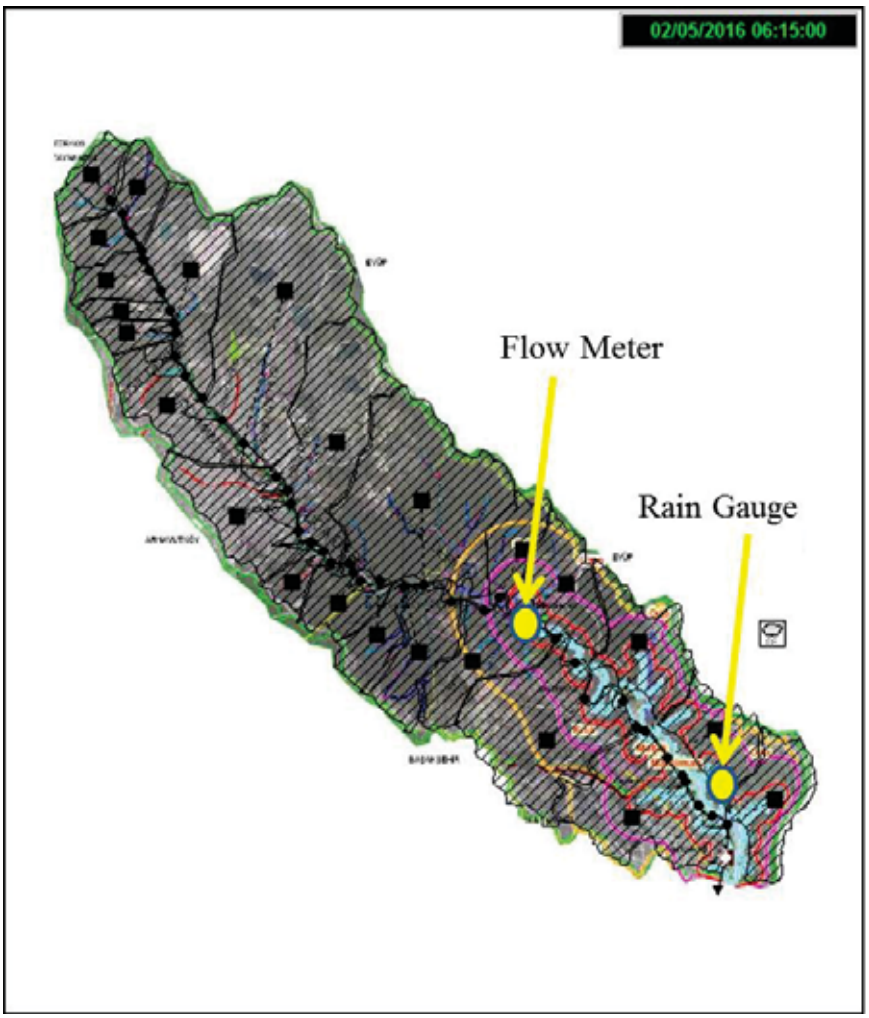

FIGURE 3
Hydrological model of Alibeyköy Watershed in EPA SWMM.

TABLE 1
Calibrated parameters for subcatchments, open channels and soil in EPA SWMM.

Water Quantity Parameters for subcatchments, open channels and soil	Type	Value
Manning's roughness coefficient for impervious area *(N)*	Asphalt	0.011
	Concrete	0.012
Manning's roughness coefficient for pervious area *(N)*	Soil	0.12
	Grass	0.27
	Woods	0.50
Depth of depression storage on impervious area *(d) (mm)*		0.09
Depth of depression storage on pervious area *(d) (mm)*		0.10
Manning's roughness coefficient for the open channel *(n)*	Concrete	0.015
	Excavated or dredged	0.04
	Natural channels	0.06
Hydraulic Conductivity *(K) (mm/hr)*		1.8

Calibration. Storm events such as rainfall and flow rate data are monitored for five months. The measured data recorded during these storm events are used to calibrate the model developed by using EPA SWMM. For the calibration of the hydrological model, Manning's roughness coefficient (*N*) for pervious and impervious area, depth of depression storage (*d*) on pervious and impervious area, Manning's roughness coefficient for conduits (*n*), and hydraulic conductivity (*K*) are selected initially according to

their typical values reported in the literature [26, 27, 28]. Then, the values of these parameters are tuned until the flow rate simulated by the model matches the measured flow rate. The final values of the calibrated parameters are listed in Table 1. During the calibration stage of the study, many trials are done manually in order to match model results with the measured data. During calibration process, we were interested in time and amount of peak flow rate and shape of flow rate curve. Simulated and measured flow rate results match with each other during rainfall event on February 05-08, 2016 as shown in Fig. 4.

Urbanization and LID Implementation Scenarios. In this part of the study, the effect of population increase on the water quantity is investigated. With the population increase, residential areas also increase which result in a rise in the impervious surfaces. Therefore, the peak of the outflow hydrograph over the catchment also increases which may cause flooding. Alibeyköy watershed area is currently composed of 23% of agricultural land, 10% of residential and industrial areas, 65% of forest and 2% of dam area. Model simulations are made for current population, which corresponds to approximately 20% of impervious area, and for estimated population, which corresponds to 40% of impervious area, and results are compared in order to examine the effect of population growth on the hydrograph. As the next step, several LID types such as retention basin (bio-retention cell), infiltration trench, vegetative swale and permeable pavement (porous pavement) are introduced into the calibrated model in order to decrease negative effects of high urbanization on the watershed. While implementing these four types of LID into the model, the relevant parameters are defined in the model and are given in Table 2. The values of these parameters are chosen by referencing EPA SWMM manual [27].

LIDs are performed on 3.7 km^2 of an area which corresponds to about 2% of the modeled watershed. The implemented LID types in the model are bioretention, vegetative swale, infiltration trench and permeable pavement and the properties of these LID types are given in Table 2. The surface layer properties are used to describe the surface properties of bioretention, vegetative swale, infiltration trench and permeable pavement; the soil layer properties are used to describe the properties of the engineered soil mixture used in bioretention and permeable pavement types of LIDs; the storage layer properties are used to define the properties of the crushed stone or gravel layer used in bioretention, infiltration trench and permeable pavement; the drain layer properties are used to describe the drain properties of bioretention, infiltration trench and permeable pavement; the pavement layer properties are used to define values for permeable pavement types of LID systems.

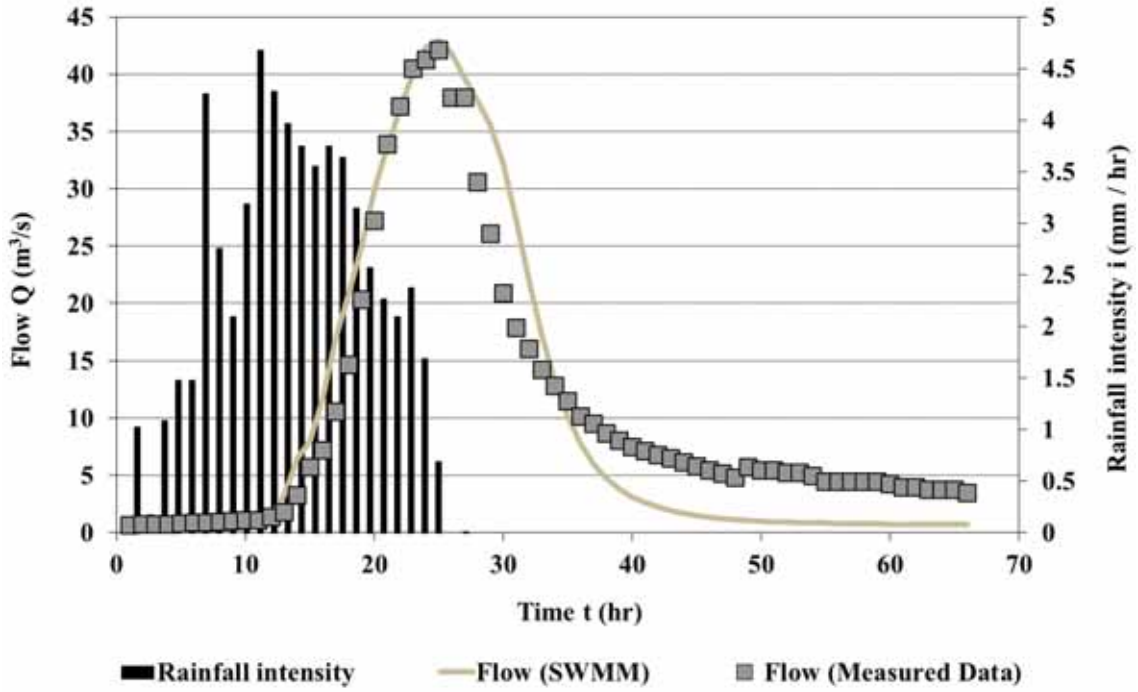

FIGURE 4
Measured and calculated flow rates during rainfall event on February 05-08, 2016 at downstream of the watershed.

TABLE 2
Properties of surface, pavement, soil and storage layers for LID implementation [27].

Layer	Parameters	LID Types			
		Vegetative Swale	Permeable Pavement	Bioretention Cell	Infiltration Trench
Surface	Bern Height (Storage Depth) (mm)	500	10	500	400
	Vegetation Volume (Fraction)	0.3	0.0	0.2	0.0
	Surface Roughness (Manning's N)	0.1	0.1	0.1	0.1
	Surface Slope (Percent)	1.0	1.0	1.0	1.0
	Swale Side Slope (run/rise)	5.0	NA	NA	NA
Soil	Thickness (mm)	NA	400	1000	NA
	Porosity (volume fraction)	NA	0.5	0.5	NA
	Field Capacity (volume fraction)	NA	0.2	0.2	NA
	Wilting Point (volume fraction)	NA	0.1	0.1	NA
	Conductivity (mm/hr)	NA	400	380	NA
	Conductivity Slope	NA	10	10	NA
	Suction Head (mm)	NA	35	19	NA
Storage	Thickness (Height) (mm)	NA	150	500	1000
	Void Ratio (voids/solids)	NA	0.75	0.75	0.75
	Seepage Rate (mm /hr)	NA	0.5	0.5	0.5
	Clogging Factor	NA	0	0	0
Drain	Flow Coefficient	NA	0	0	0
	Flow Exponent	NA	0.5	0.5	0.5
	Offset Height (mm)	NA	6	6	6
Pavement	Thickness (Height) (mm)	NA	100	NA	NA
	Void Ratio (voids/solids)	NA	0.15	NA	NA
	Impervious Surface (fraction)	NA	0	NA	NA
	Permeability (mm/hr)	NA	100	NA	NA
	Clogging Factor	NA	0	NA	NA

NA: Not Applicable

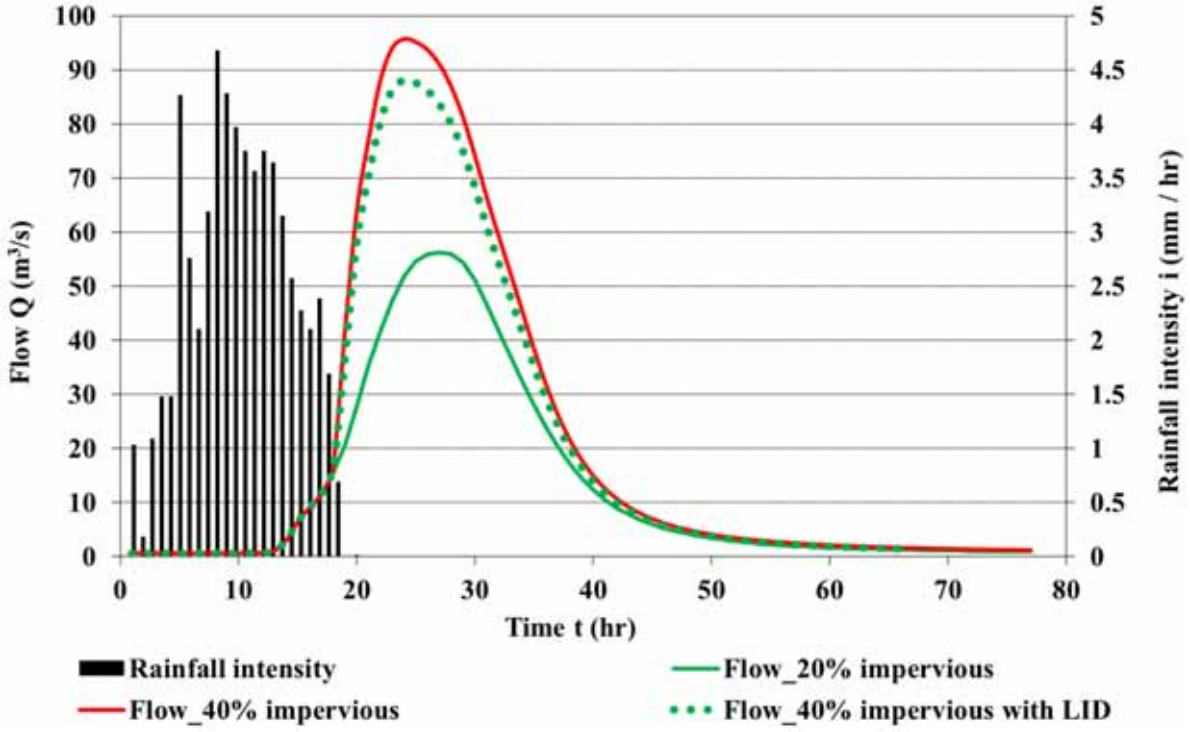

FIGURE 5
Simulated flow rate versus time at the outfall of the Alibeyköy Watershed during storm event observed between February 05-08, 2016.

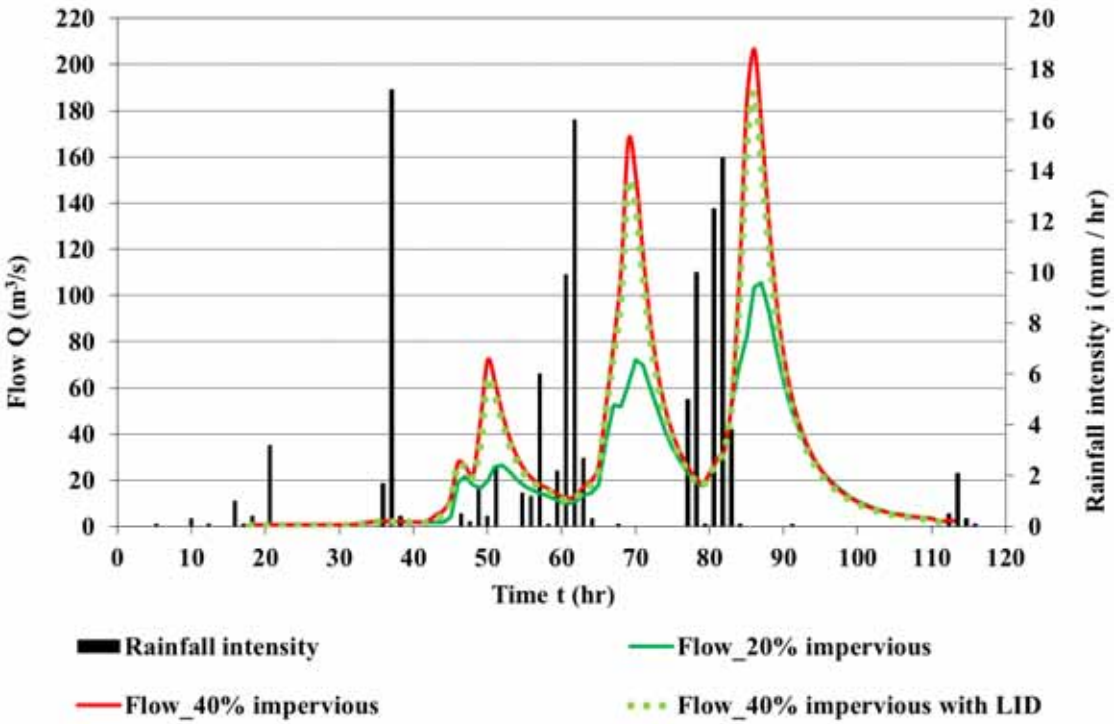

FIGURE 6
Simulated flow rate versus time at the outfall of the Alibeyköy Watershed during storm event observed between September 07-09, 2009.

TABLE 3
Peak of the hydrograph generated over Alibeyköy Watershed during rainfall events I-II.

Water Quantity	Rainfall Event I February 05-08, 2016		Rainfall Event II September 07-09, 2009	
	(m^3/s)	(%)	(m^3/s)	(%)
Peak of the hydrograph for current urbanization	56		106	
Peak of the hydrograph for projected urbanization	96		207	
Peak of the hydrograph for projected urbanization with LID	88		188	
Peak reduction after LID	8	**8.3**	19	**9.2**

RESULTS AND DISCUSSION

The simulation results are presented for the storm event observed during February 05-08, 2016 and September 07-09, 2009 to model low and high (extreme) rainfall intensity impacts, respectively. The change in surface runoff with and without LID BMP implementations are observed and compared. Effects of LID BMP implementation on runoff volume and peak flow rate are predicted.

Urbanization Effects under Typical and Extreme Storm Events. The surface runoff developed over Alibeyköy Watershed is simulated under 2 rainfall events. The first one has a low intensity measured by the rain gauge set on the field site and the second one has a high (extreme) intensity recorded at Florya Meteorological Station in Istanbul, Turkey. These rainfall events are occurred on February 05-08, 2016 and on September 07-09, 2009, respectively.

Fig. 5 shows the rainfall intensity and the corresponding flow rates at the outfall of the Alibeyköy Watershed occurred during the rainfall event on February 05-08, 2016 under current urbanization, under projected urbanization and under projected urbanization with LID implementation. Current urbanization is simulated with 20% of impervious area, and projected urbanization is simulated with 40% of impervious area. As it can be seen from this figure, the peak of the hydrograph increases from 56 m^3/s to 96 m^3/s, if the impervious area increases from 20% to 40%. After LID implementation, the peak of the hydrograph decreases from 96 m^3/s to 88 m^3/s. In other words, when 2% of LID area is considered in the watershed, the peak of the runoff generated over the catchment decreases 8.3% under the Rainfall Event I. The simulations are repeated for the storm event occurred on September 07-09, 2009 and the result is

presented in Fig. 6. As it can be seen from this figure, the peak of the hydrograph increases from 106 m^3/s to 207 m^3/s due to the urbanization. And, it decreases from 207 m^3/s to 188 m^3/s with LID implementation. In other words, when 2% of LID area is considered, the peak of the surface runoff generated over the catchment decreases 9.2% under the Rainfall Event II. The results are summarized in Table 3.

CONCLUSIONS

A hydrological model is developed for Alibeyköy Watershed in Istanbul, Turkey by using EPA SWMM in this study. Rainfall on the Alibeyköy Watershed and flow rate at downstream of main stream have been measured with rain gauge and flow meter set into the study site. Calibration of the hydrological model has been accomplished by making use of the measured data set. Then, the surface runoff for current urbanization, projected urbanization and projected urbanization with LID implementation are simulated under typical and extreme rainfall events using the calibrated model. After implementing LID type of storm water BMPs, which are bioretention, vegetative swales, infiltration trench and permeable pavement, it is found that LID implementation in the Alibeyköy Watershed results in a considerable decrease in the peak of the hydrograph and helps control peak surface runoff. Further research area of this study would include developing a calibrated water quality model for the Alibeyköy Watershed. Furthermore, there is room for extending the rainfall and flow data in Alibeyköy Watershed. The long term data will be established with the existing stations set in the field, which are still in function.

ACKNOWLEDGEMENTS

This work was supported by Scientific Research Projects Coordination Unit of Istanbul University, Project number 49485 and BEK-2016-22070. The writers would like to thank Scientific Research Projects Coordination Unit of Istanbul University, Turkish State Meteorological Service (DMI), Istanbul Metropolitan Municipality (IBB) and Istanbul Water and Sewerage Administration (ISKI) for their data support and valuable discussions in undertaking this work.

REFERENCES

[1] Qin, L., Bai, X., Wang, S., Zhou, D., Li, Y., Peng, T., Tina, Y. and Luo, G. (2015) Major problems and solutions on surface water resource utilisation in karst mountainous areas. Agricultural Water Management, 159, 55–65.

[2] Cai, Y., Yue, W., Xu, L., Yang, Z. and Rong, Q. (2016) Sustainable urban water resources management considering life-cycle environmental impacts of water utilization under uncertainty. Resources, Conservation and Recycling, 108, 21–40.

[3] Gulbaz, S. and Kazezyilmaz-Alhan, C.M. (2013) Calibrated Hydrodynamic Model for Sazlidere Watershed in Istanbul and Investigation of Urbanization Effects. Journal of Hydrologic Engineering, 18, 75-84.

[4] Shuster, W.D., Bonta, J., Thurston, H., Warnemuende, E. and Smith, D.R. (2005) Impacts of impervious surface on watershed hydrology: A review. Urban Water Journal, 2(4), 263–275.

[5] Sun, Y., Li, Q., Liu, L., Xu, C. and Liu, Z. (2014) Hydrological simulation approaches for BMPs and LID practices in highly urbanized area and development of hydrological performance indicator system. Water Science and Engineering, 7(2), 143–154.

[6] Albek, M., Bakir Ogutveren, U. and Albek, E. (2004) Hydrological modeling of Seydi Suyu watershed (Turkey) with HSPF. Journal of Hydrology, 285(1-4), 260–271.

[7] Fonseca, A., Botelho, C., Boaventura, R.A. and Vilar, V.J. (2014) Integrated hydrological and water quality model for river management: a case study on Lena River. The Science of the total environment, 485-486, 474–89.

[8] Cizek, A.R. and Hunt, W.F. (2013) Defining predevelopment hydrology to mimic predevelopment water quality in stormwater control measures (SCMs). Ecological Engineering, 57, 40–45.

[9] Masseroni, D. and Cislaghi, A. (2016) Green roof benefits for reducing flood risk at the catchment scale. Environmental Earth Sciences, 75(7), 579.

[10] Ghodsi, S.H., Kerachian, R. and Zahmatkesh, Z. (2016) A multi-stakeholder framework for urban runoff quality management: Application of social choice and bargaining techniques. Science of The Total Environment, 550, 574–585.

[11] Lee, J.M., Hyun, K.H. and Choi, J.S. (2013) Analysis of the impact of low impact development on runoff from a new district in Korea. Water Science and Technology, 68(6), 1315–1321.

[12] Jia, H., Yao, H., Tang, Y., Yu, S.L., Field, R. and Tafuri, A.N. (2015) LID-BMPs planning for urban runoff control and the case study in China. Journal of environmental management, 149, 65–76.

[13] Liu, Y., Ahiablame, L.M., Bralts, V.F. and Engel, B.A. (2015) Enhancing a rainfall-runoff model to assess the impacts of BMPs and LID practices on storm runoff. Journal of environmental management, 147, 12–23.

[14] Martin-Mikle, C.J., Beurs, K.M.D., Julian, J.P. and Mayer, P.M. (2015) Identifying priority sites for low impact development (LID) in a mixed-use watershed. Landscape and Urban Planning, 140, 29–41.
[15] Dietz, M.E. (2007) Low Impact Development Practices: A Review of Current Research and Recommendations for Future Directions. Water, Air, and Soil Pollution, 186 (1-4), 351–363.
[16] United States Environmental Protection Agency (USEPA) (2000) Low Impact Development (LID), A Literature Review. EPA-841-B-00-005. USEPA Office of Water: Washington, D.C.
[17] Yang, H.B., Dick, W.A., McCoy, E.L., Phelan, P.L. and Grewal, P.S. (2013) Field evaluation of a new biphasic rain garden for stormwater flow management and pollutant removal. Ecological Engineering, 54, 22-31.
[18] Sigmon, L., Hoopes, S., Booker, M., Waters, C., Salpeter, K. and Touchette, B. (2013) Breaking dormancy during flood and drought: sublethal growth and physiological responses of three emergent wetland herbs used in bioretention basins. Wetlands Ecology and Management, 21(1), 45-54.
[19] Joksimovic, D. and Alam, Z. (2014) Cost Efficiency of Low Impact Development (LID) Stormwater Management Practices. Procedia Engineering, 89(Lid), 734–741.
[20] Brown, R.A. and Hunt, W.F. (2012) Improving bioretention/biofiltration performance with restorative maintenance. Water Science and Technology, 65(2), 361–367.
[21] Khan, U.T., Valeo, C., Chu, A. and van Duin, B. (2012) Bioretention cell efficacy in cold climates: Part 1-hydrologic performance. Canadian Journal of Civil Engineering, 39(11), 1210-1221.
[22] Mei, Y., Yang, X.H., He, J., Guo, Y.A., Jiang, R. and Dong, Z.H., (2013) A New Assessment Model for Pollutant Removal Using Mulch in Bioretention Processes. Fresen. Environ. Bull., 22(5A), 1507-1515.
[23] Gulbaz, S. and Kazezyilmaz-Alhan, C.M. (2017) Experimental investigation on hydrologic performance of LID with rainfall-watershed-bioretention system. Journal of Hydrologic Engineering, 22(1), D4016003.
[24] Lucas, W.C. and Sample, D.J. (2015) Reducing combined sewer overflows by using outlet controls for Green Stormwater Infrastructure: Case study in Richmond, Virginia. Journal of Hydrology, 520, 473-488.
[25] Moura, N.C.B., Pellegrino, P.R.M. and Martins, J.R.S. (2016) Best management practices as an alternative for flood and urban storm water control in a changing climate. Journal of Flood Risk Management, 9(3), 243-254.
[26] Huber, W.C. and Dickinson, R.E. (1988) Storm Water Management Model, Version 4, User's Manual, Athens, GA.: Environmental Research Laboratory, Office of Research and Development, U.S. Environmental Protection Agency (EPA).
[27] Rossman, L.A. (2010) Storm Water Management Model, User's Manual, Version 5, Water Supply and Water Resources Division National Risk Management Research Laboratory, Cincinnati, Ohio, U.S. Environmental Protection Agency, EPA/600/R-05/040.
[28] Temprano, J., Arango, O., Cagiao, J., Suarez, J. and Tejero I. (2006) Stormwater quality calibration by SWMM: A case study in Northern Spain. Water SA, 32(1), 55–63.

Received: **19.05.2017**
Accepted: **21.07.2017**

CORRESPONDING AUTHOR:

Cevza Melek Kazezyılmaz-Alhan
Istanbul University
Engineering Faculty
Civil Engineering Department
Avcılar, Istanbul 34320 – TURKEY

e-mail: meleka@istanbul.edu.tr

© by PSP Volume 26 – No. 10/2017 pages 6121-6126 Fresenius Environmental Bulletin

THE EFFECT OF COAL ASH PRACTICES ON HEAVY METAL CONTENT IN THE SOIL

Duygu Boyraz-Erdem[1,*], Seyide Yilmaz[2]

[1]Namik Kemal University, Agricultural Faculty Department of Soil Science and Plant Nutrition, Tekirdag, Turkey
[2]District of Provincial Food Agriculture and Livestock Saray, Tekirdag, Turkey

ABSTRACT

The objective of this study is to define whether the ash, which is formed after burning of lignite coal, can be used as soil regulator in agricultural lands and to determine its doses if it has applicable value. A randomized experimental design with three replications was used with two different soil textures, being clay and sandy loam, and four different ash dosages (0, 5, 15 and 20%) are taken into consideration. As a result, it is defined that coal ash within two different soil textures and having four different doses didn't form heavy metal pollution according to existing regulations in terms of Ni, Zn, Cd, Pb, Hg, Cr, Sn and Cu elements. However, 15 and 20% affected the increase in Cr amount while the amount applied as 20% affected increase of Ni and Cu values to sandy loam soil texture. More than 5% coal ash is not recommended as it increases heavy metals on soils. With the usage of coal ash, which is processed as waste material in agriculture; prevention of environmental pollution, savings in natural resources are expected.

KEYWORDS:
Coal ash, soil pollution, heavy metal, soil conditioner

INTRODUCTION

Total coal reserves of Turkey is $8.2x10^9$ t according to MTA (General Directorate of Mineral Research and Exploration) data, while 1 billion tons of the need for coal burnt in industry and heaters used in homes is provided with production [1]. It is generally stated that ash amount of our lignite coals is around 15-30 % [2]. According to General Directorate of Turkish Coal Ankara Coal Sector Report 2008 data, by the year 2007, 76 % of the lignite coal production of General Directorate of Turkish Coal was consumed by using in thermal plants while 24 % was used in industry and heating sector. By 2008, it was predicted that our country needed around 17 million tons of coal needs and half of that need was imported while remaining half was covered by General Directorate of Turkish Coal and other domestic producers. If we calculate by considering that average 20 % of 17 million tons of coal we use annually is ash, approximately 3.5 million tons of ash comes out as waste material. When the volumetric space of 3.5 million tons of ash coming out in a year is calculated (1.74482 m^3 per ton), it covers 5.932.388 m^3 volume [3].

Coal ash, which is the residue material after coal is burnt for energy production and heating purposes, forms environmental pollution when left to nature in the way it is, while creating serious space problem due to its covered space when batching is made. However, ash usage as a soil regulator may fix soil tissue and water holding capacity, increases pH value of soil and enriches efficiency of the soil itself. Barman et al., [4], state that fly ash coming out of thermal plants may be used in increasing efficiency of agricultural soil due to its regulating effect on physical and chemical qualities of problematic lands.

Protection of soil and its goal-oriented use in our country are conducted in accordance with the subjects defined in Soil Protection Act and Environment Law. Legislations that are issued based on these laws, fertilizer mixable to agricultural soil, soil regulator and waste materials, qualities along with permissible amount of pollutant elements are given in detail in [5] and [6].

The effects of fly ashes on soil and plant were researched in India, fly ash was mixed into soil with doses changing between 10-50 t ha^{-1} and effects of fly ash on efficiency and development of wheat (*Triticum aestivum* L.), mustard (*Brassicajuncea* L.), lentil (*Lensesculenta Moench* L.), rica (*Oryzasativa* L.) and corn (*Zeamays* L.) plants along with certain important physical and chemical qualities of the soil were examined. According to obtained results, ash application had positive effects on efficiency together with soil qualities [7].

Sing [8] stated that using coal ash coming out of thermal plants has benefits and risks. For benefits, improvement of permeability condition of soil, improvement of soil efficiency, increasing textural qualities and aeration of soil, reducing shell and compact formation along with mass density, improving water holding capacity and porosity, optimum soil pH for plants, procurement of micronutrients like Mo- B- Mn- Fe- Zn- Cu and macronutrients like Mg- S- K- P- Ca, being alternative liming material

for plaster used for acidic soil in sodium soil and increase of organic materials along with other microbial activities may be counted. Meanwhile, its risks include toxic effect formation of heavy metal accumulation for cultivated plants, pollution of underground waters due to contamination of heavy metal to soil layers and possibility of causing soil sterility due to excessive dosage use in agricultural lands.

In this study, defining whether the ash formed after burning of lignite coal that is used in excess amounts in industry and with heating purposes can be used as a soil regulator in agricultural lands, whether it will create heavy metal pollution and if it is applicable, which doses can be worked is targeted. For this purpose, heavy metal condition of soils is examined by applying four different doses of coal ash to soil in two different texture classes. Accordingly, it is taken as a basis that the ash formed after burning of coal not forming environmental pollution, while benefiting from certain qualities within the ash in waste condition.

MATERIALS AND METHODS

A randomized experimental design with three replications was used with two different soil textures, being clay and sandy loam, and four different ash dosages are taken into consideration. Coal ash dosages to be applied to soil textures were defined as 0 % (D_1), 5 (D_2), 15 (D_3) and 20 (D_4). The 20% level, which was chosen as the highest dose, is taken into hand in order to define the condition that might give harm. Before practice, coal ash was turned into small practices by beating and better mixture was provided with the soil. Mixtures were prepared with weight calculation compared to percentage rates to be 1000 g total in each pot. Vetch plant was grown into pots.

In the study, the ash formed after burning of coal, which was taken from Tekirdag– Malkara district, for heating purposes in boiler is used as a material. Also, the soil samples as clay and sandy loam soil were taken from Tekirdag– Kapakli and Saray District. Heavy metal analysis for coal ash and soil samples was conducted before the experiment. Also the physical and chemical analyses were conducted for two soil samples.

The oven dry soil weight was determined after dried in air conditions and sieved from 2 mm sieve. The pH of coal ash and two different soil textures was calculated electrometrically in saturation extract [9] while electrical conductivity rates were measured with electrical conductivity measure device in water soluble total salt saturation extract [10]. Also, organic material amounts were assigned with Walkley– Black method [11], while soil texture analyses were determined with Bouyoucos hydrometer method [12].

Hydrofluoric, nitric, sulfuric and perchloric acids along with copper, zinc, nickel, lead and chromium amounts passing from wet decomposed soil and ash sample to solution were determined by using ICP-MS [13, 14].

Data obtained from treatments were analyzed using of variance (ANOVA). The least significant test (LSD) was used to compare and rank treatments [15]. Differences were declared significant at $p < 0.05$ or 0.01.

The obtained heavy metals data from treatments were evaluated according to [5, 6] (Table 1).

TABLE 1
Heavy metal levels of the regulations

Elements	Heavy metal levels (ppm)	
	[5]	[6]
Cu	3129	450
Zn	23464	1100
Ni	1564	120
Pb	400	150
Cr	235	350

TABLE 2
Some physical and chemical analysis results of the soil used in the experiment

Elements	Clay soil	Sandy loam soil
pH (1/2.5 soil-water)	8.14	4.70
EC (μS cm^{-1})	510.00	197.00
Organic matter (%)	0.93	1.32
Sand (%)	39.06	70.08
Silt (%)	12.73	10.16
Clay (%)	48.21	19.76
Texture Class	Clay	Sandy loam

RESULTS AND DISCUSSION

Soils used in treatment are classified in clay texture class with 48.21% clay according to texture analysis results while being classified in sandy loam texture class with 70.08% sand [16]. The soil in sandy loam texture class is classified in 4.70 medium acid classes. Organic substance amounts are in 1.32% low in sandy loam texture soil while being 0.97 very low classes in clay texture soil. Both soils are classified in salt-free class [9] (Table 2).

Zn amount measured as 4.65 ppm for sandy loam soil, 10.15 ppm for clay soil and 29.75 ppm for coal ash. The obtained data for zinc amount was far below according to Anonymous 2010 and 2014 [5, 6]. The other elements amounts as zinc for two soil types and coal ash were measured under heavy metal regulations according to [5] and [6]. Also, all elements except nickel in coal ash were higher than in two soil types (Table 3).

The soil samples were taken from pot after plant harvest and total copper (Cu), zinc (Zn), nickel (Ni), lead (Hg), and chromium (Cr) values are given

in Table 4. Copper element is a plant nutrient and considered as soil pollutant when it passes certain barrier levels in our existing legislations.

In the evaluations made according to legislations, it is seen that copper amount in treatment soils didn't pass soil pollution parameters. Texture condition of the soil and the difference between applied ash dosages $p<0.01$ was found significant. Clay soil and D_4 dosages gave the highest copper amounts than sandy loam soil and the other dosages (Figure 1). However, the interaction between texture class and applied ash dosages was not found significant in terms of statistics. According to LSD results; clay textured soil in terms of soil qualities. 20% dosage in terms of application dosages forms upper groups. This result shows that coal ash usage doesn't give any Cu pollution harm to the soil.

TABLE 3
Heavy metal analysis results of coal ash and soil samples used in the experiment

Elements	Coal ash (ppm)	Clay soil (ppm)	Sandy loam soil (ppm)
S	29.75	10.15	4.65
Zn	40.30	23.85	13.10
Ni	5.09	13.20	4.19
Pb	12.19	6.13	4.64
Cr	50.40	8.33	3.04

TABLE 4
The contents of Cr, Ni, Pb, Zn and Cu (ppm) for treatments

Soil texture	Doses	Copper (ppm)	Zinc (ppm)	Nickel (ppm)	Lead (ppm)	Chromium (ppm)
Clay	D_1	12.79	22.18 cd	13.91	7.76 b	8.33 cde
	D_2	14.46	23.83 bc	26.66	10.94 a	11.64 bcd
	D_3	20.84	35.24 a	45.51	6.97 b	19.97 a
	D_4	25.17	28.40 b	62.25	7.04 b	25.41 a
Sandy loam	D_1	4.90	14.12 e	4.20	7.90 b	2.98 f
	D_2	6.68	13.62 e	13.15	7.69 b	6.28 de
	D_3	12.66	16.82 e	34.62	7.22 b	12.08 abc
	D_4	13.54	17.58 d	44.56	7.71 b	14.16 ab
	LSD	**ns**	**4.810****	**ns**	**1.710****	**2.850****
Clay		18.32 a	27.41 a	37.08 a	8.18	16.64 a
Sandy loam		9.45 b	15.53 b	24.13 b	7.63	8.89 b
	LSD	**1.819****	**4.369****	**11.428****	**ns**	**2.258 ****
	D_1	8.847 c	18.150 b	9.05 d	7.83 ab	5.65 d
	D_2	10.572 c	18.723 b	19.91 c	9.31 a	8.96 c
	D_3	16.747 b	26.027 a	40.07 b	7.10 b	16.02 b
	D_4	19.357 a	22.985 a	53.40 a	7.38 b	19.79 a
	LSD	**2.384 ****	**3.430 ****	**8.804 ****	**1.699****	**2.011 ****

a.b.c. ……: LSD groups. ns: Not significant. ** : significant at $p < 0.01$

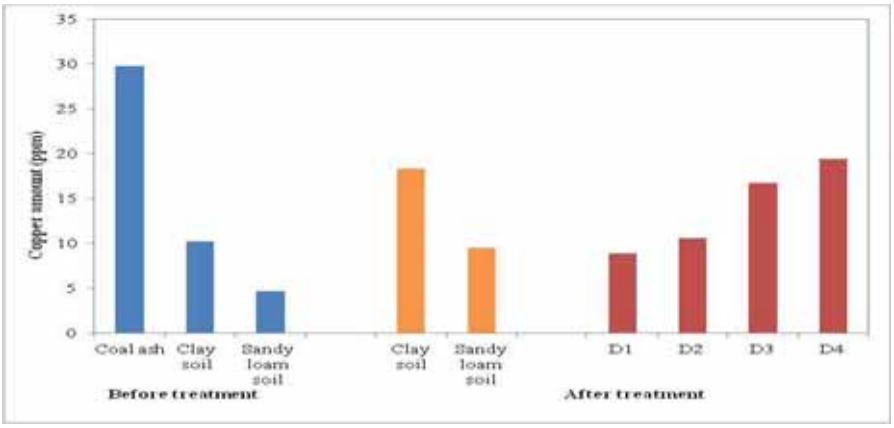

FIGURE 1
The copper amount variations between before and after treatment

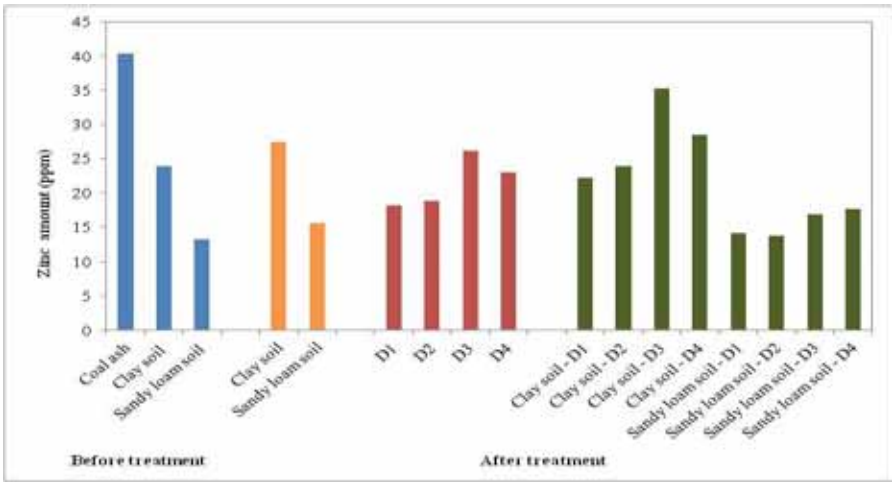

FIGURE 2
The zinc amount variations between before and after treatment

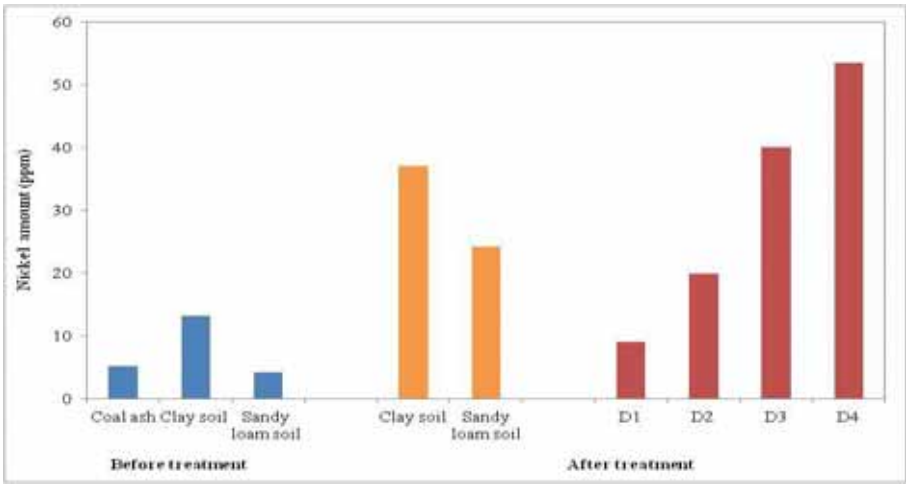

FIGURE 3
The nickel amount variations between before and after treatment

When zinc values given in Table 4 are examined, it can be seen that obtained values are lower than permissible values. Zinc values changing between 13.62 and 35.24 ppm were obtained among treatment subjects, while 1% level differences were obtained between soil textures, between different ash levels and between texture and dosage level interactions. According to LSD test results, clay soil stands forward as soil texture, while 15 and 20% levels stand forward as ash dosage and accordingly zinc values obtained in 15% ash dosage applied in clay soil stand forward as well. Even though total zinc values in all soils according to obtained results didn't pass legal values in legislations. The 15% and 20% dosage ash application shows an important increase in total zinc amounts in soil (Figure 2).

Just like zinc values, nickel values were lower than permissible values (Table 4). The heavy metal levels in coal ash, clay soil and sandy loam soil before treatment were lower than after treatment (Figure 3). Soil texture and dosage levels statistically affect nickel values changing between 4.20 and 62.25 ppm among treatment subjects while not affecting the interaction between soil texture and dosage level. Just like in copper, clay soil stands forward with 37.08 ppm among soil textures while 20% dosage level stands forward with 53.40 ppm among dosage levels.

Lead values measured in treatment subjects changed between 6.97 and 10.04 ppm. It can be said that obtained lead values were very lower than permissible values (Table 3 and Figure 4). As a result of the statistical analyses made between lead values, 1% level differences were present between soil textures, between ash levels and between texture and dosage level interactions. According to LSD test results, 5% level as coal dosage and accordingly lead values obtained in 5% ash dosage applied in clay soil stand forward.

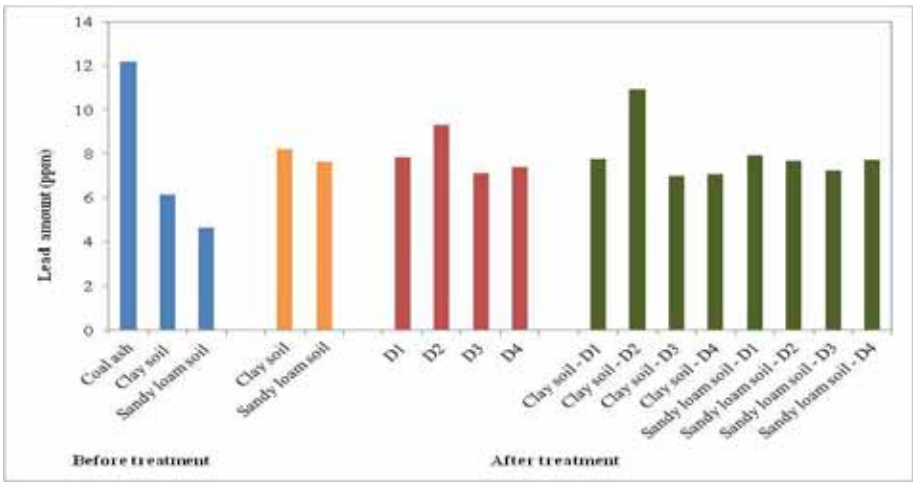

FIGURE 4
The lead amount variations between before and after treatment

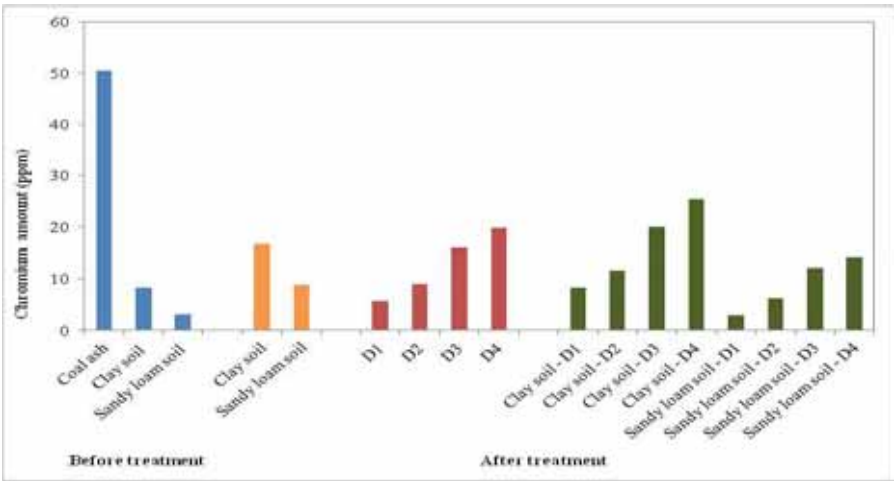

FIGURE 5
The chromium amount variations between before and after treatment

Chromium values measured in treatment changed between 2.98 and 25.41 ppm. It can be said that obtained values are lower than the permissible values given in Table 3. As a result of the statistical analyses made among chromium values, there were 1% level differences between soil textures, between different ash dosage levels and between texture and dosage levels. According to LSD test results, chromium values obtained in clay soil as a soil texture, 20% level as ash dosage and accordingly 20% ash dosage applied in clay soil stand forward.

The previous studies [8, 17, 18, 19 and 20] stated that with the mixture of coal ash to soil. Cadmium, tin, mercury, nickel, zinc, copper, lead and chromium elements among heavy metals are within permissible levels in soil. They prove with the results they offer that coal ash doesn't form heavy metal pollution when used with control.

CONCLUSION

The ash coming out of the burning of coal used in energy production, heating and industry is processed as a waste material but it is possible to use in agriculture as soil regulator and plant nutrient as it doesn't cause any heavy metal pollution.

Values of heavy metals within the ash are suitable in terms of mixing to soils according to our existing legislations. Heavy metals Cd, Hg, Zn, Pb, Cu, Sn, Cr and Ni in soil after mixture of different amount of ashes to clay and sandy loam textured soil didn't pass barrier levels and cause pollution according to existing legislation. However Ni showed important increase in soils with 20% ash dosage while Cr showed considerable increase in 15– 20% dosages in sandy loam textured soils. It is presented that by considering the fact that this increase doesn't form nickel and chromium accumulation in soils in

time and application of coal ash to land in field conditions. 5% practice on agricultural soils should have more positive effects.

With the usage of coal ash, which is processed as waste material in agriculture; prevention of environmental pollution, savings in natural resources are expected. When the expenses made by municipalities in order to remove coal ash coming out of building radiators are considered expenses and effort loss can be minimized by using coal ash in agriculture.

ACKNOWLEDGEMENTS

The authors would like to thank the Namik Kemal University Scientific Research Fund (NKU-BAP) for its financial support to the project of NKUBAP.00.24.YL.14.01

REFERENCES

[1] Anonymous (2006) 15. Komur Kongresi Bildirgesi -2006 MTA. Ankara.
[2] Karatekin, M. (1945) Cok Kullu Linyitleri Buhar Kazanlarinda Elverisli Suretle Yakan iramer Degirmenli Ocaklari. Maden Tetkik ve Arama Dergisi. 39, 58-70.
[3] Anonymous (2008) Türkiye Kömür İşletmeleri Kurumu Ankara Kömür Sektör Raporu (Linyit). www.tki.gov.tr/tr/Komur-Sektor-Raporu-2008 (Date of access:12.12.2013).
[4] Barman S.C., Kisku, G.C. and Bhargava, S.K. (1999) Accumulation of heavy metals in vegetables. Pulse and Wheat grown in Fly Ash Amended Soil. J. Environ Bio. 20(1) 15-18.
[5] Anonymous (2010) Resmi Gazete 08.06.2010 tarih ve 27605 sayili teblig.
[6] Anonymous (2014) Resmi Gazete 29.03.2014 tarih ve 28956 sayili teblig.
[7] Kalra N., Jain, M.C. Joshi, H.C., Chaundary, R., Kumar, S., Pathak, H., Sharma, S.K., Kumar, V., Kumar, R., Harit, R.C., Khan, S.A. and Hussain, M.Z. (2003) Soil Properties and Crop Productivity as Influenced by Fly Ash in Corporation in Soil. Environmental Monitoring and Assessment 87: 93-109.
[8] Sing J.S. (2012) Coal Fly Ash in Agriculture Beneficial Or Risky. Department Environmental Microbiology Ambedkar University Lucknow 226-225 Uttar Pradesh.
[9] Richards, L.A. (1954) Diagnosis and improvement of saline and alkali soils. U.S.D.A Handbook. No: 60.
[10] Soil Survey Manuel, (1951) Soil Survey Staff. U.S. Dept. Agr. Handbook 18 U.S. Govt. Printing Office. Washington D.C. USA.
[11] Saglam, M.T. (2008) Toprak ve Suyun Kimyasal Analiz Yontemleri. Namik Kemal Universitesi. Yayin No: 2. Tekirdag.
[12] Tuzuner, A. (1990) Toprak ve Su Analizi Laboratuvarlari El Kitabi. T.C. Koy Hizmetleri Genel Mudurlugu Yayinlari. Ankara.
[13] Jackson, M.L. (1958) Soil Chemical Analysis. Prentice-Hall. Inc. Englewood Cliffs. N.J. USA.
[14] Kacar, B. (1994) Bitki ve Topragin Kimyasal Analizleri. III. Toprak Analizleri. A.U. Ziraat Fakultesi Egitim Arastirma ve Gelistirme Vakfi Yayini. No: 3. Ankara.
[15] Yurtsever, N. (1984) Deneysel Istatistik Metotlari. Koy Hizmetleri Genel Mud. Yayinlari No: 56.
[16] FAO, (1984) Fertilizer and Plant Nutrition Guide. FAO Fertilizer and Plant Nutrition Bulletin. No: 9 Rome.
[17] Tuna, A. L.and Girgin, A. R., (2005) Mısırda (*Zea mays* L.) gelişme, mineral beslenme ve ağır metal içeriği üzerine Yatağan termik santral uçucu küllerinin etkisi. Ekoloji,15(57), 29-37.
[18] Im-Erb, R., Bamroongrugsa, N., Kawashima, K., Amano, T. and Kato, S. (2004) Utilisation of coal ash to improve acid soil. Songklanakarin J. Sci. Technol. 26(5), 697-708.
[19] Yunusa, I.A.M., Mele, P.M., Rab, M.A., Schefe, C.R. and Beverly, C.R. (2002) Priming of soil structural and hydrological properties by native woody species, annual crops, and a permanent pasture. Aust. J. Soil. Res. 40, 207-219.
[20] Scott I. A., Lombi, E., Carini, F. and Silva, S. (1996) Effects of fly ash treatment of soil on yields and chemical composition of chicory. Agrochimica. 40(5-6), 293-303.

Received: **22.05.2017**
Accepted: **24.07.2017**

CORRESPONDING AUTHOR

Duygu Boyraz-Erdem
Namik Kemal University
Agricultural Faculty Department of Soil Science and Plant Nutrition
Tekirdag – TURKEY

E-mail: dboyraz@nku.edu.tr

© by PSP Volume 26 – No. 10/2017 pages 6127-6134 Fresenius Environmental Bulletin

INCREASED 8-HYDROXYDEOXYGUANOSINE RESPONSES AS A MARKER OF DNA DAMAGE AFTER STRENUOUS ANAEROBIC EXERCISE IN SEDENTARY YOUNG CIGARETTE SMOKERS AND NONSMOKERS

Hayriye Cakir-Atabek[1,*], Filiz Ozdemir[2]

[1]Department of Coach Training in Sports, Faculty of Sports Science, Anadolu University, Eskişehir, Turkey
[2]Department of Biochemistry, Faculty of Pharmacy, Anadolu University, Eskişehir, Turkey

ABSTRACT

Both cigarette smoking and strenuous exercise are associated with increased oxidative stress. Therefore, we aimed to investigate the effects of strenuous anaerobic exercise on oxidative stress, assessed with 8-hydroxydeoxyguanosine (8-OHdG), in cigarette smokers and nonsmokers. Healthy male smokers (n=13) and nonsmokers (n=12) participated in this study. Each participant performed a graded treadmill exercise test to determine maximal oxygen consumption (VO_{2max}), and the Wingate anaerobic test as a strenuous exercise. Blood samples were obtained before and on completion of the test, and then again at 60 min after the test. There were no statistically significant differences in exercise performance values (VO_{2max}, peak power, average power) between the two groups ($p>0.05$). Blood lactate concentration increased significantly in both groups ($p<0.001$); however, no significant smoking status ($p>0.05$) or smoking status over time interaction ($p>0.05$) was observed for blood lactate. Level of 8-OHdG increased in both groups; significant main effect of exercise (times effects) were noted ($p<0.001$) for 8-OHdG, with higher values for smokers. Therefore, no significant smoking status ($p>0.05$) or smoking status over time interaction ($p>0.05$) was found for 8-OHdG. Consequently, strenuous anaerobic exercise exacerbated the oxidative stress damage evaluated by 8-OHdG, both in cigarette smokers and nonsmokers. Results indicated that an inactive lifestyle is as harmful as smoking itself.

KEYWORDS:
cigarette; oxidative stress; 8-OHdG; strenuous exercise; sedentary lifestyle

INTRODUCTION

Cigarette smoking has various harmful effects on health. Smoking increases free radical (FR) production and significantly increases oxidative stress under in vivo conditions [1]. It has been well documented that chronic oxidative stress has a strong relationship with numerous illnesses, such as lung cancer, chronic bronchitis, and coronary heart diseases [2]. Cigarette smokers have an increased risk of these diseases, possibly because of the increased FR production [3]. A smoker is exposed to more than 10^{15} FR in the gas phase alone. Considering the tar inhaled instead of air, this rate becomes greater than 10^{17} [4]. Previously, it has been shown that the oxidative stress biomarkers were higher in smokers [3,5-8], whereas the antioxidant defense system components (enzymes and vitamins) were lower than those in nonsmokers [3,5,6,9]. Despite a similar dietary intake, these results were unchanged [3].

Regular physical exercise is known to have many positive effects on human health. However, different types of acute aerobic or anaerobic exercises were reported to increase FR production, affect the antioxidant defense system, and cause oxidative stress [10-12]. Research that focused on the effect of exercise on oxidative stress primarily focused on individuals who did not smoke, did not use antioxidant medicines, and did not have any metabolic diseases [13-15]. Thus, there is a limited number of studies focusing on exercise-induced oxidative stress in smokers, and the findings of these studies are contradictory [2,16,17]. A limited number of studies on this topic and their conflicting results encouraged us to design this study.

The type, intensity, and duration of the exercise might affect the outcomes related to oxidative stress. In addition, the frequency of exercise and its effects (acute or chronic) might affect oxidative stress responses. From this point of view, the purpose of the current study was to compare the oxidative stress responses to strenuous anaerobic exercise between cigarette smokers and nonsmokers by measuring 8-hydroxydeoxyguanosine (8-OHdG), an indirect marker of DNA damage, before and after exercise. Our hypothesis was that the 8-OHdG responses following a single anaerobic exercise would be higher for smokers than nonsmokers.

MATERIALS AND METHODS

Participants. Thirteen cigarette smokers and 12 nonsmokers volunteered and met all criteria to be included in the study. Participants were all sedentary men, who were free of major signs and symptoms of cardiovascular and pulmonary disease [16,18], and free of orthopedic limitations that might affect exercise testing. Major exclusion criteria were current use of medications or nutritional supplements that might affect the dependent variables, and maximal oxygen consumption (VO_{2max}) higher than 50 $mL.kg^{-1}.min^{-1}$ to ensure participants' fitness status. Participants needed to regularly smoke at least five cigarettes/day [16] and to be smoking continuously without interruption at least for a year to be enrolled as a smoker. At the beginning of the study, all participants were informed about possible risks and benefits of the study, and written informed consents were obtained. The study was approved by the local ethical committee according to the principles set forth in the Helsinki Declaration.

Evaluation of Maximum Oxygen Consumption (VO_{2max}). After collecting the anthropometric data, each participant underwent a graded treadmill exercise test, using the Bruce protocol, to determine VO_{2max} ($mL.kg^{-1}.min^{-1}$) [1,14]. Oxygen consumption, carbon dioxide production, and heart rate were measured continuously using the computerized, breath-by-breath analyzing system Master-Screen-CPX (Care Fusion, Germany). The test started after all participants were informed in detail about how to use the motorized treadmill. Initially, resting oxygen consumption of the participants was recorded for 1 min prior to the test. The running speed and slope increased gradually every 3 min during the test, according to the Bruce protocol. Oxygen uptake was considered maximal when three of the following criteria were met: (a) attainment of age-predicted maximal heart rate (HR) ([220 – age] ± 10 beats/min), (b) the respiratory exchange ratio exceeded 1.20, and (c) subject became exhausted and was unable to continue testing. At the end of the test, subjects had a 3-min recovery period of walking. Following the 3-min recovery time, the mask was removed, and the individual left the treadmill. The average of respiratory parameters that were measured during the last minute was recorded as VO_{2max}.

Familiarization. Following the assessment of VO_{2max}, participants had a rest, and the strenuous anaerobic exercise test was then explained in detail. Each participant performed the first 10 s of the Wingate Anaerobic Test (WAnT) to become familiar with the exercise intensity.

Strenuous Anaerobic Exercise: Wingate Anaerobic Test (WAnT). Three to seven days after the VO_{2max} evaluation and familiarization session, the participants came to the laboratory in the morning (9:00 a.m.) to perform WAnT. The participants were instructed not to perform any strenuous physical tasks during the 48-hour period before the WAnT to avoid potential muscle soreness [13,16]. All tests were completed in the morning (9:00 a.m.-12:00 p.m.) after 8 to 10 h of overnight fasting [13,16]. On arrival at our facility, the participants had a rest period of at least 10 minutes in a sitting position [13], after which the systolic and diastolic blood pressures (SYS-BP and DIA-BP) were measured on the upper arm using a sphygmomanometer (Erka Perfect Aneroid, Germany). Then, the pretest blood samples were obtained.

The WAnT was performed on a bicycle ergometer with a mechanical brake (894 Ea, Monark, Sweden). The WAnT session started with a standardized warm-up period of 5 min of cycling at a speed of 50 to 60 rpm against no load. After the warm-up period, the participants were asked to apply sprints that lasted 3 to 4 seconds. The test was conducted as soon as the participants indicated that they were ready, after 3 to 5 min of passive resting. Necessary adjustments were made on the bicycle ergometer in accordance with body sizes, such as leg height, saddle, and handle bar adjustments, to ensure an optimal cycling position. A load that corresponded to 7.5% of total body weight was put on the bicycle for resistance during the test, and the test was then started [19,20]. As soon as the participant reached the maximum pedaling speed, the load was taken away, and the participant was instructed to continue pedaling as fast as possible despite the resistance. The duration of the test was 30 seconds. The participant was verbally motivated during the test. Maximum anaerobic power, in other words peak power (PP) and mean power (MP) were calculated automatically by the program through a computer software (Monark Exercise, Sweden) and were recorded for further analyses. Following the test, the participants rested for an hour, including 10 min of active recovery and 50 min of passive recovery, sitting on a chair.

Blood sampling and analysis. Venous blood samples were obtained before the test, within 1 min immediately after the test, and again 60 mins after the test. Samples were analyzed for whole blood lactate as an indication of the participant's efforts and for 8-OHdG as a marker of DNA damage. The blood samples collected without the use of an anticoagulant were centrifuged at 2000 *g* for 20 min at 4°C. Serum samples were separated, aliquoted into tubes, and stored at -80°C until analysis.

Analysis of blood lactate (LA). Blood lactate (LA) was analyzed based on the enzymatic-amperometric measuring method and was administered using the Biosen C-line (EKF Diagnostic GmbH, Germany) technical device.

Analysis of 8-OHdG. Serum 8-OHdG analysis was performed using an enzyme-linked immunosorbent assay kit (Enzo Life Science, Assay Design, Germany; catalogue no: ADI-EKS-350). The serum 8-OHdG assay procedure was completed as follows: Serum samples that were stored in polypropylene tubes were diluted and vortexed in sample diluent at a ratio of 1:20 (v/v). Then, 50 µL of standard solutions, zero standard (0 ng/mL), and sample solutions were added to the appropriate wells and 50 µL of pre-diluted anti 8-OHdG was added to each well, except the blank. The plate was covered and incubated for 1 h at room temperature. Then, the liquid in the wells was drained, and 300 µL of 1X washing tampon was added. The washing operation was complete after six washes. The 100 µL pre-diluted anti-mouse IgG: HRP conjugate was added to each well, except the blank. The plate was covered and incubated again for 1 h at room temperature. The washing operation was repeated (for six washes). The 100-µL TMB substrate was added to each of the wells, and the plate was incubated for 15 min in darkness at room temperature. Finally, 100 µL of stop solution-2 was added, and the absorbance was read at 450 nm. The intra-assay coefficient of variation for 8-OHdG was <10%. Assays were performed in duplicate on first thaw.

Analysis of dietary records. To rule out potentially confounding effects of diet, the subjects were required to complete dietary logs for 3 days before the test and for 24 h after the test. Subjects were encouraged to maintain their normal dietary habits during the study period. To ensure standardization of the dietary records, all subjects were instructed individually how to fill out the dietary record. The dietary logs were used to quantify the average intake of calories, protein, carbohydrate, fat, vitamin C, vitamin A, and vitamin E for both experimental groups. The diet logs were analyzed using a computerized dietary assessment program (BEBİS, version: 6.1, Turkey).

Statistical analysis. All data are presented as mean ± standard deviation (SD). The Kolmogorov-Smirnov test of normality demonstrated that the data were normally distributed. Then, independent sample t-tests were performed to determine possible group differences for the physical characteristics and for the performance variables, as well as for the total intake of calories (kcal.day^{-1}) and macronutrients [carbohydrate (g), fat (g), protein (g), vitamin C, vitamin A, and vitamin E]. The effects of strenuous anaerobic exercise on examined variables (blood LA and 8-OHdG) were analyzed using a two-way [2 (groups) x 3 (measurements)] repeated-measures analysis of variance (ANOVA). The Greenhouse–Geisser correction was used where sphericity was violated; furthermore, the Bonferroni method was applied to determine pairwise differences. All statistical analyses were performed using the 18.0 version of SPSS (Statistical Package for the Social Sciences, SPSS Inc.) for Windows. A power analysis (1-β) was performed, and the level of statistical significance was set at $p<0.05$.

TABLE 1
Descriptive characteristics of smokers and nonsmokers

Variables	Smokers (n = 13)	Nonsmokers (n = 12)
Age (years)	28.46 ± 5.96	31.42 ± 5.47
Height (cm)	176.15 ± 7.81	173.95 ± 7.60
Weight (kg)	78.17 ± 8.34	78.97 ± 11.47
Percent Body Fat (%)	18.90 ± 5.16	20.83 ± 5.02
Body Mass Index (kg/m^2)	25.24 ± 3.13	26.20 ± 3.94
Cigarettes per day	23.00 ± 8.92	NA
Years smoking	11.08 ± 6.24	NA
Resting Systolic BP (mmHg)	113.07 ± 13.77	118.75 ± 17.85
Resting Diastolic BP (mmHg)	75.38 ± 11.26	79.17 ± 9.96

Note: NA: not applicable; BP: blood pressure.

TABLE 2
Graded treadmill exercise test (Bruce protocol) and Wingate anaerobic power test values of the smokers and nonsmokers

	Smokers	Nonsmokers
Graded treadmill lexercise test (Bruce protocol)		
VO_{2max} (mL.kg^{-1}.min^{-1})	41.13 ± 5.07	42.07 ± 5.39
RER	1.34 ± 0.10	1.28 ± 0.09
Max Heart Rate (beats/min)	184.38 ± 7.60	180.25 ± 8.08
Wingate anaerobic test-WAnT		
Load (kg)	5.87 ± 0.60	5.93 ± 0.85
Peak Power (w)	923.83± 112.81	899.89 ± 148.24
Peak Power (w/kg)	11.90 ± 1.15	11.45 ± 1.16
Mean Power (w)	468.46 ± 57.52	481.43 ± 66.41
Mean Power (w/kg)	6.03 ± 0.50	6.14 ± 0.57

Note: VO_{2max}: maximal oxygen consumption; RER: respiratory exchange ratio.

RESULTS

Descriptive characteristics and test performance (graded treadmill exercise test, and Wingate anaerobic power test) values of smokers and nonsmokers are presented in Tables 1 and 2. Both groups were similar in mean age, height, weight, percent body fat, BMI, and systolic and diastolic blood pressures. There were no significant differences observed in these variables between the smokers and the nonsmokers. In addition, there were no significant differences in VO_{2max}, respiratory exchange ratio (RER), maximum heart rate, peak power, and mean power values between the two groups ($p > 0.05$). The dietary intake of the

TABLE 3
Macronutrient dietary intakes and selected antioxidants consumed for 3 days before the test in smokers and nonsmokers

	Smokers	Nonsmokers	Recommended
Calories (kcal.day^{-1})	2135.08 ± 496.16	2061.02 ± 344.66	
Carbohydrate (g.kg^{-1})	3.21 ± 1.20	3.10 ± 1.00	5-8 gr/kg ‡
Fat (g.kg^{-1})	1.12 ± 0.39	1.07 ± 0.30	1 gr/kg ‡
Protein (g.kg^{-1})	0.98 ± 0.34	0.93 ± 0.18	0.8 – 1.2 gr/kg ‡
Vitamin A (µg)	1198.71 ± 1117	1315.80 ± 1241	700 – 900 µg/d †
Vitamin C (mg)	63.73 ± 35.76	83.72 ± 35.26	75 – 90 mg/d †
Vitamin E (mg)	15.23 ± 7.16	17.55 ± 6.69	15 mg/d †

Note: Vitamin A values provide retinol equivalents; ‡ and †: Dietary Reference Intakes (DRIs) [32,33]

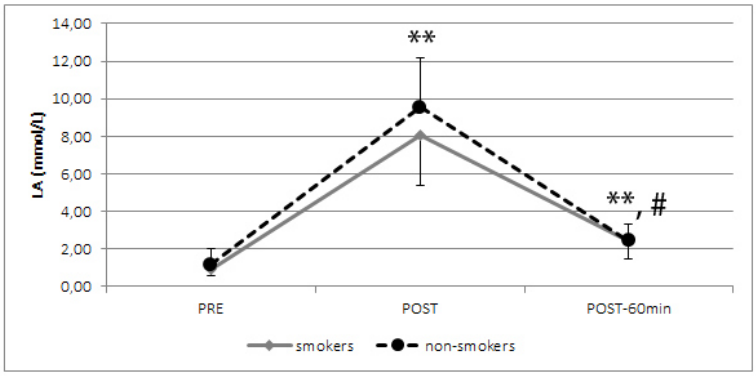

FIGURE 1
Blood lactate (LA) responses to strenuous anaerobic physical work in smokers and nonsmokers. **p< 0.001 compared with PRE values, # p<0.001 compared with POST values

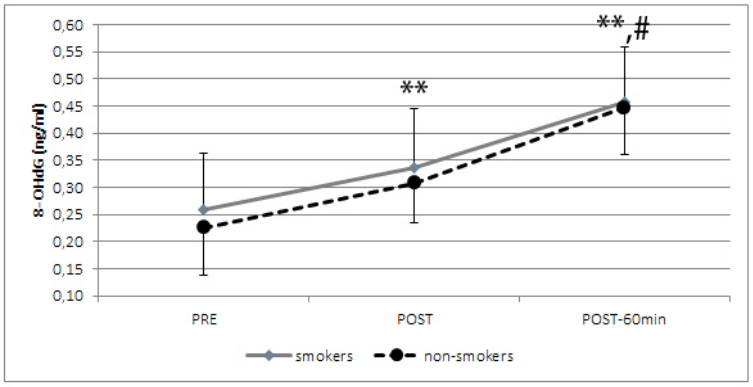

FIGURE 2
Serum 8-OHdG responses to strenuous anaerobic physical work in smokers and non-smokers. **p< 0.001 compared with PRE values, # p<0.001 compared with POST values

participants is presented in Table 3. There were no statistically significant differences for total kilocalories, macronutrients, or micronutrients between the groups ($p > 0.05$; Table 3).

The blood LA concentration increased significantly in both groups ($p < 0.001$; $1\text{-}\beta = 1.00$; Figure. 1). The mean LA level increased from 0.950 ± 0.39 mmol/L to 8.096 ± 2.71 mmol/L, and then decreased to 2.434 ± 0.92 mmol/L at 60 min after the test in smokers. Similarly, the mean LA level increased from 1.171 ± 0.82 mmol/L to 9.562 ± 2.64 mmol/L, and then decreased to 2.440 ± 0.86 mmol/L at 60 min after the test in nonsmokers. These changes were not different between the groups ($p > 0.05$); furthermore, there were no significant group x measurements interaction for blood LA ($p > 0.05$).

As illustrated in Figure. 2, serum 8-OHdG values increased significantly after the WAnT in both groups ($p < 0.001$; $1\text{-}\beta = 1.00$). The mean serum 8-OHdG levels increased from 0.259 ± 0.10 ng/mL to 0.337 ± 0.11 ng/mL, and continued to increase 60 min after the test, to 0.458 ± 0.10 ng/mL in smokers. Similarly, the mean 8-OHdG levels increased from 0.226 ± 0.09 ng/mL to 0.308 ± 0.07 ng/mL, and continued to increase at 60 min after the test, to 0.447 ± 0.09 ng/mL in nonsmokers. It has been observed that

the serum 8-OHdG levels of smokers were higher than the 8-OHdG levels of nonsmokers, but there were no significant differences between the groups ($p > 0.05$); furthermore, there were no significant group x measurements interaction for serum 8-OHdG ($p > 0.05$).

DISCUSSION

The findings of the current study indicate that strenuous anaerobic exercise increases 8-OHdG in young sedentary smokers and nonsmokers. It has been well documented that smoking increases FR production. Aside from cigarette smoking, intense physical exercise is an important stimulus of FR production that cause oxidative stress. For this reason, studies that examined the effect of exercise focused primarily on nonsmoking individuals [13,15]. However, the number of people who smoke and participate in various types of physical activities is considerable. Thus, it is important to clarify the exercise-induced oxidative stress responses of smokers. This study therefore focused on examining the effect of strenuous anaerobic exercise on individuals who smoke.

Surmen–Gur et al. [21] conducted the first study that investigated the effect of exercise on oxidative stress in smokers. Aerobic pedaling and isokinetic knee extension exercises were used as a combined physical stimulus. Oxidative stress, assessed by lipid peroxidation (MDA) level, did not differ between smokers and nonsmokers [21]. Similarly, Taito et al. [2,22] demonstrated that plasma oxidative stress, assessed by lipid hydroperoxide, did not differ between smokers and nonsmokers after maximal and moderate-intensity exercises.

In another study, an exercise with progressive intensity (Bruce protocol) was applied, and sedentary smokers (n=14; at least five cigarettes/day) and nonsmokers (n=15) were compared [16]. No significant difference was observed between the groups in terms of maximum HR and blood LA values after test. Protein carbonyl (PC) level increased at a rate of 52% for smokers and 25% for nonsmokers after the exercise, and the change in PC (%) had a positive correlation with the number of cigarettes smoked per day ($r = 0.578$, $p = 0.03$). Smoking condition and time interaction was recorded for MDA. MDA level was reported to increase (37%) only for smokers. DNA damage, assessed by 8-OHdG, was not affected by smoking and exercising at a significant level; 8-OHdG was reported to increase at a rate of 16% for smokers and 5% for nonsmokers [16]. Consequently, in the mentioned study, compared with the nonsmokers of the same age, smokers who were young, healthy, and had a sedentary lifestyle demonstrated intense oxidative stress responses for forced physical activities [16].

On the other hand, Gochman et al. [17] investigated both the effects of exercise and smoking on oxidative stress, by conducting a study on trained smokers. PC and lactate dehydrogenase (LDH) level increased for smokers (n=15) and nonsmokers (n=15) at an important level after a standard maximal exercise test; however, plasma conjugal diene level, which is one of the other indicators of oxidative stress, and lipid peroxide level increased for smokers only. Plasma antioxidant level was found to be lower at a significant level in smokers than in nonsmokers [17]. Because of the lower antioxidant capacity, the smokers could be more vulnerable to lipid peroxidation.

It is known that age, fitness status, exercise intensity, and dietary intake affect oxidative stress [16]; hence, we attempted to control these variables. The findings of the current study showed that there were no statistical differences for age between groups. In addition, the findings of our study showed that the physiological (VO_{2max}, RER, HR_{max}, blood LA) and performance (peak power and mean power) variables of smokers and nonsmokers were similar, and there were no significant differences between the two groups. These findings demonstrated that the individuals who participated in the study were at the same fitness status and they had an inactive lifestyle. Moreover, the diet analysis conducted on both groups showed that they had similar eating habits. The diet analysis proved that vitamin A, vitamin C, and vitamin E consumption was similar for both groups. Furthermore, the mean intake of antioxidant vitamin A was higher than the current Dietary Reference Intake (DRI) recommendation, and the mean intake of vitamin E was in the range of the current DRI recommendation. However, it should be pointed out that the smokers consumed fewer antioxidants than the nonsmokers did.

Furthermore, in the current study, DNA damage significantly increased in both smokers and nonsmokers. These results agree with the results of Bloomer et al. [16] with one difference: the DNA damage increment was much higher than the increment recorded in the mentioned study. The different types of exercise applied may explain this situation. The Bruce protocol differs from the anaerobic test used in this study in terms of duration (scope of exercise) and energy metabolism used. The Wingate test takes only 30 s, but it is performed at the maximum intensity. The anaerobic energy system is dominant during the test. Both energy systems have different FR production and oxidative stress formation mechanisms.

It has been well documented that oxygen metabolism in the mitochondria is related to FR production [23,24]. Ninety-five to ninety-nine percent of the consumed oxygen is converted to water by the mitochondrial cytochrome oxidase system, whereas the remaining (1–5%) parts form the superoxide radical [25]. It was emphasized that the increase in FR

production during prolonged submaximal aerobic exercise was primarily due to the large increase in oxygen consumption [24], resulting in substantially increased mitochondrial electron flux [17], and in turn increasing superoxide radical production from the mitochondria during the mitochondrial electron transport chain [17, 25-27]. Despite the lower oxygen demands, the generation of FR during anaerobic exercise is possible through other mechanisms: (a) the xanthine oxidase pathway, (b) respiratory burst of neutrophils, (c) catecholamine auto-oxidation, (d) local muscle ischemia, and (e) conversion of the weak superoxide to the strong hydroxyl radical by lactic acid [25,28,29].

Regular aerobic or anaerobic exercises are proved to strengthen the antioxidant defense system and decrease oxidative stress damage [11,15]. Despite this protective effect of exercise, the net effects of it on smoking-induced oxidative stress damage are not clear. However, the findings of this study show that intense anaerobic exercises caused oxidative damage in nonsmokers as much as in smokers. VO_{2max} values in this study were recorded as 41.13 ± 5 ($mL.kg^{-1}.min^{-1}$) for smokers and 42.07 ± 5 ($mL.kg^{-1}.min^{-1}$) for nonsmokers, and these values were lower than the VO_{2max} values of individuals who followed a formal exercise program regularly [18]. In conclusion, an inactive lifestyle might cause as much oxidative stress damage as the damage caused by smoking after forced anaerobic exercises, even if the individual is a nonsmoker. However, lack of information about passive smoke exposure in a social environment is one of the limitations of the current study. In addition, in the present study, the oxidative stress was evaluated only with the 8-OHdG (an indirect marker of DNA damage), and not with other oxidative stress indices. This factor unfortunately limits our discussion in terms of explaining the effect of intense anaerobic exercise on oxidative stress in smokers.

CONCLUSIONS

In contrast with our hypothesis**,** acute strenuous anaerobic exercise increased DNA damage at a similar level in both smokers and nonsmokers. It could be speculated that although a person does not smoke, a sedentary lifestyle is just as harmful as smoking. Recently, it has been demonstrated that aerobic exercise training of moderate intensity reduced oxidative stress induced by smoking [30,31]. Therefore, people should be encouraged to be physically active.

ACKNOWLEDGEMENTS

This study was presented at 5th International congress on cell membranes and oxidative stress: focus on calcium signaling and TRP channels, Isparta, Turkey, 2014. The authors would like to express thanks to Cihan Aygün at the Anadolu University for his assistance in dietary analysis.

Author Contributions. Hayriye Çakır-Atabek conceived and designed the experiments; Hayriye Çakır-Atabek and Filiz Özdemir performed the experiments; Hayriye Çakır-Atabek analyzed the data; Hayriye Çakır-Atabek and Filiz Özdemir contributed reagents/materials/analysis tools; Hayriye Çakır-Atabek and Filiz Özdemir wrote the paper.

Conflicts of Interest. The authors declare no conflict of interest

REFERENCES

[1] Alberg, A. (2002) The influence of cigarette smoking on circulating concentrations of antioxidant micronutrients. *Toxicology.* 180(2), 121-137.

[2] Taito, S., Domen, S., Sekikawa, K., Kamikawa, N., Oura, K., Kimura, T., Takahashi, M, Hamada, H. (2014) Cigarette smoking does not induce plasma or pulmonary oxidative stress after moderate-intensity exercise. *J. Phys. Ther. Sci*. 26(3), 413-415.

[3] Bloomer, R.J. (2007) Decreased blood antioxidant capacity and increased lipid peroxidation in young cigarette smokers compared to nonsmokers: Impact of dietary intake. *Nutr. J.* 6, 39

[4] Pryor, W.A. (1993) Stone, K. Oxidants in cigarette smoke radicals, hydrogen peroxide, peroxynitrate, and peroxynitritea. *Ann. N. Y. Acad. Sci.* 686, 12-27.

[5] Özbay, B., Dülger, H. (2002) Lipid peroxidation and antioxidant enzymes in Turkish population: Relation to age, gender, exercise, and smoking. *Tohoku J. Exp. Med*. 197(2), 119-124.

[6] Ünlü, M., Tahan, V., Akkaya, A., Demirci, M., Şahin, Ü. (1998) Plasma lipid peroxidation in adult smokers. *Turkiye Klinikleri J. Med. Sci.* 18, 105-108.

[7] Covas, M.I., Elosua, R., Fitó, M., Alcántara, M., Coca, L., Marrugat, J. (2002) Relationship between physical activity and oxidative stress biomarkers in women. *Med. Sci. Sports Exerc*. 34(5), 814-819.

[8] Çimen, F., Ulubaş, B., Eryılmaz, T., Bilgin, G. (2002) Lipid peroxidation, antioxidant activity and pulmonary function test in smokers. *Turkiye Klinikleri J. Med. Sci.* 22, 292-296.

[9] Ho, S.P., Chan-Yeung, M., Chow, K.K., Ip, M.S., Mak, J.C. (2005) Antioxidant enzyme activities in healthy Chinese adults: influence of age, gender and smoking. *Respirology.* 10(3), 305-309.

[10] Packer, L. (1997) Oxidants, antioxidant nutrients and the athlete. *J. Sports Sci.* 15(3), 353-363.
[11] Manna, I., Jana, K., Samanta, P.K. (2004) Intensive swimming exercise-induced oxidative stress and reproductive dysfunction in male Wistar rats: protective role of α-tocopherol succinate. *Can. J. Appl. Physiol.* 29(2), 172-185.
[12] Radák, Z., Asano, K., Inoue, M., Kizaki, T., Oh-Ishi, S., Suzuki, K., Taniguchi, N., Ohno, H. (1995) Superoxide dismutase derivative reduces oxidative damage in skeletal muscle of rats during exhaustive exercise. *J. Appl. Physiol.* 79(1), 129-135.
[13] Bloomer, R.J., Goldfarb, A.H., Wideman, L., McKenzie, M.J., Consitt, L.A. (2005) Effects of acute aerobic and anaerobic exercise on blood markers of oxidative stress. *J. Strength Cond. Res.* 19(2), 276-285.
[14] Dixon, C.B., Robertson, R.J., Goss, F.L., Nagle, E.F., Evans, R.W. (2006) The effect of acute resistance exercise on serum malondialdehyde in resistance-trained and untrained collegiate men. *J. Strength Cond. Res.* 20(3), 693-695.
[15] Çakir-Atabek, H., Demir, S., Pınarbaşılı, R.D., Gündüz, N. (2010) Effects of different resistance training intensity on indices of oxidative stress. *J. Strength Cond. Res.* 24(9), 2491-2497.
[16] Bloomer, R.J., Creasy, A.K., Smith, W.A. (2007) Physical work-induced oxidative stress is exacerbated in young cigarette smokers. *Nicotine Tob. Res.* 9(2), 205-211.
[17] Gochman, E., Reznick, A.Z., Avizohar, O., Ben-Amotz, A., Levy, Y. (2007) Exhaustive exercise modifies oxidative stress in smoking subjects. *Am. J. Med. Sci.* 333(6), 346-353.
[18] Pescatello, L.S., Ed. (2013) *ACSM's guidelines for exercise testing and prescription*. 9th ed. Philadelphia: Lippincott Williams & Wilkins, p.84-86,165.
[19] Inbar, O., Bar-Or, O., Skinner, J.S. (1996) *The Wingate anaerobic test.* Champaign. IL: Human Kinetics.; p.41–71.
[20] Kin-İşler, A., Ariburun, B., Ozkan, A., Aytar, A., Tandogan, R. (2008) The relationship between anaerobic performance, muscle strength and sprint ability in American football players, *Isokinetics and Exercise Science.* 16(2), 87–92.
[21] Sürmen-Gür, E., Oztürk, E., Gür, H., Pündük, Z., Tuncel, P. (1999) Effect of vitamin E supplementation on post-exercise plasma lipid peroxidation and blood antioxidant status in smokers: with special reference to haemoconcentration effect. *Eur. J. Appl. Physiol. Occup. Physiol.* 79(6), 472-478.
[22] Taito, S., Sekikawa, K., Oura, K., Kamikawa, N., Matsuki, R., Kimura, T., Takahashi, M., Inamizu, T., Hamada, H. (2013) Plasma oxidative stress is induced by single-sprint anaerobic exercise in young cigarette smokers. *Clin. Physiol. Funct. Imaging.* 33(3), 241-244
[23] Powers, S.K., Ji, L.L., Leeuwenburgh, C. (1999) Exercise training-induced alterations in skeletal muscle antioxidant capacity: a brief review. *Med. Sci. Sports Exerc.* 31(7), 987-97.
[24] Di Meo, S., Venditti, P. (2001) Mitochondria in exercise-induced oxidative stress. *Biol. Signals Recept.* 10(1-2), 125-140.
[25] Clarkson, P.M., Thompson, H.S. (2000) Antioxidants: What role do they play in physical activity and health? *Am. J. Clin. Nutr.* 72(2 Suppl), 637S–646S.
[26] Bloomer, R.J., Goldfarb, A.H. (2004) Anaerobic exercise and oxidative stress: A review. *Can. J. Appl. Physiol.* 29(3), 245-263.
[27] Jackson, M.J. (2000) Exercise and oxygen radical production by muscle. In *Handbook of oxidants and antioxidants in exercise*. Sen, C.K., Packer, L., Hanninen, O., Ed.; Amsterdam: Elsevier Science, p.57–68.
[28] Ji, L.L. (2000) Free radicals and antioxidants in exercise and sports. In *Exercise and Sport Science*. Garrett, W.E., Kirkendall, D.T., Ed.; Philadelphia, PA: Lippincott Williams and Wilkins, pp.299–317.
[29] Smith, L.L., Miles, M.P. (2000) Exercise-induced muscle injury and inflammation. In *Exercise and Sport Science*. Garrett, W.E., Kirkendall, D.T., Ed.; Philadelphia, PA: Lippincott Williams and Wilkins, pp.401–411.
[30] Toledo, A.C., Magalhaes, R.M., Hizume, D.C., Vieira, R.P., Biselli, P.J., Moriya, H.T., Mauad, T., Lopes, F.D., Martins, M.A. (2012) Aerobic exercise attenuates pulmonary injury induced by exposure to cigarette smoke. *Eur. Respir. J.* 39(2), 254-264.
[31] Koubaa, A., Triki, M., Trabelsi, H., Baati, H., Sahnoun, Z., Hakim, A. (2015) The effect of a 12-week moderate intensity interval-training program on the antioxidant defense capability and lipid profile in men smoking cigarettes or hookah: a cohort study. *ScientificWorldJournal*. 2015:639369. doi: 10.1155/2015/639369
[32] Padovani, R.M., Amaya-Farfán, J., Colugnati, F.A.B., Domene, S.M.A. (2006) Dietary reference intakes: application of tables in nutritional studies. *Braz. J. Nutr.* 19, 741-760.
[33] Deminice, R., Sicchieri, T., Mialich, M.S., Milani, F., Ovidio, P.P., Jordao, A.A. (2011) Oxidative stress biomarker responses to an acute session of hypertrophy-resistance traditional interval training and circuit training. *J. Strength Cond. Res.* 25(3), 798-804.

Received: **24.05.2017**
Accepted: **14.07.2017**

CORRESPONDING AUTHOR

Hayriye Cakir Atabek
Department of Coach Training in Sports, Faculty of Sports Science, Anadolu University, Eskişehir, Turkey

e-mail: hayriyecakir@anadolu.edu.tr

© by PSP Volume 26 – No. 10/2017 pages 6135-6140 Fresenius Environmental Bulletin

THE EFFECT OF BARLEY GRASS ON ANTIOXIDANT CAPACITY AND DNA DAMAGE IN RAT WITH RENAL FAILURE

Bahat Comba[1,*], Leyla Mis[2], Sema Uslu[3], Arzu Comba[1]

[1]Hitit University, Alaca Avni Celik Vocational High School, Department of Veterinary, Corum, Turkiye
[2]Yuzuncu Yil University Veterinary Medicine Faculty, Department of Physiology, Van, Türkiye.
[3]Cumhuriyet University, Veterinary Medicine Faculty, Department of Histology-Embryology, Sivas, Turkiye

ABSTRACT

This study was aimed to search the effect of barley grass (BG) on the Total Antioxidant (TAS)-Oxidant Status (TOS) and DNA damage (8OHdG) in rat with renal failure. The rats which are used in the study were randomly divided into 4 groups that each of has 8 rats: Control (C) group; injected i.p. with physiological saline once a day for 7 days, GM group; Gentamicin (80 mg/kg/day) was injected i.p. for 7 days, BG group; was given oral BG (250 mg/kg/day) for 4 weeks, GM+BG group was injected gentamicin (80 mg/kg/day) with i.p. for 7 days and BG (250 mg/kg/day) was given by oral for 4 weeks. After from the process of experiment for 4 weeks, blood sample and kidney tissue were taken. The analyses of urea and creatinine were done by autoanalyser; TAS, TOS levels by colorimetric kits; 8OHdG level by ELISA kits in serum. The kidney tissues were examined histologically. In the GM+BG group was statistically decreased levels of urea, creatinine, TOS ($p<0.05$) and OSI ($p<0.01$) compared to GM group. In the group of BG was determined the levels of TAS $p<0.05$ statistically increased other groups. The statistical significance was not found in the level of serum 8OHdG differences between the groups. BG decreased widespread damage to the renal glomerulus and proximal tubulus. As a result, adverse effects of high-dose gentamicin application such as kidney damage can be reduced when used barley grass.

KEYWORDS:
barley grass, DNA damage, gentamicin, kidney, TAS, TOS.

INTRODUCTION

Barley (Hordeum vulgare L.), one of the world's most extensively cultivated crops, is regarded as salt tolerant compared with other Triticeae members [1]. Barley grass (BG) is the new sprouts of barley and contain a wide range of nutrients and plant hormones. BG because of its alkaline content is reduces the intense acidity which is an important contribution in the development of cancer. Barley grass contains 3000 enzymes that are used by the body [2]. Furthermore, BG is promoted as a source of antioxidants, the most important being superoxide dismutase (SOD), catalase (CAT), vitamin E, vitamin C, and carotenoids [3].

Aminoglycoside antibiotics are frequently used in the treatment of severe infections of urinary tract [4]. Gentamicin (GM) is used to be an important aminoglycoside antibiotic against life threatening gram negative bacterial infections [5]. However, nephrotoxicity and ototoxicity is major side effect after long terapy and high dose clinical use for 10–15% of all cases of acute renal failure [6].

There is a remarkable balance between antioxidants and oxidants in a healthy body. Health problems occur due to a rise of free radicals or fall of antioxidants.Total antioxidant status (TAS) and total oxidant status (TOS) measurement is the most practical, economic and rapid practice that detects oxidant and antioxidant amounts [7;8]. It is commonly recognised that reactive oxygen species (ROS) are involved in a variety of physiological and pathological processes. ROS production can induce DNA damage, leading to a variety of chronic health problems, such as cancer, aging, chronic inflammation [9]. And today, 8-hydroxydeoxyguanosine (8OHdG) is regarded as an indicator of oxidative DNA damage [10].

Nowadays, it is a well-known that oxidative stres plays an important role in the pathophysiogenesis of kidney deases. The kidney is an organ highly vulnerable to damage caused by ROS [11].

In recent years, although many studies are available the changes in the lipid peroxidation, antioxidant enzyme activities in barley seed and its different extracts such as metanol, etanol, phenol, in vivo [12] and in vitro [1] there is limited information about whether any effect of barley grass on the urea, creatinine, TAS, TOS, DNA damage and renal histolojical examination in rat with nefrotoxicity. Therefore, in the present study, we have investigated effect of BG levels of urea, creatinine, TAS, TOS, DNA damage and renal histolojical changes in rat with with renal failure.

MATERIALS AND METHODS

Study groups. A total of 32 Wistar albino rats weighing between 200 and 250 g, were used in a climate-controlled animal care facility, with a 12 h light/dark cycle. The animals were given with standard rat chow and water, ad libitum. All animal handling procedures were approved by the local ethics committee of Yuzuncu Yil University, Van, Turkey (YYUHADEK: 2015-08)

They were randomized four groups, each containing 8 rats, as follows: Control (C) group was injected physiological saline with i.p. for 7 days; Gentamicin (GM) group, Gentamicin (80 mg/kg/day, Genta 80 mg) was injected with i.p. for 7 days; Barley Grass (BG) group was given BG (250 mg/kg/day, Now Foods, Organic Barley Grass 500 mg, USA) with orally for 4 weeks; GM+BG group gentamicin (80 mg/kg/day) was injected with i.p. for 7 days and BG (250 mg/kg/day) was given with orally for 4 weeks.

Sample collection. At the end of four weeks, blood and kidney samples were collected from all the rats and sacrificed by anesthetizing with 70 mg/kg of ketamine HCl (Ketalar, Pfizer) and xylasine HCl (Rompun, Bayer) 10 mg/kg i.p. injection.

Blood samples were taken from hearts with sterile injector and placed into tubes with coagulated. The bloods were separated into serum by centrifugation at 1800 g (3000 RPM) for 10 min. Serum was stored (-20 °C) until the analysis. The kidneys were dissected out and preserved in 10 % formalin for the histological study.

Serum analysis The serum urea and creatinine were measured by autoanalizor (Modular PP, Roche). The oxidative DNA damage 8- hydroxy-2'-deoxyguanosine (8OHdG) levels were analysis by ELISA kit (Enzo life sciences, USA); TAS, TOS values using a novel automated measurement method developed by Erel [7;8] by colorimetric kits (Rel Assay, Türkiye) in serum. The oxidative stress index (OSI) was calculated with the ratio of TOS to TAS.

Histological analysis. Kidney tissues taken from rats of all the groups were fixed in 10% buffered formaldehyde for 24 hours to histopathological examinations were blocked by the paraplastl after routine tissue processing and serially sectioned were taken at 6μm thickness. The general structures of the organs were examined with painted Crossman's modified Mallory triple stain [13].

Statistical analysis. All data were analyzed using the Kruskal-Wallis test. Dunn test was performed to determine the different groups. Statistics Calculator taken as 5 % level of significance and SPSS statistical software 16.0 for Windows was used for the calculations. The data was given as means±stantard deviation (SD).

RESULTS

Serum Findings. The mean levels of serum urea, creatinine, TAS-TOS-OSI and 8OHdG of all groups are shown in table 1. According to the table 1 the mean levels of serum of urea, kreatinin, TOS ($p<0.05$) and OSI ($p<0.01$) in GM group were determinated significantly higher than other groups. Gentamicin increased the levels of urea, creatinine, TOS-OSI but decreased the levels of TAS compared to control gropus. And these values in GM+BG group were smiliar to control group. BG supplement provided marked protective effect and improvement on these parameters. Furthermore, the mean TAS value in BG group was statistically significant for increases compared with other groups ($p<0.05$). However, there was no difference the mean levels of serum 8OHdG among the other groups.

Histolojical assessment. The score table was prepared to assess histological changes. According zero (0) =no cell damage; 1=small tubular damage (25% of affected tubulus); 2= middle tubular damage (50 % of affected tubulus); 3= intensive

TABLE 1
The values of serum urea, creatinine, TAS-TOS-OSI. 8OHdG in all groups.

	C group Mean ± SD	BG group Mean ± SD	GM group Mean ± SD	GM+BG group Mean ± SD	P value
8OHdG (ng/mL)	11.43±5.14	13.54±4.26	17.3±4.57	15.56±5.19	≥0.05
TAS (mmol Trolox Equiv/L)	0.54±0.15^{b}	0.94±0.17^{a}	0.38±0.15^{b}	0.62±0.16^{b}	≤0.05
TOS (μmol H2O2 Equiv/L)	5.38±1.42^{b}	4.43±1.51^{b}	9.21±2.26^{a}	6.42±1.78^{b}	≤0.05
OSI (Arbitrary Unit)	0.99±0.31^{b}	0.47±0.15^{c}	2.42±0.78^{a}	1.04±0.65^{b}	≤0.01
Urea (mg/dL)	31.85±3.75^{c}	34.53±4.15^{c}	65.24±4.98^{a}	45.57±2.99^{b}	≤0.05
Creatinine (mg/dL)	0.50±0.05^{b}	0.53±0.04^{b}	0.76±0.07^{a}	0.57±0.06^{b}	≤0.05

a,b,c: in the same line values with different letters show statistically significant differences.
C: Control, BG: Barley grass, GM: Genatmisin, 8OHdG (8- hydroxy-2'-deoxyguanosine), TAS - Total antioxidant status; TOS - total oxidant status; OSI -oxidative stress index

TABLE 2
The scores of histological grade tubular damage in rats (n=8)

Group	0 degree	1 degree	2 degree	3 degree
Control (C)	8	0	0	0
Barley Grass (BG)	8	0	0	0
Gentamicin (GM)	0	3	5	0
Gentamicin+Barley Grass (GM+BG)	3	3	2	0

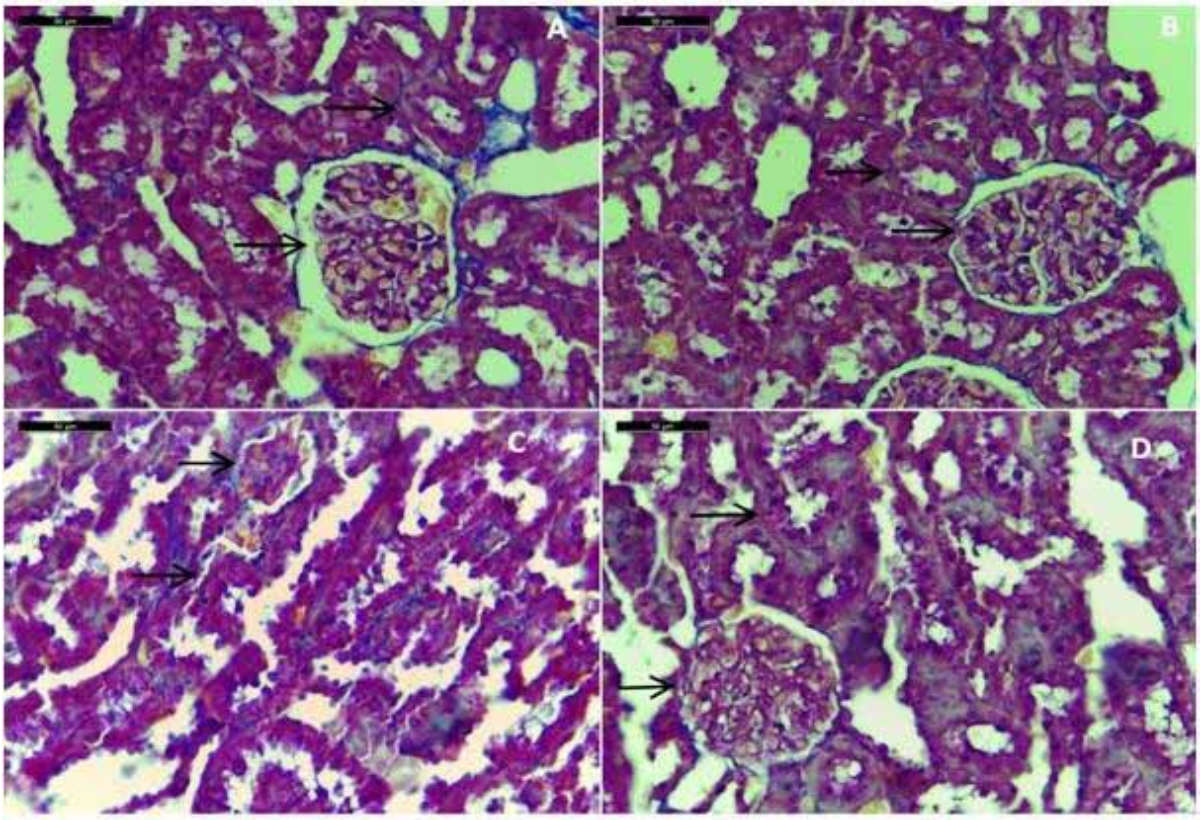

FIGURE 1
Photomicrograph of tubules proximalis and glomerulus of rat kidney section (A, B, C, D, Scala Bar 50 µm). A-Control Group: Tubules proximalis and glomerulus are normal. B-Barley Grass Group: Tubules proximalis and glomerulus are normal for rat applied barley grass (250 mg/kg) only. C-Gentamicin Group: Tubules proximalis damage eand glomerulus dejenerayon are showing for rat applied with gentamicin (80 mg/kg). D- Gentamicin + Barley Grass Group are similiar to the control goup.

tubular damage (75 % of affected tubulus) (14).

According to the histological score table were determined 37.5% 1st degree and 62.5 % 2nd degree of the rats in the GM group with kidney damage. Indeed, 37.5% of rats is similar to rats in control group, the other 37.5% 1st degree and 25% 2nd degree were showed of kidney damage in GM+BG group.

Histological changes in the kidney of rats were determined by comparing with the control group. The degenerative structure and any damage were not showed in the C group and BG group (Fig 1- A, B). The proximal tubule damage, structural changes, degeneresyon and expands in lumen of in cells of forming the wall of the tubular and abnormalities in the structure of glomerulus were determined in the GM group. (Fig 1 –C). The kidneys in groups of GM + BG were showed to be healing. The regeneration and recovery of the proximal tubule some rats in the GM+BG group was determined to be close in the control group. Furthermore, tubular epithelial cells and lumen impairments was shown to improve (Fig. 1 -D).

DISCUSSION

Gentamicin is the aminoglycoside antibiotic to be an important agent against life threatening gram negative infections [15], it may be applied single doze intravenous, intramuscular and subcutaneous in animals [16]. However, high dose gentamicin application is a major complication for nephrotoxicity [15]. It is known that the applications of gen-

tamicin 70-100 mg/kg/day for 7 days could nephrotoxicity and decline in glomerular filtration rate and increase in serum creatinine [17; 18] and urea [15; 19]. The present study indicates that high gentamicin application significantly increase in levels of serum creatinine, urea according to control group. However, these values in the GM+BG group were significantly lower than in the GM group ($p \leq 0.05$). So, BG supplement could decrease levels of serum urea and creatinine in rat with nephrotoxicity.

Reactive oxygen species (ROS) including hydroxyl radical have been implicated in the aetiology of gentamicin nephrotoxicity [20; 21; 22; 23]. In this case, ROS activity may increase and reduce the activity of antioxidant enzymes [22; 24; 25]. Free radicals can lead to loss of membrane integrity and genetic mutation [26].

In the recent years increasing interest has been observed in the role of free radicals and oxidative damage in a variety of high dose gentamicin application. In theese studies were evaluated antioxidants separately and it was determined decreases the activities of catalase (CAT), gutathione peroxidase (GSHPx), the level of glutathione (GSH) [27; 28; 29] and glutathione reductase (GR), TAS (15); but increase lipid peroxidation MDA [27; 29]. However, there was no difference in SOD activity in gentamicin nephrotoxicity rats [25; 29].

Some antioxidants can protective of this toxicity [30]. Endogenous antioxidants can partial protect the body against reactive oxygen species, so it is necessary to take extra antioxidants from the outside. Some plants has excess antioxidant enzymes [31]. There are growing interests in barley products due to their high content of phenolic compounds such as phenolic acids, proanthocyanidins, tannins, flavonols, chalcones, flavones, and amino phenolic compounds [32].

There are some studies which decrease of oxidants such as MDA and increase of antioxidants such as GSH, GSH -Px, SOD, CAT of barley grass extract [12;33;34]. But according to our knowledge, there are no published reports effect of barley grass on serum oxidative stress parameters such as TAS-TOS, OSI DNA damage and renal histological examination in rats with nefrotoxicity. Thus our results provide the first data about the effects of BG supplementation on serum TAS-TOS, OSI DNA damage and renal histological examination in rats with nefrotoxicity.

In this study the levels of serum TOS ($p \leq 0.05$) and OSI ($p \leq 0.01$) were significantly decreased while the level of serum TAS ($p \leq 0.05$) was significantly increased in BG and GM+BG groups compared to the control. There was no difference the level of serum 8OHdG among the groups, but it was higher in GM group than other groups.

Indeed, oxidative DNA damage at low levels can effectively repaire with minimal risk of error [35]. The H_2O_2, such as O_2, does not directly damage in DNA. To be effective on DNA of OH radicals must be formed in DNA or it's very close [36].

Gentamicin accumulates in the proximal renal tubular and leads to membrane damage or renal toxicity [19]. In another studies on renal histological examination reported that gentamicin causes especially varying degree of damage and damage in proximal tubules [15; 29; 37], decrease in glomerular filtration [18]. In this study proximal tubule necrosis, structural changes, degeneresyon and expands in lumen of in cells of forming the wall of the tubular and abnormalities in the structure of glomerulus were determined in the (GM) group while were displaying to be healing kidneys of rats in GM+BG group.

CONCLUSIONS

In the present study renal damage produced by gentamicin was confirmed by histological examination of the kidneys. BG decreased widespread damage to the renal glomerulus and proximal tubulus.

As a result we have tested that BG may reduce levels of serum urea, creatinine, TOS and OSI while increases TAS in rat with gentamicin nefrotoxicity. BG is also protective to renal glomerular and tubular damage. So we think that adverse effects of high-dose gentamicin application such as kidney damage can be reduced when used barley grass.

ACKNOWLEDGEMENTS

This study was supported by Yuzuncu Yil University Grant Commission of research numbered with YYUBAP- 2015-VF-B011 and it was presented at International Congress on Applied Biological Sciences, September 16-20, 2015, Skopje-Makedonya.

Conflict of interest statement. The authors declare that there is no conflict of interests regarding the publication of this article.

REFERENCES

[1] Dinler, B.S., Turkan, I., Sekmen, A.H., Konakcı, C.O. (2010) The role of ntioxidant defense systems at differential salt tolerance of *Hordeummarinum Huds*. (sea barleygrass) and *Hordeum vulgare L.* (cultivated barley), *Env and Exp Botany,* 69, 76–85.

[2] Henderson, B. (2007) Cancer-Free: Your Guide to Gentle Non-Toxic Healing, 2nd ed. Booklocker.com: Bangor, ME, USA.

[3] Acar, O., Turkan, I., Ozdemir, F. (2001) Superoxide dismutase and peroxidase activities in drought sensitive and resistant barley (*Hordeum vulgare* L.) varieties. *Acta Physiologiae Plantarum*, 23, 351–356.
[4] Nagai, J., Takano, M. (2004) Molecular aspects of renal handling of aminoglycosides and strategies for preventing the nephrotoxicity. *Drug Metab Pharm*, 19,159–70.
[5] Ali, B.H., Al-Wabel, N., Mahmoud, O., Mousa, H.M., Hashad, M. (2005) Curcumin has a palliative action on gentamicin-induced nephrotoxicity in rats. *Fundam Clin Pharmacol*, 19, 473-477.
[6] Tulkens, P.M. (1999) Nephrotoxicity of aminoglycoside antibiotics. *Toxicol Lett,* 46, 727–37.
[7] Erel, O. (2004) A novel automated direct measurement method for total antioxidant capacity using a new generation, more stable ABTS radical cation. *Clin Biochem,* 37, 277-285.
[8] Erel, O. (2005) A new automated colorimetric method for measuring total oxidant status. *Clin Biochem*, 38, 1103-1111.
[9] Yang J.L., Weissman, L., Bohr, V.A., Mattson, M.P. (2008) Mitochondrial DNA damage and repair in neurodegenerative disorders. *DNA Repair,* 7, 1110–1120.
[10] Burçak, G., Andican, G. (2004) Oxidative DNA damage and aging. *Cerrahpaşa J Med.,* 35, 159-169.
[11] Ozbek, E. (2012) Induction of oxidative stress in kidney. *Int J Nephrol,* 1-9.
[12] Shah, J.G., Patel, B.G., Patel, S.B., Patel, R.K. (2012) Antiurolithiatic and antioxidant activity of *Hordeum vulgare* seeds on ethylene glycol-induced urolithiasis in rats. *Indian J Pharmacol*, 44(6), 672–677.
[13] Bancroft, J.D., Cook, H.C. (1984) Manuel of Histological Tecniques, Churchill Livingstone Inc. New York.
[14] Karadeniz, A., Yıldırım, A., Şimşek, N., Kalkan, Y., Çelebi, F. (2008) Spirulina platensis protects against gentamicin-induced nephrotoxicity in rats. *Phytotherapy Research*, 22, 1506-1510.
[15] Chetankumar, R.A., Hetal, N.T., Vajpeyee, S.K. (2013) A study of oxidative stress in gentamicin induced nephrotoxicity and effect of antioxidant vitamin C in Wistar rats. *Natl J Physiol Pharm Pharmacol,* 3, 1, 14-20.
[16] Filazi, A., Sireli, U.T., Pehlivanlar-Onen, S., Cadırcı, Ö., Aksoy, A. (2013) Comparative pharmacokinetics of gentamicin in laying hens. *Kafkas Univ Vet Fak Derg*, 19, 3, 495-498.
[17] Khan, S.A., Priyamvada, S., Farooq, N., Khan, S, Khan, M., Yusufi, ANK. (2009) Protective effect of green tea extract on gentamicin-induced nephrotoxicity and oxidative damage in rat kidney. *Pharm Res*, 59, 254–262.
[18] Derakhshanfar, A., Bidadkosh, A., Hashempour Sadeghian, M. (2009) L-methionine attenuates gentamicin nephrotoxicity in male Wistar rat: pathological and biochemical findings. *Iranian J of Vet Res*, 10, 4, 323-328.
[19] Humes, H.D., Weinberg, M. (1986) Toxic nephropathies in the kidney Eds. BM Brenner, FC Rector p. 1491, WB Saunders Co, Philadelphia.
[20] Ramsammy, L.S., Josepovitz, C., Ling, K.Y., Lane, B.P., Kaloyanides, G.J. (1986) Effects of diphenyl-phenylenediamine on gentamicin-induced lipid peroxidation and toxicity in rat renal cortex. *J Pharmacol Exp Ther*, 238(1), 83-8.
[21] Walker, P.D., Shah, S.V. (1988) Evidence suggesting a role for hydroxyl radical in gentamicin-induced acute renal failure in rats. *J Clin Invest*. 81, 334-341.
[22] Cuzzocrea, S., Mazzon, E., Dugo, L., Serraino, I., Di Paola, R., Britti, D., De Sarro, A., Pierpaoli, S., Caputi, A., Masini, E., Salvemini, D. (2002) A role for superoxide in gentamicin mediated nephropathy in rats. *Eur J Pharmacol*, 450, 67-76.
[23] Parlakpinar, H., Tasdemir, S., Polat, A., Bay-Karabulut, A., Vardi, N., Ucar, M., Acet, A. (2005) Protective role of caffeic acid phenethyl ester (cape) on gentamicin-induced acute renal toxicity in rats. *Toxicology*, 14, 207(2), 169-77.
[24] Maldonado, P.D., Barrera, D., Medina-Campos, O.N., Hernández-Pando, R., Ibarra-Rubio, M.E., Pedraza-Chaverri, J. (2003) Aged garlic extract attenuates gentamicin induced renal damage and oxidative stress in rats. *Life Sci*, 73, 2543-2556.
[25] Pedraza-Chaverri, J., González-Orozco, A.E., Maldonado, P.D., Barrera, D., Medina-Campos, O.N., Hernández-Pando, R. (2003) Diallyl disulfide ameliorates gentamicin-induced oxidative stress and nephropathy in rats. *Eur J Pharmacol*, 473, 71-78.
[26] Vincent, M., Russell, W., Low, P., Feldman, E. (2004) Oxidative stress in the pathogenesis of diabetic neuropathy, *Endocrine Reviews*, 25, 612-628.
[27] Sandhya, P., Varalakshmi, P. (1997) Effect of lipoic acid administration on gentamicin-induced lipid peroxidation in rats. *J Appl Toxicol*, 17, 405-408.
[28] Soejima, A., Ishizuka, S., Suzuki, M., Miyake, N., Fukuoka, K., Nagasawa, T. (1998) Biochemical renal manifestations induced by consecutive administration of gentamicin in rats. *Nephron*, 80, 331-339.
[29] Farombi, E.O., Ekor, M. (2006) Curcumin attenuates gentamicin-induced renal oxidative damage in rats. *Food Chem Toxicol*, 44(9), 1443-1448.

[30] Kavutcu, M., Canbolat, O., Oztürk, S., Olcay, E., Ulutepe, S., Ekinci, C., Gökhun, I.H., Durak, I. (1996) Reduced enzymatic antioxidant defense mechanism in kidney tissues from gentamicin-treated guinea pigs, effects of vitamins E and C. *Nephron*, *72 (2),* 269-74.
[31] Osawa, T., Yoshida, A., Kawakishi, S., Yamashita, K., Ochi, H. (1995) Oxidative stress, antioxidants, aging and disease. In "Oxidative Stress and Aging," ed. by R.G. Cutler, L. Packer, J. Bertram, and A. Mori. Birkhauser Verlag, Basel/Switzerland. 367-377.
[32] Goupy, P., Hugues, M., Boivin, P., Amiot, M.J. (1999) Antioxidant composition and activity of barley (*Hordeum vulgare*) and malt extracts and of isolated phenolic compounds. *J Agr Food Chem,* 79, 1625–1634.
[33] Sato, K., Osawa, T. (2010) Dietary supplementation with pearl barley (*adlay, coix lacryma-jobi l. var ma-yuen stapf*) extract ıncreases oxidation resistance in the liver of rats ex vivo. *Food Sci. Technol. Res*, 16 (6), 613 – 616.
[34] Yang, Q., Pan, X., Kong, W., Yang, H., Su, Y., Zhang, L., Zhang, Y., Yang, Y., Ding, L., Liu, G. (2010) Antioxidant activities of malt extract from barley (*Hordeum vulgare L.*) toward various oxidative stress in vitro and in vivo. *Food Chemistry*, 118, 84–89.
[35] Halliwell, B., Gutteridge, J.M.C. (1999) Free Radicals in Biology and Medicine. 3rd ed. Oxford University Press. Inc, London.
[36] Cooke, M.S., Evans, M.D., Dizdaroglu, M., Lunec, J. (2003) Oxidative DNA damage: Mechanisms, mutation, and disease. *FASEB J*. 17, 1195-1214.
[37] Maxie, M.G., Newman, S.J. (2007) Urinary system. In Pathology of Domestic Animals, 5th ed. (Jubb KVF, Kennedy PC, Palmer N, eds.), Vol. 2, p. 438. Elsevier, Saunders, PA.

Received: **25.05.2017**
Accepted: **29.07.2017**

CORRESPONDING AUTHOR

Bahat Comba
Hitit University, Alaca Avni Celik Vocational High School, Departmant of Veterinary, Corum, Turkiye

e mail: bahatcomba@hotmail.com

© by PSP Volume 26 – No. 10/2017 pages 6141-6148 Fresenius Environmental Bulletin

EFFECTS OF FENBUTATIN OXIDE ON ANTIOXIDANT SYSTEM OF DIFFERENT TISSUES IN *Cyprinus carpio* (L., 1758)

Ferbal Ozkan-Yilmaz[1,*], Arzu Ozluer-Hunt[1], Suna Gul Gunduz[1], Mehmet Berkoz[2], Serap Yalin[3], Metin Yildirim[3]

[1]Mersin University Faculty of Fisheries, Mersin, Turkey
[2]Yuzuncu Yil University, Faculty of Pharmacy, Van, Turkey
[3]Mersin University, Faculty of Pharmacy, Mersin, Turkey

ABSTRACT

In this study, effects of sublethal concentrations of fenbutatin oxide on catalase (CAT) and superoxide dismutase (SOD) activities and lipid peroxidation in muscle, liver, kidney and brain tissues of *Cyprinus carpio* were investigated. The 96-hours LC_{50} value for fenbutatin oxide was determined as 1.544 mg/L for *C. carpio* in this study. 0.15 mg/L (1/10 of LC_{50}) and 0.30 mg/L (1/5 of LC_{50}) sublethal concentrations were applied for 96 h (4 days) in this experiment. The CAT activities in tissues were increased relation to doses applied. The SOD activities were decreased by 0.30 mg/ L. The tissue MDA levels were significantly increased in relation to dose applied.

KEYWORDS:
Cyprinus carpio, fenbutatin oxide, oxidative stress, lipid peroxidation.

INTRODUCTION

Fenbutatin oxide, (bis[tris(2-methyl-2-phenylpropyl)tin] oxide; FBTO) is an organotin acaricide with the molecular formula $C_{60}H_{78}OSn_2$. FBTO is very toxic to fish and accumulates in tissues, and it is also very toxic to aquatic organisms [1]. The accumulation and eco-toxicological effects of organotins along the food chain requires a whole classification of organotin levels tissue of organisms of lower and higher trophic stages [2].

Organotin compounds (OTCs) are one of the most widely used organometallic compounds. Over the last several decades, they have been utilized for a variety of industrial and agricultural applications including pesticides, fungicides and anti-fouling agents [3]. They are composed of an atom of tin that is covalently bonded to one or more organic chains and another functional group, such as chloride, oxide, or hydroxide, which are represented by methyl, butyl, octyl, and phenyltin groups [4]. OTCs are immunotoxic both in invertebrates and vertebrates. Mitochondria and membrane functions seem to be a preferred target of these lipophilic pollutants. The inhibition of key membrane-bound enzyme complexes such as Na, K-ATPases, accompanied by perturbation of hydromineral balance, membrane potential and bioenergetics, has been reported [5]. OTCs could be included in other biological routes occurring in cells, specifically in peroxide oxidation of lipids. The latter process is very important from the viewpoint of physiology, and it follows a radical chain mechanism. Acceleration of peroxide oxidation of lipids in cells leads to accumulation of hydroperoxides, degeneration of cell membranes, and various pathologies in organisms [6].

Reactive oxygen species (ROS), such as superoxide anion radicals, hydrogen peroxide, and hydroxyl radicals, are continuously formed in oxygen-consuming organisms. Exposure to xenobiotics or toxic chemical pollutants may produce an imbalance between these endogenous and exogenous ROS and can subsequently induce a decrease in antioxidant defenses or cause oxidative damage outright in organisms [7]. Defence systems that tend to inhibit ROS formation include the antioxidant enzymes such as catalase (CAT; EC 1.11.1.6), superoxide dismutase (SOD; EC 1.15.1.1) [8]. Lipid peroxidation (LPO) has also been used as a bioindicator of oxidative damage in aquatic organisms exposed in polluted environmental conditions. LPO can be increased in the tissues of fish, as indicated by an increased production of malondialdehyde (MDA). The most widely used test for oxidative stress is the measurement of MDA, a product of lipid peroxidation, by the thiobarbituric acid (TBA)-reacting substances assay [7].

Fish have been widely used as models to evaluate the health of aquatic ecosystems in toxicologic pathology [9]. In the present study, *Cyprinus carpio* was chosen as an experiment model, because of its wide availability and suitability for toxicity testing. We have studied the effects of sublethal concentrations of FBTO (0.15 and 0.30 mg/L) for 96 hours on oxidative stress biomarkers in muscle, liver, kidney and brain tissues of *C. carpio*.

MATERIALS AND METHODS

Chemicals. Fenbutatin oxide, (bis[tris(2-methyl-2-phenylpropyl)tin] oxide) was purchased as the Pestanal grade chemical (Sigma-Aldrich). The chemicals used for enzyme activity measurements were purchased from Sigma-Aldrich.

Toxicity test. For the toxicity tests, groups containing 10 fish were placed into glass aquarium. Fish were starved 2 days before the beginning of the experiments. Fish were divided into control and test groups. Different concentrations of FBTO were applied (0.05, 0.10, 0.50, 1.00, 1.50, 2.00 mg/L). During the 96-h experiment, the water was aerated continuously. Each test solution was renewed daily. The dead fish were removed and recorded. At the end of the experiment, median lethal concentrations (LC_{50}) were determined for 96-h. The LC_{50} values were calculated by probit analysis using SPSS Version 15.0 software. The 96-h LC_{50} value for *C. carpio* was determined as 1.544 mg/L for in this study.

Test animals and treatment. *Cyprinus carpio* (mean weight: 19.00±0.90 g; mean length 9.90±0.30 cm) were obtained from Mersin University, Fisheries Faculty, Aquaculture Department and transferred to laboratory to where the temperature was kept at 23±2°C (12:12 L:D). Throughout the experiments, dechlorinated tap water with pH value of 7.85, an alkalinity of 326 mg/L $CaCO_3$, and oxygen concentration of 6.70 mg/L was used. The fish were allowed to acclimatize to these conditions for 2 weeks. The fish were fed at a rate of 2% body weight/day with a commercial pellet diet (Camli-Yem, Izmir-Turkey) during the acclimation period. Experiments were conducted in glass aquaria containing 100 L test solution. Fish were exposed to 0.15 (1/10 of LC_{50}) and 0.30 (1/5 of LC_{50}) mg/L sublethal concentrations of fenbutatin oxide for 96 h (4 days). Stock solution was prepared by fenbutatin and diluting it in acetone to give the dosing concentrations. The water was refreshed every 2 days to compensate for the pesticide lost in the exposure medium.

Twenty-four fish were divided into three experimental groups (n: 8 in each group), as follows: Control (Cont) group; Treatment1 (T1) group (0.15 mg/L FBTO) and Treatment2 (T2) group (0.30 mg/L FBTO). The control group was exposed to acetone at the highest concentration of stock solution used in the fenbutatin oxide-exposed groups (the absence of insecticide). At the end of exposure period, eight fish were removed from each tank, and killed by transaction of the spinal cord. The muscle, liver, kidney and brain tissues of both control and treated fish were dissected. Tissues were homogenized to 1/5 (w/v) ratio in physiological saline solution (0.8 % NaCl) with homogenizer and then centrifuged at 13.500 rpm for 10 min in a Sigma 2-16K centrifuge at +4 ºC, and supernatant was used for biochemical analyses.

Enzyme Assays. The CAT activities of liver tissues were determined according to the method of Aebi [10]. The enzymatic decomposition of H_2O_2 was followed directly by the decrease in absorbance at 240 nm. The difference in absorbance per unit time was used as a measure of CAT activity. The enzyme activities are given in U/mg protein.

The SOD activity was measured by the inhibition of nitroblue tetrazolium (NBT) reduction due to O_2 generated by the xanthine/xanthine oxidase system [11]. One unit of SOD activity was defined as the amount of protein causing 50% inhibition of the NBT reduction rate. The reduction in NBT by superoxide anion to blue formazan was measured at 560 nm. The enzyme activities are given in U/mg protein.

Measurement of MDA levels. The levels of MDA homogenized tissue, as an index of LPO, were determined by TBA reaction using the method of Yagi [12]. Malondialdehyde and other aldehydes when boiled with thiobarbituric acid at acid pH give a pink-colored product that can be assayed spectrophotometrically. Briefly, a 50 µL of tissue homogenate was mixed with 750 µL of TBARS reagent. The mixture was incubated for 30 min in a boiling water bath. After cooling, the mixture was centrifuged at 3,500 rpm for 15 min. Absorption was measured at 532 nm, and the values are expressed as nanomoles of MDA/mg protein.

Protein determination. The tissue protein contents were measured only to determine the specific activity of antioxidant enzymes according to the method developed by Lowry et al. [13] using bovine serum albumin as standard. Absorbance of samples were measured at 750 nm wavelength by spectrophotometer.

Statistical analysis. The LC_{50} values were calculated by probit analysis using SPSS Version 24.0 software (SPSS Inc., USA). Data were presented as mean±standard error of the mean (SEM) and analyzed by one-way analysis of variance (ANOVA). The significant means were compared by Duncan's multiple range tests at $p<0.05$.

RESULTS

Toxicity Assay. In the present study, different concentrations of FBTO were administrated to *C. carpio*. The mortality rates of fish were calculated as a percentage after 96 hours of insecticide treatment. The mortality of *C. carpio* increased depending on the dose of fenbutatin oxide. The data were obtained from the toxicity test was evaluated using the Probit Analysis Method. The LC_{50} 96 h value for *C. carpio*

was found to be 1.544. 95% confidence limits were between 1.331-1.806 mg/L (Table 1).

Biochemical Assay. The CAT activities in tissues of fish were given in Fig. 1. FBTO did not make any significant changes in muscle tissue enzyme activity compared to control. The CAT activity of liver and brain were significantly increased (P<0.05) by 0.15 and 0.30 mg/L concentrations of FBTO, but, in kidney tissue were significantly increased (P<0.05) by 0.30 mg/L. 0.30 mg/L concentration caused a significant elevation by 46%, 34% and 44% (P<0.05), respectively, in liver, kidney and brain tissues compared to control.

The SOD activities in tissues of fish were shown in Fig. 2. FBTO did not make any significant changes in muscle tissue SOD activities compared to control. 0.30 mg/L concentration of FBO caused a significant inhibition (P<0.05) by 28% and 16% respectively, in liver and brain tissues compared to control. The SOD activity in kidney was increased (26%) by 0.30 mg/L.

TABLE 1
96 hours toxicity results of the fenbutatin oxide bioassay on *C. carpio*
(LC: Lethal concentration; SE: Standart Error)

Points of Lethal Concentration	Concentration (mg/L)	95% Confidences Limits (mg/L)	Intercept±SE
LC 1.00	0.579	0.325-0.768	1.030± 0.249
LC 5.00	0.771	0.505-0.959	
LC 10.00	0.899	0.637-1.083	
LC 30.00	1.238	1.010-1.428	
LC 50.00	**1.544**	**1.331-1.806**	
LC.80.00	2.203	1.873-2.915	
LC.90.00	2.653	2.181-3.843	
LC 99.00	4.123	3.006-7.565	

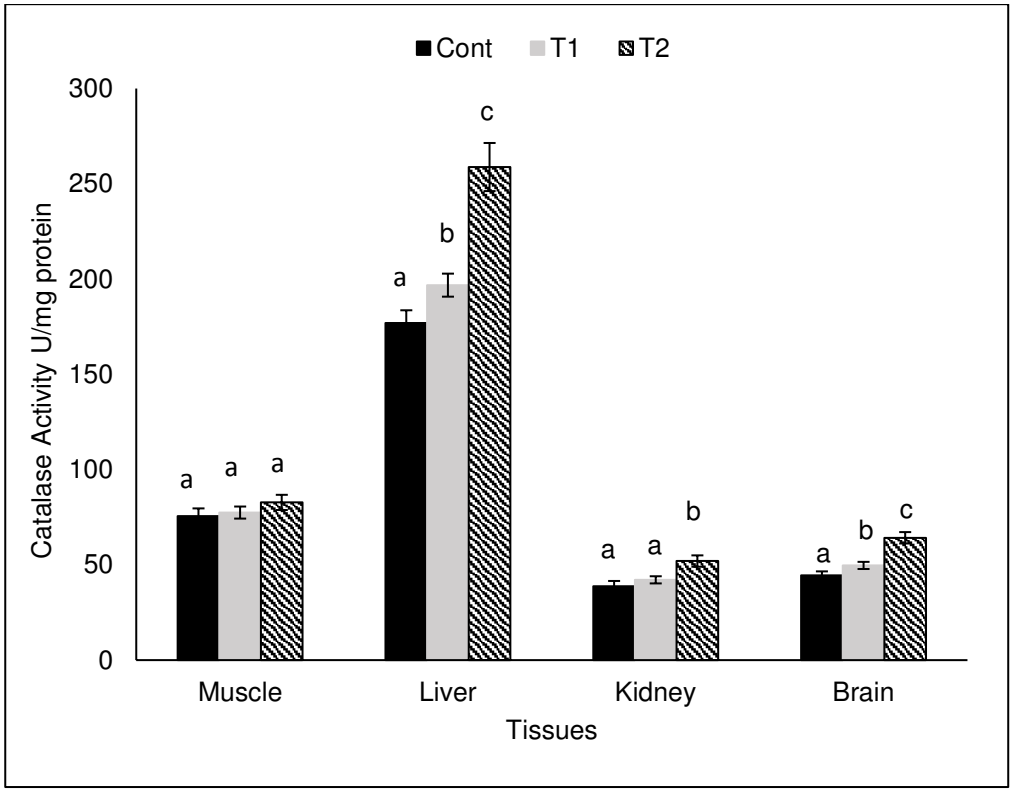

FIGURE 1
CAT activities in tissues of *C. carpio* exposed to sublethal concentrations of FBTO; 0.15 mg/L (T1) and 0.30 mg/L (T2). Each value is the mean ± standard error (n = 8). Multiple comparisons were made separately for each tissue and means with different superscript in tissues are significantly different (P< 0.05).

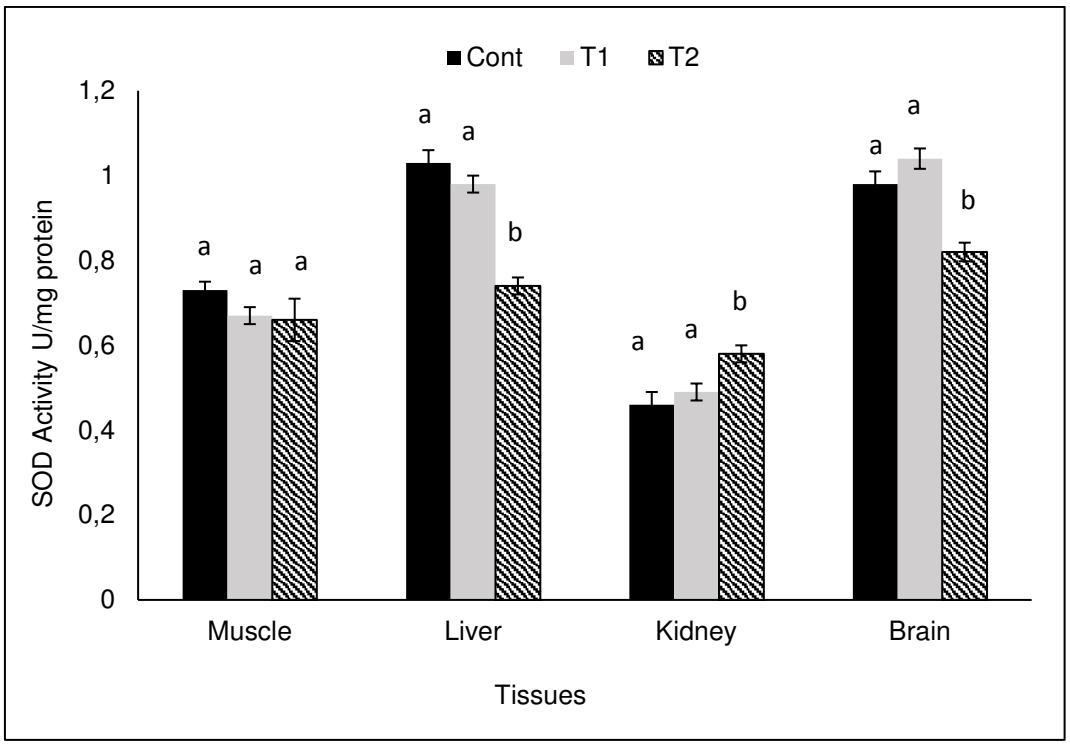

FIGURE 2
SOD activities in tissues of *C. carpio* exposed to sublethal concentrations of FBTO; 0.15 mg/L and 0.30 mg/L. Each value is the mean ± standard error (n = 8). Multiple comparisons were made separately for each tissue and means with different superscript in tissues are significantly different (P< 0.05).

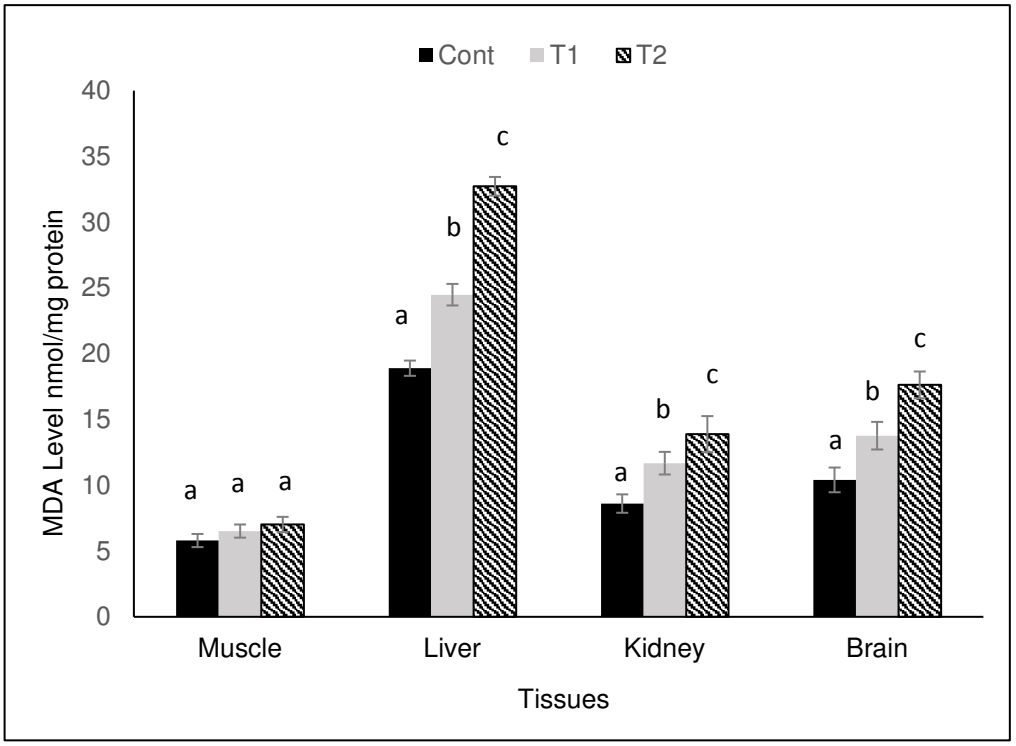

FIGURE 3
MDA levels in tissues of *C. carpio* exposed to sublethal concentrations of FBTO; 0.15 mg/L (T1) and 0.30 mg/L (T2). Each value is the mean ± standard error (n = 8). Multiple comparisons were made separately for each tissue and means with different superscript in tissues are significantly different (P< 0.05).

The levels of MDA in tissues were given in Fig. 3. The MDA levels of tissues (except muscle) were significantly increased ($P<0.05$) by both of concentrations of insecticide. 0.30 mg/L concentration of FBTO caused a significant elevation by 73%, 61% and 70% respectively, in liver, kidney and brain tissues compared to control.

DISCUSSION

Fenbutatin oxide is one of the toxic insecticide for fish. The 48-h LC_{50} values of FBTO for fish have been determined to be 1.70 µg/L for rainbow trout, 2.8 µg/L for mysid shrimp [1]. There is no data about LC_{50} values of this pesticide for *C. carpio* in previous studies. The 96-h LC_{50} value for FBTO was determined as 1.544 mg/L for *C. carpio* in this study. The different sensitivity of fish may be due to differences of sensitivity of enzymes activation [14] and species, strain, age, and sex of the animal, the dose and route of exposure, and the effect of various environmental, nutritional and physiological factors [15]. As a result of the ecological risk assessment for the 1994 Reregistration Eligibility Decision (RED), the agricultural use of FBTO was classified as restricted use due to high acute toxicity to aquatic organisms [16].

The antioxidant system responses constitute important sensors in connecting the pollutant effects and the metabolic alteration in aquatic organisms [17]. In general, the measurement of enzyme activities can provide an indication of the antioxidant status of fish and can also serve as biomarkers of oxidative stress [8]. In the present study, we observed an increase in CAT activities of liver, kidney and brain tissues following 96 h of toxicity by FBTO concentrations. SOD activities were decreased in liver and brain tissues but increased in kidney. There is no data on the effects of FBTO on antioxidant defence systems in fish. Also, there are limited data on the toxicity of OTCs in fish. Zhang et al. [18] showed that with an increase in tributyltin (TBT: one of the organotin) dose, the activities of total SOD, CAT and glutathione peroxidase (GSH-Px) in liver of *Danio rerio* were significantly decreased compared to the control. Conversely, Wang et al. [19] reported that hepatic SOD and CAT activities were significantly induced when *Sebastiscus marmoratus* were exposed to TBT for 4 days. Wang et al. [20] showed that GST activity was induced by the lower doses of TBT, while it tended to be inhibited by the higher doses of TBT. Al-Ghais and Ali [21] showed that organotin compounds (tributyltin :TBT, triphenyltin; TPT, and dibutyltin; DBT) inhibited Glutathion-S-Transferase (GST) activities of liver and kidney in *Siganus canaliculatus* and *Sparus sarba*. SOD activities in brain of *C. carpio* were slightly increased in lower concentration group and significantly decreased in the highest concentration of the TBT [22]. Compared with the control, a significant lower CAT activity was observed in fish exposed to higher concentrations [22]. Researchers have explained that the same chemical having opposite effects may be related to the differences of fish species, exposure condition and concentrations of TBT [18]. The toxicity level of OTCs may be related to its concentration, the timing of exposure, bioavailability, and sensitivity of the biota, as well as to the persistence of various compounds in the environment [4].

Similar results have also been reported in other fish species exposed to different pesticides. Zhang et al. [23] observed that CAT activity in the liver of *C. auratus* were increased although SOD activity was inhibited gradually with 2,4-dichlorophenol concentration increasing. Thomaz et al. [24] reported that CAT activity was increased and SOD activity was decreased in liver of *O. niloticus* exposed to the insecticide trichlorfon for 96 h. Lushchak et al. [25] found that the activity of CAT in liver and kidney of *C. auratus* was elevated by exposure to glyphosate. Exposure to methyl parathion resulted in a significant induction of CAT activity in *Brycon cephalus* liver [26]. Özkan et al. [27] reported that an increase in CAT activity following 96 h of toxicity by chlorpyrifos concentrations but a decrease SOD activity of liver tissue in *O. niloticus*. CAT and SOD enzymes have related functions. SOD catalyzes the dismutation of the superoxide anion radical to H_2O and H_2O_2, which is detoxified by both CAT and GSH-Px activities. Due to the inhibitory effects on ROS formation, the SOD–CAT system provides the first defense line against oxygen toxicity and usually used as an indirect biomarker indicating ROS production [8, 28]. An increase in CAT enzyme activity is probably a response toward increased ROS generation in pesticide toxicity [26]. Usually, an induction of tissue SOD activities was observed when exposed to organic pollutant [29]; however, the excess production of superoxide radicals or after their transformation to H_2O_2 causes an oxidation of the cysteine in the enzyme and deactivates SOD [20]. The decreased antioxidant enzymes result in increased oxidative stress, an indication of impaired antioxidant defense mechanism due to excessive generation of free radicals generated by pesticide [31]. The toxicity of FBTO in present study may be caused by the unbalance between free radicals and antioxidants, which might have resulted in inhibition of SOD activity.

The activity of the antioxidant enzymes could be increased or inhibited by xenobiotic exposure depending on the intensity and the duration of the stress applied, as well as the susceptibility of the exposed species. It is not a general rule that an increase in xenobiotic concentrations induces antioxidant activity [32]. Antioxidant enzymes also show tissue-specific differences in activities that reflect the functions of the tissues and the oxidative stress load that they ex-

perience [25]. In the present work, the studied enzymes responded in a different level in liver, kidney and brain tissues. The response of antioxidant system to oxidative stress in various tissues shows differences from one species to another due to the differences in free radical generation and different antioxidant potential of these tissues.

In this study, lipid peroxidation end product MDA were significantly elevated in liver, kidney and brain tissues of *C. carpio* exposed to FBTO compared with control group. Previous investigations have reported on the induction of LPO in the tissues by different OTCs. Li et al. [22] reported that a significant evaluation in MDA level in brain of *C. carpio* exposed to TBT when compared with the control. Wang et al. [20] found *Sebastiscus marmoratus* exposed to TBT for up to 7 days showed a rise in liver MDA level. MDA content was significantly increased with TBT exposure in liver of *D. rerio* [18]. Earlier investigations have reported on the induction of LPO in the tissues by different pesticides Ozkan-Yilmaz et al. [33] found that MDA levels were increased in the liver of methidathion-treated in *O. niloticus*. Hai et al. [34] reported that level of LPO was elevated in liver and brain of catfish (*Ictalurus nebulosus*) exposed to dichlorvos. Lipid peroxidation is the reaction of oxidative deterioration of membrane polyunsaturated fatty acids (PUFA). Fish tissues are characterized by high concentration of PUFA and may therefore be susceptible to lipid peroxidation [35]. Pesticide exposure could produce free radicals, which resulted in the increase in lipid peroxidation. The increase in lipid peroxidation may be attributed to alterations in the antioxidant defense system [36]. An increase in the MDA levels of tissues might be induced by the possible involvement of ROS in FBTO induced toxicity. In the present work, elevation of the MDA contents may be due to the fact that when the amount of ROS and other radicals exceeds the capacity of antioxidant enzymes. Excess production of radicals may increase in ROS level, while a rise in ROS may increase lipid peroxidation, as measured by MDA intensity [18]. Our results showed that the capacity of FBTO to produce lipid peroxidation.

In the present work, antioxidant enzymes responded in a different level in muscle, liver, kidney and brain tissues. The response of antioxidant system to oxidative stress in various tissues shows differences from one species to another due to the differences in free radical generation and different antioxidant potential of these tissues [37]. In this study, liver tissue was found to be more sensitive than other tissues. In the previous studies, it was found that liver was a more sensitive target organ to OTCs oxidative damage than kidney and muscle [38]. Also, it has been reported that organotin compounds accumulation at higher levels in liver than in most other organs [2, 39].

CONCLUSION

Fenbutatin oxide exposure can induce significant changes in activities CAT, SOD and MDA levels in the tissues of the *C. carpio*. The increasing doses are essential factors when evaluating oxidative stress responses caused by sublethal concentrations of FBTO in liver, kidney and brain tissues of fish. Compared to liver, muscle, kidney and brain was more sensitive to the oxidative damage.

The aquatic environment is contaminated by a number of foreign chemical. Fish antioxidant responses are very sensitive to environmental contamination. These are used as a biological indicator of aquatic environmental health. There is limited available data on OTCs toxicity in animals. For this reason, more detailed research is needed to explain the mechanism.

REFERENCES

[1] Environmental Protection Agency (EPA) (1994) Reregistration eligibility decision for fenbutatin oxide. September, United States EPA-738-F-94-021.

[2] Antizar-Ladislao, B. (2008) Environmental levels, toxicity and human exposure to tributyltin (TBT)-contaminated marine environment: a review. Environ. Int., 34: 292-308.

[3] Buck-Koehntop, B., Porcelli, F., Lewin, J.L., Cramer, C.J., Veglia, G. (2006) Biological chemistry of organotin compounds: interactions and dealkylation by thiols. Journal of Organometallic Chemistry, 691: 1748-1755.

[4] Graceli, J.B., Sena, G.C., Lopes, P.F.I., Zamprogno, G.C., da Costa, M.B., Godoi, A.F.L., Dos Santos, D.M., de Marchi, M.R.R., Dos Santos Fernandez, M.A. (2013) Organotins: a review of their reproductive toxicity, biochemistry, and environmental fate. Reprod. Toxicol., 36: 40-52.

[5] Pagliarani, A., Nesci, S., Vittoria Ventrella, V. (2013) Toxicity of organotin compounds: Shared and unshared biochemical targets and mechanisms in animal cells. Toxicology in Vitro, 27: 978-990.

[6] Pellerito, C., Nagy, L., Pellerito, L., Attila Szorcsik, A. (2006) Biological activity studies on organotin(IV)n+ complexes and parent compounds Journal of Organometallic Chemistry. 691: 1733-1747.

[7] Valavanidis, A., Vlahogianni, T., Dassenakis, M., Scoullos, M. (2006) Molecular biomarkers of oxidative stress in aquatic organisms in relation to toxic environmental pollutants. Ecotox. Environ. Safe. 64: 178-189.

[8] Van der Oost, R., Beyer, J., Vermeulen, N.P. (2003) Fish bioaccumulation and biomarkers in

environmental risk assessment: a review. Environ. Toxicol. Pharmacol. 13: 57-149.

[9] Peixoto, F., Alves-Fernandes, D., Santos, D., Fontainhas-Fernandes, A. (2006) Toxicological effects of oxyfluorfen on oxidative stress enzymes in tilapia *Oreochromis niloticus*. Pestic. Biochem. Phys., 85: 91-96.

[10] Aebi, H. (1974) Catalase. In: Bergmayer, H.U. (ed.) Methods of enzymatic analysis, Academic Press, New York, pp 671-684.

[11] Sun, Y., Oberley, L.W., Ying, L. (1988) A simple method for clinical assay of superoxide dismutase. Clin. Chem., 34: 497-500.

[12] Yagi, K. (1998) Simple procedure for specific enzyme of lipid hydroperoxides in serum or plasma. Methods in Mol. Biol., 108: 107-110.

[13] Lowry, O.H., Rosebrough, N.J., Farr, A.L., Randall, R.J. (1951) Protein measurement with folin phenol reagent. J. Biol. Chem., 193: 265-275.

[14] Gungordu, A. (2013) Comparative toxicity of methidathion and glyphosate on early life stages of three amphibian species: *Pelophylax ridibundus*, *Pseudepidalea viridis*, and *Xenopus laevis*. Aquat. Toxicol., 140-141: 220-228.

[15] Buhler, D.R., Williams, D.E. (1988) The role of biotransformation in the toxicity of chemicals. Aquat. Toxicol., 11: 19-28.

[16] Environmental Protection Agency (EPA) (2002) Fenbutatin oxide analysis of risks to endangered and threatened salmon and steelhead, Environmental field Branch Office of Pesticide Programs, November 29, 112 p.

[17] Lushchak, V.I. (2011) Environmentally induced oxidative stress in aquatic animals. Aquatic Toxicology, 101: 13-30.

[18] Zhang, C.N., Zhang, J.L., Ren, H.T., Zhou, B.H., Wu, Q.J., Sun, P. (2017) Effect of tributyltin on antioxidant ability and immune responses of zebrafish (*Danio rerio*). Ecotoxicology and Environmental Safety, 138: 1-8.

[19] Wang, C.G., Chen, Y.X., Li, Y., Wei, W., Yu, Q. (2005) Effects of low dose tributyltin on activities of hepatic antioxidant and phase II enzymes in *Sebastiscus marmoratus*. Bull. Environ. Contam. Toxicol., 74 (1): 114-119.

[20] Wang, C., Zhao, Y., Zheng, R., Ding, X., Wei, W., Zuo, Z., Chen, Y. (2006) Effects of tributyltin, benzo[a]pyrene, and their mixture on antioxidant defense systems in *Sebastiscus marmoratus*. Ecotoxicol. Environ. Saf., 65: 381–387.

[21] Al-Ghais, S.M., Ali, B. (1999) Inhibition of glutathione *S*-transferase catalyzed xenobiotic detoxication by organotin compounds in tropical marine fish tissues. Bull. Environ. Contam. Toxicol., 62, 207-213.

[22] Li, Z.H., Li, P., Shi Z.C. (2015) Chronic Exposure to Tributyltin Induces Brain Functional Damage in Juvenile Common Carp (*Cyprinus carpio*). PLoS ONE, 10(4): 13pp.

[23] Zhang, J., Shen, H., Wang, X., Wu, J., Xue, Y. (2004) Effects of chronic exposure of 2,4- dichlorophenol on the antioxidant system in liver of freshwater fish *Carassius auratus*. Chemosphere, 55: 167-174.

[24] Thomaz, J.M., Martins, N.D., Monteiro, D.A., Rantin, F.T., Kalinin, A.L. (2009) Cardio-respiratory function and oxidative stress biomarkers in Nile tilapia exposed to the organophosphate insecticide trichlorfon (NEGUVONs). Ecotox. Environ. Safe. 72: 1413-1424.

[25] Lushchak, O.V., Olha, I., Kubrak, O.I., Storey, J.M., Storey, K.B., Lushchak, V.I. (2009) Low toxic herbicide roundup induces mild oxidative stress in goldfish tissues. Chemosphere, 76: 932-937.

[26] Monteiro, D.A., Almeida, J.A., Rantin, F.T., Kalinin, A.L. (2006) Oxidative stress biomarkers in the freshwater characid fish, *Brycon cephalus*, exposed to organophosphorus insecticide Folisuper 600 (methyl parathion). Com Biochem Phys C 143:141-149.

[27] Ozkan, F., Gunduz, S.G., Berkoz, M., Ozluer-Hunt, A., Yalin, S. (2012) The protective role of ascorbic acid (vitamin C) against chlorpyrifos-induced oxidative stress in *Oreochromis niloticus*. Fish Physiol. Biochem. 38(3): 635-643.

[28] Pandey, S., Parvez, S., Sayeed, I., Haquer, R., Bin-Hafeez, B., Raisuddin, S. (2003). Biomarkers of oxidative stress: A comparative study of river Yamuna fish *Wallago attu* (Bl. Schn). Sci. Total Environ., 309: 105-115.

[29] Palace, V.P., Dick, T.A., Brown, S.B., Baron, C.L., Klaverkamp, J.F. (1996) Oxidative stress in Lake Sturgeon (*Acipenser fulvescens*) orally exposed to 2,3,7,8-tetrachlorodibenzofuran. Aquat. Toxicol. 35: 79-92.

[30] Dimitrova, M.S.T., Tsinova, V., Velcheva, V. (1994) Combined effect of zinc and lead on the hepatic superoxide dismutase–catalase system in carp (*Cyprinus carpio*). Comp. Biochem. Physiol. 108: 43-46

[31] Kavitha, P., Rao, V. (2008) Toxic effects of chlorpyrifos on antioxidant enzymes and target enzyme acetylcholinesterase interaction in mosquito fish, *Gambusia affinis*. Environ. Toxicol. Phar. 26: 192-198.

[32] Oruc¸ E.O., Usta, D. (2007) Evaluation of oxidative stress responses and neurotoxicity potential of diazinonin different tissues of Cyprinus carpio. Environ Toxicol Phar 23:48–55

[33] Ozkan-Yilmaz, F., Ozluer-Hunt, A., Gunduz, S.G., Berkoz, M., Yalin, S., Sahin, N.O. (2015) Effects of methidathion on antioxidant system and expression of heat shock protein 70

(HSP70) gene in the liver of *Oreochromis niloticus* L. 1758. Fresen. Environ. Bull., 24(8a): 2650-2658.

[34] Hai, D.Q., Varga, S.I., Matkovics, B. (1997) Organophosphate effects on antioxidant system of carp (*Cyprinus carpio*) and catfish (*Ictalurus nebulosus*). Comp. Biochem. Phys. C, 117: 83-88.

[35] Stephan, G., Guillaumeb, J., Lamoura, F. (1995) Lipid peroxidation in turbot (*Scophthahus maximus*) tissue: effect of dietary vitamin E and dietary n-6 or n-3 polyunsaturated fatty acids. Aquaculture, 130:251–268

[36] Ademuyiwa, O., Agarwal, R., Chandra, R., Behari, J.R. (2009) Lead induced phospholipidosis and cholesterogenesis in rat tissue. Chem. Biol. Interact., 179(2-3): 314-320.

[37] Adonaylo, V.N., Oteiza. P.I. (1999) Lead intoxication: antioxidant defenses and oxidative damage in rat brain. Toxicology, 135: 77–85.

[38] Tsuda, T., Nakanishi, H., Aoki, S., Takebayashi, J. (1986) Bioconcentration of butyltin compounds by round crucian carp. Toxicol. Environ. Chem., 12(1-2): 137-138.

[39] Strand, J., Jacobsen, J.A. (2005) Accumulation and trophic transfer of organotins in a marine food web from the Danish coastal waters. Sci. Total. Environ., 350: 72–85.

Received: **29.05.2017**
Accepted: **10.08.2017**

CORRESPONDING AUTHOR

Ferbal Ozkan-Yilmaz
Mersin University,
Faculty of Fisheries,
Department of Basic Sciences,
33169 Mersin – TURKEY

E-mail: ferbal1111@hotmail.com

© by PSP Volume 26 – No. 10/2017 pages 6149-6158 Fresenius Environmental Bulletin

EVALUATION OF TURKISH MINE WASTE MANAGEMENT POLICY WITH RESPECT TO MARINE POLLUTION

Esin Esen*

SRK Consulting Turan Gunes Bulvari No: 86/3, 06550 Yildiz, Ankara Turkey

ABSTRACT

Large volumes of wastes are produced by the mining activities and mine waste management is one of the most important environmental issues which directly affect the feasibility of the mine related to permitting. The slurries or waste materials left over after mineral is extracted from ore via physico-chemical processing are called tailings which must be safely disposed to prevent the release of contaminates into the environment. Tailings are generally stored on-land surface impoundments; can be used in backfilling the voids in exhausted underground mines and/or transferred through pipes and disposed to a watercourse under the water level subaqueously. In deep sea tailings placement (DSTP) method, the tailings are disposed to deep sea zones far from the shore. The environmental legislations are improving, forcing the mining industry to take strict measures regarding tailings management. The Turkish Regulation on Mining Wastes have been published in 2015 and is going to be in force by July 15, 2017 where DSTP is adressed as a possibility for non-hazardous wastes disposed to anoxic layer of Black Sea. This manuscript aims to provide guidance on the environmental permitting of DSTP practices as an option in Turkey's Legislation.

KEYWORDS:
Tailings, Deep Sea Tailings Placement (DSTP), Mine Waste Management, Marine Pollution.

INTRODUCTION

The extraction of metals and minerals through mining of geological resources aims to improve the quality of civilization however, the management of the residues generated at mining operations, mainly the tailings and waste-rock remains as the most important environmental issues on permitting [1, 2, 3, 4]. Potential environmental issues associated to mining activities other than wastes are air quality including dustfall [5], water use and quality, hazardous materials, land use and biodiversity, noise and vibrations energy use and visual impacts [6, 7]. Figure 1 shows the typical operations in mining.

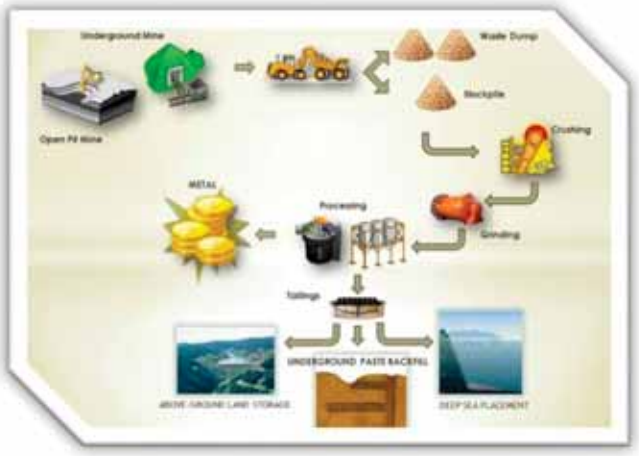

FIGURE 1
General Flow Scheme for Mining [8]

Tailings may contain suspended solid particles consisting of economically worthless minerals and a small amount of valuable minerals, dissolved solids, metal ions, chemical reactives and reaction products [9]. The heavy metals, which are important in terms of environmental pollution, contained in tailings are listed as: Boron (B), Cadmium (Cd), Chromium (Cr), Berilium (Be), Antimony (Sb), Silver (Ag), Arsenic (As), Lead (Pb), Mercury (Hg), Manganese (Mn), Nickel (Ni), Selenium (Se), Titanium (T), Uranium (U), Vanadium (V), Zinc (Zn) and Aluminum (AI) and other environmental problems encountered are the Metal Leach (ML) and Acid Rock Drainage (ARD) [9, 10, 11].

The disposal methods of tailings vary on the basis of cost, environmental factors and structural risks *i.e.* failure [1, 3]:

- On-Land disposal: Storage of tailings in dams and ponds (Tailings Storage Facility - TSF).
- Backfilling in underground mines: Filling the spaces left after ore extraction in underground mines with paste fill (dehydrated cement added dry sludge) ensures both reinforcement and waste disposal simultaneously.
- Discharge to Surface waters: Tailings disposal to the river courses is abandoned due to its environmental impacts on surface water resources [3, 12]. In USA and Canada, the disposals to lakes are being ceased due to low assimilation capacity in closed systems. In deep sea tailings placement (DSTP) method, the tailings are disposed to deep sea

zones far from the shore. It is applied in regions, where the sea is deep and close to the facility, the precipitation is high and evaporation is low, and where the land disposal methods of tailings are risky due to the stability and seismicity problems.

As of 2012, there have been approximately 3,500 TSFs in the world and until that date, significant failures have been encountered in 138 storage facilities [12]. The examples are: In 2010, due to the failure of the embankment in Hungary, 600,000-700,000 m^3 tailings have spread to the region and caused the death of 10 people. In 1998, the failure in the TSF of Los Frailes Mine, Aznalcollar region of Spain, caused 5-7 Mm^3 tailings have flown to Rio Agrio River and raised the river bed with 3 m and covered 3,500 ha of agricultural area. In 1985, TSF failure in Stava, Italy, caused the death of 268 people [1, 12].

Over the last century the volumes of tailings being generated has grown dramatically as the demand for minerals and metals has increased and lower grades of ore are being mined through advances in extraction and processing technology [13]. Being different from other industrial wastes, the tailings are produced in very big amounts. There are individual mines producing in excess of 200,000 tonnes of tailings per day [13]. Approximately 100,000 ML of postprocessing tailings slurry of the Lihr Mine on Niolam Island in Papua New Guinea is deposited annually at depth from a sub-surface pipeline (DSTP) [14]. The DSTPs are in operation in Norway with discharges from 300 000 to 4 million tons/year, where mining tailings have been deposited at 17 fjord- or near-coastal sites in Norway [2].

According to Eurostat statistics, the mining and quarrying industry produced 671,810,000 tonnes of waste in 2010, in EU (27 Member States-MS) which is equivalent to around 30% of the total waste generated in the same countries [15]. The EU (28 MS) produced over 730 million tonnes of mining waste in 2012, where 13.7 million tonnes of it is hazardous waste contribution [15].

Since tailings generally contain compounds with sulfide, they must be covered with water or an appropriate impermeable material in order to prevent their contact with air and occurrence of ARD and ML at the stage of mine closure [1, 3]. Among the important impacts related with the TSF, loss of land and habitat due to their large footprint areas, impacts on surface and underground waters and visual impacts can be mentioned. The engineering studies performed in order to ensure the short and long period stability of civil structures are among the most important issues in TSF planning.

TABLE 1
Applications of DSTP in the World as of 2012 [18]

Water environment of discharge	Mine area	Mine production	Firm
Basamuk (Astrolabe) Gulf, Bismarck Sea	Ramu Nickel and Yandera mines, Papua New Guinea	nickel-cobalt; copper- gold	Metallurgical Construction Corp., Highlands Pacific (Ramu); Marengo Mining (Yandera)
Norway fiords	Kirkenes, Kvannevann, Stjernøya, Hustadmarmor Skaland, Engebøfjellet, Repparfjorden	Iron, industrial minerals, titanium, copper	Northern Iron Ltd., LNS AS, Sibelco Nordic, Omya Group, Nordic Mining, Nussir
Senunu gulf	Batu Hijau mine, Indonesia	Copper – gold	Newmont Mining, Sumitomo Mining
Luise port	Lihir mine, Papua New Guinea	Gold	Newcrest Mining
Pigiput gulf	Simberi mine, Papua New Guinea	Gold	Allied Gold
Black Sea	Çayeli Bakır, Türkiye	Copper – zinc	Cayeli Bakir Isletmeleri A.S.

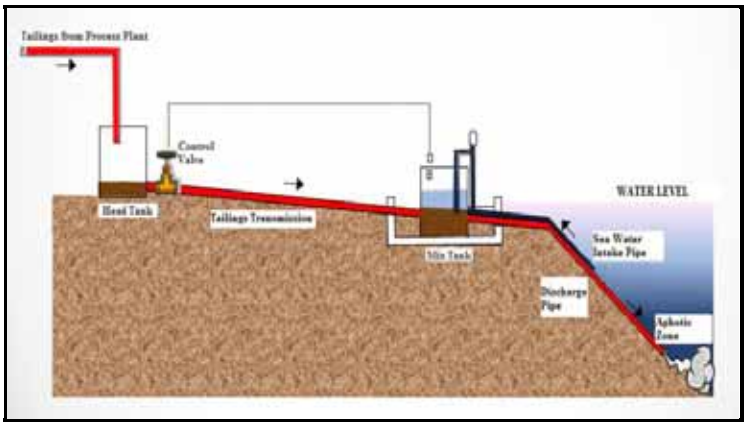

FIGURE 2
Typical DSTP Structure

The DSTP targets the trapping of tailings at the bottom of deep sea. The tailings are transported from the facility to the deep-sea environment through pipes, and discharged in the deep layer, below picnocline [10, 11, 12, 13, 14, 16, 17]. Typical DSTP structure is given in Figure 2.

The most important environmental impacts of DSTP are (i) the loss of benthic habitat on the footprint, where the tailings are stored at the sea bottom, (ii) the impacts on abundance and diversity of species, and (iii) the risk of bio-accumulation of heavy metals in the food chain.

As of 2012, there are 11 mines using the DSTP method in the world (Table 1) and all of them have obtained the legal permissions from the competent authorities in host countries. [12, 18]:

- 5 mines in Norway,
- 1 mine in England,
- 1 mine in Turkey,
- 1 Mine in Indonesia,
- 3 mines in Papua New Ginea.

The historical development of DSTP method, which has been commenced approximately 40 years ago in Philippines and Canada shows that the applications performed without mineralogical, geo-chemical and oceanographic characterization, can cause damage to the environment [11, 12]. Environmental impact from sea tailings disposal appears the lack of baseline information on the habitat, environmental conditions, and associated microbial and faunal components that are affected by the discharges. There is also a lack of scientific knowledge of the biodiversity patterns and functioning of the marine ecosystems, particularly in the deep-sea, as well as of effects of metals and chemicals on deep-sea biota [3].

Especially due to its advantages such as prevention of ARD risk by the wastes containing sulfite; in cases of construction of land based TSFs that are not geo-technically suitable; and prevention of land losses, DSTP is accepted as an alternative for the techniques of land disposal systems [1, 3].

MATERIALS AND METHOD

Assessment of International Legislation on DSTP. The evaluation of international legislation is based on the performance criteria published by World Bank's International Finance Corporation (IFC) [6, 7] and the European Union (EU) directives [19] within the framework of harmonization works in the membership process of Turkey. Besides, there are international agreements and protocols signed for the protection of seas surrounding Turkey.

Mining Wastes. EU mining waste management includes one directive (Directive 2006/21/EC on the management of waste from extractive industries - the Mining Waste Directive- "MWD") and 5 decisions in relation to the implementation of MWD [19]:

- 2009/360/EC completing the technical requirements for waste characterization;
- 2009/359/EC on the Definition of inert waste in implementation of Article 22 (1)(f),009;
- 2009/337/EC on the Criteria for the classification of waste facilities in accordance with Annex III;
- 2009/335/EC on the Technical guidelines for the establishment of the financial guarantee;
- 2009/358/EC on the Harmonization, the regular transmission of the information and the questionnaire referred to in Articles 22(1) (a) and 18.

Other relevant EU directives are listed as:

- 2012/18/EU On the control of major-accident hazards involving dangerous substances (Seveso III),
- 2010/75/EU On industrial emissions (integrated pollution prevention and control-IPPC),
- 2008/98/ EC on waste and repealing certain Directives on waste (Waste Framework Directive).

Directive 2004/35/EC on environmental liability with regard to the prevention and remedying of environmental damage (ELD) came into force in 2007 introducing the "polluter pays" principle [4]. A holder of an IPPC or waste licence for mining and related waste activities in the EU is subject to the ELD because many mining related activities are listed in Annex III of it [4].

The EU's waste management approach is based on the "waste hierarchy" which sets the following priority order for policy development: prevention [20, 21], (preparing for) reuse, recycling, recovery and, as the least preferred option, disposal (which includes landfilling and incineration without energy recovery) [19].

TSFs are divided into two categories as "Category A" and "Non-Category A" in accordance with the risk they have on public health and environment in EU Waste Legislation. For a tailings facility to be considered as Category A, (i) the effects of the accidents that may occur in the facility must be at significant levels as the result of the risk assessment; or (ii) it contains waste classified as hazardous under Directive 91/689/EEC; or (iii) it contains substances or preparations classified as dangerous under Directives 67/548/EEC or 1999/45/EC.

Additional to the Directive 2006/21/EC, EU environmental legislation includes a Best Available Techniques (BAT) reference document for the management of tailings and waste-rock in mining ctivities known as BREF (2009). DSTP operations are included within the BREF (2009) [1] suggesting it as an acceptable method for mining areas where tailings are likely to generate ARD. As a BAT example, Hustadmarmor Calcium Carbonate Mine in Norway is presented where the driving force is the lack of space for tailings deposition on land.

World Bank's IFC grants loans for private sector projects and requires Environmental and Social

Impact Assessment (ESIA) and the application of "IFC Performance Standards" in the management of environmental risks and impacts in investments. For making use of IFC financing, the project is expected to be compliant with international good sector applications, which are recognized worldwide, such as Environment, Health and Safety Guides of the World Bank Group (EHS guides). In case host country regulations are different from those indicated in EHS Guides, the project owner has to comply with the stricter one. However, where necessary, the project owner may propose alternative mitigations and measures together with the relevant scientific evidences within the ESIA process [6].

IFC also issued sectoral EHS Guidelines (2007) where DSTP may be considered as an alternative only in the absence of an environmentally and socially sound land-based alternative and based on an independent scientific impact assessment for mining [7]. If and when DSTP is considered, such consideration should be based on detailed feasibility and ESIA of all tailings management alternatives, and only if the impact assessment demonstrates that the discharge is not likely to have significant adverse effects on marine and coastal resources, or on local communities. In accordance with IFC guidelines, for DSTP to be applied the possible impacts on the sea environments and the precautions to be taken against them must be compliant with international agreements such as the United Nations Convention on the Law of the Sea (UNCLOS), 1982.

Water Quality. The basis of the EU legislation on water quality consists of Water Framework Directive (WFD) numbered 2000/60/EC [19], which also has priority in harmonization of Turkish Legislation for this sector. WFD prescribes the protection and recovery of all water masses in EU in terms of quality and amount and targets to bring all underground and surface waters to the good status as of 2015 and eliminating hazardous materials with priority from the European watercourses. Directive on Environmental Quality Standards (2008/105/EC), which is also known as the Priority Substances Directive has been enforced to reach this target. The Directive on Pollution Caused by Certain Dangerous Substances Discharged into the Aquatic Environment of the Community (76/464/EEC) has been codified and adopted as 2006/11/EC.

WFD's combined approach icludes limiting pollution at the source by the setting of emission controls with relevant legislation (i.e. Urban Waste Water Treatment Directive, the Nitrates Directive and the IPPC Directive) and by establishing water quality objectives for watercourses in compliance with good status objective [22]. The river basin management plans and programmes are at the core of all water-related legislation. Watercourses used for drinking water purposes will be subject to particular protection, linked to a requirement of complementary standards and measures to ensure safe drinking water supply, ensuring the standards of the Drinking Water Directive are met [22].

Marine Strategy Framework Directive (MSFD) (2008/56/EC) [19] has entered force in 2008. It targets to create the necessary information and application tools in line with the "Ecosystem Approach" for the transition-coastal and coastal-sea waters to ensure "Good Environmental Status" in EU marine waters until 2020 promoting international cooperation through Regional Sea Conventions (RSC):

- The Convention for the Protection of the Marine Environment in the North-East Atlantic of 1992 (further to earlier versions of 1972 and 1974) – the OSPAR Convention (OSPAR),
- The Convention on the Protection of the Marine Environment in the Baltic Sea Area of 1992 (further to the earlier version of 1974) – the Helsinki Convention (HELCOM),
- The Convention for the Protection of Marine Environment and the Coastal Region of the Mediterranean of 1995 (further to the earlier version of 1976) – the Barcelona Convention (UNEP-MAP),
- The Convention for the Protection of the Black Sea of 1992 – the Bucharest Convention.

The most important international agreements on waste disposal to the seas are: "Convention on the Prevention of Marine Pollution by Dumping of Wastes and Other Matter (London Convention, 1972)", its amendment in 1978 and London Protocol (1996). The London Protocol has been signed by 45 nations including Australia, New Zealand and Philippines [23]. Turkey is in the process of becoming a party to those agreements [24].

The purpose of London Convention is to control all marine pollution sources and to prevent marine pollution by regulating the dumping of wastes to the sea. The "gray list" and "black list" definitions are made for the wastes to categorize them in accordance with the hazard they cause in terms of environment. While the disposal of the materials in the black list is completely prohibited, the disposal of the materials in the gray list is subject to special permission from the competent authority of the host country and in compliance with certain conditions. For the disposal of other materials, a general permission is sufficient.

The London Protocol is more restrictive than London Convention. The disposal of any kind of materials except the materials included in the annex of the Protocol, or their combustion on the sea, has been prohibited. Although the sea disposal of "inert, inorganic geological material" is permitted in the protocol, tailings are not assessed within this scope. Technically, the protocol regulates the rules of dumping at the seas, platforms etc on the sea rather than the discharges to be made from the land.

Evaluation of Republic of Turkey's Legislation on DSTP. An Environmental Impact Assessment (EIA) permit is the first environmental permit required for new mining operations, as well as for major mine operation modifications. The EIA permit acts as a temporary permit for the construction of the mine. Within one year after start of the operation a Temporary Environmental Operation License application has to be made to Ministry of Environment and Urbanization (MEU). Following the application, compliance testing via an accredited laboratory is conducted for mine emissions and discharges and then "Final Environmental Operation License" is issued. The environmental licenses are managed by the MEU and cover all aspects of the environment including but not limited to waste water discharge, air pollutant emissions, noise, solid waste, hazardous waste.

Mining Waste. In line with the MWD, the MEU, published the "Regulation on Mining Wastes (RMW) (Official Gazette Date: 15.07.2015; Number: 29417). Also, Regulation on Waste Management (RWM) (Official Gazette Date: 02.04.2015; Number: 29314) has been completely harmonized with EU.

RMW classifies mining wastes in three classes as "hazardous", "non-hazardous" and "inert" wastes and addresses RWM for determination of hazardousness in which, Annex-4 provides list of wastes including mining, Annex-3/A provides the hazardousness properties and Annex-3/B provides the limit values as references for their characterization. For the determination of the geochemical properties of the waste and for the determination of ARD and ML risk, the static and kinetic tests are requested.

Leachate management is one of the most serious issues in landfill operation [25] where the leachate characterization is conducted according to the Regulation on Landfill (RL) (Official Gazette Date: 26.03.2010; Number: 27533). The land deposition of tailings in impervious impondments was subject to RL till to the enforcement of RMW.

The sea disposal of mining waste is included in Article 22 of the RMW and the conditions to comply with are defined as follows:

- As a result of waste characterization, mineral wastes which are defined as hazardous can not be disposed in the seas surrounding Turkey. Only inert and non-hazardous mineral wastes can be disposed in the anoxic layer of the Black Sea.
- There should be no geographical, topographical and geologically appropriate area in the terrestrial zone within an approximate radius of 30 km of the mine having inert and non-hazardous mineral wastes to dispose those tailings to Black Sea.
- A scientific report must be submitted to MEU representing the oceanographic and hydrodynamic conditions at the discharge location, assimilation capacity of the sea, behaviour of discharge plume and its impact on ecology and water quality.
- The receiving environment will be monitored seasonally-four times in a year for the following parameters: temperature, salinity, light transmittance, density, electrical conductivity, chlorophyll-a, pH, dissolved oxygen, hydrogen-sulfur, alkalinity, copper, zinc, mercury, lead, iron, manganese, cadmium, arsenic, total suspended solids, total organic carbon, crude oil and its derivatives. Additional parameters are required if MEU deems necessary.

For the new developing mining projects, Waste Management Plan has to be prepared in the EIA process in compliance to the RMW.

Water Quality. Turkey has announced that full harmonization of WFD under the "Environment" section and its adherence to the cited Conventions will take place following full membership of the EU and that full harmonization with the Directives under the Treaties can be done two years before the date of EU membership is finalized [24].

Regulation of Water Pollution Control (RWPC) being the most important legislation applied in the protection water resources is first issued in 1988, and the current one has been in force since 2004 (Official Gazette Date: 31.12.2004; Number: 25687). According to RWPC, the discharge standards were determined on a technological basis, each water mass was assumed to be the same and the same discharge standards were applied.

The principles related with the deep-sea discharge of the wastewaters are defined in RWPC and the criteria are established in accordance with the domestic wastewater properties. Direct discharges to the receiving environment of any kind of solid wastes, and sludge are prohibited. The dredging and disposal of the dredged materials are subject to permit of the MEU. There is a circular of MEU (2014/7) which defines the principles of deep sea discharge project preparation.

The regulatory harmonization works within the scope of marine/coastal waters performed by the Ministry of Forests and Water Affairs (MFWA) and MEU are summarized in the following pharagraphs [26].

- Regulation on Management of Surface Water Quality (RMSWQ) (Official Gazette Date: 30.11.2012; Number: 28483) has been issued targetting to identify and classify the biophysicochemical and hydromorphological qualities of surface, coastal and transitional waters; and to establish the principles and procedures for the mitigation measures to be taken to achieve good water status. By the publication of the the water quality classification articles of RWPC have been repealed.
- The chemical substances listed in Annex-1 and Annex-2 of Regulation on the Control of Pollution of Water and its Surroundings Due to Hazardous Substances (Official Gazette Date: 26.11.2005; Number: 26005) has been updated and harmonized

in 2010 (Amendment Date: 30/3/2010-No:27537).

- In order to obtain good water status, the existing quality of the water masses has to be determined as well as their quantities. It is important to establish the National Monitoring Network and to perform monitoring in an integrated way to perform monitoring within the scope of WFD. To comply with the requirements of WFD, the Regulation on the Monitoring of Surface and Underground Waters (RMSUW), which includes the procedures and principles related with the monitoring of water quality has been issued (Official Gazette Date: 11.02.2014; Number: 289105).
- The harmonization works for the Directive on the Management of Bathing Water Quality (2006/7/EC) are being performed jointly by the MEU and MFWA under the coordination of Ministry of Health (MH).

In addition to all the above legislation, the provisions of the Law on Coast (LC) numbered 3621, the Regulation on the Implementation of the Law on Coasts (RILC) (Official Gazette: 3.08.1990; Number: 20594) and the Notification on the Planning and Application Process for Coastal Structures and Facilities (NPAPCSF) (Official Gazette: 06.07.2011; Number: 27986) have to be complied with. The NPAPCSF requires, "Hydrographic and Oceanographic Report" approved by Naval Forces Command (NFC) Navigation, Hydrography and Oceanography Department.

Any mine that discharges process water into a watercourse requires discharge licence accordance to the Regulation on Environmental Permits and Licenses (Official Gazette: 10.09.2014 Number: 29115). In Turkish Legislation, it is stated clearly that discharges from waste management activities at mine sites has to be controlled in a manner that causes no deterioration to local water quality both surface waters and groundwater. The provincial directorate of Ministry of Food, Agriculture and Husbandary is included in the environmental permitting process under the Law on Water Products numbered 1380.

TECHNICAL STUDIES ON DSTP DESIGN

Since the tailings plume is heavier than the sea water, its buoyancy flux has a negative value and the plume will have the tendency of precipitating at the sea bottom. The potential impacts of DSTP depend on the receiving environment conditions as a result of the interaction of biogeochemical, ecological, bathimetric and oceanographic properties with each other [10, 11, 12, 13, 14]. For instance, in the upwelling systems, the contaminants in the tailings plume will be transported from bottom to surface therefore negative impact on fishing, and deterioration of coastal water quality is unavoidable. The potential environmental impacts of DSTP are listed as, (i) the loss of habitat at sea bottom ecosystem due to the stored footprint area of tailings, (ii) impact on the deep-sea organisms due to the metal toxicity and chemical processes which leads bio-accumulation in the food chain. Therefore, the tailings characterization and determination of the background oceanographic properties of the marine environment are the basic factors for the impact assessment of DSTP practice [11].

Water column measurements of CTD (Conductivity/ Tempretature/ Density) and sea-current have to be conducted in order to establish the hydrodynamics of the sea environment and to predict the behavior of the discharge plume [27, 28]. In addition to the oceanographic measurements, the hydrodynamic loads have to be calculated and the structural behavior against those loads has to be assessed for the design of submarine pipelines [29]. The wave and current climate has to be conducted in accordance with the measurements and meteorological data, the design wave and current properties have to be determined and hydrodynamic forces that will act on the structure have to be calculated [29]. Transportation and sinking analysis, tension and deformation analysis of the pipeline and the geological and geophysical studies have to be performed [29].

The deep sea outfall design of tailings and the domestic wastewater outfall design have different principles. In the domestic wastewater case, the outlet of the discharge, which has jet flow, through small diameter diffusers is preferred to ensure a high primary dilution (near-field dilution) with momentum principles. The waste plume, which has the tendency of rising due to its density that is lower than sea water, is subject to secondary dilution with the effect of the currents and tertiary dilution in terms of bacterial decay. The tailings include mineral solids, therefore the risk of clogging of small holes is high, and therefore the use of diffusers is not possible. A modeling study has to be performed to make predictions related with the post-discharge waste behavior.

The first phase of the post-discharge behavior of tailings consists of the near-field intense current model. The purpose of this first phase model is to simulate the behavior of the discharge plume, which creates a current due to density, after leaving the pipe, within small grids depending on the pipe diameter [28, 29].

The second phase of the discharge plume fol-

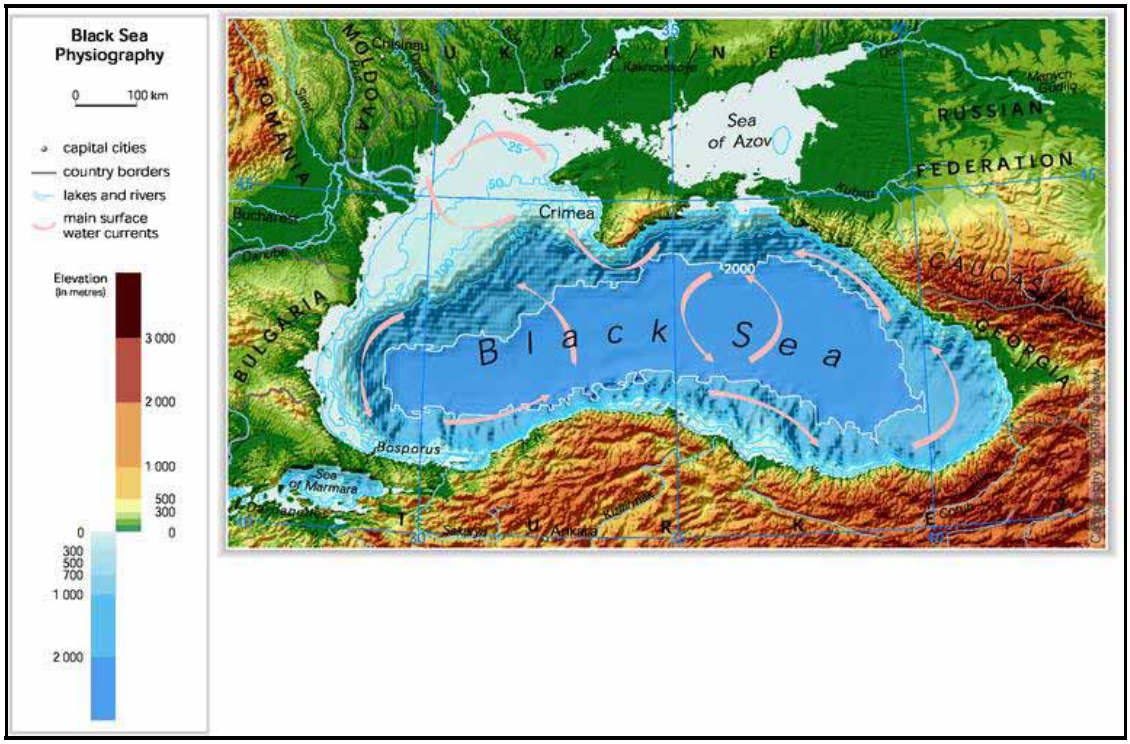

FIGURE 3
Physiography of Black Sea (http://www.eea.europa.eu/legal/copyright) [30]

lows that heavier solid particles remain in dense flow and settle after being carried to far distances by gravity and bottom slope. This behavior is simulated within bigger grids with the far–field dense current model. Lighter particles leave the dense current plume and constitute separate plumes at depths, where the medium density is the same as the density of that fluid. Consequently, the dense current containing heavy particles act as the continuity of the discharge pipe carrying the materials to deeper zones [28, 29].

Measurement of physical and biogeochemical parameters in the water column and in the sediment is important for DSTP design and for monitoring the post discharge conditions. The monitoring programme to control the environmental impact inside and around the deposit area usually covers the following parameters [1, 3]:

- water column analyses on solids content (turbidity), salinity, oxygen content and temperature, trace metals and chemicles accociated with the tailings composition,
- sediment analyses *i.e.* trace metals and chemicles accociated with the tailings composition,
- biological activity,
- bioaccumulation to analyse potential toxicity to aquatic and benthic life;
- annual video recording of the underwater pipeline and discharge point in order to observe any structural failure risks. In deep waters, where diving is risky and dangerous, ROV (remotely controlled underwater vehicle) can be used.

GENERAL PROPERTIES OF BLACK SEA

The RMW addresses DSTP applications to Black Sea on special circumstances. Black Sea is a semi enclosed sea and is connected to the Mediterranean Sea through Istanbul and Çanakkale straits and to the Azov Sea through Kerch strait (Figure 3).

Black Sea basin is receiving an abundant amount of rain. The amount of rain increases from the west towards the east and reaches an annual value of 2500 mm [31]. The main components of water balance consist of the rivers, rain and the water coming from the straits and evaporation and the water exiting through the straits. The waters are anoxic after a depth of 150 – 200 meters [31, 32].

The most important property of Black Sea, which makes it different from other seas, is that the deep basin waters are always anoxic and contain hydrogen sulfur (H_2S) in high concentrations, which increase towards the bottom [31, 32]. The basic reason of this formation is the separation of the Mediterranean Sea waters filling the entire bottom basin (>22 ppt) from the lower saline waters at the surface (18 ppt) [32]. The vertical mixtures in the Black Sea are effective up to the upper limit of halocline. Therefore, the transportation of dissolved oxygen from the oxygenated surface layer to the sulfur containing deep waters is very limited [32, 33].

Since the oxygen input does not meet the oxygen need of the aerobic bacteria, the disintegration of the precipitating organic material occurs as the result of sulfate (SO_4^{2-}) reduction by the anerobic bacteria

and an environment with H_2S occurs. In Black Sea ecosystem, the starting border of waters with H_2S is 90 – 100 m in open waters, where cyclonic eddies dominate and 160-180 m at the coasts [32]. The basic circulation on the Black Sea basin is defined with cyclonic eddies in the center; anti-cyclonic eddies along the periphery and anti-cyclonic Batum Eddie at the eastern end, surrounded by the Rim Current [34].

The limiting values of "Trophic Levels of Surface Water Masses" provided for Black Sea and Marmara in Annex-7 of the Regulation on Surface Water Quality Management, are given in Table 2.

TABLE 2
Eutrophication Criteria for Black Sea and Marmara Sea Coastal and Transition Waters (RSWM, Annex-7)

Water Quality Class	DIN (µg/l)	TP (µg/l)	Chl a (µg/l)	Secchi Disk(m)
Oligotrophic	<20	<15	<0.7	>6
Mesotrophic	20-140	15-30	0.7-3	3-6
Eutrophic	141-250	31-40	3.1-5	1.5-2.9
Hypertrophic	>250	>40	>5	<1.5

DIN: (nitrate + nitrite + ammonium)- represent the total Dissolved Nitrogen.

CONCLUSIONS

The waste management strategy has to be based on methods, which will not pose any risks on the public health and safety, where the social and environmental impacts remain within acceptable limits. As recommended in the EU legislation and IFC Standards, DSTP method can be used by researching all disposal methods scientifically with a full analysis and risk assessment. In regions where the sea is close and deep, precipitation is high, vaporization is low and land waste disposal methods are risky, DSTP method provides more advantages in comparison with other methods. Another advantage of DSTP method is the prevention of ARD and ML formation for tailings containing sulfur. The factors creating risks for the ecosystem can be eliminated with the discharge of tailings in aphotic and anoxic deep layer, where there is no upwelling.

Since the tailings discharge is heavier than the sea water, its buoyancy flux has a negative value and the discharge plume has the tendency of sinking on the sea bottom. The potential impacts of DSTP applications depend on the environmentalconditions to a great extent as the result of the interaction of the biogeochemical, ecologic, bathymetric and oceanographic properties with each other. Hence, the receiving environment quality standards have to be assessed differently in each sea region. The seas surrounding Turkey have unique biogeochemical properties that are different from each other:

- In Mediterranean Sea nutrient input is limited. The transportation with rivers in coastal areas is more effective in Western Mediterranean Sea. In Eastern Mediterranean Sea, especially on open waters, the only resource is the bottom waters, which are relatively rich in nutrients. Very strong vertical mixtures are observed in the deep basins due to the dynamic structure of Eastern Mediterranean Sea and because of the climatic conditions, and oxygen exists down to the bottom of the water column even in the deepest regions due to the effectiveness of vertical mixture [33].
- Aegean Sea basin, which is in the northeast of Mediterranean Sea, remains generally within oligotrophic limits; however, it can have more eutrophic properties in comparison with Mediterranean Sea with the effect of Black Sea waters in the north [33].
- Marmara Sea and the straits have a two – layer ecosystem. The low saline waters coming from the Black Sea are in the upper water column of 15-20 m, while the Mediterranean Sea waters entering from Çanakkale are in the bottom basin [33].
- Black Sea basin is receiving an enormous amount of rain. The amount of rain increases from the west towards the east and reaches an annual value of 2500 mm [32, 33]. The most important property of Black Sea, which makes it different from other seas, is that the deep basin waters under the oxygenated surface layer are always anoxic and contain H_2S in high concentrations, which increase towards the bottom [32, 33]. The basic reason of this formation is the separation of the Mediterranean Sea waters filling the entire bottom basin (>22 ppt) from the lower saline waters at the surface (18 ppt) [32, 33]. The vertical mixtures in the Black Sea are effective up to the upper limit of halocline. Therefore, the transportation of dissolved oxygen from the oxygen containing surface layer to the sulfur containing deep waters is very limited.

When the biogeochemical properties of the seas of our country are taken into consideration in terms of DSTP application Black Sea has an important advantage due to lack of biological life in anoxic deep bottom waters containing high concentrations of H_2S. The formation of sediments due to the reaction of dissolved metals in the H_2S containing anoxic layer provides an advantage in terms of their limited mobility in the water column. The impact on habitat will unlikely to occur due to tailinds disposal within the anoxic layer since there is no biological life. However structural risks regarding the submerged pipeline remain inherent and must be assessed cautiously and in detail.

In Mediterranean and Aegean seas any DSTP practice may have drastic impacts due to the complex oceanographic and hydrodynamic properties of those marine systems.

The method of tailings disposal is decided in

accordance with the economic and technical feasibility factors as well as the assessment of their environmental impacts and risks so as to include the period after the closure of the mine. DSTP practices have to be supported with scientific studies and must pass through very detailed assessment processes.

MEU is the coordinating authority for DSTP permits however there are quite a few governmental institutions to be consulted officially that the interactions and the duration of permitting process can not be foreseen in Turkey's environmental legislative framework which may hinder the mining.

REFERENCES

[1] European Commission, BREF (2009). The Reference Document on Best Available Techniques for Management of Tailings and Waste Rock in Mining Activities, EC, JRC, Institute for Prospective Technological Studies, Seville, Spain. 7 January 2009; http://eippcb.jrc.ec.europa.eu/reference/BREF/mmr_adopted_0109.pdf. Accessed July, 2017.

[2] European Commission BREF (2012). Establishment of guidelines for the inspection of mining waste facilities, inventory and rehabilitation of abandoned facilities and review of the BREF; document No. 070307/2010/576108/ETU/C2; Final Report; April 2012; Prepared by: DHI, in cooperation with Cantab Consulting Ltd, University of Tartu, Mecsek-Öko, Miskolc University and VTT; http://ec.europa.eu/environment/waste/mining/pdf/Inspection-Rehabilitation_BREF_report.pdf, Accessed July, 2017.

[3] European Commission MWEI-BREF (2016). Best Available Techniques Reference Document for the Management of Waste from the Extractive Industries in accordance with Directive 2006/21/EC, Joint Research Centre Institute for Prospective Technological Studies Sustainable Production and Consumption Unit; DRAFT DOCUMENT, June 2016; http://susproc.jrc.ec.europa.eu/activities/waste/documents/MWEI_BREF_Draft.pdf, Accessed July, 2017.

[4] Scannell, Y. (2004) The Regulation of Mining and Mining Waste in the European Union, pp. 92 http://law2.wlu.edu/deptimages/journal%20of%20energy,%20climate,%20and%20the%20environment/3-2-7-Scannell.pdf, Accessed July, 2017.

[5] Li, Q., Han, Y.F. and Huang, S.L. (2016) Concentration, Speciation, and Bioaccessibility of Cadmium in Dustfall from Coal Mine Areas: Case Study in Northern Anhui Province, China; Fresen. Environ. Bull., V. 25, No. 1/2016, p 163-173.

[6] International Finance Cooperation IFC (2012). Environmental, Health, and Safety (EHS) Guidelines, Jan 1, 2012.

[7] International Finance Cooperation IFC (2007). Environmental, Health, and Safety Guidelines for Mining, Dec 10, 2007.

[8] Esen, E. (2015) Deep Sea Disposal of Mineral Processing Plant Waste, Mining Turkey, March 01, 2015, 45:98-100. (In Turkish)

[9] Çetiner, E.G., Ünver, B., Hindistan, M.A. (2006) Legislation on Mine Waste: European Union and Turkey, Mining, Vol. 45, No 1, pp 23-34, March 2006. (In Turkish)

[10] Angel, B.M., Simpson, S.L., Jarolimek, C.V., Jung, R., Waworuntu, J., Batterham, G. (2013) Trace metals associated with deep-sea tailings placement at the Batu Hijau copper–gold mine, Sumbawa, Indonesia; Marine Pollution Bulletin 73; 306–313.

[11] Bernhard, D. (2014) Submarine Tailings Disposal (STD)-A Review, Minerals 2014, 4, 642-666.

[12] Vogt, C. (2012) International Assessment of Marine and Riverine Disposal of Mine Tailings, Prepared for: Secretariat of London Convention/London Protocol International Maritime Organization, London, England and United Nations Environment Programme-Global Program of Action; November 30, 2012.

[13] Engels, J. (2006) PhD thesis, University of Leeds, An Expert Management System for Surface Tailings Storage, http://www.tailings.info/basics/tailings.htm, Accessed July, 2017.

[14] Brewer, D.T., Morello, E.B., Griffiths, S., Fry, G., Heales, D., Apte, S.C., Venables, W.N., Rothlisberg, P.C., Moeseneder, C., Lansdell, M., Pendrey, R., Coman, F., Strzelecki, J., Jarolimek, C.V., Jung, R.F., Richardson, A.J. (2012) Impacts of gold mine waste disposal on a tropical pelagic ecosystem, Marine Pollution Bulletin 64 (2012) 2790–2806.

[15] European Commission (2016). Provision and Elaboration of Information for The Preparation of the "Implementation Report of Directive 2006/21/EC On the Management of Waste From Extractive Industries"; Service Request under the Multiple Framework Contract with re-opening of competition "Assistance to the Commission on the assessment of Waste Management Plans and on compliance monitoring and support of the implementation of the Waste Framework Directive"; Reference: ENV.C.2/FRA/2013/0023; FINAL REPORT, 12 April 2016 http://ec.europa.eu/environment/waste/studies/mining/waste_extractive_industries.pdf, Accessed July, 2017.

[16] Berkun, M. (2005) Submarine tailings placement by a copper mine in the deep anoxic zone of the Black Sea, Water Research, 39 (2005) 5005–5016

[17] Robinson, B., Bus, A., Diebels, B., Froehlich,

E., Grayson, R. (2004) Tailings Disposal Options for the Kensington Mine at Berners Bay Near Juneau, Alaska, https://seagrant.uaf.edu/nosb/papers/2004/midas-tailings.html, Accessed July, 2017.
[18] Troubled Waters, (2012). Published by Earthworks and MiningWatch Canada, Feb 28, 2012, https://www.earthworksaction.org/files/publications/Troubled-Waters_FINAL.pdf. Accessed July, 2017.
[19] European Commission Web Site (2017). http://ec.europa.eu/environment/waste/mining/legis.htm, http://ec.europa.eu/environment/water/water-framework/index_en.html, http://ec.europa.eu/environment/marine/eu-coast-and-marine-policy/marine-strategy-framework-directive/index_en.htm, Accessed July, 2017
[20] Zorpas, A.A., Voukkali, I. and Loizia, P. (2017) A Prevention Strategy Plan Concerning the Waste Framework Directive in Cyprus, Fresen. Environ. Bull., V. 26, No. 2/2017, p. 1310-1317.
[21] Zorpas, A.A., Lasaridi, K., Abeliotis, C., Voukkali, I., Loizia, P., Georgiou, A., Chroni, C., Phanou, K., Bikaki, N. (2014) Waste Prevention Campaign Regarding the Waste Framework Directive, Fresen. Environ. Bull., V. 23, No. 11a/2014, p. 2876-2883.
[22] Blöch, H. (2009) The Water Framework Directive: An Overview; European Commission; http://www.wecf.eu/download/2010/02/JournalEnvLawREVSep2009.pdf, Accessed July, 2017.
[23] International Maritime Organization Web Site (2017). http://www.imo.org/OurWork/Environment/LCLP/Pages/default.aspx, Accessed July, 2017.
[24] Ministry of Foreign Affairs Web Site (2017). http://www.mfa.gov.tr/avrupa-birligi-ile-su-konusu-.tr.mfa, Accessed July, 2017.
[25] Akgul, D., Mertoglu, M. and Yuzer, B. (2011) Characterization of Landfill Leachates in Turkey, Fresen. Environ. Bull., V. 20, No. 10/2011, p. 2648-2652.
[26] Development Bank of Turkey, (2014). Water Resources Management and Security Specialization Commission Report, Tenth Development Plan (2014-2018), ISBN 978-605-4667-82-6. (In Turkish)
[27] Öztürk, İ., (1996) Wastewater Pre-Treatment and Marine Discharge Systems, Istanbul Technical University, Istanbul, 1st press, ISBN: 975-561-072-3. (In Turkish)
[28] Samsunlu, A., (1995) Marine Pollution and Control, Istanbul Technical University, ISBN: 975-561-048-0. (In Turkish)
[29] Yuksel, Y., Cevik, E.O. (2009) Coastal Engineering, ISBN: 9752959972, Beta Press, Istanbul, pp 732. (In Turkish)
[30] European Environment Agency (EEA) website (2017). https://www.eea.europa.eu/data-and-maps/figures/black-sea-physiography Accessed July, 2017
[31] DAP National Marine Research and Monitoring Program (2000). 1995-1999 Synthesis Report, Editors: Ilkay Salihoglu and Erhan Mutlu, November 2000. (In Turkish)
[32] Yilmaz, A. (2002) Biogeochemistry of Turkey's Seas: Distributions and Transformations, Turkish J. Eng. Env. Sci., 26 (2002), 219 - 235. (In Turkish)
[33] TAGEM, General Directorate of Agricultural Research and Policy of Turkey (1996). Determination of the Factors Causing Water Pollution in the Black Sea Region and Investigation of the Effects on Water Products Project Report, Project Code No: TAGEM/IV/96/12/02/001. (In Turkish)
[34] Talley, L. (2011) Descriptive Physical Oceanography 6th Ed., eBook ISBN: 9780080939117, Academic Press, p. 560. http://booksite.elsevier.com/DPO/chapterS08.html, Accessed July, 2017.

Received: **30.05.2017**
Accepted: **21.07.2017**

CORRESPONDING AUTHOR

Esin Esen
SRK Consulting Turkey
Turan Gunes Bulvari No: 86/3, 06550 Yildiz,
Ankara Turkey

e-mail: esinsn@gmail.com

© by PSP Volume 26 – No. 10/2017 pages 6159-6165 Fresenius Environmental Bulletin

PROTECTIVE EFFECT OF ASTAXANTHIN AGAINST ALUMINUM INDUCED LIVER OXIDATIVE DAMAGE

H Turan Akkoyun[1,*], Aydin Sukru Bengu[2], Mahire Bayramoglu Akkoyun[3], Aykut Ulucan[2], Okan Arihan[4]

[1]Siirt University, Faculty of Veterinary Science, Department of Physiology, Siirt, Turkey
[2]Bingol University, Department of Medical Services and Technics, Vocational School of Health Services, Bingol, Turkey
[3]SiirtUniversity, Faculty of Veterinary Science, Department of Biochemistry, Siirt, Turkey
[4]Van Yuzuncu Yil University, Faculty of Medicine, Department of Physiology, Van, Turkey

ABSTRACT

In this study, protective effect of a potent anti-oxidant astaxanthine on preventing rat liver damage due to Al exposure was evaluated. In experimental design, 20 Wistar-albino rats were divided into four groups as Control, Aluminum (20 mg/kg/day i.p), Al + Astaxanthine (5 mg/kg/day AST orally, Al 20 mg/kg/day i.p) and AST (5 mg/kg/day). Study was conducted for 14 days. GSH was found significantly low in Al group compared to control and significantly high in AST and AST + Al administered groups compared to Al group($p<0.01$). When MDA levels were investigated, an increase in Al administered group compared to control ($p<0.01$) and a decrease in Al + AST group compared to Al administered group ($p<0.001$) was found. In CAT enzyme activity level, a significant decrease in Al, AST and Al + AST administered groups compared to control ($p<0.001$), an increase in AST, Al + AST groups compared to Al administered group ($p<0.001$) and also an increase in CAT enzyme activity level in AST+Al administered group compared to AST group ($p<0.001$) was determined. Due to alterations in MDA and GSH levels and CAT enzyme activity in rat liver tissue as well as positive effects of AST in liver tissue histopathological assessments, it was concluded that AST has a protective role against such toxic molecules.

KEYWORDS:
Al, Astaxanthine, rat, liver, oxidative stress.

INTRODUCTION

Al is the third most commonly found metal in water, soil and air [1]. It is found in atmosphere in a range between 0.005 to 0.18 mg/m^3, and in earth crust commonly in the form of silicate and Al oxides. Humans are exposed to this cation in a wide range of products such as medicines, crafts, kitchen tools, electrical industry, cosmetics, food packaging and drinking water [2, 3]. In addition, it is used extensively in anti-acid drugs, anti-perspirants, deodorants and as ingredients of other health care products [4]. Al absorption is quite low in animals and humans normally however various factors may alter this absorption [2]. Daily intake is thought to change between 1 to 10 mg. Al intake via respiratory pathway ends up with 0.01-5% absorption. Al has a high metabolism and metabolized Al is thought to bound transferrin and albumin proteins up to 70-90%. Although level of Al in tissues is usually low but liver, bone and lungs are tissues which have high Al accumulation [4]. Al generally has toxic effects on mammals. Its toxic effects are more prominent in brain, liver, skeletal muscle, heart, bone marrow, kidney and blood [5]. Generally, it causes altered mineral balance, behavioral disorders and play important role in physiology of neurodegenerative disorders [6]. Al in high concentrations causes oxidative stress [7] due to its negative effect on antioxidant balance system. This situation causes biochemical alterations such as attenuation of antioxidant enzyme levels in plasma and tissues and increase in lipid peroxidation [8]. In addition, over exposure to Al triggers anemia hemolysis, inhibition on aminolevulinic acid dehydratase (ALA-D) enzyme [9], genotoxicity on DNA of neurons and other cells [10] and contributes to progression of Alzheimer's disease [11]. Caretenoids are a unique group containing about 700 lipid insoluble molecules, produced in high quantities in plants and in microorganisms such as algae and planktons [12]. They are not produced in humans and other animals but consumed with diet [13]. It is thought that carotenoids have substantial impacts on various health aspects. Ingestion of fruits and vegetables with high carotenoid content reduces risk of cancer and cardiovascular disease in epidemiological studies [14]. Astaxantine (AST) (3-3 dihydroxy β-β carotene 4-4 dione) is a ketocarotenoid which causes reddish color of salmonoids, marine fishes, algae and crustaceans [15]. AST is a radical scavenger which terminates chain reaction of reactive oxygen and nitrogen species. This property gives it an antioxidant nature which poses protective effect against oxidative stress, atherosclerosis, cardiovascular disease, inflammation, diabetes, cancer and other diseases [16, 17].

Due to these mentioned properties, it was aimed to test protective role of AST in liver damage in Al administered rats.

MATERIALS AND METHODS

Animals. 20 male adult Wistar albino rats weighing 250-300 gr were used in experiments. Animals were kept in controlled environment with constant heat and temperature as well as 12 hours of light and dark cycles. Food and water were given *ad libitum*. After one week of acclimation experiments had started. Food was withdrawn 12 hours prior to experiments. An ethical permission was obtained from Bingol University Animal Experiments Ethical Committee (30.12.2015 - 2015/09). All animals were treated with humane care according to the criteria outlined in the "Guide for care and use of Laboratory Animals " prepared by the National Academy of Sciences and published by the National Institutes of Health.

Experimental Design. The rats were divided into four groups: Group I (Control group) received isotonic saline administered i.p; Group II (Al)-received 20 mg/kg/day (i.p) Al as aluminum sulfate; Group III (AST) received 5 mg/kg AST orally (i.g). Group IV (AST+Al) received 5 mg/kg/day AST orally (i.g). and Al at 20 mg/kg/day via i.p. injection concomitantly. Al and AST were applied for 14 days. The doses were selected according to the literature data [18, 19]. At the end of the experiments rats were anaesthetized with ketamine (60 mg/kg) and xylazine (10 mg/kg) (i.p.). Following decapitation under anesthesia liver samples were obtained as a block. They were washed with saline and excess fluid was removed. They were stored in deep freeze (-80^{0}C) until biochemical analyses.

BIOCHEMICAL ANALYSIS

Measurement of MDA Level. 50 mg of tissue was homogenized in a solution containing 0.15 mol/L KCl. Centrifugation was performed at 1600× g. MDA (mg/dL) was assessed according to Placer et al. [20] by the reaction of thiobarbituric acid (TBA) and recording the absorbance at 530 nm.

Measurement of CAT Level. Measurement of (CAT) activity was performed due to Aebi. [21]. 0.1 mL of supernatant was added to a quartz cuvette including 2.95 mL of 19 mmol/L H_2O_2 solution prepared in potassium phosphate buffer (0.05 M, pH 7.00). Alteration in absorbance was measured at 240 nm for 5 min with a spectrophotometer (Shimadzu UV-1201, Japan)

Measurement of GSH Level. Tissue GSH levels were measured at 412 nm according to Sedlak and Lindsay [22]. Following precipitation of samples with 50% TCA, they were centrifuged at 1000× g for 5 min. 0.5 mL of supernatant, 2.0 mL of Tris–EDTA buffer (0.2 M; pH 8.9) and 0.1 mL of 0.01 M DTNB was prepared as the reaction mixture. The solution was kept for 5 min at room temperature and evaluated at 412 nm with spectrophotometer.

Histopathological Examination. After treatment, five rats in each group were necropsied and livers were taken. Also, sample tissues were fixed in 10% neutral-buffered formalin for 48 h. The tissue samples were processed as routine protocol. Tissues were dehydrated in alcohol series, cleared in xylene and then embedded in paraffin before sectioning at 5 µm thickness by rotary microtome (Leica, RM2125) [23] The slides were stained with hematoxylin and eosin [24]. Finally, the slides were examined and photographed by using light microscopy (Leica, DM2500).

Statistical Analysis. Results are expressed as mean ± standard error of mean. Analysis of variance (ANOVA) was performed and the comparisons among the groups were carried out with post hoc Tukey's test. Statistical significance was set as $p<0.05$ or lower. SPSS 20 for Windows were used as the statistical software.

RESULTS

Comparison of GSH measurement level from liver samples between Control, Al, AST and Al+AST groups were presented in Figure 1 and Table 1. Figures and calculated values were presented as mean and mean ± sem (standard error of mean). When results are evaluated; a significant decrease in GSH value in Al administered group compared to control ($p<0.01$) was observed. Similarly, an increase in AST and AST+Al administered groups compared to Al administered group was found.

Liver tissue MDA levels for Control, Al, AST and Al+AST groups are presented in Figure 2 and Table 2. Results for groups are presented as mean ± sem (standard error of mean). When results are evaluated, MDA level was found to increase in Al administered group compared to Control ($p<0.01$). Similarly decrease observed in Al administered group compared to Al + AST administered group was significant ($p<0.001$).

Liver tissue CAT levels are presented in Figure 3 and Table 3. Results are presented as mean ±sem (Standard error of mean).

TABLE 1
GSH (EU/g protein) levels between Cont, Al, AST, Al+AST groups

Groups (n=20)	Cont	Al	AST	Al+AST
GSH (EU/gprotein)	0.0057±0.003[b]	0.0006±0.011[b]	0.0029±0.001	0.0025±0.018

[b]p<0.01

TABLE 2
MDA (µmol/L) levels between Cont, Al, AST, Al+AST groups

Groups (n=20)	Cont	Al	AST	Al+AST
MDA (µmol/L)	1.3103± 0.116[b]	1.6024±0.101[a,b]	1.4460± 0.115	1.2672± 0.097[a]

a<0.001, b<0.01

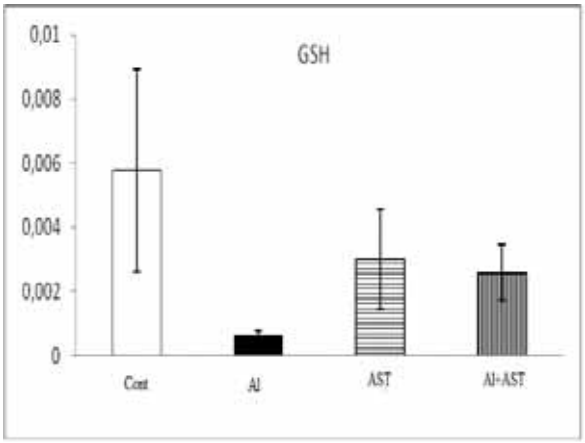

FIGURE 1
Comparison of GSH levels among groups Cont: Control, Al: Aluminum, AST: Astaxanthine, Al + AST: Aluminum + Astaxanthine.

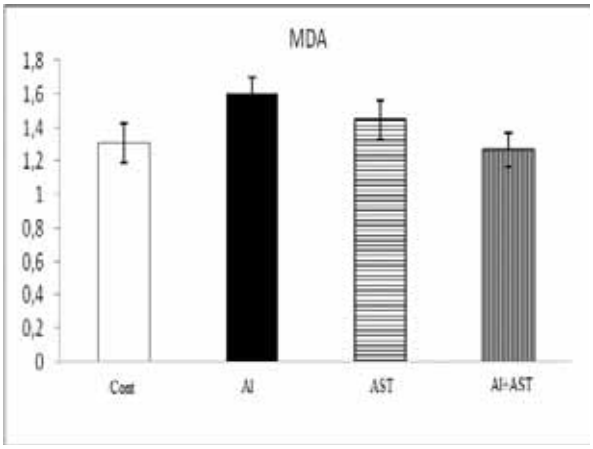

FIGURE 2
Comparison of MDA levels between Control, Aluminum, Astaxanthine, Aluminum + Astaxanthine groups.

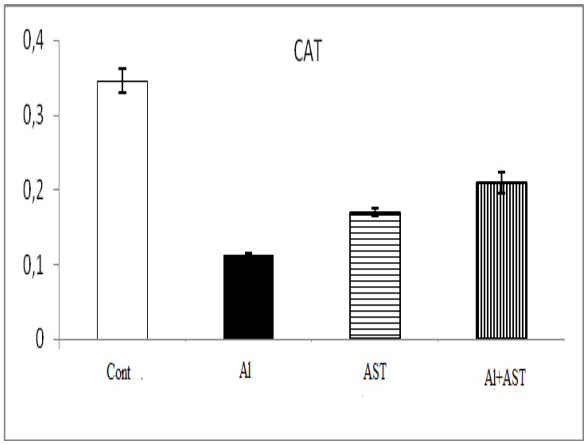

FIGURE 3
Comparison of CAT specific enzyme activity levels between groups Cont: Control, Aluminum, Astaxanthine, Aluminum + Astaxanthine

TABLE 3
CAT (IU/mg protein) enzyme activity levels between Cont, Al, AST, Al+AST groups

Groups (n=20)	Cont	Al	AST	Al + AST
CAT (IU/mgprotein)	0.3451±0.017[a]	0.1131±0.001[a,a1]	0.1700±0.005[a,a1,a2]	0.2093±0.014[a,a1,a2]

[a,a1,a2] p<0.001

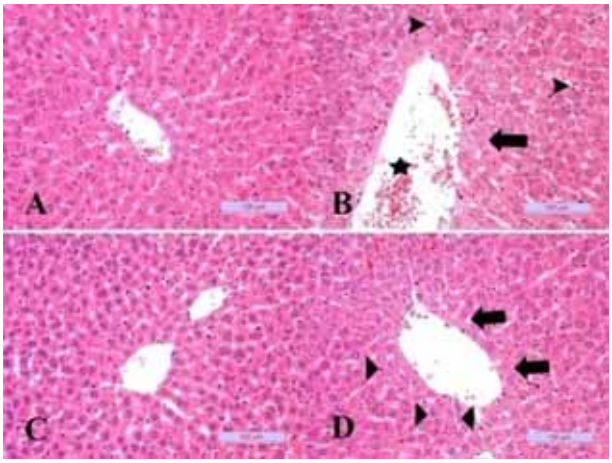

FIGURE 4
(A-B-C-D) Histopathology of liver tissues.
(4-A): Control group, normal histological structure x 20.
(4-B): Aluminum group, arrow; centrilobular hydropic degeneration of hepatocytes, arrow heads; Kupffer cells, star; vascular congestion in vena centralis x20.
(4-C): Astaxanthin group, normal histological structure x 20.
(4-D): Astaxanthin & Aluminum group, arrows; centrilobular hydropic degeneration of hepatocytes, arrow heads; Kupffer cells, x20. H&E staining.

When results are evaluated a decrease in CAT enzyme activity in Al, AST and Al + AST administered groups compared to control was observed ($p<0.001$). Similarly, an increase in enzyme activity in AST and Al + AST administered groups compared to Al administered group was detected ($p<0.001$). CAT enzyme activity was increased in AST + Al administered group compared to AST group ($p<0.001$).

In control group, in the evaluated organs no significant histopathological differences were noted. The liver tissues were observed in normal histological structure (Figure 4-A). However, in Al group in liver, centrilobular hydropic degeneration of hepatocytes, Kupffer cell hyperplasia and vascular congestion were identified (Figure-4, B). In AST group, the livers were in normal histological structure as in control group (Figure 4, C). In the concomitant AST+Al administered group in liver, mild centrilobular hydropic degeneration of hepatocytes and Kupffer cell hyperplasia were found (Figure 4-D).

DISCUSSION

Al was found to exert serious toxic effects on animals via its impact on blood, kidney, bone and brain tissues in experimental studies [25]. Especially effect of Al on Alzheimer and Parkinson diseases are well supported with experimental results [26]. Muselin et al., determined higher Al content in liver, kidney, heart, spleen and brain of rats administered Al compared to control group. In addition, administration of melatonin was found to decrease Al levels in rats in the same study. Therefore, they concluded that melatonin protects rat liver, kidney, spleen and brain tissues against Al toxication [27]. In another study, it was shown that boric acid prevented toxic effects of Al by decreasing liver marker enzymes [1]. Oxidative stress and lipid peroxidation causes great damage in body and is related with various pathological events. MDA which is an end product of lipid peroxidation occurs following exposure of fatty acids of cells to radicals. Main radicals are hydroperoxidase (ROOH), alcoxile (RO.) and peroxile (ROO.) in order. On the other hand, there exists antioxidants such as superoxide dismutase (SOD), catalase (CAT), gluthation (GSH), gluthation peroxidase (GPx) in the body which terminates activities of free radicals [28]. In literature studies in which Al administered rats were given Hesperetin and Ellagic acid, it was shown that MDA level in some tissues of rats was decreased [29]. In another study, Ellagic acid decreased MDA [30]. In another study, AST attenuated elevated MDA levels in alcohol administered mice [31]. Effect of AST on ischemia/reperfusion was also studied. Xanthine oxidase (XO) which is accepted as a marker of oxidative stress was found higher in ischemia/reperfusion administered animals in liver, whereas, it was attenuated in AST administered group [19]. In addition, in a study by Zhou et al., blood MDA levels were found high in septic rats and AST administration ameliorated this situation to a significant extent [32]. When results of our study are evaluated; MDA level was found

higher in Al administered group compared to control ($p<0.01$) and it was significantly decreased in Al+AST group compared to Al administered group ($p<0.001$). Our results are in accordance with existing literature data [19, 31, 32] however since no similar study was performed in literature we couldn't compare our results one by one. As a result, it can be stated that oxidative damage and lipid peroxidation occurred in Al administered rats.GSH is responsible from detoxification reactions in cells as an antioxidant molecule. In addition, it takes part as a cofactor in isomerization reactions of cells and it is a store for cysteine amino acid. GSH is an electron donor used in reduction of peroxidases catalyzed by GSH-Px [33]. Thus, gluthation molecule protects cells against free radicals. In literature studies GSH levels were increased following Hesperetin and Ellagic acid Al administered rats [29]. When our results are evaluated, GSH value were found significantly reduced in Al administered group compared to control ($p<0.01$). In addition, an increase in this value in AST and AST+Al administered groups compared to Al administered group was found. In a study by Ozkaya, GSH value in $AlCl_3$ + Ellagic acid group was found higher compared to control group. In the same study, no significant alteration was found in GSH value among Hesperetin administered groups. They also found higher GSH level in liver and brain tissues in Ellagic acid, $AlCl_3$+Ellagic acid and H_2O_2+Ellagic acid groups compared to control. Similarly, they found an elevated GSH level in Hesperetin, $AlCl_3$+Hesperetin, H_2O_2+Hesperetin groups compared to control. Our study results are in parallel with existing literature findings [29, 32]. In a study concerning catalase activity, an increase in serum, liver and brain catalase activity in Al administered rats compared to control was found [29]. In our study, a decrease in CAT activity in Al, AST and Al+AST administered groups compared to control was found ($p<0.001$). In addition, an increase in enzyme level in AST and Al+AST groups compared to Al administered group ($p<0.001$) as well as an increase in AST+Al administered group compared to AST group was observed ($p<0.001$). Our ameliorating results obtained with AST in Al administration are in parallel with other studies conducted with different protective molecules. Increase in catalase enzyme activity via AST+Al administration which is used in elimination of toxic hydrogen peroxide is important since catalase is a potent antioxidant enzyme. It is concluded that increased catalase activity by AST in AST+Al administration protects cells from oxidative damage. Our study is in accordance with mentioned studies above since protective molecule differs however ameliorating impact is similar when catalase is considered. In our study, histopathological findings in the liver as a result of microscopic examination, certain differences between groups were observed. In the control and AST groups, no microscopic findings were observed in the liver, while severe lesions were seen in the Al group and mild lesions in the Al + AST group.

Although Osinaka et al. [34] have reported that, Al accumulation in the liver leads to cholestasis, it has not been observed in our study. Histopathological findings such as centrilobular hydropic degeneration in hepatocytes, vascular congestion and Kuppfer cell hyperplasia, which are observed in rats' liver due to Al toxicities, Al and Al + AST groups, are similar to some Al toxicity studies [35-38] and have also been described in *Tilapia zillii* freshwater fish [39]. Although Galle et al. [40] reported in their study that Al does not produce toxic effects in the liver because it is eliminated from hepatocytes into the bile together with lysosomes, in our study it has been observed that some histopathological lesions related to Al toxication in rat livers had occurred.

Finally, it can be stated that AST protects cells from oxidative damage via blocking impact of Al in experimental rat studies and this was supported with histopathology. Therefore, this study is the first and original study in the scientific literature. Further studies should be conducted in this field.

CONCLUSIONS

AST was found to exert a protective role in liver tissues in both biochemical and histological investigation. In this manner AST can be regarded as an important protective in Al toxication which is an unintended contributor to our diets via industrial manufacturing activities and some other products such as antiperspirants.

ACKNOWLEDGEMENTS

The authors report there is no conflict of interest.

REFERENCES

[1] Turkez, H., Geyikoglu, F. and Colak, S. (2011) The protective effect of boric acid on aluminum-induced hepatotoxicity and genotoxicity in rats. Turkish Journal of Biology. 35(3), 293-301.

[2] Niu, Q., Yang, Y., Zhang, Q., Niu, P., He, S., Di Gioacchino, M. and Boscolo, P. (2007) The relationship between Bcl-2 gene expression and learning memory impairment in chronic aluminum-exposed rats. Neurotoxicity research. 12(3), 163-169.

[3] Nayak, P. (2002) Aluminum: impacts and disease. Environmental research. 89(2), 101-115.
[4] Yavuz, C.I., Vaizoglu, S.A. and Guler, C. (2013) Aluminium in Drinking Water. TAF Preventive Medicine Bulletin, 12(5), 589-596.
[5] El-Demerdash, F.M. (2004) Antioxidant effect of vitamin E and selenium on lipid peroxidation, enzyme activities and biochemical parameters in rats exposed to aluminium. Journal of Trace Elements in Medicine and Biology. 18(1), 113-121.
[6] Gomez, M., Sanchez, D.J., Llobet, J.M., Corbella, J. and Domingo, J. (1997) Concentrations of some essential elements in the brain of aluminum-exposed rats in relation to the age of exposure. Archives of gerontology and geriatrics. 24(3), 287-294.
[7] Ramu, S., Krishnaraj, K., Devika, A., Murali, A. (2014) Protective effects of Hippophaesalicifolia D. Don fruit pulp extract in Aluminium toxicity. Spatula DD-Peer Reviewed Journal on Complementary Medicine and Drug Discovery. 4(4), 207-212.
[8] Newairy, A.S.A., Salama, A.F., Hussien, H.M. and Yousef, M.I. (2009) Propolis alleviates aluminium-induced lipid peroxidation and biochemical parameters in male rats. Food and Chemical Toxicology. 47(6), 1093-1098.
[9] Farina, M., Rotta, L.N., Soares, F.A.A., Jardim, F., Jacques, R., Souza, D.O. and Rocha, J.B.T. (2005) Hematological changes in rats chronically exposed to oral aluminum. Toxicology. 209(1), 29-37.
[10] Nayak, P. and Chatterjee, A.K. (1998) Impact of Protein Malnutrition on Subcellular Nucleıc Acid and Protein Status of Brain of Alumınum - Exposed Rats. The Journal of Toxicological Sciences. 23(1), 1-14.
[11] Polizzi, S., Pira, E., Ferrara, M., Bugiani, M., Papaleo, A., Albera, R. and Palmi, S. (2002) Neurotoxic effects of aluminium among foundry workers and Alzheimer's disease. Neurotoxicology. 23(6), 761-774.
[12] Lorenz, R.T. and Cysewski, G.R. (2000) Commercial potential for Haematococcus microalgae as a natural source of astaxanthin. Trends in biotechnology.18(4), 160-167.
[13] Fassett, R.G. and Coombes, J.S. (2011) Astaxanthin: a potential therapeutic agent in cardiovascular disease. Marine drugs. 9(3), 447-465.
[14] Odeberg, J.M., Lignell, A., Pettersson, A. and Hoglund, P. (2003) Oral bioavailability of the antioxidant astaxanthin in humans is enhanced by incorporation of lipid based formulations. European journal of pharmaceutical sciences. 19(4), 299-304.
[15] Higuera-Ciapara, I., Felix-Valenzuela, L., Goycoolea, F.M. and Arguelles-Monal, W. (2004) Microencapsulation of astaxanthin in a chitosan matrix. Carbohydrate Polymers. 56(1), 41-45.
[16] Ambati, R.R., Phang, S.M., Ravi, S. and Aswathanarayana, R.G. (2014) Astaxanthin: sources, extraction, stability, biological activities and its commercial applications—a review. Marine drugs. 12(1), 128-152.
[17] Mortensen, A., Skibsted, L.H., Sampson, J., Rice-Evans, C. and Everett, S.A. (1997) Comparative mechanisms and rates of free radical scavenging by carotenoid antioxidants. FEBS letters. 418(1-2), 91-97.
[18] El-Maraghy, S.A., Gad, M.Z., Fahim, A.T. and Hamdy, M.A. (2001) Effect of cadmium and aluminum intake on the antioxidant status and lipid peroxidation in rat tissues. Journal of biochemical and molecular toxicology. 15(4), 207-214.
[19] Curek, G.D., Cort, A., Yucel, G., Demir, N., Ozturk, S., Elpek, G.O. and Aslan, M. (2010) Effect of astaxanthin on hepatocellular injury following ischemia / reperfusion. Toxicology. 267(1), 147-153.
[20] Placer, Z.A., Cushman, L.L. and Johnson, B.C. (1966) Estimation of product of lipid peroxidation (malonyldialdehyde) in biochemical systems. Analytical biochemistry. 16(2), 359-364.
[21] Aebi, H. (1984) Catalase in vitro. Methods in enzymology. 105, 121-126.
[22] Sedlak, J. and Lindsay, R.H. (1968) Estimation of total, protein-bound, and nonprotein sulfhydryl groups in tissue with Ellman's reagent. Analytical biochemistry. 25, 192-205.
[23] Anderson, G. and Bancroft, J. (2002) Tissue processing and microtomy including frozen. Theory and practice of histological techniques. London, UK: Churchill Livingstone. 85-107.
[24] Bancroft, J.D. and Gamble, M. (eds.) (2008) Theory and practice of histological techniques. Elsevier Health Sciences.
[25] Good, P.F., Perl, D.P., Bierer, L.M. and Schmeidler, J. (1992) Selective accumulation of aluminum and iron in the neurofibrillary tangles of Alzheimer's disease: a laser microprobe (LAMMA) study. Annals of neurology. 31(3), 286-292.
[26] Kurland, L.T. (1988) Amyotrophic lateral sclerosis and Parkinson's disease complex on Guam linked to an environmental neurotoxin. Trends in neurosciences. 11(2), 51-54.
[27] Muselin, F., Dumitrescu, E., Cristina, R., Alexandru, D.O.M.A. and Alexandra, T.R.I.F. (2015) Sicanlarda Melatoninin Bazi Organlarda Aluminyum Birikmesi Uzerine Koruyucu Etkisi. Istanbul Universitesi Veteriner Fakultesi Dergisi. 41(1), 26-30.
[28] Halliwell, B. and Gutteridge, J. (1984) Oxygen toxicity, oxygen radicals, transition metals and disease. Biochemical journal. 219(1), 1.

[29] Ozkaya A. (2007) Oksidatif Strese Maruz Kalan Ratların Bazı Biyokimyasal Parametrelerine Hesperetin Ve Ellagik Asidin Etkisi. Firat Universitesi. PhD.Thesis. Elazig, Turkiye.
[30] Khanduja, K.L., Gandhi, R.K., Pathania, V. and Syal, N. (1999) Prevention of N-nitrosodiethylamine-induced lung tumorigenesis by ellagic acid and quercetin in mice. Food and chemical toxicology. 37(4), 313-318.
[31] Zheng, D., Li, Y., He, L., Tang, Y., Li, X., Shen, Q. and Peng, Y. (2014) The protective effect of astaxanthin on fetal alcohol spectrum disorder in mice. Neuropharmacology. 84, 13-18.
[32] Zhou, L., Gao, M., Xiao, Z., Zhang, J., Li, X. and Wang, A. (2015) Protective effect of astaxanthin against multiple organ injury in a rat model of sepsis. Journal of surgical research. 195(2), 559-567.
[33] Öz M. (2003) DL- α-LipoikAsit ve DL- α-Tokoferol Asetat'in Yasli Albino Sicanlarin Eritrosit Membran Lipitleri Ile Karaciger ve Beyin Dokularindaki Bazi Metabolik Degisimler Uzerindeki Duzenleyici Etkileri, Firat Universitesi. Master.Thesis. Elazig, Turkiye.
[34] Osinska, E., Kanoniuk, D. and Kusiak, A. (2004) Aluminum hemotoxicity mechanisms. In Annales Universitatis Mariae Curie-Sklodowska. Sectio D: Medicina.411.
[35] Kutlubay, R., Oguz, E. O., Abban, G. and Turgut, S. (2007) Amelioration of aluminium-induced liver damage by vitamin E. Saudi medical journal. 28(2), 197-200.
[36] Laske, V., Stein, G., Muller, H., Braunlich, H., Fleck, C.H. and Linss, W. (1986) Untersuchungen Zur Aluminium schadigung der Lysosomen in verschiedenen Organen der gesunden und niereninsufficienten Ratte. In: Anke, M., Baumann, W. and Braunlich, H. (eds.) 5. Spurenelement-Symposium: New Trace Elements, University Leipzig and Jena. 792-801.
[37] Agarwal, D.R. and Jain, S. (2011) Significant liver toxicity in albino rats upon oral aluminium administration: a serious public health implication. Journal of Anatomical Society of India. 60(1), 46-49.
[38] Ogueche, P.N., Ugwu, C.E., Ezejindu, D.N., Omeje, M., Dike, C.C., Okonkwo, C.O., Maduka, H.C.C. and Obidoa, H.C.C. (2014) Aluminum Intoxication Induced Biochemical and Histopathological Alterations in Male Wistar Albino Rats Hepotocytes. Journal of Natural Sciences Research. 4, 24-6.
[39] Hadi, A.A. and Alwan, S.F. (2012) Histopathological changes in gills, liver and kidney of fresh water fish, Tilapia zillii, exposed to aluminum. International Journal of Pharmacy Life Sciences. 3(11), 2071-2081.
[40] Galle, P., Giudicelli, C.P., Nebout, T.H., Baglin, A. and Fries, D. (1987) Ultrastructural localization of aluminum in hepatocytes of hemodialyzed patients.Annales de Pathologie.7(3),163-170.

Received: **30.05.2017**
Accepted: **07.08.2017**

CORRESPONDING AUTHOR

H Turan Akkoyun
Siirt University, Faculty of Veterinary Science
Department of Physiology
TR-56100-Siirt – TURKEY

E-mail: turanakkoyun@hotmail.com

© by PSP Volume 26 – No. 10/2017 pages 6166-6174 Fresenius Environmental Bulletin

DETERMINATION OF PROBABLE REPRODUCTION SEASON OF INDIVIDUALLY TAGGED SIBERIAN, *ACIPENSER BAERII*, AND DIAMOND, *A. GUELDENSTAEDTII*, STURGEON BROODSTOCK, WHICH ARE NEWLY RISED, VIA STEROID HORMONES, HAEMATOLOGICAL CHANGES AND ULTRASOUND IMAGERY

Kubra Ak*, Ilker Zeki Kurtoglu

Recep Tayyip Erdogan University, Faculty of Fisheries Sciences, Department of Aquaculture, Rize, Turkey

ABSTRACT

In this study, it is aimed to determine the gonadal development and gender of the Siberian (*Acipenser baerii*) and diamond (*A. gueldenstaedtii*) sturgeon species by using ultrasonography and blood parameters in aquaculture conditions.

A total of 15 Siberian and 15 diamond sturgeon individuals from broodstock candidates at the ages of 4^+ years were selected and tagged. We used ultrasound examination and hematocrit, erythrocyte, leukocyte, hemoglobin values in blood, followed by calcium, sodium ions and steroids (estradiol (E_2), testosterone (T) and progesterone (P)) in blood plasma in monthly periods between December 2015 and June 2016.

Siberian sturgeon individuals were detected as 7 female and 8 male; and 7 females and 7 males were determined in diamond sturgeons, and 1 individual had no gender in ultrasound imaging.

Successful gender detection was performed by ultrasound imaging. Depending on the results of hemogram testing, probable gamete production period can be determined according to the changes of hematocrit, erythrocyte, leukocyte, hemoglobin and sex steroids. In this results, hemogram values increased between May and June in diamond sturgeon while peaking in January-February for Siberian sturgeon. However, there was no obvious change in calcium and sodium ions.

At the end of the study, it was concluded that blood analysis can be used effectively, when the main gamete maturation season of the newly produced broodstock population is decided. On the other hand, the ultrasonography is the easiest way to determine bloods' gender and maturation level.

KEYWORDS:
Maturity stage, sturgeon, ultrasonography, hematology, sex steroids.

INTRODUCTION

Sturgeons exist in the seas of Europe, Asia and America continents in northern hemisphere. They also exist along the coastal areas of Pacific and Atlantic Oceans, in the Mediterranean, in the Black Sea, Caspian Sea, and in the rivers that run to these seas and in several lakes [1].

Sturgeon are species with a high economic and ecologic value. However, overfishing, river reclamation works, water pollution, the banks built over rivers cause that this fish has almost become extinct [1].

In sturgeon species, the determination of gender and receiving gamete must be conducted without killing the fish in a reliable and practical way. The determination of gender and gonadal maturity stage especially in sturgeon species, which do not show sexual dimorphism, and which have late sexual maturity, is extremely important for broodstock management [2].

Endoscopy, gonadal biopsy, sex steroids, laparoscopy, morphology and ultrasonography methods are used to determine the gender and gonadal maturity in sturgeons [2, 3, 4, 5, 6, 7, 8].

There are many studies in the literature conducted to determine the gender and gonadal maturity in sturgeon, and many different methods have been reported in these studies. However, no studies were seen in the literature in which the changes in the blood parameters and gonadal developments were investigated in the long run in a parallel way in and out of the reproduction period of sturgeons. In this study, the purpose is to determine the gender and gonadal development by analyzing the blood parameters and using ultrasonic examinations in an 8-month period without causing any damage in Siberian (*Acipenser baerii*) and diamond (*A. gueldenstaedtii*) sturgeon species.

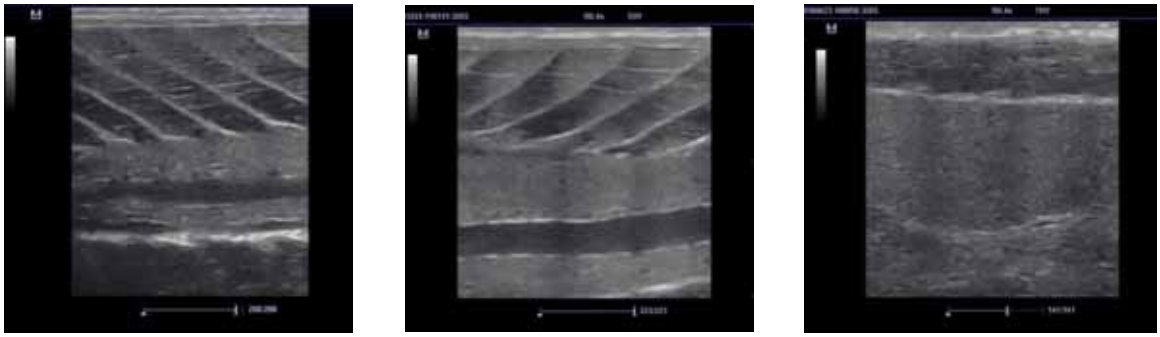

FIGURE 1
Typical ultrasonic images of testes in different maturity stages in the longitudinal views, M_1; left, M_2; mid, M_3; right

FIGURE 2
Typical ultrasonic images of ovaries in different maturity stages in the longitudinal views, F_1; left, F_2; mid, F_3; right

MATERIALS AND METHODS

The study was conducted in Recep Tayyip Erdogan University, Aquaculture Research and Application Center in November 2015-June 2016 period. The broodstock candidate fish were imported from Germany as fertilized eggs in December 2011. Fifteen of Siberian and 15 diamond sturgeon species, which had smooth body forms and which were at the age of 4^+ were selected from among the broodstock candidate fish. The average weight of the fish was 4.2±1.2 kg. The fish were tagged individually, and stocked in fiberglass tanks at the size of 3m in diameter and 1m water depth in 10 m^3/kg. The water provided from the streams was used in the caretaking of the fish.

Ultrasonographic Examinations. The fish were examined in monthly intervals. The *MINDRAY 5M* ultrasound imaging was made by using an electronic 10L4s linear probe with 8.0-12.0 MHz frequency. The examinations were made without applying any anesthetics on stretchers covered by soft towel. In ultrasound examinations, the frontal and transversal images between the 3-4th bone plates as of the ventral fin were evaluated. By using the ultrasound images, the genders and gonadal maturity levels of the fish were decided according to the morphology and echogenicity of the ovarium and testis tissues (the brightness of the tissues).

Blood Analysis. The blood samples were taken with a 2.5-ml injector from caudal vena, and transferred to heparinized tubes. The erythrocyte, leucocyte, hematocrit and hemoglobin values of the samples were measured in the PROKAN brand blood measurement device simultaneously. The samples whose blood counts were completed were centrifuged at 5,000 rpm^{-1} for 10 minutes to obtain the blood plasma. Then, samples were stocked in deep freezer (-80°C) up to analysing.

The analysis of the steroid hormones (Estradiol, testosterone and progesterone) from the blood plasma was made with Radioimmunoassay Method; and the measurement of calcium and sodium ions was made with the Spectrophotometric Method.

RESULTS

Ultrasound Imaging. In ultrasound examination of the Siberian sturgeon, it was determined that there were 7 females and 8 males; while it was determined that there were 7 females and 7 males in the diamond sturgeon, and there was 1 individual that

had not completed its gonadal maturity. The gonad stages are given in Table 1.

TABLE 1
Identification of the stages maturity of female and male Siberian and diamond sturgeon

Maturity Stages	Siberian sturgeon		Diamond sturgeon	
	Female	Male	Female	Male
1	1	3	1	-
2	6	4	5	3
3	-	1	1	4
4	-	-	-	-

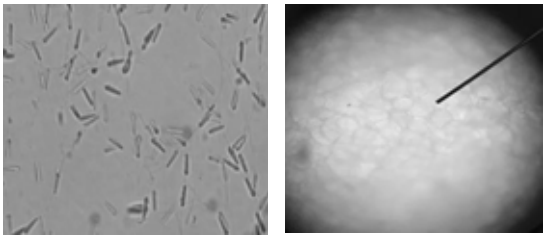

FIGURE 3
Microscopic spermatozoa and oocyte cell images

The testes in male individuals were observed to be extremely small and in the lateral part in the 1st stage. The fat tissue was observed to be in dark-grey (hypoechogenic) color. In the 2nd stage, the dark fat tissue decreased, and the testicular tissue was homogeneous and bigger. In the 3rd stage, the testicular covered the body cavity and in light-grey color (hyperechogenic). In this stage, it was determined that the spermatozoa were mature (Figure 1). In Siberian sturgeon, only one individual, which was defined as being at the end of 3rd stage, was examined in a histopathologic way. The spermatozoa in the milt that was sampled with the Stripping Method were imaged under microscope (Figure 3).

In ultrasonographic examinations in the female individuals, any mature individual in gonadal terms wasn't detected. It was observed that the ovarium tissue was surrounded by a fat tissue in the females in the 1st stage. The ovarium was in heterogenous structure and in bright color. In the ovarium tissue in the 2nd stage, the fat tissue decreased, and the ovarium tissue covered the body cavity in a bright color. In the 3rd stage, the ovarium was observed in granular structure and in dark color. Small oocytes were observed (Figure 2). In pathological sampling of a female individual, small oocytes (1.1 mm in diameter) were imaged under microscope (Figure 3).

Blood Parameters. Hemogram. In the study, the monthly changes in leucocyte, erythrocyte, hemoglobin and hematocrit values were determined in male and female Siberian and diamond (*A. gueldenstaedtii*) sturgeon species, and are given in Figure 4, Figure 5, Figure 6 and Figure 7.

The highest leucocyte value in both species was determined in the sampling of November. While the highest leucocyte amount of the female individuals in Siberian sturgeon was $58.6*10^3 \pm 12.2$ µl; the highest leucocyte amount of the male individuals was $57.3 \pm 10.4*10^3$ µl.

The lowest leucocyte value was detected in April-May. The lowest average value of the female individuals was $47.2 \pm 8.2*10^3$ µl; and $48.0 \pm 6.1*10^3$ µl in males. The lowest leucocyte amount in diamond sturgeon was detected in March. The highest leucocyte amount was $54.9 \pm 7.2*10^3$ µl in average in females; and $54.8 \pm 7.6*10^3$ µl in males; and the lowest value was $46.5 \pm 6.9*10^3$ µl in male and female individuals.

The highest erythrocyte values in Siberian and diamond sturgeons were detected in November. The highest average erythrocyte amount of female Siberian sturgeon was $1.13*10^3 \pm 0.3$ µl in November; and the lowest amount was detected in May as $0.53 \pm 0.1*10^3$ µl. The highest value in male individuals was $1.08 \pm 0.2*10^3$ µl in November; and the lowest value was detected in April with $0.57 \pm 0.1*10^3$ µl. The lowest erythrocyte value in diamond sturgeon was detected in February. The highest average value in female individuals was $0.84 \pm 0.2*10^3$ µl; and the lowest average value was $0.62 \pm 0.1*10^3$ µl; and the highest average value in males was $0.85 \pm 0.2*10^3$ µl; and the lowest value was $0.62 \pm 0.1*10^3$ µl.

The highest hemoglobin values were measured in November for both species. The lowest average values in Siberian sturgeon female and male individuals were detected in May. The highest and lowest average values for the female individuals were 17.15 g dl^{-1} and 10.14 g dl^{-1}, respectively; and the highest and lowest average values in males were 17.19 g dl^{-1} and 10.03 g dl^{-1}, respectively. The lowest hemoglobin values in diamond sturgeon were detected in March. The highest and lowest values in female individuals were 15.18 g dl^{-1} and 10.6 g dl^{-1}, respectively; and the highest and lowest values in male individuals were 15.22 g dl^{-1} and 10.5 g dl^{-1}, respectively.

The highest hematocrit rates in Siberian sturgeon individuals were detected in November; and the lowest values were detected in April. The highest average hematocrit rate of the female individuals was 25.12%; and the lowest rate was 12.03%; and in male individuals, the highest average was 25.67; and the lowest average was 12.48%. The highest hematocrit values in diamond sturgeon were detected in December; and the lowest values were detected in March. The highest average hematocrit rate of the female individuals was 18.29%; and the lowest was 12.46%; in male individuals, the highest average was 18.45%, and the lowest rate was 12.41%.

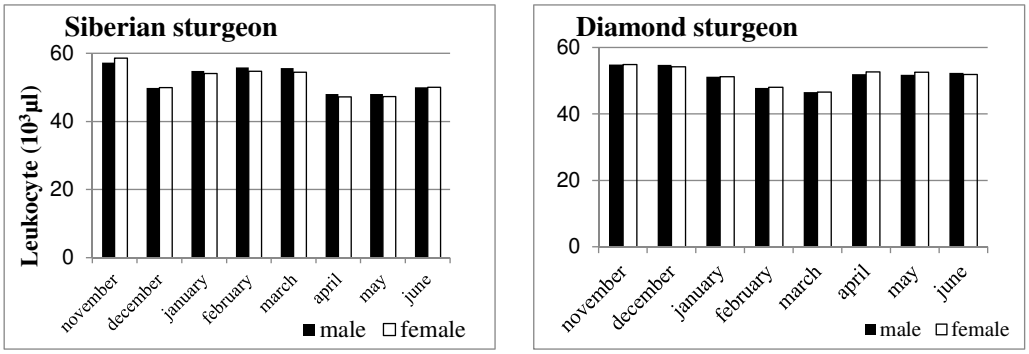

FIGURE 4
Change in the mean leukocyte concentrations in female and male sturgeon

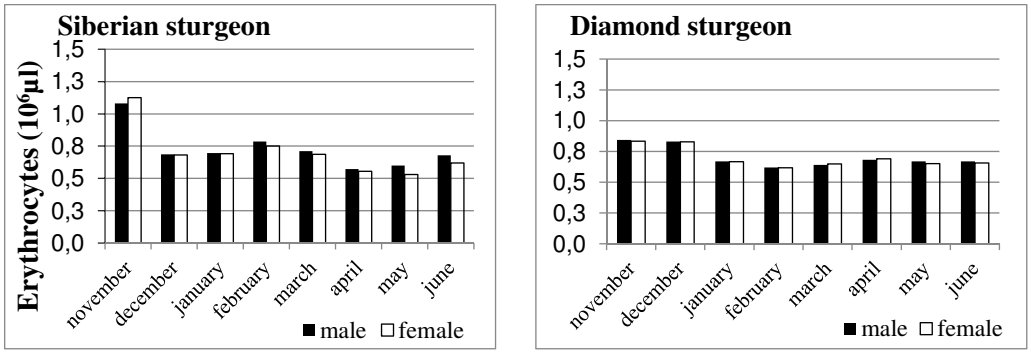

FIGURE 5
Change in the mean erythrocytes concentrations in female and male sturgeon

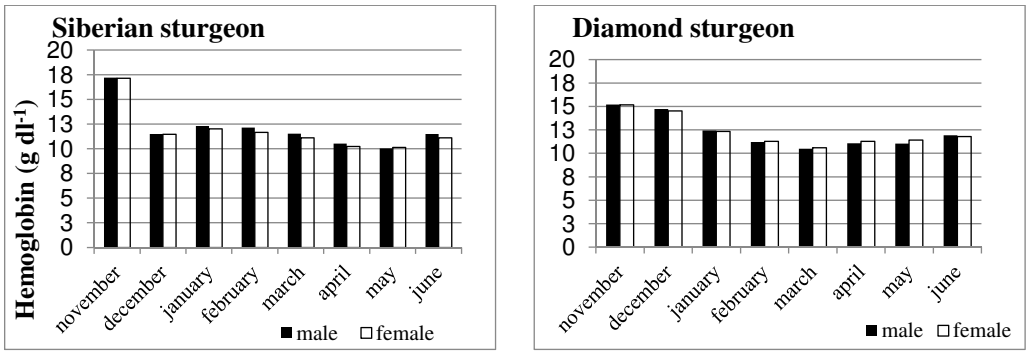

FIGURE 6
Change in the mean hemoglobin concentrations in female and male sturgeon

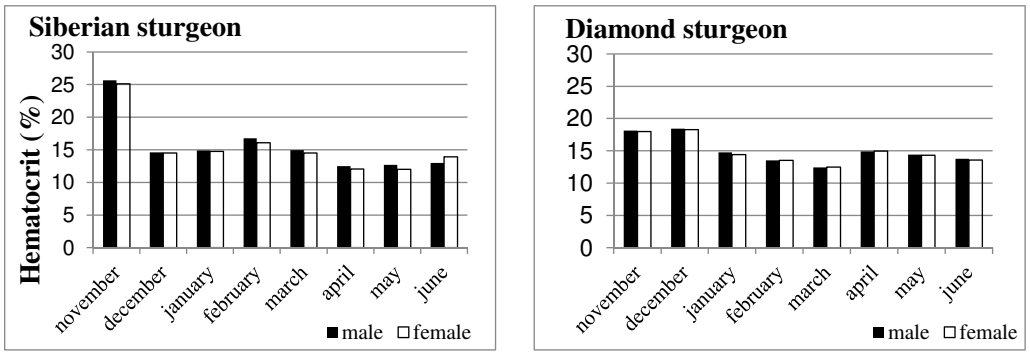

FIGURE 7
Change in the mean hematocrit concentrations in female and male sturgeon

The Analysis of the Steroid Hormones. The estradiol levels of female individuals in Siberian sturgeon were detected at the highest level in February with 199.1 pg ml^{-1}; and at the lowest level in October with 18.8 pg ml^{-1}. In male individuals, it was the highest in May with 49.0 pg ml^{-1}; and the lowest in November with 11.50 pg ml^{-1} (Figure 8). The estradiol levels in female and male individuals of diamond sturgeon showed parallel changes (Figure 8). The highest estradiol level in female and male individuals was detected in March; and the lowest value was detected in October. While the highest average value in female individuals was 153.0 pg ml^{-1}; the lowest value was 29.7 pg ml^{-1}; in male individuals, it was 57.8 pg ml^{-1} and 38.2 pg ml^{-1}, respectively.

The testosterone level in female and male individuals in Siberian sturgeon was at the highest level in June (Figure 9). While the testosterone level in male individuals was maximum with 670.0 ng dl^{-1}, the minimum value was detected in March with 398.8 ng dl^{-1}. The testosterone level in female individuals was maximum with 355.0 ng dl^{-1} and minimum in April with 181.68 ng dl^{-1}.

In diamond sturgeon, the testosterone levels of the male individuals were maximum in October with 753.7 ng dl^{-1}; and minimum in April with 351.8 ng dl^{-1}. In female individuals, the testosterone level was maximum in January with 636.3 ng dl^{-1}, and minimum in June with 230.8 ng dl^{-1} (Figure 9).

In Siberian sturgeon, the progesterone levels in female and male individuals did not differ along the study, and stayed stable at 0.1 ng ml^{-1}. No important changes were observed in the progesterone levels of the diamond (*A. gueldenstaedtii*) sturgeon, which was also the case in Siberian sturgeon. The highest progesterone level in female and male individuals was in October, and the lowest value was detected in April. The highest and lowest values in males and females were 0.21-0.11 ng ml^{-1}, and 0.22-0.11 ng ml^{-1}, respectively.

The Analysis of Sodium (Na^+) and Calcium (Ca^{++}) Ions in Blood Plasma. The calcium ion amount in Siberian sturgeon was maximum in male individuals in November, and minimum in April; and in females, maximum in December, minimum in May. In male individuals, the maximum and minimum values were measured as 19.63-9.85 mg dl^{-1}; and in females, as 16.95-11.21 mg dl^{-1} (Figure 11).

In diamond sturgeon, the maximum calcium ion levels of female and male individuals were detected in March, and minimum values were detected in October, the maximum and minimum values in female individuals were 8.45-6.76 mg dl^{-1}, respectively; and in male individuals, 8.45-6.60 mg dl^{-1}, respectively (Figure 11).

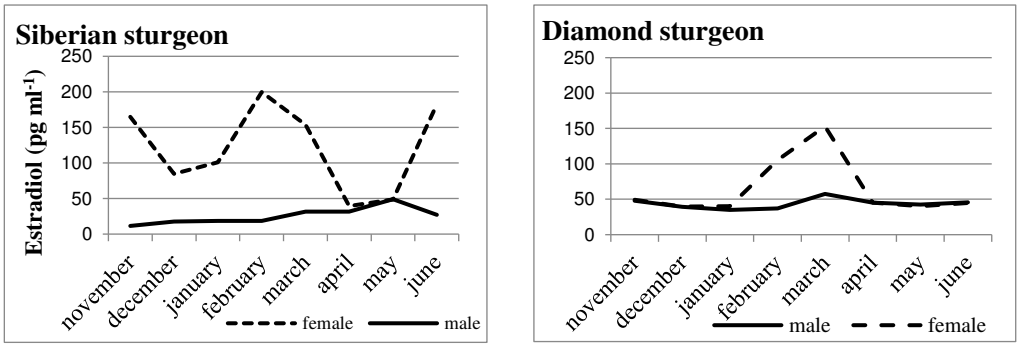

FIGURE 8
Change in the mean plasma E2 concentrations in female and male sturgeon

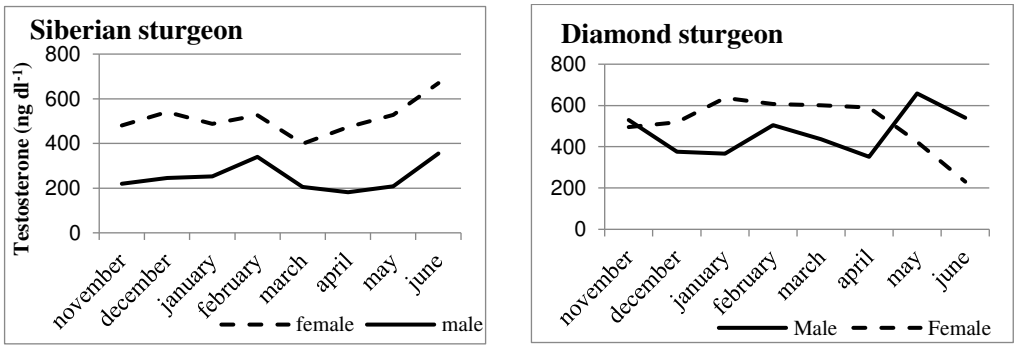

FIGURE 9
Change in the mean plasma T concentrations in female and male sturgeon

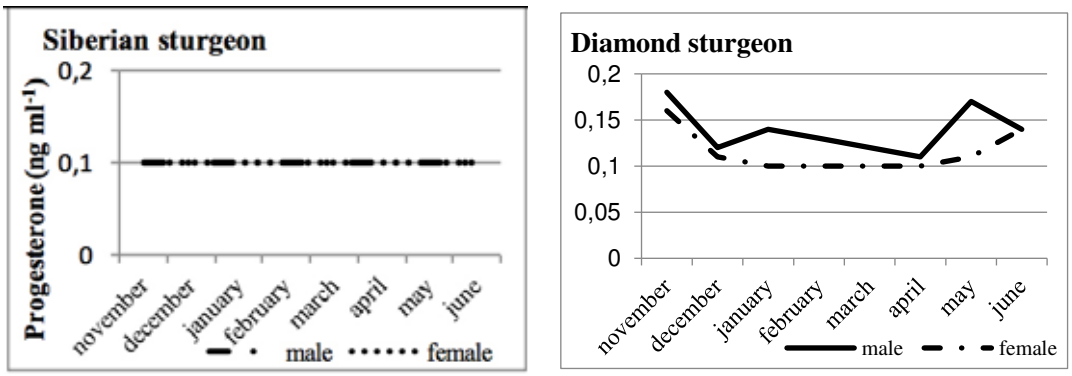

FIGURE 10
Change in the mean plasma P concentrations in female and male sturgeon

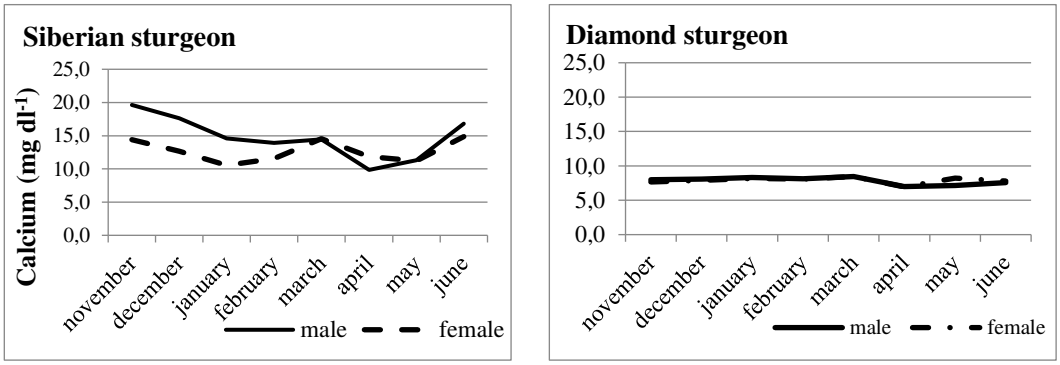

FIGURE 11
Change in the mean plasma calcium concentrations in female and male sturgeon

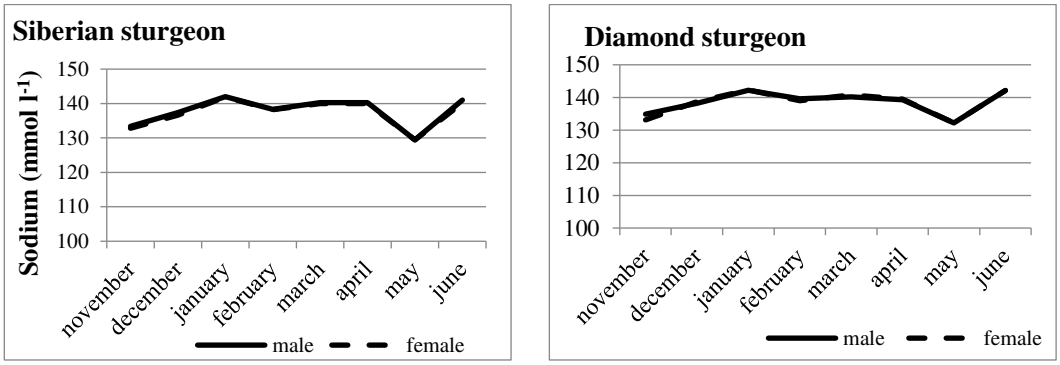

FIGURE 12
Change in the mean plasma sodium concentrations in female and male sturgeon

The sodium ion levels of female and male individuals in both species were detected to progress in similar rates. The highest sodium ion level was detected in January, and the lowest value was detected in October. In Siberian sturgeon individuals, while the maximum value for both genders was 141.86 mmol l^{-1}, the minimum value in male individuals was 118.5 mmol l^{-1}, and 120.0 mmol l^{-1} in females. In diamond sturgeon, the maximum value in females and males was 142.3 mmol l^{-1}, and the minimum values in male individuals were 133.0 mmol l^{-1}, and 120.7 mmol l^{-1} in females (Figure 12).

DISCUSSION AND CONCLUSIONS

In broodstock sturgeon species, the blood parameters and ultrasound examination may be used as a successful method in the following gamete development period by keeping the stress at minimum level and without causing any losses in fish. Several parameters like sizes of the ovarium and testis, the egg diameter and the gonadal development can be measured with ultrasound imaging method. At the same time some data related with reproductive performance like fecundity and gonadosomatic index

may be achieved with ultrasonographic imaging. [11, 12]. Many researchers recommend the determination of gender with ultrasonography since it causes less stress than the other methods and is a practical method [13, 14]. In this study, 30 broodstock candidate individuals were selected from among 1250 Siberian and diamond sturgeon species aged 4^+; and the female and male individuals were determined by using the ultrasound technique. No statistically significant differences were observed during the study course in average steroid hormones, blood parameters and sodium and calcium ion values of the female and male individuals ($p>0,05$). The gender of the species was determined by using the morphology and echogenicity (the brightness of the tissues) of the ovarium and testis tissues. The ultrasonographic imaging applications were carried out without anesthetizing. There were no deaths during the treatments.

Gender differentiation in sturgeon species is being completed up to age of 1-2 at the latest [15, 16]. However, it has been reported that the gender determination before 3 years of age is not reliable in these species. In fish rised under culture conditions, the vitellogenesis may last until the end of 3-4 years of age [15]. It must be considered that a great variation may be observed in the fish at the same age [17, 16].

The steroid hormones play important roles for hormonal control of the reproduction functions. It has been reported that the estradiol (E_2), 11-ketotestosterone (11-KT), VTG value, E_2/VTG and E_2/11KT rates may be used in determining the gender of the fish in a successful way [18, 19]. In this study, the levels of estradiol, testosterone and progesterone hormones, which are among the reproduction hormones, in and out of the reproduction season were examined in blood plasma. The estradiol level in female Siberian sturgeon individuals were measured higher than that of the male individuals. The highest estradiol level in female individuals was detected in February, and the lowest value was in October. The estradiol levels measured in April-May, which are the natural reproduction seasons of female individuals, progressed at lower levels when compared with the other months. The testosterone levels in male individuals were measured at higher levels than the female individuals during the study period. While the testosterone levels of the Siberian individuals were at high levels all during the study period, a measurable decreasing was observed in the testosterone levels in female and male individuals after March, which is reproduction season. The measured estradiol levels in male and female diamond sturgeon were similar along the study period. Although the estradiol levels of the male individuals were similar with female individuals, the estradiol levels of the female individuals were measured as relatively higher than the male individuals, just before the reproduction season in January-March. The female individuals' estradiol values rapidly decreased, and reached to similar values as male individuals in April, which is the natural reproduction season. The testosterone levels of female individuals cruised at higher levels than the male individuals all along the study. However, in April, the beginning of the reproduction season, the testosterone levels decreased in female individuals and increased in male individuals. It was also determined that there were no significant differences in females and males in terms of progesterone levels.

The changes in blood plasma, sodium and calcium ion measurements are being used efficiently in determining the maturity status. During the maturation of gonad in female *Acipenser transmontanus*, the plasma VTG and calcium concentrations increase with the onset of yolk deposition. It was reported that the calcium ion amount in the blood plasma in females that are not mature was 96 $\mu g\ ml^{-1}$, and as 175 $\mu g\ ml^{-1}$ in mature individuals [20]. Marco et al. (2010), measured the reference value of the sodium ion in blood plasma of *A. naccari x A. baerii* hybrid sturgeon individuals as 140 $\mu g\ ml^{-1}$ in average [21]. This value is similar with our obtained average values for both for *A. baerii* and for *A. gueldensatedtii*. However, the late May values, which is the end of the reproduction season for Siberian sturgeon individuals, were lower when compared with these values.

Determining the changes in blood parameters, which are changing according to environmental and biological factors, is important to reveal the stress, comfort and the physiological status of the fish. However, the data on the reference values of many species are extremely limited in the literature [13]. The data obtained in this study have revealed the change in steroid hormone levels, the changes in some blood parameters, and the changes in the sodium and calcium amounts for of the individuals both species in and out of the reproduction season.

According to the hemogram data and observed individuals gonadal development findings, the fluctuations of the hematocrit, erythrocyte, leucocyte, hemoglobin values overlapped with the possible gamete production period of the broodstock candidates. In this context, the hemogram values of the Siberian sturgeon were determined at the peak level in January-February. On the other hand, diamond sturgeon's blood parameters referred May-June duration as potential reproduction season. In the light of these findings, sperm intake from male fishes was achieved in both Siberia and diamond back fishes at the age of 4^+. It was observed that the spermatozoa were motile in the examinations made on the sperm samples. Owing to the fact that mature eggs couldn't be obtained from 4^+ year old female individuals, advanced applications related to production hadn't been realized during the study. Potential gamete maturation period can be determined following the blood parameters of the newly grown sturgeon. Thus, production planning and economic planning

process can be managed correctly when considering that the reproduction process of sturgeon fish has taken many years.

ACKNOWLEDGEMENTS

We offer our gratitude to Recep Tayyip Erdogan University BAP Coordinatorship (project number: 2015.53007.103.02.05) and Fisheries Research & Application Center Directorate, because of study finance and live material supply.

REFERENCES

[1] Dettlaff, T.A., Ginsburg, A.S. and Schmalhausen, O.I. (1993) Sturgeon fishes, Developmental Biology and Aquaculture. Springer Verlag, Berlin Heidelberg, 300.

[2] Moghim, M.A., Vajhi, R., Veshkini, A. and Masoudifard, M. (2002) Determination of sex and maturity in *Acipenser stellatus* by using ultrasonography. J. Appl. Ichthyol., 18:325-328.

[3] Webb, M.A.H., Feist, G.W., Foster, E.P., Schreck, C.B. and Fitzpatrick, M.S. (2002) Potential classification of sex and stage of gonadal maturity of wild white sturgeon using blood plasma indicators. Trans. Amer. Fish. Soc. 131:132-142.

[4] Colombo, R.E., Wills, P.S. and Garvey, J.E. (2004) Use of ultrasound imaging to determine sex of shovelnose sturgeon. Journal of Fisheries Management, 24:322-326.

[5] Wildhaber, M.L., Papoulias D.M., DeLonay A.J., Tillitt, D.E., Bryan, J.L. and Annis, M.L. (2007) Physical and hormonal examination of missouri river shovelnose sturgeon reproductive stage: a reference guide. J. Appl. Ichthyol., 23:382-401.

[6] Chebanov, M. S. and Galich, E.V. (2009) Ultrasound diagnostics for sturgeons broodstock management, p. 115. Krasnodar, Russia: Education-South.

[7] Craig, J.M., Papoulias, D.M., Thomas, M.V., Annis, M.L. and Boase, J.C. (2009) Sex assignment of Lake Sturgeon (*Acipenser fulvescens*) based on plasma sex hormone and vitellogenin levels. Journal of Applied Ichthyology, 25(Supplement 2):60–67.

[8] Petochi, T., Di Marco, P., Donadelli, V., Longobardi, A., Corsalini, I., Bertotto, D., Finoia, M.G. and Marino, G. (2011) Sex and reproductive stage identification of sturgeon hybrids (*Acipenser naccarii* × *Acipenser baerii*) using different tools: ultrasounds, histology and sex steroids. J. Appl. Ichthyol., 27:637-642.

[9] Bruch, R.M., Dick, T.A. and Choudhury, A. (2001) A field guide for the identification of stages of gonad development in Lake Sturgeon, *Acipenser fulvescens* Rafinesque, with notes on Lake Sturgeon reproductive biology and management implications. Wisconsin Department of Natural Resources, Oshkosh, and Sturgeon for Tomorrow, Appleton, Wisconsin.

[10] Chiotti, J.A., Boase, J.C., Hondorp, D.W. and Briggs A.S. (2016) Assigning sex and reproductive stage to adult Lake sturgeon using ultrasonography and common morphological measurements. North American Journal of Fisheries Management 36:21–29.

[11] Albers, J.L., Wildhaber, M.L. and DeLonay, A.J. (2013) Gonadosomatic index and fecundity of Lower Missouri and Middle Mississippi River endangered pallid sturgeon estimated using minimally invasive techniques. J. Appl. Ichthyol., 29:968-977.

[12] Bryan, J.L., Wildhaber, M.L., Papoulias, D.M., DeLonay, A.J., Tillitt, D.E. and Annis, M.L. (2007) Estimation of gonad volume, fecundity, and reproductive stage of shovelnose sturgeon using sonography and endocopy with application to the endangered pallid sturgeon. J. Appl. Ichthyol., 23:411-419.

[13] Du, H., Zhang, X., Leng, X., Zhang, S., Luo, J., Liu, Z., Qiao, X., Kynard, B. and Wei, Q. (2016) Gender and gonadal maturity stage identification of captive Chinese sturgeon, *Acipenser sinensis*, using ultrasound imagery and sex steroids. General and Comparative Endocrinology,

[14] Memiş, D., Yamaner, G., Tosun, D.D., Eryalçın, K.M., Chebanov, M. and Galich, E. (2016) Determination of sex and gonad maturity in sturgeon (*Acipenser gueldenstaedtii*) using ultrasound technique. Journal of Applied Aquaculture, 28:252-259.

[15] Doroshov, S.I., Moberg, G.P. and Van Eenennaam, J.P. (1997) Observations on the reproductive cycle of cultured white sturgeon, *Acipenser transmontanus*. Environmental Biology of Fishes, 48:265–278.

[16] Hurvitz, A., Jackson, K., Degani, G., and Levavi-Sivan B. (2007) Use of Endoscopy for gender and ovarian stage determinations in Russian Sturgeon (*Acipenser gueldenstaedtii*) grown in aquaculture. Aquaculture, 270:158–166.

[17] Amiri, B.M., Maebayashi, M. Hara, A. Adachi, S. and Yamauchi K. (1996) Ovarian development and serum sex steroid and vitellogenin profiles in the female cultured sturgeon hybrid, the bester. Journal of Fish Biology, 8:1164–1178.

[18] Cuisset, B.D., Rouault, T. and Williot, P. (2011) Estradiol, testosterone, 11-ketotestosterone, 17, 20 beta-dihydroxy-4-pregnen-3-one and vitellogenin plasma levels in females of captive European sturgeon, *Acipenser sturio*. J. Appl. Ichthyol. 27:666-672.

[19] Mola, A.E. and Hovannisyan, H.G. (2015) Measurements of serum steroid hormones (testosterone, 11-ketotestosterone, and 17b-estradiol) in farmed great sturgeon. Comparative Clinical Pathology, 24:509-513.
[20] Casenave J.L., Kroll, K.J., Van-Eenennaam, J.P. and Doroshov, S.I. (2003) Effect of ovarian stage on plasma vitellogenin and calcium in cultured white sturgeon. Aquaculture, 221:645-656.
[21] Marco, P.D., Priori, A., Finoia, M.G., Longobardş, A., Donadelli, A. and Marino G. (2010) Assessment of blood chemistry reference values for cultured sturgeon hybrids (*Acipenser naccarii* female×*Acipenser baerii* male). J. Appl. Ichthyol., 27:584-590.

Received: **31.05.2017**
Accepted: **29.07.2017**

CORRESPONDING AUTHOR

Kubra Ak
Recep Tayyip Erdogan University,
Faculty of Fisheries Sciences,
Department of Aquaculture,
53100, Rize – TURKEY

E-mail: kubra.ak@erdogan.edu.tr

© by PSP Volume 26 – No. 10/2017 pages 6175-6183 Fresenius Environmental Bulletin

COMPREHENSIVE BENEFIT EVALUATION OF VARIOUS TYPES OF MARINE DEVELOPMENT: A CASE STUDY OF JIANGSU

Sheng Gao[1], Huihui Sun[2], Lin Zhao[1], Runjie Wang[1], Baiqiong Liu[1], Min Xu[1,*]

[1]School of Geographic Science, Nanjing Normal University, Nanjing 210023, Jiangsu, China
[2]Nanjing City Vocational College, Nanjing 210028, Jiangsu, China

ABSTRACT

This study takes four main types of marine development in Jiangsu Province as an example. Discussion on a more reasonable, more objective and effective evaluation system of marine use efficiency. A more reasonable, objective and perfect marine benefit evaluation system is discussed. The social and economic benefits, the value of ecosystem services, the value of the loss of ecosystem and the value of ecological benefits are included in the evaluation of the total benefit of the calculated unit area. According to social benefit, economic benefit, resource benefit and environment benefit, the comprehensive benefit index system is constructed. On this basis, comprehensive index method and grey correlation method are adopted to evaluate the comprehensive benefits of different marine development types.

KEYWORDS:
Marine development type, comprehensive benefit evaluation, comprehensive index, grey correlation.

INTRODUCTION

Marine development is an important way for people to make full use of marine resources, but the current domestic and international related research and development of the marine economy will pay more attention to marine resources support for economic development [1], and did not fully take into account the development and utilization of marine resources and ecological environment problems caused by improper restrictions and constraints on the role of economic development.

From the point of view of calculating the total benefit of sea use type, the focus of the research on marine development at home and abroad is mainly based on the social and economic benefits and comprehensive evaluation. The social benefit, economic benefit, resource benefit and environmental benefit are all less in the study of the total benefit, and most of the comprehensive benefits around the sea reclamation. For example, Liu Qing et al. (2013) [2] comprehensive consideration of the reclamation of land for economic, social and ecological environment in three areas. The comprehensive benefit evaluation of 4 typical reclamation projects in Jiangsu province was carried out, but not included in ecological gains and losses. Meanwhile used the ratio analysis method, market value method and achievement reference method to evaluate the comprehensive benefits of reclamation. Xiao Jianhong et al. (2011) [3] use market value method and contingent valuation method. From the perspective of wetland ecosystem service function. The ecological environment value loss of reclamation project was evaluated. But there is no calculation results of ecological profit and loss. Li Jingmei et al. (2011) [4] used to bit model and willingness survey method to evaluate the environmental cost of reclamation in Jiaozhou bay. Only highlights the ecosystem service functions, not comprehensive. In addition, Qi Junting et al. (2008) [5] carried out financial evaluation and national economic evaluation on the activities of marine development. However, there is no assessment of ecological benefits in accordance with various types of marine development, Luo Xiqian et al. (2012) [6] were estimated and analyzed on the benefits of Langqi Island reclamation project, Fu qing Bay reclamation planning scheme, but neglected the ecosystem service function value accounting.

From the angle of comprehensive benefit evaluation of sea use type, the domestic and foreign researches on ocean development are mostly in the fields of engineering technology, comprehensive management and environment. However, the research on the comprehensive benefits of resources and environment caused by the development activities is less. The selection of evaluation index, the determination of index weight, the determination of safety threshold and the choice of evaluation methods should be discussed and proved [7, 8, 9]. With the development of ocean exploitation in china, more and more scholars began to study the specific development projects, and put forward some evaluation methods of marine development activities.

With the intensification of human activities, marine development has become the focus of atten-

tion of the government, especially the comprehensive benefits of marine development. However, the evaluation of the comprehensive benefits of marine development types is more ambiguous. It is mainly reflected in the uncertainty evaluation method, evaluation system, evaluation factor, evaluation criteria and the type of single evaluation. This paper selects Jiangsu province a variety of ocean development as the example and calculate the total efficiency of comprehensive benefit evaluation, improve the evaluation system, discusses the combination of various assessment methods, enriching the relevant assessment case.

MATERIALS AND METHODS

Study area and data. The coastal area of Jiangsu province is about$3.5x10^4$ km^2, Marine economic development situation is good. However, the development of marine resources in Jiangsu province is more extensive, which has a certain impact on the marine resources and environment, and reduces the marine ecological environmental services and sustainable utilization of resources. According to the present situation of the exploitation and utilization of marine resources in Jiangsu province, 4 kinds of marine development types with higher development ratio were selected, such as mariculture, offshore wind power, sewage dumping, port industry. Each type of marine development has selected several typical marine development projects, A total of 10 cases were used to evaluate the comprehensive benefits (Table 1), And the cases were selected to be representative. The relevant data are derived from the social and economic statistical data of the marine development projects, the monitoring data of the environmental protection department and the data of the sewage declaration, the actual survey data and the model calculation data.

Computational method of unit area total benefit. In this paper, the total benefit of each sea type be divided into social and economic benefits,

TABLE 1
typical marine development projects.

Major types of marine development	Item 1	Item 2	Item 3
Mariculture A	Ganyu, a sea water aquaculture project A_1	Reclamation of a sea reclamation project in Dongtai A_2	
Offshore wind power B	Wind farm project of 30 MW intertidal zone in Jiangsu, Rudong B_1	The first phase of wind farm of 150 MW inter tidal zone in Jiangsu, Rudong B_2	China three gorges 12.5MW test fan project in Jiangsu, Xiangshui B_3
Sewage dumping C	The first phase of the sewage discharge project of Nantong Port Economic Development Zone C_1	Coastal Economic Development Zone coastal industrial park 20 thousand tons/day water discharge project C_2	Tianwan Nuclear Power Plant in Lianyungang C_3
Port industry D	Jiangsu Datang Lusi power plant project D_1	Yan Da heavy equipment manufacturing Co., Ltd. D_2	

TABLE 2
Ecological damage coefficient of different types of marine development.

Development type		Damage coefficient
Marine reclamation land	Construction of sea reclamation, agricultural reclamation, waste Disposal reclamation	1
	Impermeable structure	0.8
Sea-fill	Harbor pool, storage, etc.	0.5
	Salt industry	0.6
	Mariculture	0.5
Permeable structure	Permeable structure	0.3
	Sea crossing bridge	0.3
Open type	Open culture	0.1
	Bathing beach	0.2
	Special waterway, anchorage, harbour basin and other open	0.3
Others	Submarine cable duct	0.4
	Subsea tunnel	0.4
	The sea sand mining etc.	0.7
	Sewage discharge	0.5
	Dump	0.4
	Water intake and outfall	0.4

ecological benefit value and the value of wetland ecosystem service value. The latter includes fishery resources loss value, ecological loss cost and so on. The social and economic benefits of marine development projects are directly expressed by the economic income of the sea area within the sea term unit, and the method of calculation is as follows.

$$B_i = \frac{P_i - C_i - V_i + E_i}{S_i} \quad (1)$$

In the formula, B stand for unit sea area total benefit, unit is 10000 yuan/hm^2•a. P stand for the total revenue of the project in the forecast period of the project, unit is million. C stand for the total cost of investment in marine engineering, unit is million. V stand for loss value of service function value of wetland ecosystem using sea area. E stand for ecological benefits of sea area. S stand for Sea area, unit is hm^2. The above indicators are calculated as an annual unit.

Effects on the service function of coastal wetland ecosystem. Jiangsu marine development concentrated in the coastal beach. Damage to the service function of the coastal wetland ecosystem. According to the classification system of sea area use and 11 kinds of sea use, the paper lists 10 kinds of ecological service functions. Invited 20 people engaged in wetland research, marine engineering, marine environment and marine biology professionals to assess the ecological damage caused by different ways of using sea. According to the scoring of experts, we finally determined the ecological damage coefficient of different ways of using sea (Table 2).

According to the marine engineering where the coast and sea location, development types, development area and ecological damage coefficient can be determined by marine engineering wetland ecosystem service function value loss, the formula is as follows.

$$V = \frac{v_i \sum_{j=1}^{n} s_j d_j}{S} \quad (2)$$

In the formula, V stand for Unit area wetland ecosystem service function value loss of marine project. V_i stand for Unit area ecosystem services value of marine projects, unit is ten thousand yuan/hm^2•a. S_j stand for j type of marine development area, unit is hm^2. S stand for total area of marine project. d_j stand for the damage coefficient of the wetland ecosystem service function of the J type. n stand for the project includes n kinds of marine project.

According to the research results of ecosystem service value evaluation [10], and according to Xu Min et al. (2012) [11] proposed ecological service value evaluation method, the evaluation of the ecological service value of the coastal wetland in Jiangsu was carried out separately, and the average ecosystem service value of Jiangsu beach was 40 thousand yuan/hm^2•a.

Ecological benefit value. The ecological and environmental effects of marine development activities can be divided into cost and benefit. Different types of sea use produce different ecological gains and losses. The negative ecological benefits have been included in the loss of the value of ecosystem services in the area; For the use of sea type with positive ecological benefits, The positive ecological benefit of unit area was used as the evaluation index, Such as the industrial use of offshore wind power projects in the marine and photovoltaic power generation projects, consider saving produce annual power output of standard coal for carbon emissions economic profit value as evaluation index; For offshore sewage project, then consider the use of the same standards of sewage charges processing as index, unit: ten thousand yuan/hm^2•a.

Index system and Standardized treatment. According to the evaluation index system of marine development at home and abroad [12, 13, 14, 15]. Combined with the characteristics of marine development in Jiangsu, based on the economic, social, resource and environmental costs of different types of marine development, Delphy Fa was used to select the indexes, Constructing the evaluation index system of comprehensive benefit of marine development (Table 3), The calculation method and formula of each index are referenced to the relevant literature [16], and the evaluation index value is obtained and standardized. In this paper, 10 marine development projects of the 9 indicators in the index system constitute matrix [$Y_{10\times9}$], The entropy weight method is used to get the weight value of entropy weight by matlab2010. The results are shown in Table 3.

Grade standard. The comprehensive benefit index of marine development is calculated by the linear weighted sum method [17]. The grey relational grade of marine development is calculated by entropy weight weighting method [18], which directly reflects the contribution of the evaluation index to the ecosystem. The higher the comprehensive benefit index and the correlation degree are, the higher the comprehensive benefit of marine development is, the smaller the opposite is. According to the related research results of ecological security level [19], the comprehensive benefit index and correlation degree evaluation standard of marine development project are shown in Table 4.

TABLE 3
Weight value of comprehensive benefit index of marine development.

First level index	Secondary indexes	Type of indicator	Entropy weight
Economic benefit B_1	Economic net income of marine project (ten thousand yuan / hm^2•a) X_1	+	0.0605
	Economic net income of per unit shoreline (ten thousand yuan / hm^2•a) X_2	+	0.0530
	Annual tax amount payment (ten thousand yuan/ hm^2•a) X_3	+	0.0779
	Newly employed population (people)X_4	+	0.4882
Social benefit B_2	Degree of public satisfaction (%)X_5	+	0.0691
	Social development of project (%)X_6	+	0.0986
Resource loss B_3	Area of occupied beach resources(hm2) X_7	−	0.0402
Environmental cost B_4	Maximum velocity change rate of feature points (%)X_8	−	0.0496
	Environmental change rate of dynamic sediment (%)X_9	−	0.0628

Note: +. Equity index; -. Cost index.

TABLE 4
Classification standards for comprehensive benefit evaluation of marine development projects.

Comprehensive benefit index	0~0.3	0.3~0.6	0.6~0.8	0.8~1
Safety grade	Poor	commonly	preferably	Excellent
Correlation degree	0~0.3	0.3~0.6	0.6~0.8	0.8~1
Safety grade	Poor	commonly	preferably	Excellent

TABLE 5
Total benefit of unit area of the project.

marine project		Social economic net income	Ecosystem service value loss	Ecological benefit value	total benefit of Unit area
Mariculture A	A_1	20.14	-2.3451	0	17.7949
	A_2	11.1	-1.575	0	9.525
Offshore wind power B	B_1	172.78	-1.5582	25.8835	197.1053
	B_2	162	-1.4444	39.2827	199.8383
	B_3	262.5	-1.2332	34.8829	296.1497
Sewage dumping C	C_1	52.34	-2.0045	0.3782	50.7137
	C_2	78.57	-1.8149	0.0632	76.8183
	C_3	349992	-1.649	0	349990.351
Port industry D	D_1	16142	-3.3567	0	16138.6433
	D_2	159622	-3.96	0	159618.04

Note: the above indicators are the value of unit area, unit: ten thousand yuan/hm^2•a

RESULTS AND ANALYSIS

Total benefit of unit area. Based on the calculation of the total benefit of each marine project (Table 5), it is found that the total benefit of the unit area of Lianyungang Tianwan nuclear power marine project is the largest in the types of sewage dumping, which is 3 billion 499 million 903 thousand and 510 yuan/hm^2. Secondly, Jiangsu Datang Lusi power plant project, Yanda Manufacturing Co. Ltd., heavy equipment project which belong to the type of marine industry development have a high unit area total benefit, Results are 161 million 386 thousand and 433 yuan/hm^2•a, 1 billion 596 million 180 thousand and 400 yuan/hm^2•a. However, the marine aquaculture reclamation development type in Dongtai reclamation area fangtang high reclamation for aquatic breeding project and Ganyu water aquaculture with minimum sea project benefit of unit area, respectively, 95 thousand and 250 yuan/hm^2•a, 177 thousand and 949 yuan/hm^2•a.

The study found that the average benefit per unit area of pollution dumping and industrial marine development types was the highest, reaching 1 billion 167 million 59 thousand and 610 yuan/hm^2•a and 878 million 783 thousand and 417 yuan/hm^2•a respectively. However, the value of ecosystem services of two development types per unit area is also higher, -1.8228 yuan/hm^2•a, -3.6584 yuan/hm^2•a respectively (Table 6). The higher unit area total benefit is only due to the higher net income per unit area. Compared with other types of sea use, the net economic income per unit area has an absolute advantage. The total benefit of the unit area of Mariculture Development was the lowest, which was 136 thousand and 600 yuan/hm^2•a. Ecosystem service

value loss per unit area is -1.9601 million/hm^2•a, the ecological value of unit area was 0.

In short, if we consider the unit area of social and economic net income, in accordance with the comprehensive benefits of the unit ocean area of marine development types are sorted as follows: Sewage dumping, Port industry, Offshore wind power, Mariculture.

Evaluation results of comprehensive index method. According to the comprehensive benefit index evaluation model. The weight of each index is multiplied by the standard calculation result, obtain the comprehensive index of first grade indicators for all marine development projects (Table 7) and total composite index curve (Figure 1).

It is found that the comprehensive benefit evaluation of Yan Da heavy equipment manufacturing Co., Ltd. is 0.9102 which belongs to the port industry sea type. The comprehensive benefit evaluation of Lianyungang Tianwan nuclear power plant is 0.8809 which belongs to the type of pollution dumping, between 0.8-1 and in an excellent condition.

TABLE 6
Comprehensive benefit evaluation of unit area of each marine development type.

Assessment indicators / marine development	Mariculture	Offshore wind power	Sewage dumping	Port industry
Social economic net income of unit area	15.62	199.0933	116707.6367	87882
Ecosystem service value loss value of unit area	-1.9601	-1.4119	-1.8228	-3.6584
Ecological benefit value of unit area	0	33.3497	0.1471	0
Total benefit of unit area	13.66	231.0311	116705.961	87878.3417

unit: ten thousand yuan / hm^2•a

TABLE 7
Comprehensive benefit index of various types of marine development.

Marine project	X1	X2	X3	X4	X5	X6	X7	X8	X9	ESI
A1	0.0242	0.0318	0.0156	0.0234	0.0523	0.0064	0.0397	0.0441	0.0560	0.2936
A2	0.0242	0.0318	0.0312	0.0605	0.0691	0.0365	0.0356	0.0211	0.0568	0.3668
B1	0.0363	0.0318	0.0467	0.0005	0.0504	0.0621	0.0400	0.0489	0.0593	0.3761
B2	0.0363	0.0424	0.0467	0.0039	0.0411	0.0407	0.0382	0.0485	0.0557	0.3536
B3	0.0363	0.0318	0.0623	0.0000	0.0467	0.0343	0.0400	0.0486	0.0587	0.3587
C1	0.0242	0.0212	0.0156	0.0000	0.0336	0.0944	0.0402	0.0491	0.0616	0.3398
C2	0.0242	0.0212	0.0156	0.0000	0.0454	0.0879	0.0402	0.0496	0.0628	0.3468
C3	0.0605	0.0530	0.0779	0.4882	0.0131	0.0793	0.0395	0.0447	0.0247	0.8809
D1	0.0605	0.0530	0.0779	0.0234	0.0000	0.0836	0.0344	0.0464	0.0000	0.3793
D2	0.0605	0.0530	0.0779	0.4067	0.0691	0.0986	0.0398	0.0470	0.0577	0.9102

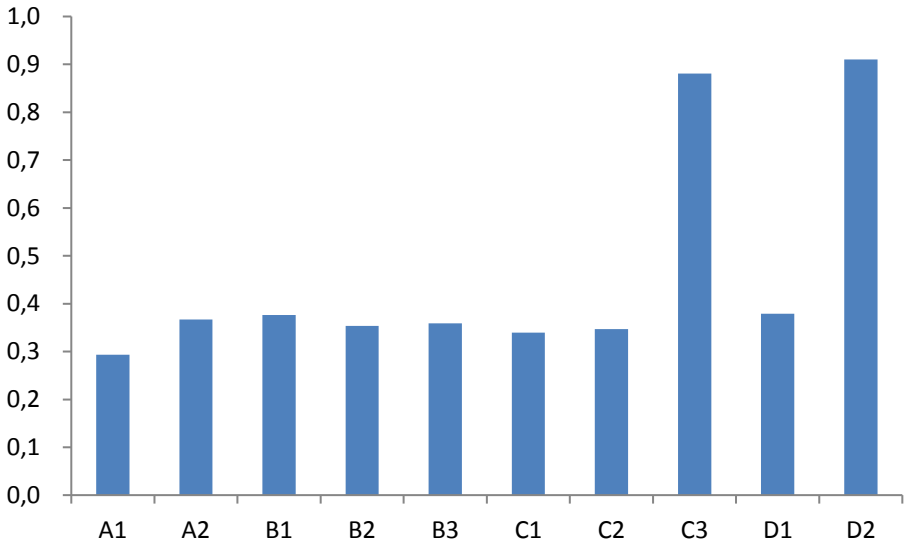

FIGURE 1
Composite index of typical marine development activities.

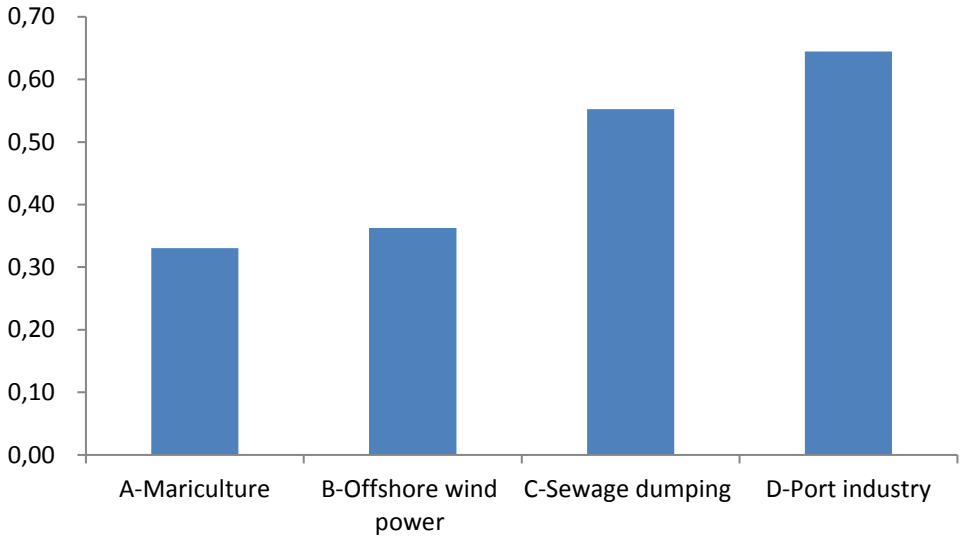

FIGURE 2
The average composite index of ocean development.

TABLE 8
Empower the correlation coefficient and associated.

Marine project	X1	X2	X3	X4	X5	X6	X7	X8	X9	Weighted correlation degree
A_1	0.024	0.027	0.026	0.168	0.047	0.034	0.014	0.018	0.023	0.3796
A_2	0.024	0.027	0.031	0.177	0.069	0.044	0.015	0.027	0.022	0.4357
B_1	0.030	0.027	0.039	0.163	0.045	0.057	0.013	0.017	0.022	0.4120
B_2	0.030	0.035	0.039	0.164	0.038	0.045	0.014	0.017	0.023	0.4049
B_3	0.030	0.027	0.052	0.163	0.042	0.043	0.013	0.017	0.022	0.4082
C_1	0.024	0.021	0.026	0.163	0.034	0.091	0.013	0.017	0.021	0.4102
C_2	0.024	0.021	0.026	0.163	0.041	0.081	0.013	0.017	0.021	0.4069
C_3	0.040	0.035	0.039	0.244	0.030	0.162	0.010	0.013	0.023	0.6060
D_1	0.040	0.035	0.039	0.125	0.026	0.189	0.011	0.013	0.031	0.5093
D_2	0.040	0.035	0.039	0.209	0.101	0.452	0.010	0.013	0.016	0.9160

In the 10 sea use projects, only the Ganyu Marine Economic Development Zone, which belongs to the sea reclamation and sea use type, has a comprehensive benefit evaluation of 0.2936, between 0-0.3 and in a bad state. The overall benefits of the remaining development projects are between 0.3-0.6 and in a general state.

Base on the results of 10 marine projects, the average comprehensive benefit index of each marine development type is calculated. Among them, the average comprehensive benefit index of port industry marine development type is 0.6448, which is between 0.6-0.8, and has better comprehensive benefits. The average comprehensive benefit index of mariculture, offshore wind power and sewage dumping marine development type is 0.3302, 0.3628 and 0.5525 respectively, all of which are between 0.3-0.6, and the comprehensive benefits are generally, as shown in Figure 2.

Evaluation results of grey correlation method. The selected evaluation index is weighted by entropy weight method, and the correlation degree is calculated by weighting method. The results are shown in Table 8.

Ranking the Weighted correlation degree by size. According to the size of weighted correlation degree, the correlation degree of the comprehensive benefit of various marine development projects is obtained (figure 3). Based on the comprehensive benefit grade standard, it is found that the correlation degree of the comprehensive benefit of the project is 0.9160, which is between 0.8-1, in excellent condition. The correlation degree of the comprehensive benefit of the sea project of Lianyungang Tianwan nuclear power plant is 0.6060 between 0.6-0.8 and is in good condition. The correlation degree of the comprehensive benefit of other marine projects is between 0.3-0.6, in general. Among them, the minimum degree of comprehensive benefit of the marine reclamation project in Ganyu was 0.3796.

FIGURE 3
The correlation degree between sea project and comprehensive benefit.

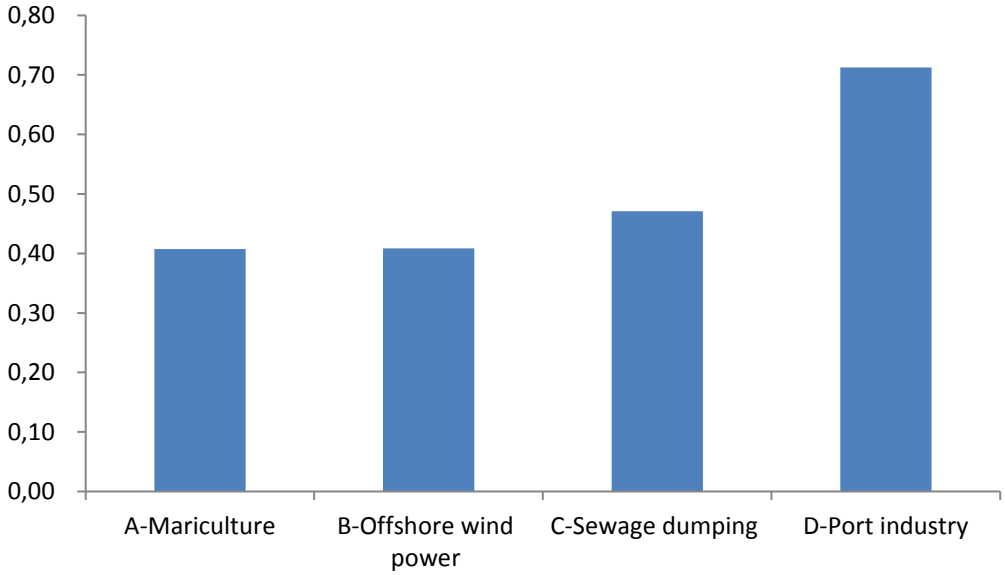

FIGURE 4
Correlation of marine development mode.

Based on the grey correlation method, the correlation degree of the comprehensive benefit of each type of marine development is obtained, as shown in Figure 4. Among them, the average value of the comprehensive benefit of the port industry marine development type is 0.7127, which is between 0.6-0.8, and has good comprehensive benefits. The correlation degree of comprehensive benefit of mariculture, offshore wind power and sewage dumping was 0.4076, 0.4084 and 0.4710 respectively, all between 0.3-0.6, with a commonly comprehensive benefit.

DISCUSSION

With the continuous development of marine activities, calculation and evaluation of comprehensive benefits of marine development types is great significance to maintain the sustainable development of marine economy and ecological environment. Different types of marine development have brought about different social and economic benefits, but also resulted in the loss of marine resources. Comprehensive benefit evaluation value can provide a reference for the development and utilization of the ocean to a certain extent. It can provide the scientific basis for the marine management department to set

up all kinds of marine functional areas. Put forward the strategic direction of the development of marine industry and optimize the adjustment proposals, to realize the coordinated development of marine economic development, marine resources utilization and marine environmental protection.

This paper selects four main types of marine development in Jiangsu province aquaculture reclamation, offshore wind power, the dumping of sewage, port industry as examples. Based on the calculation of the cost and benefit of economy, society, resources, environment and other various aspects of marine project development. Increased Net economic benefit of unit area, ecosystem service value loss value of unit area, ecological benefit value of unit area to evaluate and analyze the total benefit of marine area use, so that the connotation of the total benefit of marine types is more perfect and reasonable. On the basis of the calculation of each index value, the comprehensive benefit evaluation index system of marine development activities is constructed. The new employment population, people's support rate and other social benefits, erosion and sedimentation coefficient, the characteristics of the maximum flow rate of change and other environmental costs and other opportunity costs are incorporated into the assessment system. The comprehensive benefit of economic output and resource environment is evaluated by using the comprehensive index method and grey correlation method. It provides a scientific basis for the selection and management of marine development types in Jiangsu province and to provide reference for scientific and rational evaluation of comprehensive benefits of marine development activities. On the basis of the accurate calculation of the basic data, the objective evaluation method is used to evaluate the comprehensive benefit and enhance the reliability of the empirical results and the accuracy of the method.

CONCLUSIONS

By calculating the total benefit evaluation value and comprehensive benefit evaluation index, Objective to explore the comprehensive benefits of various types of marine development. This paper analyzes the influence of marine economic growth on marine resources, marine environment, marine ecosystem services. First, through the calculation of the total benefit value. It is found that the comprehensive benefit of the unit area of sewage dumping is the highest, which is 1 billion 167 million 59 thousand and 610 yuan/hm^2•a. Compared with other types of marine use, the main reason is that the net economic income of the unit area of nuclear power projects has absolute advantages. Followed by port industry. The total benefit of the mariculture type was 136 thousand and 600 yuan/ hm^2•a. The main reason is that the net economic income per unit area is very small.

Second, the comprehensive index method and grey correlation method are used to analyze the comprehensive benefit. It is found that the average comprehensive benefit index of Port industry is 0.6448. The average degree of correlation with comprehensive benefit is 0.7127 and the comprehensive benefit is better. However, the average comprehensive benefit index of mariculture, offshore wind power and sewage dumping were 0.3302, 0.3628 and 0.5525 respectively. The average correlation degree of comprehensive benefit was 0.4076, 0.4084 and 0.4710 respectively, which were all between 0.3-0.6 and the comprehensive benefit was commonly.

Third, the selection of the four typical types of marine development, the type of port industry has high comprehensive benefit. The main reason is that the social and economic benefits are higher than those of other types, far more than the cost of development, but it can not be denied that the development of the environmental damage and the impact is enormous. However, the economic benefits and the environmental costs caused by the sea reclamation and the dumping of sewage are relatively smaller than those of the first two types. In particular, the sea type of offshore wind power has the least impact on the ecological environment, resulting in an objective social and economic benefits.

Fourth, it is urgent to research the economic, resource and environmental comprehensive benefits of marine development activities and make a quantitative study on the comprehensive benefit of different marine development activities. It is necessary to select the types of marine development suitable for priority and encourage development according to the specific regional policies and principles, the development advantages, the importance of indicators and the actual situation.

ACKNOWLEDGEMENTS

This student was supported by the National Natural Science Foundation of China (No. 41373112) ; Jiang su Natural Science Youth Fund (No.BK20161018); Key research project of China Ocean Development Association (No.CAMAZD201613)

REFERENCES

[1] Huang, H., Chen, B., Ma, Z., Liu, Z., Zheng, S., Yu, W., Liao, J., Hu, W., Du, J. and Chen, G. (2017) Assessing the ecological security of the estuary in view of the ecological services-A case study of theXiamen Estuary. Ocean & Coastal Management. 137(1), 12-23.

[2] Liu, Q. and Xu, M. (2013) Comprehensive benefits evaluation for sea reclamation projects in Jiang su province. Journal of Nanjing

Normal University (natural science edition). 03, 125-130.
[3] Xiao, J., Chen, D., Xu, M. and Yu, Q. (2011) Evaluation on losses of ecological environment value by the sea reclamation projects. Resources and environment in the Yangtze Basin. 10, 1248-1254.
[4] Li, J. and Liu, T. (2011) The assessment of environment cost: Jiaozhou Bay's reclamation. Marine environmental science. 06, 881-885.
[5] Qi, J. (2008) The study on economic benefit evaluation about marine development activity. Ocean University of China.
[6] Luo, X. (2012) The comprehensive benefit evaluation of Lang qi Island reclamation activities. Straits science. 6(2), 68-73.
[7] Jones, K., Pan, X., Garza, A. and Lloyd-Reilley, J. (2010) Multi-level assessment of ecological coastal restoration in South Texas. Eco. Eng. 36(4), 435-440.
[8] Rombouts, I., Beaugrand, G., Artigas, L., Dauvin, J., Gevaert, F., Goberville, E. and Kirby, R. (2013) Evaluating marine ecosystem health: case studies of indicators using direct observations and modelling methods. Eco. Indic. 24, 353-365.
[9] Li, J. and Heap, A. (2014) Spatial interpolation methods applied in the environmental sciences: a review. Environmental Modelling & Software, 53(C), 173-189.
[10] Borja, A., Bricker, S., Dauer, D., Demetriades, N., Ferreira, J., Forbes, A. and Zhu, C. (2008) Overview of integrative tools and methods in assessing ecological integrity in estuarine and coastal systems worldwide. Mar. Pollut. Bull. 56 (9), 1519-1537.
[11] Xu, M., Li, P. and Lu, P. (2012) A study on the suitable scale of filling in the tidal flat of sedimentation- Taking Jiang su as an example. Beijing: Science Press. 66-92.
[12] Zuo, P., Zou, X. and Zhu, D. (2000) Study on the Frame work of lntegrated Coastal Zone Management. Marine bulletin. 19(5), 55-61.
[13] Xue, X., Lin, T. and Cao, X. (2004) Building Coastal Ecological Safety Indicator System. Journal of Xiamen University (Natural Science Edition). 18, 179-183.
[14] Huang, B. Ouyang, Z. and Zhang, z. (2009) Assessment of eco-environmental vulnerability of Hainan island, China. Chinese Journal of Applied Ecology. 20(3), 639-646.
[15] Fei, L., Min, X., Qing, L., Zai, W. and Wen X. (2014) Ecological restoration zoning for a marine protected area: A case study of Haizhouwan National MarinePark, China. Ocean&Coastal Management. 98, 158-166.
[16] Li, Y. (2015) Study on comprehensive benefits of marine resources development in Jiang su. Nanjing Normal University.
[17] Chao, W., Zhong, Y., Jian, P. and Shu, F,. (2014) Constructing an assessment indices system to analyze integrated regional carrying capacity in the coastal zones–A case in Nantong. Ocean & Coastal Management. 93, 51-59.
[18] Mi, N., Yang, M., Fan, X., Mi, W., Li, T. and Wang, T. (2016) Theory and application of the main functional subdivision of limited development ecological zones. Acta ecology sinica. 16, 5058-5066.
[19] Wang, Y., Zhou, C., Li, H. and Zhang, H. (2016) Analysis of the dominant controlling factors leading to the coal and gas out burst based on entropy weight and grey correlation method. Journal of safety and environment. 06, 5-9.

Received: **21.04.2017**
Accepted: **XX.XX.20XX**

CORRESPONDING AUTHOR

Min Xu
School of Geographic Science,
Nanjing Normal University,
Nanjing 210023 – CHINA

E-mail: xumin0895@njnu.edu.cn

© by PSP Volume 26 – No. 10/2017 pages 6184-6190 Fresenius Environmental Bulletin

ANALYSIS OF THE IMPORTANCE OF THE FACTORS THAT INFLUENCE UREA HYDROLYSIS THROUGH AN ARTIFICIAL NEURAL NETWORK

Tao Lei[1], Xihuan Sun[1,2,*], Xianghong Guo[1], Juanjuan Ma[1]

[1]College of Water Science and Engineering, Taiyuan University of Technology, Taiyuan 030024, China
[2]Jinzhong University, Jinzhong 030600, China

ABSTRACT

The importance of the factors that influence urea hydrolysis rate was analyzed to reveal the mechanism of urea hydrolysis and improve urea utilization efficiency. BP-K and DE-K prediction models were established based on the traditional backpropagation (BP) neural network model and the BP model optimized by the differential evolution algorithm (DE). The two models designed to predict the urea hydrolysis rate were validated with the measured value. The input variables in the two models were soil temperature, nitrogen amount, and moisture content, and the output variable was soil urea hydrolysis rate. Results showed that the BP-K and DE-K models possessed high accuracy and could be used to predict the urea hydrolysis rate. The simulation effect of the DE-K model was better than that of the BP-K model. The importance of the factors that affect urea hydrolysis was studied based on information on weight and the threshold value of DE-K model. The relative importance of temperature, nitrogen amount, and moisture content on urea hydrolysis was 65.87%, 25.69%, and 8.44%, respectively.

KEYWORDS:
soil urea hydrolysis rate, differential evolution algorithm, BP-K model, DE-K model, importance

INTRODUCTION

Urea is one of the most popular nitrogen fertilizers worldwide because of its low price [1], high nitrogen content [2], and other advantages. When urea is applied to soil, it is hydrolyzed into ammonium nitrogen under the catalysis of urease. A part of it is emitted into the air in the form of gas (NH_3), and the other parts are transformed into nitrate through nitrification bacteria [3]. Improper use of urea results in many problems [4], such as eutrophication of surface water [5], gaseous loss [6], denitrification loss [7], and nitrogen leaching. Thus, research on the mechanism of nitrogen transformation is highly significant.

Many studies show that temperature, moisture content, and nitrogen amount are the key factors influencing the hydrolysis process [8-10]. A high temperature equates to a fast hydrolysis rate, and a short hydrolysis process [11-13]. Because temperature influences the chemical and biological environments in soil during N transformation and cycling [14]. Some reports show that relationship between the nitrogen amount and urea hydrolysis is positive [13]. Meanwhile, some reports show an opposite result [10]. High soil moisture limits soil aeration and thus leads to a decrease in urease activity and inhibition of urea hydrolysis [15-16]. However, most previous studies only examined the causative factors without ranking their relative importance quantitatively. In this paper, the effect of the three factors on urea hydrolysis rate was quantified, the importance degrees of the factors were ranked, and the key factor was determined.

Artificial neural networks (ANNs) are models inspired by human central nervous syatems [17]. ANNs can be usd to solve a wide variety of high-dimension nonlinear problems that are hard to resolve using ordinary rule-based methods [18]. Because of the high accuracy and high convergence speed [18-19], it has been used to predict soil nitrogen loss [20], surface water pollution caused by nitrogen [21] and ammonia volatilization [22]. Published literature shows that the application of the neural network model in predicting the urea hydrolysis rate requires further study. Moreover, this model has not been used to analyze the importance of hydrolysis factors quantitatively.

The objective of this study is to establish a prediction model of urea hydrolysis rate under the coupled effect of water-temperature-nitrogen. With the artificial neural network, the backpropagation (BP) algorithm and differential evolution (DE) algorithm were used to optimize the weight and threshold matrix of the neural network. The importance of hydrolysis factors was quantitatively analyzed based on information on the optimal weight and threshold matrix.

MATERIALS AND METHODS

Soil sampling. Sandy loam samples were obtained from the Pomology Institute of Shanxi Academy of Agricultural Sciences. The samples were air dried and crushed to pass through a 10-mesh sieve. The physicochemical properties of the soil samples are shown in Table 1. pH was measured at a soil-to-water ratio of 1:5 [23]. Field capacity was determined in 0.033 MPa by the pressure membrane method [24]. Moisture content was determined by a weighing method that 5.00 g of moist soil should be dried in an oven at 105 °C for 8h [25]. NO_3^--N and NH_4^+-N were determined with a continuous flow analyzer (AA3, Bran Luebbe, Germany). All chemicals used in the experiments were of analytical reagent (AR) grade and obtained from Sinopharm Chemical Reagent Beijing Co., Ltd. (Beijing, China).

TABLE 1
Physicochemical properties of the soil

Soil type	pH	Moisture content	Field capacity	NO_3^-–N content	NH_4^+-N content
		g kg^{-1}	g kg^{-1}	mg kg^{-1}	mg kg^{-1}
Sandy loam	8.84	21.63	217.79	0.41	0.59

Treatment. The urea hydrolysis characteristics under the coupled effect of water-nitrogen-temperature were studied through a laboratory experiment. Moisture content, nitrogen amount and temperature included three levels (130.67 mg/kg, 174.23 mg/kg, and 217.79 mg/kg), four levels (130.67 mg/kg, 174.23 mg/kg, and 217.79 mg/kg) and five levels (15 °C, 20 °C, 25 °C, 35 °C, and 40 °C), respectively. The experiment has sixty treatments, and all treatments were repeated three times. A total of 151 g (oven-dry basis) of soil was added to a series of 500 mL glass beakers. The beakers were treated with urea solution and deionized water to adjust the design level. The beakers were covered with polyethylene film and incubated at different temperatures (15 °C, 20 °C, 25 °C, 35 °C, and 40 °C) for 1-7 d. The loss of soil water through evaporation was replenished with deionized water, and the residual urea content under different treatments was measured everyday. Five grams (oven-dry basis) of soil and 50 mL of ultrapure water were poured into the flasks, placed inside a mechanical shaker for 0.5 h, and oscillated at a frequency of 50 Hz. The soils and solution were separated by filtration with a filter membrane (0.45 μm), and the urea content in the pellucid filtrate was determined through high-performance liquid chromatography (Thermo Fisher Scientific Corporation, America). The specific parameter setting was as follows: sample size of 30 μl, flow rate of 1 mL min^{-1}, mobile phase (95% ultrapure + 5% acetonitrile), and chromatographic column (C18, 4.6 × 150 mm, 3 μm) with a chromatographic column temperature of 30 °C and wavelength of 190 nm.

Data analysis. A zero-order model (Equation (1)) was used to describe the dynamic process of urea hydrolysis. A regression analysis was conducted with 1stopt 7.0 software to calculate the parameters of the models from experimental data.

$$(C_0 - C_t) = a - k \times t \quad (1)$$

where C_0 and C_t are the urea contents (mg kg^{-1}) determined at time 0 and t (d), respectively; k is the reaction rate (mg kg^{-1} d^{-1}); and a is a constant.

The simulation effect of the models was evaluated with the mean-absolute-percent error (MAPE) and root-mean-square error (RMSE), which were calculated with Equation (2) and Equation (3).

$$MAPE = \frac{1}{N}\sum_{i=1}^{N}\left|\frac{W_L - W_R}{W_R}\right| \times 100\% \quad (2)$$

$$RMSE = \sqrt{\sum_{i=1}^{N}\frac{(W_L - W_R)^2}{N}} \quad (3)$$

where W_R and W_L represent the measured and calculated hydrolysis rate of urea-N (mg kg^{-1} d^{-1}), respectively, and N is the number of samples.

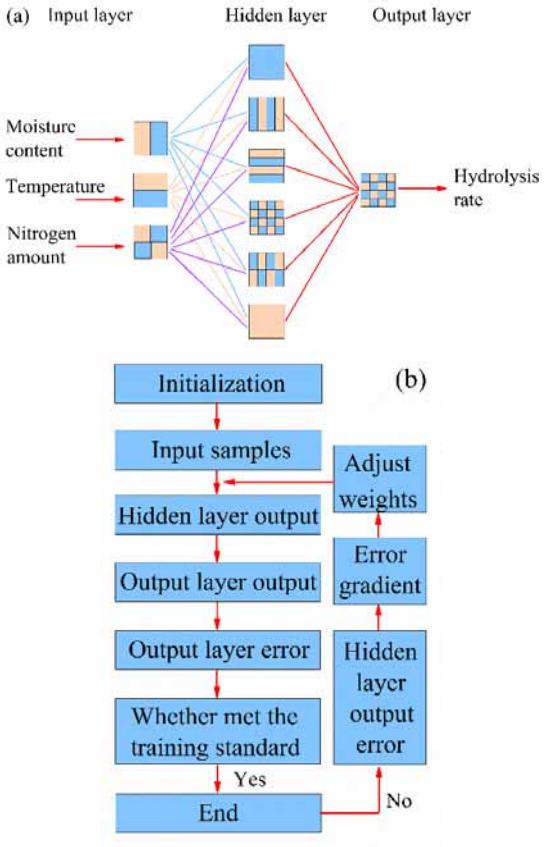

FIGURE 1
Architecture of the BP neural network

All experiments were repeated in triplicate, and the average values were reported. All data were processed in Microsoft Excel 2013. A statistical analysis

was performed with IBM SPSS Statistics 19 software, and the figures were plotted with Origin 9.1 software. Statistical significance was determined with the paired samples test. A correlation analysis was conducted with Pearson's method. Training and forecasting of the models were performed with 1stopt 7.0 software.

MODEL BUILDING

Building of the BP-K neural network model. The basic architecture of the BP neural network is illustrated in Figure 1. The network comprises three layers. The first is an input layer, which is responsible for receiving input messages and transmitting them to the hidden layer. The next is a hidden layer, in which the information is processed and transferred. The third one is the output layer, which is used for information transmission. When the output is inconsistent with the expectation, the error back-propagation mechanism works. The weight and threshold matrices of each layer are adjusted continuously until they reach the expected value.

The main idea of neural network learning is to revise the weights (ω_{ij}, T_{li}) and threshold (θ_i, θ_l) for the error function (E) to decrease along the negative gradient direction. The nodes of the BP network can be expressed as input layer node x_i, hidden layer node y_j, and output layer node O_l. The calculation formulas of the BP model are shown in Equations 4 to 9, where ω_{ij} is the network weight between input and hidden layer nodes, T_{li} is the network weight between hidden and output layer nodes, k is the number of iterations, η' is the learning rate, and δ_i' is the error gradient.

The output formula of the hidden layer node is

$$y_i = f\left(\sum \omega_{ij} x_j - \theta_i\right) = f\left(net_i\right) \quad (4)$$

The output formula of the output layer node is

$$O_l = f\left(\sum T_{li} y_i - \theta_i\right) = f\left(net_i\right) \quad (5)$$

The weight optimizing formula from the input layer to the hidden layer is

$$\omega_{ij}\left(k+1\right) = \omega_{ij}\left(k\right) + \eta' \delta_i' x_j \quad (6)$$

The threshold optimizing formula from the inp ut layer to the hidden layer is

$$\theta_i\left(k+1\right) = \theta_i\left(k\right) + \eta' \delta_i' \quad (7)$$

The weight correction formula from the hidden layer to the output layer is

$$T_{li}\left(k+1\right) = T_{li}\left(k\right) + \eta' \delta_l y_i \quad (8)$$

The threshold correction formula from the hid den layer to the output layer is

$$\theta_l\left(k+1\right) = \theta_l\left(k\right) + \eta' \delta_l' \quad (9)$$

The neurons of each layer are connected by transfer functions, such as logsig, purlin, and tanh. If the number of hidden layer nodes is selected incorrectly, simulation accuracy would be low. One could select the optimal number of hidden layer nodes by referring to the following inequality. The ideal range of hidden layer nodes is 2 to 12, as determined with Equation 10.

$$\mathrm{L} = \sqrt{\left(m+s\right)} + q \quad (10)$$

Where, L is the number of hidden layer nodes, m is the number of output layer nodes, s is the number of input layer nodes, and q is a constant between 0 and 10.

In the BP-K model, temperature, moisture content, and nitrogen amount were regarded as inputs, and urea hydrolysis rate was regarded as the output. Tanh was selected as the transfer function between input and hidden layers and between hidden and output layers. The iteration number used in the model was 5000, and the training goal was 0.00001. The 60 data sets were separated into training and validation sets in 5:1 ratios.

Building of the DE-K neural network model. The traditional BP algorithm is based on the gradient descent method. It modifies a network by calculating the objective function. This method is easy to be trapped in local minima, and the search method demonstrates slow convergence. Thus, the BP neural network algorithm needs to be optimized. The 1stopt software has been successfully applied for solving optimization problems [26-27]. The differential evolution optimization (DE) method has proved its ability in finding the global optimal solution at high speed and with high accuracy [28-29]. As a result, it is applied to solve the optimization problem of traditional neural network model in this study. The DE algorithm requires determination of some parameters (population size, mutation rate, crossover rate). In this paper, the DE algorithm parameters were as follows: population size-50, mutation rate-0.7, crossover rate-0.85.

Calculation of importance. The **DE-K** model achieved the training goal after a number of iterations. Network weights reflect the importance information of the evaluation indexes. Hence, the key point is to extract the relative importance information of each evaluation index from the weights of the network.

(1) Relative Importance Size $\partial y/\partial x_i$

$$\begin{aligned}
\partial \mathrm{y}/\partial x_i &= f(\alpha)\left[1-f(\alpha)\right]\left(\partial \textstyle\sum_{i=1}^{L}\left(T_{li}h_j-\theta_l\right)/\partial x_i\right)\\
&= f(\alpha)\left[1-f(\alpha)\right]\sum_{j=1}^{L} T_{li}\left(\partial h_j/\partial x_i\right)\\
&= f(\alpha)\left[1-f(\alpha)\right]\sum_{j=1}^{L} T_{li}\left(\partial h_j/\partial \beta_j\right)\left(\partial \beta_j/\partial x_i\right)\\
&= f(\alpha)\left[1-f(\alpha)\right]\sum_{j=1}^{L} T_{li} f\left(\beta_j\right)\left[1-f\left(\beta_j\right)\right]\left(\partial \textstyle\sum_{i=1}^{N}\left(T_{li}h_j-\theta_l\right)/\partial x_i\right)\\
&= f(\alpha)\left[1-f(\alpha)\right]\sum_{j=1}^{L} T_{li} f\left(\beta_j\right)\left[1-f\left(\beta_j\right)\right]\omega_{ij}
\end{aligned} \quad (11)$$

Where, $f(\alpha)$ is the actual output of neural network, $f(\beta_j)$ is the output of hidden layer, h is the output vector [$h = (h_1, h_2, \ldots, h_j, \ldots, h_L)^T$], X is the input

vector [$X = (x_1, x_2, \ldots, x_i, \ldots, x_N)^T$].

(2) Comparison of Relative Size $\partial y/\partial x_i$

When the training process of the neural network was completed and the inputs were provided, weight ω_{ij}, threshold T_{li}, $f(\alpha)$, and $f(\beta_j)$ became fixed values. Equation 11 was then rewritten as Equations 12 and 13.

$$\partial y/\partial x_i = f(\alpha)\left[1-f(\alpha)\right]\sum_{j=1}^{L}(\omega_{ij}T_{li})f(\beta_j)\left[1-f(\beta_j)\right] \quad (12)$$

$$(\partial y/\partial x_i)/(\partial y/\partial x_{i+1}) = \sum_{j=1}^{L}(\omega_{ij}T_{li})/\sum_{j=1}^{L}(\omega_{(i+1)j}T_{li}) \quad (13)$$

(3) Relative Importance Information of Indexe s R

The relative size of $\partial y/\partial x_i$ exerted the same effect as the relative size of $\sum_{j=1}^{L}(\omega_{ij}T_{li})$ The relative importance of evaluation index i is shown in Equation 14.

$$R_i = \sum_{j=1}^{L}(\omega_{ij}T_{li})/\sum_{i=1}^{N}\sum_{j=1}^{L}\left|\omega_{ij}T_{li}\right| \quad (14)$$

RESULTS AND DISCUSSION

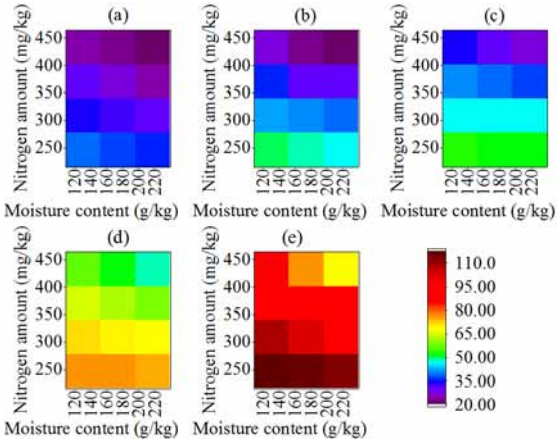

FIGURE 2
Hydrolysis rate of urea in soil under the coupled effect of water-temperature-nitrogen

Analysis of urea hydrolysis rate under the coupled effect of water-temperature-nitrogen. Figure 2 shows the urea hydrolysis rate in soil under the coupled effect of water-temperature-nitrogen. Several differences in the urea hydrolysis rate were observed for the different treatments. When the soil temperature increased, the hydrolysis rate increased monotonically. This result confirms the previous reports [11, 30]. The result is due to the enhancement of urease activity with the increase in temperature within the range of 15 °C to 40 °C [9, 31]. This increase in temperature causes an increase in the percentage of active molecules [32, 33]. The probability of effective collision between molecules also increases, and the hydrolysis reaction occurs easily [34]. Furthermore, the hydrolysis rate of urea decreased with the increase in moisture content because excessive soil moisture diluted the reactant concentration and led to a decrease in effective collision frequency between urea molecules [34]. If the nitrogen amount increases, the number of active molecules will increase, which is conducive for the hydrolysis reaction. However, the experimental results showed that the hydrolysis rate was negatively related to nitrogen amount. This negative relation may be caused by the inhibition of the noncompetitive substrate [35] or the degeneration of enzymes in high-concentration urea [36]. Urea hydrolysis rate exhibited significant ($p < 0.05$) or extremely significant ($p < 0.01$) positive correlations with temperature (r = 0.937 to 0.974). The relationship between urea hydrolysis rate and moisture content was significantly negative, except for a few cases (r = -0.942 to -1.000). Urea hydrolysis rate exhibited significant ($p < 0.05$) or extremely significant ($p < 0.01$) negative correlations with nitrogen amount (r = -0.989 to -1.000). It indicate that all of the three factors are closely related with the hydrolysis rate. Therefore, the three factors should be considered in the neural network model.

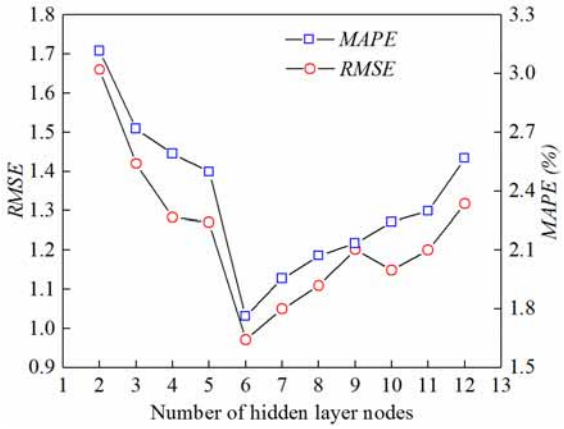

FIGURE 3
Training error of the DE-BP model under different hidden layer nodes

Determination of the best hidden layer nodes. The training error of the DE-K model under different hidden layer nodes is shown in Figure 3. When the hidden layer nodes increased from 2 to 12, the value of MAPE and RMSE initially decreased to the minimum then increased. When the number of hidden layer nodes was 6, the goal error reached the minimum value after 2384 tests and met the precision requirements. Therefore, the best topological structure of the DE-K model is 3-6-1.

Evaluation of the training results of the DE-K model. Figure 4 shows the simulation accuracy of the predicted value and observed value of hydrolysis rate. The slope of the linear equation of the BP-K and DE-K models was 0.979 and 0.996, respectively, and the determination coefficient (R^2) reached 0.991 and 0.999, respectively (Figure 4(a)). This result indicated that the measured and predicted values were in good agreement. Figure 4(b) shows that the residual

data points of the BP-K and DE-K models were distributed randomly in horizontal strip intervals of (-5, 5) and (-3, 3), respectively. This result indicated that the imitative effect was satisfactory for both models, but the residual of the DE-K model was smaller than that of the BP-K model. Figure 4(c) shows the absolute percentage error between the observed and predicted values. The maximum value of the relative error of the BP-K and DE-K models was 11.99% and 6.56%, respectively; meanwhile, the minimum value was 0.76% and 0.16%, respectively, and the average value was 4.35% and 1.64%, respectively.

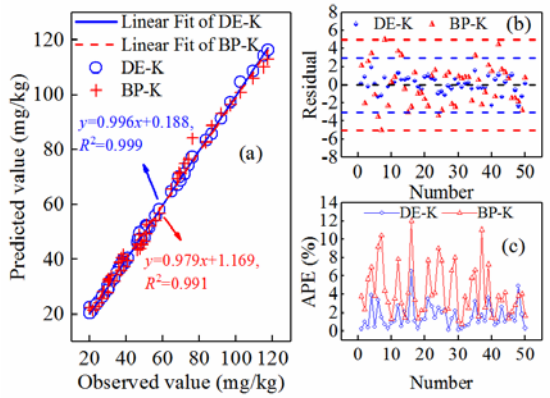

FIGURE 4
The simulation accurancy of the predicted value and observed value of hydrolysis rate ((a) linear relationship, (b) residual, (c) absolute percentage error)

The BP-K model had an *RMSE* value of 2.343, whereas that of the DE-K model was 1.246. The DE-K model had a smaller simulation error than the BP model. The *t* paired sample test results of the measured and predicted values are shown in Table 2. The absolute values of *t* for the two models were smaller than the critical *t* value $t_{0.05}(49)$ ($t_{0.05}(49) = 2.010$). The differences between the measured and predicted values were not significant. In conclusion, for the training samples, the two models exhibited high simulation accuracy and could be used to predict urea hydrolysis rate under the coupled effect of water-temperature-nitrogen.

TABLE 2
Paired sample test result of the measured and predicted values (training group)

Model	Mean	Standard deviation	Standard error mean	*t* value	df	Sig
DE-K	0.011	0.980	0.139	0.078	49	0.938
BP-K	-0.090	2.457	0.347	-0.259	49	0.797

Note. df: degrees of freedom. Sig: significance.

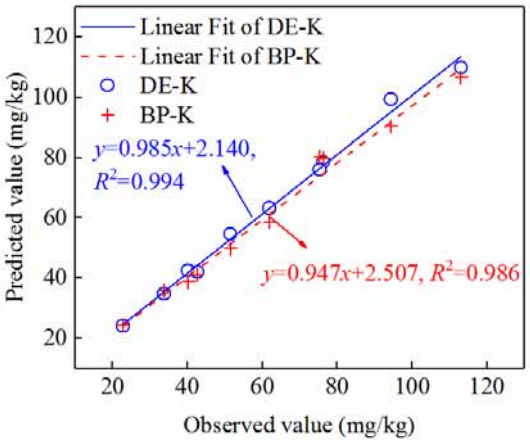

FIGURE 5
Linear relationship between predicted and observed values

Evaluation of the prediction results of the DE-K model. Figure 5 shows the linear relation between the predicted and observed values in the prediction group. The slope of the linear equation of the BP-K and DE-K models was 0.947 and 0.985, respectively, and the determination coefficient (R^2) reached 0.986 and 0.994, respectively. This result indicates that the observed and predicted values of the two models are in good agreement. The *t* paired sample test results of the observed and predicted values are shown in Table 3. The *MAPE* and *RMSE* of the DE-K model were 3.486% and 2.418, respectively; these values are smaller than those of the BP-K model. Calculation showed that the absolute *t* values of the two models were smaller than the critical value $t_{0.05}(9)$ ($t_{0.05}(9) = 2.262$); the differences between the observed and predicted values were not significant. In conclusion, for the prediction samples, the two models exhibited high simulation accuracy and could be used to predict the urea hydrolysis rate under the coupled effect of water–temperature–nitrogen. The DE-K model showed better prediction than the BP-K model.

TABLE 3
Result of statistical analysis of measured and predicted values (prediction group)

Model	*MAPE*	*RMSE*	Paired samples test		
			t value	df	Sig
BP-K	4.946%	3.459	−1.765	9	0.111
DE-K	3.486%	2.418	0.653	9	0.530

Note. ** means significant at the 0.01 levels.
df: degrees of freedom. Sig: significance.

Evaluation of the importance of the factors influencing hydrolysis. For the training and prediction samples, the simulation results of the DE-K model were better than those of the BP-K model, and the relationship between the input variables and the output variable was expressed more accurately with the DE-K model. Therefore, the weight and threshold value of the DE-K model were used to analyze

the importance of the three factors (temperature, nitrogen amount, and moisture content). It has been calculated that the percentages of the importance of temperature, nitrogen amount, and moisture content were 65.87%, 25.69%, and 8.44%, respectively. The importance of temperature was 2.56 times and 7.80 times larger than that of nitrogen amount and moisture content, respectively. In conclusion, temperature played a decisive role in the process of urea hydrolysis, whereas moisture content had a minimal effect. The analysis results for importance based on the artificial neural network model were consistent with the experimental results.

CONCLUSION

Based on the artificial neural network optimized by the BP and DE algorithm, the BP-K and DE-K models were established. Temperature, moisture content, and nitrogen amount were regarded as inputs, and the hydrolysis rate of urea was regarded as the output. The BP-K and DE-K models were validated with test data. The results showed that both models had high precision and could be used to predict the hydrolysis rate of urea under the coupled effect of water-nitrogen-temperature. The simulation effect of the DE-K model was much better than that of the BP-K model. The importance of the factors that affect urea hydrolysis was studied based on information on weight and the threshold value of DE-K model. The relative size of the three factors was in the order of temperature (65.87%) > nitrogen amount (25.69%) > moisture content (8.44%). The analysis results for importance based on the artificial neural network model were consistent with the experimental results, thus fully demonstrating the good application prospect of this method.

ACKNOWLEDGEMENTS

The research is financed by the National Natural Science Foundation of China (51579168, 51249002), the Natural Science Foundation of Shanxi Province of China (201601D011053), the Graduate Education Innovation Program of Shanxi Province of China (2016BY064), the Scientific and Technological Project of Shanxi Province of China (20140311016-6).

REFERENCES

[1] Peng, X., Maharjan, B., Yu, C., Su, A., Jin, V., Ferguson, R. B. (2015) A laboratory evaluation of ammonia volatilization and nitrate leaching following nitrogen fertilizer application on a coarse-textured soil. Agronomy Journal, 107, 871-879.

[2] Glibert, P. M., Harrison, J., Heil, C., Seitzinger, S. (2006) Escalating worldwide use of urea–A global change contributing to coastal eutrophication. Biogeochemistry, 77, 441-463.

[3] Wessen, E., Nyberg, K. A., Jansson, J. K., and Hallin, S. (2010) Responses of bacterial and archaeal ammonia oxidizers to soil organic and fertilizer amendments under long-term management. Applied Soil Ecology, 45, 193-200.

[4] Ye, Y., Li, L., Zhang, F., Sun, J., Liu, S. (2004) Effect of irrigation on soil NO_3^--N accumulation and leaching in maize/barley intercropping field. Transactions of the Chinese Society of Agricultural Engineering, 20, 105-109.

[5] Lili, W., Wenzhe, L., Zhongjiang, W., Zhiwu, W., Chao S, Yan L. (2016) Effects of digestate application depth on soil nitrogen volatilization and vertical distribution. International Journal of Agricultural and Biological Engineering, 9, 101-107.

[6] Shan, L., He, Y., Chen, J., Huang, Q., Wang, H. (2015) Ammonia volatilization from a Chinese cabbage field under different nitrogen treatments in the Taihu lake basin, China. Journal of Environmental Sciences, 38, 14-23.

[7] Dhadli, H. S., Brar, B. S., Black, T. A. (2016) N_2O emissions in a long-term soil fertility experiment under maize-wheat cropping system in Northern India. Geoderma Regional, 7, 102-109.

[8] Doak, B. W. (1952) Some chemical changes in the nitrogenous constituents of urine when voided on pasture. The Journal of Agricultural Science, 42, 162-171.

[9] Chauhan, H., Mishra, B. (1989) Ammonia volatilization from a flooded rice field fertilized with amended urea materials. Fertilizer Research, 19, 57-63.

[10] Armstrong, H. E., Horton, E. (1912) Studies on enzyme action xv.-urease: a selective enzyme. Proceedings of the Royal Society of London, 85, 109-127.

[11] Kumar, V., Wagenet, R. J. (1984) Urease activity and kinetics of urea transformation in soils. Soil Science, 137, 263-269.

[12] Sankhayan, S. D., Shukla, U. C. (1976) Rates of urea hydrolysis in five soils of India. Geoderma, 16, 171-178.

[13] Yadav, D. S., Kumar, V., Singh, M., Relan, P. S. (1987) Effect of temperature and moisture on kinetics of urea hydrolysis and nitrification. Australian Journal of Soil Research, 25, 185-191.

[14] Burns RG. 1978. Soil enzymes. London: Academic Press.

[15] Bhagat, R. M., Bhuiyan, S. I., Moody, K. (1996) Water, tillage and weed interactions in lowland tropical rice: A review. Agric Water Manage, 31, 165-184.

[16] Du, J., Gou, C., Cui, Y., Qu, D. (2007) Effects of water retaining agent on ammonia volatilization and nutrient leaching loss from N, P and K fertilizers. Journal of Agro-Environment Science, 26, 1296-1301.
[17] Goh, A. T. C. (1995) Back-propagation neural networks for modeling complex systems. Artificial Intelligence in Engineering. 9, 143-151.
[18] Vapnik, V. N. (1995) The nature of statistical learning theory. New York, N Y: Springer-Verlag.
[19] Suykens, J. A. K., Vandewalle, J. (2000) Recurrent least square support vectormachine. IEEE Transactions on Circuits and Systems-I, 47, 1109-1114.
[20] Kim, M., Gilley, J. E. (2008) Artificial Neural Network estimation of soil erosion and nutrient concentrations in runoff from land application areas. Computers and Electronics in Agriculture, 64, 268-275.
[21] Huang, J., Xu, J., Liu, X., Liu, J., Wang, L. (2011) Spatial distribution pattern analysis of groundwater nitrate nitrogen pollution in Shandong intensive farming regions of China using neural network method. Mathematical and Computer Modelling, 54, 995-1004.
[22] Boniecki, P., Dach, J., Pilarski, K., Piekarska-Boniecka, H. (2012) Artificial neural networks for modeling ammonia emissions released from sewage sludge composting. Atmospheric Environment, 57, 49-54.
[23] Li, Q., Wen, H., Hu, C. (2007) Difference between international and domestic methods in determining soil pH. Soils, 39, 488-491.
[24] Sciences IOSSCAO. (1978) Analysis of physical and chemical properties of soil. Shanghai, SHH: Shanghai Science and Technology Press.
[25] Schmugge, T. J., Jackson, T. J., Mckim, H. L. (1980) Survey of methods for soil moisture determination. Water Resources Research, 16, 961-979.
[26] Tao, R., & Tam, C-M. (2013) System reliability theory based multiple-objective optimization model for construction projects. Automation in Construction, 31, 54-64.
[27] Liang, J., Chen, X., Wang, L., Wei, X., Wang, H., Lu, S., Li, Y. (2017) Subcritical carbon dioxide-water hydrolysis of sugarcane bagasse pith for reducing sugars production. Bioresource Technology, 228, 147-155.
[28] Leema, N., Nehemiah, H. K., Kannan, A. (2016) Neural network classifier optimization using differential evolution with global information and back propagation algorithm for clinical datasets. Applied Soft Computing, 49, 834-44.
[29] Duchanoy, C. A., Moreno-Armendáriz, M. A., Urbina, L., Cruz-Villar, C. A., Calvo, H. J., Rubio, J. (2017) A novel recurrent neural network soft sensor via a differential evolution training algorithm for the tire contact patch. Neurocomputing, 235, 71-82.
[30] Lai, C. M., Tabatabai, M. A. (1992) Kinetic parameters of immobilized urease. Soil Biology and Biochemistry, 24, 225-228.
[31] Verstraeten, L. M. J., Seghers, I., Taslim, H. (1979) Mineralization of poly-(methylene-ethylidene)-polyurea. Soil Science and Plant Nutrition, 25, 1-8.
[32] Fierer, N., Craine, J. M, Mclauchlan, K., Schimel, J. P. (2005) Litter quality and the temperature sensitivity of decomposition. Ecology, 86, 320-326.
[33] Hartley, I. P., & Ineson, P. (2008) Substrate quality and the temperature sensitivity of soil organic matter decomposition. Soil Biology and Biochemistry, 40, 1567-1574.
[34] Glasstone, S., Laidler, K. J., Eyring, H. (1941) The theory of rate processes: the kinetics of chemical reactions, viscosity, diffusion and electrochemical phenomena. New York and London, NY and LON: McGraw-Hill Book Company, Incorporated.
[35] Singh, R., Nye, P. H. (1984) The effect of soil pH and high urea concentrations on urease activity in soil. European Journal of Soil Science, 35, 519-527.
[36] Lai, R. B., Kissel, D. E., Cabrera, M. L., Schwab A. P. (1993) Kinetics of urea hydrolysis in wheat residue. Soil Biology & Biochemistry, 25, 1033-1036.

Received: **03.06.2017**
Accepted: **10.08.2017**

CORRESPONDING AUTHOR

Xihuan Sun
College of Water Science and Engineering, Taiyuan University of Technology, Taiyuan 030024- China

e-mail: suntyut@126.com

© by PSP Volume 26 – No. 10/2017 pages 6191-6198 Fresenius Environmental Bulletin

EVALUATION OF PREBIOTIC POTENTIAL OF SALEP OBTAINED FROM SOME *ORCHIDACEAE* SPECIES

Buse Usta, Lutfiye Yilmaz-Ersan*

Department of Food Engineering, Faculty of Agriculture, Uludag University, 16059, Bursa, Turkey

ABSTRACT

The aim of the current study was to determine the utilization of salep from some *Orchidaceae* species by selected *Bifidobacterium* spp. Bifidobacteria were grown in Tryptone Peptone Yeast Extract (TPY) supplemented with 1% (w/v) glucose or 0.5 %, 1 % and 2 % w/v salep. The growth of the *Bifidobacterium* species was investigated by measuring the pH and optical density (OD) at 600 nm during a 48 h-fermentation, and calculating the prebiotic activity score (PAS). The results showed that the *Bifidobacterium* species could develop acidity through activation in the TPY broth containing salep. The *B. infantis* present in the TPY broth containing salep powder at 0.5-1 % was found to have the highest cell density value. In general, the PAS values obtained from the study showed similarities with those of commercial prebiotics, especially with fructooligosaccharides and inulin. The result of this study also indicates that salep can enhance the growth of some *Bifidobacterium* species.

KEYWORDS:
Prebiotic, Probiotic, *Bifidobacterium*, *Orchidaceae*, Salep

INTRODUCTION

In recent years, probiotic and prebiotic additives have gained importance in the food industry and seen an increase in consumption due to their proven beneficial effects on nutrition and health. Probiotics are live microorganisms with clinical proven benefits for the host's health and physiology when they are consumed in a sufficient amount with microbial dietary additives [1, 2, 3, 4]. Probiotics providing microbial balance in the gastrointestinal system positively affect host health by adjusting mucosal and systemic immunity. In nutrition, a multifarious microbial species have been qualified as probiotic, mainly *Lactobacillus* and *Bifidobacterium* species [5, 6].

Prebiotics, non-digestible food ingredients, are not hydrolyzed or absorbed in the upper intestinal tract and are selectively fermented by the beneficial bacteria (e.g. lactobacilli and bifidobacteria) in the colon [7, 8, 9, 10]. As fermentable substrates, prebiotics have been found to modulate colonic flora by stimulating the growth of beneficial bacteria and inhibiting the growth of pathogenic bacteria in the gut microbiota. More specifically, they act on the flora of the large intestine by increasing the number of probiotic bacteria and thereby promoting carbohydrate metabolism. As a result, i) intestinal pH is reduced, ii) bacterial balance in the large intestine is positively restored, iii) blood cholesterol level positively is aeffected, iv) uptake of minerals is enhanced, and v) risk of colorectal cancer can be reduced [7, 11, 12, 13, 14].

For a dietary substrate to be considered a prebiotic, at least three criteria must be met; i) it must not be absorbed in the small intestine, ii) it must be selective for probiotic bacteria (e.g. Lactobacilli or Bifidobacteria) in the large intestine, and iii) fermentation of the substrate should have beneficial effects on host health. The prebiotic substances can be categorized based on their chemical structure such as the chain length/degree of polymerization (DP), and mode of usage. According to their chemical nature, prebiotic substances are classified into saccharide derivates (disaccharides, oligosaccharides and polysaccharides), proteins/peptides and lipids. Depending on this classification, prebiotics are found in the food products; the substance containing a prebiotic is added or the active compound / prebiotic substance is isolated from the source and then added [15, 16, 17, 18].

Prebiotic substances are present naturally in fruits, vegetables, plant roots and seeds. Exclusively, prebiotic dietary sources are soybeans, artichoke, chicory root, raw banana, nectarine, yam, tomato, garlic, raw oats, onion, leek, wheat bran, asparagus, unrefined barley and wheat [13, 18, 19, 20]. Fructooligosaccharides (FOS), galactooligosaccharides (GOS), transgalactooligosaccharides (TOS), xylooligosaccharides (XOS), gentiooligosaccharides, lactulose (LAC), lactosucrose, inulin (INU), isomaltooligosaccharides (IMO), soybean oligosaccharides (SOS), resistant starch, glucooligosaccharides are the most used prebiotics in the food and pharmacology industry [21, 22, 23, 24, 25].

Orchidaceae commonly known as the orchid family is the largest and widespread family of flowering plants with an estimated 800 genera including nearly 25,000 species. Since orchids have exotic

beauty and long lasting flowers exhibiting an incredible range of diversity in size, shape and colour, they are grown as economically important ornamentals and cut flowers having floricultural, commercial as well as therapeutic values. All parts of orchids including leaves, roots, flowers, pseudobulbs, tubers, rhizomes and whole plants have been used as therapeutic ingredients for treating various disease, including tuberculosis, diabetes, lung cancer, stomach diseases, allergies headache and fever. Orchid products such as vanilla and salep are widely used the food and pharmaceutic industries. Salep, a Turkish word (Greek 'salapi' Arabic word 'sahlab'), is powder obtained from dried the roots or tubers of terrestrial *Orchidaceae* species, some of which have double-root tubers. Although the composition of salep is affected by the cultivar, harvesting methods and the postharvest handling procedures of the raw materials used in production, it contains glucomannan, starch, nitrogenous substance, moisture, ash and volatile oil. Salep is used in ice-cream production, confectionery and beverages as a thickening and flavoring agent, emulsifier and stabilizer. It has also therapetic importance in the treatment of diarrhea, tuberculosis, parkinson, cancer, fever and strengthening the sexual activity. Different species of orchids such as Ophrys, Orchis, Himantoglossum, Serapias, Anacamptis, Compreria, Barlia, Dactylorhiza, Aceras, and Neotinea naturally grown in Turkey are used for salep production. Salep is used mainly in a beverage as a warming drink during the winter in Turkey, Europe and England [26, 27, 28, 29, 30, 31].

Although salep has gained a great importance because of its nutritive, rheological and therapeutic properties, no work has been published on *in vivo* and *in vitro* fermentation of salep by probiotic bacteria. The objective of this study was to determine the utilization of salep from orchids grown different parts of Turkey by some selected *Bifidobacterium* species. The growth of the *Bifidobacterium* species was investigated by measuring the pH and optical density (OD) at 600 nm during 48 h-fermentation and the prebiotic activity score (PAS) was calculated.

MATERIALS AND METHODS

Microorganisms. Four species of Bifidobacteria (*Bifidobacterium bifidum*, *Bifidobacterium longum* subsp. *infantis*, *Bifidobacterium animalis* subsp. *lactis* and *Bifidobacterium longum* subsp. *longum)* were obtained from DSMZ (Deutsche Sammlung von Mikroorganismen und Zellkulturen GmbH, Braunschweig, Germany). *Bifidobacterium* species were activated according to a method suggested by DSMZ and incubated at 37°C under anaerobic conditions using an anaerobic atmosphere generation system (Anaerocult A, Merck, Darmstadt, Germany).

Culture Conditions. Salep from orchids grown different parts of Turkey region was provided by Kadem Sahlepçilik (Istanbul, Turkey). The corresponding solution was prepared by modifying it according to the work of Kaplan and Hutkins [32], Mumcu and Temiz [33]. To test the effect of the salep on the growth of the *Bifidobacterium* species, Tryptone Peptone Yeast Extract (TPY) was used as the basal medium (Table 1.). Solutions of salep and glucose were sterilized using Millipore-Stericup-GP 0.45 µm. Both were added to the TPY medium to obtain a final concentration of 0.5 %, 1 % and 2 %w/v for salep and 1 % w/v glucose as positive control. TPY broth without carbohydrates served as a negative control. The assay was performed by adding 2 % (v/v) of an overnight culture of each *Bifidobacterium* strain to separate the tubes containing TPY broth supplemented with 1% (w/v) glucose or % 0,5; % 1 and % 2 w/v salep as the sole carbon source. The experiment was completed in triplicate and the results are presented as the means±SE (standard error).

TABLE 1
Composition of TPY Broth.

TPY	g/L
Tryptone	10.00
Peptone	5.00
Yeast extract	2.50
Glucose	5.00
Tween 80	1
$K_2HPO_4.3H_2O$	2.00
$MgCl_2$	0.50
$ZnSO_4.7H_2O$	0.2
$CaCl_2$	0.15
$FeCl_3.6H_2O$	0.003
L-cysteine HCl	0.5

pH measurement. The pH of each sample was determined at 0, 12, 24, 36 and 48 h of fermentation using a pH-meter (pH 315i / SET; WTW, Germany).

Growth measurement. The cell density of the cultures was determined by monitoring the optical density at 600 nm (OD_{600}) with a spectrophotometer (Shimatzu UV 1800) at 0, 12, 24, 36 and 48 h of fermentation. The corresponding sterile TPY solutions were used as blanks for the absorbance measurements.

Prebiotic activity assay. *Bifidobacterium* species were grown in TPY medium supplemented with 1% of salep and glucose. Afterwards the 1% of the inoculum of each *Bifidobacterium* species, TPY medium with 1% salep ad glucose was added. The same process was carried out for the Enterococcus species using tryptic soya broth (TSB). Test cultures were incubated at 37°C for 24 h under anaerobic

$$PAS = \frac{\frac{((\text{Probiotic optic density}_{24\ \text{Prebiotic}}\ \text{OD 600 nm}) - (\text{Probiotic optic density}_{0\ \text{Prebiotic}}\ \text{OD 600 nm}))}{((\text{Probiotic optic density}_{24\ \text{Glucose}}\ \text{OD 600 nm}) - (\text{Probiotic optic density}_{0\ \text{Glucose}}\ \text{OD 600 nm}))}}{\frac{((\text{Enteric optic density}_{24\ \text{Prebiotic}}\ \text{OD 600 nm}) - (\text{Enteric optic density}_{0\ \text{Prebiotic}}\ \text{OD 600 nm}))}{((\text{Enteric optic density}_{24\ \text{Glucose}}\ \text{OD 600 nm}) - (\text{Enteric optic density}_{0\ \text{Glucose}}\ \text{OD 600 nm}))}}$$

conditions. Samples were taken at 0 and 24 h of fermentation, and the optical density was determined at 600 nm using a spectrophotometer. Prebiotic activity scores (PASs) were calculated according to equations above.

Statistical analysis. The data obtained was analyzed using the Minitab statistical package. The experiment was completed duplicate, and the results were presented as the means ± the standard error. A significant difference was defined as a P value of <0.01. A cluster analysis was performed following an unweighted pair group method with arithmetic average based on a dissimilarity matrix using JMP 7.

RESULTS AND DISCUSSIONS

As a result of the fermentation of probiotics, mainly the *Bifidobacterium* species, lactic, acetic, propionic and butyric acids and various by-products are produced. These acids reduce the pH of the intestinal microbiota and prevent the development of pathogenic microorganisms due to the domination of the *Bifidobacterium* species in the medium. Fig. 1-(a;c) and Fig. 2-(a;c) show that the pH values of the medium reduced during fermentation. As the microorganisms reduced the pH by rapidly producing acid during the fermentation, it was determined that *B. bifidum* which is desirable in probiotic culture selection has the highest pH value (Fig.1-c), the *B. longum* in the nutrient media, which does not contain

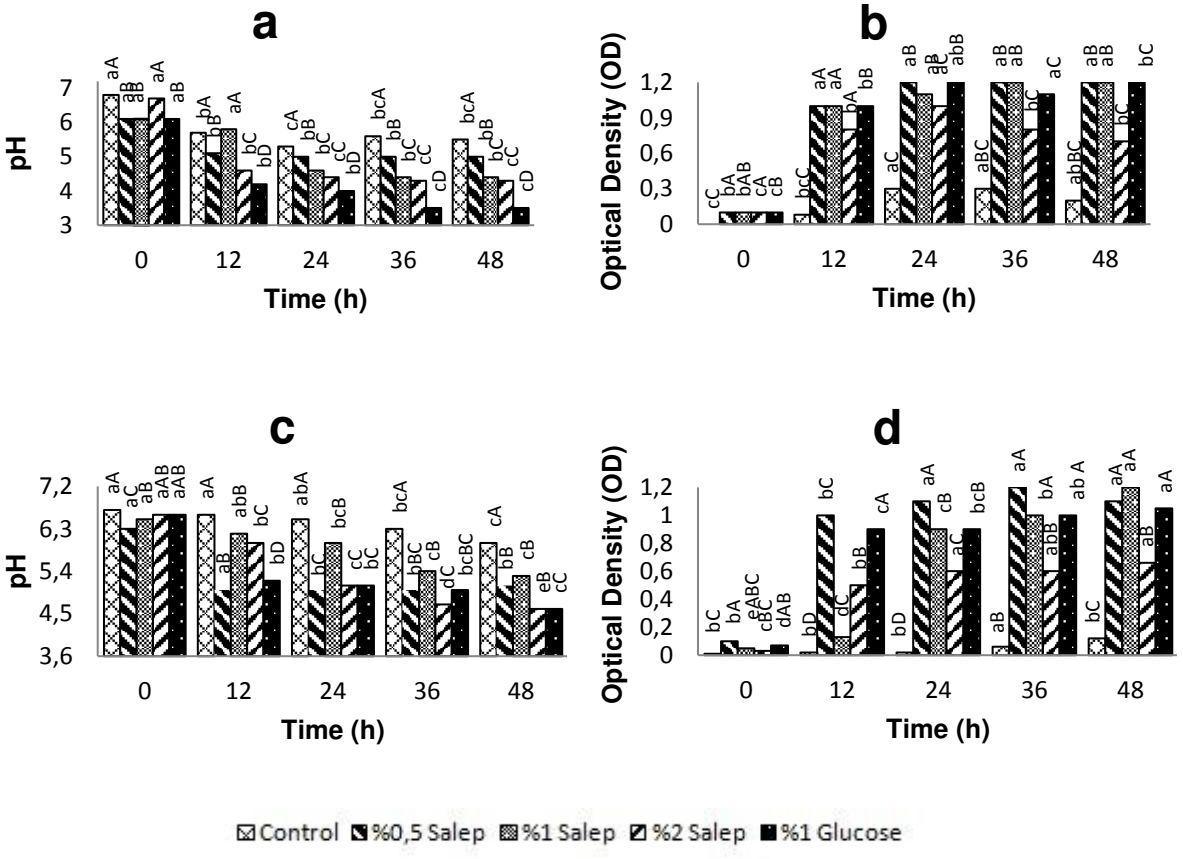

FIGURE 1

Figure 1-(a;b); pH and OD values of *B. infantis*; Figure 1-(c;d); pH and OD values of *B. bifidum*

[a,b] Different lowercase letters denote significant differences (P<0.01) between different times of fermentation

[A,B] Different capital letters denote significant differences (P<0.01) between different treatments

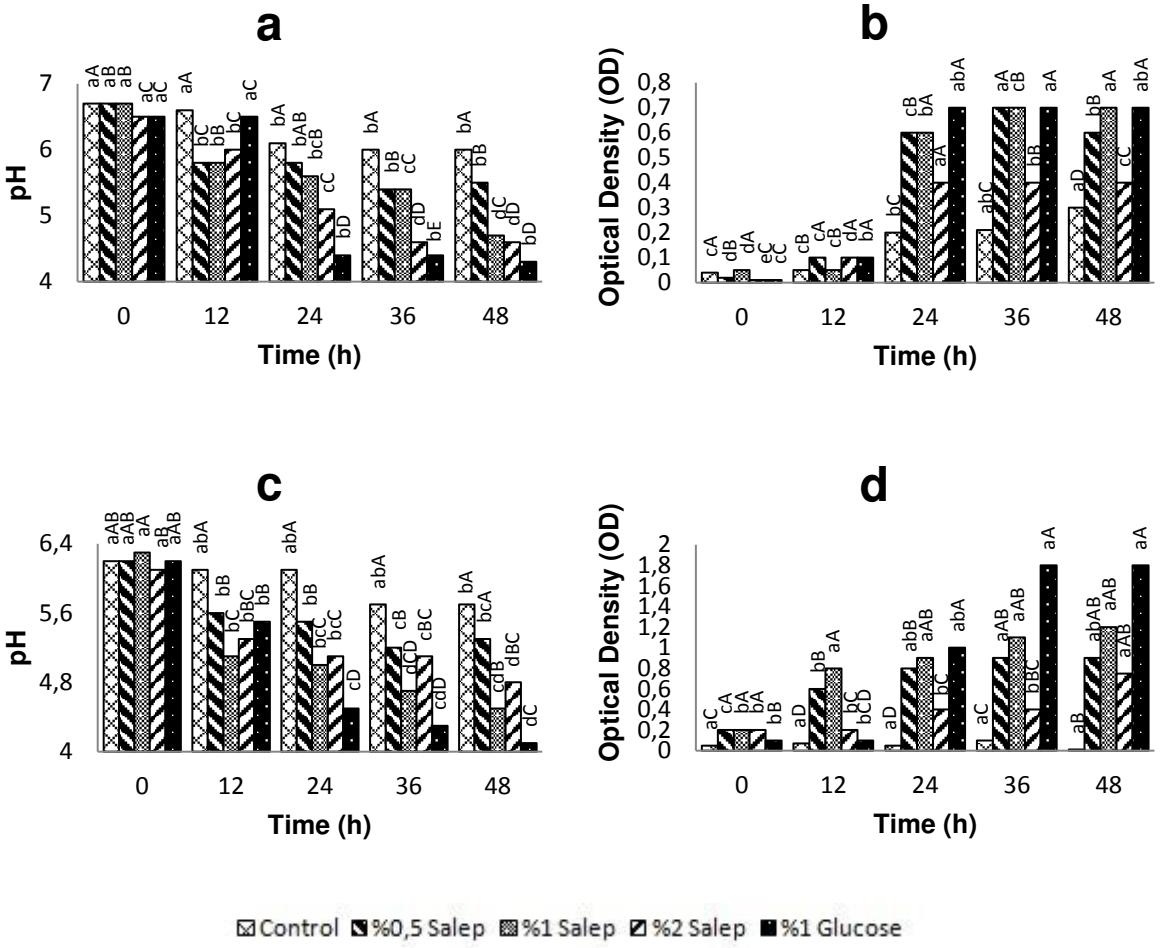

FIGURE 2

Figure 2-(a;b) pH and OD values of *B. longum*; (c;d) pH and OD values of *B. lactis*.

[a,b] Different lowercase letters denote significant differences (P<0.01) between different times of fermentation

[A,B] Different capital letters denote significant differences (P<0.01) between different treatments

prebiotic substrates, has the second highest value (Fig. 2-a) and; the *B. infantis* in the medium containing 1% glucose has the lowest pH value (Fig.1-a). The sample with *B. infantis*, which develops in the nutrient media and contains 1% and 2% salep, has next lowest pH. Of the four species compared with media containing salep, *B. infantis* grew the fastest and reached to the lowest pH during the 48 h-fermentation.

When the results were examined, it was determined that the *Bifidobacterium* species could develop acidity by activating in the nutrient media containing salep. The findings obtained in this study show that the *Bifidobacterium* species can use the carbohydrates and other components contained in the salep as well as the glucose. When the effects of the *Bifidobacterium* species and the fermentation on the development of acidity in nutrient media containing salep were examined, it was found the highest average pH value was determined at the beginning of the fermentation and the lowest average pH value was determined at the 48th hour of the fermentation.

When the pH value indicated in the results and the data obtained from previous studies by the Kaplan and Hutkins [32], Mumcu and Temiz [33] and Tzortzis et al. [34] are compared, it is apparent that the *Bifidobacterium* species could produce acid by fermenting the salep as well as the GOS and FOS can.

Indirect methods include counting, as through the standards-based counting method, in which microorganisms are often used during their logarithmic growth stages. The development curve of quickly proliferating microorganisms in the logarithmic phase and the number of proliferating cells relative to the number of dead cells is known to be lower. Therefore, the absorbance value obtained during this period quite accurately the number of living cells. Photometric measurements of the optical density are possible in a homogeneous suspension, and turbidimetric or refractometric methods can be used for this

purpose. The spectrophotometer can be used for this purpose, and an intensity loss is incurred when the monochromatic light passing through a cell suspension is measured. Fig. 1-(b; d) and Fig. 2-(b; d) show that the OD values of the medium were correlated with increased *Bifidobacterium* species during fermentation. It was determined that the *B. infantis* in the nutrient media containing 0.5-1 % salep and the *B. infantis* in the nutrient media containing 1% glucose had the highest cell density value (Fig.1-b), followed by the *B. lactis* containing 1% glucose (Fig. 2-d) and, the control groups of all the microorganisms have the lowest cell density value. When the results were examined, it was determined that in the TPY broth containing 0.5-1 % salep, the *B. infantis* had a cell density value in the same group as the positive control. These results show that *Bifidobacterium* species can develop in media containing the salep as well as they develop in glucose, which supports the bifidogenic potential.

The cell density values were determined in the study were similar to those previous to describe Lee et al [35] used chitosan oligosaccharides and FOS as a prebiotic substrate; Holt et al. [36] used the oligosaccharides obtained from alternansucrase substrates (maltitol, maltose, melibiose, raffinose); Maischberger et al. [37] used the mixtures of TOS, GOS, vivinal GOS obtained from *L. reuteri,* using the glucans obtained from the mushrooms species of *Pleurotus ostreatus* and *P. eryngii;* and Yang et al. [38] used the indigestible polysaccharides and inulin obtained from the aqueous (juicy) extracts of *Anoectochilus formasanus (Orchidaceae).* However, the results obtained here were than the findings of Crittenden et al. [39] and Kaplan and Hutkins [32].

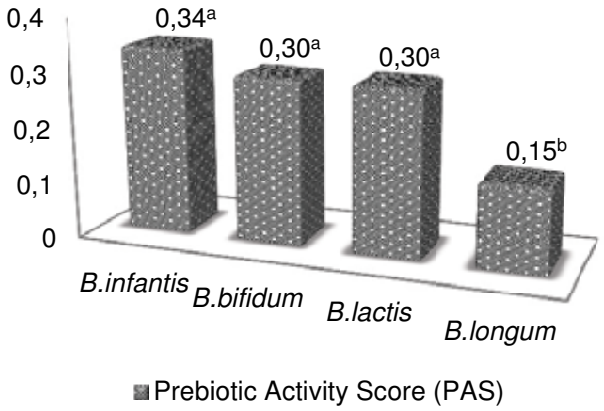

FIGURE 3
Prebiotic activity score of different *Bifidobacterium* species grown on salep.
[a,b] Different lowercase letters denote significant differences (P<0.01) among different species.

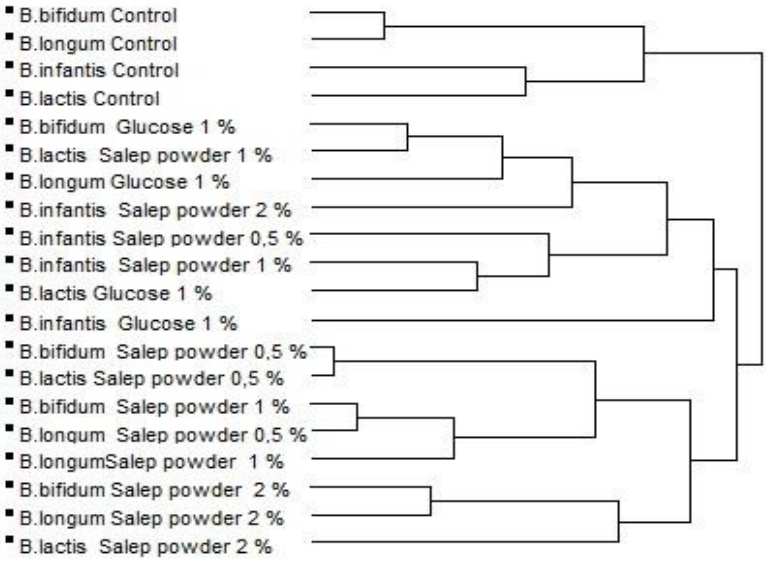

FIGURE 4
Cluster analysis of *Bifidobacterium* species

These differences may arise from differences in the probiotic microorganism species used, the different strains and their rates, the different prebiotic sources and their rates, differences in the nutrient media used or different wave lengths used in the spectrophotometric readings (e.g.$OD_{600\ nm}$, OD_{625nm}).

PAS, a quantitative score describing the prebiotic effect, compares the changes in the cell density values of dominant bacterial groups in the intestinal tract such as *Bifidobacterium* species and those of undesirable ones, such as *Coliform* species. PAS of salep against glucose with the *Bifidobacterium* species were investigated, and the species showing positive PAS are shown in Figure 3. *B. infantis, B. bifidum* and *B. lactis* (means 0.30-0.34) achieved higher PAS than *B. longum* (means 0.15). The variation between PAS of the *Bifidobacterium* species suggested differences in their metabolic capacity, specific saccharitic fermentation mechanism and transport systems for *Bifidobacterium* species.

Huebner et al. [40] studied the effects of the processing conditions of the commercial prebiotics (FOS and inulin) on prebiotic activity and found that the PAS ranged between 0.19 and 0.49. Haryadi et al. [41] determined the PAS to be 3.60 for *B. longum*; 3.58 for *L. plantarum* and 0.04 for *L. acidophilus* in nutrient media supplemented by resistant starch. Working in the *L. acidophilus* LA-5 and *B. lactis* BB-12 species, Thuaytong and Anprung [42] found the PAS to be 0.12 and 0.28 in the nutrient media containing white guava and 0.13 and 0.29 in the nutrient media containing red guava, respectively. In general, the PAS values determined in this study were similar to those determined in the above studies. As the values obtained from the study show similarities with commercial prebiotics, especially with the industrially common FOS and inulin, it seems clear that salep has prebiotic potential.

Hierarchical clustering was performed to determined if the relationship between the different concentrations of salep on the growth of *Bifidobacterium* species (Fig. 4). Cluster analysis was tested using the values of the growth parameters obtained from the measurements using pH and OD as variables. Four *Bifidobacterium* species were grouped into two clusters based on the mean values generated from the unweighted pair group mean average method of analysis. The results obtained showed the *B. bifidum* glucose of 1 % and the *B. lactis* salep of 1 %, *B. bifidum* salep of 0.5 % and the *B. lactis* salep of 0.5 %, *B. bifidum* salep powder of 1 % and the *B. longum* salep of 0.5 %, the *B. bifidum* salep of 2 % and the *B. longum* salep of 2 % to have the most similar pH and OD values.

CONCLUSIONS

To the best of our knowledge, this study provides the first demonstration of the effect of salep on the growth of *Bifidobacterium* species has been investigated. The results of this study demonstrated that all four *Bifidobacterium* species were able to utilize salep, suggesting that the salep might have the potential to promote the survival, viability and activity of Bifidobacteria and might thus potentially improve their beneficial effects on human health. A better understanding of the functionality of salep powder with prebiotic activity, the carbohydrate and monomer composition and molecular weight of the salep should be determined. Finally, more detailed studies are needed to investigate the fermentation of salep in the intestinal tract.

ACKNOWLEDGEMENTS

This study was funded in part by the Commission of Scientific Research Projects of Uludag University, Bursa, Turkey (QUAP (Z) 2013/50).

This study is a part of Buse Usta's M.Sc. thesis submitted to the Uludag University, Institute of Natural Sciences.

REFERENCES

[1] Pompei, A., Cordisco, L., Raimondi, S., Amaretti, A., Pagnoni, U.M., Matteuzzi, D. and Rossi, M. (2008) *In vitro* comparison of the prebiotic effects of two inulin-type fructans. Anaerobe,14. 280–286.

[2] Molan, A.L., Lila, M.A., Mawson, J. and De, S. (2009) *In vitro* and *in vivo* evaluation of the prebiotic acitivity of water-soluble blueberry extracts. World J Microbiol Biotechnol, 25. 1243–1249.

[3] Cianciullo, D. (2012) Effect of prebiotic and synbiotic injected in ovo on performance, meat quality and hystopathological changes in muscle of broiler chickens. University of Molise Department of Agricultural, Environmental and Food Science, Cambasso-Italy.

[4] Blatchford, P., Ansell, J., deGodoy, M.R.C., Fahey, G., Garcia-Mazcorro, J.F., Gibson, G.R., and Whelan, K. (2013) Probiotic Mechanisms, Functions, and Applications -- A Review. Int J Probiotics and Prebiotics, 8. 109–132.

[5] Mazmanian, S.K., Round, J.L., and Kasper, D.A. (2008) Microbial symbiosis factor prevents inflammatory disease. Nature,453.620–625.

[6] Ozcan, T. and Kurtuldu, O. (2014) Influence of Dietary Fiber Addition on the Properties of Probiotic Yogurt. Int J Chem Eng Appl, 5. 397–401.

[7] Pineiro, M., Asp, N.G., Redi, G., Macfarlane, S., Morelli, R., Brunser, O. and Tuohy, K. (2008) FAO Tecnical meeting on Prebiotics. J Clin Gastroenterol, 42. 156–159.

[8] Gomez, E., Tuohy, K.M., Gibson, G.R., Klinder, A. and Costabile, A. (2010) *In vitro* evaluation of the fermentation properties and potential prebiotic activity of Agave fructans. J Appl Microbiol,108. 2114–2121.
[9] Mandalari, G., Faulks, R.M., Bisignano, C., Waldron, K.W., Narbad, A. and Wickham, M. S.J. (2010) *In vitro* evaluation of the prebiotic properties of almond skins (*Amygdalus communis L.*). FEMS Microbiol Lett, 304. 116–122.
[10] Barczynska, R., Slizewska, K., Jochym, K., Kapusniak, J. and Libudzisz, Z. (2012) The tartaric acid- modified enzyme-resistant dextrin from patato starch as potential prebiotic. J Funct Foods,4.954–962.
[11] Sanders, E.M., Wijnkoop, L.I., Salminen, S., Merenstein, J.D., Gibson, G.R., Petschow, B.W., Nieuwdorp, M., Tancredi, D.J., Cifelli, C.J., Jacques, P. and Pot, B. (2014) Probiotics and prebiotics: prospects for public health and nutritional recommendations. Annals of The New York Academy of Sciences. 19-29.
[12] Serban, E.D. (2014) Gastrointestinal cancers: Influence of gut microbiota, probiotics and prebiotics. Inflammation and Gastrointestinal and Liver Cancers, 345. 258–270
[13] Canbulat, Z. and Ozcan, T. (2015) Effects of short-chain and long-chain inulin on the quality of probiotic yogurt containing *Lactobacillus rhamnosus*. J Food Process Pres, 39. 1251–1260.
[14] Rastall, R.A. and Gibson, G.R. (2015) Recent developments in prebiotics to selectively impact beneficial microbes and promote intestinal health. Curr Opin Biotechnol, 32. 42–46.
[15] Manning, T.S. and Gibson, G.R. (2004) Prebiotics. Best Pract Research Cl Ga, 18. 287–298.
[16] Al-Sheraji, S. H., Ismail, A., Manap, M.Y., Mustafa, S., Yusuf, R.M. and Hassan, F.A. (2013) Prebiotics as functional foods. J Funct Foods. 1542–1553.
[17] Das, D., Baruah, R. and Goyal, A. (2014) A food additive with prebiotic properties of an -d-glucan from *Lactobacillus plantarum* DM5. India International Journal of Biological Macromolecules. 69.
[18] Padma Ishwarya, S. and Prabhasankar, P. (2014) Prebiotics: Application in bakery and pasta products. Crit Rev Food Sci Nutr, 54. 511–522.
[19] Gibson, G.R. and Roberfroid, M. (2008) Handbook of prebiotics. Boca Raton, FL: CRC Press, 1-504.
[20] Sezen, G.A. (2013) Prebiyotik, probiyotik ve sinbiyotiklerin insan ve hayvan sağlığı üzerine etkileri. Ataturk University Journal of Veterinary Sciences, 8.248–258.
[21] Roberfroid, M. (2007) Prebiotics: The concept revisited. J Nutr, 137. 830–837.
[22] Wu, G., Chen, J., Hoffmann, C., Bittinger, K., Chen, Y. and Keilbaugh, S. (2011) Linking long-term dietary patterns with gut microbial enterotypes. Sci, 334. 105–108.
[23] Polari, L., Ojansivu, P., Makela Eckerman, C., Holmbom, B. and Salminen, S. (2012) Galactoglucomannan extracted from spruce (*Picea abies*) as a carbohydrate source for probiotic bacteria. J Agri Food Chem, 60. 11037–11043.
[24] Dwivedi, G., Fitz, L., Hegen, M., Martin, S.W., Harrold, J., Heatherington, A. and Li, C. (2014) A multiscale model of interleukin-6-mediated immune regulation in Crohn's disease and its application in drug discovery and development. CPT Pharmacometrics Syst Pharmacol, 3. 89.
[25] Kumar, H., Salminen, S., Verhagen, H., Rowland, I., Heimbach, J., Banares, S., Young, T., Nomoto, K. and Lalonde, M. (2015) Novel probiotics and prebiotics: road to the market. Curr Opin Biotechnol, 32. 99–103.
[26] Farhoosh, R. and Riazi, A.A. (2007) A compositial study on two current types of salep in Iran and their rheological properties as a function of concentration and temperature. Food Hydrocoll, 21. 660–666.
[27] Tekinsen, K. and Guner, A. (2010) Chemical composition and physicochemical properties of tubera salep produced from some *Orchidaceae* species. Food Chem,121. 468–471.
[28] Citil, O.B. and Tekinsen, K.K. (2011) A comparative study on fatty acid composition of salep obtained from some *Orchidaceae* species. Chem Nat Comp, 46. 943–945.
[29] Georgiadis, N., Ritzoulis, C., Charchari, E., Koukiotis, C., Tsioptsias, C. and Vasiliadou, C. (2012) Isolation, characterization and emulsion stabilizing properties of polysaccharides from *Orchid* roots (salep). Food Hydrocoll, 28. 68–74.
[30] Popova, E., Kim, H.H., Saxena, P.K., Engelmann, F. and Pritchard, H.W. (2016) Frozen beauty: The cryobiotechnology of orchid diversity. Biotechnol Adv, (in press).
[31] Teoh, E.S. (2016) Medicinal Orchids of Asia. Springer,1-752.
[32] Kaplan, H. and Hutkins, W.R. (2000) Fermentation of fructooligosaccharides by lactic acid bacteria and *Bifidobacteria*. Appl Environ Microbiol, 6. 2682–2684.
[33] Mumcu, S.A. and Temiz, A. (2014) Effects of prebiotics on growth and acidifying activity of probiotic bacteria. Food (in Turkish), 39. 71–77.
[34] Tzortzis, G., Goulas, K.A. and Gibson, R. (2005). Synthesis pf prebiotic galactooligosaccharides using whole cells of a novel strain, *Bifidobacterium bifidum* NCIMB 41171. Appl Microbiol Biotechnol, 68. 412–416.
[35] Lee, W.H., Park, S.Y., Jung, S.J. and Shin, S.W. (2002) Chitosan oligosaccharides, dp-28, have

prebiotic effect on the *Bifidobacterium bifidum* and *Lactobacillus* sp. Anaerobe, 8. 319–324.
[36] Holt, S.M., Miller-Fosmore, C.M. and Cote, G.L. (2005) Growth of various intestinal bacteria on alternansucrase-derived oligosaccharides. Lett Appl Microbiol, 40. 385–390.
[37] Maischberger, T., Nguyen, T., Gugler, J., Zehetner, R., Splechtna, B., Kneifel, W., Rastall, A.R. and Halritch, D. (2009) Investigations on the prebiotic effect of a novel galactooligosaccharide mixture: using pure and mixed culture fermentations: Biocatalytic synthesis of prebiotic galacto-oligosaccharides: from enzyme production to product formation. Ed: Maischberger, T., University of Natural Resource and Applied Life Sciences, Department of Food Science and Technology, Vienna, 87-104.
[38] Yang, L., Lin, W. and Lu, T. (2012) Characterization and prebiotic activity of aqueus extract and indigestible polysaccharide from *Anoectochilus formosanus.* J Agri Food Chem, 60. 8590–8599.
[39] Crittenden, R., Karppinen, S., Ojanen, S., Tenkanen, M., Fagerstrom, R., Matto, J., Saarela, M. Mattila-Sandholm, T. and Poutanen, K. (2012) *In vitro* fermentation of cereal dietary fibre carbonhydrates by probiotic and intestinal bacteria. J Sci Food Agri, 82.781–789.
[40] Huebner, J., Wehling, R.L., Parkhurst, A. and Hutkins, R.W. (2008) Effect of processing conditions on the prebiotic activity of commercial prebiotics. Int Dairy J, 18. 287–293.
[41] Haryadi Putri, W.A. and Cahyanto, N.M. (2013) Prebiotic activity of phosphorylated resistant corn starch. The 4th International Conference of Indonesian Society for Lactic Acid Bacteria (4th IC-ISLAB) Yogyakarta, Faculty of Agricultural Technology, Universitas Gadjah Mada, Yogyakarta, Indonesia, 25-26 January.
[42] Thuaytong, W. and Anprung, P. (2011) Bioactive compounds and prebiotic activity in thailand-grown red and white guava fruit (*Psidium guajava L.*). Int J Food Sci Tech,17. 205–212.

Received: **05.06.2017**
Accepted: **10.07.2017**

CORRESPONDING AUTHOR

Lutfiye Yilmaz-Ersan
Department of Food Engineering,
Faculty of Agriculture,
Uludag University,
16059, Bursa – TURKEY

E-mail: lutfiyey@uludag.edu.tr

© by PSP Volume 26 – No. 10/2017 pages 6199-6204 Fresenius Environmental Bulletin

EFFECTS OF DIFFERENT SOWING DATES ON FLOWERING PHENOLOGY OF PHACELIA (*PHACELIA TANACETIFOLIA* BENTHAM)

Ayse Genc Lermi[1,*], Sahin Palta[2]

[1]Bartin University, Vocational School, Department of Herbal and Animal Production, Bartin, Turkey.
[2]Bartın University, Faculty of Forestry, Department of Forest Engineering, Division of Watershed Management, Subdivision of Range Management, Bartin, Turkey.

ABSTRACT

This study was conducted in order to determine the flowering phenology on different sowing dates in a mild climate. The experiment was conducted in the autumn and spring vegetation periods of 2013 and 2014 in a randomized block experimental design with three replications. Flowering started on 08.04.2013–02.04.2014 and ended on 22.05.2013–26.05.2014 in the autumn sowing period. In the spring sowing period, the first flowering dates were 08.05.2013–18.05.2014, and it lasted until 31.07.2013–25.07.2014. According to the two years' results, it was determined that the average flowering period was 41.9 days. Throughout the five weeks' observation period, the peak flower density and bee density per square meter were observed in the third week, respectively, with 943.4 pcs/m^2 and 72.06 pcs/m^2. Reports of investigated traits, which obtained a value decrease with retarded sowing dates, stated that the flowering period was prolonged when phacelia should be sown in certain intervals between September–November and between the beginning of March and beginning of April for beekeeping, which is intensive in this region. It was concluded that phacelia may provide significant contributions on needs of nectar and pollen in the dearth period when the flowering period lasted.

KEYWORDS:
Bee density, flower density, flowering period, phacelia, sowing date

INTRODUCTION

Phacelia is potentially used in various agricultural practices. It is used as forage and silage in livestock feeding and used as a pollen and nectar source in beekeeping. It has significant contributions to the balance of an ecosystem through improving the biotope of beneficial insects and for biological-control activities. Phacelia is known as a great nectar source by beekeepers worldwide and is listed among the top 20 nectar plants of the world [1]. It is commonly assessed as a nectar plant both in the world and in Turkey. In Turkey, apiculture is carried out as dominantly dependent on natural flora. Pollen and nectar entities of the vegetation in natural flora of warm climate zone increase in May and June. Researchers [2] indicated that phacelia sown in October and November in the Cukurova region bloomed in March, April, and May of the next year and, thus, provided great contributions to population development of bee colonies. The researcher [3] carried out research in the Cukurova region, which has a Mediterranean climate, to investigate the effects of different sowing dates (starting from 15 September and carried out in five periods with 15 day intervals) on seed yields and potential use as bee pasture. The peak values were obtained from the plots sown on 15 November (with number of flower clusters as 98.56 pcs/m^2 and number of bees as 25.99 bee/m^2). Research [4] was carried out in the same region, noting flower densities as 5950, 6216, 4733, 8933, and 9250 flowers/m^2, respectively, for the sowing dates of 15 September, 30 September, 15 October, 30 October, and 15 November. Bee density was identified as 91, 66, 201, and 183 bee/m^2, respectively, in plots sown on 30 September, 15 October, 30 October, and 15 November. A study was carried out in the Cukurova region to investigate the relationships of honeybees (*Apis mellifera* L.) with phacelia (*Phacelia tanacetifolia* Bentham) and oilseed rape (*Brassica napus* L. Metzg.) and reported that the phacelia sown in November flowered in mid-March of the next year, the flowering lasted for 50 days, and flower density was 2722.39 flowers/m^2 in the first year of the research; flowering at the end of May lasted 38 days, and flower density was 3238.94 flowers/m^2 in the second year [5].

The experiment was carried out in a Black Sea transition zone and reported full-flowering time of phacelia as between 67–83 days, stayed in flower as between 27–39 days, and the peak values with regard to these parameters were obtained from the plants sown on 5 March [6]. The researchers [7] investigated the flowering periods and potential use of phacelia as a bee pasture under different sowing dates (7 October, 17 October, 27 October, 6 November, and

16 November) under Kahramanmaras' conditions and indicated that phacelia started flowering at the end of March and beginning of April and stayed in flower 45 days. Researchers also reported the number of flowers per m^2 during the flowering period as between 61–1662 pcs and indicated that bee density flowers per m^2 for 5 minutes varied based on flower density. Bee density was identified as seven bees/m^2 in periods with a low number of flowers and as 119 bees/m^2 in periods with peak flower density. In another study carried out in Bingol Province with intensive beekeeping, the peak plant height was reported as 53.50 cm, number of flower clusters as 71.23 pcs/plant, number of flower per clusters as 11.50 pcs/plant, number of flowers per m^2 as 8982.23, and number of bees as 116 pcs/m^2 [8].

A study was carried out in Italy with a Mediterranean climate and reported the flowering period of phacelia plants as between 38–45 days and the number of visiting bees per m^2 as more than 15 [9]. The researchers [10] carried out a study in the southeast of Great Britain in regards to flowering phenology, bee density, bee behaviors, and foraging of bees over the phacelia plants sown in different dates (between May–August). Researchers reported that flower densities exceeded 2000, 4000, and 3000 flower/m^2, respectively, in early, medium, and late sown plots. Researchers also indicated that the peak bee density reached to 29 pcs/m^2 and concluded that phacelia had a great potential as a bee foraging plant in preserved lands.

Because it is a great source of nectar and pollen and has quite long flowering durations, phacelia has long attracted the attention of beekeepers. Beekeepers need alternative nectar plants to be able to flower at different periods of the year and close to the nectar deficits. Moving from this point on, the present study was conducted to investigate the flowering phenology of phacelia in different sowing dates in mild climate regions.

MATERIALS AND METHODS

The present study was conducted in Akmanlar Village of Bartin Province in autumn and spring vegetation periods of the years 2012, 2013, and 2014. The geographical coordinates of Bartin are within 41° 37′ northern latitude and 32° 22′ eastern longitude. Experimental soils have a clay texture with medium lime content (7.01 % $CaCO_3$) and rich organic matter content (3.20%). Soils were slightly alkaline (pH 7.54), and nitrogen content was 0.29% [11]. Precipitation data for research years and long-term averages are presented in Figure 1.

Experimental design and measurements. Experiments were conducted in a randomized block design with three replications. A total of 12 different sowing dates were applied, six of which were applied in autumn, and six were applied in spring. Experiments were implemented over 36 plots each of having 10 m^2. Sowing dates were arranged as 15 September, 30 September, 15 October, 30 October, 15 November, and 30 November (for autumn) and 1 March, 15 March, 1 April, 15 April, 1 May, and 15 May (for spring). Despite the irrigations, plant emergence was not observed in both years in sowings made on 15 May. Italian-originated Stala cultivar was used as the plant material. Sowing was performed as to have 2 kg seeds per decare [6]. Row spacing was arranged at 40 cm. Irrigations were performed in both sowing periods during the periods with insufficient precipitation until the emergence and natural precipitation supplied water needs throughout the vegetation period. Together with sowing, 10 kg/da diammonium phosphate (DAP) fertilizer was applied.

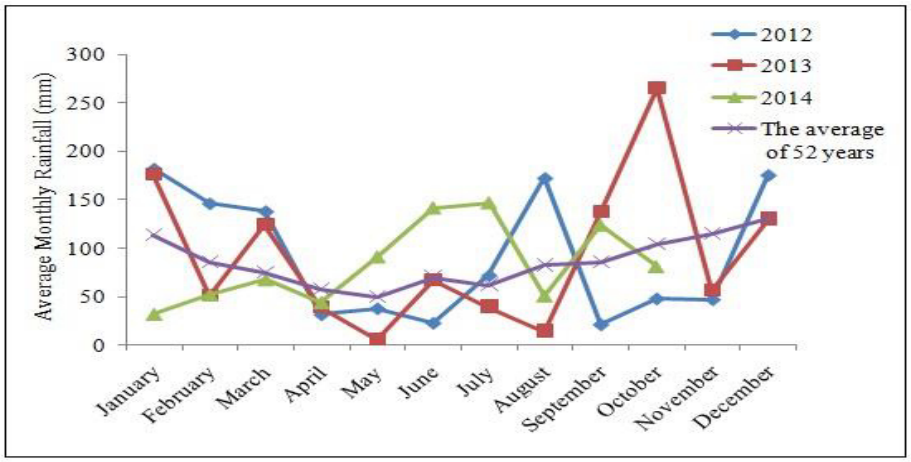

FIGURE 1
Precipitation data for the years 2012, 2013, 2014, and long-term averages for Bartin Province [11].

TABLE 1
Variance analysis for morphological and phenological traits

	Plant height (cm)	Number of side branches (per plant)	Number of flower clusters (per plant)	Number of flowers (per cluster)	Beginning of flowering (days)	Full flowering time (days)	Stayed in flower (days)
15 September	158a**	3.83a**	22.3a**	39.3d**	201a**	251a**	55a**
30 September	148b	4.0a	16.0b	70.5a	185b	237b	54a
15 October	133c	3.8a	11.1c	73.5a	175c	221c	50b
30 October	120d	3.0b	6.1d	62.3b	166d	210d	50b
15 November	114e	2.3dc	5.3de	55.5c	159e	191d	44c
30 November	102f	1.3e	5.5d	53.8c	147f	179f	40d
1 March	95g	1.3e	4.3gf	40.8d	73g	97g	30f
15 March	83h	1.3e	3.5gh	39.3d	64h	89h	31f
1 April	70ı	1.1e	2.6h	38.0d	59ı	85ı	32f
15 April	61j	2.0d	4.0gf	39.8d	50k	84j	36e
1 May	51k	2.5c	4.5ef	30.6e	55j	89h	40d
Mean	103.1	2.42	7.7	49.4	121.2	157.5	41.9
Coefficient of Variation (%)	3.63	14.89	9.72	5.72	0.75	0.61	2.67

* $P<0.05$, ** $P<0.01$.

By experimental plots, five bee colonies with medium vigor were placed before flowering. Then, bees visiting 0.5 m^2 area in plots were counted for 5 minutes during the most intense bee activities of the day (between 1:00 and 2:00 p.m.) in 5 to 7 day intervals for five weeks [7]. Observations were performed for five weeks in each plot about a week after flowering of the plot to determine the number of flowers and bees.

Morphological and phenological observations, beginning of flowering, full flowering time (days), stayed in flower (days), number of flower clusters per plant, number of florets per cluster, and number of flowers per square meter were determined in accordance with the methods recommended by [12, 13, 14, 7].

Statistical analyses. Experimental data were assessed statistically in accordance with the general linear model of SAS software at 5% and 1% significance level [15]. A least significant difference (LSD) test was used to compare the treatments.

RESULTS AND DISCUSSION

Morphological and phenological traits. Variance analysis results for two-year averages of investigated traits obtained from different sowing dates of phacelia plants are provided in Table 1. The differences between the treatments with regard to investigated characteristics were found to be significant at a 1% level. Plant heights and number of flower clusters decreased with retarded sowing dates. The peak plant height and number of flower clusters were, respectively, observed at 158 cm and 22.3 clusters in 15 September sowing. Mean plant height was identified at 103.1 cm, and mean number of flower cluster was identified at 7.7 clusters. With regard to the number of side branches, the peak values close to each other were obtained from the first three sowing dates. Researchers [13] in a study carried out with 40 cm row spacing reported mean height of phacelia plants at 67.77 cm. It is reported that the mean plant height of phacelia is 104.9 cm, number of flower clusters per plant is 41.6, and the number of flowers per cluster is 48.5 pcs. All these results show climate differences and that seed cultivars affected plant characteristics [7].

At different sowing dates, the peak beginning of the flowering day was observed at 201 days, and the number of days to full flowering time was observed at 251 days on 15 September. With regard to duration of flowering period, the peak values were observed at 55 and 54 days, respectively, in 15 September and 30 September sowing treatments. Days to beginning of flowering, days to full flowering time, and remaining in flower shortened with the retard in sowing dates (Table 1). In sowings performed at the beginning of May, the vegetative period was shorter, and the generative period was longer because of decreased precipitation and increased temperatures. The researchers revealed that the flowering period of phacelia lasted seven weeks. When it was sowing in November [16], phacelia plants started to flower at the end of March and beginning of April and stayed in flower for 45 days [7]. The flowering period of phacelia plants lasted between 38–45 days [9]. The phacelia stayed in flower for 50 days in the autumn sowing date [17]. Current findings were parallel to those of earlier reports.

The values of investigated traits were lower in spring than in autumn sowings due to shorter vegetation durations and less precipitation during spring sowings. The peak plant height in spring sowings (1 Mach to 1 May) was obtained from 1 March sowing treatment with 95 cm. The researchers [13], within the scope of their study about yield and adaptation of phacelia sown in spring with 40 cm row spacing, re-

ported the mean plant height at 67.77 cm. The researchers reported the peak plant height at 53.50 cm, number of side branches per plant at 3.16 pcs, number of flower clusters per plant at 71.23, number of flowers per cluster at 11.50 pcs, and indicated the peak values for 50 cm row spacing [8]. Findings on the number of side branches and number of flower clusters were higher than in the present values; however, those values on plant height and number of flowers per head were smaller than the present values. Such differences were mainly because of differences in row spacing, seed cultivar, climate, and ecological conditions.

The peak number of days to beginning of flowering and days to full flowering in spring sowings were obtained from 1 March treatment, respectively, at 73.3 and 97 days (Table 1). The peak number of days to flowering and the stayed-in flower of phacelia plants, respectively, as 67–83 days and 27–39 days for 5 March treatment [6]. The values obtained from spring sowings of the present study were similar to the values reported by those researchers. In addition, other researchers [17] revealed that the flowering period of phacelia stayed in flower days, and flower density is affected by sowing date and environmental conditions.

The number of flowers per square meter. The number of flowers per square meter of phacelia plants sown at different dates is provided in Table 2. In regional ecology, flowering lasted 4–5 weeks (Table 1). In all sowing dates, the number of flowers per square meter reached to maximum level 15 days after the beginning of flowering and had a decreasing trend later on. The peak number of flowers was observed in the third week and the values of the third week varied between 92 and 1475.6 flowers/m^2. With regard to sowing dates, the peak number of flowers was observed in the 30 November treatment with 1475.6 flowers/m^2 (Table 2). The number of flowers as 8982.23 pcs/m^2 [8]. The researchers reported the number of flowers of phacelia plants for three different sowing dates in Southeast Britain as over 2000 pcs in early sowing, 4000 pcs in medium sowing, and 3000 pcs in late sowing [10]. The number of flower clusters were 17.2 pcs/m^2 [13]. The researchers reported the peak number of flower was obtained 2083 pcs/m^2 from the first sowing on 7 October [7]. Different results were observed in previous studies carried out to assess the possible use of phacelia plants as bee pastures in different ecological regions. Differences could be mainly because of differences in ecological conditions and seed cultivars.

TABLE 2
Number of flowers per square meter

	1st week	2nd week	3rd week	4th week	5th week	Mean
15 September	179.3d**	843.8c**	1449.8a**	1025.6b**	534.6d**	806.6
30 September	215.5c	778.5d	1424.1a	1109.3b	678.5c	841.1
15 October	268.3a	881.5cb	1464.3a	873.6dc	737.5b	845.0
30 October	254.8b	890.0b	986.6b	878.1dc	784.3a	758.7
15 November	104.6e	900.8b	1448.1a	853.6d	524.1d	766.2
30 November	96.3e	958.8a	1475.6a	892.3c	528.3d	790.2
1 March	45.0f	687.3e	808.6c	87.3f	11.0f	327.8
15 March	36.8gf	640.5f	727.6d	96.1f	10.6f	302.3
1 April	32.6g	401.1g	275.1e	115.1fe	28.6f	170.5
15 April	38.6gf	218.5h	226.0e	126.6e	37.3f	129.4
1 May	36.6gf	175.3ı	92.0f	43.6g	21.8f	73.8
Mean	118.9	670.5	943.4	554.7	354.3	
Coefficient of Variation (%)	7.42	5.24	4.62	4.37	6.91	

* $P<0.05$, ** $P<0.01$.

TABLE 3
Number of visitor bees per square meter

	1st week	2nd week	3rd week	4th week	5th week	Mean
15 September	21.6d**	74.0a**	90.3d	102.1a**	50.8a**	67.7
30 September	23.6c	53.3c	110.6a	91.8c	47.1b	65.2
15 October	28.1b	53.6c	102.6b	100.6a	52.1a	67.4
30 October	30.1a	49.1d	96.5c	101.8a	41.5c	63.8
15 November	16.3f	51.5dc	109.1a	95.0b	32.3e	60.8
30 November	18.5e	66.3b	98.1c	72.0d	37.3d	58.4
1 March	10.6g	51.3dc	55.8e	11.8ef	4.8f	26.8
15 March	9.3hg	52.0dc	59.1e	9.1fg	4.5f	26.8
1 April	8.5hı	33.1e	26.0f	12.6e	5.6f	17.1
15 April	10.0hg	32.0e	27.8f	14.0e	6.0f	17.9
1 May	6.6ı	20.0f	16.3g	8.0g	4.0f	10.9
Mean	16.6	48.7	72.06	56.28	25.9	
Coefficient of Variation (%)	9.46	5.30	4.58	4.34	6.95	

* $P<0.05$, ** $P<0.01$

The number of flower clusters were lower in spring sowings than in autumn sowings. In spring sowing periods of both years, the number of flower clusters were high in March, but significant decreases were observed in subsequent dates.

In the autumn sowing period, flowering started on April (08.04.2013–02.04.2014) until the end of May (22.05.2013-26.05.2014); on the other hand, flowering started at the beginning of May (08.05.2013–18.05.2014) until the end of July (31.07.2013–25.07.2014). Together, with the application of spring and autumn sowings, the stayed flowering period prolonged from one and a half month to four months.

The number of visitor bees per square meter. In all sowing dates, bee density increased from the first week until the fourth week and decreased in the fifth week with decreasing dependent on flower density. The peak values were seen in the third and fourth weeks. The peak value was observed in the third week with 72.06 pcs/m^2 (Table 3), and the peak bee density was seen on 15 September treatment with 67.7 pcs/m^2. It was remarked that, in the least flowering period, bee density was 7 pcs/m^2; on the contrary, bee densities were 119 pcs/m^2 at the intense flowering period [7]. The researchers stated that bee densities per m^2 as 91, 66, 201, and 183 pcs, respectively, in plots sown on 30 September, 15 October, 30 October, and 15 November [4]. It was determined that the number of bees visiting phacelia plants per m^2 as more than 15 [9]. The peak bee density was pcs/m^2 as 29 [10]. Researchers observed bee density as 115 honeybees/m^2 [16]. Bee densities (per m^2) changed depending on differences in region, climate, and daily temperatures.

These results indicate that bee density was lower in the spring sowing period than in the autumn sowing period due to shorter vegetation duration and less flower density meters in spring and differences in climate parameters.

CONCLUSION

It was stated in this study that phacelia plants started to flower 147–201 days after sowing and stayed in flower for 40–55 days when sown in autumn; flowering started 55–73 days after sowing and stayed in flower 30–40 days when sown in spring. With different sowing periods and sowing dates, the flowering period can be prolonged from the beginning of April until the end of June.

Considering the use of phacelia as a bee pasture, it was recommended for similar ecologies that phacelia should be sown in 20–30 day intervals until the end of November in autumn and from the beginning of March until the beginning of April in 15-day intervals in spring. Within the scope of this research, phacelia could provide a significant supplementary nectar source for beekeepers in dearth periods.

ACKNOWLEDGEMENTS

The present research was supported by the Scientific Research Projects Department of Bartin University (with the project number of BAP 2012.2.65).

REFERENCES

[1] Crane, E. (1975) Honey: A Comprehensive Survey. Heinemann in Co-operation with International Bee Research Association. London. U.K. 608 pp.

[2] Kumova, U. and Korkmaz, A. (2002) Research on Bee Forage Plant (Phacelia tanacetifolia Bentham) in Turkey and its Importance in Beekeeping. Uludag Bee Journal 2(1), 11-16.

[3] Ucar, H. (1995) Value of Phacelia tanacetifolia Bentham for honeybees in Cukurova Region. University of Cukurova, Institute of Natural and Applied Science, Master Thesis, Adana.

[4] Tansi, V., Saglamtimur, T., Kumova, U. and Kizilsimşek, M. (1996) Observations on *Phacelia tanacetifolia* Bentham as a food plant for honeybees (*Apis mellifera* L.) in southern Turkey. (Development Foundation of Turkey) TKV Journal of Technical of Beekeeping. Ankara, 52, 2-6.

[5] Korkmaz, A. (2003) The Research on determination of some relations of honeybees (*Apis mellifera* L.) among the Phacelia (*Phacelia tanacetifolia* Bentham) and rape (*Brassica napus* L. Metzg.) in Cukurova region. University of Cukurova, Institute of Natural and Applied Science, PHD Thesis, Adana.

[6] Karadag, Y. and Buyukburc, U. (2003) Researches on Spring Sowing Date of Phacelia (*Phacelia tanacetifolia* Benth.) Under Tokat Conditions. II- Determination of Seed Yield Properties. Journal of Agricultural Faculty of Gaziosmanpasa, 20(1), 143-148.

[7] Kizilsimsek, M. and Ates, F. (2004) Effects of Different Sowing Dates on Flowering Period of Phacelia (*Phacelia tanacetifolia* Bentham) and Its Evaluation as Bee Pasture Under Kahramanmaras Conditions. Kahramanmaras Sutcu Imam Unıversity Journal of Sicience and Engineering, 7(1), 96-103.

[8] Bakoglu, A. and Kutlu, M.A. (2006) A Research on The Effect of Different Row Space on Some Agricultural Traits and Use of Bee Foraging in Phacelia (*Phacelia tanecetifolia* Benntham) Grown Under Irrigated Conditions of Bingol. Uludag Bee Journal February, 33-38.

[9] Orsi, S. and Biondi, A. (1987) *Phacelia tanacetifolia*: It's honey potential. Informatore-Agrario., 43:47, 53-57.
[10] Williams, I.H. and Christian, D.G. (1991) Observations on *Phacelia tanacetifolia* Bentham (Hydrophyllaceae) as a Food Plant for Honey Bees and Bombus Bees. Journal of Apicultural Research. 30(1): 3-12.
[11] Genc Lermi, A. and Palta, S. (2014) The Effects of Different Sowing Dates of Feedleneck (*Phacelia tanacetifolia* Benth.) During the Autumn and Spring Sowing Periods on the Forage Yield and Quality. International Journal of Bartin Faculty of Forestry, 16(23-24), 11-18.
[12] Bilgen, M. (1999) Effect of different sowing times on flowering characteristics of phacelia (*Phacelia tanacetifolia* Benth.) 3. Field Crops Congress Turkey. 15-18 November 1999. Adana. Volume III, 312-317.
[13] Karadag, Y. and Buyukburc, U. (1999) A research on the yield and adaptation of phacelia (*Phacelia tanacetifolia* Benth.) grown in Tokat conditions. Journal of Agricultural Faculty of Gaziosmanpasa, 16(1), 155-169.
[14] Karadag, Y. and Buyukburc, U. (2001) The effect of different row spacing on herbage and seed yields of phacelia (*Phacelia tanacetifolia* Benth.), 4th Turkey Field Crops Congress, September 17-21, Tekirdag. PAYMAS Press Istanbul. Grassland and Forage Crops 3, 143-148.
[15] Anonymous (1988). SAS/STAT User's Guide. Version 6. Fourth edition. Vol.2 SAS Institute Inc. Cary. NC. USA. 1686 p.
[16] Kumova, U., Saglamtimur, T. and Korkmaz, A. (2001) Research on honeybee (*Apis mellifera* L.) foraging preferences among varieties of phacelia (*Phacelia tanacetifolia* Bentham). Mellifera 1(1), 60-64.
[17] Kumova, U. and Korkmaz, A. (2013) The Research on determination of flowering phenology of phacelia (*Phacelia tanacetifolia* Bentham) and ıts nectar and pollen potential. Mellifera, 13(25), 30-40.

Received: **08.06.2017**
Accepted: **23.07.2017**

CORRESPONDING AUTHOR

Ayse Genc Lermi
Bartin University
Vocational School
Department of Herbal and Animal Production
Bartin, 74100 – TURKEY

E-mail: aysegenclermi@gmail.com

© by PSP Volume 26 – No. 10/2017 pages 6205-6211 Fresenius Environmental Bulletin

COMPETITIVE ADSORPTION OF HEAVY METALS IN DIFFERENT SOILS

Veli Uygur[1,*], Mehmet Ali Karaduman, Mehmet Kececi[2], Enise Sukusu[1], Metin Mujdeci[1]

[1]Soil Science and Plant Nutrition Department, Agricultural Faculty, Süleyman Demirel University, Isparta, Turkey
[2]Diroctorate of Soil Fertilizer and Water Resources Research Institute, Yenimahalle, Ankara, Turkey

ABSTRACT

Natural resources have being polluted by variety of heavy metals due to urbanization, industrialization and excessive fertilizer and pesticide usage. Since heavy metals accumulate in soils, their treats to ecosystem and human health became more serious to the time. On the other hand, at least two or more heavy metals are co-added to the soil environment. Therefore, it should be known competitive adsorption mechanism of heavy metals in soils. Their relations with soil properties can help to develop an efficient way of tackling undesirable effects of such pollution. For this aim, competitive adsorption of Cd, Cu, Ni and Zn in 36 soil samples taken from 7 different cities in Turkey with differing physico-chemical properties was investigated in this study. Scopes of 1 g soil samples were equilibrated with 25 mL solutions containing different equivalent amounts of Cd, Cu, Ni, and Zn (10^{-4}, 2.10^{-4}, 4.10^{-4}, 6.10^{-4}, 1.10^{-3}, 2.10^{-3} and 8.10^{-3} mole L^{-1}) at 25±2ºC for 24 h by using batch sorption technique. After equilibration Cd, Cu, Ni and Zn concentrations of liquid phase were determined. The conformation of the data to modified Freundlich and Langmuir models were tested by regression analysis. Results showed that both adsorption isotherms can be successfully used to describe simultaneous adsorption of the heavy metals in all soils except for Cu adsorption. Correlation analysis was made between soil physico-chemical characteristics and the parameters of the adsorption isotherms. Freundlich *n* parameters of Zn, Ni and Cd had significant negative correlation coefficients with soil pH ($p<0.01$). A significant correlation was also found between *n* parameters of Zn and Cd and carbonate content of soils. Consequently, the selectivity order of the heavy metal adsorption was found to be related to physico-chemical characteristics of soils and chemical properties of the adsorbed elements.

KEYWORDS:
Heavy metals, adsorption, soil properties, Langmuir isotherm, Freundlich isotherm

INTRODUCTION

Heavy metals are known as potentially the most toxic elements to ecosystem due to continuous increase of their concentrations and persistence in the soil environment and are therefore of great interest in ecosystem health. Heavy metal pollution in soils are related to many different anthropogenic activities [1] such as the mining activities, tanneries, atmospheric deposition, reuse of wastewater, disposal of tailings, sewage irrigation, and use of pesticides and fertilizers [2]. In most cases, several heavy metals can pollute the soils at the same time.

These simultaneously introduced heavy metals are to compete for the same sorption sites and therefore their mobility, plant availability and toxicity in the soil environment are directly relevant to their preferences on the sorption sites [3], soil physical and chemical properties [4-10], and characteristics of elements mainly hydrolyses constants [11, 12]. The occurrence of different type of functional groups on any soil component makes the situation even more complex. For example soil organic matter carries carboxyl, phenolic, and enolic hydroxy groups with different reactivity [13]. In accordance with this, the amount and timing of dissolved organic matter addition was found to play a pivotal role in determining the affinity of Cu, Ni and Zn for changing soil properties [5, 14].

The soils contain infinite number of complex mixture of soil components and the interrelations among these components characteristically result in varying physicochemical properties that could differentiate the nature of trace elements' reactions with the soils. Soil pH, the amount, type and co-presence of clay minerals, carbonate contents, organic matter, oxides, and eventually simultaneous occurrence of competing trace elements influence sorption processes [7, 12, 15-19]. The electronegativity and charge-to-radius ratio are significant consequences in determining which heavy metal is to chemisorb with the highest preference. In model system studies, the selectivity preferences of any soil component has been studied. Those reports indicate that Mn oxides shows high selectivity for Cu, Ni, Co, and Pb; whereas Fe and Al oxides and silica adsorb Pb and Cu more strongly than the other divalent metals [20]. The sorption affinity sequence of Zn<Cd<Pb on montmorillonite, which is most common clay

TABLE 1
Descriptive statistics for measured parameters of the experimental soils

Soil properties	Range	Min	Max	Mean	Std. Error	Std Dev	Variance	Skewness*		Kurtosis*	
Soluble salts (%)	0.544	0.004	0.548	0.092	0.021	0.126	0.016	2.663	0.117a	6.691	0.446 a
CEC (cmol kg^{-1})	44.38	6.99	51.37	29.53	1.512	9.074	82.34	-0.395	-0.395	0.610	0.610
Sand (%)	88.60	0.40	89.00	33.82	4.110	24.66	608.1	0.594	0.594	-0.859	-0.859
Silt (%)	66.00	4.00	70.00	31.18	2.350	14.10	198.9	0.072	0.072	0.417	0.417
Clay (%)	55.10	10.50	65.60	36.65	2.834	17.00	289.2	0.088	0.088	-1.254	-1.254
pH	5.14	4.77	9.91	7.32	0.224	1.348	1.818	-0.239	-0.239	-0.490	-0.490
OM (%)	17.25	0.25	17.50	5.78	0.843	5.057	25.57	0.659	0.659	-0.814	-0.814
CCE (%)	28.39	0.10	28.49	8.86	1.316	7.899	62.40	0.376	0.376	-0.744	-0.744
P (mg P_2O_5 kg^{-1})	66.37	0.85	67.22	9.80	1.939	11.63	135.34	3.728	0.213a	17.16	0.879 a
K (mg K_2O kg^{-1})	255.4	36.34	291.8	143.1	12.82	76.94	5921	0.354	0.354	-0.877	-0.942
Ni (mg kg^{-1})	279.6	18.70	298.3	110.6	12.58	75.49	5699	0.867	-0.347a	-0.051	-0.678 a
Cu	47.80	12.00	59.80	32.68	1.919	11.51	132.6	0.994	-0.112a	0.795	0.860 a
Zn	443.3	28.00	471.3	78.95	11.60	69.63	4848	5.379	2.170a	30.95	10.59 a
Cd	11.00	0.40	11.40	1.108	0.295	1.768	3.127	5.956	4.652a	35.64	26.47 a

* Standard error of skewness is 0.393; standard error of kurtosis is 0.768 for N=36. a: Skewed data sets were log transformed to approximate the normal distribution. CEC cation exchange capacity, CCE calcium carbonate equivalent, OM organic matter.

mineral in Turkish soils, was explained with hard-soft acid-base theory [21]. The competitive sorption of Cu (II), Pb (II) and Cr (VI) in a ternary system on montmorillonite showed Cr>Cu>Pb sequence [22]. Smectite minerals behave similarly and followed the selectivity sequence of Pb>Zn>Cd [23]. The sorption affinity of bentonite which is a smectite group clay mineral was reported as Co>Cu>Ni=Zn>Pb [24]. Raw kaolinite however adsorbed heavy metals Pb, Cd, Ni and Cu via ion exchange mechanism from the wastewater suggested by significant reduction-induced by increasing ionic strength [25]. Uddin [26] well summarised the references related to the adsorption capacities of various clay minerals and oxides towards different adsorbates (heavy metals) and their adsorption capacities were extremely different.

However, the preferences of complex systems such as soils with differing characteristics cannot be identical with those of model systems. The sorption phenomena along with the precipitation are the main factors controlling the behaviour of heavy metals in soil ecosystem. The soils showed different preference sequences due mainly to sesquioxides content [15, 27] and clay mineralogy and related traits [11, 28] and organic matter content [29, 30].

Agricultural lands are prone to simultaneous heavy metal pollution because the fertilisers especially the phosphatic ones consist of variety of heavy metals [31]. Therefore we studied the competitive adsorption of heavy metals at equivalent amounts which are present in the fertiliser and other pollution sources in differing soil properties to evaluate their potential environmental risks.

MATERIALS AND METHODS

Soil Sampling and Characterisation. Samples from the surface layer (0-20 cm) of 36 soils varying widely in their origin and properties were collected from different regions of Turkey. Soil samples were air-dried, ground to pass through a 2-mm sieve and analysed for their descriptive physico-chemical properties according to the common methods [32]. Particle size analysis was performed according to [33]. The brief descriptions of the methods are: pH and EC in saturation paste, calcium carbonate equivalent (CCE) by a manometric method with Sheibler calcimeter, organic matter (OM) by wet combustion of modified Walkley-Black method, cation exchange capacity by saturating the exchange sites with Na acetate (1 M, pH 8.2) then replacing with NH_4 (1 M, pH 7.0). Total concentration of Ni, Cd, Cu, and Zn were also determined by acid digestion and ICP-AES (Varian Series II). The descriptive statistics about the physico-chemical analyses were given in Table 1.

Adsorption Studies. Batch experiments were conducted using Cd, Ni, Cu, and Zn solutions. Scoops of 1.000 g of soil were equilibrated with 25 mL of solutions containing equivalent amounts of Cd, Ni, Cu, and Zn prepared using nitrate salts of the metals in ultrapure de-ionized water. The concentrations used were 1×10^{-4}, 2×10^{-4}, 4×10^{-4}, 6×10^{-4}, 8×10^{-3}, 1×10^{-3}, and 2×10^{-3} M. The suspensions were then equilibrated on a reciprocal shaker for 24 h at 25±2°C. After equilibration the samples were centrifuged and the supernatants were filtered through a Whatman membrane filter. The supernatants were imparted into two and in one part pH and EC of the supernatants were measured; the other parts were acidified with 0.1 mL of concentrated ultrapure HNO_3 and kept in the fridge at 4°C until the analyses. Concentrations of Cd, Ni, Cu, and Zn in the supernatants were determined with Inductively Coupled Argon Plasma-Atomic Emission Spectroscopy (ICP-AES, Varian Series II, Axial view).

The amounts of heavy metals sorbed were calculated from the difference between the added and the equilibrium concentration as shown in the equation below:

$$Si = \frac{(C_0 - C_e)xV}{W}$$

where *Si* the amounts of heavy metals adsorbed (mmol kg^{-1}), *Co* initial concentration of the metals (mmol L^{-1}), *Ce* the equilibrium concentrations of the metals (mmol L^{-1}), *V* the volume of the solution (25 mL), and *W* the dry weight (g) of the soil sample used in the sorption study.

The conformation of the sorption data to the Langmuir and Freundlich adsorption models were tested by regression analysis. The linear Langmuir model can be given as:

$Ce/Si = Ce/b+1/kb$

where *Si* is the amounts of adsorbed metals per unit mass of sorbent (mmol kg^{-1}), *Ce* is the equilibrium concentrations of metals (mmol L^{-1}), *k* and *b* bonding are energy coefficient and coefficient related to maximum adsorption, respectively.

The linear form of the Freundlich model, $Si= K_f C^n$, can be written as below:

$Log\ (Si) = Log\ K_f + n\ log\ Ce$

where K_f is the Freundlich coefficient and *n* is an empirical parameter expressing the sorption intensity of the metals [11].

RESULTS AND DISCUSSION

In general, Freundlich isotherms described the heavy metal adsorption of the soils more successfully than Langmuir isotherms. The Langmuir isotherm was inadequate in defining adsorption in some cases, most of which were Cu adsorption. The relative failure of the Langmuir isotherm could be related to non-uniform sorption sites of soils and the occurrence of both sorption and precipitation simultaneously. However, this isotherm cannot adequately describe the sorption phenomena on adsorbents having highly heterogeneous nature both in components such as organic matter, clay minerals, oxides etc. and sorption sites along with the requirement of concentration dependent correction factor [34]. The other point is soluble humic acid molecules mainly phenolic and carboxylic groups provide appreciable ability to form stable complexes with heavy metal cations [35] and the amounts of metal-chelates are to increase with the metal additions. Copper which have the higher metal-chelate complex stability constant [36] showed apparently the higher deviation from the Langmuir isotherm. The higher pH promotes such occurrence of metal-chelate complexes [36, 37] which increase the equilibrium metal concentrations leading further deviate from the heavy metals at mainly low initial concentrations. Above all application of this model may require concentration dependent factor as suggested by Sohn and Kim [34]. Particularly soils with very high buffering capacity or at initial concentration near the transition region of adsorption to precipitation reactions, Langmuir isotherm cannot satisfactorily define the sorption data. In the precipitation reactions, the Ce/Si parameter located on the Y axis in the isotherm will show a continuous decreasing tendency due to the continuous increase of Si. In this case, the slopes of the adsorption isotherm become negative as in Figure 1. This therefore does not allow calculation of the maximum adsorption capacity from the equation or other isotherm parameters. A concentration above the equilibrium concentration that the relevant phase can produce in certain conditions must be reached in order to produce an oversaturated state which provides the energy required to start precipitation of any solid phase while the adsorbent is not retained in the transition zone of the adsorption/precipitation reactions. In this case too, there are abnormal changes in the term Ce/Si (Figure 2). This leads to a poor description of the model to sorption data and thus reduces the determination coefficient (R^2=0.3484) of the regression lines.

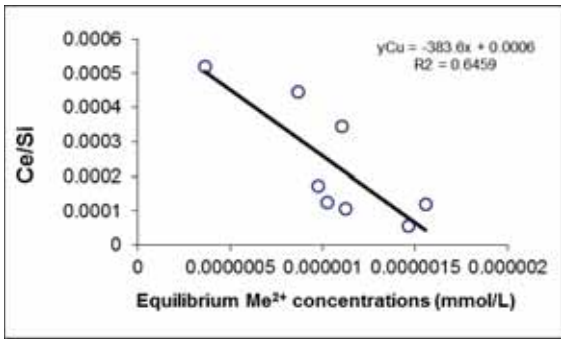

FIGURE 1
Typical poor description of Langmuir isotherm to Cu sorption data with negative slope

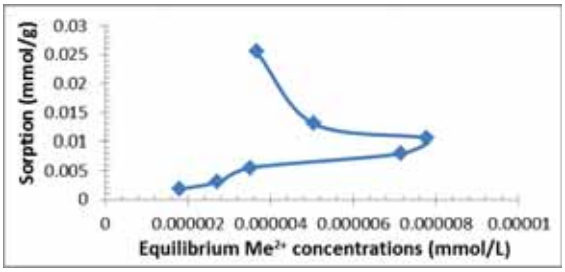

FIGURE 2
Typical poorly described adsorption/precipitation operated isotherm of Cu by Langmuir model

The assumptions made in the monolayer Langmuir adsorption model are ineffective, especially due to precipitation reactions occurring on the

TABLE 2
Freundlich isotherm parameters of heavy meals for the experimental soils

Soil	Zn			Cu			Ni			Cd		
No	n	Kf	R^2	n	Kf	R^2	n	Kf	R^2	n	Kf	R^2
1	0.6262	0.3376	0.9399	0.5295	0.997	0.901	0.4926	-0.355	0.965	0.6648	0.2617	0.9423
2	0.3801	0.2061	0.8907	0.6347	1.362	0.751	0.4215	0.3089	0.9577	0.562	1.1208	0.8217
3	0.1804	-1.2685	0.8817	0.3737	0.245	0.711	0.4051	0.5035	0.9177	0.3505	0.8426	0.9769
4	0.2475	-0.5778	0.8935	3.3453	17.75	0.665	0.1539	-1.0485	0.8434	0.2871	-1.4817	0.9067
5	0.2092	-0.8697	0.8392	0.4413	0.669	0.878	0.2038	-0.9456	0.7483	0.2247	-0.9172	0.713
6	0.378	-1.0072	0.8076	0.5681	0.18	0.834	0.9117	1.2745	0.8682	1.5798	4.0332	0.699
7	0.2429	-1.266	0.888	1.0328	3.196	0.918	0.5611	-0.0373	0.9891	0.8857	1.2259	0.9693
8	0.4706	-0.1777	0.8349	1.0078	2.979	0.818	0.6811	0.5785	0.7559	0.4647	-0.2594	0.7919
9	0.4268	-0.476	0.9395	0.58	0.7473	0.9804	0.5004	0.3037	0.9732	0.638	0.2892	0.9574
10	0.3975	-0.2365	0.9916	1.1995	4.215	0.815	0.4849	0.0579	0.9888	0.6515	0.8486	0.9648
11	0.4881	0.053	0.9791	0.8287	2.277	0.802	0.5937	0.2944	0.8143	0.5476	0.3043	0.957
12	0.5161	-0.1272	0.9374	0.4061	0.101	0.978	0.5119	-0.3145	0.9117	1.2218	2.4061	0.9494
13	0.2419	-0.6268	0.6054	1.1942	5.2442	0.8601	0.4322	-0.0223	0.8479	0.5107	0.2859	0.5936
14	0.2561	-0.6724	0.8262	0.6503	1.438	0.882	0.4427	0.1787	0.7553	0.5351	0.6662	0.6777
15	0.251	-0.7693	0.9394	2.7296	14.17	0.985	0.3718	-0.4935	0.9713	0.3793	-0.456	0.9789
16	0.1752	-1.1024	0.8757	0.4381	0.378	0.961	0.4134	-0.0361	0.8401	0.5987	0.8128	0.9156
17	0.2051	-1.0352	0.9376	0.3493	-0.08	0.911	0.4549	0.0386	0.9692	0.6153	0.7663	0.9756
18	0.2968	-0.5371	0.7785	0.7955	2.61	0.725	0.3569	-0.497	0.9026	0.7405	1.0779	0.9049
19	0.2877	-0.6476	0.9635	0.4186	0.216	0.956	0.4759	0.1933	0.8756	0.5622	0.6633	0.9026
20	0.3247	-0.8976	0.7519	1.5388	6.907	0.813	0.3427	-0.395	0.802	0.3922	-0.1858	0.8041
21	0.1846	-1.1453	0.9233	0.726	2.139	0.853	0.2992	-0.8153	0.9311	0.2244	-1.1394	0.9018
22	0.2035	-0.8173	0.9652	2.761	14.16	0.693	0.2853	-0.6039	0.9232	0.3736	-0.2818	0.9703
23	0.1211	-1.0785	0.8666	2.0429	9.306	0.813	0.4221	-0.0878	0.9131	0.4495	0.110	0.979
24	0.1781	-1.3555	0.8172	0.4045	0.031	0.936	0.6116	0.3568	0.9495	0.5621	0.3528	0.9863
25	0.6078	0.1671	0.9484	0.6347	0.811	0.984	0.5371	-0.1677	0.9516	0.8237	0.9376	0.9614
26	0.7823	0.7433	0.9205	0.9039	2.732	0.828	0.1527	-1.5202	0.7484	0.6269	-0.0523	0.8711
27	0.4183	-0.0126	0.9518	1.8441	8.193	0.707	0.4295	-0.245	0.8819	0.5975	0.5903	0.9155
28	0.2586	-0.9588	0.9262	0.5927	1.478	0.957	0.2127	-1.1521	0.891	0.4056	-0.6969	0.8364
29	0.3418	-0.2385	0.9094	0.6598	1.87	0.935	0.3199	-0.5046	0.8758	0.268	-0.7899	0.9273
30	0.1852	-1.1043	0.9443	0.4925	0.643	0.915	0.3597	-0.2987	0.8207	0.6732	1.0633	0.8813
31	0.2689	-1.024	0.8843	0.5803	0.832	0.81	0.4354	-0.2327	0.9741	0.5926	0.512	0.9531
32	0.381	-0.5275	0.9686	0.5747	1.142	0.975	0.323	-0.7473	0.9414	0.5132	-0.1744	0.9321
33	0.2129	-0.9923	0.9735	0.5719	0.988	0.9	0.5751	0.5886	0.8299	0.5798	0.8065	0.8686
34	0.2255	-0.8669	0.8677	0.4865	0.501	0.924	0.3425	-0.2915	0.9138	0.6199	1.0148	0.8441
35	0.4969	0.0463	0.9628	0.6192	1.26	0.771	0.4563	-0.4341	0.9533	0.4766	-0.2058	0.931
36	0.3819	-0.6764	0.9641	0.942	2.991	0.824	0.3333	-0.9123	0.9346	0.4236	-0.7028	0.8448
Mean	0.329			0.942			0.425			0.5728		

surface at high concentrations [38]. On the other hand, Langmuir isotherm also describes precipitation reactions [39]. However, this is not true for large concentration ranges where adsorption/precipitation reactions with precipitation reactions at low concentrations. Therefore Langmuir model did not allow comparing whole data set and the details of the Langmuir parameters are not given.

The Freundlich isotherm successfully described the sorption data of the soils indicated by very high determination coefficient of regression lines (Table 2). However the Cu sorption data of some soil samples were relatively poorly described. Table 2 shows the parameters of adsorption isotherms for Cd, Cu, Ni, and Zn by the experimental soils. Sorption isotherms for these metals by the soils exhibited apparent differences in the parameters indicating that shape of the isotherms and the amount of retained heavy metals were highly different for each metal. The ranges of Freundlich *n* parameters were 0.1211 (soil 23)-0.7823 (soil 26), 0.3493 (soil 17)-3.3545 (soil 4), 0.1527 (soil 26)-0.9117 (soil 6) and 0.2244 (soil 21)-1.5798 l/g (soil 6) for Zn, Cu, Ni, and Cd, respectively. As the average of *n* values considered, which were the average slopes of the isotherms explaining the affinity of soils for the respective metals, the adsorption for Cu was higher than the other heavy metals. The averages of the *n* values in descending order were Cu (0.942 mL g^{-1}) > Cd (0.5728 mL g^{-1}) > Ni (0.425 mL g^{-1}) > Zn (0.329 mL g^{-1}). Soil 26 showed highest affinity for Zn. Liao and Selim [40] reported that Freundlih *n* parameters changes in a very short range 0.5-0.64. Despite many soils had similar *n* values to that limit, there were some extreme soils comparatively much smaller or much higher affinity to any element in question because the soil samples were taken 7 different cities in Turkey with different climate, geology, and pedotranfer functions. Thus, the soil properties were extremely different as seen in Table 1. Lu and Xu [41] reported that the weaker competition may occur when the more available sites for almost all the metal cations in the

TABLE 3
Pearson correlations between soil properties and Freundlich isotherm parameters

		Soil Properties								Total Element Concentrations (mg/kg)			
HM	**IP**	**%Salts**	**CEC**	**Sand**	**Silt**	**Clay**	**pH**	**OM**	**CCE**	**Ni**	**Cu**	**Zn**	**Cd**
	n	-0.276	-0.321	-0.016	0.078	-0.036	**-0.493**	0.172	**-0.454**	-0.105	0.136	-0.081	0.322
Zn	***Kf***	-0.056	-0.300	-0.193	0.183	0.111	-0.212	0.094	-0.274	-0.025	-0.002	-0.027	0.291
	n	0.313	-0.032	-0.294	0.103	**0.356**	0.230	-0.214	0.325	0.319	-0.157	-0.054	-0.086
Cu	***Kf***	0.329	-0.047	-0.288	0.097	**0.355**	0.261	-0.230	**0.343**	**0.357**	-0.138	-0.052	-0.077
	n	-0.282	0.033	0.060	0.196	-0.217	**-0.459**	0.108	**-0.344**	-0.213	-0.035	-0.096	0.093
Ni	***Kf***	0.031	0.200	-0.068	0.265	-0.088	-0.165	-0.042	-0.134	-0.208	-0.209	-0.049	-0.033
	n	-0.180	-0.115	0.060	0.103	-0.119	**-0.466**	-0.005	**-0.458**	0.002	-0.215	-0.002	0.068
Cd	***Kf***	-0.130	0.117	0.161	0.047	-0.224	**-0.440**	0.206	-0.209	-0.310	0.008	0.034	-0.022

adsorption complexes. This means competition become in favour of metal with high affinity such as Pb at higher concentrations. In this study Cu generally showed distinctly higher affinity for sorption sites of the soils.

Correlation analyses between soil properties and Freundlich isotherm parameters showed that soil pH, calcium carbonate equivalent and clay content have a positive effect (Table 3). Researchers working in different parts of the world have related the preferential adsorption of heavy metals to the mineralogical properties of soils [28, 37], soil pH [42]; clay mineralogy, texture and CEC [9, 11]; pH and CEC [9, 10, 41]; and general soil properties [9, 10, 43]. Undoubtedly, initial concentration of metal ions must be an important parameter since their concentrations are pivotal criteria for metal removal processes (adsorption or precipitation). As more metal ions adsorbed the nature and affinity of surfaces are to drastically change which is one of the main causes of plateau formation with increasing concentration in the linear isotherms. There were very strong relationships ($P< 0.01$) between the Freundlich *n* parameters of Zn, Ni and Cd sorption isotherms and the soil pH. This shows that when the soil pH increases, the metal ions in the solution phase turn into less adsorptive forms or the binding energy of the sorption is to decrease. This in fact results in a decrease in the slope of the isotherm. Similarly, Hongping et al. [44] and Uygur [45] reported that increased metal adsorption over pH 6.5 where precipitation reactions were usually responsible for these increases, but the slope of the Freundlich isotherm in this region decreased. This decrease in slope is usually caused by the precipitation of carbonate and / or hydroxy phases in calcareous soils [46].

A significant negative correlation was found between the parameters of Freundlich isotherms and the carbonate content, as well as pH (Table 3). However, the positive relationship between the carbonate content and the *Kf* parameter can be interpreted as an indication that carbonates have an important effect of removing Cu from the solution phase. Indeed, it was reported that Cu-carbonates are thermodynamically stable components in calcareous environments [47, 48]. Again, the adsorption parameters of Cu correlated positively with the clay content. This is an indication that more Cu was adsorbed with increasing clay content. Copper adsorption parameters were also related to the total Ni content of the soils.

CONCLUSIONS

As a result, it has been observed that especially the Freundlich isotherm can be successfully used in describing the competitive adsorption of heavy metals. In general, the *n* coefficient at the Freundlich isotherm is a suitable parameter for comparison of their selectivity sequence.

In competitive conditions, that is, when applied to soil in quantities of more than one element, both Freundlich and Langmuir isotherms can be used. However, the Langmuir isotherm cannot adequately describe the adsorption capacity for any element with too high binding energy for a specific soil.

Heavy metals studied in the soil were adsorbed in a sequence of Cu, Cd, Ni and Zn. In other words, Cu was adsorbed in the larger quantity than the others. However, this ranking was not valid for every soil, and when soil properties change, it was also possible to change depending on the soil properties.

Adsorption isotherm parameters and pH, carbonate and clay content were important characteristics of soil properties. In contrast to the other elements, Cd showed a different behaviour than the rest that a significant correlation with soil salinity was recorded.

ACKNOWLEDGEMENT

This study is part of the MSc study by Mehmet Ali Karaduman and partially supported by Mustafa Kemal University.

REFERENCES

[1] Berti, W.R. and Jacobs, L.W. (1996) Chemistry and phytotoxicity of soil trace elements from repeated sewage sludge applications. J. Environ.

Qual. 25, 1025-1032.
[2] Kabata-Pendias, A. (2011) Trace elements in soils and plants. CRC Press, Boca Raton.
[3] Vega, F.A., Covelo, E.F. and Andrade, M.L. (2006) Competitive sorption and desorption of heavy metals in mine soils: Influence of mine soil characteristics. J. Colloid Interf. Sci. 298, 582-592.
[4] Kim, M.J. (2014) A study on the adsorption characteristics of cadmium and zinc onto acidic and alkaline soils. EnvironEarth Sci. 72, 3981-3990.
[5] Refaey, Y., Jansen, B., El-Shater, A.H., El-Haddad, A.A. and Kalbitz, K. (2014) The role of dissolved organic matter in adsorbing heavy metals in clay-rich soils. Vadose Zone J. 13, 1-12.
[6] Arenas-Lago, D., Rodriguez-Seijo, A., Cerqueira, B., Andrade, M.L. and Vega, F.A. (2015) Cd^{2+}, Cu^{2+}, and Pb^{2+} sorption, desorption and migration in Fluvisols. Span J. Soil Sci. 5, 276-295.
[7] Sahraoui, H., Andrade, M.L., Hachicha, M. and Vega, F.A. (2015) Competitive sorption and desorption of trace elements by Tunisian Aridisols Calcorthids. Environ Sci. Pollut. R. 22, 10861-10872.
[8] Li, L.H., Ma, J.C., Xu, M., Li, X., Tao, J.H., Wang, G.Z., Yu, J.T. and Guo, P. (2016) The adsorption and desorption of Pb^{2+} and Cd^{2+} in freeze-thaw treated soils. B. Environ. Contam. Tox. 96, 107-112.
[9] Cerqueira, B., Vega, F.A., Silva, L.F.O. and Andrade, L. (2013) Monometal and simul-taneous Cu and Pb soil sorption: distribution in colloidal soil components. Fresen. Environ. Bull. 22, 1090-1098.
[10] Vega, F.A., Covelo, E.F., Cerqueira, B. and Andrade, M.L. (2011) Migration rates of Cd, Cu and Pb in different soil profiles. Fresen. Environ. Bull. 20, 894-902.
[11] Usman, A.R.A. (2008) The relative adsorption selectivities of Pb, Cu, Zn, Cd and Ni by soils developed on shale in New Valley, Egypt. Geoderma 144(1-2), 334-343.
[12] Shaheen, S.M., Tsadilas, C.D. and Rinklebe, J. (2013) A review of the distribution coefficients of trace elements in soils: Influence of sorption system, element characteristics, and soil colloidal properties. Adv. Colloid Interfac. 201, 43-56.
[13] Tan, K.H. 2011. Principles of soil chemistry. CRC Press, Boca Raton.
[14] Refaey, Y., Jansen, B., Parsons, J.R., de Voogt, P., Bagnis, S., Markus, A., El-Shater, A.H., El-Haddad, A.A., and Kalbitz, K. (2017) Effects of clay minerals, hydroxides, and timing of dissolved organic matter addition on the competitive sorption of copper, nickel, and zinc: A column experiment. J. Environ. Manage. 187, 273-285.
[15] Vega, F.A., Andrade, M.L. and Covelo, E.F. (2010) Influence of soil properties on the sorption and retention of cadmium, copper and lead, separately and together, by 20 soil horizons: Comparison of linear regression and tree regression analyses. J. Hazard. Mater. 174, 522-533.
[16] Cerqueira, B., Covelo, E.F., Andrade, L. and Vega, F.A. (2011) The influence of soil properties on the individual and competitive sorption and desorption of Cu and Cd. Geoderma 162, 20-26.
[17] Diatta, J.B., Komisarek, J., and Wiatrowska, K. (2012) Evaluation of heavy metals competitive sorption and potential mobility on the basis of Cu/Cd and Zn/Pb binary systems. Fresen. Environ. Bull. 21, 1105-1109.
[18] Sdiri, A., Higashi, T., Chaabouni, R. and Jamoussi, F. (2012) Competitive removal of heavy metals from aqueous solutions by montmorillonitic and calcareous clays. Water Air Soil Poll. 223, 1191-1204.
[19] Jalali, M. and Moradi, F. (2013) Competitive sorption of Cd, Cu, Mn, Ni, Pb and Zn in polluted and unpolluted calcareous soils. Environ. Monit. Assess. 185, 8831-8846.
[20] McBride, M.B. (1994) Environmental chemistry of soils. Oxford University Press, New York.
[21] Stefan, M., Stefan, D.S., Marinescu, I.A., Belcu, M. and Vaireanu, D.I. (2008) Simultaneous sorption of cadmium, zinc and lead on montmorillonite. Rev. Roum. Chim. 53, 965-971.
[22] Zhu, J., Cozzolino, V., Pigna, M., Huang, Q., Caporale, A.G. and Violante, A. (2011) Sorption of Cu, Pb and Cr on Na-montmorillonite: competition and effect of major elements. Chemosphere 84, 484–489.
[23] Eloussaief, M., Hamza, W., Kallel, N. and Benzina, M. (2013) Wastewaters decontamination: mechanisms of Pb(II), Zn(II), and Cd(II) competitive adsorption on Tunisian smectite in single and multi-solute systems. Environ. Prog. Sustain. Ener. 32, 229–238.
[24] Vhahangwele M. and Mugera G.W. (2015) The potential of ball-milled South African bentonite clay for attenuation of heavy metals from acidic wastewaters: Simultaneous sorption of Co^{2+}, Cu^{2+}, Ni^{2+}, Pb^{2+}, and Zn^{2+} ions. J. Environ. Chem. Eng. 3, 2416–2425.
[25] Coles, C.A. and Yong, R.N. (2002) Aspects of kaolinite characterization and retention of Pb and Cd. Appl. Clay Sci. 22, 39–45.
[26] Uddin, M.K. (2017) A review on the adsorption of heavy metals by clay minerals, with special focus on the past decade. Chem. Eng. J. 308, 438-462.
[27] Lair, G.J., Gerzabek, M.H. and Haberhauer, G. (2007) Retention of copper, cadmium and zinc in soil and its textural fractions influenced by long-term field management. Eur. J. Soil Sci. 58, 1145-1154.

[28] Lafuente, A.L., Gonzalez, C., Quintana, J.R., Vazquez, A. and Romero, A. (2008) Mobility of heavy metals in poorly developed carbonate soils in the Mediterranean region. Geoderma 145, 238-244.
[29] Vega, F.A., Covelo, E.F. and Andrade, M.L. (2009) Hysteresis in the individual and competitive sorption of cadmium, copper, and lead by various soil horizons. J. Colloid Interf. Sci. 331, 312-317.
[30] Groenenberg, J.E., Koopmans, G.F., Comans, R.N.J. (2010) Uncertainty analysis of the nonideal competitive adsorption-Donnan model: effects of dissolved organic matter variability on predicted metal speciation in soil solution. Environ Sci. Technol. 44, 1340-1346.
[31] Lambert, R., Grant, C., Sauve, S., 2007. Cadmium and zinc in soil solution extracts following the application of phosphate fertilizers. Sci. Total Environ. 378, 293-305.
[32] Sparks, D. L. 1996. Methods of soil analysis. Part 3. Chemical Properties. SSSA/ASA, Wisconsin, USA.
[33] Gee, G. and J. Bauder. 1986. Particle-size analysis. In: Methods of soil analysis, physical and mineralogical methods, (2nd edn, ed: Klute A.), SSSA,Wisconsin, pp 383–409.
[34] Sohn, S. and Kim, D. 2005. Modification of Langmuir isotherm in solution systems-definition andutilization of concentration dependent factor. Chemosphere 58, 115-123.
[35] Gustafsson J.P., Pechova, P. and Berggren, D. 2003. Modeling metal bindings to soils: The role of natural organic matter. Environ. Sci. Technol. 37, 2767-2774.
[36] Kostic, I.S., Andelkovic, T.D., Nikolic, R.S., Cvetkovic, T.P., Pavlovic, D.D. and Bojic, A.L. 2013. Comparative study of binding strengths of heavy metals with humic acid. Hem. Ind. 67, 773-779.
[37] Evans, L.J., Sengdy, B., Lumsdon, D.G., Stanbury, D.A. (2003). Cadmium adsorption by an organic soil: a comparison of some humic - metal complexation models. Chem. Spec. Bioavailab. 15, 93-100.
[38] Olsen. S. R. and Khasawneh. F. E. 1980. Use and limitations of physical-chemical criteria for assessing the status of phosphorus in soils. In: The role of phosphorus in agriculture (F.E. Khasawneh, E.C. Sample and E.J. Kamprath, eds.), ASA, Madison, Wisconsin, pp 361-410.
[39] Veith, J.A. and Sposito, G. (1977) On the use of the Langmuir equation in the interpretation of adsorption phenomena. Soil Sci. Soc. Am. J. 41, 697-702.
[40] Liao, L.X. and Selim, H.M. (2009) Competitive sorption of nickel and cadmium in different soils. Soil Sci. 174, 549-555.
[41] Lu, S.G. and Xu, Q.F. (2009) Competitive adsorption of Cd, Cu, Pb and Zn by different soils of Eastern China. Environ. Geol. 57, 685-693.
[42] Serno, S., O'Day, P.A., Vlassopoulos, D., Garcia-Gonzalez, M.T. and Garrido, F. (2009) A surface complexation and ion exchange model of Pb and Cd competitive sorption on natural soils. Geochim. Cosmochim. Ac. 73, 543-558.
[43] Shaheen, S.M., Tsadilas, C.D., Mitsibonas, T. and Tzouvalekas, M. (2009) Distribution coefficient of copper in different soils from Egypt and Greece. Commun. Soil Sci. Plan. 40, 214-226.
[44] Hongping H., Jiugao, G., Xiande, X. and Jinlian, P. (2000) Experimental study of the selective adsorption of heavy metals onto clay minerals. Chin. J. Geochem. 19, 105–109.
[45] Uygur, V. (1998) Zinc adsorption/desorption chemistry in calcareous soils fromTurkey. PhD thesis, The University of Newcastle upon Tyne, UK.
[46] Uygur, V. and Rimmer, D.L. (2000) Reactions of zinc with iron-oxide coated calcite surfaces at alkaline pH. Eur. J. Soil Sci. 51, 511-516.
[47] Lindsay, W.L. (2001) Chemical equilibria in soils. Blackburn Press, New Jersey.
[48] Papadopoulos, P. and Rowell, D.L. (1989) The Reactions of copper and zinc with calcium-carbonate surfaces. J. Soil Sci. 40, 39-48.

Received: **09.06.2017**
Accepted: **23.07.2017**

CORRESPONDING AUTHOR

Veli Uygur
Department of Soil Science and Plant Nutrition, Agricultural Faculty, Suleyman Demirel University
32260, Isparta, Turkey

e-mail: veliuygur@sdu.edu.tr

© by PSP Volume 26 – No. 10/2017 pages 6212-6216 Fresenius Environmental Bulletin

THE EFFECT OF TEBUCONAZOLE ON SERUM PARAOXONASE AND AMINOTRANSFERASE ACTIVITIES IN *CYPRINUS CARPIO* (L. 1758)

Gokhan Nur[1,*], Muhitdin Yilmaz[2], Mahmut Karapehlivan[3], Inan Kaya[4] , Ozlem Nur[1], Ayla Deveci[1]

[1] Gaziantep University, Islahiye Vocational High School, Veterinary Department, Gaziantep, Turkey
[2] Sinop University, Faculty of Engineering and Architecture, Bioengineering Department, Sinop, Turkey
[3] Kafkas University, Medical Faculty, Biochemistry Department, Kars, Turkey
[4] Kafkas University, Faculty of Science and Letters, Biology Department, Kars, Turkey

ABSTRACT

The purpose of this study was to examine serum paraoxonase (PON1), alanine aminotransferase (ALT), aspartate aminotransferase (AST) activity and high density lipoprotein (HDL) levels of tebuconazole administered *Cyprinus carpio* (L. 1758). After providing adaptation of the fish in the laboratory setting for 7 days, they were divided into 3 groups, each of which included 8 fish. The fish in Group I were kept in normal water environment and those in Groups II and III were in 2 and 3 mg/L tebuconazole added water tanks, respectively, for 14 days. Blood samples were taken from the fish and serums were separated. Then, PON1, ALT, and AST activities and HDL levels were analyzed. While PON1 activity and HDL levels decreased in tebuconazole administered groups compared to Group I, increases were determined in terms of ALT and AST. Consequently, it was found that tebuconazole administrations caused significant changes in serum PON1, ALT, and AST activities and HDL levels of *Cyprinus carpio.*

KEYWORDS:
Cyprinus carpio, Tebuconazole, Paraoxonase, HDL, ALT, AST

INTRODUCTION

Pesticides have importance as a potential hazard for aquatic life. Because these chemicals are produced and used in order to destroy harmful organisms in agricultural lands [1]. Pesticides are moved by rain water, drainage water, runoff, and irrigation water and thus penetrate into aquatic environment and cause detrimental impacts on the organisms here [2, 3].

Tebuconazole is used as a fungicide against fungus threat in paddy fields. Tebuconazole, which is a fungicide with systemic effect, have an influence in such a way to inhibit ergosterol synthesis within fungus body. Tebuconazole cause detrimental impacts in aquatic environment within a long period and also toxic effects on aquatic organisms [3].

The fish have been used as indicator organisms for determination of toxicity in aquatic environments in recent years. In addition, the fish also can be used as test organism for estimating possible effects of some genotoxic agents and agricultural chemicals on human beings and hence their detoxification mechanisms are observed to have similar properties with humans [4]. Some enzymes, which are used for clinical diagnosis, are used as marker in order to reveal detrimental impacts of pesticides in toxicological studies. Chemical substances applied in experimental and non-experimental models can lead to tissue damage and increase or decrease in serum enzyme concentrations [5, 6]. Aspartate aminotransferase (AST) and Alanin aminotransferase (ALT), whose activities are measured for determination of hepatic damage in liver, are the most important ones [7].

PON1 is attached to HDL-lipids via its hydrophobic N-terminal area and metabolic changes influencing HDL are also known to affect PON1 activity [8]. Being an important element of antioxidant system, the enzyme PON1 has also the capability to detoxify organophosphate pesticides [9].

In this study, it was aimed to examine the effect of tebuconazole on serum PON1, ALT, AST activities and HDL levels of *Cyprinus carpio.*

MATERIALS AND METHODS

In this study 24 Cyprinus carpio was used in the weight of 200-250 gr caught in Cildir Lake in June 2012. By transferring the fish to laboratory, the fish were adapted to the new environment at polyethylene tanks (22-25 °C and normal photoperiod) containing water for 7 days. Table 1 shows physicochemical properties of the water used. The fish were assigned into 3 groups, each of which included 8 fish. The fish in Group I were kept in normal water environment and those in Groups II and III were in 2 and 3 mg/L tebuconazole (Folicur

EW 250) added water tanks, respectively, for 14 days [10, 11]. The water in the tanks was changed every 2 days in all groups and tebuconazole was added in the indicated quantities. There are no restrictions on the feeding of fish. Blood samples were taken from the fish at the end of study time and the samples were centrifuged at +4 ºC and 3000 rpm for 10 minutes. While PON1 activity of the obtained serum samples were analyzed according to the method reported by Eckerson [12] and Gulcu [13], AST and ALT activities and HDL levels were analyzed in automatic analyzers by using commercial kits.

TABLE 1
Physicochemical properties of the water used in tanks.

Parameter	Value
Temperature (°C)	**23±2**
pH	**7.1-7.4**
Dissolved oxygen (mg/L)	**8-9**
Total hardness (CaCO3) (mg/L)	**150-170**

Statistical analyses of the obtained results were carried out by using statistical packaged software (IBM SPSS version 20.0 for Windows). The difference between the groups was determined by nonparametric variance analysis (Kruskal-Wallis). According to the findings obtained from the test statistic, the correlations between the groups were determined by correlation analysis. In all of the tests, $p<0.05$ was accepted as significant. Results were presented as mean ± standard deviation (X±SD). The Spearman correlation coefficient was used to show the relationship between the variables.

RESULTS

The choice of tebucanazole dose selection levels below toxic values was chosen to shed light on the effects that may be encountered. Each group was examined under the same conditions, since it is not possible to conduct a controlled examination under natural conditions.

Table 2 and Figure 1 show biochemical changes occurring in the blood samples taken from the fish whose living environments were added 2 and 3 mg/L tebuconazole and the fish in the control group without tebuconazole addition 14 days later. There was a statistically significant difference between control and two tebuconazole groups in terms of all examined biochemical parameters ($P<0.05$). While AST and ALT activity increased compared to control group, PON1, and HDL levels decreased.

For PON1 activity, there was a negative correlation between the control and the 2 mg/L and 3 mg/L tebucanazole group ($r= -0.23$, $r= -0.85$). For HDL levels, there was a negative correlation between the control and the 2 mg/L and 3 mg/L tebucanazole groups ($r= -0.37$, $r= -0.16$). For AST activity, there was a positive correlation between the control and the 2 mg/L and 3 mg/L tebucanazole group ($r= 0.50$, $r= 0.36$). For ALT activity, there was a positive correlation between the control and the 2 mg/L and 3 mg/L tebucanazole groups ($r= 0.22$, $r= 0.43$).

DISCUSSION AND CONCLUSION

The overuse of pesticides causes adverse effects on all organisms including the commercially important fish. It is important for human health to examine the effects of pesticides on the fish playing an important role in food chain [14]. Determination of the effects of tebuconazole, which is the pesticide properly used against fungi in agricultural fields, on PON1, AST, and ALT activity and HDL levels in the fish is very important regarding appropriate amount of pesticide use in agricultural fields and minimizing of environmental pollution based on pesticides. Even though there are numerous studies on toxic effects of pesticides to aquatic organisms and biochemical parameters, any study investigating the effect of tebuconazole, which is used as fungicide, on PON1, AST, and ALT activities and HDL levels in the fish was not found.

TABLE 2
Serum PON1, AST, and ALT activity and HDL levels of *Cyprinus carpio* with and without tebuconazole administration.

Parameters	Control (n:8) (X±SD)	Tebuconazole (n:8) (2 mg/L) (X±SD)	Tebuconazole (n:8) (3 mg/L) (X±SD)
AST (U/L)	103±12.6^{a}	143.5±18.8^{b}	128±17.7^{b}
ALT (U/L)	14±3.7^{a}	18.5±6.75^{b}	23±5.0^{b}
PON 1 (U/L)	52±4.2^{a}	38±8.75^{b}	34.5±4.6^{b}
HDL (mg/dl)	84.5±6.1^{a}	66±6.3^{b}	62±4.1^{b}

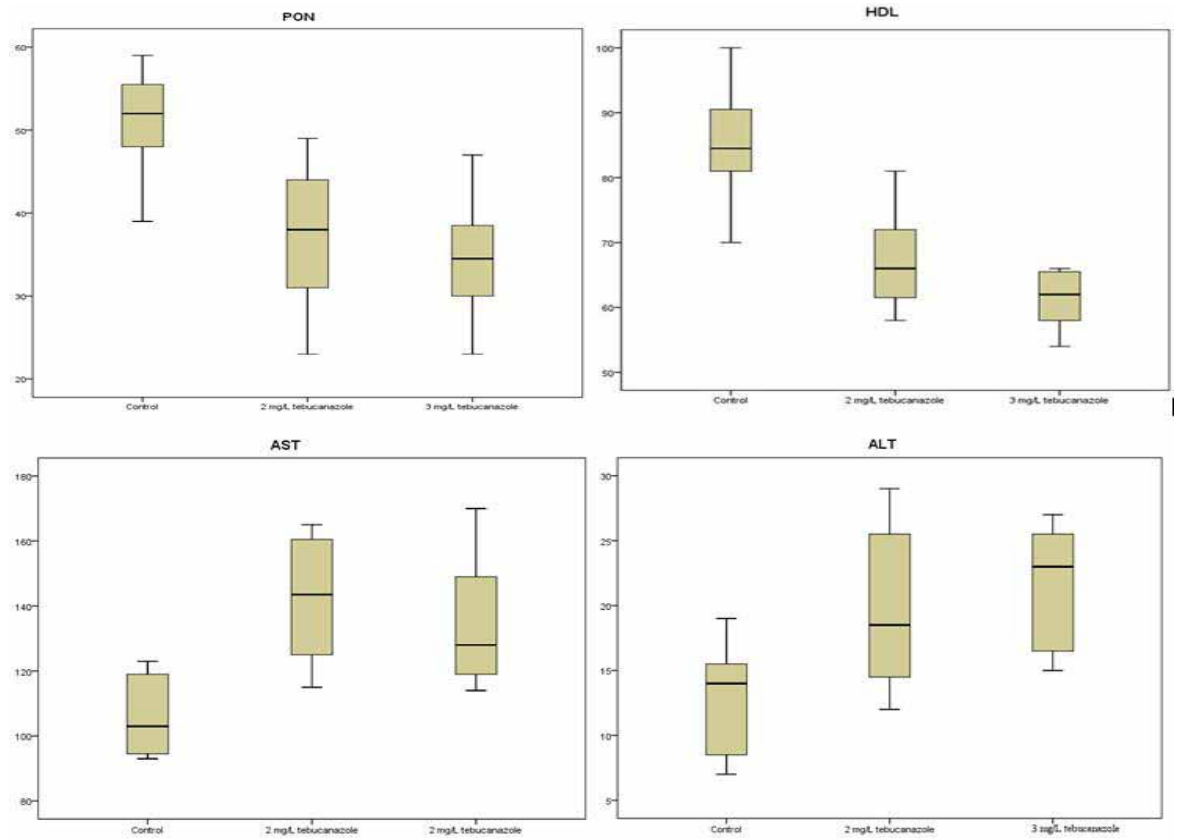

FIGURE 1
Values of biochemical parameters in control and tebuconazole groups, a: PON1, b: HDL, c: AST, d: ALT.

Because liver is the organ where several substances are synthesized and metabolized, it is functionally a vital organ. Functional disorders that may occur in the liver will influence other metabolic activities in the organism. As a result of release of some liver enzymes into blood as a result of breakdown of the cell or change in permeability of cell membrane, serum activities of cellular enzymes such as transaminases (AST, ALT), lactate dehydrogenase, and alkaline phosphatase increase [15]. Previous studies reported that serum AST and ALT levels increased in liver damage caused by chlorpyrifos-ethyl. It was determined in these studies that serum AST and ALT levels considerably increased in chlorpyrifos-ethyl group compared to control group, and AST and ALT levels decreased to levels of control group with the addition of lycopene as protective. In the light of these data, lycopene is thought to have a protective effect on liver damage caused by chlorpyrifos-ethyl [16-18]. It was reported that intracellular enzymes such as AST and ALT increased serum levels depending on liver damage caused by some metabolic disorders (like diabetes), lycopene administration as protective approximated AST and ALT levels to control group, thus lycopene had a protective effect against liver damage in metabolic disorders like diabetes [19, 20].

Oxidative damage or imbalance between the oxidant/antioxidant mechanisms have been the most important mechanisms behind pesticide and heavy metal toxicity. A decrease in serum antioxidans are accepted as an inflammatory response and also as an indicator of increased oxidative damage (21-24). Detoxification of pesticides in several organisms is carried out by enzymes such as acetylcholine-esterase, carboxylesterase, and paraoxonase (PON1). PON1 is an antioxidant enzyme found in liver, kidney, intestine and HDL on serum and its activity can change as part of the inflammatory response [25-28]. Due to the ability of hydrolyzing lipid peroxides, PON also has an important role for elimination of potential oxidants. It is stated that pesticide formulations influencing the fish living in aquatic environments inhibit acetylcholinesterase by binding covalent bonds in its active site [27-30]. This situation is reported to cause respiratory disorders depending on increase in amount of acetylcholine in neuromuscular junction [31, 32]. Determination of the effect of tebuconazole, which is the pesticide widely used for pest control in agricultural fields, on PON1, AST, and ALT activities and HDL levels in the fish is very important regarding appro-

priate amount of pesticide use in agricultural fields and minimizing of environmental pollution based on pesticides.

In the study conducted by Toni et al. [10] on exposure of *Cyprinus carpio* to tebuconazole at different concentrations, they reported that catalase concentration was decreased at 1.19 mg/L dose, superoxide dismutase decreased depending on increasing tebuconazole concentration compared to control group and consequently antioxidant system was influenced negatively. Kaya et al. [11], administered tebuconazole in their study and determined that serum total oxidant capacity and total sialic acid of *Cyprinus carpio* increased considerably compared to control group; whereas, total antioxidant capacity decreased. Deveci et al. [33, 34], administered glyphosate and zinc sulphate in their two separate studies and determined that significant changes were found in the serum PON activity, HDL, TAS and TOS levels in *Capoeta capoeta*.

In this study aiming to understand effects of tebuconazole with some biochemical parameters, it was determined that significant changes occurred in serum PON1, AST, and ALT activities and HDL levels of *Cyprinus carpio* which was administered 2 and 3 mg/L tebuconazole in their habitats for 14 days. Accordingly, it was concluded that the decrease in PON1 activity and HDL level at increasing tebuconazole concentrations could be associated with pesticide detoxification, and the increase in AST and ALT levels could be associated with liver function changes as a result of pesticide exposure of the fish.

REFERENCES

[1] Lloyd, R. (1992) Pollution and Freshwater Fish. A Buckland Foundation Book, Fishing News Books, Cornwall.

[2] Yilayaz, O. (2006) Parathion Methyl (Insektsit)'in *Capoeta Trutta* (Heckel, 1843) Uzerindeki Genotoksik Etkisinin Eritrosit Mikronukleus Testi Ile Belirlenmesi. Dogu Anadolu Bolgesi Arastirmalari Dergisi, 1-5.

[3] Bayer Crop Science Limited (2005) Information Sheet Folicur®. MAPP number 11278. CPA Guidance Notes version 3. ©EIS.

[4] Stegeman, J.J. and Lech, J.J. (1991) Cytochrome P-450 Monooxygenase Systems in Aquatic Species. Carcinogen Metabolism and Biomarkers for Carcinogen and Pollutant Exposure. Environ Healt Persp 90, 101-109.

[5] Mayer, F.L., Versteeg, D.J. and McKee, M.J., Folmar, L.C., Graney, R.L., McCume, D.C. and Rattner, B.A. (1992) Physiological and Nonspecific Biomarkers; In: Huggett, R.J., Kimerle, R.A., Mehrle, Jr., Bergman, H.L. (Eds.) Lewis Pub., 5-86.

[6] Merhan, O., Ozcan, A., Atakisi, E., Ogun, M. and Kukurt, A. (2016) The Effect of β-carotene on Acute Phase Response in Diethylnitrosamine Given Rabbits. Kafkas Univ Vet Fak Derg, 22(4), 533-537.

[7] Kim, W.R., Flamm, S.L., Bisceglie, A.M. and Jr Bodenheimer, H.C. (2008) Serum activity of alanine aminotransferase (ALT) as an indicator of health and disease. Hepatology 47(4), 1363-1370.

[8] Mackness, M.I., Mackness, B., Durrington, P.N., Connelly, P.W. and Hegele, R.A. (1996) Paraoxonase: biochemistry, genetics and relationship to plasma lipoproteins. Curr Opin Lipidol; 7, 69-76.

[9] Azarsiz, E. and Sozmen, E.Y. (2000) Paraoksonaz ve Klinik Onemi. Türk Biyokimya Dergisi; 3, 109-119.

[10] Toni, C., Ferreira, D., Kreutz, L.C., Loro, V.L. and Barcellos, L.J.G. (2011) Assessment of oxidative stress and metabolic changes in common carp (*Cyprinus carpio*) acutely exposed to different concentrations of the fungicide tebuconazole. Chemosphere, 83(4), 579-584.

[11] Kaya, I., Yilmaz, M., Koc, E., Deveci, H.A., Ersan, Y. and Karapehlivan, M. (2014) Investigation of the serum total antioxidant, oxidant and sialic acid levels of *Cyprinus carpio* (L. 1758) treated with tebuconazole (fungicide). Journal of Fisheries Sciences, 8(3), 214-219.

[12] Eckerson, H.W., Romson, J., Wyte, C.M., La Du, B.N. (1983) The human serum paraoxonase polymorphism: Identification of phenotypes by their response to salts. Am J Hum Genet; 35(2), 214-227.

[13] Gulcu, F. and Gursu, M.F. (2003) Paraoksonaz ve aril esteraz aktivite olcumlerinin standardizasyonu. Turk J Biochem; 28, 45-49.

[14] Begum, G. and Vijayaraghavan, S. (1996) Alterations in Protein Metabolism of Muscle Tissue in the Fish Clarias batrachus (Linn) by Commercial Grade Dimethoate. Bulletin Environmental Contamination and Toxicology; 57, 223-228.

[15] Comelekoglu, U. and Mazmanci, B. (2000) Pestisidlerin kronik etkisine maruz kalan tarim iscilerinde karaciger fonksiyonlarının incelenmesi. Turk J Biol; 24, 461–466.

[16] El-Banna, S.G., Attia, A.M., Hafez, A.M. and El-Kazaz, S.M. (2009) Effect of garlic consumption on blood lipid and oxidant/ antioxidant parameters in rat males exposed to chlorpyrifos. Slovak J Anim Sci; 42(3), 111-117.

[17] Khalifa, F.K., Khalil, F.A., Barakat, H.A. and Hassan, M.M. (2011) Protective role of wheat germ and grape seed oils in chlorpyrifos-induced oxidative stress, biochemical and histological alterations in liver of rats. Aust J Basic Appl Sci; 5(10), 54-66.

[18] Mansour, S.A. and Mossa, A.H. (2010) Oxidative damage, biochemical and histological alterations in rats exposed to chlorpyrifos and the antioxidant role of zinc. Pestic Biochem Physiol; 96, 14-23.
[19] Rajasekaran, S., Ravi, K., Sivagnanam, K. and Subramanian, S. (2006) Beneficial effects of aloe vera leaf gel extract on lipid profile status in rats with streptozotocin diabetes. Clin Exp Pharmacol Physiol; 33(3), 232-237.
[20] Sancheti, S., Sancheti, S. and Seo, S.Y. (2013) Antidiabetic and antiacetylcholinesterase effects of ethyl acetate fraction of Chaenomeles sinensis (Thouin) Koehne fruits in streptozotocin induced diabetic rats. Exp Toxicol Pathol; 65(1-2), 55-60.
[21] Deveci, H.A., Karapehlivan, M., Kaya, I., Kukurt, A. and Alpay, M. (2015) Akut klorprifos-etil zehirlenmesine karsi kafeik asit fenetil ester'in koruyucu etkisi. Ankara Universitesi Veteriner Fakultesi Dergisi, 62(4), 255-260.
[22] Karapehlivan, M., Ogun, M., Kaya, I., Ozen, H., Deveci, H.A. and Karaman, M. (2014) Protective effect of omega-3 fatty acid against mercury chloride intoxication in mice, Journal of Trace Elements in Medicine and Biology, 28, 94–99.
[23] Nur, G., Deveci, H.A., Ersan, Y., Merhan, O., Nazlı, M. and Nur, O. (2016) Protective Role of Caffeic Acid Phenethyl Ester against Tetramethrine-Induced Toxicity in Mice. Medicine Science, 5(4), 972-8.
[24] Uzlu, E., Karapehlivan, M., Erdogan, H.M., Kiziltepe, S., Erkilic, E.E., Deveci, H.A., Gokçe, E., Kaya, I. and Citil, M. (2016) Serum and Saliva Sialic Acid and Oxidative Stress Parameters Changes in Bulls with Foot and Mouth Disease. Kafkas Universitesi Veteriner Fakultesi Dergisi. 22(3), 321-325.
[25] Eyer, P., Szinicz, L., Thiermann, H., Worek, F. and Zilker, T. (2007) Testing of antidotes for organophosphorus compounds: Experimental procedures and clinical reality. Toxicology; 233(1-3), 108-119.
[26] Peter, J.V., Moran, J.L. and Graham, P. (2006) Oxime therapy and outcomes in human organophosphate poisoning: An evaluation using meta-analytic techniques. Crit Care Med; 34, 502-510.
[27] Marsillach, J., Camps, J., Beltran-Debon, R., Rull, A., Aragones, G., Maestre-Martinez, C., Sabench, F., Hernandez, M., Castillo, D.D., Joven, J., Mackness, M. and Mackness, B. (2011) Immunohistochemical analysis of paraoxonases-1 and 3 in human atheromatous plaques. Eur J Clin Invest; 41, 308-314.
[28] Deveci, H.A., Kukurt, A., Uzlu, E., Sozdutmaz, I., Merhan, O., Aktas, S., Alpay, M., Kaya, I. and Karapehlivan, M. (2017) Evaluation of Paraoxonase Activity, Total Sialic Acid and Oxidative Stress in Sheep with Ecthyma Contagiosa. Kafkas Univ Vet Fak Derg, 23(3), 453-457.
[29] Peter, J.V. and Cherian, A.M. (2000) Organic insecticides. Anaesth Intensive Care; 28, 11-21.
[30] Glusczak, L., Miron, D.S., Moraes, B.S., Simoes, R.R., Schetinger, M.R.C., Morsch, V.M. and Loro, V.L. (2007) Acute effects of glyphosate herbicide on metabolic and enzymatic parameters of silver catfish (Rhamdia quelen). Comparative Biochemistry and Physiology; 146:519-524.
[31] Modesto, K.A. and Martinez, C.B.R. (2010) Roundup causes oxidative stress in liver and inhibits acetylcholinesterase in muscle and brain of the fish Prochilodus lineatus. Chemosphere; 78, 294-299.
[32] Hsieh, B.H., Deng, J.F., Ger, J. and Tsai, W.J. (2001) Acetylcholinesterase inhibition and the extrapyramidal syndrome: a review of the neurotoxicity of organophosphate. NeuroToxicology; 22, 423-427.
[33] Deveci, H.A., Kaya, I., Yilmaz, M. and Karapehlivan, M. (2015) Effect of zinc sulphate on the levels of plasma paraoxonase activity, total oxidant and high density lipoprotein of transcaucasian barb (Capoeta capoeta [Guldenstaedt, 1773]). Fresen. Environ. Bull., 24(9), 2732-2735.
[34] Deveci, H.A., Unal S., Karapehlivan, M., Ayata, M.K., Gaffaroglu, M., Kaya, I. and Yilmaz, M. (2017) Effects of glyphosate (herbicide) on serum paraoxonase activity, high density lipoprotein, total antioxidant and oxidant levels in Kars Creek Transcaucasian Barbs (*Capoeta capoeta* [Guldenstaedt, 1773]). Fresen. Environ. Bull., 26(5), 3514-3518.

Received: **13.06.2017**
Accepted: **29.07.2017**

CORRESPONDING AUTHOR

Gokhan Nur
Gaziantep University,
Islahiye Vocational High School,
Veterinary Department,
Gaziantep – TURKEY

E-mail: gokhannur@gantep.edu.tr

© by PSP Volume 26 – No. 10/2017 pages 6217-6224 Fresenius Environmental Bulletin

NATURA 2000: ITS STATUS QUO, OPPORTUNITIES AND CHALLENGES FOR FOREST BIODIVERSITY IN TURKEY

Cumhur Gungoroglu*

Faculty of Forestry, Karabuk University, Karabuk, Turkey

ABSTRACT

Turkey has an impressive richness in terms of fauna and flora. Nearly 28% of total country area of Turkey is covered by the forests. The aim of this research is to present the status, opportunities and challenges for forest biodiversity in Turkey according to EU Natura 2000 concept. This concept is a European ecological network which is occurred species and habitats designated by the EU Member States based on legally binding legislation**.** The importance of directives is emerging by designation of their special conservation areas under Natura 2000 sites. Designation of sites under those Directives takes some processes. SACs designed as sites to protect EU importance plants, animals and wildlife habitats which are assessed by the Habitats Directive. SPAs are sites of conservation value for rare and threatened European bird species which are designated under the Birds Directive. The species richness and habitat diversity of Turkey's forestry is a challenge for both Turkey and EU. Turkey includes species belonging to three different floristic regions. This opportunity is not common among EU countries. The forest types of Turkey have more structured importance according to diverse vulnerable species and biogeographically distribution of habitats than European countries. It should be thought that the number of Europe's forest habitat types could be considerably increase with Turkey's forest types. Before the selecting, designing and managing, the Natura 2000 sites in Turkey are needed some research to supply the assessment criteria for national assessment of species and habitats. The existing protected areas of Turkey and important endemic plant areas are available as potential Natura 2000 sites at national level. One of the most important deficiencies is lying in the inadequacy of data that will not supply some criteria to select and design the Special Areas for Conservation at European level.

KEYWORDS:
Biodiversity and Conservation, Natura 2000 Sites, Forested Areas, Turkey

INTRODUCTION

Natura 2000 is a Community-wide network of nature protection areas that are established under the European Habitats Directive and the Birds Directive. The purpose of the network is to ensure the long-term survival of Europe's most valuable and threatened species and habitats [1, 2].

Turkey ranks among the largest countries in Europe with a surface area of 783.562 km. It is located within three biogeographical regions which are Anatolian, Mediterranean and Black Sea regions and the transition zones formed among them [3]. In these ecosystems, there are nearly 12.000 plant species and 3.000 of these are endemic. As fauna, there are 19.000 invertebrates that contain 4.000 endemic species and 1.500 vertebrates which comprise 123 endemic species [4]. Although there is planning, inventories based on preserving and improving the rich ecosystem of the country and impressions of management studies, there is not dominant systematic development directed to them. This is because previous studies dealt with only isolated preserved land approaches. Despite this, land uses continue to increase irregularly. The reasons of directly influencing the biological diversity are overgrazing of meadows and grassland, erosion, stubble burning, forest fires, agricultural practices through machines, irregular and excessive use of pesticides in agriculture, drying of wetlands, salinisation of dams, urbanisation, industrialisation, household and industrial waste, mining, tourism-recreation, supply of firewood, excessive hunting and collection of wild plants [3, 4, 5].

Turkey has an impressive richness in terms of fauna and flora. This opportunity gives to the country prestigious place between the three continents. Nearly 28% of total country area is covered by the forests [6]. The aim of this work is to present the opportunities and challenges for forest biodiversity in Turkey derived by EU Natura 2000 concept. The richness of forest biodiversity in Turkey always needs some new policy approaches to develop the protection of biodiversity for the sustainable forest management.

Conceptual framework of Natura 2000 network. Natura 2000 is an European ecological network of protected areas are designated by the EU

Member States based on legally binding legislation: The Habitats (92/43/EEC) and Birds Directives. The relevant regulations for the Natura 2000 are given under article 3 of the Habitats directive [7]. The article 3.1 clarifies Natura 2000 "*A coherent European ecological network of special areas of conservation shall be set up under the title Natura 2000. This network, composed of sites hosting the natural habitat types listed in Annex I and habitats of the species listed in Annex II, shall enable the natural habitat types and the species ' habitats concerned to be maintained or, where appropriate, restored at a favourable conservation status in their natural range*". Besides Habitats Directives is the Bird Directives as an important basis for the designation of Natura 2000 sites.

DESIGNING AND SELECTING NATURA 2000 SITES

According to Article 3 of the Habitats Directive, Natura 2000 is a coherent European ecological network of special areas of conservation (SAC) and special protection Areas for birds (SPA). SACs are sites to protect plants, animals and wildlife habitats of EU importance as designated by the Habitats Directive. SPAs are sites of conservation value for rare and threatened European bird species designated internationally under the Birds Directive [8, 9, 10]. While the designation of SPAs is based on the presence of bird species listed in the annexes of the Birds Directive including a validation stage of the EU, SACs designation (Habitats Directive) is more complex and involves several stages [7, 10, 11].

The procedure for site selection involves two separate stages: In stage one, the EU member states identify proposed Sites of Community Importance (pSCI) for inclusion in the Natura 2000 network and forward them to the European Commission together with supplementary data and maps. In stage two, the sites are assessed at EU level for their importance to the Community. A List of selected SCI's (SCIs) is then drawn up by the EU Commission in conjunction with the member states (Article 4 - 2 of the Habitats Directive). Assessment of the pSCIs in both stages is conducted in accordance with the criteria set out in Annex III of the Habitats Directive [11]. The two-staged assessment of SCI's serve selection of the most suitable sites for inclusion in the List of pSCIs. Once the lists are completed, the member states are required to comply with the provisions of national legislation to place their respective sites under protection as special areas of conservation (SACs) within a period of six years. Natura 2000 sites are selected on the basis of national lists proposed by the member states. The European Commission adopts a list of Sites of Community Importance (SCI) for each biogeographical region, which then become part of the network. Finally, the pSCIs are designated at the national level as SAC which subsequently undergo implementation measures in six years. Another important factor for selecting and designing Natura 2000 areas are the assessment criteria for national assessment of Annex I habitat types of Habitat Directive:

Representativity. Degree of representativity of the occurrence of the listed habitat type on the proposed site of Community interest, in relation to the overall occurrence of that habitat type in the physiographic province or biogeographical region.

Relative surface area. Area of the proposed site of Community interest covered by the habitat type concerned in relation to the total area covered by that habitat type in a country.

Conservation status and restorability. Degree of conservation and restoration possibilities of the habitat type concerned on the proposed site of Community interest. The 'conservation status' of individual sites in relation to habitat types can only be assessed with detailed local knowledge.

Assessment criteria for national assessment of Annex II species (Habitat Directive):

Relative population size. Population size of the species present on the proposed site of Community interest in relation to the populations present within the national territory of a country. The relative population sizes of the individual species have been determined by the EU states.

Conservation status. Degree of conservation of the features of the habitat which are important for the species concerned and restoration possibilities on the proposed site of Community interest. The 'conservation status' of individual sites in terms of their importance for species can only be assessed with detailed local knowledge.

Degree of isolation. Degree of isolation (chorological situation) of the population present on the proposed site of Community interest, in relation to the natural range of the species.

Once member states propose sites to the EU Commission for protection under the Birds Directive, the sites automatically become special protection areas (SPAs) and are included in the EU's Natura 2000 network of protection areas. SPAs are selected for the especially endangered bird species listed in Annex I of the Birds Directive. Under Article 4 (1) of the Directive, the 'most suitable territories in number and size' should be declared as special protection areas. Assessment criteria for Annex I of the Birds Directive lists (193 species and subspecies) which are:

- in danger of extinction;
- vulnerable to specific changes in their habitat;

- considered rare because of small populations or restricted local distribution;
- requiring particular attention for reasons of the specific nature of habitat

Natura 2000 and European forests. The most of forest type in Europe are semi-natural. It covers about 87 % of total European forest area [12]. These forests have been influenced by human intervention for their multiple functions, delivering multiple economic, cultural and environmental benefits over centuries. Today, it is still playing an important role to provide renewable and environmentally friendly raw materials and economic development, employment and prosperity, especially in rural areas. These forests have still a high biodiversity value and high biodiversity restoration potential, where are existing pressures [13].

Forests make up about half of the Natura 2000 Network areas. This ratio is quite high amount compared to other land types like grasslands and wetlands. The average distribution of Natura 2000 forest areas in the EU countries is 21%. For example, Germany has Natura 2000 areas in total of 55,142 km^2, of which 26,550 km^2 is forested [14].

Natura 2000 aims to assure the long-term survival of Europe's most vulnerable species and habitats, by ensuring that a sufficient number and area of their most important sites are adequately protected and positively managed. Natura 2000 sites aren't strict nature reserve sites where economic activities can take place [1]. The general principle that the conservation of flora and fauna will receive priority when managing natural resources is the basis for management of Natura 2000 areas. As long as favourable conservation status can be maintained or restored in combination with the commercial management of forests expected on most forest sites, economic activities can continue without substantial change [15]. This can be attributed to the fact that European forests are more dependent on seminatural conditions [12]. Nature conservation objectives must have priority on Natura 2000 sites, while the economic and social function of the forests should also be taken into account [16]. The implementing the land uses in Natura 2000 sites is regulated in the habitats directive. Each Natura 2000 area must have its own conservation priority plans. The success of those plans should be approved by the EU Commission at different intervals for species and habitats in considering the monitoring activities [17]. Natura 2000 management plans can be specifically designed for the site in question or integrated into other development plans, such as forest management plans [13]. This provides that the Natura 2000 conservation objectives are clearly included within sylvicultural treatments, forest conservation measurements or any land use operations in framework of a plan.

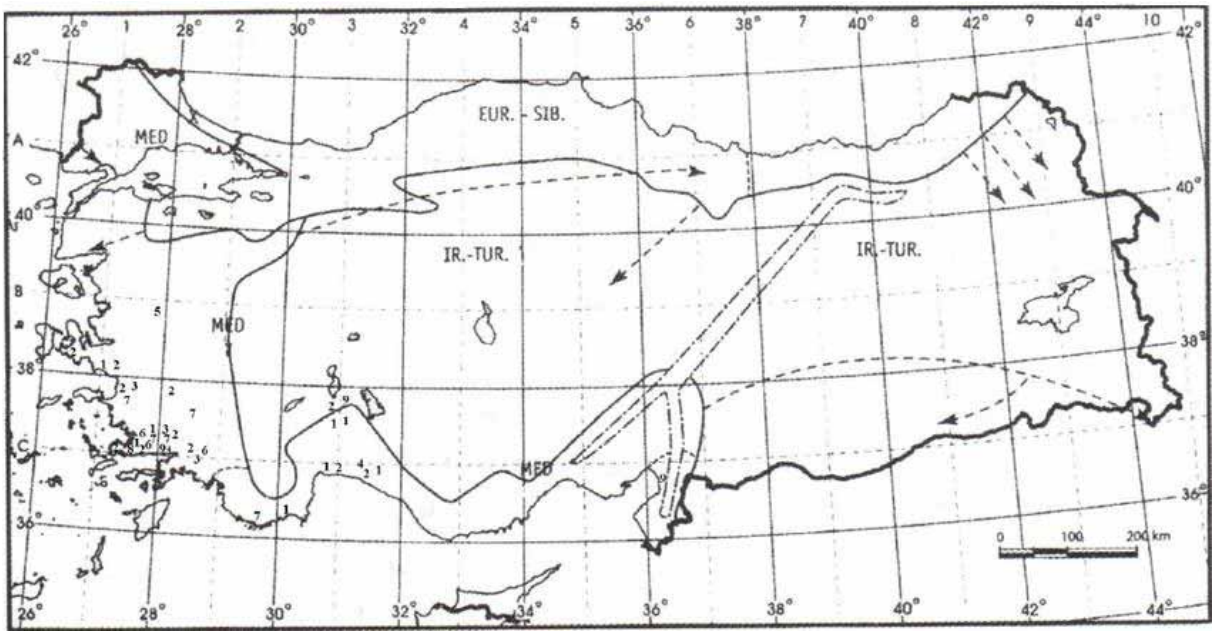

FIGURE 1
Phytogeographical areas of Turkey

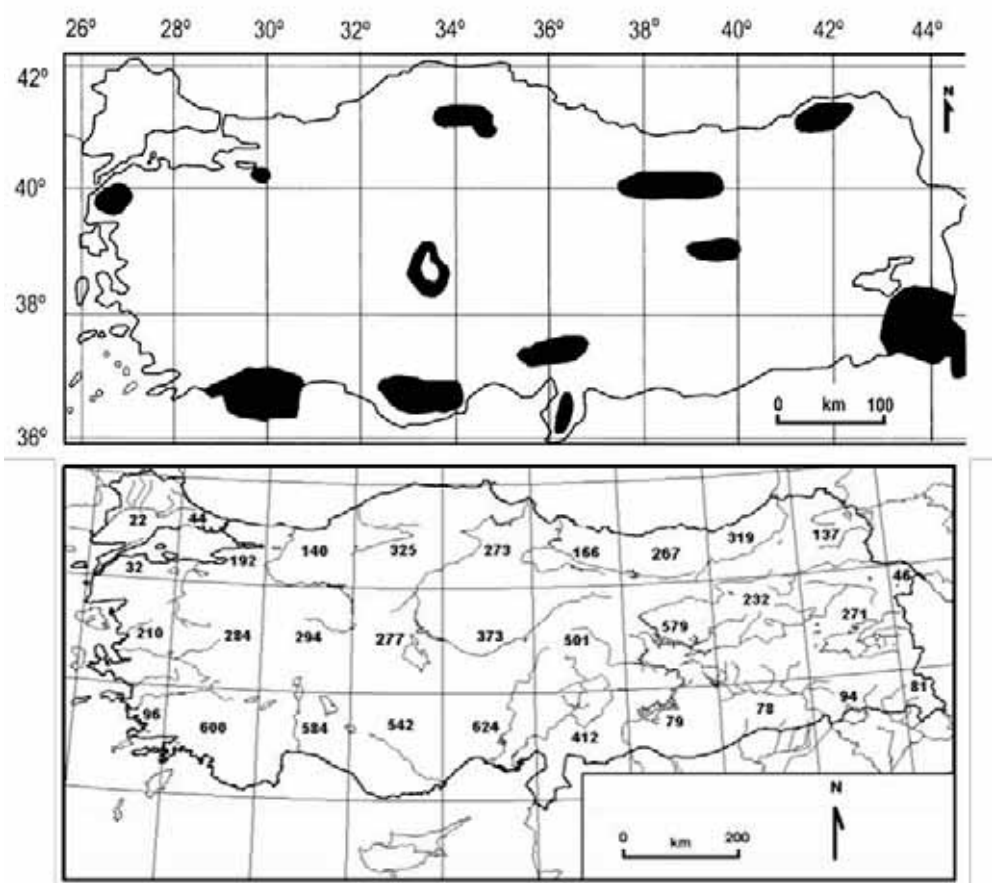

FIGURE 2
(a) The important areas for endemic plants in Turkey [20].
(b) Distribution of endemic plant numbers in Turkey [28].

OPPORTUNITIES AND CHALLENGES OF TURKISH FORESTS FOR NATURA 2000 CONCEPT

Biogeographical species distribution in country and its current status. Turkey is located within three main phytogeographical regions (Euro-Siberian, Irano-Turanian and Mediterranean) comprising the Anatolian, Mediterranean and Black Sea regions (Figure 1) and the transition zones formed among them [3, 18]. The climatic and geographical properties of these phytogeographical regions generally change according to altitudinal surfaces within short distances [19]. These variations are presenting different terrestrial and aquatic ecosystems are also found together. In these ecosystems, there are nearly 12.000 natural vascular plant taxa of which 3.694 taxa with over 30,7 % endemics are endemic [18]. As fauna, there are 19.000 invertebrates containing 4.000 endemic species and 1.500 vertebrates containing 123 endemic species [4]. Turkey has a remarkable position in the world with its richness of biological diversity [18, 19]. A significant number of endemic plant species is at risk of threatened [20]. Biogeography has important prominence in the distribution of important endemic plant areas and endemic plant numbers in the country (Figure 2). The rate of plant diversity and high endemism in Turkey, which can be compared to almost all of the European continent, is higher than in each European country. Alpine regions in Turkey are not counted within the main phytogeographical regions of the country. However, Turkey is located within the Alpine-Himalayan orogenic belt where the mountainous areas are dominant with the elevation over 1.500 meters. There are important mountain regions especially in the middle, east, northwestern and southeastern Anatolia such as Kackar, Erciyes, Aladaglar, Ararat, Cudi mountains which spread over 3000m altitude. Studies of biodiversity in Turkey are mainly carried out on protected areas. The term high mountain vegetation in Turkey refers to the asylvatic (non-forest) high mountain vegetation units of the subalpine to subnival belts, which, however, may have secondary anthropogeneous or natural extrazonal range extensions into subalpin or even montane elevations [21]. Screening and monitoring of biodiversity in Turkey have been carried out at the level of provincial regions for the last few years [22]. The full legislations

for identification and protection of biodiversity in Turkey provided currently at the level of action or master plans [23, 24]. Some inventory studies for planning and management of protected areas are also applied. There are some studies which are developed by non-governmental organizations for important areas and species [25, 26]. Data banks**,** especially for plants and animals**,** are available at the taxonomic [20] or national level [27].

Country level biogeographical properties of tree distribution. The importance of directives for Natura 2000 are emerging by designation of their special conservation areas. Designing and selecting procedures for Natura 2000 Sites are very complex and required compressive assessment criteria at national level. The first question comes to mind: How much of Turkey's data capacity can meet these criteria? Similar problems emerged after the membership of eastern European states. The experience in these countries have shown that they are obliged to notify the proposed Natura 2000 sites at national level (pSCI) to the European Commission within a few years of membership.

Turkey's forest biodiversity has some special subjects to protect the species than other EU countries. Firstly, the forest types of Turkey have important structures accordingly to diverse of species and to variability biogeographically distribution of habitats [29, 30]. Turkey has over 21 mio. hectares of forested area which comprises by over 60 tree species [6]. EU has 215 mio. hectares of forested area which comprises by over 110 tree species in 14 main biogeographical regions which include 78 forest types and some of them are divided into subtypes [31, 32]. Forest formations of the Turkey include species belonging to different floristic regions, namely Irano-Turanion, Mediterranean and Euro-Siberian. This characteristic is not seen in any of the European countries. The forest types for Irano-Turanion phyto-geographical region will only belong to Turkey, when Turkey has full membership. The Anatolian biogeographic region of Europe is commonly dominated from Irano-Turanion phyto-geographical region (Figure 3). The forest types in this biogeographical region have own features to characterize such steppe site conditions [33, 34] and existing syntaxonomical and geobotanical data base about these forests is low compared to the forests in other biogeographical regions. Likewise, it is possible to classify the new forest habitat types under Mediterranean (e.g. cedar, Taurus fir and some junipers) and Euro-Siberian regions (Oriental spruce, mixed forests e.g. by Crimean pine, Bornmueller's fir, oriental beech, scots pine, oaks) in Anatolia. The Black Sea biogeographic region of Turkey has widespread distribution from the other black sea biogeographic region in Europe (Figure 4). This biogeographic region, especially mountainous and high mountainous forests only in Turkey, will provide a characteristic new forest habitat types for Natura 2000.

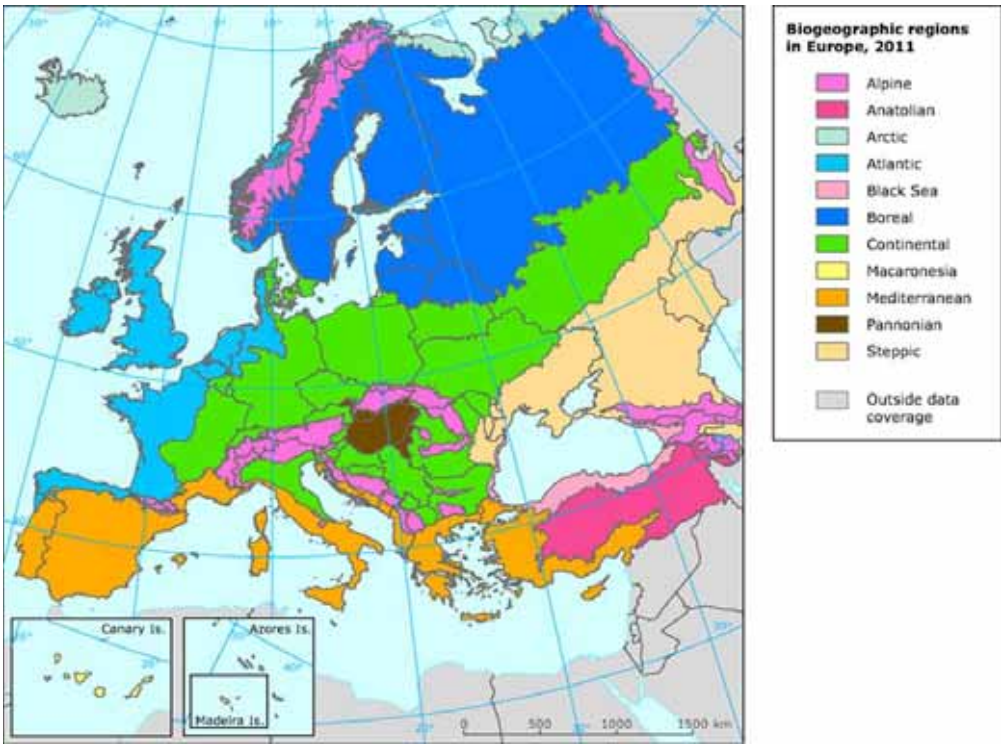

FIGURE 3
Biogeographical regions of Europe and Turkey

FIGURE 4
Physiography of the Black Sea biogeographical region

DISCUSSION AND CONCLUSION

The species richness and habitat diversity of Turkey is a challenge not only for Turkey but also for EU according to selecting, designing and managing of Natura 2000 sites. The Turkish national system for protected area is based only to conserve the areas, which are restricted by managed land use types. But, Natura 2000 concept provide the protecting the sites, as well as make possible the land uses with plan and project. They have to consider the compensatory measures to protect priority species and habitats in Natura 2000 areas the conservation status of the site, in relation to the favorable conservation status of habitats and the conservation value of species, must be maintained or improved [35]. There are other protected area types in the EU countries besides the Natura 2000 sites. SACs, SPAs and other protected area types (e.g. national park) can be overlapped on the same site. After membership of central and eastern European countries required a rapid implementation of some inventory for flora-fauna and habitats during a few years [36, 37]. The pre-existing national protected areas in these countries have become a good solution for this issue. It can be a way for Turkey in a tight time situation. But the question that arises here is, are the data in our existing national protected areas sufficient to select the Natura 2000 sites?

The existing habitat and species lists of the EU habitat and bird directives are quite lacking in terms of the species and habitats of Turkey. The species lists of EU habitat and bird directives must be widely revised for the habitats and species of Turkey. Therefore, the selecting, designing and managing of Natura 2000 sites in Turkey could provide necessity to some scientific researches more. Especially, the plants and (particular) birds of Turkey are concerning more effort for this issue. The vegetation communities with characteristic plants will be more decisive to classify the habitat types in Turkey. Therefore, it will be important the region or site specific phytosociological studies to assess the biogeographical reference of habitats and species especially in the forested area of Turkey. Additionally, species including birds must be locally identified in the population sizes, isolation grade of populations and threats, which are required for priority assessment by selecting and designing the Natura 2000 sites, and later for monitoring the species in the sites. On the other hand, it will gain importance the region and site specific ecological studies such as altitudinal distribution, bedrock and degree of human influence.

The Natura 2000 sites have cost for management. For example, the overall cost for implementing Natura 2000 in the EU-27 is estimated to be €5.8 billion per year [38]. Because of the forests' diversity in Turkey may need more forest areas to be protected by the Natura 2000 concept. It means that Turkey's biodiversity brings a considerable financial burden to the EU and Turkey. Especially, Anatolia will take place as a new European biogeographical region in the list of the Natura 2000 biogeographical regions. Additionally, several of the habitat types regarding to European biogeographical regions such Anatolia, Mediterranean, Black Sea proposed have been agreed to be variations of existing habitats and therefore some amendments to existing habitats were necessary. The species lists of EU habitat and

bird directives must be revised for the species of Turkey. Especially, the plants and particularly birds of Turkey are concerning more effort for this issue.

Alpine habitat types and their characteristic species in Turkey will be should discussed comprehensively. It should especially include secondary anthropogeneous or natural extrazonal alpine habitats and forest types with sub-alpine character such high mountainous forest types of Mediterranean, Black Sea and Anatolian biogeographical regions [39,40,41,42]. The flora-fauna and habitat studies carried out by the state and civil initiatives in Turkey are important cornerstones for the protection of the biological diversity of the country.The quality and spatial information of these studies is important for the beginning of Natura 2000 studies in Turkey. Whether Turkey is an EU member or not, such studies will provide a very important strategies and legally binding to protect the biodiversity of the country. In addition to these approaches, creating monitoring programs and building quantitative databases for conservation programs will be essential to assess future success in maintaining forest biodiversity [3]. In Europe, more seminatural forest habitat types will be protected by Natura 2000 through restoration, while in Turkey, more natural forest areas will be protected. But that does not mean that forests belonging to the seminatural oak forests in Iran-Turan phytogeographical regions of Turkey [43] will not be preserved. The existing protected areas of Turkey and important endemic plant areas are available as potential Natura 2000 sites (pSCs). One of the most important deficiencies is the inadequacy of data at various grades that will not supply some criteria to select and design the SAC's at European level. The criterion found in the most incomplete case are the relative population size and the degree of isolation.

ACKNOWLEDGEMENTS

This study has been funded in framework of the project "Practicability of EU Natura 2000 concept in the forested areas of Turkey" which is supported by the Programme "Civil Society Dialogue between EU and Turkey – IV Environment Grant Scheme (CSD-IV/ENV) TR2011/0135.15-01-2016". This project is being run by the author.

REFERENCES

[1] ec.europa.eu/environment/nature/info/pubs/docs/ nat2000/2002_faq_en.pdf
[2] Ostermann, O.P. (1998) The need for management of nature conservation sites designated under Natura 2000. Journal of Applied Ecology 35 968-973.
[3] Kaya, Z. Raynal, D.J. (2001) Biodiversity and conservation of Turkish forests. Biological Conservation 97 131-141.
[4] Kahraman, A., Onder, M. and Ceyhan, E. (2012) The Importance of Bioconservation and Biodiversity in Turkey. International Journal of Bioscience, Biochemistry and Bioinformatics 2(2), 95-99.
[5] Atmis, E., Ozden, S. and Lise, W. (2007) Urbanization pressures on the natural forests in Turkey: An overview. Urban Forestry and Urban Greening 6, 83–92.
[6] www.ogm.gov.tr/ekutuphane/Yayinlar/T% C3 %BCrkiye%20Orman%20Varl%C4%B1 %C4%9F%C4%B1.pdf
[7] eurlex.europa.eu/legalcontent/EN/TXT/PDF/ ?uri=CELEX:31992L0043&from EN
[8] www.ceeweb.org/wp-content/uploads/2011/12/ biogeo_booklet_2007.pdf
[9] eurlex.europa.eu/legalcontent/EN/TXT/PDF/ ?uri=CELEX:32011L0092&from=EN
[10] Trochet, A. and Schmeller, D.S. (2013) Effectivenes of the Natura 2000 network to cover threatened species. Nature Conservation, 4, 35-53.
[11] Tworek S., Makomaska-Juchiewicz M. and Cierlik G. (2014) How to select potential sites of community importance to the NATURA 2000 network: the issue of criteria. Ekologia (Bratislava), 33(2), 127–137.
[12] EEA (2006) European forest types. Categories and types for sustainable forest management reporting and policy. European Environment Agency, Technical report, No 9.
[13] EC (2015) Natura 2000 and Forests. Part I-II. European Commission, Technical Report - 2015 – 088.
[14] Natura 2000 (2015) Natura 2000 Barometer – update 2014. European Commission. Nature and biodiversity newsletter 37, 8-9.
[15] ec.europa.eu/environment/nature/info/pubs/ docs/nat2000/n2kforest_en.pdf
[16] ec.europa.eu/environment/nature/natura2000/ management/docs/art6/provision_of_art6 _en.pdf
[17] EC (2013) The Economic benefits of the Natura 2000 Network. Luxembourg, Publications Office of the European Union 77 p.
[18] Ture, C. and Bocuk, H. (2010) Distribution patterns of threatened endemic plants in Turkey: A quantitative approach for conservation. Journal for Nature Conservation 18, 296-303.
[19] Avci, M. (2005) Cesitlilik ve endemizm acisindan Turkiye'nin bitki ortusu. Istanbul Universitesi Edebiyat Fakultesi Cografya Dergisi 13, 27-55.
[20] Ekim, T., Koyuncu, M., Vural, M., Duman, H., Aytac, Z. and Adiguzel, N. (2000) Turkiye Bitkileri Kirmizi Kitabi. Ankara: TTKD ve Yuzuncu Yil Universitesi Yayini.

[21] Parolly, G. (2004) The High Mountain Vegetation of Turkey - a State of the Art Report, Including a First Annotated Conspectus of the Major Syntaxa. Turkish journal of botany 28 39-63.
[22] DKMP (2014) Karabukili'nin karasal ve ic su ekosistemleri biyolojik cesitlilik envanter ve izleme projesi. Doga Koruma ve Milli Parklar Genel Mudurlugu, 10. Bolge Mudurlugu, Karabuk Sube Mudurlugu, ulusal biyolojik cesitlilik envanter ve izleme projesi 357 pp.
[23] COB (2004) Turkiye Ulusal Ormancilik Programi. Cevre ve Orman Bakanligi, Ankara, 90 pp.
[24] Ulusal Biyolojik Çeşitlilik Stratejisi ve Eylem Plani. Cevre ve Orman Bakanligi, Ankara, 176 pp.
[25] Ozhatay, N., Byfield, A. and Atay, S. (2005) Turkiye'nin 122 Onemli Bitki Alani. WWF Turkiye (Dogal Hayati Koruma Vakfi), Istanbul.
[26] Eken, G., Bozdogan M., Isfendiyaroglu, S., Kilic, D.T., and Lise, Y. (2006) Turkiye'nin Onemli Doga Alanlari. Doga Dernegi, Ankara.
[27] www.nuhungemisi.gov.tr
[28] Kutluk, H. and Aytug, B. (2000) Endemik plants of Turkey, plants of the balkan peninsula: into the Next Millennium, Proceeding of the 2nd Balkan Botanical Congress, Istanbul, Turkey I (Ed. Ozhatay, N.): 285-288, Istanbul.
[29] Atalay, I., Efe, R. and Ozturk, M. (2014) Ecology and classification forests in Turkey. Procedia - Social and Behavioral Sciences 120, 788–805.
[30] Colak, A. and Rotherham I.D. (2006) A review of the Forest Vegetation of Turkey: its status past and present and its future conservation. Proceedings of the Royal Irish Academy 106B 3, 343-354.
[31] Barbati, A., Marchetti, M., Chirici, G. and Corona, P. (2014) European Forest Types and Forest Europe SFM indicators: Tools for monitoring progress on forest biodiversity conservation. Forest Ecology and Management 321, 145-157.
[32] De Rigo, D., Bosco, C., San-Miguel-Ayanz, J., Houston Durrant, T., Barredo, J.I., Strona, G., Caudullo, G., Di Leo, M. and Boc, R. (2016) Forest resources in Europe: an integrated perspective on ecosystem services, disturbances and threats. In: San-Miguel-Ayanz, J., de Rigo, D., Caudullo, G., Houston Durrant, T., Mauri, A. (eds.) European Atlas of Forest Tree Species. Publication Office of the European Union, Luxembourg.
[33] Arslan, M., Erdogan, N., Bingol, M.U. and Celik, N. (2014) Bozan Cevresi (Eskisehir) Bozuk Orman ve Bozkir Vejetasyonu. II. Ulusal Akdeniz Orman ve Cevre Sempozyumu "Akdeniz ormanlarının gelecegi: Surdurulebilir toplum ve cevre". 22-24 October 2014 –Isparta
[34] Mayer, H. and Aksoy, H. (1986) Walder der Turkei. Gustav F. Verlag. Stuttgart. 290 pp.
[35] ec.europa.eu/environment/nature/natura2000/management/docs/art6/provision_of_art6_en.pdf
[36] panda.org/downloads/n2000reportweb_he2p.pdf
[37] portals.iucn.org/library/efiles/documents/2005-117.pdf
[38] Pellegrino, D., Schirpke, U. and Marino, D. (2017) How to support the effective management of Natura 2000 sites? Journal of Environmental Planning and Management 60, 383-398.
[39] Akman, Y. (1995) Turkiye Orman Vejetasyonu. Ank. Univ. Fen Fak., Ankara
[40] Atalay, I. (2002) Turkiye'nin Ekolojik Bolgeleri. Ecoregions of Turkey. Orman Bakanligi Yayin No. 167.
[41] Kantarci, M.D. (1991) Akdeniz Bölgesi'ninYetisme Ortami Bölgesel Siniflandirilmasi. T.C. Tarim Orman ve Koyisleri Bakanligi, OGM Yayinları, Yayin No: 668, Seri No: 64, Ankara
[42] Ozturk, M., E. Yucel, C. Yarci, Celik, A. and Aksoy, A. (1998) Plant diversity in the Turkish Black Sea region and strategies for its conservation In: Kotlyakov, V., Uppenbrink, M. and Metreveli, V. (eds.) Conservation of the Biological Diversity as a Prerequisite for Sustainable Development in the Black Sea Region. Batumi-Georgia, Kluwer Acad. Publ. NATO-ASI Series 46, 155-173.
[43] Uslu. E. and Bakis, Y. (2012) Geographic distribution of Turkish Oaks. Dendrobiology 67, 41-48.

Received: **14.06.2017**
Accepted: **10.08.2017**

CORRESPONDING AUTHOR

Cumhur Gungoroglu
Faculty of Forestry,
Karabuk University,
Karabuk – TURKEY

E-mail: cumhurgungoroglu@karabuk.edu.tr

© by PSP Volume 26 – No. 10/2017 pages 6225-6233 Fresenius Environmental Bulletin

OPTIMIZATION OF MINERALIZED REFUSE ADSORBENT-FENTON-NACLO OXIDATION OF BIOLOGICALLY TREATED LANDFILL LEACHATE USING RESPONSE SURFACE METHODOLOGY

Fa-hui Nie, Qing Yu*, Wen-ting Li, Rong-rong Liu, Yong-xi Zhou

School of Civil Engineering and Architecture, East China Jiao Tong University, Nanchang, 330013, China

ABSTRACT

In this study, mineralized refuse adsorbent - Fenton-NaClO oxidation were employed to treat biologically stabilized landfill leachate. Firstly, the mineralized refuse after roasting modification was used to absorb Carbon Oxidation Demand (COD) and ammonia nitrogen (NH_3-N) in leachate treated by biochemical method, and the mineralized refuse were characterized by Scanning electron microscopy (SEM) and X-ray energy dispersive spectra (EDS) analysis. Response surface methodology (RSM) was applied to evaluate the major factors including the initial pH, reaction time, reaction temperature, H_2O_2/ Fe^{2+} molar ratio, concentration of H_2O_2 and NaClO on the removal of COD and NH_3-N in Fenton and NaClO process, and the interactions between these factors, and optimized the operating parameters as well. Under the optimum conditions of Fenton Process such as H_2O_2 concentration of 72 mmol/L, H_2O_2/ Fe^{2+} molar ratio of 3, reaction time of 1.5h and pH of 5 shows 52.68% of COD removal and 38.52% of NH_3-N removal. Finally, the removal efficiency of COD and NH_3-N reached 81.86% and 98.96% respectively by using NaClO oxidation to further remove them. The results demonstrate that the coupling of mineralized refuse adsorbent-Fenton-NaClO oxidation processes is an alternative method to eliminate the COD and NH_3-N from landfill leachate.

KEYWORDS:
mineralized refuse, SEM/EDS, Fenton, NaClO, landfill leachate, Response surface methodology

INTRODUCTION

Landfill leachate produced during the process of landfill is complicated composition of high concentration biodegradable and non-biodegradable products wastewater, characteristically rich in organic matter, phenols, NH_3-N, phosphate, heavy metals, and sulfide [1]. Traditionally, biological treatment is the main landfill leachate treatment technology due to its many advantages including various sources, low cost and simple procedures [2, 3]. However, these conventional biological treatments may not be sufficient to deal with landfill leachate before discharging into the environment. Therefore, a combination of physicochemical treatment methods have attracted more interests due to its high efficiency [4, 5].

Mineralized refuse is considered as a promising adsorption material for the strong nitrification capacity [6]. Meanwhile, it can realize resource utilization, reduce pollution cost for production enterprises, make landfill space for fresh living garbage and extend the service life of landfill. It has been widely reported that remove a large amount of NH_3-N with just little mineralized refuse in treating landfill leachate[7,8]. The mineralized refuse from Nanchang Mai Yuan landfill was chosen as adsorbent in this paper, and was used to statically absorb COD and NH_3-N in leachate treatment. However, the efficiency of removing COD and NH_3-N only by adsorption techniques can not meet the draining standard. In recent years, Fenton process, one of Advanced Oxidation Processes(AOP) techniques for removing pollutes of landfill leachate, has gained significant interest by many researchers[9-16]. Hydrogen peroxide(H_2O_2) is highly effective for the removal of pollutants, because the generation of hydroxyl radical(OH·) in Fenton process can significantly oxidize a broad range of organic and inorganic pollutants[17-19]. Landfill leachate treated by adsorption and Fenton process has a satisfactory degradation effect on COD, but the effect of removal of NH_3-N is not quite ideal, so the additional treatment is essential for further removal of NH_3-N. Based on this, many scholars[20-23] use sodium hypochlorite (NaClO) to replace the traditional chlorine series oxidant for the removal of NH_3-N, the results obtained are quite acceptable. The NaClO has the advantages of safe usage, convenient operation, good effects of oxidation and low price, simultaneously, it reduces the generation of disinfection byproducts as well[24, 25].

In this study, mineralized refuse adsorbent-Fenton-NaClO oxidation process was employed to treat the landfill leachate. In Fenton and NaClO

process, batch experiments were carried out to determine the optimal reaction parameters including the initial pH, reaction time, reaction temperature, H_2O_2/ Fe^{2+} molar ratio, concentration of H_2O_2 and concentration of NaClO through response surface methodology (RSM), and the mineralized refuse were characterized by Scanning electron microscopy (SEM) and X-ray energy dispersive spectra (EDS) analysis.

MATERIALS AND METHODS

Leachate characteristics. Leachate samples were collected from the effluent of leachate treated by biochemical method with oxidation ditch-A/O in Nanchang MaiYuan landfill. The wastewater looks brown with no obvious stench, COD ranging from 1200-1500mg/L, the concentration of NH_3-N ranging from 110-130mg/L, pH ranging from 4.5-6.5.

Mineralized refuse preparation. The mineralized refuse from Nanchang MaiYuan landfill was chosen as adsorbent in this paper, and was used to absorb COD and NH_3-N in leachate treated by biochemical method after modification. The average particle size of mineralized refuse smaller than 1mm were used for modification. The mineralized refuse was first placed into a muffle furnace for roasting at the temperature of 700℃. After roasting for 2h, remove the mineralized refuse and cool it down to room temperature, then store them in the bag until ready for use.

Experimental method. Batch experiments were performed at room temperature(25℃) in beakers with 200mL leachate sample. Magnetic stirrer(H97-A Thermostatic magnetic stirrer) was used for sample mixing. The optimum conditions of 60g/L of mineralized refuse, 30 min of mixing time and 150 rpm of mixing speed applied for mineralized refuse adsorption process. After 10 min centrifugal time, the supernatant was taken for the sample of Fenton process.

In Fenton oxidation process, the initial pH was adjusted to desired values(5.0, 6.0, 7.0), the H_2O_2 was set to achieve the concentrations of 40, 60, 80 mmol/L. Meanwhile the molar ratio of H_2O_2/Fe^{2+} was attained at intended values (3,4,5), the reaction time was adjusted to intended values (60,75,90min). After Fenton's treatment, the pH was adjusted to be 8.0 and the samples were allowed to settle for 1h. After the settling time, the supernatant was withdrawn from the beaker and was analyzed for concentration of COD and NH_3-N.

In NaClO oxidation process, after the pH values of samples were adjusted to the desired levels(5-7), the appropriate amounts of NaClO(50-70 mmol/L) were added and mixed for intended time (45-70min) under appropriate temperature (40-60 ℃). After setting 30 min, the supernatant was analyzed for concentration of COD and NH_3-N.

Calculation of the removal efficiency. The following equation can be the expression of the removal efficiency (R) of COD and NH_3-N:

$$R(\%) = \frac{C_o - C_e}{C_o} \times 100 \quad (1)$$

where C_o and C_e is the initial and final concentrations of COD and NH_3-N respectively.

BBD response surface design. Response surface methodology(RSM) is a powerful statistical-based technique for designing experiments, building model, testing the appropriateness of model and optimizing the process parameters with limited number of experiments[26, 27].As one of the most common design under RSM, Box–Behnken design (BBD) is efficient and flexible. In this study, the BBD was applied to evaluate the individual and interactive effects of independent variables on the responses in Fenton process, four main factors to three levels each one were chosen: H_2O_2 concentration(mmol/L)(A), H_2O_2/ Fe^{2+} molar ratio(B), pH(C) and reaction time(h)(D). The independent variables and their levels were presented in Table 1.

TABLE 1
Coded and actual values of the variables of the design of experiments for the Fenton process

Factor	Variables	Coded levels of variables		
		-1	0	1
A	$[H_2O_2]$(mM)	40	60	80
B	$[H_2O_2]/[Fe^{2+}]$	3：1	4：1	5：1
C	pH	5	6	7
D	Reaction time(h)	60	75	90

The second order polynomial mathematical models between related process parameters and response values by response surface methodology were established through multinomial regression analysis of experimental data(Table 2), and the following generalized form of the second-order polynomial mathematical model was used to fit the experimental data[27]:

$$Y = \beta_o + \sum_{i=1}^{k} \beta_i X_i + \sum_{i=1}^{k} \beta_{ii} X_i^2 + \sum_{i=1}^{k} \sum_{j=1}^{k} \beta_{ij} X_i X_j + \varepsilon \quad (2)$$

where Y represents predicted response (COD and NH_3-N removal efficiencies, %),β_0, β_1(i = 1, 2, 3, 4) and β_{ij} (i = 1, 2, 3, 4; j = 1, 2, 3, 4) are the model coefficients, X_i and X_j are the independent variables.

The analysis of variances (ANOVA) of RSM was employed using the software Design Expert (version 8.0.6) to analyze the results and to check the statistical significance of the developed mathematical model. The interaction between the process variables was illustrated by the three dimensional response surface plots. The optimum process parameters for Fenton process was calculated using the fitted models and validated by experiments.

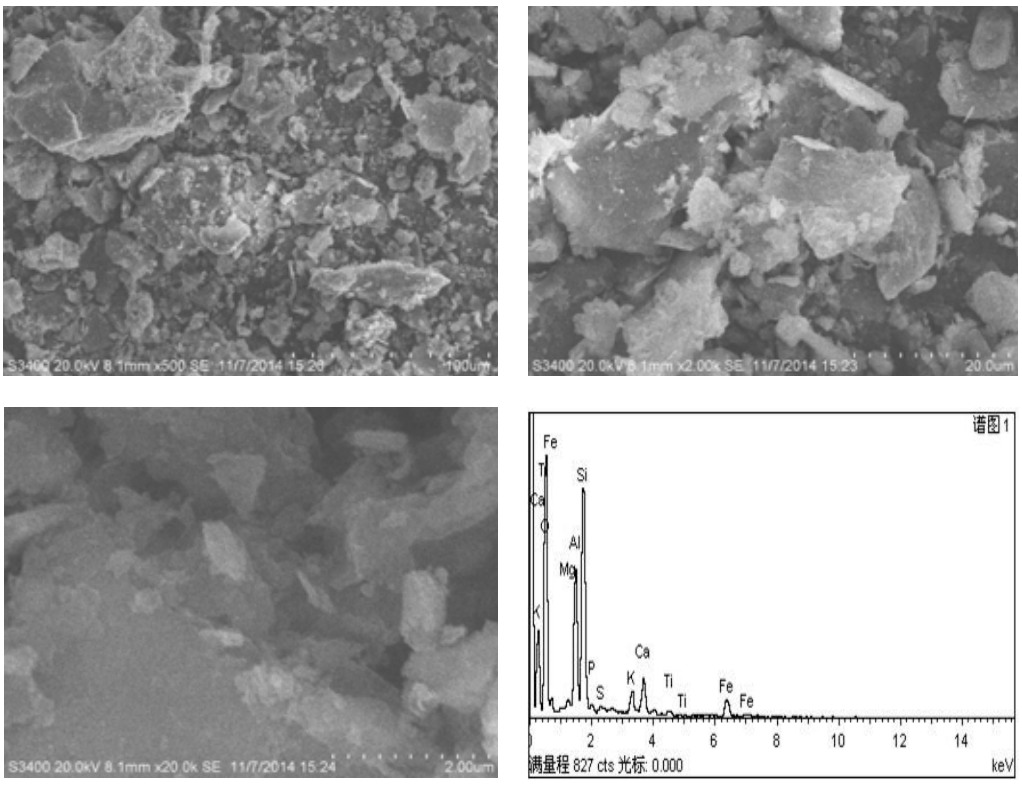

FIGURE 1(a)
SEM image and EDS pattern of adsorbent before modification

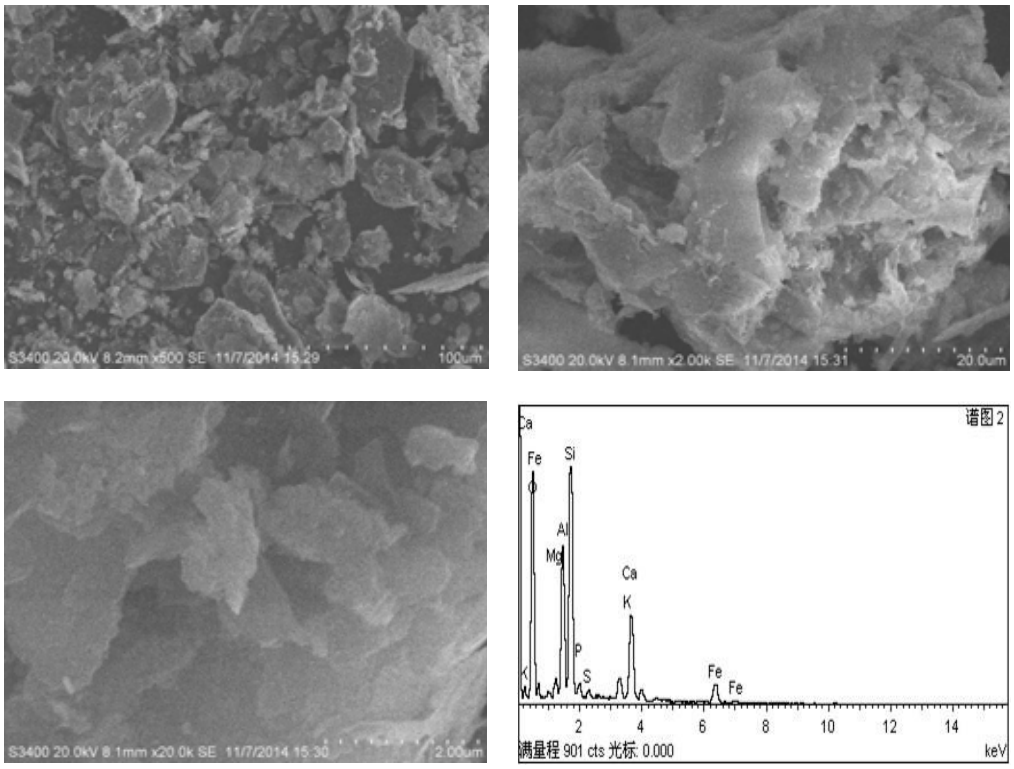

FIGURE 1(b)
SEM image and EDS pattern of adsorbent after modification

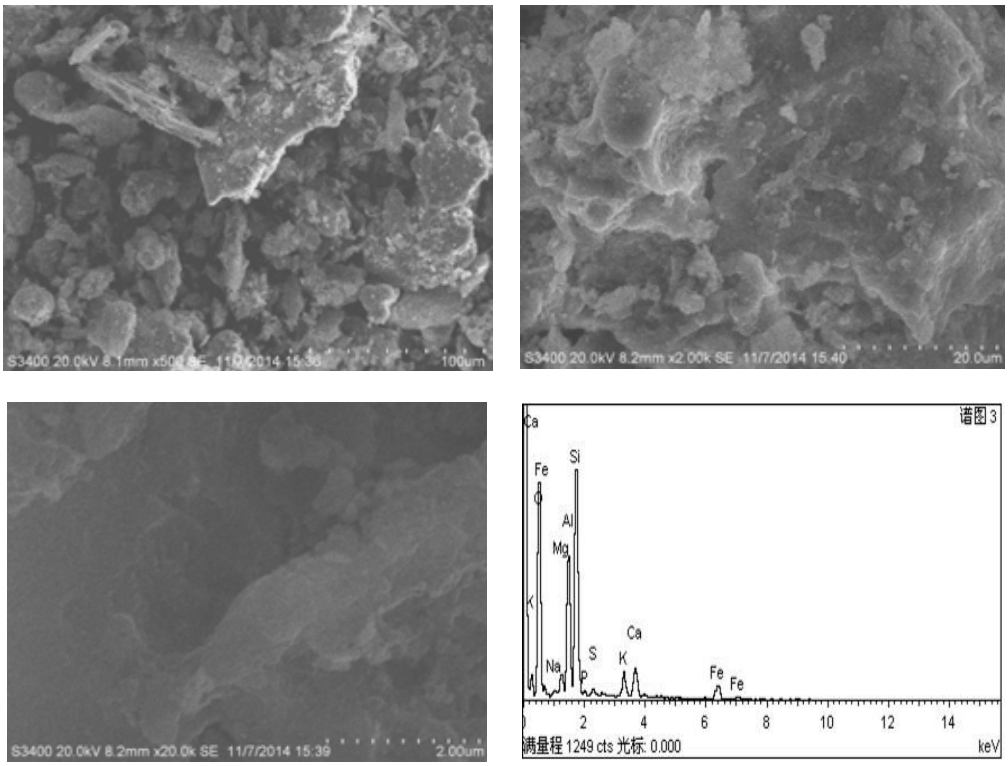

FIGURE 1(c)
SEM image and EDS pattern of adsorbent after adsorption

RESULTS AND DISCUSSIONS

Characterization of mineralized refuse. The Scanning electron microscopy(SEM) image and X-ray energy dispersive spectra(EDS) pattern of the mineralized refuse are shown in Fig. 1. As shown in Fig. 1a, the mineralized refuse before modification is mainly as particles with good dispersion and a small amount of fibrous material. The mineralized refuse has loose surface, with floccules attached. The internal structure of mineralized refuse after modification changed while fibrous material decreased. Besides, the attached floccules reduced significantly with the surface of particles getting smoother. The pore increased and penetrated into the interior pore. The surface area increased compared to the one before modification which led to enhanced adsorption. Meanwhile, after 700℃ roasting modification, the main structure of functional groups on mineralized refuse didn't change. Strength of a small amount of secondary functional groups weakened or disappeared. However, the structure of mineralized refuse before and after adsorption didn't change. Comparing the graph Fig. 1b and Fig. 1c, surface of mineralized refuse after adsorption became more compact and denser while contours of surface pores became blurred. The pore stuck together may result from some substance being generated on the surface of the adsorbent or functional groups on the adsorbent surface combined with metal ions in the filtrate after infiltration. Furthermore, the X-ray energy dispersive spectra pattern of mineralized refuse also revealed, that mineralized refuse contains elements of O, Mg, Al, Si, P, S, K, Ca, and Fe. Before and after modification as well as adsorption, the content and type of the element in the adsorbent were changed.

Analysis of response surface. Percentage removal of pollutant was calculated, and the results of RSM experiments by using the BBD design to determine the individual and interactive effects of the four independent variables including concentration of H_2O_2(mmol/L)(A), molar ratio of H_2O_2/ Fe^{2+}(B), pH(C) and reaction time(h)(D) in Fenton process, which were presented in Table 2, along with the predicted and practical values of the responses(COD removal (Y_1) and NH_3-N removal (Y_2)).The quadratic polynomial equations for the COD and NH_3-N removal percentages through the multiple regression analysis(Table 3 and 4) were obtained as follows:

$$\text{COD removal}(\%)=41.11+6.01X_1-0.82X_2-1.83X_3+0.86X_4+2.82X_1X_2-0.20X_1X_3+4.34X_1X_4-4.86X_2X_3-0.55X_2X_4+0.025X_3X_4-7.02X_1^2-1.86X_2^2+5.69X_3^2+4.06X_4^2 \quad (4)$$

$$NH_3\text{-N removal}(\%)= 21.67+1.67X_1-0.052X_2+0.086X_3-0.35X_4+5.3X_1X_2-4.73X_1X_3-0.22X_1X_4+5.27X_2X_3-6.71X_2X_4-2.89X_3X_4-0.56X_1^2+0.13X_2^2-0.02X_3^2-0.072X_4^2 \quad (5)$$

TABLE 2
BBD experimental design and results of COD and ammonia nitrogen removal efficiency

Run	Independent variables				Response (Y,%)			
					Experimental		Predicted	
	A(mmol/L) H_2O_2 concentration	B H_2O_2/Fe^{2+} ratio	C pH	D(min) Reaction time	COD removal	ammonia nitrogen removal	COD removal	ammonia nitrogen removal
1	60	4	5	90	54.16	24.49	53.52	24.03
2	60	5	6	60	43.07	29.76	42.18	28.73
3	60	3	6	90	44.59	26.75	45.53	28.15
4	60	4	7	60	48.26	24.81	48.16	24.9
5	60	3	7	75	49.44	17.08	48.8	16.64
6	60	4	5	60	52.66	19.29	51.86	18.95
7	40	3	6	75	30.94	26.07	29.86	24.91
8	80	4	5	75	48.46	27.09	47.81	27.4
9	60	4	7	90	49.86	27.09	49.92	18.43
10	60	4	6	75	40.94	21.17	41.11	21.67
11	80	4	6	60	38.31	23.45	38.98	23.28
12	40	4	6	60	35.04	18.43	35.63	19.48
13	80	4	6	90	49.26	23.19	49.36	22.14
14	60	4	6	75	40.84	22.17	41.11	21.67
15	80	4	7	75	44.54	18.08	43.77	18.12
16	60	4	6	75	41.96	22.17	41.11	21.67
17	60	3	5	75	42.78	27.3	42.72	27.02
18	60	3	6	60	42.19	15.01	42.73	15.41
19	60	4	6	75	40.86	21.67	41.11	21.67
20	40	5	6	75	23.64	14.67	42.72	14.22
21	80	5	6	75	39.91	27.36	40.25	28.15
22	80	3	6	75	35.94	17.58	36.25	17.66
23	60	5	6	90	43.29	14.65	42.81	14.62
24	60	5	5	75	49.48	15.93	50.81	16.37
25	60	4	6	75	40.96	21.17	41.11	21.67
26	60	5	7	75	36.68	26.8	37.43	27.08
27	40	4	6	90	28.64	19.07	28.66	19.24
28	40	4	5	75	34.58	14.27	35.4	14.6
29	40	4	7	75	31.44	24.17	32.14	24.23

TABLE 3
Sequential model sum of squares for responses

Source	Sum of squares	DF	Mean square	F value	Prob>F	Remarks
Sequential model sum of squares for COD removal						
Mean	49880.53	1	49880.53			
Linear	490.46	4	122.61	2.87	0.0451	
2FI	203.02	6	33.84	0.74	0.6251	Suggested
Quadratic	811.68	4	202.92	229.36	<0.0001	Aliased
Cubic	9.41	8	1.18	2.37	0.1546	
Residual	2.98	6	0.5			
Total	51398.08	29	1772.35			
Sequential model sum of squares for ammonia nitrogen removal						
Mean	13345.55	1	13345.55			
Linear	35.12	4	8.78	0.39	0.8129	
2FI	526.53	6	87.75	129.94	<0.0001	Suggested
Quadratic	2.44	4	0.61	0.88	0.5004	Aliased
Cubic	8.17	8	1.02	3.97	0.0551	
Residual	1.54	6	0.26			
Total	13919.34	29	479.98			

TABLE 4
Model summary statistics for responses

Source	Std.Dev	R^2	Adjusted R^2	Predicted R^2	PRESS	Remarks
Model summary statistics for COD removal						
Linear	6.54	0.32	0.2104	-0.0601	1608.68	
2FI	6.77	0.46	0.1553	-0.8003	2732.11	Suggested
Quadratic	0.94	0.99	0.9837	0.9555	67.53	Aliased
Cubic	0.7	1	0.9908	0.8028	299.34	
Model summary statistics for ammonia nitrogen removal						
Linear	4.74	0.06	-0.0953	-0.47	843.5	
2FI	0.82	0.98	0.967	0.9345	37.57	Suggested
Quadratic	0.83	0.98	0.9661	0.9098	51.75	Aliased
Cubic	0.51	1	0.9874	0.8608	79.89	

TABLE 5
ANOVA table for responses

Source	Y_1COD removal (%)		Y_2ammonia nitrogen removal (%)	
	F value	P value	F value	P value
Model	121.51	<0.0001	58.07	<0.0001
A	490.19	<0.0001	48.38	<0.0001
B	9.06	0.0093	0.046	0.833
C	45.18	<0.0001	0.13	0.7264
D	9.93	0.0071	2.06	0.1733
AB	35.89	<0.0001	161.64	<0.0001
AC	0.17	0.6847	128.85	<0.0001
AD	85.06	<0.0001	0.29	0.5975
BC	107.01	<0.0001	160.27	<0.0001
BD	1.34	0.2659	259.77	<0.0001
CD	0.21	0.6584	48.07	<0.0001
A^2	360.98	<0.0001	2.96	0.1072
B^2	25.38	0.0002	0.15	0.7007
C^2	237.22	<0.0001	0.043	0.8511
D^2	120.97	<0.0001	0.048	0.8297
C.V%	2.27		3.88	
PRESS	67.53		51.75	
AP	45.723		24.232	
R^2	0.9918		0.9831	
Adj-R^2	0.9837		0.9661	

The significance and adequacy of the mathematical models were performed in the form of ANOVA(Table 5). The F-value and P-value can exam the statistical significance of the fit polynomial model, the high F-values and low P-values indicates that the polynomial model adequately explains the variation in the data and represents the high significance. From Table 5, the response showing the model F value of 121.51for COD and 58.07 for NH_3-N.It showed that both models were of high significance. It could be seen that, the model Y_1 (COD removal) terms A, C, AB, AD, BC, A^2, C^2, and D^2 had significant effects on the percentage of COD removal whereas the model Y_2 terms A, AB, AC, BC, BD, and CD had significant effects on the percentage of NH_3-N removal, since the p-values of these coefficients are less than 0.05. The determination coefficients(R^2) of the models indicated that 99.18% and 98.31% of the total variability could be explained by the models for both responses. The value of the adjusted determination coefficient (adjusted R^2 = 0.9837 and 0.9661) also implied that only less than 4% of the total variations were not explained by the models. In addition, the low value of the coefficient of variation (C.V. = 2.27% and 3.88%) indicated the high precision and reliability of the experimental values.

Meanwhile, the predicted versus actual plot (Fig.2) and Normal % probability graphs (Fig. 3) can further verify that the adequacy of developed mathematical models. The experimental data is in good agreement with the predicted ones, since the data obtained was very close to the diagonal line for both graphs. Therefore, the development mathematical models could be used to describe the Fenton process robustly. The effect of four factors on COD and NH_3-N removals can be observed by three-dimensional response surface plots generated by RSM as shown in Fig.4.

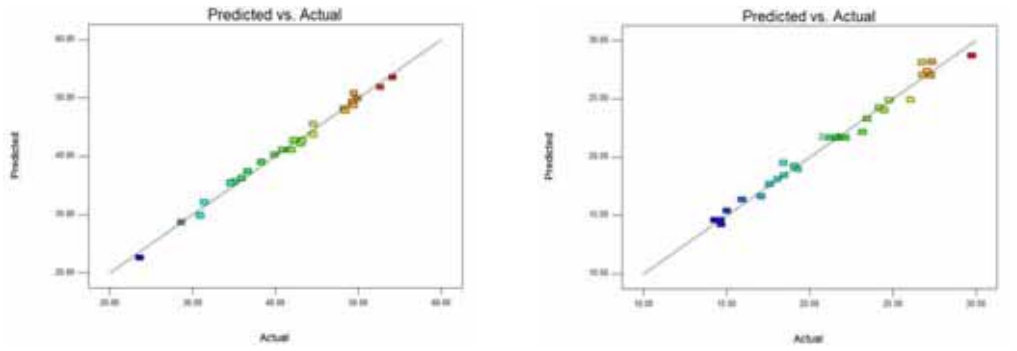

FIGURE 2
Predicted versus actual plot for responses:(a) COD removal, (b) ammonia nitrogen removal

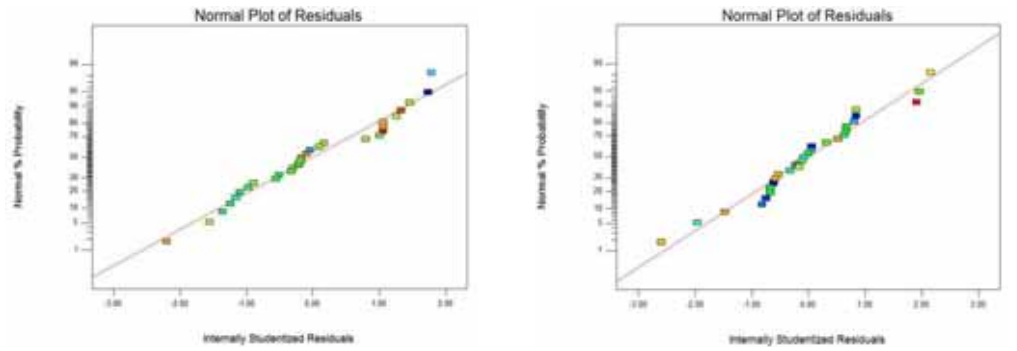

FIGURE 3
Normal % probability plots for response:(a) COD removal, (b) ammonia nitrogen removal

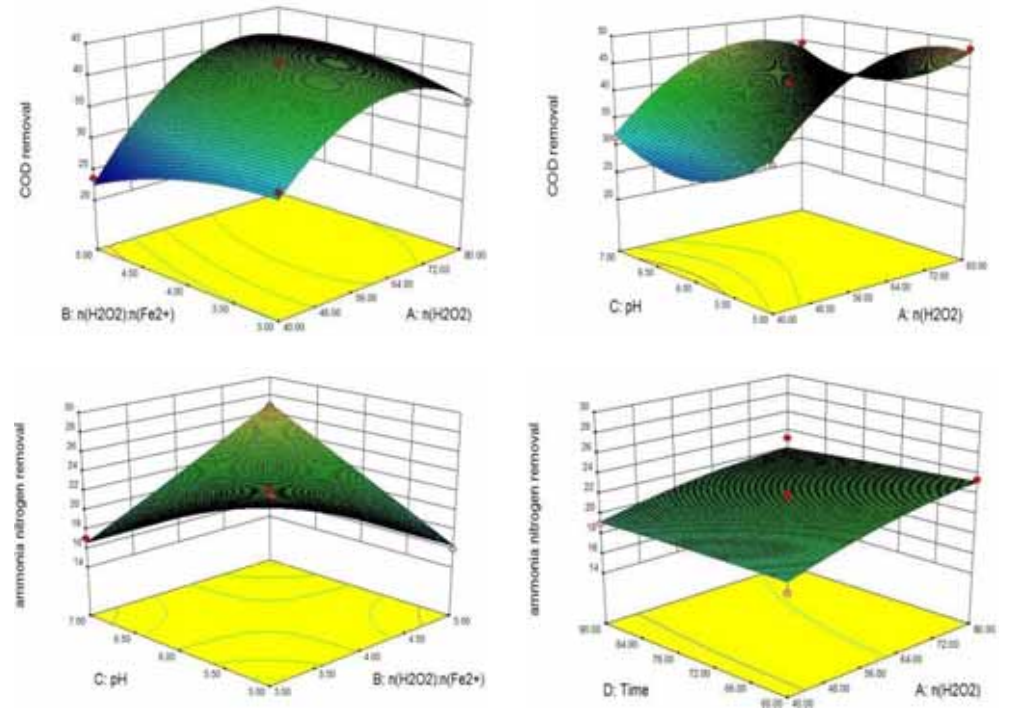

FIGURE 4
Three-dimensional response surface plot for removal of (a) COD, (b) ammonia nitrogen

Optimization of Fenton process parameters and validation of the models. In order to obtain the maximum COD removal and NH_3-N removal, the best combination was found to be the concentration of H_2O_2 71.68 mmol/L, H_2O_2/ Fe^{2+} molar ratio of 3, reaction time of 1.5h and pH of 5. Under the conditions, the removal efficiency of COD and NH_3-N were 50.27% and 36.52% respectively. But in practice, the optimal condition for concentration of H_2O_2 can be modified to 72 mmol/L. Under the modified conditions, the experimental removal efficiency of COD and NH_3-N were 52.68% and 38.52% respectively.

Optimization of NaClO process parameters and validation of the models. Similarly, RSM was also applied to evaluate the major factors including pH(5-7), concentration of NaClO (50-70mmoL/L), reaction temperature (40-60℃) and reaction time(45-75min)on the removal of COD and NH_3-N in NaClO process, and the interactions between these factors, and optimized the operating parameters as well. The results showed that the optimum conditions for NaClO process were that the concentration of NaClO is 60mmol/L, with reaction temperature 50℃, reaction time 60min and pH 6. Under the conditions, the removal efficiency of COD and NH_3-N were 82.27% and 97.48% respectively. After verification, the experimental removal efficiency of COD and NH_3-N were 83.86% and 98.96% respectively.

CONCLUSION

Biologically stabilized landfill leachate was treated by the mineralized refuse adsorbent-Fenton-NaClO oxidation. The mineralized refuse after roasting modification was used to absorb COD and NH_3-N in leachate firstly, and the removal rate of COD and NH_3-N reached up to 60.23% and 89.92% respectively under the condition of 700℃ calcination temperature. The element type and content were changed before and after modification as well as absorption respectively, with SEM/EDS, O, Mg, Al, Si, P, K, Ca and Fe tested in the aged refuse.

The Box–Behnken experimental design (BBD) and response surface methodology (RSM) were employed in this study to optimize the process variables for Fenton and NaClO oxidation process. Two quadratic models were developed with high significance and good coefficient of determination values (R^2>0.95) for both COD and NH_3-N removals. Analysis of variance showed that the response surface models were accurate for predicting experimental results, and could reflect not only the linear effects but also the interaction effects of key variables regarding the COD and NH_3-N removal of the biologically treated landfill leachate. Eventually the effluent concentration of COD and NH_3-N were reduced to 78mg/L and 0.47mg/L that meet the prescribed discharge standards of landfill pollution control standard (GB16889-2008).Therefore, it is appropriate to apply the mineralized refuse adsorbent-Fenton-NaClO oxidation process in the advanced treatment of biologically stabilized landfill leachate.

ACKNOWLEDGEMENTS

The authors gratefully acknowledge the economic support to Natural Science-Foundation of China(Project No.: 51168031) and Science and Technology Support Project of Jiangxi, China(Project No.: 20151BBF60031).

REFERENCES

[1] Kamaruddin, M.A., Yusoff, M.S., Aziz, H.A. and Hung, Y.T. (2014) Sustainable treatment of landfill leachate. Applied Water Science, 5, 113-126.

[2] Zhao, X. (2010) Photoelectrochemical treatment of landfill leachate in a continuous flow reactor. Bioresource Technology, 101, 865-869.

[3] Shokri, A., Mahanpoor, K. and Soodbar, D. (2016) Degradation of 2-nitrophenol from petrochemical wastewater by UV/$NiFe_2O_4$ supported on Clinoptilolite process. Fresen. Environ. Bull., 25, 500-508.

[4] Motling, S., Mukherjee S.N. and Dutta, A. (2014) Real life MSW Landfill leachate treatment by combined coagulation-flocculation and carbon adsorption for removal of phenol and organic load (COD). International Journal of Chemical & Environmental Engineering.

[5] Yuan, H.-P., Wang, Q.-J., Guo, S.-J., Yao, J., Zhu, N.-W. and Gong, Y. (2015) Enhancement of waste activated sludge aerobic digestion with combined Fenton oxidation and electrochemical pretreatment method. Fresen. Environ. Bull.,24, 2843-2849.

[6] Tian, J.-S., Zhang, H., Zhang, Y.-M., Ding, L. (2011) Treatment of Livestock Wastewater Using Wetland of Mineralized Refuse. Journal of Ecology & Rural Environment, 27, 95-99.

[7] Daud, N.N.N., Mansor, N.M., Ahsan, A. and Idrus, S. (2015) Leachate Treatment Using Aged Refuse (AR) as a Biofilter Medium. Polish Journal of Environmental Studies, 24, 605-609.

[8] Hassan, M. and Xie, B. (2014) Use of aged refuse-based bioreactor/biofilter for landfill leachate treatment. Applied Microbiology and Biotechnology, 98,6543-6553.

[9] Amor, C., Torres-Socias, E.D., Peres, J.A., Maldonado, M.I., Oller, I. and Malato, S. (2014) Mature landfill leachate treatment by coagula-

tion/flocculation combined with Fenton and solar photo-Fenton processes. Journal of Hazardous Materials, 286, 261–268.
[10] Gotvajn, A.Z. and Zagorc, J. (2011) Fenton's oxidative treatment of municipal landfill leachate as an alternative to biological process. Desalination, 275,269-275.
[11] He, R., Tian, B.-H., Zhang, Q.-Q. and Zhang, H.-T. (2015) Effect of Fenton oxidation on biodegradability, biotoxicity and dissolved organic matter distribution of concentrated landfill leachate derived from a membrane process. Waste Management, 38,32-239.
[12] Li, J., Lei, Z., Qin, L., Tian, X., Wang, A. and Zhou, Y. (2016) Removal of refractory organics in nanofiltration concentrates of municipal solid waste leachate treatment plants by combined Fenton oxidative-coagulation with photo – Fenton processes. Chemosphere, 146,442-449.
[13] Mohammad, R.S., Mehdi, G.L. and Omid, R. (2011) Evaluation of the main parameters affecting the Fenton oxidation process in municipal landfill leachate treatment. Waste Management & Research the Journal of the International Solid Wastes & Public Cleansing Association Iswa, 29,397-405.
[14] Soraya, M., Hamidi, A. A., Mohammed, A. Z., Leila, M., Mohammed, J.K.B. and Shuokr, Q.A. (2011) Multiple responses analysis and modeling of Fenton process for treatment of high strength landfill leachate. Water Science & Technology A Journal of the International Association on Water Pollution Research, 64, 1652-1660.
[15] Yang, D., Edualberto, R.M. and Xingmao, M. (2012) Effects of inorganic anions on Fenton oxidation of organic species in landfill leachate. Waste Management & Research the Journal of the International Solid Wastes & Public Cleansing Association Iswa, 30, 12-19.
[16] Boumechhour, F., Rabah, K., Lamine, C. and Said, B.M. (2013) Treatment of landfill leachate using Fenton process and coagulation/flocculation. Water & Environment Journal, 27, 114–119.
[17] Gao, A.-F., Peng, Z.-X., Wang, W.-P. andLi, F.-H. (2017) Online monitoring of decolorization kinetics of reactive yellow B-4RFN in Fenton process. Fresen. Environ. Bull.,26, 3415-3421.
[18] Ayas, N., Asci, Y. and Yurdakul, M. (2016) Using of Fe/ZrO2 catalyst to remove Direct Orange 26 from water by Fenton oxidation at wide pH values. Fresen. Environ. Bull.,25, 3272-3279.
[19] Ekici, P., Leupold, G. and Parlar, H.(2001) Degradability of selected azo dye metabolites in activated sludge systems. Chemosphere, 44, 721-728.
[20] Hu, X.-B., Zhao, X., Liu, K.-H. and Ye, X. (2014) Removal of ammonia nitrogen from pretreated electroplating wastewater by oxidation with sodium hypochlorite. Electroplating & Finishing, 33, 214-216.
[21] Lu, X., Liu, W.-J., Tu, Y., Guo, F.-Z., Li, Y. and Xie, L. (2011) Experimental Study on Advanced Treatment of Papermaking Wastewater by NaClO Process [J]. Environmental Science & Technology, 34, 90-92.
[22] Zhang, S.-l., Liu, D. and Cao, C. (2009) Removal of ammonia-nitrogen from wastewater by sodium hypochlorite oxidization [J]. Industrial Water & Wastewater , 44, 602-604,610.
[23] Pourmohammadbagher, A., Jamshidi, E., Ale-Ebrahim, H. and Dabir, S. (2011) Study on Simultaneous Removal of NO x and SO2 with NaClO2 in a Novel Swirl Wet System. Industrial & Engineering Chemistry Research, 50,8278-8284.
[24] Yang, T., Fu, J.-X. and Liang, J. (2005) Experiment of treatment of slightly polluted source water using sodium hypochlorite pre-oxidation process. Industrial Water & Wastewater 36,14-16.
[25] Myers, R.H. and Montgomery, D.C. (1995) Response Surface Methodology: Process and Product Optimization Using Designed Experiments. J.Wiley, 59, 185-186.
[26] Zhu, X., Tian, J., Liu, R. and Chen, L. (2011) Optimization of Fenton and electro-Fenton oxidation of biologically treated coking wastewater using response surface methodology. Separation and Purification Technology, 81,444-450.
[27] Maran, J.P., Sivakumar, V., Sridhar, R. and Immanuel, V.P. (2013) Development of model for mechanical properties of tapioca starch based edible films. Industrial Crops & Products, 42, 159-168.

Received: **15.06.2017**
Accepted: **24.07.2017**

CORRESPONDING AUTHOR

Qing Yu
School of Civil Engineering and Architecture
East China Jiao Tong University
Nanchang, 330013 – P.R.CHINA

E-mail: yuqing171984@163.com

© by PSP Volume 26 – No. 10/2017 pages 6234-6245 Fresenius Environmental Bulletin

SPATIAL AND TEMPORAL DISTRIBUTION OF PHYTOPLANKTON IN KARKAMIS DAM LAKE (SANLIURFA/TURKEY)

Feray Sonmez[1,*], Banu Kutlu[2], Ahmet Sesli[3]

[1]Fırat University, Fisheries Faculty, Department of Basic Aquatic Sciences, 23119, Elazig, Turkey
[2]Munzur University, Fisheries Faculty, Department of Basic Aquatic Sciences, Tunceli, Turkey
[3]Fisheries Research Institute, Elazig, Turkey

ABSTRACT

The environmental factors that affect the seasonal change of the phytoplankton community and composition in Karkamis Dam Lake were investigated on samples taken from five stations between January 2015 and December 2015. It was found that the phytoplankton of Karkamis Dam Lake consisted of 85 taxa belonging to Bacillariophyta (56 taxa), Chlorophyta (15 taxa), Chrysophyta (1 taxon), Cyanophyta (10 taxa), Dinophyta (2 taxa) and Euglenophyta (1 taxon). Members of Bacillariophyta and Chrysophyta increased well during spring, summer and also at the end of fall whilst Chlorophyta grew well only in summer and fall. Cyanophyta became dominant at the end of spring and in summer. However Dinophyta was remarkably conspicuous in winter as well as in spring and fall in terms of prevalence. Excessive reproduction of Cyanobacteria, which is a characteristic aspect of mesotrophic lakes, was observed in Karkamis Dam Lake in both May and July. Results of physical and chemical measurements and analysis indicated that the lake was mesotrophic based on PCA and Carlson trophic state index. Phytoplankton composition was found to be affected by environmental factors such as temperature, pH, dissolved oxygen, phosphate and nitrate through the year. Using these data, a strong model was developed for sustainable management in Karkamis Dam Lake.

KEYWORDS:
Phytoplankton, nutrient, Karkamis Dam Lake, Sanliurfa, Turkey.

INTRODUCTION

Dams are one of the most significant effects created on the hydrological regimes of streams by the humankind [1]. The genuine physico-chemical and biological characters of dam lakes are formed due to seasonal, periodical filling, emptying by humans and fluctuations on the surface levels based on these. These water movements are generally defined as unstable environments [2].

Phytoplankton reacts to the physical and chemical changes in the structure of a lake ecosystem most quickly. The changes taking place in the lake ecosystem affect the phytoplankton community first. These changes lead to a transformation in the species composition of phytoplankton and dominance of algal species community. This change influences a set of living being up to the ones on the highest levels of the food pyramid [3, 4]. Phytoplankton communities may show changes in numbers based especially on the physico-chemical (water temperature, pH, dissolved oxygen, etc.) changes in the water [5-8]. Additionally, it was reported that the hydrological factors of dam lakes such as water level, water flow and water-holding capacity are highly significant in phytoplankton development [9].

As phytoplankton reacts to environmental changes quickly, they are an important factor in determination of the environmental pollution and trophic levels of lakes and rivers. Several researchers accept dominant phytoplankton communities as indicators in determination of the trophic levels of lakes. Presence, absence or abundance of a species in a region is based on certain ecological conditions and it may be used as an indicator of environmental variables [10].

The present investigation studied the effects of environmental factors on the seasonal growth dynamics and succession of phytoplankton species in a dam lake. It is a well-known fact that monitoring of phytoplankton is a useful tool for investigating eutrophication and environmental degradation in the dam lakes. Particularly chlorophyll-a is an important parameter that can indicate the total biomass of phytoplankton and the progress of primary production. However, total phytoplankton alone is not generally enough to conduct a full investigation [11-15]. Thus such studies should include physico-chemical properties of the studied ecosystem as well.

This study aimed to determine monthly changes in the phytoplankton composition and abundance in different algal groups for the first time in the Karkamis Dam Lake established on River Euphrates.

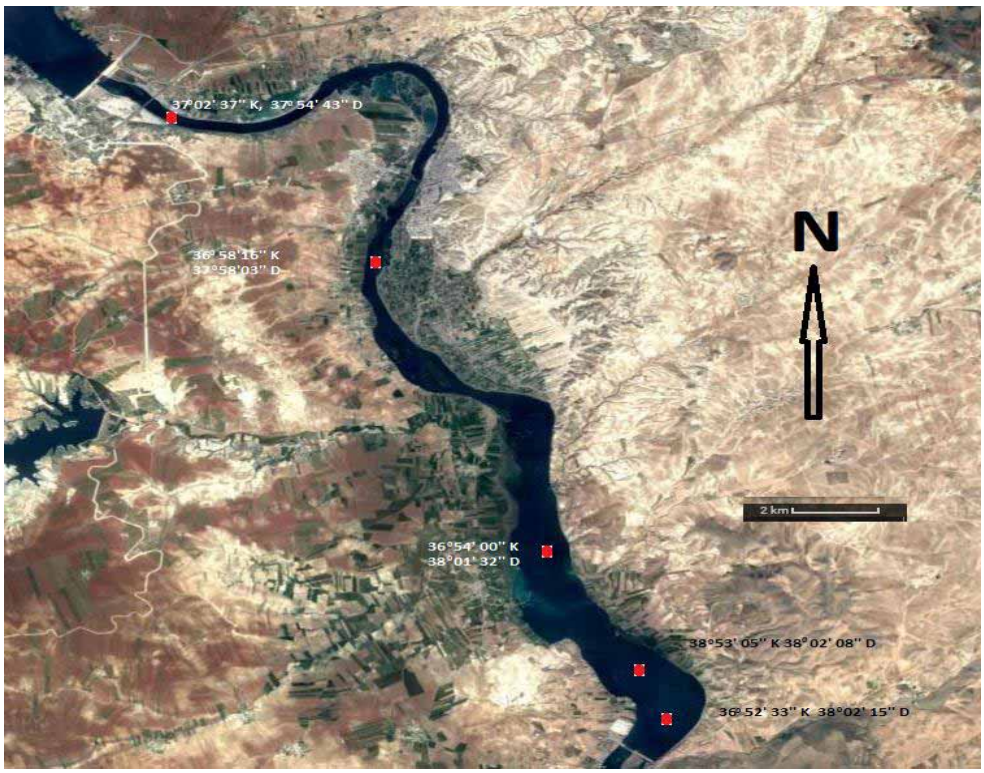

FIGURE 1
Karkamis Dam Lake and sampling stations

MATERIALS AND METHODS

Karkamis Dam Lake, which constitutes a part of the Southeastern Anatolia Project, is constructed on River Euphrates constructed in the form of concrete weight and earth fill. It is important to note that the dam is the first implementation in turkey that was carried out with the definition of a river power plant. The study was conducted at 5 stations for 12 months between January 2015 and December 2015 (Fig. 1). The selected research stations were the output water of Birecik Dam Lake, the Birecik district, before fishing farms, after fishing farms and the dam wall.

A YSI professional plus measurement device was used to measure water temperature, dissolved oxygen, oxygen saturation, pH and electrical conductivity, while a Secchi disk was used to measure light transmittance. Chlorophyll-a was measured by fluorometric determination of the acetone extract of a Whatman GF/C filter, through which a known volume of the sample was filtered [16]. Total particle nitrogen (TPN) was calculated by the difference between total nitrogen and total dissolved nitrogen (TPN=TN-TDN). Trophic index was calculated by Carlson's method [17].

Phytoplankton sampling was carried out on the surface of water by using plankton net of the brand Hydro-Bios with a brim diameter of 25 cm and pore width of 55 µm. The samples were placed in sterilized bottles and fixed by adding 4% formaldehyde. They were left for 24 hours to achieve precipitation, and then used for qualitative and quantitative analyses.

An Olympus CX21FS1 microscope was used to identify the species taken from the dam lake, and an Olympus CKX41 inverted microscope was used for counting individuals. The samples were shaken to achieve homogenous distribution, and 1 ml of sample was taken to determine the number of individuals. Average values were obtained out of five repetitions [18]. The following formula was used to determine the numbers of individuals;

$$\textbf{Lt:}\frac{250\ .(\ 2cc\ phytoplankton\ number)}{2\ .\ \pi.\ r^2.\ h}\ [18]$$

Mainly [19-32] were used for the identification of phytoplankton species. The accuracy of the current names of the species was achieved through the website www.algaebase.org [33].

Statistical analysis. The significance level for statistical analyses was 0.005. Non-parametric statistics (Wilcoxon test) were used to compare stations. The number of algal taxa present in each sample was considered as species richness. Biological diversity (H') was determined by the methodology of Shannon and Weaver [34]. The procedures of the analyses were carried out using the XLSTAT-ADA and Primer package software.

TABLE 1
Range, mean values, median and standard deviation of physical and chemical variables of Karkamis Dam Lake during the study period.

		J	F	M	A	M	J	J	A	S	D	O	N
Water temperature (°C)	**Mean**	2.7	3.4	3.3	3.0	2.8	2.6	2.12	1.6	1.7	1.8	2.8	1.9
	Min.	2.7	3.4	3.3	3.0	2.8	2.6	2.12	1.6	1.7	1.8	2.8	1.9
	Max	2.7	3.4	3.3	3.0	2.8	2.6	2.12	1.6	1.7	1.8	2.8	1.9
pH	**Mean**	2.7	3.4	3.3	3.0	2.8	2.6	2.12	1.6	1.7	1.8	2.8	1.9
	Min.	2.7	3.4	3.3	3.0	2.8	2.6	2.12	1.6	1.7	1.8	2.8	1.9
	Max	2.7	3.4	3.3	3.0	2.8	2.6	2.12	1.6	1.7	1.8	2.8	1.9
DO (mg/L)	**Mean**	2.7	3.4	3.3	3.0	2.8	2.6	2.12	1.6	1.7	1.8	2.8	1.9
	Min.	2.7	3.4	3.3	3.0	2.8	2.6	2.12	1.6	1.7	1.8	2.8	1.9
	Max	2.7	3.4	3.3	3.0	2.8	2.6	2.12	1.6	1.7	1.8	2.8	1.9
NO_3-N(mg/L)	**Mean**	2.7	3.4	3.3	3.0	2.8	2.6	2.12	1.6	1.7	1.8	2.8	1.9
	Min.	2.7	3.4	3.3	3.0	2.8	2.6	2.12	1.6	1.7	1.8	2.8	1.9
	Max	2.7	3.4	3.3	3.0	2.8	2.6	2.12	1.6	1.7	1.8	2.8	1.9
TP (mg PO_4^{-3}-P/L)	**Mean**	2.7	3.4	3.3	3.0	2.8	2.6	2.12	1.6	1.7	1.8	2.8	1.9
	Min.	2.7	3.4	3.3	3.0	2.8	2.6	2.12	1.6	1.7	1.8	2.8	1.9
	Max	2.7	3.4	3.3	3.0	2.8	2.6	2.12	1.6	1.7	1.8	2.8	1.9
Secchi Disc (m)	**Mean**	2.7	3.4	3.3	3.0	2.8	2.6	2.12	1.6	1.7	1.8	2.8	1.9
	Min.	2.7	3.4	3.3	3.0	2.8	2.6	2.12	1.6	1.7	1.8	2.8	1.9
	Max	2.7	3.4	3.3	3.0	2.8	2.6	2.12	1.6	1.7	1.8	2.8	1.9
Chlorophyll-a (µg /L)	**Mean**	2.7	3.4	3.3	3.0	2.8	2.6	2.12	1.6	1.7	1.8	2.8	1.9
	Min.	2.7	3.4	3.3	3.0	2.8	2.6	2.12	1.6	1.7	1.8	2.8	1.9
	Max	2.7	3.4	3.3	3.0	2.8	2.6	2.12	1.6	1.7	1.8	2.8	1.9

TABLE 2
The Carlson trophic state classification (TSI) of Karkamis Dam Lake [12]

	Surface	
	TSI	Level
TSI (TP)	44	M
TSI (CHL)	26	M
TSI (SD)	34	O
	0 m	
Trophic Level	Mesotrophic	

RESULTS

Physico-Chemical Parameters. Table 1 shows the physico-chemical properties of Karkamis Dam Lake. The mean values of surface water temperature were found in the range of 9.4-21.6 ºC through the year, and this was not found to be statistically significant (Wilcoxon test; P>0.05). The mean pH values were in the range of 7.85-9.13 (P>0.05). The amount of dissolved oxygen was calculated in the range of 9.1-11.8 mg L^{-1} (P>0.05). The monthly amounts of nitrite (NO_2^--N) was found in the range of 0.006-0.107 mg L^{-1}, while this range for nitrate (NO_3^--N) was 1.549-3.473 mg L^{-1}. The obtained values were analyzed statistically, and differences were not found significant(P>0.05). The mean monthly dissolved reactive phosphorus (mg PO_4^{-3}-P/L) and total phosphorus amounts were calculated as 0.007-0.022 mg L^{-1} (P>0.05) respectively.

The minimum Secchi disk depth in Karkamis Dam Lake was measured as 3 m in the 2nd station (June) and the maximum was measured as 8 m in the 3rd and 4th stations in February, April and October. The mean annual Secchi disk depth was calculated as 5.9±1.1 m and the mean monthly Secchi disk depth in the dam lake changed between 4.2±0.6 m and 7.2±1.3 m (Table 1). During the study, the differences among the sampling sites in terms of Secchi disk depth were not found statistically significant (Wilcoxon test; P>0.05).

In Karkamis Dam Lake, TSI (SD) values were in the range of 24-30, and TSI (TP) values were in the range of 23-29. The minimum value was found in the 3rd station, while the maximum was found in the 1st station. TSI (CHL) was determined to be in the range of 40-42 (Table 2).

Phytoplankton Community. During the study, the phytoplankton of Karkamış Dam Lake were from 85 taxa including 56 in Bacillariophyta, 15 in Chlorophyta, 1 in Chrysophyta, 10 in Cyanophyta, 2 in Dinophyta and 1 in Euglenophyta. 44 of these taxa were significant because they were found in all stations. The most frequently represented algae from these groups were *Gomphonema* (8 taxa), *Epithemia*, *Fragilaria*, *Navicula* and *Ulnaria* (4 taxa each), *Cymbella, Gyrosigma* and *Nitzschia* (3 taxa each) from Bacillariophyta, and *Phormidium* (3 taxa) from Cyanophyta. Based on the data, the highest number of taxa was found in the 2nd station (59 taxa), while the lowest taxa was found in the 5th station (50 taxa) (Fig.2).

Among all algae, 30 taxa from Bacillariophyta and 5 taxa from Cholorophyta were recorded in all stations. These algae are; *Asterionella formosa,Aulacoseira granulata var. angustissima, Campylodiscus noricus, Cocconeis pediculus, Cocconeis placentula, Cymatopleura solea, Cymbella affinis, Cymbella cistula, Cymbella cymbiformis, Diatoma vulgaris, Ellerbeckia arenaria, Epithemia argus, Epithemia turgida, Fragilaria acus, Fragilaria brevistriata, Fragilaria crotonensis, Gomphonema acuminatum, Gomphonema olivaceum, Gomphonema truncatum, Gyrosigma acuminatum, Gyrosigma balticum, Halamphora veneta, Navicula rhynchocephala, Nitzschia sigma, Rhoicosphenia abbreviata, Tryblionella levidensis, Ulnaria amphirhynchus*, *Ulnaria capitata, Ulnaria delicatissima var. angustissima* and *Ulnaria ulna* (30 species) from Bacillariophyta, *Microspora tumidula, Pediastrum duplex, Spirogyra affinis*, *Volvox aureus* and *Zygnema circumcarinatum* (5 species) from Chlorophyta. *Dinobryon divergens* (1 species) from Chrysophyta, *Geitlerinema amphibium, Lyngbya major, Oscillatoria limosa*, *Oscillatoria tenuis, Phormidium breve* and *Phormidium lucidum* (6 species) from Cyanophyta, and *Ceratium hirundinella* and *Peridinium cinctum* (2 species) from Dinophyta (Table 3).

Station 1. A total of 54 taxa were recorded in the 1st station belonging to Bacillariophyta (36 taxa), Chlorophyta (9 taxa), Chrysophyta (1 taxon), Cyanophyta (6 taxa), Dinophyta (2 taxa) and Euglenophyta (1 taxon). The genera represented by the highest number of species were *Gomphonema* (5 taxa), *Fragilaria* and *Ulnaria* (4 taxa each), *Cymbella* and *Epithemia* (3 taxa each) from Bacillariophyta. The number of individuals (26702 individuals/L) was the highest in March and the lowest (702 individuals/L) in January.The highest number of species (18 taxa) was recorded in July and October and the lowest (4 taxa) was in January.

Station 2. A total of 59 taxa were recorded in the 2nd station from Bacillariophyta (43 taxa), Chlorophyta (8 taxa), Chrysophyta (1 taxon), Cyanophyta (5 taxa) and Dinophyta (2 taxa). The genera represented by the highest number of species were *Gomphonema* (5 taxa), *Navicula* and *Ulnaria* (4 taxa each), *Cymbella* and *Epithemia, Fragilaria* and *Gyrosigma* (3 taxa each) from Bacillariophyta. The number of individuals to be the highest in July (5122 individuals/L) and the lowest in November (286 individuals/L), while the maximum number of taxa was recorded in July (25 taxa) and the minimum was recorded in March and April (7 taxa).

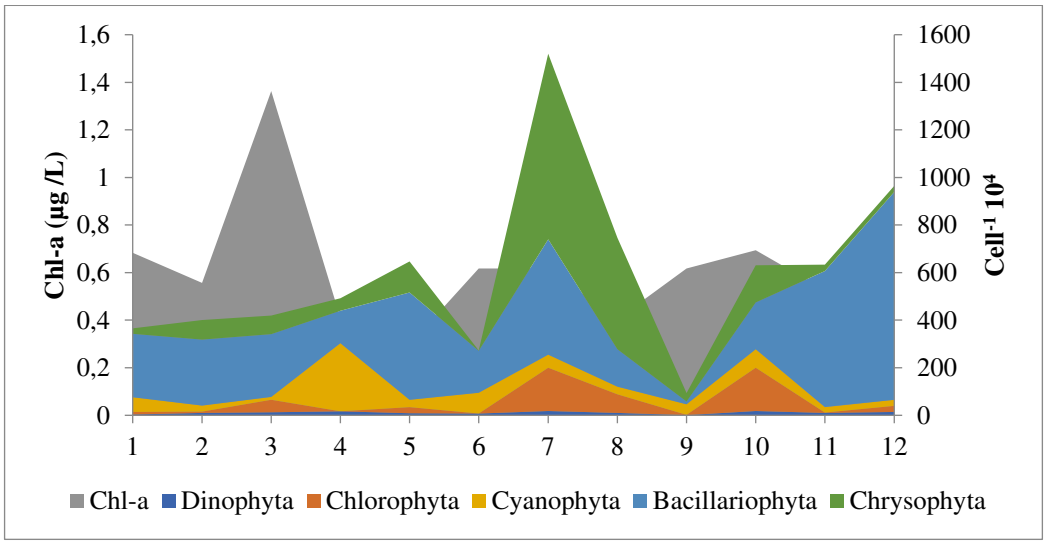

FIGURE 2
The number of planktonic algal counts and Chlorophyll–a concentration at stations

TABLE 3
The list of algae recorded in phytoplankton of Karkamis Dam Lake

	Stations				
Taxa	I	II	III	IV	V
Bacillariophyta					
Achnanthidium minutissimum (Kützing) Czarnecki	+		+		
Amphora ovalis (Kützing) Kützing			+		
Asterionella formosa Hassall	+	+	+	+	+
Aulacoseira granulata var. angustissima (O.F. Müller) Simonsen	+	+	+	+	+
Brebissonia lanceolata (C. Agardh) Mahoney & Reimer		+			
Campylodiscus noricus Ehrenberg ex Kützing	+	+	+	+	+
Cocconeis pediculus Ehrenberg	+	+	+	+	+
Cocconeis placentula Ehrenberg	+	+	+	+	+
Craticula ambigua (Ehrenberg) D.G. Mann			+		
Ctenophora pulchella (Ralfs ex Kützing) D.M. Williams & Round					+
Cyclotella meneghiniana Kützing	+			+	
Cymatopleura elliptica (Brébisson) W. Smith		+			
Cymatopleura solea (Brébisson) W. Smith	+	+	+	+	+
Cymbella affinis Kützing	+	+	+	+	+
Cymbella cistula (Ehrenberg) O. Kirchner	+	+	+	+	+
Cymbella cymbiformis C. Agardh	+	+	+	+	+
Cymbopleura cuspidata (Kützing) Krammer				+	
Diatoma vulgaris Bory de Saint-Vincent	+	+	+	+	+
Ellerbeckia arenaria (G. Moore ex Ralfs) R.M. Crawford	+	+	+	+	+
Encyonema caespitosum Kützing			+		
Epithemia adnata(Kützing) Brébisson	+				
Epithemia argus (Ehrenberg) Kützing	+	+	+	+	+
Epithemia sorex Kützing		+			
Epithemia turgida (Ehrenberg) Kützing	+	+	+	+	+
Fragilaria acus (Kützing) Lange-Bertalot	+	+	+	+	+
Fragilaria brevistriata Grunow	+	+	+	+	+
Fragilaria capucinaDesmazières	+			+	
Fragilaria crotonensis Kitton	+	+	+	+	+
Gomphonema acuminatum Ehrenberg	+	+	+	+	+
Gomphonema angustatum (Kützing) Rabenhorst				+	+
Gomphonema gracile Ehrenberg	+				+
Gomphonema grunowii R.M. Patrick & Reimer	+	+			
Gomphonema intricatum Kützing				+	
Gomphonema longiceps Ehrenberg		+			+
Gomphonema olivaceum(Hornemann) Brébisson	+	+	+	+	+
Gomphonema truncatum Ehrenberg	+	+	+	+	+
Gyrosigma acuminatum (Kützing) Rabenhorst	+	+	+	+	+
Gyrosigma balticum(Ehrenberg) Rabenhorst	+	+	+	+	+
Gyrosigma strigile (W. Smith) Cleve		+			
Halamphora veneta (Kützing) Levkov	+	+	+	+	+
Navicula capitatoradiata H. Germain		+			
Navicula oblonga (Kützing) Kützing		+			
Navicula radiosa Kützing		+	+		
Navicula rhynchocephala Kützing	+	+	+	+	+
Nitzschia intermedia Hantzsch in Cleve & Grunow				+	
Nitzschia palea (Kützing) W. Smith				+	
Nitzschia sigma(Kützing) W. Smith	+	+	+	+	+
Pleurosigma angulatum (J.T. Queckett) W. Smith		+			
Rhoicosphenia abbreviata (C. Agardh) Lange-Bertalot	+	+	+	+	+
Stauroneis phoenicenteron (Nitzsch) Ehrenberg		+			
Stephanodiscus hantzschii Grunow in Cleve & Grunow		+			
Tryblionella levidensis W. Smith	+	+	+	+	+
Ulnariaamphirhynchus (Ehrenberg) Compère & Bukhtiyarova	+	+	+	+	+
Ulnaria capitata (Ehrenberg) P. Compère	+	+	+	+	+

	Stations				
Taxa	I	II	III	IV	V
Ulnaria delicatissima var. angustissima (Grunow) M. Aboal & P.C. Silva	+	+	+	+	+
Ulnaria ulna (Nitzsch) P. Compère	+	+	+	+	+
Chlorophyta					
Chlorella vulgaris Beyerinck [Beijerinck]	+				
Coelastrum microporum Nägeli in A. Braun			+	+	
Cosmarium subcostatum var. *beckii* (Gutwinski) West & G.S. West			+		
Hydrodictyon reticulatum (Linnaeus) Bory					+
Microspora tumidula Hazen	+	+	+	+	+
Monactinus simplex (Meyen) Corda	+	+			
Pandorina morum (O.F. Müller) Bory de Saint-Vincent			+	+	
Pediastrum duplex Meyen	+	+	+	+	+
Pseudopediastrum boryanum (Turpin) E. Hegewald	+				
Scenedesmus arcuatus(Lemmermann) Lemmermann		+	+		
Spirogyra affinis (Hassall) Petit	+	+	+	+	+
Stigeoclonium tenue (C. Agardh) Kützing		+			
Tetraëdriella regularis (Kützing) Fott	+				
Volvox auerus Ehrenberg	+	+	+	+	+
Zygnemacircumcarinatum Czurda	+	+	+	+	+
Chrysophyta					
Dinobryon divergens O.E. Imhof	+	+	+	+	+
Cyanophyta					
Geitlerinema amphibium (C. Agardh ex Gomont) Anagnostidis	+	+	+	+	+
Gloeocapsa alpina Nägeli in Rabenhorst			+		
Lyngbya major Meneghini ex Gomont	+	+	+	+	+
Microcystis aeruginosa (Kützing) Kützing				+	+
*Oscillatoria limosa*C.Agardh ex Gomont	+	+	+	+	+
*Oscillatoria tenuis*C.Agardh ex Gomont	+	+	+	+	+
Phormidium breve (Kützing ex Gomont) Anagnostidis & Komárek	+	+	+	+	+
Phormidium lucidum Kützing ex Gomont	+	+	+	+	+
Phormidium subfuscum Kützing ex Gomont			+	+	
Spirulina major Kützing ex Gomont				+	
Dinophyta					
Ceratium hirundinella (O.F. Müller) Dujardin	+	+	+	+	+
Peridinium cinctum (O.F. Müller) Ehrenberg	+	+	+	+	+
Euglenophyta					
Phacus pleuronectes (O.F. Müller) Nitzsch ex Dujardin			+		
Taxa Number	54	59	56	56	50

Station 3. A total of 56 taxa were recorded in the 3rd station from Bacillariophyta (35 taxa), Chlorophyta (9 taxa), Chrysophyta (1 taxon), Cyanophyta (8 taxa), Dinophyta (2 taxa) and Euglenophyta (1 taxon). The genera represented by the highest numbers of species were *Gomphonema* (3 taxa), *Cymbella, Fragilaria* and *Ulnaria* (3 taxa each) from Bacillariophyta and *Phormidium* (3 taxa) from Cyanophyta. The highest number of individuals in the third station was recorded in March (5200 individuals/L) and the lowest was recorded in June (364 individuals/L), while the maximum number of taxa was recorded in October (17 taxa) and the minimum was recorded in June (4 taxa). It is noteworthy that, while the number of taxa was low (5 taxa) in March, this month had the highest intensity of individuals (5200 individuals/L). However, this contradictory situation is an indicator that the species *Ulnaria ulna* utilizes the environmental conditions in March better than others and it is able to show better development.

Station 4. A total of 56 taxa were recorded in the 4th station from Bacillariophyta (38 taxa), Chlorophyta (6 taxa), Chrysophyta (1 taxon), Cyanophyta (9 taxa) and Dinophyta (2 taxa). The genera represented by the highest numbers of species were *Gomphonema* (5 taxa), *Fragilaria* and *Ulnaria* (4 taxa each), *Cymbella* (3 taxa) from Bacillariophyta, and *Phormidium* (3 taxa) from Cyanophyta. The highest number of individuals in the 4th station was recorded in March (11674 individuals/L) and the lowest was recorded in October (364 individuals/L), while the maximum number of taxa was recorded in July (16 taxa) and the minimum was recorded in May (3 taxa).

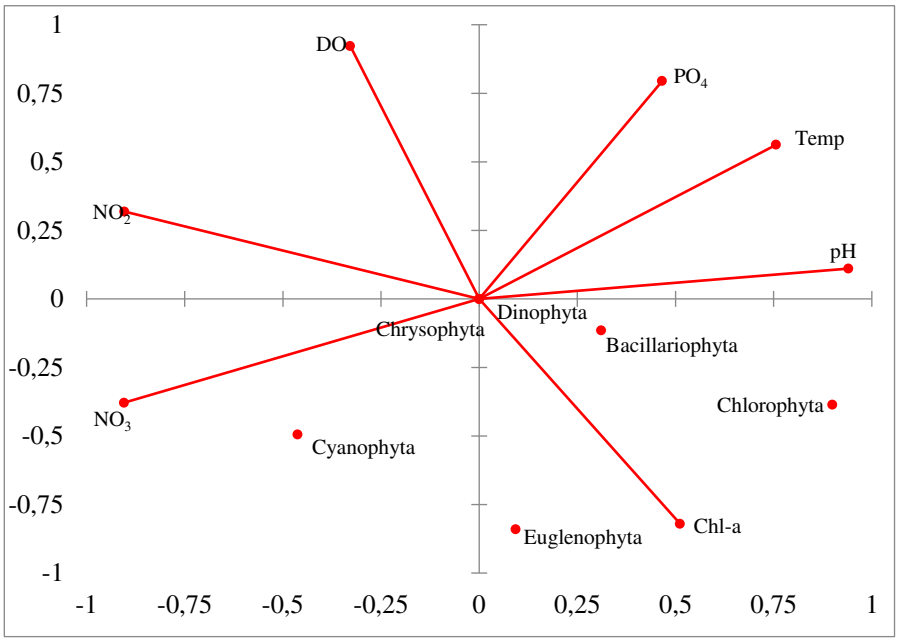

FIGURE 3
Principal component analysis (PCA) of physico-chemical variables and main phytoplankton groups. (Abbreviations: CHLa, Chlorophyll-a; DO, dissolved oxygen; nitrogen; NO_3 N, nitrate nitrogen; TP, total phosphate; TEMP, temperature; Cyanophyta; Chlorophyta; Euglenophyta; Bacillariophyta; Cryptophyta; Dinophyta; Chrysophyta)

Station 5. A total of 50 taxa were recorded in the 5th station from Bacillariophyta (34 taxa), Chlorophyta (6 taxa), Chrysophyta (1 taxon), Cyanophyta (7 taxa) and Dinophyta (2 taxa). The genera represented by the highest numbers of species were *Gomphonema* (6 taxa), *Ulnaria* (4 taxa), *Cymbella* and *Fragilaria* (3 taxa each) from Bacillariophyta. The highest number of individuals in the 5th station was recorded in March (39676 individuals/L) and the lowest was recorded in May and August (78 individuals/L), while the maximum number of taxa was recorded in April (20 taxa) and the minimum was recorded in May (2 taxa).

According to the Shannon-Wiener index, the species density of the algae in the lake was found as 1.69. The maximum density was found as 3.98 in the 4thstation in September, and the minimum density was found as 0.37 in the 3rd station in 0.37.

The influence of the measured physico-chemical variables on the abundance of phytoplankton groups was assessed using two main factors that explained 78.1% of the total variance at the lake. The first axis was closely related to Dinophyta and PO_4, and the second axis was closely related to Dinophyta and Euglenophyta (Fig.3).

DISCUSSION

The mean annual temperature of surface water of Karkamis Dam Lake was 14.3 ºC, and a mean Secchi disk depth was determined as 5.9±1.1 m. Concentrations of Chlorophyll-a changed in the range of 0.1 - 1.74 µg /L, pH in the range of 7.85 - 9.13. The mean amount of dissolved oxygen was 10 mg/L. While tropholytic reactions that consume oxygen take place in a wide hypolimnion layer in deep lakes, they take place in the entire water column in shallow lakes, which explains that shallow lakes with the same surface area store less oxygen than deep lakes do [35].

Secchi disk visibility in Karkamis Dam Lake changed throughout the study. The mean values were in the range of 5.9±1.1 m. Visibility reach 9 m in February, April and November. The light transmittance values obtained in our study were lower in comparison to those of oligotrophic lakes [36]. In the previous studies in the area, visibility values were found as 3.2 and 6.5 m [37]. Light is a major resource for phytoplankton and has a complex pattern of spatial and temporal variability [38]. Suspended matter in lake water increased in autumn and spring, resulting in minimum transparency. During the summer, the transparency was at its maximum level. There was also a significant correlation between the growth of phytoplankton and transparency in Karkamis Dam Lake since the largest populations of all algae occurred during the summer whilst individual numbers were low in winter.

The monthly phytoplankton abundance of Karkamis Dam Lake related to water temperature, light transmittance and nutrient concentration. A strong relationship was found in other studies between phytoplankton composition and water temperature [39-41] since water temperature affects abundance and

reproduction of algae directly. The seasonal succession and species composition of the phytoplankton were similar all stations during the study. The reasons for the similarities might be due to similar environmental conditions at the stations. The increase in phytoplankton during the spring and summer months in Karkamis Dam Lake could be a result of the increasing water temperature.

According to data obtained, no relation was observed between phytoplankton growth and pH level since high and low individual numbers were observed at similar pH levels [42].

Nutrients such as TN and TP were relatively high, while phytoplankton biomass and Chlorophyll-a were relatively low while diatoms were still dominating the phytoplankton in Karkamis Dam Lake. These findings suggest that phytoplankton dynamics in Karkamis Dam Lake might be affected not only by the nutrients, but also by other factors [43].

It was reported concentration of chlorophyll-a as 5-140 µg/L for eutrophic lakes, 1-15 µg/L for mesotrophic lakes and 0.3- 2.5 µg/L for oligotrophic lakes [44]. The concentration of the chlorophyll-a in Karkamis Dam Lake (0.100-1.749 µg/L) were relatively low indicating oligotrophic status of the dam lake. On the other hand, the chlorophyll-a value observed through the year (0.617 µg L^{-1}) was comparable to the one reported by Morkoyunlu Yuce et al. [37] (1.14 µg L^{-1}). It is known that, in shallow lakes and ponds, benthic material is carried into the water column as a result of water movements [45]. In this case, it may be misleading to determine the trophic state in shallow lakes only by considering light transmittance. In this study, the lake was identified to be in the limit of mesotrophic state based on the TDI and mean TDI values calculated from chlorophyll-a and Secchi disk measurement values.

The data related to the concentrations of nitrogenous compounds in Karkamis Dam Lake were similar to those of Morkoyunlu Yuce et al. [37]. The mean nitrite amount was 0.019 mg/L. The monthly average changed in the range of 0.001- 0.175 mg/L whilst the mean nitrate amount was 2.292 mg/L. The amount of dissolved reactive phosphorus was 0.034 mg/L and the mean annual total phosphorus amount in the surface water was 0.016 mg P/L. According to the data obtained from the surface water column, it was found that phosphorus is a restrictive nutrient in the dam lake, and this result agreed with those of other studies [46]. Differences of the spatial and temporal change in the parameters among stations of study were not statistically significant, and this showed that there was spatial homogeneity in the dam lake.

The largest share of the phytoplankton belonged to Bacillariophyta (56 taxa) in Karkamis Dam Lake. The highest number of taxa (59) was found in the 2nd station, while the lowest number (50) was recorded in the 5th station. The species composition of the phytoplankton of Karkamis Dam Lake showed similarities to those of many lakes and reservoirs in Turkey [47-56].

The species diversity of Bacillariophyta was the highest in spring followed by summer, and the lowest in winter and fall. *Fragilaria crotonensis* and *Asterionella formosa*, which were reported to be found in eutrophic waters by Reynolds et al. [33], were identified in Lake Karkamış in almost all seasons. *Cyclotella* species are accepted by various authors as the characteristic indicator of oligotrophic and mesotrophic lakes [57, 58]. According to the data in the literature, it was reported that *Cyclotella* species were the specific species of oligotrophic lakes, and related to the trophic status of the lake [59]. On the other hand, *Cyclotella* species are among sub-species in eutrophic lakes in Turkey [60]. *Cyclotella* was reported to be found abundantly in lakes that are poor in nutrients, and species like *Cyclotella meneghiniana* may be dominant in intermediate-sized eutrophic lakes [38]. In the shallow (the mean depth: 2 m) and nutrient-rich Karkamis Dam Lake, it was found that *Cyclotella meneghiniana* developed in fall, winter and spring in the 1st and 4th stations, where water is mixed well. A centric diatom, *Aulacoseira granulata var. angustissima* was found in the phytoplankton composition of all stations in winter and fall. It was reported that *Aulacoseira* spp. may be abundant and dominant in dam lakes with muddy conditions [57, 61]. *Ulnaria ulna* was the most significant species in all stations. *Fragilaria* species were the second most abundant species following the *Ulnaria* genus in Karkamis Dam Lake.

Chlorophyta members were observed in summer months the most. The vast majority of this group consisted of Chlorococcales members. Especially *Botryococcus braunii*, reported by Reynolds et al. [43] to prefer lakes with a clean epilimnion layer and be tolerant for muddiness, was found within the phytoplankton of Karkamis Dam Lake in almost all seasons. *Pediastrum boryanum* and *P. duplex*, reported by Rawson [62] and Bellinger and Siegee [63] to be the indicator of mesotrophic lakes. In the present study, these green algae were taxa that were frequently seen in summer, winter and spring months. Members of Volvocales were observed in summer months with noticeable appearance of *Eudorina elegans*, *Pandorina morum* and *Volvox glabator*. It was reported that these taxa are abundant in eutrophic dam lakes that are rich in minerals [43]. Especially *Pediastrum* species were found abundantly in eutrophic lakes rather than oligotrophic lakes. In our study, these algae encountered in all stations, especially in summer months.

Although Cyanophyta species were observed mostly in spring and summer months, they were encountered with much less numbers in fall and winter. Excessive Cyanophyta development in summer may be explained by sufficient amount of nutrients and high water temperature [61, 64, 65]. *Lyngbya major*

and *Oscillatoria limosa* were recorded in almost all stations in spring, while *Phormidium lucidum* occurred only in winter. Cyanophytes may have caused the color of the water to turn into green in Karkamis Dam Lake. It was shown that Cyanophyta species are found abundantly in eutrophic lakes [66, 67]. Moreover, in cases where water movements are stable and in lake environments rich in nitrate, these species reproduce with an increase in water temperature [43].

Chrysophyta species in Karkamis Dam Lake generally start to appear in stations with increasing temperature. The Chrysophyta species *Dinobryon divergens* was found in all stations, and seemed to be affected by nitrate and phosphate. Studies revealed that phosphate and nitrate have an influence on this species. This species was also observed in Karkamis Dam Lake. Additionally, Chrysophyta species that occur in the environment with decreased water temperatures were also observed in the lake [43].

Two taxa of the Dinophyta were found in the lake particularly in summer months and Dinoflagellate *Ceratium hirundinella* was observed throughout the summer and fall months. It was reported that this alga is an indicator of mesotrophic waters mostly found in the epilimnion of eutrophic lakes in summer months. Although other dinoflagellates *Peridinium* and *Ceratium* species that generally prefer eutrophic lakes were also reported in mesotrophic lakes [43, 50].

It was reported that shallowing of waters and intensity of organic matter create suitable conditions for Euglenophyta species which were reported to be found rather in shallow waters that are rich of organic matter [68]. Euglenophyta was represented with a few taxa in the phytoplankton of Lake Karkamis and *Phacus pleuronectes* was observed in the 3thstation in summer months.

The Trophic State Index developed by Carlson [17] is used today in various limnological studies to determine the efficiency of benthic habitats [69-71]. Karkamis Dam Lake was found to be a mesotrophic lake, and this result is in parallel to those in other studies in the literature [37, 71].

ACKNOWLEDGEMENTS

This study was supported as an individual project with YLTUB016-06 number by Munzur University Scientific Research Projects (MUSRP). The author specially thanks to Prof. Dr. Bulent Sen for his valuable critics and advice.

REFERENCES

[1] Perez, M.C., Bonilla, S. and Martinez, G. (1999) Phytoplankton community of a polymictic reservoir, La Plata River basin, Uruguay. Brazilian Journal of Biology. 59(4): 535-541.

[2] Geraldes, A.M. and Boavida, M.J. (1999) Limnological comparison of a new reservoir with one almost 40 years old which had been totally emptied and refilled, Lakes & Reservoirs. Research and management 4: 15-22.

[3] Habib, O.A., Tippert, R. and Murphy, K.J. (1997) Seasonal changes in phytoplankton community structure in relation to physico-chemical factors in Koch Lomond, Scotland. Hydrobiologia 350: 63-79.

[4] Burford, M.A. and Davis, T.W. (2011) Physical and chemical process promoting dominace of the toxis cyanobacterium Cylindrospermopsis raciborskii. Chinese Journal of Oceanology and Limnology 29: 883-891.

[5] Canfield, D.E., Philips, E. and Duarte, C.M. (1989) Factors influencing the abundance of blue-green algae in Florida lakes. Can. J. Fish. Aquat. Sci. 46: 1232-1237.

[6] Agusti, S., Duarte, C.M. and Canfield, D.E. (1990) Phytoplankton abundance in Florida lakes: evidence for the frequent lack of nutrient limitation. Limnology- Oceanogr.35, 181-188.

[7] Philips, E.J., Cichra, M., Aldridge, F.J., Jembeck, J., Hendrickson, J. and Brody, R. (2000) Light availability and variationsin phytoplankton standing crops in a nutrient-rich blackwater river. Limnol, Oceanogr 45,916-929.

[8] Srifa, A., Philips, E.J., Cichra, M.F. and Hendrickson, J.C. (2016) Phytoplankton dynamics in a subtropical lake dominated by cyanobacteria: cyanobacteria 'Like it Hot' and sometimes dr. Aqua. Ecol 50: 163-174.

[9] Lazar, A., Wade, N., Whitehead, A.J. and Neal, C. (2012) Reconciling observed and modeled phytoplankton dynamics in a major lowland UK river, the Thames. Hydrology Research 43(5): 576-588.

[10] Reynolds, C.S., Huszar, V., Kruk, C., Naselli-Flores, L. and Melo, S. (2002) Review towards a functional classification of the freshwater phytoplankton. Journal of Plankton Research, 24: 417-428.

[11] Skejic, S., Vilibic, I., Matijevic, S., Jozic, S., Gladan, Z.N., Morovic, M., Marasovic, I. and Prelesnik, H. (2017) Long-term regulating mechanisms of phytoplankton biomass in a traditional shellfish aquaculture area. Fresen. Environ. Bull., 24(9a), 3001-3013.

[12] Sivri, N., Seker, D.Z., Alganci, U., Basusta, N., Basusta, A. and Akgun, H. (2017) The role of spatial analysis for aquaculture: A case study of Keban Dam Lake. Fresen. Environ. Bull., 26(1), 405-412.

[13] Ozman Say, A.N., Sivri, N., Erturk, A., Seker, D.Z. and Fusheng, L. (2010) Analysis of phytoplankton distribution at the south-western coast of Istanbul utilizing GIS. Fresen. Environ. Bull., 19(9b), 2116-2122.
[14] Wu, W., Li, G., Li, D. and Liu, Y. (2010) Temperature may be the dominating factor on the alternant succession of *Aphanizomenon flos-aquae* and *Microcystis aeruginosa* in Dianchi Lake. Fresen. Environ. Bull., 19(5), 846-853.
[15] Krivokapic, S., Pestoric B., Bosak, S., Kuspilic, G. and Riser, C. W. (2011) Trophic state of Boka Kotorska Bay (south-eastern Adriatic Sea). Fresen. Environ. Bull., 20(8), 1960-1969.
[16] APHA (1995) Standart Methods for the Examination of Water and Waste water. 19th edition. America Public Health Association, Washington, DC. 1075 pp.
[17] Carlson, R.E. (1977) A trophic state index for lakes. Limnology and Oceanography 22(2): 361-369.
[18] Round, F.E. (1981) The Ecology of Algae, Cambridge University press, USA.
[19] Schilling, A.J. (1913) Dinoflagellates. Die susswasserflora Deutschlands, Osterreich und des Schweiz. A. Pascher. Heft 3. Fischer, Jena Co. Germany.
[20] Geitler, L., Pascher, A. (1925) Cyanophyceae. In: Pascher, A. Die Sußwasser-Flora, Deutschlands, Osterreichs und der Schweiz. Heft 12, VEB Gustav Fischer Verlag., Jena. Stuttgart.
[21] Prescott, G.W. (1951) Algae of the Western Great Lakes Area, Exclusive of Desmids and Diatoms. CranBrook Instıtute of Science. Bulletin No: 31 (932).
[22] Bourelly, P. (1968) Les Algues D'eau Douce Algues Jaunes et Brunes. N. Baubes, Paris.
[23] Bourelly, P. (1972) Les Algues D'eau Douce Tome:1, Editions N. Boubee and Cie3, Place Saınt-Andre-Des-Arts. Paris.
[24] Germain, H. (1981) Flora Des Diatmees Diatomophycees, Societe Nouvelle des Editions Boube'e. Paris.
[25] Streble, H. and Krauter, D. (1973) Das Laben im Wassertropfen, Mikroflora und Mikrofauna des Süßwassers Franckh'sche Verlagshandlung, W. Keller&Co., Stuttgart, 336 pp.
[26] Patrick, R. and Reimer, C.W. (1966) The diatoms of the United States, exclusive of Alaska and Hawaii, Volume 1-Fragilariaceae, Eunotiaceae, Achnanthaceae, Naviculaceae. Academy of Natural Sciences of Philadelphia Monograph: 13, USA.
[27] Patrick, R. and Reimer, C.W. (1975) The diatoms of the United States, exclusive of Alaska and Hawaii, Volume 2, Part 1-Entomoneidaceae, Cymbellaceae, Gomphonemaceae, Epithemaceae. Academy of Natural Sciences of Philadelphia Monograph 13, 213 p., USA.
[28] Krammer, K. and Lange-Bertalot, H. (1986) Bacillariophyceae. 1. Teil: Naviculaceae. in Ettl, H., Gerloff, J., Heynig, H. and Mollenhauer, D. (eds.) Susswasser flora von Mitteleuropa, Band 2/1. Gustav Fischer Verlag: Stuttgart, New York.
[29] Krammer, K. and Lange-Bertalot, H. (1988) Bacillariophyceae. 2. Teil: Bacillariaceae, Epithemiaceae, Surirellaceae. in Ettl, H., Gerloff, J., Heynig, H. and Mollenhauer, D. (eds.) Susswasserflora von Mitteleuropa, Band 2/2. VEB Gustav Fischer Verlag: Jena.
[30] Krammer, K. and Lange-Bertalot, H. (1991a) Bacillariophyceae. 3. Teil: Centrales, Fragilariaceae, Eunotiaceae. in Ettl, H., Gerloff, J., Heynig, H. and Mollenhauer, D. (eds.) Susswasserflora von Mitteleuropa, Band 2/3. Gustav Fischer Verlag: Stuttgart, Jena.
[31] Krammer, K. and Lange-Bertalot, H. (1991b) Bacillariophyceae. 4. Teil: Achnanthaceae, Kritische Erganzungen zu Navicula (Lineolatae) und Gomphonema, Gesamtliteraturverzeichnis Teil 1-4. in Ettl, H., Gartner, G., Gerloff, J., Heynig, H. and Mollenhauer, D. (eds.) Susswasserflora von Mitteleuropa, Band 2/4. Gustav Fischer Verlag: Stuttgart Jena.
[32] John, D.M., Whitton, B.A. and Brook, A.J. (2003) The Freshwater Algal Flora of the British Isles, An identification guide to freshwater and terrestrial algae. Cambridge University Press, Cambridge UK.
[33] Guiry, M.D. and Guiry, G.M. (2017) AlgaeBase. World-wide electronic publication, National University of Ireland, Galway. http://www.algaebase.org
[34] Shannon, E.C. and Weaver, W. (1963) The Mathematical Theory of Communication. Urbana, USA: University of Illinois Press.
[35] Lampert, W. and Somer, U. (2007) Limnoecology, The Ecology of Lakes and Streams, second ed. Oxford University Oxford UK.
[36] Vollenweider, R.A. and Kerekes, J.J. (1982) Eutrophication of waters: mon itoring assessment and control. Paris: Organization for Economic Co-operation and Development.
[37] Morkoyunlu Yuce, A., Ertan, O.O. and Yildirim, Z. (2015). Epiphytic and Epilithic Diatoms in Dam Lakes (Euphrates-Turkey). Yunus Research Bulletin 15(3): 45-51.
[38] Litchman, E. and Christopher, A.K. (2001) Klausmeier. Competition of Phytoplankton under Fluctuating Light. The American Natüralist (2): 170-186.
[39] Jaworska, B., Dunalska, J., Gorniak, D. And Bowszys, M. (2014) Phytoplankton dominance structure and abundance as indicators of the trophic state and ecological status of Lake Kortowskie (northeast Poland) restored with selective hypolimnetic withdrawal. Arch Pol Fish; 22 (1): 7-15.

[40] Komarkova, J., Komarek, O. and Hejzlar, J. (2003) Evaluation of the long term monitoring of phytoplankton assemblages in a canyon-shape reservoir using multivariate statistical methods. Hydrobiologia 504 (1–3): 143–157.
[41] Rakocevic, J. (2012) Spatial and temporal distribution of phytoplankton in Lake Skadar. Archives of Biological Sciences 64 (2): 585-595.
[42] Hakanson, S. (1993) Numerical methods for the inference of ph variations in mesotrophic and eutrophic lakes in Southern Sweden-A progress report. Journal Diatom Research. 8 (2): 349-370.
[43] Reynolds, C.S., Descy, J.P. and Padisak, J. (1994) Are phytoplankton dynamics in rivers so different from those in shallow lakes? In: Descy, J.P., Reynolds, C.S., Padisak, J. (eds.) Phytoplankton in turbid environments: Rivers and shallow lakes. Hydrobiologia 289: 1-7.
[44] Sakamoto, M. (1966) Primary production by phytoplankton community in some Japanese lakes and its dependence on lake depth. Arch. Hydrobiol. 62: l-28.
[45] Round, F.E. (1973) The Biology of the Algae (2nd edition). London, Edward Arnold, 278pp.
[46] Laplace-Treyture, C. and Feret, T. (2016) Performance of the Phytoplankton Index for Lakes (IPLAC): Amultimetric phytoplankton index to assess the ecological status of water bodies in France. Ecological Indicators, 69, 686-698.
[47] Cetin, A.K. and Sen, B. (1998) Diatoms (Bacillariophyta) in the phytoplankton of Keban Reservoir and their seasonal variations. Turk Bot. Science 22: 25-33.
[48] Cetin, A.K. (2000) Phytoplankton of Golbasi Lake (Adiyaman, Turkey) and their seasonal variations. Int. J. Algae 2: 87-96.
[49] Cetin, A.K. and Yildirim, V. (2000) Species composition and seasonal variation of the phytoplankton in Surgu Reservoir (Malatya, Turkey). Acta Hydrobiol. 42: 21-28.
[50] Aykulu, G., Albay, M., Akcaalan, R., Tufekci, H. and Aktan, Y. (2006) Species composition, abundance and seasonality of phytoplankton in a moderately deep Turkish lake. Nova Hedwigia 130: 325-338.
[51] Pala, G. (2007) The seasonal variations and planktonic algae on Guluskur Region of Keban Dam Lake: II-Bacillariophyta. Firat University Journal of Science, 19(1): 23-32.
[52] Sevindik Ongun, T. (2010) Phytoplankton composition of Caygoren Reservoir, Balikesir-Turkey. Turkish Journal of Fisheries and Aquatic Science, 10: 295-304.
[53] Sonmez, F. (2011) The seasonal variations of planktonic and epilithic diatoms in Kalecik Reservoir (Elazig, Turkey). Journal of Animal and Veterinary Advances, 10 (24): 3231-3235.
[54] Somek, H., Balik, S. and Ustaoglu, R. (2005) The seasonal variations and phytoplankton of Topçam Dam Lake (Cine-Aydin). Suleyman Demirel University Journal of Egirdir Fisheries Faculty, 1(1): 26-32.
[55] Atici, T. and Alas, A. (2012) A study on the trophic status and phytoplanktonic algae of Mamasin Dam Lake (Aksaray-Turkey). Turkish Journal of Fisheries and Aquatic Science, 12: 595-601.
[56] Oterler, B. (2013) The phytoplankton composition of Kadikoy Reservoir (Kesan-Edirne). Trakya University Journal of Natural Sciences, 14(2): 69-76.
[57] Hutchinson, G.E. (1967) A treatise on limnology, vol: II, introduction to lake biology and the limnoplankton John Wiley and sons. inc., New York, London, Sydney.
[58] Trifonova, I.S. (1998) Phytoplankton composition and biomass structure in relation to trophic gradient in some temperate and subarctic lakes of north-western Russia and the Prebaltic. Hydrobiologia 369/370: 99- 108.
[59] Yilmaz, N. and Aykulu, G. (2010) An investigation on the seasonal variation of the phytoplankton density on the surface water of Sapanca Lake, Turkey. Pak. J. Bot. 42(2): 1213-1224.
[60] Zaim, E. (2007) Planktonic algal flora in the Kaz Lake. Gaziosmanpasa University. Master Project. 110p, Tokat.
[61] Reynolds, C.S., Padisak, J. and Sommer, U. (1993) Intermediate disturbance in the ecology of phytoplankton and the maintenance of species diversity: a synthesis. Hydrobiologia 249: 1831-1838.
[62] Rawson, D.S. (1956) Algal indicators of trophic lake types. Limnol Oceanogr 1: 18-25.
[63] Bellinger, E.G. and Siegee D.C. (2010) Freshwater Algae. İdentifications and Use as Bioindicators. Wiley-Blackwell, Chichester, West, Sussex, UK, 284 pp.
[64] Romo, S. and Miracle, M.R. (1994) Population dynamics and ecology of subdominant phytoplankton species in a shallow hypertrophic lake (Albufera of Valencia, Spain). Hydrobiologia 273: 37-56
[65] Celik, K. and Ongun, T. (2006) Seasonal dynamics of phytoplankton assemblages across nutrient gradients in the shallow hypertrophic Lake Manyas, Turkey, Lake and Reservoir Management, 22(3): 250-260.
[66] Lathrop, R.C. (1988) Evaluations of Whole-lake nitrogen fertilization for controlling blue-green-algal blooms in a hypereutrophic lake. Canadian Journal of Fisheries and Aquatic Sciences 45: 2061-2075.
[67] Giani, A., Bird. D.F., Prairie, Y.T. and Lawrence, J.F. (2005) Empirical study of cyanobacteria toxicity along a trophic gradient of lakes. Canadian Journal of Fisheries and Aquatic Sciences 62: 2100-2109.

[68] Wetzel, R.G. (1983) Limnology. Saunders College Publishing. Philadelphia, 767 pp.
[69] Katip, A., Ileri, S., Karaer, F. and Onur, S. (2015) Determination of the Trophic State of Lake Ulubat (Bursa-Turkey). Ekoloji 24, 97.
[70] Ciagna, C., Bonotto, D.M., Camargo, A.F.M. and Sturaro, J.R. (2016) Trophic state index (TSI) and physico-chemical characteristics of a shallow reservoir in southeast Brazil. Environmental Earth Sciences 75(2): 102.
[71] Kutlu, B., Serdar, O., Aydın, R. and Danabaş, D. (2017) Determination of Trophic Status Carlson Index Induced on Uzuncayir Dam Lake (Tunceli). Yunus Research Bulletin 17(1): 83-92.

Received: **16.06.2017**
Accepted: **23.07.2017**

CORRESPONDING AUTHOR

Feray Sonmez
Firat University,
Fisheries Faculty,
Department of Basic Aquatic Sciences,
23119, Elazig – TURKEY

E-mail: feraysonmez@gmail.com

© by PSP Volume 26 – No. 10/2017 pages 6246-6252 Fresenius Environmental Bulletin

DETERMINATION OF THE ANTI-OXIDATIVE ACTIVITIES OF SIX MUSHROOMS

Celal Bal[1,*], Hasan Akgul[2], Mustafa Sevindik[2], Ilgaz Akata[3], Onder Yumrutas[4]

[1]Gaziantep University, Oguzeli Vocational School, Gaziantep, Turkey
[2]Akdeniz University, Faculty of Science, Department of Biology, Antalya, Turkey
[3]Ankara University, Faculty of Science, Department of Biology, Ankara, Turkey
[4]Adıyaman University, Faculty of Medicine, Department of Medical Biology, Adıyaman, Turkey

ABSTRACT

The objective of the present study was to determine antioxidant activities, DNA protective activities, cytotoxic effects, oxidative stress status and phenolic content of *Trametes gibbosa* (Pers.) Fr., *Fomes fomentarius* (L.) Fr., *Fuscoporia torulosa* (Pers.) T. Wagner and M. Fisch., *Daedalea quercina* (L.) Pers., *Inonotus hispidus* (Bull.) P. Karst. and *Trichaptum biforme* (Fr.) Ryvarden mushrooms. DPPH method was used to determine the antioxidant activities. DNA protective activity was determined with pBR 322 supercoil DNA. To determine the cytotoxic effects, the effects of extracts on A549 cell line were tested. Total antioxidant status (TAS), total oxidant status (TOS) and oxidative stress index (OSI) were determined. Phenolic content and other phytochemicals were screened with HPLC device. It was determined that antioxidant activities increased as the concentration of mushroom ethanol extracts increased. The highest activity was observed in *I. hispidus* EtOH extract, and the lowest activity was observed in *T. gibbosa* EtOH extract. It was determined that all mushroom ethanol extracts exhibited DNA protective effects. The highest cytotoxic effect on A549 cells was observed with *D. quercina* ethanol extract. No cytotoxic effect was observed in *I. hispidus* and *F. torulosa* species. In conclusion, it was determined that the macro-mushrooms scrutinized in the study could be used in medicinal, pharmacological, nutrition and environmental protection applications due to their strong antioxidant, DNA protective and cytotoxic activities.

KEYWORDS:
Mushroom, antioxidant, oxidant, oxidative stress, cytotoxic effect, DPPH, Phenolic compounds

INTRODUCTION

Mushrooms, which are cosmopolitan living organisms, have been used in food and medicine production for centuries [1-4]. There are limited numbers of studies on mushrooms, which have a significant pharmacological value and believed to span 140,000 species on earth [5]. However, previous studies already determined antibacterial, antifungal, antioxidant, antiviral, anti-allergenic, hypoglycemic, anti-inflammatory and immune system boosting properties of the examined species [6-11]. Mushrooms contain several secondary metabolites including phenolic compounds, polyketides, terpenes and steroids [12]. These secondary metabolites, which do not have nutritional value, have significant medical properties [13]. These secondary metabolites play a vital role in the antioxidant defence mechanisms in biological systems [14]. Mushrooms have several biological activities and when consumed, help reduce oxidative stress in vivo due to their antioxidant properties. In recent years, various nutrients were used in addition to the antioxidants produced in the human body to reduce the oxidative damage induced by free radicals [15-18]. Antioxidants may block or delay the oxidation process by blocking the initiation or spread of oxidizing chain reactions [19]. Oxidative stress could cause several serious health problems including heart diseases, neurological disorders, diabetes, leukaemia, cirrhosis, necrosis and aging [17,20]. In addition to the existing resources, examination of mushrooms for antioxidant activity and oxidative stress index (OSI) is quite important for identifying new resources.

Turkey is home to several macro-mushroom species due to the rich biodiverse environment [11]. However, number of studies on biological activities of indigenous mushrooms is extremely limited. Thus, the present study aimed to determine the biological activities of *Trametes gibbosa* (Pers.) Fr., *Fomes fomentarius* (L.) Fr., *Fuscoporia torulosa* (Pers.) T. Wagner & M. Fisch., *Daedalea quercina* (L.) Pers., *Inonotus hispidus* (Bull.) P. Karst. and *Trichaptum biforme* (Fr.) Ryvarden mushrooms, collected at the Belgrade Forest in Istanbul, Turkey. In this context, antioxidant activities, DNA protective activities, cytotoxic effects, oxidative stress status and phytochemical content of the mushroom ethanol extracts were determined.

MATERIAL AND METHODOLOGY

Sampling. Mushroom samples used in the study were collected at Belgrade forest in Istanbul. Fungarium specimens were preserved in Ankara University, Faculty of Sciences, Biology Department fungarium (Ankara, Turkey). Mushrooms were dried at 40 °C in an incubator. Then, they were pulverized with a mechanical grinder. 30 g pulverized mushroom samples were placed in magazines and extracted with ethanol in a soxhlet extractor for 6 hours at 50 °C (BUCHI Extraction System Model B-811). After extraction, the extracts were concentrated at 40 °C under high pressure on a rotary evaporator and stored at +4 °C until the experiment.

Antioxidant analyses. Mushroom DPPH free radical scavenging activities were determined with the method developed by Shimada et al. [21]. 1, 1-diphenyl-2-picrylhydrazyl (DPPH) (Sigma, Aldrich) is a stable free radical with a maximum optical absorbance at 517 nm. The presence of an antioxidant molecule in this radical medium is characterized by the change of the violet purple colour into a light yellow colour. Stock solutions containing 1 mg / mL extract were prepared with DMSO. 50 µL solution was added to 160 µL 0.039% DPPH. The solutions were incubated in the dark for 30 minutes at ambient temperature. The absorbance was read at 517 nm. The same process was repeated for all concentrations and samples. Caffeic acid and rosmarinic acid were used as reference antioxidants. Finally, DPPH free radical scavenging rates were calculated with the formula below:

SA (%)= [(ADPPH-ASample)/(ADPPH)]x100
*Scavenging activity

TAS, TOS and OSI values. Mushroom extract total antioxidant status (TAS), total oxidant status (TOS) and oxidative stress index (OSI) values were measured with Rel Assay brand commercial kits (Rel Assay Kit Diagnostics, Turkey). Trolox was used as TAS calibrator and the results were expressed as mmol Trolox equiv./L [22]. Hydrogen peroxide was used as TOS calibrator and the results were expressed as µmol H_2O_2 equiv. /L [23]. Oxidative stress index (OSI) was calculated with the following formula:

$$OSI = \frac{\text{TOS, } \mu\text{mol } H_2O_2 \text{ equiv. /L}}{\text{TAS, mmol Trolox equiv. /L X 10}}$$

DNA protective activity. Mushroom ethanol extract DNA protective activities were determined with pBR 322 supercoil DNA. 100 and 200 µg / mL standard solutions were prepared with mushroom extracts. 0.5 µg plasmid pBR 322 was added to supercoil DNA Eppendorf tubes and 10 µL standard mushroom extract solution was added. 10 µL of Fenton's agent (30 mM H2O2, 50 µM ascorbic acid and 80 µM FeCl3) was added to the prepared solution and the product was incubated for 10 minutes at ambient temperature. The final volume of the mixture was adjusted to 20 mL and allowed to stand for 30 minutes at 37 ° C. The DNA was then analysed by electrophoresis on a 1% agarose gel containing ethidium bromide [24].

Cytotoxicity assay. MTT (3- [4, 5-dimethylthiazol-2-yl]- 2, 5-diphenyl-tetrazolium bromide) was used to measure cell viability of A549 cells. In short, cells were detached using 3.0 mL Trypsin-EDTA solution (Sigma-Aldrich, MO, USA) after reaching 70-80 % confluency and cultured in 24-well plates and incubated for 24 hours. After 24 hours, varying dilutions of (5, 25, 50, 100, 200 µg/ml) the extracts were applied and cells were incubated for a further 24 hours. Control cells were only treated with the growth medium, which was not supplemented with FCS. After 48 hours of incubation, the supernatants were replaced with 1 mg/mL MTT (Sigma) dissolved in growth medium and incubated at 37°C until purple precipitate is visible. Following incubation, supernatants were removed and MTT absorbed by cells was dissolved by adding dimethyl sulfoxide (DMSO) (Sigma-Aldrich, MO, USA). Plates were read at 570 nm using an Epoch spectrophotometer (BioTek Instruments, Winooska, VT).

Phenolic content. Mushroom extracts were processed with a modified version of the method developed by Caponio et al. [25] using a SHIMADZU system HPLC device and a DAD detector: Injection volume was adjusted to 20 µL. 3% acetic acid was used as mobile phase A and methanol was used as mobile phase B (Table 1) and the flow rate was regulated to 0.8 mL per minute. Chromatographic separation was conducted with Agilent Eclipse XDB-C18 column (250x4.6 mm id 5 µM) at 30 ° C.

RESULTS AND DISCUSSIONS

DPPH activity. Mushroom ethanol extract antioxidant activity was determined with DPPH method and the % inhibition values are presented in Table 2.

It was determined that DPPH free radical scavenging effect of mushroom extracts increased due to the increase in extract concentration. *I. hispidus*, *F. torulosa* and *F. fomentarius* mushrooms exhibited higher activity when compared to the caffeic and rosmarinic acids used as standards. *T. biforme*, *D. quercina* and *T. gibbosa* mushrooms did not demonstrate any significant activity. Recent studies reported antioxidant potential of mushroom samples collected in Brazil, China, Korea, Spain,

TABLE 1
HPLC gradient program

Minute	0.1	20	28	35	50	60	62	70	73	75	80	81
%A	93	72	75	70	70	67	58	50	30	20	0	93
%B	7	28	25	30	30	33	42	50	70	80	100	7

%A: % 3 Acetic acid,% B: Methanol

TABLE 2
Dpph Free Radical Sweeping Activity Percentages of Mushroom Samples

Samples	**25**	**50**	**75**	**100**
Caffeic acid (%)	8.62±0.91	21.34±0.66	38.39±0.66	54.47±0.05
Rosmarinic acid (%)	6.03±0.15	47.72±0.76	56.44±1.98	66.33±1.01
T. biforme	nd	nd	10.40±2.49	1.37±1.78
D. quercina	nd	nd	nd	4.82±1.57
I. hispidus	25.96±2.23	42.80±6.24	66.38±4.16	79.77±0.61
F. fomentarius	34.48±0.20	49.39±1.93	71.91±7.91	75.51±3.91
F. torulosa	14.35±0.46	29.11±0.51	54.56±0.30	81.64±2.03
T. gibbosa	nd	0.15±0.46	0.30±0.81	2.54±1.22

The results indicate % inhibition values. Values are presented as mean±S.D; n=3

TABLE 3
Tas, Tos And Osi Values of Mushroom Samples

Samples	**TAS** (mmol/L)	**TOS** (µmol/L)	**OSİ** (TOS/(TASx10))
T. biforme	0.802±0.050	4.356±0.200	0.543±0.059
D. quercina	0.312±0.047	6.868±0.373	2.201±0.493
I. hispidus	2.922±0.096	6.534±0.249	0.224±0.001
F. fomentarius	3.270±0.229	2.601±0.109	0.080±0.005
F. torulosa	4.033±0.237	2.969±0.133	0.074±0.004
T. gibbosa	0.590±0.064	3.522±0.275	0.597±0.019

Values are presented as mean±S.D.; n=5

India, Portugal, Taiwan and Turkey [26]. It was demonstrated that mushrooms may contain several phytochemicals similar to plants and therefore could exhibit significant bioactivity levels [27]. Lee et al. [28] identified the DPPH free radical scavenging activity for 83 mushrooms. In that study, similar to the present study, it was determined that *Trametes* sp. possessed very low antioxidant activities. In the present study, the antioxidant activity of *D. quercina* was low, while the species with the highest activity was *F. torulosa*. Antioxidant activity of *I. hispidus* species had the second highest activity levels. It was considered that the display of different levels of antioxidant activities by different species could be due to different phytochemicals present in their structures, different regions they were collected, and the differences between the species. Study data demonstrated that among mushroom samples that were collected in Belgrade forest, *I. hispidus, F. torulosa* and *F. fomentarius* mushrooms could be used as antioxidant resources.

TAS, TOS and OSI values. TAS, TOS and OSI values of mushroom samples that were scrutinized in the study were determined with Rel Assay kits and the findings are presented in Table 3.

TAS values of mushrooms collected in the Belgrade forest demonstrated that the highest value was found in *F. torulosa* mushroom and the lowest value was found in *D. quercina* mushroom. Examination of TOS values demonstrated that the highest value was observed in *D. quercina* and the lowest value was observed in F. fomentarius mushroom. OSI values were the highest in *D. quercina* and the lowest in *F. torulosa*. In a study conducted with *Macrolepiota procera* (Scop.) Singer mushroom, collected in Antalya (Akseki) and Balikesir (Kazdağı National Park), it was determined that TAS values were 2.823 and 2.805 (mmol / L), TOS values were 10.349 and 6.596 (µmol / L), and OSI values were 0.367 and 0.235, respectively [29]. Furthermore, TAS values of *Omphalotus olearius* (DC.) Singer mushroom collected in Adana (Karaisalı) and Antalya (Konyaaltı) were 2.836 and 2.827 (mmol / L), TOS values were 8.262 and 14.210 (µmol / L), and OSI values were 0.291 and 0.503, respectively [10]. Compared to these studies, OSI values of *F. torulosa, F. fomentarius* and *I. hispidus* mushrooms were lower in our study. Furthermore, compared to these studies, *D. quercina, T. gibbosa* and *T. biforme* mushrooms had higher OSI values. Oxidative stress could occur under conditions where antioxidant compounds are ineffective in removing oxidant substances that are induced by both metabolic reactions and environmental factors [30]. The OSI value demonstrates the percentage tolerance of the internally produced antioxidant compounds and the antioxidant compounds produced due to external factors tolerance of the internally produced antioxidant compounds

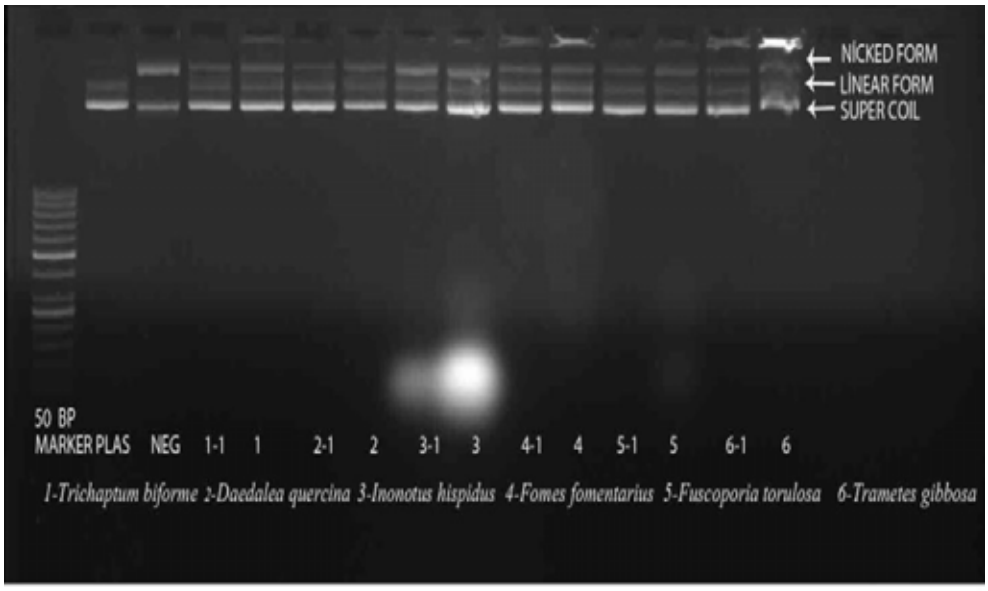

FIGURE 1
DNA protective activities of mushroom samples

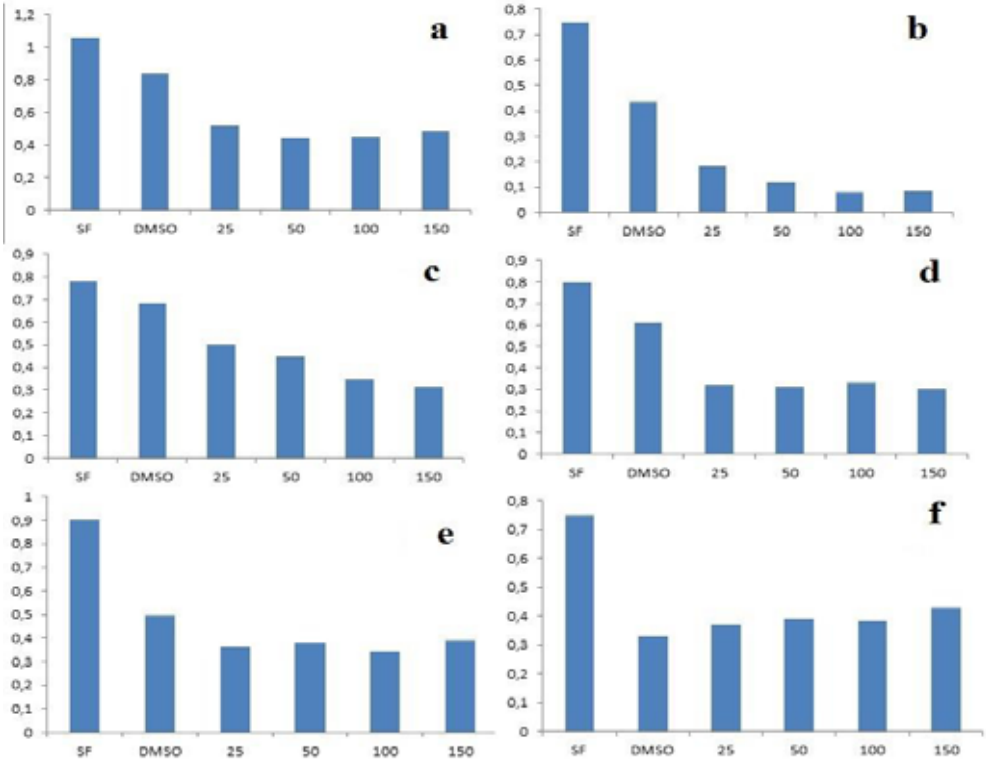

a: *T. biforme,* **b:** *D. quercina,* **c:** *I. hispidus,* **d:** *F. fomentarius,* **e:** *F. torulosa,* **f:** *T. gibbosa*

FIGURE 2
Cytotoxic effects of mushroom samples

and the antioxidant compounds produced due to external factors by the mushrooms. In the present study, the lower OSI values found in *F. torulosa, F. fomentarius* and *I. hispidus* mushrooms were due to the higher TAS values of these mushrooms. These mushrooms had a higher antioxidant capacity when compared to the other samples, resulting in a higher tolerance for the oxidant compounds. Furthermore, based on the TOS values, it could be argued that Belgrade forest was a more suitable environment for the growth of mushrooms with respect to oxidative stress when compared to Antalya, Adana and Balıkesir.

DNA protective activity. The DNA protective activities of mushroom ethanol extracts were determined using pBR 322 supercoiled DNA. The findings are shown in Figure 1.

TABLE 4
Phenolic contents of mushroom samples

Phenolic acids	1	2	3	4	5	6
Gallic acid	118.6	438.5	0.6	0.95	9.8	23.5
Catechin	2.3	67.3	13.8	9.6	2.7	3.9
Clorogenic acid	22.6	37.2	nd	27.2	42.7	70.8
Epicatechin	6.6	33.3	nd	nd	nd	8.5
Sringic acid	12.9	17.3	nd	nd	4.5	1.5
Hydroxy benzoic acid	nd	18.6	nd	nd	nd	nd
Cinnamic acid	nd	nd	15.6	nd	nd	nd
Caffeic acid	nd	nd	nd	10.3	nd	nd
Benzoic acid	nd	nd	nd	nd	170.6	nd

1: *T. biforme,* **2:** *D. quercina,* **3:** *I. hispidus,* **4:** *F. fomentarius,* **5:** *F. torulosa,* **6:** *T. gibbosa*

DNA protective activity refers to the protection of DNA against the hydroxyl radical, one of the most dangerous known radical species that exist when antioxidant compounds are present. If the hydroxyl radical is not removed from the medium, it would break the DNA in these regions by binding to the sugar phosphate backbone. In the present study, we attempted to determine the DNA protective activity using mushroom extracts. When the results were examined, it was observed that the destructive effect of the generated hydroxyl radical on DNA could be determined when the negative control is examined. In the negative control, the linear DNA form completely disappeared. However, it was clearly observed that all applied doses exhibited DNA protective activity when compared to the negative control. DNA-protective activities of macro-mushrooms were determined in previous studies as well [31]. *Gloeophyllum trabeum, Daedalea dickinsii, Pseudomerulius curtisii, Stereu sanguinolentum, Cryptoporus volvatus* and *Gloeophyllum abietinum* mushrooms were reported to have natural antioxidant and potential DNA protective activities [28]. In addition to these studies, we have identified potential DNA protective activities in the mushrooms examined in our study.

Cytotoxic action. Mushroom species extracts were prepared as standard solutions in 25, 50, 100 and 150 µg / ml concentrations and cell viability was tested with lung cancer cell line A549. The findings are presented in Figure 2.

Kaygusuz et al. [32] investigated antimicrobial, antioxidant and cytotoxic effects of *Agaricus lanipus* mushroom. The study concluded that the mushroom had high anti-proliferative and pro-apoptotic effects. *F. fomentarius* reduced cell viability at doses of 25 and 150 µg / mL, although it was determined that the effects of *F. fomentarius* were significant at 50 and 100 µg / mL concentrations. *D. quercina* extracts appeared to cause a dose-dependent decrease in cell density. The highest activity was measured at doses of 100 and 150 µg / mL. *T. biforme* extract appeared to decrease cell viability in a dose-dependent manner. The highest activity was observed at a dose of 150 µg / mL. No dose-dependent effects were observed in the experiment conducted with *T. gibbosa* extract. However, it was determined that a cytotoxic effect was observed in the cells at the dose of 25 µg / mL. Cytotoxic effects of solutions prepared with *F. torulosa* and *I. hispidus* extracts were tested on A549 cells, however it was observed that the extract doses exhibited weak cytotoxic effects on A549 cells.

Phenolic contents. Mushroom species extracts were screened with HPLC method to determine phenolic compounds. The findings are shown in Table 4.

Analyses conducted in the present study demonstrated that 9 phenolic acids were present: gallic acid, catechin, chlorogenic acid, epicatechin, syringic acid, hydroxybenzoic acid, cinnamic acid, caffeic acid and benzoic acid. The type and amount of the determined phenolic content varied based on the extract. Gallic acid and catechin were found in all mushroom extracts; the highest amount was found in *D. quercina* species. Chlorogenic acid was highest in *T. gibbosa*, but it was not found in I. *hispidus*. The highest epicatechin content was detected in *D. quercina* species, while it was not detected in *I. hispidus, F. fomentarius* and *F. torulosa* mushrooms. Syringic acid was not detected in *I. hispidus* and *F. fomentarius* mushrooms, while *D. quercina* had the highest syringic acid content. Hydroxy benzoic acid was identified only in *D. quercina*. Caffeic acid was identified in *F. fomentarius*, cinnamic acid was identified in *I. hispidus* and benzoic acid was identified in *F. torulosa*. Phenolic acids are known to have several activities, among which antioxidant activity is the prominent [33]. The highest antioxidant activities were found in *I. hispidus, F. fomentarius* and *F. torulosa* mushrooms in antioxidant activity tests. However, it was determined that *D. quercina, T. gibbosa* and *T. biforme* mushrooms, which had the highest phenolic content, demonstrated poor antioxidant activities. It could be argued that the determined phenolic substances affected antioxidant activities based on the amount and species. Furthermore, it is considered that cinnamic, caffeic and benzoic acid content determined in *I. hispidus, F. fomentarius* and *F. torulosa* mushrooms could be more predominant in

exhibited antioxidant activities when compared to others. Antioxidant activities of phenolic substances identified in the same system should be evaluated to make definite judgments.

CONCLUSION

In the present study, it was determined that I. hispidus and F. torulosa mushrooms demonstrated high antioxidant activities; the highest TAS value was found in F. torulosa, all examined extract doses demonstrated DNA protection activity, the extracts had anti-proliferative / cytotoxic effects on the A549 cells based on the dose, and finally, they contained important phenolics such as gallic acid, catechin, chlorogenic acid, epicatechin, syringic acid, hydroxy-benzoic acid, cinnamic acid, caffeic acid and benzoic acid. In conclusion, it was determined that macro- mushrooms tested in the present study could be used as natural resources in the fields of medicine, pharmacology, nutrition and cosmetics due to their strong antioxidant, DNA protective and cytotoxic activities.

ACKNOWLEDGEMENTS

The authors would like to thank Ankara University Research Fund (Project no: 15H0430001) for the financial support.

REFERENCES

[1] Dama, C.L., Kumar, S., Mishra, B.K., Shukla, K.B., Mathur, S., Doshi, (2010) A. Antioxidative enzymatic profile of mushrooms stored at low temperature. Journal of Food Science and Technology, 47, 650-655.

[2] Akata, I., Ergonul, B., Kalyoncu, D. (2012) Chemical compositions and antioxidant activities of 16 wild edible mushroom species grown in Anatolia. Int. J. Pharmacol,, 8,134-138.

[3] Tel, G., Apaydın, M., Duru, M.E. (2012) Antioxidant and Cholinesterase Inhibition Activities of Three Tricholoma Species with Total Phenolic and Flavonoid Contents: The Edible Mushrooms from Anatolia. Food Anal. Methods, 5, 495-504.

[4] Konuk, M., Afyon, A., & Yagiz, D. (2007). Minor element and heavy metal contents of wild growing and edible mushrooms from western Black Sea region of Turkey. Fresen. Environ. Bull., 16(11A), 1359.

[5] Reis, F.S., Heleno, S.A., Barros, L., Sousa, M.J., Martins, A., Buelga, C.S., Ferreira, I.C.F.R. (2011) Toward the Antioxidant and Chemical Characterization of Mycorrhizal Mushrooms from Northeast Portugal. Journal of Food Science, 76(6), 824-830.

[6] Wasser, S.P. (2002) Medicinal mushrooms as a source of antitumor and immunomodulating polysaccharides. Applied Microbiology and Biotechnology, 60, 258-274.

[7] Lee, I.K., Kim, Y.S., Jang, Y.W., Jung, J.Y., Yun, B.S. (2007) New antioxidant polyphenols from the medicinal mushroom Inonotus obliquus. Bioorganic & Medicinal Chemistry Letters, 17, 6678-6681.

[8] Sarıkürkçü, C., Çopur, M., Yıldız, D., Akata, I. (2011) Metal concentration of wild edible mushrooms in Soğuksu National Park in Turkey. Food Chemistry, 128, 731-734.

[9] Sudha, G., Vadivukkarasi, S., Shress, R.B.I., Lakshmanan, P. (2012) Antioxidant Activity of Various Extracts from an Edible Mushroom Pleurotus eous. Food Sci. Biotechnol., 21(3), 661, 668 (2012).

[10] Sun, L., Bai, X., Zhuang, Y. (2012) Effect of different cooking methods on total phenolic contents and antioxidant activities of four Boletus mushrooms. J Food Sci Technol., 51(11), 3362-3368.

[11] Sevindik, M., Akgül, H., Bal, C. (2017) Determination of Oxidative Stress Status of Ompholatus olearius Gathered from Adana and Antalya Provinces in Turkey. Sakarya University Journal of Science, 21(3), 324-327.

[12] Oke, F., Aslim, B. (2011) Protective effect of two edible mushrooms against oxidative cell damage and their phenolic composition. Food chemistry, 128(3), 613-619.

[13] Vaz, J.A., Barros, L., Martins, A., Morais, J.S., Vasconcelos, M.H., Ferreira, I.C.F.R. (2010) Phenolic profile of seventeen Portuguese wild mushrooms. Food Science and Technology, 44, 343-346.

[14] Palacios, I., Lozano, M., Moro, C., D'arrigo, M., Rostagno, M.A., Martínez, J.A., Villares, A. (2011) Antioxidant properties of phenolic compounds occurring in edible mushrooms. Food Chemistry, 128(3), 674-678.

[15] Mujić, I., Zeković, Z., Vidović, S., Radojković, M., Živković, J., Gođevac, D. (2011) Fatty acid profiles of four wild mushrooms and their potential benefits for hypertension treatment. Journal of medicinal food, 14(11), 1330-1337.

[16] Vidović, S.S., Mujić, I.O., Zeković, Z.P., Lepojević, Z.D., Tumbas, V.T., Mujić, A.I. (2010) Antioxidant properties of selected Boletus mushrooms. Food Biophysics, 5(1), 49-58.

[17] Babu, D.R., Rao, G.N. (2013) Antioxidant properties and electrochemical behavior of cultivated commercial Indian edible mushrooms. Journal of food science and technology, 50(2), 301-308.

[18] Karatas, M., Dogan, M., Emsen, B., & Aasim, M. (2015). Determination of in vitro free radical

scavenging activities of various extracts from in vitro propagated Ceratophyllum demersum L. L. Fresen. Environ. Bull, 24, 2946-2952.
[19] Aydin, E., & Turkez, H. (2011). Effects of lichenic extracts (Bryoria capillaris, Peltigera rufescens and Xanthoria elegans) on human blood cells: a cytogenetic and biochemical study. Fresen. Environ. Bull., 20, 2992-2998.
[20] Shameem, N., Kamili, A.N., Ahmad, M., Masoodi, F.A., Parray, J.A. (2015) Radical scavenging potential and DNA damage protection of wild edible mushrooms of Kashmir Himalaya. Journal of the Saudi Society of Agricultural Sciences, doi: 10.1016/j.jssas. 2015.10.005.
[21] Shimada, K., Fujikawa, K., Yahara, K., Nakamura, T. (1992) Antioxidative properties ofxanthan on the autoxidation of soybean oil in cyclodextrin emulsion. J. Agric.Food Chem., 40, 945-948.
[22] Erel, O. (2004) A novel automated direct measurement method for total antioxidant capacity using a new generation, more stable ABTS radical cation. Clinical biochemistry, 37(4), 277-285.
[23] Erel, O. (2005) A new automated colorimetric method for measuring total oxidant status. Clinical biochemistry, 38(12), 1103-1111.
[24] Lee, J.C., Kim, H.R., Kim, J., Jang, Y.S. (2002) Antioxidant property of an ethanol extract of the stem of Opuntia ficus-indica var. saboten. J. Agri. Food. Chem., 50, 6490-6496.
[25] Caponio, F., Alloggio, V., Gomes, T. (1999) Phenolic Compounds of Virgin Olive Oil: Influence of Paste Preparation Techniques. Food Chemistry, 64, 203-209.
[26] Ferreira, I.C.F.R., Barros, L., Abreu, R.M.V. (2009) Antioxidants in wild mushrooms. Cur. Med. Chem., 16, 1543-1560.
[27] Türkoğlu, A., Duru, M.E., Mercan, M. (2007) Antioxidant and antimicrobial activity of Russula delica fr: an edible wild mushroom. Eurasian Journal of Analytical Chemistry, 2, 54- 66.
[28] Lee, J., Hong, J.H., Kim, J.D., Ahn, B.J., Kim, B.S., Kim, G.H., Kim, J.J. (2013) The antioxidant properties of solid-culture extracts of basidiomycetous fungi. J. Gen. Appl. Microbiol., 59, 279-285.
[29] Akgül, H., Sevindik, M., Akata, I., Altuntaş, D., Bal, C., Doğan, M. (2016) Determination of Heavy Metal Content and Oxidative Stress Status of Macrolepiota procera (Scop.) Singer. Mushroom. Süleyman Demirel University Journal of Natural and Applied Sciences, 20(3), 504-508.
[30] Rahman, A., Hosen, I., Towhidul, M.M.I., Shekhar, H.U. (2012) Oxidative stress and human HealthAdvances in Bioscience and Biotechnology, 3, 997-1019.
[31] Lee, E.J., Jang, H.D. (2004) Antioxidant activity and protective effect of five edible mushrooms on oxidative DNA damage. Food Science and Biotechnology, 13(6), 443-449.
[32] Kaygusuz, O., Kaygusuz, M., Dodurga, Y., Seçme, M., Herken, E.N., Gezer, K. (2017) Assessment of the antimicrobial, antioxidant and cytotoxic activities of the wild edible mushroom Agaricus lanipes FH Møller & Jul. Schäff Hlaváček. Cytotechnology, 69(1), 135-144. doi:10.1007/s10616-016-0045-4.
[33] Saxena, M., Saxena, J., Pradhan, A. (2012) Flavonoids and phenolic acids as antioxidants in plants and human health. Int. J. Pharm. Sci. Rev. Res., 16(2), 130-134.

Received: **07.08.2017**
Accepted: **12.08.2017**

CORRESPONDING AUTHOR

Celal Bal
Gaziantep University, Oguzeli Vocational School and Higher Education, Gaziantep, 27310 Turkey

E-mail**:** bal@gantep.edu.tr

© by PSP Volume 26 – No. 10/2017 pages 6253-6260 Fresenius Environmental Bulletin

THE EFFECT OF PARTICLE SIZE ON PHOSPHORUS ADSORPTION KINETIC AND DESORPTION BY TURKISH NATURAL ZEOLITES

Veli Uygur*, Canan Sanli Celik, Enise Sukusu, Metin Mujdeci

Suleyman Demirel University, Agricultural Faculty, Soil Science and Plant Nutrition Department, Isparta, Turkey

ABSTRACT

Natural clinoptilolite-zeolite is widely used for enhancing crop production potential of soils by improving chemical and physical properties and treating the polluted water sources. The particle size of the adsorbents is of particular significance for manipulating the adsorption desorption characteristics of sorbed ions. Therefore we tested the effect of micronized natural clinoptilolite-zeolites samples on phosphorus (P) adsorption/desorption. Batch adsorption experiments were conducted using 1 g of adsorbent with 20 mL solution containing 0-50 mg P L^{-1} prepared in 0.01 M $CaCl_2$ background solution. The desorbability of the P was measured by 0.5 M $NaHCO_3$ solution at pH 8.5. Sorption kinetic was studied at 5 and 25 mg L^{-1} initial concentrations for 5, 10, 20, 30 min; 1, 2, 4, 8, 16, and 24 h. Both Freundlich and Langmuir sorption models fitted the sorption data well; however Langmuir model described the data with better determination coefficient. The adsorption capacity of Rota zeolite was slightly higher than Gordes zeolite's capacity. The particle size dependency of sorption capacity was apparent for Gordes zeolite. Results of kinetics study indicated that the adsorption data fit the second-order kinetic model better than the Elovich model. The sorption data indicated that these zeolite deposits have different particle size dependent-P sorption behaviour that may be used for different purposes.

KEYWORDS:
Natural clinoptilolite-zeolite; phosphorus; adsorption; desorption; particle size

INTRODUCTION

Excessive application of phosphate fertilisers, intensive livestock operations and related agricultural practices and untreated municipal effluents rich in detergents have resulted in P enrichment of arable lands, surface and ground water [1, 2]. These elevated levels of P along with high erosion potential of surface soils threaten the water sources through eutrophication. Therefore, stabilizing P in the borderline of the agricultural lands or removal of excessive P from the water bodies with highly P-reactive adsorbents is essential to maintain water-quality criteria and protect water bodies from environmental risks.

Phosphorus may be removed from the solution phase onto solids through ligand exchange (adsorption), precipitation, lattice diffusion, and anion exchange processes depending on the adsorbent type that the first two mechanisms being the most important [3]. Due to increase in the eutrophication problems in natural water resources the adsorption of P from aqueous solutions has been widely investigated in recent years in order to find efficient, environmentally friendly and low cost materials [4-11].

Phosphorus adsorption/desorption and adsorption kinetics of zeolite are determined by variety of factors such as initial P concentration, contact time, particle size, pH, adsorbent ratio, temperature, the presence of competing ions, mineralogy of zeolite, etc. [12-15]. Researchers have tried to increase the P removal efficiency of natural zeolite by surface manipulation with variety of organic and inorganic chemical compounds [14, 16-19] and particle size reduction by physical means [20]. On the other hand, modification of chemical structure in synthetic zeolite production processes to produce super P adsorbent zeolite-like minerals has been the other approach [21, 22]. Previous studies have indicated that P adsorption capacity of zeolites can differ in a very large scale from 0.37-47.2 mg g^{-1} depending on the nature of the zeolite minerals and working conditions [14, 15, 23]. The reactivity of adsorbents to any adsorbate is largely dependent on surface area and porous structure. This behaviour has prime significance when the adsorption reaction is diffusion controlled. In these circumstances increasing the sorbent surface area influence the adsorbed ions, adsorption kinetic and desorbability of adsorbed ions in question. In contrast the coarse-grained zeolite retained phosphorus at a higher level than the fine-grained zeolite in filters [20].

Since the reactions of phosphorus with zeolite are largely diffusion controlled and surface area dependent nature of adsorption phenomena it is expected that zeolite adsorption and desorption chemistry is to change depending on the physical particle size. Therefore, the aim of this work was to determine the adsorption / desorption chemistry of P in

order to determine the feasibility of micronized zeolite to be used to control mobility and pollution of P in the environment.

MATERIAL AND METHODS

Zeolite Preparation and Properties. Two natural clinoptilolite-zeolites with different sizes were kindly supplied by Rota Madencilik Sti. (RZ) and Gordes Zeolite Ltd Sti (GZ). The zeolite samples were ground to 500, 250, 106 and 53 µm stainless steel screens to obtain 250-500, 106-250, 53-106 and <53 µm micronized particle sizes. Some chemical properties of the zeolite specimens were given in Table 1. Both zeolite specimens consist of hydrated Ca, K, Na, Mg alumina-silicates, however, RZ mineralogically purer than GZ and consist of some cristobalite and tridimite up to 5% with higher porosity.

TABLE 1
Some properties of the experimental zeolites [24, 25]

Properties	Rota zeolite	Gordes zeolite
Mineral composition	**Clinoptilolite 90-95%**	**Clinoptilolite 70-85%**
Surface area (m^2 g^{-1})	39.0	40.7
Porosity (%)	47.5	39.0
CEC (cmol kg^{-1})	150-210	160-200
P content (mg kg^{-1})*	188-270	121-200

* measured in the HNO_3/HCl (3:1, V: V) digest for different particle sizes.

Adsorption. Batch sorption technique was used to determine P sorption/desorption data. One gram of subsamples of zeolites, in triplicates, were equilibrated with varying concentrations of P (0, 5, 10, 20, 30, 40 and 50 mg P L^{-1} as KH_2PO_4 prepared in 0.01 M $CaCl_2$ solution) at 20±1°C by continuous mixing on a reciprocal shaker for 24 h. The $CaCl_2$ solution was used to maintain constant ionic strength resembling typical soil solution. After equilibration the supernatants were separated by centrifugation and filtration procedures. The supernatants were then analysed for P by employing the ascorbic acid method [26] using a double beam UV/VIS spectrometer (T-80, PG Instrument). The amount of adsorbed P was calculated from the equation given below:

$$Si = \frac{(Co - Ce) \times V}{W}$$

Where *Si* is the amount of P adsorbed by unit mass of zeolite (mg kg^{-1}), *Co* initial concentration of P (mg L^{-1}), *Ce* the equilibrium concentration of P (mg L^{-1}), *V* solution volume (mL), *W* the amount of zeolite used (g).

Then the following linear adsorption equations were fitted to sorption data by regression analysis.

Langmuir: $Ce/Sim = Ce/b + 1/ab$

Freundlich model which can have non-linear form of $Si = K_f C^n$ can be written linear by taking log of the equation as: $log\ (Si) = log\ K_f + n\ log\ C_e$

Where *b* maximum P adsorption capacity (mg kg^{-1}), *a* constant related to bounding energy (L kg^{-1}), *n* a measure of adsorption intensity and *Kf* corresponding to the amount of P adsorbed (mg kg^{-1}) when the *Ce* is equal to 1 mg P L^{-1}. The Langmuir equation was modified by including the HCl+HNO_3 (1:3 v/v) soluble P to the adsorbed amounts (*Sim*) at differing initial concentrations to improve determination coefficient of the regression model [27]. To evaluate the success of the model describing the sorption data, determination coefficient of the fit along with F test was used.

Adsorption Kinetics. Phosphorus sorption kinetics of the zeolite samples were studied at 5 and 25 mg L^{-1} initial concentrations for 5, 10, 20, 30 min; 1, 2, 4, 8, 16 and 24 h. The experimental conditions were identical to those of adsorption study. The sorption data were fitted to linear Elovich, and second order models which can be written below (Ho and McKay, 2002):

Elovich equation: $qt = \beta\ ln(\alpha\ \beta) + \beta\ ln\ t$

Where *qt* is the amount of P sorbed at a time *t* (mg kg^{-1}), α initial sorption rate (mg L^{-1} min^{-1}) and β desorption constant (kg mg^{-1}). The model constants were obtained from the linear q_t versus *lnt* plot.

Pseudo-second order model: $\frac{t}{q_t} = \frac{1}{kq_e^2} + \frac{1}{q_e} t$

Where q_e and q_t are the sorption capacity of P at equilibrium and at a time *t2*, respectively, *k* is the rate constant (1 min^{-1}) for pseudo-second order sorption. The linear plot of t/q_t versus *t* gives a slope of $1/q_e$ and an intercept of $1/kq_e^2$ (l h^{-1}).

The appropriateness of the sorption kinetic models was tested with the regression analysis as described for Freundlich and Langmuir models.

Desorption. In order to determine the desorbability of the adsorbed P 0.5 M $NaHCO_3$ solution at pH 8.5 which is commonly used to extract soil available P in neutral to alkaline soils. The desorption ratio (DR) at different initial concentrations was calculated from the equation below:

$$\mathrm{DR}(\%) = \frac{Si - Sides}{Si} x100$$

where *Sides* is the amount of P desorbed by 0.5 molar $NaHCO_3$ solution. By this way it was possible to extract some information about the sorption mechanism of P as a consequence of particle size.

TABLE 2
The effect of particle size on adsorption parameters of Langmuir model

Particle size (µm)	Gördes				Rota			
	a	b	Max ads (mg kg^{-1})	R^2	a	b	Max ads (mg kg^{-1})	R^2
53	0.0056	0.0015	667	0.961	0.0021	0.0012	833	0.977
53-106	0.0062	0.0015	667	0.974	0.0025	0.0012	833	0.984
106-250	0.0065	0.0019	526	0.978	0.0028	0.0012	833	0.989
250-500	0.0099	0.0018	556	0.953	0.0035	0.0013	769	0.984

TABLE 3
The effect of particle size on Log based Freundlich model parameters

Particle size (µm)	Gördes			Rota		
	n	Kf	R^2	n	Kf	R^2
53	0.287	2.36	0.939	0.240	2.58	0.961
53-106	0.287	2.33	0.926	0.263	2.52	0.956
106-250	0.285	2.26	0.960	0.293	2.49	0.964
250-500	0.346	2.15	0.980	0.310	2.43	0.958

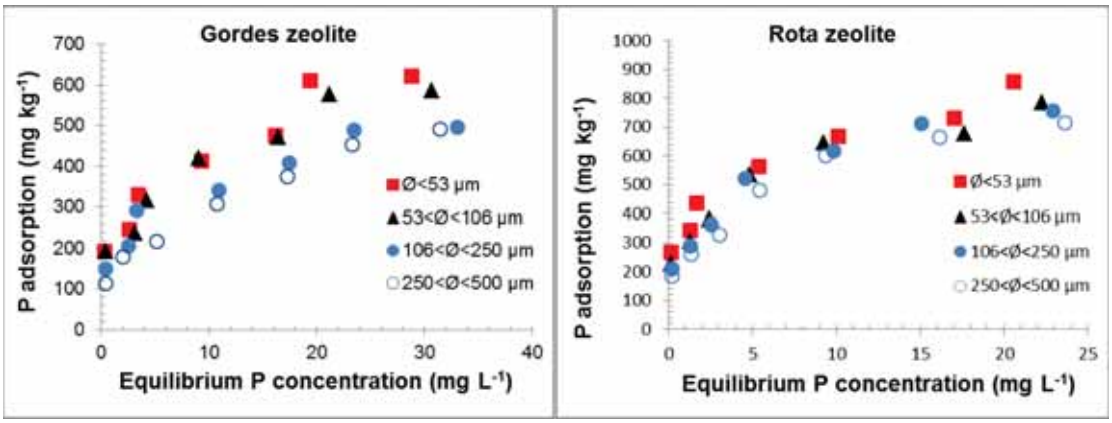

FIGURE 1
The effect of particle size on phosphorus sorption by zeolite samples

RESULTS AND DISCUSSION

Adsorption. The experimental data of phosphate ions adsorption at equilibrium onto two zeolite specimens at differing particle sizes in the solution at equilibrium are presented in Figure 1a, b. Langmuir and log based linear Freundlich isotherms were applied to the experimental data of phosphate ion adsorption at equilibrium versus phosphate ion concentration at equilibrium with 5% zeolite containing suspension. Table 2 and 3 shows calculated sorption parameters of the zeolites. Both isotherm model described the P sorption data well, however, the Langmuir model performed slightly better by considering determination coefficients. The maximum P adsorption of GZ and RZ varied between 667-526 and 833-769 mg kg^{-1} respectively. The binding energy coefficients of GZ were between 0.0056-0.0099 L kg^{-1} whereas they were 0.0021-0.0035 mL g^{-1} and increased in parallel with the increase in particle size. Sorption maxima calculated from the Langmuir equation were highly particle size dependent in GZ whereas Rota zeolite showed constant sorption maxima at differing particle size but 250-500 mm particle size. This apparent difference between two zeolites is likely to be related to porous nature of the samples and mineralogy to a lesser extent. As can be seen in Table 1 GZ has considerably smaller pore volume and higher mineralogical impurities. This means the smaller particle size resulted in the more surface sites may be reactive for P. Therefore P ions cannot access some of the surface sites in this zeolite. In contrast well developed porous structure of RZ resulted in nearly similar amount of P adsorption maximum.

The P removal by zeolite in the suspension is remarkably related to the reaction conditions, such as the initial concentration of P, initial pH value, temperature, zeolite particle size, dosage and the amount of amount and type of exchangeable cations on zeolite [13, 29, 30]. The surface modification of zeolite surfaces with either different cations or specific anion exchangers have been reported to differ P sorption maxima. However, the maximum P sorption of natural zeolites is influenced by the accompanying/saturating cations through inducing precipitation reactions [4, 6] or competing anions such as humic substances [5]. As a result, sorption

TABLE 4
The effect of particle size on phosphorus desorption percentage (%) as a function of initial phosphorus concentration

Initial P concentration (mg L^{-1})	Gordes				Rota			
	Particle size (µm)							
	<53	53-106	106-250	250-500	<53	53-106	106-250	250-500
5	268	282	109	82.1	49.2	47.5	49.1	47.5
10	112	109	51.5	68.0	40.5	40.6	42.8	40.1
20	96.7	83.1	59.5	59.1	47.8	51.7	48.5	47.7
30	83.1	77.6	47.4	45.2	38.2	36.8	46.9	51.2
40	64.5	59.9	43.7	37.2	37.9	48.4	42.0	43.8
50	77.5	76.4	61.0	50.2	34.7	43.8	47.8	50.3

maxima ranges from 370 to 47200 mg kg^{-1} were reported in the literature [14, 15, 23]. The current data are in the lower end of the reported limits.

In GZ, the Freundlich *n* parameters or the isotherm slope were highly particle sizes-dependent in both zeolite specimens, but the values of *n* were not corresponded to the particle size differences up to 250 µm for GZ but there was a steady sorption maxima in smaller particle sizes. This indicates that the smaller the particle size resulted in the lesser affinity of the surfaces to P. The increase in slope indicates that higher proportions of the added P are to be fixed by the surfaces. Log *Kf* values ranged from 2.36 to 2.15 mg kg^{-1} and 2.58 to 2.43 mg kg^{-1} for GZ and RZ, respectively. The particle sizes and the log *Kf* values were inversely related. This could be associated with the P fixed in the structural units of the zeolites which can be seen in Table 1. This is because of the reduction of the particle size enriched the solution P by releasing back the P in the structural units. Moharami and Jalali [9] determined the *Kf* value for Iranian natural zeolite as 12.63 mL g^{-1} and the *n* value as 1.56 (1 / 1.56 = 0.641). In this study, solution P was used up to an initial concentration of 250 mg L^{-1}, which resulted in higher adsorption values, since at higher concentrations P gave a precipitation reaction in the presence of $CaCl_2$. This has caused the *n* value to approach to the unity. In this study, *n (1 / n)* was found to be in the range of 0.2395-0.3455 and is quite small because of the usage of a concentration range that may disable precipitation reactions. The log *Kf* value is changed between 2.58 and 2.15, which is a very high value. Argiri et al. [6] reported an *n* value of 0.72 and the value of log *Kf* of 4.32. These values are clearly higher than the ones found in this work. This is because the amount of zeolite solution used is higher and the concentrations of P used are lower. It is therefore possible that the data obtained may be high because they studied at a concentration limit where the adsorption is promoted.

Desorption. The percentage of desorbed P were highly dependent on the initial concentration of P, particle size and zeolite origin (Table 4). At low initial concentrations (up to 10 mg P L^{-1}) and particle size below 250 µm, the desorption percentages were over 100%. This indicates that the $NaHCO_3$ solution was able to extract previously adsorbed P majority of which probably fixed in the structural units during the formation of zeolites or encapsulated in the pores. Because as the particle size decreased the higher desorption rates were observed for GZ. Increasing initial concentration up to 40 mg P L^{-1} resulted in a decrease in the desorption rate at any particle size but 50 mg P L^{-1} initial concentration behaved differently. In general both the adsorption and desorption were higher for <53 µm particle size. This point out that newly forming sorption sites induced by particle size reduction probably adsorbed P in $NaHCO_3$ extractable pool.

However, RZ behaved distinctly different comparing the GZ. The smallest particle sized RZ induced gradual decrease in desorption percentage due to increasing P loads. This corresponds to higher energy sorption of P where chemisorption and/ or precipitation processes can take place. Chemisorbed-P and/or precipitations of low solubility product solid phases limit desorbability of the ions. The desorption percentages for RZ at differing initial concentration and particle sizes were comparatively changed in a narrow range (51.7-34.7%). The ranges become even narrower when the particle size increased (Table 4) which may be attributed to evenly distribution of pores where the particle size increase limited the diffusion. The P desorption percentage of zeolite was reported to be 18.1 which was highly smaller than the current results. The desorption ratio is highly related to the sorption mechanisms [32], initial concentrations, working conditions, extracting solution [31]. Moharemi and Jalali [9] used 0.01 M $CaCl_2$ solution which can solubilize/extract far less P in the soils [33]. Moreover, Sabadash et al. [32] found negligible amounts of P desorption as distilled water is the extractant. The relatively small ratio of desorption in RZ deposit after $NaHCO_3$ extraction indicates the phosphate binding by zeolite via the mechanism of chemical sorption with insoluble compounds formation. These results confirm the conclusions concerning the formation of aluminium phosphate in the zeolite pores [34].

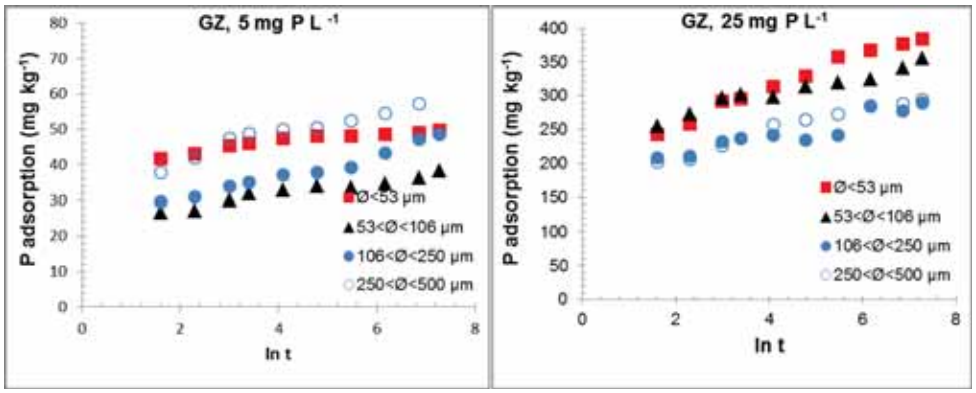

FIGURE 2
Plot of Elovich equation for sorption of phosphorus on to different sized Gordes zeolite at various initial concentrations (5 and 25 mg P L^{-1})

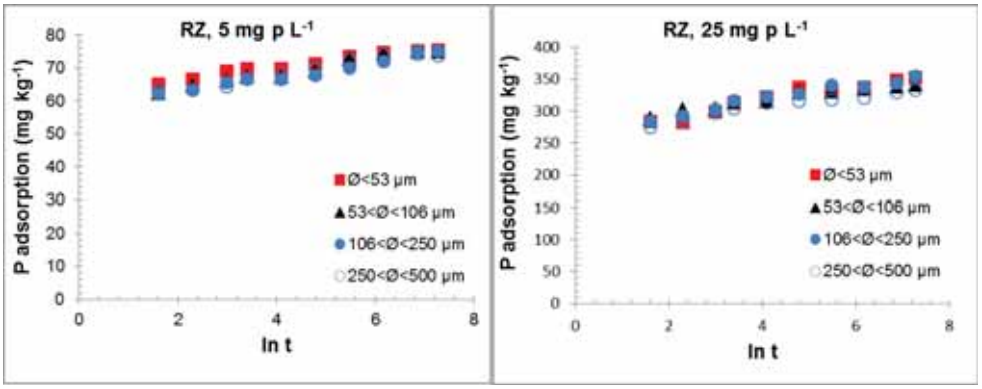

FIGURE 3
Plot of Elovich equation for sorption of phosphorus on to different sized Rota zeolite at various initial concentrations (5 and 25 mg P L^{-1})

TABLE 5
The effect of particle size, initial P concentration and zeolite type on parameters of Elovich kinetic model

Initial P concentration	Gordes zeolite				Rota zeolite		
	Particle size	α	β	R^2	α	β	R^2
	Ø<53 µm	1.299	40.8	0.894	1.859	62.59	0.968
	53<Ø<106 µm	1.853	24.14	0.933	2.315	58.91	0.968
	106<Ø<250 µm	3.249	23.64	0.971	2.287	58.07	0.967
5 mg L^{-1}	250<Ø<500 µm	3.325	35.02	0.941	2.271	58.77	0.951
	Ø<53 µm	25.32	207.6	0.983	12.54	264.2	0.932
	53<Ø<106 µm	14.99	240.4	0.941	8.887	279.9	0.951
	106<Ø<250 µm	13.8	183.4	0.872	11.81	269.3	0.956
25 mg L^{-1}	250<Ø<500 µm	17.13	176.3	0.966	9.43	266.5	0.935

Sorption Kinetics. The results of phosphate adsorption kinetic experiments at 20±1°C and for concentrations of 5 and 25 mg P L^{-1} are shown in Table 5 and 6. Figure 2 and 3 illustrate plots of the Elovich model for the differing particle size zeolite specimens at initial concentration of 5 and 25 mg P L^{-1}. In this case, a linear relationship was obtained between P sorbed, *qt*, and *ln t* over the entire sorption period, with high correlation coefficients (> 0.872) for all the lines (Table 5). It is clear that the simple Elovich equation may be used to describe the kinetics of P sorption on the natural zeolites. Table 5 shows the kinetic constants obtained from the Elovich equation. It will be seen from the data that the values of α and β varied as a function of the initial P concentration, C_0, zeolite type and particle size. Particle size dependency of Elovich model was apparent in the GZ whereas the parameters of RZ differed in relatively narrow range.

The same kinetic data were subjected to pseudo-second order equations. The determination coefficients of the regression lines, R^2, of pseudo-second kinetic model were higher in all cases (>0.998) than Elovich model. This indicates that pseudo-second model can describe the adsorption kinetics of P by different type and particle sized

TABLE 6
The effect of particle size, initial P concentration and zeolite type on parameters of pseudo-second order kinetic model

		Gordes zeolite			Rota zeolite		
Initial P concentration	**Particle size (μm)**	**q_e (mg/kg)**	**k (kg/(mg min)**	**R^2**	**q_e (mg/kg)**	**k (kg/(mg min)**	**R^2**
	Ø<53	49.5	0.277	0.999	75.8	0.262	1.000
	53<Ø<106	37.7	0.072	0.998	75.2	0.205	1.000
	106<Ø<250	48.5	0.044	0.998	75.2	0.125	0.999
5 mg L^{-1}	250<Ø<500	59.5	0.064	0.998	74.1	0.354	1.000
	Ø<53	385	0.084	0.999	357.1	0.151	0.999
	53<Ø<106	357	0.078	0.999	344.8	0.266	1.000
	106<Ø<250	286	0.071	0.999	357.1	0.147	0.999
25 mg L^{-1}	250<Ø<500	294	0.104	0.999	333.3	0.181	0.999

zeolites. Similar results have been reported by other authors [10, 35, 36]. The results in Tables 6 show the sorption rate constant, *k*, and equilibrium sorption capacity, *qe*, as a function of the initial P concentrations (C_0), particle sizes and zeolite type. Thus, on increasing the initial P concentration from 5 to 25 mg P L^{-1}, the P equilibrium sorption capacity ranges for different particle size increased from 37.7-59.5 and 74.1-75.8 to 286-385 and 333.3-357.1 mg P kg^{-1} for GZ and RZ, respectively.

CONCLUSIONS

Based on the experimental results obtained in this study the following conclusions may be drawn: Both natural clinoptilolite types can be used effectively in the removal of aqueous phosphate ions. Although RZ with comprehensive porous structure and higher purity performed better and unaffected by particle size differences and GZ exerted higher particle size dependency. Despite the sorption data were satisfactorily confirmed by both Langmuir and Freundlich models, the homogeneity of the zeolite deposits is a matter of fact in determining the success of the sorption models.

The desorption percentages were highly dependent on the zeolite type, initial P concentration and particle size. GZ had higher desorption percentages than the RZ which indicate these zeolites can adsorbe P by different mechanisms exerting changing bounding energy.

Pseudo-second order model was better performed to describe sorption kinetics of P by zeolite samples.

ACKNOWLEDGEMENT

The funding for this study provided by the Suleyman Demirel University Research Foundation with project number 4526-YL2-15 is gratefully appreciated.

REFERENCES

[1] Jarvie H.P., Sharpley, A.N., Withers, P.J., Scott, J.T., Haggard, B.E., and Neal, C. (2013) Phosphorus mitigation to control river eutrophication: murky waters, inconvenient truths, and "postnormal" science. J. Environ. Qual., 42, 295–304.

[2] Dodds, W.K. and Smith, V.H. (2016) Nitrogen, phosphorus, and eutrophication in streams. Inland Waters 6, 155-164.

[3] Sparks, D.L. (2003) Environmental Soil Chemistry. Academic Press, San Diego.

[4] Karapinar, N. (2009) Application of natural zeolite for phosphorus and ammonium removal from aqueous solutions. J. Hazard. Mater., 170, 1186-1191.

[5] Gu, Z.M., Buyuksonmez, F., Gajaraj, S. and Beighley, R.E. (2011) Adsorption of phosphate by goethite and zeolite: effects of humic substances from green waste compost. Compost Sci. Util., 19, 197-204.

[6] Argiri, A., Ioannou, Z., Gavala, P.M., and Dimirkou, A. (2013) Phosphorus removal from aqueous solutions and greek soils using modified natural minerals and its impact on the morphological characteristics of crops. Commun. Soil Sci. Plan., 44, 551-565.

[7] Drizo, A., Frost, C.A., Grace, J. and Smith, K.A. (1999) Physico-chemical screening of phosphate-removing substrates for use in constructed wetland systems, Water Res., 33, 3595–3602.

[8] Xu, D., Xu, J., Wu, J. and Muhammad, A. (2006) Studies on the phosphorus sorption capacity of substrates used in constructed wetland systems. Chemosphere, 63, 344–352.

[9] Moharami, S., Jalali, M., 2013. Removal of phosphorus from aqueous solution by iranian natural adsorbents. Chem. Eng. J., 223, 328-339.

[10] Oliveira, M., Araujo, A., Azevedo, G., Pereira, M.F.R., Neves, I.C. and Machado, A.V. (2015) Kinetic and equilibrium studies of phosphorous adsorption: effect of physical and chemical properties of adsorption agent. Ecol. Eng., 82,

527-530.
[11] Li, H., Chi, Z.F., Yan, B.X., Chakov, V. and Kuptsov, V. (2017) Removal of nitrogen and phosphorus from fluctuating degraded riverine wetland water using sphagnum floating bed. Fresen. Environ. Bull., 26, 3014-3019.
[12] Vera, I., Araya, F., Andres, E., Saez, K. and Vidal, G. (2014) Enhanced phosphorus removal from sewage in mesocosm-scale constructed wetland using zeolite as medium and artificial aeration. Environ.Technol., 35, 1639-1649.
[13] Xia, R., Na, D., Zhang, Y.H., Li, B.M., Liu, Z.D., and Lu, H.F. (2015) Nitrogen and phosphorous adsorption from post-hydrothermal liquefaction wastewater using three types of zeolites. Inter. J. Agric. Biol. Eng., 8, 86-95.
[14] Moharami, S. and Jalali, M. (2015) Use of modified clays for removal of phosphorus from aqueous solutions. Environ. Monit. Assess., 187, 639.
[15] Zhang, Y., Kou, X.Y., Lu, H.S. and Lv, X.J. (2014) The feasibility of adopting zeolite in phosphorus removal from aqueous solutions. Desalin. Water Treat., 52, 4298-4304.
[16] He, D.D., Hao, H.S., Chen, D.K., Liu, J.P., Yu, J., Lu, J.C., Liu, F., He, S.F., Li, K.Z. and Luo, Y.M. (2017) Effects of rare-earth (Nd, Er and Y) doping on catalytic performance of HZSM-5 zeolite catalysts for methyl mercaptan (CH3SH) decomposition. Appl. Catal. a-Gen., 533, 66-74.
[17] Cheng, Q.P., Li, H.X., Xu, Y.L., Chen, S., Liao, Y.H., Deng, F. and Li, J.F. (2017) Study on the adsorption of nitrogen and phosphorus from biogas slurry by NaCl-modified zeolite. Plos One 12.
[18] Bansiwal, A.K., Rayalu, S.S., Labhasetwar, N.K., Juwarkar, A.A., Devotta, S., 2006. Surfactant-modified zeolite as a slow release fertilizer for phosphorus. J. Agric. Food Chem., 54, 4773-4779.
[19] Schick, J., Caullet, P., Paillaud, J.L., Patarin, J., Freitag, S. and Mangold-Callarec, C. (2012) Phosphate uptake from water on a surfactant-modified zeolite and Ca-zeolites. J. Porous Mat., 19, 405-414.
[20] Stefanakis, A.I., Akratos, C.S., Gikas, G.D. and Tsihrintzis, V.A. (2009) Effluent quality improvement of two pilot-scale, horizontal subsurface flow constructed wetlands using natural zeolite (clinoptilolite). Micropor. Mesopor. Mat., 124, 131-143.
[21] Yang, M.J., Lin, J.W., Zhan, Y.H., Zhu, Z.L. and Zhang, H.H. (2015) Immobilization of phosphorus from water and sediment using zirconium-modified zeolites. Environ. Sci. Pollut. R., 22, 3606-3619.
[22] Xie, J., Wang, Z., Wu, D.Y. and Kong, H.N. (2014) Synthesis and properties of zeolite/hydrated iron oxide composite from coal fly ash as efficient adsorbent to simultaneously retain cationic and anionic pollutants from water. Fuel, 116, 71-76.
[23] Chen, J., Kong, H., Wu, D., Hu, Z., Wang, Z. and Wang, Y. (2006) Removal of phosphate from aqueous solution by zeolite synthesized from fly ash. J. Colloid Interface Sci., 300, 491–497.
[24] Rota Mining Ltd. Sti. (2017) http://www.rotamadencilik.com.tr/rotamadencilik_urun bilgisi.pdf. access 19.06.2017 (in Turkish).
[25] Gordes Mining Ltd. Sti. (2017) http://www.gordeszeolite.com/SF/557/2016%20Technical%20Data %20Sheet_Zeolite_ Gordes.pdf. Access 19.06.2017 (in Turkish).
[26] Murphy, J. and Riley, J.P. (1962) A modified single solution method for the determination of phosphate in natural waters. Anal. Chim. Acta, 27, 31–36.
[27] Agca, N. and Derici, R. 1999. Adıyaman Çamgazi ovası topraklarında fosfor adsorpsiyonunun değişik izotermlerle belirlenmesi. Tr. J. Agric. Forest., 23, 401-407 (in Turkish).
[28] Ho, Y.S. and McKay, G. (2002) Application of kinetic models to the sorption of copper(II) on to peat. Adsorpt. Sci. Technol., 20, 797-815.
[29] Sugiyama, S. and Hama, T. (2013) Effects of water temperature on phosphate adsorption onto sediments in an agricultural drainage canal in a paddy-field district. Ecol. Eng., 61, 94–99.
[30] Zhang, Y., He, F., Xia, X.B., Kong, L.W., Xu, D. and Wu, Z.B. (2014) Adsorption of sediment phosphorus by porous ceramic filter media coated with nano-titanium dioxide film. Ecol. Eng., 64, 186–192.
[31] Wuenscher, R., Unterfrauner, H., Peticzka, R. and Zehetner, F. (2015) A comparison of 14 soil phosphorus extraction methods applied to 50 agricultural soils from Central Europe. Plant Soil Environ. 61, 86–96.
[32] Sabadash, V., Gumnitsky, J. and Hyvlyud, A. (2016) Mechanism of phosphates sorption by zeolites depending on degree of their substitution for potassium ions. Chem. Chem. Technol., 10, 235-240.
[33] Ince, T. (2017) Atabey ovası topraklarının fosfor adsorpsiyon izotermlerinin toprak özellikleriyle olan ilişkileri ve izotermlerden fosforlu gübre ihtiyacının belirlenmesi. Süleyman Demirel Üniversitesi Fen Bilimleri Enstitüsü, Yüksek lisans Tezi, Isparta (in Turkish).
[34] Malovanyy, A., Sakalova, H., Yatchyshyn, Y., Plaza E. and Malovanyy, M. (2013) Concentration of ammonium from municipal wastewater using ion exchange process. Desalin., 329, 93-102.
[35] Köse, T.E. and Kıvanç, B. (2011) Adsorption of phosphate from aqueous solutions using calcined waste eggshell. Chem. Eng. J. 178, 34–39.

[36] Hamdi, N. and Srasra E. (2012) Removal of phosphate ions from aqueous solution using Tunisian clays minerals and synthetic zeolite. J. Environ. Sci. 24 (2012) 617–623.

Received: **26.07.2017**
Accepted: **30.07.2017**

CORRESPONDING AUTHOR

Veli Uygur
Department of Soil Science and Plant Nutrition Agricultural Faculty, Suleyman Demirel University 32260, Isparta, Turkey

e-mail: veliuygur@sdu.edu.tr

© by PSP Volume 26 – No. 10/2017 pages 6261-6265 Fresenius Environmental Bulletin

SOME MATURITY PROPERTIES OF OKUZGOZU (*VITIS VINIFERA* L. CV.) GRAPE BERRIES

Gultekin Ozdemir[1,*], Abdullah Sessiz [2], Resat Esgici[3]

[1] Dicle University, Faculty of Agriculture, Horticulture Department, 21280 Diyarbakır, Turkey
[2] Dicle University, Faculty of Agriculture, Department of Agricultural Machinery and Technologies Engineering, Diyarbakır, Turkey
[3] Dicle University, Bismil Vocational High School, Diyarbakır, Turkey

ABSTRACT

Some physical, mechanical and ripening properties of Okuzgozu (*Vitis vinifera* L. vc.) grape berries were determined. The test samples were obtained from an organic commercial vineyard in Diyarbakır province, which is located in the southeastern part of Turkey. The tests were carried out during the different phenological stages of the veraison (30 August), 15 days after veraison (15 September) and harvesting time (30 September) in 2016. Some basic important berry ripening and harvesting parameters such as the maximum berry detachment force (FDF) from cluster and berry skin firmness were measured in Newton (N) by using a pull digital force gauge. Total soluble solids content (TSSC), pH and total acidity values were determined at three different phenological stages. The results show that the size of grape berries increased with period of maturity. The average length, width and thickness were obtained as 19.42 mm, 17.57 mm, and 17.53 mm, respectively. While weight of berries, TSSC, pH and, maturity index increased, BDF, BDF/W ratio, skin firmness, and acidity decreased with phenological stages and axial dimensions. The berries detachment force was decreased from 3.56 N to 2.69 N, while berries weight increased from 3.45 g to 4.42 g depend on phenological stages. Also, there were found closely relationships between mechanical and ripening properties of berries depend on phenological stages. While DF, FDF/W and skin firmness decreased, soluble solids content (17.50-23.97 %) and pH (3.53-3.76) values increased with phenological stages, whereas the total acids were slight changed and reduced from 0.462 to 0.273 %.

KEYWORDS:
Grape, Okuzgozu, Berry, Maturity, Physical and Ripening Properties

INTRODUCTION

Grapes are the most widely grown as commercial fruit in Turkey. Also, it is valuable and important product both human diet and economy in this region. However, conventional breeding methods are dominant in vineyards activities. Especially pruning and harvesting processes in vineyards are still mainly performed by manually. These process time consuming, difficult and tiring. So, production cost is very high and labor efficiency is low. The scarcity and increased cost of hand labor and the increased competition from markets with inexpensive labor have caused commercial growers to depend on mechanization in the vineyard to ensure market competition [1-2]. We know harvesting is one of the critical stage in the management of vineyards. So, use of mechanical harvesting application should be increased in vineyards [14]. Machine harvesting offers many advantages beyond labor and cost savings since it can help improve grape yield and quality in vineyard. Percentage presence of undamaged grapes and dimensions are an important quality criteria both table grape and juice industry. Therefore, the economic value of grape mostly depends on the presence of undamaged grape fruits. To reduced harvest and post-harvest losses, we need to know some physical, mechanical and ripening properties of each grape cultivar separately. Because, these properties are important parameters for design of a pruner, harvester, sorting and grading machines. Some of these properties include the dimensional size, shape, sphericity, geometric mean diameter, surface area, mass, volume, etc. These properties generally depend on the species, variety, diameter, maturity, moisture content and cellular structure [3-4-5-15]. In addition to physical properties, we have to know some information related to grape berries detachment force from cluster and some quality criteria such as ripening, skin firmness, soluble solids content, pH, total acidity and maturity index for suitable maturity stage of grape harvesting [11]. Until now, many studies have been conducted related to mechanical and physical properties of agricultural products and biological materials such as fruits, grains and seeds [16-17]. But, published researches were not found directly physical and maturity properties of grape berry and their relations. These properties are important parameters for design of a new grapevine harvester, sorting, transporting, and grading machines. In the directions of this data, the objective of this study was to measure and determine maturity properties of

grape berries of Okuzgozu variety and their relationships at different phenological stages.

MATERIALS AND METHODS

Vineyard and samples. This study was performed with Okuzgozu (*Vitis vinifera* L) local grape variety (Figure 1). The tests samples were obtained from an organic commercial vineyard in Diyarbakır province, which is located in the southeastern part of Turkey.

FIGURE 1
View of vineyard area and Okuzgozu grape variety

The test samples were randomly harvested by manually from vineyard. Then grape clusters (Figure 2) were transported to laboratory of Department of Agricultural Machinery and Technologies Engineering, University of Dicle and it was preserved in a refrigerator at 5 ^{0}C until the time of the cutting tests.

Measurement of grape berry physical properties. The grape berry tests were carried out during the different phenological stages of the veraison (30 August), 15 days after veraison (15 September) and harvesting time (30 September) in 2016. To determine the physical properties of grape berries, 25 berries randomly taken from five grape clusters at each phenological stages during the harvest season. Length, width and thickness of grape berries were measured with a micrometer to within 0.01 mm. The geometric mean diameter, sphericity, roundness, and surface area of individual fruits were calculated using the following equations [5-6-7-8].

$$Da = \frac{(L + W + T)}{3}$$

$$Dg = (LWT)^{1/3}$$

$$\emptyset = \frac{(LWT)^{1/3}}{L} = \frac{Dg}{L}$$

$$S = \pi D_g^2$$

Where L is the length (mm), W is the width (mm), T is the thickness (mm), D_a is arithmetic mean diameter (mm), D_g is geometric mean diameter (mm), Ø is sphericity (%).

Measurement of mechanical and ripening properties of grape berries. Berry fruit detachment force (BDF), berry weight (W), and the FDF/W ratio are important mechanical and ripening properties for fruit harvesting [1-7-9], and firmness is the resistance of the individual fruit to deformation under applied forces [10]. Therefore, to determine of these parameters of Okuzgozu grape berries were measured at three different phenological stages during the harvest period. Grape berries were weighed by means of a digital balance with 0.01g (Figure 3). The maximum values of BDF force and berry skin firmness were measured in Newton (N) by using a pull digital force gauge (Model FG-20, Lutron Instrument) with stainless steel cone head (Figure 2). The digital force gauge is shown in Figure 2. After measuring the firmness and detachment force, some basic important fruit ripening and harvesting parameters, such as total soluble solids content (TSSC) (by hand refractometer), pH (by pH meter) and total acidity (by Digital Burette) values were determined at three different phenological stages [1-7-11].

FIGURE 2
View of grape cluster, force gauge, micrometer and balance

Data analysis. All data were determined using the analysis of variance (ANOVA) method and significant differences of means were compared using the least significant difference test (LSD) at 5% significance levels using the Tukey multiple range tests in JMP software, version 11.All these tests were replicated least 15 times and the average values were reported. The relationship between physical properties of grape berries and phenological stages were determined using regression analysis of Microsoft Excel (2010) program.

RESULTS AND DISCUSSION

Average some physical, mechanical and ripening properties of Okuzgozu grape berries for different phenological stages are presented in Table 1. Statistical differences were found between phenological stages and physical properties. The effect of phenological stages were found significant ($p<5$) on measured (except sphericity) all physical, mechanical and ripening properties of grape berries, namely; length, width, thickness, volume, arithmetic mean diameter, geometric mean diameter, surface area, detachment force (BDF), weight, skin firmness, TSSC, % pH, and acidity.

The main axial dimensions of berries increased gradually over the period of maturity dates (Table 1). The mean length, width and thickness values for

three phenological stages were obtained as 19.42 mm, 17.57 mm, and 17.53 mm, respectively. In addition to, the volume, arithmetic mean diameter, geometric mean diameter, surface area values were changed statistically with phenological stages. These values slightly increased with the period of maturity time. The increase in physical sizes may be due to physiological growth and increase of maturity index. However, only the change in sphericity was not found significant between phenological stages. It varied from 0.928 % to 0.950 %. As grape barriers developed uniformly in all three axial dimensions, the value of sphericity was obtained a high and almost constant [7]. Versus to increase of physical dimensions depend on phenological stages, while berries detachment force (BDF) from grape cluster, weight, BDF/W ratio, berries skin firmness, and acidity decreased, weight of berries and TSSC and, pH values increased with phenological stages and axial dimensions (Table 1).

There were observed negative relationship between detachment force (BDF) and berries weight. While the fruit weights increased, the BDF decreased with phenological stages. The berries detachment force from the grape cluster was decreased from 3.56 N to 2.69 N, berries weight increased from 3.45 g to 4.42 g depend on phenological stages. As the water content of grape berries increased with maturity, the weight of grape has increased with phenological stages. These values are valuables data for maturity criteria of Okuzgozu grape berries, because BDF/W ratio is an important parameter of fruits mechanical harvesting.

Similar results were observed for ripening properties, namely skin firmness, TSSC, pH, acidity at different phenological stages. Significant differences were found between ripening properties and maturity dates. The maximum firmness was observed as 1.28 N, when the TSS content was 17.50 %. Then the grape skin firmness slightly decreased from 1.28 N to 1.13 N with phenological stages. The situation can be explain that the water content of fruit increased and berries thickness decreased with maturity [7]. According to these results we can express that there is a high correlation between BDF/W ratio and fruit skin firmness. Also, there were found closely relationships between mechanical and ripening properties of berries depend on phenological stages. While BDF, FDF/W and skin firmness decreased, soluble solids content (17.50-23.97 %) and pH (3.53-3.76) values increased with phenological stages. At these stages, the total acids were slight changed and reduced from 0.462 to 0.273 %. Whereas, the lowest values of TSSC and pH were observed at verasion stage as 17.50 % and 3.53, respectively.

The maximum detachment force and grape skin firmness were observed at verasion stage as 3.56 N and 1.28 N, respectively. Also, while berries weight increased due to maturity, TSSC and pH increased, acidity decreased with phenological stages. Similar results were found by [1]. Researcher reported that the mean pH was in range 3.35 to 3.77 and titratable acidity was in the range of 6.44 to 7.31 $g \cdot L^{-1}$ for veraison stage [1].

TABLE 1
Mean physical, mechanical and ripening parameters of Okuzgozu grape berries at different phenological stages

	Phenological Stages				
Properties*	Veraison	15 days after Veraison	Harvest	Mean	LSD**
Length (mm)	18.80^{b}	18.90^{b}	20.57^{a}	19.42	0.795
Width (mm)	16.81^{b}	17.43^{b}	18.50^{a}	17.57	0.771
Thickness (mm)	16.66^{c}	17.58^{b}	18.44^{a}	17.53	0.752
Volume (cm^3)	3.36^{b}	3.47^{b}	4.25^{a}	3.69	0.453
Arithmetic mean dia (mm)	17.42^{b}	17.95^{b}	19.17^{a}	18.18	0.681
Geometric mean dia (mm)	17.37^{b}	17.95^{b}	19.14^{a}	18.15	0.685
Surface area (mm^2)	955.53^{b}	1019.45^{b}	1155.11^{a}	1043.36	78.58
Sphericity (%)	0.928	0.950	0.930	0.936	ns
Detachment force (BDF), N	3.56^{a}	3.05^{ab}	2.69^{b}	3.10	0.422
Weight (W) g	3.45 ^{c}	3.93^{b}	4.42^{a}	3.93	0.408
(BDF/W) N/g	1.031^{a}	0.776^{b}	0.608^{c}	0.805	0.097
Skin firmness (N)	1.28	1.18	1.13	1.196	
TSSC (%)	17.50	20.33	23.97	20.60	
Acidity (%)	0.462	0.390	0.273	0.375	
Maturity index	37.65	52.12	87.80	59.19	
pH	3.53	3.61	3.76	3.63	

*All data represent the average of three replications with 15 values.
** means followed by the same letter in each column are not significantly different by Tukey's multiple range test at the 5 % level, ns: not significant

TABLE 2
Regression equations of cutting properties as a function of three axial dimensions

Parameters*	Regression equation	R^2
Arithmetic mean diameter (mm)	Y= -4.41x 10^{-15} +0.333L+0.333 W+0.333T	1.000
Geometric mean diameter (mm)	Y= -0.08266+0.3117L+0.348W+0.345T	0.999
Surface area (mm^2)	Y= -1039+35.290 L+37.696W+41.79T	0.999
Sphericity (%)	Y= 0.9571-0.0388 L+0.0190W+0.0172T	0.994
Volume (cm^3)	Y= -6.851+0.1327 L+0.2194W+0.2347T	0.923
Detachment force (N)	Y= -1.145-0.00788 L+0.1143W+0.0979T	0.402
Weight (g)	Y= -6.192-0.1154L+0.1954W+0.2562T	0.978

*L: Length (mm), W: Width (mm), T: Thickness

In order to determine the relationships between the grape berries size and the other properties, multiple regression equations were derived from the values of three axial dimensions at different phenological stages. Theirs relationships are given in Table 2. According to the regression equations, significant and high correlations were found between investigated axial dimensions and the other physical properties and mechanical properties of berries (Table 2). As can be seen from the Table 1 and Table 2, especially, average sphericity, roundness and R^2 values were found very high at three phenological stages. Due to obtained high correlation coefficients, this equations can be used for predict the arithmetic mean diameter, geometric mean diameter, surface area, sphericity and roundness of Okuzgozu grape variety as a function of axial dimensions and maturity time. These calculations and equations can be considered in designing the prototype of sorting and separating machine and food industry for grape [2-12]. Similar results were found by [13] for Rasa grape variety.

CONCLUSION

Some physical, mechanical and ripening properties of grape berries of Okuzgozu variety and theirs relationships were determined at three phenological stages. The effect of phenological stages were found significant ($p<0.5$) on measured (except sphericity) all physical, mechanical and ripening properties of grape berries. The main size (length, width and thickness) of grape berries increased over the period of maturity dates.

Berries detachment force (BDF) from grape cluster, BDF/W ratio, berries skin firmness, and acidity decreased, while weight of berries (W), total soluble solids content (TSSC) and, pH values increased with phenological stages and axial dimensions. Soluble solids content values varied from 17.50 % to 23.97 % and pH varied from 3.53-3.76 with phenological stages. However, the total acids were slight changed and reduced from 0.462 to 0.273 % with phenological stages. As a result, these values may be used find out the optimum maturity stage for harvesting of Okuzgozu grape variety.

REFERENCES

[1] Morris, J.R. (2007) Development and commercialization of a complete vineyard mechanization system. HortTechnology. 17, 4, 411-420.

[2] Sessiz, A., Esgici, R., Ozdemir, G., Elicin, A.K., Pekitkan, F.G. (2015) Cutting properties of different grape varieties. Agriculture & Forestry, 61: (1): 211-216.

[3] Persson, S. (1987) Mechanics of cutting plant material. ASAE Publications, St Joseph, MI, USA.

[4] Morris, J.R. (2000) Past, Present, and future of vineyard mechanization. Proceeding ASEV 50 th Anniv. Ann. Mtg. Seatle, WA, 51, 155-164.

[5] Sessiz, A., Elicin, A.K., Esgici, R., Ozdemir, G., Nozdrovicki, L. (2013) Cutting Properties of Olive Sucker. Acta Technologica Agriculturae. The Scientific Journal for Agricultural Engineering, The Journal of Slovak University of Agriculture in Nitra, 16, 3, 80–84.

[6] Mohsenin, N.N. (1986) Physical properties of plant and animals materials. 2 nd edition. New York, NY: Gordon and Breach Science Publishers.

[7] Jha, S.N., Kingsly, A.R.P., Sangeeta, C. (2006) Physical and mechanical properties of mango during growth and storage for determination of maturity. Journal of Food Engineering 72, 73–76.

[8] Zare, D., Salmanizade, F., Safiyari, H. (2012) Some Phyical and mechanical properties of Russian olive fruit. World Academiy of Science, Engineering and Technology. International Journal and biological, Biomolecular, Agricultural, Food and Biotechnologicval Enginerring. 6, 9, 668-671.

[9] Sessiz, A., Özcan, M.T. (2007) Olive removal with pneumatic branch shaker and abscission chemical. Journal of Food Engineering, 76, 2, 148-153.

[10] Renny, E.P., Yahya, A., Adam, N.M., Samsuzana, A.A. (2015) Correlation of moisture content to selected mechanical properties of rice grain samples. International Journal on Advanced Science Engineering Information Technology. 5, 5, 264-267.

[11] Ozdemir, G., Sogut, A.B., Pirinccioglu, M., Kizil, G., Kizil, M. (2016) Changes in the phytochemical components in wine grape varieties during the ripening period. Scientific Papers B, Horticulture Vol. LX: 85-93.
[12] Ghahraei, O., Ahmad, D., Khalina, A., Suryanto, H., Othman, J. (2011) Cutting tests of kenaf stems. Transactions of the ASABE, 54, 1, 51-56.
[13] Khodaei, J., Akhijahani, H.S. (2012) Some physical properties of Rasa grape (*Vitis vinifera* L.). World Applied Sciences Journal 18, 6, 818-825.
[14] Ozdemir, G., Sessiz, A. Esgici, R. Elicin, A.K. (2015) Cutting properties of wine grape cultivars. Scientific Papers. Series B, Horticulture. Vol. LIX, 2015. Print ISSN 2285-5653, CD-ROM ISSN 2285-5661, Online ISSN 2286-1580, ISSN-L 2285-5653
[15] Nesvadba, N., Houska, M., Wolf, W., Gekas, V., Jarvis, D. Sadd, P.A., Johns, A.I. (2004) Database of physical properties of agro-food materials. Journal of Food Engineering 61, 497-503.
[16] Sessiz, A., Esgici, R., Kizil, S. (2007) Moisture-dependent physical properties of caper (*Capparis Ssp*) Fruit. Journal of Food Engineering, 79, 1426-1431.
[17] Sessiz, A., Esgici, R., Ozdemir, G., Elicin, A.K., Pekitkan, F.G. (2015) Cutting properties of different grape varieties. Agriculture & Forestry, 61: (1): 211-216. DOI: 10.17707 /AgricultForest. 61.1.27 Podgorica.

Received: **04.07.2017**
Accepted: **29.07.2017**

CORRESPONDING AUTHOR

Gultekin Ozdemir
Department of Horticulture, Faculty of Agriculture
University of Dicle, Diyarbakir – Turkey

e-mail:gozdemir@dicle.edu.tr

© by PSP Volume 26 – No. 10/2017 pages 6266-6271 Fresenius Environmental Bulletin

EFFECT OF TOPOGRAPHIC MAP SCALE ON QUALITY OF SOIL MAPS IN DETAILED SOIL SURVEYS OF UNDULATED LANDS

Yakup Kenan Koca[1,*], Suat Senol[2], Mahmut Dingil[3], M Eren Oztekin[3]

[1] Department of Soil Science and Plant Nutrition, Faculty of Agriculture, Dicle University, Diyarbakir, Turkey
[2] Department of Soil Science and Plant Nutrition, Faculty of Agriculture, Cukurova University, Adana, Turkey
[3] Department of Architecture and Urban Planning, Cukurova University, Adana, Turkey

ABSTRACT

Topography and slope, the most important factors that makes soil, can be identified easily by means of topographic maps. The most important factors regarding this issue are the scale and quality of cartographic material. In this study; the accuracy of slope maps provided with the use of the different scale topographic maps, one of these cartographic materials and probability of being soil boundary of those were compared. In consequence of digitizing of topographic maps through digital mapping techniques, different resolution DEM and slope maps were created. It was identified that the more resolution increased in slope maps acquired by geographic information system, the more the compatibility of slope maps with land decreased. The 2 m resolution slope map acquired by digitizing the 1:5000 scaled topographic map was determined to overlap with a high level of soil boundaries. The slope boundaries acquired from 1:25000 scaled map were found to be incompatible with land in lower levels.

KEYWORDS:
Topographic map, slope, detailed soil survey, digital mapping, GIS

INTRODUCTION

Soil surveys are complement of studies through which, all morphologic characteristics of soils are described, soils' physical and chemical properties are defined, soils are classified according to the specific classification systems and assessments of lands are performed in a variety of levels [1].

The most time and experience requiring and cost increasing factors in detailed soil mapping are identification of boundaries on land, and then drawn on available cartographic material correctly. The remote sensing (RS) techniques and geographic information systems (GIS) offering constantly new opportunities to natural resources' researchers in line with advances in computer technology, have started to be used increasingly in a more effective manner with the aim of reducing time wasted to find boundary on land in soil survey mapping and different discipline [2, 3, 4, 5, 6, 7, 8].

The soil survey and mapping studies have started in the 1950s in Turkey, schematic soil map [9] was prepared for all over Turkey In the same years, 1:800000 scale Turkey Soil Map was prepared on exploratory level by American expert H. Oakes as well [1]. Through 1:25000 scale maps, search intended soil surveys of overall country were performed and their maps were constituted between the years 1966 and 1971 by General Directorate of Soil-Water. 1:100000 scale search intended provincial land presence maps were constituted by General Directorate of Rural Services between the years 1984 and 2000. Furthermore, the detailed soil surveys of the significant plains were performed with agricultural enterprises located throughout the country.

The use of existing potential of soils unconsciously have resulted negative consequences in an irreversible manner. The most appropriate material for the studies aiming identification, classification of land and soil resources on the basis of scientific principles and prevention of their misuses and improper uses are detailed soil maps prepared on serial level. Primarily European Union member states, many countries have classified and mapped their soils. However, this has not been performed in Turkey yet. Use of unsuitable scale maps other than these mentioned maps will lead to significant mistakes in classification as well. Therefore, detailed soil surveys must be carried out throughout the country on serial level and their maps must be constituted.

In this study, it was investigated whether different scale topographic maps could be used in detailed soil mapping studies as well as digital mapping techniques and whether the slope boundaries determined with different slope classification methods could be soil boundary. For this purpose, 1:5000 and 1:25000 scale topographic map data were compared and high resolution QuickBird satellite data that belongs to the work environment was used as auxiliary cartographic material.

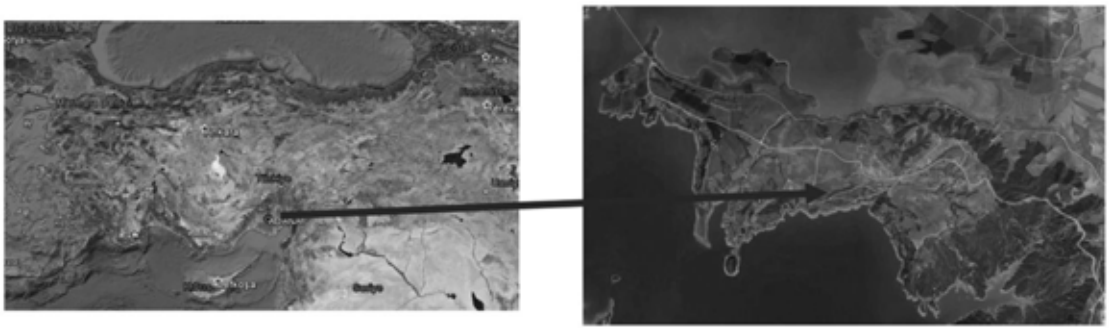

FIGURE 1
Location of study area

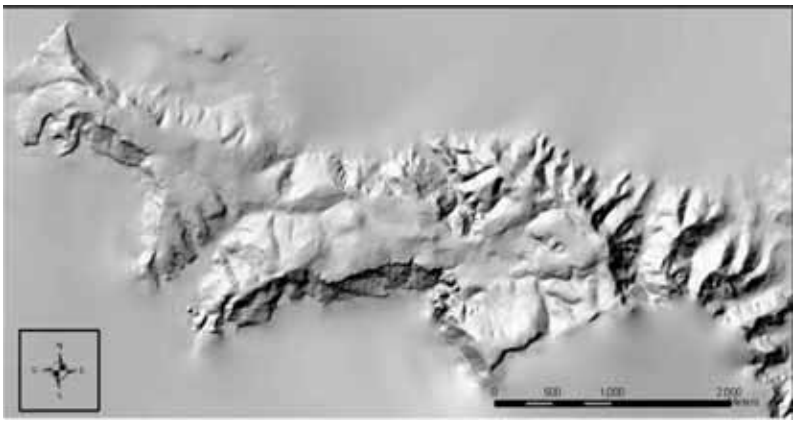

FIGURE 2
Relief map view of work area

MATERIALS AND METHODS

The study was carried out within an area of approximately 1000 ha between 37^0 03' 52" K, 35^0 22' 23" D and 37^0 26' 07" K, 35^0 17' 52" D (Figure 1).

Mediterranean climate, which is hot and dry in summers and warm and rainy in winters, is dominant in work area. The average total annual rainfall in the province of Adana is 668 mm almost half of the rainfall occurs as rain in winters. The average temperature is 19 °C in respect of the same period for many years, and it can increases up to 44 °C in summers. The lowest average temperature is 5.5 °C and occurs in January. Taking into account these data, soil moisture regime of work area was identified as Xeric, soil thermal regime of that was identified as Thermic [10].

1:25000 and 1:5000 scale topographic maps were used as the most important cartographic material and September 2010 dated QuickBird satellite image was utilized as auxiliary cartographic material in the study. Regarding Bureau works, Erdas Imagine 9.1 software was used for processing of remote sensing data; ArcMap 10.0 software was used for the process of digitizing map.

After being digitized, the counter lines on two different scale topographic map were introduced to the environment of geographic information systems. Making use of these counter lines, digital elevation models (DEM) and slope maps with different scales and resolutions belonging to work area were created. Especially prominently different areas in resulting slope classes from both maps were compared with land controls and most land compatible slope map resulted topographic map was assessed as main cartographic material. With the aim of determination whether slope boundaries resulted in classifications could also be soil boundary, slope boundaries were digitized as polygonal in office environment. At this stage, too small areas to be seen on map were eliminated and included in the neighboring polygons, most appropriate to their classes. These boundaries were transferred onto QuickBird satellite image and land works were performed.

Because of that in the surrounding area, the series were previously defined and detailed soil maps were already constituted in the areas with similar nature, a new profile identifying process wasn't performed. In order to identify whether slope map digitization resulted polygons could be soil boundaries; sampling studies were performed with auger in every boundary's center, soil and land characteristics were determined in the level of series and important phases, and mapping units were constituted.

RESULTS

In the study, in which the effects of topographic maps' scale and detail on quality of soil maps in detailed soil surveys were evaluated, the differences were found in DEM (Digital Elevation Model) and slope maps acquired with digitization of both different scale topographic maps. For the purpose of evaluation of that and comparison of the topographic data acquired from 1:5000 scale town maps with those acquired from 1:25000 scaled maps; the work area related contour lines on both topographic maps were digitized, the relief map view of the land (Figure 2) and the slope maps were resulted from these lines.

Evaluating these two slope maps, partial differences were identified in slope classifications. When two slope boundaries acquired from two different scale topographic maps belonging to a given sample area (Figure 3) were compared; it was seen that while some areas were included in similar slope classes, some of them were included in different slope classes. While it was seen in the slope map acquired from 1:5000 scale topographic map (Figure 3b) that a major part of sample area were included in class C with slope of 6 to 12%; the same area was included in class D with slope of 12 to 20% according to the slope map acquired from 1:25000 scale topographic map (Figure 3d). For the purpose of testing the accuracy of both slope maps; the sample areas were determined from the different slope defined points, transferred over the image and their coordinates were addressed at the same time. In the control phase performed in the land, predetermined points were gone their coordinates and slopes were identified. It was explored in land observations that 1:5000 scale topographic maps resulted slope classes were highly compatible with real situation on land and for this reason, this scale topographic map resulted data were used in the next stages of the study.

The different resolution slope maps were acquired from contour lines, depending on the aim of the Project. For this purpose, primarily DEM maps with 2 m, 5 m and 10 m resolutions and then slope maps with the same resolution were obtained (Figure 4). Even though there weren't so critical differences at three different resolution slope map in office environment, it was found in the land study performed with the aim of comparing the resulting slope maps with real situation on land that the most correct results were obtained through 2 m resolution slope maps. It was determined in this stage of the study that 5 m and 10 m resolution slope maps were rougher than others.

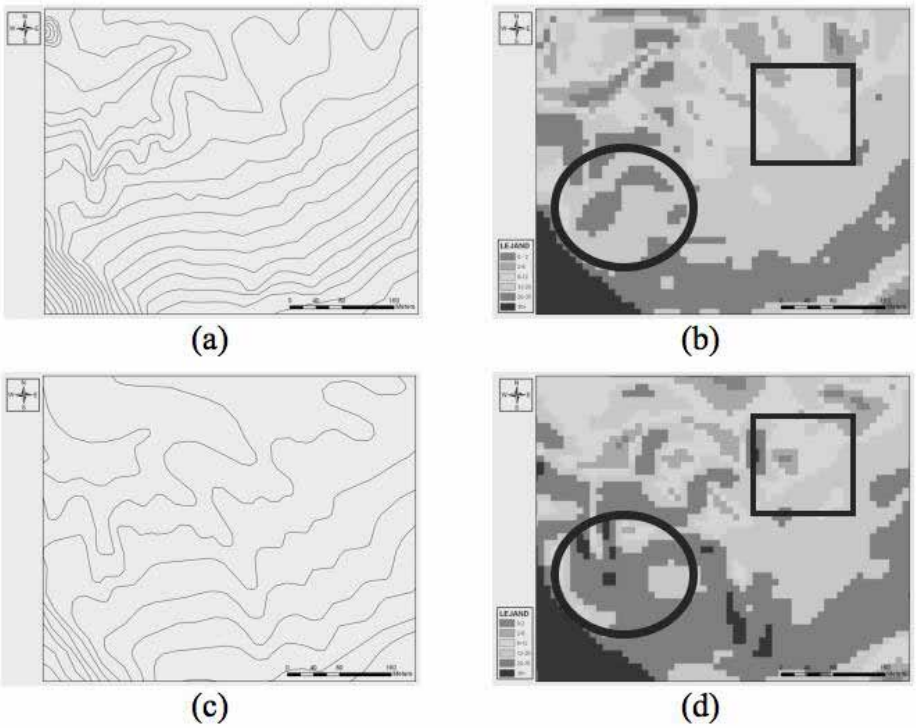

FIGURE 3
Comparison of two different scale. ((a): 1:5000 scale topographic map contour lines; (b) 1:5000 scale topographic map contour lines' slope; (c) 1:25000 scale topographic map contour lines; (d) 1:25000 scale topographic map contour lines' slope

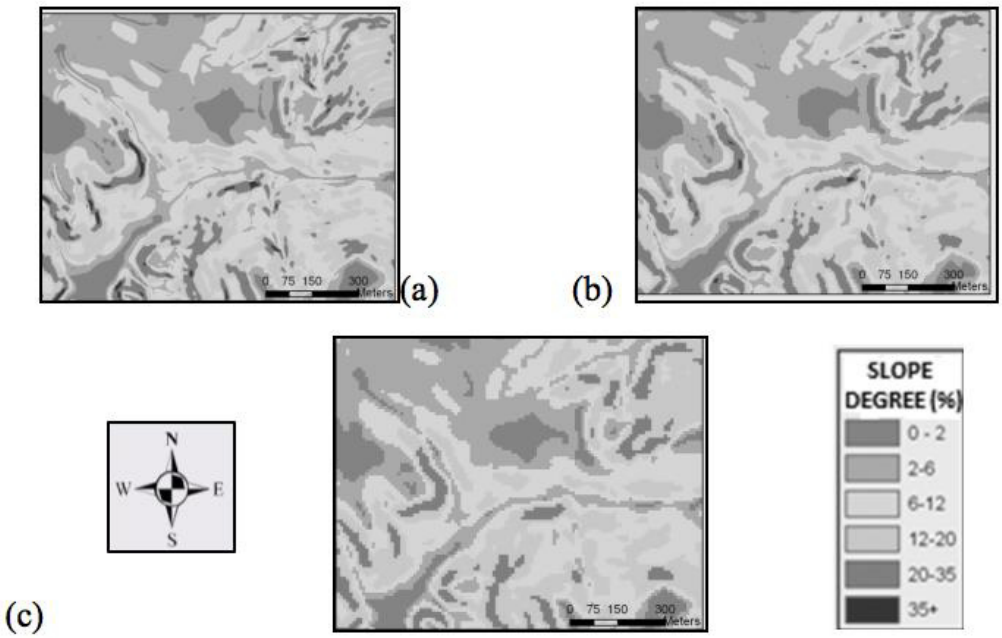

FIGURE 4
Different resolution slope maps ((a) 2 m; (b) 5 m and (c) 10 m resolutions)

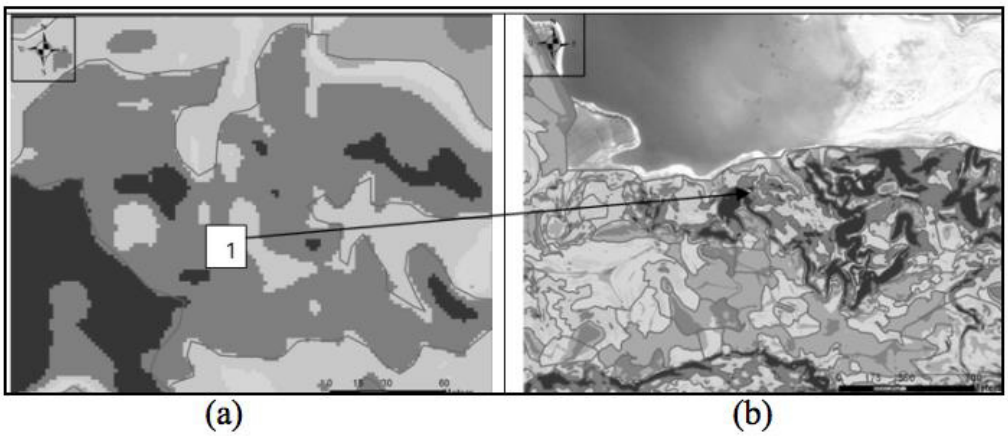

FIGURE 5
Merge of small slope boundaries

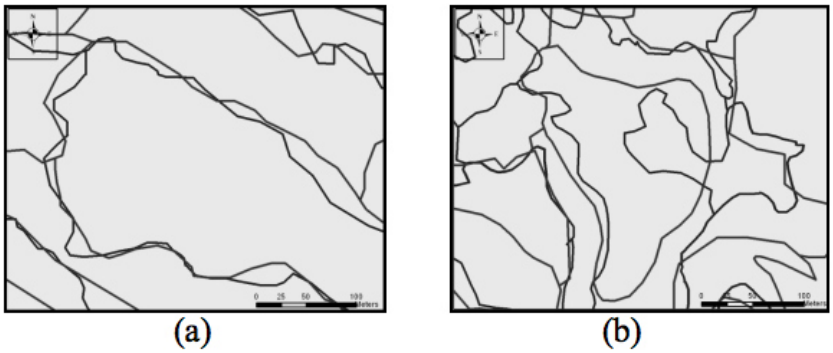

FIGURE 6
Comparison of probable and exact boundaries

The slope maps acquired in digitized form in GIS environment in order to determine that whether slope boundaries obtained in this manner could be soil boundary, were digitized as polygonal. Since display of many areas with small boundaries on map would have a negative effect on its readability and practicability [1]; small areas, not suitable for map's scale, weren't displayed on map and they were included in neighbor polygons, most appropriate to their class. The most important objective for that is to complete land works in less time and increase the quality of map. Without performing this simplification, if it is intended to control each slope with auger, controlling from a very large number of points will be required. Moreover, due to the fact that these boundaries will be eliminated before moving to printing stage, it will be useless to waste time at land.

For example, if this operation wasn't performed within the boundaries of the polygon indicated as number 1 in Figure 5a, in this case, approximately 8 to 10 control points would have to be constituted. However, as shown in Figure 5b, even if control points were constituted with such number of auger, they can't be utilized due to failing to be mapped later and this application will both increase the workforce and cause waste of time. In this way, probable soil boundaries of entire work area were identified and transferred over the satellite image that would be used as base cartographic material on land. The second land work phase defined as the one; in which symbols and boundaries of soil were determined and confirmed on land plots with probes and observations performed on land, soil mapping studies were completed [1]; was performed with satellite image over which, probable soil boundaries acquired in office environment were transferred. At this stage, controls and identifications were made with auger from the points that could represent every polygon identified and mapping units were identified.

Identification of the boundaries previously acquired in office environment, was performed in an absolutely easy manner at land works carried out with high resolution satellite data. Auger using supplied soil properties were identified and their series were specified, making use of land's legend prepared taking into account the general characteristics of predetermined soil series. Afterwards, land-soil characteristics were identified and mapping units were constituted on the basis of mapping legend. At this stage, the most important auxiliary cartographic material was satellite image. In addition, the slope maps acquired by making use of geographic information systems and contour lines, were also used as an important auxiliary cartographic material. The slope map acquired by digitization of large scaled topographic map showed significant similarity with land. Probable soil boundaries acquired by transferring slope polygons over satellite image in office environment, provided convenience on land. It was found that a little experienced surveyor could constituted mapping units correctly in easier manner by using this method. Nevertheless, in the studies performed with 1 m and higher resolution satellites, this method was found partially insufficient for 1:5000 scale topographic maps. Therefore, the probable boundaries acquired from slope map should be evaluated together with the image characteristics of cartographic material used. In addition, the differences in image characteristics involved at the same slope and that could also be defined at cartographic material, have to be analyzed and evaluated by surveyor carefully.

Saving on time was provided by high resolution satellite image of cartographic material and using slope maps acquired in digital environment. The definition point on land was easily found with auger and the polygon boundaries that would be constituted for mapping unit, were more easily and quickly confirmed. Significant overlapping of the slope boundaries that previously acquired in office environment using numerical techniques, with soil boundary appears to be the greatest factor for that. This similarity was seen in a significant part of the study (Figure 6a). Personal comments and drawing oriented differences should not mean that the boundaries are incorrect. Due to the fact that the incompatibilities between the boundaries established in the office environment and those determined after land controls, were defined as a buffer or transition zone; these boundaries could be considered as correct ones. But, incompatibilities are available in specific sections as well (Figure 6b). It was seen that these incompatibilities were much more at the areas especially where slope changed very often. It was seen that slope classes acquired from contour lines transferred to cartographic material wrongly, were also wrong. These incompatibilities were eliminated during land controls and real slope classes and boundaries were imprinted to cartographic material.

DISCUSSION

In this study performed basically for evaluation of scale differences at topographic maps used as a base for multipurpose engineering projects and for practicality of those in soil survey and mapping studies; the detailed soil survey and mapping of sloping region located in the North of the province of Adana and Cukurova University campus, was performed. Two different scale topographic maps were used for this purpose. The counter lines involved at 1:5000 and 1:25000 scale topographic maps were digitized. Through this study performed in the environment of geographic information system; firstly DEM subsequently slope maps were acquired from these counter lines mentioned. When the compatibility of the slope maps acquired from two different scale topo-

graphic maps, with real situation on land was evaluated; it was seen that the slope map acquired from the greater, that is to say, 1:5000 scale map was more compatible. Nevertheless, it was revealed that 1:25000 scale topographic maps could also be used in smaller scale studies, not necessitate any detail.

In the next stage, 2, 5 and 10 m resolution slope maps were acquired from 1:5000 scale map. It was revealed that especially 10 m resolution slope map was rougher for the studies requiring to be detailed. Although there weren't very significant differences between 2 m and 5 m resolution slope maps; 2 m resolution slope map was identified more compatible and this map was used in the rest of the study.

In the last operation before going to the land, the small boundaries on the slope map were merged with their nearest neighboring boundaries and slope boundaries were digitized. Thus, before going to the land, probable soil boundaries were identified on the basis of the slope map and transferred onto the satellite image that is a cartographic material. By this way, not only time spent on land has been shortened, but also it has facilitated less experienced researchers to find soil boundary. During the land work, these data were selected as the baseline and land observations and soil boundaries were confirmed.

REFERENCES

[1] Dinc, U. and Senol, S. (2009) Soil Survey and Mapping. University of Cukurova, Faculty of Agriculture Publication No: 161; Textbook Publication No: A-50, Adana.

[2] Harping, S., Kanemasu, E.T. and Ransom, S.Y. (1990) Separability of soils in a tall grass prairie using Spot and DEM data. Remote Sensing Env. 33, 157-163.

[3] Cullu, M.A. and Dinc, U. (1994) Determination of soil erosion using GIS and remote sensing. Seminar of 2nd RS and Using in Turkey, Uludag, Bursa.

[4] Travaglia, C., Milenova, L., Nedkov, R., Vassilev, V., Milenov, P., Radkov, R. and Pironkova, Z. (2001) Preparation of land cover database of Bulgaria through remote sensing and GIS. Environment and Natural Resources Working Paper No. 6, FAO, Rome.

[5] Senol, S., Dingil, M., Oztekin, M.E., Kapur, S., Derici, M.R., Solmaz, M.I., Dinc, A.O., Gulut, K.Y., Akca, E., Kanber, A. and Terli, H. (2009) Development of a new soil survey method by using geographic information system and remote sensing techniques for detailed mapping of sloping land in order to reduce field work and consumed time. TUBITAK Project Final Report. Project No: 106O112, Adana.

[6] Gundogan, R., Akay, A.E., Okatan, A., Yuksel, A. and Oguzkan, E.A. (2010) Land Suitability Evaluation for Reducing Soil Losses in Kahramanmaras, Turkey. Fresen. Environ. Bull. 19, 2680-2691.

[7] Ozsahin, E., Eroglu, I. and Pektezel, H. (2017) Soil Quality Index (Sqi) Analysis of Tekirdag Province Using GIS (Thrace, Turkey). Fresen. Environ. Bull. 26, 3005-3014.

[8] Comert, C., Bahar, O. and Sahin, N. (2008) Integrated Coastal Zone Management and Cage Siting for Marine Aquaculture. Fresen. Environ. Bull. 17, 12(b), 2222-2231

[9] Caglar, K.O. (1958) Soil Science. University of Ankara, Faculty of Agriculture Publication No: 10, Ankara

[10] Soil Survey Staff. (2003) Keys to Soil Taxonomy, Ninth Edition, by NRCS, US.

Received: **06.07.2017**
Accepted: **14.07.2017**

CORRESPONDING AUTHOR

Yakup Kenan Koca
Department of Soil Science and Plant Nutrition,
Faculty of Agriculture,
Dicle University,
Diyarbakir – TURKEY

E-mail: ykkoca@dicle.edu.tr

© by PSP Volume 26 – No. 10/2017 pages 6272-6285 Fresenius Environmental Bulletin

PREPARATION OF γ -Fe_2O_3/SiO_2/TiO_2 UNDER THE LOW-TEMPERATURE AND THE PHOTO-CATALYTIC DEGRADATION OF SULFAMETHAZINE IN WATER

Qingzhu Jia*, Xiaochen Jia, Hui Chen

School of Marine and Environmental Science, Tianjin University of Science and Technology, Tianjin 300457, China

ABSTRACT

In this work, the magnetic γ-Fe_2O_3/SiO_2/TiO_2 microspheres of core–shell structure with convenient recyclability were prepared by using the ultrasonic-assisted modified Stöber method and sol-gel approach, and the photo-activity of which was evaluated by through the photo-degradation of sulfamethazine in aqueous solution. Results suggested that the good superparamagnetic properties of γ-Fe_2O_3/SiO_2/TiO_2 could be reserved by the formation of γ-Fe_2O_3. The photo-degradation of sulfamethazine results demonstrated that the prepared γ-Fe_2O_3/SiO_2/TiO_2 could provide the same high UV-photo-activity as that of P25 TiO_2 because of their similar constitutes of anatase and rutile types. And the higher UV-photo-degradation rate for sulfamethazine of γ-Fe_2O_3/SiO_2/TiO_2 than that of γ-Fe_2O_3/TiO_2 further demonstrated that the SiO_2 interlining could not only block the contact of TiO_2 shell and magnetic core γ-Fe_2O_3, but also enhance the photo catalytic reactivity. Moreover, this easily recoverable γ-Fe_2O_3/SiO_2/TiO_2 could be reused at least for five times without any appreciable reduction of photo-catalytic efficiency. In combination with HPLC/ESI-MS analysis and density functional theory, photo-degradation pathway of sulfamethazine had been speculated, and some key reaction processes as the hydroxyl oxide, ammonia oxidation, splitting decomposition and open loop reactions might have occurred during the photo-degradation of sulfamethazine.

KEYWORDS:
Photo-catalyst; TiO_2; SiO_2; Sulfadimidine; Degradation pathway

INTRODUCTION

Though sulfa drugs have made a great contribution to stock breeding and disease treatment[1], its extensive use and even abuse has also brought many environmental problems. Thus, these emerging contaminants increasingly occurred in wastewater and aquatic environments[2]. However, antibiotic drugs' removal is difficult and generally inefficient in traditional wastewater treatment plant[3]; hence, sulfa antibiotics residue has caused a potential threat to aquatic organisms and human health[4].

Because of its chemical stability, innocuity safety, high photo-catalytic activity and relatively lower cost, TiO_2 photo-catalysis has been utilized widely to degrade organic contaminants from the water body[5],[6],[7],[8] . Also, in order to recycle photo-catalyst from the disposal wastewater there are increasing concerns of immobilizing TiO_2 by the coating deposited on a solid substrate such as silica gel[9], alumina[10], glass spheres[11] and/or activated carbon[12], et al. These approaches can enhance the separability of TiO_2 from the treated wastewater to some extent, however, the immobilization of TiO_2 catalytic might bring about a striking diminution of catalytic activity[13]. Thus, it is of vital challenge to develop multifunctional photo-catalysts with properties of efficient recyclability and high photo-activity.

Colloidal magnetic microsphere has recently been fascinating as composites, due to their faultless integration of sensitive magnetic response and flexible surface[14]. However, the direct contiguity of magnetic cores and TiO_2 photo-catalyst would usually lead to an unfavorable heterojunction between them giving rise to an enhancement of electron-hole recombination[15]. Hence, in order to avoid direct contiguity between TiO_2 shell and magnetic cores, it would be necessary to insert interfacial layers, such as activated carbon (due to absorbability)[16],[17], CdS (owing to visible light responsive and hetero-structure with TiO_2-based)[18], and SiO_2 (because of chemical inertness and thermo-stability)[19],[20]. In Wei et al.'s work[21], the Au-CdS-TiO_2 nanojunction with an all-solid state Z-scheme system was synthesized by the gas bubbling-assisted membrane reduction-precipitation method. By using the sol-gel method, the prepared magnetic TiO_2-WO_3/SiO_2/Fe_3O_4 nanoparticles under the high-temperature (80℃) could successfully

photo-degrade the bisphenol A from an aqueous solution[17]. But it is unstable and its catalytic efficiency is relatively low at high temperature synthesis[17]. It is necessary to develop a new γ-Fe_2O_3/SiO_2/TiO_2 photocatalyst with higher activity and very good stability.

In this present study, in order to improve the recyclability and photo-activity especially irradiated by sunlight of TiO_2-based catalyst, new hierarchically microporous magnetic γ-Fe_2O_3/SiO_2/ TiO_2 nanoparticles was prepared under the low- temperature. Structure characters of γ-Fe_2O_3/SiO_2/TiO_2 nanoparticles were systematically tested in terms of techniques such as X-ray diffraction, scanning electron microscopy, Fourier transform infrared spectroscopy, vibrating sample magnetometer and UV-vis diffuse reflectance spectra, etc. Also, the photo-activity of γ-Fe_2O_3/SiO_2/TiO_2 nanoparticles was verified by the UV/SUN-degradation of sulfamethazine, and in combination with HPLC-MS analysis, photo degradation pathway of sulfamethazine would be speculated in detail.

MATERIALS AND METHODS

Materials. Titanium isopropoxide and sulfamethazine were supplied by Adamas-beta as pure compounds (>99%). Methyl alcohol, ethanol, glacial acetic acid, tetraethyl orthosilicate (28 wt.%), isopropanol and ammonium hydroxide (25 wt.% by volume) were purchased in China. P25 TiO2 powders was bought from the manufacturer Degussa AG (Germany). Fe3O4 was directly obtained from MACKLIN. Milli-Q water was used for all preparing and after treatment processes. All the reagents were used without further purification.

Preparation of γ-Fe_2O_3/SiO_2/TiO_2 composite nanoparticles. Preparation of Fe_3O_4/SiO_2. In this work, Fe3O4 spheres could be directly bonded with amorphous silica by the ultrasound modified Stöber method. Firstly, 60mg nanosized Fe_3O_4 spheres scattered in 25mL 2-propanol were sonicated for 15min. Then, the dispersion was scattered in a mixed solution of Milli-Q water (25mL) and 2-propanol (75mL). Meanwhile, 0.8mL ammonia solution was dropwise added during 30min sonication. Next, 60μL tetraethyl orthosilicate was mixed in this solution, which was maintained during 3hr ultrasonic at 35℃. Then, they were washed three times with ethanol. Finally, the sample was dried overnight at 60℃.

Preparation of Fe_3O_4/SiO_2/TiO_2 composite nanoparticles. By using Titanium isopropoxide as titanium source, the Fe_3O_4/SiO_2/TiO_2 microspheres were prepared with an ultrasound modified sol-gel method. The process of the fore mentioned Fe_3O_4/SiO_2 as seed for the TiO_2 coating was described above. In the typical synthesis, firstly, 120mg Fe_3O_4/SiO_2 microspheres scattered in 50mL 2-propanol were sonicated for 15min at different temperatures (35℃and 65℃). Then, the dispersion was added in 50mL Milli-Q water and 130mL isopropanol, given a few glacial acetic acid, and was sonicated for 30min. Next, 6mL Titanium isopropoxide was dropwise added and sonicated for 3h. The resulting photo-catalyst was dried overnight in an oven at 80℃, 105℃ and 120℃, respectively. Then, they were washed three times by ethanol and Milli-Q water. Lastly, the Fe_3O_4/SiO_2/TiO_2 microspheres were calcined at 450℃for 2h. Additional, Fe_3O_4/ TiO_2 nanoparticles was prepared using the above approach. Simultaneously, in order to investigate the effect of calcination temperature, Fe_3O_4/SiO_2/ TiO_2 magnetic microspheres synthesized at 35℃ were calcined at 300℃, 400℃, 450℃,500℃and 600℃, respectively, for 2hr under static air.

Characterization of photo-catalysts. The characterization of the photo-catalysts was tested by the following equipment. X-ray diffraction patterns of nanoparticles were measured with a D/MAX-2500 X-ray diffractometer (XRD, Rigaku. Japan). Gold APP Instruments BET surface area were obtained with Tristar 3020 M (BET, micromeritics, America). The morphologies were performed by the scanning electron microscopy (SEM, Shimadzu Japan) equipped with an accelerating voltage of 200kV. For FT-IR, the spectra were gathered on a Fourier Transform Infrared Spectrometer (FT-IR, MultiGas 2030). Magnetic hysteresis curves were obtained with a Vibrating Sample Magnetometer (VSM, LDJ-9600, America) at 300K. UV-vis diffuse reflectance spectra (UV-vis DRS) were carried out by a Cary 60 UV-vis spectroscopy (Agilent, China).

Photocatalytic degradation sulfamethazine. Being as a representative sulfonamide, sulfamethazine was selected to assess the photo-catalytic activity of the prepared γ-Fe_2O_3/SiO_2/TiO_2 catalyst. Photolysis reactions of sulfamethazine were performed with a jacketed reactor setup. Firstly, the sulfamethazine solution (initial concentration of 10 mg/L, initial pH of 6.0) was stirred about for 30 min in the darkness with the addition of photo-catalysts γ-Fe_2O_3/SiO_2/TiO_2, in order to reach the adsorption–desorption quasi-equilibrium. The required pH of 6.0 was adjusted by adding diluted aqueous solution of NaOH and/or hydrochloric acid. Then, the UV-lamp (15W,λ=254) and/or fluorescent lamp (205W) were switched on and the photo-degradation process would be last for 2hr. Also,

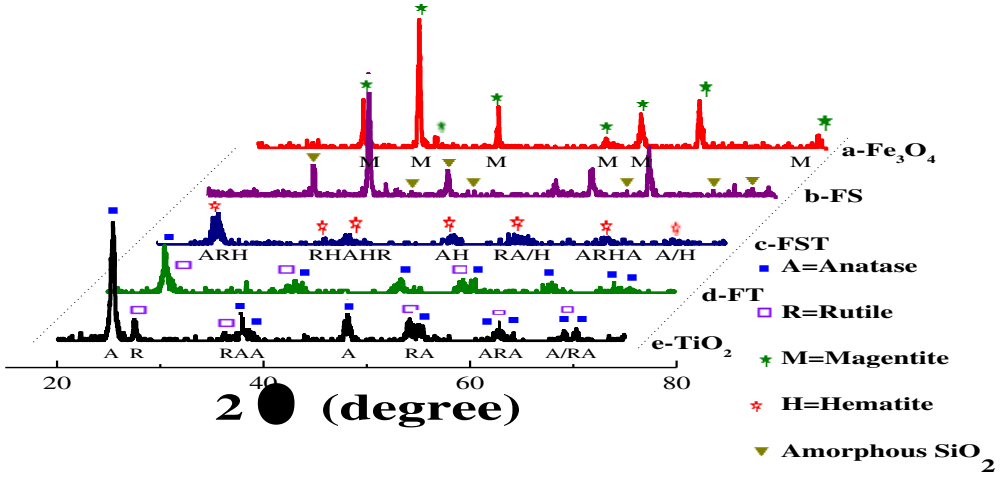

FIGURE 1
XRD patterns of various prepared samples

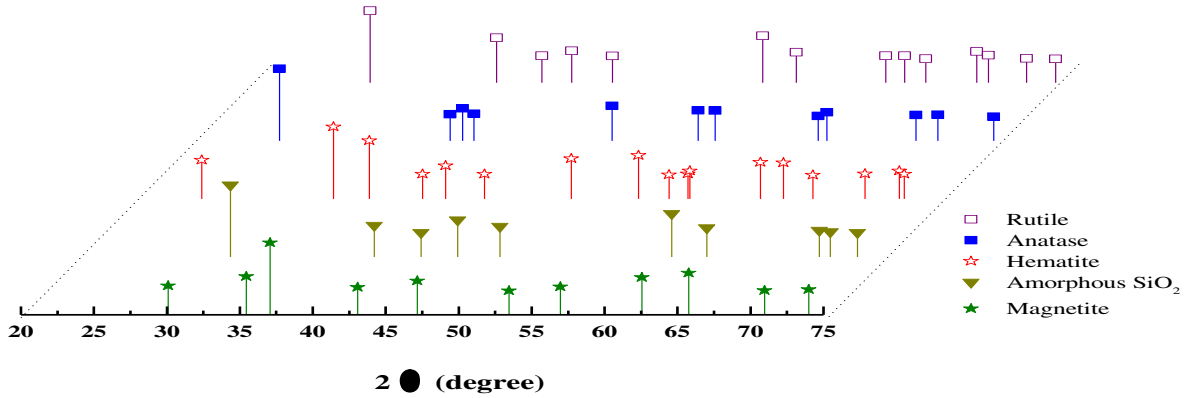

FIGURE 1A
XRD patterns of standard card with various nanoparticles.

sunlight (light intensity of 418W/m2) were used as light source about 2 hr. During the reaction process, samples obtained firstly by the magnetic separated approach were sifted through a 0.2 μm membrane for the HPLC (Ultimate 3000) analysis. Here, the mobile phase was 1 mL/min methanol and water (4:6 of V/V), and an Agela Venusil MP (C18 (2); 4.6×250 mm, 5μm) column was used, and the detector wave length was set as 268.5nm.

Quantum-mechanical calculations of sulfamethazine. According to the density functional theory, atomic charges, frontier electron densities and bond lengthes of SMZ molecule were calculated and simulated on the Pentium IV computer by ab. initio algorithm.

RESULTS AND DISCUSSION

Structure Characters of γ-Fe_2O_3/ SiO_2/TiO_2 nanoparticles. XRD. X-ray diffraction patterns (XRD) of various nanoparticles were showed in Fig.1. The standard XRD patterns of Fe_3O_4, γ-Fe_2O_3, SiO_2, rutile and anatase were showed as Fig. S1 provided as supplementary. Here, XRD patterns of P25 was used as the standard diffractogram for bulk P25 TiO_2 given by the business firm.

Fig.1 suggested the cubic spinel structure characteristic peaks of the Fe_3O_4 nanoparticles. According to XRD patterns of γ-Fe_2O_3/SiO_2/TiO_2 nanoparticle, diffractogram peaks of rutile and anatase could be detected obviously, which was similar to those of P25 TiO_2. Therefore, the new γ-Fe_2O_3/SiO_2/TiO_2 nanoparticles synthesized in our work might have the good photo-catalytic effect. Moreover, for the calcined samples of γ-Fe_2O_3/SiO_2/TiO_2 nanoparticles, diffraction peaks of Fe were showed as peaks of hematite (γ-Fe_2O_3) according to the XRD pattern standard card of γ-Fe_2O_3 (showed as Fig. 1A). These result suggested that the magnetic iron oxide core (Fe_3O_4) had been converted into hematite (γ-Fe_2O_3) after calcination, and the good superparamagnetism

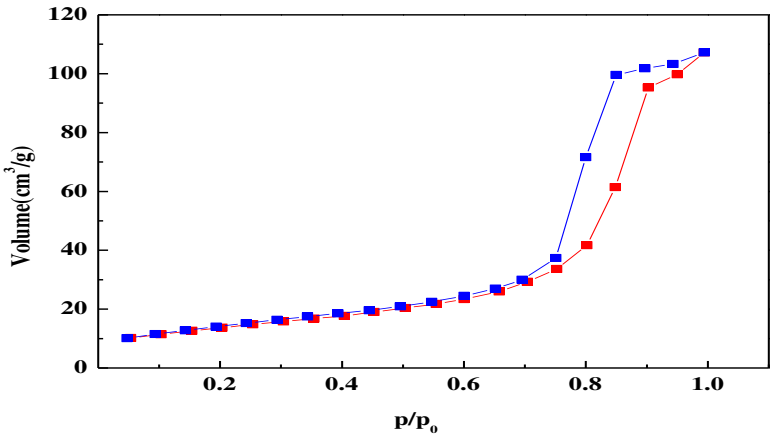

FIGURE 2
The N_2 adsorption-desorption isotherm of $TiO_2/SiO_2/\gamma\text{-}Fe_2O_3$

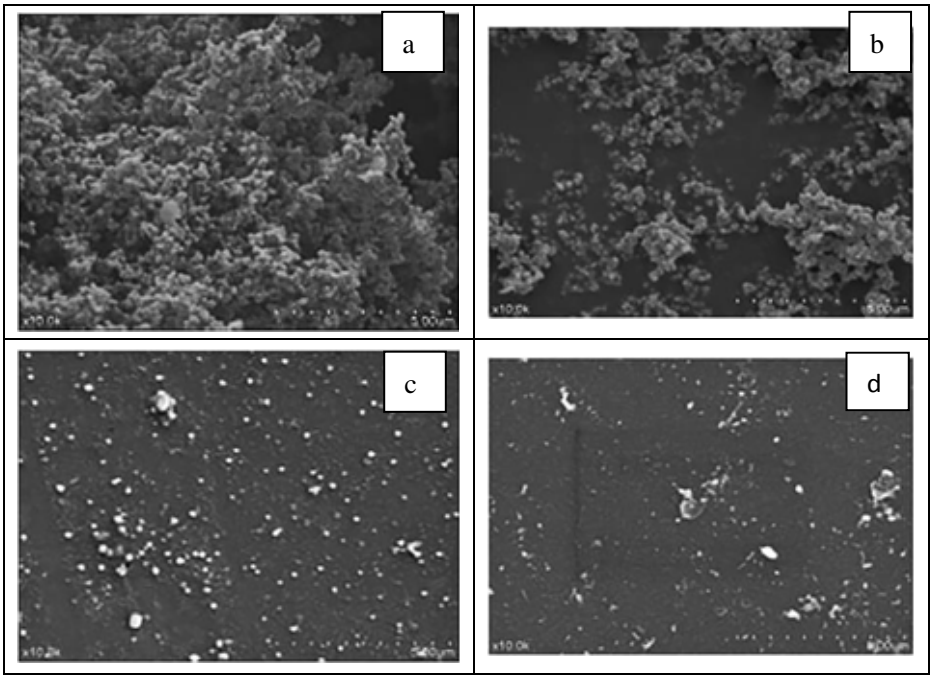

FIGURE S2
SEM pictures of samples (a) Fe_3O_4 (b) Fe_3O_4/SiO_2 (c)$\gamma\text{-}Fe_2O_3/TiO_2$ (d) $\gamma\text{-}Fe_2O_3/SiO_2/TiO_2$

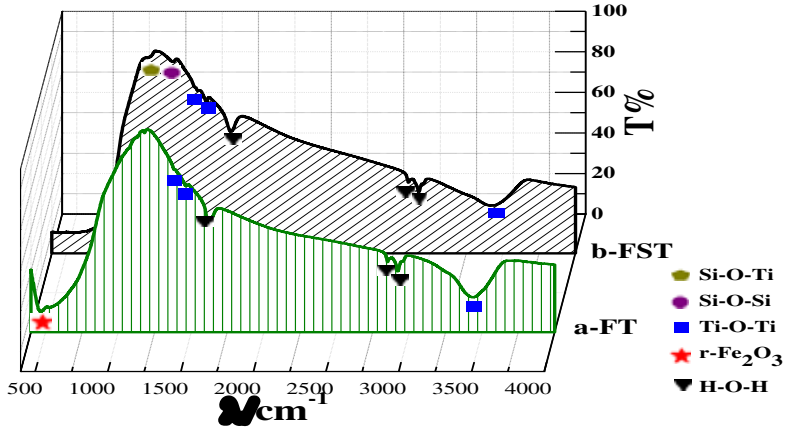

FIGURE 3
FT-IR spectra of γ-Fe2O3/SiO2/TiO2

of hematite19 in the γ-Fe_2O_3/SiO_2/TiO_2 system would ensure the high quality magnetic separation capability, which was the reason that the catalyst prepared in this present study was named as γ-Fe_2O_3/SiO_2/TiO_2 but not Fe_3O_4/SiO_2/TiO_2.

BET&SEM. In Fig. 2, the N_2 adsorption-desorption isotherm of γ-Fe_2O_3/SiO_2/TiO_2 was shown, which exhibited a type V patterns with distinct H1 hysteretic loops in accordance with the IUPAC classification, indicating the presence of agglomerates of spherical particles which is relatively uniform size. Also, the BET surface area of the γ-Fe_2O_3/SiO_2/TiO_2 particles is 49.3 m^2/g, the BJH pore volume is 0.17 cm^3/g and the pore diameter is 13.5 nm. On the other hand, the morphology of the as-preparedγ-Fe_2O_3/SiO_2/TiO_2 nanoparticles, Fe_3O_4 and other magnetic microspheres were characterized by SEM (Fig. S2, provided as supplementary), which indicated the retention of the original hierarchical structure on the nanoscale. In Fig.S2, Fe_3O_4 cores were regular spherical shape with the diameter of 50 nm, consisting of many small microspheres. And also, it could be seen that 15 nm SiO_2 layer was uniformly coated over magnetic cores of Fe_3O_4. When the loaded TiO_2 was 90%, the diameter of FST nanoparticles microspheres varied from 100 nm to 280 nm. These clusters' structures were connected likely owing to magnetic dipole interaction between neighboring nanoparticles. Also, this clusters structure character of γ-Fe_2O_3/SiO_2/TiO_2 might lead to much stronger saturation magnetization of magnetic cores than single nanoparticle[15]. Consequently, magnetic nanoparticles γ-Fe_2O_3/SiO_2/TiO_2 could be quickly separated by a magnet and the reusability of which might be ensured further.

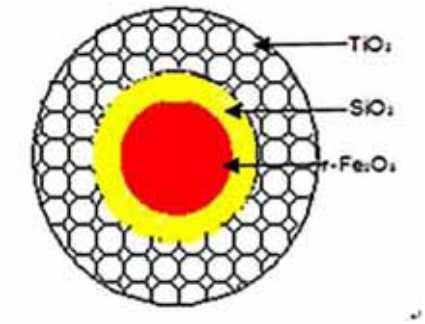

SCHEME 1
Schematic diagram of synthetic FST NPs

FTIR analysis. FTIR spectroscopy (the range of 4000-400cm^{-1}) was carried out by using the MultiGas 2030 to further identify composition information and chemical bonding of SiO_2 layers. And sequential coating TiO_2 layers of γ-Fe_2O_3/SiO_2/TiO_2 and γ-Fe_2O_3/TiO_2 were shown in Fig.3. For both γ-Fe_2O_3/SiO_2/TiO_2 and γ-Fe_2O_3/TiO_2, the high-intensity peak about at 3500cm^{-1} denoted the bending vibration of the anatase crystals. In case of γ-Fe_2O_3/TiO_2, γ-Fe_2O_3 absorption peak was detected. While for γ-Fe_2O_3/SiO_2/TiO_2, it should be noted that no γ-Fe_2O_3 absorption peaks was detected obviously, which might imply that γ-Fe_2O_3 was absolutely sheltered by SiO_2 shells; moreover, Fe and Ti bonds absorption peaks had not been recorded, implying that γ-Fe_2O_3 cores and TiO_2 shells were totally isolated by the SiO_2. Also, and 1403-1232cm^{-1} stands for the stretching modes of Si-O-Si. A band at 1052cm^{-1} was a typical stretching modes of Ti-O-Si linkage which was Si_4 structural unit connected to TiIV14. These results also implied that tetrahedral TiIV could merge into the silica framework. Hence, γ-Fe_2O_3/SiO_2/TiO_2 was core–shell structured magnetic microspheres. In addition, adsorption experiments of this work showed that this prepared photo-catalyst γ-Fe_2O_3/SiO_2/TiO_2 might have a low adsorption capacity of pollutants. Thus, combined with SEM and BET, tight outer and small porosity of the photo-catalytic structure might be speculated and showed as Scheme 1.

Magnetic hysteresis curves. Magnetic hysteresis curves were obtained by using a vibrating sample magnetometer shown as in Fig.4. The saturation magnetization of Fe_3O_4, Fe_3O_4/SiO_2 and γ-Fe_2O_3/SiO_2/TiO_2 were estimated to be 39.1emu/g, 25.7 emu/g and 6.7 emu/g at 300K temperature, respectively. The coactivity, and residual magnetization of γ-Fe_2O_3/SiO_2/TiO_2 nanoparticles were assessed to be 14.31 G and 0.15 emu/g, respectively, implying the superparamagnetism capability of γ-Fe_2O_3/SiO_2/TiO_2 nanoparticles. Benefited from properties of the higher saturation magnetization as well as narrower magnetic hysteresis curve, the magnetic core consisted of spherical γ-Fe_2O_3 nanoparticles could make quick magnetic separation and re-dispersal[19]. Hence, the γ-Fe_2O_3/SiO_2/TiO_2 nanoparticles photo-catalyst could be efficiently separated under an external magnetic field[20]. Meanwhile, once the external magnetic field was removed, magnetic microspheres could be re-dispersed in the mixture solution.

UV-Vis. The UV-vis diffuse reflectance spectra of TiO_2 and prepared γ-Fe_2O_3/SiO_2/TiO_2 nanoparticles were showed in Fig. 5. Results of Fe_3O_4@SiO_2 showed weaker absorption performance in the range of 450-750 nm. The UV–vis diffuse reflectance spectra of TiO_2 mainly concentrated on the UV range of 200nm to 400nm. Here, it should be noted that γ-Fe_2O_3/SiO_2/TiO_2 nanoparticles showed a notably wide absorption peak in the visible light region (more than 400nm). The possible reason might be that the iron ion could modify the photo absorption behavior to some extent and a

slight blue-shift at visible wavelengths could then be occurred[22]. γ-Fe_2O_3/SiO_2/TiO_2 nanoparticles prepared at synthesis temperatures of 35℃and 65℃ existed the similar absorption results, though in the normal visible light range, the absorption peak of the former was slightly higher than that of the latter.

All the above results indicated that γ-Fe_2O_3/SiO_2/TiO_2 had further enhanced photo-catalytic activity compared with P25 TiO_2 especially in the normal visible light range.

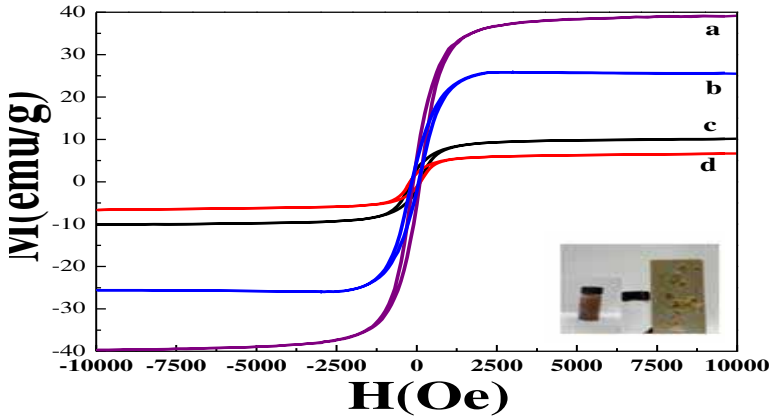

FIGURE 4
Magnetic hysteresis curves of (a) Fe_3O_4, (b) Fe_3O_4/SiO_2, (c)γ-Fe_2O_3/TiO_2, and (d) γ-Fe_2O_3/SiO_2/TiO_2 at room temperature.

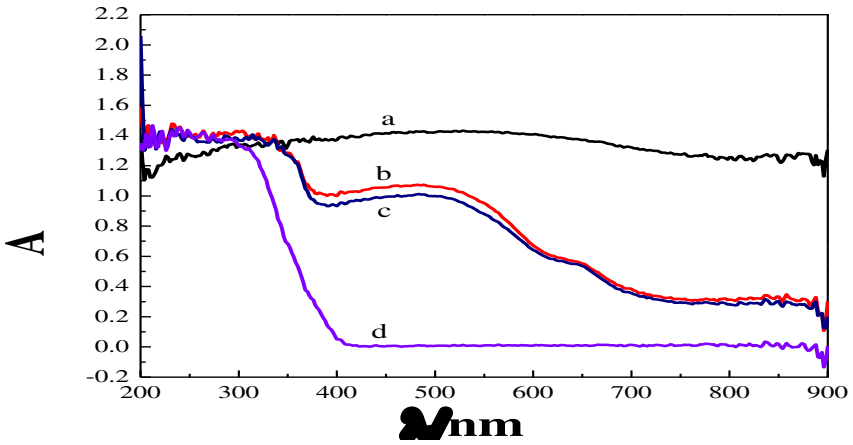

FIGURE 5
UV-VIS DRS spectras (a) Fe_3O_4/SiO_2, (b) γ-Fe_2O_3/SiO_2/TiO_2-35, (c) γ-Fe_2O_3/SiO_2/TiO_2-65 and (d) P25 TiO_2.

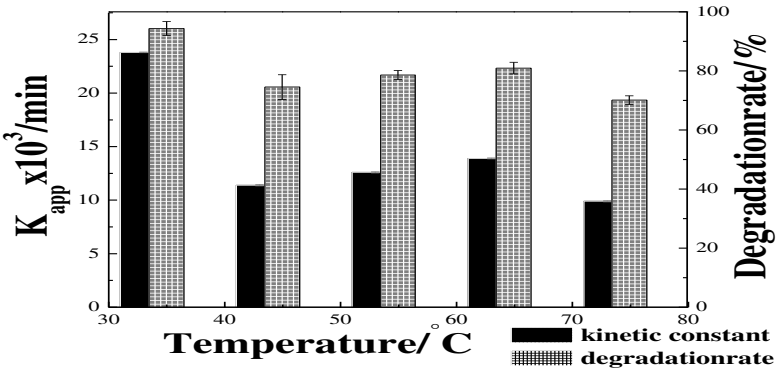

FIGURE 6
Effects of catalyst synthesis temperature on the photo-degradation of sulfamethazine

Influences of synthesis temperature and calcination temperature on the photo-catalytic property of γ-Fe_2O_3/SiO_2/TiO_2. Synthesis temperature. Irradiated with the sunshine (about 418W/m^2), the photo-activity of γ-Fe_2O_3/SiO_2/TiO_2 prepared at different synthesis temperature were investigated and the results were given in Fig.6. Fig.6 showed that the degradation rate of sulfamethazine decreased with the increasing of synthesis temperature of γ-Fe_2O_3/SiO_2/TiO_2. For theγ-Fe_2O_3/SiO_2/TiO_2 prepared at 35 the increasing of synthesisulfamethazine was about 95% after photolysis for 2h; whereas for theγ-Fe_2O_3/SiO_2/TiO_2 obtained at 65after photolysis for 2h rate could be reached. In case of the degradation kinetic constant, the former (k=0.0294 min^{-1}) was about the two times of the latter (k=0.0139 min^{-1}). These results suggested that the photo-catalytic activity of γ-Fe_2O_3/SiO_2/TiO_2 nanoparticles magnetic microsphere might be decreased with the rising of synthesis temperature. And the possible reason might be that the volatility of isopropyl alcohol would be increased if temperatures were too high, which therefore would influence the structure and photo-catalytic activity of γ-Fe_2O_3/SiO_2/TiO_2. At the same time, an interesting phenomenon was found. Compared to the γ-Fe_2O_3/SiO_2/TiO_2 of conventional synthesis process, the γ-Fe_2O_3/SiO_2/TiO_2 at low temperature synthesis better adapt to environmental changes (such as water temperature and PH), owing to firmer TiO_2 adhesion from the novel preparation method.

Moreover, our work demonstrated that if the condensing temperature of γ-Fe_2O_3/SiO_2/TiO_2 was low enough, the prepared γ-Fe_2O_3/SiO_2/TiO_2 nanoparticles would have relatively higher efficiency especially at the low-temperature synthesis condition. Accordingly, this proposed new method of γ-Fe_2O_3/SiO_2/TiO_2 nanoparticles prepared under a lower synthesis temperature instead of the traditional heat synthesis treatment was successful and hopeful.

Calcination temperature. Thermogravimetric analysis of Fe_3O_4/SiO_2/TiO_2 was showed in Fig.S3 provided as supplementary. XRD patterns of γ-Fe_2O_3/SiO_2/TiO_2 nanoparticles prepared at different calcination temperatures were described in Fig. S4 provided as supplementary, and effects of calcination temperature for γ-Fe_2O_3/SiO_2/TiO_2 on the photo-degradation of sulfamethazine were showed in Fig.7.

Fig.S3 suggested that the γ-Fe_2O_3/SiO_2/TiO_2 nanoparticles weightlessness was about 2.39% from 300℃ to 400℃ because of the crystal type transformation from amorphism to anatase, and about 1.32% weightlessness was obtained in the range of 400-500400-500-500f 400-500pe transformation from ture for γ-Fel and hopeful.w metγ-Fe_2O_3/SiO_2/TiO_2 nanoparticles weightlessness was almost zero in the range of 600℃ to 800℃.Accordingly, calcination temperature range of γ-Fe_2O_3/SiO_2/TiO_2 nanoparticles was set at 300-600a.

According to XRD patterns shown in Fig.S4, γ-Fe_2O_3/SiO_2/TiO_2 nanoparticles calcination temperature at 300℃mainly included the amorphous state TiO_2. For γ-Fe_2O_3/SiO_2/TiO_2 nanoparticles samples prepared at 450-550300℃mainly anatase and a few rutile TiO_2 were detected obviously. For d at$_2O_3$/SiO_2/TiO_2 nanoparticles of calcination temperature at 450℃, diffractogram peaks were the strongest, suggesting the better crystallinity of TiO_2. However, when calcination temperature over 60000 cry$_2$ crystal converted anatase into rutile. In summary, results shown in Fig. S4 demonstrated that the crystal form and crystallinity of TiO_2 in γ-Fe_2O_3/SiO_2/TiO_2 would be markedly affected by the calcination temperatures.

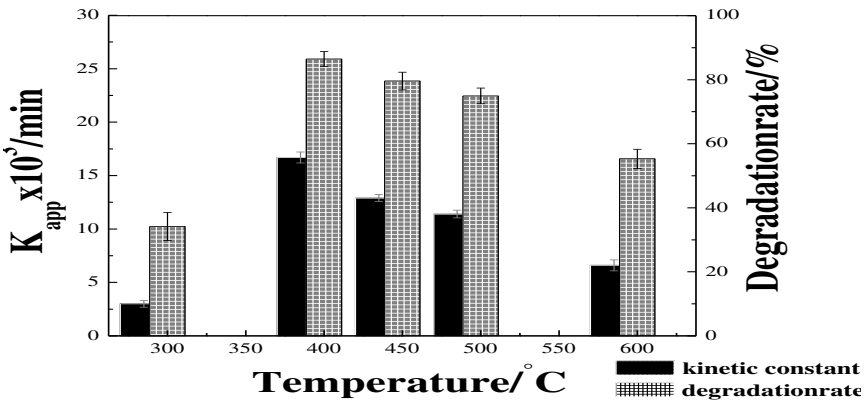

FIGURE 7
Effects of calcination temperature for γ-Fe_2O_3/SiO_2/TiO_2 on the photo-degradation of sulfamethazine

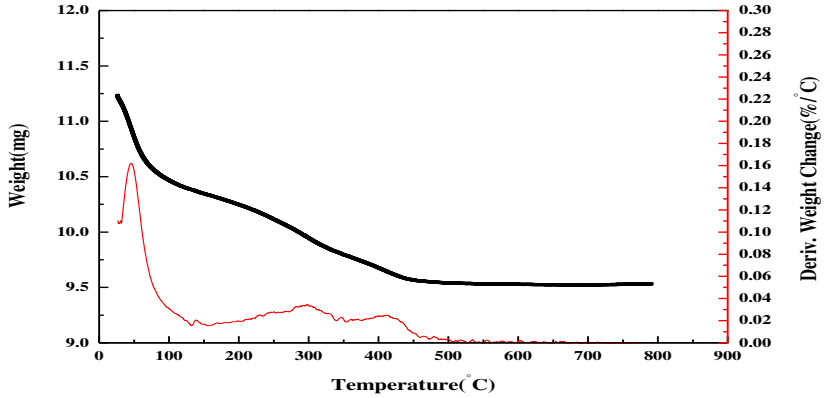

FIGURE S3
The thermogravimetric curve of $Fe_3O_4/SiO_2/TiO_2$

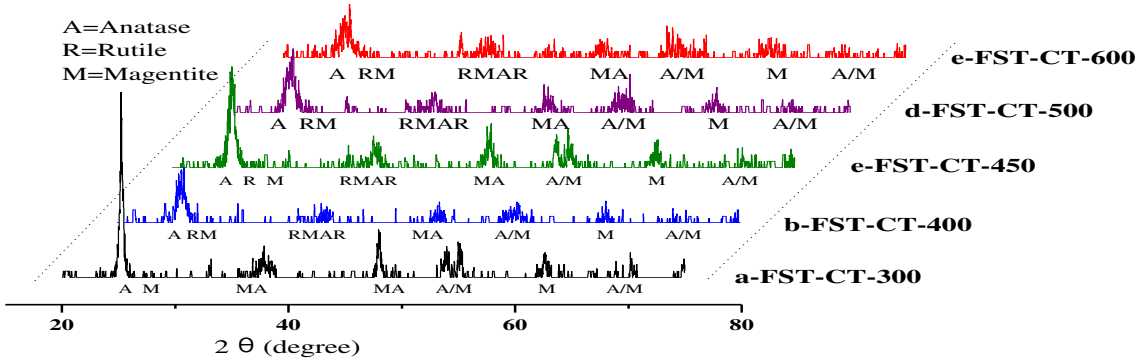

FIGURE S4
XRD patterns of γ-$Fe_2O_3/SiO_2/TiO_2$ (FST) prepared at different calcination temperatures.

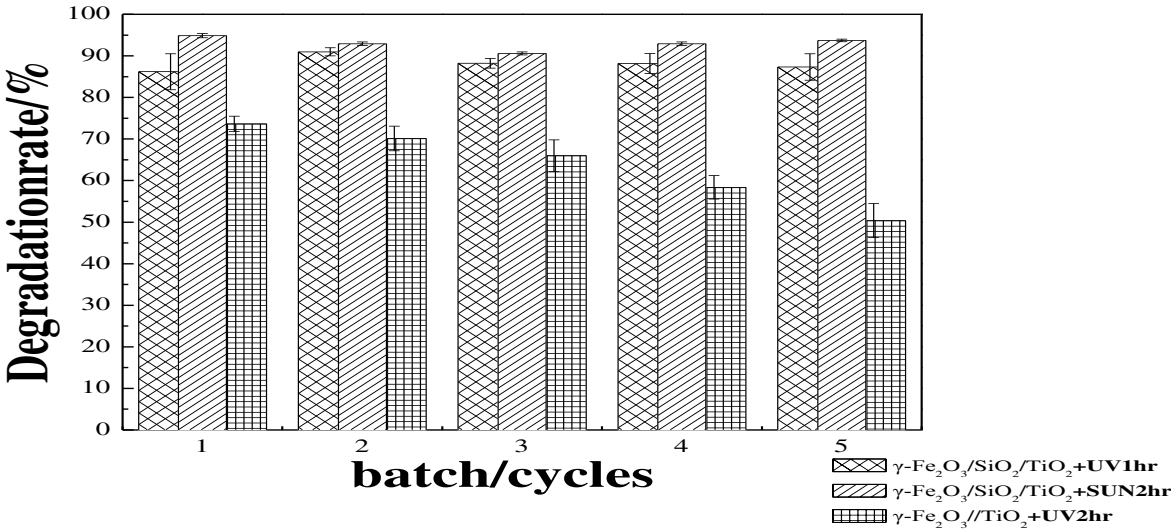

FIGURE 8
Reusability of γ-Fe_2O_3/TiO_2 (1.6g/L) and γ-$Fe_2O_3/SiO_2/TiO_2$ (2.4g/L) photo-catalysts for the photo-degradation of sulfamethazine.

Also, results shown in Fig.7 demonstrated that the photo-activity of γ-$Fe_2O_3/SiO_2/TiO_2$ was dramatically influenced by the calcination temperatures, and the high photo-activity could be obtained in the range of 400-500℃, especially for 400℃ and 450℃ γ-$Fe_2O_3/SiO_2/TiO_2$ nanoparticles, with the sulfamethazine degradation rate of 90% in the sunshine. While, for γ-$Fe_2O_3/SiO_2/TiO_2$ nanoparticles prepared at 300 and 600℃, the photo-activity was very low, and the degradation rate of sulfamethazine was only 60% after photolysis of 2hr (k=0.007 min^{-1}). Consequently, the optimal calcination temperature should be set at 450℃.

TABLE S1
The residue Fe ion of γ-Fe_2O_3/SiO_2/TiO_2 and γ-Fe_2O_3/TiO_2 systems after separation.

Fe ion mg/L \ Reuse-time	1 time	2 times	3 times	4 times	5 times
Fe ion of γ-Fe_2O_3/TiO_2	1.3375	1.214	0.832	0.900	0.876
Fe ion of γ-Fe_2O_3/SiO_2/TiO_2	0.0201	0.0008	0.0174	0.0036	0.0284

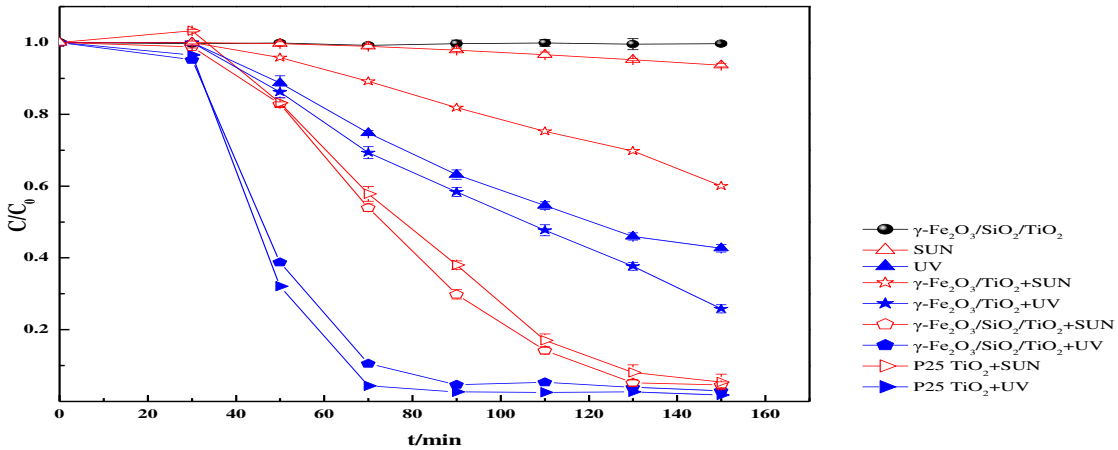

FIGURE 9
Sulfamethazine concentrations over time in dark, solar irradiation or UV condition with γ-Fe_2O_3/TiO_2, γ-Fe_2O_3/SiO_2/TiO_2 and/or P25 TiO_2

Photo-catalyst reusability. Magnetic separation process was a viable technique for reusability of synthesized photo-catalyst[23]. Fig.8 described the reusability of γ-Fe_2O_3/TiO_2 and γ-Fe_2O_3/SiO_2/TiO_2 samples on the photo-degradation of sulfamethazine in aqueous solution. Results showed that the photo-activity of γ-Fe_2O_3/TiO_2 decreased dramatically (sulfamethazine degradation rate from 75% to 50%) with the increasing of reused times under UV irradiated for 2hr; while for the γ-Fe_2O_3/SiO_2/TiO_2 samples, these γ-Fe_2O_3/SiO_2/TiO_2 could keep high photo-activity (sulfamethazine degradation rate range of 91-94%, respectively) after five times' utilization under UV irradiated for 1hr and/or solar radiation for 2 hr. Also, loss of photo-activity might be roughly ignored during the sulfamethazine degradation with γ-Fe_2O_3/SiO_2/TiO_2. In fact, not only the photo-catalytic activity, but also the magnetic and the stability largely influenced the practical application of γ-Fe_2O_3/SiO_2/TiO_2 microspheres.

On the other hand, in order to prove the stability of γ-Fe_2O_3/TiO_2 and γ-Fe_2O_3/SiO_2/TiO_2 nanoparticles photo-catalysts, the residual concentration of iron ion in solution was tested by using the atomic absorption spectrophotometer (AA-7003F, China). Table S1 (provided as supplementary) showed that the residual iron content in the γ-Fe_2O_3/TiO_2 system was about 0.8-1.4 mg/L, while in the γ-Fe_2O_3/SiO_2/TiO_2 system, the residual iron content was only about 0.003-0.02 mg/L, which might be roughly ignored. These results further suggested that the SiO_2 interlayer could protect magnetic cores from dissolution of iron ion, and γ-Fe_2O_3/SiO_2/TiO_2 nanoparticles microspheres prepared in this work were stable and reusable.

Photo-catalytic sulfamethazine. Photo-catalytic effect for sulfamethazine. In order to evaluate the photo-activity of γ-Fe_2O_3/SiO_2/TiO_2 nanoparticles prepared in this work, photo-degradation of sulfamethazine under various conditions were investigated and the results were shown as in Fig.9. Fig.9 suggested that the change of sulfamethazine concentration was very little (less than 5%) under just γ-Fe_2O_3/SiO_2/TiO_2 TiO_2 in the absence of irradiation. It was obvious that sulfamethazine removal efficiency was high as 95% (k_{uv}=0.0516min^{-1}, R^2 = 0.99) with photo-catalystics of P25 TiO_2 and γ-Fe_2O_3/SiO_2/TiO_2 for 1 hr under UV-irradiation, yet sulfamethazine removal efficiency only reached 57% if just irradiated by UV for 2 hr. Also, sulfamethazine removal efficiency was high as 70% (ksun=0.0294min^{-1}, R^2 = 0.94) with photo-catalystic of P25 TiO_2 and

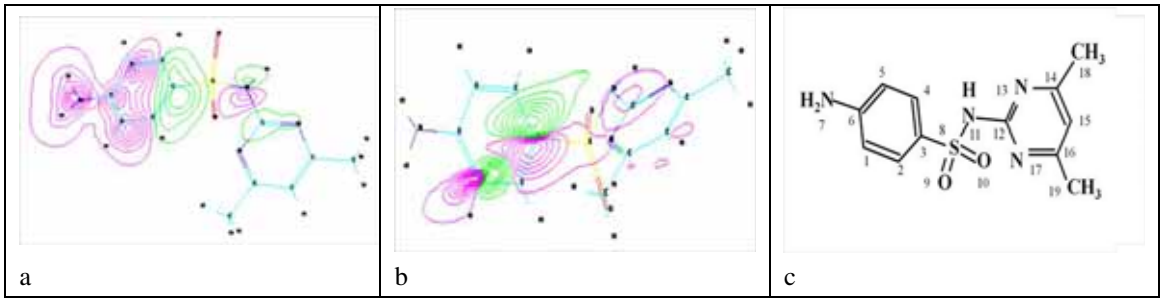

FIGURE 10
Scheme of the frontier orbital density of Sulfamethazine (a) HOMO, (b) LOMO and (c)structural formula of sulfamethazine molecule.

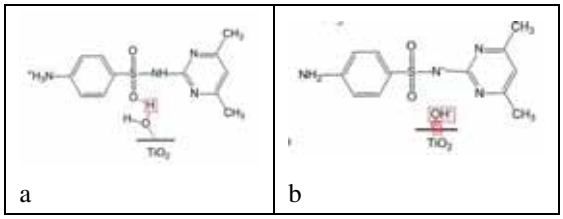

FIGURE S5
Electron reorganization of sulfamethazine of ((a)cation (b)anions) on the surface of γ-Fe_2O_3/SiO_2/TiO_2.

γ-Fe_2O_3/SiO_2/TiO_2 for 1 hr under solar irradiation. What is more, the photo-activity of prepared γ-Fe_2O_3/SiO_2/TiO_2 for 2 hr at the sunshine would reach the almost same level of γ-Fe_2O_3/SiO_2/TiO_2 for 1 hr under UV-irradiation, which further demonstrated the slight blue-shift of γ-Fe_2O_3/SiO_2/TiO_2 at visible wavelengths in the UV-vis. While, in the case of γ-Fe_2O_3/TiO_2, the lower sulfamethazine removal efficiency (75% or 40%) was obtained under condition of γ-Fe_2O_3/TiO_2/UV or γ-Fe_2O_3/TiO_2/sunshine. Compared to the performance of γ-Fe_2O_3/SiO_2/TiO_2 with their samples, our γ-Fe_2O_3/SiO_2/TiO_2 have higher activity and very good stability, due to the novel prepared method[15],[22],[23].

The photo-activity similarity of P25 TiO_2 and γ-Fe_2O_3/SiO_2/TiO_2 suggested that they might have the same crystal type of anatase and rutile, which could be certified by their XRD shown in Fig.1. Comparisons of photo-activity between γ-Fe_2O_3/SiO_2/TiO_2 and γ-Fe_2O_3/TiO_2 suggested that the SiO_2 interlayer was vital for photo-catalyst to possess both the superparamagnetic properties of internal γ-Fe_2O_3 and photo-catalytic activity of exterior TiO_2, which could not only restrain the weakening of γ-Fe_2O_3 magnetism but also prevent the weakening of photo-activity[14]. Therefore, γ-Fe_2O_3/SiO_2/TiO_2 with high photo-catalytic effect prepared in this work could realize the separation and recycling of photo-catalyst, and effectively reduce the costing of wastewater treatment.

TABLE S2
Potential cleavage sites and frontier electron density values at each position of sulfamethazine

Atom No.	Charge value	PED value
1	-0.083988	1.052891
2	-0.035062	0.944780
3	-0.094692	1.106375
4	-0.036046	0.950464
5	-0.083008	1.054081
6	0.120865	0.936789
7	-0.385078	1.545668
8	0.674793	1.981570
9	-0.330941	1.952738
10	-0.326142	1.676705
11	-0.378754	0.982929
12	0.283637	0.886688
13	-0.277453	1.033106
14	0.131882	0.903212
15	-0.106427	1.000156
16	0.136514	0.895291
17	-0.267186	1.329408
18	-0.184938	0.981180
19	-0.186343	1.035729

Degradation pathway of sulfamethazine. HOMO is the Highest Occupied Molecular Orbital, and LOMO means the Lowest Unoccupied Molecular Orbital[24]. Sometimes, HOMO and LUMO are referred to as frontier orbitals in frontier molecular orbital theory[25] . The highest molecular orbit electron in each atom has a certain charge density distribution, and the order of the size distribution would decide the location of an electrophilic rea-

gents attack individual atoms. Hence, electrophilic reaction is most likely to occur on the maximum charge density of atoms in the HOMO; similarly, nucleophilic reagent is the most easy to attack maximum charge density of atoms in the LUMO[26].

On the basis of density functional theory[24], scheme of sulfamethazine molecular model was calculated using ab initio calculation show as in Fig.10, and the atomic charge values were listed in Table S2 provided as supplementary. Also, trapping experiments of reactive species like ·OH and $\cdot O_2^-$ should be confirmed by ESR[27].

Results listed in Table S2 showed that O9 and O10 have larger electronegativity though slightly different (-0.330941 and -0.326142). Consequently, O9 and/or O10 of sulfamethazine might interact with $TiOH^{2+}$ on the TiO_2 surface during the photo-catalytic degradation of sulfamethazine, and it was possible that the new bond of -O-H…O-bond could be obtained (in Fig. S5 provided as supplementary). Also, Table S2 showed that C1, C3, N7, S8, O9, O10 and N13 have the higher front electron density. In accordance with the frontier orbital theory, the part of the high front electron density could be attacked preferentially by hydroxyl radicals; and these bonds connected with these atoms could preferentially break. Here, part of possible bond cleavage of sulfamethazine was shown in Fig.10.

In order to further analyze intermediate products, HPLC/ESI-MS analysis was carried out. The characteristic peak of HPLC/ESI-MS Ion flow chart could be shown at 2.2min, 2.5min, 5.6min, 5.9 min and 7.3min, and the corresponding intermediates are 2,4-Dimethylpyrrole, hydroquinone, N-(4,6-Dimethylpyrimidi-2-yl)Benzene-1,4-Diamine, sulphanilamide and 2-Amino-4,6-dimethylpyrimidine, respectively.

According to the theoretical analysis and HPLC/ESI-MS analysis results of this work, the main reactions in the sulfamethazine degradation process might be (1), the hydroxyl oxide (2), ammonia oxidation (3), splitting decomposition and (4), open loop, etc. Hence, degradation pathway of sulfamethazine could be speculated and also expressed in detail as Fig.11. Here, three main pathways could be summarized as follows: (1), firstly,

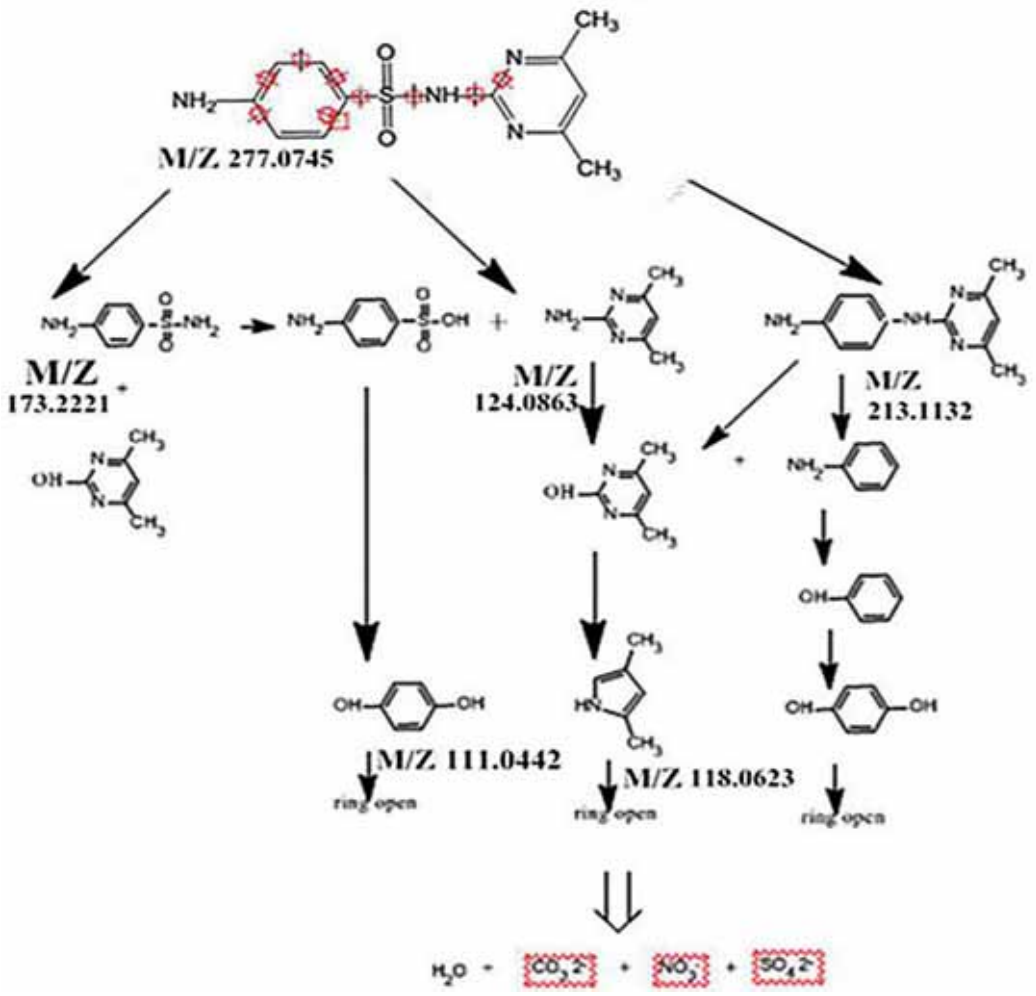

FIGURE 11
Possible pathways of sulfamethazine oxidative degradation

from the theory, intermediate products of sulfamethazine can be obtained by a hydroxyl attack on the sulfonamido-. And these products are able to yield by sulfamethazine desulfurization such as formation of 2-Amino-4, 6-dimethylpyrimidine, sulfanilamide, and N-(4,6-Dimethylpyrimidi-2-yl) Benzene-1,4-Diamine. (2), moreover, hydroxylation of the amidogen could take place owing to the attack of the hole and/or hydroxyl radical, which further led the formation of 4,6-Dimethyl-2- hydroxypyrimidine and 4-aminobenzenesulfonic acid.(3), owing to the attack of hydroxyl radical to the benzene ring, phenol and then hydroquinone could be formed successively.(4), the opening of the pyrimidine ring might be generated due to the attack of hydroxyl radicals on the ortho carbon position of the ring. Also, B Yang[28] (Vis/g-C_3N_4), Babić[29] (thin TiO_2 film) and Periša's[30] (sunlight irradiation) investigation demonstrated that desulfurization and cracking had occurred during the sulfamethazine degradation process, which was consistent with our results. On the other hand, the referenced results suggested that demethylation, heterocyclic cracking and/or the methylazolyl group reaction might be incurred during the sulfamethazine degradation process, while in our work, only the pyridine could be formed owing to the high photo degradation performance of γ-Fe_2O_3/SiO_2/TiO_2. Moreover, it should be noted that the possible ruptured position of chemical bond was consistent with intermediate products of the experimental process, which further demonstrated the theoretical guidance of the density functional theory for the experimental process.

CONCLUSIONS

In this present study, the γ-Fe_2O_3/SiO_2/TiO_2 microspheres of core–shell structure was prepared by using the ultrasonic-assisted modified Stöber method and sol-gel approach, and its photo activity was tested through the degradation of sulfamethazine. Structure characterization results showed that the good superparamagnetic property of γ-Fe_2O_3/SiO_2/TiO_2 could be reserved by the γ-Fe_2O_3, and. the SiO_2 interlining might directly block the contact of TiO_2 and γ-Fe_2O_3. The photo-degradation results of sulfamethazine demonstrated that the same high photo-activity as that of P25 TiO_2 could be obtained for our prepared γ-Fe_2O_3/SiO_2/TiO_2. The higher photo-degradation rate of γ-Fe_2O_3/SiO_2/TiO_2 than that of γ-Fe_2O_3/TiO_2 further suggested that SiO_2 interlayer could enhance the photo catalytic reactivity. Moreover, this easily magnetic-recoverable γ-Fe_2O_3/SiO_2/TiO_2 could be reused at least five times without any appreciable reduction at photo-catalytic efficiency. All these results demonstrated the successful and hopeful prospect of this prepared γ-Fe_2O_3/SiO_2/TiO_2 at lower-temperature comparing with the traditional heat synthesis approach. Additional, in combination with HPLC/ESI-MS analysis and density functional theory, degradation pathway of sulfamethazine had been speculated, and some main processes as the hydroxyl oxide, ammonia oxidation, splitting decomposition and open loop reactions might have occurred during the photo-degradation of sulfamethazine.

ACKNOWLEDGEMENTS

Thanks for the funding support of the Natural Science Foundation of China (No. 21306137).

REFERENCES

[1] Pan, X.., Qiang, Z., Ben, W., Chen, M. (2011) Residual veterinary antibiotics in swine manure from concentrated animal feeding operations in Shandong Province, China. Chemosphere; 84:695-700.

[2] Zhang, Y., Xu, J., Zhong, Z., Guo, C., Li, L., He, Y., Fan, W., Chen, Y. (2013) Degradation of sulfonamides antibiotics in lake water and sediment. Environmental Science & Pollution Research;20:2372-2380.

[3] Jian, X., Yan, X., Wang, H., Guo, C., Qiu, H., Yan, H., Yuan, Z., Li, X., Wei, M. (2015) Occurrence of antibiotics and antibiotic resistance genes in a sewage treatment plant and its effluent-receiving river. Chemosphere; 119: 1379-1385.

[4] Zhou, B.Y., Zong, C.L. (2015) Application of veterinary antibiotics in China's aquaculture industry and their potential human health risks. Environmental Science & Pollution Research: 1-12.

[5] Chen, M., Zhou, K., Lu, X., Li, Y., Feng, G., Xu, X., Chen, Z., Xu, N. (2015) The aggregation and dispersion of anatase and rutile tio_2 nanoparticles in the presence of phosphate. Fresen. Environ. Bull.;24:3205-3212.

[6] Wang, P., Bi, D., Chen, Y., Li, J. (2015) Ultraviolet irradiation of a mesoporous tio_2 membrane for removing organophosphorus pesticides from water. Fresen. Environ.Bull.; 24: 1779-1785.

[7] Nozari, M., Dehaghi, S.M. (2015) Synthesis, characterization and photocatalytic activity of pure and sb co-doped tio_2 nano photocatalyst. Fresen. Environ. Bull.;24:3505-3514.

[8] Jia, Q., Jia, X., Li, R., Chen, H., Tao, J., Wan, C. (2017) UV-photolysis of Sulfamethazine:

Effects of dissolved ions in water and the Photodegradation mechanism. Fresen. Environ. Bull.;26:3519-3528.

[9] Dawson, M., Soares, G.B., Ribeiro, C. (2013) Preparation and photocatalytical performance of TiO_2:SiO_2 nanocomposites produced by the polymeric precursors method. Journal of Nanoscience and Nanotechnology;13:5126- 5133.

[10] Hankare, P., Patil, R., Jadhav, A., Garadkar, K., Sasikala R. (2011) Enhanced photocatalytic degradation of methyl red and thymol blue using titania–alumina–zinc ferrite nano composite. Applied Catalysis B Environmental; 107:333-339.

[11] Ullah, S., Ferreira-Neto, E.P., Pasa, A.A., Alcântara, C.C., Acuna, J.J., Bilmes, S.A., Ricci, M.L.M., Landers, R., Fermino, T.Z., Rodrigues-Filho, U.P. (2015) Enhanced photo catalytic properties of core@ shell SiO_2@ TiO_2 nanoparticles. Applied Catalysis B Environmental;179:333-343.

[12] Matos, J., Montaña, R., Rivero, E. (2015) Influence of activated carbon upon the photocatalytic degradation of methylene blue under UV–vis irradiation. Environmental Science & Pollution Research;22:784-791.

[13] Kouamé, N.A., Robert, D., Keller, V., Keller, N., Pham, C., Nguyen, P. (2012) TiO_2/β-SiC foam-structured photoreactor for continuous wastewater treatment. Environmental Science & Pollution Research;19:3727-3734.

[14] Yu, X., Liu, S., Yu, J. (2011) Super- paramagnetic γ-Fe_2 O_3@ SiO_2@ TiO_2 composite microspheres with superior photocatalytic properties. Applied Catalysis B Environmental;104:12-20.

[15] Álvarez, P.M., Jaramillo, J., Lopez-Pinero, F., Plucinski, P.K. (2010) Preparation and characterization of magnetic TiO_2 nanoparticles and their utilization for the degradation of emerging pollutants in water. Applied Catalysis B Environmental;100:338-345.

[16] Quiñones, D.H., Rey, A., Álvarez, P.M., Beltrán, F.J., Plucinski, P.K. (2014) Enhanced activity and reusability of TiO_2 loaded magnetic activated carbon for solar photocatalytic ozonation. Applied Catalysis B Environmental;144:96-106.

[17] Dominguez, S., Huebra, M., Han, C., Campo, P., Nadagouda, M., Rivero, M., Ortiz, I., Dionysiou, D. (2016) Magnetically recoverable TiO_2-WO_3 photocatalyst to oxidize bisphenol A from model wastewater under simulated solar light. Environmental Science & Pollution Research:1-10.

[18] Pavani, T., Rao, K.V., Chakra, C.S., Prabhu, Y. (2016) Synthesis and characterization of γ-ferric oxide nanoparticles and their effect on Solanum lycopersicum. Environmental Science and Pollution Research:1-8.

[19] Cui, J., He, T., Zhang, X. (2013) Synthesis of Fe_3 O_4@ SiO_2@ Pt ion–TiO_2 hybrid composites with high efficient UV–visible light photoactivity. Catalysis Communications;40: 66-70.

[20] Hamzezadeh-Nakhjavani, S., Tavakoli, O., Akhlaghi, S.P., Salehi, Z., Esmailnejad- Ahranjani, P., Arpanaei A. (2015) Efficient photocatalytic degradation of organic pollu- tants by magnetically recoverable nitrogen- doped TiO_2 nanocomposite photocatalysts under visible light irradiation. Environmental Science & Pollution Research;22:18859-18873.

[21] Wei, Y., Jiao, J., Zhao, Z., Liu, J., Li, J., Jiang, G., Wang, Y., Duan, A. (2015 Fabrication of inverse opal TiO_2-supported Au@ CdS core–shell nanoparticles for efficient photocatalytic CO_2 conversion. Applied Catalysis B Environmental;179:422-432.

[22] Dominguez, S., Huebra, M., Han, C., Campo, P., Nadagouda, M., Rivero, M., Ortiz, I., Dionysiou, D. (2016) Magnetically recoverable TiO2-WO3 photocatalyst to oxidize bisphenol A from model wastewater under simulated solar light. Environmental Science and Pollution Research:1-10.

[23] Liu, H., Jia, Z., Ji, S., Zheng, Y., Li, M., Yang, H. (2011) Synthesis of TiO2/SiO2@Fe3O4 magnetic microspheres and their properties of photocatalytic degradation dyestuff. Catalysis Today;175:293-298.

[24] Ba-Abbad, M.M., Mohamad, A.B., Takriff, M.S., Kadhum, A.A.H., Jalgham, R.T.T. (2012) Comparative Study of the Adsorption Mechanism and Photochemical Oxidation of Chlorophenols on a TiO2 Nanocatalys. Inter- national Journal of Electrochemical Science; 7:11363-11376.

[25] Wu, H.-N., Wang, J., Li, H., Ma, N.-N., Zhang, T., Shi, S.-Q., Yan, L.-K., Su, Z.-M. (2016) Structure and Frontier Molecular Orbital (FMO) energies of α-Keggin-type polyoxometalate $[PW_{12}$ $O_{40}]$ $^{3-}$: A systematical study with different functionals of density functional theory. Computational & Theoretical Chemistry;1089:28-34.

[26] Du, C., Zhang, M., Min, F., Cai, C., Ge, T., Ma, X. (2014) Vibrational and quantum chemical investigations of 4.6-dimethyldibenzothiophene. International Journal of Oil Gas & Coal Technology;7:322-334.

[27] Xiaochen, J., Hui, C., Huiyu, R., Jia, Q. (2017) The Reusable γ-Fe2O3/SiO2/TiO2: Preparation and Photocatalytic Activity for the Degradation of Sulfamethazine in Water. The 2nd International Conference on Environmental Science

and Engineering; July 14th - 16th.
[28] Yang, B., Mao, X., Pi, L., Wu, Y., Ding, H., Zhang, W. (2017) Effect of pH on the adsorption and photocatalytic degradation of sulfadimidine in Vis/g-C_3N_4 progress. Environmental Science & Pollution Research International:1-13.
[29] Babić, S., Zrnčić, M., Ljubas, D., Ćurković，L., Škorić, I.(2015) Photolytic and thin TiO_2 film assisted photocatalytic degradation of sulfamethazine in aqueous solution. Environmental Science and Pollution Research;22:11372-11386.
[30] Periša, M., Babić, S., Škorić, I., Frömel, T., Knepper, T.P. (2013) Photodegradation of sulfonamides and their N^4 -acetylated metabolites in water by simulated sunlight irradiation: kinetics and identification of photoproducts. Environmental Science and Pollution Research;20:8934-8946.

Received **12.07.2017**
Accepted: **14.07.2017**

CORRESPONDING AUTHOR

Qingzhu Jia
School of Marine and Environmental Science, Tianjin University of Science and Technology, Tianjin 300457, China

e-mail: jiaqingzhu@tust.edu.cn

© by PSP Volume 26 – No. 10/2017 pages 6286-6294 Fresenius Environmental Bulletin

THE SEMI-ANALYTICAL SOLUTION OF PARTICLE TRANSPORT IN POROUS MEDIA INDUCED BY SEEPAGE

Bing Bai*, Tao Xu, Huawei Li

School of Civil Engineering, Beijing Jiaotong University

ABSTRACT

The general solution of the transport of particles induced by seepage in a semi-infinite saturated porous media is obtained by using Laplace transform and inverse Laplace transform, which takes into account the dispersion effect in the deposition kinetics. Based on the solution of an instantaneous plane source, the semi-analytical solution of the particle transport equation is derived in porous media containing a particle source whose concentration varies with time and space. The results show that the impact of the dispersion effect on the transport of particles in porous media increases with increasing dispersion coefficient, and the concentration of particles increases rather sharply for small dispersion coefficient, but more smoothly for large dispersion coefficient. In the absence of the diffusive effect in the deposition kinetics, the concentration of particles and the rate of particles deposited on the solid matrix increase than the existence of the diffusive effect.

KEYWORDS:
Saturated porous media, particle size, release source, seepage transport

INTRODUCTION

The research on the transport and deposition of particles induced by water flowing through the porous medium is of considerable practical importance in a variety of environmental, agricultural and industrial applications [1, 2]. A number of laboratory tests have been conducted to investigate the migration, absorption and release of particles in porous media, and several theoretical models have also been developed to characterize the transport process of particles, including the capillary model, isolated spherical model, and constricted tube model [3, 4]. In general, the transport of particles in porous medium can be well described by the classical deep bed filtration model [5, 6], the principle of which is based on the concept of average concentration [7, 8]. The capture of particles on the solid matrix in transport process is generally affected by many factors, such as the charge force, particle size, dispersion and bridge connection. Overall, most currently available theoretical models seem to be inadequate to describe the deposition process of particles [9–13].

Most established governing equations on the transport of particles in porous medium include the deposition kinetics (i.e., absorption process) [14, 15] induced by physical and chemical interface effects. The release of particles deposited on the solid matrix caused by the variations of physical or chemical interaction between particles and solid matrix is also investigated [16]. In reality, the hydrodynamic dispersion effect on deep bed filtration is very important due to the effects of molecular diffusion and mechanical movement, especially for the migration of particles near to wells where the dispersivity may already arise to the bed scale [17]. For this, a dispersion item is added to the mathematical models, which accounts for particle diffusion in the mass balance for particles, but neglects the dispersion flux contributing to the retention kinetics.

In this study, a mathematical model is developed to describe the seepage transport of particles in porous medium, which takes into account the dispersion effect in the process of deposition kinetics. Then, the general solution with an item of the particle source is obtained by Laplace transform and inverse Laplace transform. Based on the elementary solution of an instantaneous plane source, the semi-analytical solution of the particle transport equation is derived in a semi-infinite saturated porous media containing a particle source whose concentration varies with the coordinate and time. Some complicated particle transport problems induced by seepage, such as exponentially decayed source, can be analyzed conveniently using this solution.

MATHEMATICAL MODEL AND SOLUTION METHOD

Governing equations. Based on the advection-dispersion equation, the transport of particles in

saturated homogeneous porous media under the condition of one-dimensional hydrodynamic dispersion in a uniform flow field can be governed by the following partial differential equation [4, 6, 15]:

$$\frac{\partial C(z,t)}{\partial t} = D\frac{\partial^2 C(z,t)}{\partial z^2} - u\frac{\partial C(z,t)}{\partial z} - \frac{\rho_s}{n}\frac{\partial \sigma}{\partial t} + F(z,t) \quad (1)$$

where $C(z, t)$ is the concentration of liquid-phase particles at position z at time t (ML^{-3}), n is the porosity of the porous medium, D is the dispersion coefficient, u is the average interstitial velocity, σ is the concentration of suspended particles adsorbed on the solid matrix (MM^{-1}), ρ_s is the bulk density of the solid matrix, and $F(z, t)$ is the source of particles ($ML^{-3}T^{-1}$).

The hydrodynamic dispersion coefficient is generally assumed to be proportional to the flow velocity. Thus, let $D=\alpha_d u$, where α_d is the dispersivity. The intrinsic flow velocity u is assumed to be constant without considering the decrease of the porosity of the medium due to the particle deposition effect. If the influence of hydrodynamic dispersion given by the first item on the right-hand side of Eq. (1) is negligible, Eq. (1) can be reduced to the classical seepage model of contaminant [17, 18]. In fact, Eq. (1) takes into account both advection and dispersion of particles, and the transport flux of particles can be expressed as:

$$q_f(z,t) = u\frac{nC(z,t)}{\rho_s} - \frac{D}{\rho_s}\cdot\frac{n\partial C(z,t)}{\partial z} \quad (2)$$

where $q_f(z, t)$ is the particle flux.

Eq. (2) indicates that the transport flux of particles decreases with increasing distance in the z direction due to the effects of molecular dispersion and mechanical diffusion of particles. Because of the size-exclusion effect, some particles are adsorbed on the surface of porous medium or captured inside the pores, while the others continue to move forward with the water flow. For simplicity, the capture rate of particles is assumed to be proportional to the overall particle flux (first-order particle retention kinetics):

$$\frac{\partial \sigma(z,t)}{\partial t} = \lambda q_f(z,t) \quad (3)$$

where λ is the filtration coefficient (L^{-1}) that describes the probability of particles captured over a unit distance [12, 17]. It is related to the concentration of particles adsorbed on the solid matrix, and determined mainly by the structure of porous media. Generally, it can be expressed by the following linear equation [19]:

$$\lambda = \lambda_0(1-\xi\sigma) \quad (4)$$

where λ_0 is the initial filtration coefficient in pure porous medium, and ξ is the decay parameter of particle deposition, which is the inverse of the maximum concentration σ_m of particles deposited on the solid matrix ($\xi=1/\sigma_m$).

When the concentration of captured particles is small enough to be negligible, one can take $\xi=0$, and thus $\lambda=\lambda_0$ in this case. On the contrary, small pores are possibly filled and even blocked with the accumulation of particles on the solid matrix during the suspension flow in porous medium, resulting in a rapid decrease of the capture rate of particles, and a greater ξ should be used in this case.

Substitution Eq. (2) into Eq. (3) results in the following mass balance equation for the deposition process of particles on the solid matrix:

$$\frac{\rho_s}{n}\frac{\partial \sigma(z,t)}{\partial t} = k_d \cdot C - D_1 \cdot \frac{\partial C(z,t)}{\partial z} \quad (5)$$

where k_d is the deposition coefficient of particles, $k_d=\lambda u$; and $D_1=k_d \alpha_d$.

The second item on the right-hand side of Eq. (5) represents the dispersion effect in the deposition of particles, which warrants close attention in many engineering applications, such as migration of particles around the drawing well for the extraction of groundwater, the release of particles in a local region of aquifer stratum, etc.

Substitution Eq. (5) into Eq. (1) gives:

$$\frac{\partial C(z,t)}{\partial t} = D\frac{\partial^2 C(z,t)}{\partial z^2} + (D_1-u)\frac{\partial C(z,t)}{\partial z} - k_d \cdot C(z,t) + F(z,t) \quad (6)$$

In the case where there is no dispersion effect in the deposition of particles ($D_1=0$), Eq. (6) can be reduced to the classical advection-dispersion equation for deposition process.

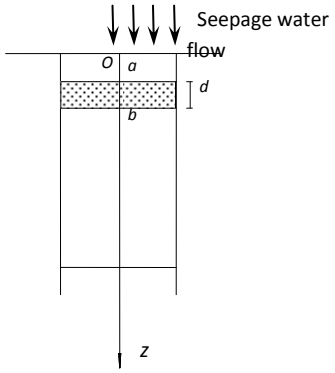

FIGURE 1
Physical model

Physical model and solutions in the Laplace transform. For the problem of one-dimensional seepage migration (Fig. 1), the concentration of particles in porous medium is obviously related to the coordinate z. Assume that the initial condition is $C(z, 0)= \sigma(z, 0)=0$ when $z>0$, and the boundary condition is $C(0, t)=0$ and $C(\infty, t)=0$.

When $C(z, 0)=0$, the Laplace transform of Eq.

(6) with respect to t is:

$$D\frac{\partial^2\overline{C}(z,p)}{\partial z^2}+(D_1-u)\frac{\partial\overline{C}(z,p)}{\partial z}-(k_d+p)\overline{C}(z,p)+\overline{F}(z,p)=0 \quad (8)$$

where $\overline{C}(z,p)=L[C(z,t)]=\int_0^\infty e^{-pt}C(z,t)\,dt$, with p being the Laplace variable.

As $\overline{C}(0,p)=0$ (i.e., $C(0,t)=0$), the Laplace transform of Eq. (8) with respect to z is:

$$D\left[s^2\overline{\overline{C}}-\frac{\partial\overline{C}(0,p)}{\partial z}\right]+(D_1-u)s\overline{\overline{C}}-(k_d+p)\overline{\overline{C}}+\overline{\overline{F}}=0 \quad (9)$$

where $\overline{\overline{C}}=\int_0^\infty e^{-sz}\overline{C}\,dz$, with s being the Laplace variable.

It follows from Eq. (9) that:

$$\overline{\overline{C}}=\frac{\frac{\partial\overline{C}(0,p)}{\partial z}}{(s+A+B)(s+A-B)}-\frac{\frac{\overline{\overline{F}}}{D}}{(s+A+B)(s+A-B)} \quad (10)$$

where $A=(D_1-u)/(2D)$ and $B=[A^2+(k_d+p)/D]^{1/2}$.

Solutions in the inverse Laplace transform. For convenience, the two items on the right-hand side of Eq. (10) are denoted as:

$$I_1=\frac{\frac{\partial\overline{C}(0,p)}{\partial z}}{(s+A+B)(s+A-B)},\quad I_2=\frac{-\frac{\overline{\overline{F}}}{D}}{(s+A+B)(s+A-B)}$$

Thus, $\overline{\overline{C}}(z,p)=I_1+I_2$. The inverse Laplace transform of I_1 with respect to z is [20]

$$L_z^{-1}(I_1)=\frac{\partial\overline{C}(0,p)}{\partial z}\cdot\frac{\exp[(B-A)z]-\exp[-(B+A)z]}{2B} \quad (11)$$

According to the convolution theorem $L^{-1}[\overline{f}(s)\cdot\overline{g}(s)]=\int_0^t f(\tau)g(t-\tau)\,d\tau$, where $\overline{f}(s)$ and $\overline{g}(s)$ are the Laplace transforms of $f(t)$ and $g(t)$ respectively, the inverse Laplace transform of I_2 with respect to z is:

$$L_z^{-1}(I_2)=-\frac{1}{2DB}\int_0^z\overline{F}(\xi,p)\{\exp[(B-A)(z-\xi)]-\exp[-(B+A)(z-\xi)]\}d\xi \quad (12)$$

As such, the inverse Laplace transform of Eq. (10) with respect to z is:

$$\overline{C}(z,p)=\frac{\partial\overline{C}(0,p)}{\partial z}\cdot\frac{\exp[(B-A)z]-\exp[-(B+A)z]}{2B}-\frac{1}{2DB}\int_0^z\overline{F}(\xi,p)\{\exp[(B-A)(z-\xi)]-\exp[-(B+A)(z-\xi)]\}d\xi \quad (13)$$

Both sides of Eq. (13) are multiplied by $2B\exp[-(B-A)z]$:

$$2B\exp[-(B-A)z]\cdot\overline{C}=\frac{\partial\overline{C}(0,p)}{\partial z}\cdot[1-\exp(-2Bz)]-\frac{1}{D}\int_0^z\overline{F}(\xi,p)\{\exp[-(B-A)\xi]-\exp[-2Bz+(B+A)\xi]\}d\xi \quad (14)$$

Let $z\to\infty$. As B–A>0, it follows from Eq. (14) that:

$$\frac{\partial\overline{C}(0,p)}{\partial z}=\frac{1}{D}\int_0^z\overline{F}(\xi,p)\exp[-(B-A)\xi]d\xi \quad (15)$$

Substituting Eq. (15) into Eq. (13) yields:

$$\overline{C}(z,p)=\frac{\exp[-(B+A)z]}{2DB}\int_0^z\overline{F}(\xi,p)\exp[(B+A)\xi]d\xi-\frac{\exp[-(B+A)z]}{2DB}\int_0^z\overline{F}(\xi,p)\exp[-(B-A)\xi]d\xi \quad (16)$$

For convenience, the two items on the right-hand side of Eq. (16) are denoted as J_1 and J_2 respectively, then, $C(z,p)=J_1+J_2$. Thus:

$$J_1=\frac{1}{2DB}\int_0^z\overline{F}(\xi,p)\cdot\exp[-A(z-\xi)]\cdot\exp[-B(z-\xi)]\cdot d\xi=\frac{1}{2\sqrt{D}}\int_0^z\exp[-A(z-\xi)]\cdot\overline{F}(\xi,p)\cdot[\frac{1}{\sqrt{p+E}}\cdot\exp(-\frac{z-\xi}{\sqrt{D}}\cdot\sqrt{p+E})]\cdot d\xi \quad (17)$$

$$J_2=-\frac{1}{2DB}\int_0^z\overline{F}(\xi,p)\cdot\exp[-A(z-\xi)]\cdot\exp[-B(z+\xi)]\cdot d\xi=\frac{1}{2\sqrt{D}}\int_0^z\exp[-A(z-\xi)]\cdot\overline{F}(\xi,p)\cdot[\frac{1}{\sqrt{p+E}}\cdot\exp(-\frac{z+\xi}{\sqrt{D}}\cdot\sqrt{p+E})]\cdot d\xi \quad (18)$$

where $E=(D_1-u)^2/(4D)+k_d$.

According to the table of Laplace transforms [20], the Laplace transform of the specific function $f(t)=\exp[-x^2/(4t)]/\sqrt{\pi t}$ is $L[f(t)]=\overline{f}(s)=\exp(-x\sqrt{s})/\sqrt{s}$. Thus, based on the displacement property of Laplace transform and the convolution theorem, the inverse Laplace transforms of Eq. (17) and Eq. (18) with respect to p are:

$$L_t^{-1}(J_1)=\frac{1}{2\sqrt{D}}\int_0^z \exp[-A(z-\xi)]\cdot\int_0^t \overline{F}(\xi,\tau)\cdot\frac{\exp[-E(t-\tau)]}{\sqrt{\pi(t-\tau)}}$$

$$\cdot\exp[-\frac{(z-\xi)^2}{4D(t-\tau)}]\cdot d\tau d\xi \qquad (19)$$

$$L_t^{-1}(J_2)=-\frac{1}{2\sqrt{D}}\int_0^z \exp[-A(z-\xi)]\cdot\int_0^t \overline{F}(\xi,\tau)\cdot\frac{\exp[-E(t-\tau)]}{\sqrt{\pi(t-\tau)}}$$

$$\cdot\exp[-\frac{(z+\xi)^2}{4D(t-\tau)}]\cdot d\tau d\xi \qquad (20)$$

Hence, the general solution of Eq. (6) can be obtained from Eq. (16):

$$C(z,t)=\int_0^z \exp[-A(z-\xi)]\cdot\int_0^t \overline{F}(\xi,\tau)\cdot\frac{\exp[-E(t-\tau)]}{2\sqrt{\pi D(t-\tau)}}\cdot$$

$$\{\exp[-\frac{(z-\xi)^2}{4D(t-\tau)}]-\exp[-\frac{(z+\xi)^2}{4D(t-\tau)}]\}\cdot d\tau d\xi \qquad (21)$$

SOURCE FUNCTION METHOD AND ITS SOLUTION

The elementary solution of an instantaneous plane source. Consider an instantaneous plane source of particles at the coordinate $z=\xi$ in one-dimensional porous medium, where the amount of particles released at time $t=\tau$ is Q (ML^{-2}) per unit area. The concentration of suspended particles induced by the seepage flow in the direction z is:

$$F(z,t)=I\cdot\delta(z-\xi)\cdot\delta(t-\tau) \qquad (22)$$

where $I=Q/n$ is the release strength of the plane source at $z=\xi$ (ML^{-2}), $\delta(t)$ is the Dirac delta function, z is the coordinate of the plane source, and t is the time.

Based on the property of Dirac delta function that $\int_\alpha^\beta f(t)\delta(t-t_0)dt=f(t_0)$ ($\alpha\le t_0\le\beta$), substituting Eq. (22) into Eq. (21) leads to the following solution for the plane source:

$$C_S(z,t)=\frac{I}{2\sqrt{\pi D(t-\tau)}}\cdot\exp(-\varpi_1)\cdot\exp(-\varpi_2)\cdot$$

$$[\exp(-\varpi_3)-\exp(-\varpi_4)] \qquad (23)$$

where $\varpi_1=(\frac{k_d}{2u}-\frac{u}{2D})(z-\xi)$,

$\varpi_2=\frac{(k_dD+u^2)^2(t-\tau)}{4Du^2}$, $\varpi_3=\frac{(z-\xi)^2}{4D(t-\tau)}$, $\varpi_4=\frac{(z+\xi)^2}{4D(t-\tau)}$.

Obviously, in the absence of the dispersion effect in the deposition kinetics of particles (D_l=0), one has $\varpi_1=-[u/(2D)](z-\xi)$ and $\varpi_2=[u^2/(4D)+k_d)](t-\tau)$. On the other hand, based on the property of Dirac delta function, substituting Eq. (21) into Eq. (2) leads to the expression of particle flux:

$$q_f(z,t)=\frac{I}{2\sqrt{\pi D(t-\tau)}}\cdot\exp(-\varpi_1)\cdot\exp(-\varpi_2)\cdot$$

$$[E_1\exp(-\varpi_3)-E_2\exp(-\varpi_4)] \qquad (24)$$

where $E_1=\frac{D_l+u}{2}+\frac{z-\xi}{2(t-\tau)}$, $E_2=\frac{D_l+u}{2}+\frac{z+\xi}{2(t-\tau)}$.

As $\sigma(z, 0)$=0, the concentration of particles adsorbed on the solid matrix can be obtained from Eq. (3):

$$\sigma(z,t)=\lambda\int_0^t q_f(z,t)\mathrm{d}t=$$

$$\frac{\lambda I}{2\sqrt{\pi D}}\int_0^t\frac{\exp(-\varpi_1)\cdot\exp(-\varpi_2)}{\sqrt{t-\tau}}\cdot[E_1\exp(-\varpi_3)-E_2\exp(-\varpi_4)]\mathrm{d}t \qquad (25)$$

When I=1, Eqs. (23)–(25) are the elementary solutions of an instantaneous plane source, also called the source function of a plane source.

Continuous source of particles with a definite thickness. Consider a particle source in porous medium distributed in the range of (a, b) with a thickness of $d=b-a$ (Fig. 1), from which particles are released continuously at a rate of $q(z, t)$ ($ML^{-3}T^{-1}$) that varies with time t and coordinate z. By using the so-called source function method [21], the transport of particles in porous medium with time t can be considered as the accumulation of release responses induced by numerous fictitious instantaneous plane sources with $I=q(z,t)\mathrm{d}z\mathrm{d}t$. Thus, the concentration of particles can be obtained by integrating Eq.(23) in the temporal and spatial domain:

$$C(z,t)=$$

$$\frac{1}{2\sqrt{\pi D}}\int_0^t\int_a^b\frac{q(\xi,\tau)}{\sqrt{t-\tau}}\cdot\exp(-\varpi_1)\cdot\exp(-\varpi_2)\cdot[\exp(-\varpi_3)-\exp(-\varpi_4)]\cdot d\xi d\tau \qquad (26)$$

where z is the calculation coordinate in porous medium, ξ is the coordinate of the plane source, and t is the elapsed time.

The flux of particles in porous medium can be obtained by integrating Eq. (24) in the temporal and spatial domain:

$$q_f(z,t)=$$

$$\frac{1}{2\sqrt{\pi D}}\int_0^t\int_a^b\frac{q(\xi,\tau)}{\sqrt{t-\tau}}\cdot\exp(-\varpi_1)\cdot\exp(-\varpi_2)\cdot[E_1\exp(-\varpi_3)-E_2\exp(-\varpi_4)]\cdot d\xi d\tau \qquad (27)$$

Similarly, the concentration of deposited particles can be solved by Eq. (25) as follows:

$$\sigma(z,t)=$$

$$\frac{\lambda}{2\sqrt{\pi D}}\int_0^t\int_a^b\int_\tau^t \frac{q(\xi,\tau)}{\sqrt{\zeta-\tau}}\cdot\exp(-\varpi_1)\cdot\exp(-\varpi_2)$$

$$\cdot[E_1\exp(-\varpi_3)-E_2\exp(-\varpi_4)]\cdot \mathrm{d}\zeta d\xi d\tau \quad (28)$$

where $\varpi_2=\frac{(k_dD+u^2)^2(\zeta-\tau)}{4Du^2}$,

$$\varpi_3=\frac{(z-\xi)^2}{4D(\zeta-\tau)},\ \varpi_4=\frac{(z+\xi)^2}{4D(\zeta-\tau)}.$$

CALCULATION EXAMPLE

Model and parameters. Consider the case in which the concentration of the particle source distributed in the range of (a, b) varies with the depth z and decays exponentially with time t (Fig. 1). Thus, the release rate can be expressed as:

$$q(z,t)=g_0\exp(-\beta t)\cdot[1+\frac{k(z-a)}{b-a}] \quad (29)$$

where g_0 is the initial release rate ($ML^{-3}T^{-1}$), β is a decay parameter (T^{-1}), k is a parameter describing the distribution of the particle source along the depth.

When β=0 and k=0, $q(z,t)=g_0$ and Eq. (29) can be reduced to a constant source. The release rate of particles decreases exponentially with t for various k values (k=–0.6, 0, 0.2, 0.6, 1.0), which can be expressed by Eq. (29). Assume that a=5 cm and b=10 cm, then d=5 cm. The factors affecting particle migration include the advection effect of seepage water flow, and the molecular movement and hydrodynamic dispersion of particles due to water flow. The relative contribution of the advection and dispersion effects differs significantly with the seepage velocity u. A dimensionless ratio called the dispersion-advection ratio is introduced as $\kappa=D/(uL)=\alpha_d/L$ to characterize the relationship between the micro heterogeneity size (dispersivity α_d) and the characteristic size L of the boundary of particle source, which in fact is the inverse of the Peclet number P_e ($\kappa=1/P_e$). For the problem in Fig. 1, one can take $L=d$.

In reality, the calculated results depend significantly on the selected parameters. Without loss of generality, it is assumed that k_d=0.02 s^{-1} and u=0.2 cm/s according to previous studies [12, 15] and different dispersion-advection ratios (κ=0.001, 0.01, 0.1, 1) or hydrodynamic dispersion coefficients (D=0.001, 0.01, 0.1, 1 cm^2/s) are considered. Multiple integrals are calculated using Mathematica 9 software (Wolfram Research).

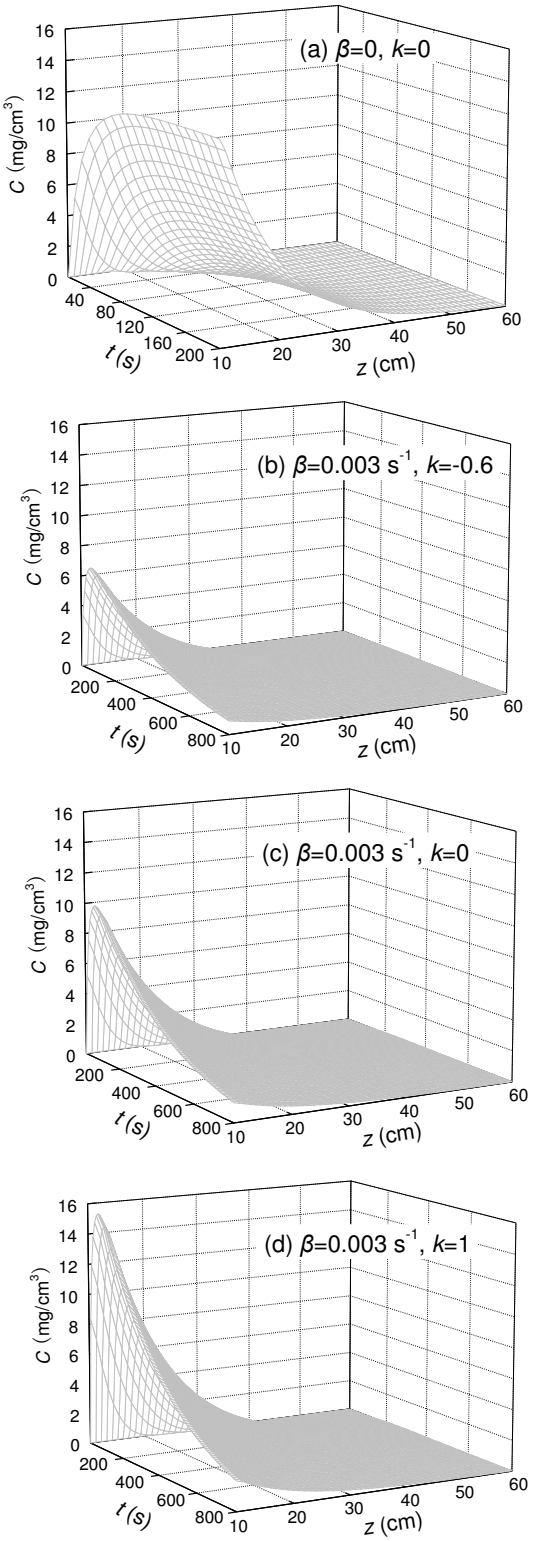

FIGURE 2
Distribution of the concentration of particles with time and space

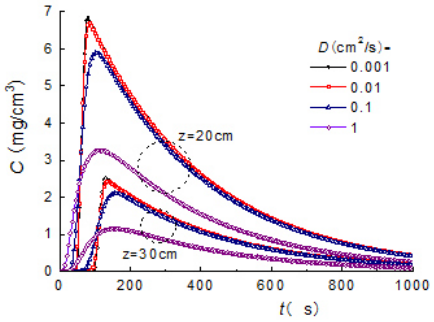

FIGURE 3
The effect of hydrodynamic dispersion on the migration process

Exponentially decayed source. Fig. 2 shows the evolution of the concentration of particles with time t along the direction z in porous medium subjected to a constant source (β=0; see Eq. (29)) or exponentially decayed source (β=0.003 s^{-1}) with k=–0.6, 0, 1, respectively. Here, the initial release rate is assumed to be g_0=1 mg/(cm^3·s). Fig. 2(a) shows that for the constant source, the concentration of particles increases with time until a plateau is reached. However, for the case of exponentially decayed source (Fig. 2(b-d)), the concentration of particles at a given depth from the surface of porous medium shows an initial sharp increase followed by a more gradual decrease to 0. It is noted that the peak concentration decreases as the depth from the surface of porous medium increases; while the time required to reach the peak increases. It is also noted that the concentration of particles is lower in the exponentially decayed source (β=0.003s^{-1}, k=0; see Fig. 2(c)) than in the constant source (β=0, k=0; see Fig. 2(a)), and more time is needed to reach the peak. In addition, the concentration of particles increases as the strength of the particle source increases (k=–0.6→0→ 1).

Fig. 3 clearly shows that the impact of the dispersion effect on particle migration increases with increasing dispersion coefficient (i.e., the increase of dispersivity λ when u=0.2 cm/s). However, the concentration of particles increases smoothly for large dispersion coefficient (e.g., D=1 cm^2/s), but sharply for small dispersion coefficient (e.g., D=0.001 cm^2/s). Moreover, the peak concentration at a given depth decrease and the time required to reach the peak increase as the dispersion coefficient increases. For example, when z=20 cm, the peak concentration is C=6.84, 6.68, 5.89, 3.26 mg/cm^3 and the time required to reach the peak is t=80, 85, 105, 115 s for the dispersion coefficients of D=0.001, 0.01, 0.1, 1 cm^2/s, respectively. It should be pointed out that the impact of dispersion effect is reduced as the depth increases from z=20 cm to z=30 cm. In addition, the dispersion effect is negligible when D<0.01 cm^2/s (i.e., λ<0.01; e.g., the comparison between D=0.001 cm^2/s and 0.01 cm^2/s in Fig. 3) due to the dominant contribution of the advection effect induced by seepage flow.

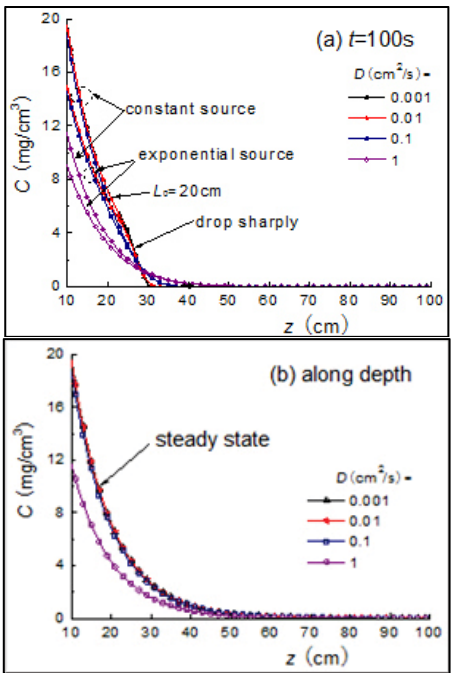

FIGURE 4
The effect of hydrodynamic dispersion on the concentration of particles

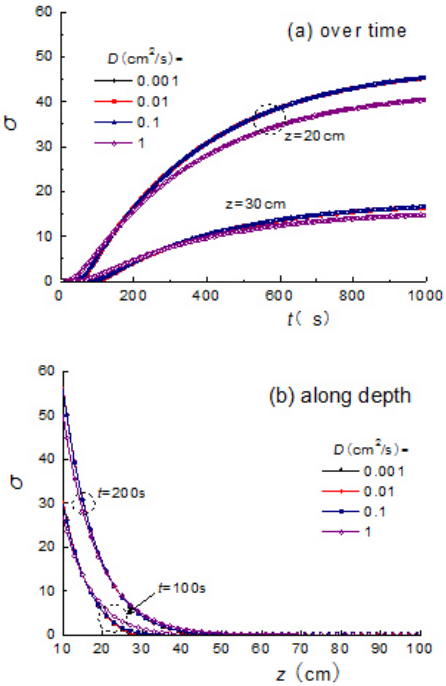

FIGURE 5
The concentration of suspend particles adsorbed on the solid matrix

Fig. 4(a) shows that the maximum concentration of particles along the depth decreases with the increase of dispersion coefficient for both

constant source and exponentially decayed source; but the penetration depth and distribution range increase, especially for the constant source. In addition, the penetration phenomenon due to the advection effect of seepage water flow is particularly obvious for small dispersion coefficients (e.g., D=0.001, 0.01 cm^2/s), and there is a clear demarcation point in the curve beyond which the concentration of particles drops more sharply. For instance, when D=0.001 cm^2/s and t=100 s, the demarcation depth is at about 23–25 cm (see Fig. 4(a)), which is slightly greater than the penetration distance induced by the convection L_0 (L_0=u·t=0.2 cm/s×100 s=20 cm). On the other hand, for the constant source, the distribution of the concentration of particles along the depth tends to be stable over time (i.e., t=∞), the maximum pollution depth is less than 86 cm (C<0.01 mg/cm^3; see Fig. 4(b)). At this moment, the vertical distributions of particle concentration are almost identical for dispersion coefficients smaller than D<0.01 cm^2/s, which is dominated by the convection effect of seepage water flow in this case.

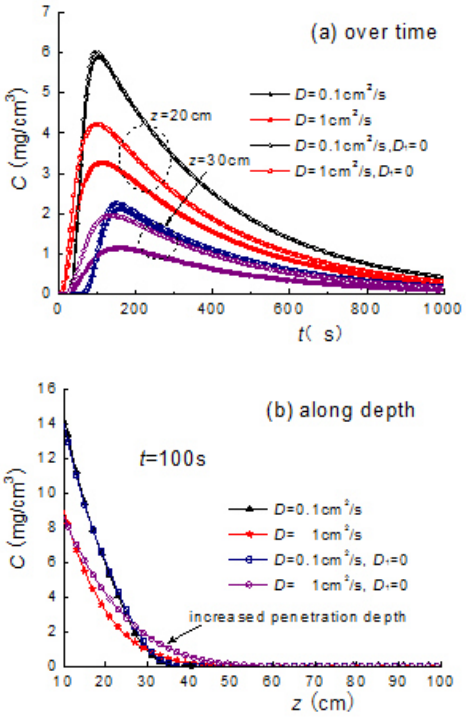

FIGURE 6
Dispersion effect in the process of hydrodynamic deposition

Fig. 5 shows that the concentration of suspended particles adsorbed on the solid matrix increases with time until a steady state is reached, but decreases sharply along the depth. Fig. 6 shows that in the absence of the dispersion effect included in the deposition kinetics (D_1=0), the concentration of particles (also can be reflected by the flux of particles in liquid phase) increases as the deposition of the particles on the solid matrix decreases. The increasing trend is more obvious for larger dispersion coefficient (D=0.1 cm^2/s and D=1 cm^2/s in Fig. 6(a)), and the peak concentration along the depth decreases slightly and the penetration depth increases a little (Fig. 6(b)). Fig. 7 shows that the concentration of particles increases with the increase of the strength of the source (i.e., k=–0.6→0→0.2→0.6→1; also see Fig. 1), but the time required to reach the peak is almost unaffected.

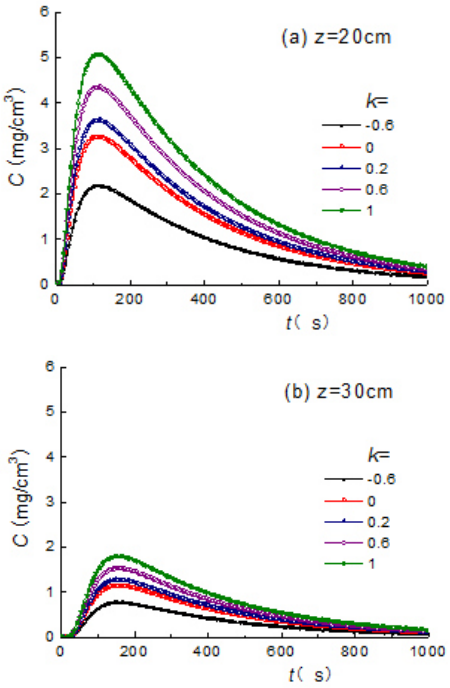

FIGURE 7
The evolution of the concentration of particles for different sources

CONCLUSIONS

Based on the solution of an instantaneous plane source, the semi-analytical solution of the particle transport equation is derived in porous media containing a particle source whose concentration varies with time and space.

The impact of the dispersion effect on the transport of particles in porous media increases with increasing dispersion coefficient, and the concentration of particles increases rather sharply for small dispersion coefficient, but more smoothly for large dispersion coefficient. The peak concentration at a given depth decreases as the dispersion coefficient increases due to the increased influence of the diffusive effect in the deposition kinetics on the migration of particles.

The maximum concentration of particles along the depth decreases with increasing dispersion coefficient for both constant source and

exponentially decayed source; but the penetration depth and distribution range increase, especially for the constant source. There is a clear demarcation point in the curve beyond which the concentration of particles drops more sharply.

In the absence of the diffusive effect in the deposition kinetics, the concentration of particles and the rate of particles deposited on the solid matrix increase than the existence of the diffusive effect, which becomes increasingly obvious with the increase of dispersion coefficient.

ACKNOWLEDGEMENTS

This work is financially supported by National Key Basic Research Program of China (2015CB057800) and the National Natural Science Foundation of China (51478034; 51279002), to which the authors are very grateful.

REFERENCES

[1] Tang, X. Y., Weisbrod, N. (2009) Colloid-facilitated transport of lead in natural discrete fractures. Environmental Pollution 157(8–9): 2266–2274.

[2] Porubcan, A. A., Xu, S. (2011) Colloid straining within saturated heterogeneous porous media. Water Research 45(4): 1796–1806.

[3] Tufenkji, N., Elimelech, M. (2004) Deviation from the classical colloid filtration theory in the presence of repulsive DLVO interactions. Langmuir 20(25): 10818–10828.

[4] Sharma, P., Flury, M., Mattson, E. D. (2008) Studying colloid transport in porous media using a geocentrifuge. Water Resources Research 44(7): 1796–1806.

[5] Bradford, S. A., Torkzaban, S., Walker, S. L. (2007) Coupling of physical and chemical mechanisms of colloid straining in saturated porous media. Water Research 41(13): 3012–3024.

[6] Guerrero, J. S. P., Pontedeiro, E. M. , Genuchten, M. , Skaggs, T. H. (2013) Analytical solutions of the one-dimensional advection-dispersion solute transport equation subject to time-dependent boundary conditions. Chemical Engineering Journal 221:487–491.

[7] Shapiro, A. A. , Bedrikovetsky, P. G. (2010) A stochastic theory for deep bed filtration accounting for dispersion and size distributions. Physica A: Statistical Mechanics and its Applications 389(13): 2473–2494.

[8] Natarajan, N., Kumar, G. S. (2011) Spatial moment analysis of colloid facilitated radionuclide transport in a coupled fracture-matrix system. International Journal of Energy and Environment 2(3): 491–504.

[9] Bolster, C. H., Mills, A. L., Hornberger, G. M., Herman, J. S. (1999) Spatial distribution of deposited bacteria following miscible displacement experiments in intact cores. Water Resources Research 35(6):1797–1807.

[10] Kumar, A., Jaiswal, D. K., Kumar, N. (2010) Analytical solutions to one-dimensional advection-diffusion equation with variable coefficients in semi-infinite media. Journal of Hydrology 380: 330–337

[11] Ovaysi, S., Piri, M. (2011) Pore-scale modeling of dispersion in disordered porous media. Journal of Contaminant Hydrology 124(1–4): 68–81.

[12] Santos, A., Bedrikovetsky, P. (2006) A stochastic model for particulate suspension flow in porous media. Transport in Porous Media 62(1): 23–53.

[13] Panfilov, M., Panfilova, I., Stepanyants, Y. (2008) Mechanisms of particle transport acceleration in porous media. Transport in porous media 74(1): 49–71.

[14] Ahfir, N. D., Benamar, A., Alem, A., Wang, H. Q. (2009) Influence of internal structure and medium length on transport and deposition of suspended particles: a laboratory study. Transport in Porous Media 76(2): 289–307.

[15] Sim, Y., Chrysikopoulos, C. V. (1998) Three dimensional analytical models for virus transport in saturated porous media. Transport in Porous Media 30(1): 87–112.

[16] Bedrikovetsky, P. G., Zeinijahromi, A., Siqueira, F. D., de Souza, A. L. S. (2012) Particle detachment under velocity alternation during suspension transport in porous media. Transport in Porous Media 91(1): 173–197.

[17] Altoé, F. J. E., Bedrikovetsky, P., Siqueira, A. G., Souza, A., Shecaira, F. S. (2006) Correction of basic equations for deep bed filtration with dispersion. Journal of Petroleum Science and Engineering 51(1–2): 68–84.

[18] Elimelech, M. (1995) Particle deposition and aggregation: measurement, modeling, and simulation. Butterworth-Heinemann, Oxford, England.

[19] Kuhnen, F., Barmettler K., Bhattacharjee S., Elimelech M., Kretzschmar R. (2000) Transport of iron oxide colloids in packed quartz sand media: monolayer and multilayer deposition. Journal of Colloid and Interface Science 231: 32–41.

[20] Spiegel, M. R. (2005) Theory and Problems of Laplace Transforms. McGraw-Hill.

[21] Bai, B. (2006) Response of saturated porous media subjected to local thermal loading on the surface of semi-infinite space. Acta Mechanica Sinica 22: 54–61.

Received: **07.03.2016**
Accepted: **17.09.2016**

CORRESPONDING AUTHOR

Bing Bai
School of Civil Engineering, Beijing Jiaotong University Beijing, 100044, P. R. China

e-mail: Baibing66@263.net

AUTHOR INDEX

A

Abdullah, H. 5900
Afify, A. E. M. R. 5841
Afzal, S. 5693
Ahmad, P. 5814
Ak, K. 6166
Akata, I. 6246
Akdeniz, N. S. 6064
Akgul, H. 6246
Akkaya Aslan, S. T. 5882
Akkoyun, H. T. 6159
Akkoyun, M. B. 6159
Al Antary, T. M. 6071
Al-Aqqad, S. 6035
Alawi, M. A. 6035
Altay, V. 5814
Arici, I. 5882
Arihan, O. 6159
Arpali, D. 6085
Arshad, M. 5693
Assareh, A. 5980
Atabek, H. C. 6127
Avramidis, P. 6093

B

Bai, B. 6286
Bal, C. 6246
Begbeg, A. 5783
Bengu, A. S. 6159
Berkoz, M. 6141
Biczak, R. 6058
Borusiewicz, A. 5824

C

Can, E. 5936
Cankilic, M. Y. 5865
Cao, Y. 6049
Celik, C. S. 6253
Celikoglu, E. 5865
Celikoglu, U. 5865
Cetin, M. 5965
Cevik, I. 6078
Changqing, M. 5987
Chen, H. 6272
Chen, Q. 5954
Chen, T.-Q. 5789
Cimen, B. 5717
Comba, A. 6135
Comba, B. 6135
Cybulska, K. 6058

D

Dai, H. 5999
Danish, M. 5693
Dasic, P. 6104
Deng, L. 5797
Deveci, A. 6212
Dikici, M. 6112
Dingil, M. 6266
Dizaji, R. N. 6112
Dong, P. 5954
Doosti, F. 5942
Du, Q. 5991
Durmaz, M. 5833

E

Emek, M. F. 5858
Ender, E. 6064
Erdem, D. B. 6121
Erdem, H. 5891
Erdogan, D. 5936
Ergin, S. 5833
Erkaya, I. A. 5769
Ertekin, I. 5754
Esen, E. 6149
Esgici, R. 6261

F

Fan, K. 5700
Fang, G. 5745
Fu, D. 5723

G

Gao, S. 6175
Ghanbari, R. 5942
Gulbaz, S. 6112
Gulser, F. 6085
Gumus, S. 6007
Gundogdu, K. S. 5882
Gunduz, S. G. 6141
Gungoroglu, C. 6217
Guo, X. 6184
Guo, X.-F. 5929
Gurcu, B. 5849

H

Hacisalihoglu, S. 6007
Huang, J. 5873

Hameed, A. 5814
Hu, X. 6017
Hu, Y. 5700
Huang, X. 5745
Huang, X.-H. 5873

I
Inan, S. 5849

J
Jaksic, T. 6104
Jamali, H. A. 5942
Jia, Q. 6272
Jia, X. 6272
Jiang, J. 5954
Jingyi, X. 6004

K
Kaiyue, Z. 5732
Kalender, S. S. 5833
Kamalak, A. 5754
Kamanbedast, A. A. 5980
Kamari, A. 5900
Karadavut, U. 5761
Karaduman, M. A. 6205
Karapehlivan, M. 6212
Karyab, H. 5942
Katsaros, D. 6093
Kaya, I. 6212
Kayis, A. F. 5769
Kazezyilmaz-Alhan, C. M. 6112
Kececi, M. 6205
Kerbachi, R. 5783
Ketin, S. 6104
Kezik, U. 6007
Khodja, M. 5783
Kirmikil, M. 5882
Kizilsimsek, M. 5754
Koc, S. 5717
Koca, Y. B. 5849
Koca, Y. K. 6266
Konswa, O. K. 5841
Kontopoulos, N. 6093
Kumar, A. J. 5723
Kurtoglu, I. Z. 6166
Kutlu, B. 6234
Kwon, Y. 5971

L
Lee, D. G. 5971
Lei, T. 6184
Lermi, A. G. 6199
Li, B.-Z. 5929
Li, H. 6286
Li, J. 6017
Li, J.-L. 5775
Li, M. 5954
Li, W. 5999
Li, W.-T. 6225
Li, Y. 5911, 5999
Li, Z.-D. 5999
Li, Z. 5917
Liang, Z. 5797
Liu, B. 6175
Liu, E. 5917
Liu, H. 5737
Liu, R.-R. 6225
Luo, Z.-W. 5775
Luo, Z. 5917
Lv, J. 5991

M
Ma, C.-M. 5999
Ma, J. 6184
Mahmooduzzafar 5814
Mao, Q.-D. 5929
Mazur, K. 5824
Mis, L. 6135
Misir, M. 6007
Misir, N. 6007
Mujdeci, M. 6205, 6253
Mukhtar, H. 5693
Mumtaz, M. W. 5693

N
Namasivayam, C. 5723
Nazef-Allaoua, M. 5783
Nie, F.-H. 6225
Noori, M. 5797
Nur, G. 6212
Nur, O. 6212

O
Oktan, E. 6007
Oktay, S. 5806
Ozdemir, F. 6127
Ozkan-Yilmaz, F. 6141
Ozluer-Hunt, A. 6141
Oztekin, M. E. 6266

Ozdemir, G. 6261
Ozer, T. 5769
Ozkan, C. O. 5754
Ozturk, C. 5754
Ozturk, M. 5814
Ozyigit, Y. 6043

P
Palta, S. 6199
Panagiotaras, D. 6093
Platkowski, M. 6058
Pu, Y. 5707

Q
Qadri, T. N. 5814
Qian, G. 5737
Qiang, W. 5732
Qingxiang, Y. 5732

R
Raza, R. A. 5693
Raza, S. A. 5693

S
Saat, A. 5965
Sagliker, H. A. 6078
Senocak, S. 5858
Senol, S. 6266
Sesli, A. 6234
Sessiz, A. 6261
Sevik, H. 5965
Sevindik, M. 6246
Shamsudin, R. 5900
Shen, Y. 5700
Shi, H. 5999
Siddiqi, T. O. 5814
Singh, R. P. 5723
Snioszek, M. 6058
Song, H.-L. 5789
Sonmez, F. 6234
Sozen, O. 5761
Strek, M. 6058
Sukusu, E. 6205, 6253
Sun, H. 6175
Sun, J. 5737
Sun, Q.-Y. 5873
Sun, X. 6184
Sun, Y. 5700
Sun, Z. 6017

T
Tameemi, F. T A. 6035
Tecimen, H. B. 5806
Telesinski, A. 6058
Thalji, T. A. 6071
Tian, M. 5999
Torun, M. B. 5891
Tuglu, M. I. 5849

U
Ulucan, A. 6159
Uslu, S. 6135
Usta, B. 6191
Uygur, V. 6205, 6253

V
Vasic, P. 6104
Vukanic, V. 6104

W
Wang, A. 5917
Wang, J. 6017
Wang, P. 6028
Wang, R. 6175
Wang, S. 5707
Wang, X. 6017
Wei, C. 5707
Wei, J. 5991
Wei, W. 6049
Wei, Z. 5987
Wen, C. 5911
Wen, X. 5745
Wu, C. 5737
Wu, J. 5707
Wu, Z. 5797
Wu, Z.-L. 5873

X
Xin, M. 5987
Xu, D. 6028
Xu, M. 6175
Xu, Q. 5700
Xu, T. 6286
Xu, X. 5707

Y

Yagmur, M. 6085
Yalcin, D. 5769
Yalcinkaya, O. 5769
Yalin, S. 6141
Yanar, K. 5754
Yang, R. 6028
Yang, X.-L. 5789
Yang, Y. 5745
Yesiloglu, T. 5717
Yildirim, M. 6141
Yildirim, N. C. 5936
Yilmaz, M. 6212
Yilmaz, S. 6121
Yilmaz-Ersan, L. 6191
Yongkui, C. 5987
Yu, J.-N. 5775
Yu, Q. 6225
Yu, X.-K. 5873
Yuan, Y. 5745
Yucesan, Z. 6007
Yumrutas, O. 6246
Yilmaz, M. 6212

Z

Zencirkiran, M. 6064
Zhang, C. 6049
Zhang, H. 5873
Zhang, H.-X. 5999
Zhang, J. 5954, 6017
Zhang, S.-X. 5999
Zhang, W. 5737, 5929
Zhang, X. 5873, 5917
Zhang, Y.-H. 5775
Zhao, L. 6175
Zheng, W. 5929
Zhou, X. 5911
Zhou, Y.-X. 6225
Zhu, J. 6049
Zhu, P. 5700
Zhu, Y. 5954
Zipeng, Z. 6004
Zubair, M. 5693

SUBJECT INDEX

A

accumulation 5814
Acid Turquoise Blue A 5700
Activated Carbon 5723
additive 5987
Adipose tissues 6035
Adjustment of FLWL 5745
Adsorption 5789, 5900, 6205, 6253
Adsorption Kinetics 5723
Aerobic stability 5754
African countries 5971
Air pollution 5693, 5833
Air quality 5965
Al 6159
alginate 5769
ALT 6212
ammonia 5911
Ammonium 5806
anaerobic digestion 5929
antibiotic 5732
Antibiotic wastewater 6004
antioxidant 6246
aquatic environment 5971
Arbutus andrachne 6078
ARGs 5732
AST 6212
Astaxanthine 6159
Autogenous shrinkage 5991

B

Balikesir 5865
Barley 6085
barley grass 6135
Basalt fiber 5991
bean 5761
Bee density 6199
Berry 6261
Best Management Practices 6112
Bifidobacterium 6191
biochemical properties 5775
biodegradability 5783
Biodegradation 5789, 6017
Biodiversity and Conservation 6217
Biofilm reactor 5707
biosorption 5769
Bohai Bay 5737
BP-K model 6184
bread wheat 5891

C

Carbon dioxide (CO_2) 5965
carbon mineralization 6078
Carbon stock 6007
CAT 5936
catalytic oxidation 6004, 6028
Cell Death 5849
central composite design (CCD) 5942
Charge neutralization 6049
chemical analyses 6104
chemical content 5761
Chemical oxygen demand (COD) 6004
Chickpea 6071
Chickpea Stored insects 6071
Chlorophyll 6043
cigarette 6127
Citrus 5717
cluster analysis 6058
Coal ash 6121
coastal sedimentology 6093
COD removal 5999
Coke wastewater 6028
co-metabolism 6017
Comprehensive benefit 5745
comprehensive benefit evaluation 6175
comprehensive index 6175
Compressive strength 5797
Contribution 5917
Copper 5769
Corn 5754
correction 5737
correlation 5783
Corrosion inhibitors 5783
Corrosion resistance 5797
creosote 6058
Cupressus sempervirens 6078
Cyprinus carpio 6141, 6212
cytotoxic effect 6246

D

DCA 5954
DCCA 5954
Decision-making model 5745
Deep Sea Tailings Placement (DSTP) 6149
Degradation pathway 6272
DE-K model 6184
desorption 6253
detailed soil survey 6266
dichlorophenol 6017
differential evolution algorithm 6184
digital mapping 6266
discharge coefficient 5980
DNA damage 6135
DPPH 6246
durum wheat 5891
dyes 5900
dynamics 5700

E

Eastern Anatolia Region 5858
Ecological requests 6064
ecological resistance 6064
Ecological restoration 5917
efficiency 5891
elevation 6078
emission measurements 5833
energy inputs 5824
Environmental effects 5693
excess sludge 5929
exploitation costs 5824

F

FAME 5865
fenbutatin oxide 6141
Fenton 6225
Fenton process 5942
ferry 5833
Fish 5849
Floc growth 6049
Floc recycling flocculation 6049
Flood Control 6112
Floodwater resource utilization 5745
flow 3D 5980
flower density 6199
flowering period 6199
Forested Areas 6217
Fresh property 5991
Freundlich isotherm 6205
FTIR 5723
Fulvic acid 5841

G

GC-ECD 6035
Genetic progress 5761
gentamicin 6135
Geochemistry 6093
Germination 6071
GIS 6266
glucose 6017
Grain yield 6085
Grape 6261
grey correlation 6175
groundwater 6104
growth 5814
GSH-Px 5936

H

H_2O_2 6004
Hardness 5797
HDL 6212
Health effects 5693
heavy metal 6121
Heavy metals 6205
hematology 6166
Heterobasidion Insulare: decolorization 5775
horizontal gene transfer 5732
human health 5971
Humic acids 5841
Hydrolytic Enzymes 5865
Hydrophilic polyurethane 5797

I

immobilization 5769
importance 6184
In Vitro Gas production 5754
In vivo antioxidant scavenging capacity 5841
Indoor air 5965
Inheritance law 5882
intermittent aeration 5873
interval partial least squares 5873
Intestine 5849
Iraq 6035
Isoelectric point 6049
Isotherms 5723

J

Jatropha Husk 5723

K

Karkamis Dam Lake 6234
kenaf bast fiber 5900
kidney 6135
kidney function 5841
Kutahya 5865

L

laccase-producing 5775
lagoons 6093
land consolidation 5882
Land use change 6007
landfill leachate 6225
Langmuir isotherm 6205
lipid peroxidation 6141
liver 6159
liver function 5841
Low Impact Development 6112
Lubricating oil 5987

M

Mann–Kendall test 5858
Marine development type 6175
marine diesel engine 5833
Marine Pollution 6149
Maturity 6261
Maturity stage 6166
Mechanical properties 5991
Membrane bioreactor 5789
Mercury 5814
metal ion 5732
Methylene Blue 5723
Metronidazole 5849
Microbial community 5707
milk production 5824
Mine Waste Management 6149
Mineralization 5806
mineralized refuse 6225
minimization 5929
monitoring 6104
Monteri Pine 5806
Morphology 6049
multi-criterial assessment 5824
Munzur Stream. 5936
Mushroom 6246

N

N:S ratio 5891
NaClO 6225
$NaClO_2$-UV/O_3 5700
narbon bean 6043
Natura 2000 Sites 6217
Natural clinoptilolite-zeolite 6253
natural transformation 5732
near-infrared spectroscopy 5873
Nitrate 5806
nutrient 5737, 6234
nutrient requirements 5775
Nutritional properties 6085
Nutritive Value 5754

O

Oak-Beech 5806
Oilfield wastewater 5999
okra 5814
Okuzgozu 6261
Olive mill wastewater 5942
one-way ANOVA test 5882
optimization 5942
Orchidaceae 6191
Organochlorine pesticides 6035
Oriental beech 6007
overlying water 5873
ownership 5882
oxidant 6246
oxidative stress 5849, 6127, 6141, 6246, 6159

P

Paraoxonase 6212
particle size 6253, 6286
Particulate matter 5693, 5965
personal care products 5971
pH 5911
phacelia 6199
Pharmaceuticals 5971
phenolic compounds 5942, 6246
phosphorus 6253
Photo-catalyst 6272
Physical and Ripening Properties 6261
physical model 5980
physicochemical properties 5783
phytoplankton 5737, 6234
pigmentation 5814
plant height 6043
Pollutant removal rate 6028
pollution indices 6093
Potential nitrification rates 5911
Prebiotic 6191
principal component analysis 6058
Probiotic 6191
Prokopos Greece 6093
Purity 6071

Q

quality 5717, 5761

R

rat 6159
release source 6286
remote sensing 6043
Removal efficiency 5707, 5999
resistance index 6058
Response surface method 5999
Response surface methodology 6225
Risk evaluation index system 5745

S

Safranbolu Bulak Mencilis Cave 5965
Salep 6191
Salmo sp 5936
Sand-fixing body 5797
SOD 5936
soil conditioner 6121
soil enzymes 6058
Soil loss 6007

Sanliurfa 6234
Saturated porous media 6286
sedentary lifestyle 6127
sediment 5911
Seeds cultivars 6071
seepage transport 6286
SEM 5723
SEM/EDS 6225
Sen's slope method 5858
sex steroids. 6166
Shilianghe reservoir 5745
ship emissions 5833
Sialkot 5693
Silage 5754
SiO2 6272
Siphon spillway 5980
slope 6266
Sludge components 5789
soil pollution 6121
soil properties 6205
soil urea hydrolysis rate 6184
solar energy 5929
sowing date 6199
Soybean 5754
spad value 5891
Spearman's rho test 5858
Start-up 5707
Stichococcus subtilis 5769
strenuous exercise 6127
sturgeon 6166
Sulfadimidine 6272
Sulphur 5891
Super-absorbent polymers 5991
Supercritical water 6028
sustainability 5824, 5965
synergistic effect 5700

T
Tailings 6149
Tarim River 5954
TAS 5936, 6135
Tebuconazole 6212
temperature 5911
The change of streamflow and sediment load 5917
The Loess hill-gully area 5917
Thermophilic 5865
thermophilic digestion 5929
tidal 5737
TiO2 6272
Topographic map 6266
TOS 5936, 6135
toxicity 5814
Trend analysis 5858
Tribochemistry 5987
Tribofilm 5987
Turkey 6217, 5882, 6234
TWINSPAN 5954

U
ultra-low sulfur diesel 5833
ultrasonography 6166
upstream slope 5980
urban landscape 6064
Urea 6085

V
variance 5761
vegetation community 5954
Viability 6071
volatile organic compounds (VOCs) 6058

W
wastewater treatment 5900
water content 6043
Watershed Modeling 6112

X
XRD 5723

Y
yield 5717, 5761

Z
Zinc 6085

1,….,9
17α-Ethinylestradiol 5789
2,4-DP 5717
3,5,6-TPA 5717
8-OHdG 6127

FEB – GUIDE FOR AUTHORS

General

FEB accepts original papers, review articles, short communications, research abstracts from the entire sphere of environmental-chemistry,-biology,-microbiology,- technology, -biotechnology and-management, furthermore, about residue analysis/ and ecotoxicology of contaminants.

Acceptance or no acceptance of a contribution will be decided, as in the case of other scientific journals, by a board of reviewers. Papers are processed with the understanding that they have not been published before (except in form of an abstract or as a part of a published lecture, review or thesis);that they are not under consideration for publication elsewhere; that their publication has been approved by all co-authors, if any, as well as-tacitly or explicitly- by the responsible authorities at the institute where the work has been carried out and that, if accepted, it will not be published elsewhere in the same form, in either the same or another language, without the consent of the copyright holders.

Language

Papers must be written in English. Spelling may either follow American (Webster) or British (Oxford) usage but must be consistent. Authors who are less familiar with the English language should seek assistance from proficient colleagues in order to produce manuscripts that are grammatically and linguistically correct.

Size of manuscript

Review articles should not exceed 30 typewritten pages. In addition up to 5 figures may be included.

Original papers must not exceed 14 typewritten pages. In addition up to 5 figures may be included.

Short-Communications should be limited to 4 typewritten pages plus not more than 1 illustration.

Short descriptions of the authors, presentation of their groups and their research activities (with photo) should together not exceed I typewritten page. Short research abstracts should report in a few brief sentences (one-fourth to one page) particularly significant findings. Short articles by relative newcomers to the chemical innovation arena highlight the key elements of their Master and PhD-works in about I page.

Book Reviews are normally written in-house, but suggestions for books to review are welcome.

Preparation of manuscript

Dear authors,

FEB is available both as printed journal and as online journal on the web. You can now e-mail your manuscripts with an attached file. Save both time and money. To avoid any problems handling your text please follow the instructions given below:

When preparing your manuscripts have the formula K/SS (Keep It Simple and Stupid) in mind. Most word processing programs such as MS-Word offer a lot of features. Some of them can do serious harm to our layout. So please do not insert hyperlinks and/or automatic cross-references, tables of contents, references, footnotes, etc.

1. Please use the standard format features of your word processor (such as standard.dot for MS Word).
2. Please do not insert automatisms or secret link-ups between your text and your figures or tables. These features will drive our graphic department sometimes mad.
3. Please only use two fonts for text or tables "Times New Roman" and for graphical presentations "Arial".
4. Stylesheets, text, tables and graphics in shade of grey
5. Turn on the automatic language detection in English (American or British)
6. Please - check your files for viruses before you send them to us!!

Manuscripts should send to:parlar@wzw.tum.de
or:parlar@prt-parlar.de

Thank you very much!

STRUCTURE OF THE MANUSCRIPT

Title page: The first page of the manuscript should contain the following items in the sequence given: A concise title of the paper (no abbreviations). The names of all authors with at least one first name spelled out for every author. The names of Universities with Faculty, City and Country of all authors.

Abstracts: The second page of the manuscript should start with an abstract that summarizes briefly the contents of the paper (except short communications). Its length should not exceed 150-200 words. The abstract should be as informative as possible. An extended repetition of the paper's title is not considered to be an abstract.

Keywords: Below the Summary up to 6 key words have to be provided which will assist indexers in cross-indexing your article.

Introduction: This should define the problem and, if possible, the frame of existing knowledge. Please ensure that people not working in that particular field will be able to understand the intention. The word length of the introduction should be 150 to 300 words.

Materials and methods:
Please be as precise as possible to enable other scientists to repeat the work.

Results: Only material pertinent to the subject must be included. Data must not be repeated in figures and tables.

Acknowledgements: Acknowledgements of financial support, advice or other kind of assistance should be given at the end of the text under the heading "Acknowledgements". The names of funding organisations should be written in full.

References: Responsibility for the accuracy of references rests with the authors. References are to be limited in number to those absolutely necessary. References should appear in numerical order in brackets and in order of their citation in the text. They should be grouped at the end of the paper in numerical order of appearance. Abbreviated titles of periodicals are to be used according to Chemical or Biological Abstracts, but names of lesser known journals should be typed in full. References should be styled and punctuated according to the following examples:

ORIGINALPAPERS:
l. Author, N.N. and Author, N.N. (Year) Full title of the article. Journal and Volume, first and last page.
BOOK OR PROCEEDING:
2. Author, N.N. and Author, N.N. (Year) Title of the contribution.
In: Title of the book or proceeding. Volume (Edition
of klitor-s, ed-s) Publisher, City, first and last page

DOCTORALTHESIS:
3. Author, N.N. (Year) Title of the thesis, University and
Faculty, City

UNPUBLISHED WORK:
Papers that are unpublished but have been submitted to a journal may be cited with the journal's name followed by "in press". However, this practice is acceptable only if the author has at least received galley proofs of his paper. In all other cases reference must be made to “unpublished work" or "personal communication".

Discussion and Conclusion: This part should interpret the results in reference to the problem outlined in the introduction and of related observations by the author/s or others. Implications for further studies or application may be discussed. A conclusion should be added if results and discussion are combined.

Corresponding author: The name of the corresponding author with complete postal address

Precondition for publishing:
A minimum number of 25 reprints must be ordered and prepaid.
1 - 4 pp.: 200,- EURO + postage/handling
5 - 8 pp.: 250,- EURO + postage/ handling
More than 8pp: 1.50 EURO/page x number of reprints +postage/ handling.
The prices are based upon the number of pages in our journal layout (not on the page numbers of the submitted manuscript).
Postage/ Handling: The current freight rate is Germany 10 €, Europe 18,00 €, International 30 €.
VAT: In certain circumstances (if no VAT registration number exists) we may be obliged to charge 7% VAT on sales to other EU member countries.MESAEP and SECOTOX members get a further discountof 20% (postage/ handling full).